

Progress in

**PHYSICAL
ORGANIC
CHEMISTRY**

VOLUME 13

Progress in

**PHYSICAL
ORGANIC
CHEMISTRY**

VOLUME 13

Editor

ROBERT W. TAFT, *Department of Chemistry
University of California, Irvine, California*

An Interscience® Publication

John Wiley & Sons

New York Chichester Brisbane Toronto

An Interscience® Publication
Copyright ©1981 by John Wiley & Sons, Inc.

All rights reserved. Published simultaneously in Canada.

Reproduction or translation of any part of this work beyond that permitted by Sections 107 or 108 of the 1976 United States Copyright Act without the permission of the copyright owner is unlawful. Requests for permission or further information should be addressed to the Permissions Department, John Wiley & Sons, Inc.

Library of Congress Cataloging in Publication Data:

Library of Congress Catalog Card Number: 63-19364

ISBN 0-471-06253-7

Printed in the United States of America

10 9 8 7 6 5 4 3 2 1

Contributors to Volume 13

J. L. M. Abboud

Department of Chemistry
Universite Cadi Iyad
Marrakech, Morocco

Marvin Charton

Department of Chemistry
Pratt Institute
Brooklyn, New York

Stephen A. Godleski

Department of Chemistry
University of Rochester
Rochester, New York

M. J. Kamlet

Explosives Chemistry Branch
Naval Surface Weapons Center/White Oak
Silver Spring, Maryland

Eiji Ōsawa

Department of Chemistry
Faculty of Science
Hokkaido University
Sapporo, Japan

Addy Pross

Department of Chemistry
Ben Gurion University of the Negev
Beer Sheva, Israel

Leo Radom

Research School of Chemistry
The Australian National University
Canberra, Australia

Wolfgang Runge
Organisch-Chemisches Institut
der Technischen Universität München
Germany

Paul V. R. Schleyer
Institut für Organische Chemie der
Universität Erlangen-Nürnberg
Erlangen, West Germany

Leon M. Stock
Department of Chemistry
University of Chicago
Chicago, Illinois

R. W. Taft
Department of Chemistry
University of California
Irvine, California

Michael R. Wasielewski
Chemistry Division
Argonne National Laboratory
Argonne, Illinois

W. Todd Wipke
Board of Studies in Chemistry
University of California
Santa Cruz, California

Introduction to the Series

Physical organic chemistry is a relatively modern field with deep roots in chemistry. The subject is concerned with investigations of organic chemistry by quantitative and mathematical methods. The wedding of physical and organic chemistry has provided a remarkable source of inspiration for both of these classical areas of chemical endeavor. Further, the potential for new developments resulting from this union appears to be still greater. A closing of ties with all aspects of molecular structure and spectroscopy is clearly anticipated. The field provides the proving ground for the development of basic tools for investigations in the areas of molecular biology and biophysics. The subject has an inherent association with phenomena in the condensed phase and thereby with the theories of this state of matter.

The chief directions of the field are: (a) the effects of structure and environment on reaction rates and equilibria; (b) mechanisms of reactions; and (c) applications of statistical and quantum mechanics to organic compounds and reactions. Taken broadly, of course, much of chemistry lies within these confines. The dominant theme that characterizes this field is the emphasis on interpretation and understanding which permits the effective practice of organic chemistry. The field gains its momentum from the application of basic theories and methods of physical chemistry to the broad areas of knowledge of organic reactions and organic structural theory. The nearly inexhaustible diversity of organic structures permits detailed and systematic investigations which have no peer. The reactions of complex natural products have contributed to the development of theories of physical organic chemistry, and, in turn, these theories have ultimately provided great aid in the elucidation of structures of natural products.

Fundamental advances are offered by the knowledge of energy states and their electronic distributions in organic compounds and the relationship of these to reaction mechanisms. The development, for example, of even an empirical and approximate general scheme for the estimation of activation energies would indeed be most notable.

The complexity of even the simplest organic compounds in terms of physical theory well endows the field of physical organic chemistry with the frustrations of approximations. The quantitative correlations employed in this field vary from purely empirical operational formulations to the approach of applying physical principles to a workable model. The most common procedures have involved

the application of approximate theories to approximate models. Critical assessment of the scope and limitations of these approximate applications of theory leads to further development and understanding.

Although he may wish to be a disclaimer, the physical organic chemist attempts to compensate his lack of physical rigor by the vigor of his efforts. There has indeed been recently a great outpouring of work in this field. We believe that a forum for exchange of views and for critical and authoritative reviews of topics is an essential need of this field. It is our hope that the projected periodical series of volumes under this title will help serve this need. The general organization and character of the scholarly presentations of our series will correspond to that of the several prototypes, e.g., *Advances in Enzymology*, *Advances in Chemical Physics*, and *Progress in Inorganic Chemistry*.

We have encouraged the authors to review topics in a style that is not only somewhat more speculative in character but which is also more detailed than presentations normally found in textbooks. Appropriate to this quantitative aspect of organic chemistry, authors have also been encouraged in the citation of numerical data. It is intended that these volumes will find wide use among graduate students as well as practicing organic chemists who are not necessarily expert in the field of these special topics. Aside from these rather obvious considerations, the emphasis in each chapter is the personal ideas of the author. We wish to express our gratitude to the authors for the excellence of their individual presentations.

We greatly welcome comments and suggestions on any aspect of these volumes.

Robert W. Taft

Contents

A Theoretical Approach to Substituent Interactions in Substituted Benzenes <i>By Addy Pross and Leo Radom</i>	1
The Systematic Prediction of the Most Stable Neutral Hydrocarbon Isomer <i>By Stephen A. Godleski, Paul v R. Schleyer, Eiji Ōsawa and W. Todd Wipke</i>	63
Electrical Effect Substituent Constants for Correlation Analysis <i>By Marvin Charton</i>	119
The Trifluoromethyl Group in Chemistry and Spectroscopy Carbon-Fluorine Hyperconjugation <i>By Leon M. Stock and Michael R. Wasielewski</i>	253
Substituent Effects in Allenes and Cumulenes <i>By Wolfgang Runge</i>	315
An Examination of Linear Solvation Energy Relationships <i>By J. L. M. Abboud, M. J. Kamlet and R. W. Taft</i>	485
Author Index	631
Subject Index	635

Progress in

**PHYSICAL
ORGANIC
CHEMISTRY**

VOLUME 13

A Theoretical Approach to Substituent Interactions in Substituted Benzenes

BY ADDY PROSS

*Department of Chemistry, Ben Gurion University of the Negev,
Beer Sheva, Israel*

AND LEO RADOM

*Research School of Chemistry, The Australian National
University, Canberra, Australia*

CONTENTS

I.	Introduction	1
II.	Previous Work	3
III.	Methods	4
	A. Quantitative Model: <i>Ab Initio</i> Molecular Orbital Theory	4
	B. Qualitative Model: Perturbation Molecular Orbital Theory	5
IV.	Monosubstituted Benzenes	9
V.	Disubstituted Benzenes	18
	A. Substituent Effects in Fluorobenzenes, Phenols, and Anilines	19
	1. Effect of π -Donor Substituents (CH ₃ , NH ₂ , OH, OCH ₃ , F)	19
	2. Effect of π -Acceptor, σ -Acceptor Substituents	27
	3. Effect of σ -Donor, π -Acceptor Substituents	29
	4. Rotational Barriers in Substituted Phenols	29
	5. Inversion Barriers in Substituted Anilines	32
	B. Substituent Effects in Cyanobenzenes	33
	C. Substituent Effects in Lithiobenzenes	36
	D. Substituent Effects in Phenoxide and Anilide Anions	38
	E. Substituent Effects in Anilinium Cations	46
	F. Effect of Substituents on Acidity and Basicity	46
VI.	Polysubstituted Benzenes	53
VII.	Concluding Remarks	57
	References and Notes	57

I. INTRODUCTION

The effect of substituents in benzene rings has been a subject of widespread interest for many years (1). Since Hammett's early work on aromatic substituent parameters (2), various experimental techniques have been employed to provide

a more detailed and quantitative understanding of how substituents interact with an aromatic ring. Both rate and equilibrium studies (3) have been carried out and, in addition, correlations based on spectroscopic properties such as nmr chemical shifts (1*b*) and ir frequencies (4) have been utilized.

Recently, with the advent of efficient programs for carrying out *ab initio* molecular orbital calculations (5), it has become possible to examine substituent effects theoretically. In one such study, Hehre et al. (6) have conducted STO-3G calculations on a large range of monosubstituted benzenes. In an extension of that work, we present here an account of similar calculations on both disubstituted and polysubstituted benzenes.

The present study attempts to assess the interactions among the substituents from both a charge and energy point of view. The theoretical energies and charge distributions not only yield energies of interaction of the substituents on the benzene ring, but analysis of σ and π charges provides an electronic rationalization of the observed energetic behavior.

An attempt is made to generalize the results with the aid of perturbation molecular orbital (PMO) theory (7). This serves as a most useful qualitative framework within which many of the quantitative results may be understood. Hopefully, as experience with PMO theory increases, its application will serve not only to rationalize results obtained from both theoretical and experimental techniques, but also to increase its predictive powers for related systems. This kind of application of PMO theory is in line with the growing tendency to use qualitative orbital arguments to understand both static and dynamic molecular properties, in addition to (and to some extent, instead of) the more conventional resonance theory.

Many of the data presented here are not readily available through experimental techniques. On the one hand, there is only a very limited amount of direct thermochemical information presently available for polysubstituted benzenes. In addition, indirect information obtained from kinetic studies is largely based on effects of substituents on a charged group. For example, the Hammett equation is concerned with substituent effects in the benzoate anion, σ^- substituent parameters are based on substituent effects in phenoxide ions, whereas σ^+ parameters are based on substituent effects in the ionic transition state for cumyl chloride solvolysis, to mention just a few (3). In fact, theoretical substituent effects discussed here confirm that charged groups on a benzene ring display significantly larger substituent effects than neutral ones, explaining the preference of experimentalists for such systems.

Finally, we draw attention to the limited objectives of the present article. We make no attempt to cover the extensive theoretical and experimental literature on substituted benzenes. Rather, we take the opportunity to examine in detail, calculations at a uniform level of theory (*ab initio* molecular orbital theory with the STO-3G basis set) for a small number of representative substituents

(H, CH₃, NH₂, OH, OCH₃, F, NO₂, CN, CHO, CF₃, Li, O⁻, NH⁻, and NH₃⁺). Some of the work reported herein has been previously published (6,8-11) but a large part of our discussion refers to previously unpublished data accumulated over a number of years from several different laboratories. The primary goal of this study has been to draw together this wide body of computational data and to attempt to understand the diverse behavior observed within a relatively simple PMO (7) framework. There are undoubtedly other frameworks within which the results could be analyzed and we make no claim that our interpretation is necessarily unique. However, regardless of the qualitative picture of substituent effects which we develop here, the quantitative data stand on their own and hopefully may be utilized by other workers to prove or disprove alternative or supplementary hypotheses concerning substituent effects in aromatic systems.

II. PREVIOUS WORK

A large number of theoretical *ab initio* calculations have been performed on benzene (12-38) and mono- and disubstituted benzenes (6,20,39-92). There appear to be no reports to date of *ab initio* calculations on polysubstituted (i.e. with more than two substituents) benzenes. Brief comment follows on some of the previous studies most closely related to the present work.

The effect of para substituents on the OH torsional barrier in phenols and nitrogen inversion barrier in anilines has been examined by Pople and co-workers (8,9). These topics are discussed in Sections V.A.4 and V.A.5. The results show that in a para-substituted benzene, a π donor and a π acceptor interact favorably with one another whereas the situation of two π donors leads to resonance saturation and a destabilizing interaction. Wepster et al. (93,94) have reached similar conclusions on the basis of experimental studies. The relative stabilities of ortho-, meta-, and para-disubstituted benzenes for the substituents CN, OH, and F have been studied by von Niessen (66) using a Gaussian lobe minimal basis set. Radom has calculated the effect of substituents on the acidities of phenols and noted good agreement with available gas-phase data (65).

Reynolds and co-workers (61,62,95-100) have used *ab initio* and other theoretical and nmr chemical shift data to examine substituent effects in substituted benzenes. Systems studied in this way include substituted benzoic acids (61), styrenes (62,98), phenylacetylenes (99), and phenylalkanes (96). Particular emphasis has been placed on the separation of field, inductive, and resonance effects.

There is also some non-*ab initio* theoretical and experimental work of direct relevance to the present study. For example, the question of the existence of π -inductive effects (1d) has been paid considerable attention by a number of

workers (95-97,101-107). Although the subject remains one of some controversy, the idea that changes in π -electron density may be induced by the σ system appears to be gaining widespread support. Katritzky, Topsom, and co-workers have utilized a method of estimating substituent interactions in para-disubstituted benzenes (4,108) based on measurements of ir intensities (109). The data provide a quantitative measure of through-conjugation in these systems.

A key paper on monosubstituted benzenes, which represents the basis of the more recent work reported here, is that by Hehre, Radom, and Pople (6). It contains a detailed analysis at the STO-3G level of substituent ring interactions in monosubstituted benzenes, and encompasses charge distributions, stabilities, and conformations of 35 substrates. Relevant results are more fully detailed in Section IV.

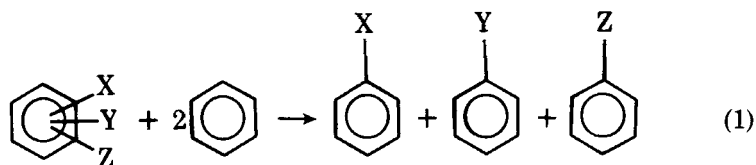
III. METHODS

A. Quantitative Model: *Ab Initio* Molecular Orbital Theory

The results described in the body of this article were all obtained within the framework of *ab initio* self-consistent-field molecular orbital theory (110). Calculations were performed with the STO-3G basis set (111) using modified versions of the Gaussian 70 system of programs (5). Molecular geometries were constructed on the basis of standard bond lengths and angles (112,113) except for the few situations noted here. For the amino substituent, calculations were carried out both for a planar model geometry and also for a model in which the three bond angles (assumed equal) about nitrogen were optimized. For the methoxy substituent, a value of 118.0° was used for the COC angle, this being the optimum value in anisole itself. Standard values of 1.28, 1.34, and 1.52 Å, obtained from STO-3G optimizations on the phenoxide, anilide, and anilinium ions, were used for the bonds C3— $\overset{\ominus}{\text{O}}1$, C3— $\overset{\ominus}{\text{N}}2$, and C3— $\overset{\oplus}{\text{N}}4$, respectively.

Charge distributions were calculated using the Mulliken population analysis (114). For most of the systems examined, it has been possible to examine not only the total atomic charges but also the separation into σ and π charges as well. Such a separation is particularly useful in the subsequent analysis of the results. Also of interest are π -overlap populations which provide a measure of double bond character. It is important to treat with caution the absolute charges obtained in the Mulliken analysis since any assignment of charges to atoms in molecules is necessarily arbitrary. As a result, absolute charges tend to be very dependent on the method used to calculate them. Relative charges, for example changes in charge distribution on substitution, are generally more meaningful and useful.

The energy data for di- and polysubstituted benzenes have been analyzed in terms of substituent interaction energies. These are given by energies of reactions of the type shown by Equation 1:



A positive value for the interaction energy implies a stabilizing interaction among the substituents. Since reaction 1 is isodesmic (24), it should be reasonably well described even at the STO-3G level of theory (115).

B. Qualitative Model: Perturbation Molecular Orbital Theory

A particularly useful model for analyzing substituent effects uses perturbation molecular orbital (PMO) theory (7). Most simply, the theory states that the interaction of two orbitals, Ψ_j and Ψ_k , results in the formation of two new orbitals, one of which is lowered in energy while the other is raised in energy compared to the interacting orbitals. For the case in which one orbital is occupied and one empty, the resultant interaction is stabilizing.

Let us discuss a specific example such as the interaction of F and CH_2^+ to form FCH_2^+ as illustrated in Fig. 1. Interaction of the F lone pair with the formally vacant orbital, $2p(\text{C}^+)$, at C^+ results in two new orbitals, one lower in energy than the initial F lone pair orbital and a second which is higher in energy than the original $2p(\text{C}^+)$ orbital. The interaction involves two electrons and is stabilizing. In general, the net stabilization energy (SE) resulting from interaction of a filled and empty orbital is given by:

$$SE = \frac{c_{rj}^2 c_{sk}^2 \beta_{rs}^2}{\Delta E} \quad (2)$$

where c_{rj} and c_{sk} represent the coefficients of the atomic orbitals on interacting atoms r and s in the molecular orbitals Ψ_j and Ψ_k , respectively, and β_{rs} represents the resonance integral associated with these atomic orbitals. ΔE represents the energy separation between the two interacting orbitals. This means that the two-electron stabilizing interaction is determined by the four parameters in Equation 2. Any factor that will reduce the energy gap between the two interacting orbitals will enhance the stabilization energy, as will factors which increase the coefficients c_{rj} and c_{sk} , and the degree of overlap, approximated by β_{rs} .

We note here two effects, which will be of particular importance in our analysis, which modify orbital energies, hence the energy gap ΔE , and hence the stabilization energy SE . (i) The first effect concerns replacement of the

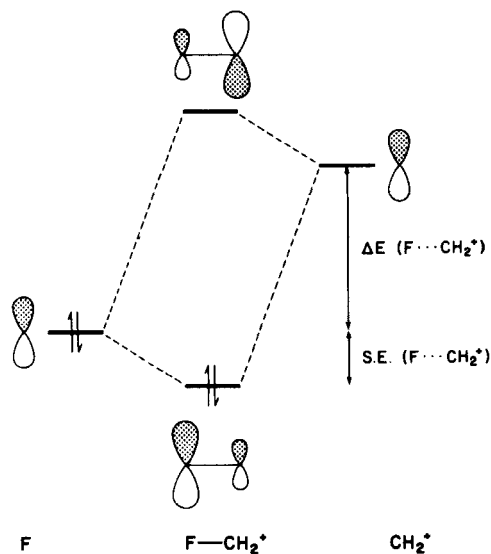


Figure 1 PMO diagram showing the interaction of an occupied F lone pair orbital with the vacant CH₂⁺ p orbital.

atoms with which either of the interacting orbitals are associated. Substitution by a less electronegative atom has the effect of increasing the energy of the orbital associated with that atom (116). This may be illustrated with reference to an extension (Fig. 2) of our original example (Fig. 1). If F is replaced by the less

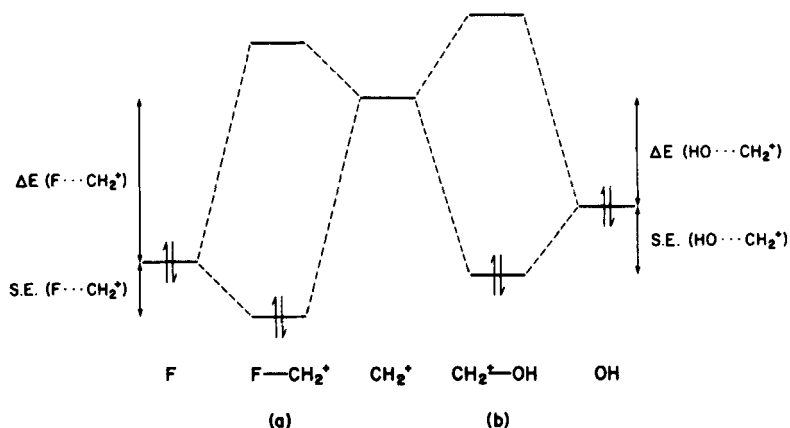


Figure 2 PMO diagram showing the relative stabilization produced by interaction (a) on an occupied F lone pair orbital and (b) of an occupied OH lone pair orbital with the vacant CH₂⁺ p orbital.

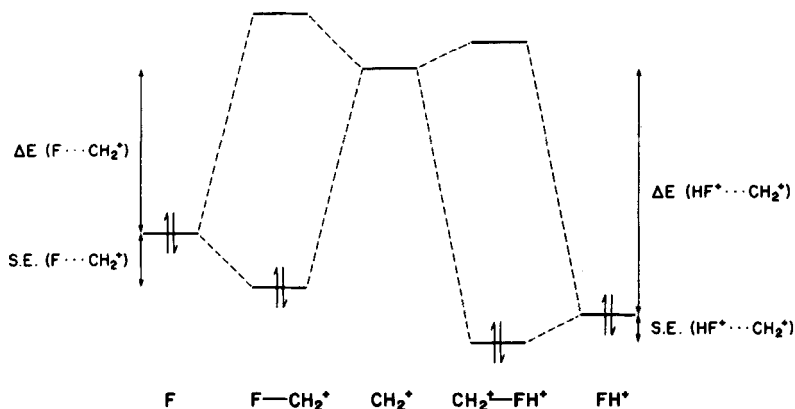


Figure 3 PMO diagram showing the effect of F protonation on the stabilization produced by interaction of an occupied F lone pair orbital with the vacant CH₂⁺ p orbital.

electronegative OH group, then an enhanced stabilizing interaction, $SE(\text{HO} \dots \text{CH}_2^+) > SE(\text{F} \dots \text{CH}_2^+)$, is anticipated as a result of the reduction in the energy gap between the interacting orbitals, $\Delta E(\text{HO} \dots \text{CH}_2^+) < \Delta E(\text{F} \dots \text{CH}_2^+)$. (ii) A second type of perturbation operates by what we term a *shielding-deshielding* mechanism. This occurs when one of the interacting moieties is substituted by an atom or group which is strongly electron-releasing or -withdrawing (117). For example, introduction of an electron-withdrawing substituent onto an existing group will lower the energy of the orbitals associated with that group (10) by a deshielding mechanism. This may be thought of in terms of enhanced nuclear-electronic attraction for the remaining electrons following electron withdrawal from an atomic center. This leads in turn to a lowering of the orbital energies. It is important to note that the lowering in energy applies not only to orbitals that can interact directly with the substituent, but it applies as well to those orbitals that are orthogonal to the interacting orbital. Returning to our example of the interaction of F with CH₂⁺: If F is now protonated to form HF⁺, then the energy of the interacting F lone pair orbital in HF⁺ is lowered by a deshielding process as shown in Fig. 3. In this case, the F lone pair orbital that interacts with the CH₂⁺ moiety is lowered as a result of protonation despite being orthogonal to the proton orbital. The effect of protonation is thus relayed to the interacting F lone pair orbital through the shielding-deshielding mechanism. Interaction of the CH₂⁺ orbital with the energetically more stable, $\Delta E(\text{FH}^+ \dots \text{CH}_2^+) > \Delta E(\text{F} \dots \text{CH}_2^+)$, FH⁺ orbital leads to less stabilization than with the F orbital: $SE(\text{FH}^+ \dots \text{CH}_2^+) < SE(\text{F} \dots \text{CH}_2^+)$.

An additional effect with which we shall have reason to be concerned and which can be usefully described in terms of PMO theory is the concept of in-

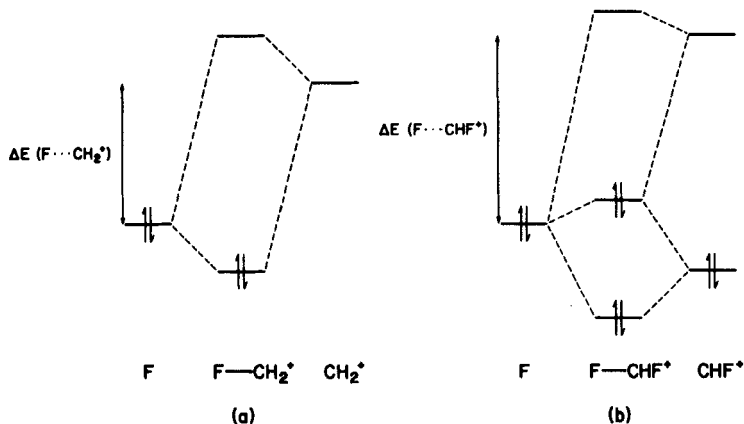


Figure 4 PMO interaction diagram showing the phenomenon of saturation arising from successive F substitution in CH_3^+ to give first (a) FCH_2^+ and then (b) F_2CH^+ .

teraction saturation. Put simply, this concept reflects the fact that the interaction of a second (identical) substituent with a given substrate is less than that of the first. For example, the effect of a second fluorine substituent in the methyl cation is less than that of the first. Interaction of the lone pair orbital of the first F substituent with $2p(\text{C}^+)$ raises the energy of the empty orbital (Fig. 1). The energy gap ΔE for interaction of a second F substituent with the acceptor orbital is thus increased, $\Delta E (\text{F} \dots \text{CH}_2^+) < \Delta E (\text{F} \dots \text{CHF}^+)$ (Fig. 4), and as a result the stabilizing interaction becomes less effective. The situation is, in fact, complicated by interaction with the filled orbital of the FCH^+ moiety, also shown in Fig. 4, but the general conclusion of diminishing interaction with successive substitution remains valid.

The quantitative *ab initio* calculations may be utilized in combination with the qualitative PMO picture to understand how the various substituents are interacting. Of particular importance is Mulliken population analysis which, as noted in Section III.A, provides a method of assigning charges to the orbitals and atoms within a molecule. Since the two-electron stabilizing interactions which we have been discussing so far involve transfer of charge from an electron donor (the filled orbital) to an electron acceptor (the empty orbital), a correlation might be expected between the degree of charge transfer, and the extent of stabilization, both of which may be monitored by the quantitative calculations. An increase in charge transfer would suggest a more favorable two-electron interaction and as a consequence greater stabilization. Similarly, a decrease in charge transfer would indicate a less favorable interaction.

For the substituted benzene systems studied here, the degree of both σ and π charge transfer between the substituent and the ring are indicative of the magnitude of the substituent-ring interaction. The effect of a second substituent may be understood by analyzing how σ and π charge transfer between the first

substituent and the ring is modified. Reduction in charge transfer would imply an unfavorable substituent-substituent interaction, while an increase in charge transfer suggests the contrary. In this context, the effect of the first substituent on the charge transfer between the second substituent and the ring must also be taken into account.

The foregoing discussion has only considered the possibility of interaction between a vacant and a filled orbital. The case in which both orbitals are occupied was not considered. Such an interaction involves four electrons and is destabilizing. This is because the increase in energy of the higher energy orbital outweighs the decrease in the orbital of lower energy (7). We note that there is no charge transfer associated with such an interaction. Most of the substituent effect behavior we observe is readily rationalized in terms of the two-electron interactions alone.

One final point is that we make no attempt to distinguish between the possible mechanisms for the transmission of the σ -effect of substituents. These are now commonly believed to encompass both field and through-bond effects (95,104). In our study, analyses associated with the field/inductive effects of a substituent are treated together under the heading of σ effects.

IV. MONOSUBSTITUTED BENZENES

A detailed account, at the STO-3G level, of conformations, charge distributions and stabilities of 35 monosubstituted benzenes, including 10 of our representative set, has been presented by Hehre et al. (6). Corresponding results for the remaining members (Li, O⁻, NH⁻, and NH₃⁺) have been obtained more recently (67,10,11). We reproduce here some of the key results for all of the substituents which will be relevant to our subsequent discussion of di- and polysubstituted benzenes. Calculated total energies and dipole moments are listed in Table 1, and Mulliken charges and overlap populations are listed in Table 2. Where more than one conformation is possible, unless otherwise specified, the energy data listed are for the most stable conformation.

For those substituents possessing π -type orbitals, the overriding conformational requirement appears to be conjugation with the ring (6). Thus OH, OCH₃, NO₂, and CHO prefer the planar conformation. The conformational preference in phenol results in a calculated rotational barrier of 5.16 kcal mole⁻¹ compared with the experimental 3.56 kcal mole⁻¹ (8). The nitrogen in aniline prefers a pyramidal configuration with a bond angle of 112.1° (experimental 113.9°) (9). The inversion barrier is calculated to be 2.72 kcal mole⁻¹ (experimental 1.61 kcal mole⁻¹) (9). The effect of substituents on the rotational barrier in phenol and inversion barrier in aniline is discussed in Sections V.A.4 and 5.

The charge data indicate that NH₂, OH, OCH₃, and F constitute a group

TABLE I
 Calculated Total Energies and Dipole Moments for Monosubstituted Benzenes^a

Substituent (X)	Conformation	Dipole moment (debyes)	Energy (hartrees)
H		0	-227.89006
CH ₃	CCCH planar	0.25	-266.47382
NH ₂	$\alpha = 112.1^\circ$ ^b	1.44	-282.20892
NH ₂	planar N	1.30	-282.20458
OH	CCOH planar	1.22	-301.72861
OH	CCOH orthogonal	1.45	-301.72039
OCH ₃	COCH trans	1.22	-340.30429
F		0.93	-325.34939
NO ₂	CCNO planar	4.26	-428.58323
NO ₂	CCNO orthogonal	3.99	-428.57408
CN		3.65	-318.44330
CHO	CCCO planar	1.90	-339.11540
CF ₃	CCCF planar	1.67	-558.85457
Li		5.12	-234.60099
O ⁻			-300.97376
NH ⁻	CCNH planar		-281.44059
NH ₃ ⁺	CCNH planar		-282.63403

^a Data taken from Ref. 6.

^b α is the optimized value of the bond angles (assumed equal) about nitrogen.

of σ acceptors and π donors and that NO₂, CN and CF₃ represent a group of σ and π acceptors. CH₃ is indicated to be a weak σ and π donor, whereas Li is a powerful σ donor and π acceptor. The charged group, O⁻, appears to be a powerful π donor and a relatively weak σ donor, whereas NH₃⁺ behaves as a powerful σ acceptor and an essentially inactive π group.

π -Electron populations for monosubstituted benzenes appear in Fig. 5. Consistent with the accepted viewpoint, π donors (CH₃, NH₂, OH, OCH₃, F, O⁻, and NH⁻) induce negative charge concentrations at ortho and para positions (π populations >1), whereas π acceptors (NO₂, CN, CHO, and CF₃) create positive charge at these positions (π populations <1).

It is of interest that a σ acceptor, such as orthogonal NO₂, which does not act as a π acceptor ($q_\pi = -0.001$), also induces positive charge at ortho and para positions. This may be attributed to the π -inductive effect, and has been noted in a number of systems (1a,4b,95-97,101-103,107,118). We use the term π -inductive effect here in the sense originally employed by Dewar (119) and Jaffe (120) and termed inductoelectromeric; that is, changes in the π -electron density which are induced by attachment of an electron-withdrawing or releasing group adjacent to the ring, and which lead to an alternation of charge density around the ring. A charged substituent such as NH₃⁺, however, appears to

TABLE 2
Mulliken Charges and Overlap Populations for Monosubstituted Benzenes^a

Substituent (X)	q_{σ}^b	q_{π}^b	$\pi(\text{Ph-X})^c$
H	-0.063	0	0
CH ₃	-0.007	-0.008	0.009
NH ₂	+0.140	-0.095	0.048
NH ₂ ^d	+0.159	-0.120	0.063
OH	+0.185	-0.102	0.052
OH ^e	+0.154	-0.049	0.022
OCH ₃	+0.192	-0.105	0.057
F	+0.215	-0.080	0.038
NO ₂	+0.227	+0.031	0.034
NO ₂ ^f	+0.241	-0.002	0.007
CN	+0.104	+0.022	0.043
CHO	-0.001	+0.032	0.047
CF ₃	+0.021	+0.011	0.017
Li	-0.265	+0.092	0.059
O ⁻	-0.021	-0.506	0.221
NH ⁻	-0.019	-0.484	0.230
NH ₃ ⁺	+0.385	-0.001	0.003

^a From Ref. 6.

^b q_{σ} and q_{π} are the total σ and π charges donated by the substituent to the ring.

^c $\pi(\text{Ph-X})$ is the Mulliken overlap population of the adjacent π -type p orbitals in the C—X bond.

^d Data refer to planar NH₂.

^e Data refer to orthogonal OH.

^f Data refer to orthogonal NO₂.

polarize the π -system as a whole so that the π -charge decreases gradually as the distance to the NH₃⁺ increases (96). This effect is apparently dominant over any contribution from the π -inductive effect. For systems for which π -electron transfer between the substituent and the ring is small, it would appear therefore that π polarization is dominant for a charged group whereas for a neutral σ -acceptor, where field effects are weaker, the π -inductive effect may be observed.

Since much of this review is concerned with substituent effects in di- and polysubstituted benzenes, a clear understanding of the orbital structure of monosubstituted benzenes is essential. This is because many of the interactions present in di- and polysubstituted benzenes may be understood in terms of the interaction between the monosubstituted benzene and the other substituent(s).

The important orbitals in monosubstituted benzenes, which will to a large extent determine the nature of any interaction with a second substituent, are

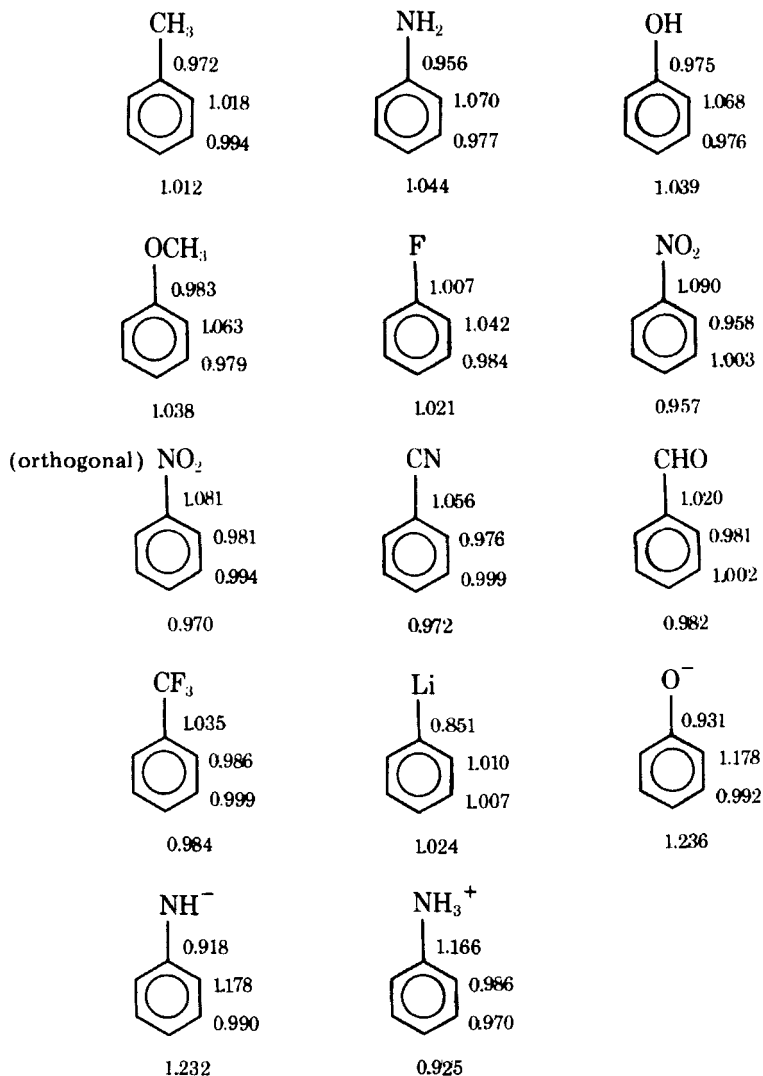


Figure 5 π -Electron populations in monosubstituted benzenes.

the highest occupied molecular orbital (HOMO) and the lowest unoccupied molecular orbital (LUMO). The molecular orbital coefficients for the HOMOs and LUMOs for the monosubstituted benzenes are listed in Figs. 6 and 7, respectively. The orbitals shown are of π symmetry, and the coefficients therefore refer to the carbon or heteroatom $2p_y$ orbital. Data for orthogonal and planar

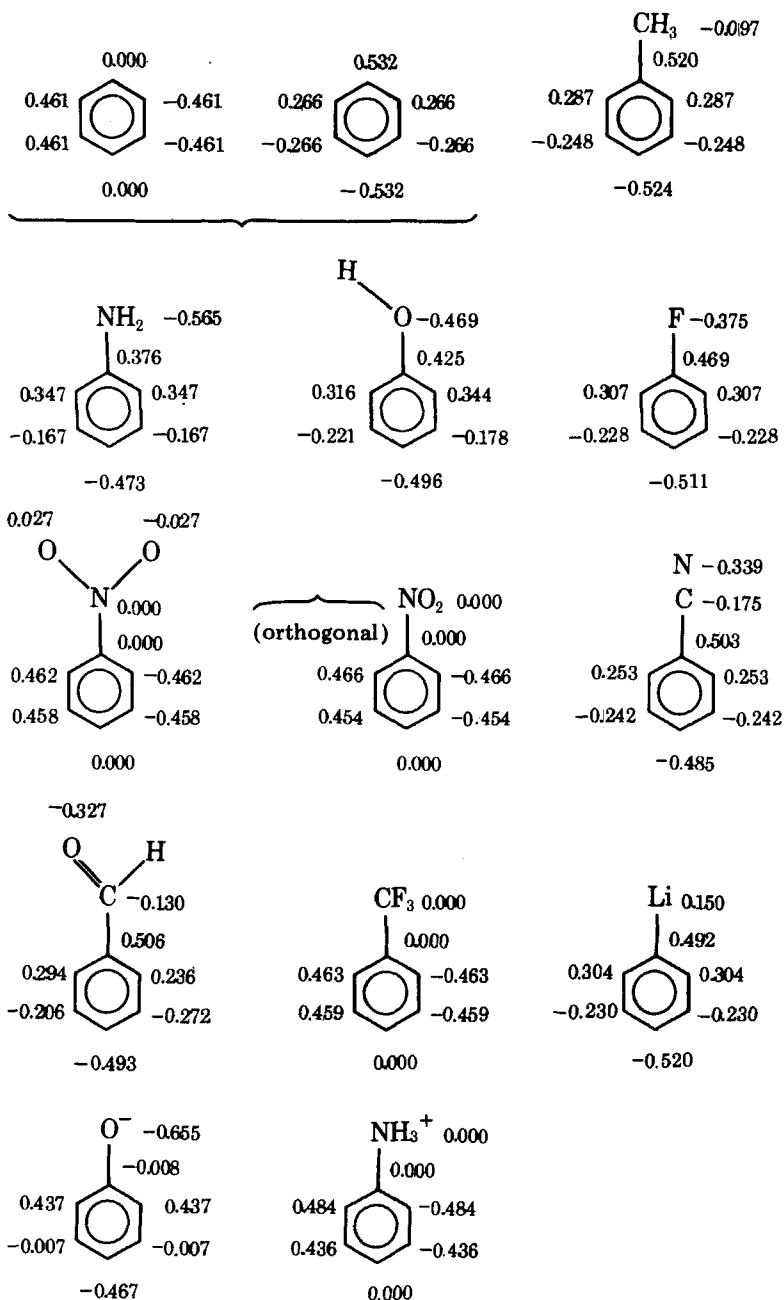


Figure 6 HOMO coefficients for monosubstituted benzenes. Data for toluene and anilinium ion are for the conformation in which a C—H or N—H bond is orthogonal to the ring. Data for aniline refer to planar N. Data for orthogonal and planar nitrobenzene refer to the level below the HOMO. The HOMOs in both cases are mainly localized on the two oxygen atoms.

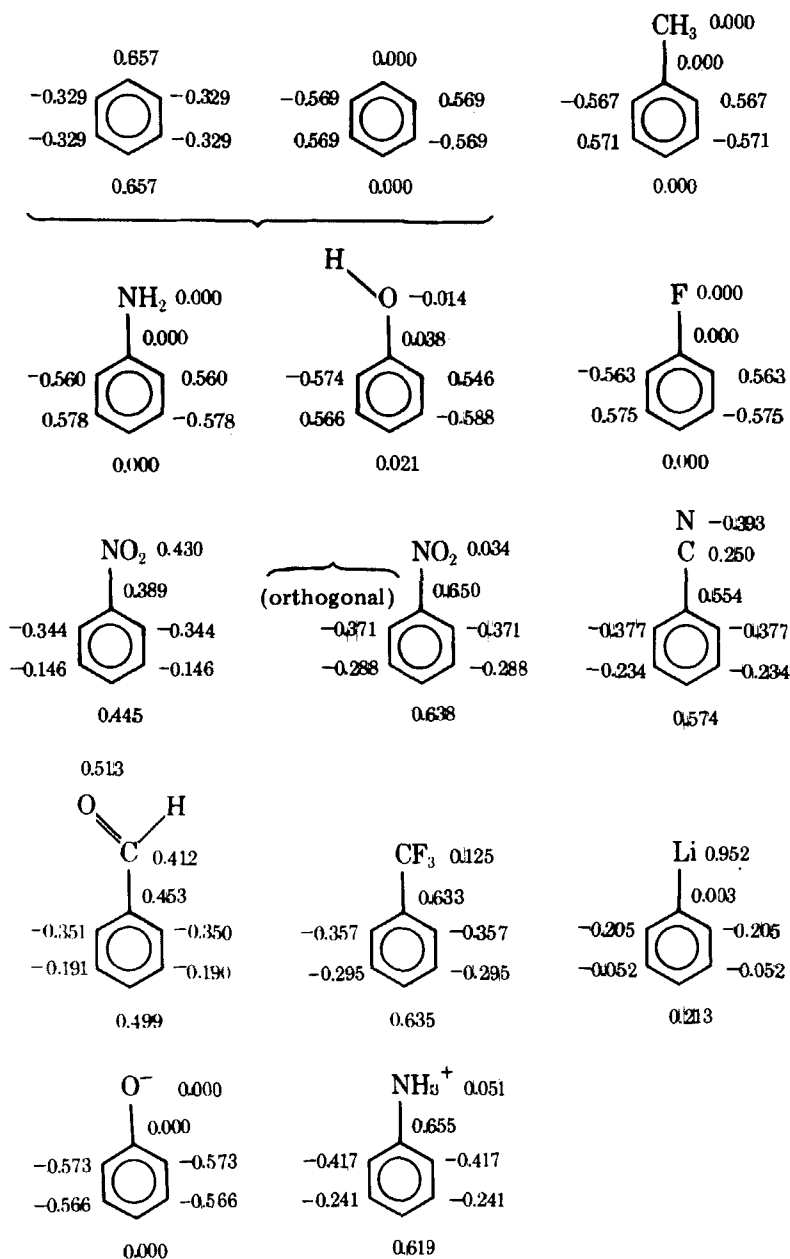


Figure 7 LUMO coefficients for monosubstituted benzenes. Data for toluene and anilinium ion are for the conformation in which a C—H or N—H bond is orthogonal to the ring. Data for aniline refer to planar N. Data for lithiobenzene refer to the level above the LUMO, this being the lowest unoccupied orbital of π symmetry.

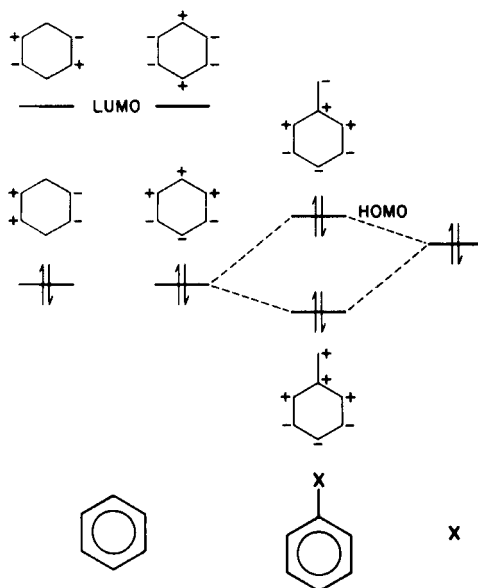


Figure 8 PMO diagram showing the interaction of benzene π -orbitals with a low-lying lone pair orbital of a substituent (X).

nitrobenzene refer to the level below the HOMO, since the HOMOs are mainly localized on the oxygen atoms. The LUMO for lithiobenzene is actually an orbital with substantial Li $2s$ character. The orbital shown in Fig. 7 is the next orbital in energy and does possess π symmetry.

From Figs. 6 and 7 it is apparent that the substituent has a significant effect on the orbital coefficients. For example, the HOMO of the phenoxide ion has essentially zero coefficients at the meta positions, whereas phenol has significant coefficients at those positions. It is instructive to examine, using the PMO model, how the general characteristics of these orbitals may be derived in a qualitative fashion.

The HOMO and LUMO orbitals of a monosubstituted benzene where the substituent, X ($= \text{NH}_2$, OH or F), is a neutral π -donor, may be obtained through interaction of the benzene HOMO and LUMO orbitals with the substituent lone pair according to the principles discussed in Section III.B. Being an occupied orbital, the lone pair orbital will be closer in energy to the occupied benzene orbitals than the unoccupied ones (Fig. 8). As a result, it will interact mainly with the occupied orbital of appropriate symmetry, to give two new orbitals. The antibonding combination of this interaction now becomes the HOMO and may be seen to conform to the quantitative data in Fig. 6. The LUMOs for aniline, phenol, and fluorobenzene are the essentially unaffected benzene LUMO, in agreement with the quantitative data (Fig. 7).

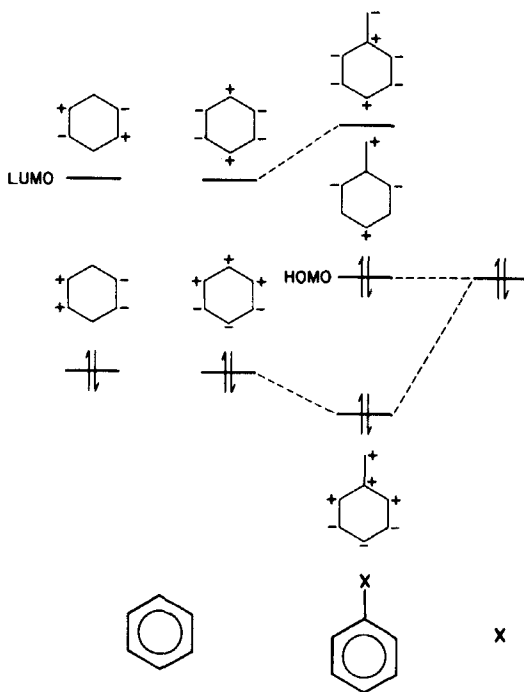


Figure 9 PMO diagram showing the interaction of benzene π -orbitals with a high-lying lone pair orbital of a substituent (X).

When the interacting orbital on the substituent, X, is higher in energy than that found in a neutral π -donor, a somewhat different interaction diagram is obtained. This is shown in Fig. 9 and is exemplified by a substituent such as O^- , which possesses a relatively high-lying occupied orbital. In this case the lone pair orbital, being in the intermediate region between the benzene HOMOs and LUMOs, will interact with both. Taking a linear combination of the benzene LUMO of appropriate symmetry with the lone pair results in a bonding combination which then may be interacted with the benzene HOMO in an antibonding combination. The result is a new nonbonding HOMO of similar energy to the original substituent orbital. The additional orbitals resulting from the benzene-substituent interaction will be a stabilized occupied orbital, and a destabilized unoccupied orbital. Examination of Figs. 6 and 7 confirms this prediction. The HOMO for phenoxide ion is essentially a nonbonding orbital with nodes at the ipso and meta positions, whereas the LUMO is just the benzene LUMO which, through symmetry, does not undergo interaction with the O^- .

Finally, analysis of the interaction of a high-lying vacant orbital with the benzene orbitals is shown in Fig. 10. Here we see that the predominant inter-

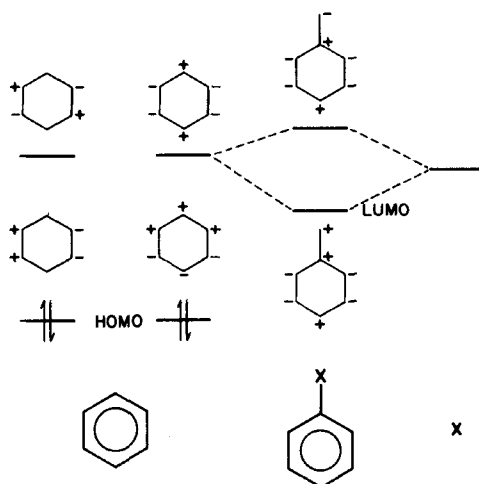


Figure 10 PMO diagram showing the interaction of benzene π -orbitals with a vacant high-lying π^* orbital of a substituent (X).

action of the vacant orbital is with the benzene LUMOs. This situation is exemplified by nitrobenzene. As a result, a relatively low-lying LUMO is produced which has the symmetry indicated. Accordingly, the quantitative data for nitrobenzene (Fig. 7) confirm the qualitative prediction. The nitrobenzene HOMO (or at least the highest occupied orbital associated with the ring in nitrobenzene) is predicted to be an essentially unaffected benzene HOMO. The quantitative data (Fig. 6) bear this out as well.

To summarize, interaction of benzene with an adjacent lone pair (e.g., NH_2 , OH , and F) will result in the formation of a new HOMO of higher energy than the unsubstituted benzene. This orbital is expected to dominate much of the chemical properties of the substituted benzene. The quantitative data (Fig. 6) indicate larger coefficients at ortho and para positions suggesting greater interactions at those positions.

For a high-lying lone pair (e.g., O^-), interaction will occur with both π and π^* benzene orbitals and will result in a high-energy nonbonding HOMO with small coefficients at the meta positions. Again, this orbital is likely to have a strong influence on the chemistry of systems in this category.

The dominant orbital in the chemistry of monosubstituted benzenes in which the interacting orbital (normally empty, e.g., NO_2 , CN , CHO) of the substituent has even higher energy, is a relatively low-lying LUMO. This orbital arises through predominant interaction with the benzene π^* orbitals.

There is one further type of substituent which may interact with the benzene ring and which needs to be considered: a powerful σ acceptor such as NH_3^+ .

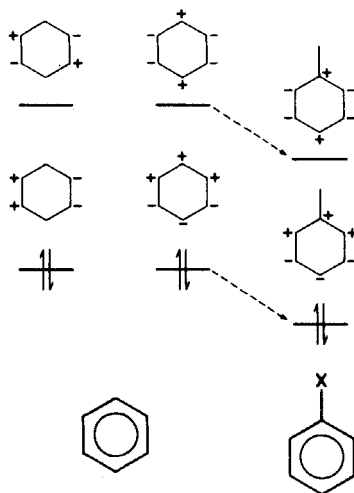


Figure 11 Effect of a powerful σ -acceptor (e.g. $X = \text{NH}_3^+$) on the π and π^* orbitals of benzene.

The effect of the NH_3^+ group on the orbitals of benzene will depend primarily on the coefficients of those orbitals at the carbon to which the NH_3^+ group is bound. For an orbital possessing a larger coefficient on the appropriate carbon atom, a large effect is anticipated since the electron-withdrawing NH_3^+ group will lower the energy of all atomic orbitals on that carbon atom by a deshielding process. As a result, the energy of the particular orbital is likely to be affected. Reference to Fig. 11 shows that, since one of the HOMOs and one of the LUMOs possess a node at the point of substitution (i.e., a zero coefficient), these two orbitals will remain unaffected. On the other hand, the remaining HOMO and LUMO exhibit a significant coefficient at the $\text{C}(2p_y)$ orbital to which the substituent is bound. As a result, those two orbitals will be lowered in energy by the deshielding process. The net result is that the HOMO for a monosubstituted benzene in which the substituent is a σ acceptor is essentially the benzene HOMO with a nodal plane passing through the ipso and para carbons while the LUMO is essentially the benzene LUMO without a nodal plane through these carbons. The qualitative predictions are borne out by the quantitative data shown in Figs. 6 and 7.

V. DISUBSTITUTED BENZENES

The consideration of substituent effects may be approached in a large number of ways due to the many possible permutations of substituent pairs. We have arbitrarily divided the discussion into a number of separate parts:

A. The effect of substituents in fluorobenzenes, phenols, and anilines, where F, OH, and NH_2 exemplify σ -accepting and π -donating groups.

B. The effect of substituents in cyanobenzenes, where CN represents a strong σ - and π -accepting group.

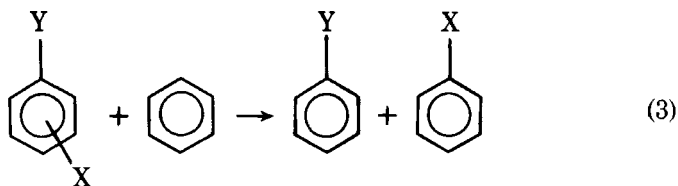
C. The effect of substituents in lithiobenzenes where Li represents a σ donor and π acceptor.

D. The effect of substituents in phenoxide ions, where O^- represents a negatively charged group.

E. The effect of substituents in anilinium ions, where NH_3^+ represents a positively charged group.

A. Substituent Effects in Fluorobenzenes, Phenols, and Anilines

Calculations were carried out on a variety of possible conformations of substituted fluorobenzenes, phenols, and anilines; the total energies, relative energies, and dipole moments are presented in Tables 3–5. Table 6 lists interaction energies, based on the lowest energy conformation of each molecule. These are calculated as energies of reaction 3:



where Y is either F, OH, or NH_2 and X is the substituent. Finally, Mulliken charges and overlap populations appear in Tables 7–9.

From the discussion on monosubstituted benzenes, it is apparent that there is a pronounced interaction between the substituents F, OH, and NH_2 with the ring. These substituents were found to be σ acceptors and π donors. The effect of an additional substituent on the interaction between the first substituent and the ring (and vice versa) will now determine whether substituent–substituent interactions are favorable or unfavorable.

1. Effect of π -Donor Substituents (CH_3 , NH_2 , OH, OCH_3 , F)

The substituents CH_3 , NH_2 , OH, OCH_3 , and F all interact favorably with the group of σ acceptors and π donors at the meta position but unfavorably at the para position. This behavior may be accounted for in terms of changes in the two-electron interaction between the π -donor substituent and π^* ring orbitals of the monosubstituted benzene. Relevant orbitals for the monosubstituted benzene (generated in Fig. 8) and the lone pair of the second substituent are shown in Fig. 12.

TABLE 3
Energy Data and Dipole Moments for Substituted Fluorobenzenes

Substituent (X)	Conformation	Dipole moment (debyes)	Total energy (hartrees)	Relative energy (kcal mole ⁻¹)
H		0.93	-325.34939	
<i>o</i> -CH ₃		0.81	-363.93313	
<i>m</i> -CH ₃		1.12	-363.93355	
<i>p</i> -CH ₃		1.19	-363.93289	
<i>o</i> -NH ₂	$\alpha = 111.8^\circ$ ^a	1.58	-379.66595	0
	planar N	1.18	-379.66125	2.95
<i>m</i> -NH ₂	$\alpha = 112.3^\circ$ ^a	1.89	-379.66916	0
	planar N	1.98	-379.66514	2.52
<i>p</i> -NH ₂	$\alpha = 112.0^\circ$ ^a	2.00	-379.66696	0
	planar N	2.24	-379.66240	2.86
<i>o</i> -OH	HOC...CF <i>cis</i>	0.75	-399.18572	0
	HOC...CF <i>trans</i>	2.11	-399.18302	1.69
	HOC...CF orthogonal	1.84	-399.17674	5.63
<i>m</i> -OH	HOC...CF <i>cis</i>	0.52	-399.18857	0
	HOC...CF <i>trans</i>	2.04	-399.18844	0.08
	HOC...CF orthogonal	1.59	-399.17988	5.45
<i>p</i> -OH	HOC...CF planar	1.42	-399.18649	0
	HOC...CF orthogonal	1.43	-399.17912	4.62
<i>o</i> -F		1.59	-422.80382	
<i>m</i> -F		0.92	-422.80871	
<i>p</i> -F		0	-422.80756	
<i>o</i> -NO ₂		4.75	-526.03684	
<i>m</i> -NO ₂		3.82	-526.04044	
<i>p</i> -NO ₂		3.41	-526.04256	
<i>o</i> -CN		4.14	-415.90122	
<i>m</i> -CN		3.22	-415.90118	
<i>p</i> -CN		2.78	-415.90254	
<i>o</i> -Li		4.80	-332.07378	
<i>m</i> -Li		5.80	-332.06223	
<i>p</i> -Li		6.04	-332.06141	

^a α is the optimized value of the bond angles (assumed equal) about nitrogen.

As noted in Section IV, interaction between the first substituent and the degenerate benzene HOMO and LUMO pairs leads to nondegenerate π and π^* levels as well as a high-energy HOMO in the monosubstituted benzene. Interaction between the lone pair of a second substituent and the monosubstituted benzene is now determined by three factors. (a) The electronegative nature of the first substituent on the ring has the effect of lowering all π and π^* orbitals through a deshielding process thus tending to create enhanced π donation by the second substituent into the π^* orbitals. In a similar manner, the electronegative second substituent leads to enhanced π donation by the first substituent. (b) The π -donor properties of the first substituent have the effect of raising the

TABLE 4
Energy Data and Dipole Moments for Substituted Phenols

Substituent (X)	Conformation	Dipole moment (debyes)	Total energy (hartrees)	Relative energy (kcal mole ⁻¹)
H	HOCC planar	1.22	-301.72861	0
	HOCC orthogonal	1.45	-301.72039	5.16
<i>o</i> -CH ₃	HOC...CCH <i>trans, trans</i>	1.00	-340.31221	0
	HOC...CCH orthogonal, <i>trans</i>	1.38	-340.30435	4.93
<i>m</i> -CH ₃	HOC...CCH <i>trans, trans</i>	1.03	-340.31283	0
	HOC...CCH <i>cis, trans</i>	1.47	-340.31271	0.08
	HOC...CCH orthogonal, <i>trans</i>	1.50	-340.30434	5.33
<i>p</i> -CH ₃	HOC...CCH <i>trans</i>	1.29	-340.31175	0
	HOC...CCH orthogonal, planar	1.55	-340.30398	4.88
<i>o</i> -NH ₂	HOC...CN <i>trans</i> , $\alpha = 111.7^\circ$ ^a	1.57	-356.04496	0
	HOC...CN orthogonal, $\alpha = 111.7^\circ$ ^a (<i>trans</i>) ^b	0.51	-356.04045	2.83
	HOC...CN orthogonal, $\alpha = 111.7^\circ$ ^a (<i>cis</i>) ^b	2.74	-356.03749	4.69
<i>m</i> -NH ₂	HOC...CN <i>trans</i> , planar NH ₂	0.50	-356.03995	3.14
	HOC...CN <i>trans</i> , $\alpha = 112.3^\circ$ ^a	1.56	-356.04877	0
	HOC...CN <i>cis</i> , $\alpha = 112.3^\circ$ ^a	2.22	-356.04856	0.13
	HOC...CN orthogonal, $\alpha = 112.3^\circ$ ^a (<i>trans</i>) ^b	0.94	-356.03996	5.52
	HOC...CN orthogonal, $\alpha = 112.3^\circ$ ^a (<i>cis</i>) ^b	2.83	-356.03955	5.79
<i>p</i> -NH ₂	HOC...CN <i>trans</i> , planar NH ₂	0.86	-356.04472	2.54
	HOC...CN <i>cis</i> , planar NH ₂	2.49	-356.04449	2.69
	HOC...CN planar, $\alpha = 111.7^\circ$ ^a	1.93	-356.04503	0
	HOC...CN orthogonal, $\alpha = 111.7^\circ$ ^a (<i>trans</i>) ^b	1.05	-356.03857	4.05
	HOC...CN planar, planar NH ₂	1.90	-356.04005	3.12
<i>o</i> -OH	HOC...COH <i>cis, trans</i>	2.15	-375.56607	0
	HOC...COH <i>trans, trans</i>	1.52	-375.56085	3.28
	HOC...COH orthogonal, <i>trans</i>	2.17	-375.55575	6.48
	HOC...COH orthogonal, <i>cis</i>	1.64	-375.56008	3.76
	HOC...COH orthogonal, orthogonal (<i>cis</i>) ^b	2.83	-375.54769	11.53
	HOC...COH orthogonal, orthogonal (<i>trans</i>) ^b	0.80	-375.54989	10.15
	HOC...COH planar, planar NH ₂	1.90	-356.04005	3.12
<i>m</i> -OH	HOC...COH <i>cis, trans</i>	1.22	-375.56850	0
	HOC...COH <i>trans, trans</i>	2.28	-375.56804	0.29
	HOC...COH <i>cis, cis</i>	1.92	-375.56784	0.41
	HOC...COH orthogonal, <i>cis</i>	1.58	-375.55936	5.74
	HOC...COH orthogonal, <i>trans</i>	2.12	-375.55932	5.76
	HOC...COH orthogonal, orthogonal (<i>cis</i>) ^b	2.77	-375.55064	11.21
	HOC...COH orthogonal, orthogonal (<i>trans</i>) ^b	0.48	-375.55109	10.92
<i>p</i> -OH	HOC...COH <i>trans</i>	0	-375.56486	0
	HOC...COH <i>cis</i>	2.39	-375.56475	0.07
	HOC...COH orthogonal, planar	1.84	-375.55810	4.24
	HOC...COH orthogonal, orthogonal (<i>cis</i>) ^b	2.71	-375.55026	9.15
	HOC...COH orthogonal, orthogonal (<i>trans</i>) ^b	0	-375.55052	9.00

TABLE 4
Energy Data and Dipole Moments for Substituted Phenols (Continued)

Substituent (X)	Conformation	Dipole moment (debyes)	Total energy (hartrees)	Relative energy (kcal mole ⁻¹)
<i>m</i> -OCH ₃	HOC...COC <i>trans, cis</i>	0.91	-414.14424	0
	HOC...COC <i>trans, trans</i>	2.14	-414.14352	0.45
	HOC...COC <i>cis, trans</i>	1.51	-414.14398	0.16
<i>p</i> -OCH ₃	HOC...COC <i>trans</i>	0.32	-414.14069	0
	HOC...COC <i>cis</i>	2.38	-414.14012	0.36
<i>o</i> -NO ₂	HOC...CN <i>trans</i>	5.45	-502.41606	0
	HOC...CN orthogonal	4.67	-502.40737	5.45
<i>m</i> -NO ₂	HOC...CN <i>cis</i>	3.14	-502.42103	0
	HOC...CN orthogonal	4.26	-502.41273	5.21
	HOC...CNO <i>cis, orthogonal</i>	2.90	-502.41203	5.65
<i>p</i> -NO ₂	HOC...CN planar	4.50	-502.42383	0
	HOC...CN orthogonal	4.14	-502.41399	6.17
	HOC...CNO planar, orthogonal	4.14	-502.41362	6.41
<i>o</i> -CN	HOC...CN <i>cis</i>	2.74	-392.28277	0
	HOC...CN <i>trans</i>	4.84	-392.28186	0.57
	HOC...CN orthogonal	4.10	-392.27338	5.89
<i>m</i> -CN	HOC...CN <i>cis</i>	2.54	-392.28128	0
	HOC...CN <i>trans</i>	4.65	-392.28099	0.18
	HOC...CN orthogonal	3.69	-392.27306	5.16
<i>p</i> -CN	HOC...CN planar	3.87	-392.28317	0
	HOC...CN orthogonal	3.54	-392.27389	5.82
	HOC...CCO <i>trans, cis</i>	3.19	-412.95469	0
<i>o</i> -CHO	HOC...CCO <i>trans, trans</i>	2.62	-412.95010	2.88
	HOC...CCO <i>cis, trans</i>	0.83	-412.95392	0
	HOC...CCO <i>cis, cis</i>	1.70	-412.95338	0.34
<i>m</i> -CHO	HOC...CCO <i>trans, cis</i>	2.38	-412.95359	0.21
	HOC...CCO <i>trans, trans</i>	3.06	-412.95332	0.38
	HOC...CCO orthogonal, <i>trans</i>	2.44	-412.94543	5.33
<i>p</i> -CHO	HOC...CCO <i>cis</i>	1.41	-412.95507	
<i>o</i> -CF ₃	HOC...CCF <i>trans, trans</i>	2.85	-632.69268	
<i>m</i> -CF ₃	HOC...CCF <i>cis, trans</i>	0.70	-632.69283	0
	HOC...CCF <i>trans, trans</i>	2.73	-632.69263	0.13
<i>p</i> -CF ₃	HOC...CCF <i>trans</i>	1.99	-632.69380	
<i>o</i> -Li	HOC...CLi <i>trans</i>	4.02	-308.45091	0
	HOC...CLi <i>cis</i>	5.83	-308.44430	4.15
	HOC...CLi orthogonal	4.99	-308.44316	4.86
<i>m</i> -Li	HOC...CLi <i>trans</i>	4.43	-308.44041	0
	HOC...CLi <i>cis</i>	6.35	-308.44019	0.14
	HOC...CLi orthogonal	5.63	-308.43209	5.22
<i>p</i> -Li	HOC...CLi planar	5.33	-308.43945	0
	HOC...CLi orthogonal	5.79	-308.43178	4.81

^a α is the optimized value of the bond angles (assumed equal) about nitrogen.

^b The terms *cis* and *trans* correspond respectively to the hydrogens of the hydroxyl group and of the substituent being located on the same or opposite sides of the ring plane.

TABLE 5
Energy Data and Dipole Moments for Substituted Anilines

Substituent (X)	Conformation ^a	Dipole moment (debyes)	Total energy (hartrees)	Relative energy (kcal mole ⁻¹)
H	$\alpha = 112.1^\circ$	1.44	-282.20892	0
	planar N	1.30	-282.20458	2.72
<i>m</i> -CH ₃	$\alpha = 112.0^\circ$, NC...CCH <i>trans</i>	1.41	-320.79298	0
	planar N, NC...CCH <i>trans</i>	1.20	-320.78866	2.71
<i>p</i> -CH ₃	$\alpha = 112.0^\circ$	1.36	-320.79196	0
	planar N	1.09	-320.78740	2.86
<i>m</i> -NH ₂	$\alpha = 112.2^\circ$, H ₂ N...NH ₂ <i>trans</i>	0.57	-336.52910	0
	$\alpha = 112.3^\circ$, H ₂ N...NH ₂ <i>cis</i>	2.68	-336.52872	0.24
	NH ₂ planar, NH ₂ $\alpha = 112.0^\circ$	1.73	-336.52473	2.74
	NH ₂ planar, NH ₂ planar	1.26	-336.52050	5.40
<i>p</i> -NH ₂	$\alpha = 111.5^\circ$, H ₂ N...NH ₂ <i>trans</i>	0	-336.52519	0
	$\alpha = 111.6^\circ$, H ₂ N...NH ₂ <i>cis</i>	2.69	-336.52496	0.14
	NH ₂ planar, NH ₂ $\alpha = 111.5^\circ$	1.57	-336.51995	3.29
	NH ₂ planar, NH ₂ planar	0	-336.51450	6.71
<i>m</i> -OCH ₃	$\alpha = 112.3^\circ$, ^b NC...COC <i>cis</i>	2.15	-394.62422	0
	$\alpha = 112.3^\circ$, ^b NC...COC <i>trans</i>	1.49	-394.62418	0.03
<i>p</i> -OCH ₃	$\alpha = 111.7^\circ$, ^b NC...COC planar	1.82	-394.62080	
<i>m</i> -NO ₂	$\alpha = 112.5^\circ$	4.80	-482.90213	0
	planar N	5.09	-482.89835	2.37
<i>p</i> -NO ₂	$\alpha = 113.2^\circ$	5.44	-482.90556	0
	planar N	6.01	-482.90257	1.88
<i>o</i> -CN	$\alpha = 113.3^\circ$	3.64	-372.76400	0
	planar N	3.34	-372.76099	1.89
<i>m</i> -CN	$\alpha = 112.4^\circ$	4.22	-372.76229	0
	planar N	4.50	-372.75840	2.44
<i>p</i> -CN	$\alpha = 112.9^\circ$	4.75	-372.76447	0
	planar N	5.31	-372.76109	2.12
<i>m</i> -CHO	$\alpha = 112.3^\circ$, NC...CCO <i>cis</i>	2.27	-393.43428	0
	$\alpha = 112.3^\circ$, NC...CCO <i>trans</i>	2.77	-393.43406	0.14
<i>p</i> -CHO	$\alpha = 112.5^\circ$, NC...CCO planar	2.91	-393.43582	
<i>m</i> -CF ₃	$\alpha = 112.3^\circ$, NC...CCF <i>cis</i>	2.44	-613.17360	
<i>p</i> -CF ₃	$\alpha = 112.5^\circ$, NC...CCF planar	2.73	-613.17466	
<i>o</i> -Li	$\alpha = 110.7^\circ$	5.27	-288.92160	0
<i>m</i> -Li	$\alpha = 111.6^\circ$	5.12	-288.91945	0
	planar N	4.64	-288.91437	3.19
<i>p</i> -Li	$\alpha = 111.6^\circ$	4.62	-288.91885	0
	planar N	3.55	-288.91376	3.19

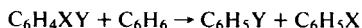
^a α is the optimized value of the bond angles (assumed equal) about nitrogen. Where for a particular isomer of aniline a number of conformations are possible, optimization was conducted on the *trans* isomer and the optimized angle used in the energy determinations of the other conformations.

^b Optimum α used was that for the corresponding OH substituent (see Table 4).

TABLE 6
Interaction Energies (kcal mole⁻¹) for Substituted Fluorobenzenes,
Phenols, and Anilines^a

Substituent (X)	Fluorobenzene	Phenol	Aniline
H	0.0	0.0	0.0
<i>o</i> -CH ₃	0.0	-0.1	
<i>m</i> -CH ₃	+0.3	+0.3	+0.2
<i>p</i> -CH ₃	-0.2	-0.4	-0.5
<i>o</i> -NH ₂	-1.4	-1.6	
<i>m</i> -NH ₂	+0.6	+0.8	+0.8
<i>p</i> -NH ₂	-0.8	-1.5	-1.6
<i>o</i> -OH	-1.4	-0.7	-1.6
<i>m</i> -OH	+0.4	+0.8	+0.8
<i>p</i> -OH	-0.9	-1.4	-1.5
<i>m</i> -OCH ₃		+0.9	+0.7
<i>p</i> -OCH ₃		-1.3	-1.5
<i>o</i> -F	-3.1	-1.4	-1.4
<i>m</i> -F	0.0	+0.4	+0.6
<i>p</i> -F	-0.7	-0.9	-0.8
<i>o</i> -NO ₂	-3.6	-3.6	
<i>m</i> -NO ₂	-1.3	-0.5	0.0
<i>p</i> -NO ₂	0.0	+1.3	+2.2
<i>o</i> -CN	-0.9	+0.6	+1.2
<i>m</i> -CN	-0.9	-0.4	+0.1
<i>p</i> -CN	-0.1	+0.8	+1.4
<i>o</i> -CHO		+0.5	
<i>m</i> -CHO		0.0	0.0
<i>p</i> -CHO		+0.7	+1.0
<i>o</i> -CF ₃		-0.3	
<i>m</i> -CF ₃		-0.2	+0.1
<i>p</i> -CF ₃		+0.4	+0.8
<i>o</i> -Li	+8.4	+7.1	+1.0
<i>m</i> -Li	+1.2	+0.5	-0.3
<i>p</i> -Li	+0.7	0.0	-0.6

^a Values represent energies for the reactions:



where Y = F, OH, or NH₂, and X is a second substituent.

energy of the ring π -acceptor orbital of appropriate symmetry (top orbital in Fig. 12) compared with its energy in benzene. This leads to a saturation effect (cf. Section III.B) and reduced π donation by a second substituent at the para position (interaction 3). Because of symmetry, the energetically more favorable interaction 2 is not allowed for the para-substituted system but is allowed for ortho or meta substitution. (c) Interaction between the lone pair and the π^* levels is also affected by the four-electron interaction between the lone pair and the

TABLE 7
 Mulliken Charges and Overlap Populations for Substituted Fluorobenzenes

Substituent (X)	$q_{\sigma}(Y)^a$	$q_{\sigma}(X)^a$	$q_{\pi}(Y)^a$	$q_{\pi}(X)^a$	$\pi(\text{Ph-Y})^b$	$\pi(\text{Ph-X})^b$
H	+0.215		-0.080		0.038	
<i>o</i> -CH ₃	+0.215	-0.017	-0.077	-0.007	0.037	0.010
<i>m</i> -CH ₃	+0.214	-0.013	-0.079	-0.009	0.039	0.010
<i>p</i> -CH ₃	+0.214	-0.007	-0.077	-0.008	0.037	0.009
<i>o</i> -NH ₂	+0.212	+0.127	-0.071	-0.092	0.031	0.044
<i>m</i> -NH ₂	+0.214	+0.137	-0.080	-0.099	0.041	0.051
<i>p</i> -NH ₂	+0.214	+0.138	-0.073	-0.092	0.033	0.045
<i>o</i> -OH	+0.212	+0.175	-0.069	-0.099	0.029	0.048
<i>m</i> -OH	+0.213	+0.182	-0.080	-0.105	0.041	0.055
<i>p</i> -OH	+0.212	+0.183	-0.074	-0.100	0.034	0.049
<i>o</i> -F	+0.204	+0.204	-0.075	-0.075	0.034	0.034
<i>m</i> -F	+0.210	+0.210	-0.080	-0.080	0.040	0.040
<i>p</i> -F	+0.211	+0.211	-0.076	-0.076	0.036	0.036
<i>o</i> -NO ₂	+0.193	+0.289	-0.090	-0.035	0.046	0.034
<i>m</i> -NO ₂	+0.203	+0.223	-0.080	+0.028	0.039	0.033
<i>p</i> -NO ₂	+0.207	+0.227	-0.086	+0.034	0.044	0.034
<i>o</i> -CN	+0.203	+0.093	-0.084	+0.026	0.042	0.044
<i>m</i> -CN	+0.207	+0.098	-0.080	+0.020	0.039	0.043
<i>p</i> -CN	+0.209	+0.101	-0.084	+0.026	0.042	0.043
<i>o</i> -Li	+0.221	-0.268	-0.073	+0.087	0.035	0.059
<i>m</i> -Li	+0.224	-0.279	-0.076	+0.087	0.037	0.057
<i>p</i> -Li	+0.221	-0.269	-0.075	+0.096	0.035	0.062

^a $q_{\sigma}(Y)$, $q_{\sigma}(X)$, $q_{\pi}(Y)$, and $q_{\pi}(X)$ are the total σ and π charges, respectively, donated by the substituent Y or X, to the ring. Y = F, X = substituent.

^b $\pi(\text{Ph-Y})$ and $\pi(\text{Ph-X})$ are Mulliken overlap populations of the adjacent π -type p orbitals in the bond joining Y and X, respectively, to the ring. Y = F, X = substituent.

HOMO (interaction 1). Greater interaction generates a new MO which cannot interact as readily with the LUMO. Such considerations may be used to explain why π donation at the ortho position is also reduced: Since the coefficients in the HOMO are greater in the ortho than in the meta position (Fig. 6), interaction 1 (Fig. 12) is larger at the ortho position.

Factor (a) would tend to enhance π donation by the second substituent to the ring in all three positions. Factor (b) would tend to enhance π donation in the meta position compared to the para position. Factor (c) would tend to enhance π donation in the meta position compared to the ortho position. The overall result is therefore: enhanced π donation at the meta position compared with the monosubstituted benzene (factor (a)), and reduced π donation at ortho and para positions, due to the greater importance of factors (b) and (c) (reducing π donation) over factor (a) (increasing π donation).

The destabilizing interaction of two π donors in a para-disubstituted benzene, which has been noted previously (8,61,62), is also illustrated by energies

TABLE 8
 Mulliken Charges and Overlap Populations for Substituted Phenols

Substituent (X)	$q_{\sigma}(Y)^a$	$q_{\sigma}(X)^a$	$q_{\pi}(Y)^a$	$q_{\pi}(X)^a$	$\pi(\text{Ph-Y})^b$	$\pi(\text{Ph-X})^b$
H	+0.185		-0.102		0.052	
<i>o</i> -CH ₃	+0.187	-0.015	-0.101	-0.007	0.050	0.010
<i>m</i> -CH ₃	+0.186	-0.011	-0.102	-0.009	0.053	0.010
<i>p</i> -CH ₃	+0.186	-0.003	-0.100	-0.007	0.050	0.009
<i>o</i> -NH ₂	+0.184	+0.130	-0.094	-0.091	0.042	0.042
<i>m</i> -NH ₂	+0.184	+0.138	-0.104	-0.099	0.055	0.052
<i>p</i> -NH ₂	+0.186	+0.140	-0.095	-0.088	0.045	0.041
<i>o</i> -OH ^c	+0.179	+0.179	-0.095	-0.095	0.043	0.043
<i>m</i> -OH ^c	+0.184	+0.184	-0.105	-0.105	0.055	0.055
<i>p</i> -OH	+0.184	+0.184	-0.096	-0.096	0.046	0.046
<i>o</i> -F	+0.175	+0.212	-0.099	-0.069	0.048	0.029
<i>m</i> -F	+0.182	+0.213	-0.105	-0.080	0.055	0.041
<i>p</i> -F	+0.183	+0.212	-0.100	-0.074	0.049	0.034
<i>o</i> -NO ₂	+0.165	+0.219	-0.121	+0.038	0.064	0.036
<i>m</i> -NO ₂	+0.172	+0.228	-0.105	+0.028	0.054	0.034
<i>p</i> -NO ₂	+0.177	+0.230	-0.115	+0.039	0.061	0.035
<i>m</i> -NO ₂ ^d	+0.172	+0.240	-0.106	-0.002	0.055	0.008
<i>p</i> -NO ₂ ^d	+0.176	+0.246	-0.111	0.000	0.059	0.007
<i>o</i> -CN	+0.175	+0.105	-0.114	+0.036	0.060	0.046
<i>m</i> -CN	+0.177	+0.101	-0.105	+0.021	0.054	0.043
<i>p</i> -CN	+0.179	+0.104	-0.111	+0.030	0.058	0.044
<i>o</i> -CHO	+0.184	-0.011	-0.107	+0.039	0.055	0.049
<i>m</i> -CHO	+0.181	-0.003	-0.103	+0.031	0.053	0.047
<i>p</i> -CHO	+0.183	0.000	-0.108	+0.041	0.056	0.049
<i>o</i> -CF ₃	+0.178	+0.013	-0.107	+0.013	0.056	0.018
<i>m</i> -CF ₃	+0.180	+0.019	-0.104	+0.011	0.053	0.017
<i>p</i> -CF ₃	+0.182	+0.024	-0.107	+0.014	0.056	0.018
<i>o</i> -Li	+0.190	-0.265	-0.092	+0.088	0.045	0.060
<i>m</i> -Li	+0.197	-0.275	-0.097	+0.087	0.049	0.056
<i>p</i> -Li	+0.194	-0.261	-0.097	+0.103	0.048	0.065

^a $q_{\sigma}(Y)$, $q_{\sigma}(X)$, $q_{\pi}(Y)$, $q_{\pi}(X)$ are the total σ and π charges, respectively, donated by the substituent, Y or X, to the ring. Y = OH, X = substituent.

^b $\pi(\text{Ph-Y})$ and $\pi(\text{Ph-X})$ are Mulliken overlap populations of the adjacent π -type p orbitals in the bond joining Y and X, respectively, to the ring. Y = OH, X = substituent.

^c Values are averaged for the two OH groups that are not equivalent.

^d Orthogonal NO₂.

of interaction of fluorobenzene, phenol, and aniline with para-substituted π donors (e.g. NH₂ and OH; Table 6). Destabilization increases in the order $\text{XC}_6\text{H}_4\text{F} < \text{XC}_6\text{H}_4\text{OH} < \text{XC}_6\text{H}_4\text{NH}_2$ (X = NH₂ and OH) consistent with the increasing π -donating ability of F < OH < NH₂.

In resonance terms, the effect may be represented as:

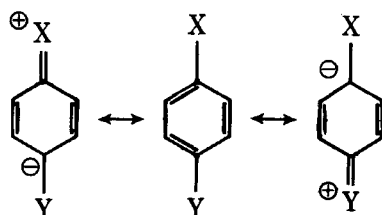
TABLE 9
 Mulliken Charges and Overlap Populations for Substituted Anilines

Substituent (X)	$q_\sigma(Y)^a$	$q_\sigma(X)^a$	$q_\pi(Y)^a$	$q_\pi(X)^a$	$\pi(\text{Ph-Y})^b$	$\pi(\text{Ph-X})^b$
H	+0.140		-0.095		0.048	
<i>m</i> -CH ₃	— ^c	— ^c	— ^c	— ^c	0.048	0.010
<i>p</i> -CH ₃	— ^c	— ^c	— ^c	— ^c	0.046	0.009
<i>m</i> -NH ₂	+0.141	+0.141	-0.098	-0.098	0.051	0.051
<i>p</i> -NH ₂	+0.142	+0.142	-0.086	-0.086	0.040	0.040
<i>o</i> -OH	+0.130	+0.184	-0.091	-0.094	0.042	0.042
<i>m</i> -OH	+0.138	+0.184	-0.099	-0.104	0.052	0.055
<i>p</i> -OH	+0.140	+0.186	-0.088	-0.095	0.041	0.045
<i>o</i> -F	+0.127	+0.212	-0.092	-0.071	0.044	0.031
<i>m</i> -F	+0.137	+0.214	-0.099	-0.080	0.051	0.041
<i>p</i> -F	+0.138	+0.214	-0.092	-0.073	0.045	0.033
<i>m</i> -NO ₂	+0.128	+0.229	-0.101	+0.029	0.051	0.034
<i>p</i> -NO ₂	+0.163	+0.233	-0.144	+0.041	0.061	0.036
<i>o</i> -CN	+0.129	+0.106	-0.111	+0.033	0.060	0.056
<i>m</i> -CN	+0.134	+0.103	-0.102	+0.022	0.051	0.043
<i>p</i> -CN	+0.136	+0.107	-0.109	+0.031	0.057	0.044
<i>m</i> -CHO	+0.137	0.0	-0.097	+0.031	0.049	0.047
<i>p</i> -CHO	+0.137	+0.004	-0.102	+0.042	0.054	0.050
<i>m</i> -CF ₃	— ^c	— ^c	— ^c	— ^c	0.050	0.017
<i>p</i> -CF ₃	— ^c	— ^c	— ^c	— ^c	0.053	0.019
<i>o</i> -Li	+0.156	-0.250	-0.082	+0.093	0.038	0.063
<i>m</i> -Li	+0.153	-0.268	-0.088	+0.090	0.043	0.057
<i>p</i> -Li	+0.149	-0.255	-0.088	+0.106	0.042	0.067

^a $q_\sigma(Y)$, $q_\sigma(X)$, $q_\pi(Y)$, and $q_\pi(X)$ are the total σ and π charges, respectively, donated by the substituent, Y or X, to the ring. Y = NH₂, X = substituent.

^b $\pi(\text{Ph-Y})$ and $\pi(\text{Ph-X})$ are Mulliken overlap populations of the adjacent π -type *p* orbitals in the bond joining Y and X, respectively, to the ring. Y = NH₂, X = substituent.

^c Values not calculable since neither substituent is planar.



whereby the substituents compete with each other for conjugation with the ring. The favorable interaction at the meta position, for which the PMO argument has been presented previously, is not readily explicable in resonance terms.

2. Effect of π -Acceptor, σ -Acceptor Substituents

π -Acceptors interact with fluorobenzenes, phenols, and anilines in the

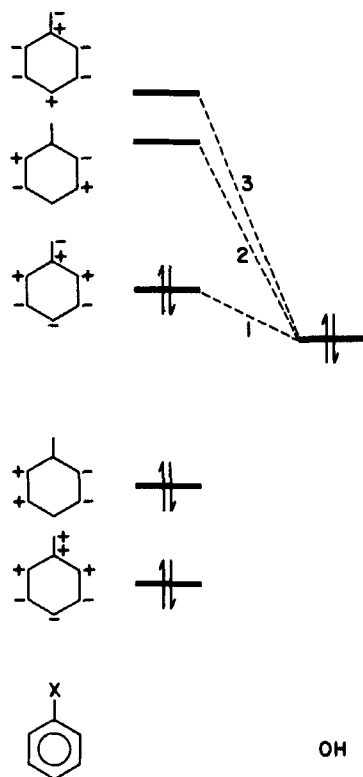


Figure 12 PMO diagram showing the interaction of a monosubstituted benzene ($X = \text{NH}_2, \text{OH}$ or F) with the OH lone pair orbital.

opposite way to π donors. The groups NO_2 , CN , CHO , and CF_3 are generally stabilizing at the para position and destabilizing at the meta position.

Here the important interaction is donation of π charge by the monosubstituted benzene HOMO into the substituent π^* orbital. Since the monosubstituted benzene HOMO is higher in energy than that of benzene (Fig. 8) the interaction is favorable. Examination of the HOMO coefficients (Fig. 6), reveals that coefficients are greater at ortho and para positions than at meta positions. As a result, greater stabilization occurs at the ortho and para positions.

At the meta positions the interaction energies are dominated by σ effects, since π interactions are small. Since σ effects are opposing for this group of substrates, destabilization generally occurs. Along the series F , OH , NH_2 the meta destabilizing interaction is observed to decrease. This supports the conclusion that the behavior at the meta position is dominated by σ effects, since σ -withdrawing power and destabilization energies decrease in the same order ($\text{F} > \text{OH} > \text{NH}_2$). Additional destabilization results from the lowering of the

ring π orbital by the σ -withdrawing F, OH or NH_2 substituent leading to reduced π -acceptance by the second substituent (e.g. NO_2).

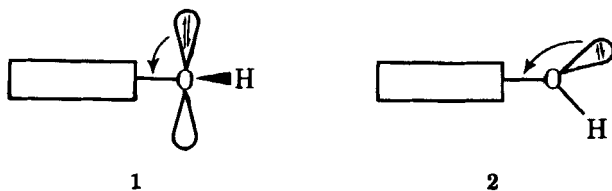
3. Effect of σ -Donor, π -Acceptor Substituents

Interaction energies with Li, the sole representative of this class of substituents, indicate that both σ and π effects are important. With F, the most electronegative group of the series, favorable interaction occurs because of the dominance of σ effects. The electron-donating Li and electron-withdrawing F act in concert. As one moves along the series F, OH, and NH_2 , π donation increases whereas σ acceptance decreases. As a result, π effects become more important. Thus the σ -donating effect of Li has the effect of raising π^* orbitals by the shielding mechanism. This results in reduced π donation, and for NH_2 the reduction results in destabilization.

The large stabilization of ortho-Li substitution in fluorobenzene and phenol are due to direct substituent interactions rather than interactions through the ring. Specifically, a very favorable two-electron stabilization occurs, brought about by donation of the F and OH in-plane lone pairs into the vacant in-plane Li $2p_x$ orbital.

4. Rotational Barriers in Substituted Phenols

An experimentally accessible probe for studying π -electron interactions in substituted phenols is the barrier to rotation about the C—O bond (8). Interaction of the p -type lone pair on oxygen with the π^* orbitals of the ring in the planar conformation (1) is more effective than interaction of the sp^2 -type lone pair on oxygen in the orthogonal conformation (2) because of poorer overlap and lower orbital energy in the latter situation.



As a consequence, phenol itself is planar, and the energy difference between the planar and orthogonal forms represents the barrier to internal rotation about the C—O bond. Substituents that increase conjugation between the OH group and the ring might be expected to increase the rotational barrier and vice versa (8).

Theoretical rotational barriers for a number of para-substituted phenols have been previously reported (8). We present here results for additional substituents and consider meta substitution as well. To examine both meta and para

TABLE 10
Effect of Substituents on Rotational Barriers (ΔV_2) and
Overlap Populations in Substituted Phenols

Substituent (X)	ΔV_2 (kcal mole ⁻¹)	π (Ph-OH)
H	0	0.052
<i>m</i> -CH ₃	+0.13	0.053
<i>p</i> -CH ₃	-0.28	0.050
<i>m</i> -NH ₂	+0.30	0.055
<i>p</i> -NH ₂	-1.11	0.045
<i>m</i> -OH	+0.45	0.055
<i>p</i> -OH	-0.95	0.046
<i>m</i> -F	+0.25	0.055
<i>p</i> -F	-0.53	0.049
<i>m</i> -NO ₂	-0.18	0.054
<i>p</i> -NO ₂	+1.02	0.061
<i>m</i> -CN	-0.07	0.054
<i>p</i> -CN	+0.66	0.058
<i>m</i> -Li	-0.01	0.049
<i>p</i> -Li	-0.35	0.048
<i>m</i> -O ⁻	+0.63	0.044
<i>p</i> -O ⁻	-4.99	0.010
<i>m</i> -NH ₃ ⁺	-0.67	0.064
<i>p</i> -NH ₃ ⁺	+1.65	0.071

substituents on a uniform basis, it is convenient to use in the comparisons the V_2 component of the barrier. This measures the average energy difference between planar and orthogonal conformations.

Theoretical values of ΔV_2 , the difference between the V_2 value for the substituted phenol and phenol itself, are listed in Table 10, together with π -overlap populations for the C—O bond. Although the theoretical V_2 values are significantly different from those obtained experimentally (e.g. for phenol the calculated barrier is 5.16 kcal mole⁻¹ compared with the experimentally determined value of 3.56 kcal mole⁻¹), the theoretical ΔV_2 values appear generally to be in good agreement with the available experimental values.

As discussed previously (Section V.A.1), π donors at the para position decrease the extent of OH-ring conjugation. It is not surprising then that para substituents such as CH₃, NH₂, OH, F, and O⁻ decrease the barrier to rotation as reflected in the ΔV_2 values. This is also reflected in the π -overlap populations (Table 10), which are a measure of the double bond character in the C—O bond. Generally those molecules with lowered rotational barriers exhibit reduced C—O double bond character. For the *p*-O⁻ substituent, a particularly powerful π donor, the rotational barrier and the π -overlap population are both close to zero.

For π acceptors at the para position the reverse applies. Enhanced conjugation (as reflected in increased π overlap) results in increased rotational barriers. For Li, which is, additionally, a powerful σ donor, the dominant effect is the raising of the π^* levels of the ring by σ donation resulting in reduced conjugation and a reduced barrier; this is despite the π -accepting effect which, however, as noted previously, is weak by comparison.

For NH_3^+ , a powerful σ -withdrawing group, the reverse occurs. The π^* levels are lowered by a deshielding effect and an increased barrier results.

For substituents at the meta position, the picture is more complicated. As was discussed previously, electron-withdrawing groups are expected to lower π^* levels in benzene leading to enhanced ring-OH conjugation and larger rotational barriers. This line of reasoning is indeed supported by the calculated π -overlap populations in the C—O bond for meta substituents NH_2 , OH, F, CN, NO_2 , and NH_3^+ which all show an increase over the value in unsubstituted phenol. Thus the double bond character in the C—O bond is increased for these meta substituents. In addition, the calculated V_2 component of the barrier increases for NH_2 , OH, and F. However, for CN, NO_2 , and NH_3^+ a decrease in rotational barrier compared with phenol is actually observed despite the increased C—O π -overlap populations. This may be explained by the fact that rotational barriers, although dependent on the degree of C—O double bond character, do depend on other factors as well. Specifically, any direct interactions between the substituents in the planar ground state will modify the rotational barrier. It would appear therefore that some destabilizing interaction between the OH and the substituent in the ground state is responsible for the reduction in barrier for *m*- NO_2 , *m*-CN, and *m*- NH_3^+ .

The data for meta Li and O^- substituents also appear anomalous. For both, electronic considerations would suggest greatly reduced rotational barriers since both are electron-releasing and hence would raise π^* levels. Indeed, the π -overlap populations confirm this expectation: Both exhibit weakened OH-ring conjugation compared with the unsubstituted phenol. Yet, despite this, the barriers are higher than in phenol. For O^- , the ΔV_2 value is actually $+0.63$ kcal mole $^{-1}$, the maximum observed at the meta position, and may be rationalized in terms of a stabilization of the ground state due to hydrogen bonding (3).

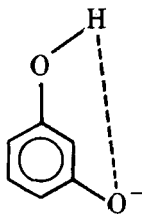


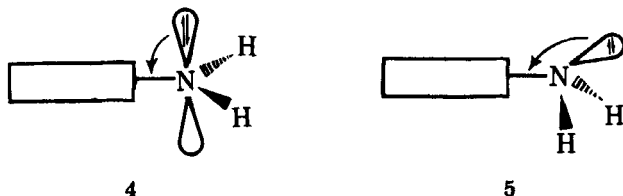
TABLE 11
Inversion Barriers and Nitrogen Bond Angles in Substituted Anilines

Substituent (X)	<i>Meta</i> isomer		<i>Para</i> isomer	
	Inversion barrier (kcal mole ⁻¹)	Bond angle (degrees)	Inversion barrier (kcal mole ⁻¹)	Bond angle (degrees)
H	2.72	112.1	2.72	112.1
CH ₃	2.71	112.0	2.86	112.0
NH ₂	2.74	112.2	3.29	111.5
OH	2.54	112.3	3.12	111.7
F	2.52	112.3	2.86	112.0
NO ₂	2.37	112.5	1.88	113.2
CN	2.44	112.4	2.12	112.9
Li	3.19	111.6	3.19	111.6
O ⁻	4.78	110.2	7.62	108.6
NH ₃ ⁺	1.21	114.4	0.82	115.3

5. Inversion Barriers in Substituted Anilines

The effect of para substituents on nitrogen inversion barriers in anilines has been reported by Hehre et al. (9). We have extended those data to include additional substituents, as well as substituents at the meta position. Although the theoretical inversion barrier in aniline (2.72 kcal mole⁻¹) is somewhat higher than the experimental value (1.6 kcal mole⁻¹), the effect of the substituent on the inversion barrier might be more reliable as in the case of the rotational barriers in substituted phenols. The nitrogen inversion barriers, as well as optimized N bond angles, are summarized in Table 11.

The results are similar to those obtained for rotational barriers in phenols although the barriers do, of course, move in opposite directions. Substituents that enhance conjugation between the NH₂ group and the ring stabilize the planar transition state (4) more than the pyramidal ground state (5) leading to a reduced barrier.



Again, we observe that at the para position, π effects are dominant. π -Donors (CH₃, NH₂, OH, and F) increase the barrier, by opposing NH₂-ring conjugation, and decrease the bond angles at N which open out as conjugation increases. For O⁻, a powerful π donor, a barrier of 7.62 kcal mole⁻¹ is observed.

TABLE 12
Calculated Total Energies and Dipole Moments for Substituted Cyanobenzenes

Substituent (X)	Conformation	Dipole moment (debyes)	Energy (hartrees)
H		3.65	-318.44331
<i>o</i> -CH ₃	NCC...CCH <i>trans</i>	3.48	-357.02765
<i>m</i> -CH ₃	NCC...CCH <i>trans</i>	3.81	-357.02741
<i>p</i> -CH ₃	NCC...CCH planar	4.04	-357.02790
<i>o</i> -NO ₂	ONCC planar	6.35	-519.12397
<i>m</i> -NO ₂	ONCC planar	3.84	-519.13212
<i>p</i> -NO ₂	ONCC planar	0.71	-519.13202
<i>o</i> -CN		5.93	-408.99116
<i>m</i> -CN		3.52	-408.99337
<i>p</i> -CN		0	-408.99337
<i>o</i> -Li		4.90	-325.16678
<i>m</i> -Li		8.06	-325.15932
<i>p</i> -Li		9.33	-325.15923

Li, a σ donor, also increases the barrier by raising π^* levels by a shielding mechanism, making conjugation less effective. π -Acceptors (NO₂ and CN), on the other hand, reduce the inversion barrier and increase the bond angle since they encourage NH₂-ring conjugation. NH₃⁺, a powerful σ acceptor, also reduces the barrier (to 0.82 kcal mole⁻¹) because of a powerful deshielding effect.

At the meta position, σ effects become more important. Thus, OH and F decrease the barrier at the meta position in contrast to the increase at the para position. At the meta position the deshielding σ -withdrawing effect is dominant, whereas at the para position it is the π effect which determines the substituent behavior.

B. Substituent Effects in Cyanobenzenes

The basic principles utilized to explain substituent effects in the π -donor/ σ -acceptor family are equally applicable to understanding substituent effects in cyanobenzenes, where the CN group represents a σ and π acceptor. Energy data are listed in Table 12. Interaction energies appear in Table 13, and Mulliken charges and overlap populations appear in Table 14.

From the interaction energies (Table 13), it appears that σ - and π -donating effects are stabilizing, whereas σ - and π -accepting effects are destabilizing. The π donors (CH₃, NH₂, OH, F) interact most favorably or least unfavorably at the ortho and para positions. This is because the LUMO for cyanobenzene (Fig. 7) has greater coefficients at these positions and hence the stabilization is more

TABLE 13
Interaction Energies (kcal mole⁻¹) for Substituted Cyano- and
Lithiobenzenes

Substituent (X)	Cyanobenzenes	Lithiobenzenes
H	0	0
<i>o</i> -CH ₃	+0.4	+0.2
<i>m</i> -CH ₃	+0.2	-0.2
<i>p</i> -CH ₃	+0.5	-0.3
<i>o</i> -NH ₂	+1.2	+1.0
<i>m</i> -NH ₂	+0.1	-0.3
<i>p</i> -NH ₂	+1.4	-0.6
<i>o</i> -OH	+0.6	+7.1
<i>m</i> -OH	-0.4	+0.5
<i>p</i> -OH	+0.8	0.0
<i>o</i> -F	-0.9	+8.4
<i>m</i> -F	-0.9	+1.2
<i>p</i> -F	-0.1	+0.7
<i>o</i> -NO ₂	-7.8	+31.7
<i>m</i> -NO ₂	-2.7	+4.4
<i>p</i> -NO ₂	-2.8	+4.3
<i>o</i> -CN	-3.4	+7.9
<i>m</i> -CN	-2.0	+3.2
<i>p</i> -CN	-2.0	+3.1
<i>o</i> -Li	+7.9	-8.5
<i>m</i> -Li	+3.2	-3.2
<i>p</i> -Li	+3.1	-3.0

favorable. This argument is supported by enhanced π donation and greater overlap populations at these positions (Table 14).

The trend from stabilizing to destabilizing interaction along the series NH₂, OH, F, is readily rationalized. While π donation decreases, σ withdrawal increases along the series, so that F substitution is destabilizing, being dominated by σ effects while NH₂ is stabilizing being dominated by π effects. OH, which is intermediate in both σ and π behaviour, is stabilizing at ortho and para positions where π effects are dominant, and destabilizing at the meta position where σ effects are most important.

For the σ and π acceptors (NO₂ and CN), there is a reduction in both σ and π charge transfer from the ring to the CN group. Both may be understood as resulting from the lowering of σ and π levels compared with the cyanobenzene parent. The σ effect lowers the energy of the ring orbitals by a deshielding process, whereas the π withdrawal has the effect of lowering the energy of the HOMO in cyano- and nitrobenzene compared with benzene, making interaction with a second π acceptor less favorable. This is analogous to the saturation effect noted earlier (Section III.B) for two π -donor substituents.

TABLE 14
Mulliken Charges and Overlap Populations for Substituted Cyanobenzenes

Substituent (X)	$q_{\sigma}(Y)^a$	$q_{\sigma}(X)^a$	$q_{\pi}(Y)^a$	$q_{\pi}(X)^a$	$\pi(\text{Ph-Y})^b$	$\pi(\text{Ph-X})^b$
H	+0.103		+0.023		0.043	
<i>o</i> -CH ₃	+0.106	-0.028	+0.025	-0.010	0.044	0.011
<i>m</i> -CH ₃	+0.104	-0.019	+0.023	-0.009	0.043	0.009
<i>p</i> -CH ₃	+0.105	-0.019	+0.025	-0.010	0.043	0.010
<i>o</i> -NH ₂	+0.106	+0.129	+0.033	-0.111	0.056	0.060
<i>m</i> -NH ₂	+0.103	+0.134	+0.022	-0.102	0.043	0.051
<i>p</i> -NH ₂	+0.107	+0.136	+0.031	-0.109	0.044	0.057
<i>o</i> -OH	+0.105	+0.175	+0.036	-0.114	0.046	0.060
<i>m</i> -OH	+0.101	+0.177	+0.021	-0.105	0.043	0.054
<i>p</i> -OH	+0.104	+0.179	+0.030	-0.111	0.044	0.058
<i>o</i> -F	+0.093	+0.203	+0.026	-0.084	0.044	0.042
<i>m</i> -F	+0.098	+0.207	+0.020	-0.080	0.043	0.039
<i>p</i> -F	+0.101	+0.209	+0.026	-0.084	0.043	0.042
<i>o</i> -NO ₂	+0.078	+0.204	+0.007	+0.028	0.044	0.035
<i>m</i> -NO ₂	+0.088	+0.218	+0.019	+0.028	0.042	0.033
<i>p</i> -NO ₂	+0.090	+0.219	+0.014	+0.025	0.043	0.033
<i>o</i> -CN	+0.086	+0.086	+0.017	+0.017	0.043	0.043
<i>m</i> -CN	+0.092	+0.092	+0.020	+0.020	0.042	0.042
<i>p</i> -CN	+0.093	+0.093	+0.017	+0.017	0.043	0.043
<i>o</i> -Li	+0.119	-0.302	+0.037	+0.074	0.044	0.050
<i>m</i> -Li	+0.120	-0.292	+0.028	+0.084	0.044	0.056
<i>p</i> -Li	+0.117	-0.294	+0.031	+0.081	0.045	0.053

^a $q_{\sigma}(Y)$, $q_{\sigma}(X)$, $q_{\pi}(Y)$, $q_{\pi}(X)$ are the total σ and π charges, respectively, donated by the substituent, Y or X to the ring. Y = CN, X = substituent.

^b $\pi(\text{Ph-Y})$ and $\pi(\text{Ph-X})$ are Mulliken overlap populations of the adjacent π -type p orbitals in the bond joining Y and X, respectively, to the ring. Y = CN, X = substituent.

TABLE 15
Calculated Total Energies and Dipole Moments for Substituted Lithiobenzenes

Substituent (X)	Conformation	Dipole moment (debyes)	Energy (hartrees)
H		5.12	-234.60099
<i>o</i> -CH ₃	HCC...CLi <i>trans</i>	5.15	-273.18513
<i>m</i> -CH ₃	HCC...CLi <i>cis</i>	5.00	-273.18438
<i>p</i> -CH ₃	HCC...CLi planar	4.88	-273.18423
<i>o</i> -NO ₂	ONCC planar	4.13	-435.34471
<i>m</i> -NO ₂	ONCC planar	8.60	-435.30113
<i>p</i> -NO ₂	ONCC planar	10.04	-435.30109
<i>o</i> -Li		7.95	-241.29837
<i>m</i> -Li		4.73	-241.30678
<i>p</i> -Li		0	-241.30716

TABLE 16
Mulliken Charges and Overlap Populations for Substituted Lithiobenzenes

Substituent (X)	$q_{\sigma}(Y)^a$	$q_{\sigma}(X)^a$	$q_{\pi}(Y)^a$	$q_{\pi}(X)^a$	$\pi(\text{Ph-Y})^b$	$\pi(\text{Ph-X})^b$
H	-0.265		+0.092		0.059	
<i>o</i> -CH ₃	-0.255	+0.019	+0.085	-0.006	0.057	0.007
<i>m</i> -CH ₃	-0.263	+0.011	+0.092	-0.007	0.059	0.009
<i>p</i> -CH ₃	-0.262	+0.010	+0.096	-0.007	0.061	0.009
<i>o</i> -NH ₂	-0.250	+0.156	+0.093	-0.082	0.063	0.038
<i>m</i> -NH ₂	-0.268	+0.153	+0.090	-0.088	0.057	0.043
<i>p</i> -NH ₂	-0.255	+0.149	+0.106	-0.088	0.067	0.042
<i>o</i> -OH	-0.265	+0.190	+0.088	-0.092	0.060	0.045
<i>m</i> -OH	-0.275	+0.197	+0.087	-0.097	0.056	0.049
<i>p</i> -OH	-0.261	+0.194	+0.103	-0.097	0.065	0.048
<i>o</i> -F	-0.268	+0.221	+0.087	-0.073	0.059	0.035
<i>m</i> -F	-0.279	+0.224	+0.087	-0.076	0.057	0.037
<i>p</i> -F	-0.269	+0.221	+0.096	-0.075	0.062	0.035
<i>o</i> -NO ₂	-0.266	+0.154	+0.066	+0.051	0.039	0.042
<i>m</i> -NO ₂	-0.302	+0.244	+0.082	+0.038	0.055	0.036
<i>p</i> -NO ₂	-0.304	+0.240	+0.076	+0.043	0.051	0.037
<i>o</i> -CN	-0.302	+0.119	+0.074	+0.037	0.050	0.044
<i>m</i> -CN	-0.292	+0.120	+0.084	+0.028	0.056	0.044
<i>p</i> -CN	-0.294	+0.117	+0.081	+0.031	0.053	0.045
<i>o</i> -Li	-0.217	-0.217	+0.112	+0.112	0.065	0.065
<i>m</i> -Li	-0.228	-0.228	+0.101	+0.101	0.064	0.064
<i>p</i> -Li	-0.237	-0.237	+0.106	+0.106	0.066	0.066

^a $q_{\sigma}(Y)$, $q_{\sigma}(X)$, $q_{\pi}(Y)$ and $q_{\pi}(X)$ are the total σ and π charges, respectively, donated by the substituent, Y or X, to the ring. Y = Li, X = substituent.

^b $\pi(\text{Ph-Y})$ and $\pi(\text{Ph-X})$ are Mulliken overlap populations of the adjacent π -type p orbitals in the bond joining Y and X, respectively, to the ring. Y = Li, X = substituent.

For Li, a powerful σ donor, the interaction energy is favorable in all positions, because of the shielding of all ring orbitals, enabling both better σ and π acceptance by CN. This is confirmed by the Mulliken charges (Table 14). The particularly large favorable interaction for *o*-Li is presumably due to direct π donation from CN π orbitals into the vacant in-plane Li $2p$ orbital.

C. Substituent Effects in Lithiobenzenes

Li is a strong σ donor and a somewhat weaker π acceptor, and lithiobenzene is therefore representative of the class of monosubstituted benzenes with these properties. Energies of substituted lithiobenzenes appear in Table 15, and Mulliken charges and overlap populations appear in Table 16.

The interaction energies for substituted lithiobenzenes, listed in Table 13, indicate that σ effects are dominant. Thus even interaction with *p*-NH₂, a strong

TABLE 17
Energy Data for Substituted Phenoxide Anions

Substituent (X)	Conformation	Total energy (hartrees)	Relative energy (kcal mole ⁻¹)
H		-300.97376	
<i>o</i> -CH ₃	OC...CCH <i>trans</i>	-399.55791	0
	OC...CCH <i>cis</i>	-399.55758	0.2
<i>m</i> -CH ₃	OC...CCH <i>cis</i>	-399.55737	0
	OC...CCH <i>trans</i>	-399.55701	0.2
<i>p</i> -CH ₃	OC...CCH planar	-399.55527	
<i>o</i> -NH ₂	$\alpha = 108.8^\circ$ ^a	-355.29011	0
	planar N	-355.27908	6.92
<i>m</i> -NH ₂	$\alpha = 110.2^\circ$ ^a	-355.29377	0
	planar N	-355.28616	4.78
<i>p</i> -NH ₂	$\alpha = 108.6^\circ$ ^a	-355.28245	0
	planar N	-355.27030	7.62
<i>o</i> -OH	OC...COH <i>cis</i>	-374.81994	0
	OC...COH <i>trans</i>	-374.80452	9.68
	OC...COH orthogonal	-374.80475	9.53
<i>m</i> -OH	OC...COH <i>trans</i>	-374.81842	0
	OC...COH <i>cis</i>	-374.81724	0.74
	OC...COH orthogonal	-374.80860	6.16
<i>p</i> -OH	OC...COH planar	-374.80537	0
	OC...COH orthogonal	-374.80510	0.17
<i>m</i> -OCH ₃	OC...COC <i>cis</i>	-413.39274	0
	OC...COC <i>trans</i>	-413.39172	0.64
<i>p</i> -OCH ₃	OC...COC planar	-413.38112	
<i>o</i> -F		-398.43470	
<i>m</i> -F		-398.44226	
<i>p</i> -F		-398.43413	
<i>o</i> -NO ₂	OC...CNO planar	-501.70523	
<i>m</i> -NO ₂	OC...CNO planar	-501.69504	0
	OC...CNO orthogonal	-501.68744	4.77
<i>p</i> -NO ₂	OC...CNO planar	-501.71545	0
	OC...CNO orthogonal	-501.69382	13.57
<i>o</i> -CN		-391.56092	
<i>m</i> -CN		-391.54948	
<i>p</i> -CN		-391.56239	
<i>o</i> -CHO	OC...CCO <i>trans</i>	-412.22252	0
	OC...CCO <i>cis</i>	-412.21219	6.5
<i>m</i> -CHO	OC...CCO <i>trans</i>	-412.20853	0
	OC...CCO <i>cis</i>	-412.20755	0.6
<i>p</i> -CHO	OC...CCO planar	-412.22225	
<i>o</i> -CF ₃	OC...CCF <i>trans</i>	-631.95691	0
	OC...CCF <i>cis</i>	-631.95012	4.3
<i>m</i> -CF ₃	OC...CCF <i>cis</i>	-631.95132	0
	OC...CCF <i>trans</i>	-631.95113	0.1
<i>p</i> -CF ₃	OC...CCF planar	-631.95718	

TABLE 17 (Continued)
 Energy Data for Substituted Phenoxide Anions

Substituent (X)	Conformation	Total energy (hartrees)	Relative energy (kcal mole ⁻¹)
<i>o</i> -Li		-307.68492	
<i>m</i> -Li		-307.66323	
<i>p</i> -Li		-307.67675	
<i>o</i> -NH ₃ ⁺	OC...CNH <i>cis</i>	-355.90631	0
	OC...CNH <i>trans</i>	-355.90315	1.98
<i>m</i> -NH ₃ ⁺	OC...CNH <i>cis</i>	-355.87367	0
	OC...CNH <i>trans</i>	-355.87346	0.13
<i>p</i> -NH ₃ ⁺	OC...CNH planar	-355.88067	

^a α is the optimized value of the bond angles (assumed equal) about nitrogen.

π donor leads to a destabilizing interaction suggesting that the lowering of ring π^* orbitals by the vacant Li $2p$ orbital is more than cancelled out by the raising of π^* levels due to the shielding effect associated with the powerful σ -electron releasing Li group. As a consequence, the stronger σ acceptors, OH, F, NO₂, and CN, all interact favorably with Li. The particularly large stabilizing interactions with these groups at the ortho positions are due to direct charge-transfer from the substituent into the Li in-plane $2p$ orbital. Not surprisingly, with Li as the second substituent, unfavorable interactions result due to opposing σ donation by each of the Li atoms into the ring.

D. Substituent Effects in Phenoxide and Anilide Anions

In the discussion up till now, we have only considered interactions between neutral substituents. This section details substituent interactions with two negatively charged groups, O⁻ and NH⁻, and examines also the differences between these two groups. Total and relative energies for substituted phenoxide and anilide ions are listed in Tables 17 and 18. Interaction energies are presented in Table 19, together with those for anilinium ions, which are discussed subsequently (Section V.E).

The most obvious result is that the energies of interaction of the charged groups with the substituents studied are considerably larger than are those of the neutral substituents. For electron-withdrawing substituents, interaction energies of over 20 kcal mole⁻¹ are common in the charged species, whereas for the neutrals, values are generally under 5 kcal mole⁻¹, except for ortho substituents where direct interactions sometimes lead to larger results.

From the charge data for monosubstituted benzenes (Table 2), it can be seen that both O⁻ and NH⁻ are powerful π donors and poor σ donors. The deprotonation of phenol to yield phenoxide has the effect of raising all the orbitals associated with the O atom, including those orthogonal to the orbitals responsible

TABLE 18
Energy Data for Substituted Anilide Anions

Substituent (X)	Conformation	Total energy (hartrees)	Relative energy (kcal mole ⁻¹)
H		-281.44059	
<i>m</i> -CH ₃	HNC...CCH <i>cis, cis</i>	-320.02420	0
	HNC...CCH <i>trans, cis</i>	-320.02423	0.02
<i>p</i> -CH ₃	HNC...CCH <i>trans</i>	-320.02205	
<i>m</i> -NH ₂	HNC...CN(H ₂) <i>cis</i> , $\alpha = 110.2^\circ$ ^{a,b}	-335.76060	0
	HNC...CN(H ₂) <i>trans</i> , $\alpha = 110.2^\circ$ ^a	-335.76048	0.08
<i>p</i> -NH ₂	HNC...CN(H ₂) planar, $\alpha = 110.2^\circ$ ^a	-335.74928	
<i>o</i> -OH	HNC...COH <i>trans, cis</i>	-355.28753	0
	HNC...COH <i>cis, trans</i>	-355.27308	2.79
<i>m</i> -OH	HNC...COH <i>trans, cis</i>	-355.28508	0
	HNC...COH <i>cis, cis</i>	-355.28492	0.10
	HNC...COH <i>trans, trans</i>	-355.28340	1.05
	HNC...COH <i>cis, trans</i>	-355.28402	0.67
<i>p</i> -OH	HNC...COH <i>trans</i>	-355.27215	
<i>m</i> -OCH ₃	HNC...COC <i>trans, cis</i>	-394.85940	0
	HNC...COC <i>cis, cis</i>	-393.85931	0.06
	HNC...COC <i>cis, trans</i>	-393.85845	0.60
	HNC...COC <i>trans, trans</i>	-393.85777	1.02
<i>p</i> -OCH ₃	HNC...COC <i>cis</i>	-393.84785	0
	HNC...COC <i>trans</i>	-393.84339	2.80
<i>o</i> -F	HNC...CF <i>cis</i>	-378.90309	0
	HNC...CF <i>trans</i>	-378.90101	1.31
<i>m</i> -F	HNC...CF <i>cis</i>	-378.90874	0
	HNC...CF <i>trans</i>	-378.90840	0.21
<i>p</i> -F	HNC...CF planar	-378.90075	
<i>m</i> -NO ₂	HNC...CN(O ₂) <i>cis</i>	-482.16075	0
	HNC...CN(O ₂) <i>trans</i>	-482.16010	0.41
<i>p</i> -NO ₂	HNC...CN(O ₂) planar	-482.18139	
<i>o</i> -CN	HNC...CN <i>trans</i>	-372.02510	0
	HNC...CN <i>cis</i>	-372.02482	0.18
<i>m</i> -CN	HNC...CN <i>cis</i>	-372.01539	0
	HNC...CN <i>trans</i>	-372.01505	0.21
<i>p</i> -CN	HNC...CN planar	-372.02838	
<i>m</i> -CHO	HNC...CCO <i>trans, trans</i>	-392.67504	0
	HNC...CCO <i>trans, cis</i>	-392.67366	0.87
	HNC...CCO <i>cis, trans</i>	-392.67484	0.13
	HNC...CCO <i>cis, cis</i>	-392.67410	0.59
<i>p</i> -CHO	HNC...CCO <i>cis</i>	-392.68867	
<i>m</i> -CF ₃	HNC...CCF <i>cis, trans</i>	-612.41737	0
	HNC...CCF <i>trans, trans</i>	-612.41711	0.16
<i>p</i> -CF ₃	HNC...CCF <i>cis</i>	-612.42346	
<i>o</i> -Li	HNC...CLi <i>trans</i>	-288.14951	
<i>m</i> -Li	HNC...CLi <i>cis</i>	-288.13005	0
	HNC...CLi <i>trans</i>	-288.12936	0.43
<i>p</i> -Li	HNC...CLi planar	-288.14389	

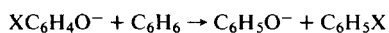
^a α is the optimized value of the bond angles (assumed equal) about nitrogen.

^b α for the *cis* isomer taken as the optimized angle for the *trans* isomer.

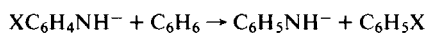
TABLE 19
Interaction Energies (kcal mole⁻¹) for Substituted Phenoxide, Anilide, and Anilinium Ions

Substituent (X)	Phenoxide anion ^a	Anilide anion ^b	Anilinium cation ^c
H	0.0	0.0	0.0
<i>o</i> -CH ₃	+0.2		
<i>m</i> -CH ₃	-0.1	-0.1	+1.5
<i>p</i> -CH ₃	-1.4	-1.4	+2.0
<i>o</i> -NH ₂	-1.6		
<i>m</i> -NH ₂	+0.7	+0.7	+2.0
<i>p</i> -NH ₂	-6.4	-6.4	+4.5
<i>o</i> -OH	+4.8	+5.3	+4.6
<i>m</i> -OH	+3.8	+3.6	0.0
<i>p</i> -OH	-4.4	-4.4	+1.4
<i>m</i> -OCH ₃	+3.0	+2.9	+1.2
<i>p</i> -OCH ₃	-4.3	-4.4	+2.8
<i>o</i> -F	+1.0	+2.0	-2.6
<i>m</i> -F	+5.8	+5.5	-3.2
<i>p</i> -F	+0.7	+0.5	-2.0
<i>o</i> -NO ₂	+24.0		
<i>m</i> -NO ₂	+17.6 (+18.6) ^d	+16.9	-12.0
<i>p</i> -NO ₂	+30.4 (+22.6) ^d	+29.9	-12.6
<i>o</i> -CN	+21.3	+19.6	-8.2
<i>m</i> -CN	+14.1	+13.5	-8.9
<i>p</i> -CN	+22.2	+21.7	-9.0
<i>o</i> -CHO	+14.7		
<i>m</i> -CHO	+5.9	+5.7	-3.6
<i>p</i> -CHO	+14.5	+14.3	-3.2
<i>o</i> -CF ₃	+11.7		
<i>m</i> -CF ₃	+8.2	+7.7	-4.9
<i>p</i> -CF ₃	+11.9	+11.5	-5.1
<i>o</i> -Li	+0.1	-1.3	+18.1
<i>m</i> -Li	-13.5	-13.5	+16.1
<i>p</i> -Li	-5.0	-4.8	+15.9

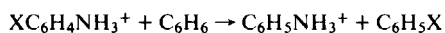
^a Values represent the energy of the reaction:



^b Values represent the energy of the reaction:



^c Values represent the energy of the reaction:



^d Corresponding values for NO₂ oriented orthogonally to the ring.

TABLE 20
 Mulliken Charges and Overlap Populations for Substituted Phenoxide Anions

Substituent (X)	$q_{\sigma}(Y)^a$	$q_{\sigma}(X)^a$	$q_{\pi}(Y)^a$	$q_{\pi}(X)^a$	$\pi(\text{Ph-Y})^b$	$\pi(\text{Ph-X})^b$
H	-0.021		-0.506		0.221	
<i>o</i> -CH ₃	-0.022	+0.068	-0.507	+0.005	0.220	0.014
<i>m</i> -CH ₃	-0.020	+0.065	-0.508	-0.003	0.222	0.101
<i>p</i> -CH ₃	-0.021	+0.085	-0.506	+0.005	0.221	0.001
<i>o</i> -NH ₂	-0.035	+0.186	-0.487	-0.058	0.212	0.016
<i>m</i> -NH ₂	-0.020	+0.191	-0.509	-0.071	0.224	0.033
<i>p</i> -NH ₂	-0.028	+0.193	-0.491	-0.044	0.216	0.002
<i>o</i> -OH	-0.046	+0.227	-0.466	-0.077	0.206	0.025
<i>m</i> -OH	-0.021	+0.233	-0.510	-0.086	0.224	0.044
<i>p</i> -OH	-0.029	+0.233	-0.490	-0.060	0.216	0.010
<i>o</i> -F	-0.032	+0.244	-0.503	-0.059	0.218	0.018
<i>m</i> -F	-0.022	+0.253	-0.513	-0.070	0.224	0.035
<i>p</i> -F	-0.026	+0.250	-0.500	-0.049	0.219	0.009
<i>o</i> -NO ₂	-0.011	+0.269	-0.597	+0.141	0.239	0.068
<i>m</i> -NO ₂	-0.027	+0.289	-0.524	+0.052	0.224	0.041
<i>p</i> -NO ₂	+0.002	+0.278	-0.589	+0.150	0.238	0.069
<i>m</i> -NO ₂ ^c	-0.026	+0.313	-0.526	+0.003	0.226	0.008
<i>p</i> -NO ₂ ^c	-0.013	+0.325	-0.548	+0.015	0.232	0.010
<i>o</i> -CN	-0.016	+0.160	-0.553	+0.081	0.233	0.066
<i>m</i> -CN	-0.025	+0.168	-0.521	+0.040	0.224	0.046
<i>p</i> -CN	-0.006	+0.167	-0.561	+0.095	0.233	0.069
<i>o</i> -CHO	-0.013	+0.048	-0.541	+0.120	0.229	0.080
<i>m</i> -CHO	-0.023	+0.060	-0.511	+0.057	0.222	0.054
<i>p</i> -CHO	-0.005	+0.055	-0.557	+0.140	0.231	0.084
<i>o</i> -CF ₃	-0.021	+0.097	-0.526	+0.029	0.228	0.030
<i>m</i> -CF ₃	-0.023	+0.094	-0.516	+0.017	0.223	0.020
<i>p</i> -CF ₃	-0.014	+0.110	-0.534	+0.034	0.228	0.033
<i>o</i> -Li	-0.086	-0.051	-0.483	+0.219	0.215	0.112
<i>m</i> -Li	-0.038	-0.055	-0.485	+0.128	0.215	0.074
<i>p</i> -Li	-0.001	-0.123	-0.559	+0.346	0.227	0.141

^a $q_{\sigma}(Y)$, $q_{\sigma}(X)$, $q_{\pi}(Y)$, and $q_{\pi}(X)$ are the total σ and π charges, respectively, donated by the substituents Y or X, to the ring. Y = O⁻, X = substituent.

^b $\pi(\text{Ph-Y})$ and $\pi(\text{Ph-X})$ are Mulliken overlap populations of the adjacent π -type orbitals in the bond joining Y and X, respectively, to the ring. Y = O⁻, X = substituent.

^c Orthogonal NO₂.

for the formation of the OH bond (10). As was described in the PMO model (Section III.B), this kind of perturbation may be thought of as a shielding process rather than one due to direct orbital interaction.

Since the principal interaction of O⁻ and NH⁻ with the ring is through the π system, it is not surprising that the interaction energies in Table 19 may be understood as resulting from perturbations to the π system. Interactions, which will tend to enhance π donation to the ring are likely to be favorable and

TABLE 21
 Mulliken Charges and Overlap Populations for Substituted Anilide Anions

Substituent (X)	$q_{\sigma}(Y)^a$	$q_{\sigma}(X)^a$	$q_{\pi}(Y)^a$	$q_{\pi}(X)^a$	$\pi(\text{Ph-Y})^b$	$\pi(\text{Ph-X})^b$
H	-0.019		-0.484		0.230	
<i>m</i> -CH ₃	-0.018	+0.060	-0.486	-0.003	0.231	0.010
<i>p</i> -CH ₃	-0.019	+0.080	-0.484	+0.007	0.229	0.011
<i>m</i> -NH ₂	-0.018	+0.188	-0.487	-0.071	0.232	0.034
<i>p</i> -NH ₂	-0.024	+0.192	-0.468	-0.045	0.223	0.003
<i>o</i> -OH	-0.038	+0.217	-0.449	-0.081	0.214	0.028
<i>m</i> -OH	-0.018	+0.229	-0.489	-0.087	0.233	0.044
<i>p</i> -OH	-0.025	+0.232	-0.468	-0.061	0.223	0.011
<i>o</i> -F	-0.028	+0.245	-0.486	-0.058	0.227	0.016
<i>m</i> -F	-0.020	+0.253	-0.493	-0.071	0.233	0.035
<i>p</i> -F	-0.023	+0.249	-0.478	-0.050	0.227	0.010
<i>m</i> -NO ₂	-0.025	+0.286	-0.510	+0.052	0.235	0.041
<i>p</i> -NO ₂	-0.001	+0.275	-0.579	+0.152	0.251	0.069
<i>o</i> -CN	-0.018	+0.152	-0.537	+0.076	0.245	0.064
<i>m</i> -CN	-0.023	+0.166	-0.504	+0.039	0.234	0.046
<i>p</i> -CN	-0.007	+0.166	-0.548	+0.095	0.245	0.069
<i>m</i> -CHO	-0.020	+0.056	-0.492	+0.055	0.231	0.053
<i>p</i> -CHO	-0.006	+0.053	-0.542	+0.139	0.243	0.084
<i>m</i> -CF ₃	-0.021	+0.090	-0.496	+0.017	0.233	0.020
<i>p</i> -CF ₃	-0.014	+0.108	-0.516	+0.034	0.239	0.032
<i>o</i> -Li	-0.090	-0.069	-0.457	+0.199	0.221	0.107
<i>m</i> -Li	-0.026	-0.076	-0.467	+0.129	0.224	0.074
<i>p</i> -Li	-0.001	-0.131	-0.544	+0.347	0.236	0.140

^a $q_{\sigma}(Y)$, $q_{\sigma}(X)$, $q_{\pi}(Y)$, and $q_{\pi}(X)$ are the total σ and π charges donated by the substituent, Y or X, to the ring. Y = NH⁻, X = substituent.

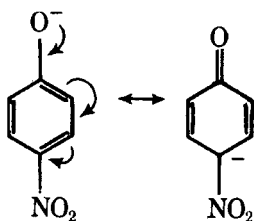
^b $\pi(\text{Ph-Y})$ and $\pi(\text{Ph-X})$ are Mulliken overlap populations of the adjacent π -type *p* orbitals in the bond joining Y and X, respectively, to the ring. Y = NH⁻, X = substituent.

vice versa. Thus monosubstituted benzenes, which have low-lying LUMOs such as C₆H₅NO₂, C₆H₅CN, C₆H₅CHO, and C₆H₅CF₃, all interact favorably with O⁻ and NH⁻, particularly at the ortho and para positions where the LUMO coefficients are greatest (Fig. 7). This is confirmed by the Mulliken charges and overlap populations for O⁻ and NH⁻, listed in Tables 20 and 21. Thus, π donation by O⁻ in phenoxide (-0.506) increases considerably with nitro substitution, particularly at the ortho (-0.597) and para (-0.589) positions.

Although it is not surprising that the π acceptors interact favorably with O⁻, it is interesting to observe the effect of a σ acceptor and to assess the importance of ring position in the transmission of the σ effect. Theoretically, this is readily done by studying interaction energies in nitrophenoxides, where the NO₂ group is constrained in a plane orthogonal to that of the ring. In contrast to planar nitrobenzene, the NO₂ group in orthogonal nitrobenzene is not a π

acceptor (π populations, Fig. 5, confirm this) and may only act as a σ acceptor. Despite this, it is apparent that orthogonal NO_2 does interact very favorably with O^- . This is because all π and π^* orbitals are lowered in energy by the NO_2 group through the deshielding mechanism, resulting in better π donation by O^- . It is interesting to note that orthogonal NO_2 in nitrophenoxide is more stabilizing at the para ($22.6 \text{ kcal mole}^{-1}$) than the meta ($18.6 \text{ kcal mole}^{-1}$) position. This may be understood by examining the LUMO coefficients in orthogonal nitrobenzene (Fig. 7). Since the coefficient at the para position (0.638) is greater than at the meta position (-0.288), a larger interaction occurs at the para position.

The more effective transmission of σ -substituent effects to ortho and para positions compared with the meta positions may be considered evidence for the π -inductive effect. Unfortunately, the term has been applied to a number of different phenomena, though most generally it is used to describe changes induced in the π -electron density of a conjugated system as a result of perturbations to the σ system (1*d*). The phenomenon in orthogonal *p*-nitrophenoxide anion may be crudely but simply understood by the following resonance structures (6):



In other words, the positive charge generated by the NO_2 group is more effectively neutralized by *p*- O^- than by *m*- O^- . Previous work supports this conclusion. Thus the orthogonal nitro group is found (6) to generate positive π charges at the ortho and para positions in benzene (Fig. 5). Pollack and Hehre (118) have noticed the effect in pyridinium ions where carbons ortho and para to the nitrogen were also found to have large positive charges.

The π donors, CH_3 , NH_2 , and OH , can be seen to interact unfavorably with O^- and NH^- at the para position, yet favorably at the meta position (with the exception of CH_3). This is similar to the pattern observed for phenols and anilines described earlier. F is stabilizing in all positions. This behavior is accountable in terms of competing σ and π effects. The effect of σ withdrawal is to lower the π^* orbitals of the ring leading to enhanced O^- π -donation. The effect of π donation by the substituent is to decrease π donation by O^- . Thus for F, a strong σ acceptor and weak π donor, the stabilizing σ effects are dominant. For NH_2 , a weak σ acceptor and strong π donor, π effects are more important. Also, π

TABLE 22
Energy Data for Substituted Anilinium Cations

Substituent (X)	Conformation	Total energy (hartrees)	Relative energy (kcal mole ⁻¹)
H		-282.63403	
<i>m</i> -CH ₃	HCC...CNH <i>trans, trans</i>	-321.22020	0
	HCC...CNH <i>cis, trans</i>	-321.22020	0
<i>p</i> -CH ₃	HCC...CNH <i>trans</i>	-321.22105	
<i>m</i> -NH ₂	HNC...CN(H ₂) <i>trans</i> , $\alpha = 114.4^\circ$ ^a	-336.95607	0
	HNC...CN(H ₂) <i>trans</i> , planar N	-336.95414	1.21
<i>p</i> -NH ₂	$\alpha = 115.3^\circ$ ^a	-336.96005	0
	planar N	-336.95874	0.82
<i>o</i> -OH	HNC...COH <i>cis, trans</i>	-356.47997	0
	HNC...COH <i>cis</i> , orthogonal	-356.46565	8.99
<i>m</i> -OH	HNC...COH <i>cis, trans</i>	-356.47264	0
	HNC...COH <i>cis</i> , orthogonal	-356.46282	6.16
	HNC...COH <i>cis, cis</i>	-356.46732	3.34
<i>p</i> -OH	HNC...COH <i>trans</i>	-356.47483	0
	HNC...COH orthogonal	-356.46398	6.81
<i>m</i> -OCH ₃	HNC...COC <i>trans, trans</i>	-395.05023	0
	HNC...COC <i>trans, cis</i>	-395.04851	1.08
<i>p</i> -OCH ₃	HNC...COC <i>trans</i>	-395.05267	
<i>o</i> -F	HNC...CF <i>cis</i>	-380.08927	0
	HNC...CF <i>trans</i>	-380.08823	0.65
<i>m</i> -F	HNC...CF <i>trans</i>	-380.08824	0
	HNC...CF <i>cis</i>	-380.08817	0
<i>p</i> -F	HNC...CF planar	-380.09024	
<i>m</i> -NO ₂	HNC...CN(O ₂) <i>cis</i>	-483.30815	0
	HNC...CN(O ₂) <i>trans</i>	-483.30811	0
<i>p</i> -NO ₂	HNC...CN(O ₂) planar	-483.30722	
<i>o</i> -CN	HNC...CN <i>cis</i>	-373.17423	0
	HNC...CN <i>trans</i>	-373.17375	0.30
<i>m</i> -CN	HNC...CN <i>cis</i>	-373.17309	0
	HNC...CN <i>trans</i>	-373.17308	0
<i>p</i> -CN	HNC...CN planar	-373.17294	
<i>m</i> -CHO	HNC...CCO <i>trans, cis</i>	-393.85546	0
	HNC...CCO <i>trans, trans</i>	-393.85369	1.11
<i>p</i> -CHO	HNC...CCO <i>cis</i>	-393.85420	
<i>m</i> -CF ₃	HNC...CCF <i>trans, trans</i>	-613.59076	0
	HNC...CCF <i>cis, trans</i>	-613.59076	0
<i>p</i> -CF ₃	HNC...CCF <i>trans</i>	-613.59050	
<i>o</i> -Li	HNC...CLi <i>trans</i>	-289.37380	0
	HNC...CLi <i>cis</i>	-289.37296	0.53
<i>m</i> -Li	HNC...CLi <i>cis</i>	-289.37058	0
	HNC...CLi <i>trans</i>	-289.37051	0
<i>p</i> -Li	HNC...CLi planar	-289.37028	
<i>o</i> -O ⁻	HNC...CO <i>cis</i>	-355.90631	0
	HNC...CO <i>trans</i>	-355.90315	1.98
<i>m</i> -O ⁻	HNC...CO <i>cis</i>	-355.87367	0
	HNC...CO <i>trans</i>	-355.87346	0.13
<i>p</i> -O ⁻	HNC...CO planar	-355.88067	

^a α is the optimized value of the bond angles (assumed equal) about nitrogen.

TABLE 23
 Mulliken Charges and Overlap Populations for Substituted Anilinium Cations

Substituent (X)	$q_{\sigma}(Y)^a$	$q_{\sigma}(X)^a$	$q_{\pi}(Y)^a$	$q_{\pi}(X)^a$	$\pi(\text{Ph-Y})^b$	$\pi(\text{Ph-X})^b$
H	+0.385		-0.001		0.003	
<i>m</i> -CH ₃	— ^c	— ^c	— ^c	— ^c	0.003	0.011
<i>p</i> -CH ₃	— ^c	— ^c	— ^c	— ^c	0.004	0.012
<i>m</i> -NH ₂	— ^c	— ^c	— ^c	— ^c	0.003	0.068
<i>p</i> -NH ₂	— ^c	— ^c	— ^c	— ^c	0.004	0.080
<i>o</i> -OH	+0.381	+0.155	-0.001	-0.111	0.004	0.058
<i>m</i> -OH	+0.383	+0.150	-0.003	-0.120	0.003	0.064
<i>p</i> -OH	+0.389	+0.155	0.000	-0.130	0.004	0.071
<i>o</i> -F	+0.379	+0.193	-0.002	-0.081	0.004	0.041
<i>m</i> -F	+0.380	+0.184	-0.002	-0.088	0.003	0.045
<i>p</i> -F	+0.384	+0.188	-0.001	-0.095	0.004	0.050
<i>m</i> -NO ₂	+0.372	+0.182	-0.002	+0.014	0.004	0.030
<i>p</i> -NO ₂	+0.372	+0.184	-0.003	+0.007	0.003	0.031
<i>o</i> -CN	+0.373	+0.068	-0.003	+0.015	0.003	0.043
<i>m</i> -CN	+0.375	+0.056	-0.002	+0.007	0.004	0.042
<i>p</i> -CN	+0.377	+0.057	-0.002	0.000	0.003	0.042
<i>m</i> -CHO	+0.383	-0.047	-0.002	+0.014	0.004	0.044
<i>p</i> -CHO	+0.383	-0.047	-0.002	+0.007	0.003	0.044
<i>m</i> -CF ₃	— ^c	— ^c	— ^c	— ^c	0.004	0.015
<i>p</i> -CF ₃	— ^c	— ^c	— ^c	— ^c	0.003	0.015
<i>o</i> -Li	+0.423	-0.326	-0.001	+0.065	0.004	0.047
<i>m</i> -Li	+0.407	-0.370	-0.001	+0.062	0.003	0.045
<i>p</i> -Li	+0.405	-0.372	0.000	+0.056	0.003	0.040
<i>o</i> -O ⁻	+0.461	-0.043	+0.007	-0.519	0.001	0.226
<i>m</i> -O ⁻	+0.452	-0.028	0.000	-0.571	0.002	0.236
<i>p</i> -O ⁻	+0.468	-0.005	+0.009	-0.615	0.000	0.245

^a $q_{\sigma}(Y)$, $q_{\sigma}(X)$, $q_{\pi}(Y)$, and $q_{\pi}(X)$ are the total σ and π charges donated by the substituent, Y or X, to the ring. Y = NH₃⁺, X = substituent.

^b $\pi(\text{Ph-Y})$ and $\pi(\text{Ph-X})$ are Mulliken overlap populations of the adjacent π -type p orbitals in the bond joining Y and X, respectively, to the ring. Y = NH₃⁺, X = substituent.

^c Values not calculable since neither substituent is coplanar with the ring.

interactions are more effective at the meta positions because of the greater interaction between the lone pair on O⁻ and the LUMO of the monosubstituted benzene at the meta position. This is due to the larger meta coefficients in the LUMOs (Fig. 7).

Finally Li, a σ donor, is destabilizing because the raising of π^* levels decreases π donation by O⁻ and NH⁻. At the para position, there is a compensating effect of π acceptance by Li. As a consequence, the destabilization at meta is larger than at para.

Comparison of interaction energies in anilides with those of phenoxides shows them to be almost identical. It is puzzling that the sensitivity of phenoxides

and anilides to substituent effects is so similar. It might have been expected that the NH^- group, a more powerful π donor than O^- , would interact more strongly with a series of substituents, leading to larger interaction energies. The reason for this unexpected result is the subject of further investigation.

E. Substituent Effects in Anilinium Cations

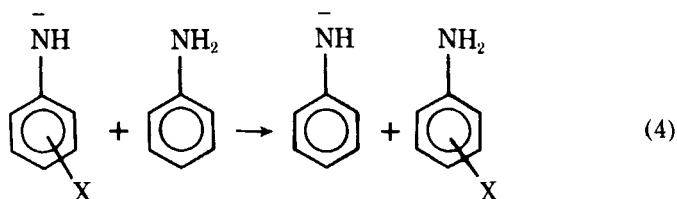
To complete our study of a wide range of substituent types, we now discuss substituent effects in a positively charged group, NH_3^+ . Total and relative energies for a range of substituted anilinium ions are listed in Table 22. Interaction energies are included in Table 19 and Mulliken charges and overlap populations are shown in Table 23.

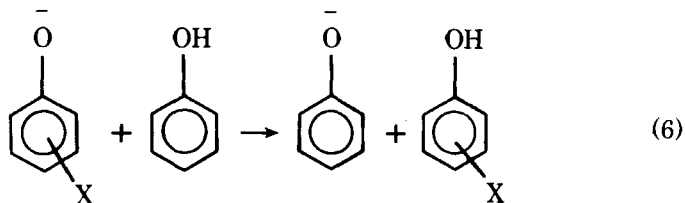
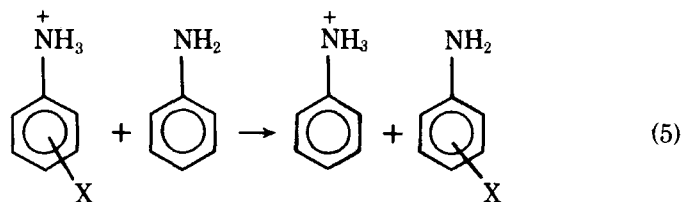
The NH_3^+ substituent can potentially act as a hyperconjugative donor or acceptor. However, the charge data for the parent anilinium ion (Table 2) show that π transfer between the NH_3^+ group and the ring is very small and that the NH_3^+ group is primarily a σ acceptor.

As for the negatively charged phenoxide and anilide ions, substituent effects in the positively charged anilinium ions are significantly greater than for related neutral systems. The data in Table 19 indicate that σ - or π -electron-releasing effects are favorable in the anilinium ions. Thus along the series NH_2 , OH , F , where the π -donating ability decreases, while the σ -withdrawing ability increases, interaction energies change from being favorable (for NH_2) to unfavorable (for F). For σ and π acceptors (NO_2 , CN , CF_3) the interaction energies are unfavorable, whereas for Li , a strong σ donor, large, favorable interactions are observed. The interaction energies may be attributed to the change in the σ -withdrawing effect of the NH_3^+ group (Table 23). An increase in the charge transfer manifests itself in a favorable interaction and vice versa.

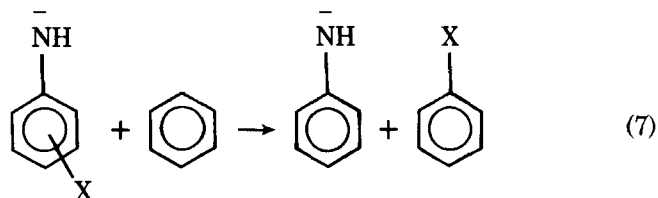
F. Effect of Substituents on Acidity and Basicity

The effect of substituents on the acidity and basicity of aniline, and on the acidity of phenol, is given, respectively, by the energy changes in reactions 4-6.

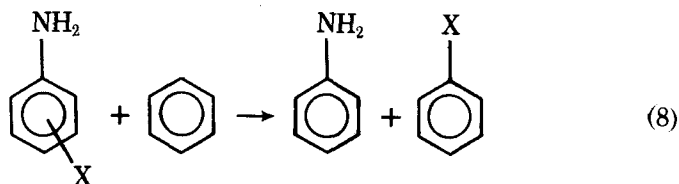




It is possible to break down the effect of substituents on acidity or basicity into the effect on the charged species on the one hand and on the corresponding neutral species on the other. For example, the effect of substituents on the acidity of aniline (reaction 4) is given by the difference between the interaction energies for the appropriate substituted anilide ion (reaction 7):



and substituted aniline (reaction 8):



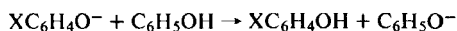
Such a breakdown is useful in determining the origin of the substituent effect.

Theoretical and gas-phase experimental results for the effect of substituents on phenol acidity (10) are listed in Table 24. Similar data for aniline acidity and basicity are given in Table 25. In general, there is good agreement between the available experimental values and the theoretical results, allowing greater confidence in those theoretical values which at present remain experimentally unverified.

TABLE 24
Effect of Substituents on Acidities of Phenols (kcal mole⁻¹)

Substituent (X)	Relative acidity ^{a,b}		
	Theoretical	Experimental	
		ICR	MS
H	0.0	0.0	0.0
<i>o</i> -CH ₃	+0.3	+0.3	+0.7
<i>m</i> -CH ₃	-0.4	-0.5	-0.4
<i>p</i> -CH ₃	-1.0	-1.2	-1.3
<i>o</i> -NH ₂	0.0		+2.1
<i>m</i> -NH ₂	-0.1	-1.3	-0.9
<i>p</i> -NH ₂	-4.9	-3.1	-4.2
<i>o</i> -OH	+5.4		+9.7
<i>m</i> -OH	+3.0		+4.2
<i>p</i> -OH	-2.9		
<i>m</i> -OCH ₃	+2.1	+1.0	+1.5
<i>p</i> -OCH ₃	-3.0	-1.1	-0.8
<i>o</i> -F	+2.4	+3.8	+3.9
<i>m</i> -F	+5.4	+4.8	+5.8
<i>p</i> -F	+1.6	+2.1	+2.6
<i>o</i> -NO ₂	+27.6		+13.9
<i>m</i> -NO ₂	+18.1 (+19.0) ^c		+15.7
<i>p</i> -NO ₂	+29.2 (+22.0) ^c		+25.8 ^d
<i>o</i> -CN	+20.7		+16.2
<i>m</i> -CN	+14.5		+14.3
<i>p</i> -CN	+21.4		+17.7
<i>o</i> -CHO	+14.2		
<i>m</i> -CHO	+5.9		+8.2
<i>p</i> -CHO	+13.8		
<i>o</i> -CF ₃	+12.0		
<i>m</i> -CF ₃	+8.4		+9.3
<i>p</i> -CF ₃	+11.5		
<i>o</i> -Li	-7.0		
<i>m</i> -Li	-14.0		
<i>p</i> -Li	-5.0		

^a Values represent the energy of the reaction:



^b Data summarized in Ref. 10.

^c Corresponding values for NO₂ oriented orthogonally to the ring.

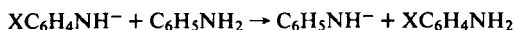
^d Estimated value.

The data indicate that most of the widely held beliefs relating to the effect of substituents on acidity and basicity are fundamentally valid. Electron-releasing groups (e.g. Li, CH₃) are acid weakening and base strengthening, whereas electron-withdrawing groups (e.g. NO₂, CN) are acid strengthening and base weakening.

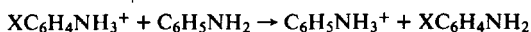
TABLE 25
Effect of Substituents on Acidities and Basicities of Anilines (kcal mol⁻¹)

Substituent (X)	Relative acidity ^a		Relative basicity ^b	
	Theoretical	Experimental ^c	Theoretical	Experimental ^c
H	0.0		0.0	
<i>m</i> -CH ₃	-0.3	-0.5	+1.3	
<i>p</i> -CH ₃	-1.0	-1.2	+2.4	+3.2
<i>m</i> -NH ₂	-0.1		+1.2	
<i>p</i> -NH ₂	-4.8		+6.1	
<i>o</i> -OH	+6.8		+6.2	
<i>m</i> -OH	+2.8		-0.8	
<i>p</i> -OH	-2.9		+2.9	
<i>m</i> -OCH ₃	+2.2		+0.6	
<i>p</i> -OCH ₃	-2.9	-0.9	+4.2	+4.0
<i>o</i> -F	+3.4		-1.1	
<i>m</i> -F	+5.0	+4.0	-3.8	-3.4
<i>p</i> -F	+1.3	+1.6	-1.1	-2.3
<i>m</i> -NO ₂	+16.9		-12.0	
<i>p</i> -NO ₂	+27.7		-14.8	
<i>o</i> -CN	+18.5		-9.3	
<i>m</i> -CN	+13.4		-9.0	
<i>p</i> -CN	+20.2		-10.4	
<i>m</i> -CHO	+5.7		-3.6	
<i>p</i> -CHO	+13.3		-4.2	
<i>m</i> -CF ₃	+7.6	+8.0	-5.0	
<i>p</i> -CF ₃	+10.7	+11.5	-5.9	
<i>o</i> -Li	-2.3		+17.0	
<i>m</i> -Li	-13.2		+16.3	
<i>p</i> -Li	-4.2		+16.5	

^a Values represent the energy of the reaction:



^b Values represent the energy of the reaction:



^c Data summarized in Ref. 122.

Decomposition of the substituent effect into the effect on the neutral molecule and the appropriate charged species, that is, either the conjugate acid or base, is revealing. For phenol acidity, the breakdown of the substituent effect into the two components indicates quite clearly that the interaction in the substituted phenoxide ion is the dominant one (10). In other words, *p*-nitrophenol is a strong acid primarily because the *p*-nitrophenoxide ion is relatively stable. The same is true for aniline acidity.

In the case of aniline basicity, comparison of substituent effects in the neutral amine versus those in the charged anilinium ion (Tables 6 and 19) in-

TABLE 26
Total Energies and Interaction Energies, E_{int} , for Polysubstituted Lithio-,
Fluoro-, and Cyanobenzenes

Substituents (X, Y, . . .)	Total energy (hartrees)	$E_{\text{int}}^{\text{a}}$ (kcal mole ⁻¹)	$E_{\text{int}}(\text{add})^{\text{b}}$ (kcal mole ⁻¹)
1,2-di-F	-422.80382	-3.1	-3.1
1,3-di-F	-422.80871	0.0	0.0
1,4-di-F	-422.80756	-0.7	-0.7
1,2,3-tri-F	-520.25823	-6.2	-6.2
1,2,4-tri-F	-520.26204	-3.8	-3.8
1,3,5-tri-F	-520.26796	-0.1	0.0
1,2,3,4-tetra-F	-617.71159	-9.9	-10.0
1,2,3,5-tetra-F	-617.71643	-6.9	-6.9
1,2,4,5-tetra-F	-617.71545	-7.5	-7.6
penta-F	-715.16496	-13.6	-13.1
hexa-F	-812.61349	-20.4	-20.7
1,2-di-CN	-408.99116	-3.4	-3.4
1,3-di-CN	-408.99337	-2.0	-2.0
1,4-di-CN	-408.99337	-2.0	-2.0
1,2,3-tri-CN	-499.53654	-8.3	-8.8
1,2,4-tri-CN	-499.53860	-7.0	-7.4
1,3,5-tri-CN	-499.54058	-5.8	-6.0
1,2,3,4-tetra-CN	-590.07972	-14.6	-16.2
1,2,3,5-tetra-CN	-590.08159	-13.4	-14.8
1,2,4,5-tetra-CN	-590.08165	-13.4	-14.8
1,2-di-Li	-241.29837	-8.5	-8.5
1,3-di-Li	-241.30678	-3.2	-3.2
1,4-di-Li	-241.30716	-3.0	-3.0
1,2,3-tri-Li	-247.99405	-18.1	-20.2
1,2,4-tri-Li	-248.00181	-13.2	-14.7
1,3,5-tri-Li	-248.00938	-8.5	-9.6
1,2,3,4-tetra-Li	-254.68925	-27.9	-34.9
1,2,3,5-tetra-Li	-254.69578	-23.8	-29.6
1,2,4,5-tetra-Li	-254.69569	-23.9	-29.4
penta-Li	-261.38405	-38.1	-52.8
hexa-Li	-268.07487	-50.7	-79.2
1-CN-2-F	-415.90122	-0.9	-0.9
1-CN-3-F	-415.90118	-0.9	-0.9
1-CN-4-F	-415.90254	-0.1	-0.1
1-CN-2,3-di-F	-513.35426	-4.8	-4.9
1-CN-2,4-di-F	-513.36045	-1.0	-1.0
1-CN-2,5-di-F	-513.35798	-2.5	-2.5
1-CN-2,6-di-F	-513.35914	-1.8	-1.8
1-CN-3,4-di-F	-513.35552	-4.0	-4.1
1-CN-3,5-di-F	-513.35907	-1.8	-1.8
1-Li-2-F	-332.07378	+8.4	+8.4
1-Li-3-F	-332.06223	+1.2	+1.2
1-Li-4-F	-332.06141	+0.7	+0.7
1-Li-2,3-di-F	-429.53038	+6.7	+6.5

TABLE 26 (Continued)
Total Energies and Interaction Energies, E_{int} , for Polysubstituted Lithio-, Fluoro-, and Cyanobenzenes

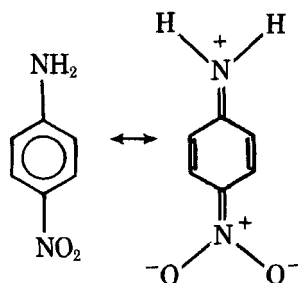
Substituents (X, Y, . . .)	Total energy (hartrees)	$E_{\text{int}}^{\text{a}}$ (kcal mole ⁻¹)	$E_{\text{int}}(\text{add})^{\text{b}}$ (kcal mole ⁻¹)
1-Li-2,4-di-F	-429.53398	+9.0	+9.1
1-Li-2,5-di-F	-429.53389	+8.9	+8.9
1-Li-2,6-di-F	-429.54631	+16.7	+16.8
1-Li-3,4-di-F	-429.51770	-1.2	-1.2
1-Li-3,5-di-F	-429.52354	+2.4	+2.4
1-F-2,3-di-Li	-338.77223	+0.6	+1.1
1-F-2,4-di-Li	-338.78068	+5.9	+5.9
1-F-2,5-di-Li	-338.78170	+6.6	+6.6
1-F-2,6-di-Li	-338.79209	+13.1	+13.6
1-F-3,4-di-Li	-338.76052	-6.7	-6.6
1-F-3,5-di-Li	-338.76952	-1.1	-0.8

^a E_{int} , the interaction energy, represents energy changes for reactions of the kind:



^b $E_{\text{int}}(\text{add})$ represents the interaction energies obtained assuming pairwise additivity, e.g., for $\text{C}_6\text{H}_3\text{XYZ}$, obtained as the sum of the interaction energies calculated for the appropriate, $\text{C}_6\text{H}_4\text{XY}$, $\text{C}_6\text{H}_4\text{YZ}$, and $\text{C}_6\text{H}_4\text{XZ}$.

dicates that the dominant effect is in the anilinium ion, rather than the aniline (11). This means that the widely held view (121) that aniline basicity is largely governed by interaction between the NH_2 group and the substituent is not valid. For example, *p*-nitroaniline is a weak base compared with aniline (-11.1 kcal mole⁻¹) due primarily to an unfavorable interaction between the NH_3^+ group and the NO_2 substituent (-8.9 kcal mole⁻¹) rather than a favorable interaction between the NH_2 and the NO_2 groups ($+2.2$ kcal mole⁻¹). So although the stabilization represented by the resonance structures:



is certainly valid, it represents only some 20% of the reduction in aniline basicity brought about by the nitro group. The key conclusion is therefore that, in general, charged group-neutral group interactions are significantly greater than those between two neutral groups.

TABLE 27
Mulliken Charges for Polysubstituted Benzenes

Substituents (X, Y, ...)	Total ^a		Per substituent ^b	
	q_{σ}	q_{π}	q_{σ}	q_{π}
F	+0.215	-0.080	+0.215	-0.080
1,2-di-F	+0.408	-0.150	+0.204	-0.075
1,3-di-F	+0.420	-0.160	+0.210	-0.080
1,4-di-F	+0.422	-0.152	+0.211	-0.076
1,2,3-tri-F	+0.598	-0.226	+0.199	-0.075
1,2,4-tri-F	+0.612	-0.229	+0.204	-0.076
1,3,5-tri-F	+0.622	-0.246	+0.207	-0.082
1,2,3,4-tetra-F	+0.618	-0.298	+0.155	-0.075
1,2,3,5-tetra-F	+0.627	-0.309	+0.157	-0.077
1,2,4,5-tetra-F	+0.618	-0.298	+0.155	-0.075
penta-F	+0.960	-0.373	+0.192	-0.075
hexa-F	+1.122	-0.444	+0.187	-0.074
CN	+0.103	+0.023	+0.103	+0.023
1,2-di-CN	+0.172	+0.034	+0.086	+0.017
1,3-di-CN	+0.184	+0.040	+0.092	+0.020
1,4-di-CN	+0.186	+0.034	+0.093	+0.017
1,2,3-tri-CN	+0.225	+0.039	+0.075	+0.013
1,2,4-tri-CN	+0.238	+0.041	+0.079	+0.014
1,3,5-tri-CN	+0.248	+0.051	+0.083	+0.017
1,2,3,4-tetra-CN	+0.264	+0.037	+0.066	+0.009
1,2,3,5-tetra-CN	+0.274	+0.042	+0.069	+0.011
1,2,4,5-tetra-CN	+0.276	+0.038	+0.069	+0.010
Li	-0.265	+0.092	-0.265	+0.092
1,2-di-Li	-0.434	+0.224	-0.217	+0.112
1,3-di-Li	-0.456	+0.202	-0.228	+0.101
1,4-di-Li	-0.474	+0.212	-0.237	+0.106
1,2,3-tri-Li	-0.561	+0.358	-0.187	+0.119
1,2,4-tri-Li	-0.593	+0.354	-0.198	+0.118
1,3,5-tri-Li	-0.593	+0.326	-0.198	+0.109
1,2,3,4-tetra-Li	-0.667	+0.501	-0.167	+0.125
1,2,4,5-tetra-Li	-0.694	+0.502	-0.174	+0.126
1,2,3,5-tetra-Li	-0.681	+0.490	-0.170	+0.123
penta-Li	-0.744	+0.636	-0.149	+0.127
hexa-Li	-0.786	+0.763	-0.131	+0.127
1-CN-2,3-di-F	+0.480	-0.134		
1-CN-2,4-di-F	+0.495	-0.143		
1-CN-2,5-di-F	+0.494	-0.137		
1-CN-2,6-di-F	+0.485	-0.144		
1-CN-3,4-di-F	+0.493	-0.134		
1-CN-3,5-di-F	+0.500	-0.146		
1-Li-2,3-di-F	+0.147	-0.060		
1-Li-2,4-di-F	+0.164	-0.060		
1-Li-2,5-di-F	+0.159	-0.063		
1-Li-2,6-di-F	+0.169	-0.066		
1-Li-3,4-di-F	+0.144	-0.053		

TABLE 27 (Continued)
Mulliken Charges for Polysubstituted Benzenes

Substituents (X, Y, ...)	Total ^a		Per substituent ^b	
	q_σ	q_π	q_σ	q_π
1-Li-3,5-di-F	+0.149	-0.073		
1-F-2,3-di-Li	-0.221	+0.142		
1-F-2,4-di-Li	-0.241	+0.131		
1-F-2,5-di-Li	-0.263	+0.132		
1-F-2,6-di-Li	-0.240	+0.123		
1-F-3,4-di-Li	-0.221	+0.150		
1-F-3,5-di-Li	-0.252	+0.120		

^a The total σ and π charges donated by the substituents to the ring.

^b The average σ and π charges per substituent donated by the substituents to the ring. Applicable only when all the substituents are the same.

VI. POLYSUBSTITUTED BENZENES

Up to now, we have been concerned with the interaction between two substituents on an aromatic ring. It would seem relevant to ask what will the effect be of adding further substituents, up to the maximum number of six? Essentially, the question which we ask is whether the effect of additional substituents is additive or nonadditive.

Total and interaction energies, E_{int} , for polysubstituted fluoro-, cyano-, and lithiobenzenes are displayed in Table 26. Also listed are interaction energies, $E_{\text{int}}(\text{add})$, obtained using results for the disubstituted benzenes and assuming pairwise additivity. For example, the interaction energy for 1,2,3-trilithiobenzene based on pairwise additivity would be the sum of twice the interaction energy in *o*-dilithiobenzene and the interaction energy in *m*-dilithiobenzene $\{-8.5 \times 2 + (-3.2) = -20.2\}$.

The interaction energies for the polyfluorobenzenes show remarkable additivity. The differences between the E_{int} and $E_{\text{int}}(\text{add})$ values for these systems do not exceed $0.5 \text{ kcal mole}^{-1}$ and in most cases are either zero or $0.1 \text{ kcal mole}^{-1}$. For the polycyanobenzenes, there are small but significant differences between the E_{int} and $E_{\text{int}}(\text{add})$ values, particularly for the tetrasubstituted molecules. Much larger deviations from pairwise additivity are observed for the polyolithiobenzenes and these increase markedly with increasing numbers of substituents. In the mixed systems, that is, monocyanodifluoro-, monolithiodifluoro-, and monofluorodilithiobenzenes, additivity appears to hold up quite well but this may be due to the small number of the "offending" lithio substituents.

Mulliken charges for the polysubstituted benzenes are shown in Table 27. The data are given as total σ and π charges donated to the ring for all molecules,

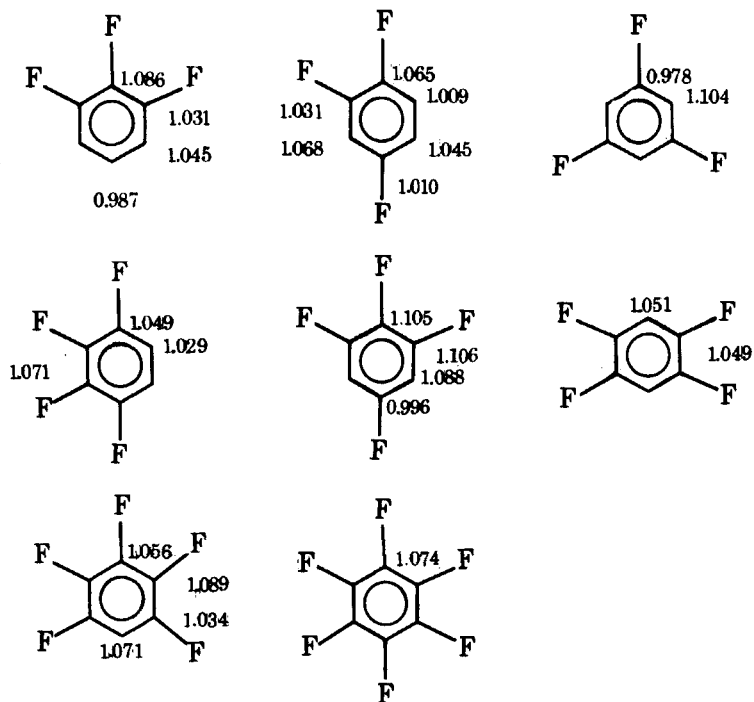


Figure 13 π -Electron populations in polyfluorobenzenes.

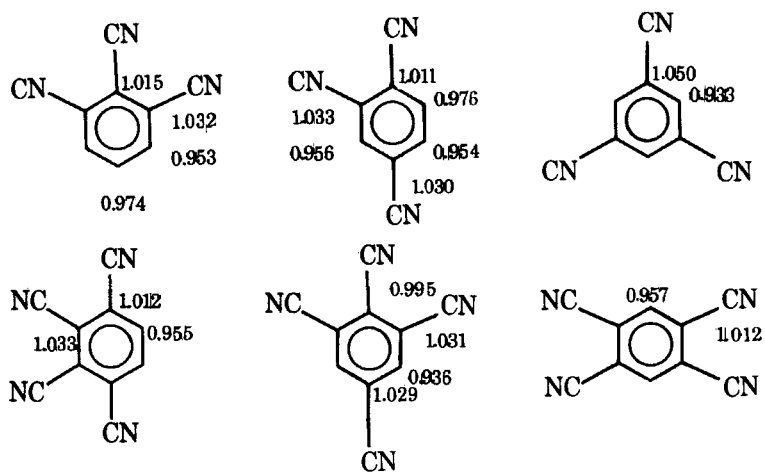


Figure 14 π -Electron populations in polycyanobenzenes.

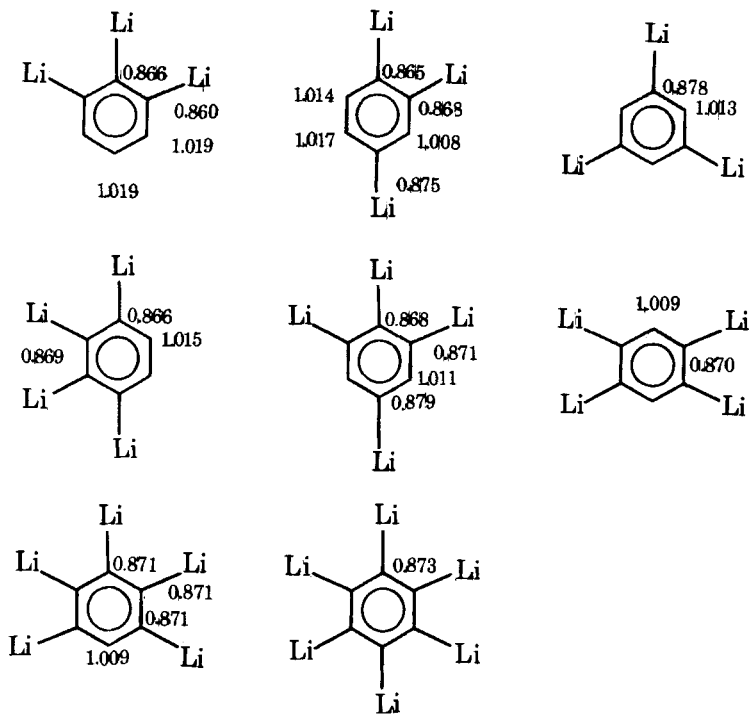


Figure 15 π -Electron populations in polythiobenzenes.

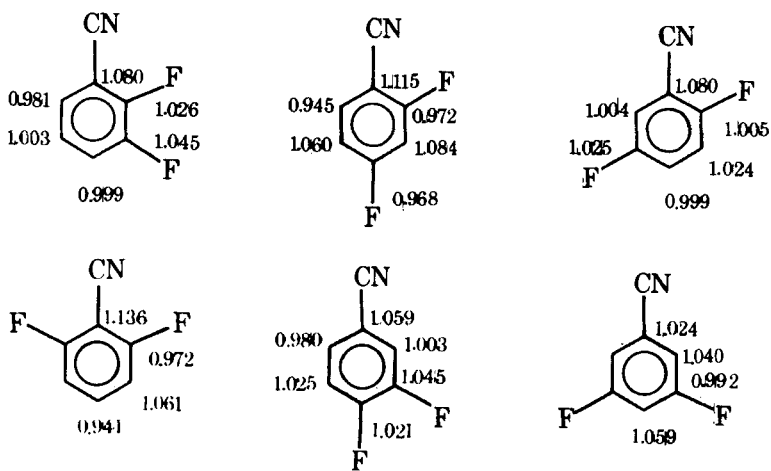


Figure 16 π -Electron populations in fluorocyanobenzenes.

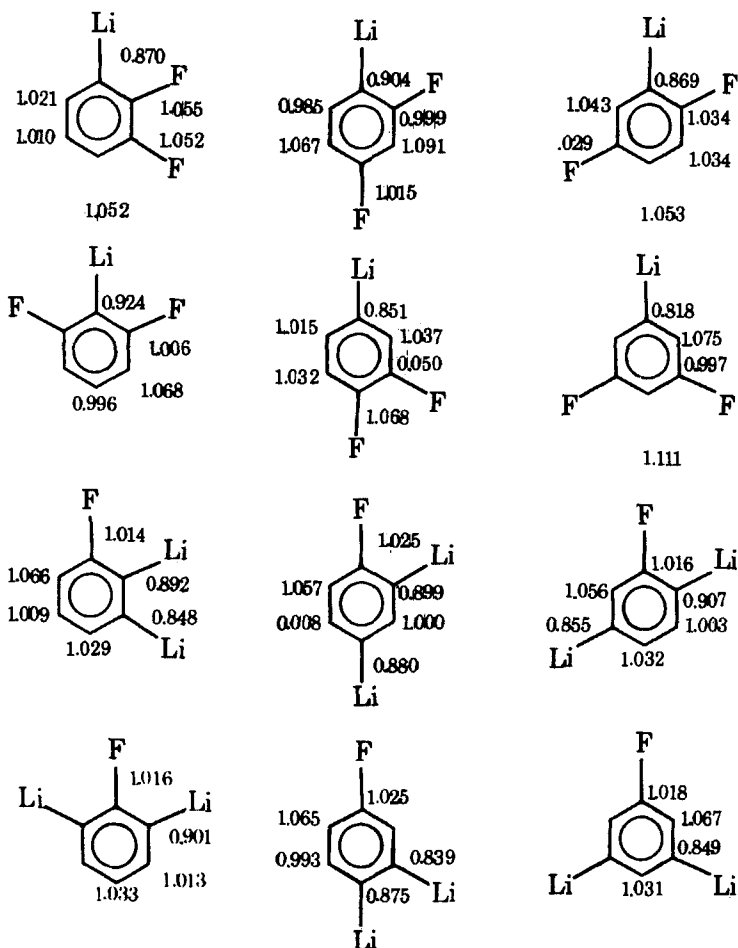


Figure 17 π -Electron populations in fluorolithiobenzenes.

as well as σ and π charges donated per substituent in the case of the polyfluoro-, polycyano-, and polythiobenzenes. Calculated π -electron populations for polyfluoro-, polycyano-, polythio-, and polysubstituted fluorocycano- and fluorolithiobenzenes are displayed in Figs. 13–17, respectively.

The relationship between the calculated charges (Table 27) and the additivity of interaction energies (Table 26) is not immediately clear. There does appear to be some correlation, however, between the variability in the values of q_π per substituent (small for F, intermediate for CN, and large for Li) and the degree to which the interaction energies are additive.

VII. CONCLUDING REMARKS

In this article we have brought together a large amount of quantitative data concerning stabilities and charge distributions in substituted benzenes as provided by *ab initio* molecular orbital calculations. It has been possible to calculate energies of interaction among the substituents in di- and polysubstituted benzenes and to probe effects such as saturation and pairwise additivity of the interactions. The theoretical data enable the effect of a substituent in a more complex reaction, such as a reaction measuring relative basicities, to be broken down into its effect on the components of the reaction. For example, the weaker basicity of para-nitroaniline compared with aniline is shown to be primarily due to destabilization of the anilinium ion by the nitro substituent rather than to the stabilization of the neutral aniline, in contrast to the common textbook explanation. Analysis of the theoretical charge distributions yields valuable information concerning the transfer of σ and π charge by a substituent to or from the ring and the effect of additional substituents on such transfer. We have attempted to construct a unifying qualitative theory of substituent effects in substituted benzenes within the framework of perturbation molecular orbital theory. Some of the results that we have obtained are well known and easily rationalized alternatively in terms of resonance theory. For example, in a para-disubstituted benzene, two π donors interact unfavorably while a π donor and a π acceptor interact favorably. On the other hand, many of the other results that we have obtained are not readily explained in resonance terms. For example, why do two amino groups meta to one another interact favorably? Our arguments based on PMO theory can be used to rationalize these and other results. Finally, we note that our discussion of this rather massive amount of data has been necessarily brief. Much of the data presented awaits more detailed analysis. We hope that our presentation here might serve as a springboard for subsequent theoretical and experimental studies of substituent effects in substituted benzenes.

ACKNOWLEDGMENTS

We are indebted to Prof. Warren J. Hehre for the generous provision of unpublished data, computational facilities, and extensive discussions.

References and Notes

1. For recent reviews see: (a) R. D. Topsom, *Prog. Phys. Org. Chem.*, **12**, 1 (1976); (b) W. J. Hehre, R. W. Taft, and R. D. Topsom, *Prog. Phys. Org. Chem.*, **12**, 159 (1976); (c) A. R. Katritzky and R. D. Topsom, *Angew. Chem., Int. Ed.*, **9**, 87 (1970); (d) A. R. Katritzky and R. D. Topsom, *J. Chem. Ed.*, **48**, 427 (1971).
2. L. P. Hammett, *Physical Organic Chemistry*, 2nd ed., McGraw-Hill, New York, 1970.

3. See, for example: J. E. Leffler and E. Grunwald, *Rates and Equilibria of Organic Reactions*, Wiley, New York, 1963.
4. (a) R. T. C. Brownlee, D. G. Cameron, R. D. Topsom, A. R. Katritzky, and A. F. Pozharsky, *J. Chem. Soc. Perkin II*, 1974, 247, and references therein; (b) R. T. C. Brownlee, G. Butt, M. P. Chan, and R. D. Topsom, *J. Chem. Soc. Perkin II*, 1976, 1486.
5. (a) W. J. Hehre, W. A. Lathan, R. Ditchfield, M. D. Newton, and J. A. Pople, Program No. 236, Quantum Chemistry Program Exchange, Indiana University, Bloomington, Indiana; (b) D. J. DeFrees, B. Levi, S. K. Pollack, E. S. Blurock, and W. J. Hehre, unpublished.
6. W. J. Hehre, L. Radom, and J. A. Pople, *J. Amer. Chem. Soc.*, 94, 1496 (1972).
7. For reviews on the PMO method, see: (a) I. Fleming, *Frontier Orbitals and Organic Chemical Reactions*, Wiley-Interscience, New York (1976); (b) N. D. Epiotis, W. R. Cherry, S. Shaik, R. Yates, and F. Bernardi, *Top. Curr. Chem.*, 70, 1 (1977); (c) *Chemical Reactivity and Reaction Paths*, G. Klopman, Ed., Wiley-Interscience, New York (1974); (d) R. F. Hudson, *Angew. Chem., Int. Ed. Engl.*, 12, 36 (1973); (e) M. J. S. Dewar and R. C. Dougherty, *The PMO Theory of Organic Chemistry*, Plenum, New York (1975).
8. L. Radom, W. J. Hehre, J. A. Pople, G. L. Carlson, and W. G. Fateley, *Chem. Commun.*, 1972, 308.
9. W. J. Hehre, L. Radom, and J. A. Pople, *Chem. Commun.*, 1972, 669.
10. A. Pross, L. Radom, and R. W. Taft, *J. Org. Chem.*, in press.
11. A. Pross, L. Radom, and R. W. Taft, unpublished.
12. J. M. Norbeck and G. A. Gallup, *J. Amer. Chem. Soc.*, 96, 3386 (1974).
13. W. C. Ermler, R. S. Mulliken, and E. Clementi, *J. Amer. Chem. Soc.*, 98, 388 (1976).
14. W. von Niessen, L. S. Cederbaum, and W. P. Kraemer, *J. Chem. Phys.*, 65, 1378 (1976).
15. W. H. Fink, *J. Chem. Phys.*, 66, 1968 (1977).
16. D. M. Hirst, *J. Chem. Soc. Faraday II*, 1977, 443.
17. G. F. Tantardini, M. Raimondi, and M. Simmonetta, *J. Amer. Chem. Soc.*, 99, 2913 (1977).
18. H. E. Popkie and J. J. Kaufman, *J. Chem. Phys.*, 66, 4827 (1977).
19. L. Praud, P. Millie, and G. Berthier, *Theor. Chim. Acta*, 11, 169 (1968).
20. W. J. Hehre and J. A. Pople, *J. Amer. Chem. Soc.*, 92, 2191 (1970).
21. S. D. Peyerimhoff and R. J. Buenker, *Theor. Chim. Acta*, 19, 1 (1970).
22. M. D. Newton, W. A. Lathan, W. J. Hehre, and J. A. Pople, *J. Chem. Phys.*, 52, 4064 (1970).
23. R. R. Gilman and J. de Heer, *J. Chem. Phys.*, 52, 4287 (1970).
24. W. J. Hehre, R. Ditchfield, L. Radom, and J. A. Pople, *J. Amer. Chem. Soc.*, 92, 4796 (1970).
25. J. M. Schulman, C. J. Hornback, and J. W. Moskowitz, *Chem. Phys. Lett.*, 8, 361 (1971).
26. P. T. van Duijnen and D. B. Cook, *Mol. Phys.*, 21, 475 (1971).
27. R. M. Stevens, E. Switkes, E. A. Laws, and W. N. Lipscomb, *J. Amer. Chem. Soc.*, 93, 2603 (1971).
28. R. E. Christoffersen, *J. Amer. Chem. Soc.*, 93, 4104 (1971).
29. R. E. Christoffersen, D. W. Genson, and G. M. Maggiora, *J. Chem. Phys.*, 54, 239 (1971).
30. M. D. Newton and E. Switkes, *J. Chem. Phys.*, 54, 3179 (1971).
31. G. Berthier, A. Y. Meyer, and L. Praud, *Jerusalem Symp. on Quantum Chem. Biochem.*, 3, 174 (1971).
32. N. W. Winter, W. C. Ermler, and R. M. Pitzer, *Chem. Phys. Lett.*, 19, 179 (1973).
33. J. M. Norbeck and G. A. Gallup, *J. Amer. Chem. Soc.*, 95, 4460 (1973).
34. I. Fischer-Hjalmar and P. Siegbahn, *Theor. Chim. Acta*, 31, 1 (1973).
35. W. C. Ermler and C. W. Kern, *J. Chem. Phys.*, 58, 3458 (1973).

36. P. J. Hay and I. Shavitt, *Chem. Phys. Lett.*, **22**, 33 (1973).
37. J. Almlöf, B. Roos, U. Wahlgren, and H. Johansen, *J. Electron. Spectrosc.*, **2**, 51 (1973).
38. L. Radom and H. F. Schaefer, *J. Amer. Chem. Soc.*, **99**, 7522 (1977).
39. J. Almlöf, *Chem. Phys.*, **6**, 135 (1974).
40. J. E. Almlöf, P. U. Isacson, P. J. Mjoberg, and W. M. Ralowski, *Chem. Phys. Lett.*, **26**, 215 (1974).
41. W. M. Ralowski, P. J. Mjoberg, and J. E. Almlöf, *J. Chem. Soc. Faraday II*, **71**, 1109 (1975).
42. W. J. E. Parr and T. Schaefer, *J. Amer. Chem. Soc.*, **99**, 1033 (1977).
43. T. Schaefer and W. J. E. Parr, *J. Chem. Phys.*, **65**, 1197 (1976).
44. T. Schaefer, J. B. Rowbotham, W. J. E. Parr, K. Marat, and A. F. Janzen, *Can. J. Chem.*, **54**, 1322 (1976).
45. W. J. E. Parr and T. Schaefer, *Can. J. Chem.*, **55**, 557 (1977).
46. D. G. Lister, P. Palmieri, and C. Zauli, *J. Mol. Struct.*, **35**, 299 (1976).
47. G. Bendazzoli, F. Bertinelli, P. Palmieri, and C. Taliani, *Chem. Phys.*, **16**, 319 (1976).
48. F. Bertinelli, P. Palmieri, A. Brillante, and C. Taliani, *Chem. Phys.*, **25**, 333 (1977).
49. D. W. Davies, *Chem. Phys. Lett.*, **48**, 565 (1977).
50. W. von Niessen, G. H. F. Diercksen, and L. S. Cederbaum, *Chem. Phys. Lett.*, **45**, 295 (1977).
51. C. R. Brundle, M. B. Robin, and N. A. Kuebler, *J. Amer. Chem. Soc.*, **94**, 1466 (1972).
52. J. Almlöf, A. Henriksson-Enflo, J. Kowalewski, and M. Sundborn, *Chem. Phys. Lett.*, **21**, 560 (1973).
53. J. M. Abboud, W. J. Hehre, and R. W. Taft, *J. Amer. Chem. Soc.*, **98**, 6072 (1976).
54. R. Cimraglia and J. Tomasi, *J. Amer. Chem. Soc.*, **99**, 1135 (1977).
55. M. M. Bursey, R. S. Greenberg, and L. G. Pedersen, *Chem. Phys. Lett.*, **36**, 470 (1975).
56. D. J. DeFrees, R. T. McIver, Jr., and W. J. Hehre, *J. Amer. Chem. Soc.*, **99**, 3853 (1977).
57. S. K. Pollack, J. L. Devlin, K. D. Summerhays, R. W. Taft, and W. J. Hehre, *J. Amer. Chem. Soc.*, **99**, 4583 (1977).
58. K. D. Summerhays, S. K. Pollack, R. W. Taft, and W. J. Hehre, *J. Amer. Chem. Soc.*, **99**, 4585 (1977).
59. S. W. Dietrich, E. C. Jorgensen, P. A. Kollman, and S. Rothenberg, *J. Amer. Chem. Soc.*, **98**, 8310 (1976).
60. J. M. McKelvey, S. Alexandratos, A. Streitwieser, Jr., J. M. Abboud, and W. J. Hehre, *J. Amer. Chem. Soc.*, **98**, 244 (1976).
61. P. G. Mezey and W. F. Reynolds, *Can. J. Chem.*, **55**, 1567 (1977).
62. W. F. Reynolds, P. G. Mezey, and G. K. Hamer, *Can. J. Chem.*, **55**, 522 (1977).
63. T. Schaefer and W. J. E. Parr, *Can. J. Chem.*, **55**, 552 (1977).
64. F. Bernardi, A. Mangini, N. D. Epiotis, J. R. Larson, and S. Shaik, *J. Amer. Chem. Soc.*, **99**, 7465 (1977).
65. L. Radom, *Chem. Commun.*, **1974**, 403.
66. W. von Niessen, *Theor. Chim. Acta*, **33**, 7 (1974).
67. I. G. John and L. Radom, *J. Amer. Chem. Soc.*, **100**, 3981 (1978).
68. F. Bernardi, A. Mangini, N. D. Epiotis, J. A. Larson, and S. Shaik, *J. Amer. Chem. Soc.*, **99**, 7465 (1977).
69. T. Schaefer, L. J. Kruczynski, and W. J. E. Parr, *Can. J. Chem.*, **54**, 3210 (1976).
70. W. M. Ralowski, P. J. Mjoberg, and J. E. Almlöf, *J. Chem. Soc. Faraday II*, **71**, 1109 (1975).
71. M. Barachi, A. Gamba, G. Moroso, and M. Simonetta, *J. Phys. Chem.*, **78**, 49 (1974).
72. A. Hinchliffe, *Chem. Phys. Lett.*, **27**, 454 (1974).
73. M. Martin, R. Carbo, C. Petrongolo, and J. Tomasi, *J. Amer. Chem. Soc.*, **97**, 1338 (1975).

74. C. Petrongolo and J. Tomasi, *Int. J. Quantum Chem., Quantum Biology Symp.*, **2**, 181 (1975).
75. B. Pullman, H. Berthod, and P. H. Courriere, *Int. J. Quantum Chem., Quantum Biology Symp.*, **1**, 93 (1974).
76. G. G. Hall, C. J. Miller, and G. W. Schnuelle, *J. Theor. Biology*, **53**, 475 (1975).
77. M. M. Bursey, R. S. Greenberg, and L. G. Pedersen, *Chem. Phys. Lett.*, **36**, 470 (1975).
78. R. S. Greenberg, M. M. Bursey, and L. G. Pedersen, *J. Amer. Chem. Soc.*, **98**, 4061 (1976).
79. W. J. E. Parr, T. Schaefer, and K. Marat, *Can. J. Chem.*, **55**, 3243 (1977).
80. W. C. Ermler and R. S. Mulliken, *J. Amer. Chem. Soc.*, **100**, 1647 (1978).
81. M. H. Palmer, W. Moyes, M. Spiers, and J. N. A. Ridyard, *J. Mol. Struct.*, **49**, 105 (1978).
82. G. M. Anderson, P. A. Kollman, L. N. Domelsmith, and K. N. Houk, *J. Amer. Chem. Soc.*, **101**, 2344 (1979).
83. J. Catalan and M. Yanez, *Chem. Phys. Lett.*, **60**, 499 (1979).
84. J. Catalan and M. Yanez, *J. Chem. Soc. Perkin II*, 741 (1979).
85. J. Catalan and M. Yanez, *J. Amer. Chem. Soc.*, **101**, 3490 (1979).
86. N. S. Chiu, J. D. Ewbank, M. Askari, and L. Schafer, *J. Mol. Struct.*, **54**, 185 (1979).
87. G. Orlandi, P. Palmieri, and G. Poggi, *J. Amer. Chem. Soc.*, **101**, 3492 (1979).
88. M. H. Palmer, W. Moyes, M. Spiers, and J. N. A. Ridyard, *J. Mol. Struct.*, **52**, 293 (1979).
89. M. H. Palmer, W. Moyes, M. Spiers, and J. N. A. Ridyard, *J. Mol. Struct.*, **53**, 235 (1979).
90. M. H. Palmer, W. Moyes, M. Spiers, and J. N. A. Ridyard, *J. Mol. Struct.*, **55**, 243 (1979).
91. C. Santiago, K. N. Houk, and C. L. Perrin, *J. Amer. Chem. Soc.*, **101**, 1337 (1979).
92. T. Schaefer and W. J. E. Parr, *Can. J. Chem.*, **57**, 1421 (1979).
93. A. J. Hoefnagel, M. A. Hoefnagel, and B. M. Wepster, *J. Amer. Chem. Soc.*, **98**, 6194 (1976).
94. B. M. Wepster, *J. Amer. Chem. Soc.*, **95**, 102 (1973).
95. W. F. Reynolds and G. K. Hamer, *J. Amer. Chem. Soc.*, **98**, 7296 (1976).
96. W. F. Reynolds, I. R. Peat, M. H. Freedman, and J. R. Lyerla, Jr., *Can. J. Chem.*, **51**, 1857 (1973).
97. W. F. Reynolds, *Tetrahedron Lett.*, 1977, 576.
98. G. K. Hamer, I. R. Peat, and W. F. Reynolds, *Can. J. Chem.*, **51**, 915 (1973).
99. D. A. Dawson and W. F. Reynolds, *Can. J. Chem.*, **53**, 373 (1975).
100. G. K. Hamer, I. R. Peat, and W. F. Reynolds, *Can. J. Chem.*, **51**, 897 (1973).
101. S. K. Dayal and R. W. Taft, *J. Amer. Chem. Soc.*, **95**, 5595 (1973).
102. J. Fukunaga and R. W. Taft, *J. Amer. Chem. Soc.*, **97**, 1612 (1975).
103. G. L. Anderson, R. G. Parish, and L. M. Stock, *J. Amer. Chem. Soc.*, **93**, 6984 (1971).
104. W. Adcock and B. D. Gupta, *J. Amer. Chem. Soc.*, **97**, 6871 (1975).
105. W. Adcock and T. C. Khor, *Tetrahedron Lett.*, 1976, 3063.
106. E. M. Shulman, K. A. Christensen, D. M. Grant, and C. Walling, *J. Org. Chem.*, **39**, 2686 (1974).
107. J. H. P. Utlely and S. O. Yeboah, *J. Chem. Soc. Perkin II*, 1978, 766.
108. T. B. Grindley, A. R. Katritzky, and R. D. Topsom, *J. Chem. Soc. Perkin II*, 1975, 443.
109. P. J. Q. English, A. R. Katritzky, T. T. Tidwell, and R. D. Topsom, *J. Amer. Chem. Soc.*, **90**, 1767 (1968).
110. C. C. J. Roothaan, *Rev. Mod. Phys.*, **23**, 69 (1951).
111. W. J. Hehre, R. F. Stewart, and J. A. Pople, *J. Chem. Phys.*, **51**, 2657 (1969).

112. J. A. Pople and M. S. Gordon, *J. Amer. Chem. Soc.*, **89**, 4253 (1967).
113. J. D. Dill, P. v. R. Schleyer, and J. A. Pople, *J. Amer. Chem. Soc.*, **98**, 1663 (1976).
114. R. S. Mulliken, *J. Chem. Phys.*, **23**, 1833 (1955).
115. L. Radom, W. J. Hehre, and J. A. Pople, *J. Chem. Soc. (A)*, **1971**, 2299.
116. W. Cherry, N. Epiotis, and W. T. Borden, *Acc. Chem. Res.*, **10**, 167 (1977).
117. R. Hoffmann, L. Radom, J. A. Pople, P. v. R. Schleyer, W. J. Hehre, and L. Salem, *J. Amer. Chem. Soc.*, **94**, 6221 (1972).
118. S. K. Pollack and W. J. Hehre, unpublished.
119. (a) M. J. S. Dewar, *J. Amer. Chem. Soc.*, **74**, 3340 (1952); (b) D. A. Brown and M. J. S. Dewar, *J. Chem. Soc.*, 1953, 2406; (c) M. J. S. Dewar and P. J. Grisdale, *J. Amer. Chem. Soc.*, **84**, 3539 (1962).
120. (a) H. H. Jaffe, *J. Chem. Phys.*, **20**, 279 (1952); (b) H. H. Jaffe, *J. Amer. Chem. Soc.*, **77**, 274 (1955).
121. For example, see: (a) J. March, *Advanced Organic Chemistry*, McGraw-Hill, New York, 1977, p. 241; (b) J. D. Roberts and M. C. Caserio, *Basic Principles of Organic Chemistry*, 2nd ed., Benjamin, New York, 1977, p. 1115; (c) A. Streitwieser and C. Heathcock, *Introduction to Organic Chemistry*, Macmillan, New York, 1976, p. 968; (d) J. B. Hendrickson, D. J. Cram, and G. S. Hammond, *Organic Chemistry*, 3rd ed., McGraw-Hill, New York, 1970, p. 313.
122. (a) R. W. Taft in *Proton Transfer Reactions*, E. Caldin and V. Gold, Eds., Chapman and Hall, London, 1975; (b) J. E. Bartmess and R. T. McIver in *Gas Phase Ion Chemistry*, M. T. Bowers, Ed., Academic, 1978; (c) J. E. Bartmess, J. A. Scott, and R. T. McIver, *J. Amer. Chem. Soc.*, **101**, 6046 (1979).

The Systematic Prediction of the Most Stable Neutral Hydrocarbon Isomer

BY STEPHEN A. GODLESKI

*Department of Chemistry, The University of Rochester,
Rochester, New York 14627*

PAUL V. R. SCHLEYER

*Institut für Organische Chemie der Friedrich-Alexander
Universität Erlangen-Nürnberg, 8520 Erlangen, West Germany*

EIJI ŌSAWA

*Department of Chemistry, Faculty of Science, Hokkaido
University, Sapporo 060, Japan*

AND W. TODD WIPKE

*Board of Studies in Chemistry, University of California, Santa
Cruz, California 95064*

CONTENTS

I. Introduction	64
II. Discussion	64
A. Experimental Methods for Determining Relative Stability of Hydrocarbons	64
B. Calculation of the Relative Stability of Isomers	65
1. Entropy	66
2. Enthalpy	67
C. Method of Prediction of Stabilomers	69
1. Generation of All Possible Isomers	70
2. Elimination of Isomers Based on Application of Basic Thermodynamic Principles of Stability	72
3. Quantification of Relative Stabilities	73
D. C_nH_{2n} and C_nH_{2n-2} Families	75
E. C_nH_{2n-4} 's	79
F. C_nH_{2n-6} 's	97
1. Aromatics	97
2. Saturated Isomers	98
3. Saturated versus Aromatic C_nH_{2n-6} 's	103

G.	C_nH_{2n-8} 's	103
	1. Aromatics	103
	2. Saturated Isomers	103
	3. Saturated C_nH_{2n-8} 's versus Aromatics	108
H.	Larger Systems	109
III.	Conclusions	114
	Acknowledgments	114
	References and Notes	115

I. INTRODUCTION

The most stable arrangement of n carbon atoms and m hydrogen atoms is of inherent interest to chemists. Theoreticians are concerned with developing means of evaluating the stability (we define stability in terms of the Gibbs free energy of the molecule ΔG_f°) of a given construction of carbon and hydrogen. Experimentalists depend on thermodynamic driving force in their efforts to create new compounds. Broad areas of research such as conformational analysis (1), aluminum halide (2), and silver ion rearrangements (3,4) and measurement of heats of formation (5) are directly concerned with determining relative stabilities of hydrocarbons.

We have developed a three-stage process for the selection of the most stable arrangement of a singlet neutral hydrocarbon, the "stabilomer" (6). The first step in the process is generation of all isomers of a given empirical formula. The second stage is elimination of isomers expected qualitatively to be unstable on the basis of structural considerations. The third step is quantification of the relative stability of the remaining candidates by computer calculations of ΔH_f° and consideration of possible entropy contributions. In this paper, we focus on cases where experimental data are available (C_2 - C_{20}).

II. DISCUSSION

A. Experimental Methods for Determining Relative Stability of Hydrocarbons

The most accurate experimental means of determining the relative stability of constitutional isomers is often by direct equilibration but this is constrained by the limit of precision of the analytical tool employed. For the most common methods (e.g., glc, nmr, ir) where the practical limit of detectability is 0.1%, $\Delta\Delta G_f^\circ$ (25°C) ($-RT \ln[A]/[B]$) must generally be in the 0-4 kcal mole⁻¹ range.

Aluminum halide catalysts can effect such equilibrations via rearrangements involving intermediate carbonium ions. A saturated precursor with the

desired empirical formula is prepared and is treated with the Lewis acid catalyst under conditions promoting thermodynamic control. The product obtained (7) usually is the most stable isomer, the stabilomer. This procedure is limited experimentally by the possibility that disproportionation or incomplete rearrangement will occur. Highly strained compounds, for example, those with three-membered rings, relieve strain by ring opening, which leads to products with fewer rings and to olefins, which give tar under the reaction conditions. Similarly, hydrocarbons containing four-membered rings are often not good candidates for isomerization (2). If the mechanistic pathway involves an inaccessibly high energy intermediate or transition state, the isomerization may not yield the stabilomer but only another isomer more stable than the starting material.

Chlorinated platinum–alumina catalysts lessen the disproportionation of highly strained precursors (8). In addition, McKervery (9) has also recently reported that polycyclic olefins undergo ring closure and rearrangement in the gas phase on a platinum–silica catalyst to saturated hydrocarbons, thus expanding the range of precursors available for isomerization. Finally, silver ion rearrangement of hydrocarbons containing three- and four-membered rings complements aluminum halide catalysis in allowing highly strained compounds to be isomerized (3,4). Experimental isomerization techniques, however, do not allow simple equilibration among aromatic, unsaturated, and saturated isomers and are not sufficiently versatile to allow for a systematic study of the relative stability of hydrocarbons.

Absolute determination of ΔG_f° is the most general method. From the experimentally determined enthalpies of formation of compounds (ΔH_f°) relative stabilities can easily be calculated (after consideration of ΔS , *vide infra*), but such experimental work requires large quantities (≥ 1 g) of extremely pure material. Also, since the heat of formation of a compound is calculated from the difference of its measured heat of combustion and the heat of combustion of its constituent elements, quantities which can be in the 1000–4000 kcal mole⁻¹ range, small experimental errors ($>0.02\%$) lead to relatively large errors in ΔH_f° (10). The measurement of heats of vaporization or of sublimation needed to convert $\Delta H_f^\circ(l)$ and $\Delta H_f^\circ(s)$ to $\Delta H_f^\circ(g)$ are also difficult experimentally (11). Premelting transitions (5i, 12) complicate matters further. As a result, reported experimental values of ΔH_f° for a given compound may differ by as much as several kilocalories per mole (e.g., adamantane and diamantane, see Table 2).

B. Calculation of the Relative Stability of Isomers

Calculation of the relative stability ($\Delta\Delta G_f^\circ$) of hydrocarbon isomers is based on estimation of the contributions of entropy (ΔS°) and enthalpy (ΔH°) ($\Delta G^\circ = \Delta H^\circ - T\Delta S^\circ$).

TABLE 1
Enthalpy, Entropy, and Free Energy of Formation of C_8H_{16} 's^a

Compound	ΔH_f° (kcal mole ⁻¹)	ΔS°_{298} (eu)	ΔG_f° (kcal mole ⁻¹)
Cyclooctane	-30.06	87.66	21.49
1,1-Dimethylcyclohexane	-43.26	87.24	8.42
<i>cis</i> -1,2-Dimethylcyclohexane	-41.15	89.51	9.85
<i>trans</i> -1,2-Dimethylcyclohexane	-43.02	88.65	8.24
<i>cis</i> -1,3-Dimethylcyclohexane	-44.16	88.54	7.13
<i>trans</i> -1,3-Dimethylcyclohexane	-42.20	89.92	8.68
<i>cis</i> -1,4-Dimethylcyclohexane	-42.22	88.54	9.07
<i>trans</i> -1,4-Dimethylcyclohexane	-44.12	87.19	7.58
Ethylcyclohexane	-41.05	91.44	9.38
1-Octene	-19.82	110.55	24.91
Propylcyclopentane	-35.39	99.73	12.57

^a Values from Ref. 25c.

1. Entropy

The contributions to the entropy (ΔS) term are ordered: $\Delta S_{\text{translational}} > \Delta S_{\text{rotational}} > \Delta S_{\text{vibrational}}$ (13). Typical entropy contributions from translational, rotational, and vibrational motions at 298°K are: 3 degrees translational freedom for compounds (standard state of 1 *M*) of molecular weights 44 (propane) and 134 (*endo*-dicyclopentadiene) are 31 and 34.2 eu (cal deg⁻¹·mole⁻¹), respectively; 3 degrees of rotational freedom, propane, 21.5 eu and *endo*-dicyclopentadiene, 27.2 eu; vibrations: 17.2 eu, *endo*-dicyclopentadiene; *n*-propane, ~5 eu (13). The translational entropy depends on the temperature, the volume available to the molecule and its mass rather than on structural features. Rotational entropy is proportional to the moment of inertia, the temperature, and the symmetry of the molecule (σ) (14). Rotational entropy has a relatively small dependence on structure; for example, the doubling of all three principal moments of inertia increases $S_{\text{rotational}}$ by only 2.1 eu. The vibrational entropy depends on the frequency of vibration and temperature. Frequencies above 1000 cm⁻¹ make a negligible contribution to S_{total} at 298°K. Only if there are several low frequency vibrations does $S_{\text{vibrational}}$ contribute significantly to S_{total} (13). The result is that structural features are often not important in contributing to ΔS and entropy differences among isomers of neutral hydrocarbons in solution or gas phase can be expected to be small. Relative values of ΔS may become important if enthalpy differences are small, and even then only rarely. Table 1 gives the enthalpy, entropy, and free energy of formation of a number of C_8H_{16} compounds, and illustrates the situation to be expected. Although the ΔH_f° 's vary by some 25 kcal mole⁻¹, the ΔS° 's vary only by 23 eu or ($T\Delta S^\circ = (298)(23)$) ~ 7 kcal mole⁻¹. In addition, the relative order of the heats of formation is largely the

same as the order of the free energies of formation. There is no correlation of the order of ΔS° and ΔG_f° .

A rare example of entropy control is afforded by the equilibration of bicyclo[2.2.2]octane, bicyclo[3.2.1]octane, and *cis*-bicyclo[3.3.0]octane (15). At 298°K the order of stability ($\Delta\Delta G^\circ$) is bicyclo[3.2.1]octane > *cis*-bicyclo[3.3.0]octane > bicyclo[2.2.2]octane. The enthalpy difference measured (15) between bicyclo[2.2.2]octane and bicyclo[3.2.1]octane is indistinguishable from zero; the greater stability of bicyclo[3.2.1]octane over bicyclo[2.2.2]octane is due entirely to more favorable entropy. Both bicyclo[2.2.2]octane and bicyclo[3.2.1]octane are less strained than *cis*-bicyclo[3.3.0]octane ($\Delta\Delta H$ measured¹⁵ = 1.9 kcal mole⁻¹) but this is counterbalanced by the high entropy of *cis*-bicyclo[3.3.0]octane. Above 378°K *cis*-bicyclo[3.3.0]octane is the most stable of the three isomers. The high entropy of the "3.3.0" system is due to its more flexible ring system. The entropy difference between the more rigid "3.2.1" and "2.2.2" systems is due primarily to symmetry. The symmetry number (σ) of bicyclo[2.2.2]octane is 6, whereas σ of bicyclo[3.2.1]octane is 1. The relative contribution to the entropy is $R \ln 6 - R \ln 1 = 3.6$ eu, which equals ($T\Delta S^\circ$) 1.1 kcal mole⁻¹; the $\Delta\Delta G^\circ_{298}$ measured (15) is 1.69 kcal mole⁻¹.

2. Enthalpy

The types of calculations available for estimating ΔH_f° 's for C₁-C₂₀ hydrocarbons easily, inexpensively, and accurately are limited. *Ab initio* MO methods (16), even those using only a minimal basis set, are not applicable because of the extreme expense in calculating such large systems with geometry search. Semiempirical MO methods such as MNDO (17), although less costly than *ab initio*, do not give reliable heats of formation (17) (e.g., the errors with cyclobutane and with norbornane and adamantane are -18.7, +2.1, and +5.5 kcal mole⁻¹, respectively) (17b). Empirical force field calculations (18,19,19a) give reliable heats of formation (generally within 2.0 kcal mole⁻¹ of the experimentally determined ΔH_f° (18)), are less expensive even than MNDO and are easy to perform.

Although the calculated heats of formation refer to the gas phase, relative enthalpies of neutral hydrocarbon isomers often do not change much in the liquid state or in solution (20).

Engler, Andose, and Schleyer (18) used force field methods to predict the heats of formation of numerous polycyclic hydrocarbons; experimental data on some of these compounds are now available. Table 2 summarizes this data and indicates the magnitude of the error expected in comparing predicted and experimental heats of formation for compounds of the type being considered. The agreement of calculated with experimental ΔH_f° 's is only fair ($\sim \pm 3$ kcal mole⁻¹) for both force fields, but experimental values often differed by a comparable

TABLE 2
 Heats of Formation of Polycyclic Alkanes

Molecule	$-\Delta H_f^\circ$ (gas) exp. (kcal mole ⁻¹)	$-\Delta H_f^\circ$ (Engler) (kcal mole ⁻¹)	$-\Delta H_f^\circ$ (Allinger) (kcal mole ⁻¹)
Adamantane	31.76 ± 0.32 ^a (30.65 ± 0.98, ^b 30.57 ± 0.79, ^c 32.96 ± 0.19 ^d)	32.50	33.82
1-Methyladamantane	40.57 ± 0.34 ^a 41.8 ± 0.6 ^e	41.82	42.89
2-Methyladamantane	35.66 ± 0.62 ^a 37.6 ± 0.70 ^e	37.94	39.04
2,2-Dimethyladamantane	44.1 ± 0.6 ^e	41.59	43.36
1,3-Dimethyladamantane	51.3 ± 0.7 ^e	51.33	51.91
1,3,5-Trimethyladamantane	61.3 ± 1.0 ^e	60.78	61.01
1,3,5,7-Tetramethyladamantane	67.15 ± 0.50 ^a 70.3 ± 1.1 ^e	70.26	70.21
Protoadamantane	20.54 ± 0.60 ^a	21.13	22.63
Diamantane	32.60 ± 0.58 ^a (36.65 ^f ± 0.42, 34.60 ^g)	37.37	38.13
4-Methyldiamantane	43.53 ± 0.30 ^a	46.82	47.21
3-Methyldiamantane	37.60 ± 0.58 ^a	42.91	43.35
1-Methyldiamantane	39.85 ± 0.85 ^a	43.56	44.43
Perhydrotriquinacene	24.47 ± 0.86 ^h	23.74	19.74
Bicyclo[3.3.1]nonane	30.46 ± 0.55 ⁱ	30.37	30.64
Bicyclo[3.3.2]decane	25.3 ± 1.7 ⁱ	26.17	25.20
Bicyclo[3.3.3]undecane (Manxane)	21.3 ± 0.5 ⁱ	25.21	22.81

^a Ref. 5a.^b Ref. 5e.^c Ref. 5f.^d Ref. 5g.^e W. Parker, W. Steele, and I. Watt, private communication. Ref. 5o.^f Refs. 5h and 5i.^g M. A. McKervey, redetermination, private communication.^h Ref. 5b.ⁱ Ref. 5c.

amount. In view of the large number of difficulties in determining ΔH_f° experimentally and the variability of these values with the investigator the calculated ΔH_f° 's offer greater consistency, comparable accuracy and are obtained with relative ease. Relative values of ΔH_f° calculated have been found to give excellent agreement with experimental fact (21). Table 3 compares ΔH_{isom} experimental (from difference of measured ΔH_f° for each compound), ΔH_{isom} calculated by force field and the values from direct isomerization. The enthalpy difference

TABLE 3
Comparison of Heats of Isomerization (kcal mole⁻¹) from Various Sources

Reaction	Experimental, ΔH_{isom}		Calculated, ΔH_{isom} (gas phase, 25°)	
	From direct isomerization data	From ΔH_f° (gas phase, 25°) differences	1971 Allinger force field	Engler force field
2-Methyladamantane → 1-Methyladamantane	-2.77 ^a (gas)	-4.91 ^b (-4.2 ^c)	-3.85 ^d	-3.88 ^d
1-Methyldiamantane → 4-Methyldiamantane	-2.14 ^{a,e} (gas)	-3.68 ^b	-2.78 ^d	-3.26 ^d
3-Methyldiamantane → 4-Methyldiamantane	-2.70 ^{a,e} (gas)	-5.93 ^b	-3.86 ^d	-3.91 ^d
Protoadamantane → Adamantane	(-11.0 ^f > 7.5 ^g solution)	-11.22 ^b	-11.19 ^d	-11.27 ^d

^a Ref. 3b. This review summarizes the available data.

^b Ref. 5a.

^c W. Parker, W. Steele and I. Watt, private communication. Ref. 5o.

^d Refs. 18 and 19.

^e These values would be 0.3–0.5 kcal mole⁻¹ larger in magnitude if theoretical instead of experimental entropies are assumed (see E. M. Engler, K. R. Blanchard, and P. v. R. Schleyer, *J. Chem. Soc., Chem. Commun.*, 1210 (1972)).

^f Indirectly estimated ΔG_{isom} from experimental data on derivatives in solution (D. Lenoir, D. J. Raber, and P. v. R. Schleyer, *J. Am. Chem. Soc.*, 96, 2149 (1974)).

^g Lower limit (ΔG) from equilibration of acetates in solution (H. J. Storesund and M. C. Whiting, *J. Chem. Soc., Perkin II*, 1452 (1975)).

calculated by the force fields is found in general to be in closer agreement with the direct isomerization data. Relative energies should be more reliably calculated than absolute enthalpies, since defects in the method tend to cancel especially for related compounds.

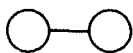
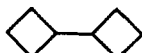
C. Method of Prediction of Stabilomers

A method for the selection of the most stable C_nH_m saturated polycyclic hydrocarbon was developed initially to assist in the prediction and the identification of the products obtained from aluminum halide isomerizations.

This method of prediction of the saturated stabilomer involves: (1) generating all possible structures; (2) elimination of isomers expected qualitatively to be unstable on the basis of structural considerations; (3) quantification of the relative stability of the remaining candidates by computer calculation of the heat of formation, ΔH_f° .

1. Generation of all Possible Isomers

For simple systems all structural possibilities can be generated manually, but for the larger systems computer methods are required, to assure completeness without redundancies. A computer program (CISGEN, constitutional isomer generator) has been developed which lists all saturated ring assemblies of a given empirical formula, and indicates the ring sizes contained in each isomer, the number of unique carbon atoms as determined by graph theoretical symmetry considerations, the number of carbon atoms of a given degree of substitution (quaternary, tertiary, etc.) and the von Baeyer (IUPAC) name (22a). The algorithm used generates constitutional cyclic saturated hydrocarbon isomers in which every bond is contained in at least one ring; that is, systems having two isolated ring assemblies are excluded (22d). In the present paper, systems such as **A** generally are more highly strained because such structures require the rings to be smaller; for example, compare **B** with **C**. Also excluded by the isomer generator were structures containing multiple bonds and/or alkyl appendages.

**A****B****C**

Details of the CISGEN algorithm are presented elsewhere (22a), but the key concept is that every cyclic isomer has a preferred systematic name (von Baeyer or spiro). Thus starting with the isomer of a given empirical formula having the "first" IUPAC name and then incrementing that name sequentially, the names of all possible isomers are generated. The "first" name has all atoms partitioned as evenly as possible into the first two bridges, other bridges contain no atoms, and superscripts are as low as possible. For example, for tricyclodecanes the first name is tricyclo[4.4.0.0^{1.3}]decane. Because of symmetry, different names may correspond to the same molecule, for example, tricyclo[4.4.0.0^{1.4}]decane and tricyclo[4.4.0.0^{1.9}]decane. These redundancies are easily recognized using the SEMA algorithm (22b) and only the first (preferred) name is retained. This results in a complete nonredundant list of isomers represented by their correct IUPAC names from which the structure can be drawn.

Structural characteristics of each isomer, such as the number of quaternary carbons or the presence or absence of three- or four-membered rings (22c), are derived by the program and used to sort the isomers. Based on the equivalence classes given by SEMA, the maximum number of ¹³C resonances are also listed for each isomer. This facilitates experimental structure determination.

Other similar programs have since become available (23) and have verified the correctness of CISGEN. The JAL-30XA program (24), which includes structures of type **A** in its generator, was also used to compute the total number of isomers. Tables 4 and 5 give the total number of possible ring structures with

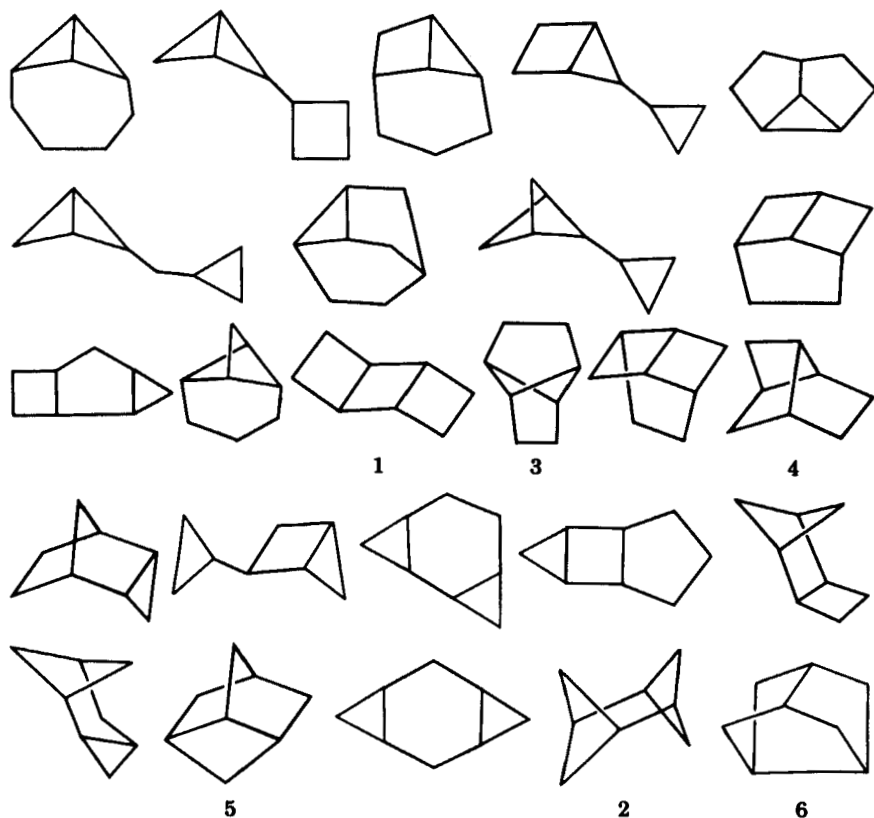
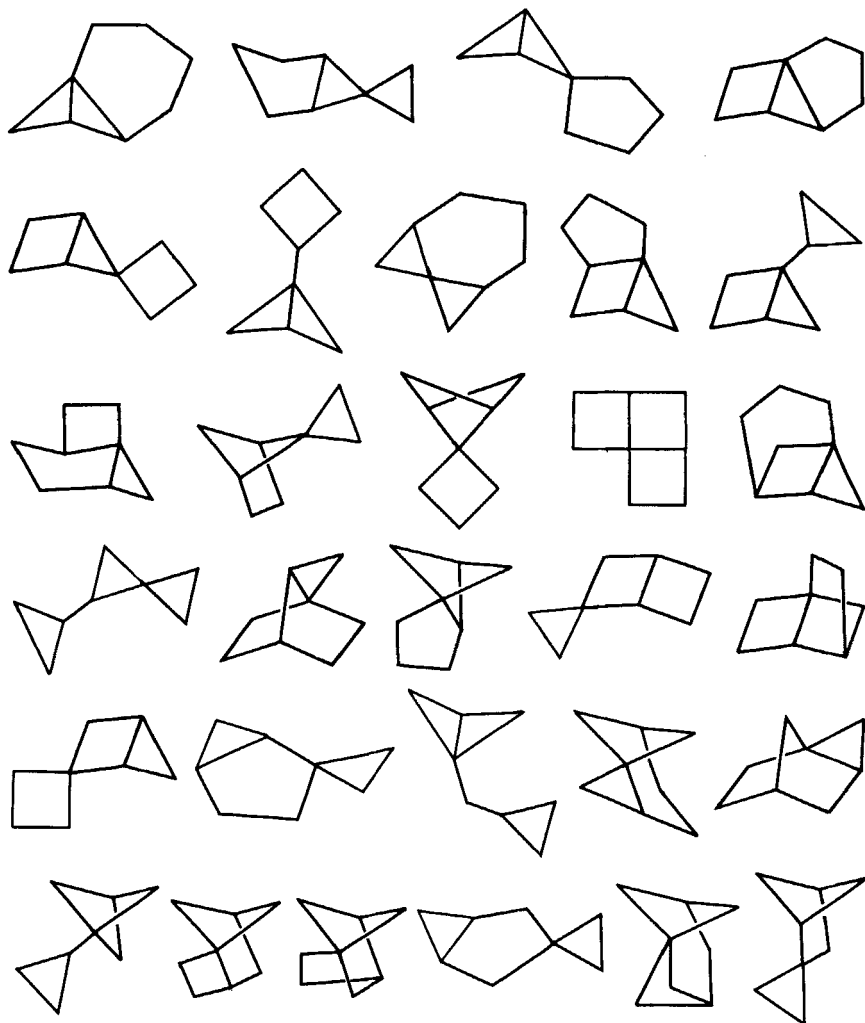


Figure 1 All possible C_8H_{12} (C_8R_3) structures including those of type A. (1) No quaternary carbon atom: 25.

and without those of type A for some representative systems. Figure 1 illustrates all possible ring structures of C_8H_{12} including type A. When type A structures are excluded, CISGEN and JAL30XA agree exactly, at least in the cases we have examined in detail.

The number of isomers increase rapidly with alkyl substitution; for example, substitution of one methyl group onto each of the 248 tricyclodecanes gives 2,889 tricyclic C_{11} 's in addition to the 434 nonalkylated tricyclodecanes (Tables 4 and 5). For the larger systems, prior experience and application of basic rules of thermodynamic stability (*vide infra*) must be relied on to generate a manageable list of likely structures.

Since CISGEN (22) as well as the other programs (23,24) only generate constitutional isomers, stereochemistry was analyzed manually. The lowest energy stereoisomers of each constitution were considered in searching for the stabilomer.



7

Figure 1 (cont.) (2) One quaternary carbon atom: 30.

2. Elimination of Isomers Based on Application of Basic Thermodynamic Principles of Stability

The relative stability ($\Delta\Delta G^\circ$) of hydrocarbon isomers is largely dominated by the enthalpy (ΔH) term (*vide supra*).

The thermodynamic stability rules are based therefore on qualitatively estimating relative ΔH_f values for isomers. Estimates are based on group increment (25) calculation of ΔH_f° and prior experience of knowing stable ring

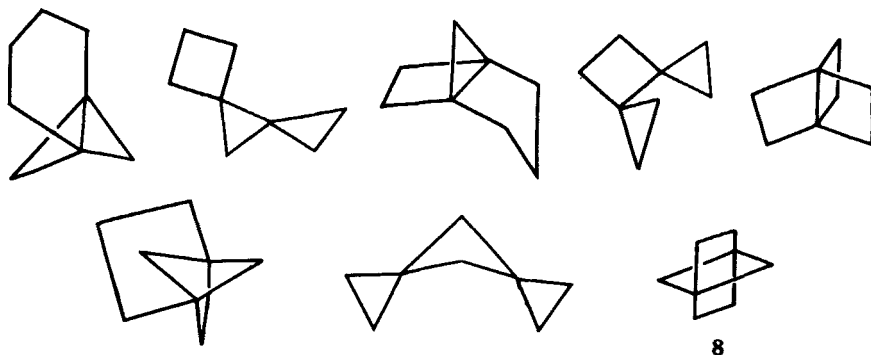


Figure 1 (cont.) (3) Two quaternary carbon atoms: 8.

structures (e.g., adamantane). Isomers containing highly strained units can be eliminated. These rules are illustrated in detail for the mono- and bicyclic isomers (*vide infra*).

3. Quantification of Relative Stabilities

The heats of formation of the remaining isomers are calculated using both Engler (18) and Allinger (19) 1971 force fields. Possible contributions of entropy (if $\Delta\Delta H_f^\circ$ is small) are included and the stabilomer is that isomer having the lowest free energy of formation.

A large body of experimental data (5,21) indicates that relative values of ΔH_f° of molecules (cf. Table 3) calculated by empirical force field methods are

TABLE 4
Calculated Number of Possible Constitutional Isomers for C_mH_n Polycyclic Hydrocarbons^a

C_mH_n $n =$	Number of possible isomers ^{a,b}				
	Tricyclic		Tetracyclic	Pentacyclic	Hexa- cyclic
8	63	(53)	162 (151)	250 (245)	
9	129	(97)	506 (447)	1144 (1091)	1613
10	248	(170)	1380 (1135)	4502	9246
11	434 ^c	(270)	3393 (2602)	15358	45175
12	728	(418)	7665 (5473)	46636	
13	1157	(614)	16057		
14	1775	(881)	31675		
15	2623	(1220)			

^a Includes only those isomers having no alkyl substituents, methyl, ethyl, etc.

^b The values without parentheses include type A structures, as given by the program JAL-30XA, Ref. 24. The values within parentheses exclude type A structures, as given by the program CISGEN, Ref. 22.

^c There are 2889 methyltricyclodecanes.

TABLE 5
 Number of Possible Constitutional Isomers for C_nH_m Polycyclic Hydrocarbons as Classified by
 the Number of Quaternary Carbon Atoms^a

Number of carbons		Number of rings			
Total	Quaternary	3	4	5	6
8	0	25	29	5	
	1	30	66	29	
	2	8	68	117	
	3		9	86	
	4			13	
9	0	52	63	19	
	1	64	227	193	27
	2	13	192	545	279
	3		24	351	765
	4			36	492
	5				50
10	0	109	198	113	19
	1	118	643	915	281
	2	21	492	2,187	2,198
	3		47	1,183	4,344
	4			104	2,243
	5				161
11	0	197 (704) ^b	536	482	115
	1	207 (1,622)	1,659	3,700	2,242
	2	30 (563)	1,103	7,380	12,529
	3		95	3,546	20,221
	4			250	8,558
	5				510
12	0	351	1,373	1,892	
	1	334	3,826	12,682	
	2	43	2,297	22,119	
	3		169	9,367	
	4			576	
13	0	581	3,159		
	1	519	8,202		
	2	57	4,405		
	3		291		
14	0	931	6,879		
	1	767	16,327		
	2	77	8,004		
	3		465		
15	0	1,423			
	1	1,103			
		97			

^a See footnotes a,b of Table 4 for details.

^b The number of structures having *one methyl* group.

TABLE 6

Compound	Strain energy ^a (kcal mole ⁻¹)
CH ₂ =CH ₂	22.36
Cyclopropane	28.13
Cyclobutane	26.90
Cyclopentane	7.19
Cyclohexane	1.35
Cycloheptane	7.57

^a Ref. 25*d*.

generally accurate to within ± 2 kcal mole⁻¹. In agreement with this, any isomer predicted to have ΔH_f° within ± 2 kcal mole⁻¹ of the isomer of lowest ΔH_f° is considered a second stabilomer possibility.

This selection process is based on simple thermodynamic principles, prior experience, and empirical force field calculations (18,19,19*a*). The methodology has evolved to include consideration of unsaturated and aromatic systems and we suggest its use not only in conjunction with but also in place of experimental determinations. The stabilomers for tricyclic, tetracyclic and pentacyclic C₈-C₂₀'s are predicted for cases where no experimental information is yet available. This computational method also allows the quantitative estimation of $\Delta\Delta H_f^\circ$ regardless of its magnitude. Finally, saturated, unsaturated and aromatic hydrocarbons can all be compared.

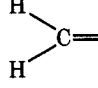
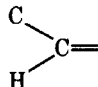
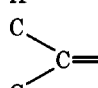
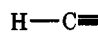
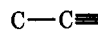
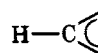
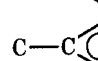
D. C_nH_{2n} and C_nH_{2n-2} Families

These simple systems illustrate the basic principles involved in determining the relative stabilities of singlet neutral hydrocarbons. By examining the application of these principles, patterns of stability emerge which aid in the prediction of the stabilomer in more complicated systems.

Tables 6 and 7 illustrate these principles. The "strain energies" (26) associated with double bonds (22 kcal mole⁻¹), and with three- and four-membered rings (28 and 27 kcal mole⁻¹, respectively) indicate that olefins will be less strained as compared with three or four-membered ring isomers. The origin of the strain of ethylene can be seen if it is considered as a "two-membered ring" and its heat of formation compared to ΔH_f° of a hypothetical strain free (CH₂)₂ (calculated from saturated group increments (25)). The strain associated with double bonds (22 kcal mole⁻¹) does not allow them to compete favorably with the strain energy of five (7 kcal mole⁻¹) or six (1.3 kcal mole⁻¹) membered rings, and the latter are preferred as "units of unsaturation." In general, six-membered rings will predominate when possible because of their low strain energy.

Group increments can be used to illustrate that branching or alkyl substitution of a framework is also favorable:

TABLE 7

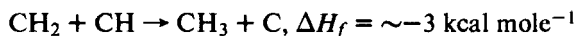
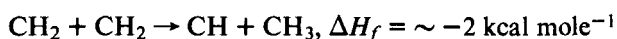
Group	ΔH_f Increment (kcal mole ⁻¹)			
	Cox and Pilcher ^a	Benson ^d	Schleyer ^b	Schleyer strain free ^c
CH ₃	-10.12		-10.12	-10.05
CH ₂	-4.92		-4.93	-5.13
CH	-1.75		-2.11	-2.16
C	-0.06		-0.23	-0.30
		6.26		
		8.59		
		10.34		
		26.93		
		27.55		
		3.30		
		5.51		

^a Ref. 25b.

^b Ref. 25d.

^c Ref. 25d, "strain free increments."

^d Ref. 25a.



that is, if no considerable additional strain is introduced, branching lowers the enthalpy of formation. This principle is limited by the fact that extensive branching invariably introduces skew interactions or ring strain and will become unfavorable when the strain energy of these interactions exceeds the 1–3 kcal mole⁻¹ lowering of the branching.

The application of these principles to the C_nH_{2n} 's is shown in Table 8. Ethylene is the C_2H_4 stabilomer and has a strain energy of 22 kcal mole⁻¹. The C_3 stabilomer of this family, propene, is more stable than its saturated isomer cyclopropane, by 7.85 kcal mole⁻¹ in accord with the thermodynamic rules of stability. 2-Methylpropene is the most stable C_4H_8 (~ 10 kcal mole⁻¹ more stable

TABLE 8
 C_nH_{2n} Stabilomers^a

Formula	Stabilomer	ΔH_f°	Saturated isomers	ΔH_f°	Unsaturated isomers	ΔH_f°
C_2H_4	ethylene	+12.45 ^b				
C_3H_6	propene	+4.88 ^b	cyclopropane	+12.73 ^b		
C_4H_8	2-methylpropene	-4.26 ^b	cyclobutane	+5.78 ^c	1-butene	-0.2 ^b
					+5.52 ^d	<i>cis</i> -2-butene
C_5H_{10}	cyclopentane	-18.37 ^c -18.09 ^d -18.44 ^b	methylcyclobutane	-1.88 ^c -1.17 ^d	<i>trans</i> -2-butene	-2.99 ^b
					2-methyl-2-butene	-10.12 ^b
C_6H_{12}	cyclohexane	-29.35 ^c -29.93 ^d -29.50 ^b	methylcyclopentane	-26.20 ^c -25.20 ^d -25.27 ^b	2,3-dimethyl-2-butene	-16.42 ^b
C_7H_{14}	methylcyclohexane	-36.99 ^c -37.06 ^d -36.98 ^b	cycloheptane	-28.26 ^c -28.50 ^d -28.21 ^b		
C_8H_{16}	<i>trans</i> -1,4-dimethylcyclohexane	-44.65 ^c -44.21 ^d -44.10 ^b -44.13 ^b	ethylcyclohexane	-41.22 ^c -41.60 ^d -41.03 ^b -29.73 ^b		
C_9H_{18}	<i>cis</i> -1,3,5-trimethylcyclohexane	-50.69 ^b	cyclooctane	-29.16 ^c -27.40 ^d		

^a All values gas phase, 25°, in kcal mole⁻¹.

^b Ref. 25b.

^c Ref. 18.

^d Ref. 19.

than cyclobutane) and again illustrates the superiority of a double bond as a unit of unsaturation relative to a three- or four-membered ring. Cyclopentane, C_5H_{10} , however, has only 7 kcal mole⁻¹ of ring strain and is more stable than any olefinic isomer. In fact, it is clear that olefins need not be considered for any higher monocyclic stabilomers. The C_6H_{12} stabilomer is cyclohexane; despite more favorable entropy and branching methylcyclopentane has too much ring strain. The C_7H_{14} , C_8H_{16} , and C_9H_{18} stabilomers are all methyl-substituted cyclohexanes. Methyl, dimethyl, and trimethyl cyclohexanes are more highly branched and have less ring strain than the cycloalkanes, $(CH_2)_n$, with $n = 7, 8, 9$. In addition, this demonstrates that polymethyl substitution is generally favored over ethyl, isopropyl, etc. substitution. Isomerization energies of dimethylcyclohexanes have been confirmed experimentally (27).

The C_nH_{2n-2} systems also follow these patterns (Table 9). Acetylene is

TABLE 9
C_nH_{2n-2} Stabilomers^a

Formula	Stabilomer	ΔH_f°	Saturated isomers	ΔH_f°	Unsaturated isomers	ΔH_f°	
C ₂ H ₂	acetylene	54.34 ^b					
C ₃ H ₄	propyne	44.39 ^b			allene	45.63 ^b	
C ₄ H ₆	1,3-butadiene	26.11 ^b	bicyclo[1.1.0]-butane	+51.90 ^b	cyclopropene	66.2 ^b	
					1,2-butadiene	38.78 ^b	
					cyclobutene	37.45 ^b	
					methylene-cyclopropene	47.92 ^b	
					1-methyl-cycloprop-1-ene	58.21 ^b	
					2-butyne	34.71 ^b	
C ₅ H ₈	cyclopentene	8.23 ^b	bicyclo[1.1.1]-pentane	50.74 ^c	2-methyl-1,3-butadiene	18.06	
			spiropentane	73.36 ^d			
			bicyclopropyl	44.25 ^b			
C ₆ H ₁₀	cyclohexene	-1.08 ^b	bicyclo[2.1.1]-hexane	30.9 ^b	1-methyl-cyclopentene	-0.6 ^b	
					bicyclo[3.1.0]-hexane		
					bicyclo[2.2.0]-hexane		
					bicyclo[3.1.1]-heptane		
C ₇ H ₁₂	norbornane	-12.99 ^c	bicyclo[3.1.1]-heptane	5.88 ^c	1-methyl-cyclohexene	-10.34 ^b	
				5.24 ^d			
C ₈ H ₁₄ ^e	bicyclo[3.2.1]-octane	-23.04 ^c	1-methyl-norbornane	-22.55 ^c	1,2-dimethyl-cyclohexene	-18.6 ^f	
	bicyclo[2.2.2]octane	-24.17 ^d		-22.78 ^d		-16.4 ^g	
		-22.45 ^c	bicyclo[4.2.0]-octane		-6.39 ^b		
		-24.22 ^d			-4.39 ^c		
	<i>cis</i> -bicyclo[3.3.0]octane	-22.61 ^c		-3.47 ^d			
C ₉ H ₁₆	1,4-dimethyl-norbornane	-32.12 ^c	<i>trans</i> -hexahydroindane	-31.42 ^b			
		-32.11 ^d		-31.47 ^c			
		-30.63 ^h	<i>cis</i> -hexahydroindane	-31.20 ^d			
				-30.38 ^b			
				-30.37 ^c			
				-29.61 ^d			
			bicyclo[3.3.1]-nonane	-30.64 ^c			
			1-methyl <i>cis</i> -bicyclo[3.3.0]-octane	-30.41 ^d			
				-30.78 ^c			
C ₁₀ H ₁₈	<i>trans</i> -decalin	-43.42 ^c	<i>cis</i> -decalin	-40.71 ^c			
		-43.78 ^d		-41.20 ^d			
		-43.50 ^b		-40.43 ^b			

TABLE 9
C_nH_{2n-2} Stabilomers^a

Formula	Stabilomer	ΔH_f°	Saturated isomers	ΔH_f°	Unsaturated isomers	ΔH_f°
			bicyclo[5.3.0]- decane	-31.37 ^b		
C ₁₁ H ₂₀	2-methyl- <i>trans</i> - decalin	-51.10 ^c -50.93 ^d				
C ₁₂ H ₂₂	2,6-dimethyl- <i>trans</i> -decalin	-58.85 ^c -58.11 ^d				

^a ΔH_f° gas phase, 25°, in kcal mole⁻¹^b Ref. 25b.^c Ref. 18.^d Ref. 19.^e Stabilomer controlled by ΔS , see text.^f ΔH_f° calculated from group increments (Ref. 25b) and ΔH_f° for 1-methylcyclohexane.^g Estimated in *J. Chem. Phys.*, 56, 106 (1972).^h M. P. Kozina, L. P. Timofeeva, S. M. Skuratov, N. A. Belikova, E. M. Milvitskaya, and A. F. Platé, *J. Chem. Thermodynamics*, 3, 563 (1971).

the C₂H₂ stabilomer and is calculated to have 57 kcal mole⁻¹ of strain energy from saturated group increments (25) (relative to a hypothetical strain free (CH)₂). The two units of unsaturation of C₃H₄ can be a triple bond (propyne, ΔH_f° 44.39 kcal mole (25b)), two double bonds (allene, ΔH_f° 45.63 (25b) or a three-membered ring and a double bond (cyclopropene, ΔH_f° 66.2 kcal mole⁻¹ (25b)) with allene and propyne about equally strained. The C₄H₆ stabilomer, 1,3-butadiene, is lower in energy than 2-butyne by 8.6 kcal mole⁻¹, cyclobutene by ~11 kcal mole⁻¹, and bicyclo[1.1.0]butane by ~25 kcal mole⁻¹. For C₅H₈ the two lowest energy units of unsaturation possible are cyclopentane and an olefin, and cyclopentene is the stabilomer (Table 9 has other candidates). The C₆H₁₀ stabilomer is cyclohexene which is ~0.4 kcal mole⁻¹ more stable than 1-methylcyclopentene and substantially more stable than any diene or saturated system. At C₇H₁₂ a saturated system not containing three- or four-membered rings can be constructed and norbornane is more stable than any cycloalkene. There are several saturated candidates of similar ΔH_f° for the C₈H₁₄ and C₉H₁₆ stabilomers but at C₁₀H₁₈ two fused six-membered rings are possible and *trans*-decalin is clearly the stabilomer. The C₁₁H₂₀ and C₁₂H₂₂ stabilomers are methyl *trans*-decalins (Table 9). The established pattern is: olefin → saturated → six-membered ring system → methyl-substituted six-membered ring system, in proceeding down a family.

E. C_nH_{2n-4}'s

The C₃H₆-C₈H₁₂ stabilomers are: C₅, cyclopentadiene, ΔH_f° 31.94 kcal mole⁻¹ (25b); C₆, 1,3-cyclohexadiene, ΔH_f° 25.38 kcal mole⁻¹ (25b) C₇, nor-

TABLE 10
Quantification of Relative Stabilities for C₈H₁₂ Stabilomer Candidates by Empirical Force Field Calculations (kcal mole⁻¹, 25°, gas)

C ₈ H ₁₂	ΔH_f°		Strain energy	
	E ^a	A ^b	E ^a	A ^b
1 ^c anti	45.39	48.97	74.55	78.35
syn	50.29	53.16	79.45	82.54
2	63.91	65.26	93.07	94.64
3	18.14	24.66	47.30	54.04
4 ^c	19.13	23.11	48.29	52.49
5 ^c	12.30	13.05	41.45	42.43
6 ^c	17.99	16.17	47.15	45.55

^a Engler force field, Ref. 18.

^b Allinger force field, Ref. 19.

^c Taken from Ref. 18.

bornene, ΔH_f° 15.12 kcal mole⁻¹ (28), or 1-methyl-1,3-cyclohexadiene, ΔH_f° 16.4 kcal mole⁻¹ (29) or nortricyclene, ΔH_f° 14.82 kcal mole⁻¹ (28) (within \pm 1 kcal mole⁻¹ co-stabilomers); C₈, bicyclo[2.2.2]oct-2-ene, ΔH_f° 4.88 kcal mole⁻¹ (30) or bicyclo[3.2.1]oct-2-ene, ΔH_f° 3.79 (31). The three-stage method of determining the saturated stabilomer is illustrated here for the C₈H₁₂ family. Of the 63 possible ring structures given in Fig. 1, those having a three-membered ring and/or more than two four-membered rings can be eliminated since they are highly strained as exemplified by **1** and **2** in Table 10. This leaves six structures **3** to **8**, of which **7** and **8** have four substituents on the same side of a carbon atom and are rejected. The remaining candidates are subjected to empirical force field calculations (Table 10). Tricyclo[3.2.1.0^{3,6}]octane (**5**, 2,6-methanonorbornane) is predicted to be the stabilomer. The prediction is supported by the rearrangement of 2-tricyclo[3.3.0.0^{3,7}]octyl esters (having the skeleton of 2,5-methanonorbornane or bisnoradamantane **6**), to the 2,6-methanonorbornane skeleton under solvolytic conditions (32). Aluminum halide rearrangement without disproportionation is often not possible with compounds containing four-membered rings and has not been attempted with the parent hydrocarbon **5**. The C₈H₁₂ adamantane relative, bisnoradamantane (**6**), with ΔH_f° calculated 17.99 kcal mole⁻¹ (Engler force field designated (E)) (18) and 16.17 kcal mole⁻¹ (Allinger 1971 force field (19) designated (A)), is predicted to be 3–5 kcal mole⁻¹ less stable than **5**.

The remaining C₉H₁₄–C₂₀H₃₆ stabilomers are dominated by the adamantane skeleton. Table 11 gives all C_{*n*}H_{2*n*-4}, C_{*n*}H_{2*n*-6}, and C_{*n*}H_{2*n*-8} (*n* = 8–20) stabilomers. Examination of the C_{*n*}H_{2*n*-4}'s shows once again the pattern of a variety of ring structures (C₈, C₉) prior to attaining the fused six-membered ring system (C₁₀), adamantane, followed by alkyl substitution of that skeleton.

Additional empirical rules of stability can be established by examining alkyl substitution of adamantanes computationally (Tables 12, 13). All alkyl groups are allowed to assume their minimum energy conformation; this is done in all cases in this paper. A comparison of Tables 12 and 13 for alkyl adamantanes $R = \text{Me, Et, } i\text{-Pr, } t\text{-Bu}$ shows the preference of adamantanes for substitution at the bridgehead (1-position). The energy advantage of bridgehead CH versus methylene CH_2 substitution by methyl (ignoring skew interactions) can be predicted (group increments) to be $\sim 3 \text{ kcal mole}^{-1}$.

1-Methyladamantane is less strained than adamantane (33). In contrast, ethyl, 2-propyl, and 1-propyl adamantane all have more strain energy than adamantane, indicating that polymethyl substituted adamantanes will generally be favored. In agreement, 1-ethyladamantane isomerizes to 1,3-dimethyladamantane (34), 1-ethyl-3-methyladamantane isomerizes to 1,3,5-trimethyladamantane (34), and 1-ethyl-3,5-dimethyladamantane isomerizes to 1,3,5,7-tetramethyladamantane (34) on treatment with aluminum bromide.

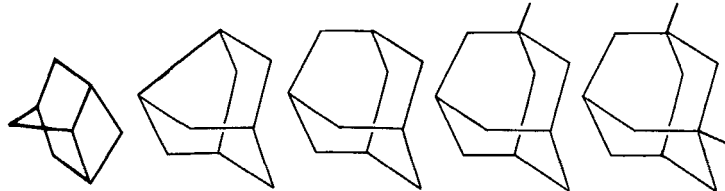

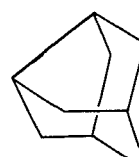
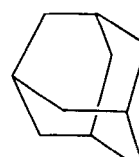
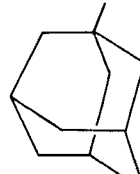
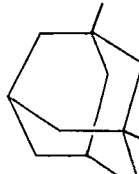
Table 12 also indicates the manner in which propyl, butyl, and pentyl carbon units prefer to be added to the bridgehead of adamantane. Although the isopropyl unit is more highly branched than the n -propyl unit, 1-(2-propyl)-adamantane possesses four skew interactions whereas the 1-(1-propyl)-adamantane derivative has a minimum energy conformation with only two skews, and is calculated to have a small energy advantage. A similar advantage is held for 1-propyl (ΔH_f° , $-49.20 \text{ kcal mole}^{-1}$ (25b)) over 2-propyl (ΔH_f° , $-48.87 \text{ kcal mole}^{-1}$ (25b)) when t -butyl is substituted for 1-adamantyl; that is, 2,2-dimethylpentane is more stable than 2,2,3-trimethylbutane.

A butyl unit can be added as n -butyl, isobutyl, *sec*-butyl, or t -butyl. *sec*-Butyl has the same skew problems as isopropyl, and is expected to be less stable than n -butyl. t -Butyl, although highly branched, has six skew interactions in its lowest energy conformation and is calculated to be higher in energy than n -butyl. A comparison of n -butyl and isobutyl indicates both have two 1-4 skew interactions. Isobutyl also has unfavorable 1-5 interactions with the adamantane skeleton and despite its higher degree of branching, 1-(2-butyl)-adamantane is calculated to be less favorable than 1-(1-butyl)-adamantane (cf. 2,2-dimethylhexane, $-53.68 \text{ kcal mole}^{-1}$ (25b) vs. 2,2,4-trimethylpentane, $-53.54 \text{ kcal mole}^{-1}$ (25b)).

Similar considerations for the pentyl, hexyl, and heptyl carbon units indicate that isopentyl, neohexyl, and neoheptyl are the optimal alkyl groups when substituted at the adamantane bridgehead.

Table 14 gives the energy difference of substituents at the 1- versus 2-positions of adamantane. Along the series Me, Et, i -Pr the energy difference between bridgehead and secondary substitution decreases. 1-Substituted Me, Et, i -Pr have 0,2,4 skew interactions, respectively, while the 2-substituted analogs all have 2 skews. As a result, the inherent advantage of 1- over 2-substitution

TABLE II
 C_nH_{2n-4} , C_nH_{2n-6} , and C_nH_{2n-8} Stabilomers ($n = 8-20$)

No. Carbons	Saturated stabilomer		ΔH_f° (kcal mole ⁻¹)		ΔH_f° Unsaturated stabilomer
			Engler ^a	Allinger ^b	
C_8H_{12}	tricyclo[3.2.1]octane (2,6-methanonorborene) ^c		12.30	13.05	bicyclo[3.2.1]-2-octene, 3.79 ^k
C_9H_{14}	noradamantane ^d		-14.22	-15.49	
$C_{10}H_{16}$	adamantane ^d		-32.55	-33.82	
$C_{11}H_{18}$	1-methyladamantane ^d		-41.92	-42.89	
$C_{12}H_{20}$	1,3-dimethyladamantane ^d		-51.33	-51.91	

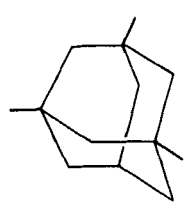
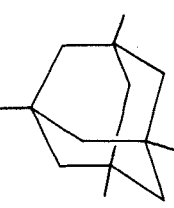
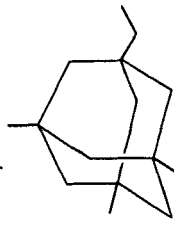
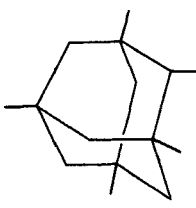
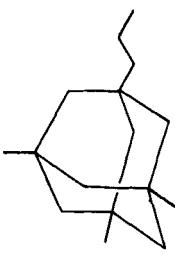
C ₁₃ H ₂₂	1,3,5-trimethyladamantane ^d		-60.78	-61.01
C ₁₄ H ₂₄	1,3,5,7-tetramethyladamantane ^d		-70.26	-70.14
83 C ₁₅ H ₂₆	1-ethyl-3,5,7-trimethyladamantane ^d		-73.41	-73.79
	1,2,3,5,7-pentamethyladamantane		-72.52	-73.07
C ₁₆ H ₂₈	1-(1-propyl)-3,5,7-trimethyladamantane		-78.78	-79.15

TABLE 11
 C_nH_{2n-4} , C_nH_{2n-6} , and C_nH_{2n-8} Stabilomers ($n = 8-20$)

No. Carbons	Saturated stabilomer	ΔH_f° (kcal mole ⁻¹)		ΔH_f° Unsaturated stabilomer
		Engler ^a	Allinger ^b	
C ₁₇ H ₃₀	1-(2-propyl)-3,5,7-trimethyladamantane	-77.62	-78.52	
	1-(1-butyl)-3,5,7-trimethyladamantane	-84.15	-84.60	
	1-(1-2-methylpropyl)-3,5,7-trimethyladamantane	-83.67	-84.11	
C ₁₈ H ₃₂	1-(4-2-methylbutyl)-3,5,7-trimethyladamantane	-90.34	-90.66	

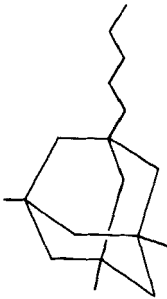
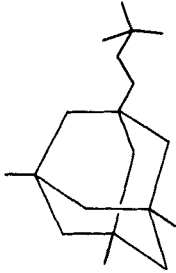
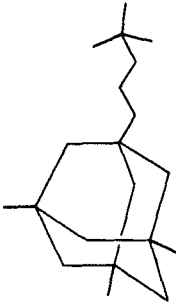
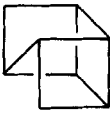
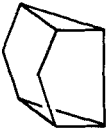
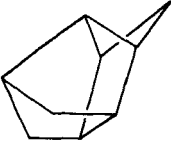
		-89.48	
		-98.11	-98.62
		-103.50	-104.11
		71.24	82.99
		48.12 ⁱ	
		31.66	39.17
			1,3,5-trimethylbenzene, -3.81
$C_{19}H_{34}$	1-(1-pentyl)-3,5,7-trimethyladamantane		
$C_{19}H_{34}$	1-(4,2,2-dimethylbutyl)-3,5,7-trimethyladamantane		
$C_{20}H_{36}$	1-(5,2,2-dimethylpentyl)-3,5,7-trimethyladamantane		
C_8H_{10}	tetraacyclo[3.3.0.0 ^{3,8} .0 ^{4,7}]octane		<i>p</i> -xylene, 4.06 ^e <i>m</i> -xylene, 4.06 ^e
C_9H_{12}	tetraacyclo[4.2.1.0 ^{2,5} .0 ^{3,7}]nonane		

TABLE 11
 C_nH_{2n-4} , C_nH_{2n-6} , and C_nH_{2n-8} Stabilomers ($n = 8-20$)

No. Carbons	Saturated stabilomer	ΔH_f° (kcal mole ⁻¹)		ΔH_f° Unsaturated stabilomer
		Engler ^a	Allinger ^b	
$C_{10}H_{14}$	tetracyclo-[5.3.1.0 ^{2,6} .0 ^{4,8}]decane	8.29	7.04	1,2,3,5-tetramethylbenzene, -10.54 ^c 1,2,4,5-tetramethylbenzene, -10.53 ^c
$C_{11}H_{16}$	2,4-ethanonoradamantane	-13.71	-13.16	pentamethylbenzene, 17.27 ^c
$C_{12}H_{18}$	2,4-ethanoadamantane	-25.52	-27.19	hexamethylbenzene, -24.00 ^c
$C_{13}H_{20}$	8-methyl-2,4-ethanoadamantane	-34.94	-36.25	ethyl, pentamethylbenzene, -26.7 ^f
	1-methyl-2,4-ethanoadamantane	-34.21	-35.51	

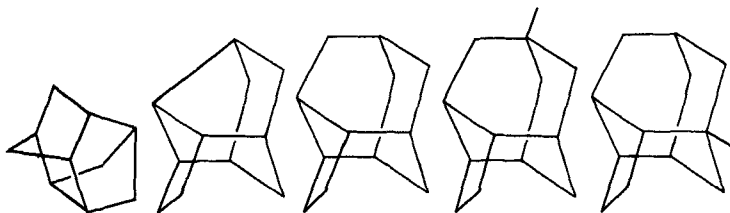
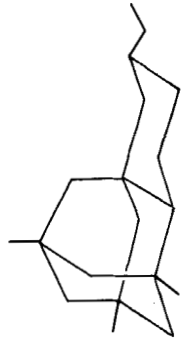
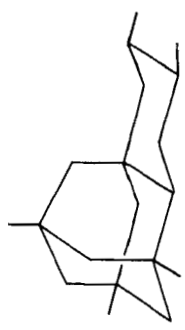
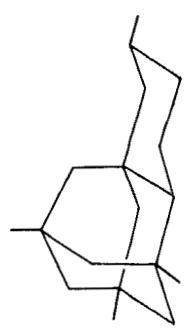
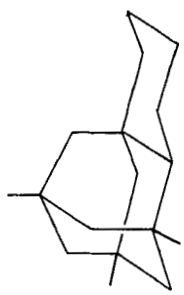


TABLE 11
 C_nH_{2n-4} , C_nH_{2n-6} , and C_nH_{2n-8} Stabilomers ($n = 8-20$)

No. Carbons	Saturated stabilomer	ΔH_f° (kcal mole ⁻¹)		ΔH_f° Unsaturated stabilomer
		Engler ^a	Allinger ^b	
$C_{17}H_{28}$	1,9,11-trimethyltetracyclo- [7.3.1.1 ^{3,11} .0 ^{3,8}]tetradecane	-72.44	-72.82	
$C_{18}H_{30}$	1,5,9,11-tetramethyltetracyclo- [7.3.1.1 ^{3,11} .0 ^{3,8}]tetradecane	-80.18	-80.01	
$C_{19}H_{32}$	<i>trans</i> -5,6-dimethyl-1,9,11-trimethyltetracyclo[7.3.1.1 ^{3,11} .0 ^{3,8}]tetradecane	-86.57	-86.37	
	5-ethyl-1,9,11-trimethyltetracyclo- [7.3.1.1 ^{3,11} .0 ^{3,8}]tetradecane	-84.50	-84.64	



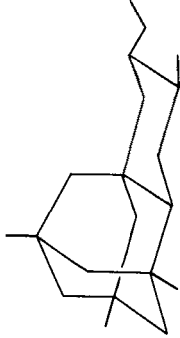
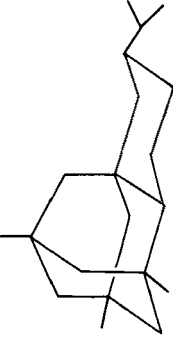
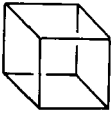
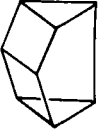
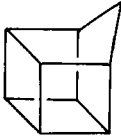
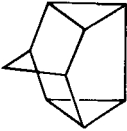
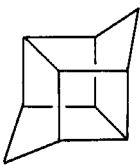
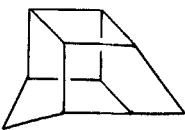
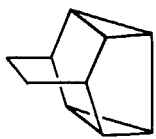
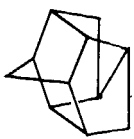
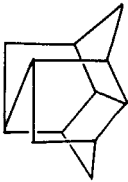
$C_{20}H_{34}$	<i>trans</i> -5-ethyl-6-methyl-1,9,11-trimethyltetraacyclo[7.3.1.1 ^{3,11} .0 ^{3,8}]-tetradecane		-90.41	-90.72
	5-(2-propyl)-1,9,11-trimethyltetraacyclo[7.3.1.1 ^{3,11} .0 ^{3,8}]-tetradecane		-89.73	-90.01
C_8H_8	cubane		148.54	
	cuneane ^g (pentacyclo[3.3.0.0 ^{2,4} .0 ^{3,7} .0 ^{6,8}] octane)		159.30 ^h 90.4 ⁱ	benzocyclobutene, + 50.6 ^f
C_9H_{10}	homocubane		95.72	hydrindene, 14.8 ^e
	pentacyclo[4.3.0.0 ^{2,4} .0 ^{3,8} .0 ^{5,7}]- nonane ^g		115.7 ^h 56.7 ⁱ	

TABLE 11
 C_nH_{2n-4} , C_nH_{2n-6} , and C_nH_{2n-8} Stabilomers ($n = 8-20$)

No. Carbons	Saturated stabilomer	ΔH_f° (kcal mole ⁻¹)		ΔH_f° Unsaturated stabilomer	
		Engler ^a	Allinger ^b		
$C_{10}H_{12}$	1,4-bishomocubane		49.86	55.03	tetralin, 6.6 ^c
			48.34	52.19	
$C_{11}H_{14}$	1,3-bishomocubane		45.31 ^d		
$C_{11}H_{14}$	pentacyclo[4,4,0,0 ²⁻⁴ ,0 ^{3,8} ,0 ^{5,7}]-decane		3.38	11.32	6-methyltetralin, -1.3 ^e
$C_{12}H_{16}$	(D ₃)trishomocubane ^d		-5.32	-4.82	5,7-dimethyltetralin, -8.6 ^f
$C_{12}H_{16}$	pentacyclo[6,4,0,0 ²⁻⁶ ,0 ^{3,11} ,0 ^{4,9}]-dodecane				

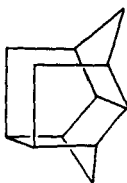
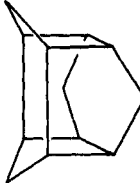
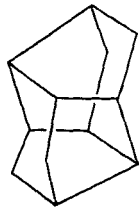
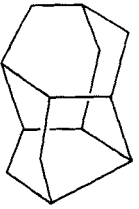
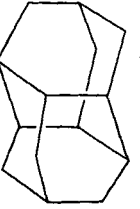

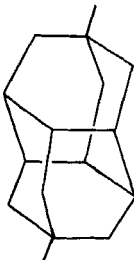
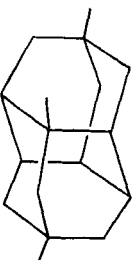
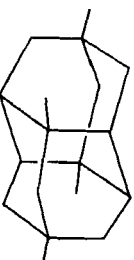
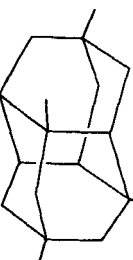
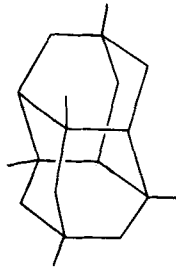

pentacyclo[5.4.1.0 ^{2,6} .0 ^{3,10} .0 ^{4,8}]- dodecane		-5.80	-1.76
pentacyclo[7.3.0.0 ^{3,7} .0 ^{4,12} .0 ^{6,10}]- dodecane		-0.57	
pentacyclo[6.3.1.0 ^{2,7} .0 ^{3,10} .0 ^{5,9}]- dodecane		3.54	3.55
C ₁₃ H ₁₈ (nordiamantane)		-18.52	5,7,8-trimethyltetralin, ^j -15.5
C ₁₄ H ₂₀ (diamantane) ^d		-37.37	-38.13 5,6,7,8-tetramethyl- tetralin, ^j -22.4
C ₁₅ H ₂₂ (4-methyldiamantane) ^d		-46.82	-47.21

TABLE II
 C_nH_{2n-4} , C_nH_{2n-6} , and C_nH_{2n-8} Stabilomers ($n = 8-20$)

No. Carbons	Saturated stabilomer	$\frac{\Delta H_f^\circ}{\text{Engler}^a}$ (kcal mole ⁻¹)	$\frac{\Delta H_f^\circ}{\text{Allinger}^b}$ (kcal mole ⁻¹)	ΔH_f° Unsaturated stabilomer
$C_{16}H_{24}$	4,9-dimethyldiamantane ^d		-56.27	-56.28
$C_{17}H_{26}$	1,4,9-trimethyldiamantane		-62.54	-62.75
$C_{18}H_{28}$	1,4,6,9-tetramethyldiamantane		-68.50	-68.83
	1,4,7,9-tetramethyldiamantane		-68.43	-68.68

$C_{19}H_{30}$	1,4,7,9,11-pentamethyldiamantane		-73.59	-73.97
$C_{20}H_{32}$	1,4,6,7,9,11-hexamethyldiamantane		-77.35	-78.49

^a Ref. 18.

^b Ref. 19.

^c Experimental evidence from solvolysis supports prediction; see Ref. 32.

^d Confirmed by AlX_3 isomerization.

^e Value from Benson's group increments, Ref. 25a.

^f ΔH_f estimated from strain energy calculated by force field and group increments.

^g Obtained from cubane derivative by silver ion rearrangement, Ref. 4.

^h From Engler force field, known to be grossly overestimated.

ⁱ From group increments, Ref. 25d.

^j ΔH_f estimated for methyltetralins from equivalent $\Delta\Delta H_f$ on going from benzene to the similarly substituted methylbenzene.

^k Ref. 25b.

TABLE 12
Calculated ΔH_f s of 1-Alkyladamantanes

1-Adamantyl-R	ΔH_f Calculated ^a		Strain energy ^a		Δ Strain energy ^a (substituted- parent system)	
	Engler ^b	Allinger ^c	Engler	Allinger	Engler	Allinger
H	-32.55	-33.82	6.87	5.94	—	—
Methyl	-41.92	-42.89	5.69	4.98	-1.18	-0.96
Ethyl	-45.05	-46.44	7.69	6.62	+0.82	+0.68
<i>n</i> -Propyl	-50.39	-51.78	7.48	6.47	+0.61	+0.53
Isopropyl	-49.05	-50.71	10.77	9.30	+3.90	+3.36
<i>n</i> -Butyl	-55.75	-57.21	7.25	6.23	+0.38	+0.29
Isobutyl	-55.36	-56.71	9.59	8.49	+1.72	+2.55
<i>t</i> -Butyl	-53.41	-55.37	14.60	12.75	+7.73	+6.81
1-Adamantyl	-53.66	-56.84	21.46	18.93	+14.59	+12.99

^a All values in kcal mole⁻¹.

^b Ref. 18.

^c Ref. 19.

is diminished in this series. 2-(2-2-dimethylpropyl)-adamantane however, suffers from an additional two 1,5-interactions and reverses the trend.

A comparison of 1-alkyladamantanes versus 2,2-methylalkylpropanes is given in Table 15. The preference for adamantyl substitution is probably due to a lessening of the repulsive nonbonded interactions between R and the ring because of a widening of the C—C—R angle in adamantane ($\sim 110^\circ$ vs. 109° in *t*-butyl).

The C₉H₁₄ noradamantane (35) demonstrates that the stabilomer can often be deduced by elimination of a CH₂ group from the homologous most stable

TABLE 13
Calculated ΔH_f s of 2-Alkyladamantanes^a

2-Adamantyl-R	ΔH_f Calculated		Strain energy		Δ Strain energy (substituted- parent system)	
	Engler ^b	Allinger ^c	Engler	Allinger	Engler	Allinger
H	-32.55	-33.82	6.87	5.94	—	—
Methyl	-37.94	-39.04	8.56	7.67	+1.69	+1.73
Ethyl	-42.40	-43.66	9.23	8.24	+2.36	+2.30
Isopropyl	-47.80	-49.11	10.91	9.74	+4.04	+3.80
<i>t</i> -Butyl	-50.65	-52.47	16.25	14.49	+9.38	+8.85
1-Adamantyl	-50.97	-53.97	23.04	20.64	+16.17	+14.70

^a All values in kcal mole⁻¹.

^b Ref. 18.

^c Ref. 19.

TABLE 14
Heat of Isomerization of 2-Alkyl to 1-Alkyladamantanes

Alkyl	ΔH Isomerization ^a	
	Engler ^b	Allinger ^c
Methyl	-3.98	-3.85
Ethyl	-2.65	-2.78
Isopropyl	-1.25	-1.60
<i>t</i> -Butyl	-1.76	-2.90

^a All values in kcal mole⁻¹.

^b Ref. 18.

^c Ref. 19.

isomer, especially if it is particularly low in energy. ΔH_f° 's for additional C₉H₁₄ saturated stabilomer candidates have been calculated (18).

Experimental verification by aluminum halide isomerization of the C₉H₁₄ (35), C₁₀H₁₆ (36), C₁₁H₁₈ (37), C₁₂H₂₀ (38), C₁₃H₂₂ (34), C₁₄H₂₄ (39), C₁₅H₂₆ (40), stabilomers as adamantane derivatives has been published. The preference for polymethyl substitution is maintained until C₁₅H₂₆, where 1-ethyl-3,5,7-trimethyladamantane (ΔH_f° , -73.41 (E), -73.79 (A) kcal mole⁻¹) is predicted to be more stable than 1,2,3,5,7-pentamethyladamantane (ΔH_f° , -72.52 (E), -73.07 (A) kcal mole⁻¹) due to the greater number of skew interactions of the latter. The predictions based on empirical force field calculations agree in every case with the experimental results. Empirical force field calculations of a large number of C₁₀H₁₆'s (41) and C₁₁H₁₈'s (42) have aided in deducing the mechanisms of their AlX₃ catalyzed rearrangements.

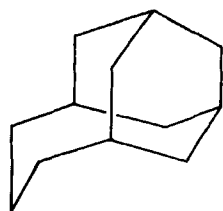
The energy differences between the alkyl adamantanes and analogs of different ring structure is very large: 1-methyladamantane is 11.86 (E) kcal mole⁻¹ more stable than homoadamantane and 1,3-dimethyladamantane is 25.01 (E) kcal mole⁻¹ more stable than 1,1-bishomoadamantane (tricy-

TABLE 15
 ΔH_f° 1-Alkyladamantanes versus 2,2-Methylalkylpropanes^a

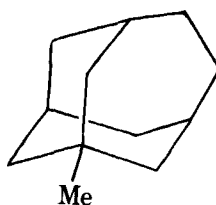
Alkyl	<i>t</i> -Butyl-alkyl			1-Adamantyl-alkyl			$\Delta\Delta$ Strain energy
	ΔH_f	Strain energy	Δ Strain energy	ΔH_f	Strain energy	Δ Strain energy	<i>t</i> -Butyl-1-adamantyl
H	-33.19	-0.88	—	-32.55	6.87	—	—
Methyl	-41.93	-1.43	-0.55	-41.92	5.69	-1.18	-0.63
Ethyl	-44.89	0.74	1.62	-45.05	7.69	0.82	-0.80
<i>i</i> -Propyl	-48.94	3.77	4.56	-49.05	10.77	3.90	-0.66
<i>t</i> -Butyl	-53.19	7.71	8.95	-53.41	14.60	7.73	-1.22

^a All values in kcal mole⁻¹ from Engler force field, Ref. 18.

clo[5.3.1.1^{3,9}]-dodecane) **9** and 12.51 (E) kcal mole⁻¹ more stable than 1-methylhomoadamantane **10**.

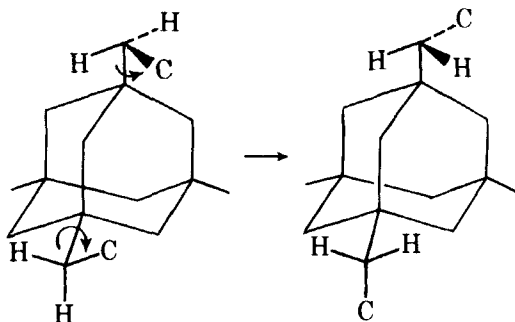


9
 ΔH_f° -26.32 (E)
 -22.36 (A)



10
 ΔH_f° -38.82 (E)
 -36.50 (A)

The C₁₆H₂₈ stabilomer is 1-(1-propyl)-3,5,7-trimethyl-adamantane consistent with the previous finding that 1-(1-propyl)-adamantane is more stable than 1-(2-propyl)-adamantane. Other C₁₆ adamantane derivatives were also investigated: 1,3-diethyl-5,7-dimethyladamantane ΔH_f° , -76.57 (E), -77.42 (A) kcal mole⁻¹; 1-(2-propyl)-3,5,7-trimethyladamantane ΔH_f° -77.62 (E), -78.52 (A) kcal mole⁻¹ is within 1 kcal mole⁻¹ (A), and considered as co-stabilomer; 1-ethyl-3,4,5,7-tetramethyl-adamantane ΔH_f° -75.66 (E) -76.68 (A) kcal mole⁻¹. The preference of the 1-propyl derivative over the 2-propyl indicates that monosubstituted adamantane is a good model for more highly substituted adamantanes, that is, that bridgehead substituents are largely noninteractive. Two conformations of the ethyl groups were investigated for 1,3-diethyl-5,7-dimethyladamantane.



The energies calculated were identical (± 0.05 kcal mole⁻¹) again indicating a lack of interaction between bridgehead groups. Finally, the ΔH_f° measured (5a) for bridgehead methyl substitution of adamantane is 8.81 kcal mole⁻¹ (ΔH_f° 1-methyladamantane - ΔH_f° adamantane), whereas the value for tetramethyl bridgehead substitution of adamantane is 35.39 kcal mole⁻¹ (ΔH_f° tetrameth-

yladamantane - ΔH_f° adamantane) or 8.84 kcal mole⁻¹ per methyl showing precise additivity and therefore no interaction.

For C₁₇H₃₀ the stabilomer is 1-(1-butyl)-3,5,7-trimethyladamantane in agreement with the model calculations. Another candidate was examined and its heat of formation is: 1,3-dimethyl-5-ethyl-7-(2-propyl)adamantane, -80.79 (E), -82.19 (A) kcal mole⁻¹.

The most stable C₁₈H₃₂ is 1-(4-2-methylbutyl)-3,5,7-trimethyladamantane (1-isopentyl-3,5,7-dimethyladamantane). Other candidates were calculated and their heats of formation are: 1,3,5,7-tetraethyladamantane -82.91 (E), -84.70 (A) kcal mole⁻¹; 1,3-dimethyl-5,7-di(2-propyl)adamantane -85.03 (E), -86.94 (A) kcal mole⁻¹; 1-(1-pentyl)-3,5,7-trimethyladamantane, -89.48 (E) kcal mole⁻¹. The 1-pentyl derivative is within ± 1 kcal mole⁻¹ of the stabilomer and must be considered as the co-stabilomer.

The C₁₉H₃₄ and C₂₀H₃₆ stabilomers are 1-(4-2,2-dimethylbutyl) and 1-(5-2,2-dimethylpentyl)-3,5,7-trimethyladamantane (1-neohexyl and 1-neoheptyl). Other candidates and their heats of formation are C₁₉H₃₄ 1,3-(2-propyl)-5-ethyl-7-methyladamantane, -88.21 (E), -90.60 (A) kcal mole⁻¹; 1-(5-2-methyl-pentyl)-3,5,7-trimethyladamantane (isohexyl), -95.78 (E) kcal mole⁻¹; C₂₀H₃₆, 1,3,5-tri(2-propyl)-7-methyladamantane, -92.43 (E), -95.31 (A) kcal mole⁻¹.

F. C_nH_{2n-6}'s

1. Aromatics

The unsaturated isomers of this family are benzene derivatives. Although normally considered to be especially stable, benzene is strained! This often ignored fact is due to the inherent strain in the double bonds forming the aromatic unit. The total strain in the double bonds can be estimated from saturated group increments (25) as 3×22.4 kcal mole⁻¹, and so, despite the ~ 32 kcal mole⁻¹ of resonance energy, benzene is strained by ~ 35 kcal mole⁻¹. Alternatively, the strain energy of benzene can be calculated by taking the difference between the heat of formation of a hypothetical strain free (CH)₆, -12.96 kcal mole⁻¹ (obtained from saturated group increments (25), 6×-2.16) and the experimentally determined (25b) ΔH_f° of +19.81 kcal mole⁻¹ to again obtain a strain value of more than 30 kcal mole⁻¹.

Table 11 lists the ΔH_f° 's for the C_nH_{2n-6} benzenoid isomers. The values for C₈-C₁₂ were obtained utilizing Benson's group increments (25a) and agree well with experimental values. Empirical force field calculations can be used to obtain a strain energy for aromatic molecules but this is not necessary when group increment values are available. The best aromatic for each C_n was selected based on group increment estimation of ΔH_f° from a list of candidates generated

by qualitative considerations. In most cases the choice was clear. A number of polyalkylated benzenes, however, were predicted to have similar energies. The choice of a single "best aromatic" from these does not affect the conclusions obtained.

The ΔH_f° for the aromatic compounds of C_{13} and C_{14} were estimated from steric energies computed by the Boyd, Andose, Mislow force field (43). It did not prove necessary to calculate further examples.

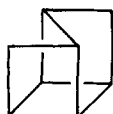
2. Saturated Isomers

In discussing the C_8H_{10} and C_9H_{12} saturated stabilomers, the limitations of the empirical force field calculations being used to obtain ΔH_f° must be considered. The strain energy of highly elaborated molecules containing three-membered rings cannot be calculated accurately using functions that compute strain based on deviations from an "ideal" C—C—C angle (18). Because of their exceptional 60° bond angles (50° deviation from ideal), their strain energy is overestimated and cyclopropanes must be considered as a separate functional group (44). The additional parameterization required has not been included into our program and ΔH_f° of highly elaborated compounds with three-membered rings is not calculated accurately. The only instances when compounds with three-membered rings may be viable saturated stabilomer candidates is for C_8H_{10} and C_9H_{12} and C_8-C_{10} (C_nH_{n-8} 's) and ΔH_f° s were estimated roughly from group increments (25). The empirical force field method estimates ΔH_f° of compounds with four-membered rings with more precision, but the absolute values of ΔH_f° are not as reliable as for compounds not containing this highly strained unit. The possibility that the predictions of C_8H_{10} (tetracyclo[3.3.0^{3,8}.0^{4,7}]octane) and C_9H_{12} (tetracyclo[4.2.1.0^{2,5}.0^{3,7}]nonane, 2,4-methanobisnoradamantane) as saturated stabilomers are in error is much greater than for the previous examples. Experimentally (45), it is known that secocubane (tetracyclo[4.2.0.0^{2,5}.0^{3,8}]octane) isomerizes to the tetracyclo[3.3.0.0^{2,8}.0^{4,6}]octane and not the predicted stabilomer. The energy of tetracyclo[3.3.0.0^{2,8}.0^{4,6}]octane can, however, only be crudely estimated because of its three-membered rings. The ΔH_f° 's of candidates for the C_8H_{10} and C_4H_{12} saturated stabilomer are included in Table 16.

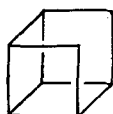
The $C_{10}H_{14}$ saturated stabilomer has been confirmed experimentally (46) ($AlBr_3$ isomerization) as tetracyclo[5.2.1.0^{2,6}.0^{4,8}]decane in agreement with the calculations. A considerable number of tetracyclodecanes have been calculated and are included in Table 17.

The $C_{11}H_{16}$, 2,4-ethanonoradamantane (47,48), and $C_{12}H_{18}$ ethanoadamantane (49) have also been verified as the saturated stabilomers of their families by AlX_3 isomerization techniques. The equilibrium ratio of 2,4-ethanonoradamantane and 2,8-ethanonoradamantane ($97:3 \pm 1$ ratio) (47,48), indicates a ~ 2 kcal mole⁻¹ differences in ΔG° . In contrast, empirical force field

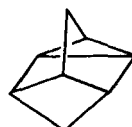
TABLE 16
 ΔH_f° of C_8H_{10} and C_9H_{12} Saturated Stabilomer Candidates^a

 C_8H_{10} Candidates

71.24 (E)
 82.99 (A)



88.76 (E)
 91.31 (A)



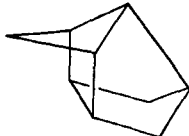
79.24 (E)



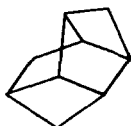
81.92 (E)



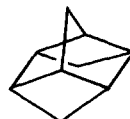
48.12 (Group Increments, Ref. 25d)

 C_9H_{12} Candidates

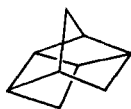
31.66 (E)
 39.17 (A)



50.47 (A)



52.71 (E)



44.18 (E)



47.79 (E)



53.03 (E)



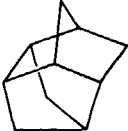
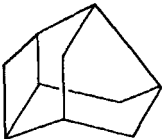
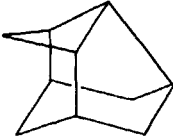
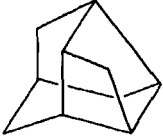
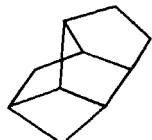
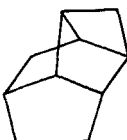

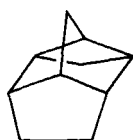
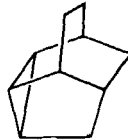
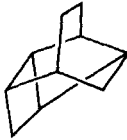
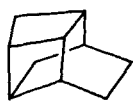
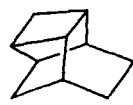
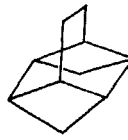
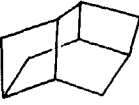
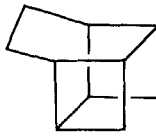
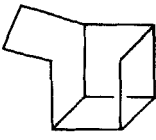
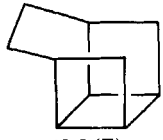
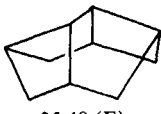
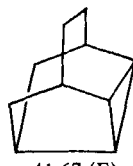
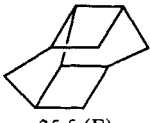


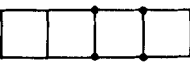
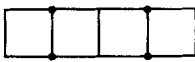
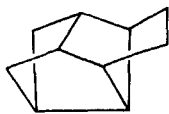
94.05 (E)

^a All values in kcal mole⁻¹, E = Engler force field, ref. 18; A = Allinger 1971 force field, ref. 19.

calculations predicted identical ΔH_f° and $\Delta\Delta S$ is expected to be near zero. This deviation between isomerization results and predicted $\Delta\Delta H_f^\circ$ is much larger than normally observed (21). ΔH_f° s of a considerable number of other $C_{11}H_{16}$ (47) and $C_{12}H_{18}$ (49) structures have been calculated by the empirical force field method.

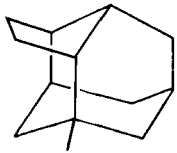
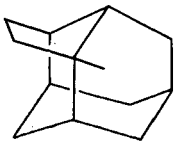
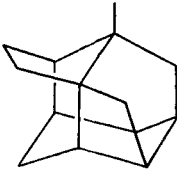
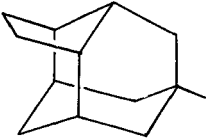
The methylethanoadamantanes ($C_{13}H_{20}$) have been isomerized using AlX_3 (50). The components of the resulting mixture have been fully identified and agree with the empirical force field calculations (assuming $\Delta S \approx 0$) prediction

TABLE 17
 ΔH_f° of C₁₀H₁₄ Saturated Stabilomer Candidates^a

			
8.29 (E)	26.40 (A)	13.52 (E) 13.54 (A)	19.57 (A)
			
16.68 (A)	26.47 (A)	15.72 (E) 17.94 (A)	20.53 (E) 21.47 (A)
			
42.57 (E) 80.73 (A)	33.6 (E)	33.55 (E)	20.87 (E) 23.74 (A)
			
58.54 (E)	30.53 (E) 31.27 (A)	58.5 (E)	51.3 (E)
			
49.5 (E)	25.48 (E) 33.03 (A)	41.67 (E)	25.5 (E)
			
32.67 (E) 37.90 (A)	81.74 (E) 87.04 (A)	69.31 (E) 75.04 (A)	64.81 (E) 70.74 (A)
			
	9.85 (E) 14.72 (A)		

^a All values in kcal mole⁻¹; E = Engler force field, ref. 18, A = Allinger 1971 force field, ref. 19.

TABLE 18
 ΔH_f° of Methyleneadamantanes^a

1-methyl-2,4-ethanoadamantane	2-methyl-2,4-ethanoadamantane
	
-34.21 (E) -35.51 (A)	-33.33 (E) -35.02 (A)
3-methyl-2,4-ethanoadamantane	5-methyl-2,4-ethanoadamantane
	
-31.44 (E) -34.21 (A)	-34.94 (E) -36.25 (A)

^a All values in kcal mole⁻¹; E = Engler force field, ref. 18, A = Allinger 1971 force field, ref. 19.

(Table 18) that a mixture of 6-methyl-2,4-ethanoadamantane, -34.94 (E), -36.25 (A) kcal mole⁻¹; 1-methyl-2,4-ethanoadamantane, -34.21 (E), -35.51 (A) kcal mole⁻¹; 1,2-trimethyleneadamantane, -34.09 (E), -35.00 (A) kcal mole⁻¹ should be present at equilibrium.

1,2-Tetramethyleneadamantane (50,51) (**11**) (tetracyclo[7.3.1.1.3¹¹.0^{3,8}]tetradecane) is the fused six-membered ring system of this family. Table 19 affords some indication of the calculated ΔH_f° difference between this structure and alternative C₁₄H₂₂'s. Although the choice is not as clear as with the adamantane system and its analogs, further alkyl substitution would only maintain or enhance the preference towards this polycyclic ring structure. 1,2-Tetramethyleneadamantane was found experimentally as a disproportionation product in the AlX₃ isomerization of diamantane (51). The AlX₃-catalyzed isomerization of a C₁₄H₂₂ precursor gave **11** in high yield (50).

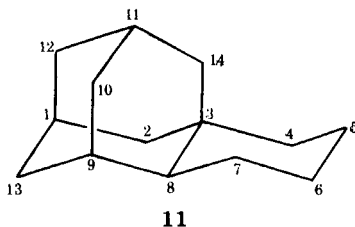
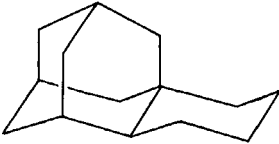
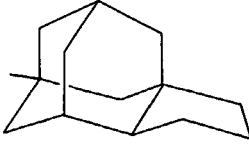
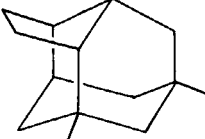
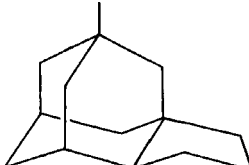


TABLE 19
 ΔH_f° of Selected $C_{14}H_{22}$'s^a

	
-45.35	-43.58
	
-43.51	-43.66

^a All values in kcal mole⁻¹; Engler force field, ref. 18.

Table 20 outlines the relative preference of alkyl substituents on the 1,2-tetramethyleneadamantane ring system, and forms the basis for the selection of the C_{15} – C_{18} saturated stabilomers. Substitution at the 5- and 6-positions was expected to be equivalent and only the former was investigated. The $C_{15}H_{24}$ saturated co-stabilomers are 1- and 11-methyltetracyclo[7.3.1.1^{3,11}.0^{3,8}]tetradecane (these isomers are interconverted by a,e isomerization about the 8-position). $AlBr_3$ isomerization studies (52) of $C_{15}H_{24}$'s showed 40% 1-methyl, 39% 11-methyl, and small amounts (<10%) of 9-methyl (–53.41 (E), –54.44 (A) kcal mole⁻¹) and 5- and 6-methyltetracyclo[7.3.1.1^{3,11}.0^{3,8}]tetradecane (–53.08 (E), –53.66 (A) kcal mole⁻¹) in excellent agreement with the calculations. The $C_{16}H_{26}$ saturated stabilomer is 1,11-dimethyltetracyclo[7.3.1.1^{3,11}.0^{3,8}]tetradecane (Table 11). $AlBr_3$ isomerization of $C_{16}H_{26}$'s (52) yielded a mixture of the 1,11-dimethyl derivative (42%) as well as small amounts (<10%) of the 1,9-, 1,6-, 9,11-, 6,11-, 5,11-, and 1,5-dimethyl derivatives.

The $C_{17}H_{28}$ saturated stabilomer is 1,9,11-trimethyltetracyclo[7.3.1.1^{3,11}.0^{3,8}]tetradecane. Model calculations predict the 1,5,11- and 1,6,11-trimethyl derivatives to be less stable but within 11 kcal mole⁻¹ and as such are co-stabilomers. 1,5,9,11- and 1,6,9,11-tetramethyltetracyclo[7.3.1.1^{3,11}.0^{3,8}]tetradecanes are the $C_{18}H_{30}$ saturated co-stabilomers.

The $C_{19}H_{32}$ saturated stabilomer is *trans*-5,6-dimethyl-1,9,11-trimethyltetracyclo[7.3.1.1^{3,11}.0^{3,8}]tetradecane. Structures calculated to be co-stabilomers (within 1 kcal mole⁻¹) and their heats of formation are: 5-ethyl-1,9,11-trimethyltetracyclo[7.3.1.1^{3,11}.0^{3,8}]tetradecane –84.50 (E), –84.64 (A) kcal mole⁻¹; 1,5,5,9,11-pentamethyltetracyclo[7.3.1.1^{3,11}.0^{3,8}]tetradecane, –83.39 (E), –83.68 (A) kcal mole⁻¹.

The $C_{20}H_{34}$ saturated co-stabilomers are 5-(2-propyl)-1,9,11-trimethyltetracyclo[7.3.1.1^{3,11}.0^{3,8}]tetradecane -89.73 (E), -90.01 (A) kcal mole⁻¹ and *trans*-5-ethyl-6-methyl-1,9,11-trimethyltetracyclo[7.3.1.1^{3,11}.0^{3,8}]tetradecane, -90.41 (E), -90.72 (A) kcal mole⁻¹.

3. *Saturated versus Aromatic C_nH_{2n-6}'s*

Initially, the aromatics are considerably more stable (C_8H_{10} , ~ 65 kcal mole⁻¹; C_9H_{12} , 35 kcal mol⁻¹) than their saturated isomers. The higher saturated analogs are able to relieve strain by forming six-membered rings, but the aromatics maintain the strain inherent in their double bonds, with the result that the saturated analogs become relatively more stable. The crossover of relative stability comes between $C_{11}H_{16}$ and $C_{12}H_{18}$. Ethanoadamantane is predicted to be more stable than hexamethylbenzene! This trend is enhanced for subsequent isomers with the saturated $C_{13}H_{20}$ and $C_{14}H_{22}$ stabilomers becoming considerably more stable than their aromatic analogs. This pattern is very similar to that observed in comparing the mono- and bicyclic saturated compounds with their olefinic isomers. The resonance energy of benzene, however, "delays" the crossover of stability for the C_nH_{2n-6} 's.

G. *C_nH_{2n-8}'s*

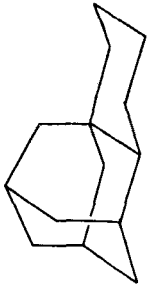
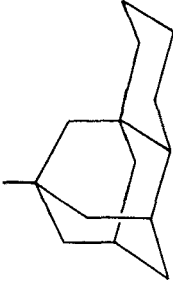
1. *Aromatics*

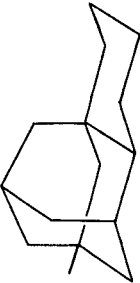
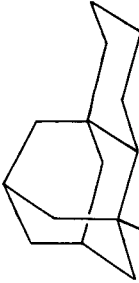
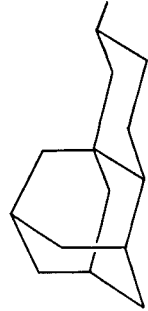
The aromatic stabilomers of this family were constructed by adding two (benzocyclobutene), three (hydrindene), and four (tetralin) methylene units of benzene. The C_nH_{2n-8} , $n = 11, 12$, etc., unsaturated stabilomers are methyl-substituted tetralins (Table 11). The ΔH_f° for benzocyclobutene was estimated from the difference of the steric energy, computed by the Boyd, An-dose, Mislow force field (43) and a group increments "strain free" ΔH_f° . The values of ΔH_f° for hydrindene and tetralin are known (25a). The ΔH_f° for the $C_{11}H_{14}$, $C_{12}H_{16}$, and $C_{13}H_{18}$ aromatic compounds were estimated assuming the same $\Delta\Delta H_f^\circ$ for the tetralin \rightarrow methyltetralin as observed for the similar benzene \rightarrow methylbenzene transformation using Benson's data (25a).

2. *Saturated Isomers*

Cubane (C_8H_8), homocubane (C_9H_{10}) and 1,8-bishomocubane pentacyclo[6.2.0.6^{3,6}.0^{5,8}]decane ($C_{10}H_{12}$) are known to isomerize readily in the presence of silver ion to the related cuneane derivatives (4). The inability to calculate elaborated three-membered ring compounds accurately does not allow a quantitative estimation of the relative stabilities of these isomers to be obtained computationally. The force field calculated ΔH_f° 's of the cubane derivatives are

TABLE 20
 ΔH_f° Calculated of Methyl-1,2-tetramethyleneadamantanes

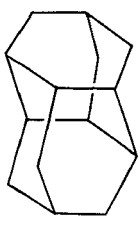
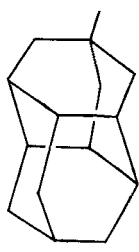
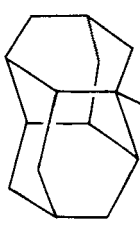
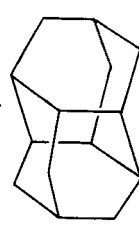
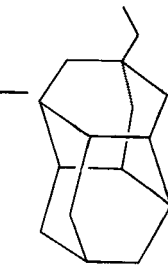
Compound	ΔH_f° (kcal mole ⁻¹)		Strain energy		Δ Strain energy (substituted parent system)	
	Engler ^a	Allinger ^b	Engler	Allinger	Engler	Allinger
 1,2-Tetramethyleneadamantane	-45.35	-46.53	9.76	9.08	0.0	0.0
 11-Methyl-1,2-tetramethyleneadamantane	-54.79	-55.60	8.51	8.12	-1.25	-0.96

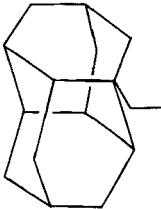
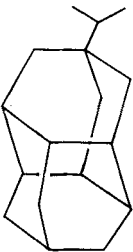
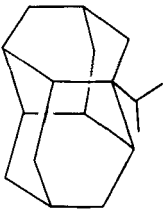
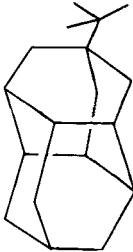
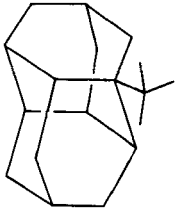
 <p>1-Methyl-1,2-tetraamethyleneadamantane</p>	-54.85	-55.68	8.45	8.04	-1.31	-1.04
 <p>9-Methyl-1,2-tetraamethyleneadamantane</p>	-53.41	-54.44	9.89	9.28	+0.13	+0.20
 <p>5-Methyl-1,2-tetraamethyleneadamantane</p>	-53.08	-53.66	9.11	8.90	-0.65	-0.18

^a Ref. 18.

^b Ref. 19.

TABLE 21
Calculated ΔH_f° of Alkyldiamantanes^a

Compound	ΔH_f°		Strain energy		Δ Strain energy (substituted-parent system)	
	Engler ^b	Allinger ^c	Engler	Allinger	Engler	Allinger
 Diamantane	-37.37	-38.13	10.69	10.25	0.0	0.0
 4-Methyldiamantane	-46.82	-47.21	9.43	9.28	-1.26	-0.97
 1-Methyldiamantane	-43.56	-44.43	12.69	12.06	+2.00	+1.81
 3-Methyldiamantane	-42.91	-43.35	12.23	11.98	+1.54	+1.73
 4-Ethyldiamantane	-49.98	-50.84	11.40	10.84	+0.71	+0.59

 <p>1-Ethyladaman- tane</p>	-46.32	-47.61	15.06	14.07	+4.37	+3.82
 <p>4-(2-propyl)dia- mantane</p>	-54.03	-55.13	14.43	13.48	+3.74	+3.23
 <p>1-(2-propyl)dia- mantane</p>	-50.18	-51.64	18.28	16.99	+7.59	+6.74
 <p>4-(2,2-methyl- propyl)-dia- mantane</p>	-58.45	-59.89	18.20	16.85	+7.51	+6.60
 <p>2-(2,2-methyl- propyl)-dia- mantane</p>	-46.75	-49.57	29.90	27.17	+19.21	+16.92

^a All values in kcal mole⁻¹.

^b Ref. 18.

^c Ref. 19.

included in Table 11 along with the ΔH_f° 's of the cuneanes estimated by simple group increments (25).

(D₃)-Trishomocubane, a molecule whose faces are all composed of five membered rings, is the C₁₁H₁₄ saturated stabilomer as determined by AlBr₃ isomerization (53,54) in agreement with the empirical force field calculations. ΔH_f° of a number of C₁₁H₁₄'s have been calculated (54).

The prediction for C₁₂H₁₆ (Table 11) is for a two component mixture at equilibrium composed of bisnordiamantane isomers (pentacyclo[6.4.0.0^{2,6}.0^{3,11}.0^{4,9}]dodecane, -5.32 (E), -4.82 (A) kcal mole⁻¹ and pentacyclo[5.4.1.0^{2,6}.0^{3,10}.0^{4,8}]dodecane, -5.80 (E), -1.78 (A) kcal mole⁻¹. Preliminary experiments (54) indicate, however, a three-component mixture. The third lowest ΔH_f° isomer, an isoasterane, is included in Table 11.

Following previous patterns the C₁₃H₁₆ stabilomer is predicted to be nordiamantane, preliminary AlX₃ rearrangement gave a single, high melting hydrocarbon (54).

The C₁₄H₂₀ saturated stabilomer, diamantane (56) is the fused six-membered ring system of the C_nH_{2n-8} family. The mechanism of the AlBr₃ isomerization to diamantane from a variety of precursors has been studied (23c,51,56,57) and as a result ΔH_f° for a large number of pentacyclic C₁₄'s has been calculated (57). These calculations indicate a clear preference for this ring system as the saturated stabilomer.

Table 21 gives the alkyl substitution energies for the diamantane skeleton. The order of preference of alkyl substitution in apical > medial > secondary. In agreement with these predictions the C₁₅ and C₁₆ C_nH_{2n-8} saturated stabilomers are known to be methyl (58) and dimethyl (59) apically substituted diamantanes.

The remaining pentacyclic stabilomers (C₁₇-C₂₀) are methyl bridgehead substituted diamantanes.

3. Saturated C_nH_{2n-8}'s versus Aromatics

The trends observed for the tetracyclics versus aromatics are duplicated for the saturated C_nH_{2n-8}'s. The strain associated with the olefin double bond is compensated by the aromatic resonance energy and the aromatics compete favorably with the saturated isomers containing four- and five-membered rings. Initially the aromatic compounds are ~100 kcal mol⁻¹ more stable (C₈H₈). The ΔH_f° difference between the saturated and aromatic C_nH_{2n-8}'s decreases and the C₁₃H₁₈ saturated stabilomer, nordiamantane, is predicted to be more stable than trimethyltetralin. The crossover for the C_nH_{2n-8}'s (C₁₃) is one carbon later than for the C_nH_{2n-6}'s which is reasonable since an additional ring must be accommodated. The saturated analogs are increasingly more stable for diamantane and its methyl derivatives.

H. Larger Systems

Although there are several examples of AlX_3 -catalyzed isomerization in large systems (e.g., ethanodiamantanes (55b,60), $\text{C}_{16}\text{H}_{22}$; triamantane (21b) $\text{C}_{18}\text{H}_{24}$) the astronomical number of isomers possible makes the chance of not getting complete thermodynamic control much greater (7). The AlX_3 isomerization of a $\text{C}_{22}\text{H}_{28}$ precursor did not give the predicted tetraadamantane (7); likewise a $\text{C}_{16}\text{H}_{20}$ isomer gave a bisethano-bisnordiamantane (**12**), heptacyclo[8.6.0.0^{2,8}.0^{3,13}.0^{4,11}.0^{5,9}.0^{12,16}]hexadecane, -4.35 (E), -0.16 (A) kcal mole⁻¹ and a caged dimer of bicyclo[2.2.2]octa-2,5-diene (**12'**), heptacyclo[7.7.0.0^{2,6}.0^{3,15}.0^{4,12}.0^{5,10}.0^{11,16}]hexadecane, -8.14 (E), -4.84 (A) kcal mole⁻¹, instead of the predicted stabilomer, a bisnortriamantane (**13**), heptacyclo[7.6.1.0^{3,8}.0^{3,13}.0^{5,12}.0^{7,11}.0^{10,14}]hexadecane, -9.42 (E), -8.60 (A) kcal mole⁻¹ (55,55a) and a $\text{C}_{21}\text{H}_{28}$ precursor gave **14** instead of the expected trimethylenetriamantane (**15**) (61). As a result the computational methods have

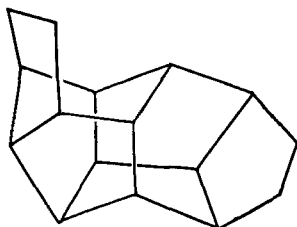
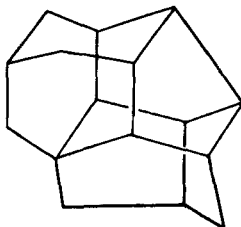
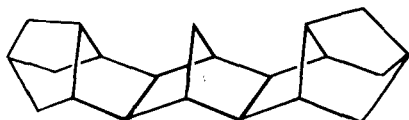
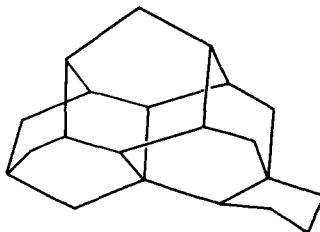
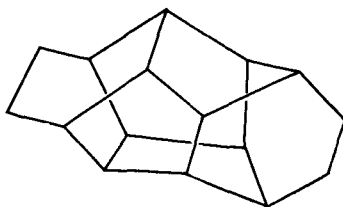
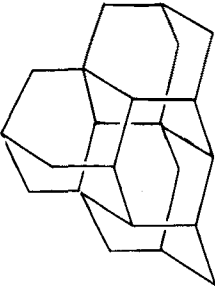
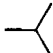
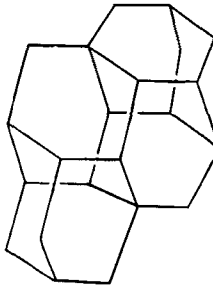

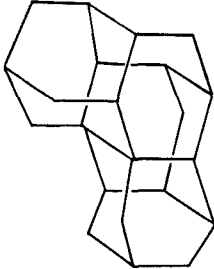

**12****13****14****15****12'**

TABLE 22
 Calculated Enthalpies and Strain Energies of Tetramantanes, Pentamantanes, and Corresponding Simple
 Alkane Conformers (kcal mole⁻¹, 25°, gas)

Adamantalogue	ΔH_f°		Strain		Alkane	ΔH_f°		Strain	
	E ^a	A ^b	E ^a	A ^b		E ^a	A ^b	E ^a	A ^b
Isotetramantane 	-53.52	-52.96	15.15	16.14	Isobutane 	-33.19 ^{c,d}	-32.21 ^{c,d}	-0.88 ^c	-0.10 ^c
Anti-tetramantane 	-51.51	-51.01	16.05	16.93	Anti- <i>n</i> -butane 	-31.04 ^c		-0.68 ^c	
Skew-tetramantane 	-46.59	-46.39	20.97	21.55	Gauche- <i>n</i> -butane 	-30.11 ^c	-29.91	0.25 ^c	0.44

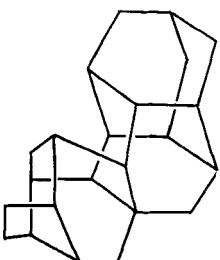
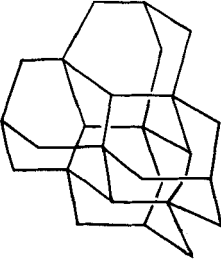

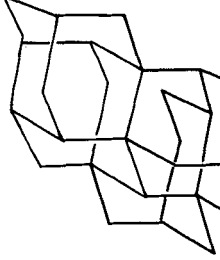

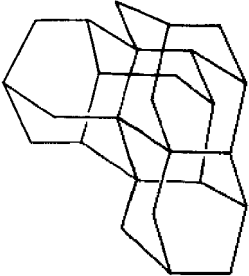

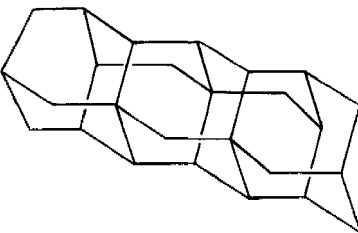

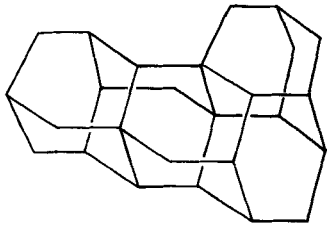
Bastardane ^f		-30.08	-29.90	36.37	36.88					
Neopentamantane		-64.85	-63.45	15.79	17.75	Neopentane	-41.93 ^{c,g}	-41.02 ^{c,g}	-1.43 ^c	-0.80 ^c
										
Gauche-anti-isopentamantane		-55.85	-54.88	22.57	24.00	Gauche-anti-isopentane	-37.29	-36.81	0.15	0.49
										

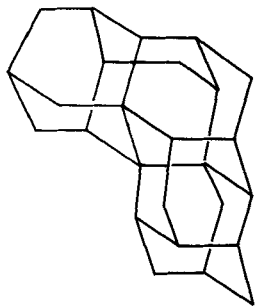
TABLE 22
 Calculated Enthalpies and Strain Energies of Tetramantanes, Pentamantanes, and Corresponding Simple
 Alkane Conformers (kcal mole⁻¹, 25°, gas)

	ΔH_f		Strain		Alkane	ΔH_f		Strain	
	E ^a	A ^b	E ^a	A ^b		E ^a	A ^b	E ^a	A ^b
Adamantylloguc									
Gauche-gauche-isopentamantane	-50.02	-49.05	28.40	29.83	Gauche-gauche-isopentane	-36.55	-36.18	0.89	1.12
 Anti-anti- <i>n</i> -pentamantane	-58.76	-57.56	18.55	20.16	 Anti-anti- <i>n</i> -pentane	-36.32 ^{c,h}	-35.94 ^{c,h}	-0.83 ^c	-0.37 ^c
									

Anti-gauche-*n*-pentamantane -53.85 -52.79 23.46 24.93 Anti-gauche-*n*-pentane -35.35 0.14 0.32



Gauche-gauche-*n*-pentamantane -49.27 -48.13 28.04 29.59 Gauche-gauche-*n*-pentane -34.55 0.94 0.82



^a Engler force field, Ref. 18.

^b Allinger force field, Ref. 19.

^c Taken from Ref. 18.

^d Experimental ΔH_f° -32.41 kcal mole⁻¹, Ref. 18.

^e E. Ōsawa, J. Collins, and P. v. R. Schleyer, *Tetrahedron*, **33**, 2667 (1977).

^f Ref. 7.

^g Experimental ΔH_f° -40.14 kcal mole⁻¹, Ref. 18.

^h Experimental ΔH_f° -35.56 kcal mole⁻¹, Ref. 18.

increased importance for these systems, allowing determination of the stabilomer in cases where experimental techniques are known to be unreliable. Table 22 gives calculations for tetramantanes and pentamantanes (62).

III. CONCLUSIONS

A methodology for predicting stabilomers has been described and utilized. Consideration of the strain of olefins indicated that unsaturated compounds will only be more stable than saturated isomers containing three- and four-membered rings; saturated isomers having only five- and six-membered rings will be preferred. Benzenoid isomers have enhanced relative stability because of resonance energy and are even favored over some saturated isomers with only five- and six-membered rings. The inherent strain energy of the double bonds comprising the aromatic unit, however, allows the saturated polycyclics to again become more stable for the larger systems.

Such predictions, based on empirical force field calculations, have been shown to be consistent with known AlX_3 isomerization results for the C_8 - C_{20} , C_nH_{2n-4} , C_nH_{2n-6} , C_nH_{2n-8} systems. In general, the force field calculations predict the products of the AlX_3 isomerizations except when high energy intermediates or transition states do not allow thermodynamic control (e.g., bastardane). The inability of our force field to calculate ΔH_f° for three-membered ring systems did not allow for a quantitative estimation of the C_8 - $C_{10}H_{2n-8}$ cuneane derivatives.

A listing of the saturated stabilomers revealed patterns of stability based on substitution of the six-membered ring system of a given family, that is, monocyclic, cyclohexane; bicyclic, *trans*-decalin; tricyclic, adamantane; tetracyclic, 1,2-tetramethyleneadamantane; pentacyclic, diamantane.

ACKNOWLEDGMENTS

This work was supported at Princeton University by the National Science Foundation, at Erlangen by the Fonds der Chemischen Industrie, and at both Princeton and Santa Cruz by the National Institutes of Health Research Resources. E.Ō. expresses gratitude to the Japan Electron Optics Co. for making the JAL-30XA program available. Computer time and computational facilities were made available by Princeton University, Hokkaido University, and the Kao Soap Co.

References and Notes

1. E. L. Eliel, N. L. Allinger, S. J. Angyal, and G. A. Morrison, *Conformational Analysis*, Interscience, New York, 1966.
2. (a) E. M. Engler and P. v. R. Schleyer, *MTP (Med. Tech. Publ. Co.) Int. Rev. Sci., Org. Chem. Ser. I*, 5, 239 (1973) and earlier reviews cited therein; (b) M. A. McKervey, *Chem. Soc. Rev.*, 3, 479 (1974); (c) R. C. Fort, Jr., *Adamantane, the Chemistry of Diamond Molecules*, Dekker, New York, 1976.
3. L. A. Paquette, *Synthesis*, 347 (1975).
4. L. A. Paquette, *MTP Int. Rev. Sci., Org. Chem. Ser. I*, 5, 127 (1973); T. Katsushima, R. Yamaguchi, M. Kawanisi, and E. Ōsawa, *J. Chem. Soc., Chem. Commun.*, 39 (1976).
5. (a) T. Clark, T. Knox, H. Mackle, M. A. McKervey, and J. J. Rooney, *J. Am. Chem. Soc.*, 97, 3835 (1975); (b) T. Clark, T. Knox, H. Mackle, and M. A. McKervey, *J. Chem. Soc., Chem. Commun.*, 666 (1975); (c) W. Parker, W. V. Steele, and I. Watt, *J. Chem. Thermodyn.*, 9, 307 (1977); (d) W. Parker, W. V. Steele, W. Stirling, and I. Watt, *J. Chem. Thermodyn.*, 7, 795 (1975); (e) R. H. Boyd, S. N. Sanwal, S. Shary-Tehrany, and D. McNally, *J. Phys. Chem.*, 75, 1264 (1971); (f) R. S. Butler, A. S. Carson, D. G. Laye, and W. V. Steele, *J. Chem. Thermodyn.*, 3, 277 (1971); (g) M. Mansson, N. Rapport, and E. F. Westrum, Jr., *J. Am. Chem. Soc.*, 92, 7296 (1970); (h) A. S. Carson, P. G. Laye, W. V. Steele, D. E. Johnston, and M. A. McKervey, *J. Chem. Thermodyn.*, 3, 915 (1971); (i) T. Clark, D. E. Johnston, H. Mackle, M. A. McKervey, and J. J. Rooney, *J. Chem. Soc., Chem. Commun.*, 1042 (1972); (j) W. D. Good, *J. Chem. Thermodyn.*, 10, 553 (1978); (k) D. J. Subach and B. J. Zwolinski, *ibid.*, 7, 493 (1975); (l) W. V. Steele, *ibid.*, 9, 311 (1977); (m) T. Bally, H. Baumgärtel, U. Büchler, E. Haselbach, W. Lohr, J. P. Maier, and J. Vogt, *Helv. Chim. Acta*, 61, 741 (1978); (n) D. R. Douslin, D. W. Scott, W. D. Good, and A. G. Osborn, *Thermodynamic Properties of Organic Compounds and Thermodynamic Properties of Fluids*, U.S. NTIS, AD Rep., AD-A03101319 (1976); (o) W. V. Steele, and I. Watt, *J. Chem. Thermodyn.*, 9, 843 (1977); (p) R. Walsh and J. M. Wells, *ibid.*, 8, 55 (1976).
6. Stabilomer (based on the German "stabil") is defined as that isomer possessing the lowest free energy of formation at 25°C in the gas phase.
7. If a high-energy intermediate or transition state exists on the reaction pathway to the stabilomer, AlX_3 treatment may yield an isomer thermodynamically more stable than the starting material (a local minimum on the potential energy surface) but not the one governed by absolute thermodynamic control (the global energy minimum), e.g., bastardane was obtained in the rearrangement of a nonacyclic decosane rather than the more stable tetramantanes, P. v. R. Schleyer, E. Ōsawa and M. G. B. Drew, *J. Am. Chem. Soc.*, 90, 5034 (1968); see also Refs. 49, 55, and 55a.
8. D. E. Johnston, M. A. McKervey, and J. J. Rooney, *J. Am. Chem. Soc.*, 93, 2798 (1971).
9. W. Burns, M. A. McKervey, and J. J. Rooney, *J. Chem. Soc. Chem. Commun.*, 965 (1975); W. Burns, T. R. B. Mitchell, M. A. McKervey, and J. J. Rooney, *ibid.*, 893 (1973); R. Hamilton, M. A. McKervey, J. J. Rooney, and J. F. Malone, *ibid.*, 1027 (1976); W. Burns, M. A. McKervey, T. R. B. Mitchell, and J. J. Rooney, *J. Am. Chem. Soc.*, 100, 906 (1978).
10. F. D. Rossini, Ed., *Experimental Thermochemistry*, Vol. I, Interscience, New York, 1956.
11. See, for example: S. H. Fishtine, *Ind. Eng. Chem.*, 55, 20, 49, 47 (1963).
12. T. Clark, M. A. McKervey, H. Mackle, and J. J. Rooney, *J. Chem. Soc., Faraday Trans. I*, 70, 1279 (1974).
13. M. I. Page, *Chem. Soc. Revs.*, 2, 295 (1973).
14. σ is the symmetry number of the molecule, and is defined as the number of proper rotations in the point group that describes the symmetry of the molecule, H. Eyring, Ed., *Physical Chemistry, An Advanced Treatise*, Vol. II, Academic, New York, 1967, p. 49.

15. P. v. R. Schleyer, K. R. Blanchard, and C. D. Woody, *J. Am. Chem. Soc.*, **85**, 1358 (1963).
16. W. J. Hehre, R. F. Stewart, and J. A. Pople, *J. Chem. Phys.*, **51**, 2657 (1969).
17. M. J. S. Dewar and W. Thiel, *J. Am. Chem. Soc.*, **99**, (a) 4899, (b) 4907 (1977).
18. E. M. Engler, J. D. Andose, and P. v. R. Schleyer, *J. Am. Chem. Soc.*, **95**, 8005 (1973).
19. N. L. Allinger, M. T. Tribble, M. A. Miller, and D. H. Wertz, *ibid.*, **93**, 1637 (1971). Reviews: (a) N. L. Allinger, *Adv. Phys. Org. Chem.*, **13** 1 (1976); (b) O. Ermer, *Structure and Bonding*, **27**, 161 (1976); (c) S. R. Miketic and K. Rasmussen, *The Consistent Force Field*, Springer, Berlin, 1977; (d) D. F. Detar et al., *Comp. and Chem.*, **1**, 139 (1977); (e) A. I. Kitaigorodsky, *Chem. Soc. Revs.*, **7**, 133 (1978).
20. See tables in Ref. 25b,c.
21. See, for example: (a) J. Slutsky, E. M. Engler, and P. v. R. Schleyer, *J. Chem. Soc., Chem. Commun.*, 685 (1973); (b) V. Z. Williams, Jr., P. v. R. Schleyer, G. J. Gleicher, L. B. Rodewald, *J. Am. Chem. Soc.*, **88**, 3862 (1966).
22. (a) W. T. Wipke, unpublished; (b) W. T. Wipke and T. M. Dyott, *J. Am. Chem. Soc.*, **96**, 4834 (1974); (c) W. T. Wipke and T. M. Dyott, *J. Chem. Inf. Comput. Sci.*, **15**, 140 (1975); (d) for examples of use, see Refs. 47–49, and 57.
23. (a) R. E. Carbart, D. E. Smith, H. Brown, and N. S. Sridharan, *J. Chem. Inf. Comput. Sci.*, **15**, 124 (1975); (b) D. H. Smith, *ibid.*, **15**, 203 (1975); N. Tanaka, T. Iizaka, and T. Kan, *Chem. Lett.*, 539 (1974); (c) N. Tanaka, T. Kan, T. Iizuka, *J. Chem. Inf. Comput. Sci.*, **3**, 162 (1979).
24. S. Sasaki, Y. Hirota, S. Ochiai, and Y. Kudo, *Bunseki Kagaku*, **21**, 916 (1972), cf. *Chem. Abstr.*, **77**, 100307p (1972). JAL-30XA is optional software available for the JNM-FX60 Fourier Transform NMR Spectrometer equipped with a 16K minicomputer (JEOLCO, Ltd).
25. (a) S. W. Benson, F. R. Cruickshank, D. M. Golden, G. R. Haugen, H. E. O'Neal, A. S. Rodgers, R. Shaw, and R. Walsh, *Chem. Rev.*, **69**, 279 (1969); (b) J. D. Cox and G. Pilcher, *Thermochemistry of Organic and Organometallic Compounds*, Academic, New York, 1970; (c) D. R. Stull, E. F. Westrum, Jr., and G. C. Sinke, *The Chemical Thermodynamics of Organic Compounds*, Wiley, New York (1969); (d) P. v. R. Schleyer, J. E. Williams, and K. R. Blanchard, *J. Am. Chem. Soc.*, **92**, 2377 (1970).
26. We define strain as the difference between the measured (or calculated) heat of formation and a strain free heat of formation computed from increments for CH₃, CH₂, CH, C derived from strain free saturated hydrocarbons. The "strain" in double bonds arises from the greater strength of two sigma bonds as compared to a π bond.
27. C. W. Beckett, K. S. Pitzer and R. Spitzer, *J. Am. Chem. Soc.*, **69**, 2488 (1947); C. Boelhouwer, G. A. M. Diepen, J. van Elk, P. Th. van Raaij, and H. I. Waterman, *Brennstoff-Chemie*, **39**, 299 (1958).
28. H. K. Hall, Jr., C. D. Smith, and J. H. Baldt, *J. Am. Chem. Soc.*, **95**, 3197 (1973).
29. Estimated from ΔH_f° cyclohexadiene (Ref. 25b) using group increment for methyl (Ref. 25b).
30. S. S. Wong and E. F. Westrum, Jr., *J. Am. Chem. Soc.*, **93**, 5317 (1971).
31. Estimated from ΔH hydrogenation, R. B. Turner, A. D. Jarrett, P. Goebel, and B. J. Mallon, *J. Am. Chem. Soc.*, **95**, 790 (1973) and ΔH_f° for bicyclo[3.2.1]octane calculated by Engler force field (Ref. 18).
32. P. K. Freeman, R. B. Kinnel, T. D. Ziebarth, *Tetrahedron Lett.*, 1059 (1970); R. R. Sauers and E. M. O'Hara, *J. Am. Chem. Soc.*, **96**, 2510 (1974); R. R. Sauers, K. W. Kelly, B. R. Sickles, *J. Org. Chem.*, **37**, 537 (1972).
33. This is true for most bridgehead substituted cage molecules we have investigated despite the expectation that replacing H by methyl should produce no difference in strain. This difference may be due to the fact that there is strain associated with the 109–110° C—C—C angle at an unsubstituted adamantane bridgehead (cf. "ideal" C—C—C angle 112°, as in isobutane) but there is no angle strain associated with the same 109–110° angle of a methyl substituted bridgehead (ideal C—C—C angle now = 109.4°) as in neopentane.

34. A. Schneider, R. W. Warren, and E. J. Janoski, *J. Am. Chem. Soc.*, **86**, 5365 (1964); A. Schneider, R. W. Warren, and E. J. Janoski, *J. Org. Chem.*, **31**, 1617 (1966); A. Schneider, R. W. Warren, and E. J. Janoski, *Trans. N.Y. Acad. Sci.*, **30**, 3 (1967).
35. P. v. R. Schleyer and E. Wiskott, *Tetrahedron Lett.*, 2845 (1967).
36. P. v. R. Schleyer, *J. Am. Chem. Soc.*, **79**, 3292 (1957); P. v. R. Schleyer and M. M. Donaldson, *ibid.*, **82**, 4645 (1960).
37. D. E. Johnston, M. A. McKervey and J. J. Rooney, *ibid.*, **93**, 2798 (1971).
38. P. v. R. Schleyer and R. D. Nicholas, *Tetrahedron Lett.*, 305 (1961); S. Landa and V. Podrozhkova, *Neftekhimiya*, **14**, 547, 551 (1974).
39. E. I. Bagrii, T. Yu. Frid, and P. I. Sanin, *Bull. Div. Chem. Sci. USSR*, 459 (1970).
40. P. v. R. Schleyer, G. J. Gleicher, and C. A. Cupas, *J. Org. Chem.*, **31**, 2014 (1966).
41. E. M. Engler, M. Farcasiu, A. Sevin, J. M. Cense, and P. v. R. Schleyer, *J. Am. Chem. Soc.*, **95**, 5769 (1973).
42. E. Ōsawa, K. Aigami, Y. Inamoto, Y. Fujikura, N. Takaishi, Z. Majerski, P. v. R. Schleyer, E. M. Engler, and M. Farcasiu, *J. Am. Chem. Soc.*, **99**, 5361 (1977).
43. R. H. Boyd, *J. Chem. Phys.*, **49**, 2574 (1968).
44. S. Chang, D. McNally, S. Shary-Tehrany, M. J. Hickey, and R. H. Boyd, *J. Am. Chem. Soc.*, **92**, 3109 (1970).
45. W. G. Dauben, C. H. Schallhorn, and D. L. Whalen, *J. Am. Chem. Soc.*, **93**, 1446 (1971).
46. E. Ōsawa, L. W. Chang, P. v. R. Schleyer, and V. V. Kane, *Tetrahedron Lett.*, 4189 (1974).
47. S. Godleski, P. v. R. Schleyer, E. Ōsawa, Y. Inamoto, and Y. Fujikura, *J. Org. Chem.*, **41**, 2596 (1976).
48. S. Godleski, P. v. R. Schleyer, and E. Ōsawa, *J. Chem. Soc., Chem. Commun.*, **38**, (1976).
49. D. Farcasiu, E. Wiskott, E. Ōsawa, W. Thielecke, E. M. Engler, J. Slutsky, P. v. R. Schleyer, and G. J. Kent, *J. Am. Chem. Soc.*, **96**, 4669 (1974); E. Ōsawa, E. M. Engler, S. A. Godleski, Y. Inamoto, G. J. Kent, M. Kausch, and P. v. R. Schleyer, *J. Org. Chem.*, **45**, 984 (1980).
50. E. Ōsawa, D. Farcasiu, P. v. R. Schleyer, E. M. Engler, A. Sevin, D. B. Ledlie, G. J. Kent, A. Togashi, Y. Tahara, T. Iizuka, N. Tanaka, T. Kan, submitted for publication.
51. T. M. Gund, V. Z. Williams, Jr., E. Osawa, and P. v. R. Schleyer, *Tetrahedron Lett.*, 3877 (1970).
52. S. S. Berman, Yu. V. Denisov and L. A. Petrov, *Neftekhimiya*, **14**, 341 (1974).
53. S. A. Godleski, P. v. R. Schleyer, E. Ōsawa, and G. J. Kent, *J. Chem. Soc., Chem. Commun.*, 976 (1974); G. J. Kent, S. A. Godleski, E. Ōsawa, and P. v. R. Schleyer, *J. Org. Chem.*, **42**, 3852 (1977).
54. E. Ōsawa, P. v. R. Schleyer, and J. Slutsky, to be submitted.
55. E. Ōsawa, A. Furusaki, T. Matsumoto, E. Wiskott, and P. v. R. Schleyer, *Tetrahedron Lett.*, 2463 (1976); (a) E. Osawa, A. Furusaki, N. Hashiba, T. Matsumoto, V. Singh, Y. Tahara, E. Wiskott, M. Farcasiu, T. Iizuka, N. Tanaka, T. Kan, and P. v. R. Schleyer, *J. Org. Chem.*, **45**, 2985 (1980).
56. T. M. Gund, E. Ōsawa, V. Z. Williams, Jr., and P. v. R. Schleyer, *J. Org. Chem.*, **39**, 2979 (1974).
57. T. M. Gund, P. v. R. Schleyer, P. H. Gund, and W. T. Wipke, *J. Am. Chem. Soc.*, **97**, 743 (1975).
58. R. Hamilton, D. E. Johnston, M. A. McKervey, and J. J. Rooney, *J. Chem. Soc., Chem. Commun.*, 1209 (1972).
59. S. A. Goscin, unpublished results, A.B. Thesis, Princeton University.
60. (a) S. T. Rao, M. Sundaralingam, E. Ōsawa, E. Wiskott, and P. v. R. Schleyer, *Chem. Commun.*, 861 (1970); (b) S. T. Rao, and M. Sundaralingam, *Acta Cryst.*, **B28**, 694 (1972).
61. J. Collins, P. v. R. Schleyer and W. Nowacki, unpublished results.
62. M. A. McKervey, *Tetrahedron*, **36**, 971 (1980).

Electrical Effect Substituent Constants for Correlation Analysis

BY MARVIN CHARTON

Department of Chemistry, Pratt Institute, Brooklyn, New York

CONTENTS

I.	Introduction	120
A.	Composition of the Electrical Effects.	120
B.	Localized Effect Parameters	121
II.	Definition of Localized Effect Substituent Constants	129
A.	Criteria for Choice of a Reference Set.	129
B.	Choice of a Reference Set	130
C.	Definition of Localized Electrical Effect Substituent Constants.	131
D.	Definition of σ_I	136
III.	Evaluation of σ_I Constants	138
A.	Methods for Evaluation of Substituent Constants.	138
B.	Secondary Sources of σ_I Constants	142
C.	Validity of the σ_I Constants in Nonprotonic Media	166
D.	Comparison of Localized Effect Substituent Constants	169
E.	Variation of σ_I Constants with Structure	172
IV.	The σ_D Constants	177
A.	Best Values of σ_m and σ_p Constants	178
B.	The σ_R Constants	182
C.	Validity of the σ_R Constants in Various Media	190
D.	Determination of σ_m and σ_p in Nonaqueous Media	196
E.	A Test of the Validity of the σ_R Constants	197
F.	Variation of the σ_R Constants with Structure	201
G.	The σ_R^0 Constants	201
H.	The σ_R^+ Constants	202
I.	The σ_R^- Constants	215
V.	Estimation of Substituent Constants	225
A.	Z Bonded to carbon	226
B.	Substituents at Elements Other Than Carbon	232
C.	Other Methods of Estimation of Substituent Constants	236
VI.	Separation of Electrical Effects	238
A.	Swain-Lupton Separation	238
B.	Exner Separation	242
VII.	Highly Variable Substituent "Constants"	245
A.	Ionic Groups	245
B.	HW Groups	246

VIII. Conclusions	246
Acknowledgment	247
Appendix	247
References	249

I. INTRODUCTION

Linear free energy relationships have been of great use to physical organic chemists in the description and rationalization of structural effects on chemical reactivity and physical properties. They are now finding ever-increasing use in attempts to predict biological activity. In describing the effect of substituents on chemical reactivity, a number of studies have found that the use of substituent parameters resulting from a separation of electrical effects into "localized" (field and/or inductive) and "delocalized" (resonance) contributions gives best results. This seems to be the case for benzene (1-3), polycyclic aromatic (4,5), heteroaromatic (5), and nonaromatic unsaturated (6) systems. It is of great interest, then, to have available the largest possible number of reliable substituent constants for the localized and delocalized electrical effects. Less reliable constants will also be of some limited use if they are clearly reported as doubtful values. Finally, methods for the estimation of unknown substituent constants are desirable. Although estimated constants are not as dependable as reliable constants determined experimentally, they are nevertheless of considerable use.

A. Composition of Electrical Effects

The factoring of the overall effect of a substituent into components seems to have been first proposed by Branch and Calvin (7). Although there are a number of possible different electrical effects (8) it is most convenient operationally to consider only two, the localized and delocalized effects. The localized effect is some combination of the inductive (through a bond) and field (through space) effects. It is the only effect that is transmitted when a substituent is bonded to sp^3 hybridized carbon. Although, of course, even electrons in σ molecular orbitals are delocalized, they are less extensively delocalized than are π electrons. To paraphrase George Orwell, all electrons are delocalized but some are more delocalized than others. Thus, when a substituent is bonded to a skeletal group atom which cannot be involved in the formation of π molecular orbitals, the substituent is said to exert only a localized electrical effect. A substituent bonded to sp^2 or sp hybridized carbon is capable of exerting in addition to the localized effect, a delocalized effect as well. If the localized effect substituent constant is represented by σ_L and the delocalized effect constant by σ_D , the overall electrical substituent effect, σ_T is given by

$$\sigma_{TX} = \lambda\sigma_{LX} \quad (1)$$

when X is bonded to sp^3 hybridized carbon and,

$$\sigma_{TX} = \lambda \sigma_{LX} + \delta \sigma_{DX} \quad (2)$$

when X is bonded to sp^2 or sp hybridized carbon.

B. Localized Effect Parameters

The first attempt at the definition of a localized effect parameter is due to Taft (9), who proposed the σ^* constants. These constants are defined by the equation

$$\sigma_X^* = \left(\frac{1}{\rho_0^*} \right) \left[\log \left(\frac{k_X}{k_{Me}} \right)_B - \log \left(\frac{k_X}{k_{Me}} \right)_A \right] \quad (3)$$

in which B and A designate base and acid catalyzed hydrolyses of carbonyl substituted esters. Equation 3 results from the combination of Equations 4 and 5,

$$\log \left(\frac{k_X}{k_{Me}} \right)_B = \rho_B^* \sigma_X^* + \delta_B E_{SX} + R_{BX} \quad (4)$$

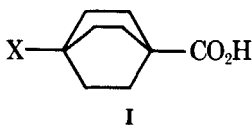
$$\log \left(\frac{k_X}{k_{Me}} \right)_A = \rho_A^* \sigma_X^* + \delta_A E_{SX} + R_{AX} \quad (5)$$

with $\rho_A^* = 0$, $R_A = R_B = 0$, and $\delta_A = \delta_B$. In these relationships, E_S is a steric parameter and R is the resonance effect. The value of ρ_0^* in Equation 3, 2.48 is obtained from the values of ρ_A from the correlation of rates of esterification of 3- or 4-substituted benzoic acids and ρ_B from the correlation of rates of base-catalyzed 3- or 4-substituted benzoate hydrolyses by the Hammett equation. This choice was determined by the desire to place the σ^* values on the same scale as the Hammett σ_m and σ_p constants. The ρ_A value, which ranges from -0.2 to $+0.5$ is assumed to be 0, averaging the available ρ_B values gives 2.48. Actually this attempt to place the σ^* values on the same scale as σ_m and σ_p is unsuccessful. The σ_m and σ_p constants apply to systems of the type XGY where X is the substituent, Y the active site (the functional group responsible for the observed phenomenon) and G is a skeletal group to which X and Y are bonded (G is m - or p -phenylene when σ_m and σ_p are defined). In the case of Eq. 3, the system studied is of the type XY, in which the substituent is bonded directly to the active site. Thus, in the case of σ_m and σ_p constants, the effect of the X group must be transmitted through G and the medium which surrounds it, whereas in XY systems this is not the case. The effect of X in XGY must therefore be attenuated relative to its effect in XY.

The Taft σ^* values have been well reviewed by Shorter (10). Their validity for alkyl groups has been a matter for considerable discussion (10-16). It seems

probable that σ^* values for alkyl groups do not accurately reflect the electrical effect of these groups.

The major disadvantages of the σ^* constants are due to their definition as the difference between two processes, one involving both the localized electrical effect and steric effects, and the other involving only steric effects. The first disadvantage is that the assumption that $\delta_A = \delta_B$ may be in error. The second is that two experimental measurements are necessary for the determination of each σ^* constant. An additional disadvantage is that σ^* values are *not* on the same scale as σ_m and σ_p values.



An alternative approach to the definition of localized effect parameters is due to Roberts and Moreland (17) who proposed the use of $pK_{a's}$ of 4-substituted bicyclo[2.2.2]octane-1-carboxylic acids, **I**, to define σ' constants. In this system the substituent, X is bonded to an sp^3 hybridized carbon atom; thus X exerts only the localized effect. As **I** is a rigid system free from conformational effects, and the substituent X and the active site CO_2H are not in proximity to each other, steric effects are not observed. Structures such as **I** are therefore ideal for the definition of localized effect parameters. The σ'_X parameters were defined from the equation

$$\sigma'_X \equiv \frac{pK_{aIX} - pK_{aIH}}{\rho'} \quad (6)$$

with ρ' set equal to ρ for the ionization of 3- or 4-substituted benzoic acids in the same medium (50% v/v aqueous ethanol) at the same temperature (25°C). Thus, if the 1,4-bicyclooctylene group is as effective in transmitting the substituent effect as is the phenylene group, the σ' constants will be on the same scale as the σ_m and σ_p constants. Whether these groups are or are not equally effective in transmitting the localized effect depends on the mode of transmission of the effect. If the predominant mode is the field effect, the 1,4-bicyclooctylene and 4-phenylene groups will transmit the localized effect equally well if their molecular geometry is very similar. According to Kirkwood and Westheimer (18), the equation

$$\log \frac{K_X}{K_H} = \frac{e\mu_X \cos\theta}{2.303RT D_E r^2} \quad (7)$$

describes the effect of substitution on the acid strength of a set of $XGCO_2H$.

In this relationship, e is the charge on a proton, μ is the moment of the

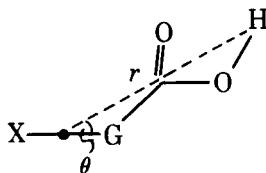


Figure 1.

X—G bond, r is the distance from the proton to the dipole (this is frequently, but not always, taken as the distance from the midpoint of the X—G bond to the ionizable proton), and θ is the angle made by the distance r with the X—G bond (Fig. 1).

Combining Equation 7 with the Hammett equation gives (19)

$$\rho\sigma_X = \frac{e\mu_X \cos\theta}{2.303 RT D_E r^2} \quad (8)$$

In a set of related compounds D_E , the effective dielectric constant must be constant throughout (that is, independent of X). The reaction constant ρ is a function of the active site Y, the medium, the temperature, the pressure, and the skeletal group G. At constant Y, medium, T , and P , ρ is a function only of G. Thus, writing Equation 8 for the 1,4-bicyclooctylene(BO) and 4-phenylene (Pn) skeletal groups, (8a and 8) and dividing Equation 8a by 8b gives

$$\frac{\rho_{Pn}}{\rho_{BO}} = \frac{D_{E_{BO}} \cos\theta_{Pn} r^2_{BO}}{D_{E_{Pn}} \cos\theta_{BO} r^2_{Pn}} \quad (9)$$

If the shapes of the Pn and BO groups are reasonably similar,

$$D_{E,BO} \cong D_{E,Pn}$$

and

$$\frac{\rho_{Pn}}{\rho_{BO}} = \frac{\cos\theta_{Pn} r^2_{BO}}{\cos\theta_{BO} r^2_{Pn}} \quad (10)$$

Furthermore, if the shapes of the Pn and BO groups are similar, it follows that

$$\cos\theta_{Pn} \cong \cos\theta_{BO} \quad (11)$$

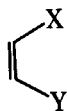
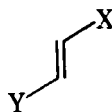
$$r_{Pn} \cong r_{BO} \quad (12)$$

and

$$\rho_{Pn} = \rho_{BO} \quad (13)$$

Calculations of r and θ do indeed show that they are not significantly different for Pn and BO.

If the predominant mode of transmission of the localized effect is the inductive effect, it is unlikely that the Pn and BO groups would be equally effective in transmitting the effect. In the BO group there are three pathways for transmitting the effect and all the carbon atoms in the group are hybridized sp^3 . Thus, if we represent the fall-off factor for the transmission as f_s , a charge q at C^4 of the BO group will have a value of $3qf_s^3$ at C^1 of the BO group. In the same manner, if f_b represents the fall-off factor of the inductive effect through a bond in the benzene ring, a charge q at C^4 will have a value of $2qf_b^3$ at C of the Pn group. It follows then that unless there is a fortuitous situation in which the larger value of the f_b compensates for the additional pathway in the BO group, the two groups will differ in their transmission of the localized effect. This seems highly unlikely. In fact, considerable evidence has accumulated which suggests that in solution in protonic solvents, the field effect is the best model for the transmission of the localized effect. Evidence for this viewpoint is summarized by Stock (20). Further evidence is provided by the observation of Charton (6), that the transmission of the localized electrical effect in *cis*-vinylene systems, **II**, differs from that in *trans*-vinylene systems, **III**; an observation which cannot be accounted for by the inductive effect.

**II****III**

Thus, the use of the bicyclooctane system for defining localized effect substituent constants scaled to the σ_m and σ_p constants is feasible. Unfortunately, the work of Roberts and Moreland reveals certain deficiencies. Only five substituents were studied by these workers, not enough to permit satisfactory definition of a fundamental set of localized effect constants. The pK_a s determined by Roberts and Moreland were apparent, not thermodynamic values. Finally, it was shown by Ehrenson, Brownlee, and Taft that, in the ionization of 3- or 4-substituted benzoic acids in various protonic solvents, the composition of the electrical effect ϵ is a function of the medium. ϵ is defined by the equation

$$\epsilon \equiv \frac{\lambda}{\delta} \quad (14)$$

where λ and δ are the coefficients of σ_L and σ_D in Equation 2. The composition of the electrical effect may also be reported in terms of the percent delocalized effect, P_D , given by the relationship

$$P_D \equiv \frac{\delta \cdot 100}{\lambda + \delta} \quad (15)$$

The σ_m and σ_p constants are defined from the ionization of the appropriately substituted benzoic acids in water at 25°. The attempt of Roberts and Moreland to place the σ' constants on the same scale as the σ_m and the σ_p constants by setting ρ' in Equation 6 equal to ρ for the 4-substituted benzoic acids requires for its success that the magnitude of the localized effect in the σ_p constants be the same as that in the σ' constants.

If Equation 2 written for σ_p is substituted in the Hammett equation

$$Q_X = \rho \sigma_{pX} + h \quad (16)$$

it gives

$$Q_X = \rho \lambda_p \sigma_{LX} + \rho \delta_p \sigma_{DX} + h \quad (17)$$

$$= L_p \sigma_{LX} + D_p \sigma_{DX} + h \quad (18)$$

To place σ' on the same scale as σ_m and σ_p it is necessary for ρ' to equal L_p . In solvents other than water, however, correlation of ionization constants of 4-substituted benzoic acids with the extended Hammett equation

$$Q_X = L \sigma_{LX} + D \sigma_{DX} + h \quad (19)$$

gives values of $L \neq L_p$. Thus, the σ' values are not likely to be on the same scale as the σ_p and σ_m values.

Taft and Lewis (21) proposed the σ_I constants based on the relationship

$$\sigma_{IX} = 0.45 \sigma_{X.CH_2}^* \quad (20)$$

Equation 20 seems to be based on (9) the equation

$$\sigma'_X = 0.45 \sigma_{X.CH_2}^* \quad (21)$$

Thus, $\sigma_{IX} \equiv \sigma'_X$. These σ_I values of Taft and Lewis, which were actually based on σ^* values, were used as a basis set by Charton (22) for the purpose of obtaining a large number of σ_I constants as a measure of the localized effect. Charton correlated pK_a s of substituted acetic acids with the σ_I constants of the basis set. The resulting correlation equation were then used to obtain many additional σ_I values. The method has four advantages: (1) There are a large number of pK_a values for substituted acetic acids available in the literature, many of which are very reliable values. (2) Only a single experimental measurement is required for the determination of a σ_I constant. (3) The synthesis and purification of substituted acetic acids is relatively easy. (4) Good values of pK_a for most substituted acetic acids are determined with relative ease. There are certain potential disadvantages, however, to the use of acetic acid pK_a s for the determination of localized effects. These are (1) The difficulty of determining

reliable pK_a values for XCH_2CO_2H when X is a strong electron acceptor group such as NO_2 . (2) The possibility of steric effects. Very large substituents such as bulky aryl groups are said to exhibit steric effects (23,24). (3) Intramolecular hydrogen bonding may occur with certain substituents. (4) The possibility that a single methylene group is insufficient to prevent the existence of the delocalized effect must be considered. Alkyl and substituted alkyl groups are known to be delocalized effect electron donors when bonded to π -bonded skeletal groups such as phenylene, vinylene, ethylene, or carbonyl. It follows, then, that when X is a π -bonded substituent, the methylene group can interact with it by the delocalized effect. The methylene group can also be expected to interact with the carbonyl group by the delocalized effect, an argument supported by the observations of Charton (6) that pK_a s of the compounds XCO_2H are best correlated by the Hammett equation. Since all alkyl and cycloalkyl groups will interact with π -bonded groups in this way, the same interactions will occur when a π -bonded substituent and a carboxyl group active site are attached to the BO skeletal group. In this case, no delocalized effect interaction involving substituent skeletal group and reaction site is possible, thus no exaltation of the delocalized effect can occur. The question is whether or not that is also the case with the methylene group.

Taft modified the definition of σ_I , redefining it as

$$\sigma_{IX} \equiv \left(\frac{1}{6.23} \right) \left[\log \left(\frac{k_X}{k_H} \right)_B - \log \left(\frac{k_X}{k_H} \right)_A \right] \quad (22)$$

He and his co-workers also observed that the F^{19} chemical shifts of 3-substituted fluorobenzenes are predominantly a function of the localized effect, and advocated their use in the determination of σ_I values (24c,24d). Many authors have determined localized effect parameters in this manner. This work of Taft and his group has been criticized by Dewar and his co-workers (24e,24f). Charton (22) has observed that a correlation of σ_I values obtained by Taft and his co-workers (24c) with those determined from acetic acid pK_a s shows that they are on a different scales. In view of the fact that 3-substituted fluorobenzenes are not entirely free from the delocalized effect, and for the other possible objections cited above, the F^{19} shielding parameters of this system should not be used to determine reliable values of the localized effect parameter.

Yukawa and Tsuno (24g,24h) have proposed as a localized effect parameter, the quantity σ_i , given by

$$\sigma_{iX} \equiv 0.74 \sigma'_X \quad (23)$$

This definition is based on the equation

$$\sigma_{pX}^0 = \sigma_{iX} + \sigma_{\pi X} \quad (24)$$

Ehrensom, Brownlee, and Taft (1) have reported a set of 26 σ_I values which they

consider to be reliable. This set is a slight modification of the values previously reported by Taft and his co-workers. The manner by which the new values were arrived at is not given.

Exner (24*i*,24*j*) has observed that for many substituents the ionization constants of 3-substituted and 4-substituted benzoic acids are related by the equation

$$\log K_{4X} - \log K_H = m(\log K_{3X} - \log K_H) \quad (25)$$

On this basis he concludes that the ratio λ_p/λ_m where λ is obtained by writing Equation 2 for σ_m and σ_p is equal to 1.14, that substituents for which Equation 24 is obeyed have a negligible delocalized effect, and that in order to place them on the same scale as σ_m and σ_p it is necessary to multiply σ_I constants by a factor of 1.10. Charton (24*k*) has pointed out that Equation 25 for those substituents which follow it is equivalent to

$$\sigma_{LX} = \frac{(m\delta_m - \delta_p)}{(\lambda_p - m\lambda_m)} \sigma_{DX} \quad (26)$$

or

$$\sigma_{LX} = c\sigma_{DX} \quad (27)$$

The Dewar–Golden–Harris (24*l*) treatment of substituent effects bases its localized effect parameters, F , on the ionization constants of 4-substituted bicyclo[2.2.2]octane-1-carboxylic acids. Thus, for bicyclooctane acids,

$$\sigma_{im} = F_X R_{im} \quad (28)$$

and

$$R_{im} = \frac{1}{r_{in}} - \frac{0.9}{r_{jn}} \quad (29)$$

where r_{in} and r_{jn} are the distances (in units of the benzene bond length) between the points in and jn shown in Fig. 2. Then,

$$\log K_X - \log Ka_H = \rho\sigma_{im} = \rho F_X R_{im} \quad (30)$$

and

$$F_X = \frac{\log Ka_X - \log Ka_H}{\rho R_{im}} \quad (31)$$

Forsyth (24*m*) has determined localized effect constants, D , by means of modifications of the original Dewar–Grisdale (24*n*) treatment. The σ_m^+ and σ_p^+ constants of Brown and Okamoto (240) constituted the experimental data used in the determination of D . These constants again require two experimental

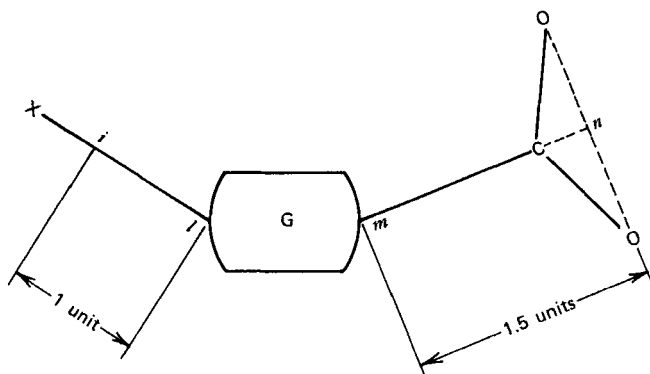


Figure 2. Dewar-Golden-Harris model for substituted carboxylic acids.

measurements for their determination and of course are not on the same scale as σ_m and σ_p .

Swain and Lupton (25) defined their localized parameter, F , by again using the 4-substituted bicyclo[2.2.2]octane-1-carboxylic acids as the model system. The pK_a values measured by Holtz and Stock (26) in 50% aqueous ethanol at 25° constituted the major part of the data which were then used to define F by means of the equation

$$F_X \equiv pK_{aX} - pK_{aH} \quad (32)$$

This equation was modified by Hansch and his co-workers (16c), who introduced the factor $1/1.65$ to place the F values on the same scale as σ_m and σ_p . Thus,

$$F_X \equiv \left(\frac{1}{1.65} \right) (pK_{aX} - pK_{aH}) \quad (33)$$

The use of the factor 1.65 seems to be due to the report of Holtz and Stock that a correlation of their pK_{aX} values with σ_I had a slope of 1.65. The value of 1.65 apparently is in error; the correct slope is 1.43 (27). This group of 14 defined F values was then correlated with σ_m and σ_p constants to give the equation

$$F_X = 1.369 \sigma_{mX} - 0.373 \sigma_{pX} - 0.009 \quad (34)$$

There are a number of problems connected with the use of the F_X values. They include: (1) Four of the 14 pK_a s used in the definition of F_X are estimated from other solvents; thus their reliability is in doubt. (2) Of the 14 groups included in the correlation which resulted in Equation 34, five have σ_m and σ_p values which were assigned errors of ± 0.1 sigma units (28) and one group had σ_m and σ_p values of unknown error. (3) The determination of new F constants requires

two experimental measurements, one for σ_m and one for σ_p . (4) Values of σ_m and σ_p determined from pK_a s of benzoic acids in solvents other than water may be in error due to the variation in the composition of the electrical effect with solvent noted previously. (5) The F constants are probably not on the same scale as the σ_m and σ_p constants.

One of the most recent attempts to define localized parameters is that of Grob and Schlageter (29). These σ^q constants are defined by the equation

$$\sigma^q = pK_{aX} - pK_{aH} \quad (35)$$

where the thermodynamic pK_a s are of the appropriately-substituted quinuclidinium ions in water at 25°. As the authors point out, this system, like the bicyclocloctane system, is free of steric and conformational effects. It has the additional advantage over the bicyclocloctane system that it is much more sensitive to electrical effects, as might be expected from a comparison of the distance from the midpoint of the X—G bond to the ionizable proton in the two systems. There are some disadvantages to the σ^q constants, however. They include: (1) The scale: As no attempt has been made to place the σ^q constants on the same scale as σ_m and σ_p constants, comparison of the magnitude of the electrical effect on reactions of saturated aliphatic systems with benzene derivatives is difficult. (2) Only 38 σ^q constants are available. (3) Grob and Schlageter have indicated that the σ^q constants of F, Cl, Br, and I are uncertain. Charton (29a) has recently attempted, unsuccessfully, to scale the localized effect and parameter constants correctly.

It is obviously desirable in view of the large number of substituent constants that have been proposed as measures of the localized electrical effect try to bring some order into the confusion which dominates this area. This is of particular importance to the many workers in other fields who would like to make use of linear free energy relationships in their own work and are overwhelmed by the morass of different constants that have been proposed.

II. DEFINITION OF LOCALIZED EFFECT SUBSTITUENT CONSTANTS

A. Criteria for Choice of a Reference Set

From the preceding discussion of previously proposed localized effect parameters, the following requirements for the reference set are readily apparent.

1. Only the localized effect can occur in the reference set.
2. The skeletal group of the reference set is rigid and therefore no conformational equilibria can occur.

3. The skeletal group causes the distance between the active site and substituent to be large enough to exclude the possibility of steric effects.
4. The reference set must permit the defined localized effect parameters to be placed on the same scale as the σ_m and σ_p constants. This permits ready comparison of substituent electrical effect magnitude of systems in which the substituent is bonded to sp^3 hybridized carbon to that in systems in which the substituent is bonded to sp^2 or sp hybridized carbon.
5. The property measured should be easy to determine accurately.
6. The members of the reference set should be easily prepared and purified.
7. The property measured should be as sensitive as possible to the substituent effect, thus making it possible to obtain reliable substituent constants for groups that exert only a small effect.
8. The members of the reference set should be stable at the conditions (medium, temperature, pressure) under which the property is measured.
9. The property measured should be a chemical property.

B. Choice of a Reference Set

The skeletal groups that best fit requirements 1, 2, and 3 are the BO group, and the quinuclidine group (Qun) which is actually a 1-aza-1,4-bicyclo[2.2.2]-octylene group. The property that best fits requirements 5 and 9 is an ionization constant. Ionization constants can generally be determined with greater ease and precision than rate constants, or most other equilibrium constants. The preparation of BO and Qun derivatives is not very simple, and there does not seem to be any preparative advantage of either of these skeletal groups. The 4-substituted quinuclidinium ion pK_{as} are very much more sensitive to substituent effects than are those of 4-substituted bicyclo[2.2.2]octane-1-carboxylic acids. The 4-halo-quinuclidinium ions may not be completely stable at the conditions under which the pK_{as} are determined, however. An important point is the requirement, 4, that the reference set must allow the defined substituent constants to be placed on the σ_m , σ_p scale. If, in accord with the greater part of the evidence, the mode of transmission of the localized electrical effect is the field effect, then the substituent constants may be placed on the σ_p scale (and therefore the σ_m scale as well) by choosing a skeletal group with the same (within 5%) values of r and θ as the 4-phenylene group attached to the same active site. As was noted previously, 4-substituted benzoic acids and 4-substituted bicyclo[2.2.2]octane-1-carboxylic acids meet this requirement. The aromatic system which corresponds to the 4-substituted quinuclidinium ion is the 4-substituted pyridinium ion. Unfortunately, the geometry of quinuclidines or quinuclidinium ions do not seem to have been examined as yet. Using the best available estimates for bond lengths and bond angles, r for the 4-substituted quinuclidinium ions

is 1.09 times r for 4-substituted pyridinium ions, although the θ values are the same. Thus, the 4-substituted bicyclo[2.2.2]octane-1-carboxylic acids are the best choice for a reference set for the definition of localized effect substituent constants.

The best set of pK_a s of these acids is that determined by Holtz and Stock in 50% w/w aqueous ethanol at 25°C. To define σ_L constants on the same scale as the Hammett σ_p constants it is necessary to set the magnitude of the localized effect on the bicyclooctane acids equal to the magnitude of the localized effect on the 4-substituted benzoic acids under the same reaction conditions. The composition of the electrical effect on the ionization of benzoic acids is solvent dependent. Thus, simply setting L in the equation

$$pK_{aX} = L \sigma_{LX} + h \quad (36)$$

equal to the value of ρ obtained by correlation of pK_a s of 4-substituted benzoic acids determined under the same conditions with σ_p constants is not satisfactory. The composition of the electrical effect in 4-substituted benzoic acids in aqueous ethanol mixtures is different from that in pure water. What is required is a method of determining L in the correlation by the extended Hammett equation of pK_a s for 4-substituted benzoic acids, and since the available data has been determined in aqueous ethanol mixtures other than 50% w/w, a method of interpolating a value of L in the latter solvent from the L values determined in various aqueous ethanol mixtures. A method for solving this problem is derived subsequently.

C. Definition of Localized Electrical Effect Substituent Constants

The localized effect substituent parameter σ_L may be defined

$$\sigma_L = \Delta \frac{pK_a}{L_t} \quad (37)$$

where L_t is the true scaling factor, and ΔpK_a is the difference in pK_a s of the substituted and unsubstituted members of the reference set. To put the σ_L constants on the same scale as the σ_p constants it is necessary to determine a value for L_t . For this purpose, let us write Equation 2 for σ_p ,

$$\sigma_p = \lambda_p \sigma_L + \delta_p \sigma_D \quad (38)$$

To set the scale, we define

$$\lambda_p \equiv \delta_p \equiv 1 \quad (39)$$

This is done to place σ_L and σ_D on the same scale as σ_p . The delocalized effect substituent constant can then be defined as

$$\sigma_D \equiv \sigma_p - \sigma_L \quad (40)$$

Let us now define an approximate set of σ_L constants designated σ'_L by the equation

$$\sigma'_L = \frac{\Delta p K_a}{L_a} \quad (41)$$

Then a set of approximate σ_D values may be defined as

$$\sigma'_D = \sigma_p - \frac{\Delta p K_a}{L_a} \quad (42)$$

The difference between L_a and L_t is the error in the approximation, E . Then

$$L_a = L_t + E \quad (43)$$

Therefore,

$$\sigma'_D = \sigma_p - \frac{\Delta p K_a}{L_t + E} \quad (44)$$

$$\sigma'_L = \frac{\Delta p K_a}{L_t + E} \quad (45)$$

Some quantity Q may be correlated with the σ'_L and σ'_D constants by means of the equation

$$Q_X = L' \sigma_{LX'} + D' \sigma_{LD'} + h \quad (46)$$

and by the σ_L and σ_D constants by means of the extended Hammett equation

$$Q_X = L \sigma_{LX} + D \sigma_{DX} + h \quad (19)$$

By substituting Equations 36 and 39 in 19; and Equations 44 and 45 in 46, we obtain

$$Q_X = \frac{(L' - D') \Delta p K_a}{L_t + E} + D' \sigma_p + h \quad (47)$$

and

$$Q_X = \frac{(L - D) \Delta p K_a}{L_t} + D \sigma_p + h \quad (48)$$

Then

$$\frac{(L' - D')}{L_t + E} \Delta p K_a + D' \sigma_p + h = \frac{(L - D)}{L_t} \Delta p K_a + D \sigma_p + h \quad (49)$$

$$\left(\frac{L' - D'}{L_t + E} \right) \Delta p K_a + D' \sigma_p = \frac{(L - D)}{L_t} \Delta p K_a + D \sigma_p \quad (50)$$

Equating coefficients gives

$$\frac{L - D}{L_t} = \frac{L' - D'}{L_t + E}; D' = D \quad (51)$$

$$\left(\frac{L' - D'}{L - D} \right) = \frac{L_t + E}{L_t} = 1 + \frac{E}{L_t} \quad (52)$$

As E approaches zero, the left side of Equation 52 approaches 1.

Values of σ'_L were calculated from the pK_a s of 4-substituted-[2.2.2]bicyclooctane-1-carboxylic acids in 50% w/w ethanol-water at 25° by setting L_a in Equation 41 equal to every odd value in the range 1.45 to 1.67. This range was chosen to include all of the choices of L_t which had been made previously from the value of 1.464 used by Roberts and Moreland to the value of 1.65 used by Hansch et al. The corresponding σ'_D values were obtained by means of Equation 42, using the σ_p values of McDaniel and Brown (28). The σ'_L and σ'_D values are given in Table 1. The pK_a values reported by Thuairé (30) for 4-substituted benzoic acids in ethanol-water mixtures and in ethanol (Table 2) were correlated with the 12 sets of σ'_L and σ'_D values obtained above by means of the extended Hammett equation. Also studied were pK_a values for 4-substituted benzoic acids in ethanol-water mixtures determined by Wepster (31). The substituents studied are: set 7; H, Me, Et, OH, OMe, Cl, Br, NO₂, CF₃, CO₂Me; Set 8 = Set 7, less CF₃; Set 6 = Set 8 less Br.

The goodness of fit is excellent, as is shown by the confidence levels of the F test and of the t tests for L and D , and also by the values of $100r^2$ (see Table 3). The values of L and D obtained are shown in Table 4. As expected from Equation 51, D is indeed constant. This is shown by carrying out t tests for the significance of the difference between \bar{D} and D . In all cases the difference was not significant. The striking and important result is that L is also constant as is shown by carrying out t tests of the difference between \bar{L} and L . Thus, the values of L and D obtained for pK_a s of benzoic acids in a given composition of ethanol-water are independent of the choice of substituent constants in the range of interest. To determine whether this is a peculiarity of the data in aqueous ethanol, pK_a s for 4-substituted benzoic acids in dioxane-water mixtures, ROH (where R = Me, Et, Pr, Bu, CH₂OH), acetone-water mixtures and 80% aqueous methylcellosolve (Table 4) were correlated with the σ'_L , σ'_D constants for $L_a = 1.45, 1.55, \text{ and } 1.67$ by means of the extended Hammett equation. Excellent correlations were obtained (Table 3). The values of L and D obtained (see Table 5) again show by means of a t test that both L and D are constant and thus, within the range of interest, L and D are independent of the choice of σ_L and σ_D values. The constancy of L may be accounted for as follows: Substituting D for D' in the left side of Equation 51 and rearranging gives

TABLE I
 Values of σ'_L and σ'_D

X	$L_a = 1.45$		1.47		1.49		1.51	
	σ_L	σ_D	σ_L	σ_D	σ_L	σ_D	σ_L	σ_D
H	0	0	0	0	0	0	0	0
Me	-0.01	-0.16	-0.01	-0.16	-0.01	-0.16	-0.01	-0.16
Et	-0.01	-0.14	-0.01	-0.14	-0.01	-0.14	-0.01	-0.14
OH	0.26	-0.63	-0.25	-0.62	0.25	-0.62	0.25	-0.62
OMe	0.32	-0.59	0.32	-0.59	0.32	-0.59	0.31	-0.58
Cl	0.51	-0.28	0.50	-0.27	0.50	-0.27	0.49	-0.49
Br	0.50	-0.27	0.50	-0.27	0.49	-0.26	0.48	-0.25
NO ₂	0.72	0.06	0.71	0.07	0.70	0.08	0.70	0.08
CF ₃	0.43	0.11	0.42	0.12	0.42	0.12	0.41	0.13
CO ₂ Et	0.32	0.13	0.32	0.13	0.32	0.13	0.31	0.14
X	$L_a = 1.53$		1.55		1.57		1.59	
	σ_L	σ_D	σ_L	σ_D	σ_L	σ_D	σ_L	σ_D
H	0	0	0	0	0	0	0	0
Me	-0.01	-0.16	-0.01	-0.16	-0.01	-0.16	-0.01	-0.16
Et	-0.01	-0.14	-0.01	-0.14	-0.01	-0.14	-0.01	-0.14
OH	0.24	-0.61	0.24	-0.61	0.24	-0.61	0.23	-0.60
OMe	0.31	-0.58	0.30	-0.57	0.30	-0.57	0.30	-0.57
Cl	0.48	-0.25	0.48	-0.25	0.47	-0.24	0.47	-0.24
Br	0.48	-0.25	0.47	-0.24	0.46	-0.23	0.46	-0.23
NO ₂	0.69	0.09	0.68	0.10	0.67	0.11	0.66	0.12
CF ₃	0.41	0.13	0.40	0.14	0.39	0.15	0.39	0.15
CO ₂ Et	0.31	0.14	0.30	0.15	0.30	0.15	0.30	0.15
X	$L_a = 1.61$		1.63		1.65		1.67	
	σ_L	σ_D	σ_L	σ_D	σ_L	σ_D	σ_L	σ_D
H	0	0	0	0	0	0	0	0
Me	-0.01	-0.16	-0.01	-0.16	-0.01	-0.16	-0.01	-0.16
Et	-0.01	-0.14	-0.01	-0.14	-0.01	-0.14	-0.01	-0.14
OH	0.23	-0.60	0.23	-0.60	0.22	-0.59	-0.22	-0.59
OMe	0.29	-0.56	0.29	-0.56	0.28	-0.55	0.28	-0.55
Cl	0.46	-0.23	0.45	-0.22	0.45	-0.22	0.44	-0.21
Br	0.45	-0.22	0.45	-0.22	0.44	-0.21	0.44	-0.21
NO ₂	0.65	0.13	0.64	0.14	0.64	0.14	0.63	0.15
CF ₃	0.39	0.15	0.38	0.16	0.38	0.16	0.37	0.17
CO ₂ Et	0.29	0.16	0.29	0.16	0.28	0.17	0.28	0.17

$$L' - L = \frac{E}{L_t} (L - D) \quad (53)$$

The largest value E may have will occur when L_t is at one extreme of the range of interest (1.45 to 1.67) and L_a is at the other. Thus, $E \leq 0.22$. For 4-substituted benzoic acids, the values of \bar{L} and \bar{D} in Tables 4 and 5 show that $L - D \leq 0.43$ (generally much less). L_t must lie in the range 1.45 to 1.67, therefore

TABLE 2
 pK_as of 4-Substituted Benzoic Acids in Various Solvents, 25°C

Set	1 ^a	2 ^b	3 ^c	4 ^d	5 ^e	9 ^f	10 ^g	11 ^h
H	5.16	5.76	6.57	7.25	10.15	5.469	7.029	4.454
NO ₂	4.06	4.58	5.27	5.93	8.90	4.369	5.849	3.585
Br	4.83	5.34	6.04	6.74	9.79	5.094	6.602	—
Me	5.37	6.00	6.80	7.46	10.48	5.684	7.239	4.656
Cl	4.83	5.38	6.10	6.62	9.75	5.089	6.639	4.207
MeO	5.45	6.09	6.88	7.59	10.55	5.794	7.390	4.813
F	4.95	5.55	6.27	6.98	9.90	—	—	—
OH	—	—	—	—	—	—	—	4.928
Set	12 ⁱ	13 ^j	14 ^k	15 ^l	16 ^e	17 ^m	18 ⁿ	
H	4.996	6.63	7.647	9.41	10.13	8.603	8.609	
NO ₂	4.039	5.29	6.682	8.349	8.85	7.463	7.468	
Br	—	6.10	7.279	9.024	9.64	8.171	8.188	
Me	5.137	—	7.819	9.624	10.32	8.814	8.802	
Cl	4.698	6.13	7.343	9.033	9.62	8.214	8.215	
MeO	5.203	7.00	7.971	9.749	10.52	8.966	8.969	
F	—	—	—	—	—	—	—	
OH	5.352	—	—	—	10.51	9.172	9.175	

^a 33.2% w/w EtOH-H₂O.^b 52.0% w/w EtOH-H₂O.^c 73.4% w/w EtOH-H₂O.^d 85.4% w/w EtOH-H₂O.^e EtOH.^f 43.5% dioxane-H₂O.^g 73.5% dioxane-H₂O.^h 10% w/w MeAc-H₂O.ⁱ 25% w/w MeAc-H₂O.^j 80% w/w MCS-H₂O.^k HOCH₂CH₂OH.^l MeOH.^m PrOH.ⁿ BuOH

Sources of the data: Sets 1-5, Ref. 30. Sets 9, 10, 14, 18, J. H. Elliott and M. Kilpatrick, *J. Phys. Chem.*, **45**, 454, 466, 472, 485 (1941). Sets 11, 12, J. F. J. Dippy, S. R. C. Hughes, and B. C. Kitchiner, *J. Chem. Soc.*, 1964, 1275. Set 13, W. Simon, G. H. Lyssy, A. Morikofer, and E. Heilbronner, *Zusammenstellung von scheinbaren Dissoziationskonstanten im Lösungsmittelsystem Methylcellosolve/Wasser*, Juris-Verlag, Zurich, 1959. Set 18, J. H. Elliott, *J. Phys. Chem.*, **46**, 221 (1942).

$$L' - L \leq \frac{(0.22)(0.43)}{1.45} \quad (54)$$

or

$$L' - L \leq 0.065 \quad (55)$$

Generally, $L' - L$ should be much less than 0.065. Furthermore, the standard

TABLE 3
Results of Correlations with the σ_L and σ_D Values

Set	$100R^2$ ^a	Set	$100R^2$ ^a	Set	$100R^2$ ^a
1	99.86	9	99.94	14	99.55
2	99.93	10	99.83	15	99.77
3	99.75	11	99.97	16	98.60
4	98.81	12	99.77	17	99.53
5	99.82	13	99.56	18	99.55

^a R is the multiple correlation coefficient. The quantity of $100R^2$ is equivalent to the percent of the data accounted for by the correlation equation. The values given are minimal values for the correlations obtained with the various sets of σ_L and σ_D in Table 1.

All sets studied had confidence levels (CL) of the F test for significance of the correlation, and Student t tests for L , D , and h of 99.9% except Set 4. For Set 4, F tests had a 99.5% CL, t_L for L_a = 1.45 through 1.51; 99.9% CL, all other L_a , 99.0% CL; t_D , 99.0% CL; t_h , 99.9% CL.

error of L is larger than $L' - L$ in all cases. It follows, then, that L should be constant and independent of the choice of σ_L and σ_D values.

D. Definition of σ_I

The constancy of L for a given solvent indicates that the best value of L for that solvent is given by \bar{L} . As we do not have a value of L available for the solvent of interest (50% w/w aqueous ethanol) we must estimate it by some interpolation method, from the \bar{L} values available for water and water-ethanol mixtures. The L s were then correlated with the equation

$$\log \bar{L} = m \log n_{EtOH} + c \quad (56)$$

where n_{EtOH} is the mole fraction of ethanol. In this correlation both the Thuairé and Wepster data were included as Wepster states that his results are in good agreement with those of Thuairé. The results of the correlation with Equation 56 are: $r = 0.9942$; $F = 429.4$ (99.9% CL); $s_{est} = 0.00947$; $s_m = 0.00868$ (99.9% CL); $s_c = 0.00630$ (99.9% CL); $m = -0.180$; $c = 0.289$; $100r^2 = 98.85$. Calculation of L for 50% w/w EtOH-H₂O from the correlation equation gives a value of -1.55 . As an alternative way of treating the data, they were correlated with the equation

$$\log \bar{L} = m \log p_{EtOH} + c \quad (57)$$

where p is the percent w/w of ethanol. The results of the correlation with Equation 57 are: $r = 0.9937$; $F = 398.1$ (99.9% CL); $s_{est} = 0.00983$; $s_{m'} = 0.0114$ (99.9% CL); $s_{c'} = 0.0190$ (99.9% CL); $m' = 0.228$; $c' = -0.191$; $100r^2 = 98.75$. Calculation of L for 50% w/w EtOH-H₂O from the correlation equation gives a value of 1.57. We have therefore averaged the two values obtaining an \bar{L} of

TABLE 4
 Values of L and D for Sets 1-8

Set L_a	1		2		3		4	
	L	D	L	D	L	D	L	D
1.45	-1.387	-1.285	-1.534	-1.380	-1.705	-1.421	-1.762	-1.448
1.47	-1.388	-1.285	-1.537	-1.380	-1.709	-1.422	-1.765	-1.453
1.49	-1.389	-1.286	-1.538	-1.382	-1.712	-1.426	-1.770	-1.453
1.51	-1.389	-1.283	-1.539	-1.380	-1.714	-1.421	-1.771	-1.449
1.53	-1.392	-1.284	-1.542	-1.380	-1.718	-1.422	-1.774	-1.454
1.55	-1.393	-1.284	-1.543	-1.379	-1.716	-1.423	-1.781	-1.447
1.57	-1.395	-1.284	-1.546	-1.380	-1.726	-1.423	-1.785	-1.451
1.59	-1.396	-1.286	-1.548	-1.382	-1.729	-1.425	-1.789	-1.452
1.61	-1.398	-1.285	-1.551	-1.380	-1.735	-1.422	-1.796	-1.449
1.63	-1.399	-1.285	-1.554	-1.381	-1.740	-1.423	-1.798	-1.454
1.65	-1.400	-1.284	-1.554	-1.379	-1.741	-1.419	-1.802	-1.446
1.67	-1.401	-1.284	-1.557	-1.379	-1.746	-1.420	-1.805	-1.451
\bar{L}, \bar{D}	-1.394	-1.285	-1.545	-1.380	-1.724	-1.422	-1.783	-1.451
Set L_a	5		6		7		8	
	L	D	L	D	L	D	L	D
1.45	-1.656	-1.540	-1.050	-1.068	-1.539	-1.395	-1.735	-1.589
1.47	-1.657	-1.542	-1.050	-1.068	-1.542	-1.394	-1.739	-1.589
1.49	-1.659	-1.542	-1.050	-1.068	-1.543	-1.395	-1.740	-1.588
1.51	-1.660	-1.540	-1.050	-1.068	-1.544	-1.395	-1.739	-1.589
1.53	-1.661	-1.541	-1.049	-1.068	-1.547	-1.393	-1.743	-1.587
1.55	-1.663	-1.540	-1.049	-1.068	-1.548	-1.394	-1.744	-1.587
1.57	-1.665	-1.540	-1.049	-1.068	-1.551	-1.395	-1.746	-1.590
1.59	-1.667	-1.541	-1.049	-1.068	-1.553	-1.394	-1.750	-1.586
1.61	-1.669	-1.540	-1.048	-1.068	-1.555	-1.394	-1.751	-1.588
1.63	-1.670	-1.542	-1.048	-1.068	-1.557	-1.395	-1.761	-1.587
1.65	-1.671	-1.539	-1.048	-1.068	-1.558	-1.392	-1.755	-1.586
1.67	-1.672	-1.541	-1.048	-1.068	-1.558	-1.392	-1.755	-1.586
\bar{L}, \bar{D}	-1.664	-1.541	-1.049	-1.068	-1.550	-1.394	-1.747	-1.587

1.56. This value is our best estimate of L_I , the true scaling factor. Inserting it into Equation 37 gives

$$\sigma_I = \frac{\Delta p K_a}{1.56} \quad (58)$$

We have reverted to the use of the subscripts I and R to designate the localized and delocalized electrical effects because of their widespread use. The use of the subscript I does not imply the inductive mode of transmission of the localized effect. We retain L and D as regression coefficients in preference to our previously employed α and β (3,5,6) or the ρ_I and ρ_R of Taft and his co-workers (1,4) because we feel they are mnemonic, simple, and available on every typewriter and computer keyboard.

TABLE 5
Values of L and D for Sets 9-18

Set	L				D			
	1.45	1.55	1.67	\bar{L}	1.45	1.55	1.67	\bar{D}
9	-1.428	-1.435	-1.445	-1.436	-1.309	-1.309	-1.309	-1.309
10	-1.518	-1.524	-1.532	-1.525	-1.424	-1.424	-1.424	-1.424
11	-1.115	-1.110	-1.102	-1.109	-1.208	-1.209	-1.209	-1.209
12	-1.192	-1.200	-1.211	-1.201	-1.068	-1.067	-1.066	-1.067
13	-1.801	-1.813	-1.830	-1.815	-1.611	-1.609	-1.608	-1.609
14	-1.244	-1.246	-1.250	-1.247	-1.205	-1.205	-1.204	-1.205
15	-1.397	-1.403	-1.412	-1.404	-1.289	-1.289	-1.289	-1.289
16	-1.649	-1.662	-1.678	-1.663	-1.424	-1.423	-1.425	-1.424
17	-1.495	-1.497	-1.501	-1.498	-1.467	-1.466	-1.465	-1.466
18	-1.479	-1.480	-1.482	-1.480	-1.468	-1.468	-1.467	-1.468

III. EVALUATION OF σ_I CONSTANTS

We now have available a small group of primary σ_I values (from set 01) which are as close to being properly scaled as is possible at the present time. This small set of primary constants is insufficient for the needs of those workers who are interested in applying correlation analysis to a very wide range of structural types. It is therefore necessary for us to make use of secondary sources. As was pointed out by McDaniel and Brown (28), the use of secondary sources may lead to large errors in the values of the σ_m and σ_p substituent constants.

In our opinion this error was due to the use of systems in which there was considerable variation in the magnitude and nature of the delocalized effect. If the sets that are to be used as secondary sources of σ_I constants are carefully limited to those systems in which only the localized effect can occur, and if they were studied in similar media at atmospheric pressure, no difficulties should arise.

A. Methods for Evaluation of Substituent Constants

There are two major approaches that have been proposed for the evaluation of substituent constants. The first consists in the choice of a reference set, from which substituent constants can be evaluated when values of the coefficients in the equation

$$Q_X = m_1\sigma_{1,X} + m_2\sigma_{2,X} + \dots + m_0 \quad (59)$$

have been determined and values of σ assigned to some reference substituent. This method is the one used by Hammett to define σ_m and σ_p constants (32). It has been used by many other authors, including Taft (9) who applied it in the

evaluation of σ^* and E_S constants. McDaniel and Brown (28) used it to obtain σ_m and σ_p constants, Stock and Brown (33) employed it in the evaluation of σ^+ constants, and Roberts and Moreland (17) in the evaluation of σ' constants. The second method was first suggested by Jaffé (34). It consists in the evaluation of substituent constants by a statistical treatment of all the available data.

This method has three disadvantages: (1) As more data accumulate, all substituent constants must be revised. Thus, the values of the constants are continually subject to change. (2) With a large body of data, the periodic revision of the substituent constants requires a large amount of time and effort even with the aid of a computer. (3) In treating the data statistically, the assumption is made that all the data can be represented by a common set of substituent constants, and that small deviations from this common set of substituent constants represent "noise" due to some combination of experimental error and of minor effects. In this averaging process, it is possible to submerge small, subtle, and important effects.

No one has yet actually applied the statistical method to the evaluation of substituent constants. The closest to it is the work of Wold and Sjostrom (35,36) who have used a large number of sets in the statistical evaluation of what they refer to as the "inductive" substituent constants. These constants are actually equivalent to the σ^0 or σ^n values. Wold and Sjostrom have argued that the statistical treatment is the best approach to the evaluation of substituent constants. In the course of their work, they have used data for ionization of benzoic acids in alcohol-water, acetone-water, and dioxane-water mixtures on the assumption that the composition of the electrical effect was the same in all of these sets. The results of Ehrenson, Brownlee, and Taft (1) and our own results show that the composition of the electrical effect varies with solvent. This would seem to throw some doubt on the results of Wold and Sjostrom and to suggest that the third objection to the statistical evaluation of substituent constants may indeed be valid.

Many authors have carried out the evaluation of substituent constants by a method somewhere between definition from a reference set and the statistical approach. Thus, Jaffé (34) assumed the validity of the original σ_m and σ_p constants and then reported mean values for additional constants. Van Bekkum, Verkade, and Wepster (37) have used essentially the same mixed method in the definition of σ^n constants, a similar treatment has been used by Taft, Ehrenson, and Glick (38) to obtain σ^0 constants. Ehrenson (89) has employed an iteration procedure in which the coefficients of Equation 59 are calculated employing Taft's σ constants. New constants were calculated from the resulting regression equations, and the procedure repeated until the substituent constants, σ_n , and the regression coefficients, m_n are unchanged. Ehrenson, Brownlee, and Taft (1) have applied this method to the evaluation of σ_R and σ_R^0 constants. They obtained σ_R^+ and σ_R^- constants by a method which is closer to the use of a

reference set, whereas additional σ_I constants were obtained from a relationship between σ_I and F^{19} shielding parameters for 3- $\text{XC}_6\text{H}_4\text{F}$.

The question then arises: What choice of method for the evaluation of substituent constants should be made. The disadvantage of the reference set method is the question of the validity of the reference set chosen; that is, is it the best model for a particular kind of substituent effect? In our opinion, when there is a good chemical reason for the choice of a reference set, and sufficient data are extant, this method is preferable. Furthermore, as noted previously, secondary values should be calculated only from those additional sets which by virtue of the known similarity of their structures to that in the defining standard set can be expected to exhibit similar substituent effects. Additionally, such secondary sets should have been studied under comparable reaction conditions. Thus, Charton (40) in the evaluation of the ν steric parameters, first demonstrated that acid catalyzed ester hydrolyses are in fact linearly related the ν parameters for groups of known van der Waals radii, $r_{\nu X}$. This reaction could therefore be used to determine apparent ν values for unsymmetric substituents, for

$$\nu \equiv r_{\nu X} - r_{\nu H} \quad (60)$$

which r_{ν} values were unknown. This collection of ν values was then shown to be applicable to base-catalyzed ester hydrolyses (13) and to acid- and base-catalyzed amide hydrolyses as well (41). Then, by application of the premise inherent in Ehrenson, Brownlee, and Taft, nucleophilic additions to a carbonyl group which result in the formation of a tetrahedral intermediate under reasonably comparable conditions, constitute a suitable series of standard sets for the definition of a particular type of steric parameter. A completely different type of transition state would generally require the definition of a different steric parameter (42).

We may now consider how to ascertain the degree of error in substituent constants which have been evaluated. When the various modifications of the statistical method are used, standard errors can readily be assigned to the resulting constants. These standard errors can be misleading, however. The constants of Wold and Sjoström show commendably small standard errors although, as was noted previously, the composition of the electrical effect varied in some of the sets studied. Furthermore, in the calculation of standard errors, no weighting was introduced to account for differences in the magnitude of errors in the data of different sets, and in fact of different values within a set when they have been determined by different methods, as frequently occurs when $\text{p}K_a$ data are used. McDaniel and Brown (28) have attempted to assign uncertainties to substituent constants obtained by the reference set method by a consideration of the errors present in the measurement of the data. This seems a useful qualitative approach.

At the present time, no clear consensus concerning the choice of method for the evaluation of substituent constants exists. We must point out, however, that the statistical method inherently requires a number of data sets that contain all of the substituents of interest. Unfortunately, as the work of Ehrenson, Brownlee, and Taft shows, data is available for a statistical treatment for very few substituents; these authors list twenty-six. Our interest in this work is to provide substituent constants for a much wider range of substituents. Thus, for our purpose, the statistical method is unsuitable.

In our search for a method for assigning errors to the substituent constants evaluated from various secondary sources, we have considered two possible approaches. In the first of these, we assume that the method normally used for compounding of errors (43) in experimental work may be applied to the evaluation of the standard error of substituent constants. For a quantity y which is obtained from the experimental measurements x_1 and x_2 by the function

$$y = x_1 - x_2 \quad (61)$$

the error is given by

$$s_y^2 = s_1^2 + s_2^2 \quad (62)$$

where s is the standard deviation. For the function

$$y' = \frac{x_1'}{x_2'} \quad (63)$$

the error is obtained from

$$s_{y'}^2 = \frac{1}{x_2'^2 s_1'^2} + \left(\frac{x_1'^2}{x_2'^2} \right) \quad (64)$$

Setting $y = x_1'$ and combining Equations 62 and 64 after setting pK_{aX} , h , and L equal to x_1 , x_2 , and x_2' , respectively,

$$s = [L^{-2} (s^2 pK_{aX} + s_h^2) + (pK_{aX} - h)^2 s_L^2 L^{-4}]^{1/2} \quad (65)$$

Alternatively, we may obtain extreme values for σ_I by means of the equation

$$\sigma_I = (pK_{aX} + s_{pK_{aX}}) - (h - s_h) \cdot (-L + s_L) \quad (66)$$

in which we have maximum and minimum absolute values of the numerator and denominator, respectively, thus giving one extreme of the range of σ . The other extreme is obtained from

$$\sigma_I = \frac{(pK_{aX} - s_{pK_{aX}}) - (h + s_h)}{(-L - s_L)} \quad (67)$$

in which the numerator and denominator have minimum and maximum values,

TABLE 6
Comparison of Errors in σ_I from Equations 65, 66, and 67

X	Error (Eq. 65)	Error (Eq. 66) ^a	X	Error (Eq. 65)	Error (Eq. 66) ^a
<i>t</i> -BuCH ₂	0.00400	0.0050	Am	0.0106	0.0140
Ph	0.00411	0.0024	CONH ₂	0.00531	0.0002
H ₂ NCONH	0.00482	0.0010	OPh	0.0118	0.0085
F	0.00807	0.0032	CN	0.00836	0.0035
SEt	0.0111	0.0103	I	0.00645	0.0013

^a Calculated from the equation $|\sigma_{Ia} - \sigma_{Ib}|/2$ where σ_{Ia} and σ_{Ib} are calculated from Equations 66 and 67, respectively.

respectively. We suggest that the value of σ_I should lie in the range defined by the values obtained from Equations 65–67. In both the preceding methods, s_L and s_h are obtained from the appropriate correlation equation, and $s_{pK_{aX}}$ is the error in the pK_a value given in the source from which it was taken. The results obtained for the calculation of the error in σ_I from the two methods are compared for several substituents in Table 6.

Although the results given by the two methods are generally of the same order of magnitude, the errors calculated from Equation 65 are usually larger. We will therefore report errors obtained by Equation 65. This equation may also be used to estimate errors in the primary σ_I values obtained from Equation 58. In this case $h = pK_{aH}$ and the errors in h and pK_{aX} are those given by Holtz and Stock (26a). The error in L is taken as the sum of the standard error of the average value of L for pK_a s of Benzoic acids in 52% w/w EtOH–H₂O and the difference between 1.56 and the L values obtained from Equations 56 and 57 (0.01) giving 0.0176.

B. Secondary Sources of σ_I Constants

The requirements for secondary sources are the same as those given previously for the reference set with the exception of the requirement that the set permit the σ_I constants to be properly scaled. The pK_a s of bicyclooctane carboxylic acids and of quinuclidines meet these requirements fairly well. The data available in the literature does not permit the evaluation of σ_I for many additional substituents. The greatest potential source of additional σ_I values consists of pK_a values of acetic acids. To use the acetic acid system as a secondary source for the evaluation of σ_I constants it must be shown that steric effects and resonance effects are absent. To establish that this is indeed the case, pK_a s of substituted acids in water at 25° were correlated with the extended Hammett equation (Eq. 19) using primary σ_I constants (Table 7) obtained from Equation 58 and σ_D constants obtained from Equation 40. Only those substituents for

TABLE 7
Values of σ_I

X	σ_I	Error ^a	pK_a^b	Set ^c
Alkyl, Cycloalkyl				
Me	-0.01	0.020	6.89 ^d	01
Et	-0.01	0.020	6.89 ^d	01
<i>c</i> -C ₃ H ₅	0.01	0.011	4.74 ^g	6
Pr	-0.01	0.003	4.8348	5
<i>i</i> -Pr	0.01	0.003	4.7673	5
Bu	-0.01	0.004	4.845	4
<i>i</i> -Bu	-0.01	0.004	4.8368	4
<i>s</i> -Bu	-0.01	0.004	4.836	4
<i>t</i> -Bu	-0.01	0.009	11.27 ^e	36
		0.008	10.24 ^f	16
Am	-0.03	0.011	4.893	6
<i>t</i> -BuCH ₂	0.00	0.004	4.788	6
AmCH ₂	-0.03	0.011	4.8945	6
<i>c</i> -C ₆ H ₁₁	0.00	U	4.801	6
<i>c</i> -C ₆ H ₁₁ CH ₂	-0.03	U	4.910	6
<i>n</i> -C ₇ H ₁₅	-0.04	0.011	4.959	6
<i>c</i> -C ₆ H ₁₁ CH ₂ CH ₂	-0.04	U	4.951	6
Vinyl, Ethynyl, Aryl; Vinyl-, Ethynyl-, Arylalkyl				
HC≡C—	0.29	0.015	9.48 ^e	36
H ₂ C=CH—	0.11	0.004	4.3521	6
MeC≡C—	0.30	0.014	3.59 ^h	6
HC≡CCH ₂ —	0.14	0.013	4.21 ^h	6
MeCH=CH—	0.07	0.011	4.507	6
H ₂ C=CMe	0.10	0.007	10.52 ^e	36
H ₂ C=CHCH ₂	0.02	0.004	4.70	4
H ₂ C=CHC≡C—	0.35	0.014	3.39 ^h	6
HC≡CCH ₂ CH ₂	0.05	0.013	4.60 ^h	6
Me ₂ C=CH—	0.05	0.011	4.600	6
EtCH=CH—	0.07	0.011	4.516	6
MeCH=CHCH ₂	0.02	0.011	4.719	6
H ₂ C=CH—CH ₂ CH ₂	0.02	0.011	4.721	6
MeC≡C—C≡C—	0.39	0.014	3.23 ^h	6
HC≡CCH ₂ CH ₂ CH ₂	0.05	0.013	4.58 ^h	6
Me ₂ C=CHCH ₂	0.00	0.011	4.800	6
Ph	0.12	0.004	4.3074	6
PhCH ₂	0.03	0.004	4.6643	6
PhC≡C—	0.33	0.014	3.44 ^h	6
PhCHMe	0.07	U	9.80 ^f	16
PhCH ₂ CH ₂	0.02	0.011	4.757	6
		0.008	10.16 ^f	16
PhCMe ₂	0.05	0.008	10.03 ^f	16
			6.26 ^{qq}	80
Ph(CH ₂) ₃	0.01	0.008	10.36 ^f	16

TABLE 7
Values of σ_I

X	σ_I	Error ^a	pK_a^b	Set ^c
1-C ₁₀ H ₇	0.14	0.011	4.2362	6
2-C ₁₀ H ₇	0.13	0.011	4.259	6
Ph(CH ₂) ₄	0.00	0.008	10.486 ^f	16
1-C ₁₀ H ₇ CH ₂	0.08	0.018	6.81	54
Haloalkyl, Halovinyl				
CCl ₃	0.36	U	—	<i>i</i>
CF ₃	0.40	0.021	6.25	01
CF ₂ H	0.32	U	7.52	16
ClCH ₂	0.17	0.004	4.10	4
BrCH ₂	0.20	0.005	3.991	4
ICH ₂	0.17	0.004	4.09	4
Cl ₂ C=CH—	0.18	U	4.04	5
CH ₂ =CCl—	0.55	U	2.55	6
Z-ClCH=CH—	0.18	U	4.07	6
E-ClCH=CH—	0.17	U	4.12	6
CCl ₃ CH ₂	0.14	U	4.21	5
CF ₃ CH ₂	0.16	U	4.156	6
MeCHBr	0.19	U	4.01 ^j	6
MeCHCl	0.15	U	4.17 ^j	6
BrCH ₂ CH ₂	0.05	U	4.58 ^k	6
ClCH ₂ CH ₂	0.07	U	4.52 ^k	6
CF ₃ CF ₂ CF ₂	0.39	U	—	<i>i</i>
Cl ₂ C=CHCH ₂	0.05	U	4.57	5
CCl ₃ CH ₂ CH ₂	0.07	U	4.52	5
BrCH ₂ CH ₂ CH ₂	0.02	U	4.72 ^k	6
ClCH ₂ CH ₂ CH ₂	0.02	U	4.70 ^k	6
CF ₃ CF ₃ CF ₃ CH ₂	0.15	U	4.18	6
Oxyalkyl				
CH(OH) ₂	0.22	0.011	9.89 ^e	36
CH ₂ OH	0.11	0.007	9.4980 ^f	16
		0.003	10.46 ^e	36
O ₂ NOCH ₂	0.20	U	3.97	6
MeCHOH	0.04	U	4.648	12
HOCH ₂ CH ₂	0.06	0.008	9.96 ^f	16
MeOCH ₂	0.11	0.014	10.46 ^e	36
AcOCH ₂	0.15	0.012	10.24 ^e	36
MeCHOHCH ₂	0.03	0.004	4.686	4
MeOCH ₂ CH ₂	0.00	0.008	10.486 ^l	16
Me ₂ CHOHCH ₂	-0.02	0.010	4.873	4
PhCHOH	0.10	0.004	4.40	4
PhOCH ₂	0.12	U	6.62 ⁿⁿ	54
TsOCH ₂	0.23	0.003	9.84 ^e	36

TABLE 7
Values of σ_I

X	σ_I	Error ^a	pK _a ^b	Set ^c
Other Substituted Alkyl				
HSCH ₂	0.12	0.011	4.32	6
NCCH ₂	0.20	0.011	3.991	6
NCS _e CH ₂	0.22	U	3.879 ^m	6
H ₂ NCOCH ₂	0.06	0.004	4.5388	6
MeSCH ₂	0.12	0.009	9.34 ^f	16
H ₂ NCONHCH ₂	0.07	0.004	4.4873	6
Me(NO ₂)NCH ₂	0.16	U	4.16 ⁿ	6
NCCH ₂ CH ₂	0.09	0.011	4.437	6
MeO ₂ CCH ₂	0.19	U	4.029	6
H ₂ NCOCH ₂ CH ₂	0.05	0.004	4.6003	6
AcNHCH ₂	0.09	0.004	4.4452	6
H ₂ NCONHCH ₂ CH ₂	0.03	0.004	4.6831	6
Me ₂ N(O)CH ₂	0.23	U	8.36 ^{mm}	16
MeO ₂ CCH ₂ CH ₂	0.07	0.007	9.839 ^{kk}	16
EtO ₂ CCH ₂	0.15	0.009	9.06 ^f	16
H ₂ NCO(CH ₂) ₃	0.04	0.004	4.6286	6
MeN(NO ₂)CH ₂ CH ₂ N(NO ₂)CH ₂	0.14	U	4.21 ⁿ	6
EtO ₂ CCH ₂ CH ₂	0.08	0.008	9.710 ^f	16
(Et ₂ PO)CH ₂	0.14	U	4.23 ^o	6
(EtO) ₂ P(O)CH ₂	0.13	U	4.28 ^o	6
EtO ₂ C(CH ₂) ₃	0.04	0.008	10.151 ^f	16
(Et ₂ PO)CH ₂ CH ₂	0.07	U	4.50 ^o	6
(EtO) ₂ P(O)CH ₂ CH ₂	0.05	U	4.57 ^o	6
EtO ₂ C(CH ₂) ₄	0.02	0.008	10.30 ^f	16
(EtO) ₂ P(O)CH ₂ CH ₂ CH ₂	0.03	U	4.68 ^o	6
PhNHCOCH ₂	0.02	U	4.701	6
PhCH ₂ SCH ₂	0.08	0.011	4.463	4
PhCHCO ₂ Me	0.11	0.010	4.36 ^p	5
(Ph ₂ PO)CH ₂	0.20	U	5.31 ^o	80
(Ph ₂ PO)CH ₂ CH ₂	0.09	U	5.81 ^o	80
MeO ₂ CCPh ₂ CH ₂	0.03	0.010	4.66 ^p	5
Et ₂ POCH ₂ CH ₂ CH ₂	0.04	U	4.62 ^o	6
Silyl, Silylalkyl				
Me ₃ Si	-0.11	U	5.22	6
Me ₃ SiCH ₂	-0.03	U	4.907	6
Me ₃ SiCH ₂ CH ₂	-0.03	U	4.886	6
Me ₃ SiOSiMe ₂ -	-0.11	U	5.22	6
Me ₃ SiCH ₂ CH ₂ CH ₂	-0.04	U	4.963	6
Me ₃ Si(CH ₂) ₄	-0.07	U	5.06 ^p	6
PhMe ₂ Si	-0.12	U	5.27	6

TABLE 7
Values of σ_I

X	σ_I	Error ^a	p <i>K</i> _a ^b	Set ^c
Carbonyl				
HO ₂ C	0.30	U	6.40	01
H ₂ NCO	0.28	0.005	3.6413	6
Ac	0.30	0.005	9.45	36
MeO ₂ C	0.32	0.015	5.867	23
Me ₂ NCO	0.28	—	8.46	38
EtO ₂ C	0.30	0.023	6.40	01
PhNHCO	0.26	U	3.717	6
Aza				
H ₂ N	0.17	0.010	10.14 ^e	36
HCONH	0.33	0.011	3.43 ^p	5
Me(NO ₂)N—	0.39	U	3.19 ⁿ	6
MeNH	0.13	0.010	10.32 ^e	36
H ₂ NCONH	0.23	0.004	3.8758	6
ClCH ₂ CONH	0.35	0.011	3.38 ^p	5
AcNH	0.28	0.005	3.6698	6
MeSCSNH	0.39	U	3.19 ^q	6
Me ₂ N	0.17	0.012	10.15 ^e	36
EtCONH	0.26	0.005	3.7176	6
EtO ₂ CNH	0.28	0.012	9.56 ^e	36
MeSCSNMe	0.44	U	2.99 ^q	6
Me(O ₂ N)NCH ₂ CH ₂ N(NO ₂)	0.39	U	3.23 ⁿ	6
Me ₂ NCSNH	0.27	U	3.71 ^q	6
(EtO) ₂ P(O)NH	0.23	U	3.85 ^r	6
PhSO ₂ NH	0.33	U	3.461	6
BzNH	0.28	U	3.66	6
PhNAc	0.23	U	3.914	13
1-C ₁₀ H ₇ NAc	0.27	U	3.693	6
2-C ₁₀ H ₇ NAc	0.29	U	3.627	6
PhNH	0.30	U	4.88 ^q	80
PhNMe	0.15	U	5.55 ^q	80
Oxa				
OH	0.24	0.0027	6.50	01
H ₂ NO—	0.16	U	4.15 ^s	6
O ₂ NO—	0.66	U	2.26	6
MeO	0.30	0.023	6.40	01
MeSO ₂ O—	0.55	0.013	2.56 ^t	6
AcO	0.38	0.014	9.00 ^e	36
EtO	0.28	0.005	3.652	4
Me ₂ C=NO—	0.30	U	3.56	6
Me ₂ NC(O)O	0.44	U	3.01 ^r	6
Me ₂ NC(S)O	0.47	U	2.87 ^r	6

TABLE 7
Values of σ_I

X	σ_I	Error ^a	pK_a^b	Set ^c
PrO	0.28	U	3.65	6
<i>i</i> -PrO	0.27	U	3.69	8
BuO	0.28	U	3.66	6
<i>s</i> -BuO	0.28	U	3.67	6
<i>c</i> -C ₅ H ₉ O	0.27	U	3.699	6
PhO	0.40	0.012	3.171	6
<i>c</i> -C ₆ H ₁₁ O	0.31	U	3.538	6
TsO	0.58	U	—	i
<i>c</i> -C ₆ H ₁₁ CH ₂ O	0.22	U	3.903	6
bicyclo[4.4.0]decyloxy	0.28	U	3.638 ^p	6
4-O ₂ NC ₆ H ₄ O	0.47	U	2.893 ^{tt}	6
OBz	0.43	U	3.04 ^{ss}	6
4-MeOC ₆ H ₄ O	0.39	U	3.213 ^{tt}	6
Phosphinyl, Thiaphosphinyl^u				
Me ₂ PO	0.30	U	3.57	6
(MeO) ₂ PO	0.36	U	3.34	6
Me(EtO)PO	0.31	U	3.52	6
Et ₂ PO	0.28	U	3.67	6
Et(EtO)PO	0.30	U	3.59	6
(EtO) ₂ PO	0.32	U	3.48	6
(Me ₂ N) ₂ PO	0.16	U	4.15	6
Pr ₂ PO	0.26	U	3.73	6
MePhPO	0.30	U	3.59	6
Ph(MeO)PO	0.32	U	3.50	6
EtPhPO	0.28	U	3.66	6
Ph(EtO)PO	0.30	U	3.57	6
Bu ₂ PO	0.25	U	3.78	6
Bu(BuO)PO	0.27	U	3.68	6
(BuO) ₂ PO	0.29	U	3.60	6
(Et ₂ N) ₂ PO	0.10	U	4.40	6
PrPhPO	0.27	U	3.68	6
BuPhPO	0.27	U	3.71	6
<i>i</i> -BuPhPO	0.26	U	3.72	6
Ph ₂ PO	0.26	U	3.74	6
(PhO) ₂ PO	0.36	U	3.35	6
Ph ₂ PS	0.28	U	4.97 ^o	80
Thia				
SH	0.27	0.011	3.68	6
F ₃ CS	0.45	U	2.95 ^v	6
NCS—	0.56	U	2.523	6
H ₂ NCOS	0.33	U	3.487	13
MeS	0.30	0.005	9.46 ^e	36
AcS	0.39	U	3.23 ^q	6

TABLE 7
Values of σ_I

X	σ_I	Error ^a	pK_a^b	Set ^c
MeC(S)S	0.45	U	7.95 ^q	6
EtS	0.26	0.011	3.74	6
Me ₂ NC(O)S	0.31	U	3.52 ^q	6
Me ₂ NC(S)S	0.36	U	3.35 ^q	6
EtOC(S)S	0.42	U	3.08 ^q	6
EtSC(S)S	0.46	U	2.94 ^q	6
CH ₂ =CHCH ₂ S	0.27	U	3.683 ^{ll}	6
PrS	0.25	0.011	3.77	6
<i>i</i> -PrS	0.26	0.011	3.72	6
CH ₂ =CHCH ₂ CH ₂ S	0.26	U	3.717 ^{ll}	6
EtO ₂ CCH ₂ S	0.28	U	3.66 ^w	6
BuS	0.26	U	3.739 ^{ll}	6
<i>s</i> -BuS	0.25	U	3.768 ^{ll}	6
CH ₂ =CH(CH ₂) ₃ S	0.26	U	3.739 ^{ll}	6
EtO ₂ CCHMeS	0.25	U	3.77 ^w	6
AmS	0.26	U	3.753 ^{ll}	6
PhS	0.31	0.011	3.52	6
<i>c</i> -C ₆ H ₁₁ S	0.32	U	3.488	6
<i>n</i> -C ₆ H ₁₃ S	0.25	U	3.758	6
EtO ₂ CCMe ₂ S	0.23	U	3.84 ^w	6
PhCH ₂ S	0.26	0.011	3.73	6
PhCH ₂ CH ₂ S	0.25	0.011	3.7945	4
Ph ₃ CS	0.12	U	4.30	6
4-O ₂ NC ₆ H ₄ S	0.35	U	3.375 ^{rr}	6
4-MeOC ₆ H ₄ S	0.27	U	2.701 ^{rr}	6
Sulfonyl, Sulfinyl				
CF ₃ SO ₂	0.71	U	1.88	6
CF ₃ SO	0.67	U	2.06 ^v	6
PhSO	0.51	U	2.732 ^{rr}	6
MeSO ₂	0.59	0.020	7.89	36
EtSO ₂	0.59	U	2.448	13
PrSO ₂	0.57	U	2.507	13
<i>i</i> -PrSO ₂	0.57	U	2.522	13
PhSO ₂	0.56	U	2.513 ^{rr}	6
4-O ₂ NC ₆ H ₄ SO	0.54	U	2.586 ^{rr}	6
4-MeOC ₆ H ₄ SO	0.50	U	2.754 ^{rr}	6
4-O ₂ NC ₆ H ₄ SO ₂	0.61	U	2.330 ^{rr}	6
4-MeOC ₆ H ₄ SO ₂	0.71	U	1.88	6
Ionic				
CO ₂ ⁻	-0.19	U	7.17	01
CH ₂ SO ₃ ⁻	0.01	U	4.74 ^x	6
CH ₂ CH ₂ SO ₃ ⁻	-0.03	U	4.91 ^x	6
⁻ O ₂ CCH ₂ CH=CH-	0.02	U	4.70 ^y	6

TABLE 7
Values of σ_I

X	σ_I	Error ^a	pK_a^b	Set ^c
Me ₃ N ⁺	1.07	U	5.007 ^z	23
SO ₃ ⁻	0.15	U	4.20	6
3,4-diphenyltetrazolium-2-thiyl	0.57	U	2.47 ^{aa}	6
Me ₃ N ⁺ CH ₂ —	0.39	U	6.91 ^{bb}	16
Me ₃ N ⁺ CH ₂ CH ₂ —	0.18	U	8.82 ^{bb}	16
Me ₂ S ⁺	0.90	U	1.15 ^{cc}	7
Bu ₃ P ⁺	0.60	U	2.34 ^{oo}	6
Ph ₃ P ⁺	0.75	U	1.77 ^{oo}	6
AsO ₃ H ⁻	0.03	U	4.670	6
Substituted Phenyl				
C ₆ F ₅	0.31	0.012	7.67 ^f	16
2,3,5,6-C ₆ F ₄ H	0.33	U	3.47 ^{dd}	6
4-BrC ₆ H ₄	0.15	0.011	4.188	6
3-ClC ₆ H ₄	0.16	0.011	4.140	6
4-ClC ₆ H ₄	0.15	0.011	4.190	6
3-FC ₆ H ₄	0.16	U	4.13 ^{dd}	6
4-FC ₆ H ₄	0.13	0.011	4.246	6
3-IC ₆ H ₄	0.16	0.011	4.159	6
4-IC ₆ H ₄	0.15	0.011	4.178	6
3-O ₂ NC ₆ H ₄	0.20	0.011	3.967	6
4-O ₂ NC ₆ H ₄	0.23	0.011	3.851	6
4-MeC ₆ H ₄	0.10	0.011	4.370	6
4-MeOC ₆ H ₄	0.11	0.011	4.361	6
4-EtC ₆ H ₄	0.10	0.011	4.373	6
4- <i>i</i> -PrC ₆ H ₄	0.10	0.011	4.391	6
4- <i>t</i> -BuC ₆ H ₄	0.09	0.011	4.417	6
Other Groups				
H	0.00	—	^{cc}	—
F	0.54	0.008	2.5857	6
Cl	0.47	0.028	6.13	01
Br	0.47	0.021	6.14	01
I	0.40	0.006	3.1752	6
N ₃	0.43	U	3.03	6
CN—	0.63	0.015	2.23 ^{ff}	6
O ₂ N	0.67	0.022	5.82	01
Me ₂ N(O)	0.58	U	—	i
F ₃ S	0.59	U	2.41 ^{gg}	6
NCS _e —	0.56	U	2.551	13
PhSe	0.26	U	3.75 ^{hh}	6
<i>c</i> -C ₆ H ₁₁ Se	0.40	U	3.187	6
NC—	0.57	0.008	2.48178	6
H ₂ P	0.18	U	4.07 ⁱⁱ	6
HO ₂ CCH ₂ CH=CH	0.13	U	4.28 ^{yj}	6

TABLE 7
Values of σ_I

X	σ_I	Error ^a	pK_a^b	Set ^c
π -(Cr(CO) ₃)Ph	0.23	U	5.02 ^{uu}	53
1-o-carboranyl	0.18	U	4.06 ^{vv}	6
HC=NOH	0.20	U	4.00 ^{ww}	6
Heteroaryl Groups				
3,4-methylenedioxy-phenyl	0.12	0.009	9.37 ^f	16
2-thienyl	0.19	U	3.89, 8.92, ^f 6.43	6,16, 54
2-furyl	0.17	U	8.89 ^f	16
3-indolyl	0.01	U	4.75	6
2-pyridylmethyl	0.10	0.009	9.52 ^f	16
2-pyridyl	0.20	0.010	8.62 ^f	16
2-pyrrolyl	0.17	U	8.95 ^f	16
3-pyrazolylmethyl	0.09	0.008	9.61 ^f	16
4-thiazolylmethyl	0.11	0.009	9.48 ^f	16
4(5)-imidazolyl	0.12	0.009	9.37 ^f	16
2-furylmethyl	0.05	U	6.97	54
2-thienylmethyl	0.06	U	6.91	54
4(5)-imidazolylmethyl	0.08	0.007	9.756 ^f	16

^a The error given is calculated from Eq. 65 when possible. The letter U indicates that the error is unknown.

^b The pK_a from which σ_I was calculated. When two or more pK_a s are given the σ_I value reported is the average of that obtained from all pK_a s. All the pK_a values and their sources are given in Ref. 22 unless otherwise noted.

^c The set in Table 9 from which L and h were taken for the calculation of σ_I .

^d Ref. 26a and b.

^e C. A. Grob and M. G. Schlageter, *Helv. Chim. Acta*, 59, 264 (1976)

^f D. D. Perrin, *Dissociation Constants of Organic Bases in Aqueous Solution*, Butterworth, London, 1965.

^g Y. E. Rhodes and L. Vargas, *J. Org. Chem.*, 38, 4077 (1973).

^h G. H. Mansfield and M. C. Whiting, *J. Chem. Soc.*, 4761 (1956).

ⁱ Calculated from Eq. 1, Table 45.

^j C. Moreau, *Bull. Soc. Chim. France*, 31, (1968).

^k H. C. Brown, D. H. McDaniel, and O. Hafliger, in *Determination of Organic Structures by Physical Methods*, E. A. Braude and F. C. Nachod, Eds. Academic, New York, 1955.

^l S. T. Lobo and R. E. Robertson, *Can. J. Chem.*, 54, 3600 (1976).

^m A. Fredga, *J. Prakt. Chem.*, (2), 121, 59, 62 (1928).

ⁿ V. Kaderabek and K. Kalfus, *Collect. Czech. Chem. Commun.*, 41, 433 (1976).

^o E. N. Tsvetkov, R. A. Malevannaya and M. I. Kabachnik, *Zhur. Obshch. Khim.*, 45, 716 (1975).

^p G. Kortum, W. Vogel, and K. Andrussow, *Pure Appl. Chem.*, 1, 190 (1961).

^q M. J. Janssen, *Rec. Trav. Chim.*, 82, 931 (1963).

^r T. Lies, R. E. Plapinger, and T. Wagner-Jauregg, *J. Amer. Chem. Soc.* 75, 5755 (1953).

which the error in the pK_a is ≤ 0.005 and for which primary σ_I values were available were included. The data used are reported in Table 8 (Set 6). The results of the correlations with Equation 19 are L , 4.07; D , 0.0381; h , 0.216; s_{est} , 0.0302; s_L , 0.0630; s_D , 0.0605; s_h , 0.0198; n , 7; r_{12} , 0.442; F , 25.77; $100r^2$, 99.92. The F test and the t tests for the significance of L and h are significant at the 99.9% CL. The t test for the significance of D is at the 20.0% CL. Thus, there is no dependence on the delocalized effect. This point is further demonstrated by the value of r_{12} , the partial correlation coefficient of σ_I on σ_R . Clearly σ_I and

^a E. Testa, B. J. R. Nicolaus, L. Mariani, and G. Pagani, *Helv. Chim. Acta*, **46**, 766 (1963).

^t J. Ashworth and B. H. W. Coller, *Trans. Faraday Soc.*, **67**, 1077 (1971).

^u All data from E. N. Tsvetkov, R. A. Malevannaya, L. I. Petrovskaya, and M. I. Kabachnik, *Zhur. Obshch. Khim.*, **44**, 1225 (1974), unless otherwise noted.

^v V. V. Orda, L. M. Yagupolskii, V. F. Bystrov, and A. V. Stepanyants, *Zhur. Obshch. Khim.*, **35**, 1628 (1965).

^w A. Solladie-Cavallo and P. Vieles, *J. Chim. Phys.*, **64**, 1593 (1967).

^x R. P. Bell and G. A. Wright, *Trans. Faraday Soc.*, **57**, 1377 (1961).

^y R. K. Resnik and B. F. Douglas, *Inorg. Chem.*, **2**, 1246 (1963).

^z C. F. Wilcox and C. Leung, *J. Amer. Chem. Soc.*, **90**, 336 (1968).

^{aa} J. W. Ogilvie and A. H. Corwin, *J. Amer. Chem. Soc.*, **83**, 5023 (1961).

^{bb} J. V. Quagliano, J. T. Summers, S. Kida, and L. M. Vallarino, *Inorg. Chem.*, **3**, 1557 (1964).

^{cc} B. Holmquist and J. C. Bruice, *J. Amer. Chem. Soc.*, **91**, 3003 (1969).

^{dd} V. P. Petrov and V. A. Koptuyug, *Reakst. Sposobnost, Organ. Khim.*, **3**, 135 (1966).

^{ee} By definition.

^{ff} J. Ashworth and B. A. W. Coller, *Trans. Faraday Soc.*, **67**, 1069 (1971).

^{gg} N. H. Ray, *J. Chem. Soc.*, **1963**, 1440.

^{hh} D. Barnes, P. G. Laye, and L. D. Pettit, *J. Chem. Soc. A*, 2073 (1969).

ⁱⁱ K. Issleib and R. Kummel, *Chem. Ber.*, **100**, 3331 (1967).

^{jj} Includes a statistical factor of 1/2.

^{kk} R. W. Hay and P. J. Morris, *J. Chem. Soc. B*, 1577 (1970).

^{ll} L. D. Pettit and C. Sherrington, *J. Chem. Soc. A*, 3078 (1968).

^{mmm} J. T. Summers and J. V. Quagliano, *Inorg. Chem.*, **3**, 1767 (1964).

ⁿⁿ K. Bowden, M. Hardy, and D. C. Parkin, *Can. J. Chem.*, **46**, 2929 (1968).

^{oo} D. Martin and C. Griffin, *J. Org. Chem.*, **30**, 4034 (1965).

^{pp} H. Hogeveen and F. Montanari, *J. Chem. Soc.*, 4864 (1963).

^{qq} A. J. Hoefnagel, J. C. Monshouer, E. C. G. Snorn, and B. M. Wepster, *J. Am. Chem. Soc.*, **95**, 5350 (1973).

^{rr} D. J. Pasto, O. McMillan, and T. Murphy, *J. Org. Chem.*, **30**, 2688 (1965).

^{ss} C. Concilio and A. Bongini, *Ann. Chim. (Italy)*, **56**, 417 (1966).

^{tt} N. N. Hayes and G. E. K. Branch, *J. Am. Chem. Soc.*, **65**, 1555 (1943).

^{uu} B. Nichols and M. C. Whiting, *J. Chem. Soc.*, 551 (1959).

^{vv} L. I. Zakharkin, Y. A. Chaporskii, and V. I. Stanko, *Izv. Akad. Nauk. SSR Ser. Khim.*, **2208** (1969).

^{ww} A. Hantzsch and A. Miolati, *Z. Physik. Chem.*, **10**, 1 (1892).

Primary σ_I values are from set 01.

TABLE 8
Data in Protonic Solvents

-
01. pK_a , 4-substituted bicyclo[2.2.2] octane-1-carboxylic acids in 50% w/w EtOH-H₂O at 25°^a:
H, 6.87; Me, 6.89; Et, 6.89; HOCH₂, 6.80; OH, 6.50; OMe, 6.40; CO₂Et, 6.40; Cl, 6.13; Br, 6.14; NO₂, 5.82; CF₃, 6.25; CO₂H, 6.40^b; CO₂⁻, 7.17.^c
1. pK_a , substituted acetic acids in H₂O at 5°^d:
H, 4.7696; Me, 4.8844; Et, 4.8030; AcNH, 3.6815; EtCONH, 3.7284; H₂NCONH, 3.9108; CN, 2.44466; MeO, 3.5381
 2. pK_a , substituted acetic acids in H₂O at 10°^d:
H, 4.7622; Me, 4.8775; Et, 4.8024; AcNH, 3.7659; EtCONH, 3.7224; H₂NCONH, 3.8996; CN, 2.44678; MeO, 3.5439
 3. pK_a , substituted acetic acids in H₂O at 15°^d:
H, 4.7582, Me, 4.8742; Et, 4.8044; AcNH, 3.6726; EtCONH, 3.7183; H₂NCONH, 3.8894; CN, 2.45231; MeO, 3.5505; F, 2.5546; Cl, 2.8847; Br, 2.87514; I, 3.1433
 4. pK_a , substituted acetic acids in H₂O at 18°^d:
H, 4.7610; Me, 4.879; Et, 4.815; Br, 2.889; I, 3.155; OH, 3.836; Ph, 4.305
 5. pK_a , substituted acetic acids in H₂O at 20°^d:
H, 4.7562; Me, 4.8735; Et, 4.7981; F, 2.5712; Cl, 2.8557; Br, 2.88729; I, 3.1583; AcNH, 3.6572; EtCONH, 3.7165; H₂NCONH, 3.8788; CN, 2.45975; MeO, 3.5591
 6. pK_a , substituted acetic acids in H₂O at 25°^d:
H, 4.7560; Me, 4.8742; Et, 4.8196; Cl, 2.8668; Br, 2.90205; OH, 3.8309; OMe, 3.5704
 7. pK_a , substituted acetic acids in H₂O at 30°^d:
H, 4.7570; Me, 4.8775; Et, 4.8286; AcNH, 3.6731; EtCONH, 3.7208; H₂NCONH, 3.8735; CN, 2.48178; MeO, 3.5834; F, 2.6038; Cl, 2.88343; Br, 2.91800; I, 3.1934
 8. pK_a , substituted acetic acids in H₂O at 35°^d:
H, 4.7625; Me, 4.8827; Et, 4.8286; AcNH, 3.6780; EtCONH, 3.7254; H₂NCONH, 3.8732; CN, 2.49550; MeO, 3.5996; F, 2.6236; Cl, 2.89984; Br, 2.93599; I, 3.2128
 9. pK_a , substituted acetic acids in H₂O at 40°^d:
H, 4.7688; Me, 4.8914; Et, 4.8554; AcNH, 3.6844; EtCONH, 3.7310; H₂NCONH, 3.8752; CN, 2.51073; MeO, 3.6126
 10. pK_a , substituted acetic acids in H₂O at 45°^d:
H, 4.7773; Me, 4.9007; Et, 4.8706; AcNH, 3.6944; EtCONH, 3.7402; H₂NCONH, 3.8804; CN, 2.52812; MeO, 3.6313
 11. pK_a , substituted acetic acids in H₂O at 50°^d:
H, 4.7870; Me, 4.9104; Et, 4.8854; AcNH, 3.7062; EtCONH, 3.7503; H₂NCONH, 3.8877; MeO, 3.6509; OH, 3.8489
 12. pK_a , 2-substituted propanoic acids in H₂O at 18°^d:
H, 4.879; Me, 4.842; Et, 4.807; Pr, 4.790; Cl, 2.879; Br, 2.971; I, 3.11; OH, 3.860
 13. pK_a , 2-substituted propanoic acids in H₂O at 25°^d:
H, 4.8742; Me, 4.848; OH, 3.8579; AcNH, 3.7151; H₂NCONH, 3.8925
 14. pK_a , 3-substituted propanoic acids in H₂O at 18°^d:
H, 4.879; Me, 4.815; Et, 4.821; Pr, 4.845; *i*-Pr, 4.8368; Cl, 4.10; Br, 3.991; I, 4.09; C₂H₃, 4.70
 15. pK_a , 3-substituted propanoic acids in H₂O at 25°^d:
H, 4.8742; Me, 4.8196; Et, 4.842; Ph, 4.6643; AcNH, 4.4451; H₂NCONH, 4.4873
 16. pK_a , substituted methylamines, in H₂O at 25°^e:
H, 10.657; CN, 5.34; CONH₂, 7.95; Me, 10.70; CH₂OH, 9.4980,^f Et, 10.69; C₂H₃, 9.49; Pr, 10.66; *i*-Bu, 10.60; Bu, 10.64; Ph, 9.35; PhCH₂, 9.84; CO₂Me, 7.59; CO₂Et, 7.64; CH₂NHAc, 9.25

TABLE 8
Data in Protonic Solvents

17. pK_a , 2-substituted ethylamines in H_2O at $25^\circ e$:
H, 10.70; Me, 10.69; Et, 10.66; *i*-Pr, 10.60; Pr, 10.64; Bu, 10.56; OH, 9.4980; NHAc, 9.25; CH₂OH, 9.96^f; Ph, 9.84
18. pK_a , 4-substituted bicyclo[2.2.2]octane-1-carboxylic acids in 50% v/v EtOH-H₂O at $25^\circ g$:
H, 6.75; OH, 6.33; CO₂Et, 6.31; Br, 6.08; CN, 5.90
19. pK_a , 4-substituted bicyclo[2.2.2]oct-2-ene-1-carboxylic acids in 50% w/w EtOH-H₂O at $25^\circ a$:
H, 6.544; Me, 6.503; Cl, 5.717; CO₂Et, 6.003; CONH₂, 5.963; CF₃, 5.785; CN, 5.495; CO₂H, 5.979^b; CO₂⁻, 6.712^c; NMe₃⁺, 4.836
20. pK_a , 4-substituted dibenzobicyclo[2.2.2]octa-2,5-diene-1-carboxylic acids in 50% w/w EtOH-H₂O at $25^\circ a$:
H, 5.750; Me, 5.777; OMe, 5.503; F, 5.258; Cl, 5.211; Br, 5.213; NO₂, 4.939
21. pK_a , 4-substituted bicyclo[2.2.2]octane-1-carboxylic acids in H_2O at $25^\circ h$:
NMe₃⁺, 4.083; CN, 4.545; Br, 4.619; CO₂Me, 4.764; CO₂H, 4.769^b; H, 5.084; CO₂⁻, 5.156^c
22. pK_a , 4-substituted bicyclo[2.2.2]octane-1-carboxylic acids in v/v MeOH-H₂O at $25^\circ h$:
NMe₃⁺, 4.517; CN, 5.008; Br, 5.103; CO₂Me, 5.257; CO₂H, 5.261^b; H, 5.612; CO₂⁻, 5.726^c
23. pK_a , 4-substituted bicyclo[2.2.2]octane-1-carboxylic acids in 50% v/v MeOH-H₂O at $25^\circ h$:
CN, 5.581; Br, 5.690; CO₂H, 5.879^b; H, 6.261; CO₂⁻, 6.427^c
24. pK_a , 4-substituted bicyclo[2.2.1]heptane-1-carboxylic acids in H_2O at $25^\circ h$:
Me₃N⁺, 3.716; CN, 4.227; Br, 4.356; CO₂Me, 4.494; CO₂H, 4.498^b; H, 4.876; CO₂⁻, 4.983^c
25. pK_a , 4-substituted bicyclo[2.2.1]heptane-1-carboxylic acids in 25% v/v MeOH-H₂O at $25^\circ h$:
Me₃N⁺, 4.113; CN, 4.663; Br, 4.816; CO₂Me, 4.964; CO₃H, 4.971^b; H, 5.391; CO₂⁻, 5.550^c
26. pK_a , 4-substituted bicyclo[2.2.1]heptane-1-carboxylic acids in 50% v/v MeOH-H₂O at $25^\circ h$:
Me₃N⁺, 4.553; CN, 5.230; Br, 5.393; CO₂Me, 5.570; CO₂H, 5.596^b; H, 6.039; CO₂⁻, 6.262^c
27. pK_a , 9-substituted-10-triptyc acids in 50% w/w EtOH-H₂O at $25^\circ i$:
H, 5.20; Me, 5.23; Cl, 4.67; Br, 4.67; NO₂, 4.40
28. pK_a , 9-substituted-10-triptyc acids in 80% w/w MCS-H₂O at $25^\circ i$:
H, 6.23; Me, 6.27; Cl, 5.70; Br, 5.69; NO₂, 5.43
29. pK_a , 6-substituted spiro[3.3]heptane-2-carboxylic acids in 50% w/w EtOH-H₂O at $25^\circ j$:
H, 6.266; CN, 5.856; Br, 5.980; CO₂Et, 6.062; Me, 6.321; CO₂H, 6.096^b; CO₂⁻, 6.450^c; CONH₂, 6.110
30. pK_a , 4-substituted cubane-1-carboxylic acids in 50% w/w EtOH-H₂O at $24.95^\circ k$:
H, 5.94; CO₂H, 5.43^b; CO₂Me, 5.40; Br, 5.32; CN, 5.14; CO₂⁻, 6.23^c
31. pK_a , 3-substituted adamantane-1-carboxylic acids in 5 w/w EtOH-H₂O at $25^\circ l$:
H, 6.81; Ph, 6.77; OH, 6.31; OMe, 6.29; I, 6.26; Br, 6.19; Cl, 6.15; F, 6.00
32. pK_a , 3-substituted adamantane-1-carboxylic acids in 50% v/v EtOH-H₂O at $25^\circ m$:
H, 6.90; Br, 6.28; OH, 6.42; NO₂, 6.00; I, 6.32; Ph, 6.81; BrCH₂, 6.75; AcNH, 6.46; MeO, 6.45; CO₂Me, 6.49; CO₂H, 6.62^f; CO₂⁻, 6.97^f

TABLE 8
Data in Protonic Solvents

33. pK_a , *trans*-4-substituted cyclohexane-1-carboxylic acids in H₂O at 24.91° n:
CO₂⁻, 5.06^c; H, 4.90; OH, 4.69; OMe, 4.66; CO₂Me, 4.66; CO₂H, 4.67^b; Cl, 4.58; CN, 4.48
34. pK_a , *trans*-4-substituted cyclohexane-1-carboxylic acids in 50% w/w MeOH-H₂O at 24.91° n:
H, 6.11; OH, 5.86; OMe, 5.82; CO₂Me, 5.87; Cl, 5.78; CN, 5.64
35. pK_a , *trans*-4-substituted cyclohexane-1-carboxylic acids in 50% v/v EtOH-H₂O at 24.91° n:
H, 6.40; OH, 6.08; OMe, 6.02; CO₂Me, 6.04; Cl, 5.90; CN, 5.74
36. pK_a , 4-substituted quinuclidinium ions in H₂O at 25° o:
H, 11.12; Me, 11.01; Et, 11.09; HOCH₂, 10.46^f; OH, 9.44^f; OMe, 9.31; Cl, 8.61; Br, 8.47; NO₂, 7.64; *i*-Pr, 11.20; CH₂Cl, 10.15; CH₂Br, 10.10; CH₂I, 10.08; C₂H₅, 10.56; C₆H₅, 10.18; CO₂Me, 9.42; CO₂Et, 9.42; CONH₂, 9.34; CN, 8.08; NHAc, 9.54; I, 8.78
37. pK_a , 4-substituted quinuclidines in 5% v/v EtOH-H₂O at 25° p:
H, 11.00; Me, 10.92; CH₂OH, 10.42; CH₂Cl, 10.08; CH₂Br, 10.00; CONH₂, 9.40; CO₂Et, 9.47; OH, 9.35; Cl, 8.57; Br, 8.46; CN, 8.05
38. pK_a , 4-substituted quinuclidines in 50% w/w EtOH-H₂O at 25° p:
H, 9.98; Me, 9.77; CH₂OH, 9.57; CH₂Cl, 8.84; CH₂Br, 8.75; CONH₂, 8.46; CO₂Et, 8.27; OH, 8.65; Cl, 7.49; Br, 7.37; CN, 7.02
39. pK_a , 4-substituted quinuclidines in 80% w/w MCS-H₂O at 25° p:
H, 8.88; CH₂OH, 8.83; CH₂Br, 8.08; CO₂Et, 7.55; OH, 8.05; Br, 6.73; CN, 6.46
40. pK_a , 4-substituted quinuclidines in 5% v/v EtOH-H₂O at 25° q:
t-Bu, 11.02; H, 10.96; Et, 10.94; Me, 10.91; Ac, 9.67; CO₂Et, 9.401; CN, 7.81
41. pK_a , 3-(substituted methyl)benzoic acids in 50% v/v EtOH-H₂O at 25° r:
H, 5.90; Ph, 5.84; CN, 5.49; Cl, 5.59; Br, 5.56; I, 5.61; OMe, 5.69
42. pK_a , 3-(substituted methyl)benzoic acids in 80% w/w MCS-H₂O at 25° r:
H, 6.82; Ph, 6.76; CN, 6.37; Cl, 6.48; Br, 6.44; I, 6.43; OMe, 6.63
43. pK_a , 4-(substituted methyl)benzoic acids in 50% v/v EtOH-H₂O at 25° s:
H, 5.78; Cl, 5.36; Br, 5.36; I, 5.41; Ph, 5.70; CN, 5.28; CONH₂, 5.44; OH, 5.56; OMe, 5.50; NHAc, 5.61
44. pK_a , 4-(substituted methyl)benzoic acids in 80% w/w MCS-H₂O at 25° s:
H, 6.82; Cl, 6.45; Br, 6.36; I, 6.41; Ph, 6.73; CN, 6.32; CONH₂, 6.69; OH, 6.70; OMe, 6.58; NHAc, 6.68
45. pK_a , *cis*-3-substituted cyclohexanecarboxylic acids in H₂O at 25° d:
H, 4.900; OH, 4.602; Me, 4.883; CO₂H, 4.401^{b,cc}; CO₂⁻, 5.159^{c,cc}
46. pK_a , substituted acetic acids in MeOH, at 25° t:
Et, 9.69; H, 9.70; Cl, 7.84; CN, 7.50; HOCH₂, 9.42; OH, 8.72
47. pK_a , substituted acetic acids in MeOH at 25° u:
H, 9.52; F, 7.99; Cl, 7.96; Br, 8.06; CH₂Cl, 9.09; CH₂Br, 9.00; CH₂I, 8.89; CHClMe, 9.18; CH₂CH₂Cl, 9.29; CHBrMe, 9.12; Me, 9.71; Et, 9.69
48. pK_a , 4-substituted bicyclo[2.2.2]octane-1-carboxylic acids in MeOH at 25° v:
Br, 9.750; CO₂Et, 9.933; CO₂H, 9.870; CO₂⁻,^f 10.268; H, 10.226; NMe₃⁺,^f 9.375; OH, 9.985; CN, 9.617
49. pK_a , 4-substituted bicyclo[2.2.2]octane-1-carboxylic acids in MeOH at 0° v:
Br, 9.946; CO₂Et, 10.077; CO₂H, 10.089; CO₂⁻,^f 10.410; H, 10.392; NMe₃⁺,^f 9.436; OH, 10.115; CN, 9.752
50. pK_a , 4-(substituted methyl)pyridinium ions in MeOH at 0.1° w:
H, 6.541; Me, 6.550; Et, 6.534; Ph, 6.228; OH,^f 6.333; CN, 5.002; NH₃⁺,^f 4.13

TABLE 8
Data in Protonic Solvents

51. pK_a , 4-(substituted methyl)pyridinium ions in MeOH at 25.0° w;
H, 6.090; Me, 6.090; Et, 6.073; Ph, 5.794; OH,^f 5.846; CN, 4.565; NH₃⁺, 3.77^f
52. pK_a , *trans*-4-substituted cyclohexanecarboxylic acids in H₂O at 25° d;
H, 3.9889; OH, 4.678; Me, 4.886; CO₂H, 4.480^{b,cc}; CO₂⁻, 5.119^{c,cc}
53. pK_a , substituted acetic acids in 50% w/w EtOH-H₂O at 25° x;
H, 5.84; Me, 6.13; Et, 6.15; Ph, 5.60; PhCH₂, 5.98; Cl, 3.95; ClCH₂, 5.35; Br, 3.84; BrCH₂, 5.22; PhO, 4.38; PhOCH₂, 5.52; I, 4.36; MeO, 4.79; OH, 4.86; SH, 4.76; CN, 3.39
54. pK_a , substituted acetic acids in 80% w/w MCS-H₂O at 25° s;
H, 6.84^f; Me, 7.18; Et, 7.30; Ph, 6.73; PhCH₂, 7.03; Cl, 5.04; ClCH₂, 6.31; Br, 4.97; BrCH₂, 6.26; PhO, 5.49; PhOCH₂, 6.62; I, 5.50; MeO, 5.70; OH, 5.78^f; SH, 5.88; CN, 4.52
55. *kr*, substituted acetic acids + diazodiphenylmethane in MeOH at 25° x
H, 1.22; Me, 0.959; Et, 1.015; Ph, 2.50; PhCH₂, 1.49; Cl, 16.1; ClCH₂, 2.96; Br, 14.9; BrCH₂, 4.30; PhO, 12.3; PhOCH₂, 2.26; I, 11.0; MeO, 6.61; OH, 5.50; SH, 5.33; CN, 23.85
56. *kr*, substituted acetic acids + diazodiphenylmethane in EtOH at 25° x
H, 0.589; Me, 0.432; Et, 0.445; Ph, 1.19; PhCH₂, 0.740; Cl, 8.18; ClCH₂, 1.52; Br, 7.65; BrCH₂, 2.09; PhO, 6.25; PhOCH₂, 1.14; I, 5.61; MeO, 3.10; OH, 2.73; SH, 2.79; CN, 13.45
57. *kr*, substituted acetic acids + diazodiphenylmethane in *i*-PrOH at 25° x;
H, 0.459; Me, 0.309; Et, 0.306; Ph, 0.821; PhCH₂, 0.538; Cl, 6.655; ClCH₂, 1.14; Br, 6.31; BrCH₂, 1.64; PhO, 4.94; PhOCH₂, 0.924; I, 4.71; MeO, 2.375; OH, 2.235; SH, 2.275; CN, 11.9
58. *kr*, substituted acetic acids + diazodiphenylmethane in *t*-BuOH at 25° x;
H, 0.2525; Me, 0.124; Et, 0.132; Ph, 0.358; PhCH₂, 0.234; Cl, 4.05; ClCH₂, 0.650; Br, 3.83; BrCH₂, 1.07; PhO, 2.575; PhOCH₂, 0.437; I, 2.68; MeO, 1.19; OH, 1.32; SH, 1.36; CN, 9.07
59. *kr*, substituted acetic acids + diazodiphenylmethane in MeOCH₂CH₂OH, at 25° x;
H, 0.257; Me, 0.188; Et, 0.189; Ph, 0.508; PhCH₂, 0.337; Cl, 6.37; ClCH₂, 0.852; Br, 5.89; BrCH₂, 1.38; PhO, 3.68; PhOCH₂, 0.526; I, 3.56; MeO, 1.65; OH, 1.94; SH, 1.74; CN, 10.75
60. *kr*, substituted acetic acids + diazodiphenylmethane in BuOCH₂CH₂OH at 25° x;
H, 0.163; Me, 0.103; Et, 0.111; Ph, 0.422; PhCH₂, 0.213; Cl, 4.23; ClCH₂, 0.576; Br, 4.03; BrCH₂, 0.832; PhO, 2.86; PhOCH₂, 0.357; I, 3.02; MeO, 1.20; OH, 1.08; SH, 1.12; CN, 6.70
61. *kr*, 4-substituted bicyclo[2.2.2]octane-1-carboxylic acids plus diazodiphenylmethane in EtOH, at 30° s;
H, 0.237; OH, 0.370; CO₂Et, 0.376; Br, 0.501; CN, 0.592
62. *kr*, ethyl-4-substituted bicyclo[2.2.2]octane-1-carboxylates + OH⁻ in 87.83% w/w EtOH-H₂O at 30° s;
H, 1.62; OH, 7.55; CO₂Et, 8.35; Br, 17.3; CN, 31.8
63. *kr*, 9-substituted-10-triopic acids + diazodiphenylmethane in MeOH at 30° y;
H, 10.1; Me, 10.2; Cl, 18.9; Br, 18.2; NO₂, 24.2
64. *kr*, 9-substituted-10-triopic acids + diazodiphenylmethane in EtOH at 30° y;
H, 3.47; Me, 3.35; Cl, 6.91; Br, 6.67; NO₂, 9.11
65. *kr*, 9-substituted-10-triopic acids + diazodiphenylmethane in *i*-PrOH at 30° y;
H, 2.03; Me, 2.14; Cl, 4.10; Br, 4.24; NO₂, 5.64
66. *kr*, 9-substituted-10-triopic acids + diazodiphenylmethane in MeOCH₂CH₂OH at 30° y;
H, 1.78; Me, 1.87; Cl, 4.28; Br, 4.09; NO₂, 5.90

TABLE 8
Data in Protonic Solvents

67.	<i>kr</i> , 9-substituted-10-triopic acids + diazodiphenylmethane in BuOCH ₂ CH ₂ OH at 30° ^y : H, 0.917; Me, 1.06; Cl, 2.27 Br, 2.24; NO ₂ , 3.24
68.	10 ³ <i>kr</i> , 4-substituted quinuclidines + Mel in MeOH at 10.00° ^z : H, 4.43; <i>t</i> -Bu, 4.21; <i>i</i> -Pr, 4.05; Et, 3.95; Me, 3.85; MeOCH ₂ , 3.57; CH ₂ OH, 3.51; Ph, 3.35; Vi, 3.25; AcOCH ₂ , 2.79; ClCH ₂ , 2.70; ICH ₂ , 2.69; BrCH ₂ , 2.68; NH ₂ , 2.60; MeNH, 2.52; TsOCH ₂ , 2.39; C ₂ H, 2.30; Me ₂ N, 2.25; AcNH, 2.22; EtO ₂ CNH, 2.19; OH, 2.11; CONH ₂ , 2.11; CO ₂ Et, 2.02; MeO, 1.70; AcO, 1.51; I, 1.48; Br, 12.9; Cl, 1.23; CN, 1.00; NO ₂ , 0.66
69.	10 ³ <i>kr</i> , 4-substituted quinuclidines + Mel in MeOH at 25° ^p : H, 10.35; Me, 10.00; CH ₂ OH, 7.56; AcOCH ₂ , 6.80; BrCH ₂ , 6.55; Me ₂ NC=O, 7.00; H ₂ NC=O, 6.85; CO ₂ Et, 5.17; OH, 6.80; OAc, 4.93; Cl, 3.70; Br, 3.67; CN, 2.73
70.	10 ⁴ <i>kr</i> , methyl- <i>trans</i> -4-substituted cyclohexane carboxylates + OH ⁻ in 1:1 MeOH-H ₂ O at 29.4° ^{bb} : <i>t</i> -Bu, 49.4; OH, 109.; CO ₂ Me, 119.; CO ₂ ⁻ , 44.0 ^f ; H, 41.9; CN, 224.
71.	10 ⁴ <i>kr</i> , methyl- <i>trans</i> -4-substituted cyclohexane carboxylates + OH ⁻ in 1:1 MeOH-H ₂ O at 50.0° ^{bb} : <i>t</i> -Bu, 221.; OH, 415.; CO ₂ Me, 463.; CO ₂ ⁻ , 165. ^f ; H, 204.; CN, 844
72.	10 ⁴ <i>kr</i> , methyl- <i>trans</i> -4-substituted cyclohexane carboxylates + OH ⁻ in 1:1 dioxane-H ₂ O at 29.4° ^{bb} : <i>t</i> -Bu, 162.; OH, 520.; CO ₂ Me, 565.; CO ₂ ⁻ , 215. ^f ; H, 194; CN, 1010.
73.	10 ⁴ <i>kr</i> , methyl- <i>trans</i> -4-substituted cyclohexane carboxylates + OH ⁻ in 1:1 dioxane-H ₂ O at 50.0° ^{bb} : <i>t</i> -Bu, 534.; OH, 1670.; CO ₂ Me, 1790.; CO ₂ ⁻ , 597. ^f ; H, 634.; CN, 3880
74.	10 ⁴ <i>kr</i> , ethyl- <i>trans</i> -4-substituted cyclohexane carboxylates + OH ⁻ in 1:1 EtOH-H ₂ O at 29.4° ^{bb} : <i>t</i> -Bu, 18.6; OH, 53.0; CO ₂ Me, 65.5; CO ₂ ⁻ , 20.2 ^f ; H, 17.6; CN, 150.
75.	10 ⁴ <i>kr</i> , ethyl- <i>trans</i> -4-substituted cyclohexane carboxylates + OH ⁻ in 1:1 EtOH-H ₂ O at 50.0° ^{bb} : <i>t</i> -Bu, 72.5; OH, 180.; CO ₂ Me, 232.; CO ₂ ⁻ , 68.4 ^f ; H, 66.1; CN, 493.
76.	10 ⁴ <i>kr</i> , ethyl- <i>trans</i> -4-substituted cyclohexane carboxylates + OH ⁻ in 1:1 dioxane-H ₂ O at 29.4° ^{bb} : <i>t</i> -Bu, 42.4; OH, 137.; CO ₂ Me, 148.; CO ₂ ⁻ , 60.6 ^f ; H, 42.4; CN, 284.
77.	10 ⁴ <i>kr</i> , ethyl- <i>trans</i> -4-substituted cyclohexane carboxylates + OH ⁻ in 1:1 dioxane-H ₂ O at 50.0° ^{bb} : <i>t</i> -Bu, 143.; OH, 442.; CO ₂ Me, 454.; CO ₂ ⁻ , 163. ^f ; H, 165.; CN, 1070.
78.	<i>kr</i> , <i>trans</i> -4-substituted cyclohexane carboxylic acids + diazodiphenylmethane in EtOH at 30° ⁿ : H, 0.357; OH, 0.484; OMe, 0.483; CO ₂ Me, 0.495; Cl, 0.564; CN, 0.622
79.	<i>kr</i> , methyl- <i>trans</i> -4-substituted cyclohexane carboxylates + OH ⁻ in 50% w/w MeOH-H ₂ O at 24.91° ⁿ : H, 2.34; OH, 5.45; CO ₂ ⁻ , 1.55; OMe, 5.83; CO ₂ Me, 7.06; CN, 11.46
80.	p <i>K</i> _a , substituted acetic acids in 50% v/v (1:1) EtOH-H ₂ O at 25° ^{dd} : PhCH ₂ , 6.06; Ph, 5.73; ClCH ₂ , 5.35; PhO, 4.46; Br, 4.13; CN, 3.61

^a H. D. Holtz and L. M. Stock, *J. Amer. Chem. Soc.*, 86, 5188 (1964); E. W. Baker, R. C. Parish, and L. M. Stock, *J. Amer. Chem. Soc.*, 89, 5677 (1967).

^b Includes statistical factor, 1/2.

^c Includes statistical factor of 2.

^d G. Kortum, W. Vogel, and K. Andrussow, *Pure Appl. Chem.*, 1, 190 (1961).

σ_R are not related. The magnitude of D provides further evidence of the unimportance of resonance effects, as does a comparison of the value of $100r^2$ obtained previously with the value obtained by correlating the data with the σ_L constants alone using Equation 36 (99.91). Results of the latter correlation have been listed in Table 9. Obviously the use of the extended Hammett equation has not resulted in any better correlation than is obtained simply with σ_I .

We may now turn our attention to the possible existence of steric effects. Very large substituents such as bulky aryl groups have been reported to show no steric effects in substituted acetic acids of the type $X^1X^2X^3\text{CCO}_2\text{H}$ in their reaction with diazodiphenylmethane (23,24). As the rate-determining step in this reaction is believed to involve proton transfer from the acid to the diazodiphenylmethane, those observations are significant. We have correlated $\text{p}K_a$ s for this type of acetic acid with the modified Taft equation in the form

$$Q_Z = Sv_Z + h \quad (68)$$

^e D. D. Perrin, *Dissociation Constants of Organic Bases in Aqueous Solution*, Butterworth, London, 1965.

^f Excluded from the correlation.

^g J. D. Roberts and W. T. Moreland Jr. *J. Amer. Chem. Soc.*, **75**, 2167 (1953).

^h C. F. Wilcox and C. Leung, *J. Amer. Chem. Soc.*, **90**, 336 (1968).

ⁱ K. Bowden and D. C. Parkin, *Can. J. Chem.*, **47**, 177 (1969).

^j C. L. Liotta, W. F. Fisher, G. H. Greene, Jr., and B. L. Joyner, *J. Amer. Chem. Soc.*, **94**, 4891 (1972).

^k T. W. Cole Jr., C. J. Mayers, and L. M. Stock, *J. Amer. Chem. Soc.*, **96**, 4555 (1974).

^l H. Stetter and J. Mayer, *Chem. Ber.*, **95**, 687 (1962).

^m M. L. Bagal and V. I. Lantvoev, *Zhur. Org. Khim.*, **9**, 291 (1973).

ⁿ S. Siegal and J. M. Komarmy, *J. Amer. Chem. Soc.*, **82**, 2547 (1960).

^o C. A. Grob and M. G. Schlageter, *Helv. Chim. Acta*, **59**, 264 (1976).

^p J. Palacek and J. Hlavaty, *Collect. Czech. Chem. Commun.*, **38**, 1985 (1973).

^q C. A. Grob, W. Simon and D. Treffert, *Angew. Chem. Internat. Ed.*, **12**, 319 (1973).

^r O. Exner, *Collect. Czech. Chem. Commun.*, **31**, 65 (1966).

^s O. Exner and J. Jonas, *Collect. Czech. Chem. Commun.*, **27**, 2246 (1962).

^t I. M. Kolthoff and M. K. Chantooni, Jr., *J. Amer. Chem. Soc.*, **98**, 5063 (1976).

^u C. Moreau, *Bull. Soc. Chim. France*, 31 (1968).

^v C. D. Ritchie and G. H. Megerle, *J. Amer. Chem. Soc.*, **89**, 1452 (1967).

^w C. D. Ritchie and P. D. Heffley, *J. Amer. Chem. Soc.*, **87**, 5402 (1968).

^x K. Bowden, M. Hardy, and D. C. Parkin, *Can. J. Chem.*, **46**, 2929 (1968).

^y K. Bowden and D. C. Parkin, *Can. J. Chem.*, **47**, 177 (1969).

^z C. A. Grob and M. G. Schlageter, *Helv. Chim. Acta*, **56**, 509 (1974).

^{aa} N. B. Chapman, B. Ehson, J. Shorter, and K. J. Toyne, *J. Chem. Soc. B*, 931 (1968).

^{bb} N. B. Chapman, B. Ehson, J. Shorter, and K. J. Toyne, *J. Chem. Soc., B*, 178 (1968).

^{cc} At 16°.

^{dd} E. N. Tsvetkov, R. A. Malevannaya, L. I. Petrovskaya, and M. I. Kabachnik, *Zhur. Obshch. Khim.*, **44**, 1225 (1974).

TABLE 9
Results of Correlations with Data in Protonic Media

Set	L	r^a	F^b	s_{est}^c	s_L^c	s_h	$100r^2$	n^c	h
1	-4.10	0.9990	3075.	0.0396	0.0740	0.0205	99.81	8	4.801
2	-4.09	0.9992	3780.	0.0356	0.0666	0.0184	99.84	8	4.795
3	-4.12	0.9994	7930.	0.0322	0.0462	0.0164	99.87	12	4.798
4	-4.06	0.9995	5059.	0.0282	0.0571	0.0145	99.90	7	4.793
5	-4.08	0.9996	14025.	0.0240	0.0345	0.0122	99.93	12	4.788
6	-4.05	0.9996	5863.	0.0283	0.0529	0.0154	99.91	7	4.791
7	-4.04	0.9997	15844.	0.0224	0.0321	0.0114	99.94	12	4.795
8	-4.01	0.9996	13903.	0.0238	0.0340	0.0121	99.93	12	4.797
9	-4.04	0.9995	6201.	0.0274	0.0513	0.0142	99.90	8	4.809
10	-4.03	0.9994	5372.	0.0294	0.0550	0.0152	99.89	8	4.819
11	-4.05	0.9987	2296.	0.0315	0.0846	0.0176	99.74	8	4.832
12	-4.04	0.9981	1607.	0.0604	0.101	0.0289	99.63	8	4.800
13	-4.06	0.9990	1497.	0.0296	0.105	0.0204	99.80	5	4.839
14	-1.72	0.9926	469.4	0.0497	0.0792	0.0207	98.53	9	4.832
15	-1.43	0.9916	234.9	0.0271	0.0935	0.0146	98.33	6	4.834
16	-9.16	0.9943	1048.	0.181	0.283	0.0601	98.87	14	10.47
17	-4.82	0.9893	323.0	0.0899	0.268	0.0347	97.88	9	10.59
18	-1.44	0.9947	280.3	0.0380	0.0862	0.0321	98.94	5	6.73
19	-1.56	0.9958	941.6	0.0540	0.0509	0.0236	99.16	10	6.452
20	-1.14	0.9807	125.8	0.0663	0.102	0.0435 ^f	96.18	7	5.778
21	-0.878	0.9969	7924.	0.0311	0.0312	0.0163	99.37	7	5.036
22	-0.982	0.9985	1644.	0.0242	0.0242	0.0127	99.70	7	5.568
23	-1.14	0.9986	1080.	0.0222	0.0347	0.0127	99.72	5	6.230
24	-1.03	0.9978	1124.	0.0307	0.0308	0.0161	99.56	7	4.824
25	-1.16	0.9986	1732.	0.0279	0.0279	0.0146	99.71	7	5.346
26	-1.37	0.9996	7128.	0.0162	0.0162	0.00847	99.93	7	6.016
27	-1.19	0.9991	1679.	0.0178	0.0289	0.0122	99.82	5	5.21
28	-1.20	0.9992	1838.	0.0172	0.0279	0.0118	99.84	5	6.25
29	-0.738	0.9932	437.9	0.0242	0.0353	0.0114	98.65	8	6.301
30	-1.43	0.9910	218.1	0.0625	0.0972	0.0349	98.20	6	5.93
31	-1.47	0.9531	59.44	0.0949	0.190	0.0691	90.83	8	6.81
32	-1.39	0.9805	95.21	0.0799	0.143	0.0498	92.25	10	6.91
33	-0.747	0.9945	545.4	0.0207	0.0320	0.0109	98.91	8	4.90
34	-0.754	0.9680	59.60 ^g	0.0431	0.0977 ^f	0.0356	93.71	6	6.09
35	-1.10	0.9911	222.0	0.0326	0.0741	0.0270	98.23	6	6.38
36	-5.28	0.9934	1276.	0.125	0.148	0.0473	98.69	19	11.03
37	-5.12	0.9915	520.0	0.135	0.225	0.0702	98.30	11	10.92
38	-5.13	0.9918	542.2	0.132	0.220	0.0688	98.32	11	9.87
39	-4.71	0.9849	161.9	0.179	0.370	0.121	97.00	7	9.07
40	-5.23	0.9931	359.0	0.156	0.276	0.0742	98.63	7	10.95
41	-0.729	0.9961	634.2	0.0146	0.0289	0.0111	99.22	7	5.91
42	-0.832	0.9745	94.16	0.0433	0.0857	0.0329	94.96	7	6.84
43	-0.905	0.9659	111.3	0.0442	0.0858	0.0303	93.30	10	5.78
44	-0.964	0.9429	64.06	0.0621	0.120	0.0425	88.90	10	6.88
45	1.42	0.9894	138.9 ^g	0.0492	0.121 ^f	0.0234 ^h	97.94	5	4.883
46	-3.92	0.9970	671.8	0.0825	0.151	0.0484	99.41	6	9.713
47	-3.19	0.9859	347.9	0.110	0.171	0.0467	97.21	12	9.594
48	-1.05	0.9941	334.2	0.0254	0.0576	0.0208	98.82	6	10.227

TABLE 9
Results of Correlations with Data in Protonic Media

Set	L	r^a	F^b	s_{est}^c	s_L^c	s_h	$100r^2$	n^e	h
49	-1.06	0.9894	186.0	0.0342	0.0776	0.0280	97.90	6	10.393
50	-2.67	0.9997	5120.	0.0187	0.0373	0.00973	99.94	5	6.529
51	-2.64	0.9993	2109.	0.0287	0.0575	0.0150	99.86	5	6.076
52	1.19	0.9819	80.49 ^g	0.0531	0.133 ^f	0.0254 ⁱ	96.41	5	4.893
53	-4.52	0.9934	975.6	0.104	0.145	0.0441	98.69	15	6.065
54	-4.58	0.9953	1163.	0.0906	0.134	0.0430	99.06	13	7.183
55	2.39	0.9948	1241.	0.0489	0.0680	0.0207 ^f	98.96	15	0.0838
56	2.50	0.9945	1178.	0.0525	0.0729	0.0222	98.91	15	-0.247
57	2.64	0.9935	985.9	0.0605	0.0840	0.0256	98.70	15	-0.390
58	2.94	0.9858	447.4	0.0999	0.139	0.0423	97.18	15	-0.729
59	2.97	0.9905	674.0	0.0823	0.114	0.0348	98.11	15	-0.601
60	3.08	0.9910	715.3	0.0828	0.115	0.0350	98.21	15	-0.805
61	0.686	0.9962	394.0	0.0152	0.0346	0.0129	99.24	5	-0.619
62	2.19	0.9927	202.8	0.0677	0.154	0.0572 ⁱ	98.54	5	0.259
63	0.556	0.9992	1791.	0.00809	0.0131	0.00555	99.83	5	1.09
64	0.631	0.9995	2841.	0.0729	0.0118	0.00500	99.89	5	0.536
65	0.638	0.9982	848.1	0.0135	0.0219	0.00924	99.65	5	0.322
66	0.756	0.9986	1052.	0.0143	0.0233	0.00984	99.72	5	0.265
67	0.761	0.9943	260.9	0.0290	0.0471	0.0199 ^j	98.86	5	-0.00267
68	-1.12	0.9823	771.3	0.0373	0.0403	0.0114	96.50	30	0.621
69	-0.923	0.9646	147.1	0.0469	0.0761	0.0240	93.04	13	1.02
70	1.22	0.9876	118.4 ^g	0.0542	0.112	0.0349	97.53	5	1.68
71	1.04	0.9960	375.3	0.0261	0.0539	0.0168	99.21	5	2.34
72	1.36	0.9789	68.70 ^g	0.0792	0.164 ^f	0.0510	95.82	5	2.29
73	1.45	0.9897	143.4 ^g	0.0586	0.121 ^f	0.0377	97.95	5	2.79
74	1.62	0.9957	346.7	0.0420	0.0869	0.0271	99.14	5	1.28
75	1.50	0.9961	381.2	0.0372	0.0770	0.0240	99.22	5	1.86
76	1.48	0.9816	79.26 ^g	0.0803	0.166 ^f	0.0517	96.35	5	1.67
77	1.47	0.9909	162.6 ^g	0.0558	0.115 ^f	0.0359	98.19	5	2.21
78	0.410	0.9897	190.8	0.0131	0.0297	0.0108	97.95	6	-0.436
79	1.20	0.9929	276.9	0.0429	0.0720	0.0230	98.58	6	0.414
80	-4.47	0.9981	1063.	0.0663	0.137	0.0485	99.63	6	6.20
4E	-4.07	0.9995	4340.	0.0302	0.0617	0.0158	99.91	6	4.791
6E	-4.06	0.9996	4902.	0.0309	0.0579	0.0172	99.92	6	4.789
11E	-4.05	0.9987	1849.	0.0341	0.0941	0.0191	99.73	7	4.832
12E	-4.04	0.9982	1399.	0.0646	0.108	0.0317	99.64	7	4.796
13E	-4.05	0.9989	877.8 ^g	0.0359	0.137 ^f	0.0248 ⁱ	99.77	4	4.839
17E	-4.99	0.9877	239.0	0.0902	0.323	0.0349	97.55	8	10.59
18E	-1.47	0.9993	1480.	0.0165	0.0382	0.0152	99.87	4	6.75
19E	-1.76	0.9963	679.6	0.0369	0.0677	0.0239	99.27	7	6.508
21E	-0.958	0.9990	1028.	0.0129	0.0299	0.0120	99.81	4	5.079
22E	-1.07	0.9995	2159.	0.00988	0.0229	0.00923	99.91	4	5.607
23E	-1.20	0.9999	3595. ^k	0.00861	0.0200 ^h	0.00854	99.97	3	6.260
24E	-1.13	0.9989	930.2 ^g	0.0159	0.0369 ^f	0.0149	99.79	4	4.871
25E	-1.26	0.9985	665.1 ^g	0.0210	0.0488 ^g	0.0196	99.70	4	5.386
26E	-1.40	0.9992	1201.	0.0174	0.0405	0.0163	99.83	4	6.035
29E	-0.726	0.9898	193.6	0.0277	0.0522	0.0180	97.98	6	6.294
30E	-1.37	0.9874	77.59 ^k	0.0668	0.155 ^h	0.0624	97.49	4	5.91

TABLE 9
Results of Correlations with Data in Protonic Media

Set	L	r^a	F^b	s_{est}^c	s_L^c	s_h	$100r^2$	n^e	h
31E	-1.52	0.9766	103.0	0.0738	0.150	0.0566	95.37	7	6.85
32E	-1.43	0.9806	175.4	0.0598	0.108	0.0386	96.16	9	6.93
33E	-0.714	0.9949	293.6	0.0180	0.0417	0.0160	98.99	5	4.89
34E	-0.776	0.9787	68.27 ⁸	0.0406	0.0940 ^f	0.0361	95.79	5	6.10
35E	-1.12	0.9941	253.7	0.0304	0.0703	0.0270	98.83	5	6.39
37E	-5.12	0.9978	1594.	0.0745	0.128	0.0429	99.56	9	10.94
38E	-5.00	0.9958	831.2	0.101	0.173	0.0579	99.16	9	9.80
39E	-4.39	0.9975	588.9	0.0183	0.181	0.0666	99.49	5	8.89
43E	-0.907	0.9654	96.00	0.0472	0.0926	0.0336	93.20	9	5.78
44E	-0.947	0.9460	59.65	0.0625	0.123	0.0445	89.50	9	6.86
46E	-3.85	0.9997	3716.	0.0334	0.0631	0.0233	99.95	4	9.67
48E	-1.05	0.9984	633.0 ⁸	0.0181	0.0419 ^f	0.0167	99.69	4	10.235
49E	-1.07	0.9909	108.1 ^f	0.0444	0.103 ^f	0.0409	98.18	4	10.399
53E	-4.52	0.9941	1010.	0.102	0.142	0.0440	98.83	14	6.07
55E	-2.40	0.9960	1489.	0.0447	0.0621	0.0192 ^f	99.20	14	0.0779
56E	2.50	0.9957	1372.	0.0486	0.0675	0.0208	99.13	14	-0.253
57E	2.64	0.9951	1219.	0.0544	0.0756	0.0233	99.03	14	-0.398
58E	2.94	0.9882	499.3	0.0946	0.131	0.0406	97.65	14	-0.739
59E	2.97	0.9941	1001.	0.0675	0.0938	0.0290	98.82	14	-0.613
60E	3.08	0.9921	750.9	0.0808	0.112	0.0347	98.43	14	-0.812
61E	0.697	0.9997	3515.	0.00508	0.0118	0.00469	99.94	4	-0.628
62E	2.24	0.9988	848.2 ⁸	0.0332	0.0767 ^f	0.0306 ^h	99.76	4	0.219
68E	-1.11	0.9835	770.5	0.0368	0.0401	0.0115	96.74	28	0.619
69E	-0.936	0.9671	129.9	0.0488	0.0821	0.0274	93.52	11	1.019
70E	1.21	0.9943	172.7 ^f	0.0446	0.0923 ^f	0.0302	98.86	4	1.668
71E	1.04	0.9980	459.9 ⁸	0.0226	0.0468	0.0153	99.60	4	2.332
72E	1.35	0.9928	136.8 ^f	0.0557	0.115	0.0377	98.56	4	2.267
73E	1.44	0.9978	452.7 ⁸	0.0328	0.0679 ^f	0.0222	99.56	4	2.775
74E	1.61	0.9984	636.7 ⁸	0.0309	0.0639 ^f	0.0209	99.69	4	1.272
75E	1.50	0.9973	369.7 ⁸	0.0377	0.0780 ^f	0.0255	99.46	4	1.855
76E	1.47	0.9959	240.3 ⁸	0.0458	0.0947 ^f	0.0310	99.17	4	1.646
77 E	1.46	0.9989	872.1 ⁸	0.0240	0.0496 ^f	0.0162	99.77	4	2.193
78E	0.422	0.9994	2568.	0.00360	0.00832	0.00320	99.88	5	-0.445
79E	1.22	0.9886	86.57 ^k	0.0531	0.132 ^h	0.0473 ^h	97.74	4	0.397

Superscripts of F , and of s indicate confidence levels (CL). In the case of s , CL of Student t test of L and h . In the absence of a superscript, the CL is 99.9%.

^a Correlation coefficient.

^b F test for significance of correlation.

^c Standard errors.

^d Percent of data accounted for by the regression equation.

^e Number of points in set.

^f 99.0% CL.

⁸ 99.5% CL.

^h 98.0% CL.

ⁱ 95.0% CL.

^j < 20.0% CL.

^k 97.5% CL.

TABLE 10
Data Used in Correlations with Equation 66

1.	<p>pK_a, XCO₂H in water at 10°^a: Me, 4.762; Et, 4.877; <i>i</i>-Pr, 4.827; <i>t</i>-Bu, 5.014; Pr, 4.803; <i>i</i>-Bu, 4.742; Am, 4.763; PrMe₂C, 5.021; <i>s</i>-BuCH₂, 4.752; <i>i</i>-Am, 4.887; AmCH₂, 4.839; <i>n</i>-C₇H₁₅, 4.794</p>
2.	<p>pK_a, XCO₂H in water at 25°^a: Me, 4.756; Et, 4.874; <i>i</i>-Pr, 4.853; <i>t</i>-Bu, 5.03; Pr, 4.817; <i>s</i>-Bu, 4.761; <i>t</i>-Am, 4.93; <i>i</i>-Bu, 4.777; Et₂CH, 4.751; Am, 4.842; PrMe₂C, 4.969; <i>s</i>-BuCH₂, 4.766; <i>i</i>-Am, 4.845; AmCH₂, 4.879; <i>n</i>-C₇H₁₅, 4.893; <i>n</i>-C₈H₁₇, 4.895</p>
3.	<p>pK_a, XCO₂H, in water at 40°^a: Me, 4.769; Et, 4.891; <i>i</i>-Pr, 4.918; <i>t</i>-Bu, 5.067; Pr, 4.854; <i>i</i>-Bu, 4.831; Et₂CH, 4.813; Am, 4.861; PrMe₂C, 5.088; <i>s</i>-BuCH₂, 4.821; <i>i</i>-Am, 4.879; AmCH₂, 4.890; <i>n</i>-C₇H₁₅, 4.88</p>
4.	<p>pK_a, XCO₂H in 50% v/v MeOH-H₂O at 40°^b: Me, 5.56; Me(<i>t</i>-BuCH₂)CH, 6.05; Me-<i>t</i>-BuCH, 6.25; Et-<i>t</i>-BuCH, 6.31; (<i>i</i>-Pr)₂CH, 6.40; Et₃C, 6.44; <i>t</i>-BuCH₂CMe₂, 6.50; (<i>t</i>-BuCH₂)₂CH, 6.56; <i>t</i>-BuCMe₂, 6.72; <i>t</i>-BuCH₂CMe<i>t</i>-Bu, 6.96</p>
5.	<p>pK_a, XCO₂H in 10% w/w MeAc-H₂O at 25°^c: Me, 4.903; Et, 4.987; <i>t</i>-Bu, 5.232; (<i>t</i>-BuCH₂)₂CH, 5.416; <i>t</i>-BuCH₂CMe-<i>t</i>-Bu, 6.167</p>
6.	<p>pK_a, XCO₂H in 25% MeAc-H₂O at 25°^c: Me, 5.233; Et, 5.440; <i>t</i>-Bu, 5.790; (<i>t</i>-BuCH₂)₂CH, 6.176; <i>t</i>-BuCH₂CMe-<i>t</i>-Bu, 6.821</p>
7.	<p>pK_a, XNH₃⁺ in water at 25°^{d,e}: Me, 10.657; Et, 10.70; Pr, 10.69; <i>i</i>-Pr, 10.67; <i>t</i>-BuCH₂, 10.24; <i>i</i>-Bu, 10.43; <i>t</i>-Bu, 10.68; Bu, 10.65; <i>i</i>-Am, 10.60; Me₂EtC, 10.72; Am, 10.62; Et₂CH, 10.42; Et₂MeC, 10.63; <i>t</i>-BuCH₂CMe₂, 10.73; Et₃C, 10.59; (<i>i</i>-Pr)₂CH, 10.23; <i>n</i>-C₆H₁₃, 10.56; <i>n</i>-C₇H₁₅, 10.66; MeAmCH, 10.67; AmMe₂C, 10.56</p>
8.	<p>pK_a, XNH₃⁺ in 43.4% MeOH-H₂O at 25°^f: Me, 9.98; Et, 9.95; Pr, 9.76; <i>i</i>-Pr, 9.67; Bu, 9.84; <i>i</i>-Bu, 9.64; Am, 9.79; <i>i</i>-Am, 9.81; <i>n</i>-C₆H₁₃, 9.87; <i>n</i>-C₆H₁₃CHMe, 9.80</p>

^a J. J. Christensen, M. O. Slade, D. E. Smith, R. M. Izatt, and J. Tsang, *J. Amer. Chem. Soc.*, **92**, 4164 (1970).

^b G. S. Hammond and D. H. Hogle, *J. Amer. Chem. Soc.*, **77**, 3384 (1955).

^c J. F. J. Dippy, S. R. C. Hughes, and A. Rozanski, *J. Chem. Soc.*, 1959, 1441.

^d Footnote e, Table 8.

^e J. J. Christensen, R. M. Izatt, D. P. Wrathall, and L. D. Hansen, *J. Chem. Soc. A*, 1212 (1969).

^f C. L. DeLigny, *Rec. Trav. Chim.* **79**, 731 (1960)

where $Z = X^1X^2X^3C$, and that the steric effect is not of the same magnitude in the acidic and basic ester hydrolysis. Significant correlations were obtained (Table 11), however the values of S were very small. The data used in the correlations are given in Table 10. Only alkyl substituted acids were examined, as we believe that the localized electrical effects of alkyl groups are constant and not significantly different from zero. The delocalized electrical effects of alkyl groups also seem to be constant. The electrical effects of alkyl groups, as we have noted previously, have been a subject for controversy. Many investigations of the structural effects of alkyl groups have been interpreted on the assumption that the σ^* values of Taft represent a good measure of alkyl group electrical effects.

TABLE 11
Results of Correlations with the Modified Taft Equation

Set	S	h	r^a	F^b	s_{est}^c	s_S^c	s_h^c	$100r^2$	n^c
1	0.192	4.677	0.6502	7.323 ^m	0.0758	0.0708 ⁱ	0.0641	42.27	12
2	0.0647	4.791	0.3003	1.388 ^h	0.0800	0.0549 ⁱ	0.0554	9.02	16
3	0.136	4.767	0.5277	4.256 ^m	0.0820	0.0659 ^m	0.0636	27.85	13
4	0.5071	5.35	0.9036	35.60	0.173	0.0850	0.181	81.65	10
5	-0.4663	0.344	0.9738	55.09 ^f	0.132	0.0628	0.110 ^m	94.84	5
6	-0.595	-0.0172	0.9934	226.0	0.0834	0.0396	0.0691 ^j	98.69	5

Footnotes a through k are given in Table 9.

ⁱ 50.0% CL.

^m 90.0% CL.

ⁿ <90.0% CL.

Charton has supplied evidence which suggests strongly that alkyl σ^* values are not a measure of electrical effects. The first line of evidence (13) consists in the derivation of the equation

$$\sigma_{alkyl}^* = m \nu_{alkyl} + c \quad (69)$$

which is applicable on the condition that the electrical effect is either constant or negligible. The ν constants were taken from a recent compilation, or estimated from equations therein (44). Equation 69 was shown to correlate the Taft σ^* alkyl values, although poorly. The results were significant at the 99.5% CL, but the correlation equation accounted for only 53.6% of the data. The failure of the σ_{alkyl}^* values to give better correlation with Equation 69 was thought due to the use of average values of (k_X/k_{Me}) obtained from rate data in different solvents. More recently (45), Charton has calculated corrected σ_{alkyl}^* values from rate constants for acidic and basic ester hydrolysis in the same solvent at the same temperature. The results obtained on correlating these corrected σ_{alkyl}^* values with Equation 69 are in fact improved, the correlation equation obtained now accounting for about 78% of the data. The failure to account for the remainder of the data may be due to slight differences in the steric effects which occur in acidic and basic ester hydrolysis. Equation 3 which defines σ^* values involves the difference between the ratios (k_X/k_{Me}) for acidic and for basic hydrolysis. Thus, the small differences in the nature of the steric effect will be magnified in the σ^* values.

The second line of evidence (14) is based on the calculation of σ^* values for amide hydrolysis. It was shown that acidic and basic amide hydrolyses do indeed have steric effects of the same magnitude (41). Values of σ_{alkyl}^* were then calculated from appropriate rate constants by means of Equation 3. The resulting σ_{alkyl}^* values were very much different from those of Taft. The latter are supposed to vary regularly with the degree of branching (9,15), whereas the former show no dependence on structure.

TABLE 12
Values of $\bar{\nu}$ and S for XCH_2CO_2H Sets

Set	$\bar{\nu}$	S	n	Set	$\bar{\nu}$	S	n
1	0.665	0.110	8	9	0.665	0.100	8
2	0.665	0.110	8	10	0.665	0.110	8
3	0.654	0.0906	12	11	0.620	0.0719	8
4	0.614	0.0757	7	12	0.798	0.195	8
5	0.654	0.0906	12	13	0.800	0.282	5
6	0.594	0.0600	7	14	0.764	0.148	9
7	0.654	0.0906	12	15	0.663	0.0513	6
8	0.654	0.0906	12				

On the basis of this evidence it seems probable that the Taft σ^* values are not a useful measure of the electrical effects of alkyl groups. The problem of the nature of the effects of alkyl substituents is a complicated one to begin with, and is made more so by semantics. Thus, many authors have reported phenomena that are a function of the degree of branching of the alkyl group. Is this dependence on branching due to electrical or steric effects? Charton has shown that the ν_{alkyl} and ν'_{alkyl} values are given by the equation

$$\nu_{\text{alkyl}} = an_{\alpha} + bn_{\beta} + cn_{\gamma} + h \quad (70)$$

This relationship shows that the steric effects of alkyl groups are dependent on the degree of branching. Obviously, then, dependence of the effect of alkyl groups on the degree of branching is not sufficient to indicate an electrical effect. To demonstrate the existence of electrical effects that are large enough to be significant and that vary with structure it is necessary to investigate a property as a function not only of alkyl group variation but as a function of other substituent types as well. If steric effects can be shown to be absent, and alkyl groups then exert reproducible significant effects that vary with branching, it may safely be concluded that electrical effects of alkyl groups that vary with structure have been clearly shown to exist. To our knowledge, no such property in the liquid phase has been reported. Examination of σ_m and σ_p values for alkyl groups support our conclusion that the electrical effects of alkyl groups are constant.

The results of the correlations with Equation 68 suggest that the pK_a s of acids of the type XCO_2H exhibit a very small dependence on steric effects, the magnitude of which is a function of the solvent. Thus, S increases with decreasing solvent polarity. In water the steric effect is obviously small. A further point concerning the significance of the steric effect is that in the substituted acetic acid sets studied (Sets 1-11, Table 8) the ν values of the CH_2X groups are close to being constant as is seen by considering the mean values of ν_{CH_2X} and their standard errors (Table 12). In arriving at these values, ν values of the $AcNHCH_2$, $H_2NCONHCH_2$ and $EtCONHCH_2$ groups were assumed equal to that of the isoamyl group. If we take 0.200 as a value of S (slightly larger than

the largest of the S values obtained in water), the steric effect of a substituent whose v_{CH_2X} values deviates from the mean by as much as 0.30 v units on its σ_I constant will be given by

$$\Delta\sigma_{IX} = \frac{S|\bar{v} - v_{CH_2X}|}{L} \quad (71)$$

Thus for substituted acetic acids in water at 25°, the maximum error to be expected is 0.015 σ units. As S is probably about 0.1 and $|\bar{v} - v_{CH_2X}|$ will generally be less than 0.30, the error in σ_I values obtained from acetic acid ionization constants should be negligible for most substituents.

We have pointed out that different transition states will generally require different steric parameters. It might be that the v_{alkyl} parameters are not the best choice for the ionization of XCO_2H . We have therefore examined the correlation of sets X-1 through X-3 with the equation

$$pK_a = an_\alpha + bn_\beta + cn_\gamma + dn_\delta + h \quad (72)$$

We have also examined the correlation of the alkyl ammonium ions, XNH_3^+ with Equation 72 (sets X-7 and X-8). The results are given in Table 13. On the basis of these results we may conclude that steric effects in XCO_2H and XNH_3^+ ionizations are generally insignificant and therefore the use of substituted acetic acids, 2- and 3-substituted propanoic acids, substituted methylammonium ions, and 2-substituted ethylammonium ions for the evaluation of localized effect substituent constants is valid in so far as steric effects are concerned. We have already remarked that the substituted acetic acids fulfill the other desirable requirements of secondary sources for the evaluation of σ_I constants. This is true also of the other systems noted previously. We have therefore made use of these secondary sources to obtain the σ_I values which are collected in Table 7 together with the primary σ_I values. In some cases, the σ_I value reported is an average value obtained from two different sources. In these cases the value reported is in our opinion, the best one available.

It cannot be overemphasized that the σ_I constants in Table 8 were defined for use in protonic media. To further establish their validity we have correlated ionization constants for various rigid systems which are free of steric and conformation effects, and are dependent only on the localized electrical effect. The sets studied include 18, 22-26, 29-40, 45, 48, and 49 (Table 8). The results of the correlations are set forth in Table 9. They are excellent and confirm the validity of the σ_I constants in Table 7. We have also examined a number of systems, in which the substituent is bonded to an sp^3 hybridized carbon atom which is in turn bonded to one or more sp^2 carbon atoms with excellent results (Sets 19, 20, 27, 28; Table 8). Results of the correlations are in Table 9. These results, coupled with those obtained for substituted acetic acids, show that a

TABLE 13
Results of Correlations with Equation 72

Set	<i>a</i>	<i>b</i>	<i>c</i>	<i>d</i>	<i>h</i>	<i>F</i> ^a	<i>R</i> ^b	<i>r</i> ₁₂ ^c	<i>r</i> ₁₃ ^c
1	0.0792	-0.0512	0.0499	-0.0363	4.757	0.884 ⁱ	0.9217 ^j	0.190	0.051
2	0.0674	-0.0580	0.0366	0.0585	4.773	8.860 ^j	0.08736	0.055	0.236
3	0.0924	-0.0420	0.0348	0.0134	4.778	15.10	0.9397	0.078	0.100
7	0.0403	-0.111	0.0237	-0.00923	10.65	10.08	0.8538	0.176	0.049
8	-0.124	-0.110	0.0357	0.0651	9.99	4.196 ^g	0.8778	0.062	0.112

Set	<i>r</i> ₁₄ ^c	<i>r</i> ₂₃ ^c	<i>r</i> ₂₄ ^c	<i>r</i> ₃₄ ^c	<i>s</i> _{est} ^d	<i>s</i> _a ^d	<i>s</i> _b ^d	<i>s</i> _c ^d	<i>s</i> _d ^d
1	0.226	0.410	0.140	0.376	0.0463	0.0165 ^f	0.0217 ^g	0.0246 ^g	0.0342 ^h
2	0.333	0.232	0.055	0.471	0.0460	0.0142	0.0180 ^f	0.0220 ^k	0.0313 ^g
3	0.252	0.256	0.058	0.399	0.0387	0.0133	0.0153 ^l	0.0191 ^k	0.0286 ^m
7	0.092	0.195	0.164	0.323	0.0857	0.0208 ^g	0.0190	0.0256 ^h	0.0423 ⁿ
8	0.284	0.302	0.218	0.395	0.0693	0.0424 ^l	0.0385 ^l	0.0370 ^h	0.0542 ^h

Set	<i>s</i> _n ^d	<i>n</i> ^e
1	0.0340	12
2	0.0323	16
3	0.0278	13
7	0.0485	20
8	0.0573	10

^a *F* test for significance of correlation. Superscript if present, indicates CL; if absent, CL = 99.9%.

^b Multiple correlation coefficient.

^c Partial correlation coefficient. Superscript when present indicates CL, when absent, CL <90.0%.

^d Standard errors. Superscript when present indicates CL of Student *t* test. When absent, CL is 99.9%.

^e Number of points in set.

^j 99.5% CL.

^f 99.0% CL.

^k 80.0% CL.

^g 90.0% CL.

^l 95.0% CL.

^h 50.0% CL.

^m 20.0% CL.

ⁱ 97.5% CL.

ⁿ <20.0% CL.

single *sp*³ hybridized carbon atom interposed between the substituent and a π -bonded group is sufficient to prevent delocalization involving the entire system. To further establish this point we have investigated systems of the type XCH₂ArY (sets 41–44, 50, 51; Table 8). The results in Table 9 support this argument for proton transfer reactions.

The σ_I constants reported in Table 1 are free of delocalized effects. They are also generally free of steric effects the exceptions being *very* large groups

whose σ_I constants were determined from acetic acid or methylammonium pK_a 's. It must be pointed out in this regard that substituents of the type ZCH_2 do not constitute a problem.

Rate constants for reactions of rigid systems free of steric and conformational effects have also been examined. The sets studied are given in Table 8, results of the correlations in Table 9. These results support those obtained for the ionization constant data. It must be noted that both ionization constants and rate constants of *trans*-4-substituted cyclohexane-1-carboxylic acids and their esters have been included as sets free of steric and conformation effects. The freedom of these sets from conformational effects rests on the knowledge that their members all exist predominantly in the diequatorial conformation.

Certain types of substituent seem to show frequent deviations in correlations. Such groups include ionic groups and substituents containing the hydroxyl group, for example, OH, CH_2OH , and CO_2H . To provide further information on the variability of these substituents we have correlated all the sets in Table 8 which contained any of these groups with the exclusion of the suspect groups. The results are presented in Table 9 (these sets are designated E). Of the fifty sets studied, 27 gave significantly improved correlation, 19 were unchanged and 4 gave worse correlation, as determined by the value of $100r^2$ (a difference in $100r^2 > 0.25$ was considered significant). On the basis of these results, it would seem best to follow the procedure following with ionic or hydroxyl substituents.

1. Correlate the data set excluding the points for the suspicious groups.
2. Correlate the data set adding the suspicious points one by one.

Suspicious points may be included in the final correlation if:

- a. Student *t* tests of the differences between the regression coefficients obtained in the correlation of Step 1 and that of Step 2 shows that the differences are not significant.
- b. The correlation obtained in Step 2 does not have a significantly smaller value of $100r^2$ than does that obtained in Step 1.

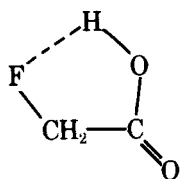
The variability of the substituent effect for ionic or hydroxylic substituents is certainly due at least in part to the medium. The solvation of ionic groups will depend strongly on the nature of the solvent and the ionic strength of the medium, whereas hydroxylic groups will be sensitive to the extent to which they can hydrogen bond to the solvent.

C. Validity of the σ_I Constants in Nonprotonic Media

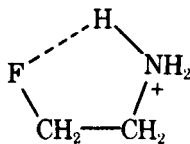
The results described previously clearly establish the validity of the σ_I values reported in Table 1 for use in a wide variety of protonic solvents, including water,

water-alcohol mixtures, and pure alcohols. There are certain exceptions that must be noted, however. Charged (ionic) substituents frequently show deviations in other solvents. For this reason the constants for all such substituents are considered to be uncertain. The constant for the hydroxyl group varies considerably with the nature of the medium. The value reported in Table 7 is restricted to water. When it is used in nonaqueous protonic media it must be considered uncertain. Topsom (46) has noted the very large dependence of substituent constants for OH on the medium. It is quite likely that similar deviations will occur for the NH_2 and NHAc groups. Nonprotonic media are conveniently divided into dipolar aprotic solvents, nonpolar aprotic solvents, and the gas phase.

To assess the validity of the σ_I constants in nonprotonic media we have examined the available data on acidity and rates of reaction of carboxylic acids with diphenyldiazomethane. The data are collected in Table 14; the results of the correlation are in Table 15. The data for the dipolar aprotic solvents seem to show that the σ_I constants are valid in this type of medium. The solvents for which data are available include acetonitrile, dimethylsulfoxide, ethyl acetate and dimethylformamide. Unfortunately, only two sets of data in a nonpolar aprotic solvent are available (sets XIV-8 and 10). The results obtained for these sets are excellent (XIV-8) and very good (XIV-10). However, this is of course not conclusive. The results obtained for the correlation of ΔG_{600} values for the gas phase reaction of substituted acetic acids with water give fairly good results on the exclusion of the value for $\text{X} = \text{F}$. The ionization potentials of 4-substituted quinuclidines also give fairly good results when the values for OH and I are excluded. The failure of the value for $\text{X} = \text{F}$ to fit the correlation equation for the ΔG_{600} of substituted acetic acids may be due to the existence of intramolecular hydrogen bonding giving rise to the species IV, which is analogous to the species V. These were proposed to account for nonadditivity on the proton affinities of the compounds $\text{CF}_n\text{H}_{3-n}\text{CH}_2\text{NH}_2$ (47). The failure of the OH group to fit the correlation equation for the ionization potentials of 4-substituted quinuclidines is in accord with the strong medium dependence of this group.



IV



V

The data in non-protonic media have also been correlated with the exclusion of hydroxylic groups. The results are set forth in Table XV, these sets are des-

TABLE 14
Data in Nonprotonic Media

1. pK_a , substituted acetic acids in MeCN at 25°^a:
Et, 22.73; H, 22.3; Cl, 18.8; CN, 18.04; HOCH₂, 21.00; OH, 19.3
2. pK_a , substituted acetic acids in Me₂SO at 25°^a:
Et, 12.86; H, 12.6; Cl, 9.0; CN, 8.50; HOCH₂, 11.47; OH, 10.20
3. pK_a , 4-(substituted methyl)pyridinium ions in DMF at 15.0°^b:
H, 4.963; Me, 4.981; Et, 5.009; OH, 4.528; Ph, 4.768; CN, 3.609; NH₃⁺, 3.901^f
4. pK_a , 4-(substituted methyl)pyridinium ions in DMF at 35.0°^b:
H, 4.819; Me, 4.831; Et, 4.831; OH, 4.235; Ph, 4.625; CN, 3.571; NH₃⁺, 3.617^f
5. ΔG°_{600} , Substituted acetate ions \pm H₂O, 600°^c:
H, 45.2; Me, 46.4; Et, 47.3; ClCH₂CH₂, 48.1; MeCHCl, 51.4; ClCH₂, 52.5; F, 56.; Cl, 58.; Br, 59.1
6. kr , substituted acetic acids + diazodiphenylmethane in Me₂SO at 30°^d:
H, 0.00429; Me, 0.00368; Et, 0.00335; Ph, 0.0118; PhCH₂, 0.00520; Cl, 0.433; ClCH₂, 0.0237; Br, 0.390; BrCH₂, 0.0360; PhO, 0.168; PhOCH₂, 0.0158; I, 0.356; MeO, 0.0492; OH, 0.0419; HS, 0.0436; CN, 0.731
7. kr , substituted acetic acids + diazodiphenylmethane in EtOAc at 30°^d:
H, 0.00402; Me, 0.0333; Et, 0.0323; Ph, 0.126; PhCH₂, 0.0678; Cl, 4.28; ClCH₂, 0.3215; Br, 4.35; BrCH₂, 0.525; PhO, 1.39^f; PhOCH₂, 0.0972; I, 2.295; MeO, 0.3775^f; OH, 1.70^f; HS, 0.755; CN, 14.6
8. kr , substituted acetic acids + diazodiphenylmethane in PhMe, at 30°^d:
H, 0.294; Me, 0.160; Et, 0.155; Ph, 1.37; PhCH₂, 0.491; Cl, 302.; ClCH₂, 7.36; Br, 282.; BrCH₂, 8.58; PhO, 93.2; I, 101.; MeO, 12.1
9. Ionization potentials 4-substituted quinuclidines^e:
H, 8.05; Me, 8.06; Et, 8.05; *i*-Pr, 7.99; *t*-Bu, 7.97; C₂H, 8.30; Ph, 8.13; OH, 8.48^f; CH₂OH, 8.17; OAc, 8.42; Cl, 8.55; Br, 8.46; I, 8.35^f; CN, 8.71; NO₂, 8.81
10. 10⁴ kr , *trans*-4-substituted cyclohexanecarboxylic acids in PhMe at 30°^{aa}:
H, 11.1; *t*-Bu, 10.5; CO₂Et, 26.0; CO₂Me, 27.5; Br, 60.2; CN, 110.

^a Footnote t, Table 8.

^b C. D. Ritchie and G. H. Megarle, *J. Amer. Chem. Soc.*, 89, 1447 (1967).

^c P. Kebarle, in *Environmental Effects on Molecular Structure and Properties*, D. Reidel, Dordredt, 1976, p. 81.

^d Footnote x, Table 8.

^e G. Bieri and E. Heilbronner, *Helv. Chim. Acta*, 57, 546 (1974).

^f Excluded from the correlation.

ignated E. Of the six sets studied, four gave improved correlation and two showed no change.

The results obtained are certainly not conclusive; they are indicative, however. Although much more data is required for absolute certainty, it seems very likely that most of the σ_I constants reported in Table 7 are applicable in dipolar aprotic solvents and probably in nonpolar aprotic solvents and in the gas phase as well. Certain substituents do have effects that are strongly dependent on the media. Those groups include charged substituents and protonic substituents capable of hydrogen bond formation.

TABLE 15
Results of Correlations of Data in Nonprotonic Media

Set	L	h	r^a	F^b	s_{est}^c	s_L^c	s_h^c	$100r^{2d}$	n^e
1	-7.56	22.30	0.9899	145.9 ^g	0.342	0.626 ^f	0.209	97.99	5
2	-7.39	12.57	0.9951	305.7	0.231	0.422	0.141	99.03	5
3	-2.35	5.000	0.9941	336.8	0.0652	0.128	0.0330	98.83	6
4	-2.21	4.820	0.9967	61.08	0.0454	0.0892	0.0230	99.35	6
5	25.6	46.8	0.9835	177.2	1.03	1.92	0.480	96.72	8
6	4.19	-2.39	0.9915	759.2	0.109	0.152	0.0463	98.32	15
7	4.39	-1.36	0.9951	1022.	0.0957	0.137	0.0413	99.03	12
8	6.48	-0.582	0.9909	540.2	0.176	0.279	0.0779	98.18	12
9	1.12	8.02	0.9873	426.3	0.0469	0.0541	0.0182	97.48	13
10	1.65	1.00	0.9826	111.8	0.0835	0.156	0.0549	96.55	6
1E	-7.80	22.48	0.9982	551.1 ^g	0.176	0.332 ^f	0.123	99.64	4
2E	-7.54	12.68	0.9984	642.0 ^g	0.158	0.298 ^f	0.110	99.69	4
3E	-2.39	4.99	0.9978	677.4	0.0459	0.0918	0.0239	99.56	5
4E	-2.18	4.83	0.9981	807.6	0.0384	0.0768	0.0200	99.63	5
6E	4.19	-2.393	0.9916	701.3	0.114	0.158	0.0488	98.32	14
9E	1.12	8.02	0.9877	397.5	0.0482	0.0563	0.0196	97.55	12

For footnotes, see Tables 9 and 11.

D. A Comparison of Localized Effect Substituent Constants

It is of interest to compare the various sets of localized effect parameters with regard to scale. This may be done by means of the equation

$$\sigma_{LX} = m_L \sigma_{IX} + h_L \quad (73)$$

where the σ_{LX} are the various localized electrical effect parameters reviewed previously (Section I.B). The σ_{IX} constants are those defined or evaluated here (Table 7). In the case of σ' and σ_I^q , the values of m_L and h_L can be calculated as follows: These σ_L constants are defined by the equation

$$\sigma_{LX} = \frac{pK_{aX} - pK_{aH}}{L} \quad (74)$$

Now

$$pK_{aX} = L\sigma_{IX} + h \quad (75)$$

and

$$h = pK_{aH} + E \quad (76)$$

Then,

$$pK_{aX} - pK_{aH} = L\sigma_{IX} + E \quad (77)$$

and

$$\sigma_{LX} + \frac{L}{L'\sigma_{IX}} + \frac{E}{L'} \quad (78)$$

which is equivalent to Equation 73 with

$$m_L = L/L', h_L = E/L' \quad (79)$$

In the case of the $\sigma_{I,Ch}$ (Charton), $\sigma_{I,EBT}$, $\sigma_{I,Ex}$ (Exner), F , (Hansch), F_{DGH} (Dewar, Golden, Harris), and σ_X^* constants, they were simply correlated with Equation 73. Results of these correlations and values of m_L and h_L calculated from Equation 79 are collected in Table 17. The constants used are set forth in Table 16. In addition to the σ_X^* constants, which probably contain a delocalized effect increment, the $\sigma_{XCH_2}^*$ constants were correlated with Equation 73, as they should be free of any contribution from the delocalized effect. The m_L values obtained show that the σ' and $\sigma_{I,EBT}$ values are on the same scale as the σ_p values. Of even greater interest is the observation that the $\sigma_{I,Ch}$; σ_I^q , $\sigma_{I,EBT}$; and σ' values are in good agreement with the σ_I values, the $\sigma_{XCH_2}^*$ and $\sigma_{I,Ex}$ values are only in fair agreement, and the F_H , F_{DGH} and σ^* values deviate considerably from the σ_I values. To clarify the significance of this point we have examined the correlation of data sets from Tables 8 and 13 for systems which are free of steric and conformational effects and in which only the delocalized effect can occur with the F_H and in some cases with the $\sigma_{I,Ex}$ constants. The results of the correlations are presented in Tables 18 and 19. Values of $100r^2$ are compared for correlations with F_H , $\sigma_{I,Ex}$, and σ_I in Table 20. With regard to the F_H constants the results are overwhelming. A large preponderance of the sets studied give better correlation with σ_I than with F_H . Of the ten sets with 10 or more substituents, nine gave significantly better results with σ_I . Of the 56 sets correlated with both F_H and σ_I , 40 gave better results with σ_I compared with F_H . The results obtained with the $\sigma_{I,Ex}$ constants, although less dramatic, nevertheless show that σ_I gives better results. Of the eight sets with 9 or more members, three give significantly better results with σ_I , two with $\sigma_{I,Ex}$, and three show no significant difference. Of the 23 sets correlated with both σ_I and $\sigma_{I,Ex}$, nine give significantly better results with σ_I , two with $\sigma_{I,Ex}$, and 12 show no difference.

Correlations have also been carried out with both the F_H and $\sigma_{I,Ex}$ constants with the exclusion of ionic and hydroxylic groups. The results of these correlations are presented in Tables 18 (F_H) and 19 ($\sigma_{I,Ex}$); these sets are designated E. Forty E sets were correlated with F_H , there were 16 sets previously correlated with F_H which contained no hydroxylic or ionic groups. Of this total of 56 sets free of suspicious substituents, 42 gave best correlation with σ_I , seven with F_H , and seven did not show any significant difference. These results confirm the marked superiority of the σ_I constants over the F_H constants.

Twenty-one E sets were correlated with $\sigma_{I,Ex}$; there were two sets previously

TABLE 16
Values of σ_L

$\sigma_{I,EBT}^a$:

NMe₂, 0.06; NH₂, 0.12; NHAc, 0.26; OMe, 0.27; PhO, 0.38; SMe, 0.23; Me, -0.04; Ph, 0.10; F, 0.50; Cl, 0.46; Br, 0.44; I, 0.39; H, 0; SiMe₃, -0.10; SCF₃, 0.42; SOCF₃, 0.64; SF₅, 0.57; CF₃, 0.45; SO₂Me, 0.59; Ac, 0.28; CO₂Et, 0.30; CO₂Et, 0.30; CO₂H, 0.30; CN, 0.56; NO₂, 0.65; CO₂Me, 0.30

$\sigma_{I,Ch}^b$:

Et, -0.05; Me, -0.05; H, 0; PhCH₂, 0.04; Ph, 0.10; F, 0.52; Cl, 0.47; Br, 0.45; I, 0.39; *t*-Bu, -0.07; OH, 0.25; MeO, 0.25; NHAc, 0.28; CN, 0.58; EtCONH, 0.25; H₂NCONH, 0.21; *i*-Pr, -0.03; CONH₂, 0.27; EtO, 0.27; CH₂=CHCH₂, 0.00; CH₂=CH, 0.09; H₂NCOCH₂, 0.05; CH₂Cl, 0.15; CH₂Br, 0.18; CH₂I, 0.16

σ_X^c :

CCl₃, 2.65; CO₂Me, 2.00; Ac, 1.65; PhC₂, 1.35; NCCH₂, 1.300; ClCH₂, 1.05; BrCH₂, 1.00; ICH₂, 0.85; Ph, 0.60; HOCH₂, 0.555; H, 0.490; PhCH₂, 0.215; Me, 0; Et, -0.10; *i*-Pr, -0.19; *t*-Bu, -0.30

$\sigma_{XCH_2}^c$:

MeSO₂CH₂, 1.32; NCCH₂, 1.300; FCH₂, 1.10; HO₂CCH₂, 1.05; ClCH₂, 1.050; BrCH₂, 1.000; *i*-CH₂, 0.85; CF₃CH₂, 0.92; PhOCH₂, 0.85; AcCH₂, 0.60; HOCH₂, 0.555; MeOCH₂, 0.520; ClCH₂CH₂, 0.385; PhCH₂, 0.215; PhCH₂CH₂, 0.02; HCH₂, 0; MeCH₂, -0.100; EtCH₂, -0.115; *i*-PrCH₂, -0.125; PrCH₂, -0.130; *t*-BuCH₂, -0.165

$\sigma_{I,Ex}^d$:

Me, -0.06; Et, -0.06; *i*-Pr, -0.07; *t*-Bu, -0.08; H, 0; Ph, 0.10; PhCH₂, -0.08; ClCH₂, 0.11; NH₂, 0.11; NMe₂, 0.11; NHAc, 0.29; OH, 0.28; OMe, 0.31; OAc, 0.40; SH, 0.28; SMe, 0.22; F, 0.56; Cl, 0.51; Br, 0.50; I, 0.43; HC≡C, 0.20; PhC≡C, 0.14; CF₃, 0.46; CN, 0.61; Ac, 0.34; CONH₂, 0.31; CO₂H, 0.34; CO₂Me, 0.35; CO₂Et, 0.35; NO₂, 0.70; MeSO₂, 0.64

F_H^e :

H, 0; Me, -0.04; Et, -0.05; OH, 0.29; OMe, 0.26; CO₂Et, 0.33; Cl, 0.41; Br, 0.44; NO₂, 0.67; CF₃, 0.38; CO₂H, 0.33; CH₂OH, 0.00; F, 0.43; I, 0.40; CN, 0.51; *i*-Pr, -0.05; *t*-Bu, -0.07; CONH₂, 0.24; CH₂Cl, 0.10; CH₂Br, 0.10; CH₂I, 0.09; CO₂Me, 0.33; Ac, 0.32; HC≡C, 0.19; Ph, 0.08; CH₂=CH, 0.07; OEt, 0.22; MeSO₂, 0.54; MeS, 0.20; NHAc, 0.28; OAc, 0.41; OPh, 0.34; Pr, -0.06; Bu, -0.06; PhCH₂, -0.08; SH, 0.28; EtS, 0.23; NH₂, 0.02; NHMe, -0.11; NMe₂, 0.10

F_{DGH}^f :

Me, -0.087; F, 4.85; Cl, 4.95; Br, 4.92; I, 4.57; OH, 2.48; OMe, 3.16; CN, 5.57; NO₂, 7.09; CO₂H, 3.13; CO₂Et, 3.18; NH₂, 0.317; NHAc, 3.22

^a Ref. 1.

^b Ref. 22.

^c Ref. 9.

^d O. Exner, in *Advances in Linear Free Energy Relationships*, N. B. Chapman and J. Shorter, Eds., Plenum, New York, 1972, p. 1.

^e Ref. 26c.

^f Ref. 24e.

TABLE 17
Values of m_L , h_L , and Correlation Statistics for σ_L Constants

L	m_L	h_L	r^a	F^b	s_{est}^c	s_{mL}^c	s_{hL}^c	$100r^2$	n^e
σ'	0.984	0.0137	0.9947 ^q	280.3 ^q	—	—	—	98.94 ^q	5 ^q
σ_q	5.28	0.09	0.9934 ^q	1276. ^q	—	—	—	98.69 ^q	19 ^q
σ_I	5.884	-0.0222	0.9452	117.3	0.282	0.543	0.105 ^j	89.34	16
$\sigma_{I,Ch}$	1.038	-0.0247	0.9960	2833.	0.0172	0.0195	0.00531	99.19	25
$\sigma_{I,EBT}$	1.008	-0.0239	0.9908	1227.	0.0295	0.0288	0.0116 ^m	98.16	25
F_{Hansch}	1.062	-0.0624	0.9625	478.4	0.0551	0.0486	0.0149	92.64	40
$\sigma_{I,Ex}$	1.173	-0.0593	0.9742	540.9	0.0516	0.0504	0.0168 ^f	94.91	31
σ_I	0.728	0.0101	—	—	—	—	—	—	—
F_{DGH}	10.63	-0.202	0.9695	172.4	0.514	0.810	0.326 ^o	94.00	13
σ_{X,CH_2}^*	2.349	-0.0568	0.9794	471.0	0.108	0.108	0.0347 ^p	95.93	22

For footnotes a to n, see Tables 9 and 11.

^o 20.0% CL.

^p 80.0% CL.

^q Values are from Set 8-18, for σ , Set 8-36 for σ_I^q .

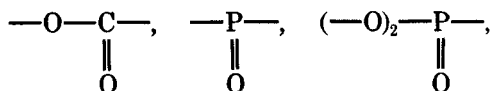
correlated with $\sigma_{I,Ex}$ which contained no hydroxylic or ionic groups. Of this total of 23 sets, free of suspicious substituents, ten gave best correlation with σ_I , two with $\sigma_{I,Ex}$ and eleven showed no significant difference. Again, the σ_I constants give significantly better results than do the $\sigma_{I,Ex}$ constants.

Values of $100r^2$ for $\sigma_{I,F}$ and $\sigma_{I,Ex}$ E sets are again compared in Table 20.

We believe that these results show that the σ_I constants given in Table 7 constitute the best available parameters for the localized electrical effect at the present time.

E. Variation of σ_I Constants with Structure

The σ_I constants for alkyl groups (only those groups for which the error could be estimated were considered) are constant, and $\bar{\sigma}_{I,Ak}$ has a value, not significantly different from zero (see Table 21). It is significant that these constants give a good fit even with pK_a s of $XCH_2NH_3^+$, where L is -9.16 and therefore the reaction is very sensitive to σ_I values of groups of the type AkW where W is O, S,



---SO₂---, etc., and Ak varies also have constant σ_I values (See Table 7). These observations support the conclusion that the localized electrical effect of alkyl groups, in solution at least, is in fact constant.

TABLE 18
Results of Correlations with the F_H Constants

Set	L	h	r^a	F^b	s_{est}^c	s_L^c	s_h^c	$100r^2$	n^e
18	-1.61	6.78	.9895	141.1 ^g	.0532	.136 ^f	.0488	97.92	5
19	-1.82	6.482	.9920	496.4	.0742	.0817	.0333	98.41	10
20	-1.20	5.752	.9934	375.7	.0389	.0621	.0242	98.69	7
21	-1.05	5.068	.9922	318.4	.0489	.0586	.0270	98.45	7
22	-1.17	5.605	.9955	557.2	.0414	.0496	.0229	99.11	7
23	-1.27	6.254	.9972	530.2	.0316	.0550	.0188	99.44	5
24	-1.23	4.863	.9947	465.5	.0476	.0570	.0263	98.94	7
25	-1.39	5.390	.9969	807.5	.0408	.0488	.0225	99.38	7
26	-1.63	6.067	.9959	604.8	.0553	.0662	.0305	99.18	7
27	-1.19	5.19	.9989	134.4	.0199	.0325	.0131	99.78	5
28	-1.21	6.22	.9990	1546.	.0187	.0306	.0124	99.81	5
29	-0.785	6.305	.9844	187.5	.0366	.0573	.0176	96.90	8
30	-1.60	5.96	.9964	551.9	.0395	.0679	.0231	99.28	6
31	-1.65	6.82	.9572	65.67	.0907	.204	.0671	91.63	8
32	-1.36	6.88	.9861	282.3	.0476	.0810	.0276	97.24	10
33	-0.838	4.92	.9921	375.7	.0248	.0432	.0138	98.43	8
34	-0.861	6.10	.9671	57.74 ^g	.0437	.113 ^f	.0384	93.52	6
35	-1.25	6.40	.9830	114.8	.0450	.117	.0395	96.63	6
36	-5.00	10.79	.9828	481.7	.202	.228	.0681	96.59	19
37	-4.93	10.68	.9772	190.5	.220	.357	.102	95.49	11
38	-4.87	9.61	.9646	120.4	.273	.443	.126	93.05	11
39	-4.38	8.84	.9606	59.72	.288	.567	.174	92.27	7
40	-4.97	10.81	.9692	77.49	.328	.564	.148	93.94	7
41	-0.776	5.90	.9972	892.4	.0123	.0260	.00908	99.44	7
42	-0.900	6.83	.9912	279.8	.0256	.0538	.0188	98.24	7
43	-0.949	5.78	.9401	60.86	.0582	.122	.0399	88.38	10
44	-1.01	6.87	.9194	43.73	.0733	.153	.0502	84.53	10
45	-1.34	4.904	.9709	49.28 ^f	.0810	.191 ^f	.0398 ^m	94.26	5
48	-1.16	10.26	.9756	78.95	.0513	.131	.0464	95.18	6
49	-1.17	10.43	.9711	66.31 ^g	.0562	.143 ^f	.0508	94.31	6
50	-2.83	6.454	.9967	453.3	.0625	.133	.0310	99.34	5
51	-2.80	6.002	.9961	385.4	.0669	.142	.0331	99.23	5
52	-1.10	4.907	.9597	34.94 ^f	.0788	.186 ^f	.0387 ^m	92.09	5
61	0.764	-0.642	.9876	118.6 ^g	.0275	.0712 ^f	.0252	97.53	5
62	2.46	0.177	.9940	249.7	.0611	.156	.0560	98.81	5
63	0.557	1.022	.9947	278.3	.0204	.0334	.0135	98.93	5
64	0.633	0.550	.9960	368.2	.0202	.0330	.0133	99.19	5
65	0.639	0.337	.9945	270.2	.0238	.0389	.0157	98.90	5
66	0.756	0.283	.9924	196.3	.0330	.0540	.0218	98.49	5
67	0.761	0.0157	.9876	118.6 ^g	.0427	.0698	.0282 ^o	97.53	5
68	-0.938	0.527	.9364	177.9	.0727	.0704	.0188	87.68	30
69	-0.852	0.968	.9207	50.12	.0755	.120	.0372	84.78	13
71	1.21	1.70	.9801	73.18 ^g	.0684	.142 ^f	.0429	96.06	5
72	1.03	2.35	.9802	73.46 ^g	.0580	.120 ^f	.0363	96.08	5
73	1.39	2.30	.9995	318.0	.0119	.0246	.00745	99.91	5
74	1.46	2.81	.9968	461.4	.0329	.0681	.0206	99.35	5
75	1.61	1.31	.9981	123.4 ^g	.0699	.145 ^f	.0438	97.63	5
76	1.49	1.88	.9841	92.36 ^g	.0748	.155 ^f	.0468	96.85	5

TABLE 18
Results of Correlations with the F_H Constants

Set	L	h	r^a	F^b	s_{est}^c	s_L^c	s_h^c	$100r^2$	n^e
77	1.50	1.69	.9943	264.7	.0445	.0923	.0279	98.88	5
78	1.48	2.23	.9933	221.7	.0479	.0992	.0300	98.67	5
79	0.472	-0.448	.9954	428.0	.00879	.0228	.00772	99.07	6
80	1.34	0.385	.9968	629.6	.0286	.0533	.0160	99.37	6
3 ^r	-2.32	4.949	.9666	56.97 ^g	.154	.308 ^f	.0749	93.44	6
4 ^r	-2.23	4.779	.9910	220.0	.0753	.150	.0365	98.21	6
9 ^r	1.06	8.08	.9788	251.0	.0605	.0672	.0212	95.80	13
10 ^r	1.60	1.05	.9465	34.39 ^g	.145	.273 ^f	.0918	89.58	6
18E	-1.61	6.78	.9900	98.02 ^k	.0636	.163 ^h	.0610	98.00	4
19E	-1.85	6.486	.9829	142.8	.0794	.155	.0504	96.62	7
21E	-1.05	5.091	.9982	552.4 ^g	.0176	.0449 ^f	.0168	99.64	4
22E	-1.17	5.620	.9980	498.1 ^g	.0205	.0525 ^f	.0197	99.60	4
23E	-1.32	6.262	.9997	1769. ^k	.0123	.0314 ^h	.0122 ^h	99.94	3
24E	-1.24	4.885	.9972	350.3 ^g	.0259	.0662 ^f	.0248	99.43	4
25E	-1.38	5.401	.9964	279.9 ^g	.0323	.0827 ^f	.0310	99.29	4
26E	-1.54	6.051	.9965	286.6 ^g	.0356	.0911 ^f	.0342	99.31	4
29E	-0.759	6.287	.9875	156.5	.0308	.0607	.0195	97.51	6
30E	-1.52	5.93	.9937	158.3 ^f	.0471	.120 ^f	.0452	98.75	4
31E	-1.65	6.83	.9584	56.31	.0979	.220	.0735	91.84	7
32E	-1.36	6.88	.9893	321.9	.0446	.0758	.0262	97.87	9
33E	-0.797	4.90	.9907	159.0 ^g	.0244	.0632 ^f	.0220	98.15	5
34E	-0.860	6.10	.9671	43.34 ^f	.0504	.131 ^f	.0455	93.53	5
35E	-1.25	6.40	.9864	108.0 ^g	.0463	.120 ^f	.0417	97.30	5
37E	-5.13	10.74	.9806	174.8	.221	.388	.116	96.15	9
38E	-4.98	9.59	.9733	126.0	.253	.443	.133	94.74	9
39E	-4.43	8.76	.9816	79.49 ^g	.218	.497	.168	96.36	5
43E	-0.949	5.77	.9480	62.12	.0576	.120	.0400	89.87	9
44E	-1.01	6.85	.9495	64.08	.0605	.126	.0420	90.15	9
48E	-1.15	10.249	.9839	60.74 ^k	.0577	.147	.0553	96.81	4
49E	-1.17	10.415	.9782	44.40 ^k	.0684	.175 ⁱ	.0656	95.69	4
61E	0.762	-0.638	.9884	84.39 ^k	.0324	.0829 ^h	.0311	97.68	4
62E	2.46	0.181	.9941	168.5 ^f	.0741	.189 ^f	.0710 ^f	98.83	4
68E	-0.943	0.524	.9369	165.2	.0742	.0733	.0199	87.78	25
69E	-0.932	0.987	.9531	69.45	.0641	.112	.0367	90.84	9
70E	1.22	1.701	.9800	48.37 ^k	.0831	.175 ⁱ	.0535	96.03	4
71E	1.04	2.361	.9831	57.84 ^k	.0652	.137 ^h	.0420	96.66	4
72E	1.38	2.297	.9998	4853.	.00942	.0198	.00607	99.96	4
73E	1.47	2.810	.9968	313.0 ^g	.0394	.0830 ^f	.0254	99.37	4
74E	1.63	1.313	.9903	101.9 ^f	.0767	.161 ^f	.0494	98.08	4
75E	1.51	1.893	.9884	84.88 ^k	.0780	.164 ^h	.0502	97.70	4
76E	1.49	1.682	.9945	180.0 ^f	.0529	.111 ^f	.0340	98.90	4
77E	1.48	2.229	.9933	147.1 ^f	.0581	.122 ^f	.0374	98.66	4
78E	0.471	-0.447	.9956	341.2 ^g	.00984	.0255 ^f	.00887	99.13	5
79E	1.36	0.386	.9969	316.3 ^g	.0280	.0766 ^f	.0253 ^f	99.37	4
3E ^r	-2.51	4.920	.9973	547.4	.0510	.109	.0253	99.45	5
4E ^r	-2.32	4.767	.9965	428.8	.0526	.112	.0260	99.31	5
9E ^r	1.09	8.06	.9837	300.1	.0552	.0629	.0206	96.77	12

For footnotes a-q, see Tables 9, 11, and 17.

^r From Table 14; all other data sets are in Table 8.

TABLE 19
Results of Correlations with the $\sigma_{L,Ex}$ Constants

Set	L	h	r	F	s_{est}	s_L	s_h	$100r^2$	n
19	-1.63	6.507	.9940	577.8	.0604	.0679	.0333	98.80	9
20	-1.04	5.755	.9805	124.4	.0667	.0937	.0421 ^f	96.14	7
21	-1.00	5.110	.9962	523.9	.0322	.0438	.0242	99.24	6
22	-1.10	5.636	.9972	719.4	.0301	.0409	.0226	99.45	6
23	-1.26	6.300	.9962	521.5	.0406	.0552	.0305	99.24	6
24	-1.16	4.901	.9970	666.5	.0331	.0450	.0249	99.40	6
25	-1.28	5.415	.9975	812.7	.0331	.0449	.0249	99.51	6
26	-1.49	6.091	.9954	428.8	.0531	.0721	.0399	99.08	6
29	-0.643	6.287	.9886	215.5	.0262	.0438	.0162	97.73	6
33	-0.656	4.89	.9909	270.1	.0188	.0399	.0154	98.18	7
34	-0.705	6.09	.9670	57.61 ⁸	.0437	.0929 ^f	.0365	93.51	6
35	-1.03	6.38	.9901	200.0	.0343	.0729	.0287	98.04	6
36	-4.53	10.82	.9927	943.3	.141	.147	.0536	98.54	16
37	-4.40	10.75	.9876	276.9	.175	.264	.0963	97.53	9
38	-4.30	9.68	.9801	171.0	.218	.329	.120	96.07	9
48	-0.992	10.24	.9916	236.4	.0301	.0646	.0255	98.34	6
49	-1.00	10.41	.9893	183.8	.0344	.0737	.0292	97.87	6
68	-0.932	5.60	.9754	372.7	.0503	.0483	.0160	95.15	21
69	-0.853	1.015	.9690	107.8	.0525	.0822	.0317	93.90	9
79	0.386	-0.439	.9943	346.3	.00976	.0207	.00816	98.86	6
3 ^r	-2.03	4.937	.9847	128.2	.105	.179	.0500	96.98	6
4 ^r	-1.92	4.764	.9956	456.5	.0525	.0898	.0251	99.13	6
9 ^r	0.975	8.07	.9871	380.8	.0492	.0500	.0182	97.44	12
19E	-1.54	6.480	.9908	268.0	.0584	.0939	.0366	98.17	7
21E	-0.898	5.081	.9991	1069.	.0126	.0275	.0118	99.81	4
22E	-0.998	5.609	.9997	3161.	.00817	.0178	.00766	99.94	4
23E	-1.12	6.260	.9998	2226. ^k	.0109	.0238 ^h	.0108 ^f	99.96	3
24E	-1.06	4.874	.9995	2182.	.0104	.0226	.00975	99.91	4
25E	-1.18	5.389	.9992	1254.	.0153	.0333	.0144	99.84	4
26E	-1.31	6.038	.9997	2865.	.0113	.0246	.0106	99.93	4
29E	-0.647	6.284	.9916	234.8	.0252	.0422	.0158	98.32	6
33E	-0.661	4.89	.9921	188.5	.0224	.0481	.0199	98.43	5
34E	-0.716	6.10	.9972	51.67 ^f	.0464	.0996 ^f	.0411	94.51	5
35E	-1.04	6.39	.9906	157.4 ⁸	.0385	.0826 ^f	.0341	98.13	5
37E	-4.40	10.78	.9894	281.2	.174	.262	.0980	97.91	8
38E	-4.30	9.65	.9822	164.1	.222	.335	.125	96.47	8
48E	-0.994	10.248	.9945	269.6	.0282	.0605	.0246	98.90	5
49E	-0.999	10.404	.9904	153.8 ⁸	.0376	.0806 ^f	.0327	98.09	5
68E	-0.933	5.59	.9758	358.5	.0513	.0493	.0164	95.22	20
69E	-0.846	10.05	.9741	111.4	.0511	.0802	.0319	94.89	8
78E	0.391	-0.444	.9988	129.4	.00507	.0109	.00449	99.77	5
3E ^r	-2.11	4.915	.9960	370.9	.0619	.109	.0305	99.20	5
4E ^r	-1.92	4.762	.9954	324.8	.0603	.107	.0300	99.08	5

For footnotes, see Tables 9, 11, 17, and 18.

TABLE 20
Comparison of Correlations with σ_I , $\sigma_{I,Ex}$, and F

Set	$100r^2$			n^a	Set	$100r^2$			n^a
	F	$\sigma_{I,Ex}$	σ_I			F	$\sigma_{I,Ex}$	σ_I	
18	97.92		98.94	5	48	95.18	98.34	98.82	6
19	98.41	98.80	99.16	10,9 ^c	49	94.31	97.87	97.90	6
20	98.69	96.14	96.18	7	50	99.34		99.94	5
21	98.45	99.24	99.37	7,6 ^c	51	99.23		99.86	5
22	99.11	99.45	99.70	7,6 ^c	52	92.09		96.41	5
23	99.49	99.24	99.72	5,6 ^c	3 ^a	93.44	96.98	98.83	6
24	98.94	99.40	99.56	7,6 ^c	4 ^a	98.21	99.13	99.35	6
25	99.38	99.51	99.71	7,6 ^c	9 ^a	95.80	97.44	97.48	13,12 ^c
26	99.18	99.08	99.93	7,6 ^c	61 ^d	97.53		99.24	5
27	99.78		99.82	5	62	98.81		98.54	5
28	99.81		99.84	5	63	98.93		99.83	5
29	96.90	97.73	98.65	8,7 ^c	64	99.19		99.89	5
30	99.28		98.20	6	65	98.90		99.65	5
31	91.63		90.83	8	66	98.49		99.72	5
32	97.24		92.25	10	67	97.53		98.86	5
33	98.43	98.18	98.91	8,7 ^c	68	87.68	95.15	96.50	30,27 ^b ,21 ^c
34	93.52	93.51	93.71	6	69	84.78	93.90	93.04	13,11 ^b ,9 ^c
35	96.63	98.04	98.23	6	10 ^a	89.58		96.55	6
36	96.59	98.54	98.69	19,16 ^c	70	96.06		97.53	5
37	95.49	97.53	98.30	11,9 ^c	71	96.08		99.21	5
38	93.05	96.07	98.37	11,9 ^c	72	99.91		95.82	5
39	92.27		97.00	7	73	99.35		97.95	5
40	93.94		98.63	7	74	97.63		99.14	5
41	99.44		99.22	7	75	96.85		99.22	5
42	98.24		94.96	7	76	98.88		96.35	5
43	88.38		93.30	10	77	98.67		98.19	5
44	84.53		88.90	10	78	99.07	98.86	97.95	6
45	94.26		97.94	5	79	99.37		98.58	6
18E	98.00		99.87		48E	96.81	98.90	99.69	
19E	96.62	98.17	99.27		49E	95.69	98.09	98.18	
21E	99.64	99.81	99.81		61E	97.68		99.94	
22E	99.60	99.94	99.91		62E	98.83		99.76	
23E	99.94	99.96	99.97		68E	87.78	95.22	96.74	
24E	99.43	99.91	99.79		69E	90.84	94.89	93.52	
25E	99.29	99.84	99.70		70E	96.03		98.86	
26E	99.31	99.93	99.83		71E	96.66		99.60	
29E	97.51	98.32	97.98		72E	99.96		98.56	
30E	98.75		97.49		73E	99.37		99.56	
31E	91.84		95.37		74E	98.08		99.69	
32E	97.87		96.16		75E	97.70		99.46	
33E	98.15	98.43	98.99		76E	98.90		99.17	
34E	93.53	94.51	95.79		77E	98.66		99.77	
35E	97.30	98.13	98.83		78E	99.13	99.77	99.88	
37E	96.15	97.91	99.56		79E	99.37		97.74	
38E	94.74	96.47	99.16		3aE	99.45	99.20	99.56	

TABLE 20
Comparison of Correlations with σ_I , $\sigma_{I,Ex}$, and F

Set	$100r^2$			n^a	Set	$100r^2$			n^a
	F	$\sigma_{I,Ex}$	σ_I			F	$\sigma_{I,Ex}$	σ_I	
39E	96.36		99.49		4aE	99.31	99.08	99.63	
43E	89.87		93.20		9aE	96.77	97.44	97.55	
44E	90.15		89.50						

All sets from Table 9 unless otherwise noted.

^a From Table 15. The number of data points is the same for correlation with each σ_L parameter unless other values are given.

^b Number of points correlated with F_H .

^c Number of points correlated with $\sigma_{I,Ex}$.

^d Begins a series of correlations that involve rate constants. Sets 61-80.

These $\bar{\sigma}_{I,AKW}$ values are also very useful in predicting σ_I values for substituents for which experimental data are unavailable. They are also of assistance in determining the reliability of an uncertain experimental value. If an uncertain σ_I value deviates greatly from the $\bar{\sigma}_I$ value for that type of substituent it can probably be rejected.

IV. THE σ_D CONSTANTS

Ehrenson, Brownlee, and Taft (1) have presented arguments for the existence of four distinct types of σ_D constant. The cause of this multiplicity of delocalized effect substituent constants is the nature of the interaction between substituent constant and active site. When substituent and active site are bonded to a skeletal group such that a lowest-energy molecular orbital exists which encompasses skeletal group, substituent, and active site an "exaltation" of the delocalized effect is possible. This exaltation will occur if:

1. The substituent is an electron donor and the active site a strong electron acceptor by resonance, or
2. The substituent is an electron acceptor and the active site a strong electron donor by resonance. Delocalized effect substituent constants for use in these two cases are designated σ_R^+ and σ_R^- , respectively.

If the active site is separated from the π -bonded moiety of the skeletal group by some group of atoms that does not allow the existence of a lowest-energy π molecular orbital that encompasses both substituent and active site, a third type of delocalized effect substituent constant, the σ_R^0 constant, is required. The σ_R constants (written $\sigma_{R,BA}$ by Ehrenson, Brownlee, and Taft) defined from the

TABLE 21
 Mean Values of $\sigma_{I, Akw}$

Substituent Type, X	$\bar{\sigma}_I^a$	s^b	n^c	$\bar{\sigma}_{I, Akw}^d$
Ak	-0.0133 ^e	0.0137	12	-0.01
AkO	0.277	0.0236	10	0.28
AkS	0.268	0.0249	9	0.27
AkSO ₂	0.580	0.0115	4	0.58
Ak ₂ PO	0.273	0.0222	4	0.27
AkPhPO	0.276	0.0152	5	0.28
(AkO) ₂ PO	0.323	0.0351	3	0.32
AkOCO	0.310	0.0141	2	0.31
4-AkPn	0.0975	0.005	4	0.10
2-AkVn	0.0700	0	2	0.07
AkCONH	0.270	0.0141	2	0.27

^a Mean value of σ_I .

^b Standard error.

^c Number of σ_I values.

^d Best value of σ_I for the substituent type.

^e Only substituents for which the estimated error in σ_I is known were included.

equation

$$\sigma_{RX} = \sigma_{pX} - \sigma_{IX} \quad (80)$$

constitute a fourth case. The σ_p constants are defined from the ionization constants of 4-substituted benzoic acids in water. The carboxyl group is a weak electron acceptor group. It is possible, then, for an electron donor group to interact with the carboxyl group to produce a significant exaltation of the resonance effect. Thus, the σ_R constants are in a sense intermediate between the σ_R^0 and σ_R^+ constants. This suggests that delocalized effect weak donor active sites should when bonded to an appropriate skeletal group bearing an acceptor substituent, constitute a fifth case. This fifth case would then require another type of resonance effect substituent constant, which might be designated $\sigma_R^{\delta-}$, the δ^- indicating the weak donor nature of the active site. No need for such resonance effect constants has been demonstrated so far.

A. Best Values of σ_m and σ_p Constants

About twenty years ago McDaniel and Brown (28) published their non-classic compilation of σ_m and σ_p constants based on the ionization constants of the corresponding benzoic acids. Since that time considerable numbers of new determinations of substituted benzoic acid ionization constants have appeared. As σ_R constants are readily determined from Equation 80, it seemed worthwhile

TABLE 22
Values of \bar{L}/\bar{D}

Set	\bar{L}/\bar{D}	Solvent
1	1.085	33.2% w/w EtOH-H ₂ O
2	1.120	52.0% w/w EtOH-H ₂ O
3	1.212	73.4% w/w EtOH-H ₂ O
4	1.228	85.4% w/w EtOH-H ₂ O
5	1.080	EtOH
6	0.982	8.05% w/w EtOH-H ₂ O
7	1.112	44.1% w/w EtOH-H ₂ O
8	1.101	70.3% w/w EtOH-H ₂ O
9	1.097	43.5% w/w dioxane-H ₂ O
10	1.071	73.5% w/w dioxane-H ₂ O
11	0.917	10% w/w MeAc-H ₂ O
12	1.126	25% w/w MeAc-H ₂ O
13	1.128	80 w/w MCS-H ₂ O
14	1.035	HOCH ₂ CH ₂ OH
15	1.089	MeOH
16	1.168	EtOH
17	1.022	PrOH
18	1.008	BuOH

to reexamine the available data and report a new collection of σ_m and σ_p constants based on the best available data now extant. Before doing so we must call attention to our results in Tables 4 and 5. Correlation of $\text{p}K_a$ values for 4-substituted benzoic acids were carried out with σ'_L and σ'_D constants defined by Equations 41 and 42. Equation 42 becomes equivalent to Equation 80 if L_a is replaced by L_t . Since the L' and D' values obtained by correlation with Equation 46 were shown to be essentially constant no matter what the choice of L_a , it follows that the \bar{L} and \bar{D} values given in Tables 4 and 5 are equivalent to the L_p and D_p values obtained by correlation with Equation 19. (With σ_R in place of σ_D). The ratio \bar{L}/\bar{D} is easily seen by inspection (See Table 22) to differ significantly from unity in many solvents. From Equations 17 and 18 we see that

$$L_p = \rho\lambda_p, D_p = \rho\delta_p \quad (81)$$

Then from Equations 39 and 81.

$$\frac{L_p}{D_p} = 1 \quad (82)$$

We are forced to the conclusion that " σ_p " constants calculated from $\text{p}K_a$ data in solvents for which $L_p/D_p \neq 1$ must contain some error. The same should be true of " σ_m " constants, although to a lesser extent. We therefore will use as a basis set of σ_m and σ_p values those which can be calculated from $\text{p}K_a$ values determined in aqueous solution. The $\text{p}K_a$ values used to define σ_m and σ_p con-

TABLE 23
Values of σ_m from Benzoic Acid pK_a s in Water at 25°

X	σ_m	Error ^a	pK_a	X	σ_m	Error ^a	pK_a
Me	-0.06	0.0099	4.252 ^b 4.269 ^c 4.252 ^d	<i>t</i> -Bu	0.00	0.0053	4.199 ^e
<i>c</i> -C ₃ H ₅	-0.08	0.0099	4.28 ^e	CH ₂ =CHCH ₂	-0.06	0.0043	4.266 ^f
Ac	0.38	0.0400	3.825 ^h	CH ₂ =CMe	-0.05	0.0043	4.248 ^f
NH ₂	-0.21	U	4.41 ^g	Me ₃ Si	0.11	0.0053	4.089 ^e
OMe	0.11	0.0053	4.093 ^b 4.043 ^d	CHO	0.25	0.0300	3.951 ⁱ
PO(OEt) ₂	0.47	U	3.73 ^k	OH	0.13	0.0053	4.076 ^b
NMe ₃ ⁺	1.04	U	3.76 ^l	OPh	0.25	0.0082	3.951 ^j
F	0.34	0.0053	3.865 ^b	PO(OMe) ₂	0.46	U	3.74 ^k
Br	0.34	0.0053	3.809 ^j 3.809 ^c 3.810 ^d 3.810 ^b	SMe ₂ ⁺	1.11	U	3.09 ^l
			3.460 ^b	NH ₃ ⁺	0.90	U	3.30 ^g
NO ₂	0.74	0.0077	3.447 ^{m,n} 3.460 ^d	Cl	0.37	0.0071	3.822 ^j 3.837 ^d 3.826 ^c 3.834 ^b
			4.1998 ⁱ 4.203 ^e 4.202 ^d	I	0.35	0.0053	3.856 ^b 3.855 ^{m,n}
H	0	0.0016 ^o		CN	0.61	0.0053	3.598 ^j 3.596 ^c

^a The error given is estimated from Eq. 62 when possible. The letter U indicates that the error is unknown. It must be noted that for all ionic substituents the error is assumed to be unknown.

^b T. Matsui, H. C. Ko, and L. G. Hepler, *Can. J. Chem.*, 52, 2906 (1974).

^c J. M. Wilson, N. E. Gore, J. E. Sawbridge, and F. Cardenas-Cruz, *J. Chem. Soc. B*, 852 (1967).

^d P. D. Bolton, K. A. Fleming, and F. M. Hall, *J. Am. Chem. Soc.*, 94, 1033 (1972).

^e J. M. Wilson, A. G. Briggs, J. E. Sawbridge, P. Tickle, and J. J. Zuckerman, *J. Chem. Soc. A*, 1024 (1970).

^f G. M. Brauer, G. Durany, and H. Argentar, *J. Res. Natl. Bur. Stand., A*, 71A, 79 (1967).

^g J. Smejkal, J. Jonas, and J. Farkas, *Collect. Czech. Chem. Commun.*, 29, 2950 (1964).

^h L. G. Bray, J. F. J. Dippy, and S. R. C. Hughes, *J. Chem. Soc.*, 265 (1957).

ⁱ A. A. Humffray, J. J. Ryan, J. P. Warren, and Y. H. Yung, *Chem. Commun.*, 610 (1965).

^j G. Kortum, W. Vogel, and K. Andrussov, footnote p, Table 7.

^k V. A. Palm, Ed. *Tables of Rate and Equilibrium Constants of Heterolytic Organic Reactions* Vol. I Moscow, 1975.

^l M. Hojo, M. Utaka, and Z. Yoshida, *Tetrahedron*, 27, 4255 (1971).

^m D. H. Everett and W. F. K. Wynne-Jones, *Trans. Faraday Soc.*, 35, 1380 (1939).

ⁿ J. J. Christensen, L. D. Hansen, and R. M. Izatt, *Handbook of Proton Ionization Heats and Related Thermodynamic Quantities*, Wiley-Interscience, New York, 1976.

^o Standard error of mean of values for H.

^p R. A. Robinson and K. P. Ang, *J. Chem. Soc.*, 2314 (1959).

^q J. Christensen, D. P. Wrathall, R. M. Izatt, and D. O. Tolman, *J. Phys. Chem.*, 71, 3001 (1967).

^r E. E. Sager and V. E. Bower, *J. Res. Natl. Bur. Stand., A*, 64A, 351 (1960).

TABLE 24
Values of σ_p from Benzoic Acid pK_a s in Water at 25°

X	σ_p	Error ^a	pK_a	X	σ_p	Error ^a	pK_a
Me	-0.17	0.0059	4.370 ^d	Et	-0.15	0.0400	4.353 ^j
			4.362 ^c	<i>i</i> -Pr	-0.15	0.0400	4.354 ^j
<i>t</i> -Bu	-0.19	0.0019	4.389 ^e	<i>c</i> -C ₃ H ₅	-0.22	0.0201	4.42 ^g
CH ₂ =CHCH ₂	-0.12	0.0043	4.326 ^f	SiMe ₃	0.01	0.0019	4.192 ^e
CHO	0.45	0.0300	3.75 ⁱ	Ac	0.50	0.0400	3.700 ^h
NH ₂	-0.63	U	4.83 ^q	OH	-0.38	0.0142	4.582 ^j
OMe	-0.28	0.0112	4.494 ^d				4.580 ^c
			4.478 ^{m,n}	PO(OMe) ₂	0.59	U	3.61 ^k
			4.492 ^r	PO(OEt) ₂	0.57	U	3.63 ^k
MeSO	0.54		3.66 ^s	H ₂ NSO ₂	0.73	0.0201	3.97 ^t
Me ₃ N ⁺	0.97	U	3.245 ^u	SMe ₂ ⁺	1.14	U	3.06 ^l
			3.21 ^l	SO ₃ ⁻	0.48	U	3.72 ^y
SO ₂ ⁻	-0.07	U	4.27 ^w	NH ₃ ⁺	0.71	U	3.49 ^q
F	0.06	0.0400	4.141 ^j	Cl	0.22	0.0019	3.9863 ^j
Br	0.22	0.0238	4.0020 ^j				3.985 ^c
			3.961 ^d				3.986 ^d
			4.002 ^c	I	0.24	0.0481	3.927 ^p
CN	0.65	0.0019	3.5510 ^j				3.995 ^{d,n}
			3.550 ^c	NO ₂	0.77	0.0102	3.442 ^j
E—O ₂ NCH=CH	0.26	0.0400	3.94 ^x				3.442 ^j
EtCO	0.48	U	3.72 ^y				3.442 ^j
<i>i</i> -PrCO	0.47	U	3.73 ^y				3.424 ^d
				<i>t</i> -BuCO	0.32	U	3.88 ^y
				CH ₂ OH	0.04	U	4.16 ^z

For footnotes, see Table 23.

stants are the best available at the present time as determined by the magnitude of the experimental error reported. Where two or more values of comparable reliability are available, the average value was used to define the substituent constant. The defining equations are in water at 25°.

$$\sigma_m \equiv -(pK_{a,3-X} - pK_{aH}) \quad \sigma_p \equiv -(pK_{a,4-X} - pK_{aH}) \quad (83)$$

The σ_m constants are reported in Table 23, the σ_p constants in Table 24.

^s M. Hojo, M. Utaka, and Z. Yoshida, *Tetrahedron*, 27, 4031 (1971).

^t H. Zollinger and C. Wittwer, *Helv. Chim. Acta*, 39, 347 (1956).

^u A. V. Willi, *Zeit. Physik. Chem.*, N. F. 26, 42 (1960).

^v H. Zollinger, W. Buchler, and C. W. Wittwer, *Helv. Chim. Acta*, 36, 1711 (1973).

^w B. J. Lindberg, *Acta Chem. Scand.*, 24, 2852 (1970).

^x R. Stewart and L. G. Walker, *Can. J. Chem.*, 35, 1561 (1957).

^y K. Borwden and M. J. Shaw, *J. Chem. Soc. B*, 161 (1971).

^z J. P. Girault and G. Dana, *J. Chem. Soc. Perkin Trans. II*, 993 (1977).

To determine the magnitude of the error in σ_m and σ_p values due to the variation of L/D with solvent we have calculated these constants from the equations

$$\sigma_m = \frac{pK_{mX} - h}{\rho}, \quad \sigma_p = \frac{pK_{pX} - h}{\rho} \quad (84)$$

and compared the values obtained with the values calculated from the equations

$$\sigma_p = \sigma_I + \sigma_R \quad (85)$$

and obtained from Equations 38 and 39, and Equation 86 was

$$\sigma_m = 0.999\sigma_I + 0.388\sigma_R + 0.0130 \quad (86)$$

obtained by the correlation of the best σ_m values of the basis set (calculated from pK_a data with errors ≤ 0.04 , σ_m values for OH and Me_3Si were excluded). The results of the correlation were: R , 0.9951; F , 506.8; r_{12} , 0.040; s_{est} , s_λ , s_δ , s_c , 0.0295; 0.0335; 0.0388; 0.0142; $100r^2$, 99.0; the intercept c is not significant.

In calculating the values of the σ_m and σ_p constants of the basis sets, when more than one reliable pK_a was available the pK_a s were averaged. The errors in the resulting σ_m and σ_p values were estimated by means of Equation 62. In using Equation 62, the value of S was taken as the experimental error in the pK_a when only a single pK_a value was available for the substituent. When two or more values of pK_a were available, the larger of the two quantities, the largest experimental error or the standard error of the mean was assigned to S . The $pK_{a,H}$ value used in Equation 83 for calculating the basis set σ_m and σ_p values (4.202) was an average of the best experimental values. The values used are given in Table 23.

B. The σ_R Constants

Values of σ_R were calculated from Equation 80 using the σ_p values in Table 24 or from the equation

$$\sigma_{RX} = (pK_{aX} - L\sigma_{IX} - h)/D \quad (87)$$

when the pK_a values used were obtained in other solvents or at other temperatures. In addition to σ_R values obtained from benzoic acid pK_a s, a number of values were obtained from the pK_a s of *trans*-3-substituted acrylic acids. The values of L and D required by Equation 87 were obtained by correlation of appropriate pK_a s with Equation 88

$$Q_X = L\sigma_{IX} + D\sigma_{RX} + h \quad (88)$$

The data used are given in Table 25 when possible. The results of the correlations

TABLE 25
Data Used in Correlations with Eq. 88

1.	pK_a , 4-XC ₆ H ₄ CO ₂ H in 8.05% w/w aq. EtOH at 25° a
1m.	pK_a , 3-XC ₆ H ₄ CO ₂ H in 8.05% w/w aq. EtOH at 25° a
2.	pK_a , 4-XC ₆ H ₄ CO ₂ H in 44.1% w/w aq. EtOH at 25° a
2m.	pK_a , 3-XC ₆ H ₄ CO ₂ H in 44.1% w/w aq. EtOH at 25° a
3.	pK_a , 4-XC ₆ H ₄ CO ₂ H in 70.3% w/w aq. EtOH at 25° a
3m.	pK_a , 3-XC ₆ H ₄ CO ₂ H in 70.3% w/w aq. EtOH at 25° a
4.	pK_a , 4-XC ₆ H ₄ CO ₂ H, 44.1% w/w aq. EtOH, 25° b: H, 5.72; Me, 5.96; CH ₂ CN, 5.46; CH ₂ Br, 5.54; CF ₃ , 4.92; Ac, 5.09 ^c ; NO ₂ , 4.43; NHAc, 5.81; NH ₂ , 6.47; NHCHO, 5.65; OH, 6.25; OMe, 6.03; OEt, 6.04; CN, 4.67; SO ₂ Me, 4.61; OPh, 5.50 ^c
5.	pK_a , 4-XC ₆ H ₄ CO ₂ H, 44.1% w/w aq. EtOH, 25° d: H, 5.80; Me, 6.00; MeO, 6.12; Br, 5.35; NO ₂ , 4.53; CN, 4.70; Ac, 5.10
6.	pK_a , 4-XC ₆ H ₄ CO ₂ H, water, 20° e: H, 4.205; Br, 4.005; Cl, 3.991; CN, 3.551; OH, 4.585; NO ₂ , 3.444; Me, 4.376; <i>t</i> -Bu, 4.425; Me ₃ Si, 4.116
7.	pK_a , 4-XC ₆ H ₄ CO ₂ H, water, 30° e: H, 4.203; Br, 4.002; Cl, 3.981; CN, 3.541; OH, 4.576; NO ₂ , 3.440; Me, 4.349; <i>t</i> -Bu, 4.354; Me ₃ Si, 4.060
8.	pK_a , 4-XC ₆ H ₄ CO ₂ H, 80% w/w aq. MCS, 25° b: H, 6.63; Me, 6.83; CH ₂ CN, 6.33; CH ₂ Br, 6.37; CF ₃ , 5.72; NO ₂ , 5.29; NHAc, 6.84; NH ₂ , 7.77; NHCHO, 6.70; OH, 7.29; OMe, 7.03; OEt, 7.08; CN, 5.52; SO ₂ Me, 5.49
9.	pK_a , <i>trans</i> -3-XCH=CHCO ₂ H, water, 25° f: H, 4.255; Cl, 3.79; Br, 3.71; I, 3.74; OMe, 4.85; NO ₂ , 2.58; CF ₃ , 3.15; Ac, 3.238; Me, 4.693; Et, 4.695; <i>i</i> -Pr, 4.701
10.	pK_a , 4-XC ₆ H ₄ CO ₂ H, in 50% aq. BCS at 25° g H, 5.65; Cl, 5.24; MeO, 5.99; NO ₂ , 4.44; Ph, 5.66
11.	pK_a , 4-XC ₆ H ₄ CO ₂ H in 33.2% w/w aq. EtOH at 25° hi;
11m.	pK_a , 3-XC ₆ H ₄ CO ₂ H in 33.2% w/w aq. EtOH at 25° h: H, 5.16; NO ₂ , 4.14; Br, 4.71; Me, 5.29; Cl, 4.78; MeO, 5.06; F, 4.74
12.	pK_a , 4-XC ₆ H ₄ CO ₂ H in 52.0% w/w aq. EtOH at 25° hi;
12m.	pK_a , 3-XC ₆ H ₄ CO ₂ H in 52.0% w/w aq. EtOH at 25° h: H, 5.76; NO ₂ , 4.67; Br, 5.27; Me, 5.92; Cl, 5.37; MeO, 5.72; F, 5.36
13.	pK_a , 4-XC ₆ H ₄ CO ₂ H in 73.4% w/w aq. EtOH at 25° hi;
13m.	pK_a , 3-XC ₆ H ₄ CO ₂ H in 73.4% w/w aq. EtOH at 25° h: H, 6.57; NO ₂ , 5.37; Br, 5.96; Me, 6.62; Cl, 6.03; MeO, 6.48; F, 6.07
14.	pK_a , 4-XC ₆ H ₄ CO ₂ H in 85.4% w/w aq. EtOH at 25° hi;
14m.	pK_a , 3-XC ₆ H ₄ CO ₂ H in 85.4% w/w aq. EtOH at 25° h: H, 7.25; NO ₂ , 6.03; Br, 6.77; Me, 7.32; Cl, 6.67; MeO, 7.14; F, 6.70
15.	pK_a , 4-XC ₆ H ₄ CO ₂ H in EtOH, at 25° h;
15m.	pK_a , 3-XC ₆ H ₄ CO ₂ H in EtOH, at 25° h: H, 10.15; NO ₂ , 8.82; Br, 9.46; Me, 10.37; Cl, 9.61; MeO, 10.13; F, 9.71
16.	pK_a , 4-XC ₆ H ₄ CO ₂ H in 43.5% w/w aq. dioxane at 25° i;
16m.	pK_a , 3-XC ₆ H ₄ CO ₂ H in 43.5% w/w aq. dioxane at 25° i: NO ₂ , 4.496; I, 5.072; Br, 4.999; Cl, 4.986; F, 5.057; Me, 5.611; OH, 5.469; H, 5.469
17.	pK_a , 4-XC ₆ H ₄ CO ₂ H, in 73.5% w/w aq. dioxane at 25° ij;
17m.	pK_a , 3-XC ₆ H ₄ CO ₂ H in 73.5% w/w aq. dioxane at 25° j: NO ₂ , 5.969; I, 6.573; Br, 6.502; Cl, 7.497; F, 6.541; Me, 7.174; OH, 7.051; H, 7.029

TABLE 25
Data Used in Correlations with Eq. 88

18.	pK_a , 4- $\text{XC}_6\text{H}_4\text{CO}_2\text{H}$, in 10% w/w aq. MeAc at 25° ^{i,k} :
18m.	pK_a , 3- $\text{XC}_6\text{H}_4\text{CO}_2\text{H}$, in 10% w/w aq. MeAc at 25° ^k : H, 4.454; Me, 4.486; NO ₂ , 3.695; OH, 4.460; OMe, 4.311; Ac, 4.062; F, 4.064; Cl, 4.043
19.	pK_a , 4- $\text{XC}_6\text{H}_4\text{CO}_2\text{H}$ in 25% w/w aq. MeAc, at 25° ^{i,k} :
19m.	pK_a , 3- $\text{XC}_6\text{H}_4\text{CO}_2\text{H}$, in 25% w/w aq. MeAc at 25° ^k : H, 4.996; Me, 5.040; NO ₂ , 4.182; OH, 4.951; OMe, 4.830; Ac, 4.565; F, 4.620; Cl, 4.565
20.	pK_a , 4- $\text{XC}_6\text{H}_4\text{CO}_2\text{H}$, in 80% w/w aq. MCS at 25° ^{i,l} :
20m.	pK_a , 3- $\text{XC}_6\text{H}_4\text{CO}_2\text{H}$ in 80% w/w aq. MCS at 25° ^l : OH, 6.74; F, 6.07; Cl, 5.99; Br, 5.97; I, 6.05; NO ₂ , 5.44; NH ₂ , 6.96; OMe, 6.55; H, 6.63
21.	pK_a , 4- $\text{XC}_6\text{H}_4\text{CO}_2\text{H}$, in HOCH ₂ CH ₂ OH at 25° ^{i,m} :
21m.	pK_a , 3- $\text{XC}_6\text{H}_4\text{CO}_2\text{H}$ in (HOCH ₂) ₂ at 25° ^m : NO ₂ , 6.716; I, 7.157; Br, 7.103; Cl, 7.128; F, 7.199; Me, 7.737; OH, 7.681; H, 7.647
22.	pK_a , 4- $\text{XC}_6\text{H}_4\text{CO}_2\text{H}$, in MeOH at 25° ^{i,n} :
22m.	pK_a , 3- $\text{XC}_6\text{H}_4\text{CO}_2\text{H}$ in MeOH at 25° ⁿ : NO ₂ , 8.366; I, 8.884; Br, 8.851; Cl, 8.856; F, 8.944; Me, 9.507; OH, 9.574; H, 9.41
23.	pK_a , 4- $\text{XC}_6\text{H}_4\text{CO}_2\text{H}$ in EtOH at 25° ^{i,o} :
23m.	pK_a , 3- $\text{XC}_6\text{H}_4\text{CO}_2\text{H}$ in EtOH at 25° ^o : NO ₂ , 8.88; I, 9.47; Br, 9.47; Cl, 9.52; F, 9.53; Me, 10.20; OH, 10.31; H, 10.25
24.	pK_a , 4- $\text{XC}_6\text{H}_4\text{CO}_2\text{H}$ in PrOH at 25° ^{i,p} :
24m.	pK_a , 3- $\text{XC}_6\text{H}_4\text{CO}_2\text{H}$ in PrOH at 25° ^p : H, 8.603; NO ₂ , 7.450; I, 7.986; Br, 7.973; Cl, 7.997; F, 8.081; Me, 8.698; OH, 8.768
25.	pK_a , 4- $\text{XC}_6\text{H}_4\text{CO}_2\text{H}$ in BuOH at 25° ^{i,q} :
25m.	pK_a , 3- $\text{XC}_6\text{H}_4\text{CO}_2\text{H}$ in BuOH at 25° ^q : NO ₂ , 7.509; I, 8.043; Br, 8.031; Cl, 8.024; F, 8.193; Me, 8.704; OH, 8.768; H, 8.609
26.	pK_a , 4- $\text{XC}_6\text{H}_4\text{CO}_2\text{H}$ in 26.5% aq. dioxane at 25° ^{i,j} :
26m.	pK_a , 3- $\text{XC}_6\text{H}_4\text{CO}_2\text{H}$ in 26.5% w/w aq. dioxane at 25° ^j : NO ₂ , 3.931; I, 4.448; Br, 4.387; Cl, 4.379; F, 4.409; Me, 4.944; OH, 4.810; H, 4.820
27.	Gas phase acidity, 4- $\text{XC}_6\text{H}_4\text{CO}_2\text{H}$ ^r : H, 23.7; Me, 24.8; OMe, 24.4; OH, 19.6; F, 20.8; Cl, 19.3; NH ₂ , 26.0; NO ₂ , 12.0; CN, 12.8
27m.	Gas phase acidity, 3- $\text{XC}_6\text{H}_4\text{CO}_2\text{H}$ ^r : H, 23.7; Me, 24.4; OMe, 23.2; OH, 22.4; F, 19.9; Cl, 19.0; NH ₂ , 25.2; NO ₂ , 14.1; CN, 13.5
28.	pK_a , 4- $\text{XC}_6\text{H}_4\text{CO}_2\text{H}$ in MeNO ₂ at 25° ^s : NO ₂ , 12.08; CO ₂ Et, 12.58; Br, 12.90; Cl, 12.98; OH, 13.27; H, 13.20; Me, 13.64; Me, 13.60; NH ₂ , 14.98; NMe ₂ , 15.04
28m.	pK_a , 3- $\text{XC}_6\text{H}_4\text{CO}_2\text{H}$, in MeNO ₂ at 25° ^s : NO ₂ , 11.70; Br, 12.57; Cl, 12.43; OH, 12.98; H, 13.20; NH ₂ , 13.60
29.	log K_{BHA} , 4- $\text{XC}_6\text{H}_2\text{CO}_2\text{H}$ in PhH at 25° ^t : H, 5.26; NH ₂ , 4.45; Br, 5.86; Cl, 5.82; CN, 6.53; NMe ₂ , 4.89; F, 5.61; I, 5.85; OMe, 4.92; Me, 5.03; NO ₂ , 6.80
29m.	log k_{BHA} , 3- $\text{XC}_6\text{H}_4\text{CO}_2\text{H}$, in PhH at 25° ^t : H, 5.26; NH ₂ , 4.93; Br, 6.06; Cl, 6.06; CN, 6.56; F, 5.94; I, 6.05; OMe, 5.38; Me, 5.13; NO ₂ , 6.83
30.	pK_a , 4- $\text{XC}_6\text{H}_4\text{CO}_2\text{H}$ in 12.7 mole % aq. dioxane at 25° ^u : H, 5.85; Me, 6.01; Cl, 5.56; OAc, 5.31; CN, 4.94; NO ₂ , 4.79; SO ₂ Me, 4.86

TABLE 25
Data Used in Correlations with Eq. 88

30m.	pK_a , 3- $XC_6H_4CO_2H$ in 12.7 mole % aq. dioxane at 25° ^u ; H, 5.85; Me, 6.01; Cl, 5.35; OAc, 5.43; CN, 5.13; NO ₂ , 4.88; SO ₂ Me, 5.03
31.	pK_a , 4- $XC_6H_4CO_2H$ in 20 mole % aq. dioxane at 25° ^u ; H, 6.81; Me, 7.04; Cl, 6.55; OAc, 6.30; CN, 5.89; NO ₂ , 5.69; SO ₂ Me, 5.82
31m.	3- $XC_6H_4CO_2H$ in 20 mole % aq. dioxane at 25° ^u ; H, 6.81; Me, 6.97; Cl, 6.37; OAc, 6.45; CN, 6.05; NO ₂ , 5.85; SO ₂ Me, 5.93
32.	pK_a , 4- $XC_6H_4CO_2H$ in 33.4 mole % aq. dioxane at 25° ^u ; H, 8.11; Me, 8.31; Cl, 7.83; OAc, 7.58; CN, 7.14; NO ₂ , 6.96; SO ₂ Me, 7.07
32m.	pK_a , 3- $XC_6H_4CO_2H$ in 33.4 mole % aq. dioxane at 25° ^u ; H, 8.11; Me, 8.29; Cl, 7.62; OAc, 7.69; CN, 7.24; NO ₂ , 7.05; SO ₂ Me, 7.20
33.	pK_a , 4- $XC_6H_4CO_2H$ in 50 mole % aq. dioxane at 25° ^u ; H, 9.82; Me, 9.97; Cl, 9.49; OAc, 9.33; CN, 8.83; NO ₂ , 8.61; SO ₂ Me, 8.72
33m.	pK_a , 3- $XC_6H_4CO_2H$ in 50 mole % aq. dioxane at 25° ^u ; H, 9.82; Me, 9.92; Cl, 9.25; OAc, 9.47; CN, 8.95; NO ₂ , 8.71; SO ₂ Me, 8.89
34.	pK_a , 4- $XC_6H_4CO_2H$ in aq. DMSO at 25° ^v (by spectrophotometry): H, 4.64; Cl, 4.36; OH, 5.05; NO ₂ , 3.66; SMe, 4.66; SO ₂ Me, 3.72
35.	pK_a , 4- $XC_6H_4CO_2H$ in aq. DMSO at 25° ^v ; H, 5.87; Me, 6.07; Cl, 5.48; OMe, 6.18; NO ₂ , 4.80; <i>i</i> -Pr, 6.06; <i>t</i> -Bu, 6.05; F, 5.67; Br, 5.44; I, 5.44
36.	pK_a , 4- $XC_6H_4CO_2H$ in aq. DMSO at 25° ^v ; H, 6.97; Me, 7.17; Cl, 6.50; OMe, 7.33; NO ₂ , 5.73; <i>i</i> -Pr, 7.16; <i>t</i> -Bu, 7.15; F, 6.72; Br, 6.54; I, 6.51
37.	pK_a , 4- $XC_6H_4CO_2H$ in aq. DMSO at 25° ^v ; H, 8.97; Me, 9.22; Cl, 8.42; OMe, 9.41; NO ₂ , 7.49; SMe, 9.00; SO ₂ Me, 8.19; SO ₂ Me, 7.72; <i>i</i> -Pr, 9.17; <i>t</i> -Bu, 9.23; F, 8.70; Br, 8.42
38.	pK_a , 4- $XC_6H_4CO_2H$ in aq. DMSO at 25° ^v ; H, 10.44; Me, 10.79; Cl, 9.73; OH, 11.41; OMe, 11.05; NO ₂ , 8.71; <i>i</i> -Pr, 10.77
39.	pK_a , 4- $XC_6H_4CO_2H$ in aq. DMSO at 25° ^v (by spectrophotometry): H, 9.12; Me, 9.41; Cl, 8.54; OH, 9.98; OMe, 9.61; NO ₂ , 7.53; SMe, 9.16; SO ₂ Me, 7.01; SO ₂ Me, 7.27; <i>i</i> -Pr, 9.43; Br, 8.50; I, 8.54; CN, 7.70
40.	k_r , 4- $XC_6H_4CO_2H$ + Ph ₂ CN ₂ in MeAc at 37° ^w ; NO ₂ , 8.09; F, 0.713; H, 0.363; Me, 0.184; OMe, 0.125; NH ₂ , 0.0228
41.	pK_a , 4-X-2,6-dimethylbenzoic acids ^a : PrO, 5.48; Me, 5.38; AcNH, 5.21; H, 5.18; Br, 4.78; MeO ₂ C, 4.56
42.	pK_a , 4-XPnCO ₂ H, 75% v/v aq. MeOH, 39.8° ^v ; Br, 5.579; NO ₂ , 4.920; MeO, 6.304; Me, 6.169; H, 5.995; Bz, 5.373; AcNH, 6.063; CF ₃ , 5.30

^a B. M. Wepster, private communication.

^b O. Exner, *Coll. Czech. Chem. Commun.*, 31, 65 (1966).

^c Excluded from the correlation.

^d Ref. 28.

^e Footnotes, c,e, Table 23, footnote p, Table 7.

^f Tabulated by M. Charton in *Prog. Phys. Org. Chem.*, 10 81 (1973).

^g E. Berliner and E. A. Blommers, *J. Am. Chem. Soc.*, 73, 2479 (1951).

^h R. Thuaire, *C. R. Acad. Sci., Paris*, 267, 993 (1968).

ⁱ Data in Table 2.

^j J. H. Elliott and M. Kilpatrick, *J. Phys. Chem.*, 485 (1941).

are reported in Table 26. The σ_R values obtained are given in Table 27, when two or more σ_R values of equal reliability were available. The average value is reported in the table. The error in the σ_R values was estimated where possible by means of the equation

$$s = \left[\frac{(S^2_{pK_a} + \sigma^2_{IX}S_L^2 + L^2S^2\sigma_{IX} + S_H^2)}{D^2} + \frac{(pK_a - L\sigma_{IX} - h)^2S_D^2}{D^4} \right]^{1/2} \quad (89)$$

which was obtained by the same method as was Equation 65 (43). The σ_I values required for the calculation of σ_R are generally from Table 7. In some cases estimated values were used. Thus, from the σ_I values for $H_2C=CH$, Ph, 1- $C_{10}H_8$, 2- $C_{10}H_8$, we can obtain an average value of σ_I of 0.13 with a standard error of 0.013 for the σ_I values of substituents containing only H and sp^2 -hybridized carbon. For carbonyl groups of the type ZCO, inspection of the values available shows that they lie in the range 0.26 to 0.32. It has been shown that in systems of the type



where X is a substituent, Y the active site, and G some group to which Y and the carbonyl group are attached and in

^k J. F. J. Dippy, S. R. C. Hughes, and B. C. Kitchiner, *J. Chem. Soc.*, 1964, 1275.

^l W. Simon, G. H. Lyssy, A. Morikofer, and E. Heilbronner, *Zusammenstellung von scheinbaren Dissoziationskonstanten im Lösungsmittelsystem Methylcellulose/Wasser*, Juris-Verlag, Zurich, 1959.

^m J. H. Elliott and M. Kilpatrick, *J. Phys. Chem.*, 45, 472 (1941).

ⁿ J. H. Elliott, and M. Kilpatrick, *ibid.*, 45, 454 (1941).

^o J. H. Elliott, and M. Kilpatrick, *ibid.*, 45, 466 (1941).

^p J. H. Elliott and M. Kilpatrick, *ibid.*, 46, 221 (1942).

^q J. H. Elliott and M. Kilpatrick, *ibid.*, 45, 472 (1941).

^r T. B. McMahon and P. Kebarle, *J. Am. Chem. Soc.*, 99, 2222 (1977).

^s A. G. Kozachenko, E. I. Matrossov, and M. I. Kabachnik, *Izv. Akad. Nauk, SSR. Ser. Khim.*, 2240 (1976).

^t M. M. Davis and M. Paabo, *J. Org. Chem.*, 31, 1804 (1966).

^u K. Kalfus, M. Vecera and O. Exner, *Collect. Czechoslov. Chem. Commun.*, 25, 382 (1970).

^v M. Hojo, M. Utaka, and Z. Yoshida, *Tetrahedron*, 27, 2713, 4031, 4255 (1971).

^w N. B. Chapman, M. R. J. Dack, D. J. Newman, J. Shorter, and R. Wilkinson, *J. Chem. Soc., Perkin Tran. II*, 962, (1974).

^x J. D. Roberts and C. M. Regan, *J. Am. Chem. Soc.*, 76, 939 (1954).

^y W. N. White, R. Schlitt, and D. Gwynn, *J. Org. Chem.*, 26, 3613 (1961); W. A. Sheppard, *J. Am. Chem. Soc.*, 92, 5419 (1970).

TABLE 26
Results of Correlations with Eq. 88

Set	$-L$	$-D$	h	R^a	F^b	r_{12}^c	S^d	S_L^d
1	1.09	1.05	4.37	0.9998	8241.	0.052	0.0102	0.0126
1M	1.09	0.398	4.38	0.9983	1489.	0.011	0.0187	0.0210
2	1.58	1.35	5.49	0.9976	1226.	0.094	0.0381	0.0395
2M	1.62	0.684	5.55	0.9923	350.9	0.119	0.0604	0.0628
3	1.74	1.46	6.27	0.9945	500.0	0.034	0.0649	0.0728
3M	1.74	0.808	6.30	0.9951	509.7	0.011	0.0523	0.0587
4	1.69	1.36	5.74	0.9979	1278.	0.381	0.0459	0.0680
5	1.69	1.36	5.81	0.9981	512.7	0.196	0.0480	0.0756
6	0.958	1.05	4.186	0.9978	673.2	0.025	0.0295	0.0352
7	0.902	1.07	4.148	0.9966	442.0	0.025	0.0355	0.0423
8	1.62	1.75	6.58	0.9974	1045.	0.381	0.0587	0.0870
9	2.34	2.10	4.34	0.9986	1434.	0.099	0.0446	0.0592
10	1.63	1.39	5.67	0.9994	905.2 ⁸	0.086	0.0280	0.0525 ^h
11	1.44	1.24	5.16	0.9987	749.7	0.091	0.0293	0.0453
11M	1.36	0.628	5.17	0.9904	103.0	0.091	0.0645	0.0997
12	1.58	1.35	5.77	0.9996	2524.	0.091	0.0175	0.0271
12M	1.46	0.769	5.77	0.9930	141.7	0.091	0.0603	0.0932
13	1.76	1.39	6.57	0.9988	850.5	0.091	0.0327	0.0506
13M	1.57	0.771	6.53	0.9964	273.9	0.091	0.0461	0.0712
14	1.79	1.46	7.23	0.9940	164.0	0.091	0.0767	0.119
14M	1.59	0.738	7.22	0.9922	126.2	0.091	0.0684	0.106
15	1.73	1.46	10.20	0.9974	381.6	0.091	0.0491	0.0759
15M	1.83	0.993	10.16	0.9940	164.2	0.091	0.0706	0.109
16	1.49	1.29	5.474	0.9991	1663.	0.019	0.0234	0.0355
16M	1.35	0.564	5.485	0.9969	403.3	0.015	0.0334	0.0508
17	1.59	1.40	7.031	0.9974	562.8	0.019	0.0434	0.0658
17M	1.49	0.617	7.045	0.9992	1537.	0.015	0.0189	0.0287
18	1.19	1.12	4.481	0.9966	363.0	0.017	0.0444	0.0692
18M	1.04	0.378	4.440	0.9967	381.6	0.017	0.0266	0.0415
19	1.24	1.01	4.997	0.9981	647.3	0.017	0.0318	0.0496
19 M	1.09	0.390	4.973	0.9956	281.9	0.017	0.0322	0.0503
20	1.90	1.64	6.64	0.9977	660.1	0.301	0.0559	0.101
20M	1.72	0.775	6.63	0.9983	857.5	0.301	0.0328	0.0592
21	1.30	1.20	7.635	0.9975	599.4	0.019	0.0351	0.0532
21M	1.34	0.559	7.635	0.9971	425.3	0.015	0.0324	0.0491
22	1.45	1.37	9.406	0.9965	428.4	0.019	0.0470	0.0713
22M	1.49	0.779	9.390	0.9957	286.0	0.015	0.0455	0.0691
23	1.68	1.43	10.09	0.9955	332.9	0.019	0.0587	0.0889
23M	1.75	0.905	10.09	0.9935	190.9	0.015	0.0652	0.0990
24	1.56	1.43	8.592	0.9965	426.3	0.019	0.0499	0.0757
24M	1.64	0.847	8.573	0.9946	227.6	0.015	0.0561	0.0852
25	1.54	1.42	8.597	0.9969	489.1	0.019	0.0461	0.0698
25M	1.53	0.859	8.571	0.9952	258.3	0.015	0.0498	0.0757
26	1.31	1.18	4.386	0.9993	1109.	0.020	0.0243	0.0392
26M	1.24	0.486	4.387	0.9978	577.0	0.015	0.0255	0.0388
27	15.3	11.1	23.2	0.9942	172.1	0.071	0.704	1.05

TABLE 26
Results of Correlations with Eq. 88

Set	$-L$	$-D$	h	R^a	F^b	r_{12}^c	S^d	S_L^d
27M	13.7	7.72	23.2	0.9875	78.40	0.071	0.866	1.29
28	1.56	2.36	13.23	0.9946	230.4	0.274	0.132	0.214
28M	2.05	0.959	13.20	0.9972	175.7 ^h	0.330	0.0780	0.155 ^h
29	-2.00	-1.53	5.28	0.9988	1496.	0.226	0.0396	0.0572
29M	-2.13	-0.934	5.29	0.9988	1459.	0.226	0.0347	0.0502
30	1.32	1.40	5.81	0.9987	583.7	0.464	0.0352	0.0580
30M	1.38	0.417	5.89	0.9954	217.0	0.403	0.0491	0.0784
31	1.38	1.57	6.80	0.9996	1691.	0.464	0.0220	0.0363
31 M	1.35	0.679	6.83	0.9982	550.6	0.403	0.0319	0.0509
32	1.41	1.59	8.08	0.9992	893.5	0.464	0.0309	0.0510
32M	1.49	0.678	8.14	0.9985	684.7	0.403	0.0312	0.0498
33	1.47	1.53	9.77	0.9977	331.3	0.464	0.0515	0.0850
33M	1.48	0.677	9.82	0.9965	283.9	0.403	0.0481	0.0768
34	1.26	1.15	4.64	0.9969	324.1	0.435	0.0500	0.0968
35	1.44	1.24	5.85	0.9973	652.9	0.129	0.0354	0.0451
36	1.61	1.42	6.93	0.9977	744.8	0.129	0.0373	0.0476
37	1.82	1.56	8.96	0.9911	248.5	0.112	0.0918	0.106
38	2.34	2.33	10.42	0.9949	195.9	0.064	0.113	0.176
39	2.27	2.16	9.08	0.9928	308.5	0.311	0.116	0.154
40	-1.90	-1.76	-0.459	0.9952	156.5	0.068	0.107	0.171 ^h
41	1.50	1.35	0.830	0.9979	355.8	0.288	0.0298	0.0731
42	1.41	1.28	5.973	0.9977	538.0	0.157	0.0396	0.0666

Set	S_D^d	S_h^d	$100r^{2c}$	n^f	P_R	Error
1	0.0116	0.00521	99.95	11	49.1	0.7
1M	0.0246	0.00878	99.67	13	26.7	1.8
2	0.0411	0.0152	99.51	15	46.1	1.7
2M	0.0758	0.0241	98.46	14	29.7	3.5
3	0.0736	0.0304	98.91	14	45.6	2.7
3M	0.0689	0.0246	99.03	13	31.7	2.9
4	0.0434	0.0287	99.57	14	44.6	1.8
5	0.0749	0.0324	99.61	7	44.6	2.9
6	0.0440	0.0145	99.56	9	52.3	2.6
7	0.0530	0.0175	99.33	9	54.3	3.3
8	0.0555	0.0368	99.48	14	51.9	2.3
9	0.0655	0.0229	99.72	11	47.3	1.7
10	0.0532 ^h	0.0230	99.89	5	46.0	2.1
11	0.0496	0.0217	99.73	7	46.3	2.2
11M	0.109 ^h	0.0478	98.10	7	31.6	6.0
12	0.0296	0.0130	99.62	7	46.1	1.2
12M	0.102	0.0446	98.61	7	34.5	5.1
13	0.0553	0.0242	99.77	7	44.1	2.0
13M	0.0779 ^h	0.0341	99.28	7	32.9	3.6
14	0.130	0.0568	98.79	7	44.9	4.7

TABLE 26
Results of Correlations with Eq. 88

Set	S_D^d	S_h^d	$100r^{2e}$	n^f	P_R	Error
14M	0.116 ^h	0.0506	98.44	7	31.7	5.4
15	0.0830	0.0363	99.48	7	45.8	3.1
15M	0.119	0.0523	98.80	7	35.2	4.7
16	0.0333	0.0171	99.82	9	46.4	1.4
16M	0.0538	0.0244	99.38	8	29.5	3.0
17	0.0616	0.0316	99.47	9	46.8	2.5
17M	0.0304	0.0138	99.84	8	29.3	1.6
18	0.0535	0.0292	99.32	8	48.5	3.0
18M	0.0321	0.0175	99.35	8	26.7	2.5
19	0.0383	0.0209	99.62	8	44.9	2.1
19M	0.0389	0.0212	99.12	8	26.4	2.9
20	0.0689	0.0524	99.55	9	46.3	2.5
20M	0.0404	0.0307	99.65	9	31.1	1.8
21	0.0498	0.0256	99.50	9	48.0	2.4
21M	0.0520	0.0236	99.42	9	29.4	3.0
22	0.0667	0.0343	99.30	9	48.6	2.9
22M	0.0732	0.0332	99.13	8	34.3	3.6
23	0.0832	0.0427	99.11	9	46.0	3.2
23M	0.105	0.0476	98.71	8	34.1	4.4
24	0.0708	0.0364	99.30	9	47.8	2.9
24M	0.0902	0.0409	98.91	8	34.0	4.0
25	0.0654	0.0336	99.39	9	48.0	2.7
25M	0.0801	0.0363	99.04	8	36.0	3.7
26	0.0350	0.0180	99.86	6	47.4	1.7
26M	0.0411	0.0186	99.57	8	28.2	2.6
27	1.07	0.514	98.85	7	42.0	4.7
27M	1.32 ^h	0.633	97.51	7	36.0	6.9
28	0.136	0.0908	98.93	8	60.0	5.2
28M	0.118 ⁱ	0.0780	99.43	5	31.9	4.4
29	0.0462	0.0286	99.77	10	43.3	1.6
29M	0.0405	0.0250	99.76	10	30.5	1.5
30	0.118 ^h	0.0274	99.74	6	51.5	5.0
30M	0.138 ⁱ	0.0381	99.09	7	23.2	7.9
31	0.0736	0.0171	99.91	6	53.2	2.9
31M	0.0893 ^h	0.0247	99.64	7	33.5	4.7
32	0.103	0.0241	99.83	6	53.0	4.0
32M	0.0875	0.0242	99.71	7	31.3	4.3
33	0.172 ^h	0.0401	99.55	6	51.0	6.6
33M	0.135 ⁱ	0.0373	99.30	7	31.4	6.7
34	0.0820	0.0493	99.39	7	47.7	4.2
35	0.0593	0.0201	99.47	10	46.3	2.6
36	0.0626	0.0213	99.53	10	46.9	2.4
37	0.127	0.0512	98.22	12	46.2	4.4
38	0.169	0.0738	98.99	7	49.9	4.5
39	0.149	0.0741	98.56	12	48.8	4.1
40	0.136	0.0797	99.05	6	48.1	4.7

TABLE 26
Results of Correlations with Eq. 88

Set	S_D^d	S_h^d	$100r^{2e}$	n^f	P_R	Error
41	0.0604	0.0210	99.58	6	47.3	2.6
42	0.0596	0.0265	99.54	8	47.6	2.7

^a Multiple correlation coefficient.

^b F test for significance of correlation. Confidence level < 99.9 is shown by superscript.

^c Partial correlation coefficient of σ_I on σ_R .

^d Standard errors of the estimate, L , D , h . Superscript indicates a CL of the Student t test of L , D , h if less than 99.9.

^e Percent of data accounted for by correlation equation.

^f Number of points in the set.

^g 99.5% CL.

^h 99.0% CL.

ⁱ 98.0% CL.

^j 95.0% CL.



itself, the substituent exerts a predominantly localized electrical effect. The delocalized effect, however, is significant. Thus, the value of σ_I for alkanoyl groups, aroyl groups, and the formyl group must lie between the values for MeO_2C (0.32) and H_2NCO (0.28). We have chosen to set σ_I for these groups equal to 0.30. The value of σ_I of 0.54 for MeSO was estimated from the correlation of $\sigma_{I,XSO}$ with σ_{I,XSO_2} . The statistics for the correlation line were $m = 1.02$, $c = -0.0605$, $r = 0.9837$, $s_m = 0.131$, $s_c = 0.0798$, $100r^2 = 96.79$, $n = 4$. In some cases the σ_I values used were the average values of AkW groups from Table 21. We have rejected some $\text{p}K_a$ values that gave σ_R constants that deviated sharply from the great majority of the constants for the same type of substituent.

C. Validity of the σ_R Constants in Various Media

Correlations of the sets of 4-substituted benzoic acid $\text{p}K_a$ s in various protonic solvents with Equation 88 are generally excellent, with 29 of 35 sets giving values of $100r^2$ greater than 99.00. The results obtained for the 3-substituted benzoic acid sets are somewhat inferior to those obtained for the 4-substituted benzoic acids (16 sets of a total of 23 gave correlations with $100r^2$ values greater than 99.00); nevertheless, the results are very good. We may conclude from these results that the applicability of these σ_R values to data in protonic media is valid. What little data is available in dipolar aprotic solvents (sets 28, 28m in nitromethane, set 40 in acetone) gave very good results. The available data in non-

TABLE 27
Values of σ_R , σ_m , σ_p

X	σ_R	Error ^a	pK_a^b	Set ^c	σ_m	σ_p
Alkyl, Cycloalkyl						
Me	-0.16	0.021	—	01		
Et	-0.14	0.045	—	01	-0.05	
<i>c</i> -C ₃ H ₅	-0.19	U	5.93 ^d	01,4		
Pr	-0.16	0.023	4.703 ^f	9	-0.06	-0.17
<i>i</i> -Pr	-0.16	0.040	—	01	-0.04	
<i>c</i> -C ₄ H ₇	-0.13	U	5.91 ^d	4	-0.05	-0.14
<i>t</i> -Bu	-0.18	0.009	—	01		
<i>c</i> -C ₅ H ₉	-0.13	U	5.91 ^d	4	-0.05	-0.14
<i>t</i> -BuCH ₂	-0.17	0.025	— ^e	2	-0.05	-0.17
EtMe ₂ C	-0.17	0.025	— ^e	2	-0.06	-0.18
<i>c</i> -C ₆ H ₁₁	-0.15	U	— ^e	2	-0.05	-0.15
<i>n</i> -C ₇ H ₁₅	-0.12	0.024	— ^e	2	-0.07	-0.16
Et ₃ C	-0.19	0.025	— ^e	2	-0.07	-0.20
Vinyl, Ethynyl, Aryl, Vinylalkyl, Ethynylalkyl, Arylalkyl						
HC≡C—	-0.04	0.037	3.75 ^g	9	0.29	0.25
CH ₂ =CH—	-0.15	0.020	— ^e	2	0.06	-0.04
MeC≡C—	-0.27	0.034	4.20 ^g	9	0.21	0.03
CH ₂ =CHCH ₂	-0.14	0.006	—	01		
E—MeCH=CH	-0.16	0.029	4.50 ^g	9	0.02	-0.09
H ₂ C=CMe—	-0.05	U	5.71	5	0.09	0.05
Ph	-0.11	0.020	— ^e	2	0.09	0.01
PhCH ₂	-0.13	0.019	— ^e	2	-0.01	-0.10
PhC≡C	-0.21	U	5.47 ^h	4	0.26	0.12
3-PhC ₆ H ₄	-0.14	U	5.65 ⁱ	10	0.09	-0.01
4-PhC ₆ H ₄	-0.22	U	5.77 ⁱ	10	0.06	-0.09
Haloalkyl						
CCl ₃	0.08	U	5.85 ^h	8	0.40	0.44
CF ₃	0.11	0.046	— ^e	2	0.46	0.51
ClCH ₂	-0.08	0.039	5.54 ^h	4	0.15	0.09
		0.042	6.46 ^h	8		
BrCH ₂	-0.10	0.023	— ^e	2	0.17	0.10
ICH ₂	-0.09	0.039	5.59 ^h	4	0.15	0.08
		0.042	6.42 ^h	8		
CF ₂ CF ₂ CF ₃	0.09	U	3.229 ^f	9	0.44	0.48
Oxyalkyl						
060HOCH ₂	-0.07	U	—	01	0.10	0.04
AcOCH ₂	-0.09	0.043	6.50 ^h	8	0.13	0.06
PhOCH ₂	-0.11	U	6.57 ^h	8	0.09	0.01
MeOCH ₂	-0.10	0.041	5.68 ^h	4,8	0.08	0.01
		0.043	6.59 ^h			

TABLE 27
Values of σ_R , σ_m , σ_p

X	σ_R	Error ^a	pK_a ^b	set ^c	σ_m	σ_p
Other Substituted Alkyl						
NCCH ₂	-0.04	0.023	— ^e	1	0.20	0.16
		0.043		2		
H ₂ NCCH ₂	-0.12	0.041	6.69 ^h	8	0.03	-0.06
$\begin{array}{c} \parallel \\ \text{O} \end{array}$						
AcNHCH ₂	-0.14	0.041	6.68 ^h	8	0.05	-0.05
(EtO) ₂ P(O)CH ₂	-0.07	U	5.61 ^j	4	0.12	0.06
PhSO ₂ CH ₂	-0.15	U	6.37 ^h	8	0.24	0.14
Ph ₂ P(O)CH ₂	-0.19	U	5.66 ^j	4	0.14	0.01
Silyl, Silylalkyl						
Me ₃ Si	0.12	U	—	01		
Me ₃ SiCH ₂	-0.23	U	— ^e	2	-0.11	-0.26
Carbonyl						
CO ₂ H	0.11	0.037	3.397 ^k	9	0.36	0.41
Ac	0.20	0.040	—	01		
CO ₂ Me	0.11	0.038	— ^e	1,2	0.38	0.43
CO ₂ Et	0.11	0.038	3.396 ^k	9	0.36	0.41
EtCO	0.18	U	—	01		
<i>i</i> -PrCO	0.17	U	—	01		
<i>t</i> -BuCO	0.12	U	—	01		
PhCO	0.11	U	5.90 ^l	8	0.36	0.41
HCO	0.15	U	—	01		
H ₂ NCO	0.08	U	4.65 ^{aa}	41		
Aza						
NH ₂	-0.80	U	—	01		
HCONH	-0.40	0.027	— ^e	2	0.19	-0.07
H ₂ NCONH	-0.47	0.037	7.03 ^h	8	0.06	-0.24
ClCH ₂ CONH	-0.42	0.056	5.70 ^h	4	0.20	-0.07
		0.046	6.75 ^h	8		
AcNH	-0.35	0.023	— ^e	2	0.16	-0.07
Me ₂ N	-0.88	0.028	— ^e	2	-0.16	-0.71
EtO ₂ CNH	-0.48	0.053	5.91 ^h	4	0.11	-0.20
		0.044	6.94 ^h	8		
PhNH	-0.86	U	— ^e	1,2	-0.02	-0.56
PhSO ₂ NH	-0.36	U	5.70 ^h	4,8	0.20	-0.03
			6.63 ^h			
BzNH	-0.47	U	6.95 ^h	8	0.11	-0.19

TABLE 27
Values of σ_R , σ_m , σ_p

X	σ_R	Error ^a	pK_a^b	Set ^c	σ_m	σ_p
Oxa						
HO	-0.62	0.031	—	01		
MeO	-0.58	0.026	—	01		
MeSO ₂ O	-0.24	0.068	5.16 ^b	4,8	0.47	0.31
		0.056	6.06 ^h			
AcO	-0.23	0.045	6.36 ^h	8	0.30	0.15
EtO	-0.57	0.021	— ^c	2	0.07	-0.29
PrO	-0.52	U	4.46 ^m	6	0.09	-0.24
BuO	-0.58	U	4.52 ^m	6	0.07	-0.30
AmO	-0.60	U	4.55 ^m	6	0.06	-0.32
PhO	-0.48	0.030	— ^e	2	0.23	-0.08
BzO	-0.30	U	6.41 ^h	8	0.33	0.13
Phosphinyl, Thiophosphinyl						
(MeO) ₂ PO	0.21	U	4.88 ^j	01,4	0.45	0.57
(EtO) ₂ PO	0.24	U	4.90 ^j	01,4	0.43	0.56
Bu ₂ PO	0.28	U	4.94 ^j	4	0.37	0.53
(BuO) ₂ PO	0.28	U	4.87 ^j	4	0.41	0.57
Ph ₂ PO	0.34	U	4.79 ⁿ	4	0.40	0.60
			4.88 ^o			
Ph ₂ PS	0.22	U	4.97 ^o	4	0.38	0.50
Thia						
F ₃ CS	-0.01	U	4.98 ^p	4	0.46	0.44
			5.01 ^t			
NCS	-0.16	U	4.97 ^h	4	0.51	0.40
			6.00 ^h			
MeS	-0.38	U	5.74 ^q	4	0.17	-0.08
AcS	-0.02	U	5.10 ^h	4	0.39	0.37
EtS	-0.30	U	5.71 ^r	4	0.16	-0.04
<i>i</i> -PrS	-0.27	U	5.66 ^r	4	0.17	-0.01
4-O ₂ NC ₆ H ₄ S	-0.11	U	5.30 ^s	4	0.32	0.24
PhS	-0.24	U	5.54 ^s	4	0.23	0.07
Sulfonyl, Sulfinyl						
CF ₃ SO ₂	0.21	U	4.24 ^t	4	0.80	0.92
			4.17 ^h			
			4.35 ^r			
MeSO ₂	0.11	0.033, 0.057	— ^e	1,2	0.65	0.70
PhSO ₂	0.12	U	4.63 ^s	4	0.62	0.68
CF ₃ SO	-0.03	U	4.65 ^t	4	0.67	0.64
MeSO	0.00	U	— ^e	01		

TABLE 27
Values of σ_R , σ_m , σ_p

X	σ_R	Error ^a	pK_a^b	Set ^c	σ_m	σ_p
4-O ₂ NC ₆ H ₄ SO	0.06	U	4.74 ^s	4	0.58	0.60
PhSO	-0.07	U	4.97 ^s	4	0.50	0.44
Ionic						
NMe ₃ ⁺	-0.11	U	—	01		
SMe ₂ ⁺	0.24	U	—	01		
SO ₃ ⁻	0.33	U	—	01		
CO ₂ ⁻	0.23	U	4.300 ^k	9	-0.09	0.04
Substituted Phenyl						
4-MeC ₆ H ₄	-0.13	0.031	5.69 ^u	10	0.06	-0.03
4-EtC ₆ H ₄	-0.12	U	5.67 ^v	10	0.07	-0.02
4- <i>i</i> -PrC ₆ H ₄	-0.09	U	5.64 ^v	10	0.08	0.01
4- <i>t</i> -BuC ₆ H ₄	-0.08	U	5.64 ^v	10	0.07	0.01
4-MeOC ₆ H ₄	-0.19	0.022	5.75 ^u	10	0.05	-0.08
4-ClC ₆ H ₄	-0.03	0.025	5.47 ^u	10	0.15	0.12
3-ClC ₆ H ₄	-0.06	U	5.49 ^v	10	0.15	0.10
4-BrC ₆ H ₄	-0.03	0.026	5.47 ^u	10	0.15	0.12
4-IC ₆ H ₄	-0.05	U	5.49 ^v	10	0.14	0.10
3-IC ₆ H ₄	-0.10	U	5.55 ^v	10	0.13	0.06
4-FC ₆ H ₄	-0.07	U	5.56 ^v	10	0.12	0.06
3-FC ₆ H ₄	-0.06	U	5.49 ^v	10	0.15	0.10
4-O ₂ NC ₆ H ₄	0.03	0.032	5.25 ^u	10	0.25	0.26
3-O ₂ NC ₆ H ₄	0.00	0.030	5.35 ^u	10	0.21	0.20
C ₆ F ₅	-0.35	0.046	5.99 ^{bb}	42		
Other Groups						
H	0	—	—	01		
F	-0.48	0.041	—	01		
Cl	-0.25	0.028	—	01		
Br	-0.25	0.032	—	01		
I	-0.16	0.048	—	01		
CN	0.08	0.008	—	01		
NO ₂	0.10	0.024	—	01		
N ₃	-0.31	U	5.45 ^h 6.41 ^h	4,8	0.32	0.12
SF ₅	0.03	U	4.70 ^h	4	0.61	0.62
π -Cr(CO) ₃ Ph	-0.09	U	6.36 ^y	8	0.21	0.14
<i>o</i> -carboranyl	0.07	U	5.86 ^z	3	0.22	0.25
Heteroaryl Groups						
2-furyl	-0.19	U	5.71 ^x	4	0.13	0
2-thienyl	-0.19	U	5.67 ^j	4	0.11	-0.02

protic solvents is limited to two sets in PhH (sets 29, 2m) Two sets of gas phase acidities are also available (29, 29m). Very good results were obtained with the data in benzene. The gas phase results were not as good. It must be pointed out again that the OH group is a very badly behaved substituent in any solvent other than water, and therefore the σ_R value reported in Table 27 should be restricted to water or solvents with a high water concentration.

With regard to ionic substituents, the medium dependence is so large that

^a Estimation of error for σ_R values obtained from Eq. 80 and the σ_p values given in Table 24 were calculated from Eq. 65 (these values are from set 01). Estimates of error for the σ values obtained from Eq. 87 were calculated from Eq. 89.

^b When more than one pK_a value is reported, the σ_R value is the average of the values calculated from the reported pK_a s.

^c The set in Table 26 from which the values of L , D , and h required for the calculation of σ_R were taken.

^d R. C. Hahn, T. F. Corbin, and H. Schter, *J. Am. Chem. Soc.*, **90**, 3404 (1968).

^e Private communication, B. M. Wepster; the pK_a values used to calculate the σ_R constants will be published by Prof. Wepster. We believe the maximum error for these values is 0.02.

^f Footnote p, Table 7.

^g Footnote h, Table 7.

^h O. Exner, *Collect. Czechoslov. Chem. Commun.*, **31**, 65 (1966); O. Exner and L. Lakomy, *ibid.*, **35**, 1371 (1970).

ⁱ D. J. Byron G. W. Gray, and R. C. Wilson, *J. Chem. Soc. C*, 831 (1966); *ibid.*, 837 (1966).

^j Footnote k, Table 23.

^k G. Dahlgren and F. A. Long, *J. Am. Chem. Soc.*, **82**, 1303 (1960).

^l Footnote y, Table 23.

^m G. W. K. Cavill, N. A. Gibson, and R. S. Nyholm, *J. Chem. Soc.*, 2466 (1949).

ⁿ J. J. Monagle, J. V. Mengenhauser, and D. A. Jones Jr., *J. Org. Chem.*, **32**, 2477 (1967).

^o E. N. Tsvetkov, D. I. Lobanov, M. M. Makhamatkhanov, and M. I. Kabachnik, *Tetrahedron*, **25**, 5623 (1969).

^p W. A. Sheppard, *J. Am. Chem. Soc.*, **85**, 1314 (1963).

^q F. G. Bordwell and G. D. Cooper, *J. Am. Chem. Soc.*, **73**, 5184 (1951); *ibid.*, **74**, 1058 (1952).

^r V. Baliah, S. Shanmaganathan, and R. Varadachari, *J. Phys. Chem.*, **61**, 1013 (1957).

^s H. Szmant and G. Suld, *J. Am. Chem. Soc.*, **78**, 3400 (1956).

^t L. M. Yagupolskii, B. F. Bistrov, A. V. Stelanyants, and O. A. Fialkov, *Zhur. Obshch. Khim.*, **34**, 3682 (1964).

^u Footnote g, Table 25.

^v Calculated from the equation $pK_{ax}(25^\circ) = mpK_{ax}(20^\circ) + c$, $m = 0.827$; $c = 1.00$; $r = 0.9916$; $s = 0.0290$; $s_m = 0.0441$ (99.9% CL); $s_c = 0.0246$; $100r^2 = 98.32$; $n = 8$; $F = 351.9$ (99.9% CL), using data from footnote *i*.

^x T. Fringuelli, G. Marino, and A. Taticchi, *J. Chem. Soc. B*, 2304 (1971).

^y S. P. Gubin, V. S. Khandkarova, and A. Z. Kreindlin, *J. Organomet. Chem.*, **64**, 229 (1974).

^z M. F. Hawthorne, T. E. Berry, and P. A. Wegner, *J. Am. Chem. Soc.*, **87**, 4746 (1965).

^{aa} Footnote x, Table 25.

^{bb} Footnote y, Table 25.

all substituent constants for these groups must be considered uncertain. The values of σ_R reported for groups of this type are best used in the medium in which the pK_a values used to calculate them were determined, if at all.

D. Determination of σ_m and σ_p in Nonaqueous Media

It was noted previously that composition of the electrical effect in the ionization of 4-substituted benzoic acids varied with the medium. As a measure of the composition of the electrical effect we will use P_D , defined in Equation 15. From Equations 17 and 18,

$$L = \rho\lambda, D = \rho\delta \quad (90)$$

and

$$\frac{D \cdot 100}{L + D} = \frac{\rho\delta \cdot 100}{\rho\lambda + \rho\delta} \equiv P_D \quad (91)$$

The justification for the use of P_D is given in the Appendix.

In the specific case of the σ_R constants, P_D will be written P_R . Values of P_R are reported in Table 26. Estimates of the error in P_R were made by means of the equation (43)

$$S = 100 \left(\frac{1}{(L + D)^2} \left(\frac{S_D^2 + (D^2[S_D^2 + S_L^2])}{(L + D)^2} \right) \right)^{1/2} \quad (92)$$

Values of the estimated error S are also given in Table 26. Inspection of the P_R values for 4-substituted benzoic acid sets in protic solvents shows clearly that certainly in 13 sets and probably in 14 others, P_R is smaller than the value of 50.0 obtained for water from Equations 15 and 39. In only one set is P_R unquestionably greater than 50.0, and in only five other sets is it probably greater. Thus, in general, in mixed aqueous and nonaqueous protic solvents, the delocalized effect makes less of a contribution to the overall electrical effect than it does in water. A value of 28.0 for the P_R of 3-substituted benzoic acids can be calculated from Equations 15 and 86. Eight sets definitely and 10 sets probably have P_R values greater than 28.0 whereas 4 sets have values probably smaller. In general, in protic solvents other than water, the delocalized effect makes more of a contribution to the overall electrical effect than it does in water. We may gain further insight into the question of the variations of the electrical effect by defining the quantities

$$C_L = \frac{L_m}{L_p}, C_D = \frac{D_m}{D_p} \quad (93)$$

and examining their variation with solvent. Values of C_L , D_D and the error in these quantities estimated from Equation 64 are given in Table 29. The values of C_L in water-ethanol and water-dioxane mixtures do not generally show a

significant variation from the value of 1.00 for pure water which may be calculated from Equations 39, 86, 90, and 93.

$$C_L = \frac{\lambda_m}{\lambda_p}, C_D = \frac{\delta_m}{\delta_p} \quad (94)$$

The values of C_D do differ significantly from the value of 0.39 obtained for pure water by means of Equation 94. In fact, a plot of C_D versus moles of hydroxyl group per liter (M_{OH}) shows a reasonably linear relationship with C_D increasing as the molarity of the hydroxyl group decreases. This is not the case for C_L values in aqueous ethanol or aqueous dioxane and although in pure hydroxylic solvents C_L is linear, in M_{OH} , the slope of the line is much smaller than is that for C_D in the same media. Correlations of C_L and C_D with the equation

$$C = m M_{OH} + d \quad (95)$$

are reported in Table 30. M_{OH} for a solution is defined by the equation

$$M_{OH} = \sum n_i M_i \quad (96)$$

where M_i is the molarity of the i th component of the solvent and n_i is the number of OH groups in a molecule of the i th component. The values of MeOH used in the correlations with Equation 95 are reported in Table 31. The values of C_L and C_D are taken from Table 29. We may conclude from these observations that the solvent dependence of the composition of the electrical effect in benzoic acid ionizations in protic media is probably due to an action on the delocalized effect. The overall effect is that

$$\frac{dL}{dMd} \neq \frac{dD}{dMd} \quad (97)$$

That is, the rate of change of the localized effect coefficient, L , with the medium, Md , is different from that of the delocalized effect coefficient, D , with Md .

Inspection of the σ_m and σ_p constants in Table 28 which were calculated from the simple Hammett equation with those calculated from Equations 86 and 86 shows that in the case of the σ_p constants, significant deviations ($\cong \pm 0.03$) occur in 14 of the 37 groups examined. In the case of the σ_m values, significant deviations were almost always encountered. In the basis of this analysis, we would strongly suggest that mixed protic solvents should not be used for the determination of σ_m constants and that their use for σ_p constants should be avoided.

E. A Test of the Validity of the σ_R Constants

The best possible test of the σ_R constants would be their application to a set of data that would be dependent only on σ_R . It is difficult to find such a set of data under ordinary circumstances. We may obtain such data sets, however,

TABLE 28
Comparison of Hammett σ Constants

X	$pK_{a,m}^a$	σ_m^b	σ_m^c	Δ_m^d	σ_p^e	σ_p^c	Δ_p^f
<i>c</i> -C ₄ H ₇	5.91	-0.05	-0.17	0.124	-0.14	-0.17	0.034
<i>c</i> -C ₅ H ₉	5.95	-0.05	-0.20	0.152	-0.14	-0.17	0.034
PhC ₂	5.51	0.26	0.10	0.158	0.12	0.13	-0.010
(EtO) ₂ P(O)CH ₂	5.59	0.12	0.05	0.073	0.06	0.03	0.027
Ph ₂ P(O)CH ₂	5.65	0.14	0.01	0.134	0.01	0.00	0.011
Bu ₂ PO	5.15	0.37	0.35	0.019	0.53	0.50	0.033
(BuO) ₂ PO					0.57	0.54	0.025
Ph ₂ PS	5.24	0.38	0.29	0.091	0.50	0.48	0.024
MeS	5.53	0.17	0.09	0.081	-0.08	-0.06	-0.023
AcS	5.18	0.39	0.33	0.059	0.37	0.39	-0.016
EtS					-0.04	-0.04	-0.004
<i>i</i> -PrS					-0.01	0.00	-0.009
4-O ₂ NC ₆ H ₄ S					0.24	0.25	-0.008
PhS					0.07	0.08	-0.012
PhSO ₂					0.68	0.71	-0.031
CF ₃ SO	4.74	0.67	0.63	0.035	0.64	0.70	-0.057
4-O ₂ NC ₆ H ₄ SO					0.60	0.63	-0.035
PhSO					0.44	0.48	-0.036
SF ₅	4.82	0.61	0.58	0.030	0.62	0.66	-0.043
2-furyl	5.65	0.13	0.01	0.124	0.00	-0.04	0.036
2-thienyl	5.61	0.11	0.03	0.077	-0.02	-0.01	-0.012
<i>t</i> -BuCH ₂		-0.05	-0.22	0.171	-0.17	-0.18	0.010
EtMe ₂ C		-0.06	-0.22	0.161	-0.18	-0.19	0.007
<i>c</i> -C ₆ H ₁₁					-0.15	-0.16	0.009
<i>n</i> -C ₇ H ₁₅					-0.16	-0.17	0.013
Et ₃ C		-0.07	-0.27	0.200	-0.20	-0.21	0.008
Ph		0.09	0.00	0.091	0.01	0.01	0.004
PhCH ₂					-0.10	-0.11	0.011
CH ₂ =CH					-0.04	-0.04	-0.005
CF ₃		0.46	0.39	0.068	0.51	0.52	-0.013
BrCH ₂		0.17	0.14	0.033	0.10	0.10	-0.003
Me ₃ SiCH ₂		-0.11	-0.24	0.132	-0.26	-0.27	0.010
HCONH					-0.07	-0.03	-0.042
AcNH		0.16	0.14	0.016	-0.07	-0.06	-0.007
Me ₂ N					-0.71	-0.65	-0.061
EtO		0.07	0.03	0.036	-0.29	-0.25	-0.041
PhO		0.23	0.10	0.134	-0.08	-0.03	-0.052

^a The sources of the $pK_{a,m}$ values are the same as those of the $pK_{a,p}$ values used to calculate both σ_R and σ_p . The latter are reported in Table 27.

^b Calculated from Eq. 86. Substituents from *c*-C₄H₇ through 2-thienyl had their σ_m and σ_p constants calculated from set 30-7, the remaining σ_m and σ_p constants were calculated from set 30-8.

^c Calculated from Eq. 84 using the ρ and h values obtained from correlations reported in Table 30 (sets 7 and 8 for 44.1% aq. EtOH). The data used in the correlations are from footnotes a, Table 25 and those from footnote b are reported in Table 31.

^d $\Delta_m \equiv \sigma_m^b - \sigma_m^c$.

^e Calculated from Eq. 85.

^f $\Delta_p \equiv \sigma_p^e - \sigma_p^c$.

TABLE 29
Values of C_L ; $S_{C,L}$; C_D ; $S_{C,D}$

Set ^a	C_L	$S_{C,L}$ ^b	C_D	$S_{C,D}$ ^b	Set	C_L	$S_{C,L}$	C_D	$S_{C,D}$ ^b
1	1.00	0.023	0.379	0.024	21	1.03	0.067	0.466	0.049
2	1.03	0.057	0.507	0.060	22	1.03	0.087	0.569	0.066
3	1.00	0.080	0.553	0.062	23	1.04	0.110	0.633	0.0904
11	0.944	0.081	0.506	0.091	24	1.05	0.097	0.592	0.076
12	0.924	0.064	0.570	0.077	25	0.994	0.085	0.605	0.069
13	0.892	0.061	0.555	0.064	26	0.947	0.047	0.412	0.038
14	0.888	0.121	0.505	0.103	27	0.895	0.944	0.695	0.754
15	1.06	0.102	0.680	0.099	28	1.31	0.298	0.406	0.075
16	0.906	0.047	0.437	0.044	29	1.07	0.066	0.610	0.039
17	0.937	0.064	0.441	0.035	30	1.05	0.085	0.298	0.105
18	0.873	0.070	0.338	0.034	31	0.978	0.051	0.432	0.065
19	0.879	0.060	0.386	0.041	32	1.06	0.064	0.426	0.070
20	0.905	0.097	0.473	0.041	33	1.01	0.100	0.442	0.117

^a Numbers refer to Tables 25 and 26.

^b Errors in C_L and C_D , respectively.

by making use of a technique that seems to have first been employed in a different sense by Hartman and Traylor (48). Let us consider a set of substituents for which the localized effect is constant, whereas the delocalized effect varies over a considerable range. Such a set of substituents may be termed an isocalized

TABLE 30
Results of Correlations with Equations 16, 95, 98

Set	—Slope	Int.	r^a	F^b	S_{est}^c	S_{slope}^c	S_{int}^c	$100r^{2d}$	n^e
1	0.000101	0.981	0.0222	0.00 ^f	.0653	.0616 ^g	.00393	0.05	10
2	0.00602	0.727	0.8930	31.50	.0436	.00107	.0383	79.75	10
3	0.000665	0.995	0.2100	0.23 ^f	.0554	.00138 ^h	.0435	4.41	7
4	0.00103	0.454	0.8866	18.37	.00964	.000241 ⁱ	.00757	78.60	7
5	0.000601	1.04	0.3748	0.82 ^f	.0258	.000665 ^j	.0192	14.04	7
6	0.00566	0.701	0.9186	27.03	.0423	.00109 ⁱ	.0314	84.39	7
7	1.45	5.66	0.9908	535.0	.0995	.0625	.0293	98.17	12
8	1.45	5.46	0.9915	1273.	.0639	.0406	.0151	98.30	24
9	1.30	5.26	0.9750	173.4	.0923	.0989	.0310	95.07	11
10	1.63	6.13	0.9892	182.4	.0852	.121	.0485	97.85	6

Superscripts of F and of S indicate confidence levels (CL). In the case of S , CL refers to Student t test of slope and intercept. In the absence of a superscript, CL is 99.9%. For superscripts a through e, see Table 9.

^f <90.0.

^g <20.0.

^h 20.0.

ⁱ 99.0.

^j 50.0.

TABLE 31
Data Correlated with Equations 16, 95, 98

1,2.	<i>M</i> _{OH} , aqueous ethanol ^a : 0, 55.5; 8.05,52.0; 33.2,42.0; 44.1,37.6; 52.0,34.5; 70.3,27.9 ^b ; 73.4,26.8 ^b ; 85.4,22.5 ^b ; 100,17.1
3,4.	<i>M</i> _{OH} , aqueous dioxane ^c : 0, 55.5; 6.87,40.8; 12.7,32.4; 13.6,31.4; 20,25.0; 33.4,16.1; 36.2,14.7; 50,9.42
5,6.	<i>M</i> _{OH} , hydroxylic solvents: H ₂ O, 55.5; HOCH ₂ CH ₂ OH, 35.7; MeOH, 24.7; EtOH, 17.1; PrOH, 13.0; BuOH, 10.9.
7.	<i>pK</i> _a , 3-, or 4-substituted benzoic acids in 44.1% w/w aq. EtOH at 25°C ^d : H, 5.72; 4-Me, 5.96; 4-NO ₂ , 4.43; 4-NH ₂ , 6.47; 4-OH, 6.25; 4-OMe, 6.03; 4-CN, 4.67; 3-CN, 4.82; 3-Me, 5.90; 3-NO ₂ , 4.60; 3-NH ₂ , 5.79; 3-OMe, 5.59
9.	<i>pK</i> _a , 4-substituted benzoic acids in 44.1% w/w aq. EtOH at 25°C ^d ; $\sigma_{IX} = 0.30$: Ac, 5.09; CO ₂ Et, 5.00; PhC ₂ , 5.47; OEt, 6.04; OMe, 6.03; NHAc, 5.81 Bz, 5.05; CO ₂ H, ^e 5.20; CO ₂ Me, ^f 5.07; HCONH, 5.65; C ₂ H, ^g 5.410;
10.	<i>pK</i> _a , 4-substituted benzoic acids in 80% w/w aq. MCS, 25°C ^d ; $\sigma_{IX} = 0.30$: OEt, 7.08; OMe, 7.03; NHAc, 6.84; Bz, 5.95; CO ₂ H, 5.93; HCONH, 6.70

Data for set 8 are taken from Ref. 31.

^a Percent w/w, *M*_{OH}.

^b Values interpolated from smooth curve drawn through plot of mole percent versus *M*_{OH}.

^c Values calculated assuming solution density 1.00 (mole percent, *M*_{OH}).

^d Footnote *b*, Table 25, unless otherwise indicated.

^e Includes statistical factor 1/2.

^f E. Z. Katsnelson, Ch. S. Frankovskii, and G. M. Timofeeva, *Zh. Org. Khim.*, 6, 1892 (1970).

^g J. A. Landgrebe and R. H. Rynbrandt, *J. Org. Chem.*, 31, 2585 (1966).

set. A convenient isocalized set consists of those groups for which $\sigma_I = 0.30 \pm 0.03$. We may now correlate *pK*_a values of 4-substituted benzoic acids bearing isocalized substituents with the equation

$$Q_X = D\sigma_R + h' \quad (98)$$

which is obtained from Equation 88 by setting σ_I equal to the constant *C*_I. Then,

$$h' = L C_I + h \quad (99)$$

Only those *pK*_a values that have not been used to calculate σ_R values are acceptable in the set. Sufficient data are extant for two such sets. The data are given in Table 31, the correlations in Table 30 (sets 9, 10). The results obtained are highly significant (99.9% CL) and would undoubtedly have given even better results had the data been determined in the same laboratories under exactly the same conditions. It is also encouraging to compare the *D* values obtained from correlation by Equation 98 with those obtained from correlation with Equation 88

Set	Values of $-D$		Values of $-L$	
	Eq. 88	Eq. 98	Eq. 88	Eq. 98
4	1.36	1.30	1.69	1.60
8	1.75	1.63	1.62	1.50

The differences in D are not significant. From Equation 99 values of L may be calculated. These values are compared above with those resulting from correlation with Equation 88. Again, the values are not significantly different. We conclude that the correlations with Equation 98 support the validity of the σ_R constants and indicate that they are correctly scaled.

F. Variation of the σ_R Constants with Structure

The σ_R values for alkyl groups are constant within experimental error. The σ_R values of groups AkW where Ak is an alkyl group and W is O, O₂P(O), CO, OC(O), and 4-C₆H₄ are also constant. Values of $\sigma_{R,AkW}$ are reported in Table 32. They may be used to predict σ_R constants for many groups for which experimental data are unavailable.

G. The σ_R^0 Constants

When the σ_R^0 and σ_R constants reported by Ehrenson, Brownlee, and Taft are compared with each other it is immediately apparent that the values are the same for delocalized effect acceptor groups and for delocalized effect donor groups other than oxa, aza, and F. If this is indeed the case, we can readily place the σ_R^0 constants on the same scale as the σ_R constants by correlating data for

TABLE 32
Mean Values of $\sigma_{R,AkW}$

Substituent Type	$\bar{\sigma}_R^a$	S^b	n^c	$\sigma_{R,AkW}^d$
Ak	-0.161	0.0209	9	-0.16
AkO	-0.570	0.0300	5	-0.57
(AkO) ₂ PO	0.263	0.0208	3	0.26
AkCO	0.183	0.0153	3	0.18
CO ₂ Ak	0.100	0.	2	0.11
4-AkC ₆ H ₄	-0.105	0.0238	4	-0.11

^a Mean value of σ_R .

^b Standard error of the mean.

^c Number of σ_R values used to determine the mean

^d Best value of σ_R for substituent type.

sets of the type XG_1G_2Y with σ_I and σ_R , assuming that for substituents other than oxa, ($-\text{OZ}$), aza(NZ^1Z^2), F, SR,

$$\sigma_R^0 \equiv \sigma_R \quad (100)$$

and choosing G_1 as a π -bonded part and G_2 as an insulating part of the skeletal group G. Typical G_2 groups are CH_2 , CH_2CH_2 , CH_2CMe_2 . A number of correlations of rate and equilibrium data for sets of this type have been carried out with the equation

$$Q_X = L \sigma_{IX} + D \sigma_{RX}^0 + h \quad (101)$$

The data used are presented in Table 33, results of correlations in Table 34. The results obtained are generally excellent and confirm the validity of Equation 100. Substituents that obey Equation 100 include Me, Et, *i*-Pr, *t*-Bu, Ph, Cl, Br, I, cC_3H_5 , Ac, NO_2 , CN, SO_2Me , and H. Although generalization from so small a collection of substituents is dangerous, it seems likely that for groups with $\sigma_R > -0.30$, Equation 100 is obeyed.

Values of σ_R^0 for oxa, aza, F, and SMe groups may now be calculated from the correlation equations reported in Table 34; the constants are given in Table 35. It should be noted that for AkW groups in Table 32 for which W is *not* oxa, aza, or thia, average σ_R values are available. They are, of course, according to Equation 100 equal to the average σ_R^0 values. Thus, a large number of σ_R^0 values are actually available. The applicability of those σ_R^0 values which are not identical to σ_R to dipolar aprotic and nonpolar media and to gas phase data is unknown since no chemical reactivity data sets are available for examination.

H. The σ_R^+ Constants

From our previous discussion it seemed quite likely that delocalized effect acceptor groups should obey the equation

$$\sigma_R^+ \equiv \sigma_R \quad (102)$$

It seemed possible that those delocalized effect donor groups for which $\sigma_R < 0.20$ would also obey Equation 102. If this is the case we may again properly scale our σ_R^+ constants by correlations involving suitable data sets with those σ_R^+ values that are obtainable from Equation 102. We therefore examined the correlation of rates of solvolysis of 4-substituted cumyl chlorides with the equation

$$Q_X = L \sigma_{IX} + D \sigma_R^+ + h \quad (103)$$

If the substituents in the set are restricted to H, Me, Et, Pr, I, C_2H_5 , CO_2Me , CO_2H , CO_2Et , NO_2 , CN, SiMe_3 , an excellent correlation is obtained. The data

TABLE 33
Data Used in Correlations with Equation 101

1.	pK_a , thermodynamic, 4- $\text{XC}_6\text{H}_4\text{CH}_2\text{CO}_2\text{H}$ in 10% v/v aq. EtOH at 25° a: H, 4.50; Me, 4.57; CN, 4.11; NHCHO, 4.42; NHAc, 4.44; NO ₂ , 4.05; OMe, 4.55; OPh, 4.50; F, 4.43; Cl, 4.37; Br, 4.36; I, 4.36
2.	pK_a , thermodynamic, 4- $\text{XC}_6\text{H}_4\text{CH}_2\text{CO}_2\text{H}$ in 50% v/v aq. EtOH at 25° a: H, 5.47; Me, 5.56; <i>i</i> -Pr, 5.60; <i>t</i> -Bu, 5.60; <i>t</i> -BuCH ₂ , 5.61; CN, 4.95; NH ₂ , 5.61; NMe ₂ , 5.63; NHCHO, 5.36; NHAc, 5.43; NO ₂ , 4.86; OMe, 5.53; OPh, 5.44; F, 5.36; Cl, 5.28; Br, 5.28; I, 5.25
3.	pK_a , thermodynamic, 4- $\text{XC}_6\text{H}_4\text{CH}_2\text{CO}_2\text{H}$ in 75% v/v aq. EtOH at 25° a: H, 6.20; Me, 6.32; <i>i</i> -Pr, 6.32; <i>t</i> -Bu, 6.32; <i>t</i> -BuCH ₂ , 6.31; CN, 5.58; NH ₂ , 6.39; NMe ₂ , 6.39; NHCHO, 6.12; NHAc, 6.18; NO ₂ , 5.51; OMe, 6.30; OPh, 6.16; F, 6.06; Cl, 5.95; Br, 5.96; I, 5.95
4.	10^3kr , 4- $\text{XC}_6\text{H}_4\text{CH}_2\text{OBz} + \text{OH}^-$ in 70% v/v aq. MeAc at 25° b: H, 6.74; Me, 5.13; Et, 5.02; <i>i</i> -Pr, 4.88; <i>t</i> -Bu, 4.56; NO ₂ , 43.2; CN, 33.9; SOMe, 24.7; SO ₂ Me, 36.8; Br, 13.2; Cl, 12.8; Ph, 7.35; MeS, 7.57
5.	10^2kr , 4- $\text{XC}_6\text{H}_3\text{CH}_2\text{CO}_2\text{Et} + \text{OH}^-$ in 60% v/v aq. MeAc at 25° c: Me, 3.30; Et, 3.26; <i>i</i> -Pr, 3.80; <i>t</i> -Bu, 2.96; Ph, 4.78; Cl, 8.23; Br, 8.7; H, 4.36; Ac, 13.2; NO ₂ , 27.0
6.	kr , 4- $\text{XC}_6\text{H}_4\text{CH}_2\text{CO}_2\text{H} + \text{Ph}_2\text{CN}_2$ in EtOH at 26.05° d: Me, 0.76; MeO, 0.75; H, 0.81; Cl, 1.05; Br, 1.08; I, 1.10; NO ₂ , 1.53
7.	pK_a , 4- $\text{XC}_6\text{H}_4\text{CH}_2\text{CO}_2\text{H}$ in 50% v/v aq. EtOH at 25° e: H, 5.63; Et, 5.78; Me, 5.74; <i>c</i> -C ₃ H ₅ , 5.72; NO ₂ , 5.01; Br, 5.38
8.	$\log K_e$, 4- $\text{XC}_6\text{H}_4\text{CH}_2\text{NHC}_6\text{H}_3-2, 4'-(\text{NO}_2)_2$ in aq. H ₂ SO ₄ at 25° f: H, 4.90; Br, 5.28; Cl, 5.29; CN, 6.10; F, 4.99; Me, 4.70; NO ₂ , 6.23; OMe, 4.51
9.	kr , 4- $\text{XC}_6\text{H}_4\text{CH}_2\text{NH}_2 + 1\text{-Cl-2,4:C}_6\text{H}_3(\text{NO}_2)_2$ in azeotropic EtOH at 45° g: H, 18.8; Br, 11.6; Cl, 11.0; CN, 5.9; F, 14.4; OMe, 25.4; Me, 23.3; NO ₂ , 5.4
10.	pK_a , 4- $\text{XC}_6\text{H}_4\text{CH}_2\text{CO}_2\text{H}$ in H ₂ O at 25° h: H, 4.3074; Me, 4.370; Et, 4.373; <i>i</i> -Pr, 4.391; <i>t</i> -Bu, 4.417; F, 4.246; Cl, 4.190; Br, 4.188; I, 4.178; OMe, 4.361; NO ₂ , 3.851
11.	pK_a , 4- $\text{XC}_6\text{H}_4\text{CH}_2\text{NMe}_2\text{H}^+$ in 50% w/w aq. MeOH at 25° i: Me, 8.33; H, 8.20; F, 7.96; Br, 7.76; Cl, 7.80; CN, 7.18; NO ₂ , 7.04
12.	pK_a , 4- $\text{XC}_6\text{H}_4\text{CMe}_2\text{CH}_2\text{CO}_2\text{H}$ in 50% v/v aq. EtOH at 25° j: H, 6.26; NO ₂ , 5.90; CN, 5.95; Me, 6.31; <i>t</i> -Bu, 6.31; Cl, 6.16; NH ₂ , 6.33; NHAc, 6.20; OMe, 6.28; F, 6.19
13.	pK_a , 4- $\text{XC}_6\text{H}_4\text{CH}_2\text{NH}_3^+$ in H ₂ O at 25° k: H, 9.38; Br, 9.13; Cl, 9.14; CN, 8.52; F, 9.30; Me, 9.54; MeO, 9.51; NO ₂ , 8.50
14.	10^2kr , 4- $\text{XC}_6\text{H}_4\text{CH}_2\text{OAc} + \text{OH}^-$ in 56% w/w aq. MeAc at 25° l: H, 69.0; F, 90.0; Cl, 106.8; Br, 103.2; I, 103.7; CN, 197.0; <i>i</i> -Pr, 35.8; MeO, 49.9; Me, 48.76; NO ₂ , 266.0
15.	10^3kr , 4- $\text{XC}_6\text{H}_4\text{CH}_2\text{CO}_2\text{Et} + \text{OH}^-$ in 84.5% w/w aq. EtOH at 24.8° m: H, 9.20; F, 17.0; Cl, 22.2; Br, 23.9; I, 23.2; NO ₂ , 71.5; Me, 7.48; <i>t</i> -Bu, 8.12; MeO, 8.10; NH ₂ , 4.59; NMe ₃ ⁺ , 69.5
16.	10^3Kr , 4- $\text{XC}_6\text{H}_4\text{CH}_2\text{CO}_2\text{Et} + \text{OH}^-$ in 60% w/w aq. EtOH at 24.8° m: H, 21.6; Cl, 49.3; I, 47.6; NO ₂ , 160.; Me, 17.5; <i>t</i> -Bu, 17.0
17.	10^2kr , 4-XPnCH ₂ CO ₂ Et + OH ⁻ in 56% w/w aq. MeAc at 25° n: H, 4.48; Me, 3.18; OMe, 3.93; F, 6.96; Cl, 9.71; Br, 10.10; Ac, 13.0; NO ₂ , 26.2; <i>t</i> -Bu, 2.19; NMe ₂ , 2.58; NH ₂ , 3.11; Ph, 4.95; I, 6.89; CN, 21.7; NMe ₃ ⁺ I ⁻ , 51.7
18.	kr , 4-XPnCH ₂ CH ₂ CO ₂ Et + OH ⁻ in 87.8% v/v aq. EtOH at 30° o: H, 5.98; Me ₃ N ⁺ , 20.7; NO ₂ , 19.2; Cl, 9.20; F, 8.02; MeO, 4.99; Me, 4.98; OEt, 4.87; NH ₂ , 3.69; Me ₂ N, 4.04

used are set forth in Table 36; results of the correlation in Table 37. In defining σ_R^+ constants we must choose our scale. In the traditional definition of σ_P^+ constants this choice was made by correlating the data with σ_m values. Inherent in this method are certain assumptions:

$$\sigma_m = \sigma_m^+ \quad (104)$$

$$\rho_m = \rho_p \quad (105)$$

In applying the separation of electrical effects to the Hammett equation written for use with σ_P^+ constants

$$Q_X = \rho \sigma_{PX}^+ + h \quad (106)$$

we obtain from Equation 2 and 106

$$Q = \rho_\lambda \sigma_{IX} + \rho \delta \sigma_{RX}^+ + h \quad (107)$$

which is equivalent to Equation 103.

Thus, if the value of D is larger than the value of L , as is the case in cumyl chloride solvolysis, this has been traditionally accounted for by a corresponding increase in δ . The same result can be achieved however, (in terms of defining a useful scale of σ_R^+ constants) by simply setting $\lambda_p = \delta_p = 1$, and allowing the increased electronic demand of an electronically deficient active site to be accounted for by an increased value of D . This is the method which we have used. The resulting constants are set forth in Table 38.

The results of the correlations show that the H, Me₃Si, CO₂H, CO₂Me,

^a A. J. Hoefnagel and B. M. Wepster, *J. Am. Chem. Soc.*, **95**, 5357 (1973).

^b Y. Yukawa, T. Tsuno, and M. Sawada, *Bull. Chem. Soc. Japan*, **45**, 1198 (1972).

^c Y. Yukawa, Y. Tsuno, and M. Sawada, *Bull. Chem. Soc., Japan* **39**, 2274 (1966).

^d R. M. O'Ferrall and S. I. Miller, *J. Am. Chem. Soc.*, **85**, 2440 (1963).

^e Y. Kusuyama and Y. Ikeda, *Bull. Chem. Soc. Japan*, **46**, 204 (1973).

^f A. Fischer, M. P. Hartshorn, U. M. Senanayake, and J. Vaughan, *J. Chem. Soc. B*, 833 (1967).

^g A. Fischer, R. S. H. Hickford, G. R. Scott and J. Vaughan, *J. Chem. Soc. B*, 466 (1966).

^h Footnote d, Table 8.

ⁱ D. G. Lee and R. Srinivasan, *Can. J. Chem.*, **51**, 2542 (1973).

^j A. J. Hoefnagel, J. C. Monshouwer, E. C. G. Snorn, and B. M. Wepster, *J. Am. Chem. Soc.*, **95**, 5350 (1973).

^k L. F. Blackwell, A. Fischer, I. J. Miller, R. D. Topsom, and J. Vaughan, *J. Chem. Soc.*, 3588 (1964).

^l E. Tommila and C. N. Hinshelwood, *J. Chem. Soc.*, 1801 (1938); E. Tommila, *Ann. Acad. Sci. Fennicae Ser. A*, **59**, No. 4,3 (1942) [CAS 38,6172^a (1942)].

^m J. G. Watkinson, W. Watson, and B. L. Yates, *J. Chem. Soc.*, 5437 (1963).

ⁿ R. O. C. Norman and P. D. Ralph, *J. Chem. Soc.*, 5431 (1963); R. O. C. Norman, G. K. Radda, D. A. Brimacombe, P. D. Ralph, and E. M. Smith, *J. Chem. Soc.*, 3247 (1961).

^o R. Fuchs and J. A. Caputo, *J. Org. Chem.*, **31**, 1524 (1966).

TABLE 34
 Results of Correlations with Equation 101

Set	$-L$	$-D$	h	R^a	F^b	r_{12}^c	s_{est}^c	s_L^d
1	0.568	0.573	4.49	0.9988	805.3	0.208	0.0116	0.0180
2	0.800	0.738	5.47	0.9983	1013.	0.342	0.0182	0.0229
3	0.915	0.781	6.19	0.9990	1832.	0.342	0.0152	0.0191
4	-1.06	-0.893	0.836	0.9994	3943.	0.494	0.0141	0.0171
5	-1.03	-0.814	0.651	0.9979	833.6	0.212	0.0230	0.0307
6	-0.369	-0.222	-0.0847	0.9965	214.9	0.049	0.0117	0.0189
7	0.866	0.574	5.65	0.9966	221.5	0.360	0.0316	0.0500
8	-1.68	-1.77	4.95	0.9978	344.7	0.224	0.0530	0.0828
9	0.753	0.539	1.272	0.9974	291.2	0.234	0.0237	0.0372
10	0.551	0.624	4.290	0.9974	585.8	0.145	0.0146	0.0189
11	1.49	1.25	8.16	0.9980	373.4	0.224	0.0427	0.0667
12	0.435	0.450	6.24	0.9973	281.8	0.480	0.0171	0.0271
13	1.15	1.28	9.35	0.9951	151.9	0.224	0.0555	0.0868
14	-0.866	-0.712	1.775	0.9820	67.41	0.261	0.0648	0.0910
15	-1.16	-0.662	0.997	0.9971	348.9	0.122	0.0325	0.0471
16	-1.13	-0.753	1.360	0.9989	662.4	0.274	0.0231	0.0360
17	-1.15	-0.790	0.604	0.9847	111.8	0.223	0.0691	0.0921
18	-0.700	-0.641	0.774	0.9915	144.5	0.071	0.0361	0.0544

Set	s_D^d	s_h^d	$100r^2$	n^f	P_R	Error
1	0.0323	0.00893	99.75	7	50.2	3.3
2	0.0504	0.0112	99.66	10	48.0	3.7
3	0.0422	0.00933	99.81	10	46.0	2.8
4	0.0370	0.00793	99.89	12	45.7	2.1
5	0.0527	0.0114	99.58	10	44.1	3.2
6	0.0371 ^h	0.00922 ^h	99.31	6	37.8	6.8
7	0.116 ⁱ	0.0222	99.33	6	39.9	8.8
8	0.152 ^h	0.0409 ^h	99.57	6	51.3	5.1
9	0.0761 ^h	0.0183	99.49	6	41.7	6.5
10	0.0459	0.00929	99.49	9	53.1	4.5
11	0.122 ^h	0.0330	99.60	6	45.6	5.0
12	0.0591 ^h	0.0124	99.47	6	50.8	7.7
13	0.159 ^h	0.0429	99.02	6	52.7	7.6
14	0.181 ⁱ	0.0446	96.42	8	45.1	12.8
15	0.102 ^h	0.0234	99.43	7	36.3	6.0
16	0.0819 ^h	0.0172	99.77	6	40.0	4.7
17	0.150 ^h	0.0385	96.96	10	40.7	8.6
18	0.0630	0.0266	98.30	8	47.8	5.6

For footnotes, see Table 26.

CO₂Et, CN, NO₂, Me, Et, *i*-Pr, I, CH=CH₂, Pr, Bz, PhCH₂, CONH₂, PhC₂, SO₂Me, *c*-C₄H₇, *c*-C₅H₉, and *c*-C₆H₁₁ groups obey Equation 102. We have observed only one alkyl group, *t*-Bu, and two delocalized effect electron acceptor groups, Ac, and CF₃, which definitely do *not* obey Equation 102. We consider

TABLE 35
Values^a of σ_R°

X	σ_R°	Error ^b	pK_a^c or $\log kr$	Set ^d
Aza				
NH ₂	-0.42	0.040,0.036	5.61;6.39	2,3
NHCHO	-0.24	0.032,0.036,0.032	4.42,5.36,6.12	1,2,3
NHAc	-0.25	0.029,0.035,0.030	4.44,5.43,6.18	1,2,3
NMe ₂	-0.44	0.042,0.037	5.63,6.39	2,3
Oxa				
OH	-0.46	0.044,0.051,0.049	4.59,5.59,6.39	1,2,3
OMe	-0.44	0.042,0.048,0.045	4.55,5.53,6.30	1,2,3
OEt	-0.44	0.086	0.688	18
OPh	-0.42	0.039,0.043,0.037	4.50,5.44,6.16	1,2,3
Other				
F	-0.44	0.040,0.046,0.038	4.43,5.36,6.06	1,2,3
MeS	-0.31	0.024	0.879	4
NMe ₃ ⁺	-0.32	U	1.316	18

^a These values are for those substituents that do not obey Eq. 100. When no value for error is given in the reference from which the data were taken, and a pK_a or $\log kr$ value used to calculate a new σ constant is from the same source as the data that were used to obtain the correlation equation, the value of s_{est} obtained from the regression analysis is used as the best estimate of the error in pK_a or $\log kr$.

^b Estimated from Eq. 89.

^c From which the substituent constant was calculated.

^d The set of Table 34 from which the L , D , and h values required for calculation of σ_R° were taken. The pK_a and $\log kr$ values used to calculate σ_R° values were all taken from the sources given for the corresponding sets in Table 33.

a group with a value of Δ_D , defined as

$$\Delta_D \equiv \sigma_D - \sigma_R \quad (108)$$

of ≤ 0.03 , to obey Equation 102. The values of Δ for *t*-Bu and CF₃ are 0.04 and 0.05, respectively, for Ac, -0.14. Thus *t*-Bu and CF₃ show barely significant deviations from Equation 102. A large negative value of Δ (≥ -0.10) is also observed for MeSO, NHAc, NMe₂, NH₂, 4-BrC₆H₄, 4-ClC₆H₄, MeS, 3-, and 4-O₂NC₆H₄, and styryl. Large positive Δ values are observed for NHBz, F, and CH₂SO₂Ph. The remaining groups show small values of Δ . A positive value of Δ indicates that the substituent is less effective as an electron donor relative to those groups that obey Equation 102. A negative value of Δ indicates that a group is a more effective electron donor relative to those groups that obey Equation 102. On the basis of our admittedly limited results we suggest that alkyl groups and delocalized effect electron acceptor groups should generally obey

TABLE 36
Data used in Correlations with Eq. 103

1. kr , 4-XC₆H₄CMe₂Cl + H₂O in 90% aq. MeAc at 25°^a:
H, 12.4; Me₃Si, 10.0; CO₂H, 0.154; CO₂Me, 0.0750; CO₂Et, 0.0806; CN, 0.0126; NO₂, 0.00319; Me, 322.; Et, 273.; *i*-Pr, 233.; I, 3.03; Vi, 62.5
2. $krel$, 4-XC₆H₃SiMe₃ in H₂SO₄-H₂O-AcOH at 50.18°^b:
NO₂, 0.000122; NMe₃⁺, 0.000384; CO₂H, 0.00148; Br, 0.104; I, 0.165; Cl, 0.190; F, 0.95; H, 1.00; Ph, 2.83; Me, 18.0; MeO, 1010.; Me₃SiCH₂, 202.
3. 10⁴ kr , 4-XC₆H₄CONHCl rearrangement in water at 30°^c:
MeO, 67.4; EtO, 70.9; Me, 23.64; Et, 23.00; H, 8.045; F, 4.297; Cl, 2.428; Br, 2.219; NO₂, 0.1218
4. ΔG^\ddagger , internal rotation, 4-XC₆H₄+CHOH, 25°^d:
Me, 67.36; Et, 66.32; *i*-Pr, 66.07; *t*-Bu, 65.73; F, 64.73; Ph, 62.89; Cl, 60.76; Br, 60.59; CF₃, 49.50; H, 61.30
5. pK_a , 4-XC₅H₄NH⁺ in water at 25°^e:
H, 5.21; Me, 6.03; Et, 6.03; Pr, 6.05; *i*-Pr, 6.04; MeO, 6.58; NH₂, 9.12; Cl, 3.83; Br, 3.75; Bz, 3.35; CN, 1.86; NO₂, 1.39; PhCH₂, 5.59; Ph, 5.35; Ac, 3.51; CO₂Me, 3.49
6. 10⁴ kr , 4-XC₅H₄N + EtI in PhNO₂ at 60°^f:
H, 3.15; Me, 6.65; NH₂, 50.7; MeO, 8.20; CN, 0.107; Bz, 0.755; PhCH₂, 4.46; *i*-Pr, 6.02; Ph, 3.45; Ac, 0.740
7. pK_a , 4-XC₅H₄NH⁺ in water at 25°^h:
Ac, 3.58; NH₂, 9.19; Br, 3.96; Cl, 4.09; CN, 2.14; Me, 5.88; H, 5.35
8. pK_a , 4-XC₅H₄NH⁺ in water at 25°^h:
H, 5.14; Me, 5.95; Br, 3.74; Cl, 3.79; CONH₂, 3.43; CO₂Et, 3.30; CN, 1.83
9. pK_a , 4-XC₅H₄NH⁺ in water at 20°ⁱ:
H, 5.278; NH₂, 9.2524; Me, 6.10; MeO, 6.62; NO₂, 1.61; SMe, 5.97; SO₃Me, 1.62
10. pK_a , 4-XC₅H₄NH⁺ in water at 25°ⁱ:
H, 5.229; NH₂, 9.1141; Me, 6.03; MeO, 6.58; Br, 3.68; CN, 1.48; NO₂, 1.23; Cl, 3.83; Ac, 3.505
11. pK_a , 4-XC₅H₄NH⁺ in 9.0 mole% aq MeOH at 25°^h:
H, 4.92; Me, 5.72; Br, 3.55; Cl, 3.58; HOCH₂, 5.14; CONH₂, 3.24; CO₂Et, 3.10; CN, 1.66
12. pK_a , 4-XC₅H₄NH⁺ in 19.4 mole % aq. MeOH at 25°^h:
H, 4.59; Me, 5.45; Br, 3.24; Cl, 3.28; HOCH₂, 4.87; CONH₂, 7.95; CO₂Et, 2.78; CN, 1.41
13. pK_a , 4-XC₅H₄NH⁺ in 27.2 mole % aq. MeOH at 25°^h:
H, 4.37; Me, 5.20; Br, 2.99; Cl, 3.04; HOCH₂, 4.63; CONH₂, 2.73; CO₂Et, 2.55; CN, 1.24
14. pK_a , 4-XC₅H₄NH⁺ in 36.0 mole % aq. MeOH at 25°^h:
H, 4.14; Me, 4.96; Br, 2.71; Cl, 2.75; HOCH₂, 4.46; CONH₂, 2.59; CO₂Et, 2.32; CN, 1.10
15. pK_a , 4-XC₅H₄NH⁺ in 51.1 mole % aq. MeOH at 25°^h:
H, 3.81; Me, 4.61; Br, 2.40; Cl, 2.44; HOCH₂, 4.17; CONH₂, 2.31; CO₂Et, 2.03; CN, 0.9
16. pK_a , 4-XC₅H₄NH⁺ in 69.2 mole % aq. MeOH at 25°^h:
H, 3.63; Me, 4.43; Br, 2.22; Cl, 2.23; HOCH₂, 4.04; CONH₂, 2.21; CO₂Et, 1.96
17. kr , 4-XC₅H₄N + *n*-C₁₂H₂₅Br in DMF at 50°^j:
NH₂, 6.76; Me, 5.05; Et, 4.85; H, 2.94; Bz, 2.17; CO₂Me, 1.76; CO₂Et, 1.52; CN, 1.29
18. 10⁵ kr , 4-XC₅H₄N + *n*-C₁₂H₂₅Br in MeOH at 50°^j:
NH₂, 3.03; Me, 0.874; Et, 0.847; H, 0.500; Bz, 0.339; CO₂Me, 0.384; CO₂Et, 0.329; CN, 0.253

TABLE 36
Data used in Correlations with Eq. 103

-
19. 10^5 *kr*, 4- $\text{XC}_5\text{H}_4\text{N}$ + *n*- $\text{C}_{12}\text{H}_{25}\text{Br}$ in Me OH at 75°^j:
NH₂, 27.4; Me, 8.82; Et, 9.02; H, 5.65; Bz, 4.23; CO₂Me, 4.54; CO₂Et, 3.86; CN, 2.72
20. 10^5 *kr*, 4- $\text{XC}_5\text{H}_4\text{N}$ + *n*- $\text{C}_{12}\text{H}_{25}\text{Br}$ in MeOH at 100°^j:
NH₂, 194.; Me, 61.3; Et, 67.4; H, 48.3; Bz, 37.8; CO₂Me, 35.9; CO₂Et, 29.4; CN, 21.9
21. $\delta\Delta G_i^\ddagger$, 4- $\text{XC}_5\text{H}_4\text{N}$ proton affinity, gas phase^k:
NMe₂, 14.6; OMe, 6.7; Me, 4.0; H, 0; Cl, -3.1; CF₃, -7.8; CN, -10.5
22. 10^{-3} *kr*, deprotonation of 4- $\text{XC}_5\text{H}_4\text{NH}^+$ in strongly acid aqueous solution^l:
NMe₂, 0.008156; NH₂, 0.0131; *t*-Bu, 3.42; Me, 3.07; H, 32.0; Cl, 563.; Br, 528.; CO₂H, 1570.; CO₂Me, 1230.; CN, 71900.
23. $-\text{p}K_a$, 4- $\text{XC}_6\text{H}_4\text{-C}(\text{OH})_2$ in H₂SO₄^m:
OEt, 4.36; *t*-Bu, 4.48; Me, 4.52; *i*-Pr, 4.52; Ph, 4.65; H, 4.70; F, 4.92; Cl, 4.97; I, 4.95; CF₃, 5.34
24. $-\text{p}K_a$, 4- $\text{XC}_6\text{H}_4\text{-C-PhOH}$ in aq. H₂SO₄ⁿ:
OEt, 5.48; OMe, 5.48; Me, 5.77; H, 6.11; F, 6.04; I, 6.23; Cl, 6.27; Br, 6.37; CN, 6.81; NO₂, 7.02
25. *kr*, 9-(4'- XC_6H_4)-9,10-dimethylphenanthronium ion rearrangement in 1:10 HSO₃F-SO₂FCI at -50°^o:
H, 25.; Me, 40.; MeO, 10000.; Cl, 0.63; F, 25.; CF₃, 0.0032
26. $\text{p}K_{R^+}$, 4-substituted malachite green^p:
H, 7.07; Me₃N⁺, 6.15; NO₂, 6.00; Cl, 6.80; OMe, 7.87; OH, 8.06; Me₂N, 9.46; F, 7.15; Br, 6.82; I, 6.89; Me, 7.32
-

^a L. M. Stock and H. C. Brown, *Adv. Phys. Org. Chem.*, **1**, 35 (1963).

^b F. B. Deans, and C. Eaborn, *J. Chem. Soc.*, 2299 (1959).

^c T. Imamoto, Y. Tsuno, and Y. Yukawa, *Bull. Chem. Soc. Japan*, **44**, 1639 (1971).

^d J. M. Sommer, R. P. Post, and T. Drakenberg, *J. Mag. Res.* **21**, 93 (1976).

^e A. Fischer, W. J. Galloway, and J. Vaughan, *J. Chem. Soc.*, 3591 (1964).

^f A. Fischer, W. J. Galloway, and J. Vaughan, *J. Chem. Soc.*, 3596 (1964).

^g M. R. Chakrabarty, C. S. Handloser, and M. W. Mosher, *J. Chem. Soc. Perkin Trans. II*, 938 (1973).

^h C. Tissier and M. Tissier, *C. R. Acad. Sci. Paris*, **281**, 749 (1975).

ⁱ Footnotes *f* and *p*, Table 7; footnote *n*, Table 23; A. Albert and G. B. Barlin, *J. Chem. Soc.*, 238 (1959); A. Albert and J. N. Philips, *J. Chem. Soc.*, 1294 (1956); G. B. Barlin and W. V. Brown, *J. Chem. Soc. B*, 1435 (1968); J. M. Essery and K. Schofield, *J. Chem. Soc.*, 2225 (1963); R. W. Green, *Aust. J. Chem.*, **22**, 721 (1969); H. H. Perkampus and O. Prescher, *Ber. Bunsenges. Phys. Chem.*, **72**, 429 (1968).

^j K. Murai, S. Takeuchi, and C. Kimura, *Nippon Kagaku Kaishi*, 75 (1973).

^k E. M. Arnett, B. Chawla, L. Bell, M. Taagepera, W. J. Hehre, and R. W. Taft, *J. Am. Chem. Soc.*, **99**, 5729 (1977).

^l J. J. Delpuech and G. Serratrice, *Bull. Soc. Chim. Fr.*, 2500 (1974).

^m R. I. Zalewski, *Bull. Acad. Pol. Sci.*, **20**, 853 (1972).

ⁿ J. Mindl and M. Vecera, *Collect. Czech. Chem. Commun.*, **35**, 950 (1970).

^o V. G. Shubin, D. V. Korchagina, B. G. Derenbyaev, G. I. Borodkin, and V. A. Koptyug, *Zhur. Org. Khim.*, **9**, 1041 (1973).

^p H. H. Freedman, *Carbonium Ions*, G. A. Olah and P. v. R. Schleyer (Eds.), Vol. IV, Wiley, New York, 1973, p. 1501.

TABLE 37
Results of Correlation with Eq. 103

Set	$-L$	$-D$	h	R^a	F^b	r_{12}^c	s_{est}^d	s_L^d
1	4.64	7.22	1.257	0.9982	1282.	0.421	0.117	0.154
2	4.83	7.21	-0.102	0.9954	428.1	0.058	0.218	0.285
3	2.35	2.44	0.9508	0.9990	1494.	0.021	0.0452	0.0619
4	15.9	3.34	61.07	0.9893	160.5	0.247	0.862	1.24
5	5.17	4.23	5.33	0.9976	1158.	0.218	0.124	0.145
6	2.27	1.42	0.572	0.9938	279.7	0.106	0.0917	0.163
7	4.62	4.32	5.25	0.9991	1117.	0.205	0.117	0.207
8	5.04	4.59	5.19	0.9983	586.9	0.004	0.0951	0.169
9	5.14	4.33	5.29	0.9989	908.0	0.322	0.158	0.257
10	5.44	4.41	5.28	0.9981	775.0	0.308	0.180	0.278
11	4.99	4.55	4.98	0.9986	865.3	0.088	0.0838	0.143
12	4.97	4.56	4.68	0.9989	1130.	0.088	0.0732	0.125
13	4.93	4.44	4.45	0.9993	1705.	0.088	0.0588	0.100
14	4.94	4.16	4.25	0.9985	825.6	0.088	0.0834	0.142
15	4.82	3.99	3.93	0.9976	519.6	0.088	0.102	0.174
16	4.84	3.74	3.80	0.9933	148.6	0.166	1.46	0.298
17	0.435	1.27	0.502	0.9961	315.6	0.279	0.0581	0.111 ⁱ
18	0.541	0.728	0.219	0.9920	153.5	0.279	0.0525	0.0995 ^h
19	0.527	0.636	0.829	0.9896	118.0	0.279	0.0533	0.101 ^h
20	0.493	0.586	1.720	0.9870	94.47	0.279	0.0551	0.105 ^h
21	16.2	14.4	0.803	0.9944	175.7	0.227	1.13	2.08 ^h
22	-5.17	-4.33	1.252	0.9895	164.1	0.211	0.427	0.676
23	-1.12	-1.04	4.70	0.9972	619.4	0.197	0.055	0.0387
24	-1.12	-1.45	6.07	0.9944	308.2	0.183	0.0610	0.0901
25	4.77	7.39	0.427	0.9985	503.6	0.240	0.150	0.292
26	1.25	2.11	7.01	0.9968	473.1	0.224	0.0881	0.134

Set	S_D^d	S_h^d	$100r^{2e}$	n^f	P_R	Error
1	0.299	0.0480	99.65	12	60.9	3.1
2	0.316	0.123 ^k	99.01	11	59.9	3.4
3	0.0609	0.0283	99.80	9	50.9	1.6
4	2.18	0.434	97.87	10	17.4	11.6
5	0.177	0.0540	99.53	14	45.0	2.2
6	0.0806	0.0458	98.76	10	38.5	2.9
7	0.119	0.0814	99.82	7	48.3	1.9
8	0.276	0.0628	99.66	7	47.7	3.3
9	0.149	0.117	99.78	7	45.7	2.1
10	0.167	0.124	99.61	9	44.8	2.2
11	0.234	0.0516	99.71	8	47.7	2.8
12	0.205	0.0450	99.78	8	47.8	2.5
13	0.164	0.0362	99.85	8	47.4	2.0
14	0.233	0.0513	99.70	8	45.7	2.9
15	0.286	0.0628	99.52	8	45.3	3.7
16	0.450 ^h	0.0982	98.67	7	43.6	5.9
17	0.0558	0.0307	99.21	8	74.5	6.3
18	0.0503	0.0295	98.40	8	57.4	6.4

TABLE 37
Results of Correlation with Eq. 103

Set	S_D^d	S_A^d	$100r^{2e}$	n^f	P_R	Error
19	0.0512	0.0300	97.93	8	54.7	6.9
20	0.0529	0.0310	97.42	8	54.3	7.7
21	0.966	0.807 ^k	98.87	7	47.1	4.7
22	0.300	0.241 ^h	97.91	10	45.6	4.8
23	0.0411	0.0131	99.44	10	48.1	2.3
24	0.0769	0.0444	98.88	10	56.4	4.0
25	0.244	0.1068	99.70	6	60.8	2.8
26	0.0797	0.0635	99.37	9	62.8	3.8

For footnotes a-j, see Table 26.

^k 50.0% CL.

Equation 102. Values of Δ are given in Table 38. Certain relationships between Δ and the Pauling electronegativity are observed. Thus, for groups of the type WZ where W is a second period element (O,N,F) and Z is H, Ak, or a lone pair, and for the halogen substituents, the equation

$$\Delta = m\chi + d \quad (109)$$

is obeyed. These results suggest that for second period elements with at least one lone pair, the lower the electronegativity, the more strongly the substituent can function as an electron donor. This is also the case in the halogen substituents, although to a lesser extent as overlap of a p orbital in Cl, Br, and I with a π orbital is less effective than it is in the case of the second period element, F.

Our results confirm the conclusion of Ehrenson, Brownlee, and Taft that pyridinium ions are best correlated by Equation 103. In regard to this point we must consider a recent publication of Johnson, Roberts, and Taylor (49) which claims that the proper treatment of pyridine substituent effects requires the use of the equation

$$\log \left(\frac{k}{k^0} \right) = \rho\sigma \quad (110)$$

for all substituents other than localized and delocalized effect electron acceptor groups (LaDa groups). The latter being represented by the equation

$$\log \left(\frac{k}{k^0} \right) = \rho\sigma_I \quad (111)$$

Equation 110 is simply the Hammett equation in its original form. Equation 111, is the original form of Equation 36. As evidence for this argument they cite the following points: (1) The quantity $\log (k/k^0)_1 / \log (k/k^0)_2$ for ionization of 4-substituted pyridinium ions [1] and 4-substituted quinuclidinium ions [2] with

TABLE 38
Values^a of σ_R^+

X	σ_R^+	Error ^b	$\log k$ or pK^c	Set ^d	Δ (Eq. 108)
Alkyl					
<i>t</i> -Bu	-0.13	0.019	2.250 ^e	1	0.05
<i>c</i> -C ₃ H ₅	-0.27	U	3.190 ^f	1	-0.08
Aryl					
Ph	-0.17	0.019	1.907 ^e	1	-0.06
PhCH=CH	-0.30	U	5.92 ^g	9	
Substituted Alkyl					
CH ₂ OH	-0.15	0.028	5.32 ^f	8	-0.08
CH ₂ CH ₂ OH	-0.15	0.028	5.60 ⁱ	8	
CH ₂ CH ₂ CH ₂ OH	-0.15	U	5.84 ⁱ	8	
CH ₂ SiMe ₃	-0.30	U	3.540 ^j	1	-0.07
CH ₂ CO ₂ Et	-0.08	U	4.86 ^k	9	
CH ₂ SO ₂ Ph	0.01	U	3.75 ^l	9	0.14
Electron Acceptor Groups					
Ac	0.06	0.018	3.51 ^m	5	-0.14
CF ₃	0.15	0.025	-1.686 ^e	1	0.04
Aza					
NH ₂	-1.10	0.050	9.12 ^m	5	-0.30
NHMe	-1.16	0.050	9.65 ⁿ	9	
NMe ₂	-1.22	0.053	9.70 ⁿ	9	-0.34
NHAc	-0.47	0.037	5.87 ^o	9	-0.12
NHBz	-0.34	U	5.32 ^o	9	0.13
Oxa					
OH	-0.64	0.061	8.06 ^p	26	-0.02
OMe	-0.66	0.036	4.620 ^e	1	-0.08
OEt	-0.65	0.040	6.67 ^q	9	-0.08
Thia					
MeS	-0.55	0.030	3.836 ^e	1	-0.17
PhCH ₂ S	-0.36	U	5.41 ^r	9	
Sulfinyl					
MeSO	-0.10	U	2.94 ^s	9	-0.10
Substituted Aryl					
4-BrC ₆ H ₄	-0.14	0.020	1.603 ^{t,z}	1	-0.11

TABLE 38
Values^a of σ_R^+

X	σ_R^+	Error ^b	log <i>k</i> or p <i>K</i> ^c	Set ^d	Δ (Eq. 108)
3-ClC ₆ H ₄	-0.12	0.020	1.398 ^{t,z}	1	-0.06
4-ClC ₆ H ₄	-0.15	0.020	1.642 ^{t,z}	1	-0.12
3-O ₂ NC ₆ H ₄	-0.15	U	4.90 ^u	9	-0.15
4-O ₂ NC ₆ H ₄	-0.18	U	4.87 ^u	9	-0.21
4-MeC ₆ H ₄	-0.20	0.021	2.225 ^{t,z}	1	-0.07
4-MeOC ₆ H ₄	-0.27	0.022	2.677 ^{t,z}	1	-0.08
Ionic					
CO ₂ ⁻	0.06	U	1.702 ^e	1	
NMe ₃ ⁺	-0.31	U	-0.793 ^e	1	-0.28
			6.15 ^p	26	
CH ₂ NMe ₃ ⁺	-0.02	U	3.242	10	
SO ₃ ⁻	0.23	U	3.44 ^w	10	
Other					
F	-0.37	0.026	1.423 ^e	1	0.11
Cl	-0.21	0.028	0.577 ^e	1	0.04
Br	-0.19	0.025	0.412 ^e	1	0.06
CH=NOH	-0.12	U	4.77 ^x	9	
π -Cr((O) ₃ Ph	-0.18	U	1.524 ^y	1	-0.09

^a These values are for those substituents that do not obey Eq. 102.

^b Estimated from Eq. 89.

^c From which the substituent constant was calculated.

^d The set of Table 27 from which the *L*, *D*, and *h* values required for calculation of σ_R^+ were taken.

^e Footnote a, Table 36.

^f Footnote d, Table 27.

^g A. R. Katritzky, D. J. Short, and A. J. Boulton, *J. Chem. Soc.*, 1516 (1960).

^h Footnote h, Table 36.

ⁱ M. Tissier and C. Tissier, *Bull. Soc. Chim. France*, 3155 (1967).

^j M. A. Cook, C. Eaborn, and D. R. M. *J. Organomet. Chem.*, 24, 293 (1970).

^k R. A. Jones and A. R. Katritzky, *Aust. J. Chem.*, 17, 455 (1964).

^l S. Golding, A. R. Katritzky, and H. Z. Kucharska, *J. Chem. Soc.*, 3090 (1965).

^m Footnote e, Table 36.

ⁿ Footnote f, Table 7.

^o R. A. Jones and A. R. Katritzky, *J. Chem. Soc.*, 1317 (1959).

^p Footnote p, Table 36.

^q K. Clarke and K. Rothwell, *J. Chem. Soc.*, 1885 (1960).

^r R. A. Jones and A. R. Katritzky, *J. Chem. Soc.*, 3610 (1958).

^s G. B. Barlin and W. V. Brown, *J. Chem. Soc. B*, 1435 (1968).

^t T. Inukai, *Bull. Chem. Soc. Japan*, 35, 400 (1962).

^u A. R. Katritzky and P. Simmons, *J. Chem. Soc.*, 1511 (1960).

^v R. B. Barlow and J. T. Hamilton, *Brit. J. Pharmacol.*, 18, 510 (1962).

^w R. F. Evans and H. C. Brown, *J. Org. Chem.*, 27, 3127 (1962).

LaDa groups is a constant. (2) the pK_a s of [1] give a linear plot with the pK_a s of [2] when only LaDa groups are considered. The groups involved are NO_2 , SO_2Me , CN , CO_2Me , CO_2Et , Ac . (3) The quantity α defined by the equation

$$\frac{\log (K_{4Ad}/K_H)}{\log (K_{3Ad}/K_H)} = \frac{\sigma_{4Ac}}{\sigma_{3Ac}} = \alpha \quad (112)$$

has a value of 0.95 ± 0.11 . (4) A correlation of pK_a data for [1] with Equation 110 using σ_I constants for LaDa groups and σ_p constants for other groups gave $r = 0.998$, $s_p = 0.12$.

If we consider the σ_R^+ values of the LaDa groups which were studied, they are NO_2 , 0.10; CN , 0.08; SO_2Me , 0.11; CO_2Me , 0.11; CO_2Et , 0.11, Ac , 0.06. The average value of σ_R^+ for these groups is 0.095 with a standard error of 0.0207. Thus, the resonance effect of the groups in question is in fact fairly constant. Then, applying the *LD* equation in the form

$$\log (K_X/K_H) = L\sigma_{IX} + D\sigma_{RX}^+ \quad (113)$$

Since σ_{RX}^+ is constant,

$$\log \left(\frac{K_X}{K_H} \right)_1 = L_1 \sigma_{IX} + c^* \quad (114)$$

Thus,

$$\frac{\log (K_X/K_H)_1}{\log (K_X/K_H)_2} = \frac{L_1 \sigma_{IX} + c^*}{L_2 \sigma_{IX}} \quad (115)$$

$$= \frac{L_1}{L_2} + \frac{c^*}{L_2 \sigma_{IX}} \quad (116)$$

As σ_R^+ is smaller than the σ_{IX} values which range from 0.30 to 0.67 and from Table 37, D_1 with values of -4.2 to -4.6 is less than L_2 for which we have a value of -5.28 (set 36, Table 9), we can write

$$\frac{\log (K_X/K_H)_1}{\log (K_X/K_H)_2} = \frac{L_1 + c^*/\sigma_{IX}}{L_2} = \frac{L_1}{L_2} \quad (117)$$

We find it particularly significant that if the arguments of Johnson, Roberts, and Taylor were correct, the localized effect would be greater in pyridines than in quinuclidines, that is, they state that $L_2/L_1 = 1.19$. We find that L_1 lies in the range -4.6 to -5.4 , varying with temperature and that at 25° the average

^x S. F. Mason, *J. Chem. Soc.*, 22 (1960).

^y S. P. Gobin, V. S. Khandkorova, and A. Z. Kreindlin, *J. Organomet. Chem.*, 64, 229 (1974).

^z The error in $\log kr$ for these points is assumed equal to s_{est} for Eq. 1.

value is -5.22 . This does not differ significantly from the value of L_2 of -5.28 ; thus $L_1/L_2 \cong 1$. If we calculate values of $c^*/L_2\sigma_{IX}$ for the six LaDa groups and add them to the value of L_1/L_2 obtained from the L_1 and L_2 values given previously, the result is 1.19 . This is in complete agreement with the figure reported by Johnson, Roberts, and Taylor. The average value of $c^*/L_2\sigma_{IX}$ is 0.196 with a standard error of 0.073 ; the values range from 0.118 to 0.263 .

The linear relationship between pK_{a_1} and pK_{a_2} is easily understood as from Equations 103 and 36

$$pK_{a_1} = L_1 \sigma_{IX} + D_1 \sigma_{RX^+} + h_1 \quad (118)$$

$$pK_{a_2} = L_2 \sigma_{IX} + h_2 \quad (119)$$

$$\sigma_{IX} = \frac{pK_{a_2} - h_2}{L_2} \quad (120)$$

Then

$$pK_{a_1} = \frac{L_1}{L_2} pK_{a_2} = D_1 \sigma_{RX^+} + h_1 - \frac{h_2}{L_2} \quad (121)$$

or, as σ_{RX^+} is constant,

$$pK_{a_1} = m pK_{a_2} + d \quad (122)$$

We may now combine Equations 112 and 113 to obtain

$$\alpha = \frac{L_1 \sigma_{IX} + D_1 \sigma_{RX^+}}{L_3 \sigma_{IX} + D_3 \sigma_{RX^+}} \quad (123)$$

where L_3 and D_3 are the coefficients obtained from the application of Equation 113 to 3-substituted pyridines. Then letting $D_3 = aD_1$,

$$\alpha = \frac{L_1 \sigma_{IX} + c^*}{L_3 \sigma_{IX} + a c^*} \quad (124)$$

which may be rearranged to

$$(\alpha L_3 - L_1)\sigma_{IX} = c^*(1 - \alpha a) \quad (125)$$

If we let

$$L_1 = \alpha L^* \quad (126)$$

we may obtain

$$\frac{1}{\alpha} = \left(\frac{L_3 - c^*}{c^*} \right) \sigma_{IX} + a \quad (127)$$

As L_3 , c^* , and L^* are all constants, it follows that $1/\alpha$ is linear in σ_{IX} . Thus no conclusion concerning the nature of resonance effects of LaDa groups in pyri-

dines can be reached on the basis of an analysis of α *unless and until* a substituent is examined for which σ_R^+ has been evaluated from reactions other than those of pyridines and has been shown to be significantly different from the σ_R^+ value of 0.095 for the groups cited previously. We would suggest that to be significantly different such a group should have a σ_R^+ value of not less than three times the standard error in σ_R^+ and should be an LaDa group. Thus, we may set a minimum value of σ_R^+ of 0.16. It would be best if the group involved were to have an even higher σ_R^+ value. To minimize experimental difficulties in the determination of pyridinium pK_a values, it would be best to choose a group for which σ_I is about 0.30. Phosphinyl groups which show σ_I values in the range 0.2 to 0.4 and σ_R values in the range 0.2 to 0.3 are likely candidates.

Finally, the results of the correlations for pyridinium pK_a s given in Table 37 are certainly as good as those obtained by Johnson et. al. We may therefore conclude that the results of those authors are explainable in terms of a constant σ_R^+ value for the LaDa groups studied and therefore their conclusions are not warranted on the basis of the evidence presented.

The results of the correlations clearly demonstrates the applicability of the σ_R^+ constants in protic solvents. Sets 6 and 17 suggest that they are also applicable in dipolar aprotic solvents whereas set 21 indicates that they may be applied to work in gas phase. These latter results are only suggestive however, further work is required to establish beyond any doubt the applicability of the σ_R^+ constants in dipolar aprotic and nonpolar aprotic solvents and in the gas phase.

The only AkW substituent type for which even a minimal amount of data is available is OAc for which we may tentatively suggest a value of -0.66 .

I. The σ_R^- Constants

On the basis of the work of Ehrenson, Brownlee, and Taft, we chose the pK_a values of anilinium ions as the basis set for the definition of σ_R^- values. To scale these values we again considered the possibility that for some substituents the equation

$$\sigma_{RX} = \sigma_{RX}^- \quad (128)$$

is obeyed. From our previous discussion we would expect delocalized effect electron donor groups to obey Equation 128. We have correlated the best available pK_a values of substituted anilinium ions in water at 25° with the equation

$$Q_X = L\sigma_{IX} + D\sigma_{RX}^- + h \quad (129)$$

Good correlation was obtained with a set including the Me, *t*-Bu, OMe, OEt, Ph, CH₂Ph and PhCH=CH groups. The σ_{IX} and σ_{RX}^- values were too strongly

correlated to permit the use of this set for the definition of σ_R^- values. Therefore, we looked for other types of substituent which might obey Equation 1. It seemed possible that groups with σ_R values close to 0 and electron acceptors which were not of the π type (SiAk₃, CHI₃) might also obey Equations 128. In fact, the SF₅ and SCF₃ groups, for which $\sigma_R \cong 0$, and the SiMe₃ and CF₃ groups, which are delocalized effect electron acceptors of the non- π type do obey Equation 129 and the resulting eleven-point set shows no significant correlation between σ_I and σ_R^- . A problem remains, however, as the hydrogen point does not lie on the line in this set. We may remedy this deficiency as follows: Let us represent the delocalized effect constants of those substituents that obey Equation 128 as σ_{RbX}^- . They obey the correlation equation

$$Q_X = L\sigma_{IX} + D'\sigma_{RbX}^- + h' \quad (130)$$

and $Q_H \neq h'$. Now the desired delocalized effect constants denoted σ_R^- , result in the applicability of Equation 129 and $Q_H = h$. Then

$$D'\sigma_{RbX}^- + h' = D\sigma_{RX}^- + h \quad (131)$$

or

$$\sigma_{RX}^- = \frac{D'}{D}\sigma_{RbX}^- + \frac{h' - h}{D} \quad (132)$$

As D and D' are both constants, we may write

$$\frac{D'}{D} \equiv r \quad (133)$$

and

$$\sigma_{RX}^- = r\sigma_{Rb,X}^- + \left(\frac{h' - h}{D}\right) \quad (134)$$

When $X = H$, from Equation 132, and the fact that $\sigma_{RH}^- \equiv 0$,

$$r\sigma_{RbX}^- = \left(\frac{h' - h}{D}\right) \quad (135)$$

and

$$\sigma_{RX}^- = r\sigma_{RbX}^- - r\sigma_{RbH} \quad (136)$$

$$= r(\sigma_{RbX}^- - \sigma_{RbH}) \quad (137)$$

We may evaluate σ_{RbH} from Equation 138 which is obtained from Equations 133 and 135;

$$\sigma_{RbH}^- = -\left(\frac{h' - h}{D'}\right) = \left(\frac{h' - Q_H}{D'}\right) \quad (138)$$

with h' and D' obtained from the correlation with Equation 129 using the groups that obey Equation 128 and choosing the best available value of Q_H . We find $\sigma_{RbH}^- = 0.07$; thus from Equation 22,

$$\sigma_{RX}^- = r(\sigma_{RbX}^- + 0.07) + h \quad (139)$$

Substituting Equation 139 in Equation 129 gives

$$Q_X = L\sigma_{IX} + rD(\sigma_{RbX}^- + 0.07) + h \quad (140)$$

$$= L\sigma_{IX} + D'(\sigma_{RB}^- + 0.07) + h \quad (141)$$

We have therefore chosen as our basis set of σ_R^- constants, those groups that obey the equation

$$\sigma_{RX}^- = \sigma_R + 0.07 \quad (142)$$

and the H group for which $\sigma_{RH}^- = 0$. This set (set 1, Table 39) gave an excellent correlation with Equation 129, with Q_H lying on the regression line.

The results obtained for anilinium and N,N-dimethylanilinium ions in water are excellent with the correlation equations accounting for more than 99.2% of the variance (see Table 40). The results in other protonic media for these systems are not as good, with the correlation equations accounting for more than 97.4% of the variance. In dipolar aprotic media, the results are still poorer with 96.1–97.1% of the variance accounted for. The results in toluene are very good, the results in benzene are not significant, possibly due to an error in the pK_a value for $X = Cl$. Examination of systems of the type $X-CH_6H_4NHZa$ where Za is a constant delocalized effect acceptor substituent shows excellent results in protic solvents and in two of the three sets in dipolar aprotic solvents available. Data for carbon acids are limited to one set in water and three in other protonic solvents, with results ranging from very good to excellent.

Ehrenson, Brownlee, and Taft have reported that their σ_R^- values do not give results with phenol which are comparable to the results obtained with other systems. We have examined a number of set of substituted phenol ionization constants in water and other protic solvents and one set in a dipolar aprotic solvent. The results are fairly comparable with those obtained for NH_3^+ , NMe_2H^+ , and $NHZa$ as active groups. We would suggest that the σ_R^- values can be applied successfully to phenolic reactivities and that the differences observed by Ehrenson, Brownlee, and Taft may be due in part to the data examined. Best results are obtained when the data have all been obtained in the same laboratory or alternatively when only those values are considered for which the error is known and is not more than 0.05 pK units. The one set of pK_a data for 4-substituted benzene thiols in water also gives excellent results. We conclude then, that the σ_R^- constants are applicable to ionization constants of active sites of the type NH_3^+ , $NMeCH^+$, $NHZa$, $CHZa$, OH , and SH ; and probably to other

TABLE 39
Data Used in Correlations with Equation 129

1. pK_a , 4- $\text{XC}_6\text{H}_4\text{NH}_3^+$ in water at 25° ^a:
H, 4.596; Me, 5.084, *t*-Bu, 4.95; OMe, 5.31; OEt, 5.32; SF₅, 2.17; SCF₃, 2.78; SiMe₃, 4.36; Ph, 4.24; PhCH₂, 4.78; PhCH=CH, 4.18; CF₃, 2.75
2. pK_a , 4- $\text{XC}_6\text{H}_4\text{NH}_3^+$ in water at 30° ^b:
H, 4.506; Me, 4.987; MeS, 4.31; MeSO₂, 1.46; Bz, 2.12; Br, 3.80; Cl, 3.92; F, 4.56; I, 3.71; MeO, 5.24; NO₂, 0.97
3. pK_a , 4- $\text{XC}_6\text{H}_4\text{NH}_3^+$ in water at 20° ^b:
H, 4.686; Me, 5.187; NH₂, 6.01; Bz, 2.24; Br, 3.95; Cl, 4.07; F, 4.73; I, 3.87; MeO, 5.44; NO₂, 1.04
4. pK_a , 4- $\text{XC}_6\text{H}_4\text{NH}_3^+$ in ethanol^c:
OEt, 4.33; Me, 4.00; H, 3.97; Cl, 3.55; Br, 3.72; CO₂Me, 2.74
5. pK_a , 4- $\text{XC}_6\text{H}_4\text{NH}_3^+$ in chloroform^c:
OEt, 3.36; Me, 3.35; H, 3.20; Cl, 3.00; Br, 2.76; CO₂Me, 2.46
6. pK_a , 4- $\text{XC}_6\text{H}_4\text{NH}_3^+$ in toluene^c:
OEt, 3.12; Me, 3.15; H, 3.00; Cl, 2.80; Br, 2.75; CO₂Me, 2.50
7. pK_a , 4- $\text{XC}_6\text{H}_4\text{NH}_3^+$ in benzene^c:
OEt, 3.04; Me, 3.00; H, 2.86; Cl, 3.00; Br, 2.76; CO₂Me, 2.57
8. pK_a , 4- $\text{XC}_6\text{H}_4\text{NH}_3^+$ in acetonitrile at 25° ^d:
H, 10.57; Me, 11.25; Cl, 9.56; Br, 9.39; F, 10.41; I, 9.40; OMe, 12.05; Ac, 8.13; CO₂Et, 8.18; NO₂, 6.21; CF₃, 8.16
9. pK_a , 4- $\text{XC}_6\text{H}_4\text{NH}_3^+$ in nitromethane at 25° ^e:
H, 9.06; Me, 9.80; Cl, 7.97; OMe, 10.28; NO₂, 5.18; CF₃, 6.90; CO₂Me, 6.73; NH₂, 11.55; CN, 5.72
10. pK_a , 4- $\text{XC}_6\text{H}_4\text{NMe}_2\text{H}^+$ in water at 25° ^f:
Me, 5.63; H, 5.07; Br, 4.23; OMe, 5.85; CHO, 1.612; CN, 1.78; NO₂, 0.61; CF₃, 2.67
11. pK_a , 4- $\text{XC}_6\text{H}_4\text{NMe}_2\text{H}^+$ in 50% v/v aqueous ethanol at 20° ^g:
Me, 4.94; H, 4.35; Br, 3.52; Cl, 3.33; I, 3.43; SiMe₃, 3.98; OMe, 5.14
12. pK_a , 4- $\text{XC}_6\text{H}_4\text{NHSO}_2\text{Ph}$ in 50% w/w aq. EtOH at 20° ^h:
H, 9.98; MeO, 10.34; Me, 10.27; Br, 9.22; Cl, 9.28; NO₂, 7.30; F, 9.71
13. pK_a , 4- $\text{XC}_6\text{H}_4\text{NHSO}_2\text{C}_6\text{H}_4\text{Me-4}'$ in 50% w/w aq. EtOH at 20° ^h:
H, 10.17; MeO, 10.58; Me, 10.47; Br, 9.43; Cl, 9.48; NO₂, 7.50; F, 9.92
14. pK_a , 4- $\text{XC}_6\text{H}_4\text{NHSO}_2\text{C}_6\text{H}_4\text{F-4}'$ in 50% w/w aq. EtOH at 20° ^h:
H, 9.72; MeO, 10.08; Me, 10.01; Br, 8.90; Cl, 8.99; NO₂, 7.04; F, 9.47
15. pK_a , 4- $\text{XC}_6\text{H}_4\text{NHSO}_2\text{C}_6\text{H}_4\text{Cl-4}$ in 50% w/w aq. EtOH at 20° ^h:
H, 9.55; MeO, 9.95; Me, 9.84; Br, 8.81; Cl, 8.86; NO₂, 6.87; F, 9.27
16. pK_a , 4- $\text{XC}_6\text{H}_4\text{NHSO}_2\text{C}_6\text{H}_4\text{NO}_2\text{-3}'$ in 50% w/w aq. EtOH at 20° ^h:
H, 8.76; MeO, 9.13; Me, 9.10; Br, 8.06; Cl, 8.09; NO₂, 6.14; F, 8.43
17. pK_a , 4- $\text{XC}_6\text{H}_4\text{NHBz}$ in dimethyl sulfoxide at 25° ⁱ:
MeO, 19.8; Me, 19.6; H, 19.3; F, 18.9; Cl, 18.3; Br, 18.1; CO₂, 17.2; NO₂, 15.4
18. pK_a , 4- $\text{XC}_6\text{H}_4\text{NHCO}_2\text{Me}$ in dimethylsulfoxide at 25° ^j:
MeO, 20.9; Me, 20.8; H, 20.3; F, 19.8; Cl, 19.5; Br, 19.2; NO₂, 16.2; I, 19.1; Ac, 18.4
19. pK_a , 4- $\text{XC}_6\text{H}_4\text{NHCO}_2\text{Me}$ in dimethoxyethane at 25° ^j:
MeO, 15.4; Me, 15.3; H, 15.0; Cl, 14.4; NO₂, 12.2; Ac, 13.5
20. pK_a , 2-(4'- XC_6H_4)-1,3-indandione in 1% aq. methanol at 20° ^k:
H, 4.13; Cl, 3.72; Br, 3.65; I, 3.57; MeO, 4.25; NO₂, 2.39
21. pK_a , 2-(4- XC_6H_4)-1,3-indandione in 50% aq. ethanol at 20° ^k:
H, 4.29; Cl, 3.58; Br, 3.50; I, 3.46; MeO, 4.56; NO₂, 1.61

TABLE 39
Data Used in Correlations with Equation 129

22. pK_a , 4- $\text{XC}_6\text{H}_4\text{CHMeNO}_2$ in 30.9 mole % aq. MeOH at 23° ^l:
H, 8.52; Me, 8.55; F, 8.36; Cl, 8.23; NO₂, 7.49; CF₃, 8.05
23. pK_a , 4- $\text{XC}_6\text{H}_4\text{CH}(\text{NO}_2)_2$ in water at 20° ^m:
H, 3.89; Me, 4.04; F, 3.65; Br, 3.43; Cl, 3.42; MeO, 4.04; CN, 2.73; NO₂, 2.63
24. pK_a , 4- $\text{XC}_6\text{H}_4\text{NH}_3^+$ in 1% aq. ethanol at 25° ^h:
H, 4.63; F, 4.61; Cl, 3.95; Br, 3.86; I, 3.77; Me, 5.08; Et, 5.00; OH, 5.48; OMe, 5.36; CN, 1.71;
CO₂Me, 2.49; CO₂Et, 2.52; NO₂, 0.96
25. pK_a , 4- $\text{XC}_6\text{H}_3\text{OH}$ in water at 25° ^o:
H, 9.998; Me, 10.262; NO₂, 7.149; MeO, 10.209; Cl, 9.378; F, 9.810; *t*-Bu, 10.232; Ac, 9.047;
Bz, 7.95; CHO, 7.620; Br, 9.340; SCF₃, 8.66
26. pK_a , 4- $\text{XC}_6\text{H}_4\text{OH}$ in water at 25° ^p:
NO₂, 6.99; CN, 7.85; NH₂, 10.44; Ac, 8.01; MeO, 10.12; I, 9.21; Br, 9.27; Cl, 9.35; Et, 10.18;
H, 9.89
27. pK_a , 4- $\text{XC}_6\text{H}_4\text{OH}$ in water at 25° ^q:
H, 10.00; NO₂, 7.16; Br, 9.34; Me, 10.28; Cl, 9.42; MeO, 10.20; F, 9.81
28. pK_a , 4- $\text{XC}_6\text{H}_4\text{OH}$ in 33.2% w/w aq. ethanol at 25° ^q:
H, 10.96; NO₂, 7.43; Br, 9.97; Me, 11.27; Cl, 10.02; MeO, 10.79; F, 10.44
29. pK_a , 4- $\text{XC}_6\text{H}_4\text{OH}$ in 52.0% aq. ethanol at 25° ^q:
H, 11.44; NO₂, 7.87; Br, 10.41; Me, 11.75; Cl, 10.49; MeO, 11.26; F, 10.96
30. pK_a , 4- $\text{XC}_6\text{H}_4\text{OH}$ at 85.4% w/w aq. ethanol at 25° ^q:
H, 12.44; NO₂, 9.07; Br, 11.63; Me, 12.75; Cl, 11.73; MeO, 12.51; F, 12.14
31. pK_a , 4- $\text{XC}_6\text{H}_4\text{OH}$ in ethanol at 25° ^q:
H, 15.12; NO₂, 11.90; Br, 14.27; Me, 15.25; Cl, 14.31; MeO, 15.29; F, 14.82
32. pK_a , 4- $\text{XC}_6\text{H}_4\text{OH}$ in methanol at 25° ^r:
t-Bu, 14.543; H, 14.356; Br, 13.501; CHO, 11.906; NO₂, 11.400; Me, 14.54
33. pK_a , 4-*X*-2,6-(*t*-Bu)₂C₆H₂OH in methanol at 25° ^r:
t-Bu, 17.512; H, 17.201; Br, 15.804; CHO, 12.267; NO₂, 10.888
34. pK_a , 4- $\text{XC}_6\text{H}_4\text{OH}$ in DMSO at 25° ^s:
MeO, 17.58; Me, 16.96; H, 16.47; Cl, 16.10; Br, 15.24; Ac, 13.68; CN, 13.01; NO₂, 11.27
35. pK_a , 4- $\text{XC}_6\text{H}_4\text{OH}$ in water at 20° ^l:
H, 10.04; Me, 10.35; Et, 10.38; Pr, 10.25; *i*-Pr, 10.24; Bu, 10.40; *s*-Bu, 10.37; *t*-Bu, 10.25;
c-C₆H₁₁, 10.30; Cl, 9.45; OMe, 10.25; NO₂, 7.20
36. pK_a , 4- $\text{XC}_6\text{H}_4\text{NMe}_2\text{H}^+$ in 14.8 mole % aq. dioxane at 25° ^u:
Me, 4.60; H, 4.14; Br, 2.95; NO₂, -0.75; Cl, 3.09; SCF₃, 1.40; CF₃, 1.56; C₆H₅, 2.33
37. pK_a , 4- $\text{XC}_6\text{H}_4\text{SH}$ in water at 25° ^v:
Me, 6.820; OMe, 6.775; H, 6.615; Cl, 6.135; Br, 6.020; Ac, 5.330; NO₂, 4.715

^a R. A. Benkeser and H. R. Krysiak, *J. Am. Chem. Soc.*, 75, 2421 (1953); P. D. Bolton and F. M. Hall, *Aust. J. Chem.*, 20, 1797 (1967); B. Gutbezahl and E. Grunwald, *J. Am. Chem. Soc.*, 75, 559 (1953); W. A. Sheppard, *J. Am. Chem. Soc.*, 84, 3072 (1962); 85, 1314 (1963); B. M. Wepster, *Rec. Trav. Chim.*, 76, 357 (1957); V. A. Dadali, L. M. Litvinenko, and N. G. Korzhenskaya, *Teor. i Eksperimeikhim.*, 8, 154 (1972); E. V. Titov, L. M. Litvinenko, V. I. Ribachenko, and M. V. Poddubnaya, *Ukr. Khim. Zhur.*, 33, 287 (1967).

^b A. I. Biggs, *J. Chem. Soc.*, 2572 (1961); P. D. Bolton and F. M. Hall, *Aust. J. Chem.*, 20, 1797 (1967); E. E. Sager and T. J. Siewers, *J. Res. Natl. Bur. Stand.*, 45, 489 (1950); S. Shanmuganathan and N. Vanajakshi, *Proc. Ind. Acad. Sci.*, 69A, 212 (1969); A. V. Willi and H. Meier, *Helv. Chim. Acta*, 39, 318 (1956).

active sites in which formation of a lone pair on the atom attached to the skeletal group occurs. Furthermore, a system with an active site such as NHZa, CHZa, OH, and SH, can be used as a secondary source of σ_R^- values. All of the available σ_R^- values are collected in Table 41.

With regard to the applicability of the σ_R^- values in aprotic solvents, the available data suggest that these constants are in fact satisfactory, although somewhat poorer results may be obtained. Whether the cause of these poorer results lies in the quality of the data or in solvent induced deviations in the σ_R^- values is uncertain at present. Solvent induced variations in certain groups such as OH and NH₂ are of course likely, and the behavior of ionic groups is again very strongly dependent on the medium.

Our results suggest that alkyl groups, alkoxy groups, and probably aryl and arylvinylene groups, SiX₃, CHI₃, phosphinyl and sulfinyl groups obey Equation 142. Thus, a fairly large number of σ_R^- values is actually available.

^c A. S. Chernobrov, and L. N. Gindin, *Izv. Sibirskogo Otdel. Akad. Nauk SSR, Ser. Khim. Nauk*, 14 (1974).

^d V. A. Bren, E. N. Malisheva and V. I. Minkin, *Reakts. Sposobnost. Org. Soedin.*, 4, 523 (1967).

^e B. A. Korolev and B. I. Stepanov, *Izv. Vissh. Uchen. Zardevii. Khim. Khim. Tekhnol.*, 11, 1193 (1968).

^f M. M. Fickling, A. Fischer, B. R. Mann, J. Packer, and J. Vaughan, *J. Am. Chem. Soc.*, 81, 4226 (1959); J. D. Roberts, R. L. Webb, and E. A. McElhill, *J. Am. Chem. Soc.*, 72, 408 (1950); W. Rubaszewska and Z. R. Grabowski, *Rocz. Chem.*, 33, 781 (1959).

^g R. A. Benkeser and H. R. Krysiak, *J. Am. Chem. Soc.*, 87, 2410 (1965).

^h G. Dauphin, A. Kergomard, and H. Veschambre, *Bull. Soc. Chim. France*, 3395 (1967).

ⁱ E. S. Petrov, E. N. Teleschov, S. G. Tadevosyin, N. N. Shelganova, A. I. Pravednikov, and A. I. Shatenshtein, *Zhur. Org. Khim.*, 12, 568 (1977).

^j T. I. Lebedeva, V. A. Kolesova, L. L. Gerasimovich, Kefchiyan, E. S. Petrov, Y. A. Streikheev, and A. I. Shatenshtein, *Zhur. Org. Khim.*, 13, 1137 (1977).

^k Y. Linaberg, O. Neiland, A. Veis, and G. Vanag, *Dokl. Akad. Nauk. SSR*, 154, 1385 (1964); Y. Linaberg, Dissertation (See *Tables of Rate and Equilibrium Constants of Heterolytic Organic Reactions*, V. Palm (Ed) Vol. II: Part I, Moscow, 1976).

^l F. G. Bordwell, W. J. Boyle, and K. C. Yee, *J. Am. Chem. Soc.*, 92, 5926 (1970).

^m G. I. Kolesetskaya, I. V. Tselinskii, and L. I. Bagal, *Reakt. Sposobnost. Org. Soedin*, 6, 387 (1969).

ⁿ A. de Courville, *C. R. Acad. Sci. Paris Ser. C*, 262, 1196 (1966).

^o Footnote n, Table 23.

^p C. Van Hoodonk and L. Ginjaar, *Rec. Trav. Chim.*, 86, 444 (1967).

^q R. Thuair, *J. Chim. Phys.*, 23 (1972).

^r P. D. Bolton, C. H. Rochester, and B. Rossall, *Trans. Faraday Soc.*, 66, 1348 (1970).

^s K. Kalfus, J. Socha, and M. Vecera, *Collect. Czech. Chem. Commun.*, 39, 275 (1974).

^t P. Demerseman, N. Platzler, J. P. Bachelet, A. Cheutin, and R. Royer, *Bull. Soc. Chim. France*, 201 (1970).

^u W. A. Sheppard, *J. Am. Chem. Soc.*, 87, 2410 (1965).

^v P. DeMaria, A. Fini, and F. M. Hall, *J. Chem. Soc. Perkin Trans. II*, 1969 (1973).

TABLE 40
Results of Correlations with Eq. 129

Set	$-L$	$-D$	h	R^a	F^b	r_{12}^c	s_{est}^d	s_L^d
1	3.50	3.36	4.61	0.9963	601.8	0.030	0.102	0.140
2	3.51	3.28	4.57	0.9992	2426.	0.106	0.0653	0.0943
3	3.70	3.42	4.76	0.9996	4129.	0.047	0.0495	0.0734
4	1.72	1.89	3.88	0.9882	62.28 ^g	0.311	0.109	0.237 ^h
5	1.38	1.07	3.22	0.9804	37.19 ^h	0.311	0.0908	0.198 ^h
6	1.01	0.735	3.04	0.9946	137.3 ^g	0.311	0.0335	0.0732
7	0.486	0.605	2.92	0.8908	5.762 ^l	0.311	0.111	0.243 ^m
8	4.89	3.88	10.86	0.9855	135.1	0.056	0.315	0.481
9	4.56	4.13	9.39	0.9848	112.6	0.367	0.405	0.636
10	4.34	4.07	5.13	0.9989	1139.	0.316	0.112	0.181
11	4.56	4.26	4.38	0.9872	76.81	0.775 ^l	0.143	0.371
12	2.90	2.18	10.02	0.9990	1042.	0.011	0.0559	0.0860
13	2.89	2.21	10.22	0.9986	688.7	0.011	0.0690	0.106
14	2.92	2.18	9.76	0.9982	549.9	0.011	0.0771	0.119
15	2.90	2.20	9.60	0.9987	741.5	0.011	0.0665	0.102
16	2.90	2.10	8.84	0.9984	608.1	0.011	0.0719	0.111
17	4.15	3.08	19.34	0.9980	623.2	0.030	0.109	0.168
18	4.50	2.96	20.54	0.9878	120.8	0.054	0.258	0.396
19	2.94	2.20	15.10	0.9960	186.4	0.233	0.144	0.249
20	1.82	1.36	4.12	0.9984	464.5	0.284	0.0484	0.101
21	2.87	2.11	4.29	0.9992	948.0	0.284	0.0530	0.110
22	1.06	0.715	8.51	0.9924	97.16 ^g	0.238	0.0628	0.0984 ^h
23	1.53	0.961	3.92	0.9933	184.1	0.135	0.0753	0.111
24	3.77	3.42	4.71	0.9993	3554.	0.076	0.0598	0.0768
25	2.84	2.51	9.93	0.9967	683.1	0.031	0.101	0.135
26	2.80	2.25	9.88	0.9939	283.1	0.300	0.144	0.221
27	2.90	2.33	10.01	0.9981	515.5	0.011	0.0819	0.126
28	3.76	2.47	10.94	0.9938	159.2	0.011	0.175	0.269
29	3.78	2.52	11.42	0.9933	148.0	0.011	0.183	0.282
30	3.45	2.64	12.43	0.9954	215.5	0.011	0.147	0.226
31	3.23	2.56	15.04	0.9988	827.2	0.011	0.0715	0.110
32	3.00	2.55	14.26	0.9983	434.4	0.392	0.106	0.177
33	6.02	5.59	17.03	0.9990	514.9 ^g	0.326	0.186	0.333 ^h
34	4.83	4.50	16.63	0.9885	106.5	0.241	0.392	0.611
35	3.64	2.89	10.04	0.9917	266.4	0.148	0.129	0.168
36	5.64	5.08	4.20	0.9883	83.87	0.106	0.344	0.592
37	2.07	1.52	6.621	0.9987	777.5	0.138	0.0490	0.0803

Set	s_D^d	s_n^d	100 r^2	n	P_R	Error
1	0.136	0.0398	99.26	12	49.0	2.4
2	0.0602	0.0407	99.84	11	48.3	1.2
3	0.0468	0.0303	99.92	10	48.0	0.9
4	0.183 ^h	0.0729	97.65	6	52.4	6.7
5	0.153 ^h	0.0610	96.12	6	43.7	7.7
6	0.0565	0.0225	98.92	6	42.1	3.9

TABLE 40
Results of Correlations with Eq. 129

Set	s_D^d	s_h^d	100 r^2	n	P_R	Error
7	0.187 ^j	0.0747	79.34	6	55.5	23.2
8	0.289	0.193	97.12	11	44.2	4.3
9	0.429	0.259	96.99	10	47.5	6.5
10	0.129	0.0712	99.78	8	48.4	2.0
11	0.408	0.0746	97.46	7	48.3	5.5
12	0.0702	0.0391	99.81	7	42.9	1.7
13	0.0867	0.0483	99.71	7	43.3	2.1
14	0.0969	0.0540	99.64	7	42.7	2.3
15	0.0835	0.0466	99.73	7	43.1	2.0
16	0.0903	0.0503	99.67	7	42.0	2.2
17	0.119	0.0712	99.60	8	42.6	2.0
18	0.264	0.165	97.58	9	39.7	4.4
19	0.182	0.0935	99.20	6	42.8	4.4
20	0.0742	0.0476	99.68	6	42.8	2.9
21	0.0812	0.0520	99.84	6	42.4	2.0
22	0.0829 ^h	0.0430	98.48	6	40.3	5.5
23	0.0840	0.0524	98.66	8	38.6	4.0
24	0.0529	0.0309	99.86	13	47.6	1.0
25	0.0810	0.0515	99.35	12	46.9	2.0
26	0.146	0.0907	98.78	10	44.6	3.7
27	0.103	0.0573	99.61	7	44.6	2.4
28	0.220	0.122	98.76	7	39.6	4.2
29	0.230	0.128	98.67	7	40.0	4.3
30	0.185	0.103	99.08	7	43.3	3.7
31	0.0898	0.0501	99.76	7	44.2	1.9
32	0.165	0.0580	99.66	6	45.9	3.6
33	0.292 ^h	0.123	99.81	5	48.1	3.1
34	0.450	0.255	97.71	8	48.2	6.2
35	0.258	0.0502	98.34	12	44.3	4.5
36	0.658 ^h	0.239	97.67	7	47.4	7.3
37	0.0584	0.0319	99.74	7	42.3	2.0

For footnotes a-j, see Table 26.

^k 50% CL.

^l 90.0% CL.

^m 80.0% CL.

Data are available for the determination of a $\overline{\sigma_{RAkW}}$ value for the CO₂Ak group; the resulting value is 0.31 with a standard error of 0.005.

It is of interest to compare the delocalized electrical effect of those substituents that do not obey Equation 142 with those that do. For this purpose we define

$$\Delta \equiv \sigma_R^- - (\sigma_R + 0.07) \quad (143)$$

TABLE 41
Values^a of σ_R^-

X	σ_R^-	Error ^b	pK_a^c	Set ^d	Δ
Carbonyl					
Ac	0.41	U	2.19 ^e	1	0.14
Bz	0.41	U	2.17 ^f	1	0.23
CO ₂ H	0.31	0.031	2.501 ^g	1	0.13
CO ₂ Me	0.30	0.029	2.465 ^h	1	0.12
CO ₂ Et	0.31	0.034	2.508 ^h	1	0.13
CO ₂ Pr	0.31	0.029	2.487 ^h	1	
CO ₂ Bu	0.31	0.029	2.472 ^h	1	
CHO	0.53	U	1.76 ^e	1	0.31
CONH ₂	0.23	U	8.56 ⁱ	25	0.08
Substituted Alkyl					
CH ₂ OH	-0.08	0.026	9.82 ^j	25	-0.08
CH ₂ CH=CH ₂	-0.14	0.023	10.23 ^k	25	-0.07
Vinyl					
CH ₂ =CMe	-0.07	0.024	0.824 ^k	25	-0.09
Aza					
NH ₂	-0.55	0.033	5.86 ^l	1	0.18
NHPh	-0.49	U	5.20 ^m	1	0.30
NMePh	-0.25	U	4.94 ^m	1	
NMe ₂	-0.30	0.0508	10.08 ⁿ	26	0.51
Oxa					
OH	-0.45	0.039	5.29 ^o	1	0.10
Phosphonyl					
POMe ₂	0.25	U	8.45 ^p	26	
PO(OEt) ₂	0.29	U	8.28 ^q	25	-0.02
Thia					
NCS	-0.09	U	8.57 ^r	25	0
MeS	-0.24	0.024	4.35 ^s	1	0.07
AcS	-0.02	U	8.88 ^r	25	-0.07
PhS	-0.08	0.023	3.80 ^m	1	0.09
4-O ₂ NPhS	0.12	U	2.99 ^t	1	0.16
4-MeOPhS	-0.08	U	3.94 ^t	1	
EtS	-0.10	U	4.00 ^u	2	0.13
<i>i</i> -PrS	-0.07	U	3.89 ^u	2	0.13
<i>t</i> -BuS	0.06	U	3.44 ^u	2	

TABLE 41
Values^a of σ_R^-

X	σ_R^-	Error ^b	pK_a^c	Set ^d	Δ
Sulfonyl, Sulfinyl					
SO ₂ Me	0.35	0.039	1.364 ^s	1	0.17
SO ₂ CF ₃	0.63	U	-0.01 ^v	1	0.35
SO ₂ Et	0.34	U	1.38 ^u	2	
SO ₂ - <i>i</i> -Pr	0.36	U	1.40 ^u	2	
SOMe	0.05	U	8.28 ^w	25	-0.02
Aryl					
4-O ₂ NC ₆ H ₄	0.04	U	3.67 ^t	1	-0.06
4-MeOC ₆ H ₄	-0.01	U	4.25 ^t	1	0.11
Ionic					
NMe ₃ ⁺	-0.45	U	2.146 ^x	1,25	-0.41
SMe ₂ ⁺	0.03	U	7.30 ^y	25	-0.28
Other					
F	-0.58	0.037	4.65 ^z	1	-0.17
Cl	-0.30	0.041	3.982 ^z	1	-0.12
Br	-0.28	0.036	3.888 ^z	1	-0.10
I	-0.18	0.026	3.812 ^z	1	-0.09
CN	0.26	0.030	1.739 ^{aa}	1	0.11
NO ₂	0.37	0.043	1.00 ^{bb}	1	0.20

^a These values are for those substituents that do not obey Eq. 142.

^b Estimated from Eq. 89.

^c From which the substituent constant was calculated.

^d The set in Table 40 from which the *L*, *D*, and *h* values used to calculate the substituent constant were taken.

^e J. M. Vandenberg, C. Heinrich, and S. G. Van den Berg, *Anal. Chem.*, 26, 726 (1954).

^f E. E. Sager and T. J. Siewers, *J. Res. Nat. Bur. Stand.*, 45, 489 (1950).

^g M. L. Deviney, R. C. Anderson, and W. A. Felsing, *J. Am. Chem. Soc.*, 79, 237 (1957).

^h R. A. Robinson and A. I. Biggs, *Aust. J. Chem.*, 10, 128 (1957).

ⁱ L. A. Cohen and W. M. Jones, *J. Am. Chem. Soc.*, 85, 339 (1963).

^j G. R. Sprengling and C. W. Lewis, *J. Am. Chem. Soc.*, 75, 570 (1953).

^k G. M. Brauer, H. Argentar, and G. Durany, *J. Res. Nat. Bur. Stand.*, 68A, 619 (1964).

^l A. V. Willi, *Z. Physik. Chem. (Frankfurt)*, 27, 233 (1961). Includes a statistical factor of 2.

^m E. V. Titov, L. M. Litvinenko, V. A. Ribachenko, and M. V. Poddubnaya, *Ukr. Khim. Zhur.*, 33, 287 (1967).

ⁿ Footnote p, Table 7.

^o M. Gillois and P. Rumpf, *Bull. Soc. Chim. France*, 112 (1954).

^p E. N. Tsvetkov, Dissertation, in *Tables of Rate and Equilibrium Constants of Heterolytic Organic Reactions*, Vol. I Part I, V. A. Palm (Ed.), Moscow, 1975; E. N. Tsvetkov, M. M. Ma-

in an analogous method previously applied to comparison of σ_R^+ . These values are given in Table 41. From these Δ values we may draw some generalizations. Relative to those groups that obey Equation 142, (1) $pp\pi$ type delocalized acceptors such as ZCO, CN, NO₂, are stronger electron acceptors. (2) ZSO₂ groups are stronger electron acceptors. (3) Aza groups (NH₂, NMe₂, NHPH, and probably NHZ in general) are poorer electron acceptors. (4) The halogens are better electron donors. (5) Alkylthio and arylthio groups are poorer electron donors.

V. ESTIMATION OF SUBSTITUENT CONSTANTS

The need for substituent constants of groups for which experimentally determined values are unavailable continually recurs. To supply this need methods of estimation of substituent constants are required. The first successful attempt to estimate substituent constants is due to Charton (50). The basis of this method is that a data set with substituents of the type ZW, where Z is variable and W is constant, can be treated in two equivalent ways. The system has the form ZWGY. The substituent can be taken to be Z, and the skeletal group to be WG; or, the substituent can be assumed to be ZW, and the skeletal group to be G. In that case, let the composite substituent constant, $\sigma_{T,ZW}$ represent the effect of the ZW group, and the composite substituent constant, σ'_{TZ} represent the effect of the Z group. From the simple Hammett equation, some quantity Q which is to be correlated is given by,

$$Q_{ZW} = \rho_{WG}\sigma'_{TZ} + h_Z \quad (144)$$

$$= \rho_G\sigma_{TZW} + h_H \quad (145)$$

khamatkhonov, D. I. Lobanov, and M. I. Kabachnik, *Izv. Akad. Nauk SSR, Ser. Khim.*, 178 (1970).

^q G. D. Freedman and H. H[†] Jaffé, *J. Am. Chem. Soc.*, 77, 920 (1955). At 23°.

^r F. G. Bordwell and P. J. Bolton, *J. Am. Chem. Soc.*, 78, 854 (1956).

^s F. B. Bordwell and G. D. Cooper, *J. Am. Chem. Soc.*, 74, 1058 (1952).

^t L. M. Litvinenko, E. V. Titov, R. S. Cheshko, M. V. Shavinskaya, and V. I. Ribachenko, *Zhur. Org. Khim.*, 2, 1857 (1966).

^u S. Shanmugnathan and N. Vanajakshi, *Proc. Ind. Acad., Sci.*, 69, 212 (1969).

^v W. A. Sheppard, *J. Am. Chem. Soc.*, 85, 1314 (1963).

^w F. G. Bordwell and P. J. Bolton, *J. Am. Chem. Soc.*, 79, 717 (1957).

^x A. V. Willi, *Z. Physik. Chem. (Frankfurt)*, 26, 42 (1960).

^y F. G. Bordwell and P. J. Bolton, *J. Am. Chem. Soc.*, 78, 87 (1956).

^z Footnote n, Table 23.

^{aa} M. M. Fickling, A. Fischer, B. R. Mann, J. Packer, and J. Vaughan, *J. Am. Chem. Soc.*, 81, 4226 (1959).

^{bb} A. I. Biggs, *J. Chem. Soc.*, 2572 (1961).

Then

$$\rho_G \sigma_{TZW} + h_H = \rho_{WG} \sigma'_{TZ} + h_{HW} \quad (146)$$

However,

$$h_{HW} = \rho_G \sigma_{THW} + h_H \quad (147)$$

Then

$$\rho_G \sigma_{TZW} = \rho_{WG} \sigma'_{TZ} + \rho_G \sigma_{THW} \quad (148)$$

or

$$\sigma_{TZW} = \frac{\rho_{WG}}{\rho_G} \sigma'_{TZ} + \sigma_{THW} \quad (149)$$

$$= \rho' \sigma'_{TZ} + \sigma_{THW} \quad (150)$$

σ_{THW} is constant. Substituting Equation 2 in Equation 150 gives

$$\sigma_{TZW} = \rho' \lambda \sigma_{IZ} + \rho \delta' \sigma_{DZ} + a \quad (151)$$

$$= L \sigma_{IZ} + D \sigma_{DZ} + a \quad (152)$$

As σ_{IZW} and σ_{DZW} are special cases of σ_{TZW} with $\delta = 0$ for the former and $\lambda = 0$ for the latter, it follows that

$$\sigma_{IZW} = L \sigma_{IZ} + D \sigma_{DZ} + a \quad (153)$$

$$\sigma_{DZW} = L' \sigma_{IZ} + D' \sigma_{DZ} + a' \quad (154)$$

A. Z Bonded to Carbon

When in a set of ZW groups, W is CH₂, CH, C, C=O, C₆H₄, CH=CH, or C≡C, no problem arises as the σ_I and σ_D constants have been shown applicable to skeletal groups of this type in this work or elsewhere (6). When Z is bonded to an sp^3 -hybridized carbon atom our previous results suggest that the delocalized effect is insignificant. Thus, we expect that for σ_{I,ZCH_2} and σ_{DZCH_2} ,

$$\sigma_{IZCH_2} = L \sigma_{IZ} + a \quad (155)$$

$$\sigma_{DZCH_2} = L' \sigma_{IZ} + a' \quad (156)$$

These equations are indeed obeyed. Results of correlations with them are given in Table 43; the groups in each set are reported in Table 42. Both σ_{RZCH_2} and $\sigma_{RZCH_2}^+$ groups were studied (sets 1R, 1RP) with very good results. The σ_R and σ_R^+ values for the Me₃SiCH₂ group do not fit on either of the appropriate re-

TABLE 42

 σ_{ZW} Sets^a

-
1. σ_{1,ZCH_2}
Cl, Br, I, OH, OMe, SMe, NHAc, OAc, Ph, H, Me, Et, Vi, *i*-Pr, H₂NCO, H₂NCNH,
t-Bu ||
O
- 1R. σ_{R,CH_2Z}
H, Me, Vi, *t*-Bu, CN, Br, Cl, I, MeO, PhO, OAc, NHAc, CONH₂, Ph, Et
- 1RP. σ_{R^+,ZCH_2}
CH₂OH, CH₂CH₂OH, CO₂Et, SO₂Ph, H, Me, Et
2. σ_{1,Z^1Z^2CH}
H, H; Me, Me; Me, Et; Me, Br; Me, Cl; F, F; Me, OH; Ph, OH; Ph, Me; Ph, CO₂Me
- 3R. $\sigma_{1,Z^1Z^2Z^3C}$
H, H, H; Me, Me, Me; Me, Me, Ph; F, F, F; Cl, Cl, Cl
4. $\sigma_{1,ZC=O}$
H, Me, Cl, F
- 4R. $\sigma_{R,ZC=O}$
OH, OMe, OEt, Me, H, Ph, Et
- 4RM. $\sigma_{R^-,ZC=O}$
OH, OEt, OMe, NH₂, Me, Ph
5. $\sigma_{1,ZNH}$
H, Me, H₂NCO, Ac, EtO₂C, PhSO₂, Bz, HCO
- 5R. $\sigma_{R,ZNH}$
H, H₂NCO, Ac, EtO₂C, PhSO₂, Ph, Bz, HCO
6. $\sigma_{1,ZO}$
H, H₂N, O₂N, Me, MeSO₂, Et, Pr, *i*-Pr, Bz
- 6R. $\sigma_{R,ZO}$
H, Me, MeSO₂, Ac, Et, Pr, Ph, Bz
7. σ_{1,Z^1Z^2PO}
Me, MeO, Et, EtO, Pr, Bu, (Me₂N)₂PO
8. $\sigma_{1,ZS}$
H, CF₃, CN, CONH₂, Me, Ac, Et, Pr, *i*-Pr, Ph, PhCH₂, ViCH₂
- 8R. $\sigma_{R,ZS}$
CF₃, CN, Me, Ac, Et, *i*-Pr, Ph
9. σ_{1,ZSO_2}
Me, Et, Pr, *i*-Pr, Ph, 4-MeOPn, CF₃
10. $\sigma_{1,ZC\equiv C}$
H, Me, Vi, MeC₂, Ph
11. $\sigma_{1,Z-CH=CH}$
H, Me, Et, Ph, Cl, HO₂CCH₂
12. $\sigma_{1,3-ZC_6H_4}$
H, Cl, F, I, NO₂
- 12R. $\sigma_{1,3-ZC_6H_4}$
H, Cl, F, O₂N
13. $\sigma_{1,4-ZC_6H_4}$
Br, Cl, F, I, O₂N, Me, MeO, Et, *i*-Pr, *t*-Bu, H
- 13R. $\sigma_{R,4-ZC_6H_4}$
Br, Cl, F, I, O₂N, Me, Et, *i*-Pr, H
- 13RP. $\sigma_{R^+,4-ZC_6H_4}$
Br, Cl, Me, MeO, H

TABLE 42
 σ_{ZW} Sets^a

51.	$\sigma_{R^{\circ}, Z^1Z^2N}$ H, H; H, CHO; H, Ac; Me, Me
61.	$\sigma_{R^{\circ}, ZO}$ H, Me, Et, Ph
81.	$\sigma_{R^{\circ}, ZS}$ CF ₃ , CN, Me, Ac, Et, Ph
131.	$\sigma_{R^{\circ}, A-ZC_6H_4}$ H, MeO, Me, Cl, Br

gression lines. This group is more of an electron donor than would be expected and is possibly functioning in a different manner from the other ZCH₂ groups in so far as its delocalized effect is concerned. When dealing with multiply substituted methyl groups, the problem is more difficult. A number of authors

TABLE 43
Results of Correlations with Eqs. 145, 155, 156, 160, 161

Set	<i>L</i> or <i>P</i>	<i>h</i>	<i>r</i> ^a	<i>F</i> ^b	<i>s</i> _{est} ^c	<i>s</i> _{<i>L</i> or <i>P</i>} ^c	<i>s</i> _{<i>h</i>} ^c	100 <i>r</i> ²	<i>n</i> ^e
1	0.416	-0.0103	0.9867	515.3	0.0126	0.0183	0.00490 ^k	97.36	16
1R	0.164	-0.156	0.9421	86.79	0.0132	0.0176	0.00567	88.75	13
1RP	0.288	-0.160	0.9752	96.93	0.0153	0.0293	0.00716	95.09	7
2	0.297	0.00482	0.9691	123.5	0.0270	0.0268	0.0119 ^h	93.92	10
3	0.248	0.00398	0.9977	657.4	0.0159	0.00969	0.00932 ^h	99.55	5
3R	0.173	-0.167	0.9991	1090.	0.00806	0.00524	0.00563 ⁱ	99.82	4
4Rc	-0.401	0.160	0.9433	40.35 ^l	0.0140	0.0726 ⁱ	0.00625	88.97	7
4RM	0.197	0.439	0.9964	554.4	0.00662	0.00835	0.00543	99.28	6
5c	0.235	0.153	0.9722	86.07	0.0181	0.0254	0.0118	94.51	7
6Rc	0.277	-0.532	0.9576	66.21	0.0500	0.0340	0.0208	91.69	8
7c	0.489	0.320	0.9392	37.43 ^l	0.0238	0.0799 ^l	0.0116	88.22	7
8	0.466	0.260	0.9627	126.5	0.0271	0.0414	0.00978	92.68	12
8R	0.870	-0.175	0.9331	33.67 ^l	0.0555	0.150 ⁱ	0.0213	87.07	7
9	0.420	0.645	0.9853	165.9	0.0104	0.0326	0.00579	97.07	7
10	0.311	0.300	0.9668	42.97 ⁱ	0.0119	0.0475 ⁱ	0.00725	93.47	5
6Ac	-1.41	7.08	0.9731	71.50	0.127	0.166 ⁱ	0.0683	94.70	6
6Bc	-1.52	5.99	0.9064	18.42 ^m	0.218	0.355 ^o	0.111	82.16	6
51	0.392	-0.0992	0.9926	133.2 ⁱ	0.0160	0.0340 ⁱ	0.0221 ⁿ	98.52	4
81	0.729	-0.0564	0.9075	18.68 ^m	0.0705	0.318 ^o	0.0380 ^p	82.36	6
131	0.718	-0.116	0.9444	24.74 ^m	0.0198	0.144 ^o	0.0167 ⁱ	89.19	5

For Footnotes a-j, see Tables 9 and 30.

^k 90.0% CL.

^l 99.5% CL.

^m 97.5% CL.

ⁿ 95.0% CL.

^o 98.0% CL.

^p 80.0% CL.

have suggested that the effects of the Z groups in CHZ^1Z^2 and $\text{CZ}^1\text{Z}^2\text{Z}^3$ are not additive. The nonadditivity may mean that when $\sigma_{\text{IZ}^1} = \sigma_{\text{IZ}^2} = \sigma_{\text{IZ}^3}$, unless $Z = H$, the equation

$$\sigma_{Z_n C} = m n_Z = a \quad (157)$$

where n_Z is the number of Z groups, is not obeyed. This equation would result if the effect of Z groups were proportional to their number. Thus,

$$\sigma_C Z_n = L_1 \sigma_{\text{IZ}^1} + L_2 \sigma_{\text{IZ}^2} + L_3 \sigma_{\text{IZ}^3} + a \quad (158)$$

If $L_1 = L_2 = L_3$, and Z is either constant or 0,

$$\sigma_{CZ_n} = (L_1 \sigma_{\text{IZ}^1}) n_Z + a \quad (159)$$

which is equivalent to eq. 157.

For CHZ^1Z^2 and for $\text{CZ}^1\text{Z}^2\text{Z}^3$ the equations

$$\sigma_{Z^1 Z^2 CH} = L_2 \sum \sigma_{\text{IZ}} + a_2 \quad (160)$$

$$\sigma_{Z^1 Z^2 Z^3 C} = L_3 \sum \sigma_{\text{IZ}} + a_3 \quad (161)$$

are not obeyed. Equations 160 and 161 result when $L_1 = L_2$ or if $L_1 = L_2 = L_3$ and σ_{IZ^1} need not equal σ_{IZ^2} which need not equal σ_{IZ^3} . If Equation 160 is not obeyed, the equation

$$\sigma_{\text{CHZ}^1\text{Z}^2} = L_1 \sigma_{\text{IZ}^1} + L_2 \sigma_{\text{IZ}^2} + a \quad (162)$$

should be obeyed. We have correlated $\sigma_{\text{ICHZ}^1\text{Z}^2}$ constants with Equation 162. The results are given in Table 44. They show clearly that L_1 is not significantly different from L_2 . Then as $L_1 = L_2$, Equation 160 is obeyed. We observed, however, that the values of L_1 , L_2 , and L_3 are 0.416, 0.297, and 0.248. The L_1 and L_2 values are significantly different. Thus, Equation 157 is not obeyed. Results of the correlations with Equations 160 and 161 are presented in Table 43, the sets studied are given in Table 42. The $\sigma_{\text{RZ}^1\text{Z}^2\text{Z}^3\text{C}}$ groups are also successfully correlated by Equation 161 (set 3R, Table 43).

For $W = \text{C}=\text{O}$, $\text{C}\equiv\text{C}$, $\text{CH}=\text{CH}$, 3- C_6H_4 , and 4- C_6H_4 , correlations with Equation 153 and 154 were carried out. The first problem to be solved is the choice of σ_D value. The $\sigma_{\text{I},4\text{-ZC}_6\text{H}_4}$ constants are best correlated by σ_R^0 (set 13, Table 44). The $\sigma_{\text{I},3\text{-ZC}_6\text{H}_4}$ constants give equally good results with σ_R and σ_R^0 (sets 12-1, 12-2, Table 44). In the case of $W = \text{C}\equiv\text{C}$ and $\text{CH}=\text{CH}$, no substituents for which $\sigma_R \neq \sigma_R^0$ were available. Good results for $\sigma_{\text{I,ZCH}=\text{CH}}$ were obtained with σ_R . For the $\sigma_{\text{I,ZC}\equiv\text{C}}$ values the term in σ_R was not significant (set 10, Table 44) and the constants were therefore correlated with σ_{IZ} (set 10, Table 43). This may be due to insufficient variation in Z. The range in $\sigma_{\text{I,ZC}=\text{O}}$ for the groups available is too small (0.04 σ units) to make it possible to obtain a useful equation for estimating $\sigma_{\text{IZC}=\text{O}}$ values. The $\sigma_{\text{R,ZC}=\text{O}}$ and $\sigma_{\text{R,ZC}=\text{O}}$ constants introduce a new problem. It has been clearly demonstrated both by

TABLE 44
Results of Correlations with Equations 154, 162, 88, 103, 129

Set	L or L_1	D or L_2	h	R^a	F^b	r_{12}^c	s_{est}^d
2	0.320	0.293	0.00629	0.9513	38.08	0.510	0.0361
4R	-0.604	-0.193	0.152	0.9669	28.71 ⁱ	0.949 ⁱ	0.0120
5	0.155	0.217	0.156	0.9837	74.85	0.763 ^j	0.0154
5R	0.456	1.43	-0.757	0.9689	38.36	0.620	0.0587
6	0.434	0.241	0.299	0.9745	56.51	0.393	0.0419
6R	0.301	0.398	-0.534	0.9580	27.87 ⁱ	0.858 ^k	0.0545
7	0.563	0.201	0.309	0.9595	23.22 ^g	0.729 ^m	0.0218
11	0.271	0.278	0.117	0.9828	42.55 ^g	0.694	0.00925
12	0.112	0.0445	0.120	0.9988	415.9 ⁱ	0.197	0.00196
12z	0.112	0.0474	0.120	0.9989	443.2 ⁱ	0.187	0.00190
12Rz	0.153	0.0761	-0.110	0.9993	383.2 ⁱ	0.188	0.00281
13z	0.138	0.137	0.120	0.9954	427.1	0.148	0.00431
13Rz	0.180	0.111	-0.0988	0.9661	41.98	0.183	0.0155
13Rp	0.139	0.218	-0.167	0.9983	299.0 ⁱ	0.356	0.00427
5A	-1.18	-1.26	7.73	0.9881	82.63	0.615	0.0708
5B	-0.723	-1.12	6.47	0.9996	1267.	0.636	0.0134
8B	-0.951	-1.01	5.55	0.9902	75.18 ⁱ	0.747	0.0570
9B	-0.810	-0.330	4.63	0.9957	114.8 ^g	0.137	0.0334

Set	s_L^d	s_D^d	s_h^d	100 r^2	n^f
Set2	0.664 ^g	0.0773 ^g	0.0175 ^h	90.49	11
4R	0.111 ^g	0.0545 ^j	0.00808	93.49	7
5	0.0477 ⁱ	0.0422 ^g	0.00979	96.77	8
5R	0.169 ^j	0.293 ^g	0.0419	93.88	8
6	0.0593	0.0572 ^g	0.0208	94.96	9
6R	0.183 ^l	0.171 ^m	0.0252	91.77	8
7	0.0898 ^g	0.0314 ^g	0.0128	92.07	7
11	0.0310 ^g	0.0710 ^j	0.00809	96.60	6
12	0.00395 ^g	0.00443 ^g	0.00187	99.76	5
12z	0.00382 ^g	0.00456 ^g	0.00182	99.77	5
12Rz	0.00566 ^j	0.00677 ^m	0.00278 ^k	99.87	4
13z	0.0519	0.00858	0.00234	99.07	11
13Rz	0.0199	0.0342 ^k	0.00890	93.33	9
13RP	0.00953 ^g	0.00925 ^g	0.00323	99.67	5
5A	0.215 ^g	0.217 ^g	0.0644	97.64	7
5B	0.0418 ^g	0.0442 ^g	0.0129	99.92	5
8B	0.187 ^k	0.280 ^j	0.0508	98.04	6
9B	0.0758 ^g	0.0359 ^k	0.0277	99.14	5

Footnotes a-f are from Table 26.

^g 99.0% CL.

^h 20.0% CL.

ⁱ 99.5% CL.

^j 95.0% CL.

^k 98.0% CL.

^l 80.0% CL.

^m 90.0% CL.

Ehrens, Brownlee, and Taft, and in this work as well, that when a delocalized effect donor substituent and a delocalized effect acceptor active site are attached to a *para*-phenylene skeletal group, σ_R^+ constants must be used for optimal correlation. If a delocalized effect acceptor substituent and a delocalized effect donor active site are attached to a *para*-phenylene skeletal group, the σ_R^- constants are required for best results. Then considering ZW, when Z is a delocalized effect donor and W a delocalized effect acceptor, we might require for best correlation, the σ_R^+ constants, whereas if Z is a delocalized effect acceptor and W a delocalized effect donor, the σ_R^- constants may be necessary.

The carbonyl group is a delocalized effect electron acceptor; we have therefore examined the correlation of $\sigma_{R,ZC=O}$ and $\sigma_{R^-,ZC=O}$ with Equation 154 using both σ_{RZ} and σ_{RZ}^+ values. Best results were obtained with σ_R^+ ; however, σ_I and σ_R were colinear (set 4R, Table 44). Correlation was therefore carried out with a composite substituent constant with good results. The definition of suitable composite substituent constants is described in Section V.B. The

TABLE 45
Equations for the Estimation of Substituent Constants

1.	$\sigma_{I,ZCH_2} = 0.416 \sigma_{I,Z} - 0.0103$
2.	$\sigma_{R,ZCH_2} = 0.164 \sigma_{I,Z} - 0.156$
3.	$\sigma_{R^+,ZCH_2} = 0.288 \sigma_{I,Z} - 0.160$
4.	$\sigma_{I,Z^1Z^2CH} = 0.297 \Sigma \sigma_{I,Z} + 0.00482$
5.	$\sigma_{I,Z^1Z^2Z^3C} = 0.248 \Sigma \sigma_{I,Z} + 0.00398$
6.	$\sigma_{R,Z^1Z^2Z^3C} = 0.173 \Sigma \sigma_{I,Z} - 0.167$
7.	$\sigma_{R,ZCO} = -0.461 \sigma_{20}^+ + 0.160$
8.	$\sigma_{R^+,ZCO} = 0.197 \sigma_R^+ + 0.439$
9.	$\sigma_{I,ZNH} = 0.236 \sigma_{40}^- + 0.153$
10.	$\sigma_{R,ZNH} = 0.456 \sigma_{I,Z} + 1.43 \sigma_{RZ} - 0.757$
11.	$\sigma_{I,ZO} = 0.434 \sigma_{IZ} + 0.241 \sigma_{RZ} + 0.299$
12.	$\sigma_{R,ZO} = 0.277 \sigma_{60}^- - 0.532$
13.	$\sigma_{I,Z_2PO} = 0.489 \sigma_{30}^+ - 0.320$
14.	$\sigma_{I,ZS} = 0.466 \sigma_{IZ} + 0.260$
15.	$\sigma_{R,ZS} = 0.870 \sigma_{RZ} - 0.175$
16.	$\sigma_{I,ZSO_2} = 0.420 \sigma_{R^+,Z} + 0.645$
17.	$\sigma_{I,ZC\equiv C} = 0.311 \sigma_{IZ} + 0.300$
18.	$\sigma_{I,ZCH=CH} = 0.271 \sigma_{IZ} + 0.278 \sigma_{RZ} + 0.117$
19.	$\sigma_{I,3-ZC_6H_4} = 0.112 \sigma_{IZ} + 0.0474 \sigma_{R^0,Z} + 0.120$
20.	$\sigma_{R,3-ZC_6H_4} = 0.153 \sigma_{IZ} + 0.0761 \sigma_{R^0,Z} - 0.110$
21.	$\sigma_{I,4-ZC_6H_4} = 0.138 \sigma_{IZ} + 0.137 \sigma_{R^0,Z} + 0.120$
22.	$\sigma_{R,4-ZC_6H_4} = 0.180 \sigma_{IZ} + 0.111 \sigma_{R^0,Z} - 0.0988$
23.	$\sigma_{R^+,4-ZC_6H_4} = 0.139 \sigma_{IZ} + 0.218 \sigma_{R^+,Z} - 0.167$
24.	$\sigma_{R^0,Z^1Z^2N} = 0.392 \sigma_{R,Z^1Z^2N} - 0.0992$
25.	$\sigma_{R^0,ZO} = 0.267 \sigma_{R,ZO} - 0.290$
26.	$\sigma_{R^-,ZS} = 0.729 \sigma_{R,ZS} - 0.0564$

$\sigma_{R,ZC=O}^-$ constants gave an excellent correlation with σ_{RZ}^+ alone (set 4RM, Table 43). A comparison of the results obtained for $\sigma_{R,ZC=O}$ and $\sigma_{R,ZC=O}^-$ shows some striking differences. Thus, $\sigma_{R,ZC=O}$ is predominantly dependent on σ_I ($P_R^+ = 20$) whereas $\sigma_{R,ZC=O}^-$ is dependent only on σ_{RZ}^+ ($P_R^+ = 100$). The former is increased by donor Z and decreased by acceptor Z , with the latter, the exact reverse occurs.

The $\sigma_{R,3-ZC_6H_4}$ and $\sigma_{R,4-ZC_6H_4}$ constants are best correlated by Equation 154 using σ_R^0 constants (sets 12R, 13R, Table 44). Unfortunately, there are insufficient data available to permit examination of σ_R , σ_R^+ , and σ_R^- for many W of interest such as $CH=CH$, $C\equiv C$, and CH . Those correlation equations which are best suited for the estimation of new σ_I and σ_D constants are set forth in Table 45. It must be emphasized that these equations should give reasonable estimates when used for interpolation. Extrapolated substituted constants estimated from these equations are *uncertain*.

B. Substituents at Elements Other Than Carbon

In the case of groups W such as O , NH , S , $P=O$, and SO_2 , the substituent is bonded to an element other than carbon. Before correlations with Equations 153 and 154 can be carried out, it is necessary to establish the applicability of the σ_I , σ_R , σ_R^+ , and σ_R^- constants to substituents which are bonded to N , O , P , and S . The applicability of σ_I and σ_R constants defined from substituent effects at carbon to substituents bonded to phosphorus has been clearly demonstrated by the work of Charton and Charton (51–53). These authors have examined the correlation of ionization potentials of Z^1Z^2W and $Z^1Z^2Z^3W$, where W is O , S , and N (54). The results in this case are not sufficient to establish the applicability of σ_I and σ_R constants as the O , S , and N were both skeletal groups and active sites. We have therefore examined the correlation of pK_a s of acids of the type 4- ZW where W is NH , O , S , and SO_2 , with Equations 88 and 129 in the case of NH , O , and S ; and Equations 88 and 103 in the case of SO_2 . The data used in the correlations are presented in Table 46. In the case of $W = NH$, very much better correlation is obtained with the σ_R^- constants (sets 5Am and 5Bm, Table 44) than with the σ_R values (sets 5A and 5B, Table 44). The results show that the σ_I and σ_R^- constants are indeed applicable to substituent effects at nitrogen. The case in which $W = O$ presents a new problem. When correlations with σ_I and σ_R or σ_R^- are carried out the partial correlation coefficients of σ_I on σ_R or σ_R^- constants (r_{12} values) show that the σ_I and σ_R or σ_R^- constants are linear in each other. This situation results from the small number of points and the limited types of Z groups available. To overcome this difficulty we may make use of composite substituent constants. Rearranging Equation 91 we obtain

TABLE 46
 pK_a Values of 4-ZWC₆H₄CO₂H at 25°^a

5A.	W = NH H, 7.77; CHO, 5.70; Ac, 6.84; CO ₂ Et, 6.94; CONH ₂ , 7.03; Bz, 6.95; MeSO ₂ , 6.63; PhSO ₂ , 6.63
5B.	W = NH H, 6.47; CHO, 5.65; Ac, 5.81; CO ₂ Et, 5.91; MeSO ₂ , 5.65; PhSO ₂ , 5.70
6A.	W = O H, 7.29; Me, 7.03; Et, 7.08; Ac, 6.36; Bz, 6.41; MeSO ₂ , 6.06; PhSO ₂ , 6.07
6B.	W = O H, 6.25; Me, 6.03; Et, 6.04; Ph, 5.50; CF ₃ , 5.25; MeSO ₂ , 5.16; PhSO ₂ , 5.22
8B.	W = S Me, 5.74; CN, 4.97; CF ₃ , 4.98; Ac, 5.10; Ph, 5.54; 4-O ₂ NPn, 5.30
9B.	W = SO ₂ Me, 4.68 ^b ; F, 4.33 ^c ; CF ₃ , 4.24; Ph, 4.63; NH ₂ , 4.85

^a A sets are in 80% w/w aqueous MCS; B sets are in 44.1% w/w aqueous EtOH. Data are from footnotes h, q, s, t, Table 27 unless otherwise noted.

^b F. G. Bordwell and G. D. Cooper, *J. Am. Chem. Soc.*, 73, 5184 (1951); 74, 1058 (1952).

^c Footnote u, Table 25.

$$\frac{P_D}{100} (\lambda + \delta) = \delta \quad (163)$$

or

$$\left(\frac{P_D}{100}\right) \lambda = \delta \left(\frac{1 - P_D}{100}\right) \quad (164)$$

Then

$$\delta = \left(\frac{P_D}{100 - P_D}\right) \lambda \quad (165)$$

$$= \frac{P_D}{P_L} \lambda \quad (166)$$

If for convenience we choose to define

$$\lambda \equiv 1 \quad (167)$$

Then

$$\delta = \frac{P_D}{P_L} \quad (168)$$

The composition of some composite substituent constant σ_T is given by Equation 2. Then substituting Equations 167 and 168 into Equation 2 gives

$$\sigma_T = \sigma_I + \left(\frac{P_D}{P_L} \right) \sigma_D \quad (169)$$

We represent these composite substituent constants by the symbol σ_n^d where d is nothing, 0, +, or - depending on whether σ_R , σ_R^0 , σ_R^+ , or σ_R^- is used to calculate σ_n^d . The subscript n is the value of P_D . Thus, σ_{30} is a composite substituent constant with a percent delocalized effect of 30, obtained from σ_I and σ_R , whereas σ_{20}^+ is a composite substituent constant obtained from the σ_I and σ_R^+ constants with a 20% delocalized effect. Values of σ_n^d are tabulated for a number of common groups in Table 47. These constants are useful when σ_I and σ_D are linear in each other, when it is desirable to reduce the number of variables in the correlation equation to increase the number of degrees of freedom, and for plotting data to permit a graphical estimate of the composition of the electrical effect. Correlations with these constants are carried out by means of the simple Hammett equation as in Equation 145.

The $\sigma_{I,ZNH}$ constants gave a highly significant correlation with Equation 129 (set 5, Table 44). The value of r_{12} showed that σ_I and σ_R^- were colinear. A significant correlation was obtained, however, with the σ_{40}^- constants (set 5c, Table 43). The $\sigma_{R,ZNH}$ constants give good correlation with Equation 88 (set 5R, Table 44). The $\sigma_{I,ZO}$ constants also give good correlation with Equation 88 (set 6, Table 44), whereas the $\sigma_{R,ZO}$ constants give best results with Equation 129 (set 6Rm, Table 44). In the latter case, the r_{12} values show that σ_I and σ_R^- are highly colinear. Good results were obtained with the σ_{60}^- constants, however (set 6Rc, Table 43). The $\sigma_{I,ZPO}$ constants gave a good correlation with Equation 103. The r_{12} value indicates some slight colinearity between σ_I and σ_R^+ . The results of a correlation with σ^+ were good. The $\sigma_{I,ZR}$ constants gave a good correlation with σ_{IZ} (set 8, Table 43). The $\sigma_{R,ZS}$ constants were best correlated by σ_{RZ} (set 8R, Table 43). The $\sigma_{R,ZS}$ constants show no correlation with any combination of σ_I and σ_D constants. The σ_{I,ZSO_2} give good results with $\sigma_{R,Z}^+$ alone (set 9, Table 43). The correlation equations useful in the estimation of substituent constants are given in Table 45.

It is of interest to note that the W groups, CO, PO, and SO₂ which are all electron acceptor groups give best results in all cases with σ_R^+ . The best results for the electron donor W groups NH and O may be with either σ_{RZ} or $\sigma_{R,Z}$.

In obtaining the best correlation equations it has frequently been necessary to exclude members of a set. In many cases the range of variation in σ_{ZW} is limited. For these reasons the percent of the data accounted for by the correlation equations is not as great as we would wish. We must emphasize again that the equations in Table 45 are intended for the estimation of otherwise unavailable substituent constants. Unless the number of data points in the set is large, $100r^2$ is >99.00%, and the new constant to be estimated can be found by interpolation rather than by extrapolation, all substituent constants estimated by means of

TABLE 47
Values of σ_n^d

X	n = 10	20	30	40	50	60	70	80	90
Me	-0.03	-0.05	-0.08	-0.12	-0.17	-0.25	-0.38	-0.65	-1.45
Et	-0.03	-0.05	-0.07	-0.10	-0.15	-0.22	-0.34	-0.57	-1.27
Pr = Me									
<i>i</i> -Pr	-0.01	-0.03	-0.06	-0.10	-0.15	-0.23	-0.36	-0.63	-1.43
Bu = Me									
ViCH ₂	0.00	-0.02	-0.04	-0.07	-0.12	-0.19	-0.31	-0.54	-1.24
Ph	0.11	0.09	0.07	0.05	0.01	-0.05	-0.14	-0.32	-0.87
PhCH ₂	0.02	0.00	-0.03	-0.06	-0.10	-0.17	-0.27	-0.49	-1.14
CF ₃	0.41	0.43	0.45	0.47	0.51	0.57	0.66	0.84	1.39
CHO	0.32	0.34	0.36	0.40	0.45	0.53	0.65	0.90	1.65
CONH ₂	0.29	0.30	0.31	0.33	0.36	0.40	0.47	0.60	1.00
Ac	0.32	0.35	0.39	0.43	0.50	0.60	0.77	1.10	2.10
CO ₂ Et	0.31	0.33	0.35	0.37	0.41	0.47	0.56	0.74	1.29
Bz = CO ₂ Et									
NH ₂	0.08	-0.03	-0.17	-0.36	-0.63	-1.03	-1.70	-3.03	-7.03
NMe ₂	0.07	-0.05	-0.21	-0.42	-0.71	-1.15	-1.88	-3.35	-7.75
OH	0.17	0.09	-0.03	-0.17	-0.38	-0.69	-1.21	-2.24	-5.34
OMe	0.24	0.16	0.05	-0.09	-0.28	-0.57	-1.05	-2.02	-4.92
OEt	0.22	0.14	0.04	-0.10	-0.29	-0.58	-1.05	-2.00	-4.85
OPh	0.35	0.28	0.19	0.08	-0.08	-0.32	-0.72	-1.52	-3.92
MeS	0.26	0.21	0.14	0.05	-0.08	-0.27	-0.59	-1.22	-3.12
PhS	0.28	0.25	0.21	0.15	0.07	-0.05	-0.25	-0.65	-1.85
MeSO ₂	0.60	0.62	0.64	0.66	0.70	0.76	0.85	1.03	1.58
PhSO ₂	0.57	0.59	0.61	0.64	0.68	0.74	0.84	1.04	1.64
CF ₃ SO ₂	0.73	0.76	0.80	0.85	0.92	1.03	1.20	1.55	2.60
MeSO	0.54	0.54	0.54	0.54	0.54	0.54	0.54	0.54	0.54
4-MeOPh	0.09	0.06	0.03	-0.02	-0.08	-0.18	-0.33	-0.65	-1.60
H	0	0	0	0	0	0	0	0	0
CN	0.58	0.59	0.60	0.62	0.65	0.69	0.76	0.89	1.29
NO ₂	0.68	0.70	0.71	0.74	0.77	0.82	0.90	1.07	1.57
F	0.49	0.42	0.33	0.22	0.06	-0.18	-0.58	-1.38	-3.78
Cl	0.44	0.41	0.36	0.30	0.22	0.10	-0.13	-0.53	-1.78
Br = Cl									
I	0.38	0.36	0.33	0.29	0.24	0.16	0.03	-0.24	-1.04
SF ₅	0.59	0.60	0.60	0.61	0.62	0.64	0.66	0.71	0.86

Values of σ_n^+

Ph	0.10	0.08	0.05	0.01	-0.05	-0.14	-0.28	-0.56	-1.41
CF ₃	0.42	0.44	0.46	0.50	0.55	0.63	0.75	1.00	1.75
NH ₂	0.05	-0.11	-0.30	-0.56	-0.93	-1.48	-2.40	-4.23	-9.73
NMe ₂	0.03	-0.14	-0.35	-0.64	-1.05	-1.66	-2.68	-4.71	-10.81
OH	0.17	0.08	-0.03	-0.19	-0.40	-0.72	-1.25	-2.32	-5.52
OMe	0.23	0.14	0.02	-0.14	-0.36	-0.69	-1.24	-2.34	-5.64
OEt	0.21	0.12	0.00	-0.15	-0.37	-0.70	-1.24	-2.32	-5.57
SMe	0.24	0.16	0.06	-0.07	-0.25	-0.53	-0.98	-1.9	-4.65

TABLE 47
 Values of σ_n^d

X	<i>n</i> = 10	20	30	40	50	60	70	80	90
4-MeOPn	0.08	0.04	-0.01	-0.07	-0.16	-0.30	-0.52	-0.97	-2.32
SOMe	0.53	0.52	0.50	0.47	0.44	0.39	0.31	0.14	-0.36
F	0.50	0.45	0.38	0.29	0.17	-0.02	-0.32	-0.94	-2.79
Cl	0.45	0.42	0.38	0.33	0.26	0.16	-0.02	-0.37	-1.42
Br	0.45	0.42	0.39	0.34	0.28	0.19	0.03	-0.29	-1.24
I \equiv I, σ_n									
Values of σ_n^-									
Me	-0.02	-0.03	-0.05	-0.07	-0.10	-0.15	-0.22	-0.37	-0.82
Et	-0.02	-0.03	-0.04	-0.06	-0.08	-0.12	-0.17	-0.29	-0.64
Pr \equiv Me									
<i>i</i> -Pr	0.00	-0.01	-0.03	-0.05	-0.08	-0.13	-0.20	-0.35	-0.80
Ph	0.12	0.11	0.10	0.09	0.08	0.06	0.03	-0.04	-0.24
PhCH ₂	0.02	0.02	0.00	-0.01	-0.03	-0.06	-0.11	-0.21	-0.51
CF ₃	0.42	0.45	0.48	0.52	0.58	0.67	0.82	1.12	2.02
CHO	0.36	0.43	0.53	0.65	0.83	1.10	1.54	2.42	5.07
CONH ₂	0.31	0.34	0.38	0.43	0.51	0.63	0.82	1.20	2.35
Ac	0.35	0.40	0.48	0.57	0.71	0.92	1.26	1.94	3.99
CO ₂ Et	0.33	0.38	0.43	0.51	0.61	0.77	1.02	1.54	3.09
Bz \equiv Ac									
NH ₂	0.11	0.03	-0.07	-0.20	-0.38	-0.66	-1.11	-2.03	-4.78
MeS	0.27	0.24	0.20	0.14	0.06	-0.06	-0.26	-0.66	-1.86
PhS	0.30	0.29	0.28	0.26	0.23	0.19	0.12	-0.01	-0.41
MeSO ₂	0.63	0.68	0.74	0.82	0.94	1.12	1.41	1.99	3.74
MeSO	0.55	0.55	0.56	0.57	0.59	0.62	0.66	0.74	0.99
CF ₃ SO ₂	0.78	0.87	0.98	1.13	1.34	1.66	2.18	3.23	6.38
NO ₂	0.71	0.76	0.83	0.92	1.04	1.23	1.53	2.15	4.00
CN	0.60	0.64	0.68	0.74	0.83	0.96	1.18	1.61	2.91
F	0.48	0.40	0.29	0.15	-0.04	-0.33	-0.81	-1.78	-4.68
Cl	0.44	0.40	0.34	0.27	0.17	0.02	-0.23	-0.73	-2.23
Br	0.44	0.40	0.35	0.28	0.19	0.05	-0.18	-0.65	-2.05
I	0.38	0.36	0.32	0.28	0.22	0.13	-0.02	-0.32	-1.22

the equation in Table 45 are uncertain. This does not diminish the utility of the estimated constants. An educated guess is preferable to total ignorance.

C. Other Methods of Estimation of Substituent Constants

In some cases we observe the relationship

$$\sigma_{D,ZW} = a_1 \sigma_{R,ZW} + a_0 \quad (170)$$

Sets of $\sigma_{D,ZW}$ that obey Equation 170 are given in Table 42. From Equations 154 and 170 and the equation

$$\sigma_{R,ZW} = L\sigma_{IZ} + D\sigma_{DZ} + h \quad (171)$$

we obtain

$$L'\sigma_{IZ} + D'\sigma_{DZ} + a' = a_1L\sigma_{IZ} + a_1D\sigma_{DZ} + a_1h + a_0 \quad (172)$$

Thus,

$$L' = a_1L, D' = a_1D, a' = a_1h + a_0 \quad (173)$$

From Equation 91

$$P_{D,\sigma_{DZW}} = \frac{D' \cdot 100}{L' + D'} = \frac{a_1D \cdot 100}{a_1L + a_1D} = P_{D,\sigma_{RZW}} \quad (174)$$

Then Equation 170 may be expected to hold only when:

1. Both $\sigma_{R,ZW}$ and $\sigma_{D,ZW}$ are a function of the same type of $\sigma_{D,Z}$ (thus, both are a function of σ_R , or σ_R^- , etc.)
2. Equation 174 is obeyed, thus $\sigma_{D,ZW}$ and $\sigma_{R,ZW}$ have the same percent delocalized effect and therefore the same composition.

When Equation 170 is obeyed, we may use it to estimate $\sigma_{D,ZW}$ constants. Again, constants may be fairly well estimated by interpolation; those obtained by extrapolation are uncertain. Correlations with Equation 170 are given in Table 43. Equations suitable for the calculation of substituent constants are set forth in Table 45.

Values of σ_I and σ_R can be estimated when the corresponding σ_m and σ_p values are known. For the reasons discussed in Section IV.D, such estimates are unreliable. If the correlation equations are known, better estimates can be made from the equations;

$$Q_m = L_m \sigma_{IX} + D_m \sigma_{DX} + h_m \quad (175)$$

$$Q_p = L_p \sigma_{IX} + D_p \sigma_{DX} + h_p \quad (176)$$

when the rate or equilibrium constants for the *meta*- and *para*-substituted compounds, Q_m and Q_p are known. Solving Equation 175 for σ_{IX} gives

$$\sigma_{IX} = \frac{Q_m - D_m \sigma_{DX} - h_m}{L_m} \quad (177)$$

Substituting Equation 177 into Equation 176 gives

$$Q_p = \frac{L_p}{L_m} (Q_m - D_m \sigma_{DX} - h_m) + D_p \sigma_{DX} + h_p \quad (178)$$

Solving for σ_{DX} gives

$$\sigma_{DX} = \frac{Q_p - (L_p/L_m)(Q_m - h_m) - h_p}{D_p - [(h_p D_m)/L_m]} \quad (179)$$

With σ_{DX} known, Equation 177 can be used to calculate σ_{IX} . Constants obtained in this manner are uncertain.

Finally, we may note that AkW groups show essentially no variation in σ with change in the Ak group and that the average values given for σ_{AkW} in Tables 21 and 32 and on p. 215 make possible the calculation of fairly reliable values for a large number of groups of this type.

VI. SEPARATION OF ELECTRICAL EFFECTS

A. Swain-Lupton Separation

There are three other major sets of localized and delocalized effect substituent constants: those proposed by Swain and Lupton (25) and modified by Hanch and his co-workers, those of Exner (24*i,j*), and those of Ehrenson, Brownlee, and Taft (1). Regarding the modified Swain-Lupton constants (MSL constants) a number of papers have appeared which suggest that these constants are incorrect. As, in spite of this, the SL and MSL constants continue to be used, we review here the arguments which show that they are incorrectly scaled and do not successfully separate electrical effects. The SL separation is based on the claim that the delocalized electrical effect of the trimethylammonio group is zero. It is suggested that the ultraviolet spectrum of the phenyltrimethylammonium ion supports this conclusion. It is further suggested that the localized electrical effect of a substituent in the *meta* position of a benzene derivative is greater than the effect of the same group in the *para* position since the mode of transmission is the field effect. Finally, the SL approach requires the trimethylammonio group to be no more dependent on the medium than dipolar groups such as methoxy, cyano, and nitro.

With regard to the delocalized electrical effect of the NMe_3^+ group, as it is isoelectronic with the tertiary butyl group which is well known to be a delocalized effect electron donor (thus, σ_R , σ_R^+ , σ_R^- , and σ_R^0 for the *t*-Bu are -0.18 , -0.13 , -0.11 , and -0.18 , respectively), it would also be a delocalized electron effect donor group. In support of this contention are studies of infrared spectra of *para*- and *meta*-substituted benzenes (55,56,62), pK_a measurements (57,58) and nmr results (59-61), and SCF-MO calculations indicating that NH_3^+ is an electron donor by the delocalized effect (61) which supports the argument that NMe_3^+ is.

Our results for σ_R , σ_R^+ , σ_R^- and σ_R^0 for NMe_3^+ are -0.11 , -0.31 , -0.45 , and -0.32 . It is very nearly certain that the NMe_3^+ group is indeed a delocalized effect donor group and therefore the basic assumption of the SL and MSL approaches is *wrong*.

With regard to the effect of medium on σ_m and σ_p values for NMe_3^+ ; Table

TABLE 48
 σ Values for the NMe_3^+ Group and the Corresponding C_L Values

σ_m	Source	σ_p	Source	Solvent	C_L^e
0.88 ± 0.2	<i>a</i>	0.82 ± 0.2	<i>a</i>	50% v/v EtOH-H ₂ O	1.07
1.03	<i>b</i>	0.98	<i>b</i>	H ₂ O	1.05
1.18	<i>b</i>	1.05	<i>b</i>	50% v/v EtOH-H ₂ O	1.12
1.08	<i>c</i>	0.94	<i>c</i>	50% v/v EtOH-H ₂ O	1.15
1.01	<i>b</i>	0.86	<i>b</i>	65% v/v DMSO-H ₂ O	1.17

^a Ref. 28.

^b M. Hojo, M. Utake, and Z. Yoshida, *Tetrahedron*, 27, 4255 (1971).

^c Values reported by J. D. Roberts, A. Clement, and J. J. Drysdale, as corrected in *b*.

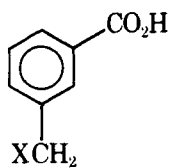
^d C. F. Wilcox Jr. and J. S. McIntyre, *J. Org. Chem.*, 30, 777 (1965).

^e Calculated from Eq. 180.

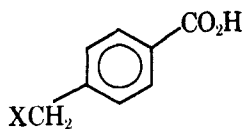
48 reports those values now available. The range in σ is 0.2–0.3. The values used by Swain and Lupton to define SL constants are those given by McDaniel and Brown who suggested errors of $\pm 0.2 \sigma$ units for them. Little credence at best can be placed in constants based on so unreliable a foundation.

Regarding the argument that the field effect transmits the localized effect more effectively from the *meta* than from the *para* position, in benzene derivatives, our results for the C_L values obtained from benzoic acids in water and aqueous mixed solvents show that C_L is not significantly different from 1.00. Further evidence on this point is available from field effect calculations and from a consideration of model systems.

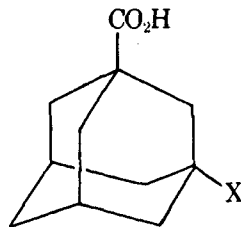
Suitable model systems for the estimation of C_L should be free of the delocalized effect and should have a geometry closely resembling that of the *meta*- or *para*-substituted benzoic acids. There are two model systems that meet these requirements. They are the 3- and 4-substituted methyl benzoic acids, **VI** and **VII**; and the 3-substituted adamantane-1-carboxylic acids, **VIII**, and 4-substituted bicyclo[2.2.2]octane-1-carboxylic acids (**I**). In both model systems, the delocalized effect is unimportant. The geometry of the substituted methylbenzoic acids is only approximately similar to that of the corresponding benzoic acids. The geometry of **I** is very similar to that of 4-substituted benzoic acids, as was noted previously; that of **VIII** is fairly close to that of 3-substituted benzoic acids.



VI



VII



VIII

TABLE 49
Evaluation of C_L from Model Systems

Model System		Sets ^a	Solvent ^b	$-L_m$	$-L_p$	C_L
<i>m</i>	<i>p</i>					
VI	VII	41, 43	A	0.729	0.905	0.806
VI	VII	42, 44	B	0.832	0.964	0.863
VIII	I	31, 01	C	1.47	1.55	0.948
VIII	I	32, 01	A	1.39	1.56	0.891
VIII	I	32, 18	A	1.39	1.44	0.965

^a From Table 8; L values from Table 9.

^b A, 50% v/v aq. EtOH; B, 80% w/w aq. MCS; C, 50% w/w aq. EtOH.

Values of C_L calculated from the model systems are given in Table 49. If the assumption of Swain and Lupton were valid,

$$\sigma_{m, NMe_3^+} = L_m \sigma_{I, NMe_3^+}$$

$$\sigma_{p, NMe_3^+} = L_p \sigma_{I, NMe_3^+}$$

and

$$C_L = \frac{\sigma_{m, NMe_3^+}}{\sigma_{p, NMe_3^+}} \quad (180)$$

Values of C_L calculated from Equation 180 are given in Table 48. The average C_L value of 1.112 ± 0.051 is obtained. This value is very much different from the average values obtained for the model systems or the average value obtained for the 3- and 4-substituted benzoic. They are 0.835, 0.935, and 1.00, respectively.

We may now consider the calculations of the field effect as a means of estimating C_L . All such calculating as we have remarked previously (Section I) are based on the work of Kirkwood and Westheimer (KW). These calculations are also sensitive to the choice of the location of the dipole and of the charge. The original KW work located the charge (the proton to be removed) on an axis through the carbonyl carbon of the benzoic acid, and C¹ and C⁴ of the ring, 1.45 Å from the carboxyl carbon. This KW model has been used by a number of authors (26a, 26b, 63). Charton (19, 24k) modified the model slightly using the actual location of the proton as the site of the charge (KW* model). Bowden (64) located the charge on the KW axis 0.89 Å from the carboxyl carbon (KWB model). Wiberg (65) located the charge on either oxygen atom in the carboxylate ion (KWW model). Wells, Ehrenson, and Taft (4) do not indicate where they have located the charge. They have shifted the location of the dipole to varying distances from the ring (KWWET method). The argument for this is that the location of the dipole must itself be uncertain. All the other methods described previously locate the dipole at the midpoint of the X—C bond (where X is the

TABLE 50
 Field Effect Calculations of C_L

Method	C_L	Method	C_L
KW	0.967	KW*	0.945
KWB	1.010	KWW*	1.004
KW(1)	0.956	KW(2)	0.936

substituent) as is shown in Fig. 1. In any consideration of the field effect model, the following point must be made. L values can be successfully calculated from the equation

$$L_G = \frac{\cos\theta_G \phi_{G^0}}{r_G^2} \quad (181)$$

where G is some skeletal group, G^0 is the reference skeletal group, *para*-phenylene, and

$$\phi_{G^0} = \frac{L_{G^0} r^2_{G^0}}{\cos\theta_{G^0}} \quad (182)$$

with r and θ defined in Figure 1. These calculations were carried out with the KW* method. Bowden (64) has also carried out successful calculations which are equivalent to the calculation of L using the KWB method. In both methods, the dipole midpoint is located as in the original KW method, at the midpoint of the X—C bond. The very success of the original Hammett equation, in which the members of a single data set frequently vary greatly in the size, shape, and degree of partial charge on the substituent, shows that small variations in molecular size and shape are not significant. We would suggest that in view of the successful calculations of Bowden and of Charton, the original choice of location of the dipole by Kirkwood and Westheimer is best. From Equation 181 and 182, with $G = meta$ -phenylene, we obtain,

$$\frac{L_m}{L_p} = C_L = \frac{\cos\theta_m r_p^2}{\cos\theta_p r_m^2} \quad (183)$$

Values of C_L calculated by the KW, KW*, KWB, and KWW* model (in which the proton is located at the midpoint of the C—X bond rather than at the X group as in the original Wiberg model) are given in Table 50. Also given are modifications of the KW method in which the proton is located at 1.65 (KW1) and 1.95 (KW2) Å from the carbonyl carbon on the axis defined previously. The results indicate a C_L value of about 1 in agreement with the value observed for the benzoic acids in aqueous media, as we have noted previously. The values from the model systems are also in better agreement with a C_L of 1 than with a C_L value of about 1.1. This is particularly true for the VIII, I model system which

reflects the geometry of the *meta*- and *para*-phenylene groups much more accurately than does the VI, VIII model system. Thus, all of these results, although not conclusive, support the argument against the SL separation. As we have already shown that the MSL-F constants give very much poorer correlations, than do the σ_I constants given here, and we have reviewed a number of papers which claim that NMe_3^+ is a delocalized effect donor, we can only conclude that the SL and MSL constants are incorrectly scaled and inferior to those given in this work.

B. Exner Separation

There remains the question of the validity of the Exner approach. We have noted earlier that Charton has shown that Exner's equation (Eq. 25) can be accounted for if σ_{IX} is proportional to σ_{RX} . To shed further light on this point we have examined the correlation with Equation 36 of a number of sets (of benzoic acid $\text{p}K_{a,s}$) containing isodelocalized substituents. The sets studied are in Table 51; the results of the correlations are given in Table 52. The correlations are very good; they provide further evidence for the validity of the σ_I and σ_R constants reported here. The arguments of Exner concerning Equation 25, in which he assumes that the delocalized effect of the groups which obey Equation 25 is negligible, is a special case of a more general relationship. We may write Equation 88 for $\text{p}K_{a,3}$ and $\text{p}K_{a,4}$ of 3- and 4-substituted benzoic acids.

$$\text{p}K_{a,3X} = L_3 \sigma_{IX} + D_3 \sigma_{RX} + h \quad (184)$$

$$\text{p}K_{a,4X} = L_4 \sigma_{IX} + D_4 \sigma_{RX} + h \quad (185)$$

If an isodelocalized data set is used, σ_{RX} is a constant, and

$$\text{p}K_{a,3X} = L_3 \sigma_{IX} + D_3 C^* + h = \sigma_3 \sigma_{IX} + h' \quad (186)$$

$$\text{p}K_{a,4X} = L_4 \sigma_{IX} + D_4 C^* + h = L_4 \sigma_{IX} + h'' \quad (187)$$

Then,

$$\frac{(\text{p}K_{a,4X} = h'')}{L_4} = \sigma_{IX} \quad (188)$$

and

$$\text{p}K_{a,3X} = \frac{L_3}{L_4} \text{p}K_{a,4X} - \frac{L_3 h''}{L_4} + h' \quad (189)$$

or

$$\text{p}K_{a,3X} = C_L \text{p}K_{a,4X} + a_0 \quad (190)$$

TABLE 51
Data Used in Correlations with Equations 36 and 191

1M.	A, $\sigma_R = 0.10$ CCl ₃ , 5.95; CF ₃ , 5.95; CO ₂ H, 6.09; NO ₂ , 5.44; SO ₂ Me, 5.61; CN, 5.65
1P.	A, $\sigma_R = 0.10$ CCl ₃ , 5.85; CF ₃ , 5.72; CO ₂ H, 5.93; NO ₂ , 5.29; SO ₂ Me, 5.49; CN, 5.52
2M.	B, $\sigma_R = 0.10$ CF ₃ , 5.08; CO ₂ Et, 5.12; NO ₂ , 4.60; SO ₂ Me, 4.77; CN, 4.82; SiMe ₃ , 6.00
2P.	B, CF ₃ , 4.92; CO ₂ Et, 5.00; NO ₂ , 4.43; SO ₂ Me, 4.67; CN, 4.67; SiMe ₃ , 5.80
3M.	C, $\sigma_R = 0.10$ NO ₂ , CN, CO ₂ Me
3P.	C, $\sigma_R = 0.10$ NO ₂ , CN, CO ₂ Me, SO ₂ Me
4M.	B, NO ₂ , CF ₃ , CN, CO ₂ Me, SO ₂ Me
4P.	B, $\sigma_R = 0.10$ NO ₂ , CF ₃ , CN, CO ₂ Me, SO ₂ Me, SiMe ₃
5M.	D, $\sigma_R = 0.10$ NO ₂ , CN, CO ₂ Me, SO ₂ Me
5P.	D, $\sigma_R = 0.10$ NO ₂ , CN, CO ₂ Me, SO ₂ Me
6M.	A, $\sigma_R = -0.15$ Me, 6.82; PhCH ₂ , 6.76; SCN, 5.82; I, 6.05
6P.	A, $\sigma_R = -0.15$ Me, PhCH ₂ , SCN, I, 6.15
7M.	B, $\sigma_R = -0.15$ Me, 5.90; PhCH ₂ , 5.84; SCN, 4.99; I, 5.26; <i>c</i> -hexyl, 5.93
7P.	B, $\sigma_R = -0.15$ Me, 5.96; PhCH ₂ , 5.88; SCN, 4.97; <i>i</i> -Pr, 5.89; <i>c</i> -hexyl, 5.89
8M.	B, $\sigma_R = -0.15$ Me, 5.60; Et, 5.65; <i>i</i> -Pr, 5.71; Ph, 5.46; I, 5.05
8P.	B, $\sigma_R = -0.15$ Me, 5.69; Et, 5.70; <i>i</i> -Pr, 5.71; Ph, 5.45; I, 5.11; PhCH ₂ , 5.62; Vi, 5.51
9M.	D, $\sigma_R = -0.15$ Me, 6.41; Et, 6.43; <i>i</i> -Pr, 6.44; Ph, 6.15; I, 5.74
9P.	D, $\sigma_R = -0.15$ Me, 6.50; Et, 6.49; <i>i</i> -Pr, 6.48; Ph, 6.21; I, 5.79; PhCH ₂ , 6.37
10M.	A, $\sigma_R = -0.25$ Me ₃ SiCH ₂ , 6.98; MeSO ₂ O, 5.96; AcO, 6.19; Cl, 5.99; Br, 5.97
10P.	A, $\sigma_R = -0.25$ Me ₃ SiCH ₂ , 7.03; MeSO ₂ O, 6.06; AcO, 6.36; Cl, 6.13; Br, 6.10
11M.	B, $\sigma_R = -0.25$ Me ₃ SiCH ₂ , 6.02; MeSO ₂ O, 5.12; AcO, 5.17; Cl, 5.11; Br, 5.11
11P.	B, $\sigma_R = -0.25$ Me ₃ SiCH ₂ , 6.10; MeSO ₂ O, 5.16; AcO, 5.30; Cl, 5.20; Br, 5.27; PhS, 5.54

All data are pK_a s at 25° for (M) 3-XC₆H₄CO₂H and (P) 4-XC₆H₄CO₂H.
 A. 80% w/w aq. MCS. B. 44.1% w/w aq. EtOh. C. 8.06% w/w aq. EtOH. D. 75% v/v aq. EtOH.
 pK_a s for sets 3M, 3P, 4M, 4P, 5M, 5P, 8M, 8P, 9M, 9P, are from B. M. Wepster, private

TABLE 52
Results of Correlations of Isodelocalized Sets with Equation 36

Set	$-L$	h	r^a	F^b	s_{est}^c	s_L^c	s_h^c	100 r^2 ^d	n^e
1M	1.61	6.54	0.9915	233.1	0.0350	0.106	0.0529	98.31	6
1P	1.62	6.41	0.9900	196.3	0.0383	0.116	0.0579	98.00	6
2M	1.73	5.76	0.9918	240.6	0.0712	0.112	0.0536	98.36	6
2P	1.66	5.59	0.9932	290.9	0.0623	0.0976	0.0469	98.64	6
3M	1.19	4.39	0.9997	1471. ^m	0.0793	0.0311 ^o	0.0168 ⁱ	99.93	3
3P	1.03	4.23	0.9996	2683.	0.0520	0.0198	0.0110	99.93	4
4M	1.74	5.54	0.9944	353.0	0.0589	0.0926	0.0447	98.88	6
4P	1.55	5.33	0.9995	3826.	0.0159	0.0251	0.0121	99.90	6
5M	2.03	6.38	0.9693	31.08 ⁿ	0.0957	0.365 ⁿ	0.202 ⁱ	93.95	4
5P	1.68	6.10	0.9978	461.4 ^l	0.0204	0.0780 ⁱ	0.0432	99.57	4
6M	1.80	6.80	0.9988	833.2 ^l	0.0302	0.0623 ⁱ	0.0214	99.76	4
6P	1.48	6.79	0.9957	230.3 ^l	0.0473	0.0977 ⁱ	0.0336	99.14	4
7M	1.62	5.90	0.9991	1660.	0.0211	0.0398	0.0122	99.82	5
7P	1.69	5.92	0.9988	1230.	0.0239	0.0482	0.0121	99.76	5
8M	1.48	5.65	0.9819	80.43 ^l	0.0580	0.166 ⁱ	0.0309	96.40	5
8P	1.46	5.68	0.9900	247.2	0.0332	0.0929	0.0152	98.02	7
9M	1.71	6.41	0.9921	187.6	0.0436	0.125	0.0233	98.43	5
9P	1.72	6.46	0.9924	260.4	0.0380	0.107	0.0182	98.49	6
10M	1.88	6.91	0.9922	191.1	0.0626	0.136 ^o	0.0573	98.45	5
10P	1.75	6.98	0.9940	247.0	0.0512	0.111	0.0469	98.80	5
11M	1.68	5.95	0.9884	84.56 ^m	0.0844	0.183 ^o	0.0791	97.69	4
11P	1.68	6.05	0.9959	364.4	0.0407	0.0879	0.0361	99.18	5

For footnotes, see Tables 9, 30, and 43.

where

$$h' = D_2C^* + h, h'' = D_4C^* + h \quad (191)$$

Thus, Exner claims $1/C_L = 1.14$ or $C_L = 0.877$. We have carried our correlations with Equation 191; the results are presented in Table 53 (sets 1–11). A Student t test shows that certainly in five and probably two more sets, the C_L values observed are significantly different from the value given by Exner (See

communication. Other pK_a values are from footnotes, h, q, s, t, Table 28, unless otherwise noted.

^a J. D. Roberts and C. M. Regan, *J. Am. Chem. Soc.*, 75, 4102 (1953).

^b F. G. Bordwell and P. J. Bolton, *J. Am. Chem. Soc.*, 78, 854 (1956).

^c Footnote l, Table 25.

^d J. J. Monagle, J. V. Mengenhauer, and D. A. Jones Jr., *J. Org. Chem.*, 32, 2477 (1967).

^e Footnote d, Table 27.

^f E. N. Tsvetkov, D. I. Lobanov, M. M. Makhamatkhonov, and M. I. Kabachnik, *Tetrahedron*, 25, 5623 (1969).

^g W. Bright and H. T. Briscoe, *J. Am. Chem. Soc.*, 37, 787 (1933).

TABLE 53
Results of Correlations with Equation 190

Set	C_L	a_0	r^a	F^b	s_{est}^c	$s_{C_L}^c$	$s_{a_0}^c$	100 r^{2d}	n^e	t^g
1	0.990	0.190	0.9961	512.1	0.0237	0.0437	0.247 ^j	99.22	6	2.586 ^k
2	1.04	-0.0402	0.9981	1063.	0.0341	0.0319	0.157 ^g	99.63	6	5.110 ⁱ
3	1.17	-0.535	1.000	20534.	0.00212	0.00813 ⁱ	0.0301 ⁿ	100.00	3	36.04 ^o
4	1.12	-0.441	0.9956	447.9	0.0523	0.0530	0.250 ^p	99.11	6	4.585 ^o
5	1.19	-0.913	0.9530	19.79 ⁿ	0.118	0.268 ⁿ	0.139 ^h	90.82	4	1.168 ^j
6	1.21	-1.40	0.9984	628.2 ^l	0.0347	0.0482 ⁱ	0.310 ⁿ	99.68	4	6.909 ⁿ
7	0.954	0.252	0.9956	226.0 ^j	0.0518	0.0634 ⁱ	0.361 ^h	99.12	4	1.215 ^j
8	1.01	-0.0766	0.9873	116.1 ^l	0.0485	0.0935 ⁱ	0.517 ^g	97.48	5	1.422 ^j
9	0.980	0.0653	0.9983	873.4	0.0204	0.0332	0.209 ^h	99.66	5	3.102 ^k
10	1.07	-0.585	0.9969	482.7	0.0396	0.0489	0.310 ^j	99.38	5	3.947 ⁿ
11	1.01	-0.133	0.9940	164.1 ⁱ	0.0609	0.0786 ⁱ	0.428 ^h	98.80	4	1.692 ^j

For footnotes a-p. see Tables 9, 30, and 43.

^g Student t test for significance of difference between C_L observed and the Exner C_L value of 0.877. Superscript indicates confidence level.

Table 53). Another argument against the validity of Exner's conclusions is that if the value of 0.877 were valid, the values obtained here should be equally likely to be larger or smaller than it. This is not the case; C_L for all of the sets studied is larger than 0.877.

Finally, a correlation of σ_{IX} with σ_{RX} for the groups studied by Exner was significant at the 99.9% confidence level. Thus, for the groups studied by Exner, a variant of Equation 25

$$\sigma_{IX} = c\sigma_{RX} + h \quad (192)$$

is obeyed. It seems to us that this conclusively refutes the claims of Exner.

VII. HIGHLY VARIABLE SUBSTITUENT "CONSTANTS"

There are two types of substituent that show a very great dependence on the nature of the medium. They are ionic groups and HW groups.

A. Ionic Groups

All ionic substituent "constants" are very variable, probably due to their dependence upon the type of solvent and the ionic strength of the solution. It is for this reason that we have labeled all substituent constants for these groups uncertain, no matter how small the error reported for the ionization constants from which they were determined. Use of these constants should be avoided when

possible. We would suggest that if they must be used, it is under the following conditions.

1. The medium in which they are to be used is as similar as possible to that in which the ionization constants from which they were calculated is determined.
2. A comparison of the regression coefficients obtained for the set including the ionic groups shows no difference.
3. Their inclusion does not result in a meaningful change in the value of $100r^2$ for the set from the value obtained when they are excluded.

The "constants" reported in the tables were listed largely to provide an estimate of the effect of these groups.

B. HW Groups

Groups of this type include $W = O$, NH , OCH_2 , and $\text{---}OC \overset{O}{\parallel}$. Of these, the worst offender is the OH group for which $W = O$. We would suggest that the rules given in the section preceding for ionic groups be applied to the OH group as well. The other groups mentioned, CO_2H , CH_2OH , and NH_2 are to our knowledge, much better behaved than is the OH group. All the σ values for the latter are considered uncertain. We propose that the other groups simply be treated with caution.

VIII. CONCLUSIONS

The substituent constants presented here are the best obtainable from chemical reactivities at the present time. They are generally applicable in protic solvents. The sparse data available suggests that they are probably applicable in dipolar aprotic and nonpolar solvents and in the gas phase. These statements do not apply to ionic substituents or to the OH group, all of which are strongly dependent on medium. The σ_I constants reported here are the best choice for any correlation of substituent effects of groups attached to sp^3 hybridized carbon. The σ^* constants are inferior and *should not be used*. The evidence presented here clearly indicates that the *use of Swain-Lupton constants* or their modifications *should be discontinued*. The "correction" proposed by Exner for σ_I and σ_R constants is in error. These "corrected" constants should not be used.

A number of equations have been proposed for the estimation of substituent

constants that are unavailable from experimental data. Constants calculated from these equations are *uncertain*. The work on these estimation equations emphasizes the applicability of the σ_I and σ_D constants to substituents bonded to elements other than carbon. There is a remarkable lack of quantitative chemical reactivity data for such systems.

The remarks of Ehrenson, Brownlee, and Taft (1), and of Charton (66) with regard to the use of well-characterized data sets cannot be sufficiently underscored. Although certainly some data are better than none, no definitive conclusion concerning structural effects can be reached.

Much remains to be done with regard to the σ_R^0 , σ_R^+ , and σ_R^- constants for which the paucity of experimental data is amazing, and the quality of much of what is available is poor. As more experimental data becomes available, not only can more substituent constants be obtained but, at least as important, the equations for the estimation of substituent constants can be refined. The availability of large numbers of reliable substituent constants very much increases the utility of correlation analysis as a method of predicting substituent effects on chemical reactivity, biological activity and physical properties.

ACKNOWLEDGMENT

The author gratefully acknowledges the aid of Prof. Bart M. Wepster, Laboratory of Organic Chemistry, Delft University of Technology who make available many unpublished pK_a values; Prof. R. D. Topsom, Department of Chemistry, LaTrobe University (Australia), for helpful discussion; Prof. R. W. Taft, Department of Chemistry, University of California, Irvine, for making available unpublished results; B. I. Charton, Chemistry Department, Pratt Institute, for assistance in many of the correlations, and Prof. T. Fujita, Department of Agricultural Chemistry, Kyoto University for his comments on part of the manuscript. Finally, many thanks are due to the Pratt Institute Computer Center in general and Donald Owings in particular for their helpfulness and patience.

APPENDIX

The Use of P_D as a Measure of the Composition of the Electrical Effect

We may conveniently express the composition of the overall substituent effect and compare the composition in different data sets by choosing a reference substituent X^0 and then calculating the contributions of the different component substituent effects to the value of Q (the correlatable quantity), for X^0 . Consider the case of the LD Equation (Equation 19)

$$Q_{X^0} = L\sigma_{IX^0} + D\sigma_{DX^0} + h \quad (193)$$

Then the contribution of the localized and delocalized electrical effects will be given by

$$Q_{X^0} - h = L\sigma_{IX^0} + D\sigma_{DX^0} \quad (194)$$

We must now select a reference substituent. For this purpose we choose the hypothetical group X_r for which

$$\sigma_{I,X_r} \equiv \sigma_{D,X_r} = 1 \quad (195)$$

Then

$$Q_{X_r} - h = L + D \quad (196)$$

The fraction of the overall electrical effect due to the delocalized effect is then given by

$$\frac{|D|}{|L| + |D|} = f_D \quad (197)$$

and on multiplying by 100, we obtain

$$P_D = \frac{|D| \cdot 100}{|L| + |D|} \quad (198)$$

Thus comparing P_D values is equivalent to comparing the substituent effect on different data sets of the hypothetical reference group X_r .

The method can be extended to any type of correlation equation. For the general case, consider the correlation equation

$$Q = \sum_{i=1}^n a_i F_i + a_0 \quad (199)$$

where a_i and F_i are coefficients and parameters respectively. The hypothetical reference substituent (or solvent, etc) R has the property

$$a_1 \equiv a_2 \equiv \dots \equiv a_1 \equiv \dots \equiv a_n \equiv 1 \quad (200)$$

and we may write

$$P_{a_i} = \frac{|a_i| \cdot 100}{\sum_{i=1}^n |a_i|} \quad (201)$$

where P_{a_i} is the percent of the i th variable's contribution to the overall effect.

The advantages of P_D as a measure of substituent effect composition are:

1. It is simply related to the ϵ values which are also used as a measure of substituent effect composition (Ehrenson, Brownlee and Taft¹ used λ in place of ϵ , $\lambda \equiv \rho_R/\rho_I$). Thus,

$$P_D = \frac{\epsilon \cdot 100}{\epsilon + 1} \quad (202)$$

2. Values lie in the range 0 to 100, they are more conveniently tabulated than ϵ values which lie in the range 0 to ∞ .

3. P_D is quickly and easily calculated.

References

1. S. Ehrenson, R. T. C. Brownlee, and R. W. Taft, *Prog. Phys. Org. Chem.*, **10**, 1 (1973).
2. J. Shorter, in *Correlation Analysis in Chemistry: Recent Advances*, N. B. Chapman and J. Shorter (Eds.) Plenum, New York, 1978, p. 119.
3. M. Charton, *Prog. Phys. Org. Chem.*, **8**, 235 (1971).
4. P. R. Wells, S. Ehrenson, and R. W. Taft, *Prog. Phys. Org. Chem.*, **6**, 147 (1968).
5. M. Charton, in *Correlation Analysis in Chemistry: Recent Advances*, N. B. Chapman and J. Shorter (Eds.) Plenum, New York, 1978, p. 175.
6. M. Charton, *Prog. Phys. Org. Chem.*, **10**, 81 (1973).
7. G. E. K. Branch and M. Calvin, *The Theory of Organic Chemistry*, Prentice-Hall, New York, 1941, p. 183.
8. A. R. Katritzky and R. D. Topsom, *J. Chem. Ed.*, **48**, 423 (1971).
9. R. W. Taft, *Steric Effects in Organic Chemistry* M. S. Newman (Ed), Wiley, New York, 1956.
10. J. Shorter, *Advances in Linear Free Energy Relationships*, N. B. Chapman and J. Shorter (Eds.), Plenum, London, 1971.
11. C. D. Ritchie, *J. Phys. Chem.*, **65**, 2091 (1961).
12. C. D. Ritchie and W. F. Sager, *Prog. Phys. Org. Chem.*, **2**, 323 (1964).
13. M. Charton, *J. Am. Chem. Soc.*, **97**, 3691 (1975).
14. M. Charton, *J. Am. Chem. Soc.*, **99**, 5687 (1977).
15. A. J. Macphee and J. E. Dubois, *Tetrahedron Lett.*, 2471 (1976).
16. F. G. Bordwell and H. E. Fried, *Tetrahedron Lett.*, 1121 (1977).
17. J. D. Roberts and W. T. Moreland Jr., *J. Am. Chem. Soc.*, **75**, 2167 (1953).
18. J. G. Kirkwood and F. H. Westheimer, *J. Chem. Phys.*, **6**, 506 (1938).
19. M. Charton, Dissertation, Stevens Institute of Technology, Hoboken, New Jersey, 1962.
20. T. W. Cole Jr, C. J. Mayers and L. M. Stock, *J. Am. Chem. Soc.*, **96**, 4555 (1974); L. M. Stock, *J. Chem. Ed.*, **49**, 400 (1972).
21. R. W. Taft and I. C. Lewis, *J. Am. Chem. Soc.*, **80**, 2436 (1958).
22. M. Charton, *J. Org. Chem.*, **29**, 1222 (1964).
23. K. Bowden, N. B. Chapman and J. Shorter, *J. Chem. Soc.*, 5239 (1963); 3370 (1964).
24. K. Bowden and R. Young, *Can. J. Chem.*, **47**, 2775 (1969).
- 24a. R. W. Taft, *J. Phys. Chem.*, **64**, 1805 (1960).
- 24b. R. W. Taft, N. C. Deno, and P. S. Skell, *Ann. Rev. Phys. Chem.*, **9**, 292 (1958).
- 24c. R. W. Taft, E. Price, I. R. Fox, I. C. Lewis, K. K. Anderson, and G. T. Davis, *J. Am. Chem. Soc.*, **85**, 509 (1963).
- 24d. R. T. C. Brownlee and R. W. Taft, *J. Am. Chem. Soc.*, **92**, 7007 (1970).

- 24e. W. Adcock and M. J. S. Dewar, *J. Am. Chem. Soc.*, **89**, 379 (1967).
- 24f. M. J. S. Dewar and A. P. Marchand, *J. Am. Chem. Soc.*, **88**, 3318 (1966).
- 24g. Y. Yukawa and Y. Tsuno, *Nippon Kagaku Zasshi*, **86**, 873 (1965).
- 24h. Y. Yukawa and Y. Tsuno, *Mem. Inst. Sci. Ind. Res. Osaka Univ.*, **23**, 71 (1966).
- 24i. O. Exner, *Tetrahedron Lett.*, 815 (1963).
- 24j. O. Exner, *Collect. Czech. Chem. Commun.*, **31**, 65 (1966).
- 24k. M. Charton, *Chem. Tech.*, 502 (1974).
- 24l. M. J. S. Dewar, R. Golden, and J. M. Harris, *J. Am. Chem. Soc.*, **93**, 4187 (1971).
- 24m. D. A. Forsyth, *J. Am. Chem. Soc.*, **95**, 3594 (1973).
- 24n. M. J. S. Dewar and P. J. Grisdale, *J. Am. Chem. Soc.*, **84**, 3539, 3548 (1962).
- 24o. H. C. Brown and Y. Okamoto, *J. Am. Chem. Soc.*, **80**, 4979 (1958).
25. C. G. Swain and E. G. Lupton, *J. Am. Chem. Soc.*, **90**, 4318 (1968).
- 26a. H. D. Holtz and L. M. Stock, *J. Am. Chem. Soc.*, **86**, 5188 (1964).
- 26b. F. W. Baker, R. C. Parish, and L. M. Stock, *J. Am. Chem. Soc.*, **89**, 5677 (1967).
- 26c. C. Hansch, A. Leo, S. H. Unger, K. H. Kim, D. Nikaitani, and E. J. Lien, *J. Med. Chem.*, **16**, 1207 (1973).
27. W. Altenberg, Thesis, Pratt Institute, Brooklyn, New York, 1972.
28. D. H. McDaniel and H. C. Brown, *J. Org. Chem.*, **23**, 420 (1958).
29. C. A. Grob and M. G. Schlageter, *Helv. Chim. Acta*, **59**, 264 (1976).
30. R. Thuair, *C. R. Acad. Sci. Paris*, **267**, 993 (1968).
31. B. M. Wepster, private communication. Most of these pKa values have now been published in A. J. Hoefnagel, R. A. Hoefnagel, and B. M. Wepster, *J. Org. Chem.*, **42**, 4720 (1978).
32. L. P. Hammett, *J. Am. Chem. Soc.*, **59**, 96 (1937).
33. L. M. Stock and H. C. Brown, *Adv. Phys. Org. Chem.*, **1**, 35 (1963).
34. H. H. Jaffé, *Chem. Rev.*, **53**, 191 (1953).
35. S. Wold and M. Sjoström, *Chem. Scripta*, **2**, 49 (1972).
36. S. Wold and M. Sjoström, *Chem. Scripta*, **6**, 114 (1974).
37. H. VanBekkum, P. E. Verkade, and B. M. Wepster, *Rec. Trav. Chim. Pays-Bas*, **78**, 815 (1959).
38. R. W. Taft, S. Ehrenson, I. C. Lewis, and R. E. Glick, *J. Am. Chem. Soc.*, **81**, 5352 (1959).
39. S. Ehrenson, *Prog. Phys. Org. Chem.*, **2**, 195 (1964).
40. M. Charton, *J. Am. Chem. Soc.*, **97**, 1552 (1975).
41. M. Charton, *J. Org. Chem.*, **41**, 2906 (1976).
42. M. Charton, *J. Am. Chem. Soc.*, **97**, 3694 (1975).
43. E. B. Wilson Jr. *An Introduction to Scientific Research*, McGraw-Hill, New York, 1952, p. 272.
44. M. Charton, in *Design of Biopharmaceutical Properties through Prodrugs and Analogs*, E. B. Roche (Ed.), American Pharmaceutical Society, Washington, D.C., 1977, p. 228.
45. M. Charton, unpublished results.
46. R. D. Topson, *Prog. Phys. Org. Chem.*, **12**, 1 (1976).
47. R. H. Staley, M. Taagepere, W. G. Henderson, I. Koppel, J. L. Beauchamp, and R. W. Taft, *J. Am. Chem. Soc.*, **99**, 326 (1977).
48. G. D. Hartman and T. G. Traylor, *J. Am. Chem. Soc.*, **97**, 6147 (1975).
49. C. D. Johnson, I. Roberts, and P. G. Taylor, *J. Chem. Soc., Chem. Commun.*, 897 (1977).
50. M. Charton, *J. Org. Chem.*, **28**, 3121 (1963).
51. M. Charton, *J. Org. Chem.*, **34**, 1877 (1969).
52. M. Charton and B. I. Charton, *Phosphorus and Sulfur*, **3**, 367 (1977).
53. M. Charton and B. I. Charton, *J. Org. Chem.*, **43**, 1161, 2383 (1978).
54. M. Charton and B. I. Charton, *J. Org. Chem.*, **34**, 1882 (1969).

55. P. J. Q. English, A. R. Katritzky, T. T. Tidwell, and R. D. Topsom, *J. Am. Chem. Soc.*, **90**, 1767 (1968).
56. N. C. Cutress, T. B. Brindley, A. R. Katritzky, M. V. Sinnott, and R. D. Topsom, *J. Chem. Soc. Perkin Trans. II*, 2255 (1972).
57. S. Oae and C. C. Price, *J. Am. Chem. Soc.*, **80**, 3425 (1958).
58. W. A. Sheppard, private communication.
59. R. W. Taft, private communication.
60. G. Fraenkel and J. P. Kim, *J. Am. Chem. Soc.*, **88**, 4203 (1966).
61. A. Ricci, F. Bernardi, R. Danielli, D. Macciantelli, and J. H. Ridd, *Tetrahedron*, **34**, 193 (1978).
62. A. R. Katritzky and R. D. Topsom, *Angew. Chem. Intl. Ed.*, **9**, 87 (1970).
- 63a. F. H. Westheimer and M. W. Shookhoff, *J. Am. Chem. Soc.*, **61**, 555 (1969).
- 63b. F. H. Westheimer, *J. Am. Chem. Soc.*, **61**, 1977 (1939).
- 63c. S. Siegel and J. Komormy, *J. Am. Chem. Soc.*, **82**, 2547 (1960).
- 63d. C. L. Liotta, W. F. Fisher, G. A. Greene Jr., and B. L. Joyner, *J. Am. Chem. Soc.*, **94**, 4891 (1974).
64. K. Bowden, *Can. J. Chem.*, **41**, 2781 (1963).
65. K. B. Wiberg, *Physical Organic Chemistry*, Wiley, New York, 1964, pp. 282-285.
66. M. Charton, *Chem. Tech.*, 245 (1975).

The Trifluoromethyl Group in Chemistry and Spectroscopy. Carbon-Fluorine Hyperconjugation^a

BY LEON M. STOCK

Department of Chemistry, University of Chicago, Chicago, Illinois 60637

AND MICHAEL R. WASIELEWSKI

Chemistry Division, Argonne National Laboratory, Argonne, Illinois 60439

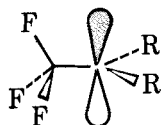
CONTENTS

I.	Introduction	254
II.	The Contributions	255
III.	Patterns of Chemical Reactivity	260
	A. Aromatic Compounds	260
	B. Aliphatic Compounds	264
	C. Summary	266
IV.	Physical and Spectroscopic Properties	267
	A. Dipole Moments	267
	B. Infrared Intensity Measurements	269
	C. Nuclear Magnetic Resonance	269
	D. Photoelectron Spectroscopy	271
	E. Electron Paramagnetic Resonance	273
	1. Coupling Constant Tensors, Solid State Results	275
	2. Aliphatic Free Radicals	279
	3. Nitroxide Radicals	289
	4. Nitrobenzene Anion Radicals	292
	5. Other Radicals	298
	6. Direction Interactions	302
	7. Theoretical Interpretation	304
	F. Summary	308
V.	Conclusion	309
	References	309

^a Work at the Argonne National Laboratory performed under the auspices of the Division of Basic Energy Sciences of the Department of Energy. Work at the University of Chicago performed under the auspices of the Block Foundation.

I. INTRODUCTION

The influence of the trifluoromethyl group on the chemical and spectroscopic properties of stable molecules and reactive intermediates has been under active study for more than 25 years. This chemistry is intriguing because several contributions including the polar effect, the π inductive effect, carbon-fluorine hyperconjugation, and 1,3 pp interactions may affect the behavior of this substituent. Consequently, this group and related groups have received special attention in work directed toward the assessment of the relative importance of these contributions. The matter is well illustrated by the course of the work on carbon-fluorine hyperconjugation, the idea that electron density can be delocalized to the formally saturated trifluoromethyl group in electron-rich molecules and ions. This concept was proposed in 1950 by Roberts, Webb, and McElhill



I

to account for the seemingly enhanced electron-withdrawing properties of the trifluoromethyl group (1). By 1970, however, several investigators had expressed reservations concerning the importance of this effect in reaction chemistry. Sheppard and Sharts (2) and Holtz (3,4) discussed these reservations in critical reviews of the evidence for carbon-fluorine hyperconjugation as a factor in the chemistry of both aliphatic and aromatic molecules. They concluded that carbon-fluorine hyperconjugation played no significant role in the determination of the stability or reactivity of aliphatic organofluorine compounds or of aromatic compounds with perfluoroalkyl substituents. Yagupol'skii, Il'chonko, and Kondratenko focused their attention on the Hammett and Taft sigma constants for the perfluoroalkyl groups and suggested, in contrast to the other reviewers, that carbon-fluorine hyperconjugation influenced the chemistry of molecules with trifluoromethyl groups (5). Diverse interpretations have also been advanced for the spectroscopic properties of molecules, ions, and radicals with trifluoromethyl groups. To illustrate, large coupling constants are observed in the electron paramagnetic resonance spectra (epr) of radicals with β -fluorine atoms as shown by the result for 2,2,2-trifluoroethyl radical, II, with $a_{\beta}^F = 29.9\text{G}$ (6). Holtz



II

pointed out that the interpretation of these large constants was uncertain because the evidence concerning the dependence of these constants on the dihedral angle between the p orbital and the carbon-fluorine bond axis, θ , was conflicting and

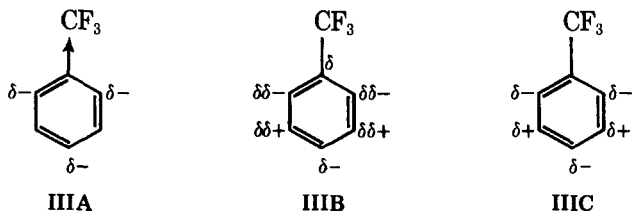
because the relationship between the spin density distribution and the charge density distribution was not well defined (4). Spectroscopists, on the other hand, have usually discussed the coupling constants on the basis of carbon-fluorine hyperconjugation or 1,3 *p p* interactions. In recent years, many of the issues concerning the interpretation of the epr results have been resolved and new observations concerning the influence of trifluoromethyl groups on reaction rates, on equilibrium constants, on nmr chemical shifts, and on other physiochemical properties have been reported. These contributions and related observations are discussed in this review.

II. THE CONTRIBUTIONS

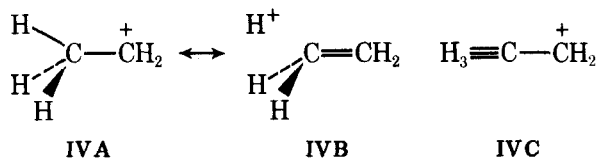
Topsom recently discussed the concepts that are central to an understanding of the origin of electronic substituent effects (7). For the trifluoromethyl group, attention must be given to several of the conventional interactions including the direct field effect, the pi inductive effect, the hyperconjugative interaction, and other factors that originate in the nonbonding fluorine atoms.

The trifluoromethyl group and other perfluoroalkyl groups exert large direct field effects which originate in the large dipole moments of these groups. The magnitude of this contribution is defined empirically by the σ_I constant for the trifluoromethyl group, 0.45. This constant is only about 10% less than the σ_I constant for the fluorine atom. Consequently, the trifluoromethyl group exerts a major polar effect on conventional equilibrium and rate processes.

The pi inductive effect is a composite of several interactions including the π_σ effect which involves the polarization of the sigma framework with resultant changes in the distribution of the electron density of the pi electron system; the π_F effect which involves the direct polarization of the pi electron system in the field of the polar substituent; and the π_{orb} effect which originates in the repulsive interaction between electron density on the substituent and the pi electron system. All these interactions require consideration in the analysis of the behavior of the trifluoromethyl group. The π_σ effect of this group produces negative pi charges at the 2, 4, and 6 positions, **IIIA**, of benzene. The π_F effect polarizes the pi electron system as shown in **IIIB**. The π_{orb} effect produces yet another pi electron effect with a negative pi charges at the 2, 4, and 6 positions, **IIIC**. Sheppard has stressed this interaction in his discussion of the behavior of the trifluoromethyl group (2,8). Quantitative estimates of the importance of the pi inductive effect are difficult to make because the magnitude of this effect depends on the character of the pi electron system to which the substituent is bonded. Furthermore, Topsom and his students and others have pointed out that it is often impractical to consider the mutually dependent interactions of the pi inductive effect, **IIIA-IIIC**, as experimentally separable.



The concept of carbon-fluorine hyperconjugation is related to the concepts of carbon-hydrogen and carbon-carbon hyperconjugation. These ideas are now widely employed in the interpretation of the chemistry and spectroscopy of electron-deficient compounds and intermediates (9-11). The notion that carbon-fluorine hyperconjugation may play a similar role in the chemistry of electron-rich molecules remains controversial. Carbon-hydrogen hyperconjugation is qualitatively described by structures **IVA-IVB** and **IVC**. Structures **IVA** and **IVB** are the conventional valence bond representations. In structure **IVC**, the methyl group is represented as a hypothetical $C\equiv H_3$ group to illustrate the most popular, qualitative, orbital viewpoint (9,10). In this model, the three hydrogen atom $1s$ orbitals are used to form three orthogonal group orbitals. Two of these orbitals have the proper symmetry for interaction with the p orbitals of the other carbon atoms. The energy levels are sketched in Fig. 1.



Two conformations, **VA** and **VB**, must be considered in the discussion of hyperconjugation. For the ethyl carbonium ion, the interactions labeled 1 and 2 in Fig. 1 between the $2p$ orbital, p_x , and $\sigma\pi_x$ in **VA** and between the $2p$ orbital, p_y , and $\sigma\pi_y$ are dominant and stabilize the ion. The situation is more interesting when an electronegative substituent such as a fluorine atom is introduced. Hoffmann and Rossi and their associates have argued that, to a first approximation, the energies of $\sigma\pi_y$ and $\sigma\pi_y^*$ are unchanged for the monofluoroethyl derivatives, **VIA** and **VIB** (11,12). However, the energies of $\sigma\pi_x$ and $\sigma\pi_x^*$ are both reduced as shown in Fig. 2. Under the influence of the electronegative substituent, $\sigma\pi_x$ becomes more localized on the fluorine atom and $\sigma\pi_x^*$ on the carbon atom. For an anion the interactions labeled 1 and 2 in Fig. 2 between the p_x and p_y orbitals and the $\sigma\pi_x$ and $\sigma\pi_y$ orbitals are repulsive but less so for **VIB** than for **VIA**. Also the attractive interactions labeled 3 and 4 in Fig. 2 between p_x and p_y and the $\sigma\pi_x^*$ and $\sigma\pi_y^*$ orbitals are more favorable for **VIB** than for **VIA** (11). The result is a major conformational preference for the **B** conformer of the anion (13). This model focuses on the influence of an electronegative sub-

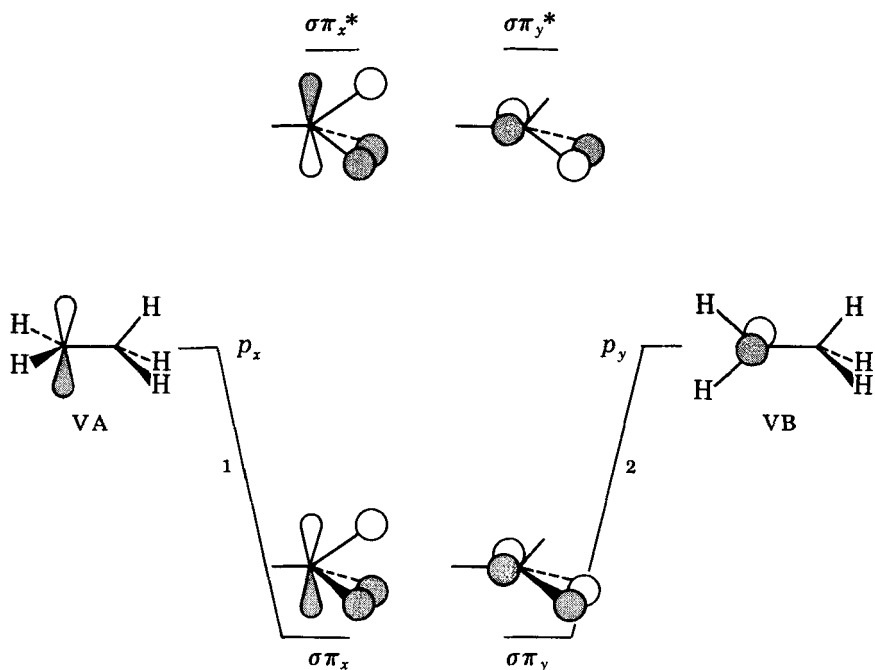


Figure 1 An interaction diagram for the p_x and p_y orbitals of a carbon atom and the methyl group orbitals.

stituent on the energy content of the group orbitals. It is deficient in the sense that it does not consider the orbitals of the substituent. Rossi and Wood have argued that the neglect of the nonbonding electrons of fluorine or chlorine atoms is not a serious matter because extended Hückel analyses and *ab initio* calculations employing an STO-3G basis set indicate that the overlap population between the p orbital and the nonbonding electrons of these halogen atoms is quite small in the 2-haloethyl radicals (12). It is not clear whether or not the nonbonding orbitals could be neglected in a qualitative description of the corresponding anions. In any case, this model for the discussion of hyperconjugation of the CH_2F group conveys the important idea that the interaction between the carbon atom p orbitals and the antibonding orbitals of an alkyl group is more likely when electronegative substituents are present.



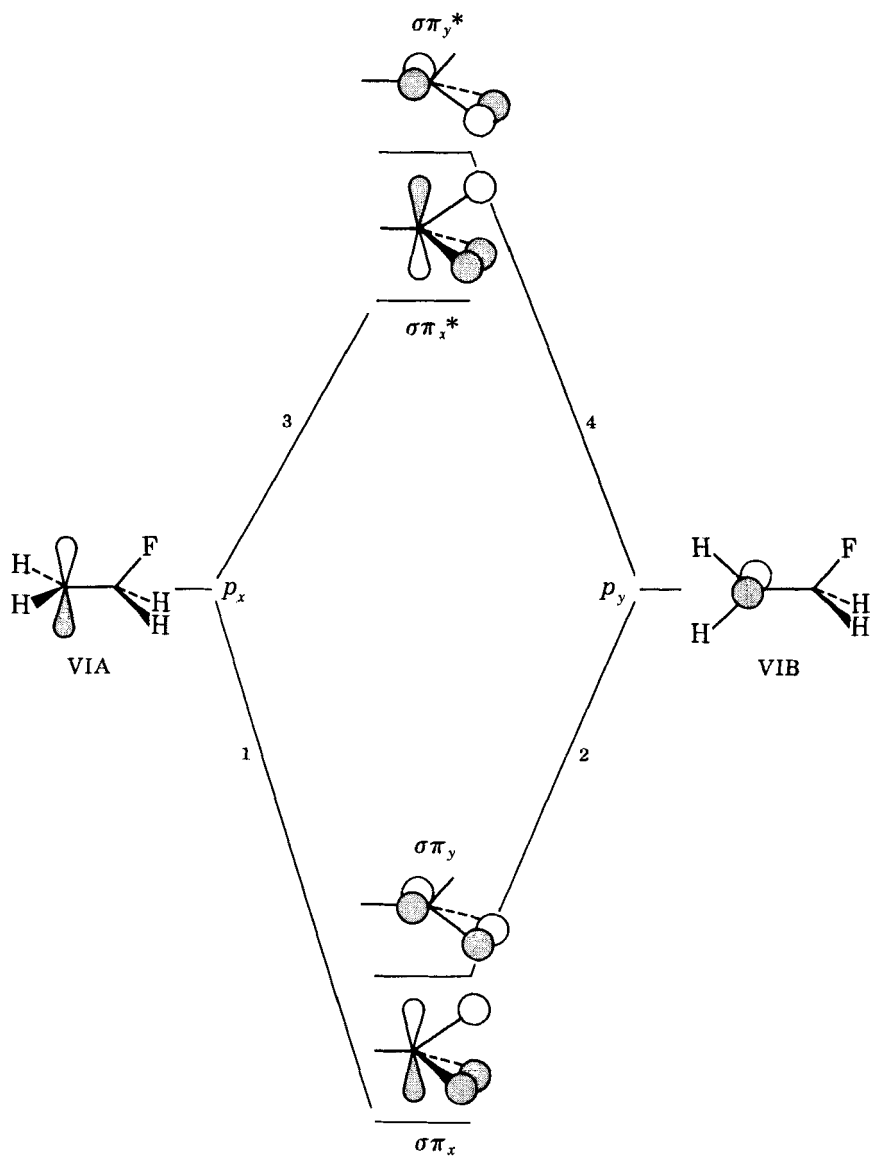


Figure 2 An interaction diagram for the p_x and p_y orbitals of a carbon atom and the fluoromethyl group orbitals.

hand, the unoccupied orbitals of the trifluoromethyl group have energy contents comparable with the energy content of the p_x or p_y orbitals of the other carbon atoms. This point is well illustrated by the fact that the calculations based on the INDO approach reveal that the energy contents of the singly occupied molecular orbitals of the model radicals $\text{H}_2\text{CO}^\cdot$ and $\text{H}_2\text{NO}^\cdot$ are 0.10 au and -0.46 au, respectively (14), compared to estimates of 0.30 or 0.27 au for the energy content of the lowest unoccupied π^* molecular orbital of the trifluoromethyl group in fluoroform (14,15). Thus, it is not unreasonable to propose that electron delocalization to an unoccupied, antibonding molecular orbital influences the chemistry and spectroscopy of molecules, ions, and radicals with trifluoromethyl groups.

Finally, it is necessary to consider the role of 1,3 $p-p$ interactions since many investigators have commented on their possible importance. In an important sense these interactions are implicitly included in the more complete model for the description of carbon-fluorine hyperconjugation. On the other hand, chemical interest in the finer dissection of phenomena has prompted the consideration of these interactions as separable from hyperconjugation. For the 2,2,2-trifluoroethyl carbanion, this interaction would involve the interaction



VII

of two closed shell units, the doubly occupied orbital centered on the carbon atom and the nonbonding orbitals of the fluorine atom. Intuition suggests that an interaction of this kind would not be effective for the stabilization of the anion. However, such an interaction would be more important in an electron-deficient species such as a free radical or a carbonium ion. It is interesting to note in this connection that March has pointed out that there are no known cases where β -fluorine atoms participate in solvolytic reactions leading to carbonium ions (16).

III. PATTERNS OF CHEMICAL REACTIVITY

A. Aromatic Compounds

Considerable effort has been devoted to the determination of rate and equilibrium constants for benzene derivatives with *meta*- and *para*-trifluoromethyl substituents in a search for an exalted substituent effect which would provide evidence for special electron delocalization. Resonance interactions are generally detectable by such procedures. To illustrate, two sigma constants $\sigma_{p-\text{NO}_2}$ and $\sigma_{p^--\text{NO}_2}$ with values of 0.78 and 1.24, respectively are necessary to describe the behavior of the nitro group quantitatively by the Hammett equation

TABLE I
Hammett Sigma Constants for the Trifluoromethyl Groups^a

Reaction	Sigma constants			Ref.
	σ_{m-CF_3}	σ_{p-CF_3}	$\sigma_{p-CF_3}/\sigma_{m-CF_3}$	
Equilibria				
Ionization, Benzoic Acids, 50% EtOH-H ₂ O, 25°	0.42	0.53	1.26 ^b	8
Ionization, Anilines, H ₂ O, 25°	0.47	0.63	1.34 ^b	8,18
Ionization, Phenols, H ₂ O, 25°	0.45	0.56	1.25 ^c	19,20
Rate				
Exchange, Substituted Toluenes, C ₆ H ₁₁ NHLi, C ₆ H ₁₁ NH ₂ , 50°	0.47	0.61	1.29 ^b	3,4,21
Exchange, Substituted C ₆ H ₅ CH(CF ₃) ₂ , CH ₃ OD, (CD ₃) ₂ SO, 23-66.5°	0.40	0.50	1.20 ^d	22
Substitution, Substituted 2-Nitrochlorobenzenes, C ₆ H ₅ SNa, CH ₃ OH, 35°	0.44	0.63	1.43 ^b	23

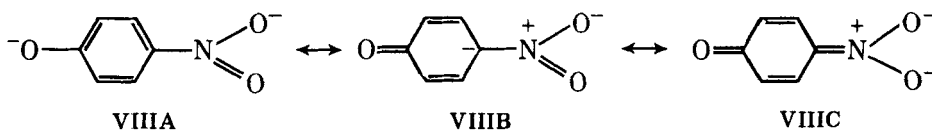
^a Only reactions for which the results for both *meta*- and *para*-trifluoromethyl are known are presented.

^b Holtz reexamined the original data and recalculated the σ constants on the basis of the ρ values for other reliable groups; Ref. 3.

^c Ref. 20b.

^d Calculated from the results presented in Ref. 22.

(17). The smaller value is appropriate for reactions in which only a modest negative charge is delocalized into the benzene ring. The larger value is appropriate for reactions in which a substantial negative charge is delocalized into the benzene ring. The data for the *p*-nitro group in electrophilic substitution reactions and other electron-deficient processes are well accommodated by the smaller value. On the other hand, the data for nucleophilic substitution reactions and other electron-rich processes such as the dissociation constants for phenols and anilinium ions require the larger value and indicate the importance of structures such as **VIIIC** in the description of the *p*-nitrophenolate anion. The ratio, σ_p/σ_m is also enhanced when resonance interactions influence the behavior of the *para* substituent. The values of σ_{p-CF_3} and σ_{m-CF_3} necessary to accommodate the experimental results for aromatic reaction chemistry are summarized in Table I.



The experimental results for the equilibrium reactions have been examined in some detail. In particular, Liotta and his students carefully investigated the behavior of the phenols (20). They redetermined the dissociation constants for

TABLE 2
Thermodynamic Quantities for the Dissociation Reactions of
Trifluoromethylphenols in Water at 25°^a

Substituent	p <i>K</i> _a	$\Delta\bar{H}^\circ$, from p <i>K</i> _a	kcal mole ⁻¹ from Calorimetry	$\Delta\bar{S}^\circ$, from p <i>K</i> _a	cal (deg mole) ⁻¹ from Calorimetry
<i>p</i> -CF ₃	8.675	5.12 ± 0.3	4.99 ± 0.08	-22.7 ± 1.0	-23.0 ± 0.2
<i>m</i> -CF ₃	8.950	5.16 ± 0.1	5.24 ± 0.08	-23.7 ± 0.4	-23.3 ± 0.2

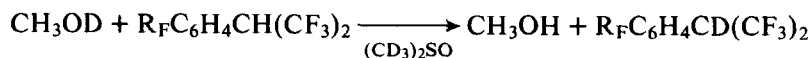
^a Ref. 20*b*.

the *m*- and *p*-trifluoromethylphenols and measured the enthalpy and entropy of ionization by two methods (20*b*). Their results are presented in Table 2.

The enthalpy and entropy of the dissociation reaction are not unusual in any respect (20*b*). Accordingly, these dissociation constants can be discussed with some confidence.

Generally the σ_p/σ_m ratio is between 1.2 and 1.3 for substituents for which resonance delocalization is impossible or unimportant (17). For the equilibrium reactions, the σ_p/σ_m ratio for the trifluoromethyl group ranges from 1.25 for the phenols to 1.34 for the anilines. These results suggest that the polar effect of the trifluoromethyl group is dominant even in reactions that are electron-rich.

The results obtained in the work on isotopic exchange reactions and nucleophilic substitution reactions, in general, support this conclusion. To illustrate, the rate constants for the isotopic exchange reaction studied by Klambunde and Burton (22) are linearly related to the Hammett σ constants, Fig.



4. Several experimental tests suggest that charge delocalization to the aromatic nucleus is modest. However, the ρ value, 4.0, is large and the σ_p/σ_m ratio is unchanged from the ratio observed for the benzoic acids. The results for the tritium exchange reactions of the toluenes are similar (3,4,21).

The investigations of the nucleophilic substitution reactions have yielded more interesting results. Unfortunately, both the *meta*- and *para*-trifluoromethyl groups have been studied in only one reaction. The results of this study (23) and other work by the Miller group (24) and the Brioux group (25) indicates that somewhat larger values of $\sigma_{p-\text{CF}_3}$ (0.63, 0.65, 0.72, 0.73, 0.74) are required to accommodate the data for reactions such as the sodium methoxide substitution of 2-nitro-4-trifluoromethylchlorobenzene. Thus, the data for the substitution reactions with very electron-rich transition states which resemble the benzenonium intermediate, IX, are compatible with the idea that the trifluoromethyl group exhibits an enhanced substituent effect.

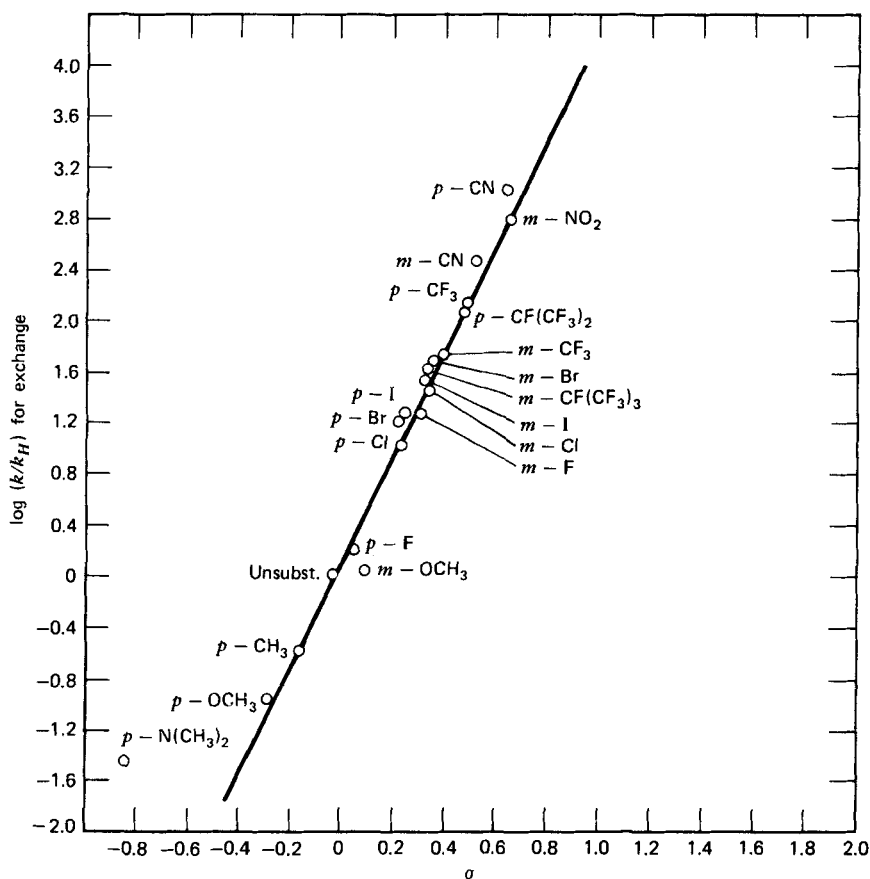
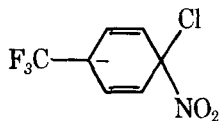


Figure 4 The relationship between the rates of proton exchange of *meta*- and *para*-substituted 2-phenyl-1,1,1,3,3,3-hexafluoropropanes and the Hammett sigma constants.



IX

Sheppard has pointed out that the observations for other perfluoroalkyl groups are relevant to a discussion of the influence of the trifluoromethyl group (2,8). His work and contribution of others indicate that the perfluoroalkyl groups, CF_2CF_3 , $\text{CF}(\text{CF}_3)_2$ and $\text{C}(\text{CF}_3)_3$, exhibit substituent effects which are as large or larger than the effects of the trifluoromethyl group. This point is illustrated by the Hammett sigma constants presented in Table 3.

TABLE 3
Hammett Sigma Constants for the Perfluoroalkyl Groups^a

Reaction	Substituent constants					
	$\sigma_{m-CF_2CF_3}$	$\sigma_{p-CF_2CF_3}$	$\sigma_{m-CF(CF_3)_2}$	$\sigma_{p-CF(CF_3)_2}$	$\sigma_{m-C(CF_3)_3}$	$\sigma_{p-C(CF_3)_3}$
1. Benzoic Acids			0.37 ^b	0.53 ^b	0.35 ^c	0.53 ^c
2. Aniline	0.52 ^{b,d}	0.69 ^{b,d}	0.52 ^b	0.68 ^b	0.39 ^c	0.71 ^c

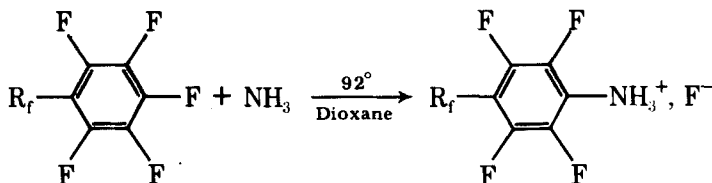
^a See Ref. 5 for a more complete evaluation of the substituent constants for the perfluoroalkyl groups.

^b Ref. 8.

^c Ref. 26.

^d For dimethylaniline.

In other work, Chambers, Waterhouse, and Williams (27) found that all the perfluoroalkyl groups influenced the nucleophilic substitution reactions of substituted perfluorobenzenes similarly, Table 4.



The fact that the trifluoromethyl and other perfluoroalkyl groups behave similarly has received attention in discussions of the influence of the trifluoromethyl group. Both Sheppard (2,8) and Holtz (3) have argued that the equivalent behavior of these two groups is incompatible with an important role for carbon-fluorine hyperconjugation. Their arguments are based on the idea that the energies of the antibonding orbitals for the perfluoroalkyl groups would be appreciably higher than those for the trifluoromethyl group.

B. Aliphatic Compounds

Two research groups have investigated the rates of the base-catalyzed hydrogen atom exchange reactions of aliphatic fluorocarbons (3,4,28,29). The results for a selected series of compounds are presented in Table 5.

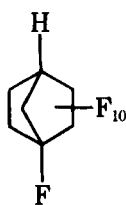
The dependence of the reaction rate on the degree of fluorine atom substitution is remarkable. Andreades concluded that the large substituent effects could not be attributed to polar effects alone (29). However, the observations of Holtz and Streitwieser (4,28) indicate that this conclusion was premature. For example, 1-hydril-F-bicyclo[2.2.1]heptane, **X**, is 10^4 more reactive than the 1,4-dihydril compound, **XI**. Clearly, the dipolar field effect of the 4 fluorine atom in **X** has a major influence on the reaction rate and the short range inductive

TABLE 4
Relative Rates of Ammonolysis of Substituted Pentafluorobenzenes^a

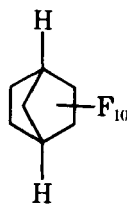
Compound	Relative rate
C ₆ F ₅ CF ₃	1.00
C ₆ F ₅ CF ₂ CF ₃	2.14
C ₆ F ₅ CF(CF ₃) ₂	1.49
C ₆ F ₅ C(CF ₃) ₃	2.58

^a Ref. 27.

and field effects of the fluorine atoms on these reactions are very large indeed.



X



XI

Streitwieser and Holtz have discussed the reactivity patterns of the acyclic and the bicyclic molecules (4,28). They proposed largely on the basis of Bredt's rule that the rate constant for tris(trifluoromethyl)methane should be much larger than the rate constant for the bicyclic compound, X, if carbon-fluorine hyperconjugation were important. The observation that these compounds ex-

TABLE 5
Relative Rates of Sodium Methoxide-Catalyzed
Hydrogen Atom Exchange of Perfluoroalkanes in
Methanol at 0°C^{a,b}

Compound	Relative rate
CF ₃ H	1.00
CF ₃ (CF ₂) ₆ H	9.8
(CF ₂) ₂ CFH	1.6 × 10 ⁶
(CF ₃) ₃ CH	1 × 10 ¹¹
HC ₇ F ₁₀ H ^c	3.0 × 10 ⁷
FC ₇ F ₁₀ H ^d	2.6 × 10 ¹¹
FC ₈ F ₁₂ H ^e	2 × 10 ¹³

^a Extrapolated from data at other temperatures, Ref. 4.

^b Refs. 4,28,29.

^c 1,4-Dihydryl-F-bicyclo[2.2.1]heptane.

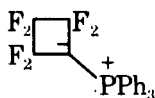
^d 1-Hydryl-F-bicyclo[2.2.1]heptane.

^e 1-Hydryl-F-bicyclo[2.2.2]octane.

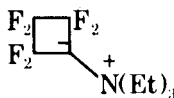
hibited the same rate constants prompted their conclusion that hyperconjugation was unimportant. This conclusion was also premature because, as pointed out by Yagupo'skii, Il'chenko, and Kondratenko (5), the formation of the anion does not require the rehybridization of the bridgehead carbon atom to sp^2 geometry. In this situation, the anions of tris(trifluoromethyl)methane and **X** would have similar geometry and the role of carbon-fluorine hyperconjugation need not be greatly different. Moreover, the net polar influences of the fluorine atoms and the impact of changes in the hybridization of the *tertiary* carbon atoms in these aliphatic molecules are different to assess quantitatively (30). We are forced to conclude that the information now available for aliphatic molecules cannot be used for a confident decision concerning the role of carbon-fluorine hyperconjugation in the stabilization of anions.

C. Summary

As discussed, the results for the aliphatic molecules are difficult to interpret. Consequently, even though rather remarkable observations have been made in the aliphatic series, for example the finding that the perfluorocyclobutane ylides,



XIII A



XIII B

XIII A and **XIII B**, are stable (31,32), the equilibrium and rate observations for the aromatic compounds must be given primary consideration until additional quantitative information is available concerning the reactions of other aliphatic compounds. The evidence for an enhanced stabilization of electron-rich molecules and ions by the *para*-trifluoromethyl group is marginal. The dissociation constants for the phenols indicate that the group exhibits quite normal behavior. The related observations for the anilines, in contrast, suggest a modest increase in its substituent effect. The results obtained in the studies of nucleophilic side-chain and nucleophilic substitution reactions are more suggestive. Whereas the rate data obtained for the exchange reactions are characteristic of normal behavior, the work on the nucleophilic substitution reactions is compatible with an enhanced substituent effect for the *para*-trifluoromethyl group. All the evidence suggests that the transition states for these substitution reactions are very electron-rich. Thus, we infer that an important electron excess is necessary for the detection of a significant enhancement of the influence of the trifluoromethyl group and that the observed increase is real. Yagupol'skii, Il'chenko, and Kondratenko have argued for the same conclusion on the basis of the fact that self-consistent analyses of the substitution reactions yield σ_R^0 values of 0.1 for the trifluoromethyl group.

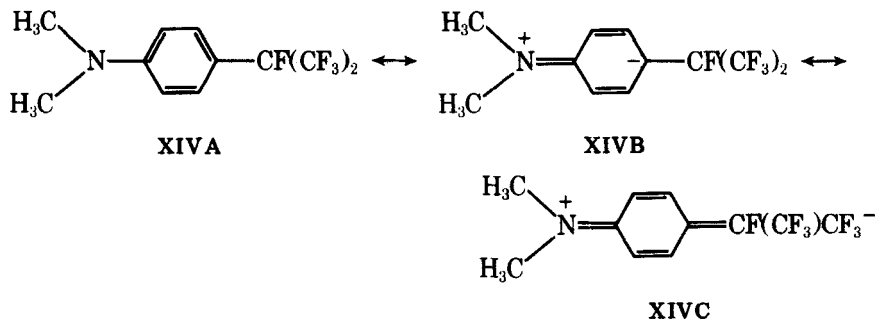
TABLE 6
Dipole Moments of Selected Substituted Benzenes

Compound	Dipole moment (D)		
	Exptl ^a	Calcd	Interaction ^b
C ₆ H ₅ NO ₂	3.93		
C ₆ H ₅ N(CH ₃) ₂	1.58		
C ₆ H ₅ CF ₃	2.61		
C ₆ H ₅ CF(CF ₃) ₂	2.68		
4-(CH ₃) ₂ NC ₆ H ₄ NO ₂	6.89	5.31	1.59
4-(CH ₃) ₂ NC ₆ H ₄ CF ₃	4.62	3.97	0.66
4-(CH ₃) ₂ NC ₆ H ₃ CF(CF ₃) ₂	4.71	4.09	0.63
3-(CH ₃) ₂ NC ₆ H ₄ CF ₃	3.75	3.52	0.30
3,5-(CH ₃) ₂ NC ₆ H ₃ (CF ₃) ₂	4.58	3.97	0.62

^a Refs. 1,3,33.

^b Calculated as described by Ibbitson, Ref. 33.

cording to this argument, because the electronegativity of the fluorine atom and the trifluoromethyl group differ. On this basis, Holtz proposed that pi inductive effects were responsible for the enhanced dipole moments (3). Subsequently, Ibbitson and his associates investigated the dipole moments of selected *meta*-trifluoromethyl derivatives of N,N-dimethylaniline (33). Their results and the related data are presented in Table 6.



The interaction moments directed along the major axis of the ring that are necessary to account for the observed moments of the *meta* derivatives of the trifluoromethylaniline compounds are appreciable. The values of 0.62 for the for the 3,5-ditrifluoromethyl derivative and 0.30 for the 3-trifluoromethyl derivative are comparable with the interaction moment, 0.66, assessed for N,N-dimethyl-4-trifluoromethylaniline. Inasmuch as resonance interactions are impossible in the *meta* derivatives, Ibbitson and his associates concluded that all the observed interaction moments for the trifluoromethyl groups are the consequence of pi inductive effects which are operative in both the *meta* and *para* positions. Unfortunately, no data are available for the *meta*-perfluoro-

roisopropyl substituent. Topsom and Katritzky have proposed that the enhanced moment in the *meta* compounds results from an induced increase in the interaction between the dimethylamino group and the pi system under the influence of the field of the trifluoromethyl group (34). Whichever of these explanations is correct, it seems clear that a pi inductive effect rather than fluorine hyperconjugation is responsible for the enhanced dipole moments (35).

B. Infrared Intensity Measurements

In an empirical approach, Topsom and Katritzky and their associates have related the intensities of selected infrared absorptions to the σ_R^0 substituent constant. They estimate that σ_R^0 for the trifluoromethyl group is 0.11 on the basis of the infrared intensities for monosubstituted benzenes (36). In more recent work, this group has examined the infrared intensities of *para*-disubstituted compounds (34). They have found that there is a mutual interaction between the trifluoromethyl group and other substituents in the benzene nucleus such that a single σ_R^0 value cannot adequately describe the influence of the group on the intensity of the infrared absorption intensities without modification of the empirical expressions to incorporate parameters which measure the substituent's tendency to accept further upon increased demand (37). Regrettably, the mutual interaction considerably limits the utility of the infrared intensity measurements for the confident characterization of the manner in which the trifluoromethyl group effects electron withdrawal.

C. Nuclear Magnetic Resonance

The evidence for fluorine hyperconjugation derived from nmr measurements available in 1970 was not definitive (3,4). Taft and his associates had originally argued that the fluorine substituent chemical shifts (SCS) of *p*-fluorine atoms in molecules with substituents which are capable of resonance interactions, for example the nitro group, exhibited a special solvent dependence and shifted to lower field as the polar character of the solvent was increased (38,39). The fluorine substituent chemical shift for the aromatic fluorine atom in 4-fluorobenzotrifluoride, indeed, exhibits a small downfield shift from 4.95 in 3-methylpentane to 5.75 in nitromethane to 6.05 in 75% aqueous methanol. For comparison, the substituent chemical shift for the fluorine atom in 4-fluoronitrobenzene exhibits a shift from 9.00 in 3-methylpentane to 10.55 in nitromethane to 11.20 in 75% aqueous methanol (39). Holtz concluded on these grounds that fluorine hyperconjugation, structure XVC, might contribute to the determination of the substituent chemical shift. However, Brownlee, Dayal, and Taft subsequently showed that the effects of dipolar aprotic solvents on the

TABLE 7
Substituent Chemical Shifts for Trifluoromethyl, Nitro, Cyano, Carboxy Derivatives of
Fluorobenzene, 4-Fluorobiphenyl, 1- and 2-Fluoronaphthalene

Compound	Substituent chemical shift (ppm)					
	DMF	CF ₃ ^a		NO ₂ ^{a-d}	CN ^{a-d}	CO ₂ H ^{a-d}
		C ₆ H ₆	Calcd			
1-Fluoronaphthalene						
3-Subst (3 α)	-3.70	-3.26	-2.57	-4.87	-3.68	-1.01
4-Subst (4 α)	-8.28	-7.24	-6.56	-12.77	-11.34	-8.19
5-Subst (5 α)	-3.03	-2.20	-3.17	-3.47	-2.41	-1.80
7-Subst (7 α)	-1.71	-1.90	-1.49	-3.39	-2.35	-1.52
2-Fluoronaphthalenes						
4-Subst (4 β)	-0.09	0.00	-1.70	-0.79	-0.80	+0.72
5-Subst (5 β)	-1.67	-1.42	-1.99	-2.34	-2.70	-0.16
6-Subst (6 β)	-3.99	-3.67	-3.03	-6.54	-5.45	-3.26
7-Subst (7 β)	-2.37	-2.15	-1.91	-3.25	-3.05	-1.24
8-Subst (8 β)	-4.72	-4.80	-3.85	-6.76	-5.32	-3.46
4-Fluorobiphenyl ^a						
3'-Subst	-1.35	-1.37	-1.84	-2.08	-1.80	-0.80
4'-Subst	-1.65	-1.68	-2.05	-2.74	-2.24	-1.40
Fluorobenzene						
3-Subst	-2.48	-2.28	—	-3.28	-2.70	—
4-Subst	-5.70	-5.15	—	-10.30	-9.80	-6.05

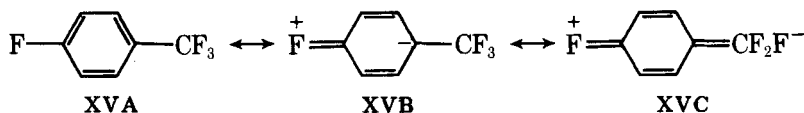
^a Many of these data are summarized in Ref. 41.

^b For the work on the biphenyls, see Refs. 41 and 43.

^c For the work on the naphthalenes, see Refs. 41, 42, and 44.

^d For the work on the benzenes, see Refs. 38 and 39.

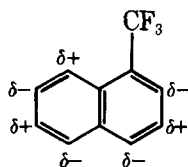
chemical shift did not involve pi electron delocalization and that dipolar interactions were the predominant factor (40). Therefore, the bases for the original suggestion have been removed. It is pertinent that Sheppard had previously pointed out that the shifts for the fluorine atoms of the trifluoromethyl group are insensitive to solvent effects (8). Accordingly, the fluorine substituent chemical shifts for the benzotrifluorides do not provide evidence for fluorine hyperconjugation.



The substituent chemical shifts for 4-fluoro-3'-trifluoromethylbiphenyl and 4-fluoro-4'-trifluoromethylbiphenyl and 1-fluoro- and 2-fluoronaphthalenes with substituent trifluoromethyl groups have recently become available (41). These results are summarized in Table 7 together with results for nitro, cyano, and carboxyl groups. The substituent chemical shifts calculated for the triflu-

romethyl derivatives of the fluoronaphthalenes and fluorobiphenyls are included for comparison. The calculated values are based on the analysis of Adcock and Dewar (42).

Adcock and his associates have examined these results in detail. They conclude that the new observations do not permit an unequivocal decision concerning the origin of the influence of the trifluoromethyl group. However, they do argue for a significant pi electron interaction. Their suggestion is based on several lines of argument. First, they point out that the shift for the fluorine in the 4β compound is -0.09 , an unusual result, which they infer arises from the induction of alternate pi electron density at the positions *meta* to the trifluoro-



XVI

methyl substituent, XVI. Second, they point out that there is an empirical relationship between the observations for the trifluoromethyl group and the corresponding data for the nitro, cyano, and carboxyl groups. The SCS data for the trifluoromethyl group parallel the results for the cyano group for the biphenyl and the 3α , 5α , 7α , 5β , 7β , 8β naphthalene series whereas the SCS data for the trifluoromethyl group and the carboxyl group are related for the 4α , 4β , and 6β series. Adoption of the idea that the shifts in the first group (3α etc.) are dictated by polar effects and that the shifts in the second group (4α etc.) are dictated by pi electron effects leads to their suggestion that the polar effect of the trifluoromethyl group is greater than that of the carboxyl group and approaches that of the cyano group. The same criteria indicate that the pi electron effect of the trifluoromethyl group is less than that of either the cyano or carboxyl groups. They suggest that the polar and pi electron effects are qualitatively in accord with $\sigma_I = 0.45$ and $\sigma_R^0 = 0.08$ for the trifluoromethyl group. These values are, of course, closely related to the values assessed in other empirical analyses of substituent effect data (5).

D. Photoelectron Spectroscopy

In another approach, Holmes and Thomas measured the core binding energies of the nuclei in trifluoromethylbenzene, 1,3- and 1,4-di(trifluoromethyl)benzene by X-ray photoelectron spectroscopy (esca) in the vapor phase to assess the charge distribution (45). Clark and his associates had previously described the esca spectrum of trifluoromethylbenzene in condensed phase (46). Their analysis of the poorly resolved signals of the aromatic carbon atoms re-

TABLE 8
Core-Electron Ionization Potentials for Trifluoromethylbenzene Derivatives

Compound	Ionization potential (eV)		
	Fluorine	Carbon	Aromatic carbon
Benzene			290.38 ^a
C ₆ H ₅ CF ₃	693.88 ^a	298.24 ^a	291.02 ^a
	690.8 ^b	293.8 ^b	
1,3-C ₆ H ₄ (CF ₃) ₂	694.14 ^a	298.64 ^a	291.48 ^a
1,4-C ₆ H ₄ (CF ₃) ₂	694.17 ^a	298.58 ^a	291.48 ^a

^a Ref. 45.

^b Ref. 46.

quired a deepseated deconvolution and these results are not discussed. The results for the other nuclei are presented in Table 8.

There are some serious discrepancies between the results obtained in the two investigations. Certain of these differences can be attributed to the study of a condensed phase in one study and vapor phase molecules in the other. However, the relative values also differ. For instance, the difference between the ionization potential for the carbon 1s electrons in benzene and in the substituent group of trifluoromethylbenzene is 7.86 ± 0.09 eV for the vapor phase work and 8.9 ± 0.3 eV for the condensed phase work. Lesser discrepancies are observed between the results for the other ionization potentials.

The ionization potentials can be analyzed by a point charge model to estimate the charge distribution. This analysis is based on the elementary idea that the core-electron binding energy of an atom in trifluoromethylbenzene relative to the core-binding energy of a related atom in an appropriate reference com-

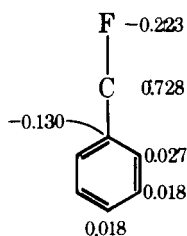
TABLE 9
Atomic Charges for Atoms in Trifluoromethylbenzenes^a

Atom	Atom charges			
	C ₆ H ₅ CF ₃		1,3-C ₆ H ₄ CF ₃	1,4-C ₆ H ₄ CF ₃
	Exptl	CNDO/2	Exptl	Exptl
F	-0.223		-0.238	-0.220
CF ₃	0.728		0.772	0.735
C ₁	-0.130	-0.051	-0.128	-0.124
C ₂	0.027	0.028	0.043	0.043
C ₃	0.018	0.005	-0.128	0.043
C ₄	0.018	0.022	0.033	-0.124
C ₅	0.018	0.005	0.023	0.043
C ₆	0.027	0.028	0.033	0.043
H	-0.007		0.001	-0.019

^a Ref. 45.

pound, benzene, depends on the charges induced on the atom and its neighbors by the substituent. Adoption of this idea and the notion that all the hydrogen atoms in each molecule are constrained to have the same charge enables the calculation of the charge distribution in these molecules on the basis of the observed potentials. The results are presented in Table 9.

The atomic charges, XVII, assessed in this way indicate that carbon atom C₁ is modestly electron-rich compared to a carbon atom in benzene. The charges at the other aromatic carbon atoms are positive compared to the carbon atoms in benzene. Holmes and Thomas have critically assessed this conclusion by an



XVII

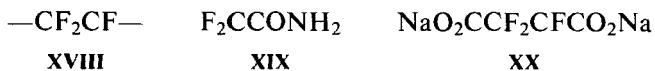
examination of the assumptions implicit in the point charge model. They conclude that the result that the ring is slightly negative is independent of any reasonable assumptions that might be made about relaxation effects or unresolved lines. The conclusion that the trifluoromethyl group acts as a feeble electron donor is not unique to the esca work on the aromatic molecules. Related work on fluorinated ethanes and ethenes yields the same result (47).

The charge distribution deduced from the esca data implies that the dipole moment for trifluoromethylbenzene is 1.49 D with the fluorine atoms at the negative terminus (48). This value is only about 50% of the known dipole moment. This is apparently a common problem. Often the charge distributions assessed in the analysis of the esca results do not correspond with known dipole moments. Most explanations focus on the idea that molecular dipole moments are especially sensitive to the distribution of lone pair electron density whereas the core ionization potentials depend more critically on the charge distribution in the vicinity of the nucleus (48). Nevertheless, the discrepancy between the estimated and known moments is disconcerting.

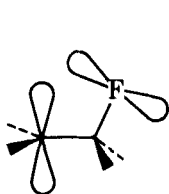
E. Electron Paramagnetic Resonance Spectroscopy

Electron paramagnetic resonance spectroscopy offers a very powerful method for the examination of the structures of radicals and for the distribution of spin and charge density in radicals and radical ions. The early observations that spin density appeared at the α - and β -fluorine atoms in radiation damaged

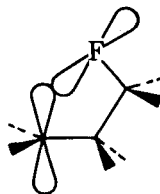
teflon (49), in difluoroacetamide radical (50), in the perfluorosuccinate radical (51), and in other radicals in the solid state and in solution were generally inter-



preted as evidence for conjugation and hyperconjugation, respectively. Reservations, however, were voiced concerning the latter interpretation (52). It is now well recognized that the epr coupling constants depend critically on the structure of the radical. Information concerning the geometry at the central atom, the influence of electron-withdrawing substituents, the angular relationship between key orbitals, and other factors is essential for an appreciation of the results. At first, the ideas concerning the geometric dependence of the β -fluorine atom coupling constants derived from experiments on radicals in the solid state were applied in the interpretation of the coupling constants observed for radicals in solution. These results were discussed in detail by Iwasaki in 1971 (52*b*). Since then, the spectra of many organic radicals with fluorine atoms have been reported. Recent contributions have, we believe, identified the factors that affect, often in subtle ways, the spectroscopic observations. These contributions enable a more confident interpretation of the data and provide evidence concerning the relative importance of four mechanisms which have been considered in discussions of the delocalization of electron charge or electron spin density. First, electron spin density may be delocalized to a β -fluorine atom by a 1,3 *pp* interaction between the *p* orbital of the radical center and the nonbonding *p* orbitals of the fluorine atom, **XXI**. Second, electron spin density may appear at



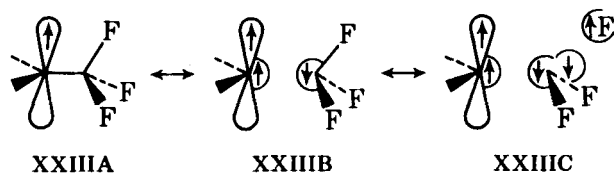
XXI



XXII

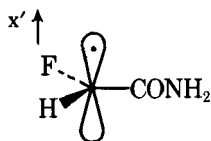
a fluorine atom that is remote from the radical site through a direct interaction of this same kind as sketched for the 3-fluoropropyl radical, **XXII**. Third, electron spin density may be delocalized by hyperconjugation. Generally, this interaction involves charge transfer as well as spin transfer. The orbital energies are sufficiently variable that it is necessary to consider delocalization from the bonding orbitals of the fluoroalkyl groups to the pi system of the radical or radical ion and delocalization to the antibonding orbitals of the fluoroalkyl groups from the pi system. Fourth, spin polarization of the sigma bond electrons between the radical center and the fluorine atom may place spin density at the β -fluorine atom, **XXIII**. The experimental evidence concerning the relevance of these four

interactions in the analysis of β -fluorine atom coupling constants is discussed in this section.



1. Coupling Constant Tensors, Solid State Results

The study of radicals trapped in single crystals of their precursors has shown that the hyperfine tensors for both α - and β -fluorine atoms are much more anisotropic than the tensors for related α - and β -hydrogen atoms. This feature is well illustrated for the α -atoms by the observations for monofluoroacetamide radical, XXIV, shown in Table 10.



XXIV

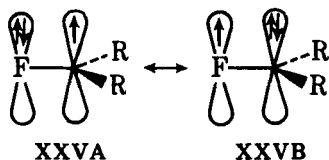
The anisotropic hyperfine tensor components for the α -fluorine atom are 133, -60 , and -72 G, respectively. The direction of the maximum principal element for the fluorine atom is parallel to the axis of the carbon $2p$ orbital and is almost axially symmetric with respect to the perpendicular axis, x' in XXIV. Iwasaki (52b) and Kispert (54) have discussed these results and other observations for α -fluorine atoms. Iwasaki concludes that the large anisotropy and the large positive coupling constants (55) have a common origin in the delocalization of spin density by direct overlap, XXV. It is pertinent that theory suggests that the anisotropic components for a fluorine atom are 1080, -540 , -540 G, respectively. The results for the acetamide radical, consequently,

TABLE 10
Hyperfine Tensors for Monofluoroacetamide^a

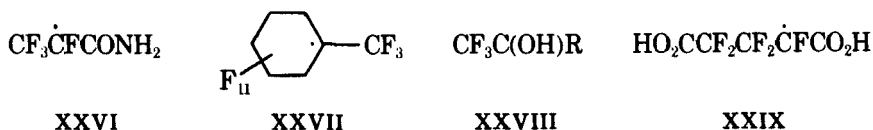
Tensor	Hydrogen direction	Value (G)	Tensor	Fluorine direction	Value (G)
A_1	\parallel C—H Bond	-11	A_1	\parallel C $2p$ Orbital	189
A_2	\parallel C $2p$ Orbital	-23	A_2	\perp C—F Bond	-4
A_3	\perp C—H Bond	-34	A_3	\parallel C—F Bond	-16
A_0	Isotropic	-23	A_0	Isotropic	56

^a Ref. 53.

suggest that about 10% of the spin density is delocalized to the fluorine atom. Thus, the available data quite convincingly indicate that the dominant mechanism for spin delocalization to α -fluorine atoms involves their nonbonding electrons.



The irradiation of alcohols, acids, amides, fluorocarbons, and other compounds has provided other radicals for study. Work on single crystals oriented in magnetic fields yielded the spectroscopic data for the perfluorosuccinate, **XX**, and the perfluoropropionamide, **XXVI** (51,56). The study of unoriented materials has yielded additional information concerning the coupling behavior of α - and β -fluorine atoms in perfluoromethylcyclohexyl radical, **XXVII**, hydroxyalkyl derivatives, **XXVIII**, the perfluoroglutarate, **XXIX** (57,58) as well as the 2,2,2-trifluoroethyl radical (59) and other related substances (54).



The original observations for the perfluorosuccinate, the most thoroughly studied radical of this kind, have been widely discussed (52,60). Subsequent studies, however, have revealed that the coupling constants determined in the original studies at ambient temperature represent average values of the actual coupling constants for two distinctly different conformations of the radical which may be resolved at lower temperature (61,62). The principal values and the anisotropic components for the β -fluorine atoms components for the β -fluorine atoms of the perfluorosuccinate, the perfluoropropionamide, and the trifluoroethyl radical are summarized in Table 11.

The β -fluorine atoms of the perfluorosuccinate and the other radicals all exhibit large anisotropy with nearly axial symmetry. The crystal structure of the host, sodium perfluorosuccinate, has recently been determined (63). Unfortunately, rearrangements occur upon radical formation and these rearrangements considerably restrict the usefulness of the crystallographic data for the definition of the structure of the radical. In the absence of structural information, workers in this area have been forced to make certain assumptions in the analysis of the data. The procedures used in the case of the succinate have been thoroughly discussed (52,60-62). The principal challenge has been to assign the structures of the two radicals which are conformationally stable at low

TABLE 11
Experimental Findings for the α - and β -Fluorine Nuclei in the Solid State

Radical	Principal value (G)	Anisotropic component (G)
Perfluorosuccinate, XX, 27^oa		
β -F ₁	62.9	28.1
	22.9	-11.9
	18.6	-16.2
	34.8 (isotropic)	
β -F ₂	71.4	31.0
	26.8	-13.6
	22.9	-17.5
	40.4 (isotropic)	
α -F	150.4	79.3
	58.9	-12.2
	3.9	-67.2
	71.1 (isotropic)	
Perfluorosuccinate, structure XXXA, -196^ob		
β -F ₁	122	58
	41	-29
	41	-29
	68 (isotropic)	
β -F ₂	9	8
	-3	-4
	-2	-3
	1.4 (isotropic)	
α -F	217	148
	-2	-71
	-7	-76
	69.3 (isotropic)	
Perfluorosuccinate, structure XXXB, -196^o		
β -F ₁	125	55
	44	-26
	41	-26
	70 (isotropic)	
β -F ₂	14	
	-1	-5
	-2	-6
	3.7 (isotropic)	
α -F	224	152
	-4	-75
	-5	-76
	71.6 (isotropic)	
Perfluoropropionate, XXVI^c		
	36	14
	17	5
	14	-8
	22 (isotropic)	

TABLE 11
Experimental Findings for the α - and β -Fluorine Nuclei in the Solid State

Radical	Principal value (G)	Anisotropic component (G)
2,2,2-Trifluoroethyl, II ^d	48.0	27.6
	20.4	-8.3
	17.7	-11.0
	28.7 (isotropic)	

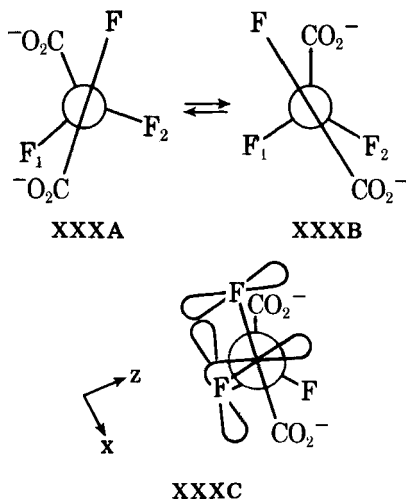
^a Refs. 51, 52, 54, and 61.

^b Refs. 61 and 62.

^c Refs. 51 and 56.

^d Ref. 59.

temperature.^d At present, the data appears to be most compatible with a torsional oscillatory motion of the α -fluorine atom with a corresponding motion of the β -fluorine atoms as shown in XXXA and XXXB. This conformational equilibrium accounts for the fact that the two isomers are about equally abundant at -196° , that there is one large and one small β -fluorine atom coupling interaction in each conformer, and that a partially averaged coupling interaction is observed at higher temperature (62). In addition, it has been noted that overlap between the α -fluorine atom and the carbon atom $2p$ orbital and one β -fluorine atom $2p$ orbital can occur most effectively in these conformations, XXXC. The implicit suggestion is that delocalization occurs through a direct interaction between the nonbonding orbitals of the α - and β -fluorine atoms as well as through a more traditional interaction involving the spin density in the carbon $2p$ orbital.



^d A third conformationally stable radical also can be observed when the irradiation is carried out at low temperature. The structure of this radical has not been assigned (61).

It is clear that a major effort has been made to define the geometry of the key interactions which may be responsible for spin delocalization to β -fluorine atoms. There are certain obvious problems. First, the structure of the radical is not well defined. The radical center may, in fact, be pyramidal. Second, the direct delocalization of spin density from neighboring but nonbonded atoms, for example, the α -fluorine atom or the carboxyl group, presumably influences the results. In view of these difficulties, it seems unwise to weight the solid state observations unduly in the interpretation of the origin of the coupling interaction. Nevertheless, all the results for radicals in solid state indicate that the hyperfine tensors are highly anisotropic. The data for the succinate and other radicals suggest that both the isotropic and the anisotropic coupling constants are very small for β -fluorine atoms that are very close to the nodal plane of the p orbital at the radical center. These features of the results must be incorporated into the ultimate interpretation.

Several workers have suggested that the large anisotropy indicates that spin density is delocalized to β -fluorine atoms dominantly through 1,3 $p p$ interactions (51,52,56). In this regard, Iwasaki has shown that the conformational dependence of the maximum overlap integral between a carbon p orbital and the fluorine p orbitals is given by Equation 1 where S_0 and S are defined

$$S_{CF}^2(\max) = S_0^2 + S^2 \cos^2 \theta_F \quad (1)$$

by the well known overlap integrals for specific geometric relationships between the carbon and fluorine atoms (63). If it is assumed that the spin density in the fluorine p orbital is proportional to the value of $S_{CF}^2(\max)$ and that this is the dominant coupling mechanism then the isotropic coupling constant should also be proportional to $S_{CF}^2(\max)$. This analysis predicts $A_{\beta-F}^0(\theta_F = 0^\circ)/A_{\beta-F}^0(\theta_F = 90^\circ)$ to be about 6 for molecules with conventional bond angles and bond distances (52,63,64). The information now available for the perfluorosuccinate in the solid state and other radicals in solution suggests that the ratio is greater than 50. Thus, the idea that 1,3 $p p$ interactions are dominant cannot be readily accepted.

2. Aliphatic Free Radicals

The epr spectra of many relatively simple fluoromethyl and fluoroethyl radicals and related substances have been examined in solution. Interest in this chemistry has been particularly keen since the spectroscopic results yield important clues concerning the structures of the radicals, rotation and inversion barriers, and the factors governing spin delocalization. Representative results which have been selected to portray the variations in experimental results and the small, but important influence of temperature on the a values are presented in Table 12.

The structures of the simple alkyl radicals are strongly dependent upon

TABLE 12
The Coupling Constants for the Nuclei of Selected Aliphatic Radicals in Solution

Radical	Coupling constant (G)					g	Ref.
	a_{α}^F	a_{β}^F	a_{α}^H	a_{β}^H	a^C		
CH ₃ , -177°			23.0		38.3	2.0026	65,66
CH ₂ F, -188°	64.3		21.1		54.8	2.0045	65
CHF ₂ , -188°	84.2		22.2		148.8	2.0041	65
CF ₃ , -90°	144.1						67
CF ₃ , -188°	142.4				271.6	2.0031	65
CH ₂ CH ₃ , -113°			22.4	27.0		2.0026	68
CH ₂ CH ₃ , -178°					39.1	2.0026	66
CH ₂ CH ₂ F, -60°		47.1	22.3	26.9			70
CH ₂ CH ₂ F, -60°		47.8	22.5	27.4			71
CH ₂ CH ₂ F, -122°		45.4	22.2	27.9		2.0025	69
CH ₂ CHF ₂ , -60°		49.5	23.4	12.3			72
CH ₂ CHF ₂ , -60°		48.7	23.4	12.3			71
CH ₂ CF ₃ , -60°		29.9	23.9				70,71
CH ₂ CF ₃ -113°		29.6	23.8			2.0023	68
CH ₂ CF ₃ , -125°		29.8	23.8			2.0023	69
CHFCH ₃ , -106°	59.2		17.3	24.5		2.0037	68
CHFCH ₃ , -106°	66.2	25.3	21.5			2.0036	68
CF ₂ CH ₃ , -78°	94.0			14.0		2.0036	68
CH(CH ₃)CH ₂ F, -60°		85.3	22.1	15.9 ^a			71
CH(CH ₃) ₂ , -113°							
CF(CH ₃) ₂ , -48°	60.9			21.1		2.0036	68
CH(CF ₃) ₂ , -113°		22.6	24.6			2.0022	68
CF(CF ₃) ₂ , -60°	67.4	19.2				2.0033	73
CF(CF ₃) ₂ , 25°	70.3	19.8				2.0031	74
C(CH ₃) ₃ , -163°				22.8	49.5		75
C(CF ₃) ₃ , 26°				18.7	44.3	2.0020	74
C(CF ₃) ₃ , -60°				17.9		2.0015	73
CF ₂ CF ₃ , -10°	87.7	11.4				2.0037	67
CF ₂ CF ₃ , -60°	84.9	11.2				2.0054	73
CF ₂ CF ₂ CF ₃ , -60°	93	15					73
CF ₂ CF ₂ CF ₃ , -60°	86.2	15.1					67
CF ₂ OSi(C ₂ H ₅) ₃ , -86°	147.6						74
CCl ₂ CF ₃ , -81°		18.6				2.0080	68
CCl ₂ CH ₃ , -108°				19.7		2.0073	68
CCl ₂ F, -60°	84.6						70
(CF ₂) ₂ CF,	64.5	29.4					76
(CF ₂) ₃ CF,	67.8	39.9 ^d					76
(CF ₂) ₂ CCl,	5.5 ^e	33.4					76
(CF ₂) ₃ CCl,	5.1 ^e	36.2 ^f					76

^a The value of a^{CH_3} is 25.7 G.

^b The value of a_{γ}^F is 4 G.

^c The value of a_{γ}^F is 3.6 G.

^d The value of a_{γ}^F is 6.1 G.

^e For a_{α}^{Cl} .

^f The value of a_{γ}^F is 5.1 G.

the nature of the substituents on the α -carbon atom. Fessenden and Schuler showed that a^C for the carbon atom of the methyl radical and its fluorinated derivatives changed from 38.5 G for the methyl radical to 271.6 G for the trifluoromethyl radical (65). The methyl radical is virtually planar (66,77,78). However, the trifluoromethyl radical is distinctly pyramidal. Good evidence has also been presented that the *t*-butyl radical is also pyramidal with an inversion barrier of about 600 cal mole⁻¹ (75,79-81). Krusic and Meakin and Wood and Lloyd have pointed out that this conclusion and related results for the bromine derivative, XXXI, which is also nonplanar have important conse-



XXXI

quences because these data imply that the stereoselectivity observed in the reactions of these radicals need not be the result of halogen bridging (82-84) but rather a natural consequence of rotational isomerism in a bent radical structure (82,85,86).

Two explanations have been proposed for the nonplanarity of radicals with electronegative substituents on the α -carbon atom. Pauling has argued that these radicals are not planar because the increased polarity of the carbon-substituent bond should favor an increase in the *s* character of the singly occupied orbital (87). Dewar and Bingham have proposed, to the contrary, that the conjugative destabilization resulting from the presence of two or three donor substituents on the α -carbon atom could also account for the nonplanarity (88). Subsequent work by Krusic and Bingham has revealed that the latter explanation appears to be generally more applicable (89). They have pointed out that there is a disproportionate change in a_α^H and a^C between the monofluoro and difluoromethyl radicals, that a^C for the tris(trifluoromethyl)methyl radical, about 44 G, is smaller than that for the *t*-butyl radical, about 49 G, that the coupling constant for the central carbon atom, a^C , for the tris derivative increases with temperature, a normal result for planar geometry and finally that the a_α^F values for radicals of the RCF₂ class appear to be correlated by the σ_R^0 resonance constants rather than the inductive constants, Table 13.

Although the relationship between a_α^F and σ_R^0 is not highly precise, this parameter provides a much better correlation of the data than σ_I . The results for the amido and ethereal substituents with almost identical σ_I values but very different values of σ_R^0 and a_α^F are particularly striking in this regard.

There is, however, a clear discrepancy. The value of a_α^F for the 1,1-difluorobenzyl radical, 51 G, contrasts strikingly with the other observations. Kispert, Liu, and Pittmann have discussed this result and the observations for other radicals of this class (91*b*). They suggest that the 1,1-difluorobenzyl radical is planar on the basis of the small value of a_α^F and the finding that approximate molecular orbital calculations indicate a preference for the planar structure.

TABLE 13
The Values of a_{α}^F for Selected Radicals of the RCF₂ Class

Radical	a_{α}^F (G)	σ_R^0 ^a	$\sigma_I^?$
H ₂ NCOCF ₂ ^b	68	0.14 ^d	0.30 ^d
F ₃ CCF ₂ ^c	85	0.08	0.45
HCF ₂ ^c	84	0.00	0.00
H ₃ CCF ₂ ^c	94	-0.11	-0.04
H ₅ C ₆ CF ₂ ^b	51	-0.11	0.10
CICF ₂ ^c	85	-0.23	0.46
FCF ₂ ^c	142	-0.34	0.50
Et ₃ SiOCF ₂ ^c	148	-0.45 ^e	0.27 ^e

^a Ref. 90.

^b Ref. 91a.

^c See Table 12.

^d Estimate based on σ_I for CO₂R.

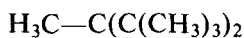
^e Estimate based on σ_I for OCH₃.

However, the fact that a_o^H and a_p^H for this radical are about 5 G suggests strongly that there is substantial charge delocalization to the phenyl nuclei. A large delocalization of spin density would, of course, have an appreciable influence on a_{α}^F . Moreover, the approximate molecular orbital analyses reveal that the increase in energy for the difluorobenzyl radical is only 0.1 kcal mole⁻¹ or less for a 5° out-of-plane deformation (91b). Consequently, the results seem equivocal and the 1,1-difluorobenzyl radical may be pyramidal.

The available evidence supports the view that conjugative destabilization effects rather than electronegativity considerations dictate the geometry of these radicals and that the trifluoromethyl group, a traditional electron-withdrawing group, does not induce a major distortion from planarity. Deviations from planarity apparently are modest except for radicals with two or more donor substituents bonded to the radical center. Thus, radicals with structures of the class of RCF₂ and RCl₂ may be expected to be distinctly nonplanar whereas other radicals such as the 1,2,2,2-tetrafluoroethyl radical have only modest deviations from planar geometry.

The epr spectra of many radicals have been investigated over a broad temperature range to define the energy barriers for rotation and inversion. The results for a selected group of radicals and reference molecules are summarized in Table 14.

Neither the ethyl radical (76,92,93) nor radicals with large steric requirements such as XXXII exhibit line broadening effects in low temperature



XXXII

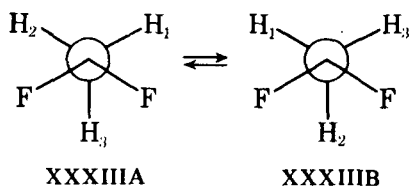
epr spectra (68). These results indicate that the energy barriers for rotation about

TABLE 14
 Rotational Energy Barriers for Alkyl Radicals

Radical	Phase	Rotational barrier (kcal mole ⁻¹)	Method	Ref.
CH ₃ CH ₂	solution	not observed	esr line shape	76,92,93
CH ₂ FCH ₂	solution	1.1, 1.2	esr line shape	94
CF ₂ HCH ₂	solution	1.4, 1.7	esr line shape	94
CH ₃ CHF	solution	not observed	esr line shape	68
CH ₃ CF ₂	solution	2.2	esr line shape	68, 94
CF ₃ CH ₂	solution	not observed	esr line shape	69, 70
CF ₃ CF ₂	solution	2.8	esr line shape	69, 94
(CH ₃) ₂ CF	solution	not observed	esr line shape	68
((CH ₃) ₃ C) ₂ - CCH ₃	solution	not observed	esr line shape	68
CH ₃ CCl ₂	solution	not observed	esr line shape	68
CH ₃ CH ₃	gas	2.9	thermodynamics	95
CH ₃ CH ₂ F	gas	3.3	microwave spectrum	96
CH ₃ CHF ₂	gas	3.2	microwave spectrum	96
CH ₃ CF ₃	gas	3.5	microwave spectrum	97

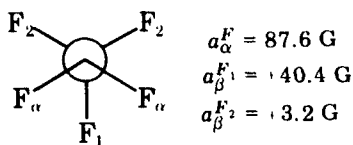
the carbon-carbon bonds in unsubstituted alkyl radicals are quite small, presumably less than 1 kcal mole⁻¹. The inversion barriers for the nonplanar unsubstituted alkyl radicals are also apparently rather small as illustrated by the inversion barrier, 0.6 kcal mole⁻¹, estimated for the *t*-butyl radical (75,79-82).

Line-broadening effects are discernible in the epr spectra of many radicals with α - and β -fluorine atom substituents as shown by the results in Table 14. Fluorine atoms at the radical site cause an increase in the barrier to rotation. Line-broadening effects have been observed for the 1,1-difluoroethyl, and 1,1,2,2,2-pentafluoroethyl radicals and other perfluoroalkyl radicals (67,68,94). No line-broadening effects have been detected, however, for the 1-fluoroethyl or the 1,2,2,2-tetrafluoroethyl radicals (68). A detailed analysis of the epr observations for the 1,1-difluoroethyl radical indicates that rotation of the methyl group is apparently responsible for the line broadening rather than the inversion of the carbon atom center (68,94). Meakin and Krusic also concluded that ro-



tational motion or possibly rotational motion coupled with inversion is responsible for the line width variation in the spectrum of perfluoroethyl radical (67). Their

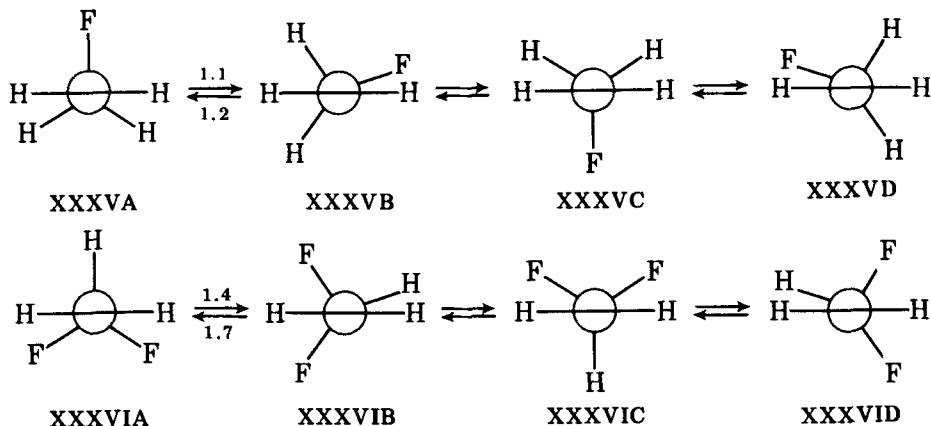
analysis of the data yielded the coupling constants for the nonequivalent nuclei in conformation **XXXIV** (67,94) and an estimate of the energy barrier for rotation, 2.9 kcal mole⁻¹.



XXXIV

Edge and Kochi and Biddles and his co-workers also examined the temperature dependence of a_{β}^F in the 2-fluoroethyl, 2,2-difluoroethyl, 2,2,2-trifluoroethyl, and 3-fluoro-2-propyl radicals (69,71). They established that a_{β}^F for the planar 2,2,2-trifluoroethyl radical is independent of temperature over a broad range of temperature. However, rotation may be restricted in the solid at 4.2°K (61). The a_{β}^F values of the other fluoroethyl derivatives exhibit a novel temperature dependence (Table 15).

The results suggest that the preferred conformations of these radicals differ somewhat as shown in **XXXVB** and **XXXVIB**. There are selective line-broadening effects which establish the small energy barriers to rotation about the carbon-carbon bonds as shown in the equations (94).



It is most interesting that there is a fourfold barrier to rotation with structures **XXXVB** and **XXXVIB** regarded as shallow minima on the potential surface. Although certain assumptions are required for the estimation of the energy barriers, the derived values are certainly accurate enough for the establishment of the relative barrier heights. The findings that the 2-fluoroethyl radical exhibits a small preference for the eclipsed form is intriguing. This observation suggests that some special features favor the adoption of the more sterically crowded eclipsed structure.

TABLE 15
Temperature Dependence of the Coupling Constants
for Fluoroethyl Radicals^a

Radical	da_{β}^F/dT	da_{β}^H/dT
F ₃ CCH ₂	Zero	—
F ₂ CHCH ₂	Negative	Positive
FCH ₂ CH ₂	Positive	Negative

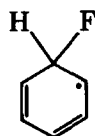
^a Refs. 69, 71.

Many investigators have tested the applicability of Equation 2 for the

$$a_{\beta}^F = \rho_C^F (B_0^F + B_2^F \langle \cos^2 \theta_F \rangle) \quad (2)$$

prediction of the coupling constants of β -fluorine atoms. a_{β}^F is the hyperfine coupling constant for the β -fluorine atom, B_0^F and B_2^F are empirical constants, θ_F is the dihedral angle between the axis of the carbon p orbital and the carbon-fluorine bond axis, and ρ_C^F is the spin density in the carbon p orbital. The data for ethyl radicals with one, two, or three fluorine atoms have been discussed by Biddles and his associates (71) and by Chen and his associates (94). While quantitative theoretical work is hindered by the fact that the INDO model considerably overestimates the a_{β}^F values (98), self-consistent analyses of the experimental data lead quite clearly to the conclusion that the B_2^F constants depend strongly on the degree of fluorine atom substitution with estimates of this constant ranging from 106 G for 2-fluoroethyl radical to 60 G, 2,2,2-fluoroethyl radical (71,94).

Yim and Wood have also pointed out that it is remarkable that a_{β}^F for the tris(trifluoromethyl)methyl radical, 19.2 G, is actually less than a_{β}^H for the *t*-butyl radical, 22.9 G (99). This observation coupled with the fact that a_{β}^H is only 19.3 G for the perfluorocyclohexadienyl radical, **XXXVII**, compared to 47.9 G for the unsubstituted radical, **XXXVIII**, provides more evidence for the view that electronegativity has an important influence on the coupling constants of both β -fluorine and β -hydrogen atoms and the B_2^F and B_2^H constants (100).^c



XXXVII



XXXVIII

The analyses of the data for the β -fluoroethyl radicals have generally been based on the idea that Equation 2 is applicable for the description of the angular dependence of the a_{β}^F constants. Approximate molecular orbital theory suggests,

^c This point is discussed in subsequent sections.

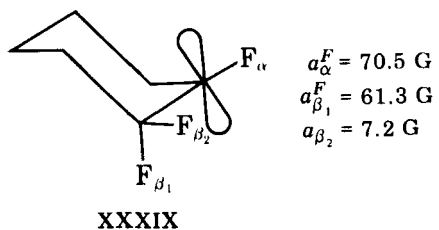
however, that B_0^F is quite small compared to B_2^F and an approximate form of Equation 2 has been used by some workers to examine the experimental results.

$$a_\beta^F = \rho_C^F B_2^F \langle \cos^2 \theta_F \rangle \quad (3)$$

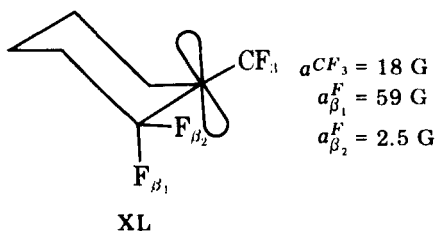
Unfortunately, only a few aliphatic radicals of known geometry have been studied to clarify the dependence on θ_F and the relative values of B_0^F and B_2^F . In one relevant study, Krusic and his associates determined the a_β^F constants for the perfluorocyclopropane, 29.4 G, and perfluorocyclobutane, 39.9 G (76). These constants must be compared with the value, 19.8 G, for the perfluoroisopropyl radical (73,74). Although ring strain effects influence the results, the observation that a_β^F for the cyclobutane is about twice the value for the acyclic radical strongly suggests that the B_2^F/B_0^F ratio is large. In another relevant study, Chachaty and his group examined the perfluorinated radicals, **XXXIX** and **XL**, in the solid state at low temperature (57,101). Their analyses of the spectra suggest that a_β^F depends critically on the dihedral angle, θ_F . Atom F_{β_1} is in a highly favored position for spin delocalization. The other fluorine atom, F_{β_2} , exhibits a much smaller coupling constant. The sign of $a_{\beta_1}^F$ may be presumed to be positive. The sign of $a_{\beta_2}^F$ cannot be assigned with confidence. Chachaty and his associates have fit the results for **XL** to Equation 4 on the basis of the assumption that B_0^F

$$a_\beta^F = -23 + 82 \langle \cos^2 \theta_F \rangle \quad (4)$$

and B_2^F are the same for the three different β -fluorine atoms (59,101). This agreement may be fortuitous for several reasons including the point that B_2^F is not expected to be constant for these different radicals. Nevertheless, the large differences in the a_β^F constants for the cyclohexyl radicals provide convincing evidence for a major dependence on the dihedral angle.



$$\begin{aligned} a_\alpha^F &= 70.5 \text{ G} \\ a_{\beta_1}^F &= 61.3 \text{ G} \\ a_{\beta_2}^F &= 7.2 \text{ G} \end{aligned}$$

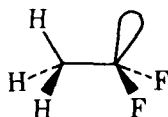


$$\begin{aligned} a^{CF_3} &= 18 \text{ G} \\ a_{\beta_1}^F &= 59 \text{ G} \\ a_{\beta_2}^F &= 2.5 \text{ G} \end{aligned}$$

These experimental observations for the fluoroalkyl radicals reveal that the values of the epr constants depend on several factors the most important of which is the number and kind of substituents on the α -carbon atom. Appropriate substitution patterns cause the radical center to be nonplanar with resultant novel a_β^F values. In these cases the fluorine substituents at the radical center affect a large reduction in the a_β^F values as a consequence of a decreased interaction

CF ₃ CH ₂	CF ₃ CF ₂	CH ₃ CH ₂	CH ₃ CF ₂
29.6 G	11.4 G	27.0 G	14.0 G

between the nuclei of the methyl or trifluoromethyl groups and the reaction center, **XLI**. Substitution at the β -carbon atom center also has a large influence on the coupling constants of the other β -nuclei as illustrated by the results for the substituted ethyl radicals. The radicals without electronegative atoms at the radical center may be regarded as essentially planar. The most economical interpretation stresses the idea that the extent of spin delocalization depends on the energy levels of the bonding and antibonding orbitals of the fluoromethyl, difluoromethyl, and trifluoromethyl groups relative to the energy level of the carbon p orbital. Qualitatively, the donor abilities of these groups decrease sharply as the degree of fluorine atom substitution increases. Their ability to accept charge density from the singly occupied carbon p orbital increases sharply, however, as the degree of fluorine atom substitution increases because the unoccupied antibonding molecular group orbitals approach the energy of the carbon $2p$ orbital. The former interaction is expected to be more important in these radicals with the result that B_2^F decreases with increasing fluorine atom substituents. The available data for the simple alkyl radicals are, of course, compatible with a distinct dependence on θ_F and are in accord with the idea that a_β^F depends on $\langle \cos^2\theta_F \rangle$ in the same general way that a_β^H depends on $\langle \cos^2\theta_H \rangle$. However, the experimental results cannot be used to establish the angular dependence unambiguously because B_2^F depends on the degree of fluorine substitution and on the stereochemical characteristics of the radical center. Thus, a_β^F is diminished as the radical center becomes pyramidal. The results suggest that a_β^F decreases by about 1 G for each degree of deformation from planarity.

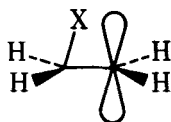
**XLI**

All these factors make it especially difficult to deduce the structures of radicals from the coupling constants. Not long ago several groups argued that the unusually small values of a_β^H for 2-fluoroethyl and 2-chloroethyl radical indicated that these radicals possessed distorted, bridged structures, **XLII** (69,70,92). The reduced a_β^H values were related to the increased distance between

TABLE 16
Long-Range Coupling Interactions in Aliphatic Radicals

Radical	Coupling constants (G)							Ref.
	a_{α}^H	a_{β}^H	a_{γ}^H	a_{α}^F	α_{β}^F	α_{γ}^F	a_{δ}^F	
FCH ₂ CH ₂ CH ₂	22.3	28.2	0.5			1.0		69
F ₃ CCH ₂ CH ₂	22.9	26.6				0.4		102
F ₂ CCF ₂ CF ₂				86.2	15.1	3.6		73,74
F ₃ CCH(CH ₃)CH ₂	22.7	28.0				1.7		94

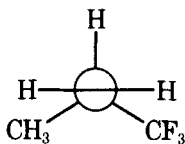
the β -hydrogen atoms and the radical center in the bridged structure. It is now recognized that the small a_{β}^H values are merely the consequence of the introduction of electronegative substituents on the β -carbon atom.^f



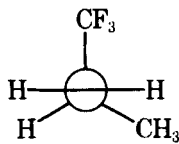
XLII

The question of longer range interactions to fluorine atoms as well as chlorine and bromine atoms has been examined by Kochi and his associates (69,94,102). Typical results for a selected group of compounds with fluorine atoms are summarized in Table 16.

The coupling constants for the γ -fluorine atoms appear to be significantly greater than the coupling constants for the γ -hydrogen atoms (94). This finding may be rationalized in two ways. On the one hand, the a_{γ}^F values may be large because direct 1,4 $p-p$ interactions are significant. Alternatively, these values may be appreciable because the interactions between the carbon p orbital and the group orbitals of the alkyl group, in this instance the CH₂(CH₂F) group, may be effective for the indirect propagation of spin density to the remote fluorine atoms. In the absence of a sign determination or other evidence it is difficult to distinguish between these interpretations. The evidence discussed on p. 303 suggests that the direct $p-p$ interaction is more important even though the a_{β}^H values indicate that the trifluoride preferentially adopts conformation **XLIIIA** rather than **XLIIIB** in which the direct interaction could be maximized.



XLIIIA

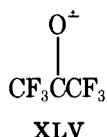
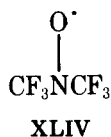


XLIIIB

^f This explanation appears to be secure because, as discussed subsequently, p. 295, small values of a_{β}^H are observed even when bridging interactions are impossible

3. Nitroxide Radicals

The spectra of many fluorinated nitroxide radicals have been reported in recent years. The spectrum of the parent molecule of this series, bistrifluoromethylnitroxide, was first reported in 1965 (103). Scheidler and Bolton observed that the spectrum of this radical was temperature dependent (104). They found that a^N decreased whereas a_β^F increased with a decrease in temperature. This novel observation prompted their suggestion that fluorine atom nitrogen atom $p p$ interactions were responsible for the coupling interactions because such interactions would restrict rotation about the nitrogen-carbon bond at low temperature with a resultant enhancement of the a_β^F constant (104). They also pointed out that a^N for bistrifluoromethylnitroxide is only about 9 G whereas a^N for di-*tert*-butylnitroxide is about 15 G (105). This large difference was attributed to a greater degree of spin delocalization from the nitrogen atom to the trifluoromethyl group than from the nitrogen atom to the *tert*-butyl group. However, there is no firm evidence concerning the stereochemistry at the radical centers in these substances. Indeed, Underwood and Vogel have argued, on the basis of approximate molecular orbital theory, that bistrifluoromethylnitroxide has a pyramidal radical center but that there is only a small difference between the energy content of the planar and pyramidal forms (106). Consequently, the temperature variations and the differences in the values of a^N and a_β^F may reflect changes in stereochemistry. Considerations of this and other kinds prompted Bolton and his students to reject the interpretation of the data based on 1,3 $p p$ interactions in favor of an explanation based on carbon-fluorine hyperconjugation. The new interpretation emerged from a comparison of the coupling constants of bistrifluoromethylnitroxide and hexafluoroacetone ketyl, XLV (Table 17).



The values of a_β^F are very different for the nitroxide and the ketyl even though the radicals are isoelectronic. This fact led Knolle and Bolton (108) to adopt a proposal of Morokuma (14). He pointed out that the energy difference between the lowest unoccupied molecular orbital of the trifluoromethyl group and the highest occupied molecular orbital of the carbonyl and nitroxide fragments in these compounds differed greatly. The interaction between these or-

TABLE 17
Coupling Constants for Bistrifluoromethylnitroxide and
Hexafluoroacetone Ketyl

Constant	XLV ^a	Constant	XLIV ^b
a^F	34.9 G	a^F	8.3 G
$a_{CF_3}^C$	8.0 G	$a_{CF_3}^C$	5.1 G
a_{CO}^C	23.3 G	a^N	9.5 G

^a Refs. 107 and 108.

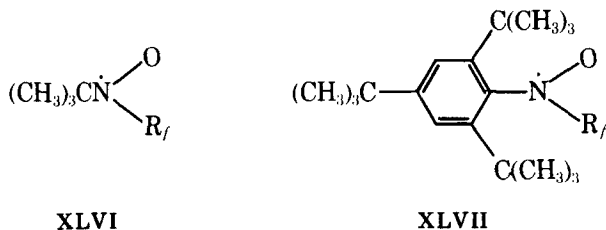
^b Refs. 104 and 108.

bitals is more significant in the ketyl than in the nitroxide to the end that a_β^F for the ketyl is much greater than a_β^F for the nitroxide. This hyperconjugation model predicts that electron transfer occurs with electron density delocalized from the singly occupied antibonding orbital of the radical center to the antibonding orbital of the trifluoromethyl group. The predictions of approximate molecular orbital theory support this interpretation. The energy content of an electron localized in the singly occupied carbon-oxygen antibonding molecular orbital is estimated to be 0.10 au compared to -0.46 au for an electron in the nitrogen-oxygen antibonding orbital. The most effective interaction, according to this explanation, occurs with an unoccupied antibonding pi orbital of the trifluoromethyl group estimated at 0.30 au (14).

The computations undertaken by Morokuma and by Underwood and his group support the idea that a_β^F for the nitroxide, XLIV, adheres to Equation 5 as shown in Fig. 5 (14,106).

$$a_\beta^F = -6.6 + 115 \langle \cos^2 \theta_F \rangle \quad (5)$$

Several investigations have been undertaken to estimate the angular dependence of a_β^F through the study of nitroxides in which the dihedral angle may be defined by the molecular geometry or severely restricted by steric constraints (109-111). Klabunde, for example, photolyzed perfluoroalkyl iodides in the presence of 2-nitroso-2-methylpropane to obtain *t*-butylperfluoroalkylnitroxides, XLVI (110). Terabe and Konaka also used this approach in a study of alkyl and perfluoroalkylnitroxides with aryl groups containing *o*-methyl or *o*-*t*-butyl substituents, XLVII (111). Typical results are summarized in Table 18.



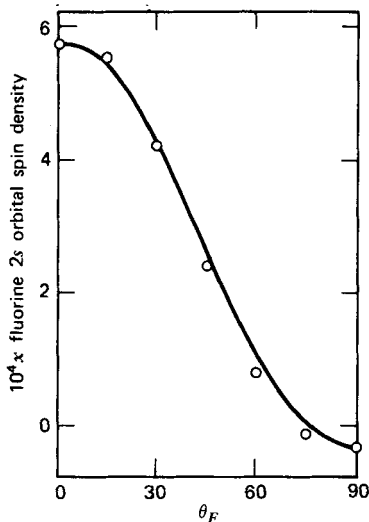


Figure 5 The relationship between the calculated fluorine atom 2s orbital spin density and the dihedral angle, θ_F , for bistrifluoromethylnitroxide (106).

The coupling constants for these radicals exhibit only a modest temperature dependence. The experimental results for the perfluoroisopropyl derivatives suggest that the β -fluorine atoms are oriented quite differently in **XLVI** and **XLVII**. Klabunde has pointed out that the steric interactions in the *t*-butyl derivative **XLVI** are minimized when the single β -fluorine atom is near the nodal plane of the nitrogen atom 2*p* orbital (110). Terabe and his associates have noted that the isopropyl derivative of **XLVII** exhibits a preference for the conformer in which the dihedral angle between the carbon-hydrogen bond and the nitrogen atom 2*p* orbital is 0° (112,113). They argue that the perfluoroisopropyl group should have the same conformational preference. These conformational as-

TABLE 18
Coupling Constants for Selected Nitroxides with Perfluoroalkyl Groups

Perfluoroalkyl group	Coupling constant (G)				
	XLVI ^a		XLVII ^b		
	a^N	a_β^F	a^N	a_β^F	a_γ^F
CF ₃	12.0	12.0	9.4	9.4	
CF ₃ CF ₂	11.3	21.2	9.6	27.2	0.7
(CF ₃) ₂ CF	12.1	2.3	9.7	48.4	- ^c

^a Ref. 110.

^b Ref. 111.

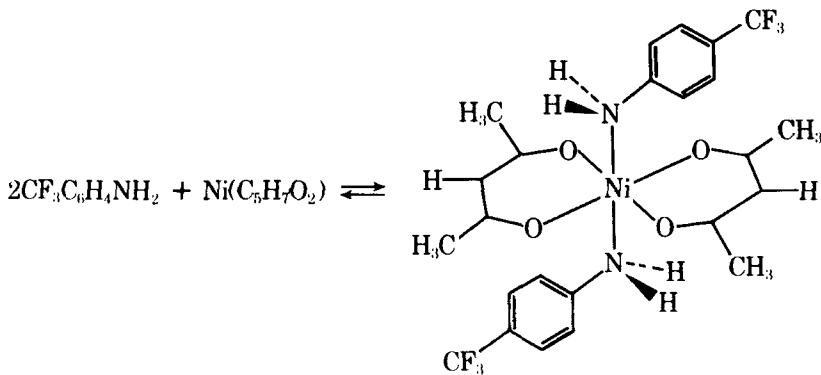
^c Unresolved.

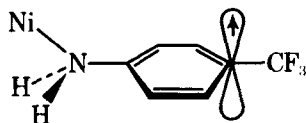
signments suggest that a_{β}^F depends on the dihedral angle with a small value when θ_F is 90° in accord with the conclusion reached in the analysis of the results for the fluoroalkyl radicals. The observations for the nitroxides are also akin to the results for the fluoroalkyl radicals in the sense that the B_2^F parameters depend on the number and kind of electronegative atoms on the substituent carbon atom (111-113). However, it must be noted that the stereochemistry at the nitrogen atom has not been established for these nitroxide radicals. This unresolved issue creates quite serious problems for the confident interpretation of the spectroscopic data.

4. Nitrobenzene Anion Radicals

The interpretation of the experimental a_{β}^F constants for the fluoroalkyl and nitroxide radicals is complicated because the stereochemistry at the radical center is not well defined. This complication does not exist for radicals derived from aromatic compounds. Consequently, several research groups have investigated aromatic radicals to characterize the factors governing spin delocalization to β -fluorine atoms. One aspect of this work concerns the epr spectra of nitrobenzene anion radicals. Another concerns the contact chemical shifts of paramagnetic transition metal complexes. The latter approach was initiated by Eaton, Josey, and Sheppard who examined stable bis(phenylaminotroponimato)-nickel(II) complexes (55a). More recently, we have examined the contact chemical shifts in the nmr spectra of nickel acetylacetonate complexes of aniline derivatives (55b).

The contact chemical shift measurements establish both the magnitude and the sign of the coupling constant. In brief, this approach depends upon favorably rapid ligand exchange and electron relaxation rates (114,115). When these processes are rapid the nmr resonances of the amine ligand are shifted but the lines are not unduly broadened. The extent of the shift depends on the pi spin





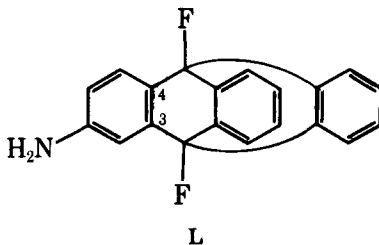
IL

density at the *para* carbon atom, **IL**. The contact shifts for the hydrogen and fluorine atoms in these complexes can be predicted from the Bloembergen-McConnell expression

$$\sigma_i = \frac{\Delta H_i}{H} = \frac{-a_i(\gamma_e/\gamma_N)g\beta S(S-1)}{3kT} \quad (6)$$

where the chemical shift, $\Delta H_i/H$, is measured relative to the shift in the uncomplexed ligand (or other suitable reference compound), S is the total spin quantum number, and the other symbols have their usual significance (114,115).

The contact shifts for the fluorine atoms relative to the shift for the *ortho* hydrogen atoms in the same molecule for the fluoroanilines, the trifluoromethylanilines, and the amino-9,10-difluorotriptycene, **L**, are summarized in Table 19.



L

TABLE 19
Relative Fluorine Atom Contact Chemical Shifts for Nickel Acetylacetonate Complexes^a

Compound	σ_i/σ_{2-H}		
	2-F	3-F	4-F
2-Fluoroaniline	-1.72 ± 0.06		
3-Fluoroaniline		0.95 ± 0.01	
4-Fluoroaniline			-2.85 ± 0.09
2-Trifluoromethylaniline	-1.04 ± 0.21		
3-Trifluoromethylaniline		0.43 ± 0.01	
4-Trifluoromethylaniline			-1.63 ± 0.01
L ^b		0.0094 ± 0.007	0.083 ± 0.001

^a Ref. 55b.

^b Numbered as shown in **L**.

The contact shifts for the fluorine and the 2-hydrogen atoms are related by Equation 7

$$\frac{\sigma_i}{\sigma_{2-H}} = \left(\frac{a_i^F}{a_2^H} \right) \left(\gamma_H / \gamma_F \right) \quad (7)$$

The a_2^H constant is negative in all these molecules. Thus, the σ_i / σ_{2-H} values for the fluoroanilines establish that a_2^F and a_4^F are positive whereas a_3^F is negative. Indeed, the signs of the three α -fluorine atom coupling constants are opposite to the signs of the corresponding α -hydrogen atom coupling constants in aniline. The observations for the fluoroanilines correspond exactly with the results obtained by Eaton and his associates (55a). The available information is in accord with the idea discussed on p. 275 that spin delocalization from the aromatic pi electron system to the fluorine nonbonding p orbitals is principally responsible for the coupling interaction.

The contact chemical shifts for the trifluoromethylanilines indicate that $a_{2-CF_3}^F$ and $a_{4-CF_3}^F$ are positive whereas $a_{3-CF_3}^F$ is negative. The signs reflect the fact that $\rho_{C_2}^{\pi}$ and $\rho_{C_4}^{\pi}$ are positive whereas $\rho_{C_3}^{\pi}$ is negative. Thus, B_2^F , the dominant term in Equation 2 is positive in all three cases. This conclusion is supported by the conclusions reached in the study of stable nickel complexes by Eaton and his group (55a).

The fluorine atoms in the triptycene, **L**, are constrained to the nodal plane of the pi electron system of the aryl amine fragment of the structure. The contact chemical shifts of these fluorine atoms are very much smaller than the shifts of the corresponding fluorine atoms in the trifluoromethylanilines. The shift for the fluorine atom in the position *meta* to the amino group is barely perceptible and the result cannot be discussed with confidence. The shift observed for the fluorine atom in the *para* position establishes that a_{β}^F for the fluorine atom in the nodal plane, $\theta_F = 90^\circ$, is very small and negative. It is opposite in sign to the a_{β}^F constants for the *para*-trifluoromethyl group. The ratio $a_{\beta-CF_3}^F$ ($\langle \theta_F \rangle = 45^\circ$) / $a_{\beta}^F(\theta_F = 90^\circ)$ is about -20 . This observation indicates that B_0^F is negative and rather small compared to B_2^F . It is regrettable that there are no other measurements available to test the reliability of this conclusion.

The coupling constants for the methyl- and trifluoromethylnitrobenzene anion radicals are summarized in Table 20.

The coupling constants of the nitrogen atoms in all the trifluoromethyl compounds are about 20% less than the constants for the methylnitrobenzene anion radicals. The fact that the a^N value is smallest for the *para* isomer is

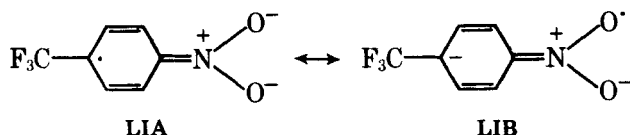


TABLE 20
Coupling Constants for the Methyl and Trifluoromethyl Derivatives of
Nitrobenzene Anion Radicals in Acetonitrile

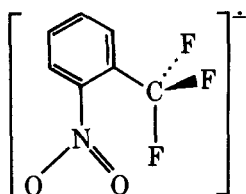
Substituent	Coupling constant (G)							
	a^N	a_2^H	a_3^H	a_4^H	a_5^H	a_6^H	$a_{CH_3}^H$	$a_{CF_3}^F$
2-CH ₃ ^a	11.3		3.32	3.74	1.04	3.32	3.32	—
3-CH ₃ ^a	10.7	3.39	—	3.84	1.09	3.39	1.09	—
4-CH ₃ ^b	10.7	3.39	1.11	—	1.11	3.39	3.98	—
2-CF ₃ ^{c,d}	8.32	—	0.87	3.90	1.23	3.20	—	8.51
3-CF ₃ ^c	8.84	3.01	—	4.05	1.00	3.21	—	1.20
4-CF ₃ ^c	8.00	3.20	0.92	—	0.92	3.20	—	8.00

^a Ref. 116.

^b Ref. 117.

^c Ref. 118.

^d Anomalous line broadening observed.



LII

compatible with a delocalization of spin and charge density from the aromatic pi system, to the trifluoromethyl group.

Janzen and Gerlock found that the epr spectrum of 2-trifluoromethylnitrobenzene anion radical exhibits a distinct alternation in line width (118). They related this alternation to the restriction of rotation about the carbon-carbon bond, **LII**. They also pointed out that there may be an important interaction between the oxygen and fluorine atoms which leads to the direct delocalization of spin density to the trifluoromethyl group.^g

The observations made in the work on the fluoroalkyl and nitroxide radicals suggests that the delocalization of spin density to β -hydrogen and β -fluorine atoms depends importantly on the electronegativity of the other atoms in the alkyl group. This aspect of epr spectroscopy has also been investigated by the study of the a_β^H constants for the 4-substituted nitrobenzene anion radicals (Table 21).

The a_β^H values are customarily analyzed on the basis of Equation 8:

$$a_\beta^H = \rho_C^\pi (B_0^H + B_2^H \langle \cos^2 \theta_H \rangle) \quad (8)$$

^g This interaction is discussed in more detail on p. 302.

TABLE 21
Coupling Constants for 4-Substituted Nitrobenzene Anion Radicals at Ambient Temperature

4-Substituent	Coupling constant (G)					Ref.
	a^N	a_2^H	a_3^H	a_β^H	a_β^X	
H	10.32	3.39	1.09	3.97 ^a	—	117
CH ₃	10.70	3.39	1.11	3.98	—	117
CH ₂ CH ₃	10.71	3.37	1.11	2.96	—	117
CH ₂ C(CH ₃) ₃	10.73	3.33	1.12	2.14	—	119
CH ₂ C(CH ₃) ₃ , -35°	10.96	3.40	1.10	2.06	—	119
CH ₂ N(CH ₃) ₂	12.38	3.33	1.19	2.62	1.20 ^b	119
CH ₂ OH	13.70	3.40	1.15	2.75	—	120
CH ₂ F	8.8	3.5	0.9	1.7	27.4 ^{c,d}	121
CH ₂ F, -35°	9.65	3.35	1.02	1.75	25.73 ^{c,d}	119
CHF ₂	8.2	3.4	1.0	1.0	14.6 ^c	121
CF ₃	8.0	3.2	0.9	—	9.1 ^c	118
CH ₂ N ⁺ (CH ₃) ₃ , -35°	11.2	3.31	1.00	1.52	2.85 ^b	119

^a For the 4-hydrogen atom.

^b For nitrogen atom.

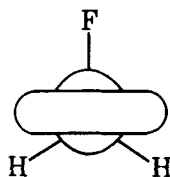
^c For fluorine atom.

^d Temperature dependent.

where ρ_C^π is the spin density at the 4 position, B_0^H and B_2^H are constants near -1.5 and 50 G, respectively, and $\langle \theta \rangle$ is the average dihedral angle. Often, it is assumed that B_0^H is negligible and that ρ_C^π and B_2^H are essentially constant for the substituted (XCH_2^-) and unsubstituted (CH_3^-) groups. Under these circumstances, a_β^H for the substituted radical is related to $a_{CH_3}^H$ by Equation 9:

$$a_\beta^H = (\cos^2\theta_1 + \cos^2(\theta_1 + 120^\circ))a_{CH_3}^H \quad (9)$$

This expression predicts that the minimum value of a_β^H , 2 G, is realized when the nitrotoluene anion radical adopts conformation **LIIA**.



LIIA

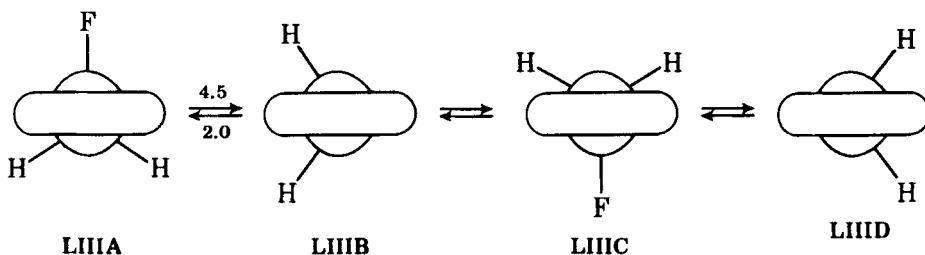
The experimental a_β^H values are all appreciably smaller than the constant for toluene. The values for the radicals with the most electron-withdrawing substituents are, actually, less than the minimum allowable value based on Equation 9. The result for the saturated trimethylammonium derivative which exhibits the smallest a_β^H value in this series excludes an interpretation based on

bridging (82–84). These findings suggest that the electronegative groups localize electron density in the carbon–hydrogen bonds with a consequent reduction in the interaction between the aromatic pi electron system and the carbon–hydrogen bonds as predicted by qualitative models based on hyperconjugation.

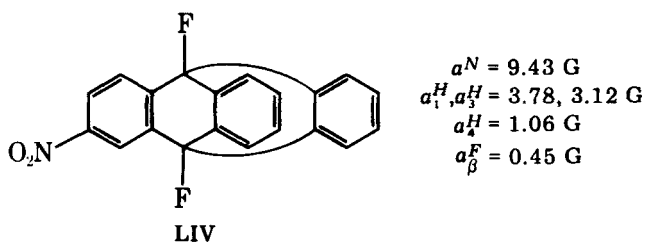
The spectroscopic results for the mono-, di-, and trifluoromethyl derivatives presented in Table 21 reveal that the a_{β}^F constants range from 9 to 27 G. These observations are very similar to the observations for the mono-, di-, and trifluoroethyl radicals for which a_{β}^F ranges from 30 to 48 G. Both series of data indicate that B_2^F is inconstant. This feature of the results is especially clear from the a_{β}^F constants for the nitrobenzene anion radicals. Analysis of the data for the trifluoromethyl derivative on the basis of Equation 3 with $(\cos^2\theta_F)$ as 0.5 and $\rho_{C_4}^F$ as 0.14 (122) suggests that B_2^F is about 115 G. This parameter predicts that the maximum value of a_{β}^F for the monofluoro derivative is 17 G. The observed value is 27 G. All these results are consistent with the idea that the introduction of electronegative atoms exerts a profound influence on the coupling interaction and that electron density is localized in the more electronegative substituent groups. This feature is apparent in the coupling constants of both the hydrogen and fluorine atoms of these groups.

The anion radical of 4-nitrobenzyl fluoride is not stable at ambient temperature. Moreover, the epr spectrum of this radical exhibits a very prominent temperature dependent line width effect at -5° (55*b*). The resonance lines associated with the dominant β -fluorine atom constant and the β -hydrogen atoms are increasingly broadened from the outer wings of the spectrum to the center. Chen and his associates discussed the origin of a similar line width effect in 2-fluoroethyl radical (94). The observations for both these radicals are consistent with the existence of a fourfold potential barrier. As already discussed, the data for the 2-fluoroethyl radical indicate that the eclipsed conformer, **XXXVB**, is slightly more stable than the staggered form, **XXXVA**, and that the rotational barrier is about 1.1 kcal mole⁻¹. The rotational barrier is much more pronounced for the anion radical. The barrier heights are estimated to be 2.0 and 4.5 kcal mole⁻¹, respectively. The results clearly require that the staggered form, **LIIIA**, be more stable than the eclipsed conformer, **LIIIB**. For comparison, the energy barrier for sterically hindered rotation about the aryl carbon–alkyl carbon bond of the anion radical of neopentylbenzene is only 2.4 kcal mole⁻¹ (55*b*). Thus, the barriers for rotation are strongly increased by the introduction of the electronegative fluorine atom into the alkyl group. In addition, the influence of the fluorine atom on the rotational barrier is greater in the anion radical than in the simple alkyl radical. These findings confirm the essential idea that the introduction of electronegative groups considerably alters the extent of electron delocalization. Moreover, the results for monofluoromethylnitrobenzene anion radical confirm the prediction of the qualitative theory of hyperconjugation advanced by Hoffmann and his associates (11) that the rotational barriers should

be larger for electronegatively substituted anions than for electronegatively substituted radicals.



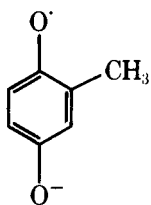
The anion radical of 2-nitro-9,10-difluorotriptycene, **LIV**, has also been investigated to establish the value of a_{β}^F for a molecule with the fluorine atom constrained to the nodal plane (55*b*). The constants for the nitrogen and hydrogen atoms differ only slightly from the values of the related constants for fluoromethylnitrobenzene anion radical, Table 21. The single fluorine atom coupling constant is assigned to the fluorine atom in the *para* position because the spin density at this position is about threefold greater in magnitude than the spin density at the position *meta* to the nitro group. Moreover, this assignment is in accord with the contact chemical shift data for the closely related amine, **L**. The a_{β}^F constant is presumably negative. The difference in the values of a_{β}^F for the triptycene derivative, -0.45 , and for the monofluoromethyl derivative, 25.7 G, is striking. The epr observations and the nmr observations both provide strong support for the view that the coupling interaction decreases to a very small and negative value when the fluorine atom is constrained to the nodal plane of the pi electron system. This result is incompatible with interpretations that stress $1,3 p p$ interactions but is fully consistent with explanations based on the concept of hyperconjugation.



5. Other Radicals

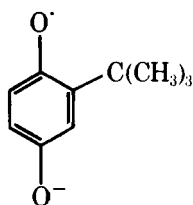
Ketyls, semidiones, semiquinones, and azo radicals with fluorine atoms have been studied in several laboratories. Certain of the more prominent features of these investigations are discussed in this section.

Early work established that a_{β}^F for semiquinone **LVII** was modest compared to the constants for the corresponding hydrogen and carbon nuclei in **LV** and **LVI** (123). These results infer that the β -hydrogen atom $1s$ orbital spin population and the β -carbon atom $2s$ orbital spin populations are about an order of magnitude greater than the β -fluorine atom spin population of 0.002.^h The a_{β}^H and a_{β}^F constants observed for fluoroalkyl radicals and nitrobenzene anion radicals also indicate, in general, that ρ_{1s}^H is much greater than ρ_{2s}^F .



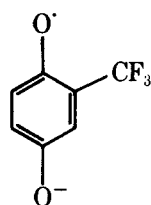
LV

$$a_{\beta}^H = 1.8 \text{ G}$$



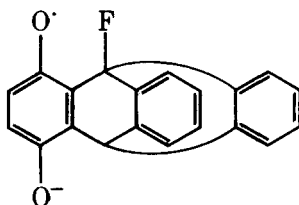
LVI

$$a_{\beta}^C = 0.7 \text{ G}$$



LVII

$$a_{\beta}^F = 2.7 \text{ G}$$

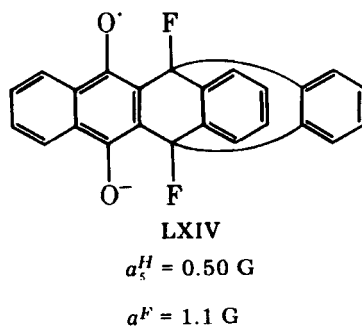
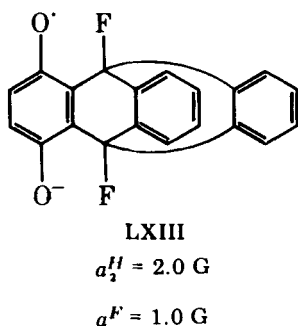
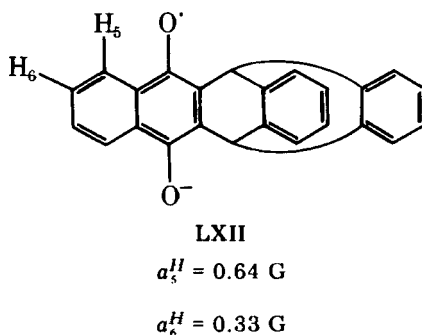
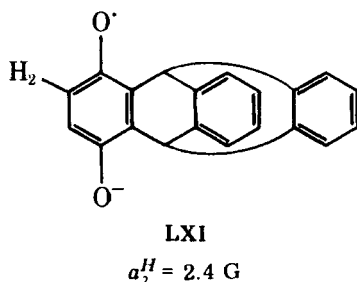
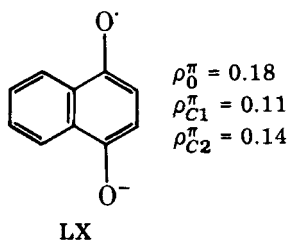
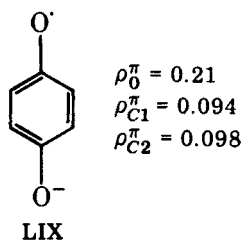


LVIII

Semiquinone **LVIII** was investigated in another attempt to establish the a^F value for a β -fluorine atom constrained unambiguously to the nodal plane of the π electron system (124). The observed a_{β}^F constant, 0.85 G, is only about fourfold smaller than the constant for the trifluoromethylsemiquinone, 2.7 G. This result contrasts sharply with the observations for the nitrobenzene and aniline derivatives discussed in Section IV.E.4. There are two viable interpretations. On the one hand, the result is compatible with an important role for p p interactions between the carbon atom p orbital and the nonbonding p orbitals of the fluorine atom (63,64). On the other hand, the fluorine and oxygen atoms are virtually in contact in semiquinone **LVIII**. Accordingly, a direct interaction between the p orbitals of these atoms may contribute to the delocalization of spin density to the fluorine atom (64). This interpretation is especially viable because ρ_0^{π} for benzosemiquinone is 0.21, more than twice the value of ρ_{C2}^{π} (125).

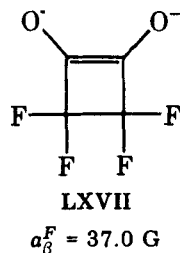
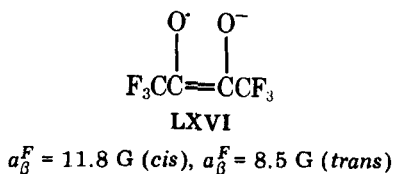
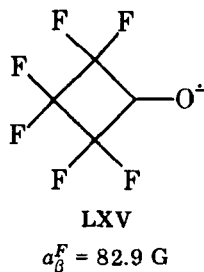
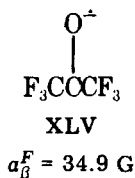
^h This analysis is based on the fact that the a values are determined exclusively by s orbital spin density. The coupling constants for unit spin densities are 508 and 17,000 G, respectively, for the hydrogen and fluorine nuclei. Hence, $\rho_{1s}^H = a^H/508$ and $\rho_{2s}^F = a^F/17,000$ (62).

A recent experimental observation suggests that the direct interaction is more important (55*b*). The epr spectra of several benzosemiquinones and naphthosemiquinones were analyzed. The analysis is based on the fact that the ρ_0^π and ρ_{C2}^π values of benzosemiquinone, **LIX**, and naphthosemiquinone, **LX**, differ appreciably (125). Under the assumption that the same spin density distribution prevail in the triptycene derivatives, **LXI-LXIV**, it is expected that a_β^F will exhibit a 40% increase if the spin density ρ_{C2}^π is the dominant consideration but a modest decrease if ρ_0^π is the critical factor. The results for these semiquinones and the unsubstituted derivatives, **LXI-LXII**, establish that the fluorine has a noticeable influence on the spin density distribution (55*b*). Nevertheless, the fact that the a_β^F parameters are comparable for **LXIII** and **LXIV** strongly infers that the spin density at the oxygen atom rather than at the carbon



atom is the dominant factor in spin delocalization in these anion radicals. The differences between the results for the nitrobenzenes and the semiquinones with a fluorine atom in the nodal plane apparently arise from a direct interaction between the oxygen and fluorine atom in the semiquinone which is excluded in the nitrobenzene and aniline (55*b*).

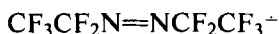
Several groups have addressed the issue of the angular dependence of a_{β}^F through the study of other radicals of rigid structure. Gerlock and Janzen recorded the esr spectra of the perfluorinated ketyls **XLV** and **LXV** (107,108,126). Although the results are certainly influenced by ring-strain, the fact that a_{β}^F is much larger for the cyclobutane provides further evidence for the view that the maximum value of a_{β}^F is realized when θ_F is small. In a similar investigation, Russell and his students examined the somewhat analogous semidiones **LXVI** and **LXVII** (126,127). They also observed that the rigid molecule with the smaller dihedral angle, **LXVII**, exhibited the larger coupling constant. Gerlock, Janzen, and Ruff reported that a_{β}^F constants for several perfluoroazoalkane radical anions including **LXVIII** and **LXIX** (129). In this instance, the a_{β}^F values do not differ appreciably. However, the radicals, **LXX** and **LXXI**, have larger a_{β}^F constants. Unfortunately, there is no secure approach for the assignment of their conformational preferences. It is pertinent that two nitroxides with perfluoroisopropyl groups **XLVI** and **XLVII**, Table 18, apparently exhibit opposite conformational preferences. Accordingly, no definite conclusion can be drawn from the observations for **LXX** and **LXXI**. Nevertheless, the results for these ketyls, semidiones, and azo radicals do generally support the view that a_{β}^F is largest for the conformations with the smallest dihedral angles between the p orbitals on the carbon and nitrogen atoms and the carbon-fluorine bonds.





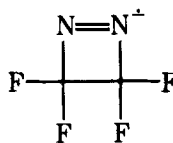
LXVIII

$$a_{\beta}^F = 18.0 \text{ G}, a^N = 8.4 \text{ G}$$



LXX

$$a_{\beta}^F = 35.2 \text{ G}$$



LXIX

$$a_{\beta}^F = 21.9 \text{ G}, a^N = 7.4 \text{ G}$$

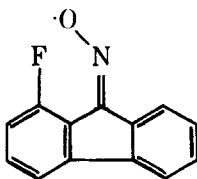


LXXI

$$a_{\beta}^F = 62.5 \text{ G}$$

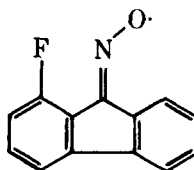
6. Direct Interactions

The notion that spin density can be delocalized by a direct interaction between two spatially proximate nonbonded atoms has been mentioned in the discussion of the coupling constants for several radicals. For example, Janzen and Gerlock related the motional modulation of the coupling constants of the β -fluorine atoms of 2-trifluoromethylnitrobenzene anion radical to a direct interaction of this kind (118). Direct interactions may also contribute to the delocalization of spin density from oxygen to fluorine atoms in the semiquinones, semifuraquinones, fluorinated nitroxides, and the perfluorosuccinate radical. Independent evidence indicates that the spin density at the oxygen atoms in these radicals and radical ions is large. To illustrate, ρ_0^{\cdot} is about 0.2 for benzosemiquinone (125) and about 0.5 for the nitroxide (14). Although it is difficult to develop secure experimental evidence for the direct interaction, there are many very suggestive observations concerning its importance. Norman and Gilbert prepared the isomeric iminoxy radicals, LXXII and LXXIII (130). The a^F values for these two sigma radicals differ greatly. Only the proximate fluorine atom is coupled. Clearly, the direct interaction mechanism offers the most reasonable explanation. Some thoughtful investigators have been reluctant to extrapolate this conclusion for these sigma radicals to the interpretation of the observations for pi radicals. Nevertheless, other evidence for direct delocalization has slowly accumulated from the careful analysis of the data for several different pi radicals.



LXXII

$$a^F = 13.5 \text{ G}$$



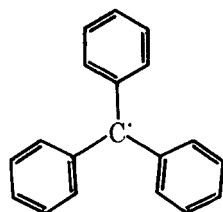
LXXIII

$$a^F = 0 \text{ G}$$

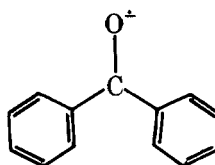
TABLE 22
Coupling Constants for 2- and 4-Fluorine Atoms of
Triphenylmethyl and Diphenylnitroxide Radicals^a

Substituent	Coupling constant (G)	
	LXXIV	LXXV
2,6-Difluoro	2.11	4.13
4-Fluoro	6.26	7.42

^a Refs. 131 and 132.



LXXIV



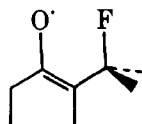
LXXV

Critical examination of the coupling constants for the triptycene derivatives, **LXIII** and **LXIV**, suggests not only that the direct interaction is important but also that the sign of the coupling constant in this case is negative (55*b*). In other work, Kulkarni and Trapp investigated the esr spectra of fluorine atom derivatives of the triphenylmethyl and diphenylketyl radicals (131,132). Their observations are presented in Table 22.

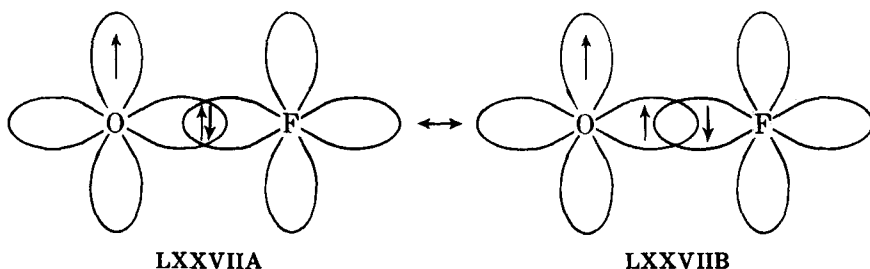
The a_2^f constants are unusually small compared to the a_4^f constants. The spin densities calculated by approximate molecular orbital theory for the 2 and 4 carbon atoms of the trityl and diphenylketyl radicals are, however, essentially the same. Kulkarni and Trapp, accordingly, conclude that a direct transfer of spin density occurs from the radical center to the fluorine atoms in the *ortho* positions. The interpretation implies that the direct interaction yields negative spin density in the fluorine 2*s* orbital.

These inferences are complemented by nmr findings. Mallory has discussed the salient nmr observations and their most probable interpretation. He has concluded that the direct interaction is the dominant factor for long-range fluorine-fluorine coupling (133). Application of this explanation to the results for the semiquinones discussed in Section IV.E.6 suggests that the *p* orbitals on the proximate oxygen and fluorine atoms, **LXXVI**, combine to yield two molecular orbitals which are both doubly occupied and which do not contribute to the stabilization of the radical. However, the electron pair in this molecular orbital may be spin polarized by spin density, $\rho_0^{\bar{\sigma}}$, in the orthogonal *p* orbital of the oxygen atom in a fashion similar to the spin polarization of the electron density

in a carbon-hydrogen bond in a pi radical (134). The favored electron configuration, **LXXVIIIB**, places negative spin density at the fluorine atom in accord with the implications of the experiments.



LXXVI



LXXVIIA

LXXVIIIB

7. Theoretical Interpretation

The experimental results discussed in the previous sections present a challenge for theoretical interpretation. Generally, the experimental data for radicals with β -fluorine atoms have been examined on the basis of the empirical two-term expression, Equation 2, which is presented here for convenient dis-

$$a_{\beta}^F = \rho^{\pi}(B_0^F + B_2^F \langle \cos^2 \theta_F \rangle) \quad (2)$$

cussion. The experimental results indicate that the second term is dominant. The dependence on the cosine of the dihedral angle is implied experimentally by the small values of a_{β}^F for various radicals in which the fluorine atom is constrained to the nodal plane and by the large a_{β}^F constants for other radicals in which the fluorine atom exhibits a preference for the staggered conformation. The B_2^F parameters estimated from the results for six well-studied radicals with trifluoromethyl groups are summarized in Table 23.

Clearly, these approximate B_2^F values depend importantly on the structure of the radical. Quite different values are observed for fluoroalkyl radicals, nitroxide radicals, nitrobenzene anion radicals, ketyls, and so forth. This conclusion would not be altered by the consideration of the angle independent term or by the reconsideration of the estimated spin densities. Furthermore, the values of B_2^F are not the same for closely related radicals such as the mono-, di-, and trifluoroethyl radicals or the mono-, di-, and trifluoromethylnitrobenzene anion radicals as already discussed. The B_2^F value estimated for monofluoromethyl-

TABLE 23

Radical	a_{β}^F (G)	$\rho^{\pi a}$	B_2^F (G) ^b
(CF ₃) ₂ NO	8.3	0.3	55
CF ₃ COCOFCF ₃ ⁻	8.5	0.3	57
CF ₃ CH ₂ ⁻	29.9	1.0	60
CF ₃ C ₆ H ₄ O ₂ ⁻	2.7	0.08	68
CF ₃ C ₆ H ₄ NO ₂ ⁻	8.0	0.14	115
(CF ₃) ₂ CO ⁻	34.9	0.5	140

^a Estimated on the basis of the experimental results for other derivatives and approximate molecular orbital theory.

^b Estimated from the expression, $B_2^F = 2\rho^{\pi}a_{\beta}^F$.

nitrobenzene anion radical is 164 G, about 50% greater than the B_2^F value appropriate for the trifluoromethyl derivative. In addition, the experimental data for nitroxides, nitrobenzene anion radicals, and the contact shift work on aniline derivatives suggest that the first, angle independent term in Equation 2 is definitely small and two experiments suggest that B_0^F is negative. The analysis of the coupling behavior of β -fluorine atoms is complicated by the existence of direct interactions between nonbonded atoms. The observations for semiquinone derivatives suggest that these interactions may be appreciable even for pi radicals.

Although it is regrettable that the data for radicals in the solid state have been derived in the absence of secure information about the structures of the host crystals and that there are no data concerning the anisotropy of the tensors for radicals with monofluoroalkyl groups or with fluorine atoms constrained to a definite position by structure, the known tensors reveal that the coupling interactions of β -fluorine atoms are much more anisotropic than the interactions of β -hydrogen atoms. To illustrate, a_{β}^F is 28.7 G for the trifluoroethyl radical and a_{β}^H is 27.0 G for the ethyl radical. On the other hand, the principal elements of the corresponding anisotropic tensors for comparable radicals for 19.3, -11.0, and -8.3 G, respectively, for the β -fluorine atom and 6.5, -2.5, and -3.0 G, respectively, for the β -hydrogen atom. These results may be directly compared because the magnetogyric ratios for the hydrogen and fluorine nuclei are essentially equal. Careful examinations of the data for the fluorine atoms indicate that the maximum principal elements of the tensors lie along the axes of the nonbonding p orbitals of the fluorine atoms. A literal interpretation of the experimental findings for the trifluoroethyl radical suggests that the $2s$ orbital spin density is about 0.002 and that the $2p$ orbital spin density is about 0.04. These results infer that no more than about 5% of the spin density is delocalized to the β -fluorine atom in this radical.

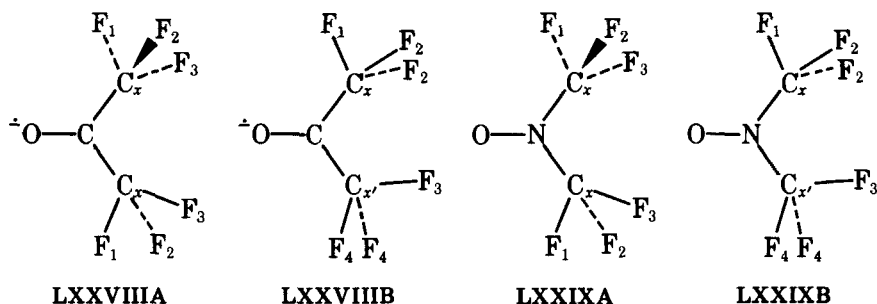
Most theoretical examinations of the experimental results have employed the INDO approach (98). Several different investigators have noted that the

TABLE 24
Spin Densities Calculated for Nuclei of Conformers of Trifluoromethyl Nitroxide and Ketyl^a

Atomic orbital	2s Orbital spin density, 10 ⁴			
	Conformational isomer			
	LXXVIII A	LXXVIII B	LXXIX A	LXXIX B
F ₁	5.5	-0.1	1.0	-0.1
F ₂	23.9	17.8	5.0	3.8
F ₃	5.7	-0.3	1.1	-0.3
F ₄	—	17.4	—	3.5
Average	11.7	11.7	2.4	2.4

^a Ref. 14.

application of this theory for the prediction of the isotropic a_{β}^F values for trifluoromethyl groups in different radicals indicate that the calculated constants adhere to Equation 2 and that almost negligible values are predicted for β -fluorine atoms in the nodal plane (135). These features are illustrated by the results shown in Fig. 5 and by the spin densities calculated for the conformers of the nitroxide and ketyl radicals summarized in Table 24.



These results and the related finding that the calculated a_{β}^F constants for the monofluoroethyl radical also conform to Equation 2 establish the general correspondence between the predictions of the theory and the experimental results concerning the dominance of the angle dependent term and the dependence on the cosine of the dihedral angle. However, there is a notable problem. The B_2^F constants predicted by theory are not usually in reasonable agreement with the experimental results. Part of this disagreement arises in the initial selection of a scaling factor for the conversion of the calculated spin density to the coupling constant (98). However, the problem appears to be more deepseated because no single scaling factor will provide generally satisfactory agreement. Hence, we must rely on an intuitive interpretation of the theoretical calculations.

The fact that the coupling constants for the trifluoromethyl ketyl and the nitroxide differed so much (Table 23) prompted Morokuma to examine the

matter. He pointed out, as discussed on p. 289, that the energies of the singly occupied orbitals of these radicals differed appreciably and that the large difference in the a_{β}^F values for these radicals originated in the correspondingly large difference in the interaction between these singly occupied orbitals and the orbitals of the trifluoromethyl group (14). He proposed that, in general, the interpretation of the epr data for radicals with β -fluorine atoms would require special consideration of the relative energies of these interacting orbitals. This key suggestion provides a basis for the discussion of the data and for an understanding of the limitations of the INDO approach for the calculation of the β -fluorine atom coupling constants. First, the variability of B_2^F for the trifluoromethyl derivatives originates in the variations in the energy content of the singly occupied orbitals. The variability of B_2^F for the mono-, di-, and trifluoromethyl derivatives has a similar origin because the electronegative atoms have a major influence on the energies of the orbitals of the fluoroalkyl groups. In these circumstances, the a_{β}^F values reflect the differences in the effectiveness of the interaction of the singly occupied orbital both with the bonding as well as the antibonding orbitals of the fluoroalkyl groups. It has been pointed out that the fact that the empirical B_2^F parameters are greater for the monofluoromethyl derivatives than for the trifluoromethyl derivatives implies that the electronegative atoms localize electron density and thereby diminish spin and electron density delocalization. For the trifluoromethyl group, it is notable that the spin delocalization may occur with special efficiency between two antibonding orbitals as illustrated by the results for the trifluoromethylketyl and for trifluoromethylnitrobenzene anion radical. In other cases, the orbital energies may differ appreciably such that spin delocalization is hindered as proposed for the corresponding nitroxide. Second, we note that this factor has an important bearing on the interpretation of the deviations of the experimental results from the predictions of the INDO theory. Clearly, the results present a considerable challenge for any theory because many interactions must be computed with great accuracy if the ultimate spin densities and coupling constants are to be in good agreement with the experimental findings. In this case, the problem is especially critical because at least two major orbital interactions must be accurately assessed. Although the INDO method yields reasonable results, it is evident that there are limitations to its scope.

The results obtained in the investigation of radicals in the solid state convincingly demonstrate that spin density is delocalized to the $2p$ orbitals of the β -fluorine atoms. An interpretation based on carbon-fluorine hyperconjugation between the orbital at the radical center and the e orbitals of the trifluoromethyl groups constructed from $2p_z$ orbitals, for example, $\Psi_{E_a}(2p_z)$ or $\Psi_{E_b}(2p_z)$ in Fig. 3, provides an attractive qualitative explanation for this aspect of the results. However, the findings of recent *ab initio* computations concerning the nature of the orbitals of the trifluoromethyl fragment of fluorofrom suggest that the

e orbitals with the appropriate energy have a mixed $2s$ and $2p$ character (15). Presumably, all modern theoretical methods will yield orbitals which have a highly mixed character. In this situation, spin delocalization quite naturally introduces spin density into formally unoccupied antibonding molecular orbitals of the trifluoromethyl group with both s and p character.

The distinction between delocalization to an e orbital with p character by carbon-fluorine hyperconjugation and delocalization by a $1,3 p p$ interaction is a fine one. However, the experimental observations obtained for monofluorides with the fluorine atom located in the nodal plane reveal that the isotropic a_{β}^F constant is very small and probably negative. Strictly speaking, such results are incompatible with the idea that a $1,3 p p$ interaction is generally responsible for the delocalization of spin density because this interaction, as described in Equation 1, does not reduce to zero or change sign as a consequence of rotation of the carbon-fluorine bond into the nodal plane. Thus, we infer that carbon-fluorine hyperconjugation offers a more satisfactory explanation for spin delocalization.

F. Summary

The physical measurements yield quite intriguing information concerning the behavior of the trifluoromethyl group. The work on the dipole moments of benzotrifluoride and its derivatives seems unequivocal. The similar properties of molecules with the trifluoromethyl group in the *meta* and *para* positions strongly suggests that pi inductive interactions rather than carbon-fluorine hyperconjugation is responsible for the modestly enhanced dipole moments observed in the compounds with donor substituents. The substituent chemical shifts observed in the nmr spectra of substituted fluorobenzenes, fluorobiphenyls, and fluoronaphthalenes and the esca spectra of the derivatives of benzotrifluoride are all consistent with an interpretation of this kind. The results do not require the postulation of a special acceptor resonance effect for the trifluoromethyl group in these uncharged molecules. This conclusion corresponds closely with the conclusion reached in the discussion of the chemical reactions of molecules with trifluoromethyl groups.

The interpretation of the epr data is more challenging. These spectroscopic data strongly suggest that spin delocalization occurs in radicals and in radical anions through carbon-fluorine hyperconjugation. The extent of spin delocalization apparently depends critically on the structure of the radical. The delocalization is enhanced when, in a formal sense, the energy content of the orbital containing the odd electron and the unoccupied orbitals of e symmetry of the fluoroalkyl group approach one another. In this instance, spin and electron density appear to be delocalized to the trifluoromethyl group.

V. CONCLUSION

The chemical and physical measurements concerning the behavior of the trifluoromethyl group and related fluoroalkyl groups are in good agreement. The chemical equilibrium and rate data concerning the dissociation constants of benzoic acids, phenols, and anilines as well as the rate constants for the reactions of aliphatic and aromatic compounds can be understood on the basis of the field and pi inductive effects of this very polar group. The influence of this substituent appears to be enhanced only in very electron-rich transition states such as the one leading to the benzenanion intermediate in nucleophilic aromatic substitution reactions. The spectroscopic properties of uncharged, stable molecules similarly can be rationalized on the basis of polar and pi inductive effects. However, the favored interpretation for the epr data centers on carbon-fluorine hyperconjugation. Qualitatively, the interaction which appears to be especially relevant involves the transfer of spin as well as charge density from the radical center to an antibonding molecular orbital of the trifluoromethyl group. We infer that this charge transfer is a significant factor only in electron-rich transition states and intermediates.

References

1. J. D. Roberts, R. L. Webb, and E. A. McElhill, *J. Am. Chem. Soc.*, **72**, 408 (1950).
2. W. A. Sheppard and C. M. Sharts, *Organic Fluorine Chemistry*, Benjamin, New York, 1969, Chapter 2.
3. D. Holtz, *Chem. Rev.*, **71**, 139 (1971).
4. D. Holtz, *Prog. Phys. Org. Chem.*, **8**, 1 (1971).
5. L. M. Yagupol'skii, A. Ya. Il'chenko, and N. V. Kondratenko, *Russ. Chem. Rev.*, **43**, 32 (1974).
6. The results of several independent studies are presented by M. Jinguji, K. C. Lin, C. A. McDowell, and P. Raghunathan, *J. Chem. Phys.*, **65**, 3910 (1976).
7. R. D. Topsom, *Prog. Phys. Org. Chem.*, **12**, 1 (1976).
8. W. A. Sheppard, *J. Am. Chem. Soc.*, **87**, 2410 (1965).
9. R. S. Mulliken, C. A. Rieke, and W. G. Brown, *ibid.*, **63**, 41 (1941).
10. C. A. Coulson, *Valence*, Oxford, 1952, pp. 310-314.
11. R. Hoffmann, L. Radom, J. A. Pople, P. von R. Schleyer, W. J. Hehre, and L. Salem, *J. Amer. Chem. Soc.*, **94**, 6221 (1972).
12. A. R. Rossi and D. E. Wood, *ibid.*, **98**, 3452 (1976).
13. Approximate calculations suggest that there is a 9 kcal mole⁻¹ preference for the **B** conformation of the 2-fluoroethyl carbanion (Ref. 11).
14. K. Morokuma, *J. Amer. Chem. Soc.*, **91**, 5412 (1969).
15. L. C. Snyder and H. Basch, *Molecular Wave Functions and Properties*, Wiley, 1972, pp. 346-350.
16. J. March, *Advanced Organic Chemistry*, 2nd ed., McGraw-Hill, 1977, p. 284.
17. (a) L. P. Hammett, *Physical Organic Chemistry*, 2nd ed., McGraw-Hill, New York, 1970,

- Chapter 11. (b) J. E. Leffler and E. Grunwald, *Rates and Equilibria of Organic Reactions*, Wiley, New York, 1963, p. 381.
18. D. D. Perrin, *Dissociation Constants of Organic Bases in Aqueous Solution*, Butterworths, London, 1965.
 19. A. I. Biggs and R. A. Robinson, *J. Chem. Soc.*, 1961, 388.
 20. (a) C. L. Liotta and D. F. Smith, Jr., *Chem. Commun.*, 1968, 416. (b) C. L. Liotta, D. F. Smith, Jr., H. P. Hopkins, Jr., and K. A. Rhodes, *J. Phys. Chem.*, 76, 1909 (1972).
 21. A. Streitwieser, Jr., and H. F. Koch, *J. Amer. Chem. Soc.*, 86, 404 (1964).
 22. K. J. Klabunde and D. J. Burton, *ibid.*, 94, 820 (1972).
 23. A. M. Porto, L. Altieri, A. J. Castro, and J. A. Brioux, *J. Chem. Soc., B*, 1966, 963.
 24. (a) J. Miller, *Aust. J. Chem.*, 9, 61 (1956). (b) J. Miller and W. Kai-Yan, *J. Chem. Soc.*, 1963, 3492. (c) K. C. Ho and J. Miller, *Aust. J. Chem.*, 19, 423 (1966).
 25. W. R. Greizerstein, R. A. Bonelli, and J. A. Brioux, *J. Amer. Chem. Soc.*, 84, 1026 (1962).
 26. L. M. Yagupol'skii, N. V. Kondratenko, N. I. Delyagina, B. L. Dyatkin, and I. L. Knunyants, *J. Org. Chem. (USSR)*, 9, 669 (1973).
 27. R. D. Chambers, J. S. Waterhouse, and D. L. H. Williams, *Tetrahedron Lett.*, 1974, 743.
 28. A. Streitwieser, Jr., and D. Holtz, *J. Amer. Chem. Soc.*, 89, 692 (1967).
 29. S. Andreas, *ibid.*, 86, 2003 (1964).
 30. Holtz (3,4) has discussed the problems associated with the variations in hybridization and polar effects among the molecules presented in Table 5. We do not believe that sufficiently reliable corrections can be made to permit a confident decision concerning the actual impact of the change in the dihedral angle on the reaction rate.
 31. Stable phosphoranes have been reported by several groups. (a) W. J. Middleton and W. H. Sharkey, *J. Org. Chem.*, 30, 1384 (1965). (b) G. H. Birum and C. N. Matthews, *ibid.*, 32, 3554 (1967). (c) M. A. Howells, R. D. Howells, N. C. Baenziger, and D. J. Burton, *J. Amer. Chem. Soc.*, 95, 5366 (1973).
 32. D. J. Burton, R. D. Howells, and P. D. Vander Valk, *ibid.*, 99, 4830 (1977).
 33. J. D. Hepworth, J. A. Hudson, D. A. Ibbitson, and G. Hallas, *J. Chem. Soc. Perkin II*, 1972, 1905.
 34. T. J. Broxton, D. G. Cameron, R. D. Topsom, and A. R. Katritzky, *J. Chem. Soc., Perkin II*, 1974, 256.
 35. The Kerr constants for benzotrifluoride have been determined by K. E. Calderbank and R. K. Pierens, *J. Chem. Soc. Perkin II*, 1972, 293. These results do not distinguish between the various electronic factors governing the interaction of the trifluoromethyl group.
 36. R. T. C. Brownlee, R. E. J. Hutchinson, A. R. Katritzky, T. T. Tidwell, and R. D. Topsom, *J. Amer. Chem. Soc.*, 90, 1757 (1968).
 37. R. T. C. Brownlee, D. G. Cameron, R. D. Topsom, A. R. Katritzky, and A. F. Pozharsky, *J. Chem. Soc. Perkin II*, 1974, 247.
 38. R. W. Taft, E. Price, I. R. Fox, I. C. Lewis, K. K. Andersen, and G. T. Davis, *J. Amer. Chem. Soc.*, 85, 709 (1963).
 39. R. W. Taft, E. Price, I. R. Fox, I. C. Lewis, K. K. Andersen, and G. T. Davis, *ibid.*, 85, 3146 (1963).
 40. R. T. C. Brownlee, S. K. Dayal, J. L. Lyle, and R. W. Taft, *ibid.*, 94, 7208 (1972).
 41. W. Adcock, J. Alste, S. Q. A. Rizvi, and M. Aurangzeg, *ibid.*, 98, 1701 (1976).
 42. W. Adcock and M. J. S. Dewar, *ibid.*, 89, 379 (1967).
 43. M. J. S. Dewar and A. P. Marchand, *ibid.*, 88, 3318 (1966).
 44. W. Adcock, P. D. Bettess, and S. Q. A. Rizvi, *Aust. J. Chem.*, 23, 1921 (1970).
 45. S. A. Holmes and T. D. Thomas, *J. Amer. Chem. Soc.*, 97, 2337 (1975).
 46. D. T. Clark, D. Kilcast, and W. K. R. Musgrave, *Chem. Commun.*, 516 (1971).

47. D. W. Davis, M. S. Banna, and D. A. Shirley, *J. Chem. Phys.*, **60**, 237 (1974).
48. We are indebted to Professor Thomas for a discussion of the origin of the discrepancy between the calculated and observed dipole moments.
49. E. E. Schneider, *J. Chem. Phys.*, **23**, 978 (1955).
50. R. J. Lontz and W. Gordy, *ibid.*, **37**, 1357 (1962).
51. M. T. Rogers and D. H. Whiffen, *ibid.*, **40**, 2662 (1964).
52. (a) Iwasaki, M., *Mol. Phys.*, **20**, 503 (1971). (b) Iwasaki, M., *Fluorine Chem. Rev.*, **5**, 1 (1971).
53. R. J. Cook, J. R. Rowlands, and D. H. Whiffen, *Mol. Phys.*, **7**, 31 (1963).
54. Kispert, L. D., *Electron Spin Resonance Studies of Fluorine-Containing Radicals in Single Organic Crystals*, American Chemical Society Symposium Series, No. 66, J. W. Root Ed., 1978.
55. Several independent determinations of the sign of the α -fluorine coupling constant have been made. The contact chemical shifts of the fluorine atoms of paramagnetic bis(fluorophenylaminotroponiminato)nickel(II) complexes and of the nickel acetylacetonate complexes of *o*-, *m*-, and *p*-fluoroaniline as well as observations of chemically induced dynamic nuclear polarization in products obtained from fluorinated benzyl radicals are all in accord with the assignment of a positive sign. (a) D. R. Eaton, A. D. Josey, and W. A. Sheppard, *J. Amer. Chem. Soc.*, **85**, 2689 (1963). (b) M. R. Wasielewski, Thesis University of Chicago Library (1975). (c) M. R. Brinkman, D. Bethell, and J. Hayes, *J. Chem. Phys.*, **59**, 3431 (1973). (d) J. Bargon and K. G. Seifert, *J. Phys. Chem.*, **77**, 2877 (1973).
56. R. J. Lontz, *J. Chem. Phys.*, **45**, 1339 (1966).
57. C. Chachaty, A. Forchioni, and M. Shiotani, *Can. J. Chem.*, **48**, 435 (1970).
58. C. Chachaty and M. Shiotani, *J. Chim. Phys.*, **68**, 300 (1971).
59. M. Jinguji, K. C. Lin, C. A. McDowell, and P. Raghunathan, *J. Chem. Phys.*, **65**, 3910 (1976).
60. J. E. Wertz and J. R. Bolton, *Electron Spin Resonance*, McGraw-Hill, 1972, Chapters 7 and 8.
61. L. D. Kispert and M. T. Rogers, *J. Chem. Phys.*, **54**, 3326 (1971).
62. (a) C. M. Bogan and L. D. Kispert, *J. Phys. Chem.*, **77**, 1491 (1973). (b) L. D. Kispert, private communication.
63. M. Iwasaki, *J. Am. Chem. Soc.*, **92**, 6348 (1970).
64. D. Kosman and L. M. Stock, *ibid.*, **92**, 409 (1970).
65. R. W. Fessenden and R. H. Schuler, *J. Chem. Phys.*, **43**, 2704 (1965).
66. R. W. Fessenden, *J. Phys. Chem.*, **71**, 74 (1967).
67. P. Meakin and P. J. Krusic, *J. Amer. Chem. Soc.*, **95**, 8185 (1973).
68. K. S. Chen and J. K. Kochi, *ibid.*, **96**, 794 (1974).
69. D. J. Edge and J. K. Kochi, *ibid.*, **94**, 6485 (1972).
70. A. J. Bowles, A. Hudson, and R. A. Jackson, *Chem. Phys. Lett.*, **5**, 552 (1970).
71. I. Biddles, J. Cooper, A. Hudson, R. A. Jackson, and J. T. Wiffen, *Mol. Phys.*, **25**, 225 (1973).
72. A. Hudson and K. D. J. Root, *Advan. Mag. Res.*, **5**, 1 (1971).
73. R. V. Lloyd and M. T. Rogers, *J. Amer. Chem. Soc.*, **95**, 1512 (1973).
74. P. J. Krusic and R. C. Bingham, *ibid.*, **98**, 230 (1976).
75. D. E. Wood and R. F. Sprecher, *Mol. Phys.*, **26**, 1311 (1973).
76. P. J. Krusic, private communication.
77. G. Herzberg, *Proc. Roy. Soc., London Ser. A*, **262**, 291 (1961).
78. T. Koenig, T. Balle, and W. Snell, *J. Amer. Chem. Soc.*, **97**, 662 (1975).
79. D. E. Wood, L. F. Williams, R. F. Sprecher, and W. A. Lathan, *ibid.*, **94**, 6241 (1972).
80. C. Hesse and J. Roncin, *Mol. Phys.*, **19**, 803 (1970).

81. P. J. Krusic and P. Meakin, *J. Amer. Chem. Soc.*, **98**, 228 (1976).
82. P. S. Skell, *Free Radicals*, Wiley-Interscience, New York, 1973, Chapter 26.
83. L. Kaplan, *Bridged Free Radicals*, Dekker, New York, 1972.
84. D. D. Tanner, E. V. Blackburn, Y. Kosugi, and T. C. S. Ruo, *J. Amer. Chem. Soc.*, **99**, 2714 (1977).
85. R. V. Lloyd, D. E. Wood, and M. T. Rogers, *ibid.*, **96**, 7130 (1974).
86. R. V. Lloyd and D. E. Wood, *ibid.*, **97**, 5986 (1975).
87. L. Pauling, *J. Chem. Phys.*, **51**, 2767 (1969).
88. R. C. Bingham and M. J. S. Dewar, *J. Amer. Chem. Soc.*, **95**, 7182 (1973).
89. P. J. Krusic and R. C. Bingham, *ibid.*, **98**, 230 (1976).
90. S. Ehrenson, R. T. C. Brownlee, and R. W. Taft, *Prog. Phys. Org. Chem.*, **10**, 1 (1973).
91. (a) C. M. Bogan and L. D. Kispert, *J. Chem. Phys.*, **57**, 3109 (1972). (b) L. D. Kispert, H. Liu, and C. U. Pittman, Jr., *J. Amer. Chem. Soc.*, **95**, 1657 (1973).
92. P. J. Krusic and J. K. Kochi, *ibid.*, **93**, 846 (1971).
93. P. J. Krusic, P. Meakin, and J. P. Jesson, *J. Phys. Chem.*, **75**, 3438 (1971).
94. K. S. Chen, P. J. Krusic, P. Meakin, and J. K. Kochi, *ibid.*, **78**, 2014 (1974).
95. K. S. Pitzer, *Discuss. Faraday Soc.*, **10**, 66 (1951).
96. D. R. Herschbach, *J. Chem. Phys.*, **25**, 358 (1956).
97. H. T. Minden and B. P. Dailey, *Phys. Rev.*, **82**, 338 (1951).
98. This now well-known feature of the INDO model, J. A. Pople, and D. L. Beveridge, *Approximate Molecular Orbital Theory*, McGraw-Hill, New York, 1970 has caused considerable difficulty in the quantitative analysis of the experimental results.
99. M. B. Yim and D. E. Wood, *J. Amer. Chem. Soc.*, **98**, 3457 (1976).
100. M. B. Yim and D. E. Wood, *ibid.*, **97**, 1004 (1975).
101. C. Chachaty, A. Forchioni, and M. Shiotani, *C.R. Acad. Sci. Paris Ser. C*, **268**, 1181 (1969).
102. K. S. Chen, D. Y. H. Tang, L. K. Montgomery, and J. K. Kochi, *J. Amer. Chem. Soc.*, **96**, 2201 (1974).
103. (a) W. E. Blackley and R. R. Reinhard, *ibid.*, **87**, 802 (1965). (b) W. D. Blackley, *ibid.*, **88**, 480 (1966).
104. P. J. Scheidler and J. R. Bolton, *ibid.*, **88**, 371 (1966).
105. H. Lemaire, A. Rassat, and P. Servoz-Gavin, *J. Chim. Phys.*, **59**, 1247 (1962).
106. G. R. Underwood, V. L. Vogel, and I. Krefting, *J. Amer. Chem. Soc.*, **92**, 5019 (1970).
107. E. G. Janzen and J. L. Gerlock, *J. Phys. Chem.*, **71**, 4577 (1967).
108. W. R. Knolle and J. R. Bolton, *J. Amer. Chem. Soc.*, **91**, 5411 (1969).
109. E. T. Strom and A. L. Bluhm, *Chem. Commun.*, 115 (1966).
110. K. J. Klabunde, *J. Amer. Chem. Soc.*, **92**, 2427 (1970).
111. S. Terabe and R. Konaka, *Bull. Chem. Soc. Japan*, **46**, 825 (1973).
112. S. Terabe, K. Kuruma and R. Konaka, *J. Chem. Soc. Perkin II*, 1252 (1973).
113. S. Terabe and R. Konaka, *J. Amer. Chem. Soc.*, **93**, 4306 (1971).
114. E. de Boer and H. van Willigen, *Prog. Nucl. Magn. Reson. Spectroscopy*, **2**, 111 (1967).
115. G. N. LaMar, W. De W. Horrocks, Jr., and R. H. Holm, *NMR of Paramagnetic Molecules*, Academic, New York, 1973.
116. T. Fujinaga, Y. Deguchi, and K. Umemoto, *Bull. Chem. Soc., Japan*, **37**, 822 (1964).
117. L. M. Stock and P. E. Young, *J. Amer. Chem. Soc.*, **94**, 7686 (1972).
118. E. G. Janzen and J. L. Gerlock, *ibid.*, **89**, 4902 (1967).
119. L. M. Stock and M. R. Wasielewski, *ibid.*, **97**, 5620 (1975).
120. P. L. Kolker and W. A. Waters, *J. Chem. Soc.*, 1136 (1964).
121. E. A. Polenov, B. I. Shapiro, and L. M. Yagupol'skii, *Zhur. Strukt. Khim.*, **12**, 163 (1971).

122. The values of $\rho_{\text{C}_4}^{\text{C}}$ may be estimated on the basis of the $a_{\text{C}_4}^{\text{C}}$ constants (Ref. 119).
123. L. M. Stock and J. Suzuki, *J. Amer. Chem. Soc.*, **87**, 3909 (1965).
124. The corresponding semifuraquinone has also been studied (Ref. 64).
125. M. Broze, Z. Luz, and B. L. Silver, *J. Chem. Phys.*, **46**, 4891 (1967).
126. J. L. Gerlock and E. G. Janzen, *J. Phys. Chem.*, **72**, 1832 (1968).
127. G. A. Russell, J. L. Gerlock and G. R. Underwood, *J. Amer. Chem. Soc.*, **94**, 5209 (1972).
128. G. A. Russell and J. L. Gerlock, *ibid.*, **96**, 5838 (1974).
129. J. L. Gerlock, E. G. Janzen, and J. K. Ruff, *ibid.*, **92**, 2558 (1970).
130. R. O. C. Norman and B. C. Gilbert, *J. Phys. Chem.*, **71**, 14 (1967).
131. S. V. Kulkarni and C. Trapp, *J. Amer. Chem. Soc.*, **92**, 4801 (1970).
132. S. V. Kulkarni and C. Trapp, *ibid.*, **92**, 4809 (1970).
133. F. B. Mallory, *ibid.*, **95**, 7747 (1973).
134. This interaction is discussed by Wertz and Bolton, in Chapter 6, Ref. 62.
135. These calculations have been carried out by several groups including Morokuma (14), Hudson and his associates (71), Krusic and Kochi and their co-workers (94), Underwood and his students (106), and others.

Substituent Effects in Allenes and Cumulenes*

BY WOLFGANG RUNGE

*Organisch-Chemisches Institut der Technischen Universität
München, Germany†*

CONTENTS

I. Introduction	316
II. Descriptions of Molecular Properties of Cumulenes on the Basis of a Geometrophysical Model	318
A. The Concepts and the Model	318
1. The Model	318
2. Isomerism, Completeness, and Qualitative Completeness	323
B. Vector Properties of Allenes and Cumulenes	331
1. Dipole Moments	331
2. A Vector Addition Model for Bond Moments in Allenes	336
C. Scalar Molecular Properties of Allenes	340
1. Carbon and Hydrogen Electron Densities	340
2. ¹³ C Chemical Shifts	346
3. ¹ H Chemical Shifts	349
4. Nuclear-Nuclear Spin-Spin Coupling Constants	351
5. Ionization and Excitation Energies	354
D. Pseudoscalar Molecular Properties of Allenes	360
1. Molar Rotations and Optical Rotatory Dispersion	360
E. Comparisons between Observed and Calculated Molecular Properties of Allenes	365
F. Correlations of Substituent Effects in Allenes with Those in Ethylenes, Benzenes, and Related Compounds	377
G. Effects of Isoelectronic or Isovalent Substitutions in the Allenic Skeleton	383
1. NMR-Chemical Shifts of Ketenes, Ketene Imines, Carbodiimides, Diazo-compounds, and Thioketenes	383
2. Electron Densities	391
3. Ionization and Excitation Energies	395
H. Effects of Increase in Chain Lengths of the Cumulenic Skeleton	399
1. NMR Spectral Data and Electron Densities in Butatrienes and Pentatetraenes	399
2. Excitation and Ionization Energies	406

* Dedicated to the memory of Richard Kuhn (1900-1967), Nobel prize laureate and pioneer in the field of stereochemistry and physical organic chemistry of cumulenes.

† Present address: Studiengruppe für Systemforschung, D-6900 Heidelberg, Germany.

III. Some Interpretations of Substituent Effects on Molecular Properties of Cumulenes	407
A. Levels of Interpretations	407
B. π - σ Separabilities in Cumulenes	409
C. Electron Density Distributions	412
D. Ionization Energies and Electron Affinities	418
E. Excitation Energies	425
F. Nuclear Magnetic Resonances	427
1. Chemical Shifts	427
2. Nuclear Spin-Spin Coupling Constants	435
G. Molar Rotations	444
Acknowledgment	448
References	448
Appendix	453
A. Summary of Unpublished Material	453
B. Chemical Compound Index	454

I. INTRODUCTION

During the last two decades investigations of substituent effects on molecular properties and chemical reactivities of aromatic (2) and nonaromatic unsaturated (3) systems have been a central concern of physical organic chemistry. The presentations of such topics are an essential part of this series of *Progress in Physical Organic Chemistry* (2-4).

It is the purpose of the present contribution to give an overview of substituent effects on spectroscopic properties and electron density distributions (including dipole moments) of cumulenes. The magnitudes of such substituent effects and electronic interactions may aid in predictions of chemical properties, such as reaction rates and equilibria.

The kinds of cumulenes covered with this treatment include allenes, butatrienes, and pentatetraenes on the one side, and ketenes, ketene imines, carbodiimides, diazocompounds, and thioketenes on the other side. The molecular spectra under consideration include photoelectron (pe), electronic uv absorption spectra, ^{13}C -, ^{15}N - (^{14}N -), and ^1H -nmr spectra as well as molar rotations and optical rotatory dispersions (ORD). Molecular properties related to theoretical indices (not observables), such as electron densities, are discussed on a semi-empirical CNDO/S or *ab initio* STO-3G MO level.

Concerning physical organic chemistry of allenes and cumulenes the situation has been (and partly continues to be) quite different from that of aromatic or nonaromatic unsaturated systems. It was only in 1973 that Charton (3) has characterized the field in the following way:

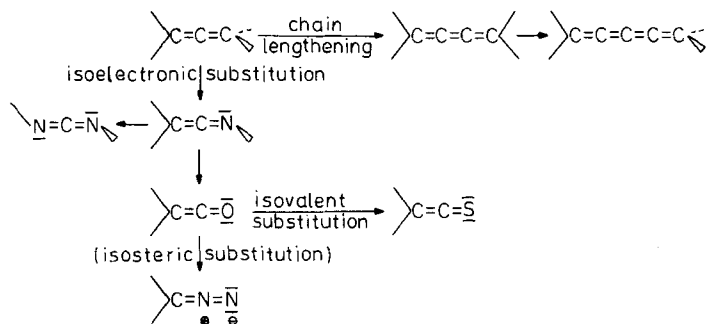
"There are absolutely *no data sets* for substituted allenes or cumulenes in the literature. This is a situation which should be remedied at the earliest opportunity, as data on these systems would be of considerable interest." (Italics added.)

Since then a wealth of data has appeared in the literature and a summary of the material is necessary and timely, especially as the synthetic chemistry of these molecular systems has become the subject of considerable interest (5).

However, apart from missing data there is a further aspect which has counteracted research in physical organic chemistry of cumulenes. The whole problem is adequately described by Weimann and Christofferson (6):

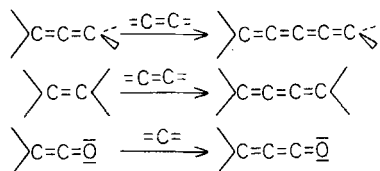
“Rationalization of the observed physical and chemical characteristics of organic cumulenes in terms of molecular structure theory has been beset by various difficulties. These difficulties arise in part owing to a *lack of data* on molecules in this series but are also due to a *lack of a unified theoretical treatment* that is consistent with available data on the various members of this series.” (Italics added.)

As, in general, the measure of progress in science is not so much the accumulation of knowledge (and data) as its systematization, this contribution tries to present a consistent treatment and systematization of now available spectroscopic properties and electron density distributions in allenes and cumulenes. The conceptional framework for such a treatment is based on a geometry-oriented, algebraic model for the description of scalar (7-11) and pseudoscalar (1c,12,13) molecular properties of allenes. In this approach, firstly, substituent effects (ligand-specific parameters) and other parameters are treated as only formally defined elements of the model whose numerical values are determined experimentally. These values then may be used for the semiempirical calculations of the various molecular properties. In a further step the ligand-specific parameters and the other parameters are interpreted physically (a posteriori). From a systematic point of view the results deduced for the allenes form the basis for the discussions of the molecular properties of the other cumulenes, as the molecular properties of cumulenes may be related to those of allenes either by a process of increase in chain length of the molecular skeleton or an isoelectronic (isovalent) substitution in the heavy atom grouping of the cumulenic molecular skeleton.



Furthermore, for cumulenes one may introduce a concept of homology

which is associated with a conservation of symmetry, if one differentiates between antiplanar (D_{2d}) and planar (D_{2h}) hydrocarbon systems. For the D_{2h} compounds ethylene would be the parent compound for the homologous series. In a similar way homology is found for other systems, for example, ketenes. Therefore, owing



to symmetry conservation, concepts of homology may achieve a more quantitative status for the discussions of molecular properties than in case of aliphatic homologous series (with flexible alkyl chains).

Following the "Introduction to this Series" for the practicing organic chemist the present contribution is intended to cover simple procedures to predict molecular properties of arbitrarily substituted cumulenes; for those interested in physical organic chemistry this contribution shall clarify geometrophysical aspects associated with substituent effects without going too much into mathematical details and shall provide insights into the nature of the substituent effects in cumulenes on a semiquantitative level involving usual substituent parameter approaches or MO calculations.

II. DESCRIPTIONS OF MOLECULAR PROPERTIES OF CUMULENES ON THE BASIS OF A GEOMETROPHYSICAL MODEL

A. The Concepts and the Model

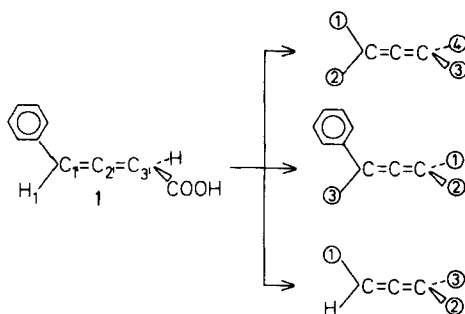
1. The Model

A basic concept in science is to relate the properties of a system to properties of appropriately selected subsystems.

On the molecular level the treatment of properties of compounds is based on a conceptional dissection of the molecule into a skeleton or frame with n ligand sites to which the ligands (substituents) are attached. The ligands may be atoms or groups of atoms. Changing the ligands gives rise to observable "substituent effects."

With respect to the quantitative discussions of particular molecular properties a given molecule may be dissected conceptionally in different ways according to the invariants (the skeletons) and the variables (the ligands) of the

observable phenomena under consideration. For instance, 4-phenyl-but-2,3-dienoic acid (**1**) may be viewed as a four-site allenic skeleton with one phenyl group, one carboxylic group, and two hydrogens with respect to the treatment of the ^{13}C chemical shifts $\delta_{\text{C}21}$, of the allenic central atom (Section II.C.2) or the molar rotations $[\phi]_D^{25}$ at the wavelength of the sodium *D* line (Section II.D.1). Alternatively, **1** may be thought of as a three-site skeleton with one carboxylic group and two hydrogen atoms, if the intense lowest-energy uv absorption bands (the π, π^* bands) of phenylallenes are discussed (Section II.C.5). Similarly, **1** may be viewed as a three-site skeleton with one phenyl group, one carboxylic group, and one hydrogen atom, if the ^1H chemical shifts $\delta_{\text{H}1}$ are taken into consideration (Section II.C.3).



The first level for the description of molecules by models which allows the introduction of mathematical structures for the phenomena of interest concerns the skeleton. The restriction to a spatially rigid skeleton makes possible a systematic treatment on the basis of symmetry arguments. This then allows a consistent representation of complex molecular properties for chemically different skeletons (e.g., allenes and pentatetraenes), provided the ligands and their relative arrangements in space are identical.

A detailed discussion of the structural chemistry of allenes and cumulenes (*1b*) has revealed that upon arbitrary substitutions the cumulenic double bonds in allenes, butatrienes, and ketenes retain their linear arrangements and their bond lengths within experimental errors. Furthermore, the antiplanar arrangements of the ligands in allenes (and surely also in pentatetraenes) are not affected by substitutions.

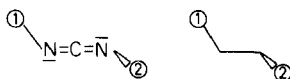
The geometry of ketene imines (and carbodiimides) exhibits a complex behavior, depending upon the types of ligands and the positions of their attachments (at the carbon or nitrogen atom) (*1b*). However, ligands bonded via carbon to the ketene imine (and carbodiimide) skeleton do not seem to influence the nonplanar geometry of these kinds of molecules. Therefore, the preceding empirical findings justify the use of a spatially rigid skeleton of cumulenes for the treatments of substituent effects. Then the introduction of methods of

symmetry for the quantitative discussions of molecular properties of cumulenes are very attractive, as such approaches have become one of the most general and effective methods for theoretical investigations (14).

The fundamental significance of symmetry methods arises from their capacity to reveal the invariants of transformations and to describe the inner structure of ideal systems. The concept of symmetry has two opposing aspects: transformation (change) and conservation (invariance). That which is conserved during a change is an invariant, the set of transformations which keeps something invariant is the symmetry group G . Then, different ways of distinguishing the structural sublevels associated with one particular object lead to different definitions of its symmetry group. That means the theory of symmetry considers that all transformations of a system are executed at the level of a certain set of elements which are equivalent in some particular respect. Fundamental for the whole theories of symmetry therefore is the concept of relative equality; that is, any particular object may or may not exhibit a specific symmetry depending upon the properties singled out and on the internal structure which we happen to be considering. Thus, in case of **1** we have seen that for allenes the molecular skeleton may have the symmetry D_{2d} or C_s , depending upon whether we discuss four-site or three-site systems.

The symmetry of the skeleton, that is, the point-symmetry group G of the arrangement of the ligand sites, defines a class of molecules which may be characterized by a geometrical figure. The individual members of the class are determined by a specification of the ligands at the various sites. If we refer to a particular molecular property, where the number of ligand sites of the skeletons is identical with the coordination number of the skeletons, the allenes and pentatetraenes may become representatives for the molecular class with the skeletal symmetry D_{2d} of an irregular tetrahedron. Ketene imines may be represented by an irregular pyramid of symmetry C_s , whereas the planar butatrienes and ketenes (diazocompounds, thioketenes) are related to a rectangle (of symmetry D_{2h}) or a C_{2v} -triangle, respectively (Fig. 1).

All these molecular skeletons are achiral. According to the preceding separations of molecules the two-site skeleton of carbodiimides is chiral and therefore represents a special case. It has a C_2 -symmetry and may be represented by a helical line.



As a consequence, any ligand combination in carbodiimides gives rise to chiral molecules, whereas of the other molecular systems the nonplanar allenes, pentatetraenes, and ketene imines may become chiral only through certain arrangements of (achiral) ligands. The planar systems are always achiral, if we restrict ourselves to achiral ligands.

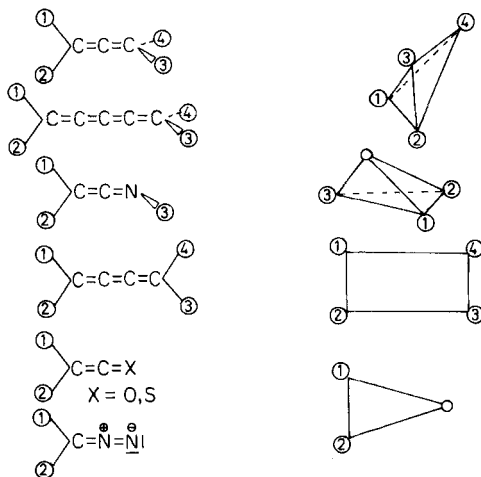


Figure 1 Representations of molecular skeletons of cumulenes by geometrical figures.

These remarks are of interest, as the molecular properties which are treated in this contribution are scalar as well as pseudoscalar (chiral) in character.

Scalar molecular properties (energies, nmr shifts, etc.) do not depend on the orientations of the molecules in space and give identical values for molecules and their mirror images. For pseudoscalar properties (molar rotations) the experimental measurements of the corresponding numerical values of the molecules (or mixtures thereof) give the value zero, if the objects are achiral (or the mixtures racemic) and give identical values with opposite signs, if the chiral molecules (or mixtures) are enantiomeric, regardless of the orientation of the molecules in space (1*c*). According to Ruch (15) experiments of the last kinds with chiral molecules are termed "chirality observations."

Symmetry operations on the (achiral) molecular skeleton subject the molecules to rotations or rotation-reflections by which the skeleton is brought into coincidence with itself. For a rigid skeleton such operations (from the symmetry group *G*) may be represented by interchanges of the ligands, that means permutations (from a permutation group *S*) of the ligands among the sites. In general, a permutation of the ligands gives a different isomer, but there may be some permutations whose effect is the same as simply rotating the molecules and/or replacing it by its mirror image (enantiomerism). The truly different isomers produced in this way are called "permutation isomers" (constitutional isomers).

Now, the further level of the analytical descriptions of molecular properties is concerned with the ligands and the permutation operations with the ligands. If the symmetry arrangements of the ligand sites are not influenced by the ligands or certain types of ligands in specific positions relative to each other, the nature

of the ligands determines the overall symmetry and shape of the molecule which means that the site symmetry has to be retained. Then, for instance, in case of allenes and pentatetraenes the mirror planes of the cumulenic skeleton must be identical with the mirror planes of the ligands at the particular sites. In this way, the geometrical model imposes a constraint on the set of real molecules whose molecular properties can be investigated by means of the model theory. Situations that will affect the preceding conditions include any deformations of valence or dihedral angles by neighboring ligands, changes of conformations, or rotamer populations owing to specific arrangements of ligands relative to each other.

Furthermore, as most investigations are performed in solution, also steric hindrances of solvation or other solvent effects (e.g., hydrogen bonding effects), have to be taken into consideration, if real experimental situations are treated.

If more than one orientation of a ligand is possible this means that, in relation to the time scale of the experiment, one of the following must hold: either

1. the ligand must possess sufficient symmetry to make all properties of interest invariant under rotations, or
2. properties of interest refer to time- or ensemble-averages to which all orientations contribute equally, or
3. for a given distribution of ligands, a single orientation is strongly preferred.

In Ref. 1*b* it has been shown, especially for the allenes, that most of the chemically interesting substituents achieve only one preferred conformation (cf. also Ref. 16). Therefore, apart from the rigidity of the skeletons, another important restricting condition for a unified treatment of substituent effects in cumulenes is met.

As a consequence one may establish a geometrical model of points in space for the molecules which disregards the spatial extension of the ligands and also their actual dispositions in space.

If one accepts the preceding premises of the geometrical model any molecular property \mathfrak{F} may be related to intrinsic properties $\sigma(R_i)$ of the ligands R at the various sites i . And thus one may think of a description of the molecular property \mathfrak{F} in terms of a real function $F(\sigma(R_1), \dots, \sigma(R_n))$ of the ligands or parameters thereof. The scalar parameter $\sigma(R_i)$ is a "substituent constant" and may be treated as an undefined element; that is, it achieves a fixed numerical value for a given experiment, but lacks any information about the physical quality which is represented by $\sigma(R)$. The property \mathfrak{F} may be a scalar or pseudoscalar molecular property. A function of the ligands that describes a pseudoscalar molecular property of molecules with a common achiral skeleton is called a "chirality function" χ (15). On this level of describing molecular

properties it may take many forms. We only have the geometrical requirement that its numerical value for a chiral property is invariant under rotations of the molecule, but changes sign when the molecule is replaced by its mirror image. The geometrical model introduced in this subsection therefore defines a molecular skeleton as a spatial arrangement of points (sites) and a particular molecule is an indexed set where definite numbers are assigned to the sites. A permutation of the ligands corresponds to a reassignment of the ligand sites by numbers, that is, concerning the molecular property \mathfrak{F} a permutation results in interchanges among the arguments of the function $F(\sigma(R_1), \dots, \sigma(R_n))$.

In particular, the model includes stereochemical aspects, as it covers constitutions and configurations of molecules, that is, the sequential arrangement of atoms in the molecules regardless of their directions in space (constitution) and the relative positions of atoms and/or groups (represented by points) in space (configuration).

For the ideal model discussed so far relations between the structure of systems and their properties are governed by relations to symmetry. To describe real situations, however, a transition from geometric to geometrophysical (material) spaces is necessary which brings in the problems of interactions between the parts of an integral system. This may have the effect that, on the geometrophysical level, only some of the relationships valid for the geometrical level can be realized. That means, the symmetry group of a system determined as the result of physical experiments may be incorrectly taken as the geometric group. Then, for material spaces the symmetry of the geometric structure (subject to correct definition) is the minimum symmetry of the properties and relationships associated with the structure in question.

Another difficulty with the geometrical model lies in the fact that symmetry conditions are only necessary, but not sufficient for the realization of phenomena. Phenomena predicted by the symmetry of a system may not be observed or may be unstable. These are facts of principal restrictions for any analysis of physical phenomena in terms of geometry-oriented, algebraic models. Therefore, any formal analysis of the conditions of symmetry does not relieve anyone of the necessity of making a careful study of the actual physical situation and finding those additional aspects which actually enter as factors for physical systems.

A certain set of such factors will become evident, if one looks at the phenomena of isomerisms for the different types of molecules.

2. *Isomerism, Completeness, and Qualitative Completeness*

For a given set of ligands permutations of the ligands among the sites in allenes (pentatetraenes), ketene imines, and butatrienes give rise to isomers. The types of isomerisms discussed on the basis of the geometrical model are illustrated in Fig. 2 for dimethylallenes and dimethylbutatrienes. The molecules

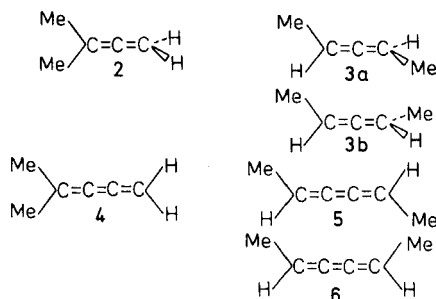


Figure 2 Types of isomerisms of allenes and butatrienes.

in horizontal lines (**2** and **3**, **4** and **5**) are related to each other as constitutional isomers (or structural isomers), as the constituting atoms of the compounds are connected differently. The molecules arranged vertically (**3a** and **3b**, **5** and **6**) are stereoisomers, as they differ in the positions of their otherwise identically connected atoms in space. The molecules **3a**, **3b** and **5**, **6**, respectively, differ only by an interchange of geminal ligands.

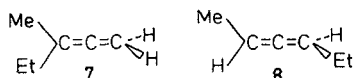
The stereoisomeric relation of the nonplanar D_{2d} -molecules **3a** and **3b** is an enantiomerism. Both these isomers are chiral and are related to each other as object and mirror image. As enantiomers have identical scalar properties (energies, nmr shifts, etc.), but different pseudoscalar properties an experimental differentiation of these chiral molecules is bound to rely on chiral properties, such as optical rotations. The planar E-dimethylbutatriene (**5**) and Z-dimethylbutatriene (**6**) exhibit *cis-trans* isomerism (geometrical isomerism). **5** and **6** differ in their scalar molecular properties.

On investigating such isomeric molecules or even more complicated isomeric allenes or butatrienes with four different ligands one may not only be interested in a corresponding molecular property of one permutation isomer, but additionally one may think of relations between the properties of different isomers.

Relations between the enantiomeric allenes **3a** and **3b** clearly are governed by symmetry, as **3a** and **3b** behave as object and mirror image. Therefore, all the chiral properties χ of **3a** and **3b** are related to each other according to Equation 1, their scalar properties being identical. (The enumeration of ligand sites for the allenic D_{2d} -skeleton is given in Fig. 1).

$$\chi(\text{Me,H,Me,H}) + \chi(\text{Me,H,H,Me}) = 0 \quad (1)$$

Let us now turn to the constitutionally isomeric 1,1-dimethylallene (**2**) and 1,3-dimethylallene (**3a**) or the corresponding pair 3-methyl-penta-1,2-diene (**7**) and hexa-2,3-diene (**8**) and ask for relations between scalar properties of these molecules.



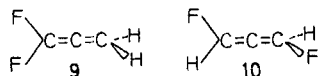
For instance, concerning the ^{13}C chemical shifts δ_{C_2} of the allenic central atoms it has been suggested (17) that "for a given alkyl substituent there is a fair linear relationship between the number of these substituents and δ_{C_2} of the allenes." And more specifically with respect to the preceding example, "there is a strikingly regular upfield shift of the sp carbon with increasing number of substituents, 3 ppm for each added methyl group" (18). This apparent "additivity rule" for the ^{13}C chemical shifts of the allenic central atoms of alkylallenes would give rise to Equation 2.

$$\delta_{C_2}(\text{Me,Me,H,H}) - \delta_{C_2}(\text{Me,H,Me,H}) = 0 \quad (2)$$

If, however, one compares the ^{13}C chemical shifts δ_{C_2} of the methyl-ethyl-allenes **7** and **8** (Table 16), their corresponding ^{13}C -chemical shifts are distinctly different.

If one takes also the constitutionally isomeric difluoroallenes **9** and **10** (Table 16) into consideration (19), one notes a marked nonadditivity of the ^{13}C chemical shifts δ_{C_2} with respect to the number of the fluoro substituents.

$$\delta_{C_2}(\text{F,F,H,H}) - \delta_{C_2}(\text{F,H,F,H}) \neq 0 \quad (3)$$



From these examples one can infer that one must choose a sufficient range of substituents to find the general aspects of the physical phenomena of interest; that is, generalizations from results obtained for a series of very similar substituents, say alkyl groups, may not be a representative for the whole physical effect.

As a last example related to the preceding problem of relationships between scalar molecular properties of constitutional isomers, one observes that also in case of the molar refractions R_D of the methyl-ethyl-allenes **7** and **8** a nonadditivity holds (20).

$$R_D(\text{Et,Me,H,H}) - R_D(\text{Et,H,Me,H}) \neq 0 \quad (4)$$

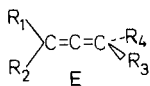
The problems of the mathematical structure governing the relationships between arbitrarily multisubstituted constitutional isomers have been treated for scalar and pseudoscalar properties in Ref. 7 and Refs. 15*b* and 15*c*, respectively.

In mathematical terms in Equations 1 and 2 the functions representing definite molecular properties are linearly dependent, whereas in Equations 3 and 4 they are linearly independent of each other. The essential differences between the Equations 1-4 are that in (1) symmetry arguments are applicable,

whereas for (2)–(4) they are not applicable. Within quantum theory as the basis of our understanding of molecular structure (rather than simply its determination) predictions of linear dependencies between observable properties of molecules only can rely on symmetry arguments (21).

The chemist uses symmetry every time he recognizes which parts (atoms, groups) in a molecule are equivalent (e.g., in nmr experiments) or which kinds of molecules can be transformed into mirror images with the characteristics of enantiomerism. Then, symmetry reduces the number of necessary measurements to be performed on parts of the molecules, if the properties of all the parts should be determined. Symmetry is a sufficient prerequisite to predict linear dependencies between observables within the same molecule or between observables of different molecules. Therefore, in the absence of definite symmetry relations there are no a priori reasons to assume linear dependencies between observables. For instance, one should assume linear independencies between functions representing molecular properties of constitutional isomers. On the other hand, it must be admitted that there may exist linear dependencies between observables accidentally. They may be found in some cases for certain molecular classes or a definite set of ligands within one particular class of molecules, for example, alkyl groups. The essential point for a strict mathematical treatment of properties of molecules that may exhibit certain types of isomerism is that, in the absence of symmetry relations, linear dependencies between observables cannot be predicted on the basis of any (algebraic or quantum-theoretical) arguments. They may exist, but can only be realized a posteriori (for instance, by inspection of the numerics). Therefore, without any prejudice a quantitative treatment of molecular properties has to start from the assumption of linear independencies of the functions describing properties of constitutional isomers. Without going too much into mathematical details the consequences of the preceding considerations are illustrated for the particular example of the allenes (and pentatetraenes). They are easily extended to ketene imines. The possibility of *cis-trans* isomerism for butatrienes gives rise to complications which have not yet been treated adequately in the literature.

Let R_i be a real number characterizing the ligand R at the site i and $F(R_1, \dots, R_4)$ a real function of the variables R_i representing a scalar property of a reference molecule \mathbf{E} . The property under consideration shall allow the dissection of the allenes into four ligands and the rigid skeleton of symmetry D_{2d} .



Then, the symmetry operations by which the skeleton is brought into coincidence with itself may be represented by permutations from a permutation group S .

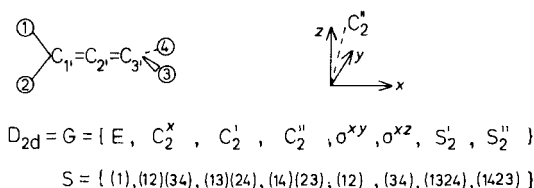


Figure 3 Representation of the geometric point-symmetry group G of the allenic skeleton by a permutation group S .

S is a subgroup of the symmetric group S_n , the group of all permutations of ligands among the n ($=4$) sites of the skeleton. Even permutations from S represent rotations, odd permutations mirror reflections or rotation reflections (Fig. 3).

According to the usual conventions (7,15) application of a permutation s_μ from a (left) coset of S in S_4 transforms the molecule **E** into a nonenantiomeric permutation (constitutional) isomer **P** with the molecular property $s_\mu \cdot F(R_1, R_2, R_3, R_4) = F(R_{\mu(1)}, R_{\mu(2)}, R_{\mu(3)}, R_{\mu(4)})$. As in general the number of distinct (nonenantiomeric) isomers having n different ligands is given by the index $|S_n \cdot S|$, in case of the allenes three different isomers may be generated from **E** (Fig. 4) (for instance by application of the permutations $s_1 = (1)$, $s_2 = (234)$, $s_3 = (243)$).

In this way, a mathematical structure may be introduced which is related not only to the transformations under the point group of the molecular skeleton $G \simeq S$, but under the larger group of all permutations of the ligands among the n sites. These last permutations from S_n , but not from S have no counterparts in geometrical transformations.

According to the preceding considerations the functions $F(R_{\nu(1)}, \dots, R_{\nu(n)})$ which have been constructed with the aid of all the different representative permutations s_ν from the cosets $\{s_\nu \cdot S\}$ ($S_n = \cup_\nu \{s_\nu \cdot S\}$) and which describe molecular properties of constitutional isomers should be *linearly independent* from each other (apart from accidental cases). For instance, for the mixture of type (a) of nonenantiomeric allenes in Fig. 4 Equation 5 should hold.

$$F(R_1, R_2, R_3, R_4) + F(R_1, R_3, R_4, R_2) + F(R_1, R_4, R_2, R_3) \neq \text{const.} \quad (5)$$

In particular, for any pair of nonenantiomeric isomers, such as **2** and **3a**, **7** and **8**, **9** and **10**, Equation 6 should be valid.

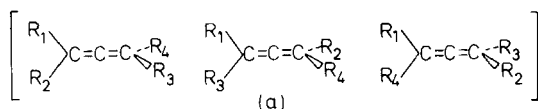


Figure 4 The possible constitutionally isomeric allenes with four different ligands.

$$F(R_1, R_2, R_3, R_4) - F(R_1, R_3, R_2, R_4) \neq 0 \text{ and no constant} \quad (6)$$

The property of functions (namely linear independency) which hence are sufficiently general to describe actual physical situations has been termed "completeness" in case of scalar molecular properties (7). So far, we have treated molecular properties disregarding the actual physical constitution of the skeleton. We only have been concerned with the symmetry arrangement of the ligand sites. Conceptionally, on this level, the skeleton may be represented by the fix-point of all the symmetry operations from the symmetry group G of the skeleton. In case of the allenes this geometrical point is identical with the allenic central atom $C_{2'}$. Therefore, all the preceding considerations also apply to molecular properties related to this particular point, such as the ^{13}C chemical shifts $\delta_{C_{2'}} = F(C_{2'} | R_1, R_2, R_3, R_4)$. For point-properties $F(C_{i'} | R_1, R_2, R_3, R_4)$ of the other nuclei (the terminal carbon atoms $C_{1'}$ and $C_{3'}$) our considerations have to be slightly modified. If we refer in particular to the ^{13}C chemical shifts of the allenic carbon atoms, the skeletal nuclei may be partitioned into two sets of symmetry-equivalent nuclei $\{C_{2'}\}$ and $\{C_{1'}, C_{3'}\}$. If instead of thinking of only one function $F(C_{2'} | R_1, \dots, R_4)$, that is, a one-dimensional vector space which transforms appropriately under the symmetry operations from D_{2d} , one should take a two-dimensional vector space into consideration which is constructed from $F(C_{1'} | R_1, \dots, R_4)$ and $F(C_{3'} | R_1, \dots, R_4)$. Referring again to pairs of constitutional isomers completeness may be expressed in terms of Equations 7a and 7b.

$$F(C_{2'} | R_1, R_2, R_3, R_4) - F(C_{2'} | R_1, R_3, R_2, R_4) \neq 0 \text{ and no constant} \quad (7a)$$

$$\begin{bmatrix} F(C_{1'} | R_1, R_2, R_3, R_4) \\ + \\ F(C_{3'} | R_1, R_2, R_3, R_4) \end{bmatrix} - \begin{bmatrix} F(C_{1'} | R_1, R_3, R_2, R_4) \\ + \\ F(C_{3'} | R_1, R_3, R_2, R_4) \end{bmatrix} \neq 0 \text{ and no constant} \quad (7b)$$

Equations 6 and 7 have been verified experimentally for molar refractions (22) and ^{13}C chemical shifts of variously substituted allenes (8). With respect to an approximation of the functions F which shall describe real molecular properties the term "constitutional isomerism order" k has proven to be useful (7,9,10). It provides a further transition step from a geometrical to a geometrophysical model. The "constitutional isomerism order" k is a characteristic for the phenomenon of constitutional isomerism of a given class of molecules with a n -ligand skeleton. It defines the maximum number of identical ligands which may occur for constitutionally isomeric molecules. Then, $N = (n - k)$ is the minimum number of ligands which via definite interactions give contributions to (observable) properties thus allowing the differentiation of constitutionally isomeric molecules. This definition does not involve any arguments that extend the geo-

metrical character of the point-model of molecules. Especially, it does not specify the term "interaction" in terms of distances of ligand sites or spatial requirements of ligands, and so on.

In case of the allenic D_{2d} systems we have $n = 4$ and $k = 2$ ($N = 2$); for ketene imines we have $n = 3$ and $k = 2$ ($N = 1$). Therefore, any approximation ansatz for the description of molecular properties of allenic D_{2d} systems must at least involve two-particle functions (pair-terms). In short, the constitutional isomerism order k allows a specification of the conditions that follow from the requirement of completeness. From the assumption of completeness one only can infer that one-particle functions (ligand-specific parameters, i.e., substituent constants) do not suffice to describe the whole physical situation for complex, multisubstituted molecules.

For instance, an approximation of the ^{13}C chemical shifts of the allenic central atoms in terms of Equation 8 would give identical results for all the possible constitutionally isomeric allenes, that is, would give rise to linear dependencies.

$$\delta_{\text{C}_2'} = \rho + \sum_{i=1}^4 \sigma(\text{R}_i) \quad (8)$$

In Equation 8 ρ is a constant and the $\sigma(\text{R}_i)$ substituent constants for the different ligands R attached to the sites i .

In general, it is common practice to use an equation such as (8) to get a simple tool for the predictions of ^{13}C chemical shifts. The usual way would be to apply a least-squares procedure to determine the substituent constants $\sigma(\text{R}_i)$. However, this data-fitting based on a simple formula is accompanied by a loss of information about the actual physical situation which shall be described.

In this article the discussion of substituent effects is related consistently to definite models for the description of observable physical effects, that is, the treatment of substituent effects is intended to give insights into physical phenomena as well as procedures for the predictions of numerical values of definite molecular properties.

All these considerations for scalar molecular properties have counterparts in the discussions of pseudoscalar molecular properties. Pseudoscalar properties are related to the chirality of the molecules under consideration, that is, to effects of enantiomerism. A chiral object cannot be superimposed onto its mirror image by rotation (and/or translation). Therefore, an object is achiral, if only the position in space is altered on reflection or rotation-reflection. It is achiral, if its symmetry group contains no planes of reflection and/or improper rotations (14a,15). As a consequence, chiral allenes are of the types (b)–(d) in Fig. 5.

The maximum number of identical ligands which may occur for chiral molecules is the "chirality order" o (15). It is a characteristic for the chirality phenomenon of a given molecular class with n ligands. Then, $N = (n - o)$ is the

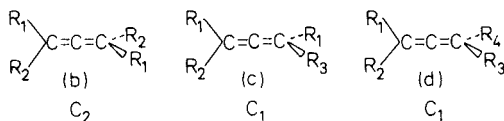


Figure 5 Types of chiral allenes and their symmetries.

minimum number of ligands which according to their simultaneous contributions are necessary for the description of a chiral property. In case of D_{2d} -molecules (allenes, pentatetraenes) we have $o = 2$ and consequently a chirality function $\chi'(9)$ must involve at least pair-terms $\omega(R_i, R_j) = \omega(R_j, R_i)$.

$$\chi'(R_1, R_2, R_3, R_4) = \sum_{i \neq j} \omega(R_i, R_j) \quad (9)$$

If one assigns one ligand-specific parameter $\lambda(R_i)$ to each substituent attached to the site i of the allenic D_{2d} -skeleton, the chirality function χ' (10a) may or may not accurately describe an interesting chiral property of allenes; it does, however, possess the necessary transformation properties in doing so. It is invariant under rotations of the D_{2d} -molecules, but changes sign if the molecules are replaced by their mirror images (cf. Fig. 3).

$$\chi'(R_1, R_2, R_3, R_4) = [\lambda(R_1) - \lambda(R_2)][\lambda(R_3) - \lambda(R_4)] \quad (10a)$$

$$\chi'(R_1, R_2, R_3, R_4) = \omega(R_1, R_3) - \omega(R_1, R_4) - \omega(R_2, R_3) + \omega(R_2, R_4) \quad (10b)$$

The expression 10a, for instance, results from 10b, if there is no correlation between the ligands.

$$\omega(R_i, R_j) = \lambda(R_i) \cdot (R_j) \quad (11)$$

From Equation 10a it is easily seen that the functions χ' give a zero identity (12), regardless of the nature of the ligands. This means that the functions χ' for the constitutionally isomeric allenes of type (a) (Fig. 4) exhibit linear dependencies. Therefore, it may be expected that the above function χ' for chiral properties is in general unable to describe effects associated with constitutional isomerism of chiral allenes. It is "qualitatively incomplete", as Ruch and Schönhofer (15b) have termed this property. Their treatment of chiral molecular properties is based on the concept of "qualitative completeness" of chirality functions, that is, on linear independencies of the functions describing pseudoscalar properties of constitutionally isomeric molecules. Furthermore, they have shown that the requirement of qualitative completeness is equivalent to the fact that, apart from accidental cases, any ensemble of chiral molecules gives a nonzero chirality observation, regardless of whether this ensemble contains only molecules of one kind or is a mixture of (nonenantiomeric) chiral constitutional isomers (such as the mixture of type (a) in Fig. 4).

$$\chi'(R_1, R_2, R_3, R_4) + \chi'(R_1, R_3, R_4, R_2) + \chi'(R_1, R_4, R_2, R_3) = 0 \quad (12)$$

With the apparatus outlined in the preceding subsections a consistent treatment of substituent effects on molecular properties of multisubstituted cumulenes is possible.

In treating the various properties, first, the most general structure of an adequate ansatz for the description of the physical effect under consideration is deduced. It contains only formally defined elements (ligand-specific parameters, pair-terms, etc.). Then, in a semiempirical fashion, the parameters are evaluated from a restricted set of experimental data. These parameters are used to predict corresponding properties of further molecules. At last, the parameters are interpreted physically a posteriori.

Such a procedure of treating substituent effects has several important features: (a) As it is related to a detailed model it reveals the limitations of the proposed methods lucidly and avoids misinterpretations of "substituent effects" (sets of numerical values) resulting from purely numerical data-fitting processes which start from "simple" formulas; (b) for numerical purposes the method may be extended successively; that is, new parameters may be evaluated without the necessity to readjust the old ones (the set of numerical values of the parameters is not related to a restricted set of molecules which when subjected to a least-squares fit shall reproduce the experimental values for this given set).

B. Vector Properties of Allenes and Cumulenes

1. Dipole Moments

The study of substituent effects on vector molecular quantities usually refer to electric dipole moments. However, dipole moments of allenes are also intimately related to the discussion of the basis of the geometric model underlying the treatments of scalar and pseudoscalar molecular properties (Section II.A).

In treating substituent effects in different molecular classes one relies essentially on the transferability of ligand qualities and bond properties; that is, one assigns an intrinsic (scalar) point property σ to each ligand R or a group dipole moment to a bond R—C. Both these qualities are characterized by definite numbers and disregard different rotamer populations of the substituents in the various molecular classes.

Rotamer populations enter essentially into the molecular dipole moments, as they depend sensitively on the actual spatial orientations of the substituents. Therefore, a comparison between the dipole moments of allenes with those in structurally related systems allows insights in how far substituent constants in the various molecular classes are transferable. In many cases, molecular prop-

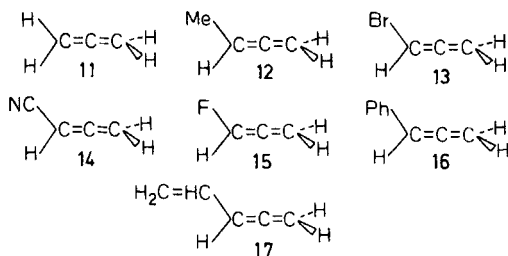
erties of allenes $R_1R_2C=C=CH_2$ or $RHC=C=CH_2$ may be compared with those of ethylenes $R_1R_2C=CH_2$ or benzenes, RPh , respectively (22-25). For the purpose of comparisons related to ligand conformations one may distinguish substituents with an axial rotation symmetry, such as H, F, Cl, Br, I, Me, *t*-Bu, CF_3 , CN, unsaturated groups which are locally planar, such as $H_2C=CH$, COMe, COOMe, and which achieve preferred molecular conformations of C_s -symmetry, but may exhibit *s-cis* or *s-trans* forms, and furthermore saturated groups which may exhibit gauche conformations, such as Et, MeO, MeS, CH_2Cl , CH_2OH , and thus give molecular conformations without symmetry.

For allenes with axially symmetric groups there are fair linear correlations between the magnitudes of their dipole moments μ (D) and those in correspondingly substituted ethylenes and benzenes (9). The directions of the dipole moments in allenes and ethylenes are also very similar. Therefore, for such substituents a discussion of substituent effects on molecular properties may strictly rely on substituent constants transferred from benzenes to allenes (and other cumulenes).

$$\mu(R_1R_2C=C=CH_2) = 1.10 \mu(R_1R_2C=CH_2) - 0.02 \text{ (D)} \quad (13)$$

$$\mu(RCH=C=CH_2) = 1.12 \mu(RPh) - 0.04 \text{ (D)} \quad (14)$$

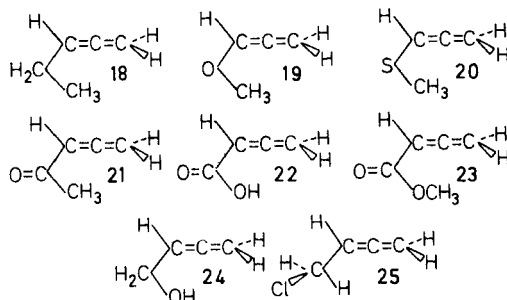
The preceding correlations are based upon the experimental dipole moments of 1,1-dimethylallene (**2**) ($\mu = 0.549$ D (27)), allene (**11**) ($\mu = 0$ D), methylallene (**12**) ($\mu = 0.401$ D (28)), bromoallene (**13**) ($\mu = 1.5 \pm 0.10$ D (29)), and cyanoallene (**14**) ($\mu = 4.28$ D (30)). 1,1-Difluoroallene (**9**) ($\mu = 2.07$ D (31*a*)) and fluoroallene (**15**) ($\mu = 1.97$ D (31*b*)) do not follow the regression line (13). However, allenes with fluoro groups often behave irregularly (Section II.C.2).



From the correlations (13) or (14), dipole moments of allenes with axially symmetric substituents may be predicted. Furthermore, it has been shown (9) that dipole moments obtained from the preceding regressions agree well with dipole moments μ (CNDO/S) of allenes calculated with the semiempirical CNDO/S procedure. (Dipole moments calculated with the *ab initio* STO-3G MO method give inferior results.)

Also for other allenes where conformational effects of the substituents may be disregarded, such as phenylallene (**16**), or where the allene and the corresponding ethylene exhibit the same conformational preference for their substituents, for example, vinylallene (**17**) with a preferred *s-trans* arrangement (*1b*), the correlations (13) and (14) are useful for estimating dipole moments of allenes.

For other molecules (**18–25**) with substituents like XCH_3 ($X = CH_2, O, S$), COR ($R = CH_3, OH, OCH_3$), and CH_2X ($X = OH, Cl$) the allenes exhibit rotamer populations that are different from those in ethylenes (and also in benzenes). In allenes the corresponding molecules exhibit one preferred conformation, whereas in ethylenes there is often observed a mixture of different rotamers (*1b*). Therefore, for these last ligands substituent constants have to be established which are different from those used for other planar aromatic and nonaromatic unsaturated systems. Similar arguments are also valid with respect to substituent effects in other cumulenes.



A particularly striking example for the decisive influence of conformational effects is found for the group CH_2Cl . 4-Chloro-buta-1,2-diene (**25**) ($\mu = 2.02$ D (29)) exhibits only one preferred conformation with a gauche arrangement of the chloro group, whereas 3-chloro-propene ($\mu = 1.08$ D (29)) exists in two rotameric forms, a C_s -conformation with the chloro group *syn* to the ethylenic moiety and a gauche conformation (*1b*). Generally, dipole moments of arbitrarily substituted allenes may be calculated via correlation (15) (linear correlation coefficient $r = 0.9641$) which has been based on the experimental dipole moments μ (exp.) of the compounds **9**, **10** ($\mu = 1.77$ D (31*b*)), **14**, **15**, **25**, and the moments $\mu(\text{CNDO/S})$ calculated with the CNDO/S-procedure (9) (cf. Table 1).

$$\mu(\text{exp.}) = 1.19 \mu(\text{CNDO/S}) - 0.63 \text{ for allenes} \quad (15)$$

As calculated dipole moments in comparison with experimental values represent sensitive tests of the qualities of the molecular wavefunctions obtained from a particular quantum-chemical procedure, correlation (15) is a basis for confidence in theoretically calculated quantities with the CNDO/S-method.

TABLE 1
Calculated Dipole Moments of Allenes $R_1R_2C=C=CR_3H$ with the CNDO/S-Scheme

Compd.	R ₁	R ₂	R ₃	μ (CNDO/S) (D)	Ref.
14	CN	H	H	4.04	9
15	F	H	H	2.12	— ^a
16	Ph	H	H	0.18	— ^a
17 ^b	H ₂ C=CH	H	H	(-) 0.24	9
18 ^c	Et	H	H	(-) 0.26 ^d	9
19	MeO	H	H	0.92	9
20	MeS	H	H	1.36	9
21 ^b	COMe	H	H	4.07	9
23 ^b	COOMe	H	H	2.25	9
24 ^c	CH ₂ OH	H	H	1.88	9
25	CH ₂ Cl	H	H	1.93	— ^a
26	CF ₃	H	H	2.81	9
27	Me ₃ Si	H	H	(-) 0.53	9
28	HC≡C	H	H	0.59	9
29	HC≡CC≡C	H	H	0.93	— ^a
30	Cl	H	H	1.22	9
31 ^c	C ₃ H ₅	H	H	(-) 0.66	— ^a
32 ^f	POCl ₂	H	H	4.08	— ^a
33 ^g	NCO	H	H	1.33	— ^a
34 ^h	SO ₂ Me	H	H	4.74	— ^a
9	F	F	H	2.54	9
10	F	H	F	2.23	— ^a
35	Ph	Ph	H	0.31 ⁱ	33
36	Ph	H	Cl	1.39	— ^a
37	Ph	H	CN	4.37	— ^a
38	Ph	H	Me	1.00	34
39	Ph	H	MeO	1.37 ^j	— ^a
1	Ph	H	COOH	2.14 ^j	— ^a
40	Me	H	Cl	1.83	— ^a
41	Me	Me	CN	5.31	— ^a

^a This work.

^b *s-trans* conformation.

^c Concerning the conformation cf. Ref. 9.

^d STO-3G calculation.

^e Conformation of symmetry C_s with perpendicular planes of the allenic and cyclopropyl moieties.

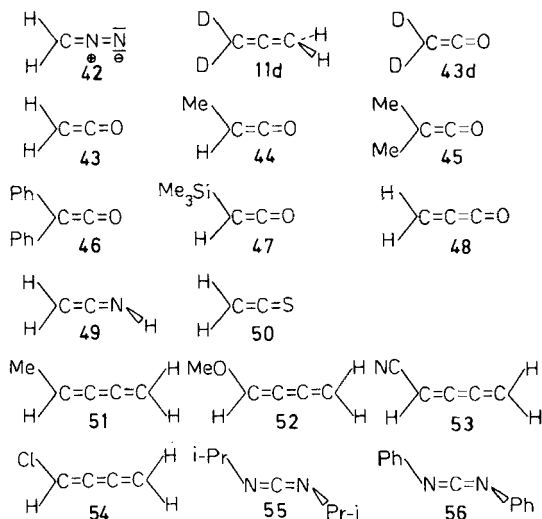
^f *s-cis* conformation of symmetry $C_s(1c)$.

^g *s-cis* conformation (1c).

^h Conformation of C_s -symmetry with an *anti* arrangement of the allenic and the methyl groups.

ⁱ CNDO/2 calculation.

^j INDO calculation.



In Table 1 a summary of (calculated) dipole moments of allenes is displayed. For monosubstituted compounds $\text{RHC}=\text{C}=\text{CH}_2$ the directions of the dipole moments are such that the group R represents the negative end of the dipole. A negative sign in parenthesis indicates that R is the positive end of the dipole.

In Table 2 dipole moments of other cumulenes are given which are either experimental values or result from semiempirical or *ab initio* MO calculations. The experimental dipole moments of the ketenes **43d**, **43–46** are related to those of correspondingly substituted allenes (**2**, **11**, **11d**, **12**, **35**) according to correlation (16) ($r = 0.9931$).

$$\mu(\text{R}_1\text{R}_2\text{C}=\text{C}=\text{O}) = 0.95 \mu(\text{R}_1\text{R}_2\text{C}=\text{C}=\text{CH}_2) + 1.43 \quad (16)$$

If one neglects the calculated dipole moment of methoxybutatriene (**52**) and uses the CNDO/2 value for **54** (which seems to be more reasonable than the CNDO/S value) there is a correlation (17) ($r = 0.9818$) between the calculated dipole moments of butatrienes and the experimental dipole moments of correspondingly substituted ethylenes.

$$\mu(\text{calc.})(\text{RCH}=\text{C}=\text{C}=\text{CH}_2) = 1.01 \mu(\text{exp.})(\text{RHC}=\text{CH}_2) + 0.43 \quad (17)$$

The experimental dipole moments of carbodiimides, such as **55** and **56**, have been of interest primarily in connection with the question of their molecular structures (*1b*). Comparisons between experimental and calculated dipole moments confirmed that the carbodiimides have no planar structures, but have their substituents in perpendicular planes (*1b*).

TABLE 2
Experimental and Calculated Dipole Moments of Cumulenes

Compd.	$\mu(\text{exp.})(\text{D})$	Ref.	$\mu(\text{calc.})(\text{D})$	Ref.
11d	0.003	34		
42	1.50	35	1.28 1.99 ^c 1.98	— ^a 38a 38d
43	1.414	36	1.30 ^b 2.06 ^c 2.90 ^c 1.81 ^c 1.62 ^c	37a 38a 38b 38c 38e
43d	1.442	36		
44	1.79	39	1.35 ^b	37a
45	1.94	40		
46	1.76	41		
47			0.73 ^d (1.53) ^e	— ^a
48	2.14	42a		
49			1.62	— ^a
50	0.02	42b	1.63 ^d	— ^a
51			1.16	— ^a
52			0.52	— ^a
53			4.26	— ^a
54			3.33 ^d (2.10) ^b	— ^a , 44
55	2.08	43a,43b		
56	1.70	43a		

^a This work, CNDO/S calculations.

^b CNDO/2 calculations.

^c *Ab initio* calculations with various basis sets.

^d CNDO/S calculations including *d* orbitals.

^e CNDO/S calculations neglecting *d* orbitals.

2. A Vector Addition Model for Bond Moments in Allenes

When dealing with the problem of predicting the dipole moment of a molecule with a known structure two fundamental properties of the dipole moment are pertinent:

1. It is a vector quantity, of which usually only the absolute magnitude is known.
2. It is a property of the whole molecule.

When the dipole moment has been determined from the Stark effect in microwave spectroscopy, its direction is experimentally fixed. Most other experimental methods give only the absolute magnitude of the vector, the direction being merely hypothetical or even unknown.

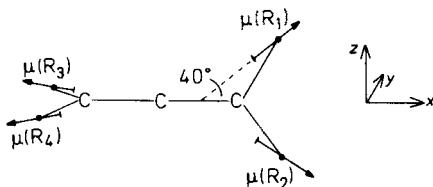


Figure 6 Origins and directions of the group moments in allenes according to the D_{2d} model.

Symmetry arguments, however, facilitate the problem of the direction of the vector (45). With respect to allenes the following rules are important.

- a. If the molecule has a mirror plane (e.g., allenes of symmetry C_s) the dipole moment is situated in this plane.
- b. If the molecule has a rotation axis (e.g., allenes of symmetry C_{2v} or C_{2v}) the dipole moment is directed along the axis.
- c. If the molecule has a rotation-reflection axis (e.g., allenes of symmetry D_{2d}) the dipole moment is zero.

A most widely used method for the prediction of molecular dipole moments is the empirical "vector addition" of bond moments (45). It involves the concept of point dipoles situated in the directions of the individual bonds and assumes that the magnitudes of the dipoles are transferable from one molecule to another. For allenes a somewhat modified approach has been established which is of relevance in connection with the discussion of influences of electrostatic field effects on spectroscopic properties of allenes (24,25) (Section III.D). This model uses fixed origins and fixed orientations for all the different (point dipole) bond moments in substituted allenes. As the origins of the point dipoles the positions of the hydrogen atoms in allene (11) have been used (24). The directions of the dipole moments are assumed to make an angle of 40° with the $C=C=C$ axis (Fig. 6) which represents an average value of experimental directions of dipole moments in differently substituted allenes (24).

The vector addition model for allenes conforms to the concepts of the D_{2d} -molecular models outlined in Section II.A. Within the preceding model it suffices to characterize each substituent by one numerical (positive or negative) value $\mu(R)$, the magnitude of the group moment of the substituent R in the allenic system.

In Table 3 a summary of group moments for chemically relevant substituents for allenes and other cumulenes is given. The values correspond to the molecular dipole moments in monosubstituted allenes which are either experimentally determined or from the correlations given in Section II.B.1. They have been fixed numerically to be similar, as far as possible, to other group moments used for aromatic and nonaromatic unsaturated compounds (45).

TABLE 3
 Group Moments and Substituent Constants for Allenes and Cumulenes

R	$\mu(\text{R})(\text{D})$	σ_I	σ_R^0	σ_R^-
H	0	0	0	0
F	1.97 ^a	0.50	-0.34	-0.45
Cl	1.75 ^b	0.46	-0.23	-0.23
Br	1.60 ^a	0.44	-0.19	-0.19
I	1.52 ^b	0.39	-0.16	-0.11
CF ₃	2.88 ^b	0.45	0.08	0.17
Me ₃ Si	-0.43 ^b	-0.10	0.06	0.14
HC≡C	0.84 ^b	0.22		
H≡CC≡C	1.00 ^c	0.27		
NC	4.28 ^a	0.56	0.13	0.33
Me	-0.40 ^a	-0.040	-0.11	-0.11
Et	-0.62 ^b	-0.048	-0.13	-0.13
<i>i</i> -Pr	-0.84 ^b	-0.056		
<i>t</i> -Bu	-0.89 ^b	-0.065		
C ₃ H ₅	-0.70 ^c	-0.050		
CH ₂ Cl	2.02 ^a	0.25	-0.03	
CH ₂ OH	1.80 ^c	0.22		
H ₂ C=CH	-0.06 ^b	(-0.01)	-0.19	
Ph	0.18 ^b	0.10	-0.11	0.04
COOH	2.30 ^c	0.33	0.14	0.34
COOMe	2.30 ^c	0.33	0.14	0.34
COMe	4.00 ^c	(0.52)	0.16	0.47
NCO	1.33 ^c	0.33	-0.21	
MeO	1.00 ^c	0.27	-0.45	-0.45
MeS	1.35 ^c	(0.33)	-0.20	-0.14
POCl ₂	4.00 ^c	(0.52)	0.10	0.32
MeSO ₂	4.80 ^c	0.59	0.12	0.38

^a Experimental values.

^b From correlations (13) or (14).

^c Highly probable values based on CNDO/S or STO-3G calculations.

With the exceptions of the groups CF₃ and MeS the group moments $\mu(\text{R})$ in Table 3 exhibit two good linear correlations (Fig. 7) with the polar substituent constants $\sigma_I(2b,4a)$ depending upon whether the substituents are of the $-I^-$ and $+I^+$ -type or the $-I^+$ or $+I^-$ -type (37a). The corresponding σ_I values of the substituents under consideration are given in Table 3. Parameters in parentheses are rescaled σ_I values for substituents which take account of the orientational contributions of the polar effects in cumulenic systems, that is, which take the different conformations of the substituents in cumulenes and ethylenes into account.

Considering all one sees that for the cumulenes the usual σ_I scale (2b,4a) should be valid for most of the chemically relevant substituents. In addition, in

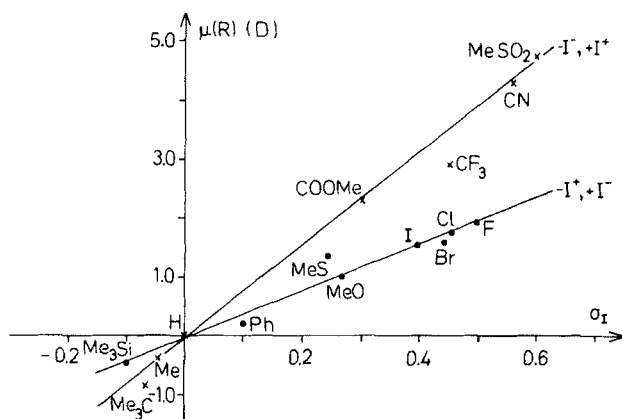


Figure 7 Correlations of the group moments and the polar substituent constants σ_r .

Table 3 also resonance substituent constants σ_R^0 and σ_R^- for most of the substituents are given. These values are used in Section III when observable substituent effects are interpreted semiquantitatively. In most cases these resonance constants are identical with those given by Taft and co-workers (2,4) for aromatic systems.

On the basis of the vector sum in Equation 18 the molecular dipole moments of substituted allenes should be predictable with the bond moments from Table 3.

$$\mu(R_1, R_2, R_3, R_4) = [\mu(R_1) + \mu(R_2) - \mu(R_3) - \mu(R_4)] \cdot \cos 40^\circ \mathbf{i} + [\mu(R_3) - \mu(R_4)] \cdot \sin 40^\circ \mathbf{j} + [\mu(R_1) - \mu(R_2)] \mathbf{k} \quad (18)$$

In case of 1,1-dimethylallene (**2**) (-0.549 vs. -0.613) and 1,3-difluoroallene (**10**) (1.77 vs. 1.79) a good agreement between experimental and calculated dipole moments is observed. A larger deviation is found for 1,1-difluoroallene (**9**) (2.07 vs. 3.02). However, such discrepancies are always observed if two strongly polar groups are in geminal positions in the molecule (45).

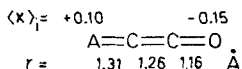
The effects of increasing the chain lengths of the cumulenic skeletons on the dipole moments, for example, the transition from ketenes to methylene ketenes, may be rationalized, at least qualitatively, on the basis of Flygare's method (46) of calculating electric dipole moments by summing empirically derived reduced-atom dipole moments. In this approach the center of mass (CM) of the corresponding molecule is the reference point (i.e., the origin of the dipole moment).

A crude, but particularly simple illustration of the effect of increase in chain length may be presented for the cases of ketene (**43**) and methylene ketene (**48**) treating the methylene groups H_2C as pseudo-atoms A of atomic mass 14. For $\text{A}=\text{C}=\text{O}$ (ketene) the center of mass coincides to a good approximation with

the *sp* carbon atom, whereas for A=C=C=O (methylene ketene) the center of mass is situated approximately in the middle of the C=C bond. Then, according to Equation 19, $\langle x \rangle_i$ being the reduced-atomic dipoles of the atoms *i* (in Å) of distance *x* from the center of mass, the atomic contributions of the two *sp* carbon atoms in **48** cancel.

$$\mu = -|e| \sum_i \langle x \rangle_i \quad (19)$$

In **48** we choose the reduced-atom dipole of the oxygen atom to be -0.15 Å (the average value for oxygen in O=C=O (-0.20) and O=C=X (-0.10) (46)). The reduced-atom dipole of the pseudoheteroatom A is chosen to be $+0.10$ Å (enlarging the value of $+0.05$ Å for an *sp*² carbon atom in C=C (46)). This last value takes the influence of the neighboring *sp* carbon atom as well as the neighboring hydrogen atoms in the group H₂C (=A) into account.



Then, Flygare's method (46) gives

$$\begin{array}{l} \mu(\mathbf{48}) \\ \mu(\mathbf{43}) \end{array} \approx 1 + \frac{(0.10 + 0.15) r_{\text{C}=\text{C}}/2}{0.10 r_{\text{A}=\text{C}} + 0.15 r_{\text{C}=\text{O}}} \approx 1.52 \quad (20)$$

From Equation 20 one predicts a value of $\mu = 2.15$ D for **48**, in excellent agreement with the experimental value (Table 2). However, in view of the crudeness of the approximations in the calculation this excellent agreement between experimental and theoretical dipole moments of **48** must be regarded as fortuitous.

C. Scalar Molecular Properties of Allenes

1. Carbon and Hydrogen Electron Densities

Electron densities and their relations to experimentally observable effects play an important role in the discussions of molecular properties. Electron density distributions in molecules may be related to dipole moments (47), that is, observables. However, the most widely used concept of charges attributed to atoms in a molecule associates the electron density distributions to a set of (theoretically determined) indices characteristic for the atoms in the molecule.

An often-used method of calculating atomic charges in molecules is the "population analysis" (47). The gross population of an atomic orbital is given by the Equations 21 and 22,

$$q_{\mu\mu} = P_{\mu\mu} + \sum_{\mu \neq \nu} P_{\mu\nu} \cdot S_{\mu\nu} \quad (21)$$

$$P_{\mu\nu} = 2 \sum_i^{occ} c_{\mu i} \cdot c_{\nu i} \quad (22)$$

where $S_{\mu\nu}$ represents the overlap integral and $P_{\mu\nu}$ an element of the first-order density matrix. The net charge q_A of an atom A results from Equation 23, Z_A being the atomic number and Q_{AA} the gross atomic population.

$$q_A = Z_A - \sum_{\mu}^A q_{\mu\mu} = Z_A - Q_{AA} \quad (23)$$

If a "zero differential overlap" (ZDO) approximation (47) is invoked, as in semiempirical CNDO theories, the gross atomic population reduces to the electron density P_{AA} (24).

$$P_{AA} = 2 \sum_{\mu}^A \sum_i^{occ} c_{\mu i}^2 \quad (24)$$

In case of the allenes it has been shown (9) that semiempirical CNDO/S electron densities P_{AA} of the carbon and hydrogen atoms as well as the π electron densities P_{AA}^{π} correlate linearly with *ab initio* STO-3G gross atomic populations Q_{AA} and π orbital populations Q_{AA}^{π} , respectively. The corresponding values for ketene (43) also fall on the regression lines.

$$P_{CC}(\text{CNDO/S}) = 0.722 Q_{CC}(\text{STO-3G}) - 0.365 \quad (r = 0.9593) \quad (25)$$

$$P_{HH}(\text{CNDO/S}) = 0.530 Q_{HH}(\text{STO-3G}) + 0.476 \quad (r = 0.9447) \quad (26)$$

$$P_{CC}^{\pi}(1',2')(\text{CNDO/S}) = 1.253 Q_{CC}^{\pi}(\text{STO-3G}) - 0.248 \quad (r = 0.9784) \quad (27)$$

$$P_{CC}^{\pi}(3')(\text{CNDO/S}) = 0.047 Q_{CC}^{\pi}(\text{STO-3G}) + 0.925 \quad (r = 0.9561) \quad (28)$$

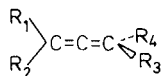
For the π electron densities, however, one must differentiate between the carbon atoms $C_{1'}$ and $C_{2'}$ near the position of substitution and the remote carbon atom $C_{3'}$ (9).

As a result, informations of comparable quality may be obtained from both types of calculations, regardless of the different definitions adopted for the charge densities. For these reasons in the present chapter electron density distributions in cumulenes are discussed on the basis of semiempirical CNDO/S data, which allow a consistent and facile treatment also for larger molecules. Notably, CNDO/S electron densities do not correlate with CNDO/2 or INDO electron densities (Section II.G.2).

Concerning a systematic discussion of substituent effects in allenes the (theoretically defined) total electron densities may be treated as point-properties of the atoms in the molecules; that is, they may be treated as numerical values associated to definite points (or regions) which are arranged in space according to the requirements of the D_{2d} -model (Section II.A).

If one discusses the total CNDO/S electron densities of the allenic carbon

atoms in arbitrarily substituted allenes the requirement of completeness in



connection with the constitutional isomerism order $k = 2$ for the D_{2d} -systems makes at least two-particle functions for the descriptions of carbon electron densities in allenes necessary. In Ref. 9 the Equations 29 and 30 as the simplest ansätze conforming to the preceding requirements have been suggested as approximations for the predictions of electron densities of CNDO/S quality, C_c denoting the allenic central atom (C_2) and C_i (C_1, C_3) the terminal ones.

$$\tilde{P}_{CC}(C_c) = \rho^P + \sum_{i=1}^4 \sigma^P(R_i) + \tau^P(R_1, R_2) + \tau^P(R_3, R_4) \quad (29)$$

$$\begin{aligned} \tilde{P}_{CC}(C_i) = & \alpha^P + \beta^P(R_1) + \beta^P(R_2) + \gamma^P(R_1, R_2) \\ & + \mu^P(R_3) + \mu^P(R_4) + \nu^P(R_3, R_4) \end{aligned} \quad (30)$$

In these expressions $\sigma^P(R_i)$, $\beta^P(R_j)$, and $\mu^P(R_k)$ represent ligand-specific parameters ("substituent effects") of the corresponding ligands at the ligand sites i , j , and k , respectively. $\tau^P(R_i, R_j)$, $\gamma^P(R_k, R_l)$, and $\nu^P(R_m, R_n)$ are pair-terms for geminal substituents. ρ^P and α^P are constants.

For the predictions of electron densities the necessary parameters have been determined from CNDO/S electron densities of a restricted set of monosubstituted and 1,1-disubstituted allenes using the conventions (31) and (32) (9):

$$\sigma^P(H) = \beta^P(H) = \mu^P(H) = 0 \quad (31)$$

$$\tau^P(R, H) = \gamma^P(R, H) = \nu^P(R, H) = 0 \text{ for arbitrary R} \quad (32)$$

The relevant parameters are summarized in Table 4, which are identical with the computerized CNDO/S electron densities for the particular molecules.

CNDO/S electron densities of complex allenes predicted with these parameters on the basis of Equations 29 and 30 agree well with those obtained from direct quantum-chemical CNDO/S computations (cf. Table 14). With respect to the CNDO/S level most pair-terms (τ^P , γ^P , ν^P) are small compared with the one-particle functions. Therefore, for numerical purposes they seem to be not so relevant as, for instance, in case of the ^{13}C chemical shifts of the allenic carbon atoms (Section II.C.2) which are described by approximation ansätze similar to Equations 29 and 30. In the light of the discussions in Section II.A the preceding findings concerning the pair-terms must be viewed as accidental and cannot be predicted a priori. For instance, the neglect of the pair-terms may no longer be justified, if one uses a different computational procedure for the evaluation of the electron densities (such as the INDO or MINDO/3 scheme).

TABLE 4
Parameters for the Predictions of Carbon Total Electron Densities of Allenes, Obtained from
Monosubstituted and 1,1-Disubstituted Compounds $R_1R_2C=C=CH_2$ (in $10^{-3} e$) (9)

Compd.	R_1	R_2	$\sigma^P(R)$	τ^P (R_1, R_2)	$\beta^P(R)$	γ^P (R_1, R_2)	$\mu^P(R)$	ν^P (R_1, R_2)
11	H	H	$\rho^P =$ 3.940			$\alpha^P =$ 4.099		
12	Me	H	+24		-45		+13	
18	Et	H	+10		-50		+29	
31 ^a	C ₃ H ₅	H	-45		-6		+59	
24	CH ₂ OH	H	+27		-42		-14	
25 ^b	CH ₂ Cl	H	+15		-61		+1	
26	CF ₃	H	-24		+12		-26	
27	Me ₃ Si	H	-9		+35		+26	
17	H ₂ C=CH	H	+8		-52		+3	
16	Ph	H	-4		-43		+14	
57 ^a	α -Np	H	-2		-37		+12	
28	HC≡C	H	-9		-65		-4	
29	HC≡CC≡C	H	-11		-65		-6	
58	COO [⊖]	H	+4		-72		+67	
22	COOH	H	-22 ^c		-40 ^c		-17 ^c	
			-40 ^d		-34 ^d		-24 ^d	
23	COOMe	H	-24 ^c		-44 ^c		-20 ^c	
			-38 ^d		-39 ^d		-24 ^d	
21	COMe	H	-16 ^c		-42 ^c		-12 ^c	
			-35 ^d		-31 ^d		-24 ^d	
14	CN	H	-27		-60		-23	
33 ^a	NCO	H	+8		-101		+16	
15	F	H	+86		-299		-59	
30	Cl	H	-4		-69		-12	
19	MeO	H	+53		-153		+15	
20	MeS	H	+2		-30		+12	
34 ^a	MeSO ₂	H	-44		-61		-55	
32 ^b	POCl ₂	H	-84		-24		-53	
2	Me	Me		+2		+3		-1
7 ^a	Et	Me		+21		-6		-20
59	Ph	Me		+6		+2		-4
9	F	F		-1		-3		+2

^a This work.

^b From Ref. 11.

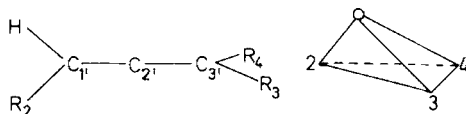
^c *s-trans* form.

^d *s-cis* form.

From the substituent constants (σ^P , β^P , μ^P) in Table 4 one sees that substitution in the allenic system is accompanied by electron density redistributions which comprise the whole C=C=C cumulenenic skeleton.

Taking the electron densities of the hydrogen atoms of Allenes into con-

sideration for a quantitative treatment one has to start from a dissection of the molecules into a three-site skeleton ($n = 3$) resembling an irregular pyramid of symmetry C_s (9).

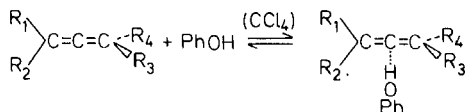


For such systems the constitutional isomerism order is $k = 2$. Consequently, the simplest ansatz for the description of a point-property of an allenic hydrogen atom conforming to the requirement of completeness only contains one-particle functions ($N = 3 - 2$). In Ref. 9 it has been shown that for the predictions of CNDO/S electron densities of allenic hydrogens indeed one-particle functions suffice; that is, the hydrogen electron densities may be calculated according to Equation 33.

$$\bar{P}_{HH} = \beta^P + \alpha^P(R_2) + \gamma^P(R_3) + \gamma^P(R_4) \quad (33)$$

In Equation 33 β^P is a constant, $\alpha^P(R_2)$ and $\gamma^P(R_i)$ are ligand-specific parameters for the substituents attached to the ligand sites 2 or $i = 3, 4$, respectively. These parameters have been determined from the CNDO/S hydrogen electron densities of monosubstituted allenes ($\alpha^P(H) = \gamma^P(H) = 0$). They are given in Table 5. From the numerical values one can see that substitution affects both the kinds of allenic hydrogen atoms to a comparable extent which again indicates the pronounced substituent effects across the whole allenic heavy-atom grouping.

The concept of electron densities is important in the interpretation of chemical reactions or equilibria, acidities, and basicities. For instance, alkylallenes act as monofunctional π bases in equilibria with phenol to give hydrogen bonded complexes (48).



The hydrogen bonding is to the allenic central atom (48). As expected from the known positive inductive effects of the alkyl groups the basicity of alkylallenes increase with increasing substitution as a result of accumulation of negative charge density at the central atom (Table 6). With respect to the general model of molecular properties of allenes it should be noted that, again, the constitutionally isomeric ethyl-methyl-allenes **7** and **8** exhibit distinctly different thermodynamic data for the preceding equilibrium. This means that the actual physical situation cannot be described in terms of only a sum of substituent effects. The structure of the observables of the equilibrium is reflected by linear

TABLE 5
Parameters for the Predictions of Hydrogen Electron Densities of Allenes, Obtained from
Monosubstituted Compounds $RHC=C=CH_2$ (in $10^{-3} e$) (9)

Compd.	R	$\alpha^P(R)$	$\gamma^P(R)$
11	H	$\beta^P = 0.965$	
12	Me	+1	+6
18	Et	+4	+9
31 ^a	C ₃ H ₅	-2	+1
24	CH ₂ OH	-7	+5
25 ^b	CH ₂ Cl	-6	0
26	CF ₃	-15	-10
27	Me ₃ Si	+5	+6
17	H ₂ C=CH	-1	+1
16	Ph	+2	+2
57 ^a	α -Np	-6	+2
28	HC \equiv C	-13	-2
29	HC \equiv CC \equiv C	-14	-3
58	COO ^e	+16	+29
22	COOH	-10 ^c (+2) ^d	-10 ^c (-12) ^d
23	COOMe	-11 ^c (+2) ^d	-8 ^c (-9) ^d
21	COMe	-9 ^c (+9) ^d	-6 ^c (-9) ^d
14	CN	-17	-10
33 ^a	NCO	-12	+1
15	F	+4	-2
30	Cl	-13	-3
19	MeO	-14	+9
20	MeS	-10	+3
34 ^a	MeSO ₂	-22	-18
32	POCl ₂	-15	-22

^a This work.

^b From Ref. 11.

^c *s-trans* form.

^d *s-cis* form.

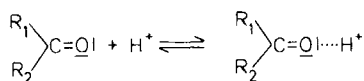
correlation (34) ($r = 0.9172$) of the equilibrium enthalpies with the total electron densities $\bar{P}_{CC}(2')$ obtained from Equation 29 (Fig. 8).

$$-\Delta H = 2.942 \bar{P}_{CC}(2') - 10.144 \quad (34)$$

The preceding equilibrium of alkylallenes shows a formal analogy with the initial reaction step of an acidic hydrolysis of saturated carboxylic acid esters $R'(RO)C=O$ or protonation reactions of carbonyl compounds $R_1R_2C=O$. This similarity concerns the position of the attack of the proton relative to the positions of the substituents and the kinds of atoms involved in that reactions. In both the cases (C and O) the attacked atoms have perpendicular p AOs in the LCAO expansions of their two outermost occupied orbitals.

TABLE 6
Thermodynamic Parameters for the Equilibria of Alkylallenes and Phenol
(in CCl₄; T = 27°C) (48)

Compd.	R ₁	R ₂	R ₃	R ₄	-ΔF(kcal mole ⁻¹)	-ΔH(kcal mole ⁻¹)	-ΔS (eu)
60	<i>n</i> -Pr	H	H	H	-0.89	1.49	8.0
7	Et	Me	H	H	-0.76	1.51	7.6
8	Et	H	Me	H	-0.73	1.59	7.8
61	Me	Me	Me	H	-0.72	1.61	7.8
62	Me	Me	Me	Me	-0.63	1.78	8.1



A conventional treatment of the allene-phenol equilibrium would suggest that the free energy of the equilibrium depends upon the sum of the σ_I substituent constants (correlation (35); $r = 0.9473$).

$$\Delta F = 0.965 - 2.161 \sum_i \sigma_I(R_i) \quad (35)$$

Though satisfying from a numerical point of view, correlation (35) disregards an essential physical effect associated with the constitutional isomerism in allenes and must be subjected to a criticism which has been given in connection with Equation 8. Any numerical improvement of the preceding correlation (35) using instead of a single-parameter approach a dual-substituent parameter (DSP) approach (2,4) also buries these physical problems.

2. ¹³C Chemical Shifts

The chemically most important observable phenomena associated with point-properties of the allenic carbon atoms with physical structures corresponding to those of the total electron densities are the ¹³C chemical shifts. Therefore, the simplest approximations for the (semiempirical) descriptions

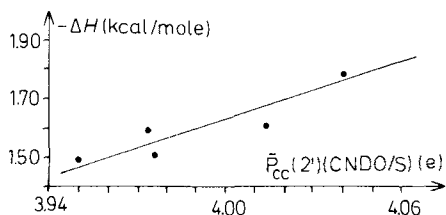


Figure 8 Correlation of the alkylallene-phenol equilibrium enthalpies and the total electron densities of the allenic central atoms.

of the ^{13}C chemical shifts in arbitrarily substituted allenes must have the same analytical forms as those used for the predictions of electron densities (Equations 29 and 30).

In Refs. 7 and 8 it has been shown that ^{13}C -chemical shifts of allenes are adequately described by the Equations (36)–(38)

$$\sigma^{\text{C}}(\text{H}) = \beta^{\text{C}}(\text{H}) = \mu^{\text{C}}(\text{H}) = 0 \quad (36a)$$

$$\tau^{\text{C}}(\text{R},\text{H}) = \gamma^{\text{C}}(\text{R},\text{H}) = \nu^{\text{C}}(\text{R},\text{H}) = 0 \text{ for arbitrary R} \quad (36b)$$

$$\bar{\delta}_{\text{C}_c} = \rho^{\text{C}} + \sum_{i=1}^4 \sigma^{\text{C}}(\text{R}_i) + \tau^{\text{C}}(\text{R}_1,\text{R}_2) + \tau^{\text{C}}(\text{R}_3,\text{R}_4) \quad (37)$$

$$\bar{\delta}_{\text{C}_i} = \alpha^{\text{C}} + \beta^{\text{C}}(\text{R}_1) + \beta^{\text{C}}(\text{R}_2) + \gamma^{\text{C}}(\text{R}_1,\text{R}_2) \\ + \mu^{\text{C}}(\text{R}_3) + \mu^{\text{C}}(\text{R}_4) + \nu^{\text{C}}(\text{R}_3,\text{R}_4) \quad (38)$$

Following the procedure outlined for the evaluation of the parameters for the calculations of the electron densities (Section II.C.1) the ^{13}C chemical shift parameters may be obtained from a restricted set of monosubstituted and 1,1-disubstituted allenes (or from molecules with four identical ligands). Then, these parameters may be used, without any further numerical adjustment processes, to calculate the ^{13}C chemical shifts of other allenes. Evidently, the one-particle functions $\sigma^{\text{C}}(\text{R})$, $\beta^{\text{C}}(\text{R})$, and $\mu^{\text{C}}(\text{R})$ are identical with the (experimental) "substituent chemical shifts" (SCS).

A summary of the ^{13}C chemical shift parameters is given in Table 7. Comparisons between experimental and calculated ^{13}C chemical shifts of allenes may be found in Tables 16 and 17 (Section II.E). These comparisons clearly demonstrate the physical competence of the ansätze, (37) and (38), for the description of ^{13}C chemical shifts of allenes. Only the fluoroallenes do not follow these lines (8). The apparent discrepancies are discussed in Section II.E.

^{13}C chemical shifts of cyclic allenes (49) cannot be incorporated into the preceding treatment.

From the numerical values of the parameters in Table 7 one can see that the pair-terms make essential contributions to the overall observable ^{13}C chemical shifts of allenes. They may become as large as the substituent chemical shifts.

Furthermore, the bulk of data for constitutional isomers shows that, in by far the most cases, there are no linear dependencies between the experimental ^{13}C chemical shifts of constitutionally isomeric allenes. For practical purposes of organic chemistry an important aspect of nmr chemical shifts is that they allow a differentiation of the various constitutional isomers. Using Equation 38 one can see easily that such a criterion (i.e. differences in nmr shifts of the isomers) does not suffice to characterize the physical situation appropriately. An ansatz neglecting the pair-terms (γ^{C} , ν^{C}) in Equation 38 obviously fulfills the re-

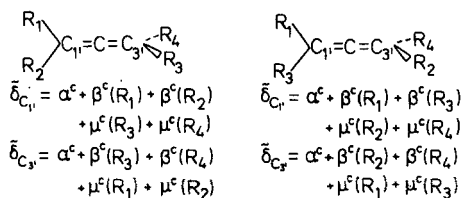
TABLE 7
 Parameters for the Calculations of ^{13}C Chemical Shifts of Allenes (in ppm) (8)

R	$\sigma^C(\text{R})$	$\beta^C(\text{R})$	$\mu^C(\text{R})$	R',R''	τ^C (R',R'')	γ^C (R',R'')	ν^C (R',R'')
H	$\rho^C = 212.6$	$\alpha^C = 73.5$					
Me	-3.2	+10.7	-0.1	Me,Me	+0.5	-1.0	-0.9
Et	-3.8	+18.1	+1.2	Et,Me	+0.5	-2.1	-0.2
<i>n</i> -Pr ^a	-3.1	+16.4	+1.1				
<i>i</i> -Pr	-4.8	+24.3	+2.7				
<i>n</i> -Bu ^a	-3.6	+16.1	+0.3				
<i>t</i> -Bu	-5.6	+28.9	+3.5				
<i>n</i> -Pe ^a	-3.2	+16.9	+1.5				
CH ₂ SMe ^b	-3.0	+15.1	+2.6				
CMe ₂ CH=CH ₂ ^c	-7.8	+26.2	+3.3				
				COOH,Me	+0.9	-5.2	-1.7
Li ^d	-16.2	+13.7	-30.3	COOH,Et	+0.9	-5.6	-1.7
COOH	+5.1	+14.6	+5.9	COOMe,Me	+0.9	-1.5	-1.0
COOMe	+4.9	+12.8	+5.5	COOMe,Et	+0.9	-2.5	-1.0
COONa	+4.2	+20.1	+5.1	Ph,Me	+2.7	-4.7	-2.0
CN	+6.0	-6.1	+7.2	Ph,Et	+2.9	-5.0	-1.5
Ph	-3.0	+20.5	+5.3	Ph,Ph	+3.9	-6.9	-5.7
				Ph,COOMe	+2.1	-6.4	-3.6
<i>p</i> -ClC ₆ H ₄ ^e	-3.0	+19.6	+5.4				
<i>p</i> -MeC ₆ H ₄ ^e	-2.5	+20.8	+5.7				
PhMeN ^f	-8.6	+32.5	+13.5				
MeO	-11.5	+49.5	+17.9	MeO,Me	-1.4	+0.4	-4.9
EtO	-10.3	+48.2	+16.1	MeO,Et	-1.9	-6.8	-4.9
				MeO, <i>i</i> -Pr	-0.3	-9.3	-5.5
MeS	-5.7	+15.0	+7.4	MeS,Me	-0.1	+0.7	-0.7
				MeS,Et ^b	+0.4	+0.6	+0.1
				MeS, <i>i</i> -Pr ^b	-0.6	+0.6	-1.8
F	-13.3	+55.0	+19.1	F,F	+5.5	-28.6	-8.2
Cl	-5.2	+15.2	+11.3				
Br	-5.7	-1.6	+9.6				
I ^g	-4.0	-38.8	+4.9				
Me ₃ Si ^g	+1.4	+8.4	-5.7				

^a Ref. 18.^b Ref. 17.^c Ref. 50.^d Ref. 52.^e Ref. 51.^f Ref. 53.^g Ref. 54.

quirement of predicting different ^{13}C chemical shifts for the terminal carbon atoms of constitutionally isomeric allenenes.

However, in this case, the sums ($\delta_{C_1'} + \delta_{C_3}$) are identical for both the preceding molecules; that is, there are linear dependencies contrary to the ex-



perimental facts. For this particular case three measurements of ^{13}C chemical shifts of allenic terminal atoms would suffice to predict the shift of the fourth atom with certainty.

This last example should emphasize the problem inherent in verbal descriptions of physical phenomena, if one seeks for a mathematical approach to describe the apparent phenomena adequately.

3. ^1H Chemical Shifts

The proton chemical shifts of the allenic hydrogen atoms represent point-properties of the molecules which are expected to exhibit similar structural features as the hydrogen electron densities (Section II.C.1). Therefore, on the basis of the general geometrical model an ansatz comparable with that of Equation 33 would be attractive for semiempirical calculations of proton chemical shifts of allenes. However, symmetry conditions are only necessary, but not sufficient for the realization of physical properties of systems or the structure of physical phenomena, respectively. In particular, a purely geometrical treatment does not suffice to describe the whole physical situation in case of the proton chemical shifts (10). In addition, there exists a "boundary condition" for the experimentally observable effects associated with proton chemical shifts. In Ref. 10 it has been suggested that proton chemical shifts do not only depend upon the types of ligands attached to the molecular skeleton and their arrangements in space but, additionally, upon a point-property of at least the atom to which the hydrogen atom under consideration is bonded. This conditions is simply a generalization of the well-known fact that often proton chemical shifts may be related to π electron densities or total electron densities of the carbon atoms to which they are bonded.

Therefore, an adequate description (Equation 39) of the proton chemical shifts $\bar{\delta}_H(R_2, R_3, R_4)$ of allenes requires two contributions which are independent from each other. The proton shifts depend upon a certain point-property $P(H|R_2, R_3, R_4)$ of that proton and point-properties $Q(C_i|H_1, R_2, R_3, R_4)$ of the carbon atoms of the allenic skeleton.

$$\bar{\delta}_H(R_2, R_3, R_4) = P(H|R_2, R_3, R_4) + Q(C_i|H_1, R_2, R_3, R_4) \quad (39)$$

Both the contributions of Equation 39 have to be "complete" with respect to the geometrical situations of the underlying molecular skeletons (P with respect

TABLE 8
Parameters for the Calculations of ^1H Chemical Shifts of Allenes (in ppm) (10)

R'	R''	$\alpha^H(\text{R}')$	$\gamma^H(\text{R}')$	$\omega^H(\text{R}',\text{R}'')$
H		$\beta^H = 4.67$		
Me		+0.27	-0.17	
Me	Me			+0.07
Et		+0.36	-0.12	
Et	Me			+0.09
<i>n</i> -Pr		+0.29	-0.07	
<i>i</i> -Pr		+0.45	0.0	
<i>t</i> -Bu	Me			+0.07
<i>t</i> -Bu		+0.52	+0.09	
<i>t</i> -Bu	Me			-0.01
CH_2OH^a		+0.63	+0.18	
CH_2Cl^b		+0.76	+0.30	
CH_2Br^c		+0.74	+0.27	
$\text{CH}_2\text{CH}_2\text{OH}^d$		+0.46	0.0	
COOH		+0.97	+0.56	
COOH	Me			+0.09
COOH	Et			+0.14
COOMe		+0.97	+0.56	
COOMe	Me			-0.06
COOMe	Et			-0.03
CHO		+1.00	+0.60	
CHO	Me			+0.01
COMe		+1.00	+0.60	
CN		+0.30	+0.36	
$\text{H}_2\text{C}=\text{CH}$		+1.29	+0.25	
$\text{H}_2\text{C}=\text{CH}$	Me			+0.07
Ph		+1.36	+0.43	
Ph	Me			+0.06
Ph	Et			-0.01
Ph	Ph			-0.24
MeO		+1.76	+0.75	
MeO	Me			+0.11 ^e
MeO	Et			+0.07
MeO	<i>i</i> -Pr			-0.13
Cl		+1.33	+0.47	
Br		+1.26	+0.26	
I		+1.02	-0.19	
PhMeN ^f		+2.15	+0.67	
Me_3Si		+0.02	-0.46	
MeS		+1.23	+0.36	
Et_2P		+0.53	-0.09	
Cl_2P		+1.58	+0.88	
Et_2PO^g		+1.01	+0.36	
Ph_2PO^g		+1.19	+0.12	
Cl_2PO^g		+1.58	+0.87	
$(\text{EtO})_2\text{PO}^g$		+0.78	+0.37	

to the three-site pyramidal C_s -situation, Q with respect to the four-site D_{2d} -situation).

Then, it has been shown (10) that the simplest ansatz (40) for the description of proton chemical shifts of allenes must involve a pair-term $\omega^H(R_3, R_4) = \omega^H(R_4, R_3)$ for the geminal substituents at the ligand-sites 3 and 4.

$$\tilde{\delta}_H = \beta^H + \alpha^H(R_2) + \gamma^H(R_3) + \gamma^H(R_4) + \omega^H(R_3, R_4) \quad (40)$$

In Equation 40 β^H is a constant, $\alpha^H(R)$ and $\gamma^H(R)$ are ligand-specific parameters which correspond to the substituent chemical shifts ($\alpha^H(H) = \gamma^H(H) = 0$; $\omega^H(R, H) = 0$).

The parameters have been obtained from a restricted set of allenes and are given in Table 8. There one sees that the interaction terms become especially important in case of alkylallenes, contrary to many other observations where molecular properties of alkyl compounds are almost additive in increments for the alkyl groups.

Predicted proton chemical shifts of allenes on the basis of Equation 40 agree well with experimental values (10) (cf. also Table 19). Therefore, one may conclude that the extended algebraic model reflects the physical situation appropriately.

As the experimental 1H -chemical shifts δ_{H_4} of the methylene group protons in allenes are related to the ^{13}C -chemical shifts δ_{C_3} of the methylene carbon atoms (10), the corresponding proton and ^{13}C chemical shift parameters, $\mu^C(R)$ and $\gamma^H(R)$, respectively, reflect similar physical effects.

$$\delta_{H_4} = 0.051 \delta_{C_3} + 0.810 \text{ for } RCH=C=CH_2 \quad (41)$$

In case of alkylallenes also the 1H and ^{13}C chemical shifts of the α atoms exhibit a linear correlation (10).

$$\delta_{H_1} = 0.0176 \delta_{C_1'} + 3.4050 \text{ for } AlkHC=C=CH_2 \quad (42)$$

4. Nuclear-Nuclear Spin-Spin Coupling Constants

So far, molecular properties have been considered which are either properties of the whole molecule or of a single atom (a "point") within the molecule.

^a From $H_2C=C=CHCH_2OH$ (55a).

^b From $H_2C=C=CHCH_2Cl$ (56).

^c From $BrHC=C=CHCH_2Br$ (55b).

^d From $H_2C=C=CHCH_2CH_2OH$, band centers (59).

^e From $EtCH=C=CMe(MeO)$ and $PhHC=C=COMe(i-Pr)$ (57).

^f From $PhMeNHC=C=CH_2$ in C_6D_6/Et_2O (53).

^g From correspondingly monosubstituted allenes (58).

Nuclear–nuclear spin–spin coupling constants $J(AB)$ between two atoms A and B in a molecule are interesting quantities which depend simultaneously upon point-properties of two nuclei of the molecule. Within the geometrophysical model adopted for the description of molecular properties of allenes the coupling constants offer two alternatives as to the primitive concepts for our ideal model of a deductive geometrical system. Again, we may take the concept “point” as the essential undefined element of the model, or we may additionally introduce the concept “line” into the geometrical model. The concept “line” would be the chemical equivalent of “bond,” whereas “point” is the equivalent of “atom.”

From a pragmatic point of view it is more advantageous to restrict oneself to the concept “point” as the single primitive element of the model. Then, deductions concerning spin–spin coupling constants may be related to arguments that have already been given for properties of single points in molecules.

For the discussions of other properties involving two atoms in the molecules, such as force constants which are definitely properties of bonds, however, it may turn out that an adequate geometrical model should be based on the concept “line.”

Accepting the preceding arguments we factor the function $\tilde{J}(AB)$ which shall describe the observable phenomenon “spin–spin coupling constant” into functions, $P(A)$ and $Q(B)$, respectively, of only one argument. $P(A)$ and $Q(B)$ represent point-properties of the atoms A and B involved in the spin–spin coupling.

$$\tilde{J}(AB) = P(A) \cdot Q(B) \quad (43)$$

It should be noted that on the basis of an algebraic (geometrical) model there is no a priori justification for an ansatz like Equation 43. The most general form of the two-variable function $\tilde{J}(AB)$ should contain a correlated pair-function $j(AB)$.

$$\tilde{J}(AB) = f(A) \cdot g(B) + j(AB) \quad (44)$$

However, in relation to the quantum theory of spin–spin couplings (60) the factorization in Equation 43 is quite natural, since in the spin Hamiltonian the interaction energy between two nuclei A and B is directly proportional to the dot product of the corresponding operators, namely $E_{AB} = J(AB) \mathbf{I}_A \cdot \mathbf{I}_B$, where \mathbf{I}_A and \mathbf{I}_B do not depend upon the electronic wavefunctions.

Ansatz (43) is the basis for many empirical findings, such as the observations that one-bond carbon–hydrogen couplings ${}^1J({}^{13}\text{CH})$ are related to the hybridizations of the corresponding carbon atoms (61) or that carbon–carbon couplings ${}^1J({}^{13}\text{C}^{13}\text{C})$ parallel the product $s_C \cdot s_C$ of the hybridizations of the carbon atoms (62) or that sometimes carbon–nitrogen couplings may be related to the hybridizations $s_C \cdot s_N$ (63).

Furthermore, coupling constants may also be related to the product of

calculated electron densities ($J(AB) \sim P_{AA}P_{BB}$) (64). Ansatz (43) has non-trivial consequences, if, for instance, one-bond carbon-proton $^1J(^{13}\text{CH})$ (54,65) and four-bond proton-proton coupling constants $^4J(\text{HH})$ (11,65) of allenes are discussed. For an investigation of the substituent effects on $^1J(^{13}\text{CH})$ the most general forms of the functions P and Q in Equation 45 are known from the previous treatments.

$$^1\tilde{J}(^{13}\text{CH}) = P(\text{H}|\text{R}_2, \text{R}_3, \text{R}_4) \cdot Q(\text{C}|\text{H}_1, \text{R}_2, \text{R}_3, \text{R}_4) \quad (45)$$

They are identical with those of Equations 30 and 33. Then, one may immediately infer that in case of the one-bond carbon-proton couplings of allenes there are interactions across the allenic system. That means, the simplest ansatz for the description of these couplings as deduced from Equation 45 generally contains pair-terms of the form $\pi^J(\text{R}_2, \text{R}_3)$, whereas the molecular properties discussed so far have contained only pair-terms for geminal substituents, such as $\rho^J(\text{R}_3, \text{R}_4)$ in Equation 46.

$$\begin{aligned} ^1\tilde{J}(^{13}\text{CH}) = & \gamma^J + \kappa^J(\text{R}_2) + \delta^J(\text{R}_3) + \delta^J(\text{R}_4) + \rho^J(\text{R}_3, \text{R}_4) \\ & + \pi^J(\text{R}_2, \text{R}_3) + \pi^J(\text{R}_2, \text{R}_4) + \tau^J(\text{R}_2, \text{R}_3, \text{R}_4) \end{aligned} \quad (46)$$

Furthermore, Equation 46 contains a triple-term ($\tau^J(\text{H}, \text{R}, \text{R}') = \tau^J(\text{R}, \text{H}, \text{R}') = \tau^J(\text{R}, \text{R}', \text{H}) = 0$).

In Table 9 parameters for the predictions of one-bond carbon-proton couplings of allenes are summarized. From the numerical values of the parameters one can see that the interactions $\pi^J(\text{R}_2, \text{R}_3)$ across the allenic system are only significant, if a phenyl group is involved. In this case the "cross-terms" $\pi^J(\text{Ph}, \text{R})$ are comparable in magnitude with the pair-terms $\rho^J(\text{Ph}, \text{R})$ reflecting geminal interactions. The triple-terms τ^J are also only of relevance, if allenes with a phenyl group are taken into consideration. The one-particle functions $\delta^J(\text{R})$ reflecting the substituent effects on the carbon atom remote from the substituents are rather small.

A comparison between calculated and observed one-bond carbon-proton couplings in multiply substituted allenes is given in Table 20. This comparison gives credit to the preceding treatment of coupling constants. In quite the same way it may be concluded that also the four-bond proton-proton coupling constants $^4J(\text{HH})$ of allenes $\text{R}_2\text{HC}=\text{C}=\text{CHR}_3$ involve interactions across the allenic skeleton (11).

$$^4\tilde{J}(\text{HH}) = \gamma^J + \kappa^J(\text{R}_2) + \kappa^J(\text{R}_3) + \pi^J(\text{R}_2, \text{R}_3) \quad (47)$$

The substituents show a small, but significant influence on the four-bond proton-proton couplings in allenes (Table 10). Again, only interaction terms $\pi^J(\text{Ph}, \text{R})$ involving a phenyl group exhibit significant magnitudes. For alkylallenes and chloro-alkylallenes the allenic four-bond couplings $^4J(\text{HH})$ are

TABLE 9
Parameters for the Calculations of One-Bond Carbon-Proton
Coupling Constants of Allenes (in Hz)^a

R	$\kappa^J(\text{R})$	$\delta^J(\text{R})$	R',R''	$\rho^J(\text{R}',\text{R}'')$	$\pi^J(\text{R}',\text{R}'')$
H	$\gamma^J = 168.2$				
Me	-8.3	-1.7	Ph,Me	+7.2	+6.1
Et	-10.2	-4.2	Ph,Et	+8.6	+6.1
Ph	-8.3	-5.2	Ph,COOMe		+3.0
COOMe	+4.3	+3.4	Ph,COOH		+3.0
COOH	+4.3	+3.4	Alk,Alk ^c	+2.0	0.0
CN	+11.8	-1.7	COOH,Alk ^c	0.0	0.0
Me ₃ Si	-20.2	+0.8	COOMe,COOMe ^d		0.0
Cl ^b	+38.7	+1.9	Alk,Br		0.0
Br	+44.8	-1.8			
I	+36.6	+0.9			
MeO	+33.4	-0.7		$\tau^J(\text{Ph,COOR,Alk}) = -9.0^{\text{c,d}}$	
MeS	+23.1	-3.0			

^a The parameters κ^J and δ^J have been obtained from the experimental values of $^1J(^{13}\text{CH})$ in CDCl_3 for monosubstituted allenenes in Ref. 54; the pair-terms have been determined in this work; $\tau^J(\text{R}_1,\text{R}_2,\text{R}_3) = 0$ for arbitrary R and R \neq Ph.

^b From Ref. 65.

^c Alk = Me, Et.

^d R = H, Me.

additive in the substituent effects, that is, in the ligand-specific parameters $\kappa^j(\text{R})$ (11).

As a resume of the discussions of spin-spin coupling constants one may state that strict deductions from a well-defined geometrophysical point model have led to nontrivial qualitative predictions and quantitative interpretations which are corroborated by experiments (Table 20).

5. Ionization and Excitation Energies

If one wants to describe substituent effects on ionization and electronic excitation energies (from the chemically interesting pe and uv spectra) according to the geometrical model used so far, one is immediately confronted with the problem of dissecting the molecules appropriately into ligands and the skeleton, that is, with the problem of finding the invariants for the description of the phenomena.

For a treatment of the ionization energies one has to refer to particular molecular orbitals (MOs), in case of electronic excitation energies one has to refer to "chromophores," Chromophores also play the key role, if substituent effects on intensities of uv bands or cd bands in circular dichroism spectroscopy are considered.

TABLE 10
Substituent Effects on Four-Bond Proton-Proton Coupling Constants
in Allenes (in Hz) (11)^a

R	$\kappa^j(\text{R})$	R	$\kappa^j(\text{R})$
H	$\gamma^j = -7.00$		
Me	+0.33	PhMeN	+0.90
Et	+0.23	MeO	+1.10
CH ₂ Cl	+0.41	MeS	+0.60
Ph	+0.05	Cl	+0.96
H ₂ C=CH	+0.36	Br	+0.94
COOMe	+0.35	I	+0.73
COOH ^b	+0.35	Me ₃ Si	-0.02
COMe	+0.50	Cl ₂ PO	+0.39
CN	+0.21	Ph ₂ PO	+0.20

^a $\pi^j(\text{Me,Me}) = 0$; $\pi^j(\text{Me,Cl}) = 0$; $\pi^j(\text{Ph,Me}) = -0.30$; $\pi^j(\text{Ph,COOH}) = -0.20$; $\pi^j(\text{Ph,MeO}) = -0.35$; $\pi^j(\text{Ph,Ph}_2\text{PO}) = +0.25$.

^b Estimated from $\kappa^j(\text{COOMe}) = \kappa^j(\text{COOH})$.

Both the properties (ionization and excitation energies) are related to subsystems of the molecules which comprise more than one constituent atom. Attention is focussed to electronic subsystems of the molecules. Therefore, one cannot expect that analyses of ionization and excitation energies may be established which cover all kinds of interesting molecules in the general manners discussed so far. In particular, it is quite clear that mesomeric substituents (or substituents that interact essentially mesomerically with the skeleton) restrict the possibilities for the conceptional dissection of the molecules into the ligands and the skeleton (which may be a MO or a chromophore). By definition mesomeric substituents extend the range of delocalization of π systems. Therefore, the originally defined invariant (the MO or chromophore) is changed by the introduction of a mesomeric group to the extent of the capability of that group for mesomeric interactions. Therefore, one cannot adopt the geometrical model outlined in the preceding subsections, if the substitution is associated with considerable changes of the particular MOs or chromophores by π -conjugation interactions, spiro conjugation effects, and so on.

For some special cases, however, the geometrophysical model may be well suited. Two such cases are provided by the ionization energies of alkylallenes (from pe spectra) and the uv spectra of phenylallenes. The pe spectra of alkylallenes are discussed more qualitatively, whereas the uv spectra of phenylallenes are treated quantitatively.

Pe spectra are usually interpreted in terms of Koopmans' approximation which relates the vertical ionization energy $I_v(i)$ to the negative orbital energy ϵ_i of the MO i from an SCF procedure.

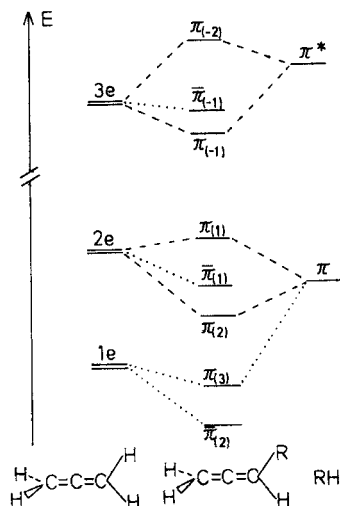


Figure 9 Orbital diagram correlating the a'' (π) and a' ($\bar{\pi}$) orbitals in monosubstituted allenes with the allenic e orbitals and the substituents' a'' orbitals (dashed lines denote strong, dotted lines weak mesomeric interactions).

$$I_v(i) = -\epsilon_i \quad (48)$$

On substituting hydrogen by σ -inductive alkyl groups the electronic states of allene (**11**) are only slightly perturbed thus retaining the widely spread distribution of state characteristics of the D_{2d} -chromophore ($1c$) and corresponding orbital system. Nevertheless, concerning the allenic outermost orbitals, these perturbations result in an effective reduction of symmetry which removes the degeneracies of molecular orbitals and electronic states.

In Fig. 9 an orbital diagram correlating the outermost (occupied and unoccupied) degenerate e orbitals of allene (**11**) with orbitals of corresponding symmetries in the molecules RH to give the outermost orbitals of a monosubstituted allene is displayed.

As a result of substitution the e orbitals in **11** are split into $\pi(a'')$ and $\sigma(a')$ orbitals. The σ orbitals correlating with the allenic e orbitals are usually referred to as $\bar{\pi}(a')$ orbitals (1c,22,24) (Sections III.B and III.D). Dashed lines in Fig. 9 illustrate possibilities for strong π conjugation interactions, whereas dotted lines represent weak mesomeric interactions (π -type interactions) (Section III.D).

Pe spectroscopy allows the lucid study of substituent effects on the energies of the highest energy occupied π and σ orbitals $\pi_{(1)}$ and $\bar{\pi}_{(1)}$, respectively. By symmetry (of a rigid molecular model) the corresponding orbital energies $\epsilon(\pi_{(1)})$ and $\epsilon(\bar{\pi}_{(1)})$ should be identical for allenes with a C_2 rotational symmetry (the corresponding orbitals become degenerate). The symmetry situation for both

these orbitals is comparable with that of the allenic terminal carbon atoms, that is, the symmetries of the $\pi_{(1)}$ and $\bar{\pi}_{(1)}$ orbitals (reflecting the "skeleton") are C_{2v} . Therefore, the treatment of substituent effects on $\epsilon(\pi_{(1)})$ and $\epsilon(\bar{\pi}_{(1)})$ follows the lines discussed for the ^{13}C chemical shifts of the allenic terminal atoms (Section II.C.2). The most general ansätze for the descriptions of substituent effects should have the forms given in Equations 49a and 49b.

$$- \epsilon(\pi_{(1)}) = I_v(\pi_{(1)}) = \alpha^I + \beta^I(\text{R}_1) + \beta^I(\text{R}_2) + \gamma^I(\text{R}_1, \text{R}_2) \\ + \mu^I(\text{R}_3) + \mu^I(\text{R}_4) + \nu^I(\text{R}_3, \text{R}_4) \quad (49a)$$

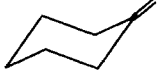
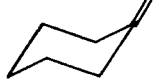
$$- \epsilon(\bar{\pi}_{(1)}) = I_v(\bar{\pi}_{(1)}) = \alpha^I + \beta^I(\text{R}_3) + \beta^I(\text{R}_4) + \gamma^I(\text{R}_3, \text{R}_4) \\ + \mu^I(\text{R}_1) + \mu^I(\text{R}_2) + \nu^I(\text{R}_1, \text{R}_2) \quad (49b)$$

In this way substituent effects of the groups R on the orbital system comprising the adjacent formal double bond in the allene ($\beta^I(\text{R})$) and those on the orbital system comprising the nonadjacent formal double bond ($\mu^I(\text{R})$) are introduced. A consequence of the preceding ansätze, (49a) and (49b), is the prediction that the sums of the ionization energies ($I_v(\pi_{(1)}) + I_v(\bar{\pi}_{(1)})$) for the constitutionally isomeric allenes, such as 1,1-dimethylallene (**2**) and 1,3-dimethylallene (**3**), should be rather different. This is borne out by experiments as can be seen from Table 11 where ionization energies of allenic hydrocarbons are summarized. A more detailed treatment of ionization energies of alkylallenes is not possible owing to the scarcity of data. Furthermore, a consistent treatment of substituent effects is impossible because the overall observable effects in pe spectroscopy of methylallenes are due to two contributions resulting from the intrinsic substituent effects of the alkyl groups and an additional contribution from the Jahn-Teller effect in these molecules (especially in methylallenes) (66).

For a rough numerical estimation of ionization energies of alkylallenes one may restrict oneself to an addition of ligand-specific parameters, the effect of the methyl group being -0.50 eV ($\beta^I(\text{Me})$) for the adjacent "double bond" orbital and -0.10 eV for the nonadjacent "double bond" ($\mu^I(\text{Me})$) ($\beta^I(\text{Et}) = -0.65$ eV; $\mu^I(\text{Et}) = -0.10$ eV). The typical value for the substituent effect $\mu^I(\text{Me}) = -0.10$ eV is also observed for $I_v(\pi_{(1)})$ in molecular systems, such as the alkenylidene-cyclohexanes **65** and **66** and the phenylallenes **16** and **38**. The methyl effect (-0.50 eV) is also observed for $I_v(\bar{\pi}_{(1)})$ in **16** and **38** or **65** and **66**, respectively.

More interesting with regard to the structure of the phenomenon and the substituent effects are the electronic excitation energies $\tilde{\nu}_{uv}$ of phenylallenes obtained from uv absorption spectra. For these systems the analysis of the lowest-energy uv bands with intensities $\epsilon \geq 10^4$ is based upon a separation of the phenylallenes into the "phenylallene chromophore" (1c,73) as the skeleton with three ligand-sites (cf. Section II.A). Therefore, the geometric situation underlying the observable effects is analogous to those used for the proton

TABLE 11
Vertical Ionization Energies of Allenic Hydrocarbons from Photoelectron
Spectroscopic Data (in eV)

Compd.	R ₁	R ₂	R ₃	R ₄	$I_v(\pi_{(1)})$	$I_v(\bar{\pi}_{(1)})$	Ref.
11	H	H	H	H	10.07	10.07	24
12	Me	H	H	H	9.33(9.57) ^a	10.06	66,(67)
3	Me	H	Me	H	9.13(9.26) ^a	9.13(9.26) ^a	66,(68)
2	Me	Me	H	H	8.95	9.86	66
61	Me	Me	Me	H	8.69(8.90) ^b	9.24	66
62	Me	Me	Me	Me	8.47	8.47	66
18	Et	H	H	H	9.22(9.42) ^a	9.96	24,(68)
63	HC≡CCH ₂	H	H	H	9.65	10.30	69
31	C ₃ H ₅	H	H	H	8.83	9.75	70
64	C ₃ H ₅	H	Me	Me	8.78	8.98	70
16	Ph	H	H	H	8.29	9.77	71
38	Ph	H	Me	H	8.15	9.15	71
65			H	H	8.80	9.56	72
66			Me	H	8.66	9.10	72
67	<i>t</i> -Bu	<i>t</i> -Bu	H	H	8.55(8.75) ^b	9.30	66

^a From electron impact data.

^b Alternative values owing to uncertainties in fixing the values for the vertical ionization energies.

chemical shifts (Section II.C.3) and also the one-bond carbon-proton coupling constants (Section II.C.4).

The particular excited state associated with the uv bands of interest of the phenylallenes correlates with ${}^1B_{1u}$ in benzene (71,73,25). It results mainly from a (electric dipole allowed) π, π^* transition. However, this excited state also contains a small, but significant admixture of the $\bar{\pi}, \bar{\pi}^*$ excitation which is essential for an understanding of the circular dichroism of phenylallenes (1c,73). (It corresponds to a mixture of the $\pi_{(1)} \rightarrow \pi_{(-1)}$ and $\bar{\pi}_{(1)} \rightarrow \bar{\pi}_{(1)}$ excitations according to the orbital diagram in Fig. 9). For convenience we term the corresponding uv absorption bands the “ π, π^* -bands.”

For the semiempirical description of the substituent effects on the π, π^* - bands of phenylallenes

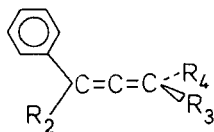


TABLE 12
Parameters for the Calculations of the UV Absorption Positions
of the π, π^* -Bands in Phenylallenes (in cm^{-1})

R	$\alpha^E(\text{R})$	$\gamma^E(\text{R})$
H	$\beta^E = 40400$	
Me	-600	-500
Ph	-1200	-1200
CN		+600
COOH		+100
MeO		-300
Cl		-1500
Br		-3100
I		-4900

one may expect Equation 50 to hold which follows from arguments given for the electron densities of the allenic hydrogen atoms (Section II.C.1; Equation 33).

$$\Delta E(\pi, \pi^*) = \beta^E + \alpha^E(\text{R}_2) + \gamma^E(\text{R}_3) + \gamma^E(\text{R}_4) \quad (50)$$

Relevant parameters are summarized in Table 12. A comparison between experimental and calculated uv absorption band positions $\tilde{\nu}_{uv}(\pi, \pi^*)$ is given in Section II.E (Table 21).

This treatment may also be applied successfully to 1,1-diphenylallenes ($\text{R}_2 = \text{Ph}$). Therefore, there arises the natural question of the justification of this finding, as a formal discussion of 1,1-diphenylallenes would suggest that both the geminal phenyl groups are equivalent. Then, one would expect a chromophore which comprises an electronic subunit with both the phenyl groups, that is, a chromophore different from that underlying the discussion of the uv spectra of phenylallenes with no geminal aryl groups. However, structural chemistry (1*b*) shows that the two geminal phenyl groups in allenes are not equivalent. One phenyl ring is twisted by about 19° relative to the allenic plane. This is comparable to the situation when a methyl group is geminal to the phenyl ring. Such a spatial orientation allows to retain the mesomeric interactions of phenylallene (16) to a large extent. The second phenyl group in 1,1-diphenylallenes, however, is twisted by about 50° (1*b*) thus reducing resonance interactions between this phenyl group and the allenic π system considerably.

Larger deviations between observed and calculated uv absorption frequencies of the π, π^* -bands in phenylallenes on the basis of Equation 50 are only found for molecules with bromo and iodo groups (Table 21). An interpretation of this finding is not straightforward. The discrepancies may be due to the inadequacy of Equation 50 which would suggest the introduction of an interaction term $\omega^E(\text{R}_3, \text{R}_4)$ into Equation 50. However, there are no physical

reasons from which the necessity of the incorporation of such pair-term may be strictly deduced. The other possibility is that the phenylallene chromophoric system undergoes some changes that depend upon the types of substituents attached to the molecular system. As we deal explicitly with excited states properties the last explanation is rather attractive. As excited electronic states are spatially much more diffuse than the electronic ground state, excited-states properties are much more sensitive to perturbations than ground-state properties.

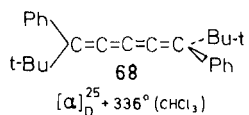
As a last remark with respect to the treatment of scalar molecular properties of allenes on the basis of a well-defined geometrophysical model it should be emphasized that there is a large variety of informations from such a model which is unexpected from an attitude that relates scalar molecular properties to functions involving more or less an addition of ligand-specific parameters. For instance, the treatments of proton chemical shifts δ_H (Equation 40), the one-bond carbon-proton coupling constants $^1\tilde{J}(^{13}\text{CH})$ (Equation 46), and the uv absorption frequencies $\Delta E(\pi, \pi^*)$ of phenylallenes (Equation 50) are all based upon a three-site skeleton which may be represented on a geometrical level by an irregular pyramid of symmetry C_s . The structures of the functions that describe the particular phenomena, however, are quite different. The analytical forms of these functions may be strictly deduced from the geometrical model in connection with the phenomenologically physical features of the effects without any reference to a particular quantum-mechanical theory.

D. Pseudoscalar Molecular Properties of Allenes

1. Molar Rotations and Optical Rotatory Dispersion

Of the molecules (with an achiral skeleton) under consideration only allenes, pentatetraenes, and ketene imines may become chiral through an appropriate arrangement of (achiral) ligands and thus offer the opportunity to investigate substituent effects on chiral (pseudoscalar) properties.

So far, there is reported no chiral ketene imine with only achiral substituents in the literature (1c). In case of pentatetraenes only one example is found in the literature (1c). It is the compound **68** (74).



For allenes, however, there exists a rather great number of studies of substituent effects on molar rotations $[\phi]_D^{25}$ measured at the wavelength of the sodium D line or optical rotatory dispersion (ORD) $[\phi]_\lambda^{25}$ ($\lambda \geq 330 \text{ nm}$) (1c,12,13). A

detailed discussion of chiroptical properties of cumulenes is given in Ref. 1c. The present subsection summarizes and specifies the results for $[\phi]_D^{25}$ from Refs. 1c, 1d, 12, 13 within the context of the consistent description of arbitrary molecular properties of allenes.

In Section II.A.2 it has been demonstrated that Equation 10a has the correct transformation properties to describe chiral properties of D_{2d} systems. However, it has been stressed that the corresponding function is "qualitatively incomplete," as it exhibits linear dependencies for constitutionally isomeric molecules.

For the allenes it has turned out that a qualitatively complete chirality function χ for the description of the optical rotations is made up additively of two components φ_1 and φ_2 (15). If χ is developed in terms of polynomials of the lowest degree in two different ligand-specific parameters $\lambda(R)$ and $\mu(R)$ the corresponding expression is given by Equation 51. With such an ansatz it is easily shown (1c) that the function χ for three constitutionally isomeric allenes (of type (a)) with four different ligands are linearly independent (cf. Fig. 4).

$$\chi(R_1, R_2, R_3, R_4) = \varphi_1(R_1, R_2, R_3, R_4) + \varphi_2(R_1, R_2, R_3, R_4) \quad (51a)$$

$$\begin{aligned} \chi(R_1, R_2, R_3, R_4) = & \epsilon_1[\lambda(R_1) - \lambda(R_2)][\lambda(R_3) - \lambda(R_4)] \\ & + \epsilon_2[\mu(R_1) - \mu(R_2)][\mu(R_2) - \mu(R_3)][\mu(R_3) - \mu(R_1)] \\ & \times [\mu(R_1) - \mu(R_4)][\mu(R_2) - \mu(R_4)][\mu(R_3) - \mu(R_4)] \end{aligned} \quad (51b)$$

In Equation 51b the $\epsilon_i = \pm 1$ ($i = 1, 2$) are sign factors that may be determined experimentally or on the basis of a quantum-mechanical theory. The μ term in Equation 51b has a special feature. It vanishes for chiral allenes with two identical ligands. For such kinds of allenes the λ component of Equation 51b represents a qualitatively complete chirality function and is, from the point of view of the general theory, the strict expression for the calculations of molar rotations of allenes.

However, on the basis of the material now being available, it has been shown (1c, 12, 13) that the molar rotations $[\phi]_D^{25}$ of arbitrarily substituted allenes may be calculated using only the λ term of Equation 51b, that is, using a "shortened" expression corresponding to the "qualitatively incomplete" function (10a). Therefore, for the predictions of molar rotations $[\phi]_D^{25}$ of allenes one only needs a set of λ -parameters which is given for a wide range of chemically interesting substituents in Table 13 (1c, 1d, 12, 13). For a consistent treatment the molar rotations should be measured in ethanol (12, 13). Rotations measured in other solvents may be related to the "ethanol standard" according to Equation 52.

$$\chi(S) = \frac{(n_D^2(S) + 2)}{(n_D^2(\text{EtOH}) + 2)} \cdot \chi(\text{EtOH}) \quad (52)$$

TABLE 13
Parameters for the Calculations of Molar Rotations at the Wavelength of the Sodium *D* Line
(in Ethanol) for Allenes (1c, 1d)

R	$\lambda(R)$	R	$\lambda(R)$	R	$\lambda(R)$
H	0	COOH	+15.4	NCO	+12.4
Me	+7.7	COOMe	+16.5	Ph ₂ PO	+31.0 ^a
Et	+12.6	COONa	+19.3	Cl ₂ PO	+27.5
<i>n</i> -Pr	+7.7	Ph	+44.3	(HO) ₂ PO	+24.5
<i>i</i> -Pr	+16.5	<i>p</i> -ClC ₆ H ₄	+44.3	F	-17.3
<i>n</i> -Bu	+12.6	<i>p</i> -BrC ₆ H ₄	+44.3	Cl	-2.5
<i>t</i> -Bu	+18.9	<i>p</i> -MeC ₆ H ₄	+42.3	Br	+9.2
<i>n</i> -Pe	+7.7	α -Np	+82.9	MeO	-21.1
<i>n</i> -Hex	+12.6	HC \equiv CC \equiv C	+37.5	MeS	+9.2
<i>n</i> -Und	+15.4	MeC \equiv CC \equiv C	+37.5	MeSO ₂	+15.8
CH ₂ OH	+9.5	HC \equiv C	+21.8	PhSO ₂	+15.8 ^b
CH ₂ OAc	+9.5	H ₂ C=CH	+25.6		
CH ₂ SMe	+7.7	COMe	+10.4		
CH ₂ COOMe	+9.5	CN	+19.1		
CH ₂ Cl	+7.5 ^c				
(CH ₂) ₂ OH	+12.6				
(CH ₂) ₃ OH	+9.3				
(CH ₂) ₄ OH	+7.7				
(CH ₂) ₄ OAc	+7.7				
(CH ₂) ₃ COOMe	+9.3				
CMe ₂ CH=CH ₂	+26.2 ^d				

^a Estimated value (1d).

^b $\lambda(\text{PhSO}_2) = \lambda(\text{MeSO}_2)$.

^c Cf. Section III.G.

^d From correlations (53a).

The fact that the λ term suffices for a numerical description of molar rotations of allenes is not quite unexpected on the basis of the following interpretation. An expression corresponding to the μ -polynomial of Equation 51b represents the qualitatively complete chirality function for a molecular class with the skeleton of the regular tetrahedron, for example, for methane derivatives with a T_d skeletal symmetry (15). On the other hand, the sum of the λ term and the μ term represents the qualitatively complete chirality function of a molecular class with the symmetry D_{2d} of an irregular tetrahedron. Then, the μ term may be viewed as some sort of contribution associated with a regular T_d symmetry of the ligand arrangement, whereas the λ term may be interpreted as a contribution which represents the deviation from the regular T_d situation (12). Owing to the cumulated double bonds the symmetry situation in allenes differs considerably from the T_d situation. Therefore, it may be assumed that the λ term describes the relevant part of the phenomenon and the μ term should be small compared with the λ term and probably negligible for numerical purposes. In

this context it should be stressed again that any algebraic theory does not claim that (qualitatively) incomplete functions for the description of molecular properties do not exist or do not suffice for the numerical treatment of observable effects. The very point is that their existence cannot be predicted a priori on the basis of any (group theoretical and/or quantum theoretical) arguments or criteria. Related to these arguments the findings that for the calculations of molar rotations of allenes the incomplete chirality function suffices must be regarded as accidental.

The incompleteness of the λ term with respect to its ability to cover effects associated with constitutional isomerism in allenes may be illustrated lucidly by the correlations (53) of the λ parameters with the ^{13}C chemical shift parameters $\sigma^C(\text{R})$ for the calculations of the ^{13}C shifts of the allenic central atoms (Equation 37) (1c,8,13).

$$\lambda(\text{R}) = -3.47 \sigma^C(\text{R}) - 0.85 \text{ for inductive groups} \quad (53a)$$

$$\lambda(\text{R}) = -3.53 \sigma^C(\text{R}) + 33.76 \text{ for mesomeric groups} \quad (53b)$$

Equation 53a is valid for σ -inductive alkyl groups and hydrogen, whereas Equation 53b is valid for mesomeric groups bonded via carbon to the allenic skeleton.

In Section II.C.2 it has been shown that an ansatz with only one-particle functions cannot describe adequately the ^{13}C chemical shifts of the allenic central atoms. The $\sigma^C(\text{R})$ parameters cannot account for the observable differences in the ^{13}C chemical shifts of constitutionally isomeric allenes. For this purpose a further contribution to the physical phenomenon described by the pair-term τ^C is necessary. This means that the λ term for the calculations of molar rotations of allenes neglects all effects associated with constitutional isomerism. In particular, the success of the λ formula reflects the fact that the molar rotations are rather independent from geminal interactions in allenes.

The semiempirical treatment of molar rotations $[\phi]_D^{25}$ of allenes on the basis of chirality functions may be easily extended to the rotatory dispersion $[\phi]_\lambda^{25}$ in the transparent region ($\lambda \geq 330$ nm) (1c,13) introducing the wavelength dependencies of the $\lambda(\text{R})$ parameters according to Equations 54a and 54b.

$$[\lambda(\text{R})]_\lambda = 0.224 [\lambda(\text{R})]_D \cdot \left(1 + \frac{1.20 \cdot 10^6}{\lambda^2} \right) \quad (54a)$$

R = H, alkyl, COOH, COOMe, COONa, NCO, $(\text{CH}_2)_n\text{X}$

$$[\lambda(\text{Ar})]_\lambda = 0.100 [\lambda(\text{Ar})]_D \cdot \left(1 + \frac{3.21 \cdot 10^6}{\lambda^2} \right) \quad (54b)$$

Ar = C_6H_5 , *p*- YC_6H_4 (Y = Me, Cl, Br)

In Equations 54a and 54b, respectively, $[\lambda(\text{R})]_D$ or $[\lambda(\text{Ar})]_D$ represent the

corresponding parameters calculated for the wavelength (589 nm) of the sodium *D* line which are given in Table 13. The wavelength dependencies of the $\lambda(\mathbf{R})$ parameters have been determined evaluating the parameters for some selected wavelengths and then using a fitting procedure based upon a two term function $a \cdot (1 + b/\lambda^2)$. Then it has turned out that, with the exceptions of the aryl groups, the wavelength dependencies of most of the substituents may be described by almost identical constants *a* and *b*.

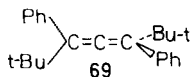
As the algebraic treatment of molecular properties outlined in Section II.A is based upon a classification of molecules according to the symmetry of the skeleton and the number of ligands attached to the skeleton, it is immediately obvious that the molar rotations of pentatetraenes should be described by an approximation ansatz corresponding to that of Equation 51*b*. Referring to pentatetraenes with two identical ligands, such as **68**, their molar rotations should be given by Equation 55 ($[\phi]_D^{25} - \bar{\chi}$),

$$\bar{\chi}(\mathbf{R}_1, \mathbf{R}_2, \mathbf{R}_3, \mathbf{R}_4) = [\bar{\lambda}(\mathbf{R}_1) - \bar{\lambda}(\mathbf{R}_2)][\bar{\lambda}(\mathbf{R}_3) - \bar{\lambda}(\mathbf{R}_4)] \quad (55)$$

involving ligand-specific parameters $\bar{\lambda}(\mathbf{R})$ for the pentatetraene D_{2d} -system. With respect to the general concepts of substituent effects, relating molecular properties to intrinsic properties of ligands, it would be interesting to investigate the influence of the very similar allene and pentatetraene skeletons on the molar rotations, the ligand set being constant. One therefore has to ask for the effect on the molar rotation of an allene when simply lengthening the cumulenenic chain. Ideally this transformation does not affect the distance between the geminal ligand-sites (1 and 2 or 3 and 4, respectively) thus retaining the structural integrity of the system.

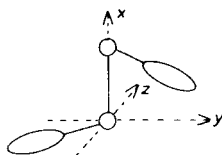
In case of molecular dipole moments (Section II.B.2) of ketene (**43**) and methylene ketene (**48**) which are related to each other by a homology (chain lengthening of the skeleton) retaining the overall symmetry it has been shown that the physical properties only differ by a scalar factor (Equation 20). The magnitude of this factor is determined by the overall length of the cumulenenic skeleton.

Corresponding arguments should hold for the molar rotations of the pentatetraene **68** and the similarly substituted allene **69**. Furthermore, it may be conjectured that the molar rotations of pentatetraenes and allenes are related to each other by a constant factor *b*: $[\phi]_D$ (pentatetraene) = *b* · $[\phi]_D$ (allene).



The factor *b* may be determined from physical theories of optical rotations (75). In particular, coupled oscillator (75), polarizability (76) or free-electron theories (77) of molar rotations in the transparent region for helical line models of molecules consisting of *N* interacting units *i, j, ...* involve relations of the

rotations to a sum of terms which include the position vectors r_{ij} from unit i to unit j . These units may be represented by spheres and/or ellipsoids.



According to all the preceding theories the order of magnitude of the molar rotation $[\phi]_D^{25}$ of the pentatetraene **68** in relation to that of the allene **69** (both having the same helicity) should approximately be given by the ratio of the distances between the ligands with respect to the x -axis (x_{13}), that is, the cumulenenic bond axis. Assuming the ligand sites to be identical with the positions of the hydrogen atoms in the parent compounds one obtains with $r_{CC}(1'2') = 1.31 \text{ \AA}$, $r_{CC}(2'3') = 1.26 \text{ \AA}$, $r_{CH} = 1.07 \text{ \AA}$, and the angle $\text{HC}_1\text{H} = 120^\circ$ (1*b*)

$$\frac{[\phi]_D(\text{pentatetraene})}{[\phi]_D(\text{allene})} \approx \frac{x_{13}(\text{pentatetraene})}{x_{13}(\text{allene})} \approx 1 + \frac{2}{3.69} r_{CC}(2'3') \approx 1.7 \quad (56)$$

On the basis of this crude model the theoretical molar rotation of the pentatetraenes should be given by Equation 57 with the parameters $\lambda(R)$ which are also used for the allenes.

$$\bar{\chi}(R_1, R_2, R_3, R_4)(\text{pentatetraenes}) = 1.7 [\lambda(R_1) - \lambda(R_2)][\lambda(R_3) - \lambda(R_4)] \quad (57)$$

Using the λ values from Table 13 one calculates for the pentatetraene **68** $\bar{\chi}_D + 1130^\circ(\text{CHCl}_3)$ which is in excellent agreement with the experimental value $[\phi]_D^{25} + 1104^\circ(\text{CHCl}_3)$ (74).

Such an agreement surely is fortuitous, as the oversimplified model is expected to predict the molar rotations of pentatetraenes to only within $\pm 50\%$. Starting from a strict quantum-theoretical interpretation of the $\lambda(R)$ -parameters for alkyl groups (Section III.G) it may be predicted that alkyl substituted pentatetraenes should exhibit rotations that are about twice as large as those of correspondingly substituted allenes. Considering all, however, one may assume that Equation 57 is a good approximation for the optical rotations of pentatetraenes.

E. Comparisons between Observed and Calculated Molecular Properties of Allenes

A comparison between experimental molecular properties of allenes and calculated values for the properties treated in Sections II.C and II.D serves two

purposes. Firstly, a data compilation of experimental spectroscopic properties of chemically interesting allenes is given which may meet the practicing organic chemist's needs. Secondly, an assessment of the scopes and limitations of the models underlying the calculations is possible which may lead to further developments and understandings. In particular, if the approximation formulas for the molecular properties are quantitatively confirmed for a number of molecules which is appreciably greater than the number of the parameters to be used, discrepancies between calculated and experimental values for certain compounds may hint at valuable chemical informations concerning conformational effects, solvent effects, specific ligand interactions, and so on. In this context the quantum-chemically determined electron densities are also viewed as "experimental" molecular properties.

For purposes of comparisons between experimental and theoretical values also regression analyses have been performed which list the slopes a and intercepts b for Equation 58 as well as the linear correlation coefficients r for the corresponding molecular property P . Also standard deviations σ_y and σ_x for the y - and x -fields are given. Then, equations of the type (58) may be used to obtain the "best" values for the corresponding molecular property.

$$P(\text{exp.}) = a\bar{P}(\text{calc.}) + b \quad (58)$$

In Tables 14 and 15 comparisons between carbon and hydrogen CNDO/S electron densities P_{CC} and P_{HH} , respectively, and the predicted (Equations 29, 30, 33) values \bar{P}_{CC} and \bar{P}_{HH} are summarized. Electron densities for monosubstituted and 1,1-disubstituted allenes have been used for the evaluations of the corresponding parameters and therefore may be obtained from Tables 4 and 5.

Correspondingly, calculated ^{13}C chemical shifts $\bar{\delta}_{C_i}$ (Equations 37 and 38) and observed values δ_{C_i} are given in Tables 16 and 17. These tables contain only allenes with substituents which appear at least in two different molecules. With the exceptions of the fluoroallenes there is an overall good agreement between calculated and observed ^{13}C chemical shifts of arbitrarily substituted allenes. Discrepancies between calculated and experimental values have also been observed for the fluoroallenes in case of their dipole moments (Section II.B.2). On the other hand, the fluoroallenes behave quite "normal," if calculated and predicted electron densities are considered (Tables 15 and 16). Larger deviations between calculated and observed chemical shifts are also found for the methoxyallenes **39** and **114**, especially for the central atoms. This means that, for instance, for the interval $\delta_{C_2} \leq 190$ ppm the parameter set given in Table 7 for the fluoro substituents is not appropriate for an adequate description of the ^{13}C chemical shifts of allenes with more than two fluoro groups. The last statement, however, does not concern the analytical forms of the ansätze for the predictions of ^{13}C chemical shifts of fluoroallenes. This shall be illustrated for

TABLE 14
Calculated CNDO/S ($P_{CC}(i')$) and Predicted ($\bar{P}_{CC}(i')$) Carbon Electron Densities of Allenes (9)

Compd.	R ₁	R ₂	R ₃	R ₄	$\bar{P}_{CC}(2')$	$P_{CC}(2')$	$\bar{P}_{CC}(1')$	$P_{CC}(1')$	$\bar{P}_{CC}(3')$	$P_{CC}(3')$
3	H	Me	Me	H	3.988	3.988	4.067	4.065	4.067	4.065
70	H	Me	COOH	H	3.917 ^a	3.918 ^a	4.030 ^a	4.026 ^a	4.078	4.079
40	H	Me	Cl	H	3.960	3.943	4.049	4.052	4.057	4.057
71	H	COOH	COOH	H	3.846 ^a	3.853 ^a	4.041 ^a	4.042 ^a	4.041 ^a	4.042 ^a
41	H	CN	Me	Me	3.963	3.956	4.064	4.071	3.989	3.987
72 ^c	H	Ph	Ph	H	3.932	3.937	4.070	4.063	4.070	4.063
38	H	Ph	Me	H	3.960	3.956	4.069	4.068	4.068	4.066
1	H	Ph	COOH	H	3.914 ^b	3.912 ^b	4.039 ^b	4.035 ^b	4.073 ^b	4.073 ^b
37	H	Ph	CN	H	3.889 ^a	3.900 ^a	4.032 ^a	4.026 ^a	4.079 ^a	4.079 ^a
36	H	Ph	Cl	H	3.909	3.913	4.033	4.032	4.053	4.058
39	H	Ph	MeO	H	3.932	3.934	4.044	4.042	4.044	4.047
73	H	COOH	Ph	Me	3.989	3.986	4.071	4.067	3.960	3.957
10	H	F	F	H	3.944 ^b	3.941 ^b	4.082 ^b	4.087 ^b	3.996 ^b	3.990 ^b
74	F	F	F	F	4.112	4.116	3.741	3.741	3.741	3.741
					4.282	4.288	3.382	3.385	3.382	3.385

^a *s-cis* conformation.

^b *s-trans* conformation.

^c This work.

$$P_{CC}(i') = 0.9981 \bar{P}_{CC}(i') + 0.0072$$

$$r = 0.9994$$

$$\sigma_y = 0.1367$$

$$\sigma_x = 0.1369$$

TABLE 15
 Calculated CNDO/S ($P_{HH}(i)$) and Predicted ($\tilde{P}_{HH}(i)$) Hydrogen Electron
 Densities of Allenes (9)

Compd.	$\tilde{P}_{HH}(1)$	$P_{HH}(1)$	$\tilde{P}_{HH}(4)$	$P_{HH}(4)$
2 ^c	0.977	0.977		
7 ^d			0.980	0.979
3	0.972	0.971	0.972	0.971
70	0.954 ^a	0.954 ^a	0.973 ^a	0.972 ^a
40	0.963	0.962	0.958	0.957
71	0.956 ^a	0.956 ^a	0.956 ^a	0.956 ^a
41	0.960	0.959		
72 ^d	0.969	0.970		
38	0.973	0.972	0.968	0.967
1	0.957 ^b	0.960 ^b	0.957 ^b	0.956 ^b
	0.955 ^a	0.957 ^a	0.969 ^a	0.971 ^a
37	0.957	0.959	0.950	0.951
36	0.964	0.965	0.960	0.955
39	0.976	0.976	0.953	0.952
73	0.963	0.962		
10	0.967	0.967	0.967	0.967

^a *s-cis* form.

^b *s-trans* form.

^c From Ref. 71.

^d This work.

$$P_{HH}(i) = 0.9832 \tilde{P}_{HH}(i) + 0.0159$$

$$r = 0.9824$$

$$\sigma_y = 0.0078$$

$$\sigma_x = 0.0078$$

simplicity for the ^{13}C chemical shifts of central atoms of 1,3-disubstituted allenes. For this special case the desired ansatz for the description of the molecular property corresponds to a series expansion in one independent parameter $\sigma(\text{R})$ (the substituent constant). One then chooses a suitable origin for the expansion such that the first order of the expansion suffices for an adequate description of the molecular property under investigation. In most cases the origin is identical with the value for the unsubstituted compound, that is, the parent molecule (allene (11)). In general, $\sigma(\text{R})$ is taken as an undefined element and one does not know the physical quality that is represented by $\sigma(\text{R})$. Therefore, one is not able to choose with certainty a center of reference (an origin for the expansion in $\sigma(\text{R})$) such that the linear expression in $\sigma(\text{R})$ for arbitrary ligands R is a good approximation. This is illustrated in Fig. 10, where for simplicity the relation between the ^{13}C chemical shifts and the variable $\sigma(\text{R})$ is given as a polynomial ($\delta_{C_2} = \sum_{i=0}^n \rho_i \cdot \sigma^i(\text{R})$). Then, we see that, for instance, for the interval $\sigma_2 \leq \sigma(\text{R}) \leq \sigma_1$ around the point ρ_0 we can substitute the actual curve (resembling a third-degree polynomial) to a good approximation by a straight line $\tilde{\delta}_{C_2}$, i.e.

TABLE 16
 Calculated ($\bar{\delta}_{C_2}$) and Experimental (δ_{C_2}) ^{13}C Chemical Shifts^a of the
 Central Atoms of Allenes (in ppm) (8)

Compd.	R ₁	R ₂	R ₃	R ₄	$\bar{\delta}_{C_2}$	δ_{C_2}
12	Me	H	H	H	209.4	209.4
2	Me	Me	H	H	206.7	207.2
3	Me	H	Me	H	206.2	206.5
61	Me	Me	Me	H	203.5	203.5
62	Me	Me	Me	Me	200.8	200.0
18	Et	H	H	H	208.8	208.8
75	Et	H	Et	H	205.0	204.0
7	Et	Me	H	H	206.1	206.3
8	Et	H	Me	H	205.6	204.9 ^b
76	<i>i</i> -Pr	H	H	H	207.8	207.8
60	<i>n</i> -Pr	H	H	H	209.5	209.5 ^c
22	COOH	H	H	H	217.7	217.7
23	COOMe	H	H	H	217.5	216.1 ^d
71	COOH	H	COOH	H	222.8	221.1
78	COOMe	H	COOMe	H	222.4	219.7
79	COOMe	Me	H	H	215.2	214.6
80	COOMe	Et	H	H	214.6	213.8
81	Me	H	COOMe	Me	212.0	211.0
82	Et	H	COOMe	Et	210.8	209.6
83	Me	H	COOMe	Et	211.4	210.5
84	Et	H	COOMe	Me	211.4	210.1
85	Et	Me	COOMe	H	210.5	210.2 ^e
86	Et	Me	COOMe	Et	207.1	207.1
87	<i>i</i> -Pr	H	COOH	Et	210.0	209.9
88	CMe ₂ CH=CH ₂	H	H	H	204.8	204.8 ^f
89	CMe ₂ CH=CH ₂	H	Me	H	201.6	203.8 ^f
90	CMe ₂ CH=CH ₂	H	Me	Me	198.9	200.4 ^f
91	CMe ₂ CH=CH ₂	H	Et	Me	198.3	199.7 ^f
92	CMe ₂ CH=CH ₂	H	H	<i>n</i> -Pr	201.7	202.9 ^f
16	Ph	H	H	H	209.6	209.6
59	Ph	Me	H	H	209.1	209.1
38	Ph	H	Me	H	206.4	206.2
93	Ph	Me	Ph	H	206.1	206.6 ^e
94	Ph	Ph	Ph	Ph	208.4	208.3
1	Ph	H	COOH	H	214.7	216.3
73	Ph	Me	COOH	H	214.2	213.9
77	Ph	H	COOH	Me	212.2	212.1
95	Ph	Et	COOH	H	213.8	215.2
96	Ph	H	COOH	Et	211.8	211.8
97	Ph	Me	COOH	Et	211.3	210.8
98	Ph	Et	COOH	Me	211.5	212.6
99	Ph	Et	COOH	Et	210.9	212.1
100	Ph	Ph	COOH	H	214.6	214.5
101	Ph	Me	COOMe	H	214.0	214.0
102	Ph	H	COOMe	Me	212.2	212.4

TABLE 16
 Calculated ($\bar{\delta}_{C_2}$) and Experimental (δ_{C_2}) ^{13}C Chemical Shifts^a of the
 Central Atoms of Allenes (in ppm) (8)

Compd.	R ₁	R ₂	R ₃	R ₄	$\bar{\delta}_{C_2}$	δ_{C_2}
103	Ph	Et	COOMe	H	213.6	213.8
104	Ph	H	COOMe	Et	211.6	211.9
105	Ph	Me	COOMe	Me	211.7	211.5
106	Ph	Et	COOMe	Et	210.7	210.5
107	Ph	Et	COOMe	Me	211.3	211.2
108	Ph	Me	COOMe	Et	211.1	210.8
109	Ph	COOMe	Et	Me	210.1	209.1
110	Ph	Ph	COOMe	Ph	214.5	214.5
19	MeO	H	H	H	201.1	201.1
111	MeO	Me	Et	H	192.7	192.7 ^e
39	MeO	H	Ph	H	198.1	194.7
112	MeO	Et	Ph	H	192.4	192.4
113	MeO	<i>i</i> -Pr	Ph	H	193.0	192.0
114	MeO	<i>i</i> -Pr	Ph	Me	192.5	188.8
30	Cl	H	H	H	207.4	207.4
115	Cl	H	Et	Me	199.9	199.1
13	Br	H	H	H	206.9	206.9
116	Br	H	Et	Me	201.1	199.1
20	MeS	H	H	H	206.9	206.9
117	MeS	H	Me	H	203.7	202.0
118	MeS	Me	H	H	203.6	203.6
15	F	H	H	H	199.3	199.3 ^g
10	F	H	F	H	186.0	175.6 ^g
9	F	F	H	H	191.5	191.5 ^g
119	F	F	F	H	178.2	148.9 ^g
74	F	F	F	F	170.4	117.2 ^g

^a In general measured in CDCl₃.

^b This work.

^c Ref. 18.

^d Ref. 54.

^e Ref. 57.

^f Ref. 50.

^g From Ref. 19 based upon $\delta_{C_2} = 212.6$ ppm for **11**.

$$\delta_{C_2} = 1.0039 \bar{\delta}_{C_2} - 1.0560$$

$$r = 0.9877 \text{ (omitting the fluoroallenes)}$$

$$\sigma_y = 6.6950$$

$$\sigma_x = 6.5873$$

for the interval around ρ_0 we can interpolate linearly ($\bar{\delta}_{C_2} = \rho_0^C + \rho_1 \cdot \sigma(R)$; $\rho_0 = \rho_0^C$ being the intercept and ρ_1 the slope, for example, $\rho_1 \cdot \sigma(R) = \sigma^C(R)$).

Now we see that for the interval $\sigma_3 \leq \sigma(R) \leq \sigma_2$ we also may interpolate linearly. However, the slope and the intercept of the corresponding straight line are different from the former ones. Consequently, linear approximations of $\bar{\delta}_{C_2}$

TABLE 17
 Calculated ($\bar{\delta}_{C_V}$) and Experimental (δ_{C_V}) ^{13}C Chemical Shifts^a of the
 Terminal Atoms of Allenes (in ppm) (8)

Compd.	$\bar{\delta}_{C_V}$	δ_{C_V}	$\bar{\delta}_{C_Y}$	δ_{C_Y}
12	84.2	84.2	73.4	73.4
2	93.9	93.9	72.4	72.6
3	84.1	84.9	84.1	84.9
61	93.8	94.1	83.1	83.5
62	92.8	91.6	92.8	91.6
18	91.6	91.6	74.7	74.7
75	92.8	93.2	92.8	93.2
7	100.2	100.2	74.4	74.4
8	91.5	92.2 ^b	85.4	86.1 ^b
76	97.8	97.8	76.2	76.2
60	89.9	89.9 ^c	74.6	74.6 ^c
22	88.1	88.1	80.0	80.0
23	86.3	87.4 ^d	79.0	79.2 ^d
71	94.0	94.0	94.0	94.0
78	91.8	92.1	91.8	92.1
79	95.5	95.5	77.9	77.9
80	101.9	101.9	79.2	79.3
81	88.6	88.7	96.4	95.0
82	97.3	97.3	103.1	103.1
83	89.9	90.2	101.7	101.8
84	95.0	95.7	96.7	96.3
85	107.8	106.5 ^e	87.2	87.6 ^e
86	105.9	106.1	102.8	102.7
87	103.2	103.1	103.3	103.3
88	99.7	99.7 ^f	76.8	76.8 ^f
89	99.6	100.4 ^f	87.4	87.8 ^f
90	98.6	99.1 ^f	97.2	97.1 ^f
91	100.6	101.0 ^f	103.5	103.4 ^f
92	100.8	101.0 ^f	93.2	93.3 ^f
16	94.0	94.0	78.8	78.8
59	100.0	100.0	76.7	76.7
38	93.9	94.2	89.5	89.5
93	105.3	104.3 ^e	97.2	96.6 ^e
94	112.5	112.5	112.5	112.5
1	99.9	99.0	93.4	91.4
73	105.9	104.9	91.3	90.0
77	98.1	98.6	98.9	99.1
95	113.0	113.0	93.1	91.2
96	99.4	98.4	106.5	106.3
97	105.4	104.6	103.8	104.0
98	111.2	111.3	102.1	98.6
99	112.5	112.9	105.6	105.5
100	113.5	113.5	93.0	91.3
101	105.5	105.5	89.5	89.5
102	98.4	97.4	100.8	99.1

TABLE 17
 Calculated ($\bar{\delta}_{C_1}$) and Experimental (δ_{C_1}) ^{13}C Chemical Shifts^a of the
 Terminal Atoms of Allenes (in ppm) (8)

Compd.	$\bar{\delta}_{C_1}$	δ_{C_1}	$\bar{\delta}_{C_3}$	δ_{C_3}
103	112.6	112.6	91.3	91.3
104	99.7	99.0	107.2	105.9
105	104.4	103.7	98.7	97.0
106	112.8	112.4	106.9	105.7
107	111.5	110.9	100.5	99.7
108	105.7	105.4	105.1	103.8
109	106.4	106.9	101.3	102.7
110	114.8	114.8	105.3	105.3
19	123.0	123.0	91.4	91.4
111	135.3	135.3	104.5	104.5
39	128.3	126.1	111.9	109.0
112	139.6	139.7	108.2	108.2
113	143.3	143.4	109.1	108.4
114	141.3	141.0	115.1	114.1
30	88.7	88.7	84.8	84.4
115	89.6	87.9	111.5	113.9
13	71.9	71.9	83.1	83.1
116	73.0	71.8	109.8	113.2
20	88.5	88.5	80.9	80.9
117	88.4	90.3	91.6	93.1
118	99.9	99.9	80.1	80.1
15	128.5	128.5	92.6	92.6 ^g
10	147.6	130.9	147.6	130.9 ^g
9	154.9	154.9	103.5	103.5 ^g
119	174.0	144.5	158.5	132.5 ^g
74	184.9	139.3	184.9	139.3 ^g

^a In general measured in CDCl_3 .

^b This work.

^c Ref. 18.

^d Ref. 54.

^e Ref. 57.

^f Ref. 50.

^g Based upon $\delta_{C_1} = \delta_{C_3} = 73.5$ ppm for **11**.

$$\delta_{C_1} = 0.9921 \bar{\delta}_{C_1} + 0.6150$$

$$r = 0.9980$$

$$\sigma_y = 13.6240$$

$$\sigma_x = 13.7050$$

in ligand-specific parameters for the interval $[\sigma_3, \sigma_2]$ have to use other values $\bar{\sigma}^C(\text{R})$ for the substituent constants related to this last interval ($\bar{\delta}_{C_2} = \bar{\rho} + \rho_1 \cdot \bar{\sigma}(\text{R}) = \bar{\rho}^C + \bar{\sigma}^C(\text{R})$). Furthermore, one sees that around the value $\sigma(\text{R}) = \sigma_2$ both approximations $\bar{\delta}_{C_2}$ and $\bar{\delta}_{C_2}$, respectively, are equivalent in that they

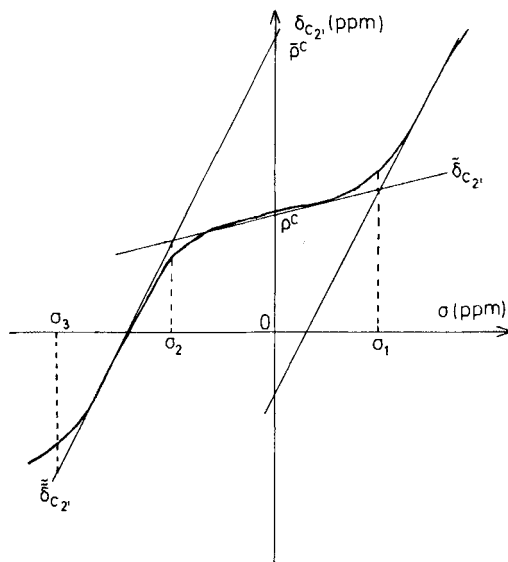


Figure 10 Approximations for a polynomial which represents the ^{13}C chemical shifts of the allenic central atoms by different straight lines for different intervals.

both are not well suited for the calculations of ^{13}C chemical shifts of the allenic central atoms.

Based upon these qualitative arguments one may suggest that the ^{13}C chemical shifts of allenes with more than one fluoroatom should be described by Equations 58a and 59 which correspond concerning their analytical forms to the Equations 37 and 38.

$$\bar{\delta}_{C_c} = \bar{\rho}^C + \sum_{i=1}^4 \bar{\sigma}^C(R_i) + \bar{\tau}^C(R_1, R_2) + \bar{\tau}^C(R_3, R_4) \quad (58a)$$

$$\begin{aligned} \bar{\tau}_{C_i} = & \bar{\alpha}^C + \bar{\beta}^C(R_1) + \bar{\beta}^C(R_2) + \bar{\gamma}^C(R_1, R_2) \\ & + \bar{\mu}^C(R_3) + \bar{\mu}^C(R_4) + \bar{\nu}^C(R_3, R_4) \end{aligned} \quad (59)$$

With the following parameters involving only fluoroatoms (and $\bar{\sigma}^C(\text{H}) = 0$; $\bar{\tau}^C(\text{F}, \text{H}) = 0$) the ^{13}C chemical shifts of the multiply substituted fluoroallenes (**9**, **10**, **74**, **119**) may be reproduced (Table 18).

In Table 19 calculated (Equations 40) and observed ^1H chemical shifts of allenes are summarized. There is an overall good agreement between predicted and experimental values. The results in Table 20 show that Equation 46 is suited for the description of one-bond carbon-proton spin-spin coupling constants of allenes. Only for the bromoallene **116** there is a larger deviation between the

TABLE 18
 Calculated ($\bar{\delta}_{C_i}$) (Equations 58 and 59) and Experimental^a (δ_{C_i}) ¹³C Chemical Shifts of
 Fluoroallenes (in ppm)

Compd.	$\bar{\delta}_{C_2}$	δ_{C_2}	$\bar{\delta}_{C_1}$	δ_{C_1}	$\bar{\delta}_{C_3}$	δ_{C_3}
10	175.6	175.6	130.9	130.9	130.9	130.9
9	191.5	191.5	154.9	154.9	103.5	103.5
119	146.5	148.9	137.7	144.5	132.5	132.5
74	117.4	117.4	139.3	139.3	139.3	139.3

^a From Ref. 19.

calculated and observed couplings which may be due to the neglect of the interaction π^J between the ligands at the different terminal carbon atoms of the allenic system.

Equation 50 for the calculation of the uv absorption spectral positions of the π, π^* -bands of phenylallenes (Table 21) seems to be of lower quality than all the other ansätze for the predictions of scalar molecular properties of allenes. On the other hand, Equation 50 is of the simplest analytical form for this particular phenomenon. It exhibits a pure additivity in ligand-specific parameters. Therefore, taking also interaction terms into account could improve the agreement between calculated and observed values. However, significant interactions are only observed for molecules (**166**, **167**) with geminal heavy halogen atoms (Br, Br; Br, I). Therefore, it seems that ansatz (50) is adequate for the description of the π, π^* -band positions of phenylallenes in general, but that for geminal bromo and iodo atoms there are additional contributions to the physical effect.

As an example for the calculation of pseudoscalar molecular properties of allenes in Table 22 calculated and experimental molar rotations at the wavelength of the sodium *D* line are given. Concerning the range of the numerical values for the variously substituted allenes there is a striking difference compared with the numerical values for scalar properties.

In case of scalar molecular properties the variation (in terms of the standard deviations) is of the order of a typical ("average") substituent constant (σ), whereas for the particular pseudoscalar molecular property it is related to the square of an average value of the substituent constant (λ^2). This follows from Equation 51. For the calculation of the linear regression $[\phi]_D/\chi$ in Table 22 the compounds **137** and **138** have been omitted, as in these cases solvent and conformational effects influence the experimental rotations (1c, 13). For **96** and **135** the values in acetonitrile (13) have been used.

As a summary it may be stated that strict methods of symmetry are powerful for the quantitative treatment of various scalar and pseudoscalar molecular properties of allenes, not only for some model systems, but for chemically interesting and complex molecules.

TABLE 19
 Calculated ($\bar{\delta}_H$) and Experimental (δ_H) ^1H Chemical Shifts^a of Allenic Hydrogen Atoms
 (in ppm) (10)

Compd.	R ₁	R ₂	R ₃	R ₄	$\bar{\delta}_{H_1}$	δ_{H_1}
12	H	Me	H	H	4.94	4.94
					4.50	4.50 ^b
2	H	H	Me	Me	4.40	4.40
18	H	Et	H	H	5.03	5.03
					4.55	4.55 ^b
7	H	H	Et	Me	4.51	4.51
60	H	<i>n</i> -Pr	H	H	4.96	4.96
					4.60	4.60 ^b
76	H	<i>i</i> -Pr	H	H	5.12	5.12
					4.67	4.67 ^b
120	H	<i>t</i> -Bu	H	H	5.19	5.19
					4.74	4.74 ^b
121	H	H	<i>t</i> -Bu	Me	4.56	4.56
122	H	CH ₂ CH ₂ OH	H	H	5.13	5.13
					4.67	4.67
24	H	CH ₂ OH	H	H	5.30	5.30
					4.85	4.85 ^b
23	H	COOMe	H	H	5.64	5.64
					5.23	5.23
79	H	H	COOMe	Me	5.00	5.00
80	H	H	COOMe	Et	5.14	5.14
22	H	H	COOH	H	5.64	5.64
					5.23	5.23 ^b
123	H	H	COOH	Me	5.15	5.15
124	H	H	COOH	Et	5.25	5.25
125	H	CHO	H	H	5.67	5.67
					5.27	5.27 ^b
126	H	H	CHO	Me	5.21	5.21
14	H	CN	H	H	4.97	4.97
					5.03	5.03 ^b
16	H	Ph	H	H	6.03	6.03
					5.10	5.10 ^b
59	H	H	Ph	Me	4.99	4.99
103	H	COOMe	Ph	Et	5.96	5.96
127	H	Ph	Ph	Ph	6.65	6.65
19	H	MeO	H	H	6.43	6.43
					5.42	5.42 ^b
128	H	H	MeO	Et	5.32	5.32
30	H	Cl	H	H	6.00	6.00
					5.14	5.14 ^b
13	H	Br	H	H	5.93	5.93
					4.93	4.93 ^b
129	H	I	H	H	5.69	5.69
					4.48	4.48 ^b
130	H	Cl ₂ P	H	H	6.25	6.25
					5.55	5.55 ^b

TABLE 19
 Calculated ($\bar{\delta}_H$) and Experimental (δ_H) ^1H Chemical Shifts^a of Allenic Hydrogen Atoms
 (in ppm) (10)

Compd.	R ₁	R ₂	R ₃	R ₄	$\bar{\delta}_{H_1}$	δ_{H_1}
3	H	Me	Me	H	4.77	4.89
75	H	Et	Et	H	4.91	5.10
81	H	Me	COOEt	Me	5.27	5.35
83	H	Me	COOEt	Et	5.35	5.51
84	H	Et	COOEt	Me	5.36	5.43
85	H	COOEt	Et	Me	5.48	5.45
82	H	Et	COOEt	Et	5.44	5.54
131	H	<i>i</i> -Pr	COOEt	Et	5.80	5.50
132	H	<i>i</i> -Pr	COOEt	Me	5.16	5.39
133	H	COOEt	Me	Me	5.37	5.30
71	H	COOH	COOH	H	6.20	6.21
134	H	Me	COOH	Me	5.42	5.50
135	H	Me	COOH	Et	5.52	5.51
136	H	Et	COOH	Me	5.51	5.63
137	H	Et	COOH	Et	5.61	5.72
87	H	<i>i</i> -Pr	COOH	Et	5.70	5.60
138	H	COOH	Et	Me	5.48	5.37
139	H	CH ₂ CH ₂ OH	Me	Me	4.84	4.89 ^c
140	H	CH ₂ OH	<i>n</i> -Pr	H	5.23	5.31 ^d
141	H	CH ₂ OH	Et	Me	5.14	5.31 ^{b,d}
38	H	Ph	Me	H	5.05	5.29 ^d
72	H	Ph	Ph	H	5.84	6.03
1	H	Ph	COOH	H	5.37	5.47 ^b
73	H	COOH	Ph	Me	6.46	6.43
95	H	COOH	Ph	Et	6.59	6.65
100	H	COOH	Ph	Ph	6.07	6.00 ^b
77	H	Ph	COOH	Me	5.96	5.88
96	H	Ph	COOH	Et	5.94	5.97
101	H	COOEt	Me	Ph	6.26	6.15
104	H	Ph	COOEt	Et	6.51	6.58
93	H	Ph	Ph	Me	6.61	6.63
142	H	Ph	Me	Me	5.96	5.84
143	H	Me	CHO	Me	6.44	6.43
41	H	CN	Me	Me	6.35	6.46
144	H	CN	Et	Me	5.76	5.93
145	H	CN	<i>t</i> -Bu	Me	5.38	5.56
146	H	H	HC=CH ₂	Me	4.76	4.90
112	H	Ph	MeO	Et	4.87	5.10
147	H	MeO	Et	H	4.94	5.17
148	H	MeO	<i>n</i> -Pr	H	4.82	4.82
					6.73	6.60
					6.31	6.59
					5.78	5.86 ^b
					6.36	6.59
					5.71	5.79 ^b

TABLE 19
Calculated ($\bar{\delta}_H$) and Experimental (δ_H) ^1H Chemical Shifts^a of Allenic Hydrogen Atoms
(in ppm) (10)

Compd.	R ₁	R ₂	R ₃	R ₄	$\bar{\delta}_{H_1}$	δ_{H_1}
39	H	MeO	Ph	H	6.86	7.06
					6.78	6.94
40	H	Cl	Me	H	5.83	5.93
					5.41	5.53 ^b
115	H	Cl	Et	Me	5.84	5.78
149	H	Cl	<i>t</i> -Bu	Me	5.91	5.90
150	H	Cl	Ph	Ph	6.62	6.42
151	H	Me	Br	H	5.86	5.91
					5.20	5.32 ^b
152	H	Br	Me	Me	5.66	5.85
116	H	Br	Et	Me	5.73	5.90
153	H	Br	CH ₂ Br	H	6.21	6.21
					5.67	5.67 ^b
154	H	Br	<i>t</i> -Bu	Me	5.84	5.83
155	H	Br	Ph	Ph	6.55	6.39
156	H	Br	Ph	H	6.36	6.20
					6.29	6.20
157	H	Br	Ph	Me	6.18	6.15
158	H	Br	CH ₂ OH	H	6.11	6.21
					5.56	5.67 ^b
159	H	I	Me	H	5.52	5.60
					4.75	5.00 ^b
160	H	Cl ₂ P	Me	Me	5.98	6.27

^a Usually measured in CCl₄.

^b δ_{H_4} .

^c Ref. 59.

^d Ref. 55a using the proton chemical shifts of *n*-PrCH=C=CHCH₂OH and *n*-PrCH=C=CDCH₂OH.

^e Ref. 55b.

$$\delta_H = 0.9790 \bar{\delta}_H + 0.1530$$

$$r = 0.9857$$

$$\sigma_y = 0.6033, \sigma_x = 0.6075$$

F. Correlations of Substituent Effects in Allenes with Those in Ethylenes, Benzenes, and Related Compounds

The one-particle functions used for the approximation ansätze for the calculations of molecular properties of allenens according to the algebraic model are (in almost every case) experimental values of the corresponding substituent effects, that is, differences between the observed properties *P* for substituted allenens RHC=C=CH₂ (or R₁R₂C=C=CH₂) and the corresponding values for allene H₂C=C=CH₂. Therefore, empirical correlations of molecular

TABLE 20
 Calculated (${}^1\tilde{J}({}^{13}\text{CH})$) and Experimental^a (${}^1J({}^{13}\text{CH})$) One-Bond Carbon-Proton Coupling
 Constants of Allenes (in Hz)

Compd.	R ₁	R ₂	R ₃	R ₄	${}^1\tilde{J}({}^{13}\text{CH})$	${}^1J({}^{13}\text{CH})$
2	H	H	Me	Me	166.8	166 ^b
8	H	Et	Me	H	156.3	156.3
					155.7	155.7 ^c
38	H	Ph	Me	H	164.3	164.5
					160.8	162.7 ^c
59	H	H	Ph	Me	168.5	168.0
124	H	H	COOH	Et	167.4	166.1
135	H	Me	COOH	Et	159.1	157.8
137	H	Et	COOH	Et	157.2	159.0
96	H	Ph	COOH	Et	159.2	160.8
1	H	Ph	COOH	H	166.3	166.3
					170.3	172.3 ^c
71	H	COOH	COOH	H	175.9	175.0
73	H	COOH	Ph	Me	168.6	170.2
104	H	Ph	COOMe	Et	159.2	155.4
80	H	H	COOMe	Et	167.4	167.5
102	H	Ph	COOMe	Me	161.7	163.8
84	H	Et	COOMe	Me	159.7	162.1
116	H	Br	Et	Me	209.1	213.2
23	H	COOMe	H	H	172.5	172.5
					171.6	171.6 ^c
18	H	Et	H	H	158.0	158.0
					164.0	164.0
16	H	Ph	H	H	159.9	159.9
					163.0	163.0 ^c
13	H	Br	H	H	213.0	213.0
					167.0	167.0 ^c

^a In CDCl₃, the values for the multiply substituted Allenes are from this work, the experimental conditions are described in Ref. 54a.

^b Ref. 78.

^c ${}^1J({}^{13}\text{C}_3\text{H}_4)$.

$${}^1J({}^{13}\text{CH}) = 0.9916 {}^1\tilde{J}({}^{13}\text{CH}) + 1.5883$$

$$r = 0.9926$$

$$\sigma_y = 11.0114$$

$$\sigma_x = 11.0228$$

properties of Allenes with those in related molecules may be used to estimate unknown substituent constants for allenic systems and thus may be used to estimate properties of Allenes which until now have not been reported in the literature.

Usually molecular properties of Allenes $\text{RHC}=\text{C}=\text{CH}_2$ or $\text{R}_1\text{R}_2\text{C}=\text{C}=\text{CH}_2$, respectively, are compared with those in correspondingly substituted ethylenes, benzenes, acetylenes, and carbonyl compounds (9,17,22-

TABLE 21
 Calculated ($\Delta\bar{E}(\pi,\pi^*)$) and Experimental ($\bar{\nu}(\pi,\pi^*)$) UV Absorption Positions^a of the π,π^*
 Bands in Phenylallenes $\text{PhR}_2\text{C}=\text{C}=\text{CR}_3\text{R}_4$ (in cm^{-1})

Compd.	R ₂	R ₃	R ₄	$\Delta\bar{E}(\pi,\pi^*)$	$\bar{\nu}(\pi,\pi^*)$	Ref.
16	H	H	H	40400	40400	71
59	Me	H	H	39800	39800	71
38	H	Me	H	39900	39900	71
72	H	Ph	H	39200	39200	80,1c
35	Ph	H	H	39200	39200	81
1	H	COOH	H	40500	40500	73
36	H	Cl	H	38900	38900	25
156	H	Br	H	37300	37300	82
161	H	I	H	35500	35500	83
100	Ph	COOH	H	39300	40000 ^b	84
162	Ph	COOH	Ph	38100	38000	85
127	Ph	Ph	H	38000	38500 ^c	86
163	Ph	Me	Me	38200	38600	— ^d
72	Me	COOH	H	39400	41000	73
77	H	COOH	Me	40000	40500	73
157	Me	Br	H	36700	36900	79
150	Ph	Cl	H	37700	37500	87
155	Ph	Br	H	36100	35600	87
164	Ph	I	H	34300	33200	87
165	Ph	Cl	Br	34600	35300	87
166	Ph	Br	Br	33000	34500	87
167	Ph	I	Br	31200	33700	87

^a Generally measured in ethanol or methanol.

^b The synthesis of **100** is described in Ref. 84, the uv spectrum in ethanol is from this work.

^c In *n*-heptane.

^d This work.

$$\bar{\nu}(\pi,\pi^*) = 0.8871 \Delta\bar{E}(\pi,\pi^*) + 4543$$

$$r = 0.9541$$

$$\sigma_y = 2416, \sigma_x = 2599$$

25,31,32,54,65,80). In Table 23 a summary of linear correlations between molecular properties of allenes, ethylenes, benzenes, and carbonyl compounds is given. Generally, these correlations are only valid for mono- and 1,1-disubstituted allenes with a mirror plane symmetry, so that one can strictly distinguish π and σ electronic states of the molecules. Furthermore, it may be expected that such kinds of correlations are only valid for molecules with comparable rotamer populations, i.e. comparable spatial ligand arrangements (Section II.B).

A general shortcoming of such data fitting by regression analyses is the fact that interesting effects related to notable differences in the substituent effects in the various molecular classes may be buried. One such particular example concerns the uv absorption position of the π,π^* bands in phenylallenes (**16**) and

TABLE 22
 Calculated (χ) and Experimental ($[\phi]_D^{25}$) Molar Rotations of Allenes Having the (S)
 Configuration^a (in deg) (1c)

Compd.	R ₁	R ₂	R ₃	R ₄	χ	$[\phi]_D^{25}$	Solvent
3	Me	H	Me	H	+62.3	+53.3	neat
72	Ph	H	Ph	H	+1962	+1958	EtOH
1	Ph	H	COOH	H	+675	+673	EtOH
73	Ph	Me	COOH	H	+564	+515	EtOH
95	Ph	Et	COOH	H	+488	+496	EtOH
168	Ph	Me	COOH	Me	+282	+280	EtOH
99	Ph	Et	COOH	Et	+88.8	+88.8	EtOH
98	Ph	Et	COOH	Me	+244	+253	EtOH
97	Ph	Me	COOH	Et	+102	+103	EtOH
77	Ph	H	COOH	Me	+342	+374	EtOH
96	Ph	H	COOH	Et	+124	+157	EtOH
					+124	+117	MeCN
106	Ph	Et	COOMe	Et	+124	+124	EtOH
107	Ph	Et	COOMe	Me	+279	+300	EtOH
108	Ph	Me	COOMe	Et	+143	+154	EtOH
169	Ph	Et	COONa	Et	+212	+211	EtOH
170	Ph	Et	COONa	Me	+368	+354	EtOH
171	Ph	Me	COONa	Et	+256	+249	EtOH
138	Et	Me	COOH	H	+77.7	+124	CHCl ₃
135	Me	H	COOH	Et	+21.6	+34.4	EtOH
					+21.6	+25.7	MeCN
136	Et	H	COOH	Me	+97.0	+100.0	EtOH
137	Et	H	COOH	Et	+35.3	+74.9	EtOH
134	Me	H	COOH	Me	+59.3	+63.5	EtOH
172	<i>n</i> -Hex	H	COOH	H	+194	+244 ^b	
173	Me	H	COOH	<i>n</i> -Bu	+45.6 ^c	+47.2	CHCl ₃
85	Et	Me	COOMe	H	+83.3	+111	CHCl ₃
174	Me	H	CH ₂ OH	H	+72.4	+76.0	MeOH
175	Me	H	CH ₂ CH ₂ OH	H	+97.0	+84.0	MeOH
176	<i>n</i> -Und ^c	H	CH ₂ CH ₂ OH	H	+194	+194	neat
177	<i>n</i> -Und ^c	H	(CH ₂) ₃ COOMe	H	+143	+139	EtOH
178	CH ₂ OAc	H	(CH ₂) ₃ COOMe	H	+91.0	+84.9	CH ₂ Cl ₂
179	CH ₂ OAc	H	(CH ₂) ₄ OAc	H	+75.3	+86.0	CH ₂ Cl ₂
180	HC≡CC≡C	H	CH ₂ OH	H	+366	+448	CH ₂ Cl ₂
181	HC≡CC≡C	H	CH ₂ CH ₂ OH	H	+473	+475	EtOH
182	HC≡CC≡C	H	(CH ₂) ₃ OH	H	+349	+350	EtOH
183	HC≡CC≡C	H	(CH ₂) ₄ OH	H	+289	+288	EtOH
184	MeC≡CC≡C	H	CH ₂ CH ₂ OH	H	+473	+496	EtOH
185	HC≡CC≡C	H	CH ₂ COOMe	H	+356	+456	EtOH
186	<i>p</i> -MeC ₆ H ₄ SO ₂	H	Me	H	+125	+150	CH ₂ Cl ₂
187	Ph ₂ PO	H	Ph	H	+1373	+1620 ^b	

^a Enumeration of ligand sites according to Fig. 1.

^b Unknown solvent; the values for χ correspond to those in ethanol as the solvent.

^c *n*-Und = CH₃(CH₂)₁₀.

$$[\phi]_D^{25} = 1.0482 \chi + 0.0830$$

$$r = 0.9940$$

$$\sigma_r = 394.13$$

$$\sigma_\chi = 373.73$$

TABLE 23
Correlations of Molecular Properties of Allenes with Those in Related Molecules

Molecular Property	Correlation	r	Eq.	Ref.
Dipole moments	$\mu(R_1R_2C=C=CH_2) = 1.10 \mu(R_1R_2C=CH_2) - 0.02$	1.0000	(13)	9
Vertical ionization energies	$\mu(RHC=C=CH_2) = 1.12 \mu(RPh) - 0.04$	0.9991	(14)	9
	$I_0(\pi_{(1)})(RHC=C=CH_2)^a = 0.84 I_0(\pi_{(1)})(RHC=CH_2) + 1.14$	0.9923	(60)	24
	$I_0(\pi_{(2)})(RHC=C=CH_2)^a = 0.91 I_0(\pi_{(2)})(RHC=CH_2) + 0.91$	0.9991	(61)	24
	$I_0(\pi_{(1)})(RHC=C=CH_2)^a = 1.33 I_0(\pi(b_1))(RPh) - 2.44$	0.9884	(62)	b
	$I_0(\tilde{\pi}_{(1)})(RHC=C=CH_2)^a = 1.49 I_0(\pi(a_2))(RPh) - 3.70$	0.8904	(63)	24
Excitation energies	$\Delta E(\pi, \pi^*)(R_1R_2C=C=CH_2) = 0.90 \Delta E(\pi, \pi^*)(R_1R_2C=CH_2) + 0.64$	0.9852	(64)	22,24
¹³ C nmr	$^1J(^{13}C_1, H_2)(RHC=C=CH_2) = 0.99 \ ^1J(^{13}C_1, H_2)(RHC=CH_2) + 13.1$	0.9983	(65)	54,65
Spectral data	$^2J(^{13}C_2, H_2)(RHC=C=CH_2) = 0.98 \ ^2J(^{13}C_2, H_2)(RHC=CH_2) - 0.8$	0.9924	(66)	54,65
	$\delta_C(R_1R_2C=C=CH_2) = 0.0431 \delta_C(R_1R_2C=O) + 182.6$	0.9091	(67)	— ^{b,c}
	$\delta_C(RHC=C=CH_2) = 0.423 \delta_C(RHC=CH_2) + 160.4$	0.9534	(68)	— ^b
	$\delta_C(RHC=C=CH_2) = 1.019 \delta_C(RHC=CH_2) - 47.9$	0.9671	(69)	— ^b

^a Concerning the labeling of the orbitals cf. Fig. 9.

^b This work.

^c The ¹⁷O-resonances are from Ref. 88; downfield shifts relative to H₂O are chosen to be positive.

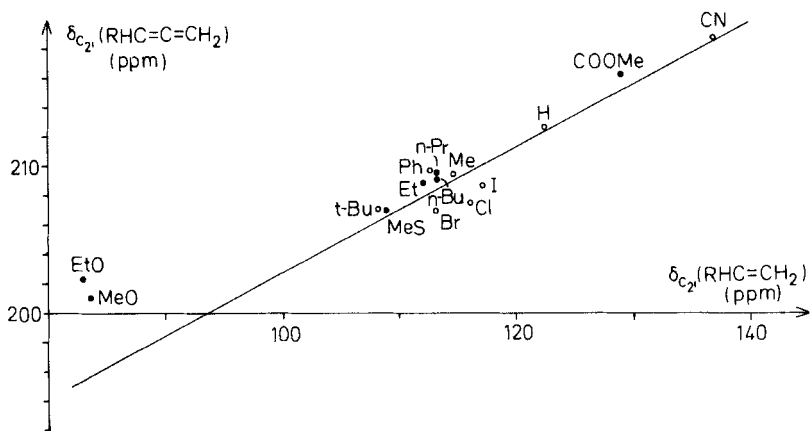


Figure 11 Correlation of the ^{13}C chemical shifts of the β carbon atoms in allenes and ethylenes.

styrene $\text{PhHC}=\text{CH}_2$, if the α hydrogen is substituted by a methyl group. In α -methyl-phenylallene (**59**) the uv absorption $\bar{\nu}(\pi, \pi^*)$ is bathochromically shifted by 600 cm^{-1} (71) relative to **16**, whereas in α -methyl-styrene the corresponding π, π^* band is hypsochromically shifted by about 1100 cm^{-1} (71).

Most of the correlations relate properties of allenes to corresponding properties of unsaturated systems with a carbon atom skeleton. Formally more interesting is the correlation of the ^{13}C chemical shifts of the allenic central atoms with the ^{17}O chemical shifts in carbonyl compounds. Qualitative similarities have also been observed for the $\bar{\pi}_{(1)}$ ionization energies in allenes and the lone-pair n_0 ionization energies in carbonyl derivatives (24) and the lowest-energy

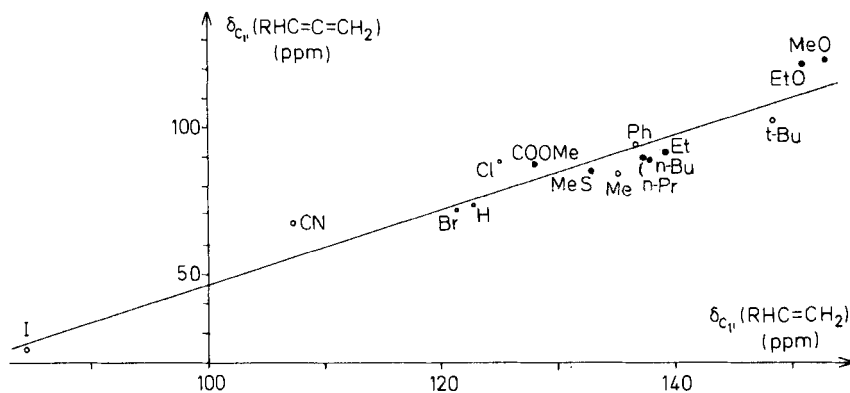


Figure 12 Correlations of the ^{13}C chemical shifts of the α carbon atoms of allenes and ethylenes.

weak uv bands resulting from electric dipole forbidden, magnetic dipole allowed transitions in both kinds of molecules (the $\pi, \bar{\pi}^*$ and $\bar{\pi}, \pi^*$ transitions in allenes and n, π^* transitions in carbonyl compounds) (24,73). Conformational effects are also quite similar in allenes and carbonyl derivatives (1b).

The correlations (68) and (69) have been evaluated taking only substituents with the rotational symmetry C_{3v} or $C_{\infty v}$ into account. They are displayed in Figs. 11 and 12.

Furthermore, in Figures 11 and 12 also the ^{13}C chemical shifts of allenes and ethylenes with substituents which exhibit different conformations in both the kinds of molecules (Section II.B) are given. However, including all kinds of substituents in the regression analyses for the ^{13}C chemical shifts gives correlations of inferior qualities.

G. Effects of Isoelectronic or Isovalent Substitutions in the Allenic Skeleton

1. *NMR-Chemical Shifts of Ketenes, Ketene Imines, Carbodiimides, Diazocompounds, and Thioketenes*

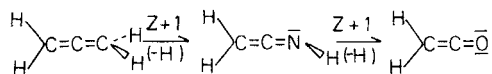
The algebraic model adopted so far (Section II.A) for the analyses of (scalar and pseudoscalar) molecular properties of allenes has been based upon a concept of symmetry that is related to Euclidean geometry (orthogonal groups). In deducing mathematical expressions for the predictions of numerical values for the particular properties the molecular skeleton does not contribute directly to the mathematical ansätze. Relevant for the treatment was the point-symmetry of the (ideal) point arrangement of the skeletal ligand-sites and their number n (the coordination number of the skeleton).

However, one must be aware of the fact that the symmetry group of a system determined as a result of physical experiments may be incorrectly taken as that of the geometrical figure (subjected to a correct definition). The symmetry of the geometrical structure may give only a minimum symmetry of the properties and relationships associated with the physical structure in question.

In the present subsection dealing explicitly with isoelectronic substitution (89) within the allenic frame it will be shown that the methods and ideas of symmetry are advantageously extended on dispensing with the conditions that during corresponding transformations the metric properties of the objects (frames) under consideration be preserved. Then, one can construct, for instance, affine, projective, or topological geometries as a set of invariant propositions (axioms, theorems, and the consequences derived from these) which remain unchanged in making a corresponding transformation. For this purpose one can define groups of generalized compound transformations for the material spaces so obtained. It is quite natural to take these groups as the symmetry groups of

the material objects. Then one shall define the symmetry group "as the group of permissible one-to-one transformations preserving the structural integrity of the systems under consideration" (Ref. 14a, p. 308).

If one investigates the effect of isoelectronic substitution within the allenic functionality (allene \rightarrow ketene imine \rightarrow ketene), one considers structural units that are equivalent concerning the number of heavy atoms, the linear arrangement of the heavy atoms, and the total number of electrons for these molecules or correspondingly substituted molecules. The relevant (nongeometrical)



transformations relating these last kinds of molecules concerns changes in nuclear charges Z of the heavy atoms and internuclear distances $r_{\text{C}=\text{X}}$. To a good approximation the $\text{C}=\text{C}$ bond lengths and bond angles in all these three kinds of cumulenes remain identical (1b).

Restricting to ketene imines with substituents R_1 (R_2) and R_3 bonded via carbon atoms to the skeleton and lying in perpendicular planes it has been shown (89a) that, as a result of the isoelectronic principle, approximation ansätze for the calculations of ^{13}C chemical shifts of ketene imines (89b) and ketenes (89a, 89c, 89d) may be simply deduced from corresponding expressions for allenes, that is, from Equations 37 and 38. For ketene imines they have the analytical forms of Equations 70 and 71, for ketenes of Equations 72 and 73.

$$\bar{\delta}_{\text{C}_1'} = \alpha_7 + \beta_7(\text{R}_1) + \beta_7(\text{R}_2) + \gamma_7(\text{R}_1, \text{R}_2) + \mu_7(\text{R}_3) \quad (70)$$

$$\bar{\delta}_{\text{C}_2'} = \rho_7 + \sigma_7(\text{R}_1) + \sigma_7(\text{R}_2) + \tau_7(\text{R}_1, \text{R}_2) + \pi_7(\text{R}_3) \quad (71)$$

$$\bar{\delta}_{\text{C}_1'} = \alpha_8 + \beta_8(\text{R}_1) + \beta_8(\text{R}_2) + \gamma_8(\text{R}_1, \text{R}_2) \quad (72)$$

$$\bar{\delta}_{\text{C}_2'} = \rho_8 + \sigma_8(\text{R}_1) + \sigma_8(\text{R}_2) + \tau_8(\text{R}_1, \text{R}_2) \quad (73)$$

The subscripts of the parameters in Equations 70–73 refer to the nuclear charges ($Z = 7, 8$) of the heteroatoms in the corresponding cumulenes. The corresponding parameters for allenes then are denoted by $Z = 6$.

In deducing the above equations the electron lone-pairs in ketene imines and ketenes have the status of formal ligands according to the isoelectronic principle (89,90). Furthermore, it has been shown that all the isoelectronic systems under consideration exhibit quantitatively a systematic variation of their corresponding physical properties with nuclear charges. That means, the parameters p_Z from Equations 70–73 are simply related to the corresponding parameters $p_{Z=6}$ used for the calculations of the ^{13}C chemical shifts of allenic systems (Table 7) according to Equation 74. The slopes b_Z represent the sensitivities of the allenic ^{13}C chemical shift parameters towards changes in the nuclear charge of one terminal carbon atom.

TABLE 24
 Relationships of ^{13}C Chemical Shift Parameters^a for Allenes, Ketene Imines,
 and Ketenes with Nuclear Charges of the Heavy Atoms in the Cumulenic
 Functionality (89a)

$\alpha_Z = \alpha_{Z=6} - 35.5 (Z - 6)$	
$\beta_Z(\text{Alk}) = \beta_{Z=6}(\text{Alk}) - 1.00 (Z - 6)$	
$\beta_Z(\text{Ph}) = \beta_{Z=6}(\text{Ph}) + 3.00 (Z - 6)$	
$\gamma_Z(\text{Alk,Alk}) = \gamma_{Z=6}(\text{Alk,Alk}) + 1.50 (Z - 6)$	Alk = alkyl
$\gamma_Z(\text{Ph,R}) = \gamma_{Z=6}(\text{Ph,R}) + 0.35 (Z - 6)$	R = Me, Et, Ph
$\mu_Z(\text{R}) = \mu_{Z=6}(\text{R}) - 5.00 (Z - 6)$	
$\rho_Z = \rho_{Z=6} - 9.30 (Z - 6)$	
$\sigma_Z(\text{Alk}) = \sigma_{Z=6} + 5.25 (Z - 6)$	
$\sigma_Z(\text{Ph}) = \sigma_{Z=6} + 4.20 (Z - 6)$	
$\tau_Z(\text{Alk,Alk}) = \tau_{Z=6}(\text{Alk,Alk}) - 1.00 (Z - 6)$	
$\tau_Z(\text{Ph,R}) = \tau_{Z=6}(\text{Ph,R}) - 2.40 (Z - 6)$	
$\pi(\text{Ph}) = \sigma_{Z=6}(\text{Ph}) - 9.60 = -12.60$	
$\pi(\text{Alk}) = \sigma_{Z=6}(\text{Alk}) - 13.0$	

^a The parameters $p_{Z=6}$ are those for allenes from Table 7.

$$p_Z = p_{Z=6} + b_Z \cdot (Z - 6) \quad (74)$$

The parameters p_Z have been determined empirically (89a). Relations corresponding to that of Equation 74 are given for inductive alkyl groups and the phenyl group in Table 24. Explicit numerical values for the corresponding parameters are given in Ref. 89a. They are easily calculated using the allenic values in Table 7.

In Table 25 comparisons between experimental and predicted ^{13}C chemical shifts of ketene imines and ketenes on the basis of Equations 70–73 are given. They exhibit excellent agreements between calculated and observed values.

Consequently, isoelectronic substitution may be regarded as a symmetry principle (subject to our broader concept of symmetry given previously) which, when applied to a series of isoelectronic species, allows a systematic treatment of corresponding physical properties of isoelectronic molecules on the basis of algebraic arguments. Thus structural insights into physical phenomena are given not only for one molecular class, but for the whole family of isoelectronic systems.

The isoelectronic principle as formulated qualitatively in Ref. 90 has a quantum-theoretical foundation (91). Relations of the expressions (70)–(74) which have been based essentially on algebraic arguments to quantum-theoretically derived expressions are discussed in Ref. 89a.

As the proton chemical shifts of the hydrogen atoms in the methylene group of cumulenes are linearly correlated to the ^{13}C chemical shifts of the methylene carbons (10), the proton chemical shifts of allene (11), ketene imine (49) (10), and ketene (43) (10) also vary systematically with the nuclear charges (Fig. 13).

TABLE 25
 Calculated ($\bar{\delta}_{C_1'}$) and Experimental ($\delta_{C_1'}$) ^{13}C Chemical Shifts of Ketene Imines
 $\text{R}_1\text{R}_2\text{C}=\text{C}=\text{NR}_3^a$ and Ketenes $\text{R}_1\text{R}_2\text{C}=\text{C}=\text{O}$ in CDCl_3 (in ppm) (89a)

Compd.	R ₁	R ₂	R ₃	$\bar{\delta}_{C_1'}$	$\delta_{C_1'}$	$\bar{\delta}_{C_2'}$	$\delta_{C_2'}$
188	H	H	Ph	37.3	36.9	190.7	189.2
189	Me	H	Ph	48.0	48.0	192.8	193.4
190	Et	H	Ph	55.4	56.0	192.2	192.9
191	Ph	H	Ph	61.8	60.4	191.9	190.4
192	Ph	Ph	Ph	78.8	77.8	194.6	190.2
193	Et	Me	Ph	64.5	65.5	193.8	195.4
194	Me	Me	Ph	58.2	58.2	194.4	195.5
195	Ph	Me	Ph	67.1	67.1	194.3	193.9
196	Ph	Ph	Me	73.4	74.4	191.0	186.7
197	Ph	Me	<i>i</i> -Bu	64.5	64.3	189.1	187.8
198	Et	Me	<i>i</i> -Bu	61.9	62.5	188.6	191.8
43	H	H		2.5	2.5	194.0	194.0
44	Me	H		11.2	10.9	201.1	200.0
199	Et	H		18.6	18.6	200.7	200.0
45	Me	Me		21.9	19.8	207.1	206.2
200	Et	Me		28.2	26.9	207.5	206.1
201	Ph	Me		33.7	33.8	204.6	205.6
202	Ph	Et		40.8	42.1	204.2	205.7
46	Ph	Ph		49.3	47.0	203.9	201.3

^a Ketene imines: **188–198**.

$$\delta_{C_1'} = 1.0150 \bar{\delta}_{C_1'} - 0.8820$$

$$r = 0.9990$$

$$\sigma_y = 22.8322$$

$$\sigma_x = 22.4909$$

$$\delta_{C_2'} = 0.9470 \bar{\delta}_{C_2'} + 9.9983$$

$$r = 0.9400$$

$$\sigma_y = 6.4985$$

$$\sigma_x = 6.7108$$

If we use the ligand-specific parameters for the calculations of proton chemical shifts of allenes from Table 8, the proton chemical shifts of ketene imines (89,92) may be estimated to a good approximation by Equation 75, which takes into consideration that the substituent effects in ketene imines are generally larger than those in allenes.

$$\bar{\delta}_H(\text{RHC}=\text{C}=\text{NR}') \approx 3.5 + (\beta^H(\text{R}) + 0.3) \quad (75)$$

The correlation between experimental proton shifts of ketene imine and allenes is given by Equation 76 ($r = 0.9769$).

$$\delta_H(\text{RHC}=\text{C}=\text{NR}') = 1.10 \delta_H(\text{RHC}=\text{C}=\text{CH}_2) - 1.61 \quad (76)$$

On the basis of the isoelectronic principle interpolating between the ^{13}C chemical shifts of allene ($Z = 6$) ($\delta_C = 212.6$ ppm relative to TMS) and carbon dioxide **204** ($Z = 8$) ($\delta_C = 125$ ppm (93)) one would expect the ^{13}C chemical shift of carbodiimide (**203**) which cannot be isolated owing to tautomerism with cyanamide $\text{H}_2\text{NC}\equiv\text{N}$ to be observed near 169 ppm. If one assumes that the

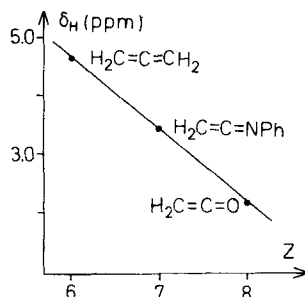
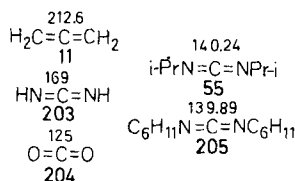
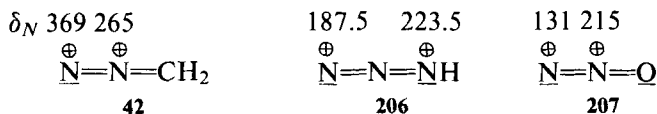


Figure 13 Relation of the proton chemical shifts of triatomic cumulenes to the nuclear charges of one terminal atom.



isopropyl group shifts the ^{13}C nmr resonance of the carbon atom of carbodiimides by about 18 ppm to higher field, as is observed for ketene imines ($\pi(\text{Alk})$; Table 24), then this gives a rough estimate of $\delta_{\text{C}} = 176$ ppm for **203** using the ^{13}C chemical shifts of the carbodiimides **55** and **205** (93a) as references. This gives credit to the value of 169 ppm for **203** whose deduction from the isoelectronic principle seems to be more sound. More ^{13}C chemical shift data of carbodiimides are reported in Refs. 93b and 93c.

The isoelectronic principle may also be used as a guideline for comparisons of ^{14}N - (or ^{15}N -) chemical shifts of diazocompounds (94,95). Accordingly, the positions of the ^{14}N nmr resonances of diazomethane (**42**) are related to those of hydrazoic acid (**206**) and dinitrogen mono-oxide (**207**) (relative to $^{14}\text{NH}_4^+$; $\delta_{^{14}\text{N}}(\text{Me}_4\text{N}^+) = \delta_{^{14}\text{N}}(\text{NH}_4^+) - 18$ (95)).



The relations between the ^{14}N chemical shifts of **42**, **206**, and **207** are displayed in Figure 14. The relation for the central nitrogen atoms is sufficiently linear, whereas for the terminal nitrogen atoms a linear relation can only approximately reproduce the observed trend.

As is observed for the ^{13}C chemical shifts of corresponding molecules (**11**, **49**, **43**) the compound with the methylene group ($Z = 6$) (**42**) exhibits the lowest field positions for the ^{14}N resonances, and the compound with the oxygen atom

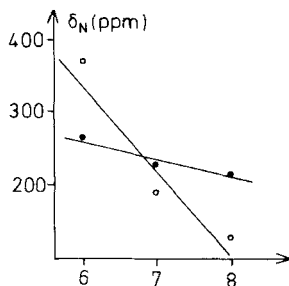


Figure 14 Relations of the ^{14}N chemical shifts of diazomethane ($Z = 6$), hydrazoic acid ($Z = 7$), and dinitrogen mono-oxide ($Z = 8$) to the nuclear charges of one terminal atom.

(207) the highest field positions. Again, the variations of δ_N with nuclear charges are greater for the terminal atoms than for the central ones.

Based on the isoelectronic principle it is clear that carbodiimides, such as dicyclohexylcarbodiimide (205) ($\delta_N = +75$ ppm in CCl_4 relative to NH_4^+ (61b)), resonate at considerably lower field than isocyanates ($\delta_{N(\text{MeNCO})} = -8.5$ ppm in benzene relative to NH_4^+ (61b)). Diazomethane (42) is not only isoelectronic with ketene (43), but also isosteric (96). Therefore, one may expect close similarities for all their corresponding molecular properties. Concerning nmr shifts the central carbon atom of ketene (43) exhibits its resonance near that of carbon monoxide $\ominus \text{C} \equiv \text{O} \text{I}^{\oplus}$ (89c, 89d). Similarly, the central nitrogen atom of diazomethane (42) has a resonance position near the nitrogen ($\text{IN} \equiv \text{NI}$) resonance ($\delta_N = 283$ ppm (94a)). More nitrogen (-15) chemical shifts of carbodiimides may be found in Ref. 93c.

Substituent effects on the ^{13}C chemical shifts of the terminal carbon atoms in diazocompounds (89e) are very close to those in ketenes. The experimental ^{13}C chemical shifts in both the kinds of molecules are related to each other according to Equation 77 ($r = 0.9982$). Diazocompounds exhibit also very high-field carbon resonance positions (e.g., $\delta_C(\text{H}_2\text{CN}_2) = 23.1$ ppm (89e)).

$$\delta_C(\text{R}_1\text{R}_2\text{C}=\overset{\oplus}{\text{N}}=\overset{\ominus}{\text{N}}\text{I}) = 0.87 \delta_C(\text{R}_1\text{R}_2\text{C}=\text{C}=\text{O}) + 21.5 \quad (77)$$

The results presented so far have revealed that, on the basis of the isoelectronic principle, it is possible to deduce qualitatively and quantitatively relations between molecular properties and substituent effects within a family of isoelectronic molecules.

The acceptance of the isoelectronic principle as a symmetry principle has important consequences for the investigation of the structures of physical phenomena on the basis of algebraic arguments, as has been shown for the treatments of ^{13}C chemical shifts of allenes, ketene imines, and ketenes that are scalar in character. For pseudoscalar molecular properties the isoelectronic principle would have farer reaching consequences. Take, for instance, the carbodiimides

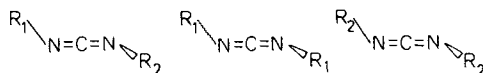
(with an arrangement of the ligands in perpendicular planes and in an arbitrary



configuration (*S*)). According to the conventional theories (15) (cf. Section II.A) the carbodiimides should be viewed as representatives of a molecular class with $n = 2$ ligand-sites and a skeletal symmetry C_2 ; that is, the skeleton is chiral. Consequently, it is not possible to treat, for instance, the molar rotations of carbodiimides by the conventional procedures (15), since these treatments are restricted to achiral skeletons (subject to the geometrical definition relying on coordination numbers of the skeletons). Taking the broader concept of symmetry, the isoelectronic principle suggests that the structure of the phenomenon of molar rotations of carbodiimides should be related to that of allenes regarding the electron lone-pairs as formal ligands. Therefore, from the λ -formulas (10a) and (51a) for allenes with two identical ligands and the convention $\bar{\lambda}(e) = 0$ molar rotations of carbodiimides should be given by Equation 78

$$\chi(R_1, R_2) = \epsilon \cdot \bar{\lambda}(R_1) \cdot \bar{\lambda}(R_2) \text{ for carbodiimides} \quad (78)$$

In Equation 78 $\epsilon = \pm 1$ is a sign factor. Until now no chiral carbodiimides have been isolated (1b, 1c). To test the preceding predictions concerning chiral properties of carbodiimides Equation 78 should be a guideline for planning experiments with chiral carbodiimides. Ansatz (78) can be easily tested on the basis of the molar rotations of three molecules with two different ligands.



Using the same arguments, for instance, molar rotations of ketene imines with two identical ligands should be given by Equation 79, assuming for the lone-pair $\bar{\nu}(e) = 0$ ($R_1 = R_3$)

$$\begin{aligned} \chi(R_1, R_2, R_3) &= \epsilon \cdot [\bar{\lambda}(R_1) - \bar{\lambda}(R_2)] [\bar{\nu}(R_3) - \bar{\nu}(e)] \\ &= \epsilon \cdot \bar{\nu}(R_3) [\bar{\lambda}(R_1) - \bar{\lambda}(R_2)] \end{aligned} \quad (79)$$

According to the conventional theory (15) ketene imines should be viewed as systems with $n = 3$ ligand-sites and an achiral skeleton of symmetry C_s . The structure of a (qualitatively complete) chirality function for such a system (15b) is given by Equation 80a.

$$\begin{aligned} \chi(R_1, R_2, R_3) &= \epsilon_1 [\bar{\lambda}(R_1) - \bar{\lambda}(R_2)] \\ &+ \epsilon_2 [\bar{\mu}(R_1) - \bar{\mu}(R_2)] [\bar{\mu}(R_1) - \bar{\mu}(R_3)] [\bar{\mu}(R_2) - \bar{\mu}(R_3)] \end{aligned} \quad (80a)$$

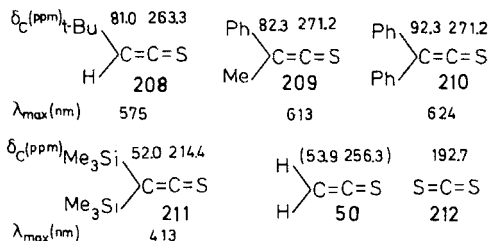


Figure 15 ^{13}C -chemical shifts and the longest wavelength uv band positions of thioketenes. (The values for thioketene (**50**) are calculated).

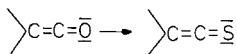
Then, for $R_1 = R_3$ one has

$$\chi(R_1, R_2, R_3) = \sigma_1 [\lambda(R_1) - \lambda(R_2)] \quad (80b)$$

Related to Equation 80b the optical rotations of ketene imines (with $R_1 = R_3$) should not depend upon the kinds of substituents attached to the nitrogen atom, that is, ligand-site 3. This is definitely different from the situation reflected by Equation 79.

Until now, unfortunately, no chiral ketene imines (with achiral ligands) have been synthesized (1b, 1c).

A further chemically interesting process involving molecular skeletons is "isovalent (isovalence electronic) substitution" which does not affect the number of heavy atoms and the number of valence electrons. In connection with the cumulenes the most important isovalent substitution process is the transition from ketenes to thioketenes which retains the overall geometry of the corre-



sponding molecules. Concerning ^{13}C chemical shifts both the molecular systems exhibit qualitatively corresponding substituent effects for both the carbon atoms; that is, if in ketenes a substituent induces high-field shifts of the ^{13}C resonances the same is observed in thioketenes. Based upon the ^{13}C resonances of the thioketenes **208–211** (97) (Fig. 15) the following correlations between ^{13}C chemical shifts in thioketenes and ketenes are observed ($r = 0.9931$ for Equation 81a, $r = 0.9950$ for Equation 81b; for the *t*-butylketene *t*-BuHC=C=O resonances calculated with Equations 72 and 73 have been used: $\delta_{C_1} = 29.4$, $\delta_{C_2} = 198.9$ ppm).

$$\delta_{C_1}(R_1R_2\text{C}=\text{C}=\text{S}) = 0.90 \delta_{C_1}(R_1R_2\text{C}=\text{C}=\text{O}) + 51.6 \quad (81a)$$

$$\delta_{C_2}(R_1R_2\text{C}=\text{C}=\text{S}) = 1.53 \delta_{C_2}(R_1R_2\text{C}=\text{C}=\text{O}) - 40.4 \quad (81b)$$

From these equations the ^{13}C chemical shift positions for the parent compound, thioketene (**50**), may be estimated which are also given in Fig. 15. An-

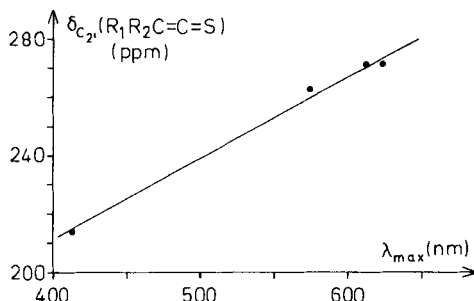


Figure 16 Correlation of the ^{13}C chemical shifts of the central atoms in thioketenes and their longest wavelength uv band positions.

other estimate of the $^{13}\text{C}_{2'}$ resonance position corroborates the value for **50** given in Fig. 15. The difference between the ^{13}C chemical shifts of ketene (**43**) ($\delta_{C_2'} = 194.0$ ppm) and carbon dioxide (**204**) ($\delta_{\text{C}} = 125$ ppm) amounts to 69 ppm which is close to the difference of 64 ppm between the ^{13}C resonance positions of thioketene (**50**) and carbon disulfide (**212**) (Fig. 15).

Most remarkably, the central atom ^{13}C resonances ($C_{2'}$) of thioketenes are far more sensitive towards substituents than the ^{13}C resonances of the other cumulenenic *sp* central atoms. The substituent induced variations cover about 60 ppm, in contrast to 40 ppm for correspondingly substituted ketenes and about 10 ppm for similar allenes.

Furthermore, the effect of isovalent substitution on the ^{13}C chemical shifts in ketenes is very pronounced when compared with the effect in the related isocyanates $\text{RN}=\text{C}=\text{O}$. The ^{13}C chemical shift positions of isocyanates and corresponding isothiocyanates are very close ($\delta_{\text{C}}(\text{MeN}=\text{C}=\text{O}) = 121.5$ ppm, $\delta_{\text{C}}(\text{MeN}=\text{C}=\text{S}) = 128.7$ ppm (61)).

Interestingly, the $^{13}\text{C}_{2'}$ -resonances of thioketenes exhibit a linear correlation (82) ($r = 0.9961$) with the positions of the longest wavelength uv band positions (in nm given in Fig. 15) of the thioketenes (Fig. 16). A corresponding correlation cannot be observed neither for ketenes nor allenes.

$$\delta_{C_2'}(\text{R}_1\text{R}_2\text{C}=\text{C}=\text{S}) = 0.279 \lambda_{\max}(\text{R}_1\text{R}_2\text{C}=\text{C}=\text{S}) + 100.1 \quad (82)$$

2. Electron Densities

The electron density distributions in ketenes and ketene imines may be discussed on the basis of the isoelectronic principle in quite the same way as has been done for the ^{13}C chemical shifts in the preceding subsection.

In this regard it is quite evident that the CNDO/S electron densities of the carbon and hydrogen atoms of allene (**11**) (54), ketene imine (**49**) (89a), and ketene (**43**) (54) are related to the nuclear charges of one terminal atom of the

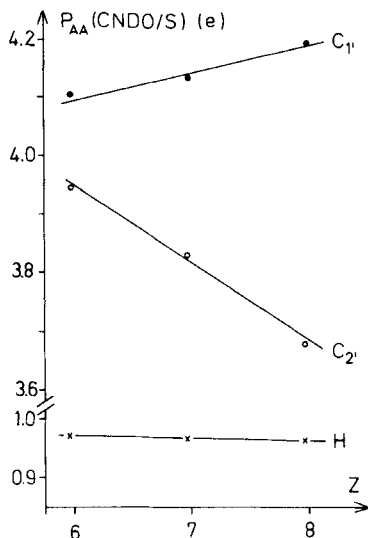


Figure 17 Total CNDO/S electron densities in allene ($Z = 6$), ketene imine ($Z = 7$), and ketene ($Z = 8$) in relations to the nuclear charges of a terminal heavy atom.

cumulenic skeleton (Fig. 17). The hydrogen atom electron densities vary only by $0.001 e$ changing Z by $(Z + 1)$.

Consequently, one could treat substituent effects on carbon electron densities in ketene imines and ketenes in the same manner as is outlined for the ^{13}C chemical shifts; that is, one should start from approximation ansätze used for the predictions of electron densities of allenes (Section II.C.1). Then these ansätze have to be adapted to the structural situations in the heterocumulenes (e.g. corresponding in form to Equations 70-73). At last, relations of the parameters to the nuclear charges (as in Table 24) have to be established. Until now, however, there are no data for electron densities of substituted ketene imines in the literature.

For some selected ketenes the CNDO/S electron densities are summarized in the Appendix (Part A). The CNDO/S carbon and oxygen electron densities in ketenes exhibit the linear correlations (83a)-(83c) with those in correspondingly substituted mono- and 1,1-disubstituted allenes, which reflect the close similarities of both these three-atomic cumulenic functionalities.

$$P_{CC}(1')(R_1R_2C=C=O) = 0.867 P_{CC}(1')(R_1R_2C=C=CH_2) + 0.626 \quad (r = 0.9382) \quad (83a)$$

$$P_{CC}(2')(R_1R_2C=C=O) = 0.876 P_{CC}(2')(R_1R_2C=C=CH_2) + 0.216 \quad (r = 0.9863) \quad (83b)$$

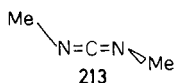
$$P_{OO}(3')(R_1R_2C=C=O) = 1.208 P_{CC}(3')(R_1R_2C=C=CH_2) + 1.253 (r = 0.9586) \quad (83c)$$

In particular, the substituent effects of the methyl and the phenyl groups on the electron densities are very similar in ketenes and allenes. Major differences are associated with the acceptor group COOH which is responsible for the only moderate correlation coefficients in Equations 83a and 83c. This is probably due to the fact that the ketene functionality acts as a stronger π donor (89d) than the allenic moiety and thus, bonded to an acceptor, the electron density variations in the ketene group are more pronounced than in the allenic group.

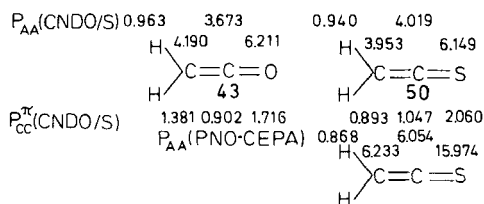
Electron density distributions on the CNDO/S level in diazocompounds are only available for diazomethane (**42**) (54). Electron densities of substituted diazocompounds have been evaluated on the INDO level (95). As there exists no correlations of INDO and CNDO/S electron densities (tested for the phenylallenes **16**, **38–40** in Table 1 and diazomethane (**42**)), the substituent effects on the (INDO) electron density distributions in diazo-compounds (95) cannot be compared with the substituent effects on the CNDO/S electron densities in ketenes and allenes.

Similar arguments also apply, if one wants to compare the CNDO/2 electron densities of dimethylcarbodiimide (**213**) (99) with CNDO/S electron density distributions in other cumulenes. There cannot be observed any correlation ($r \geq 0.85$) between CNDO/2 (37a) and CNDO/S electron densities (tested for ketene (**43**), ethylene, formaldehyde ($H_2C=O$), formic acid (HCOOH), and diazomethane (**42**) (101)).

Consistent discussions of electron density distributions in cumulenes have to rely on semiempirical CNDO/S electron densities or ab initio STO-3G atomic populations (Equations 25–28).



According to CNDO/S calculations (including d orbitals for sulfur) (Appendix, Part A) isovalent substitution in the ketene functionality has a remarkable effect.



The CNDO/S electron density distribution in **50** is largely due to a transfer

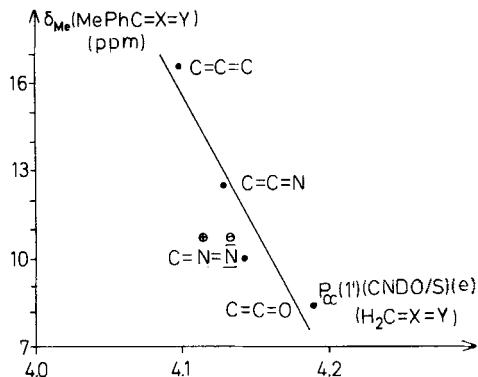


Figure 18 Relation between methyl carbon-13 chemical shifts in methyl-phenyl-cumulenes and the CNDO/S total electron densities of the terminal carbon atoms of the parent compounds.

of $\pi(p_z)$ electron density from the terminal carbon atom into the sulfur d orbitals (d_{xz}) of corresponding symmetry.

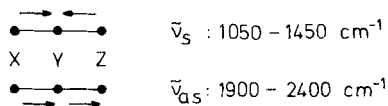
The CNDO/S electron density distribution is in sharp contrast to the one resulting from PNO-CEPA-MO calculations (100) for **50** which give the terminal carbon atom a considerably negative partial charge and sulfur a positive charge. (Notably both the calculations give reasonable ionization energies identified with the negative orbital energies.)

As relative charge densities within molecules cannot be deduced reliably from chemical reactions, if second-row atoms are involved, one has to look for other indicators relating electron densities to molecular spectroscopic properties in order to discuss the above problems of the electron densities in **50**.

For molecular skeletons with only first-row heavy atoms (C, N, O) the CNDO/S procedure gives reasonable electron density distributions. Then, if one relates the total CNDO/S electron densities of the terminal carbon atoms in the parent cumulenic systems $H_2C=X=Y$ (**11**, **42**, **43**, **49**; X, Y = C, N, O) to the ^{13}C chemical shifts of the methyl carbon atoms in corresponding methyl-phenyl compounds $MePhC=X=Y$ (Fig. 18), a total electron density of about $4.15 e$ is estimated for the terminal carbon atom in thioketene (**50**) (δ_{CH_3} ($MePhC=C=S$) = 10.5 ppm (97a)). This is near the PNO-CEPA value for **50**. Therefore, it seems that the calculated CNDO/S electron density distribution does not reflect the actual situation in the cumulenic skeleton, if a second-row atom is a constituent atom of the cumulenic frame.

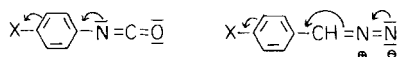
Electron density distributions in molecules are often used to discuss qualitatively chemical reactivities. In particular, electron densities may be used as indications of a proton to attack a molecule at different sites. For instance, the electron density distribution in ketene (**43**) with its pronounced negative charges at the terminal carbon and oxygen atoms, respectively, is expected to allow C protonation (**43b**) as well as O protonation (**43a**).

of the heavy atoms of the molecular skeletons. For instance, the vibrational frequencies of cumulenes $X=Y=Z$ ($X, Y, Z = C, N, O$) in the range $1900\text{--}2400\text{ cm}^{-1}$ exhibit such a behavior. These vibrational frequencies are fundamental for the identifications of these molecular systems by infrared (ir) spectroscopy (109a). The vibrations may be associated with coupled stretching modes in the $X=Y$ and $Y=Z$ subsystems, respectively, of the linear triatomic vibrators $X=Y=Z$.



The symmetric stretching mode $\tilde{\nu}_s$ involves no change in dipole moment in symmetrically substituted allenes and carbodiimides. So, it will not be infrared active, though it should appear in the Raman spectrum. In asymmetric substituted allenes and carbodiimides (i.e., in molecules with no center of symmetry,) this mode is also active in the infrared. The asymmetric stretching mode $\tilde{\nu}_{as}$ is generally observed as a strong infrared band.

The integrated ir absorption intensities ($\lg A$) of the $\tilde{\nu}_{as}$ vibrations in p -substituted phenylheterocumulenes, such as isocyanates, carbodiimides, ketene



imines, and diazocompounds, exhibit Hammett $\rho\sigma$ plots (109b). The absorption intensity is dependent on the change of the dipole moment during the vibration of the chemical bond, substituents favoring a dipole of a bond (e.g., π electron acceptors, such as NO_2 , CN) increase the integrated absorption intensity A .

For cumulenic skeletons one observes linear correlations of the asymmetric stretching frequencies $\tilde{\nu}_{as}$ with the nuclear charges for the series allene (**11**) (106), N -phenyl-ketene imine (**188**) (89b), and ketene (**43**) (107), ketene imine (**188**) (89b), dimethylcarbodiimide (**213**) (108), and phenylisocyanate (**218**) (110) as well as allene (**11**), dimethylcarbodiimide (**213**), and carbon dioxide (**204**) (109a) (Fig. 19). From the first two series one sees that the introduction of a nitrogen atom into the cumulenic skeleton has a constant effect of shifting $\tilde{\nu}_{as}$ by 100 cm^{-1} to longer wavenumbers.

The validity of the preceding relations is guaranteed by the fact that the infrared excitation $\tilde{\nu}_{as}$ is concerned with a motion retaining the overall linear heavy atom arrangement of the cumulenic frame.

In case of uv electronic excitation the situations are expected to be more complicated as the electronic excitations of the small cumulenic parent compounds may be associated with changes in geometry (111). In most cases the lowest energy electric dipole allowed π, π^* transitions of these cumulenes are accompanied, among others, by bending motions of the cumulenic skeletons (111).

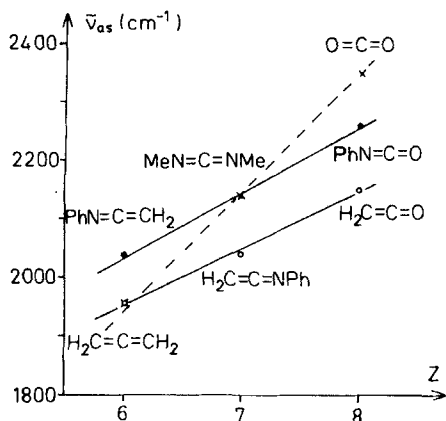


Figure 19 Relations of infrared frequencies of the asymmetric $X = Y = Z$ vibrations to nuclear charges of the terminal carbon atoms of isoelectronic series.

Changes in molecular conformations upon uv electronic excitations are probably of minor importance or, alternatively, conformational changes with regard to the chromophores are comparable for the lowest-energy weak electric dipole forbidden uv transitions in the cumulenes. There can be observed fairly linear correlations for these last transitions within a series of corresponding isoelectronic molecules (Fig. 20).

To have a consistent set of molecules for this correlation the lowest-energy uv bands $\bar{\nu}(\pi, \pi^*)$ which result from π, π^* transitions of the dimethyl derivatives **2** (71), **214** (112), and **45** (113) have been used. Typical isoelectronic shifts are also observed, if the positions of the π, π^* bands in phenyl derivatives are taken into consideration. Isoelectronic substitution (**16** → **215** → **216**) within the phenylallene chromophore (Section II.C.5) results in bathochromic shifts of the π, π^* bands.

Ph \bar{N} =C=CH ₂	Ph \bar{N} =C= $\bar{N}H$	Ph \bar{N} =C= \bar{O}
188	217	218
PhHC=C=CH ₂	PhHC=C= $\bar{N}H$	PhHC=C= \bar{O}
16	215	216

From CNDO/S calculations for **16** (71) and **216** (from this work) which are assumed to give the correct relative positions of the uv bands it is expected that the π, π^* bands in **16**, **215**, and **216** are shifted according Equation 85.

$$\bar{\nu}(\pi, \pi^*)(PhHC=C=X) = 40400 - 700(Z - 6) \text{ for } \mathbf{16}, \mathbf{215}, \mathbf{216} \quad (85)$$

Using the substituent constants $\alpha^E(R)$ (from Table 12) for the predictions of the π, π^* -band positions and a substituent constant $\bar{\gamma}^E(R) = (\gamma^E(R) + 2500)$ cm⁻¹ for all the groups attached to the nitrogen atom in ketene imines the π, π^*

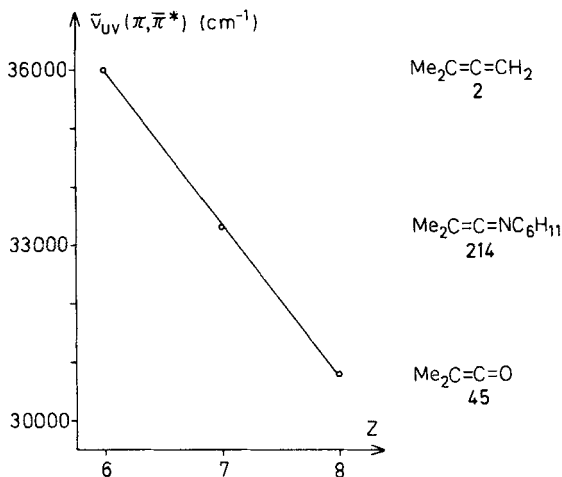


Figure 20 Correlation of the longest wavelength uv absorption positions of triatomic cumulenes and the nuclear charges of one terminal atom.

uv absorptions may be easily estimated. This is done for some ketene imines (112,115) and diphenylketene (**46**) (116) in Table 26.

Another way of looking at isoelectronic substitutions within the phenylallene chromophore would be the change of the α CH unit in phenylallene (**16**) by N to give N-phenyl-ketene imine (**188**). This kind of substitution within the phenylallene chromophore is associated with a hypsochromic shift of the π, π^* band (e.g. from 40400 cm⁻¹ in **16** to 44000 cm⁻¹ in **218** (114)). The isoelectronic substitution of the methylene group in N-phenyl-ketene imine (**188** \rightarrow **217** \rightarrow **218**) results in a relatively small π, π^* band variation (**190**: 43300 cm⁻¹ (115), **218**: 44000 cm⁻¹ (114)).

As expected for isosteric molecules diphenyldiazomethane (**220**) (117) exhibits a uv spectrum which is very similar to that of diphenylketene (**46**), in particular, if the π, π^* bands are taken into consideration.

TABLE 26
Predicted^a ($\Delta E(\pi, \pi^*)$) and Experimental ($\tilde{\nu}(\pi, \pi^*)$) UV Absorption Positions of the π, π^* Bands in Phenyl-Substituted Ketene Imines and Ketenes (in cm⁻¹)

Compd.	R ₁	R ₂	R ₃	$\Delta E(\pi, \pi^*)$	$\tilde{\nu}(\pi, \pi^*)$	Ref.
197	Ph	Me	<i>i</i> -Bu	36100	36200	112,115
192	Ph	Ph	Ph	34800	33000	112
219	Ph	Ph	<i>i</i> -Bu	35500	35400	112
46	Ph	Ph		37800	38100	116

^a $\tilde{\gamma}^E(i\text{-Bu}) = 3000 \text{ cm}^{-1}$, $\tilde{\gamma}^E(\text{Ph}) = 3700 \text{ cm}^{-1}$ for ketene imines, $\Delta E(\pi, \pi^*) = 40400 - 700(Z - 6) + \alpha^E(\text{R}) + \tilde{\gamma}^E(\text{R})$.



Isovalent substitution in **46** (**46** → **210**) shifts the π, π^* band bathochromically by about 1400 cm^{-1} (**210**: $\tilde{\nu}(\pi, \pi^*) = 36360 \text{ cm}^{-1}$ (96*c*)).

The isoelectronic principle as a mean to predict—at least qualitatively—trends of molecular properties probably is also applicable to ionization energies or orbital energies, respectively.

Calculated FSGO orbital energies for allene (**11**), ketene imine (**49**), and ketene (**43**) give the typical diagrams, if they are plotted versus the atomic numbers of one terminal atom (6). CNDO/S orbital energies for these last molecules, however, do not follow such a pattern (**11**: $\epsilon(\pi_{(1)}) = -10.28 \text{ eV}$, $I_v(\pi_{(1)}) = 10.07 \text{ eV}$; **49**: $\epsilon(\pi_{(1)}) = -9.59 \text{ eV}$; **43**: $\epsilon(\pi_{(1)}) = -9.57 \text{ eV}$, $I_v(\pi_{(1)}) = 9.60 \text{ eV}$ (118)). The CNDO/S result is expected, as concerning orbital energies (ionization energies) of the corresponding $\pi_{(1)}$ orbitals the molecules **11**, **49**, **43** represent no proper isoelectronic series (Section III.B).

The vertical ionization energies (in eV) of the π HOMOs in ketenes from pe spectra (Section III.D) are related to those of the correspondingly substituted allenes according to Equation 86 ($r = 0.9633$).

$$I_v(\pi_{(1)})(\text{R}_1\text{R}_2\text{C}=\text{C}=\text{O}) = 0.881 I_v(\pi_{(1)})(\text{R}_1\text{R}_2\text{C}=\text{C}=\text{CH}_2) + 0.752 \quad (86)$$

In general, the substituent effects $\Delta I_v(\pi_{(1)}) (= I_v(\text{RHC}=\text{C}=\text{X}) - I_v(\text{H}_2\text{C}=\text{C}=\text{X}))$ on the ionization energies in ketenes are smaller (for R = H, Me, Ph, Cl) than those in allenes according to Equation 87 ($r = 0.9907$).

$$\Delta I_v(\pi_{(1)})(\text{RHC}=\text{C}=\text{O}) = 0.831 \Delta I_v(\pi_{(1)})(\text{RHC}=\text{C}=\text{CH}_2) - 0.041 \quad (87)$$

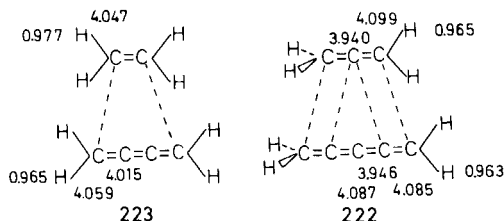
Geminal methyl groups shift the ionization energies of the π HOMOs in ketenes (**43** → **45**) as in allenes (**11** → **2**) by about 1.1 eV. The same effect is observed for the ionization energies of diazomethane (**42**) ($I_v(\pi_{(1)}) = 9.00 \text{ eV}$ (119)) and dimethyldiazomethane (**221**) ($I_v(\pi_{(1)}) = 7.88 \text{ eV}$ (120)).

H. Effects of Increase in Chain Lengths of the Cumulenic Skeleton

1. NMR Spectral Data and Electron Densities in Butatrienes and Pentatetraenes

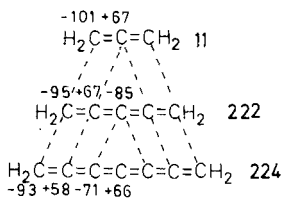
If the total CNDO/S electron densities of butatriene (**223**) and pentatetraene (**222**) are compared with those of ethylene ($\text{H}_2\text{C}=\text{CH}_2$) (71) and allene (**11**) (54,71), one observes numerical similarities of the terminal carbon atoms in **11** and **222** on the one side and ethylene and **223** on the other side. The ter-

minal carbon atoms in the antiplanar systems **11** and **222** bear a more negative charge than those in the planar systems.



Furthermore, the two inner carbon atoms ($C_{2'}$, $C_{4'}$) in **222** exhibit similar electron densities as the central atom in allene (**11**). The carbon atoms considered in the preceding hydrocarbons which seem to be electronically equivalent all have the same neighbor-atom topology. However, as the example of **11** and **222** shows, electronically equivalent atoms of molecules need not be geometrically equivalent. This remark concerns the central atoms in **11** and **222**.

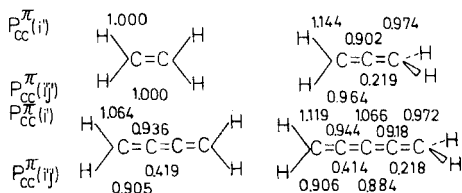
The preceding carbon electron density pattern for cumulenic systems may be extended to higher cumulenes. For instance, the CNDO/2 charge densities (in units of $10^{-3} e$) (121) for allene (**11**), pentatetraene (**222**), and heptahexaene (**224**) give a corresponding pattern with regard to the "similarities" of skeletal atoms.



In general, the total carbon charge densities alternate their signs along the chain in antiplanar D_{2d} cumulenes, whereas in planar D_{2h} systems there seems to be no corresponding alternation.

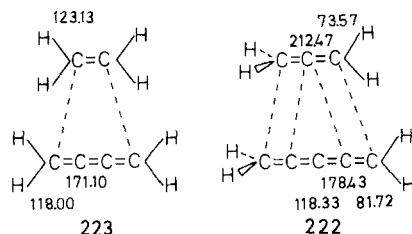
All these patterns which establish relationships between point-properties of the different carbon atoms in cumulenes visualize homology concepts for the two series of cumulenes with different skeletal symmetries (D_{2d} or D_{2h} , respectively).

The CNDO/S π electron densities for ethylene and butatriene (**223**) as well as the p_z electron densities for allene (**11**) and pentatetraene (**222**) exhibit



qualitatively the same patterns as the total electron densities. The $\pi(p_z)$ bond orders in the cumulenes show a strongly alternating character. Interestingly, the cumulenic subsystems $\text{H}_2\text{C}=\text{C}=\text{C}=\text{H}_2$ in the planar and antiplanar cumulenes **222** and **223** have the same π bond orders for the corresponding units.

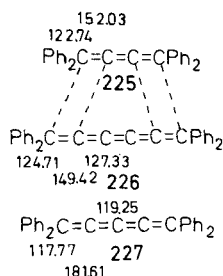
Concerning hydrogen electron densities one observes a close similarity for all the cumulenic hydrocarbons **11**, **222**, and **223**. Their hydrogen electron densities are distinctly more positive than that of ethylene. Qualitatively, the equivalencies of the various carbon atoms in the cumulenes (and ethylene) are also reflected by their ^{13}C nmr resonance positions (relative to TMS).



Correspondingly, electronic equivalencies based on similar ^{13}C nmr resonances may be established for higher cumulenes, such as the tetraphenyl derivatives **225** and **226** (121).

On the other hand, it seems that in higher cumulenes (**226**, **227**) inner carbon atoms (C_3 , C_4) tend to become more or less electronically equivalent showing an average ^{13}C nmr position of $\delta_{\text{C}} \approx 120$ ppm, irrespectively of whether the cumulene is of the planar or antiplanar type. Generally, the terminal carbon-13 atom resonances of all the cumulenes under consideration (including ethylene) are related to their total CNDO/S electron densities according to Equation 88 ($r = 0.9842$) (Fig. 21).

$$\delta_{\text{C}_i} = -910.1 P_{\text{CC}}(1')(\text{CNDO/S}) + 3803.8 \quad (88)$$



Owing to the problems discussed in Section II.G.2 thioketene (**50**) has been omitted in the regression (88). From Equation 88 a total electron density of $P_{\text{CC}}(1') = 4.120$ for **50** may be deduced which supports the assumption of a negative partial charge for the terminal carbon atom in **50**. Whereas the ^{13}C

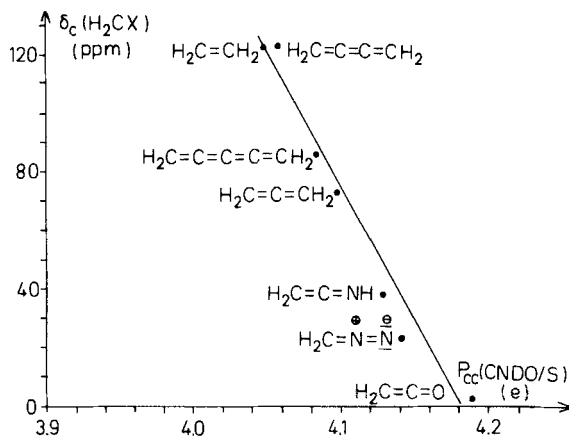


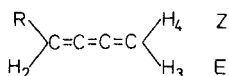
Figure 21 Correlation of the ^{13}C chemical shifts of the methylene group carbon atoms in cumulenes and the CNDO/S total electron densities of these atoms.

chemical shifts of the terminal carbon atoms of the three-atomic cumulenes are correlated with the ^1H chemical shifts of the methylene group protons (10) the proton chemical shifts of butatriene (**223**) (123) and pentatetraene (**222**) (122) do not follow this line. The ^{13}C chemical shifts $\delta_{\text{C}'}$ in **222** and **223** are markedly different, their methylene proton shifts, however, are almost identical ($\delta_{\text{H}} = 5.20$ ppm (123), $\delta_{\text{H}} = 5.33$ ppm (127 *e*) for **223**; $\delta_{\text{H}} = 5.22$ ppm (122) for **222**).

The substituent effects on the total CNDO/S electron densities in the butatrienes **223** and **51-55** (Section V.A) correlate regarding the terminal carbon atoms and the α protons roughly with those in allenes (Fig. 22). Therefore, the total (CNDO/S) electron density substituent effects in butatrienes correspond approximately to the constants $\beta^{\text{P}}(\text{R})$ and $\mu^{\text{P}}(\text{R})$ (Table 4) and $\alpha^{\text{P}}(\text{R})$ (Table 5) for allenes. This indicates comparable mechanisms for the transmissions of the substituent effects in both kinds of molecules. The terminal carbon atoms of butatrienes are those atoms which are of particular chemical interest, as especially they are involved in addition reactions of these cumulenes (124,125).

For the substituent effects on the electron densities of the inner carbon atoms of butatrienes no appropriate analogies with other systems have been found until now.

In monosubstituted butatrienes the electron densities of the remote methylene hydrogen atoms (H_3 , H_4) which are in *E*- or *Z*-positions relative to



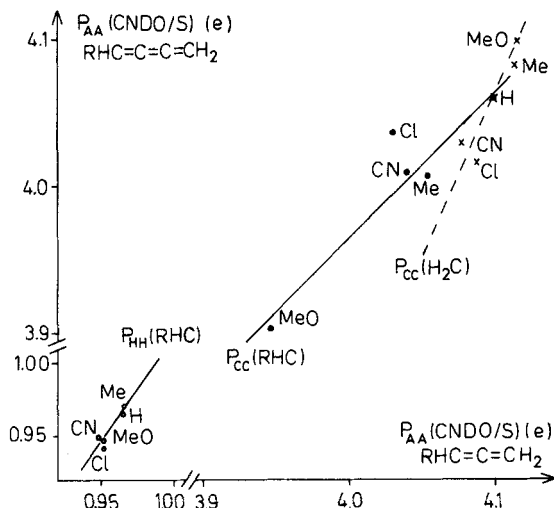
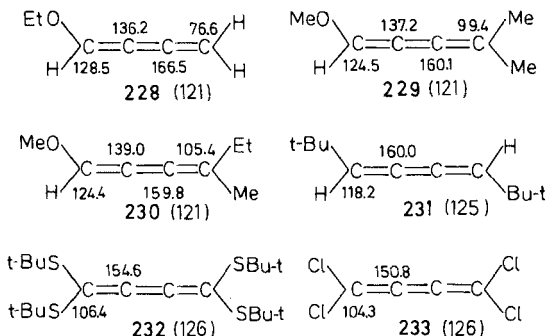


Figure 22 Correlations of CNDO/S electron densities in butatrienes and allenes.

the substituent R differ only by 0.001 e . The CNDO/S electron densities of these hydrogen atoms, for example, $P_{HH}(3)$, are related to the carbon electron densities $P_{CC}(4')$ according to Equation 89 ($r = 0.9967$).

$$P_{HH}(3)(\text{RHC}=\text{C}=\text{C}=\text{CH}_2) = 0.274 P_{CC}(4')(\text{RHC}=\text{C}=\text{C}=\text{CH}_2) - 0.148 \quad (89)$$

Concerning the substituent effects on the ^{13}C chemical shifts of butatrienes (121, 125b, 126) and pentatetraenes only some qualitative deductions are possible. (References for the ^{13}C shifts of the particular butatrienes are given in parentheses near the numbers of the compounds.)

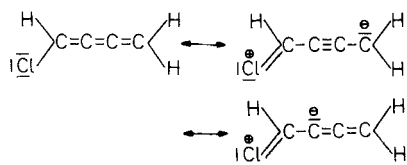


The δ_{C} values of *cis/trans* (*Z/E*) isomeric butatrienes seem to be very similar: $|\delta_{\text{C}}(\text{Z}) - \delta_{\text{C}}(\text{E})| \leq 0.4$ ppm (121).

As the example of ethoxybutatriene (**228**) shows, especially the β and δ carbon atoms in butatrienes seem to be affected by substitution, the effect on the δ atom being rather pronounced. The ^{13}C resonances for the β and δ atoms in butatrienes with π donors are shifted to higher field. The shift of the β carbon atom in **228** is comparable with that of the β atom in ethyl vinyl ether (Et-OHC=CH₂: δ_{C_1} = 150.8, δ_{C_2} = 82.6 ppm). Assuming to a first approximation the substituent effects of EtO and MeO to be identical the effects of alkyl groups on the ^{13}C chemical shifts of directly bonded butatrienoic carbon atoms seem to be of the usual magnitude, that is, $\sim +11$ ppm for Me and $\sim +18$ ppm for Et (cf. **228** \rightarrow **230**). On the other hand, the substituent effect of EtO on the α carbon ($\sim +10$ ppm) in butatriene is remarkably smaller than that in ethylene or allene which amount to $\sim +38$ ppm and $+48$ ppm (Table 7), respectively. Owing to the availability of a larger set of data the substituent effects on the ^1H chemical shifts (relative to TMS) of butatrienes (123,125,127) may be described in more detail than those on ^{13}C chemical shifts. The proton chemical shifts δ_{H_1} of the α protons in monosubstituted butatrienes correlate ($r = 0.9962$) with those in corresponding allenes.

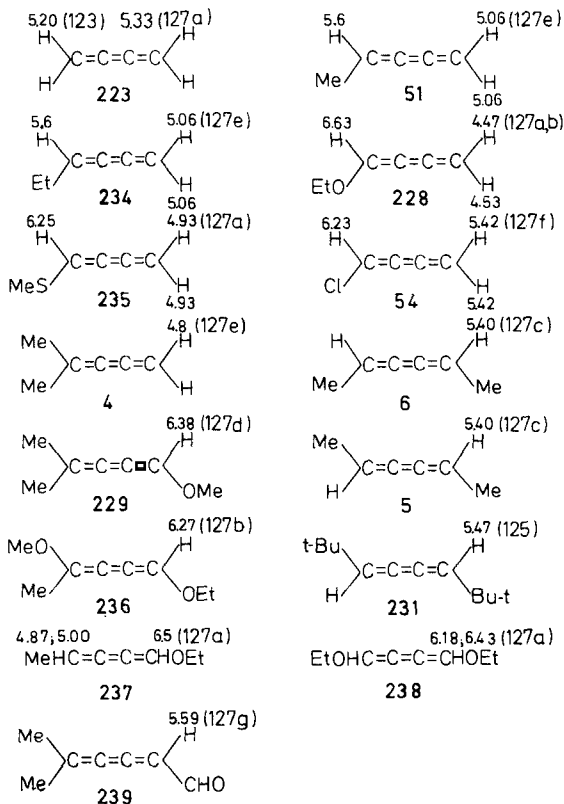
$$\delta_{H_1}(\text{RHC}=\text{C}=\text{C}=\text{CH}_2) = 0.71 \delta_{H_1}(\text{RHC}=\text{C}=\text{CH}_2) + 2.05 \quad (90)$$

The substituent effects on the α protons in butatrienes correspond to $0.71 \alpha^H(\text{R})$ in Table 8 (R = H, Me, Et, MeO, MeS, Cl, CHO (from **4**, **229**, and **239**)); that is, they are reduced compared with those in allenes. Concerning the remote hydrogen atoms (H₃, H₄) one observes, if ever, only a slight difference between the ^1H chemical shifts of the *Z*- and *E*-protons (**228**). The substituent effects on the proton shifts of these last hydrogen atoms show an unexpected behavior: The π donors Me, Et, EtO shift the resonances to higher field, whereas the π donors Cl and MeS yield low-field shifts. Therefore, simple resonance theory which stresses a negative π electron density at the δ carbon atoms of butatrienes with π donors does not seem to be appropriate to represent the electron density distributions in butatrienes with second-row substituents (Cl, MeS) (Section III.C).

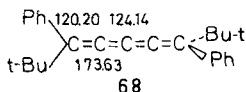


For alkyl-substituted butatrienes the ^1H chemical shifts seem to be additive in substituent effects (cf. **51**, **4-6**, **229**). The proton shifts of the rotamers **5** and **6**, furthermore, do not allow a differentiation of both the stereoisomers.

For alkoxy-substituted butatrienes (**237**, **238**), however, distinct differences



between the *Z*- and *E*-isomers may be observed. For pentatetraenes only some ^{13}C nmr data are available (121,122,128,129). No systematic discussions of substituent effects are possible. Furthermore, if the ^{13}C chemical shifts of **222**, **227**, and **68** (128a) are taken into consideration, the β and δ carbons exhibit ^{13}C resonances which are unexpected based on comparisons with ^{13}C chemical shift trends for the central atoms in correspondingly substituted allenes.



For **227** one observes a low-field shift, whereas for **68** a high-field shift is observed. Analogies with allenes would suggest high-field shifts for the carbons of these molecules. Therefore, more ^{13}C data for pentatetraenes are necessary before any reliable conclusions are possible.

It is interesting to note that a formal pattern for the ^{13}C resonance positions similar to that of allene (**11**) and pentatetraene (**222**) is also found for carbon dioxide (**204**) and carbon suboxide (**240**) (130).

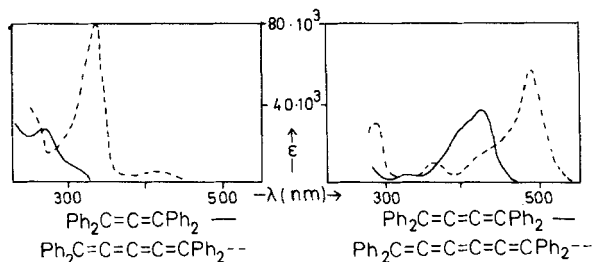
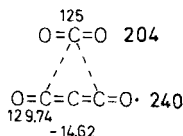


Figure 23 Ultraviolet absorption spectra of tetraphenylcumulenes (131).



2. Excitation and Ionization Energies

If excited states of the higher cumulenes are considered, for example, from electronic uv spectra, concepts of homology for the two series of (planar and antiplanar) cumulenes may also be found.

If one looks at the uv spectra of tetraphenylallene (**94**) and tetraphenylpentatetraene (**227**) on the one side and tetraphenylbutatriene (**225**) and tetraphenylhexapentaene (**226**) (131) on the other side (Fig. 23), one can see lucidly that within the corresponding class of cumulenes the uv spectra are qualitatively very similar. The same feature is observed for cumulenenic hydrocarbons **241–244** (132).

For the tetraphenylsystems in Fig. 23 in each case the longest wavelength intense uv absorption of the higher homologue is shifted bathochromically by 70 nm, the uv maxima in cyclohexane being (131): 265 nm (**94**) versus 335 nm (**227**) and 420 nm (**225**) versus 490 nm (**226**).

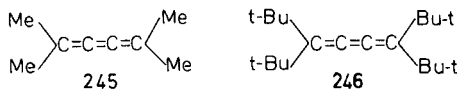
In general, there is no regular bathochromic shift for the molecules $\text{Ph}_2\text{C}=(\text{C})_n=\text{CPh}_2$, if only the chain length (n) is taken into consideration. The pentatetraene **227** exhibits its intense maximum at a considerably shorter wavelength than the butatriene **225**.

n	Compd.	Band 1 (nm)	Band 2 (nm)
1	241	271.5	
2	242	339	238
3	243	400.5	284
4	244	465	326

In the series of the D_{2h} cumulenes **241–244** the high-intensity longer

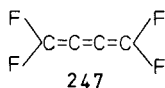
wavelength uv maxima are shifted by about 64 nm, whereas the other high-intensity shorter wavelength bands are shifted by about 44 nm with increasing chain length.

Ultraviolet spectra of butatriene (**223**) (127*f*,133), alkylated butatrienes, such as **231** (125), **245** (133,134*a*), and **246** (134*b*), chlorobutatriene (**54**) (127*f*), the methoxyderivative **229** (127*d*) and the CHO derivative **239** (135) have not yet been interpreted.



Tentatively, one can assign the two intense bands in the ranges of 230–235 nm ($\epsilon \approx 9000 - 13000$) and 250 – 300 nm ($\epsilon \approx 20000 - 30000$) to excited states resulting from electric dipole allowed transitions. As the positions of the shorter wavelength bands are largely unaffected by substitution, they may be associated with $\sigma \rightarrow \sigma^*$ ($\bar{\pi}_{(1)} \rightarrow \bar{\pi}_{(-1)}$) transitions, whereas the more intense longer wavelength bands should be related to $\pi \rightarrow \pi^*$ ($\pi_{(1)} \rightarrow \pi_{(-1)}$) transitions (which is corroborated by CNDO/S calculations of butatrienes in this work). As expected the π, π^* band undergoes pronounced bathochromic shifts in the presence of mesomeric groups. Alkyl groups shift the π, π^* band position additively by about 5 nm to longer wavelength. As in case of ethylenes ($\text{H}_2\text{C}=\text{CH}_2 \rightarrow \text{H}_2\text{C}=\text{CHCHO}$) the CHO group shifts the π, π^* band of butatrienes by about 50 nm to ~ 290 nm (125).

Ionization energies (from pe spectra) of cumulenes are only available for butatriene (**223**) ($I_v(\pi_{(1)}) = 9.30$ eV (133)), tetramethylbutatriene (**245**) ($I_v(\pi_{(1)}) = 7.70$ eV (133)), tetra-*t*-butylbutatriene (**246**) ($I_v(\pi_{(1)}) = 7.23$ eV (133)), tetrafluorobutatriene (**247**) ($I_v(\pi_{(1)}) = 9.30$ eV (136)), and pentatetraene (**222**) ($I_v(3e) = 9.15$ eV (137)). Therefore, the lack of data prevents a discussion of substituent effects on ionization energies of these last systems.



III. SOME INTERPRETATIONS OF SUBSTITUENT EFFECTS ON MOLECULAR PROPERTIES OF CUMULENES

A. Levels of Interpretations

In the preceding sections it has been tried to give a systematization of the knowledge (and data) on spectroscopic properties of cumulenes rather than a

sole accumulation. For some molecular properties this systematization could be based on a "classification theory" using a geometrophysical model with only formally defined elements, such as ligand-specific parameters. In many cases the classification theory also serves purposes of a "computation theory"; that is, it may be used to predict spectroscopic properties of cumulenes.

In the subsequent subsections substituent effects on definite molecular properties are interpreted in terms of current concepts of electronic theories; that is, the overall observable substituent effects are related to intrinsic properties of the substituents. For this purpose two levels of semiquantitative approaches are used:

- a. the substituent constant concept characterizing each ligand by two different numerical values which reflect the polarity influence and the charge-transfer ability of the ligands (4) and
- b. quantum-chemical calculations based on all-valence electron procedures.

In general, three distinct substituent scales are taken into consideration, the group electronegativity order (χ_R), the polar effect scale (σ_I), and the (various) resonance effect scales (σ_R).

Concerning quantum-chemical procedures there is, in our opinion, a rather exclusive relationship between the rigor of a given quantum-chemical approach and the breadth of applicability of that approach. Therefore, it is important to establish whether in the hierarchy of theories there exist a range wherein the theories are both tractable, in the sense of being readily usable by anyone measuring spectroscopic properties, and also sufficiently reliable and quantitative to yield really incisive chemical information. We believe that such a range does exist and that the semiempirical CNDO/S-MO scheme lies in this range provided one is primarily interested in relative changes of properties for a series of related molecules.

Within the last decade the development of *ab initio* computations has tended to overshadow the usefulness of semiempirical procedures. And also in this contribution results of *ab initio* STO-3G calculations are taken into consideration (especially in connection with spin-spin coupling constants). However, the advantage of semiempirical methods mainly lies in the possibility of a semiquantitative classification of electronic ground state and excited states properties within classes of molecules which also include larger chemically relevant compounds.

Furthermore, semiempirical MO procedures often describe the situations numerically more accurate than *ab initio* methods with small basis sets (STO-3G, STO-4.31G), especially if molecules with second-row atoms (Si, S, Cl) are considered.

The results of the quantum-chemical calculations are used in two ways:

- a. the observables of interest are calculated or
- b. the calculations provide a set of indices which may be related to spectroscopic properties.

Indices of interest comprise (total and π) electron densities (atomic populations), bond orders (overlap populations), and HOMO electron densities, the last ones being of interest for discussions of chemical reactivities.

B. π - σ Separabilities in Cumulenes

A fundamental concept for the discussion of the electronic structure of (planar) unsaturated compounds is the π - σ separation (138). Then, qualitative arguments concerning the π electronic systems are mainly based on valence-bond (VB) theory, on hybridization and conjugation. In hydrocarbons the π states of the conjugated system are constructed synthetically from p_z atomic orbitals (AOs) of the constituent carbon atoms of the molecule (xy being the molecular plane), that is, from atomic basis functions that are antisymmetric with respect to the nuclear plane. For these systems the molecular plane coincides with the nodal plane of the π electronic states which, by virtue of their symmetry, are also antisymmetric with respect to mirror reflection at the molecular plane. In " π electronic theories" some shortcomings for certain nonplanar molecules (e.g., compounds with methyl groups) have been overcome by the introduction of the concept of "hyperconjugation."

All these well-established concepts obviously are useful for the discussion of the planar cumulenes, such as ketenes, diazocompounds, thioketenes, and butatrienes. For nonplanar cumulenes (allenes, ketene imines, carbodiimides, pentatetraenes) the situation is not so simple, as the proper classification of electronic states depends essentially on the substitution patterns of the molecules (1c,24,25,73). The usual concepts based on VB arguments have led to classifications and analytical descriptions of allenic electronic systems (or orbitals) in terms of "two perpendicular, isolated π systems," especially in terms of two-center ethylenic π systems (24). Sometimes, "hyperconjugation" of the "ethylenic" $C=C$ π system with the CH_2 group orbitals of corresponding symmetry has been taken into consideration (24).

From a quantum-theoretical point of view only the state property is observable, and this is determined by the overall symmetry of the molecule under consideration. In planar molecules the π - σ separation is physically relevant, as it is connected with state properties which are associated with projection operators for the antisymmetric (a'') and symmetric (a') representation of the symmetry group C_s . In nonplanar allenes only for molecules of C_s symmetry, for example, monosubstituted compounds $RHC=C=CH_2$, there exists a correspondingly physically relevant and unique $\pi(a'')$ - $\sigma(a')$ classification (24).

For these last systems π and σ interactions may be strictly differentiated which is important for the discussions of substituent effects.

In general, all the $\sigma(a')$ orbitals in monosubstituted allenes correlating with allenic e orbitals have been termed $\bar{\pi}$ orbitals. Such a denotation for σ orbitals (!), especially the outermost occupied and unoccupied orbitals, may be chosen for three reasons: (a) LCAO expansions of these orbitals involve essentially p_y AOs giving rise to π -type overlap, (b) the orbitals have low ionization energies (~ 10 eV) typical for real π orbitals, and (c) the $\bar{\pi}$ orbitals often are involved in addition reactions in quite the same way as is observed for π systems, such as ethylenes.

For a discussion of the situation in complex allenes take for simplicity a 1,3-disubstituted allene with identical ligands. These molecules are (at least) of symmetry C_2 . Then, symmetry suffices to state that the electronic states (orbitals) have lost a typical feature of π systems: They have no longer nodal planes. Furthermore, in allenes of symmetry C_2 , such as **3** or **72**, the resulting a and b orbitals are accidentally degenerate (1c,66).

Degenerate orbitals are also found in tetrasubstituted allenes, that is, allenes of symmetry D_{2d} (cf. Fig. 9). However, the (e) degeneracy of these last molecules is due to symmetry.

Corresponding arguments apply to pentatetraenes. In all these D_{2d} -systems the chemically interesting (outermost) orbitals have no nodal planes. Then, of course, in isoelectronic 1,3-disubstituted carbodiimides the situation is comparable with that in 1,3-disubstituted allenes and corresponding reasonings apply and similar findings are expected. From pe spectra it has been shown recently (99) that, indeed, the outermost a and b orbitals in symmetric carbodiimides are degenerate.

The situation for 1,3-disubstituted allenes with different ligands becomes complex and is discussed, for instance, for γ -substituted phenylallenes in Ref. 1c. Symmetry arguments lead to the expectation that in such 1,3-disubstituted allenes the π - σ separability breaks down. But, symmetry does not allow any statement about the extent of the breakdown. For γ -substituted phenylallenes $\text{PhHC}=\text{C}=\text{CHX}$ it has been shown (1c) that the orbitals correlating with the $\pi(a'')$ orbitals in phenylallene (**16**) retain to a good approximation their nodal planes and thus may be treated and classified (with respect to their nodal plane symmetry) like π orbitals. The question about the extent of the possibility for a "quasi" π - σ separation of orbitals is of fundamental importance for the quantitative treatment of the circular dichroism of chiral allenes (1b,73).

Ketene imines introduce a further formal difficulty. In ketene imine (**49**) of symmetry C_s the orbitals may be strictly classified as a'' (π) and a' (σ). If we compare the π structure of cumulenes the relevant mirror plane of the molecules involves the $\text{H}_2\text{C}=\text{C}=\text{C}$ subunit whose atoms all lie in that plane, for instance in ketenes. In **49**, however, the corresponding CH_2 hydrogen atoms are

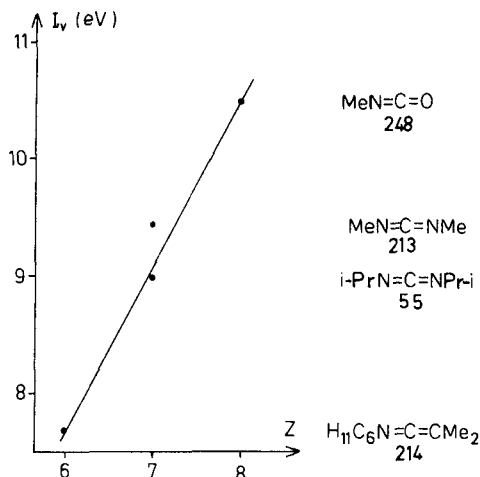
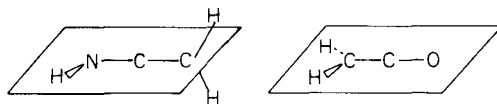
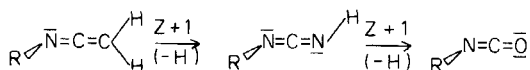


Figure 24 Ionization energies of an isoelectronic series of nitrogen containing heterocumulenes.

situated above and below the symmetry plane which is relevant for the π - σ separation.



Therefore, with respect to (π) orbitals (or ionizations of corresponding orbitals) allene (**11**), ketene imine (**49**), and ketene (**43**) represent no proper isoelectronic series (Section II.G.3). And consequently, with respect to the preceding problems the correct application of the isoelectronic principle requires that concerning π ionizations ketene imines should be compared with carbodiimides and isocyanates.



Unfortunately, there are no data for strictly comparable molecules available. However, as can be seen from Fig. 24, the ionization energies of the molecules **214** (140), **213** (99), **55** (99), and **248** (139) reflect sufficiently that we have a proper isoelectronic series. In arbitrarily substituted ketene imines one generally must expect that it is impossible to classify MOs according to the existence of a nodal plane as " π -type" orbitals. Only detailed experimental and/or theoretical analyses can give insights of whether one may classify certain orbitals as " π -type" orbitals (Section III.D).

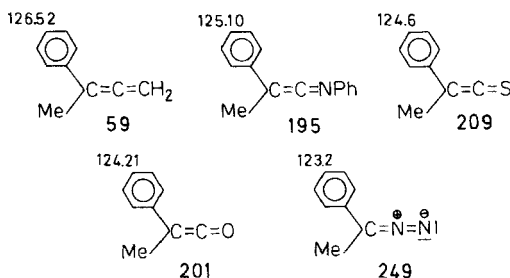
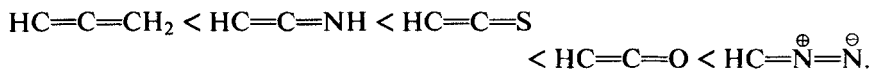
C. Electron Density Distributions

Conceptually electron density distributions of molecules play a key role in the discussion of molecular properties, of spectroscopic properties as well as chemical reactivities and equilibria.

The present section is concerned with the electron density distributions in monosubstituted cumulenes on a CNDO/S level (which is equivalent to a discussion on an *ab initio* STO-3G level (Section II.C.1)). Emphasis is on the π electronic systems in allenes, ketenes, and butatrienes. Of particular importance with respect to π electron densities is the fact that the cumulenic functionalities under consideration act as π donors as may be deduced from the ^{13}C chemical resonance positions of the *para* carbon atoms in phenyl substituted cumulenes (8,89b,89d,89e).

In case of the allenic moiety one may characterize the $\text{H}_2\text{C}=\text{C}=\text{CH}$ group quantitatively in terms of its polar (σ_I) and resonance (σ_R^0) effect. From the $\text{p}K_a$ value ($\text{p}K_a = 3.69$ (141)) of allenecarboxylic acid (**22**) one may deduce $\sigma_I(\text{H}_2\text{C}=\text{C}=\text{CH}) = +0.07$ interpolating linearly between the $\text{p}K_a$ values of $\text{H}_2\text{C}=\text{CHCOOH}$ ($\text{p}K_a = 4.25$ (142), $\sigma_I = -0.01$) and $\text{MeC}\equiv\text{CCOOH}$ ($\text{p}K_a = 2.65$ (142), $\sigma_I = 0.22$). Then, from the *para* carbon-13 resonance of phenylallene (**16**) (8) (and using $\Delta\delta_{C_p} = 4.1 \sigma_I + 19.7 \sigma_R^0$ from Ref. 4a) one obtains $\sigma_R^0(\text{H}_2\text{C}=\text{C}=\text{CH}) = -0.12$.

Concerning the π donor characteristics of the various triatomic cumulenic groups one deduces from the $^{13}\text{C}_p$ chemical shifts of α -methyl-phenyl compounds (89b,89e,97a) the following series of increasing π donating ability:



Therefore, the triatomic functionalities behave like electron-rich molecular systems, whereas typical unsaturated moieties, such as benzenes and ethylenes, act as rather indifferent systems with respect to their π donating or accepting abilities.

With regard to the electron density at the terminal carbon atom the π donor

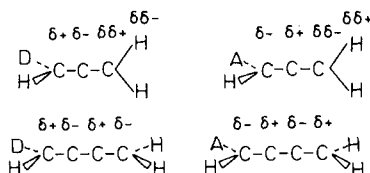


Figure 25 π electron density distributions in allenes and butatrienes with typical donors (D) and acceptors (A).

character of the butatrienyl group seems to be similar to that of the ethylenic group (Section II.H.1).

The electron density distributions in monosubstituted allenes are discussed in Ref. 9. In allenes the π system of the cumulenic moiety comprises the $C=C$ and the CH_2 subunits, that is, in VB terms there is a "hyperconjugation" of the $C=C$ π system with the CH_2 group orbitals of corresponding symmetry.

The main effect of substitution is alternating polarization of the whole allenic π system, that is, charge alternation along the allenic "four-center" π system. In Fig. 25 the π electronic charge redistribution for an allene with a typical donor (MeO) D and a typical acceptor (CN) A is displayed.

For ketenes, however, such an alternating polarization is not observed. The alternating polarization within the allenic CH_2 subunit is lucidly illustrated by the linear correlation (90a) of the (CNDO/S) π electron density $P_{CC}^{\pi}(3')$ at C_3' and the hydrogen electron density $P_{HH}(3)$ at H_3 which is determined essentially by π interactions (9).

$$P_{HH}(3) = -1.17 P_{CC}^{\pi}(3') + 2.052 \text{ for allenes} \quad (90a)$$

A corresponding charge redistribution upon substitution is also observed for butatrienes (Fig. 25).

In general, in allenes and butatrienes the charge redistributions of the π and the σ electronic systems follow a linear response system. For allenes the π electron density $P_{CC}^{\pi}(2')$ is inversely linearly related to the σ electron density $P_{CC}^{\sigma}(2')$ at that atom and directly proportional to the σ electron density $P_{CC}^{\sigma}(3')$ at C_3' (9). The σ electron density $P_{CC}^{\sigma}(1')$ at the substituted atom is related to the (group) electronegativity of the substituent.

For the butatrienes one observes relationships of the π electron densities at C_1' and C_2' with those at C_3' and C_4' , respectively (Fig. 26). Furthermore, all the π electron densities $P_{CC}^{\pi}(i')$ ($i' = 2', 3', 4'$) are correlated with the σ electron densities $P_{CC}^{\sigma}(i')$ ($i' = 2', 3', 4'$) at the same carbon atom (Fig. 27). DSP analyses (4) of the overall (CNDO/S) π charge transfer $\Sigma \Delta P^{\pi}$ in allenes and butatrienes and the substituent effect on the π electron densities $\Delta P_{CC}^{\pi}(2')$ ($= P_{CC}^{\pi}(2')(\text{RHC}=\text{C}=\text{CH}_2) - P_{CC}^{\pi}(2')(\text{H}_2\text{C}=\text{C}=\text{CH}_2)$) at the allenic central atoms give the following results (using units of $10^{-3} e$). In allenes, the π charge

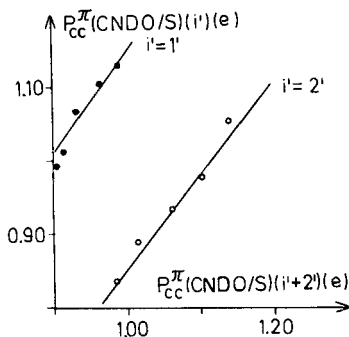


Figure 26 Correlations of the π electron densities at the atoms 1' and 3', respectively, with those at the atoms 2' and 4'.

transfer $\Sigma \Delta P^{\pi} (= \Sigma_{i=1}^3 \Delta P_{CC}^{\pi}(i') + 2 \Delta P_{HH}(3))$ is preferentially related to only the resonance substituent constants $\sigma_R^-(4)$ ($r = -0.9472$ omitting F) (Fig. 28).

$$\Sigma \Delta P^{\pi} = -143.02 \sigma_R^- - 1.71 \text{ for allenes} \quad (91a)$$

A strict DSP analysis gives ($R^2 = 0.8846$)

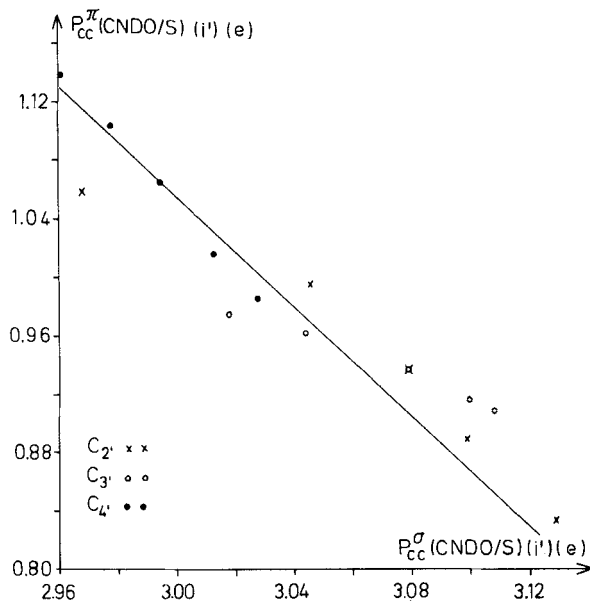


Figure 27 Correlations of the π electron densities of the atoms 2'-4' in butatrienes with the σ electron densities of the corresponding atoms.

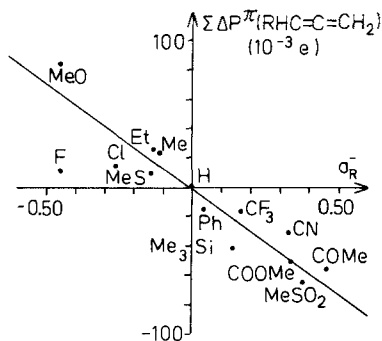


Figure 28 Relation of the π charge transfer in allenes to the resonance substituent constants σ_R^- .

$$\sum \Delta P^\pi = -6.20 + 15.57 \sigma_I - 150.22 \sigma_R^- \text{ for allenes} \quad (91b)$$

These findings stress quantitatively the fact that the allenes act as “electron-rich” molecules. The π charge transfer for the more “neutral” ethylenes and benzenes, on the other hand, are related to σ_R^0 (4). A proportionality to σ_R^0 seems also to be valid for $\sum \Delta P^\pi$ of butatrienes (Fig. 29). If one neglects the chloro group which may give rise to problems owing to its d AOs, for butatrienes a correlation (92) ($r = 0.9999$) is found which is in line with expectations resulting from the little π donor character of butatriene.

$$\sum \Delta P^\pi = -218.95 \sigma_R^0 + 0.57 \text{ for butatrienes} \quad (92)$$

As is observed for benzenes the substituent effect $\Delta P_{CC}^\pi(2')$ on the π electron densities of the allenic central atoms is markedly affected by polar effects, however, it is related to σ_R^- ($R^2 = 0.8419$).

$$\Delta P_{CC}^\pi(2') = 19.72 - 53.42 \sigma_I - 207.26 \sigma_R^- \text{ for allenes} \quad (93)$$

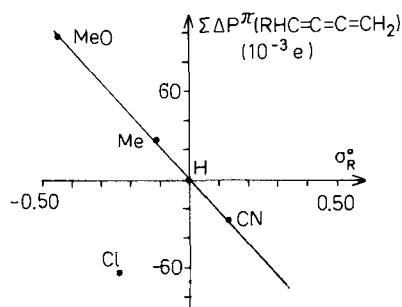


Figure 29 Relation of the π charge transfer in butatrienes to the resonance substituent constants σ_R^0 .

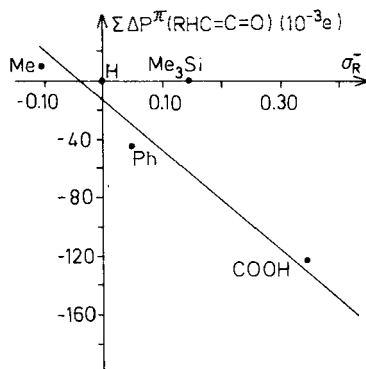
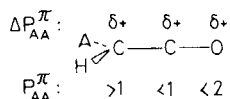


Figure 30 Relation of the π charge transfer in ketenes to the resonance substituent constants σ_R^- .

The preceding correlations are only of medium to good quality. However, it must be kept in mind that the substituent constants σ_R^0 and σ_R^- are essentially those derived from benzene derivatives. Therefore, the set of substituent constants from Ref. 4 may not represent the "best" values for cumulenes.

Though the (CNDO/S) total electron density distribution in substituted ketenes follow that in allenes (Section II.G.2), the π electron density redistribution in ketenes upon substitution is unusual. This is probably due to the strong π donor character of the ketene functionality, to the fact that the $C=C=O$ group has a "three-center" π system which is isoelectronic with that of an allyl anion, and, furthermore, that a strongly electronegative heteroatom is part of the cumulenic skeleton. There is no π charge alternation upon substitution and there are no correlations between π and σ electron densities of the atoms in substituted ketenes. In particular, all the substituents which can accept π electron density (Ph, COOH, Me_3Si) make the three ketenic heavy atoms more positive than those in ketene (43). The terminal carbon atom in ketenes, however, retains a strongly negative charge ($P_{CC}^\pi(1') > 1$).



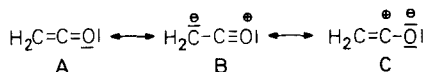
If the Me_3Si group is neglected, the π charge transfer in substituted ketenes is related to the σ_R^- constants (Fig. 30) according to Equation 94 ($r = -0.9606$).

$$\sum \Delta P^\pi = -302.16 \sigma_R^- - 20.85 \text{ for ketenes} \quad (94)$$

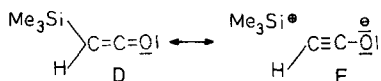
Owing to the limited number of CNDO/S calculations no full DSP analysis of the electron density data of ketenes is meaningful.

The π electron density of the inner carbon atom $P_{CC}^\pi(2')$ follows qualitatively σ_R^- .

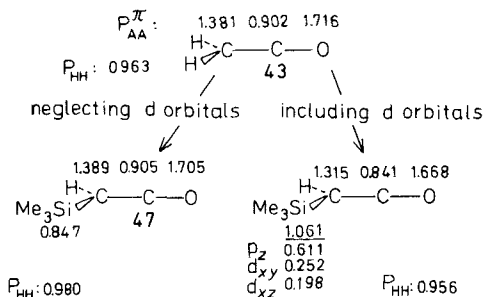
The π electron density redistribution in substituted ketenes cannot adequately be described by canonical forms. Usually it is assumed (89*c*,89*d*) that resonance form **B** is of particular importance for the description of the π elec-



tronic structure in ketene (**43**). For trimethylsilylketene (**47**), for instance, Brady (143) has offered that the trimethylsilyl group is electron donating and that **47** should be formulated in terms of resonance structures **D** and **E** with a positive

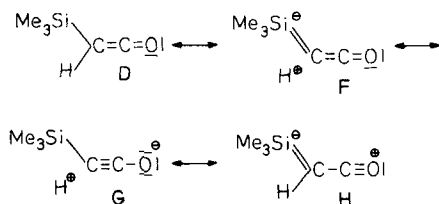


silicon atom. The CNDO/S MO calculations give another picture of the situation in **47**. From the relations of ^{13}C chemical shifts of trimethylsilylallene



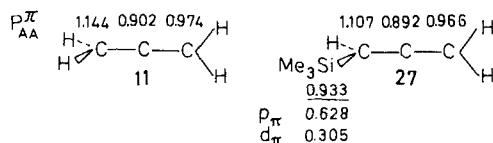
(**27**) and trimethylsilylketene (**47**) with CNDO/S data (Section II.F.1) one may have confidence that the calculations including *d* AOs reflect the electronic situations in both these systems more accurately than calculations neglecting *d* orbitals.

The CNDO/S calculations (with *d* AOs) strongly emphasize the electron withdrawing character of the trimethylsilyl group in ketenes ($\Sigma\Delta P^\pi = -175 \cdot 10^{-3} e$). Then, one must conclude that the Si atom in **47** bears a negative charge due to interaction of the ketene π system and the empty *d* orbitals on the silicon atom. Furthermore, it is seen that the hydrogen atom becomes more positive than in ketene (**43**). Therefore, the CNDO/S calculations suggest a description of **47** in terms of the canonical forms **D**, **F**, **G**, **H** which give the Si-C

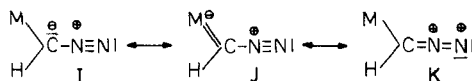


bond a partial double bond character. Especially resonance forms **F** and **H** could be the reason for the relative stability of the aldoketene **47** (143). Usually, aldoketenes are very unstable.

Also in trimethylsilyllallene (**27**) (9) the Me_3Si group acts as an electron withdrawing substituent ($\Sigma\Delta P\pi = -43 \cdot 10^{-3} e$). However, in this last case the $p\pi-d\pi$ back donation does not suffice to make the silicon atom negative.



The canonical form **H** corresponds to the form **J** which is discussed for the description of diazocompounds with metal substituents **M**, such as the trimethylsilyl group (117a).



D. Ionization Energies and Electron Affinities

When dealing with substituents effects on ionization energies (144) one should properly relate the observed data to substituent constants reflecting the substituent's abilities to stabilize positively charged systems. Fair linear correlations between vertical ionization energies of benzenes (from pe spectra) and (σ^+) substituent constants have been obtained for some substituents (such as NMe_2 , NH_2 , MeO , Me , H , CF_3 , CN , NO_2) but not for others (such as F , Cl , Br , I , OH) (144a). As a consequence, a further set of σ constants ($\sigma_{I.P.}^+$) has been introduced (144a). To be consistent with the contents of this article one should apply a DSP approach with the σ_R^+ constants (4) for the treatment of substituent effects on ionization energies. However, the convenient substituent constant approach for ionization energies of π HOMOs is bound to fail, apart from those cases where the molecules have alkyl substituents or similar σ -inductive groups. The reasons have been discussed in Section II.C.5.

For a large variety of (inductive and mesomeric) groups a discussion of substituent effects on ionization energies in terms of σ constants is not possible. Therefore, concerning ionization energies (or electron affinities) one has to adopt another approach to substituent effects. This approach is presented in detail for ionization energies from pe spectra of allenes in Ref. 24. It is a three-parameter model of substituent effects which involves short-range and long-range inductive effects as well as resonance effects and uses a "composite molecule" (LCMO) approach on a HMO level. Furthermore, it assumes the validity of Koopmans'

approximation (Equation 48) which relates the vertical ionization energies $I_v(i)$ to the negative (SCF) orbital energies ϵ_i . According to Koopmans' approximation the SCF LUMO energy should be approximately equal to the vertical electron affinity $A_v(j)$ of the neutral species.

To a good approximation the sum of the vertical ionization energies and the vertical electron affinities of corresponding π orbitals (i and $-i$) in unsaturated molecules is constant.

$$I_v(\pi_{(i)}) + A_v(\pi_{(-i)}) = \text{const.} \approx 8.2 \text{ eV} \quad (95)$$

The values of this constant are given as 7.7 eV (145a) and 8.2 eV (145b). In the light of newer results on electron affinities the last value seems to be more appropriate.

Of particular importance for the numerical evaluation of the parameters of the previously mentioned model of substituent effects on orbital energies (or ionization energies, respectively) is the observation that the ionization energies of the highest-energy σ orbitals ($\bar{\pi}_{(1)}$) of allenes are related to the group moments $\mu(\text{R})$ of the substituents R (as defined in Table 3). The substituent effect $\Delta I_v(\bar{\pi}_{(1)}) = I_v(\bar{\pi}_{(1)})(\text{RHC}=\text{C}=\text{CH}_2) - I_v(2e)(\text{H}_2\text{C}=\text{C}=\text{CH}_2)$ is given by Equation 96 (24).

$$\Delta I_v(\bar{\pi}_{(1)}) = 0.25 \mu(\text{R}) \text{ for allenes} \quad (96)$$

Additionally, the ionization energies of the low-energy π orbitals ($\pi_{(3)}$) correlating with the $1e$ orbital in allene (11) (Fig. 9) show a rough correlation with the group moments ($r = 0.8452$).

$$\Delta I_v(\pi_{(3)}) = 0.23 \mu(\text{R}) \text{ for allenes} \quad (97)$$

All these findings can be rationalized within the LCMO model of substituent effects on orbital energies of monosubstituted allenes $\text{RHC}=\text{C}=\text{CH}_2$ which starts from semilocalized π orbitals (group orbitals) of the fragments R and $\text{HC}=\text{C}=\text{CH}_2$.

Furthermore, it is assumed that (a) substituted allenes exist in the gas phase in one single preferred conformation and (b) that second-order inductive interactions between π levels are negligible.

The parameters of interest characterizing the different substituent effects on the orbital energies have been obtained by solving the simplified secular Equation 98 which describes three interacting π orbitals (the substituent highest-energy π orbital (π_R) and the a'' components of the allenic $1e$ and $2e$ orbitals $\pi(2e)$ and $\pi(1e)$, respectively).

$$\begin{vmatrix} (A'_C + \Delta A'_C) - \epsilon & B''_{CR} & 0 \\ B''_{CR} & A'_R - \epsilon & B'_{CR} \\ 0 & B'_{CR} & (A'_C + \Delta A'_C) - \epsilon \end{vmatrix} = 0 \quad (98)$$

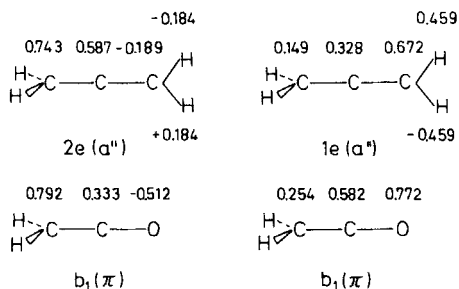


Figure 31 CNDO/S LCAO coefficients for the a'' components of the allenic e orbitals and the π orbitals in ketene.

In Equation 98 $A''_C = \langle \pi(2e) | \mathcal{H} | \pi(2e) \rangle = -10.07$ eV, $A'_C = \langle \pi(1e) | \mathcal{H} | \pi(1e) \rangle = -14.50$ eV, and $A_R = \langle \pi_R | \mathcal{H} | \pi_R \rangle$ represent the Hückel Coulomb integrals of the allenic π system and the π HOMO of the substituents. \mathcal{H} is the effective Hückel Hamilton operator. For A_R the negative vertical ionization energies of the highest occupied orbitals of the molecules HR have been used (24).

The resonance integrals $B'_{CR} = \langle \pi(2e) | \mathcal{H} | \pi_R \rangle$ and $B'_{CR} = \langle \pi(1e) | \mathcal{H} | \pi_R \rangle$ are measures of the conjugative power of the substituents. Both these resonance integrals are related to each other by the (p_z) CNDO/S LCAO coefficients $c_{\mu i}$ of the $1e$ and $2e$ orbitals of allene (11) at the center of substitution. The CNDO/S LCAO coefficients of the a'' components of the allenic e orbitals and the π orbitals of ketene (43) are given in Fig. 31.

Then, for the allenes one has

$$B'_{CR} = 0.140/0.743 \quad B''_{CR} = 0.189 B'_{CR} \quad (99)$$

From Equation 99 one may infer that the π orbitals correlating with $1e$ in allene can only be influenced to a small extent by π conjugative effects.

In the secular Equation 98 $\Delta A''_C$ and $\Delta A'_C$ represent modifications of the corresponding Coulomb integrals of the molecular skeleton owing to nonresonance interactions with the substituents.

The nonresonance interactions are separated into a short-range V_{SR} and a long-range terms V_{LR} . V_{SR} comprises the σ -inductive effect transmitted through the R-C bond in $\text{RHC}=\text{C}=\text{CH}_2$ and affecting only the carbon atom μ ($= 1'$) directly bonded to the substituent (Fig. 32). Apart from electrostatic effects this parameter also includes exchange contributions (24).

The short-range substituent effect is characterized by a parameter $\delta\alpha_\mu(\text{R})$ which may be related to the difference between the CNDO/S π (p_z) electron densities at $C_{1'}$, that is, the substituent effect $\Delta P''_{CC}(1')$ (24).

$$\delta\alpha_{\mu(\text{R})} = -6.67 \Delta P''_{CC}(1') \quad (\text{in eV}) \quad (100)$$

The σ -inductive parameters $\delta\alpha_\mu(\text{R})$ show a rough correlation with the inductive

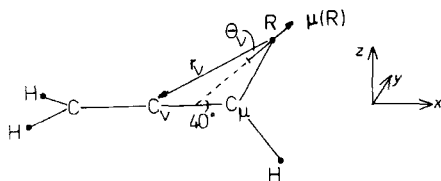


Figure 32 Definitions of quantities related to short-range and long-range inductive effects in allenes according to the D_{2d} model.

parameters α'_R (145a) which have been evaluated from electronic spectra (24).

The long-range inductive effect V_{LR} is a field effect. This field effect is evaluated on a point-dipole approximation. Then, the total inductive modification of the Coulomb integrals for the orbitals i (for arbitrary molecular classes) is given by Equation 101 (24).

$$\Delta A_C^i = c_{\mu i}^2 \cdot \delta \alpha_{\mu}(\mathbf{R}) + \sum_{\nu \neq \mu} \left(\frac{e \cdot c_{\nu i}^2}{\epsilon} \right) \frac{\mathbf{r}_{\nu} \cdot \boldsymbol{\mu}(\mathbf{R})}{r_{\nu}^3} \quad (101)$$

In Equation 101 e represents the charge of an electron, ϵ is an effective dielectric constant of the framework of the molecule which has been determined to be $\epsilon = 1.98$ (24). $\mathbf{r}_{\nu} \cdot \boldsymbol{\mu}(\mathbf{R})$ is the scalar product of the bond dipole moment $\boldsymbol{\mu}(\mathbf{R})$ of the C-R bond (as defined in Section II.B.2) and the position vector \mathbf{r}_{ν} (Fig. 32). The sum is over all atoms ν not bonded to the substituent R.

From Equation 101 (in connection with the values from Fig. 31) one can see that the ionization energies of the $\pi_{(3)}$ orbitals of allenes must be essentially determined by a long-range electrostatic field effect, as, apart from the small resonance contribution, also the short-range effect must be rather small ($c_{\mu i}^2 \approx 0.02$).

Introducing Θ_{ν} as the angle between the vectors \mathbf{r}_{ν} and $\boldsymbol{\mu}(\mathbf{R})$ one can write for the electrostatic field effect of the substituent

$$V_{LR} = - \sum_{\nu \neq \mu} \left(\frac{e c_{\nu i}^2}{\epsilon} \right) \frac{\cos \Theta_{\nu}}{r_{\nu}^2} \boldsymbol{\mu}(\mathbf{R}) \quad (102)$$

Using fixed orientations and origins for all the group moments of the different substituents (Section II.B.2) expression (102) is essentially of the form found empirically for the ionization energies $I_{\nu}(\bar{\pi}_{(1)})$ and $I_{\nu}(\pi_{(3)})$ (Equation 96 and 97).

In Table 27 a summary of the σ -inductive parameters and the resonance integrals B''_{CR} for allenes is given. These resonance integrals can be converted to values for other molecular systems with the help of the CNDO/S LCAO coefficients for atom $C_{1'}$ of the particular π MOs similar to Equation 99. For instance, in case of ketenes we have for the π HOMO

TABLE 27
Resonance and σ -Inductive Substituent Effects for the Calculations of Orbital Energies (24)
and Vertical Ionization Energies of Allenes $\text{RHC}=\text{C}=\text{CH}_2$ (24,66,70,71) (in eV)

R	$\delta\alpha_\mu(\text{R})$	B'_{CR}	A_{R}	$I_v(\pi_{(1)})$	$I_v(\bar{\pi}_{(1)})$
H	0	0		10.07	10.07
F ^a	+0.30	-1.82 ^b	-15.77		
Cl	+0.06	-1.60	-12.74	9.57	10.55
Br	+0.06	-1.41	-11.69	9.46	10.38
I	+0.03 ^c	-1.26	-10.38		
$\text{HC}\equiv\text{C}^{\text{a}}$	+0.03	-1.37	-11.40		
CN	-0.19	-1.39	-13.60	10.35	11.16
Me	+0.28	-1.00	-12.99	9.33(9.57)	10.06
Et	+0.37	-1.12	-11.65	9.22(9.42)	9.96
$\text{C}_3\text{H}_5^{\text{a}}$	+0.12	-1.29	-10.52	8.83	9.75
$\text{H}_2\text{C}=\text{CH}$	+0.17	-1.33	-10.51	8.88	10.04
Ph	+0.20	-1.27	-9.25	8.29	9.77
MeO	+0.45	-1.72	-10.96	8.75	10.33
MeS	+0.13	-1.36	-9.45	8.22	10.40
COOMe	-0.30	-1.32	-15.20	10.02	10.95

^a This work.

^b From correlation (105).

^c Estimated value.

$$B''_{\text{CR}}(\text{ketenes}) = 0.792/0.743 B''_{\text{CR}} = 1.066 B''_{\text{CR}} \quad (103)$$

The preceding three-parameter model of substituent effects on orbital energies has been used successfully for the calculations of the ionization energies resulting from the removals of electrons from π orbitals of substituted allenes (on the basis of Equation 98 and using the parameters from Table 27 and the group moments from Table 3).

If one is interested in only approximate values of the orbit energies of the π HOMOs, a reduced procedure may be used based on the "truncated" secular Equation 104. This shortened procedure reproduces the π HOMO orbital energies within 0.3 eV.

$$\begin{vmatrix} (A''_{\text{C}} + \Delta A''_{\text{C}}) - \epsilon & B''_{\text{CR}} \\ B''_{\text{CR}} & A_{\text{R}} - \epsilon \end{vmatrix} = 0 \quad (104)$$

For substituted ketenes $\text{RHC}=\text{C}=\text{O}$ Equation 104 gives the values that are listed in Table 28 ($A''_{\text{C}}(\text{ketene}) = -9.63$ eV (146)). The full procedure using a 3×3 secular equation (with $A''_{\text{C}}(\text{ketene}) = -14.60$ eV (146)) gives, for instance, for chloroketene (**251**) the value $\epsilon(\pi_{(1)}) = -9.07$ eV.

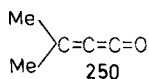
With respect to ionization energies it is interesting to note that the vertical ionization energies of the π HOMOs of dimethylketene (**45**) ($I_v(\pi_{(1)}) = 8.38$

TABLE 28
Comparisons of Calculated (Equation 104) and Experimental^a
Ionization Energies of Ketenes RCH=C=O (in eV)

Compd.	R	$-\epsilon(\pi_{(1)})$	$I_v(\pi_{(1)})$
44	Me	9.17	8.95
216	Ph	8.10	8.17
251	Cl	9.02	9.35

^a From Ref. 118.

eV (118)) and isopropylidene ketene (**250**) ($I_v(\pi_{(1)}) = 8.4$ eV (100e)) are almost identical, that is, there seems to be an only small effect of homology.



The resonance parameters B''_{CR} from Table 27 correlate linearly with the ¹³C chemical shift parameters $\mu^C(\text{R})$ for the C_{3'} atoms in monosubstituted allenes (24).

$$B''_{CR} = -1.06 - 0.04 \mu^C(\text{R}) \quad (105)$$

Therefore, the parameters B''_{CR} are related to the (group) electronegativities $\chi(\text{R})$ of the substituents (24).

For numerical calculations of orbital energies of the highest-energy occupied orbitals the CNDO/S procedure gives excellent results for allenes (24,71). Also for the ketenes **43–45**, **216**, diazomethane (**42**), thioketene (**50**), butatriene (**223**), and pentatetraene (**222**) there is an excellent agreement between I_v and $-\epsilon$ for the highest-energy occupied orbitals. These findings also give credit to the CNDO/S results for the orbital energies of ketene imine (**49**) (Section II.G.3).

For the calculations of orbital energies of lower-energy orbitals the *ab initio* STO-3G method is more appropriate (24,133,137).

For arbitrary cumulenes the ionization energies (with $I_v \leq 11.5$ eV) are related to the negative CNDO/S orbital energies according to Equation 106.

$$-\epsilon(\text{CNDO/S}) = 0.86 I_v + 1.57 \quad (106)$$

Until now there are no data on electron affinities of allenes (or other cumulenes) in the literature. From Equation 95 one would estimate a value of $A_v(3e) = -1.87$ eV for the 3e orbital in allene (**11**). This is more negative than the value found for ethylene ($A_v = -1.55$ eV (147)) by -0.32 eV. CNDO/S calculations give a difference of -0.19 eV for the LUMO orbital energies of allene (**11**) and ethylene.

The substituent effects on the electron affinities of the lowest-energy π and

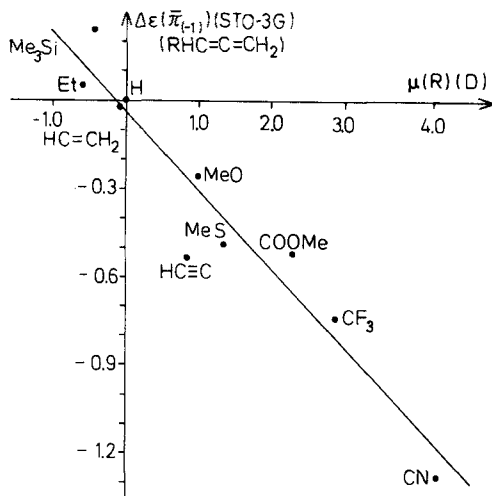


Figure 33 Relation of the substituent effects on the STO-3G $\bar{\pi}_{(-1)}$ orbital energies and the group moments of the substituents.

σ orbitals ($\pi_{(-1)}$ and $\bar{\pi}_{(-1)}$) correlating with $3e$ in **11** may be reasonably estimated using CNDO/S or STO-3G calculations.

Concerning the relations of the substituent effects to intrinsic properties of the substituents, the case of the electron affinity $A_v(\bar{\pi}_{(-1)})$ in allenes is of particular interest. From the model outlined in this section one would expect a correlation of $A_v(\bar{\pi}_{(-1)})$ with the group moments, similar to the case of $I_v(\bar{\pi}_{(1)})$. Such a correlation is observed, if the substituent effect $\Delta A_v(\bar{\pi}_{(-1)})$ is identified with that on the CNDO/S or STO-3G orbital energies $\Delta\epsilon(\pi_{(-1)})$ (Fig. 33). Omitting the chloro group one finds ($r = -0.9567$)

$$\Delta\epsilon(\bar{\pi}_{(-1)})(\text{STO-3G}) = -0.27 \mu(R) - 0.04 \quad (107)$$

which is close to the substituent effect on the orbital energies of $\bar{\pi}_{(1)}$ (Equation 96).

Concerning substituent effects the pe spectra of symmetrical alkyl carbo-diiimides (**99**) show the expected trends. As has been mentioned in Section III.B the outermost a and b orbitals of the C₂-cumulenes are accidentally degenerate.

The pe spectra of ketene imines (**140**) also show the expected features. The

R	I_v (eV)	
	194	H
252	Me	7.92
253	MeO	7.83

first band usually is observed in the range between 7.5 and 8.0 eV. The effects

of the *para* substituents in the N-aryl ketene imines **194**, **252**, **253** on the highest occupied orbitals comprising the out-of-phase combination of the nitrogen lone-pair with the C=C group orbital are rather small. Relative to N-cyclohexyl-dimethylketene imine (**214**) ($I_v = +7.85$ eV (140)) the HOMO is stabilized in the aryl compounds, probably as a result of the electron-withdrawing effect of the phenyl group relative to the alkyl group. This interpretation is supported by a decreasing ionization energy of ketene imines with increasing π donating ability of the *para* substituent.

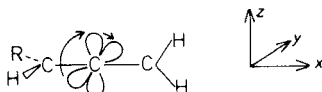
E. Excitation Energies

Electronic excitations of allenes $\text{RHC}=\text{C}=\text{CH}_2$ which are relevant for uv absorption spectroscopy in the near ultraviolet may be achieved via magnetic dipole allowed, electric dipole forbidden electronic transitions (of the $\pi \rightarrow \sigma^*(\pi, \bar{\pi}^*)$ or $\sigma \rightarrow \pi^*(\bar{\pi}, \pi^*)$ type leading to $^1A''$ excited states) or electric dipole allowed, magnetic dipole forbidden transitions (π, π^* transitions giving $^1A'$ excited states) (1c, 23, 24, 25, 71, 73). The former ones are associated with weak uv bands ($\epsilon \approx 1 - 100$) in the range of 220–300 nm, whereas the last ones correspond to strong uv bands ($\epsilon > 5000$). Usually, the two longest wavelength uv bands in monosubstituted allenes are related to $^1A''(\pi, \bar{\pi}^*)$ and $^1A''(\bar{\pi}, \pi^*)$ states.

The $^1A''(\pi, \bar{\pi}^*)$ excited states, for instance, are associated with single electronic configurations (in the sense of configuration interaction (CI)) of energies $^1\Delta E(\pi, \bar{\pi}^*)$.

$$^1\Delta E(\pi, \bar{\pi}^*) = \epsilon(\bar{\pi}^*) - \epsilon(\pi) - J(\pi, \bar{\pi}^*) + 2K(\pi, \bar{\pi}^*) \quad (108)$$

In Equation 108 J and K are the Coulomb and the exchange integrals for the MOs π and $\bar{\pi}^*$, respectively. To a good approximation these $\pi, \bar{\pi}^*$ and $\bar{\pi}, \pi^*$ transitions are localized at the allenic central atom and thus resemble atomic $p_z \rightarrow p_y$ and $p_y \rightarrow p_z$ quantum jumps, respectively (1c, 24, 73). Therefore, these electronic transitions in allenes may be compared with the n, π^* transitions of carbonyl compounds.



Owing to different localization properties of the orbitals in the other cumulenes this last statement is no longer valid for all the cumulenes under consideration. Evidently, the circulating charge densities associated with the $\pi, \bar{\pi}^*$ and $\bar{\pi}, \pi^*$ transitions in allenes induce a magnetic field in the x direction.

In most cases (24) the uv band positions $^1\Delta E(\pi, \bar{\pi}^*)$ (in eV) of allenes

RHC=C=CH₂ correlate with the ionization energies $I_v(\pi)$ of the π HOMOs.

$${}^1\Delta E(\pi, \bar{\pi}^*)(\text{RHC}=\text{C}=\text{CH}_2) = 0.53 I_v(\pi) - 0.26 \quad (109)$$

Consequently, for both these molecular properties the same kinds of substituent effects are operative.

A qualitative interpretation of Equation 109 is straightforward. Accumulating π electron density at the allenic central atoms through π donors increase the facilities for the $\pi, \bar{\pi}^*$ electronic jumps, that is, the uv band shifts of the $\pi, \bar{\pi}^*$ bands to longer wavelengths parallel qualitatively the π donor characteristics of the substituents.

In general, the energetical order of the ${}^1A''$ excited states in allenes is ${}^1A''(\pi, \bar{\pi}^*) < {}^1A''(\bar{\pi}, \pi^*)$ for allenes with π donors and ${}^1A''(\pi, \bar{\pi}^*) > {}^1A''(\bar{\pi}, \pi^*)$ for acceptors (23,24,71), whereas for mesomerically rather indifferent substituents (Ph, HC≡C) both these excited states have comparable energies (24,71).

If one uses the quantum-chemical expression (108) for an interpretation of Equation 109, further insights are possible. According to Equations 108 and 109 the term $[\epsilon(\bar{\pi}^*) - J(\pi, \bar{\pi}^*) + 2K(\pi, \bar{\pi}^*)]$ must be constant (or parallel $\epsilon(\pi)$). On the other hand, $\epsilon(\bar{\pi}^*)$ varies considerably with the substituents' group moments (Equation 107). Consequently, the change of $\epsilon(\bar{\pi}^*)$ must be balanced by the changes in the Coulomb and exchange integrals J and K , respectively, so that $[\epsilon(\bar{\pi}^*) - J(\pi, \bar{\pi}^*) + 2K(\pi, \bar{\pi}^*)]$ remains constant (or parallels $\epsilon(\pi)$). CNDO/S calculations support the assumption that the last mentioned term remains constant. A discussion of the relative importance of polar and resonance substituent effects on the $\pi, \bar{\pi}^*$ uv bands in allenes therefore would be bound to underestimate the relevance of electrostatic field effects, as such a treatment would reflect the situation expressed by Equation 109.

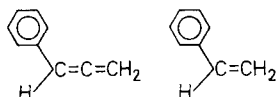
A calculation of the $\pi, \bar{\pi}^*$ transition energies with the CNDO/S procedure fails to give numerical agreements with the experimental values, as in CNDO theories the exchange integrals involving p_z and p_y AOs vanish identically. However, the CNDO/S method usually gives the correct sequences of excited states for the individual molecules and reproduces the substituent effects on the ${}^1A''(\pi, \bar{\pi}^*)$ and ${}^1A''(\bar{\pi}, \pi^*)$ excited states energies ${}^1\Delta E(A'')$ (in eV) of allenes (23-25,71) fairly well ($r = 0.8795$).

$${}^1\Delta E(A'') = 1.14 \widetilde{{}^1\Delta E}(A'')(CNDO/S) + 0.16 \text{ for allenes} \quad (110)$$

Phenylallenes have been omitted in the preceding regression, as for these molecules the CNDO/S calculations reproduce the experimental values satisfyingly (71).

The substituent effects on the π, π^* uv bands of monosubstituted allenes (24,25,71) follow the lines observed for corresponding ethylenes (Equation 63).

The π, π^* bands (excited state ${}^1A'(\pi, \pi^*)$) in allenes contain a small admixture of the $\bar{\pi}, \bar{\pi}^*$ excitations (1c, 23, 24, 71, 73). However, this admixture has only a very small influence on the energies. Therefore, the identical uv band positions of the π, π^* bands in allenes and ethylenes may be compared referring to the single electronic excitations $\pi \rightarrow \pi^*$ of energies $\Delta E(\pi, \pi^*)$. Then, in case of phenylcompounds one sees that the identical π, π^* uv band positions are due to comparable shifts of the π HOMOs and π LUMOs in phenylallene (**16**) and styrene and that in both the molecules the interaction terms $[-J(\pi, \pi^*) + 2K(\pi, \pi^*)]$ are almost identical which may also be inferred from the different ionization energies of both these phenylderivatives and Equation 95.



$\epsilon(\pi^*) - \epsilon(\pi) - J(\pi, \pi^*) + 2K(\pi, \pi^*)$		
$\frac{\Delta E(\pi, \pi^*)}{\Delta E(\pi, \pi^*)}(\text{CNDO/S})$	5.013	4.937
$\Delta E(\pi, \pi^*)(\text{exp.})$	5.00	5.04
$\epsilon(\pi^*)$	-0.895	-1.018
$\epsilon(\pi)$	-8.749	-8.874
$I_v(\pi)$	8.29	8.48
$-J(\pi, \pi^*) + 2K(\pi, \pi^*)$	-2.917	-2.843

F. Nuclear Magnetic Resonances

1. Chemical Shifts

Apart from its potential in structure elucidation nuclear magnetic resonance, especially ${}^{13}\text{C}$ nmr, is an interesting tool in dealing with questions of electronic structures and bonding.

It is the intention of this section to give a summary of interpretations of nmr effects (chemical shifts and coupling constants) observed in cumulenes. Since the general physical theory of nuclear magnetic resonance for complex molecules comprises several molecular variables emphasis is on discussions of well-defined situations which enable valid comparisons and semiquantitative deductions to be made. Though the relationships of chemical shifts to charge densities continues to receive attention, it can be said that chemical shifts do not correlate in general with charge densities (4c).

Direct quantum-theoretical calculations of chemical shifts, in particular ${}^{13}\text{C}$ - and ${}^{14}\text{N}$ - (${}^{15}\text{N}$ -) chemical shifts on an *ab initio* or semiempirical CNDO/S level give reasonable agreements with available experimental data in most cases (148). Such direct calculations are reported in the literature for alkylallenes

(149), fluoroallenes (19) for the carbon shifts and diazomethane (42) (148d) for the nitrogen shifts. These calculations, however, neglect structural aspects and do not offer relations of the observable chemical shifts to intrinsic properties of the substituents or other chemically interesting indices.

To interpret chemical shifts in terms of substituent constants or quantum-chemical indices it suffices to start from the most general expression (111) ("Ramsey's formula" (60a)) for the nmr shielding constant σ_A of an atom A in a molecule, where σ_A represents the trace of a tensor.

$$\sigma_A = \sigma_A^d + \sigma_A^p \quad (111)$$

In Equation 111 the diamagnetic shielding constant σ_A^d is similar to Lamb's formula for atoms and involves only the ground-state molecular wavefunction $|\Psi_0\rangle$.

$$\sigma_A^d = \frac{e^2}{3 m c^2} \sum_i \langle \Psi_0 | r_i^{-1} | \Psi_0 \rangle \quad (112)$$

In Equation 112 e , m , c are the electronic charge, electronic mass, and the speed of light, respectively. The sum is over all electrons in the molecule.

The paramagnetic term σ_A^p involves the mixing of ground-state $|\Psi_0\rangle$ and excited states $|\Psi_n\rangle$ (of energies E_0 and E_n , respectively) by the applied magnetic field. As this last term is derived via quantum-theoretical perturbation theory σ_A^p is a sum over products of matrix elements of appropriate operators \mathfrak{A} and \mathfrak{B} divided by the corresponding energy term ($E_n - E_0$):

$$\sum_n \langle 0 | \mathfrak{A} | n \rangle \langle n | \mathfrak{B} | 0 \rangle (E_n - E_0)^{-1}.$$

The diamagnetic shielding term σ_A^d of atom A is a property which is assumed (150) to depend essentially only on the kinds of nearest neighbor atoms B , that is, the ones bonded directly to A .

Though σ_A^d may influence the absolute resonance position of an atom A in nmr experiments it may be stated that the substituent effects on ^{13}C and ^{14}N chemical shifts are largely determined by σ_A^p for all those atoms whose neighbor topologies are retained upon substitution, for instance C_2' and C_3' in monosubstituted allenes.

To evaluate σ_A^p it is necessary to have a detailed knowledge of the eigenfunctions of all the excited electronic states (including the continuum). This is obviously impracticable for most cases. Therefore, approximations are required.

The approximate LCAO MO theory of nmr shielding by Karplus and Pople (151) contains contributions from (MO) excitation energies $\Delta E(i \rightarrow j)$ and from LCAO coefficients as well as electron densities, A reduction in $\Delta E(i \rightarrow j)$ increases the contribution of the corresponding component to σ_A^p , whereas a

general decrease in the magnitude of the LCAO coefficients acts in the opposite sense.

Only in special cases of extremely low-lying excited states (resulting from magnetically allowed transitions) chemical shifts follow changes in the longest-wavelength transitions ($\lambda(i \rightarrow j) \sim 1/\bar{\nu}(i \rightarrow j)$). In general, all the factors listed previously influence nmr chemical shifts simultaneously.

If, on the other hand, there exists a series of related molecules with substituents of similar character, for example, σ -inductive alkyl groups, so that it may be assumed that for all these molecules the relevant excited states have comparable magnitudes, one may replace all of the electronic excitation energies ($E_n - E_0$) by a single average value ΔE^{av} ("average excitation energy (AEE) approximation"). This, then, simplifies the discussions of the substituent effects on nmr chemical shifts considerably. For such cases it may be expected that there exist relations of nmr chemical shifts to electron densities. Within the AEE approximation the Karplus-Pople equations for σ_A^p reduce to the well-known expression (113) (with the symbols having their usual meanings (151)).

$$\sigma_A^p = - \frac{e^2 \hbar^2}{2m^2 c^2 \Delta E^{av}} \langle r^{-3} \rangle_{2p} \sum_B Q_{AB} \quad (113)$$

The link of σ_A^p to electron densities is essentially given by the dimensions of the $2p$ orbital (in the $\langle r^{-3} \rangle_{2p}$ term). The sum $\sum Q_{AB}$ involves changes in bond orders of the atom A to adjacent atoms B . For a series of closely related molecules variations in the sum over Q_{AB} may be assumed to be small in comparisons to variations in $\langle r^{-3} \rangle_{2p}$.

If we refer to the three parameters (excitation energies, electron densities, and bond orders) which determine the substituent effects on ^{13}C (and ^{14}N) chemical shifts we have seen that in case of thioketenes with their extreme long-wavelength transitions excitation energies govern the behavior of the ^{13}C chemical shifts of the central atoms (Section II.G.1, Equation 82).

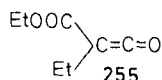
Also in case of the ^{13}C chemical shifts of C_2 in ketenes and ^{14}N chemical shifts of diazocompounds (relative to NH_4^+) there are qualitative trends following the longest-wavelength uv bands.

	δ_{C_2} (ppm)	λ_{max} (nm)	Ref.
$\text{H}_2\text{C}=\text{C}=\text{O}$ 43	194.0	320	(38c,38e)
$\text{Me}_2\text{C}=\text{C}=\text{O}$ 45	206.2	325	(113)
$\text{Ph}_2\text{C}=\text{C}=\text{O}$ 46	201.3	400	(116)
$\text{Me}_3\text{SiHC}=\text{C}=\text{O}$ 47	179.3	292	(98)

	$\delta_{N_2'}$ (ppm)	$\delta_{N_3'}$ (ppm)	λ_{\max} (nm)	Ref.
$H_2C=N=N^{\oplus}N^{\ominus}$ 42	265	369	400	(94a)
$EtOOCCHC=N=N^{\oplus}N^{\ominus}$ 254	245	336	353	(94a)
	242.69	358.92		(94b)
$Ph_2C=N=N^{\oplus}N^{\ominus}$ 220	274	414	525	(94a)

In case of diazocompounds the ^{14}N chemical shifts of both the nitrogen atoms follow qualitatively the uv band positions.

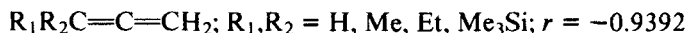
In case of ketenes the corresponding trend seems to be restricted to alkylketenes and trimethylsilylketene (**47**) whose longest-wavelength uv band is estimated from CNDO/S calculations (and additionally from correlation (110)). The calculated uv band position of **47** seems to be reasonable, as **47** is a colorless liquid (143b), whereas in general ketenes are yellow or orange. A hypsochromic shift of the longest-wavelength uv band of ketene (**43**) is also observed in carboalkoxy substituted ketenes, such as **255** which is a colorless liquid (152). The same substituent effect on the longest-wavelength uv bands is also observed in diazocompounds (**42** \rightarrow **254**).



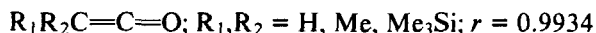
The example of diphenylketene (**46**) shows that, in general, the $^{13}C_{2'}$ chemical shifts of ketenes are not only determined by excitation energies. The same holds for allenes, where the situation becomes even more complex, as there are (at least) two low-energy uv bands which are associated with $^1A''$ excited states and which are separated by only 4000–9000 cm^{-1} and sometimes are of comparable energy (23,24,71).

Therefore, it seems quite natural that one has to restrict oneself to allenes and ketenes with certain types of ligands (e.g., alkyl groups and Me_3Si , mesomeric groups bonded via carbon to the cumulenic skeleton (Ph, COOH, COOMe, CN), and mesomeric groups with heteroatoms (F, Cl, MeO, MeS)), if one wants to establish relations of ^{13}C chemical shifts of the allenic and kетенic central atoms to total CNDO/S electron densities $P_{CC}(2')$ (Equations 114–117).

$$\delta_{C_{2'}} = -106.50 P_{CC}(2')(\text{CNDO/S}) + 631.64 \quad (114)$$



$$\delta_{C_{2'}} = 416.28 P_{CC}(2')(\text{CNDO/S}) - 1335.91 \quad (115)$$



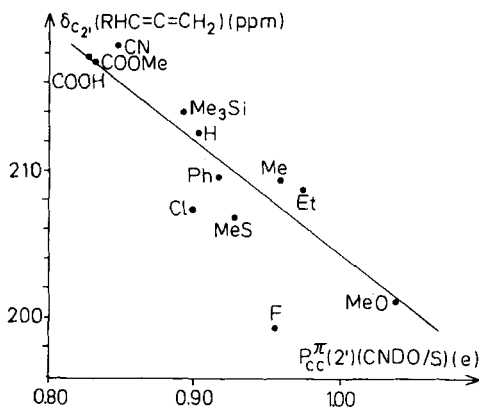


Figure 34 Correlation of the ^{13}C chemical shifts of the allenic central atoms and their CNDO/S π electron densities.

$$\delta_{C_2'} = -401.39 P_{CC}(2')(\text{CNDO/S}) + 1789.62 \quad (116)$$

$\text{RHC}=\text{C}=\text{CH}_2$; R = Ph, COOMe, COOH, CN; $r = -0.9927$

$$\delta_{C_2'} = -94.20 P_{CC}(2')(\text{CNDO/S}) + 578.04 \quad (117)$$

$\text{RHC}=\text{C}=\text{CH}_2$; R = F, Cl, MeO, MeS; $r = -0.9904$

On the other hand, there are rather fair linear correlations for $\delta_{C_2'}$ of monosubstituted allenes (Fig. 34) and ketenes with arbitrary substituents with the π electron densities $P_{CC}^{\pi}(2')$. Only the fluoro group exhibits a larger deviation.

$$\delta_{C_2'}(\text{RCH}=\text{C}=\text{CH}_2) = -77.18 P_{CC}^{\pi}(2') + 281.48 \quad (118)$$

R arbitrary; $r = -0.9081$

$$\delta_{C_2'}(\text{RHC}=\text{C}=\text{O}) = 223.20 P_{CC}^{\pi}(2') - 8.19 \quad (119)$$

R = H, Me, Me₃Si; $r = 0.9987$

Another quantum-chemical index that is also of relevance for chemical reactivity and which involves intuitively relationships to the low-energy uv excitations $\pi \rightarrow \bar{\pi}$ in allenes and ketenes are the π HOMO electron densities $c_{2',\pi}^2$, that is, the squares of the CNDO/S LCAO coefficients for the central atoms of the π HOMOs. The ^{13}C chemical shifts of allenes and ketenes exhibit also relations to these last indices, if the substituents are differentiated as has been done for P_{CC} .

Further semiquantitative insights into the natures of the substituent effects on the ^{13}C chemical shifts of allenes may be obtained from substituent parameter

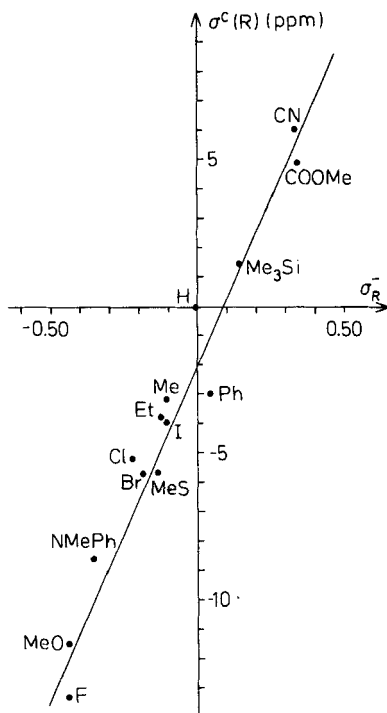


Figure 35 Correlation of the substituent effects on the ^{13}C chemical shifts of the allenic central atoms and the resonance substituent constants σ_R^- ($\sigma_R^-(\text{NMePh}) \approx \sigma_R^-(\text{NHCOMe})$).

approaches or DSP approaches, respectively. The substituent effects $\Delta\delta_{C_2} = \sigma^C(\text{R})$ (Table 7) on the central allenic carbon resonances exhibit a close relationship to the resonance constants σ_R^- ($r = 0.9786$) (Fig. 35),

$$\Delta\delta_{C_2} = \sigma^C(\text{R}) = 22.08 \sigma_R^- - 1.75 \quad (120)$$

A full DSP analysis gives ($R^2 = 0.9508$)

$$\sigma^C(\text{R}) = -1.63 + 0.04 \sigma_I + 20.85 \sigma_R^- \quad (121)$$

that is, the substituent effect on the ^{13}C chemical shifts of the allenic central atoms seems to be rather insensitive to polar effects. This finding is in contrast to substituent effects on ^{13}C chemical shifts of the *para* carbon atoms of benzenes RPh, where one observes a more pronounced influence of σ_I ($\Delta\delta_{C_p} = 4.1 \sigma_I + 19.7 \sigma_R^0(4a)$).

An interpretation of the pair-terms $\tau^C(\text{R}_i, \text{R}_j)$ (Equation 37) for the calculations of ^{13}C chemical shifts has been given in Ref. 8, at least for some cases where one can factor $\tau^C(\text{R}_i, \text{R}_j)$ into a product ($\tau^C(\text{R}_i, \text{R}_j) = \delta^C(\text{R}_i) \cdot \delta^C(\text{R}_j)$).

Then, for a given mesomeric substituent M $\tau^C(M,R)$ correlates with Taft's steric constants $E_s(R)$ (8). In particular, for phenylallenes $\tau^C(Ph,R)$ may be related to the angle of twist $\Theta(Ph,R)$ of the phenyl group which results from the steric bulk of the neighboring ligand (1b).

$$\tau^C(Ph,R) = 3.59 \sin 2 \Theta(Ph,R) \quad (122)$$

At this point it should be noted again that the pair-terms in the treatments of molecular properties of allenes are the consequences of the geometrophysical model which is independent from any considerations about distances of ligands, topological effects, steric bulks of ligands, and so on. Only for special cases the numerical values of the pair-terms may reflect distance and volume effects, that is, an a posteriori interpretation of the pair-terms hints to steric effects.

The substituent effect $\Delta\delta_{C\gamma} = \mu^C(R)$ on the ^{13}C resonances of the γ carbon atoms in monosubstituted allenes has been suggested to be related to the group electronegativities $\chi(R)$ according to Equation 123 (assuming $\chi(H) = 2.20$).

$$\mu^C(R) = 22.20 [1 - \exp - (\chi(R) - 2.20)] \quad (123)$$

As the proton chemical shifts δ_{H_4} of the methylene group protons are related to the ^{13}C chemical shifts $\delta_{C\gamma}$ (Equation 41), also the H_4 proton chemical shifts of monosubstituted allenes correlate with the group electronegativities (10).

Interpretations of the substituent effects on the ^{13}C resonances of the α carbon atoms (C_1) are complicated, as the neighbor topology of these atoms are often changed and, therefore, the overall observable effects are due to changes in the paramagnetic and the diamagnetic shielding constants. If one restricts oneself to systems where the neighbor topology is retained upon substitution, for example, compounds with only substituents bonded via carbon to the allenic skeleton, the substituent constants $\beta^C(R)$ exhibit relations to the polar substituent constants σ_I (8). Correlations with σ_I are also observed for the α proton chemical shifts (δ_{H_2}) in alkylallenes (10).

If one restricts oneself to substituents bonded only via first- and second-row atoms (F, C, O, N, Si, S, Cl) to the allenic skeleton (omitting Br and I with their pronounced "heavy atom" shifts (61)) some more insights into the ^{13}C nmr substituent effects on the α carbon atoms may be obtained. For this purpose one can use the approximation for σ_A^d as proposed by Flygare and Goodisman (150b).

$$\sigma_A^d = \sigma_A^d(\text{free atom}) + \frac{e^2}{3mc^2} \sum_{B \neq A} \frac{Z_B}{R_{AB}} \quad (124)$$

In Equation 124 σ_A^d (free atom) is constant for the atom A , Z_B the nuclear charge of atom B , and R_{AB} is the bond distance between the atoms A and B . The sum is over all atoms B which are directly linked to A .

TABLE 29
Reduced Substituent Effects on α Carbon Atoms in Monosubstituted
Allenes $\text{RHC}=\text{C}=\text{CH}_2$ (in ppm)

R	$[\beta^C(\text{R})]$	R	$[\beta^C(\text{R})]$
Me	+39.1	MeO	+94.5
Et	+46.5	MeS	+91.0
Ph	+48.6	F	+109.0
COOMe	+41.2	Cl	+97.5
CN	+22.3	Me ₃ Si	+69.8

According to Equation 124 the diamagnetic shielding terms for the $\text{C}_{1'}$ atoms differ only in the expression $Z_{R'}/R_{R'C}$ for the monosubstituted allenes, where R' denotes the atom of the substituent R which is bonded to $\text{C}_{1'}$. Then, one can introduce "reduced" substituent constants (125) which give only the paramagnetic shielding contribution to the $\text{C}_{1'}$ resonance; that is, for the allenes we have

$$[\beta^C(\text{R})] = \beta^C(\text{R}) + \frac{e^2}{3mc^2} \left[\frac{Z_{R'}}{R_{R'C}} - \frac{Z_H}{R_{HC}} \right] \quad (125)$$

In Table 29 a summary of such "reduced" substituent effects $[\beta^C(\text{R})]$ on ^{13}C chemical shifts of α carbon atoms of allenes is given.

Irrespective of the crudeness of approximation (124) for the calculations of $[\beta^C(\text{R})]$ one may conclude that $[\beta^C(\text{R})]$ is not governed by (group) electronegativities of the substituents.

If one differentiates the substituents under consideration and restricts oneself to the $[\beta^C(\text{R})]$ constants of the heterosubstituents, a DSP approach gives the correlation (126a) ($R^2 = 0.9752$).

$$[\beta^C(\text{R})] = 75.75 + 39.82 \sigma_I - 22.06 \sigma_R^- \quad (126a)$$

All the heterosubstituents are of the $-I^+$ - or $+I^-$ -type (37a) having σ_I and σ_R^- constants of different signs. These types of substituents affect the σ electron density and the π electron density at $\text{C}_{1'}$ in the same way. On the other hand, as the other substituents bonded via carbon to the allenic skeleton are of the $+I^+$ - or $-I^-$ -type which influence the σ electron density and the π electron density at $\text{C}_{1'}$ differently, it seems quite natural that the constants $[\beta^C(\text{R})]$ for these last groups exhibit another relation, (126b) ($R^2 = 0.8260$) to σ_I and σ_R^- .

$$[\beta^C(\text{R})] = 48.65 - 83.31 \sigma_I + 62.96 \sigma_R^- \quad (126b)$$

In this way all the ^{13}C SCS of allenes ($\beta^C(\text{R})$, $\sigma^C(\text{R})$, and $\mu^C(\text{R})$) have been related to usual substituent constants.

A detailed discussion of substituent effects on nmr chemical shifts in butatrienes is only possible for the proton chemical shifts. As the difference in the

^1H nmr resonances for the remote *Z* and *E* protons (H_4 and H_3 , respectively) is very small, the stereochemical positions of these hydrogen atoms may be disregarded in butatrienes to a good approximation, if substituent effects are taken into consideration. Then, it turns out that in butatrienes the δ proton chemical shifts are related to the (CNDO/S) π electron densities at the neighboring carbon atoms C_4' ($r = -0.8877$).

$$\delta_{\text{H}_4}(\text{RHC}=\text{C}=\text{C}=\text{CH}_2) = -5.58 P_{\text{C}_4'}^{\pi}(\text{CNDO/S}) + 11.04 \quad (127)$$

2. Nuclear Spin-Spin Coupling Constants

Substituent effects on spin-spin coupling constants (60) of unsaturated molecules are usually discussed in terms of factors that influence primarily the σ electronic structures of the compounds; that is, they are related to polarities, electronegativities, and aspects of hybridizations. For one-bond couplings involving only carbon and hydrogen atoms it is assumed that of the several terms that may influence the spin-spin couplings the Fermi contact term is dominant (60,61,153). A MO treatment of Ramsey's second-order treatment of the couplings (60*b*,60*c*) relates the coupling constants $^1J(\text{AB})$ of the nuclei *A* and *B* via the Fermi contact term to the square of the atom *A* *s*-atom *B* *s* element of the first-order density matrix, that is, to the square of the bond orders P_{sAsB}^2 (Equation 22) and a factor $f_A f_B$ which involves the total electron densities of the atoms *A* and *B* (153). The expression $f_A f_B P_{sAsB}^2$ includes changes in hybridizations and effective nuclear charges, as P_{sAsB}^2 reflects the percent *s*-character of the atoms *A* and *B* and the term f_A is related to the effective nuclear charge of *A* via the electron density (153).

In general, the electron density factor $f_A f_B$ is assumed to be more of a correction than a dominant influence for spin-spin couplings (153). Overall trends of substituent effects on one-bond couplings follow essentially changes in P_{sAsB}^2 . Neglecting problems associated with the signs of the coupling constants and the question of whether only the Fermi contact term or also the orbital and spin dipolar terms contribute to the spin-spin mechanism variations in P_{sAsB}^2 often reflect substituent effects on long-range couplings $^nJ(\text{AB})$ ($n \geq 2$).

More empirical approaches relate coupling constants $^nJ(\text{AB})$ ($n \geq 1$) to the products of the electron densities $P_{AA} P_{BB}$ of the atoms involved in the couplings (64) or differences in P_{AA} and P_{BB} (11).

Furthermore, it has been shown recently (154) that (one-bond and long-range) coupling constants may be related to Mulliken overlap populations Q_{sAsB} obtained from ab initio MO procedures.

For vicinal proton-proton couplings, in particular, correlations with the π bond orders between the carbon atoms which are linked to the relevant protons are observed (155).

In most cases, carbon-carbon coupling constants may also be related to

TABLE 30
 One-Bond Coupling Constants in Cumulenes (in Hz)

Compd.		$^1J(^{13}\text{CH})$	Ref.	$^1J(^{13}\text{C}^{13}\text{C})$	Ref.
	$\text{H}_2\text{C}=\text{CH}_2$	+156.4	61	+67.2	62a
11	$\text{H}_2\text{C}=\text{C}=\text{CH}_2$	+168.2	61	+98.7	157
223	$\text{H}_2\text{C}=\text{C}=\text{C}=\text{CH}_2$	+170.9	123		
43	$\text{H}_2\text{C}=\text{C}=\text{O}$	+171.5	89c,89d		
42	$\text{H}_2\text{C}=\overset{\oplus}{\text{N}}=\overset{\ominus}{\text{N}}$	+195.1	158	-20.2 ^{a,b}	156

^a $^1J(^{13}\text{C}^{15}\text{N}), ^1J(^{13}\text{C}^{14}\text{N}) = +14.4$ Hz.

^b $^1J(^{13}\text{C}^{15}\text{N}) = -24.0$ Hz (95).

$P_{s,ASB}^2$ or hybridizations, respectively (62,153), as also in these cases the Fermi contact term is dominant.

The situation for carbon–nitrogen couplings is complicated (63b). Concerning one-bond carbon–nitrogen couplings it has been suggested that the Fermi contact term is dominant for all CN systems for which isosteric CC systems exist (156). In particular, in most CN systems with formal lone-pairs apart from the Fermi contact term the orbital and spin dipolar terms are operative and non-negligible (63b,156).

In Table 30 a summary of one-bond CH and CC coupling constants of cumulenes is given. For comparisons also corresponding values for ethylene are listed. The one-bond carbon–proton spin–spin coupling constants of the methylene systems $\text{H}_2\text{C}=\text{T}$ in Table 30 may be related to the square of the carbon $2s$ -hydrogen $1s$ bond orders according to Equation 128 ($r = 0.9441$).

$$^1J(^{13}\text{CH})(\text{H}_2\text{C}=\text{T}) = 644.1 P_{s,CH}^2(\text{CNDO/S}) - 35.1 \quad (128)$$

From Equation 128 one may estimate the one-bond CH couplings for the other methylene systems considered in this work. The calculated coupling constants of some cumulenes are given in Table 31.

The calculated value of **49** may be compared with the experimental CH coupling of N-phenyl-ketene imine (**188**) ($^1J(^{13}\text{CH}) = 172.0$ Hz (89b)). If one assumes a substituent effect of -5 Hz for the phenyl group as in phenylallene

 TABLE 31
 Calculated (Equation 128) One-Bond Coupling Constants in Cumulenes (in Hz)

Compd.		$^1J(^{13}\text{CH})$	Compd.		$^1J(^{13}\text{C}^{13}\text{C})^a$
49	$\text{H}_2\text{C}=\text{C}=\text{NH}$	+175.3	11	$\text{H}_2\text{C}=\text{C}=\text{CH}_2$	+108.5
50	$\text{H}_2\text{C}=\text{C}=\text{S}$	+159.4	43	$\text{H}_2\text{C}=\text{C}=\text{O}$	+113.3
222	$\text{H}_2\text{C}=\text{C}=\text{C}=\text{C}=\text{CH}_2$	+164.9	223	$\text{H}_2\text{C}^*=\text{C}^*=\text{C}=\text{CH}_2$	+120.7

^a Calculated values from Ref. 153b.

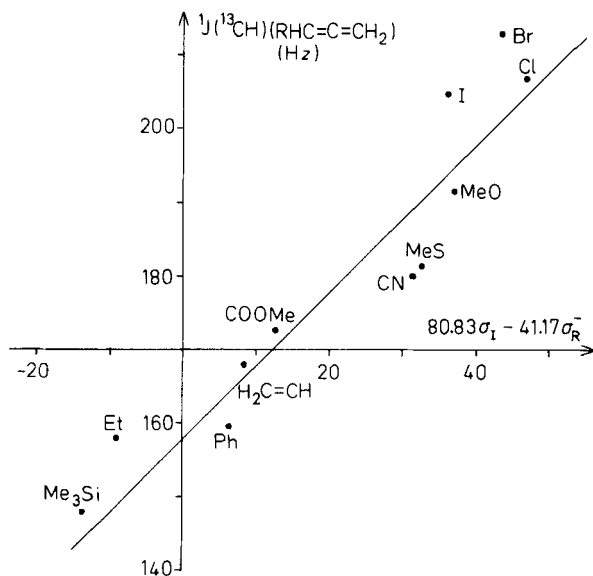


Figure 36 DSP correlation for one-bond carbon-proton coupling constants of allenes.

(16) (Table 9) an estimate of $^1J(^{13}\text{CH})$ for **49** would give a value of 177 Hz which is close to the calculated value for **49** in Table 31.

Concerning the two different one-bond carbon-proton coupling constants $^1J(^{13}\text{C}_1\text{H}_2)$ and $^1J(^{13}\text{C}_3\text{H}_3)$ in monosubstituted allenes $\text{RHC}=\text{C}=\text{CH}_2$ the correlation of $^1J(^{13}\text{CH})$ and P_{SCSH}^2 is of a poor quality, if all the first-row and second-row substituents are taken into consideration (54a). Only the coupling constants $^1J(^{13}\text{C}_1\text{H}_2)$ for first-row substituents may be adequately related to P_{SCSH}^2 (54a). This last correlation can be improved, if the factor f_{CFH} is additionally taken into account.

On the other hand, it has turned out that both the one-bond carbon-proton coupling constants of monosubstituted allenes are correlated with the Mulliken overlap populations Q_{SCSH} obtained from ab initio STO-3G calculations ($r = 0.9330$). Correlation (129) includes first- and second-row substituents (54b).

$$^1J(^{13}\text{CH})(\text{RHC}=\text{C}=\text{CH}_2) = 1064.9 Q_{SCSH}(\text{STO-3G}) - 142.0 \quad (129)$$

In Ref. 54a it has been suggested that $^1J(^{13}\text{C}_1\text{H}_2)$ may be roughly related to the polar substituent constants σ_I , if one differentiates between $-I^-$ (and $+I^-$) substituents and $-I^-$ (and $+I^+$) substituents. If one omits the hydrogen atom in the regression a DSP approach relates the one-bond carbon-proton coupling constants $^1J(^{13}\text{C}_1\text{H}_2)$, that is, the substituent constants $\kappa^J(\text{R})$ (Table 9), to σ_I and σ_R^- ($R^2 = 0.8573$) (Fig. 36).

TABLE 32
 CNDO/S Total and π Electron Densities of Ketenes $R_1R_2C=C=O$ and Thioketene

Compd.	R_1	R_2	$P_{CC}(1')$	$P_{CC}(2')$	$P_{OO}(3')$	P_{HH}	$P_{CC}^*(1')$	$P_{CC}^*(2')$	$P_{OO}^*(3')$
43	H	H	4.190	3.673	6.211	0.963	1.381	0.902	1.716
44	Me	H	4.184	3.694	6.225	0.967	1.351	0.935	1.723
45	Me	Me	4.118	3.703	6.241		1.325	0.963	1.730
47	Me ₃ Si	H	4.239	3.640	6.209	0.956	1.315	0.841	1.668 ^a
			4.232	3.698	6.231	0.980	1.389	0.905	1.705 ^b
264	COOH	H	4.135	3.628	6.172	0.962	1.340	0.859	1.678
216	Ph	H	4.142	3.659	6.214	0.966	1.341	0.907	1.698
201 ^c	Ph	Me	4.098	3.691	6.226				
50 ^d	H	H	3.953	4.019	6.149	0.940	0.893	1.047	2.060 ^a

^a CNDO/S calculation including d orbitals.

^b CNDO/S calculation neglecting d orbitals.

^c Dihedral angle $\theta = 30^\circ$.

^d Thioketene, $P_{OO} \rightarrow P_{SS}$.

$${}^1J({}^{13}C_1, H_2)(RHC=C=CH_2) = 157.92 + 80.83 \sigma_I - 41.17 \sigma_R^- \quad (130)$$

This is a surprising result, not so much with respect to the fact that the resonance effect σ_R^- has an influence on the coupling constants (which is expected from the factor $f_C f_H$), but concerning the amount of the contribution of σ_R^- ($\lambda = -0.51$).

Substituent effects on one-bond carbon-proton coupling constants in diazocompounds seem to be similar to those in allenes. For instance, ${}^1J({}^{13}CH)$ in diazo acetic acid ester (**254**) is increased relative to the value in diazomethane (**42**) by about 8 Hz ($\delta_C = 46.3$ ppm (89b), ${}^1J({}^{13}CH) = 203.3$ Hz for **254** (94b)).

One-bond carbon-carbon coupling constants ${}^1J({}^{13}C^{13}C)$ also show good correlations with P_{SCSC}^2 (153b).

If one assumes a value of ${}^1J({}^{13}C^{13}C) = 104$ Hz for ketene (**43**) which follows from the calculated values in Table 31 (${}^1J({}^{13}C^{13}C)$ (**43**) = ${}^1J({}^{13}C^{13}C)$ (**11**) + 5 Hz), one obtains Equation 131. It is based upon the couplings of ethylene, allene, and ketene.

$${}^1J({}^{13}C^{13}C) = 834.8 P_{SCSC}^2 (\text{CNDO/S}) - 32.3 \text{ for cumulenes} \quad (131)$$

From correlation (131) a value of ${}^1J({}^{13}C^{13}C) = 97.2$ Hz for the C_1, C_2' coupling in butatriene (**223**) may be deduced.

Electron density effects on carbon-carbon coupling constants in cumulenes seem to play a minor role. For instance, there are observed almost no effects on the carbon-carbon couplings comparing allene (**11**) and 1,1-dimethylallene (**2**) (${}^1J({}^{13}C_2, {}^{13}C_3) = +99.5$ Hz (159)).

The one-bond carbon-nitrogen-15 spin-spin couplings in diazocompounds

are also dominated by the Fermi contact term (94*b*,156), that is, one may expect relationships of ${}^1J({}^{13}\text{C}^{15}\text{N})$ to P_{SCSN}^2 , irrespectively of the negative sign of ${}^1J({}^{13}\text{C}^{15}\text{N})$ in diazocompounds. Apart from diazomethane (**42**) (Table 30) there is only one further compound for which a carbon–nitrogen coupling is reported, namely diazo acetic acid ester (**254**) (${}^1J({}^{13}\text{C}^{15}\text{N}) = -21.4$ Hz (94*b*,95)).

Despite the progress made in theoretical treatments of spin–spin couplings (160) empirical correlations between the couplings and structural and theoretical parameters remain useful for larger chemically relevant molecules. In particular, these empirical correlations often allow rather precise numerical predictions.

In monosubstituted allenes the two-bond carbon–proton couplings ${}^2J({}^{13}\text{C}_2\text{H}_2)$ exhibit a pronounced substituent effect, whereas the couplings ${}^2J({}^{13}\text{C}_2\text{H}_3)$ are not much affected by the substituents, that is, all the values ${}^2J({}^{13}\text{C}_2\text{H}_3)$ are close to that in allene (**11**) (${}^2J({}^{13}\text{CH}) = -3.9$ Hz (65)).

For the two-bond carbon–proton coupling constants in monosubstituted allenes correlation (132) ($r = -0.9339$) with the Mulliken overlap populations Q_{SCSH} (in units of 10^{-2}) is observed (54*b*).

$${}^2J({}^{13}\text{CH})(\text{RHC}=\text{C}=\text{CH}_2) = -64.35 Q_{\text{SCSH}}(\text{STO-3G}) - 78.61 \quad (132)$$

A DSP approach for the two-bond couplings ${}^2J({}^{13}\text{C}_2\text{H}_2)$ (from Ref. 54*a*) reveals that, from the statistical point of view, this last coupling should be related to σ_R^0 (and σ_I) and not to σ_R as in the preceding cases. This seems to be a real effect for long-range couplings, as also in case of the four-bond proton–proton couplings in allenes a DSP treatment suggests relations to σ_R^0 (11).

In the DSP approach for ${}^2J({}^{13}\text{C}_2\text{H}_2)$ the hydrogen atom and the trimethylsilyl group exhibit larger deviations and have been omitted in the regression (Fig. 37).

The DSP approach stresses a predominance of resonance contributions to the substituent effects on two-bond carbon–proton couplings in allenes ($R^2 = 0.8798$).

$${}^2J({}^{13}\text{C}_2\text{H}_2)(\text{RHC}=\text{C}=\text{CH}_2) = 0.63 + 0.43 \sigma_I - 19.51 \sigma_R^0 \quad (133)$$

The fact that in the substituent parameter approaches, especially for coupling constants (${}^1J({}^{13}\text{C}_1\text{H}_2)$, ${}^2J({}^{13}\text{C}_2\text{H}_2)$, ${}^4J(\text{H}_2\text{H}_3)$), the parent compound allene (**11**) exhibits a larger deviation from the regression lines may be due to the particular electronic situation of the hydrogen atoms in allenes. In monosubstituted allenes the $1s$ AOs of H_2 are always part of the σ electronic system whereas in **11** this proton may also be involved in the π system (“hyperconjugation”). The substituent constants in the semiquantitative approaches, however, are derived from compounds with a strict π – σ separation, where the $1s$ AOs of hydrogen only take part in the σ system.

A rather remarkable substituent effect is also operative in case of the two-bond proton–proton coupling constants ${}^2J(\text{HH})$ in allenes (161). The

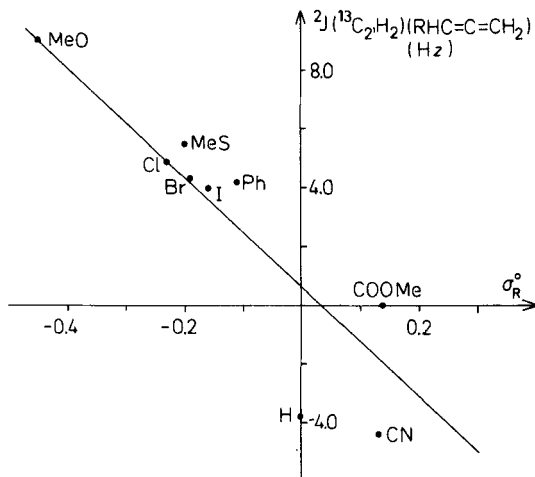


Figure 37 DSP correlation for two-bond carbon-proton coupling constants of allenes.

geminal coupling is dominated by π conjugative effects, as one observes a relation of ${}^2J(\text{HH})$ with the square of the (CNDO/S) hydrogen electron densities P_{HH}^2 (Fig. 38). The electron density variations at the hydrogen atom of the methylene group of allenes, in turn, result from π hyperconjugative interactions with the substituent orbitals of corresponding symmetry (Section III.C; Equation 90).

Whereas in allenes the $1s$ AOs of the methylene hydrogen atoms may become part of the molecule's π system, in planar ethylene, ketene (43), diazomethane (42), and butatriene (223) the methylene proton $1s$ AOs are always part of the σ system. The influence of the molecular skeleton on the CH_2 two-bond proton-proton couplings in these last cumulenes should be determined by electron populations of the H_2CX units which are determined by the antisymmetric or symmetric group orbitals of the hydrogen $1s$ AOs ($1s_H \mp 1s_{H'}$) (162).

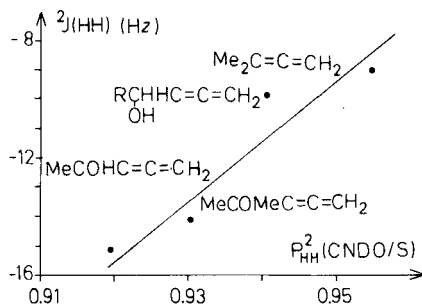
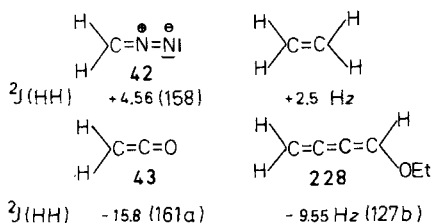


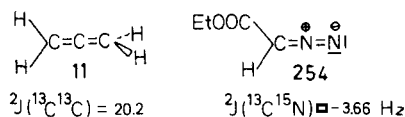
Figure 38 Relation of the geminal proton-proton coupling constants in allenes to the squares of the hydrogen electron densities.

Using CNDO/S wavefunctions for the approach given in Ref. 162 for geminal couplings only a qualitative trend for ${}^2J(\text{HH})$ in planar cumulenes may be deduced.



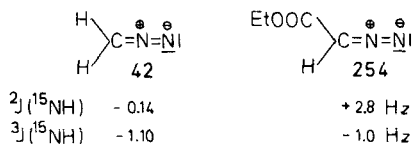
The Pople–Bothner–By approach (162) with CNDO/S wavefunctions, however, corroborates the suggestion (158) that in diazomethane ${}^2J(\text{HH})$ has a positive sign.

Two-bond carbon–carbon or carbon–nitrogen-15 coupling constants of cumulenes are only available for allene (**11**) (157) and ethyl diazoacetate (**254**) (94b).



Interestingly with respect to these coupling constants is the fact that the ratio of one-bond and two-bond couplings (${}^1J({}^{13}\text{CX})/{}^2J({}^{13}\text{CX})$, $\text{X} = {}^{13}\text{C}, {}^{15}\text{N}$) in these cumulenes seems to be constant (and of the order of five). Such a finding is expected on the basis of the isoelectronic principle.

Two-bond proton–nitrogen-15 coupling constants in diazocompounds may be assumed to follow qualitatively trends observed for ${}^2J({}^{13}\text{C}_2\text{H}_2)$ in allenes. Such an example is found for ${}^2J({}^{15}\text{NH})$ in diazomethane (**42**) (158) and ethyl diazoacetate (**254**) (94b). In **254** ${}^2J({}^{15}\text{NH})$ is more positive than in **42**, comparable to the situation in allene and allenecarboxylic acid ester.



As the signs of the coupling constants in **42** and **254** have been deduced from comparisons with results from quantum-chemical calculations, one cannot be quite sure that the preceding deductions are correct.

The three-bond proton–nitrogen-15 coupling constants in diazocompounds seem to be rather insensitive to substituent effects as is also the case for the three-bond carbon–proton couplings in allenes (54,65).

If one takes the two different three-bond carbon-proton coupling constants in allenes into consideration only a poor correlation with overlap populations Q_{SCSH} is observed. Taken separately, however, the two different three-bond CH couplings of allenes exhibit acceptable correlations with overlap populations (54*b*). Omitting the cyano group from the regression one obtains for the couplings involving no atom which is directly linked to a substituent the correlation (134) ($r = -0.8989$, Q_{SCSH} in units of 10^{-4}).

$${}^3J({}^{13}\text{C}_3\text{H}_2)(\text{RHC}=\text{C}=\text{CH}_2) = -8.19 Q_{SCSH}(\text{STO-3G}) + 20.02 \quad (134)$$

The other three-bond CH coupling is related to the overlap population according to Equation 135 ($r = 0.9316$, Q_{SCSH} in units of 10^{-4}).

$${}^3J({}^{13}\text{C}_1\text{H}_3)(\text{RHC}=\text{C}=\text{CH}_2) = 22.43 Q_{SCSH}(\text{STO-3G}) - 27.00 \quad (135)$$

A correlation of coupling constants with STO-3G Mulliken overlap populations has also been observed in case of the four-bond proton-proton couplings of allenes (11) (Q_{SHSH} in units of 10^{-3}).

$${}^4J(\text{H}_2\text{H}_3)(\text{RHC}=\text{C}=\text{CH}_2) = -1.04 Q_{SHSH}(\text{STO-3G}) - 13.26 \quad (136)$$

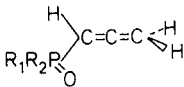
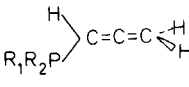
Using a DSP approach it has been shown (11) that ${}^4J(\text{HH})$ in allenes is related to σ_I and σ_R^0 according to Equation 137; that is, the substituent effect $\kappa^j(\text{R})$ (Table 10) on the four-bond couplings is affected by polar and resonance factors to a comparable amount.

$$\kappa^j(\text{R}) = 1.10 \sigma_I - 1.38 \sigma_R^0 + 0.11 \quad (137)$$

The substituent effect $\kappa^j(\text{R})$ on the four-bond HH couplings in allenes exhibits also a correlation with the difference in the CNDO/S electron densities (in units of 10^{-3}) of the protons involved in the coupling (11).

$$\kappa^j(\text{R}) = 0.0431(P_{\text{HH}}(2) - P_{\text{HH}}(3)) + 0.11 \quad (138)$$

Four-bond phosphorus-proton couplings ${}^4J(\text{PH})$ in allenes are reported in Ref. 163 for allenic phosphineoxides (phosphonylallenes) **256–259**, **32** and allenic phosphines (phosphinylallenes) **260–263**, **130**.

						
	R ₁	R ₂	${}^4J(\text{PH})$	R ₁	R ₂	${}^4J(\text{PH})$
256	Et	Et	-10.35	Me ₂ N	Me ₂ N	+5.0
257	Ph	Ph	-11.2	EtO	EtO	-0.56
258	Me ₂ N	Me ₂ N	-11.92	Et	Et	-1.4
259	EtO	EtO	-13.70	Ph	Ph	-3.04
32	Cl	Cl	-18.23	Cl	Cl	-3.64

For the allenes with the phosphorus substituents also four-bond proton-proton coupling constants are given in Ref. 163.

The couplings ${}^4J(\text{PH})$ in the phosphonylallenes **32** and **256–259** may be related to the polar substituted constants σ_I ($r = -0.9660$) (163) of the groups linked to the phosphorus atom.

$${}^4J(\text{PH})(\text{R}_2\text{POCH}=\text{C}=\text{CH}_2) = -15.19 \sigma_I - 10.52 \quad (139)$$

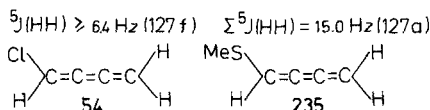
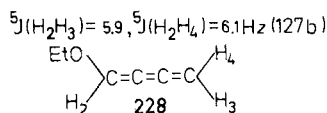
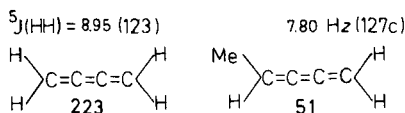
For the phosphinylallenes, on the other hand, correlations of ${}^4J(\text{PH})$ and the Hammett σ_p constants have been observed (163). Based on the small sample of phosphinylallenes **260–263**, **130** the four-bond phosphorus-proton coupling may be described by Equation 140 ($R^2 = -0.9158$) using a DSP approach.

$${}^4J(\text{PH})(\text{R}_2\text{PHC}=\text{C}=\text{CH}_2) = -3.75 - 9.14 \sigma_I - 15.90 \sigma_R^0 \quad (140)$$

In both these kinds of allenic phosphorus derivatives the substituent effects on the four-bond couplings ${}^4J(\text{PH})$ are additive, that is, for $\text{R}_1 \neq \text{R}_2$ the substituent effect is given by $\frac{1}{2}[\text{R}_1^1\text{PHC}=\text{C}=\text{CH}_2 + \text{R}_2^2\text{PHC}=\text{C}=\text{CH}_2]$.

Substituent effects on long-range coupling constants of butatrienes may be extracted from the literature for five-bond proton-proton couplings. In general, the two five-bond couplings involving protons *cis* or *trans* to the substituents seem to differ only slightly. Therefore, to find trends in substituent effects on ${}^5J(\text{HH})$ in butatrienes averages ${}^5\bar{J}(\text{HH})$ of both these last couplings may be used. In particular, one may assume a value of ${}^5J(\text{HH}) = 7.5$ Hz for **235**. Then, it turns out that ${}^5J(\text{HH})$ in butatrienes are correlated with the CNDO/S π bond orders $P_{CC}^\pi(1'4')$ between the terminal carbon atoms of the cumulenic skeleton ($r = -0.9347$ using ${}^5J(\text{HH}) = 6.4$ Hz for **54**).

$${}^5J(\text{HH})(\text{RHC}=\text{C}=\text{C}=\text{CH}_2) = -112.10 P_{CC}^\pi(1'4') - 38.48 \quad (141)$$



A more illustrative interpretation of ${}^5J(\text{HH})$ may be extracted from the correlations of ${}^5J(\text{HH})$ in butatrienes and the four-bond couplings ${}^4J(\text{HH})$ in allenes ($r = -0.9921$)(Fig. 39).

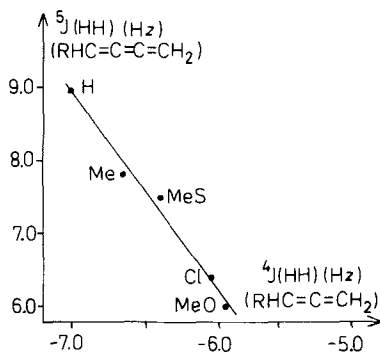


Figure 39 Correlation of the five-bond proton-proton couplings in butatrienes and the four-bond proton-proton couplings in allenes.

$${}^5J(\text{HH})(\text{RHC}=\text{C}=\text{C}=\text{CH}_2) = -2.58 {}^4J(\text{HH})(\text{RHC}=\text{C}=\text{CH}_2) - 9.21 \quad (142)$$

G. Molar Rotations

Discussions of substituent effects on molecular properties considered so far have been performed on a quantitative level. In case of molar rotations of allenes, at least allenes with σ -inductive groups, a quantitative interpretation of the substituent constant $\lambda(\text{R})$ is possible. This interpretation is based upon a quantum-theoretical treatment of the molar rotation of (*S*)-(+)-1,3-dimethylallene (**3a**) (164). According to the theory the parameter $\lambda(\text{Me})$ is related to the group anisotropic polarizability $\Delta\alpha(\text{Me})$ and a factor $\kappa(\text{Me})$ which reflects the polarity of the $\text{C}_{sp^2}\text{-C}_{sp^3}$ bond between the allenic terminal carbon atom and the ligand carbon atom.

$$\lambda(\text{Me}) = G \cdot \kappa(\text{Me}) \cdot \Delta\alpha(\text{Me}) \quad (143)$$

In Equation 143 G is a geometrical factor depending upon the particular molecular skeleton. Considering G for allenes and pentatetraenes it is this factor from which one may deduce that for correspondingly substituted alkylated pentatetraenes and allenes the molar rotations of the former ones (κ and $\Delta\alpha$ being identical) must be larger. A numerical evaluation of G (165) for pentatetraenes and allenes gives:

$$\bar{\lambda}(\text{R})(\text{pentatetraenes}) \approx 1.4 \lambda(\text{R})(\text{allenes})$$

As the group anisotropic polarizabilities for alkyl groups are almost identical, the substituent effects of the alkyl groups on molar rotations are largely due to the factor $\kappa(\text{R})$, that is, to polarity effects (1c,13). The λ parameter for alkyl

TABLE 33
 CNDO/S Total and π Electron Densities of Butatrienes $\text{RHC}_1=\text{C}=\text{C}=\text{CH}_2$ and Pentatetraene

Compd.	R	$P_{CC}(1')$	$P_{CC}(2')$	$P_{CC}(3')$	$P_{CC}(4')$	$P_{HH}(2)$	$P_{HH}(3)$	$P_{CC}(1')$	$P_{CC}(2')$	$P_{CC}(3')$	$P_{CC}(4')$	$P_{CC}(5')$
223	H	4.059	4.015	4.015	4.059	0.965	0.965	1.064	0.936	0.936	1.064	
51	Me	4.006	4.041	4.015	4.082	0.970	0.970	1.010	0.995	0.915	1.104	
52	MeO	3.903	4.026	4.017	4.098	0.947	0.975	0.994	1.058	0.908	1.139	
54	Cl	4.036	3.962	3.994	4.015	0.942	0.950	1.141	0.833	0.976	0.987 ^b	
53	CN	4.009	3.987	4.006	4.029	0.949	0.955	1.107	0.888	0.962	1.016	
222 ^a	H	4.085	3.946	4.087	4.087	0.963		1.119	0.944	1.066	0.918	0.972

^a Pentatetraene.

^b CNDO/S calculation including d orbitals.

groups may be related to group dipole moments (13). Using the values for the polar substituent constants in Table 3 one finds for alkyl groups and hydrogen

$$\lambda(\text{Alk}) = -293.71 \sigma_I - 1.06 \quad (144)$$

For a more general treatment of the λ parameters for the calculations of molar rotations of allenes one must differentiate between σ inductive and mesomeric groups.

If only substituents bonded via carbon to the allenic skeleton are taken into consideration, correlations of the λ parameters and the CNDO/S π electron densities of the allenic central atoms in monosubstituted compounds $\text{RHC}=\text{C}=\text{CH}_2$ have been observed (1c,13).

$$\lambda(\text{R}) = 190.3 P_{\text{CC}}^{\pi}(2')(\text{RHC}=\text{C}=\text{CH}_2) - 173.0 \text{ for inductive groups} \quad (145a)$$

$$\lambda(\text{R}) = 344.0 P_{\text{CC}}^{\pi}(2')(\text{RHC}=\text{C}=\text{CH}_2) - 269.3 \text{ for mesomeric groups bonded via carbon} \quad (145b)$$

The most general correlations of the λ parameters with quantum-chemical indices, however, are those that involve the π HOMO CNDO/S electron densities at the allenic central atoms, that is, the squares of the CNDO/S LCAO coefficients $c_{2,\pi}^2$ for the π HOMO (1c). In this case the correlation for mesomeric groups includes substituents bonded via heteroatoms to the allenic skeleton. Equation 145b is no longer valid, if also heterosubstituents are taken into account.

$$\lambda(\text{R}) = 247.3 c_{2,\pi}^2(\text{CNDO/S})(\text{RHC}=\text{C}=\text{CH}_2) - 77.8 \text{ for inductive groups} \quad (146a)$$

$$\lambda(\text{R}) = -379.6 c_{2,\pi}^2(\text{CNDO/S})(\text{RHC}=\text{C}=\text{CH}_2) + 121.6 \text{ for mesomeric groups} \quad (146b)$$

Equation 146a has been used to deduce the (tentative) value $\lambda(\text{CH}_2\text{Cl}) = +7.5$ given in Table 13.

A DSP analysis relates the $\lambda(\text{R})$ parameters of those mesomeric groups whose parameters have been shown to give reliable molar rotations of allenes to the σ_I and σ_R constants (Fig. 40). Only the carbomethoxy group exhibits a larger deviation from the DSP correlation. From Equation 147 ($R^2 = 0.6827$ including COOMe) one can see that also in case of mesomeric groups the $\lambda(\text{R})$ parameters are more affected by polar than by resonance effects. Irrespectively of the crudeness of the correlation (147) the DSP analysis of the $\lambda(\text{R})$ parameters is the first trial to extend usual substituent parameter approaches for scalar molecular properties to pseudoscalar molecular properties.

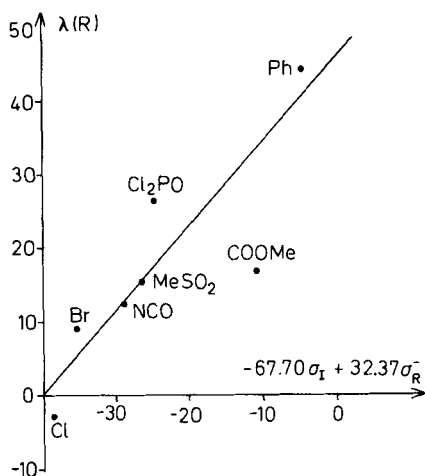
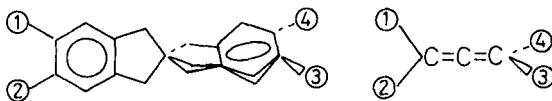


Figure 40 DSP plot of the $\lambda(R)$ parameters of mesomeric groups which serve calculations of molar rotations of allenes.

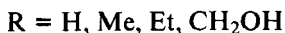
$$\lambda(R) = 42.35 - 67.70 \sigma_I + 32.37 \sigma_R^- \quad (147)$$

The reliability of the suggested λ -parameters in Table 13 for the calculations of the optical rotations of allenes may be demonstrated additionally by the following finding. It has been shown recently (166) that also the molar rotations of spiro-2,2'-biindenes may be described to a very good approximation by the "shortened" expression (10a) of the qualitatively complete chirality function (51). Both systems, allenes and spiro-biindenes, represent unsaturated molecules with a four-site molecular skeleton of symmetry D_{2d} .



Referring to the $\bar{\lambda}$ -parameters given in Ref. 166 for the calculations of the molar rotations of the spiro-biindenes (in acetone as the solvent) and the parameters $\lambda(R)$ for the allenes in Table 13 two good correlations (148a) and (148b) are observed ($r = 0.9733$ and $r = 0.9804$, respectively).

$$\lambda(R)(\text{allenes}) = 2.54 \bar{\lambda}(\text{spiro-biindenes}) - 0.19 \quad (148a)$$



$$\lambda(R)(\text{allenes}) = 7.13 \bar{\lambda}(\text{spiro-biindenes}) - 50.16 \quad (148b)$$



ACKNOWLEDGMENT

Thanks are due to Dr. W. Kosbahn (München, Germany), Prof. A. Dondoni (Ferrara, Italy), Dr. G. Seybold (Ludwigshafen, Germany), Dr. D. Haase (Berlin, Germany), and Prof. J. C. Jochims (Konstanz, Germany) for making material available prior to publication. In particular, the author is greatly indebted to Dr. W. Kosbahn who makes feasible CNDO/S computations at the Leibniz-Rechenzentrum der Bayerischen Akademie der Wissenschaften, München, Germany.

References

1. (a) This is Part IV of the series *Essays on Cumulenes*; (b) Part I: W. Runge, in *The Chemistry of Ketenes, Allenes, and Related Compounds*, S. Patai (Ed.), Wiley, London, New York, Chapter 2, (1979); (c) Part II: W. Runge, in *The Chemistry of Ketenes, Allenes, and Related Compounds*, S. Patai (Ed.), Wiley, London, New York, Chapter 3, (1979); (d) Part III: W. Runge, in *The Chemistry of Allenes*, S. R. Landor (Ed.), Academic, London, Chapter 6, (1979).
2. (a) P. R. Wells, S. Ehrenson, and R. W. Taft, *Progr. Phys. Org. Chem.*, **6**, 147 (1968); (b) S. Ehrenson, R. T. C. Brownlee, and R. W. Taft, *Progr. Phys. Org. Chem.*, **10**, 1 (1973).
3. M. Charton, *Progr. Phys. Org. Chem.*, **10**, 81 (1973).
4. (a) R. D. Topsom, *Progr. Phys. Org. Chem.*, **12**, 1 (1976); (b) W. J. Hehre, R. W. Taft, and R. D. Topsom, *Progr. Phys. Org. Chem.*, **12**, 159 (1976); (c) G. L. Nelson and E. A. Williams, *Progr. Phys. Org. Chem.*, **12**, 229 (1976); (d) W. F. Reynolds and G. K. Hamer, *J. Amer. Chem. Soc.*, **98**, 7296 (1976); (e) R. T. C. Brownlee, G. Butt, M. P. Chan, and R. D. Topsom, *J. C. S. Perkin Trans. II*, 1486 (1976).
5. (a) Houben-Weyl, *Methoden der organischen Chemie, Alkine, Di- und Polyine, Allene, Kumulene*, Vol. V, 2a, 4th ed., Georg Thieme Verlag, Stuttgart, Germany, 1977; (b) S. Patai (Ed.), *The Chemistry of Ketenes, Allenes, and Related Compounds*, Wiley, London, New York, (1979); (c) S. R. Landor (Ed.), *The Chemistry of Allenes*, Academic, London, in press.
6. L. J. Weimann and R. E. Christoffersen, *J. Amer. Chem. Soc.*, **95**, 2074 (1973).
7. W. Runge and J. Firl, *Ber. Bunsenges. Phys. Chem.*, **79**, 907 (1975).
8. W. Runge and J. Firl, *Ber. Bunsenges. Phys. Chem.*, **79**, 913 (1975).
9. W. Runge, W. Kosbahn, and J. Kroner, *Ber. Bunsenges. Phys. Chem.*, **81**, 841 (1977).
10. W. Runge, *Z. Naturforsch.*, **32b**, 1296 (1977).
11. W. Runge, *Z. Naturforsch.*, **33b**, 932 (1978).
12. E. Ruch, W. Runge, and G. Kresze, *Angew. Chem. Int. Ed. Engl.*, **12**, 20 (1973).
13. W. Runge and G. Kresze, *J. Amer. Chem. Soc.*, **99**, 5597 (1977).
14. (a) A. V. Shubnikov and V. A. Koptsik, *Symmetry in Science and Art*, Plenum, New York, 1974; (b) L. von Bertalanffy, *General Systems Theory*, George Branziller, New York, 1968.
15. (a) E. Ruch and A. Schönhofer, *Theor. Chim. Acta*, **10**, 91 (1968); (b) E. Ruch and A. Schönhofer, *Theor. Chim. Acta*, **19**, 225 (1970); (c) E. Ruch, *Acta. Chem. Res.*, **5**, 49 (1972); (d) E. Ruch, *Angew. Chem.*, **89**, 67 (1977).
16. P. Klabeo, A. Phongsatha, B. N. Cyvin, S. J. Cyvin, and H. Hopf, *J. Mol. Struct.*, **43**, 1 (1978).

17. R. Steur, J. P. C. M. van Dongen, M. J. A. de Bie, W. Drenth, J. W. de Haan, and L. J. M. van de Ven, *Tetrahedron Lett.*, 3307 (1971).
18. J. K. Crandall and S. A. Soika, *J. Amer. Chem. Soc.*, **94**, 5084 (1972).
19. A. P. Zens, P. D. Ellis, and R. Ditchfield, *J. Amer. Chem. Soc.*, **96**, 1309 (1974).
20. A. A. Petrov and A. V. Fedorova, *Russ. Chem. Rev.*, **33**, 1 (1964).
21. (a) A. Messiah, *Quantum Mechanics*, Vols. I, II, North-Holland, Amsterdam, 1965; (b) M. Hamermesh, *Group Theory and Its Applications to Physical Problems*, Pergamon, London, 1962; (c) L. Jansen and M. Boon, *Theory of Finite Groups. Application in Physics*, North-Holland, Amsterdam, 1967.
22. W. Runge, Habilitation Thesis, Technische Universität München, Germany, 1975.
23. W. Runge, W. Kosbahn, and J. Winkler, *Ber. Bunsenges. Phys. Chem.*, **79**, 381 (1975).
24. J. Kroner, W. Kosbahn, and W. Runge, *Ber. Bunsenges. Phys. Chem.*, **81**, 826 (1977).
25. W. Runge, unpublished.
26. N. B. Chapman and J. S. Shorter (Eds.), *Advances in Linear Free Energy Relationships*, Plenum, London, 1972.
27. J. Demaison and H. D. Rudolph, *J. Mol. Spectrosc.*, **40**, 445 (1971).
28. D. R. Lide and D. E. Mann, *J. Chem. Phys.*, **27**, 874 (1957).
29. M. Charton, *J. Org. Chem.*, **30**, 552 (1965).
30. A. Bouchy, J. Demaison, G. Roussy, and C. Barriol, *J. Mol. Struct.*, **18**, 211 (1973).
31. (a) J. R. Durig, Y. S. Li, C. C. Tong, A. P. Zens, and P. D. Ellis, *J. Amer. Chem. Soc.*, **96**, 3805 (1974); (b) P. D. Ellis, Y. S. Li, C. C. Tong, A. P. Zens, and J. R. Durig, *J. Chem. Phys.*, **62**, 1311 (1975).
32. P. Beltrame, P. L. Bertrame, and M. G. Cattania, *Gazz. Chim. Ital.*, **105**, 59 (1975).
33. H. Dickerson, S. Ferber, and S. F. Richardson, *Theor. Chim. Acta*, **42**, 333 (1976).
34. E. Hirota and C. Matsumura, *J. Chem. Phys.*, **59**, 3038 (1973).
35. A. P. Cox, L. F. Thomas, and J. Sheridan, *Spectrochim. Acta*, **14**, 542 (1959).
36. H. P. Johnson and M. W. P. Strandberg, *J. Chem. Phys.*, **20**, 687 (1952).
37. (a) J. A. Pople and M. Gordon, *J. Amer. Chem. Soc.*, **89**, 4253 (1967); (b) W. J. Hehre and J. A. Pople, *J. Amer. Chem. Soc.*, **92**, 2191 (1970).
38. (a) J. H. Letcher, M. L. Unland, and J. R. Van Wazer, *J. Chem. Phys.*, **50**, 2185 (1969); (b) J.-M. André, M. Cl. André, G. Leroy, and J. Weiler, *Int. J. Quant. Chem.*, **3**, 1013 (1969); (c) C. E. Dykstra and H. F. Schaefer, *J. Amer. Chem. Soc.*, **98**, 2689 (1976); (d) S. R. Walsh and W. A. Goddard, *J. Amer. Chem. Soc.*, **97**, 5319 (1975); (e) L. R. Harding and W. A. Goddard, *J. Amer. Chem. Soc.*, **98**, 6093 (1976).
39. B. Bak, J. J. Christiansen, K. Kunstmann, L. Nygaard, and J. Rastrup-Andersen, *J. Chem. Phys.*, **45**, 883 (1966).
40. K. P. R. Nair, H. D. Rudolph, and H. Dreizler, *J. Mol. Spectrosc.*, **48**, 571 (1973).
41. R. Huisgen, L. A. Feiler, and P. Otto, *Tetrahedron Lett.*, 4485, 4491 (1968).
42. (a) G. L. Blackman, R. D. Brown, R. C. F. Brown, F. W. Eastwood, and G. L. McMullen, *J. Mol. Spectrosc.*, **68**, 488 (1977); (b) K. Georgiou, H. W. Kroto, and B. M. Landsberg, *J. Mol. Spectrosc.*, **77**, 365 (1979).
43. (a) F. Feichtmeyer and F. Würstlin, *Ber. Bunsenges. Phys. Chem.*, **67**, 434 (1963); (b) W. C. Schneider, *J. Amer. Chem. Soc.*, **72**, 761 (1950).
44. F. Karlsson, R. Vestin, and A. Borg, *Acta Chem. Scand.*, **26**, 3394 (1972).
45. O. Exner, *Dipole Moments in Organic Chemistry*, Georg Thieme Publishing, Stuttgart, Germany, 1975.
46. T. O. Gierke, H. L. Tigelaar, and W. H. Flygare, *J. Amer. Chem. Soc.*, **94**, 330 (1972).
47. S. P. McGlynn, L. G. Vanquickenborne, H. Konishita, and D. G. Carroll, *Introduction to Applied Quantum Chemistry*, Holt, Rinehart, and Winston, New York, 1972.
48. Z. Yoshida, N. Ishibe, and H. Ozoe, *J. Amer. Chem. Soc.*, **94**, 4948 (1972).

49. C. Charrier, D. E. Dorman, and J. D. Roberts, *J. Org. Chem.*, **38**, 2644 (1973).
50. R. Faure, M. Malacria, J. Grimaldi, M. Bertrand, and E.-J. Vincent, *C. R. Acad. Sci., Ser. C*, **280**, 1243 (1975).
51. T. Okuyama, K. Izawa, and T. Fueno, *Bull. Chem. Soc. Japan*, **47**, 410 (1974).
52. J. P. C. M. van Dongen, H. W. D. van Dijkman, and M. J. A. de Bie, *Rec. Trav. Chim.*, **93**, 29 (1974).
53. T. Bottin-Strzalko, M. J. Pouet, and M. P. Simonnin, *Org. Magn. Res.*, **8**, 120 (1976).
54. (a) W. Runge and W. Kosbahn, *Ber. Bunsenges. Phys. Chem.*, **80**, 1330 (1976); (b) W. Runge, *Z. Naturforsch.*, **34b**, 118 (1979).
55. (a) J. S. Cowie, P. D. Landor, and S. R. Landor, *J. C. S. Perkin Trans. I*, 720 (1973); (b) P. D. Landor, S. R. Landor, and P. Leighton, *J. C. S. Perkin Trans. I*, 1628 (1975).
56. R. C. Ferguson, *J. Phys. Chem.*, **68**, 1594 (1964).
57. H. Reeps, Dissertation Thesis, Technische Universität München, Germany, 1976.
58. M. P. Simonnin and C. Charrier, *Org. Magn. Res.*, **1**, 27 (1969).
59. L.-J. Olsson, A. Claesson, and C. Bogentoft, *Acta Chem. Scand.*, **B28**, 765 (1974).
60. (a) N. F. Ramsey, *Phys. Rev.*, **91**, 303 (1953); (b) J. A. Pople and D. P. Santry, *Mol. Phys.*, **8**, 1 (1964); (c) J. N. Murrell, *Progr. Nucl. Magn. Reson. Spectrosc.*, J. W. Emsley and L. H. Sutcliffe (Eds.), Vol. 6, Pergamon, Oxford, 1971.
61. (a) J. B. Stothers, *Carbon-13 NMR Spectroscopy*, Academic, New York, London, 1972; (b) G. Webb and M. Witanowski (Eds.), *Nitrogen-NMR*, Plenum, London, New York, 1973.
62. (a) H. Günther and W. Herrig, *Chem. Ber.*, **106**, 3938 (1973); (b) M. D. Newton, J. M. Schulman, and M. M. Manus, *J. Amer. Chem. Soc.*, **96**, 17 (1974); (c) J. M. Schulman and M. D. Newton, *J. Amer. Chem. Soc.*, **96**, 6295 (1974).
63. (a) G. Binsch, J. B. Lambert, B. W. Roberts, and J. D. Roberts, *J. Amer. Chem. Soc.*, **86**, 5564 (1964); (b) J. M. Schulman and T. Venanzi, *J. Amer. Chem. Soc.*, **98**, 4701 (1976).
64. P. Lazzaretti and F. Taddei, *Org. Magn. Res.*, **3**, 125 (1971).
65. N. J. Koole and M. J. A. de Bie, *J. Magn. Res.*, **23**, 9 (1976).
66. F. Brogli, J. K. Crandall, E. Heilbronner, E. Kloster-Jensen, and S. A. Soika *J. Electron Spectrosc. Related Phenomena*, **2**, 455 (1973).
67. J. Collin and F. P. Lossing, *J. Amer. Chem. Soc.*, **79**, 5548 (1957).
68. J. Collin and F. P. Lossing, *J. Amer. Chem. Soc.*, **81**, 2064 (1959).
69. P. Bischof, R. Gleiter, H. Hopf, and F. T. Lenich, *J. Amer. Chem. Soc.*, **97**, 5467 (1975).
70. M. J. S. Dewar, G. J. Fonken, T. B. Jones, and D. E. Minter, *J.C.S. Perkin Trans. II*, 764 (1976).
71. W. Runge, W. Kosbahn, and J. Kroner, *Ber. Bunsenges. Phys. Chem.*, **79**, 371 (1975).
72. D. J. Pasto, T. P. Fehlner, M. E. Schwartz, and H. F. Baney, *J. Amer. Chem. Soc.*, **98**, 530 (1976).
73. W. Runge and J. Winkler, *Ber. Bunsenges. Phys. Chem.*, **79**, 610 (1975).
74. (a) K. Bertsch and J. C. Jochims, *Tetrahedron Lett.*, 4379 (1977); (b) K. Bertsch, M. A. Rahman, and J. C. Jochims, *Chem. Ber.*, **112**, 567 (1978).
75. D. J. Caldwell and H. Eyring, *The Theory of Optical Activity*, Wiley-Interscience, New York, 1971.
76. J. Applequist, *J. Chem. Phys.*, **58**, 4251 (1973).
77. N. L. Balasz, T. R. Brocki, and I. Tobias, *Chem. Phys.*, **13**, 141 (1976).
78. E. I. Snyder and J. D. Roberts, *J. Amer. Chem. Soc.*, **84**, 1582 (1962).
79. D. K. Black, S. R. Landor, A. N. Patel, and P. F. Whiter, *Tetrahedron Lett.*, 483 (1963).
80. (a) S. F. Mason and G. W. Vane, *Tetrahedron Lett.*, 1593 (1965); (b) T. L. Jacobs and S. Singer, *J. Org. Chem.*, **22**, 1424 (1957).
81. W. M. Jones, M. H. Grasley, and W. S. Brey, *J. Amer. Chem. Soc.*, **85**, 2754 (1963).
82. P. M. Greaves and S. R. Landor, *DMS UV Atlas organischer Verbindungen*, Vol. II, Butterworths, London and Verlag Chemie, Weinheim, Germany, D10/51, 1966.

83. C. S. L. Baker, P. D. Landor, S. R. Landor, and A. N. Patel, *J. Chem. Soc.*, 4348 (1965).
84. W. Runge, G. Kresze, and E. Ruch, *Liebigs Ann. Chem.*, 1361 (1975).
85. G. Kresze, W. Runge, and E. Ruch, *Liebigs Ann. Chem.*, 756, 112 (1972).
86. T. L. Jacobs, D. Dankner, and S. Singer, *Tetrahedron*, 20, 2177 (1964).
87. H. Kollmar and H. Fischer, *Tetrahedron Lett.*, 4291 (1968).
88. H. A. Christ, P. Diehl, H. R. Schneider, and H. Dahn, *Helv. Chim. Acta*, 44, 865 (1961).
89. (a) W. Runge, *Org. Magn. Res.*, 13, (1980), in press; (b) J. Firl, W. Runge, W. Hartmann, and H.-P. Utikal, *Chem. Lett.*, 51, (1975); (c) J. Firl and W. Runge, *Angew. Chem.*, 85, 671 (1973); (d) J. Firl and W. Runge, *Z. Naturforsch.*, 29b, 393 (1974); (e) J. Firl, W. Runge, and W. Hartmann, *Angew. Chem.*, 86, 274 (1974).
90. H. A. Bent, *J. Chem. Educ.*, 43, 170 (1966).
91. (a) B. J. Laurenzi, *Theor. Chim. Acta*, 13, 106 (1969); (b) B. J. Laurenzi and A. F. Saturno, *J. Chem. Phys.*, 53, 574 (1970); (c) A. F. Saturno and B. J. Laurenzi, *J. Chem. Phys.*, 55, 2255 (1971); (d) B. J. Laurenzi, *Theor. Chim. Acta*, 28, 81 (1972).
92. J. L. Reilly, G. R. Krow, and K. C. Ramey, *J. Org. Chem.*, 37, 2364 (1971).
93. (a) F. A. L. Anet and I. Yavari, *Org. Magn. Res.*, 8, 327 (1976); (b) I. Ruppert, *Angew. Chem.*, 89, 336 (1977); (c) I. Yavari and J. D. Roberts, *J. Org. Chem.*, 43, 4689 (1978).
94. (a) J. Mason and J. G. Vinter, *J.C.S. Dalton Trans.*, 2522 (1975); (b) R. L. Lichter, P. R. Srinivasan, A. B. Smith, R. K. Dieter, C. T. Denny, and J. M. Schulman, *J.C.S. Chem. Commun.*, 366 (1977).
95. T. L. Albright and W. J. Freeman, *Org. Magn. Res.*, 9, 75 (1977).
96. J. R. Platt, *J. Chem. Phys.*, 19, 101 (1951).
97. (a) G. Seybold, personal communication; (b) G. Seybold and C. Heibl, *Angew. Chem.*, 87, 171 (1975); (c) G. Seybold and C. Heibl, *Chem. Ber.*, 110, 1225 (1977).
98. Yu. K. Grishin, S. V. Ponomarev, and S. A. Lebedev, *J. Org. Chem. USSR*, 10, 402 (1974).
99. A. Schouten and A. Oskam, *Inorg. Chim. Acta*, 22, 149 (1977).
100. (a) H. Bock, B. Solouki, G. Bert, and P. Rosmus, *J. Amer. Chem. Soc.*, 99, 1663 (1977); (b) P. Rosmus, B. Solouki, and H. Bock, *Chem. Phys.*, 22, 453 (1977); (c) H. Bock, B. Solouki, G. Bert, T. Hirabayashi, S. Mohma, and P. Rosmus, *Nachr. Chem. Tech. Lab.*, 26, 634 (1978).
101. H. M. Niemeyer, *Helv. Chim. Acta*, 59, 1133 (1976).
102. A. C. Hopkinson, *J.C.S. Perkin Trans. II*, 795 (1973).
103. (a) G. A. Olah, K. Dunne, Y. K. Mo, and P. Szilagyi, *J. Amer. Chem. Soc.*, 94, 4200 (1972); (b) G. A. Olah and P. W. Westermann, *J. Amer. Chem. Soc.*, 95, 3766 (1973).
104. (a) G. Diderich, *Helv. Chim. Acta*, 55, 2103 (1972); (b) J. R. Mohrig, K. Keegstra, A. Maverick, R. Roberts, and S. Wells, *J.C.S. Chem. Commun.*, 780, (1974).
105. (a) W. Kosbahn, Habilitation Thesis, Technische Universität München, Germany, 1976; (b) W. Kosbahn, manuscript in preparation.
106. (a) S. J. Cyvin, *J. Chem. Phys.*, 29, 583 (1958); (b) K. Tanabe and S. Saeki, *Bull. Chem. Soc., Japan*, 47, 1847 (1974).
107. C. B. Moore and G. C. Pimentel, *J. Chem. Phys.*, 38, 2816 (1963).
108. G. Rapi and G. Sbrana, *J. Amer. Chem. Soc.*, 93, 5213 (1971).
109. (a) D. H. Williams and I. Fleming, *Spectroscopic Methods in Organic Chemistry*, McGraw-Hill, Maidenhead, 1966; (b) S. Stankovsky and S. Kovacs, *Tetrahedron*, 29, 4175 (1973).
110. G. W. Chantry, E. A. Nicol, D. J. Harrison, A. Bouchy, and G. Roussy, *Spectrochim. Acta*, 30A, 1717 (1974).
111. J. W. Rabalais, J. M. McDonald, V. Scherr, and S. P. McGlynn, *Chem. Rev.*, 71, 73 (1971).
112. L. A. Singer and G. A. Davis, *J. Amer. Chem. Soc.*, 89, 598 (1967).

113. P. J. Lillford and D. P. N. Satchel, *J. Chem. Soc. (B)*, 1016 (1970).
114. J. W. Rabalais, J. M. McDonald, and S. P. McGlynn, *J. Chem. Phys.*, *51*, 5103 (1969).
115. W. Runge, unpublished results.
116. Sh. Nadzhimutdinov, N. A. Slovokhotova, and V. A. Kargin, *Russ. J. Phys. Chem.*, *40*, 479 (1966).
117. (a) M. Regitz, *Diazoalkane*, Georg Thieme Verlag, Stuttgart, Germany, 1977; (b) G. L. Closs and R. A. Moss, *J. Amer. Chem. Soc.*, *86*, 4042 (1964).
118. H. Bock, T. Hirabayashi, S. Mohmad, and B. Solouki, *Angew. Chem.*, *89*, 106 (1977).
119. J. Bastide and J. P. Maier, *Chem. Phys.*, *12*, 177 (1976).
120. E. Heilbronner and H.-D. Martin, *Chem. Ber.*, *106*, 3376 (1973).
121. J. P. C. M. van Dongen, M. J. A. de Bie, and R. Steur, *Tetrahedron Lett.*, 1371 (1973).
122. J. L. Rippoll and A. Thuillier, *Tetrahedron*, *33*, 1333 (1977).
123. S. G. Frankiss and I. Matsubara, *J. Phys. Chem.*, *70*, 1543 (1966).
124. H. Fischer, in *The Chemistry of Alkenes*, S. Patai (Ed.), Interscience, London, 1964, p. 1025.
125. H. Yamazaki, *J.C.S. Chem. Commun.*, 841 (1976).
126. A. Roedig, G. Zaby, and W. Scharf, *Chem. Ber.*, *110*, 1484 (1977).
127. (a) R. Mantione, A. Alves, P. P. Montijn, G. A. Wildschut, H. J. T. Bos, and L. Brandsma, *Rec. Trav. Chim.*, *89*, 97 (1970); (b) M. L. Martin, F. Lefevre, and R. Mantione, *J. Chem. Soc. (B)*, 2049 (1971); (c) W. R. Roth and H.-D. Exner, *Chem. Ber.*, *109*, 1158 (1976); (d) P. P. Montijn, J. H. van Boom, L. Brandsma, and J. F. Arens, *Rec. Trav. Chim.*, *86*, 115 (1967); (e) P. P. Montijn, L. Brandsma, and J. F. Arens, *Rec. Trav. Chim.*, *86*, 129 (1967); (f) R. Vestin, A. Borg, and T. Lindblom, *Acta Chem. Scand.*, *22*, 685 (1968); (g) E. M. Kosower and T. S. Sorensen, *J. Org. Chem.*, *28*, 687 (1963).
128. (a) G. Karich and J. C. Jochims, *Chem. Ber.*, *110*, 2680 (1977); (b) K. Bertsch, G. Karich, and J. C. Jochims, *Chem. Ber.*, *110*, 3304 (1977).
129. M. v. Herrath and D. Rewicki, *Liebigs Ann. Chem.*, 589 (1977).
130. E. A. Williams, J. D. Cargioli, and A. Ewo, *J.C.S. Chem. Commun.*, 366 (1975).
131. R. Kuhn, H. Fischer, and H. Fischer, *Chem. Ber.*, *97*, 1760 (1964).
132. F. Bohlmann and K. Kieslich, *Chem. Ber.*, *87*, 1363 (1954).
133. F. Brogli, E. Heilbronner, E. Kloster-Jensen, A. Schmelzer, A. S. Manocha, J. A. Pople, and L. Radom, *Chem. Phys.*, *4*, 107 (1974).
134. (a) L. Skattebol, *Tetrahedron*, *21*, 1357 (1965); (b) H. D. Hartzler, *J. Amer. Chem. Soc.*, *93*, 4527 (1971); (c) E. Schaumann and W. Walter, *Chem. Ber.*, *107*, 3562 (1974).
135. E. H. Kosower, G.-S. Wu, and T. S. Sorensen, *J. Amer. Chem. Soc.*, *83*, 3151 (1961).
136. H. Basch, G. Bieri, E. Heilbronner, and T. B. Jones, *Helv. Chim. Acta*, *61*, 46 (1978).
137. G. Bieri, J. D. Dill, E. Heilbronner, J. P. Maier, and L. L. Rippoll, *Helv. Chim. Acta*, *60*, 629 (1977).
138. W. Kutzelnigg, G. Del. Re, and G. Berthier, *Topics Current Chem.*, *22*, 1 (1971).
139. T. Kobayashi and S. Nagakura, *J. Electron Spectrosc. Rel. Phenomena*, *7*, 488 (1975).
140. A. Battaglia, G. Distefano, and A. Dondoni, unpublished results, personal communication.
141. E. R. H. Jones, G. H. Whitham, and M. C. Whiting, *J. Chem. Soc.*, 4628 (1957), 1226 (1966).
142. H. A. Staab, *Einführung in die theoretische organische Chemie*, Verlag Chemie, Weinheim, Germany, 1962, p. 616.
143. (a) W. T. Brady, *J. Org. Chem.*, *42*, 733 (1977); (b) R. A. Ruden, *J. Org. Chem.*, *39*, 3607 (1974).
144. (a) T. W. Bentley and R. A. W. Johnstone, *J. Chem. Soc. (B)*, 263 (1971); (b) H. W. Gibson, *Can. J. Chem.*, *51*, 3065 (1973); (c) R. Egdell, J. C. Green, and C. N. R. Rao, *Chem. Phys. Lett.*, *33*, 600 (1975); (d) D. Betteridge and M. Thompson, *J. Mol. Struct.*, *21*, 341 (1974).

145. (a) J. N. Murrell, *The Theory of Electronic Spectra of Organic Molecules*, Methuen, London, 1963; (b) R. Daudel, *Quantum Theory of Chemical Reactivity*, D. Reidel Publishing Company, Dordrecht-Holland and Boston-USA, 1973.
146. D. Hall, J. P. Maier, and P. Rosmus, *Chem. Phys.*, **24**, 373 (1977).
147. P. D. Burrow and K. D. Jordan, *Chem. Phys.*, **36**, 594 (1975).
148. (a) R. Ditchfield and P. D. Ellis, *Topics in ¹³C NMR Spectroscopy*, G. Levy (Ed.), Vol. 1, Wiley, New York, 1974, p. 1; (b) K. A. K. Ebraheem and G. A. Webb, *Progr. Nucl. Magn. Reson. Spectrosc.*, **11**, 149 (1977); (c) K. A. K. Ebraheem and G. A. Webb, *Org. Magn. Res.*, **9**, 241, 248 (1977).
149. J.-C. Simon and M. Rajzmann, *J. Chim. Phys.*, **71**, 1429 (1974).
150. (a) J. Mason, *J. Chem. Soc. (A)*, 1038 (1971); (b) W. H. Flygare and J. Goodisman, *J. Chem. Phys.*, **49**, 3122 (1968); (c) K. A. K. Ebraheem, G. A. Webb, and M. Witanowski, *Org. Magn. Res.*, **8**, 317 (1976).
151. (a) M. Karplus and J. A. Pople, *J. Chem. Phys.*, **38**, 2803 (1963); (b) J. A. Pople, *Mol. Phys.*, **8**, 301 (1964).
152. H. Staudinger and St. Bereza, *Chem. Ber.*, **42**, 4908 (1909).
153. (a) G. E. Maciel, J. W. McIver, N. S. Ostlund, and J. A. Pople, *J. Amer. Chem. Soc.*, **92**, 1 (1970); (b) G. E. Maciel, J. W. McIver, N. S. Ostlund, and J. A. Pople, *J. Amer. Chem. Soc.*, **92**, 11 (1970).
154. K. D. Summerhays and G. E. Maciel, *Mol. Phys.*, **24**, 913 (1972).
155. (a) H. Günther and G. Jikeli, *Chem. Rev.*, **77**, 599 (1977); (b) H. Günther, H. Schmickler, M.-E. Günther, and D. Cremer, *Org. Magn. Res.*, **9**, 420 (1977).
156. W. Runge and J. Firl, *Z. Naturforsch.*, **31b**, 1515 (1976).
157. R. D. Bertrand, D. M. Grant, E. L. Allred, J. C. Hinshaw, and A. Brent Strong, *J. Amer. Chem. Soc.*, **94**, 997 (1972).
158. J. P. Jacobsen, K. Schaumburg, and J. T. Nielsen, *J. Magn. Res.*, **13**, 372 (1974).
159. F. J. Weigert and J. D. Roberts, *J. Amer. Chem. Soc.*, **94**, 6021 (1972).
160. P. D. Ellis and R. Ditchfield, *Topics in ¹³C NMR Spectroscopy*, Vol. 2, Wiley, New York, 1976, p. 434.
161. (a) E. L. Allred, D. M. Grant, and W. Goodlett, *J. Amer. Chem. Soc.*, **87**, 673 (1965); M. L. Martin, G. J. Martin, and R. Couffignal, *J. Mol. Spectrosc.*, **34**, 53 (1970); (c) M. L. Martin, G. J. Martin, and R. Couffignal, *J. Chem. Soc. (B)*, 1282 (1971).
162. J. A. Pople and A. A. Bothner-By, *J. Chem. Phys.*, **42**, 1339 (1965).
163. M. P. Simonin and B. Borecka, *Org. Magn. Reson.*, **1**, 27 (1969).
164. D. Haase and E. Ruch, *Theor. Chim. Acta*, **29**, 247 (1973).
165. D. Haase, personal communication.
166. H. Neudeck, B. Richter, and K. Schlögl, *Mh. Chem.*, **110**, 931 (1979).

APPENDIX

A. Summary of Unpublished Material

The appendix gives first a summary of material that has not yet been published, but has been used in the text dealing with "Substituent Effects in Allenes and Cumulenes." Some details of this material may be of interest for further investigations.

Secondly, there is a chemical compound index. This is intended to provide

easy location of the cumulenes treated in the preceding chapters and fast access to the various spectral (and other) informations.

All indices lead to the number under which the corresponding cumulene has been registered in this work.

To retrieve the compounds, the molecular formulas are the relevant entries which are listed in the usual form (starting with C and H and then the other atoms according to alphabetical order).

Chemical names are given as systematic names and, additionally, sometimes as preferred names which relate the chemical names to the structures of the molecules according to the separation into the cumulenic skeleton and the ligands, for example:

<u>Systematic Name</u>	<u>Preferred Name</u>
buta-1,2-diene	methylallene
penta-1,2,3-triene	methylbutatriene

Regarding the present contribution as a data compilation we have two classification schemes:

1. the chemical classification according to the substances and the molecular classes, and
2. the physical classification according to the physical phenomena.

Then, the Chemical Compound Index gives a direct file for asking what kinds of molecular properties are discussed for the particular compounds. On the other hand, the Contents gives the inverted file, as via its entries all compounds may be found for which a definite molecular property is listed.

B Chemical Compound Index

C1 H2 N2

Diazomethane (42)

- Dipole moment 336,
- Carbon chemical shift 388,
- Nitrogen chemical shift 387-388, 428, 429
- One-bond carbon-hydrogen coupling 436,
- One-bond carbon-nitrogen coupling 436,
- Two-bond proton-proton coupling 441,
- Two-bond nitrogen-proton coupling 441,
- Three-bond nitrogen-proton coupling 441,
- UV Absorption spectrum 429;

Carbodiimide (203)

Carbon chemical shift 385.

C1 O1

Carbon monoxide

Carbon chemical shift 388.

C1 O2

Carbon dioxide (204)

Carbon chemical shift 385, 405,

IR Absorption spectrum 396.

C1 S2

Carbon disulfide (212)

Carbon chemical shift 391.

C2 H1 Cl O

Chloro ketene (251)

PE Spectrum 423.

C2 H2 O

Ketene (43)

Dipole moment 336,

Total electron density 394, 431, 438,

π Electron density 417, 431, 438,

Carbon chemical shift 386, 429, 431,

Proton chemical shift 385,

One-bond carbon-hydrogen coupling 436,

One-bond carbon-carbon coupling 436, 438,

Two-bond proton-proton coupling 441,

PE Spectrum 399,

UV Absorption spectrum 429,

IR Absorption spectrum 396,

Protonation reaction 395.

C2 H2 S

Thio ketene (50)

Dipole moment 336,

Total Electron density 393-394, 401, 438,

π Electron density 438,

Carbon chemical shift 390,

One-bond carbon-hydrogen coupling 436.

C2 H3 N

Ketene imine (vinylideneamine) (49)

Dipole moment 336,
One-bond carbon-hydrogen coupling 436,
Orbital energy 399,
Barrier of stereoisomerization 395.

C2 H3 N1 O1

Methylisocyanate (248)

Carbon chemical shift 391,
Nitrogen chemical shift 387,
PE Spectrum 411.

C2 H3 N1 S1

Methyl thioisocyanate

Carbon chemical shift 391.

C2 H4

Ethylene

Total electron density 399,
 π Electron density 400,
 π Bond order 400,
Carbon chemical shift 401,
One-bond carbon-hydrogen coupling 436,
One-bond carbon-carbon coupling 436,
Two-bond proton-proton coupling 441.

C2 D2 O

Dideuterioketene (43d)

Dipole moment 336.

C3 H F3

Trifluoroallene (119)

Carbon chemical shift 370, 372, 374.

C3 H2 D2

1,1-Dideuterioallene (11d)

Dipole moment 336.

C3 H2 F2

1,1-Difluoroallene (9)

Dipole moment 332, 334, 339,
Total electron density 343,
Carbon chemical shift 348, 370, 372;

1,3-Difluoroallene (10)

Dipole moment 333, 334, 339,
Total electron density 367, 368,

Carbon chemical shift 370, 372, 374.

C3 H2 O1

Methylene ketene (propadienone) (48)

Dipole moment 336, 340.

C3 H2 O3

Carboxylketene (propa-2,3-dienoic acid-3-one) (264)

Total electron density 438,

π Electron density 438.

C3 H3

Allenyl anion (11a)

Barrier of stereoisomerization 395.

C3 H3 Br

1-Bromo-propa-1,2-diene (bromoallene) (13)

Dipole moment 332,

Carbon chemical shift 348, 370, 372,

Proton chemical shift 350, 375,

One-bond carbon-proton coupling 354, 378,

Two-bond carbon-proton coupling 439,

Four-bond proton-proton coupling 355,

PE spectrum 422.

C3 H3 Cl

1-Chloro-propa-1,2-diene (chloroallene) (30)

Dipole moment 334,

Total electron density 343, 345, 431

Carbon chemical shift 348, 370, 372, 431,

Proton chemical shift 350, 375,

One-bond carbon-proton coupling 354,

Two-bond carbon-proton coupling 439,

Four-bond proton-proton coupling 355,

PE Spectrum 422.

C3 H3 Cl2 O1 P1

Dichlorophosphonylallene (dichloroallenyl-phosphineoxide) (32)

Dipole moment 334,

Total electron density 343, 345,

Proton chemical shift 350,

Four-bond proton-proton coupling 355,

Four-bond phosphorus-proton coupling 422.

C3 H3 Cl2 P1

Dichlorophosphinylallene (dichloroallenyl-phosphine) (130)

Proton chemical shift 375,
Four-bond phosphorus-proton coupling 442.

C3 H3 F1

1-Fluoro-propa-1,2-diene (fluoroallene) (15)

Dipole moment 332, 334,
Total electron density 343, 345, 431,
Carbon chemical shift 348, 370, 372, 431.

C3 H3 I1

1-Iodo-propa-1,2-diene (iodoallene) (129)

Carbon chemical shift 348,
Proton chemical shift 350, 375,
One-bond carbon-proton coupling 354,
Four-bond proton-proton coupling 355.

C3 H3 Li1

Allenyllithium

Carbon chemical shift 348.

C3 H4

Propa-1,2-diene (allene) (11)

Total electron density 343, 345, 399-400, 431,
 π Electron density 400, 418,
 π Bond order 400,
Carbon chemical shift 348, 386, 401, 431,
Proton chemical shift 350, 385,
One-bond carbon-proton coupling 354, 436,
One-bond carbon-carbon coupling 436,
Two-bond carbon-proton coupling 439,
Two-bond carbon-carbon coupling 441,
Four-bond proton-proton coupling 355,
PE Spectrum 358, 399, 422,
IR Absorption spectrum 396,
Electron affinity 423-424.

C3 H4 O1

Methylketene (44)

Dipole moment 336,
Total electron density 431, 438,
 π Electron density 431, 438,
Carbon chemical shift 386, 431,
PE Spectrum 423.

C3 H6 N2

Dimethylcarbodiimide (213)

PE Spectrum 411,
IR Absorption spectrum 396;

Dimethyldiazomethane (221)

PE Spectrum 399.

C3 F4

Tetrafluoroallene (74)

Total electron density 367,
Carbon chemical shift 370, 372, 374.

C3 O2

Carbon suboxide (240)

Carbon chemical shift 405.

C4 H3 Cl1

1-Chloro-buta-1,2,3-triene (chlorobutatriene) (54)

Dipole moment 336,
Total electron density 445,
 π Electron density 445,
Proton chemical shift 404,
Five-bond proton-proton coupling 443,
UV Absorption spectrum 406.

C4 H3 F3

4,4,4-Trifluoro-buta-1,2-diene (trifluoromethylallene) (26)

Dipole moment 334,
Total electron density 343, 345.

C4 H3 N1

Buta-2,3-dienonitrile (cyanoallene) (14)

Dipole moment 332, 334,
Total electron density 343, 345, 431,
Carbon chemical shift 348, 431,
Proton chemical shift 350, 375,
One-bond carbon-proton coupling 354,
Two-bond carbon-proton coupling 439,
Four-bond proton-proton coupling 355,
PE Spectrum 422.

C4 H3 N1 O1

Allenylisocyanate (33)

Dipole moment 334,
Total electron density 343, 345.

C4 H3 O2

Buta-2,3-dienoate (buta-2,3-dienoic acid anion) (58)

Total electron density 343, 345.

C4 H4

Buta-1,2,3-triene (butatriene) (223)

Total electron density 399, 445,
 π Electron density 400, 445,
 π Bond order 400,
Carbon chemical shift 401,
Proton chemical shift 402, 404,
One-bond carbon-hydrogen coupling 436,
One-bond carbon-carbon coupling 436, 438,
PE Spectrum 406,
UV Absorption spectrum 406.

C4 H4 Br2

1,4-Dibromo-buta-1,2-diene (153)

Proton chemical shift 377.

C4 H4 O1

Buta-2,3-dienal (125)

Proton chemical shift 350, 375.

C4 H4 O2

Buta-2,3-dienoic acid (allenecarboxylic acid) (22)

Total electron density 343, 345, 431,
Carbon chemical shift 348, 369, 371, 431,
Proton chemical shift 375,
pK_a-Value 412.

C4 H5 Br1

4-Bromo-buta-2,3-diene (3-bromo-1-methylallene) (151)

Proton chemical shift 377.

C4 H5 Br1 O1

4-Bromo-buta-2,3-dien-1-ol (158)

Proton chemical shift.

C4 H5 Cl1

4-Chloro-buta-1,2-diene (chloromethylallene) (25)

Dipole moment 333, 334,
Total electron density 343, 345,

Proton chemical shift 350,

Four-bond proton-proton coupling 355.

4-Chloro-buta-2,3-diene (3-chloro-1-methylallene) (40)

Dipole moment 334,

Total electron density 367, 368,

Proton chemical shift 377.

C4 H5 I1

4-Iodo-buta-2,3-diene (3-iodo-1-methylallene) (159)

Proton chemical shift 377.

C4 H6

Buta-1,2-diene (methylallene) (12)

Dipole moment 332,

Total electron density 343, 345, 431,

Carbon chemical shift 348, 369, 371, 431,

Proton chemical shift 350, 375,

Four-bond proton-proton coupling 355,

PE Spectrum 358, 422.

C4 H6 N2 O2

Ethyl diazoacetate (diazoacetic acid ethyl ester) (254)

Carbon chemical shift 438,

Nitrogen chemical shift 429,

One-bond carbon-hydrogen coupling 438,

One-bond carbon-nitrogen coupling 438-439,

Two-bond carbon-nitrogen coupling 441,

Two-bond nitrogen-hydrogen coupling 441,

Three-bond nitrogen-hydrogen coupling 441,

UV Absorption spectrum 429.

C4 H6 O1

Methyl-allenyl-ether (methoxyallene) (19)

Dipole moment 334,

Total electron density 343, 345, 431,

Carbon chemical shift 86, 348, 370, 372, 431,

Proton chemical shift 350, 375,

One-bond carbon-proton coupling 354,

Two-bond carbon-proton coupling 439,

Four-bond proton-proton coupling 355,

PE Spectrum 422;

Buta-2,3-dien-1-ol (hydroxymethylallene) (24)

Dipole moment 334,

Total electron density 343, 345,
Proton chemical shift 350, 375;

Dimethylketene (45)

Dipole moment 336,
Total electron density 438,
 π Electron density 438,
Carbon chemical shift 386, 429,
PE Spectrum 422,
UV Absorption spectrum 397, 429;

Ethylketene (199)

Carbon chemical shift 386.

C4 H6 O2 S1

Methyl-allenyl-sulfone (methylsulfonylallene) (34)

Dipole moment 334,
Total electron density 343, 345.

C4 H6 S1

Methyl allenyl sulfide (methylallenyl thioether) (20)

Dipole moment 334,
Total electron density 343, 345, 431,
Carbon chemical shift 348, 370, 372, 431,
Proton chemical shift 350,
One-bond carbon-proton coupling 354,
Two-bond carbon-proton coupling 439,
Four-bond proton-proton coupling, 355,
PE Spectrum 422.

C4 C14

Tetrachlorobutatriene (perchlorobutatriene) (233)

Carbon chemical shift 404.

C4 F4

Tetrafluorobutatriene (perfluorobutatriene) (247)

PE Spectrum 406.

C5 H3 N1

Penta-2,3,4-trienonitrile (cyanobutatriene) (53)

Dipole moment 336,
Total electron density 445,
 π Electron density 445.

C5 H4

Penta-1,2-dien-4-yne (allenylacetylene) (28)

Dipole moment 334,
Total electron density 343, 345;

Penta-1,2,3,4-tetraene (pentatetraene) (222)

Total electron density 399-400, 445,
 π Electron density 400, 445,
 π Bond order 400,
Carbon chemical shift 401,
Proton chemical shift 402,
One-bond carbon-proton coupling 436,
PE Spectrum 406.

C5 H4 O4

Penta-2,3-diendioic acid (1,3-allene-dicarboxylic acid) (71)

Total electron density 367, 368,
Carbon chemical shift 369, 371,
Proton chemical shift 376,
One-bond carbon-proton coupling 378.

C5 H6

Penta-1,2,4-triene (vinylallene) (17)

Dipole moment 334,
Total electron density 343, 345,
Proton chemical shift 350,
One-bond carbon-proton coupling 354,
Four-bond proton-proton coupling 355,
PE Spectrum 422;

Penta-1,2,3-triene (methylbutatriene) (51)

Dipole moment 336,
Total electron density 445,
 π Electron density 445,
Proton chemical shift 404,
Five-bond proton-proton coupling 443.

C5 H6 O1

Penta-1,2-dien-4-one (acetylallene) (21)

Dipole moment 334,
Total electron density 343, 345,
Proton chemical shift 350,
Two-bond proton-proton coupling 439,
Four-bond proton-proton coupling 355;

Methyl-butatrienyl-ether (methoxybutatriene) (52)

Dipole moment 336,

Total electron density 445,

π Electron density 445;

2-Methyl-buta-2,3-dienal (126)

Proton chemical shift 350, 375;

3-Methyl-buta-1,2-dien-1-one (isopropylidene ketene) (250)

PE Spectrum 422-423.

C5 H6 O2

Methyl-buta-2,3-dienoate (carbomethoxyallene) (23)

Dipole moment 334,

Total electron density 343, 345, 431,

Carbon chemical shift 348, 369, 371, 431,

Proton chemical shift 350, 375,

One-bond carbon-proton coupling 354, 378,

Two-bond carbon-proton coupling 439,

Four-bond proton-proton coupling 355,

PE Spectrum 422;

Penta-2,3-dienoic acid (3-methyl-1-allenecarboxylic acid) (70)

Total electron density 367, 368;

2-Methyl-buta-2,3-dienoic acid (123)

Carbon chemical shift 348,

Proton chemical shift 350, 375.

C5 H6 S1

Methyl-butatrienyl-sulfide (235)

Proton chemical shift 404,

Five-bond proton-proton coupling 443.

C5 H7 Br1

1-Bromo-3-methyl-buta-1,2-diene (152)

Proton chemical shift 377.

C5 H7 Cl2 P1

1-Dichlorophosphinyl-3-methyl-buta-1,2-diene (160)

Proton chemical shift 377.

C5 H8

3-Methyl-buta-1,2-diene (1,1-dimethylallene) (2)

Dipole moment 332, 339,

Total electron density 343, 368,

Carbon chemical shift 348, 369, 371,

Proton chemical shift 350, 375,

One-bond carbon-proton coupling 378,

One-bond carbon-carbon coupling 438,
Two-bond proton-proton coupling 439,
PE Spectrum 358,
UV Absorption spectrum 397;

Penta-2,3-diene (1,3-dimethylallene) (3)

Total electron density 367, 368,
Carbon chemical shift 369, 371,
Proton chemical shift 376,
PE Spectrum 358,
Molar rotation 380,

Penta-1,2-diene (ethylallene) (18)

Dipole moment 334,
Total electron density 343, 344, 431,
Carbon chemical shift 348, 369, 371, 431,
Proton chemical shift 350, 375,
One-bond carbon-proton coupling 354, 378,
Four-bond proton-proton coupling 355,
PE Spectrum 358, 422.

C5 H8 O1

Penta-3,4-dien-1-ol (122)

Proton chemical shift 350, 375;

Penta-2,3-dien-1-ol (174)

Molar rotation 380;

Ethyl-methyl-ketene (200)

Carbon chemical shift 386;

Ethyl-allenyl-ether (ethoxyallene)

Carbon chemical shift 348.

C5 H8 S1

Methyl-4-buta-1,2-dienyl-sulfide

Carbon chemical shift 348;

Methyl-1-buta-1,2-dienyl-sulfide (117)

Carbon chemical shift 370, 372;

Methyl-3-buta-1,2-dienyl-sulfide (118)

Carbon chemical shift 348, 370, 372.

C5 H10 O1 Si1

Trimethylsilylketene (47)

Dipole moment 336,
Total electron density 431, 438,

π Electron density 417, 431, 438,
Carbon chemical shift 431,
UV Absorption spectrum 429, 430.

C5 H13 O1 P1

Diethylphosphonyllallene (diethylallenyl-phosphineoxide) (256)

Proton chemical shift 350,
Four-bond phosphorus-proton coupling 442.

C6 H6

Hexa-1,2-diene-5-yne (propargylallene) (63)

PE Spectrum 358.

C6 H7 N1

4-Methyl-penta-2,3-dienonitrile (3,3-dimethyl-1-cyanoallene) (41)

Dipole moment 334,
Total electron density 367, 368,
Proton chemical shift 376.

C6 H8

2-Methyl-penta-2,3,4-triene (1,1-dimethylbutatriene) (4)

Proton chemical shift 404;

(E)-Hexa-2,3,4-triene (trans-1,4-dimethylbutatriene) (5)

Proton chemical shift 404;

(Z)-Hexa-2,3,4-triene (cis-1,4-dimethylbutatriene) (6)

Proton chemical shift 404;

Cyclopropylallene (31)

Dipole moment 334,
Total electron density 343, 345,
PE Spectrum 358, 422;

3-Methyl-penta-1,2,4-triene (1-methyl-1-vinylallene) (146)

Proton chemical shift 350, 376;

Hexa-3,4,5-triene (ethylbutatriene) (234)

Proton chemical shift 404.

C6 H8 O1

2-Methyl-penta-2,3-dienal (143)

Proton chemical shift 376;

Ethyl-butatrienyl-ether (ethoxybutatriene) (228)

Carbon chemical shift 403,
Proton chemical shift 404,
Two-bond proton-proton coupling 441,

Five-bond proton-proton coupling 443.

C6 H8 O2

Methyl 2-methyl-buta-2,3-dienoate (79)

Carbon chemical shift 348, 369, 371,

Proton chemical shift 350, 375;

2-Ethyl-buta-2,3-dienoic acid (124)

Carbon chemical shift 348,

Proton chemical shift 350,

One-bond carbon-proton coupling 378;

2-Methyl-penta-2,3-dienoic acid (134)

Proton chemical shift 376,

Molar rotation 380.

C6 H9 Br1

3-Methyl-5-bromo-penta-3,4-diene (116)

Carbon chemical shift 370, 372,

Proton chemical shift 377,

One-bond carbon-proton coupling 378.

C6 H9 Cl1

3-Methyl-5-chloro-penta-3,4-diene (115)

Carbon chemical shift 370, 372,

Proton chemical shift 377.

C6 H10

Hexa-2,3-diene (1-methyl-3-ethyl-allene) (8)

Carbon chemical shift 369, 371,

One-bond carbon-proton coupling 378,

Allene-phenol equilibrium constant 346;

3-Methyl-penta-1,2-diene (1-methyl-1-ethyl-allene) (7)

Total electron density 343, 368,

Carbon chemical shift 348, 369, 371,

Proton chemical shift 350, 375,

Allene-phenol equilibrium constant 346;

Hexa-1,2-diene (n-propylallene) (60)

Carbon chemical shift 348, 369, 371,

Proton chemical shift 350, 375,

Allene-phenol equilibrium constant 346;

4-Methyl-penta-2,3-diene (trimethylallene) (61)

Carbon chemical shift 369, 371,

PE Spectrum 358,

Allene-phenol equilibrium constant 346;

4-Methyl-penta-1,2-diene (isopropylallene) (76)

Carbon chemical shift 348, 369, 371,

Proton chemical shift 350, 375.

C6 H10 O1

3-Methoxy-penta-3,4-diene (128)

Proton chemical shift 375;

5-Methoxy-penta-3,4-diene (3-ethyl-1-methoxyallene) (147)

Proton chemical shift 376;

Hexa-3,4-dien-1-ol (175)

Molar rotation 380.

C6 H10 S1

Tert. butyl- thioketene (208)

Carbon chemical shift 390,

UV Absorption spectrum 390;

Methyl-3-penta-3,4-dienyl-sulfide (1-ethyl-1-thiomethoxyallene)

Carbon chemical shift 348.

C6 H12 Si1

Trimethylsilylallene (27)

Dipole moment 334,

Total electron density 343, 345, 431,

π Electron density 418,

Carbon chemical shift 348, 431,

Proton chemical shift 350,

One-bond carbon-proton coupling 354,

Four-bond proton-proton coupling 355.

C7 H4

Hepta-1,2-diene-4,6-diyne (29)

Dipole moment 334,

Total electron density 343, 345;

Hepta-1,2,3,4,5,6-hexaene (heptahexaene) (224)

Total electron density 400.

C7 H5 N1 O1

Phenyl isocyanate (218)

UV Absorption spectrum 398,

IR Absorption spectrum 396.

C7 H8 O1

5-Methyl-hexa-2,3,4-trienal (239)

Proton chemical shift 404,
UV Absorption spectrum 406.

C7 H8 O4

Dimethyl penta-2,3-diendioate (1,3-dicarbomethoxyallene) (78)

Carbon chemical shift 369, 371.

C7 H9 N1

4-Methyl-hexa-2,3-dienonitrile (144)

Proton chemical shift 376.

C7 H9 N2 O1 P1

Bis-dimethylamino-phosphonyllallene (258)

Four-bond phosphorus-proton coupling 442.

C7 H10 O1

5-Methoxy-2-methyl-penta-2,3,4-triene (229)

Carbon chemical shift 404,
Proton chemical shift 404,
UV Absorption spectrum 406;

5-Ethoxy-penta-2,3,4-triene (237)

Proton chemical shift 404.

C7 H10 O2

Methyl 2-ethyl-buta-2,3-dienoate (80)

Carbon chemical shift 348, 369, 371,
Proton chemical shift 350, 375,
One-bond carbon-proton coupling 378;

Methyl 2-methyl-penta-2,3-dienoate (81)

Carbon chemical shift 369, 371,
Proton chemical shift 376;

2-Ethyl-penta-2,3-dienoic acid (135)

Proton chemical shift 376,
One-bond carbon-proton coupling 378,
Molar rotation 380;

2-Methyl-hexa-2,3-dienoic acid (136)

Proton chemical shift 376,
Molar rotation 380;

4-Methyl-hexa-2,3-dienoic acid (138)

Proton chemical shift 376,
Molar rotation 380.

C7 H10 O3

Carboethoxy-ethyl-ketene (255)

UV Absorption spectrum 430.

C7 H12

2,4-Dimethyl-penta-2,3-diene (tetramethylallene) (62)

Carbon chemical shift 369, 371,

PE Spectrum 358

Allene-phenol equilibrium constant 346;

Hepta-3,4-diene (1,3-diethylallene) (75)

Carbon chemical shift 369, 371,

Proton chemical shift 376;

4,4-Dimethyl-penta-1,2-diene (tert. butylallene) (120)

Carbon chemical shift 348,

Proton chemical shift 350, 375;

Hepta-1,2-diene (n-butylallene)

Carbon chemical shift 348;

3,4-Dimethyl-penta-1,2-diene (1-methyl-1-isopropyl-allene)

Proton chemical shift 350.

C7 H12 O1

2-Methoxy-hexa-2,3-diene (111)

Carbon chemical shift 370, 372;

5-Methyl-hexa-3,4-dien-1-ol (139)

Proton chemical shift 376;

Hepta-2,3-dien-1-ol (140)

Proton chemical shift 376;

4-Methyl-hexa-2,3-dien-1-ol (141)

Proton chemical shift 376;

6-Methoxy-hexa-4,5-diene (148)

Proton chemical shift 376.

C7 H12 S1

1-Isopropyl-1-thiomethoxyallene

Carbon chemical shift 348.

C7 H13 O2 P1

Diethoxyphosphinylallene (diethoxyallenyl-phosphine) (261)

Four-bond phosphorus-proton coupling 442.

C7 H13 O3 P1

Diethoxyphosphonyllallene (diethylphosphonoallene) (259)

Proton chemical shift 350,

Four-bond phosphorus-proton coupling 442.

C7 H13 P1

Diethylphosphinylallene (diethylallenyl-phosphine) (262)

Proton chemical shift 350,

Four-bond phosphorus-proton coupling 442.

C7 H14 N2

Diisopropylcarbodiimide (55)

Dipole moment 336,

Carbon chemical shift 385-386,

PE Spectrum 411.

C7 H15 N2 P1

Bis-dimethylaminophosphinylallene (bis-dimethylamino-allenyl-phosphine) (260)

Four-bond phosphorus-proton coupling 442.

C8 H6 O1

Octa-2,3-diene-5,7-diyne-1-ol (180)

Molar rotation 380;

Phenylketene (216)

Total electron density 438,

π Electron density 438,

PE Spectrum 423,

UV Absorption spectrum 397.

C8 H7 N1

N-Phenyl ketene imine (N-1-vinylideneaniline) (188)

Carbon chemical shift 386,

Proton chemical shift 385,

One-bond carbon-hydrogen coupling 436,

IR Absorption spectrum 396;

C-Phenyl ketene imine (2-phenyl-vinylidene-amine) (215)

UV Absorption spectrum 397.

C8 H8

Styrene

PE Spectrum 427,

UV Absorption spectrum 427.

C8 H8 N2

Methyl-phenyl-diazomethane (249)

Carbon chemical shift 412.

C8 H12

Vinylidene cyclohexane (65)

PE Spectrum 358;

2-Methyl-4-cyclopropyl-buta-2,3-diene (64)

PE Spectrum 358;

4,4-Dimethyl-hexa-1,2,5-triene (88)

Carbon chemical shift 348, 369, 371;

2,5-Dimethyl-hexa-2,3,4-triene(tetramethylbutatriene) (245)

PE Spectrum 406,

UV Absorption spectrum 406.

C8 H12 O1

2-Methyl-6-methoxy-hexa-3,4,5-triene (230)

Carbon chemical shift 403.

C8 H12 O2

Methyl 2-ethyl-penta-2,3-dienoate (83)

Carbon chemical shift 369, 371,

Proton chemical shift 376;

Methyl 2-methyl-hexa-2,3-dienoate (84)

Carbon chemical shift 369, 371,

Proton chemical shift 376,

One-bond carbon-proton coupling 378;

Methyl 4-methyl-hexa-2,3-dienoate (85)

Carbon chemical shift 369, 371,

Proton chemical shift 376,

Molar rotation 380;

Ethyl 4-methyl-penta-2,3-dienoate (13)

Proton chemical shift 376;

2-Ethyl-hexa-2,3-dienoic acid (137)

Proton chemical shift 376,

One-bond carbon-proton coupling 378,

Molar rotation 380.

C8 H12 O2

(E)-2-Methoxy-5-ethoxy-penta-2,3,4-triene (236)

- Proton chemical shift 404;
Diethoxybutatriene (238)
Proton chemical shift 404.
C8 H13 Br1
1-Bromo-3,4,4-trimethyl-penta-1,2-diene (154)
Proton chemical shift 377.
C8 H13 Cl1
1-Chloro-3,4,4-trimethyl-penta-1,2-diene (149)
Proton chemical shift 377.
C8 H14
3,4,4-Trimethyl-penta-1,2-diene (121)
Proton chemical shift 350, 375;
Octa-1,2-diene (*n-pentylallene*)
Carbon chemical shift 348.
C8 H18 S1 Si2
Bis-trimethylsilyl-thioketene (211)
Carbon chemical shift 390,
UV Absorption spectrum 390.
C9 H7 Br1
3-Bromo-1-phenylallene (156)
Proton chemical shift 377,
UV Absorption spectrum 359, 379.
C9 H7 Cl1
3-Chloro-1-phenylallene (36)
Dipole moment 334,
Total electron density 367, 368,
UV Absorption spectrum 359, 379;
p-Chloro-phenylallene
Carbon chemical shift 348.
C7 H9 I1
3-Iodo-1-phenylallene (161)
UV Absorption spectrum 359, 379.
C8 H9
Phenylallene (16)
Dipole moment 334,
Total electron density 343, 345, 431,

Carbon chemical shift 348, 369, 371, 431,
Proton chemical shift 350, 375,
One-bond carbon-proton coupling 354, 378,
Two-bond carbon-proton coupling 439,
Four-bond proton-proton coupling 355,
PE Spectrum 358, 422, 427,
UV Absorption spectrum 359, 397, 427.

C9 H8 O1

Nona-3,4-diene-6,8-diyne-1-ol (marasin) (181)

Molar rotation 380;

Methyl-phenyl-ketene (201)

Total electron density 438,
 π Electron density 438,
Carbon chemical shift 386, 412.

C9 H8 S1

Methyl-phenyl-thioketene (209)

Carbon chemical shift 390, 394, 412,
UV Absorption spectrum 390.

C9 H9 N1

N-Phenyl-methyl-ketene imine (N-1-propenylideneaniline) (189)

Carbon chemical shift 386.

C9 H13 N1

4,5,5-Trimethyl-hexa-2,3-dienonitrile (145)

Proton chemical shift 376.

C9 H14

Propenylidene cyclohexane (66)

PE Spectrum 358;

5,5-Dimethyl-hepta-2,3,6-triene (89)

Carbon chemical shift 369, 371.

C9 H14 O2

Methyl 2-ethyl-hexa-2,3-dienoate (82)

Carbon chemical shift 369, 371;

2-Ethyl-5-methyl-hexa-2,3-dienoic acid (87)

Carbon chemical shift 369, 371,
Proton chemical shift 376;

2-n-Butyl-penta-2,3-dienoic acid (173)

Molar rotation 380.

C9 H17 N1

N-isobutyl-methyl-ethyl-ketene imine (isobutyl-N-(2-methyl-1-butenylidene)amine) (198)

Carbon chemical shift 386.

C10 H7 N1

4-Phenyl-buta-2,3-dienonitrile (3-cyano-1-phenylallene) (37)

Dipole moment 334,

Total electron density 367, 368,

UV Absorption spectrum.

C10 H8

p-Methyl-phenylallene

Carbon chemical shift 348.

C10 H8 O2

Methyl nona-3,4-diene-6,8-dienoate (185)

Molar rotation 380;

4-Phenyl-buta-2,3-dienoic acid (phenylallenecarboxylic acid) (1)

Dipole moment 334,

Total electron density 367, 368,

Carbon chemical shift 369, 371,

Proton chemical shift 376,

One-bond carbon-proton coupling 378,

Four-bond carbon-proton coupling 355,

UV Absorption spectrum 359, 379,

Molar rotation 380.

C10 H9 Br1

1-Bromo-3-phenyl-buta-1,2-diene (157)

Proton chemical shift 377,

UV Absorption spectrum 379.

C10 H10

4-Phenyl-buta-2,3-diene (3-methyl-1-phenylallene) (38)

Dipole moment 334,

Total electron density 367, 368,

Carbon chemical shift 369, 371,

Proton chemical shift 376,

One-bond carbon-proton coupling 378,

Four-bond proton-proton coupling 355,

PE Spectrum 358,

UV Absorption spectrum 359, 379;

2-Phenyl-but-2,3-diene (1-methyl-1-phenylallene) (59)

Total electron density 343,
Carbon chemical shift 348, 369, 371, 412,
Proton chemical shift 350, 375,
One-bond carbon-proton coupling 378,
UV Absorption spectrum 379, 382.

C10 H10 O1

3-Methoxy-1-phenylallene (39)

Dipole moment 334,
Total electron density 367, 368,
Carbon chemical shift 370, 372,
Proton chemical shift 377,
Four-bond proton-proton coupling 355,
UV Absorption spectrum 359;

Deca-3,4-diene-6,8-diyne-1-ol (methyl marasin) (184)

Molar rotation 380;

Deca-4,5-diene-7,9-diyne-1-ol (182)

Molar rotation 380;

Ethyl-phenyl-ketene (202)

Carbon chemical shift 386.

C10 H11 N1

N-Phenyl-ethyl-ketene imine (N-1-butenylideneaniline) (190)

Carbon chemical shift 386,
UV Absorption spectrum 398;

N-Phenyl-dimethyl-ketene imine (N-(2-methyl-1-propenylidene)aniline) (194)

Carbon chemical shift 386,
PE Spectrum 424-425;

Phenyl-methyl-allenyl-amine (N,N-methyl-phenyl-aminoallene)

Carbon chemical shift 348,
Proton chemical shift 350,
Four-bond proton-proton coupling 355.

C10 H16

2,5,5-Trimethyl-hepta-2,3,6-triene (90)

Carbon chemical shift 369, 371.

C10 H16 O2

Methyl 2-ethyl-4-methyl-hexa-2,3-dienoate (86)

Carbon chemical shift 369, 371;

Ethyl 2,5-dimethyl-hexa-2,3-dienoate

Proton chemical shift 375;

Deca-2,3-dienoic acid (172)

Molar rotation 380.

C10 H17 N1

N-Cyclohexyl-dimethyl-ketene imine (cyclohexyl-N-(2-methyl-1-propenylidene)amine) (214)

PE Spectrum 411, 425,

UV Absorption spectrum 397.

C11 H10 O2

4-Phenyl-penta-2,3-dienoic acid (73)

Total electron density 367, 368,

Carbon chemical shift 369, 371,

Proton chemical shift 376,

One-bond carbon-proton coupling 378,

Molar rotation 380;

2-Methyl-4-phenyl-buta-2,3-dienoic acid (77)

Carbon chemical shift 369, 371,

Proton chemical shift 376,

UV Absorption spectrum 379,

Molar rotation 380.

C11 H12

2-Methyl-4-phenyl-buta-2,3-diene (142)

Proton chemical shift 376.

C11 H12 O1

Undeca-5,6-diene-8,10-diyne-1-ol (183)

Molar rotation 380.

C11 H12 O2 S1

Buta-1,2-dienyl-p-tolyl-sulfone (4-p-tolylsulfonyl-buta-2,3-diene) (186)

Molar rotation 380.

C11 H13 N1

N-Phenyl-methyl-ethyl-ketene imine (N-(2-methyl-1-butenylidene)-aniline) (193)

Carbon chemical shift 386;

N-p-Tolyl-dimethyl-ketene imine (N-(2-methyl-1-propenylidene)-p-toluidine) (252)

PE Spectrum 424-425.

C11 H13 N1 O1

N-p-Methoxy-phenyl-dimethyl-ketene imine (N-(2-methyl-1-propenylidene)-p-methoxy-aniline) (253)

PE Spectrum 424–425.

C11 H16 O4

Methyl-hepta-5,6-dienoate-7-ol-acetate (178)

Molar rotation 380.

C11 H18

3,6,6-Trimethyl-octa-3,4,7-triene (91)

Carbon chemical shift 369, 371;

7,7-Dimethyl-nona-4,5,8-triene (92)

Carbon chemical shift 369, 371.

C11 H18 O2

Ethyl 2-ethyl-5-methyl-hexa-2,3-dienoate (131)

Proton chemical shift 375.

C11 H20

3-Tert. butyl-4,4-dimethyl-penta-1,2-diene (1,1-di-tert. butylallene) (67)

PE Spectrum 358.

C12 H12 O2

4-Phenyl-hexa-2,3-dienoic acid (95)

Carbon chemical shift 369, 371,

Proton chemical shift 376,

Molar rotation 380;

2-Ethyl-4-phenyl-buta-2,3-dienoic acid (96)

Carbon chemical shift 369, 371,

Proton chemical shift 376,

Molar rotation 380;

Methyl 4-phenyl-penta-2,3-dienoate (101)

Carbon chemical shift 369, 371,

Proton chemical shift 376;

Methyl 2-methyl-4-phenyl-buta-2,3-dienoate (102)

Carbon chemical shift 369, 371,

One-bond carbon-proton coupling 378,

2-Methyl-4-phenyl-penta-2,3-dienoic acid (168)

Molar rotation 380.

C12 H14 O2

3-Methoxy-5-phenyl-penta-3,4-diene (112)

Carbon chemical shift 370, 372,

Proton chemical shift 376.

C12 H18 O4

Octa-2,3-diene-1,8-diol-diacetate (179)

Molar rotation 380.

C12 H20

(E)-2,2,7,7-Tetramethyl-octa-3,4,5-triene (*trans-di-tert. butylbutatriene*)
(231)

Carbon chemical shift 404,

Proton chemical shift 404,

UV Absorption spectrum 406.

C12 H22 N2

Dicyclohexylcarbodiimide (205)

Carbon chemical shift 386,

Nitrogen chemical shift 387.

C13 H10

α -Naphthylallene

Total electron density 343, 345.

C13 H10 N2

Diphenylcarbodiimide (56)

Dipole moment 336;

Diphenyldiazomethane (220)

Nitrogen chemical shift 429,

UV Absorption spectrum 429.

C13 H13 Na1 O2

Sodium 2-methyl-4-phenyl-hexa-2,3-dienoate (170)

Molar rotation 380;

Sodium 2-ethyl-4-phenyl-penta-2,3-dienoate (171)

Molar rotation 380.

C13 H14 O2

2-Ethyl-4-phenyl-penta-2,3-dienoic acid (97)

Carbon chemical shift 369, 371,

Molar rotation 380;

2-Methyl-4-phenyl-hexa-2,3-dienoic acid (98)

Carbon chemical shift 369, 371,

Molar rotation 380;

Methyl 4-phenyl-hexa-2,3-dienoate (103)

Carbon chemical shift 370, 372,
Proton chemical shift 375;

Methyl 2-ethyl-4-phenyl-buta-2,3-dienoate (104)

Carbon chemical shift 370, 372,
Proton chemical shift 376,
One-bond carbon-proton coupling 378;

Methyl 2-methyl-4-phenyl-penta-2,3-dienoate (105)

Carbon chemical shift 370, 372.

C₁₃ H₁₆ O₁

2-Methyl-3-methoxy-5-phenyl-penta-3,4-diene (113)

Carbon chemical shift 370, 372.

C₁₃ H₁₇ N₁

N-Isobutyl-methyl-phenyl-ketene imine (isobutyl-N-(2-phenyl-1-propenylidene)amine) (197)

Carbon chemical shift 386,
UV Absorption spectrum 398.

C₁₄ H₁₀ O₁

Diphenylketene (46)

Dipole moment 336,
Carbon chemical shift 386, 429,
UV Absorption spectrum 398, 429.

C₁₄ H₁₀ S₁

Diphenylthioketene (210)

Carbon chemical shift 390,
UV Absorption spectrum 390, 399.

C₁₄ H₁₁ N₁

N-Phenyl-phenyl-ketene imine (N-(2-phenyl-1-vinylidene)aniline) (191)

Carbon chemical shift 386.

C₁₄ H₁₅ Na₁ O₂

Sodium 2-ethyl-4-phenyl-hexa-2,3-dienoate (169)

Molar rotation 380.

C₁₄ H₁₆ O₂

2-Ethyl-4-phenyl-hexa-2,3-dienoic acid (99)

Carbon chemical shift 369, 371,
Molar rotation 380;

Methyl 2-methyl-4-phenyl-hexa-2,3-dienoate (107)

Carbon chemical shift 370, 372,

Molar rotation 380;

Methyl 2-ethyl-4-phenyl-penta-2,3-dienoate (**108**)

Carbon chemical shift 370, 372,

Molar rotation 380;

Methyl 2-phenyl-4-methyl-hexa-2,3-dienoate (**109**)

Carbon chemical shift 370, 372.

C₁₄ H₁₈ O₁

2-Methyl-3-methoxy-5-phenyl-hexa-3,4-diene (**114**)

Carbon chemical shift 370, 372.

C₁₅ H₁₀ Br₂

1,1-Dibromo-3,3-diphenylallene (**166**)

UV Absorption spectrum 379.

C₁₅ H₁₀ Br₁ Cl₁

1-Bromo-1-chloro-3,3-diphenylallene (**165**)

UV Absorption spectrum 379.

C₁₅ H₁₀ Br₁ I₁

1-Bromo-1-iodo-3,3-diphenylallene (**167**)

UV Absorption spectrum 379.

C₁₅ H₁₁ Br₁

1-Bromo-3,3-diphenylallene (**155**)

Proton chemical shift 377,

UV Absorption spectrum 379.

C₁₅ H₁₁ Cl₁

1-Chloro-3,3-diphenylallene (**150**)

Proton chemical shift 377,

UV Absorption spectrum 379.

C₁₅ H₁₁ I₁

1-Iodo-3,3-diphenylallene (**164**)

UV Absorption spectrum 379.

C₁₅ H₁₂

1,1-Diphenylallene (**35**)

Dipole moment 334,

UV Absorption spectrum 379;

1,3-Diphenylallene (**72**)

Total electron density 367, 368,

Proton chemical shift 376,

UV Absorption spectrum 359, 379,
Molar rotation 380.

C15 H13 N1

N-Phenyl-methyl-phenyl-ketene imine (N-(2-phenyl-1-propenylidene)-aniline) (195)

Carbon chemical shift 386, 412;

N-Methyl-diphenyl-ketene imine (methyl-N-(2,2-diphenyl-1-vinylidene)-amine) (196)

Carbon chemical shift 386.

C15 H13 O1 P1

Diphenylphosphonyllallene (diphenylallenyl-phosphineoxide) (257)

Proton chemical shift 350,

Four-bond proton-proton coupling 355,

Four-bond phosphorus-proton coupling 442.

C15 H18 O2

Methyl 2-ethyl-4-phenyl-hexa-2,3-dienoate (106)

Carbon chemical shift 370, 372,

Molar rotation 380.

C16 H12 O2

4,4-Diphenyl-buta-2,3-dienoic acid (100)

Carbon chemical shift 369, 371,

Proton chemical shift 376,

UV Absorption spectrum 379.

C16 H14

2,4-Diphenyl-buta-2,3-diene (93)

Carbon chemical shift 369, 371,

Proton chemical shift 376.

C16 H30 O1

Hexadeca-3,4-dien-1-ol (176)

Molar rotation 380.

C17 H16

2-Methyl-4,4-diphenyl-buta-2,3-diene (163)

UV Absorption spectrum 379.

C18 H19 N1

N-Isobutyl-diphenyl-ketene imine (isobutyl-N-(2,2-diphenyl-1-vinylidene)-amine) (219)

UV Absorption spectrum 398.

C19 H34 O2

Methyl octadeca-5,6-dienoate (methyl laballenoate) (177)

Molar rotation 380.

C20 H15 N1

Triphenyl-ketene imine (N-(2,2-diphenyl-1-vinylidene)aniline) (192)

Carbon chemical shift 386,

UV Absorption spectrum 398.

C20 H36

Tetra-tert. butylbutatriene (246)

PE Spectrum 406,

UV Absorption spectrum 406.

C20 H36 S4

Tetrakis-(tert. butylthio)-butatriene (232)

Carbon chemical shift 404.

C21 H16

Triphenylallene (127)

Proton chemical shift 375,

UV Absorption spectrum 379.

C21 H17 O1 P1

3-Diphenylphosphonyl-1-phenylallene (187)

Four-bond proton-proton coupling 355,

Molar rotation 380.

C22 H16 O2

2,4,4-Triphenyl-buta-2,3-dienoic acid (162)

UV Absorption spectrum 379.

C22 H36

Bis-(2,2,6,6-tetramethyl-cyclohexylidene-1)-butatriene (241)

UV Absorption spectrum 406.

C23 H18 O2

Methyl 2,4,4-triphenyl-buta-2,3-dienoate (110)

Carbon chemical shift 370, 372.

C24 H36

Bis-(2,2,6,6-tetramethyl-cyclohexylidene-1)-hexapentaene (242)

UV Absorption spectrum 406.

C25 H28

2,2,8,8-Tetramethyl-3,7-diphenyl-nona-3,4,5,6-tetraene (68)

Carbon chemical shift 360,
Molar rotation 360.

C27 H20

Tetraphenylallene (94)

Carbon chemical shift 369, 371,
UV Absorption spectrum 406.

C26 H36

Bis-(2,2,6,6-tetramethyl-cyclohexylidene-1)-octaheptaene (243)

UV Absorption spectrum 406.

C28 H20

Tetraphenylbutatriene (225)

Carbon chemical shift 402,
UV Absorption spectrum 406.

C28 H36

Bis-(2,2,6,6-tetramethyl-cyclohexylidene-1)-decanonaene (244)

UV Absorption spectrum 406.

C29 H20

Tetraphenylpentatetraene (227)

Carbon chemical shift 402,
UV Absorption spectrum 406.

C30 H20

Tetraphenylhexapentaene (226)

Carbon chemical shift 402,
UV Absorption spectrum 406.

H1 N3

Hydrazoic acid (206)

Nitrogen chemical shift 387.

N2

Nitrogen

Nitrogen chemical shift 388.

N2 O1

Dinitrogen mono-oxide (207)

Nitrogen chemical shift 387.

An Examination of Linear Solvation Energy Relationships

BY M. J. KAMLET,

*Explosives Chemistry Branch,
Naval Surface Weapons Center/White Oak
Silver Spring, Maryland 20910*

AND J. L. M. ABBOUD,

*Universite Cadi Iyad,
Boulevard de Safi, Marrakech, Morocco*

AND R. W. TAFT,

*University of California,
Irvine, Irvine, California 92717*

CONTENTS

Introduction	485
I. Dipolar Contributions to Solvent Effects	488
A. Reaction Rates and Equilibria	488
1. Theoretical Approach	488
2. Empirical Approach	500
B. Physical Properties	507
1. Theoretical Approach	507
2. Empirical Approach	511
C. Toward a Generalized Scale of Solvent Polarities	522
II. Linear Solvation Energy Relationships (LSER)	533
A. General Formalism	533
B. Methodology	535
1. The β Scale of Solvent HBA Basicity	535
2. The π^* Scale of Solvent Polarity	558
3. The α Scale of Solvent HBD Acidity	587
4. Additional Correlations with π^* , α , and β	604
5. Concluding Remarks	617
References	623

INTRODUCTION

Nearly a century ago, Menshutkin (1) showed that the rate of quaternarization of amines by alkyl halides,



is a very solvent-sensitive property.

Since then, the generality and importance of solvent effects on chemical reactivity and physical properties of species in dilute solutions has been widely acknowledged. Solvent-solute interactions for reactants and for products account for observed shifts in chemical equilibria; those involving reactants and transition states determine changes in the rates of elementary processes. Shifts of the absorption and/or fluorescence maxima originate in differential solvent-solute interactions of the ground and electronically excited states of a dissolved species. The perturbations induced by the solvents are reflected by concurrent variations of such physical properties of the solute as ir, nmr, and epr spectra and partial molar properties.

Since chemists are generally concerned with solvent effects in equilibria and reaction rates, the role of solvents is adequately expressed and visualized in terms of chemical potentials (2).

If a process such as Equation 2 is studied in highly dilute solution in two solvents, S_1 and S_2 , the corresponding changes in free energy can be written as in Equations 3 and 4:



$$\Delta G^\circ(S_1, T) = \mu_C^\circ(S_1, T) - \mu_A^\circ(S_1, T) - \mu_B^\circ(S_1, T) \quad (3)$$

$$\Delta G^\circ(S_2, T) = \mu_C^\circ(S_2, T) - \mu_A^\circ(S_2, T) - \mu_B^\circ(S_2, T) \quad (4)$$

The standard state used for all the chemical potentials appearing in Equations 3 and 4 is one of infinite dilution, that is, the one in which all the solute molecules are completely surrounded by and interact only with solvent molecules (3). Under those conditions, for a given species, say A, the difference $\mu_A^\circ(S_2, T) - \mu_A^\circ(S_1, T)$ is a measure of its differential solvation by S_2 and S_1 .

The difference $\Delta G^\circ(S_2, T) - \Delta G^\circ(S_1, T)$ can be expressed as a function of the differential solvation of reactants and products:

$$\Delta G^\circ(S_2, T) - \Delta G^\circ(S_1, T) = [\mu_C^\circ(S_2, T) - \mu_C^\circ(S_1, T)] - [\mu_A^\circ(S_2, T) - \mu_A^\circ(S_1, T)] - [\mu_B^\circ(S_2, T) - \mu_B^\circ(S_1, T)] = \rho(T) \quad (5)$$

Since $\rho(T)$ is the limiting value of $-RT \ln(K_x)_{s_2} / (K_x)_{s_1}$ at infinite dilution, it measures the shift of equilibrium (Equation 2) on going from S_1 to S_2 , as shown schematically in Fig. 1.

Equation 5 simplifies when only an "isomerization" process is considered:



$$\rho(T) = [\mu_{A'}^\circ(S_2, T) - \mu_{A'}^\circ(S_1, T)] - [\mu_A^\circ(S_2, T) - \mu_A^\circ(S_1, T)]$$

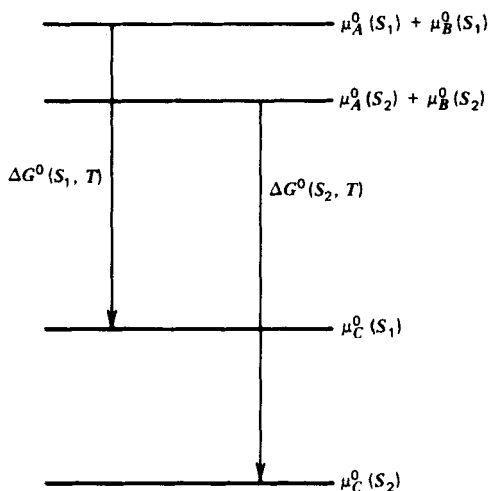
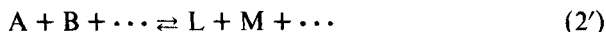


Figure 1 Solvent effects on chemical potentials of solutes.

In general, for any process:



$$\rho(T) = \Delta G^{\circ}(S_2, T) - \Delta G^{\circ}(S_1, T) = \Delta^{S_1 \rightarrow S_2} (\mu_L^{\circ} + \mu_M^{\circ} + \dots) - \Delta^{S_1 \rightarrow S_2} (\mu_A^{\circ} + \mu_B^{\circ} + \dots)$$

The principle is the same for any other state change, including spectroscopic ones.

If reaction proceeds through a transition state C^{\ddagger} , according to



the activated complex theory (4), equations formally identical to 3 and 4 are applicable, except for the fact that μ_c° is replaced by $\mu_{c^{\ddagger}}^{\circ}$. Equation 5' follows:

$$\rho(T) = \Delta G^{\ddagger}(S_2, T) - \Delta G^{\ddagger}(S_1, T) = [\mu_{C^{\ddagger}}^{\circ}(S_2, T) - \mu^{\circ}(S_1, T)] - [\mu_A^{\circ}(S_2, T) - \mu_A^{\circ}(S_1, T)] - [\mu_B^{\circ}(S_2, T) - \mu_B^{\circ}(S_1, T)] \quad (5')$$

Likewise, $\rho_{tr}(T)$ is also the limiting value of $-RT \ln (k_1)_{S_2} / (k_1)_{S_1}$ at infinite dilution. Changes in partial molar quantities involved in processes 2' and 6 are easily derived from Equation 5 and 5'.

These same equations formally bring the quantitative study of solvent effects on equilibria and rates of elementary processes to that of solvent effects on the chemical potentials of the dissolved species or, in other words, to that of the energetics of solvent-solute interactions. In the forthcoming section, we restrict ourselves to the study of polar species (excluding "free ions") in polar

media and attention is directed toward the effects of dipolar forces (excluding hydrogen-bonding and/or charge-transfer).

I. DIPOLAR CONTRIBUTIONS TO SOLVENT EFFECTS

A. Reaction Rates and Equilibria

1. Theoretical Approach

The Reaction Field (R.F.) (5). Consider a solute molecule A with a non-zero dipole moment μ_A surrounded by the molecules of a polar solvent S(μ_S). The distribution of S molecules* around the molecule A creates an electrostatic field E_R . This field (a) is colinear and proportional to μ_A and (b) has the same orientation as the electrostatic field produced by μ_A :

$$E_R = C(S, A) \mu_A \quad (6')$$

Furthermore, E_R interacts with the solute dipole leading to a decrease of the internal energy of the system.** Following Onsager (5), the electrostatic field E_R is known as "reaction field." The great physical significance of this concept originates in the fact that it embodies the electrostatic fields of a practically infinite number of solvent molecules.

An exact determination of the magnitude of E_R requires at least the knowledge of the structure of the cybotactic environment of the solute. This information is generally unavailable but a reasonable statistical estimate can be obtained under some simplifying conditions.

The Theory of Onsager (5): In the case of a nonpolarizable solute, the model is quite simple: The solute molecule A is assumed to be a point dipole μ_A located at the center of a cavity of radius a . The potential ψ created by the dipole and its surroundings has to satisfy Laplace's equation:

$$\Delta\psi = 0 \quad (8a)$$

where ψ is a continuous, finite function. A further condition for the solution ψ is the continuity of the displacement vector when crossing the boundary of the cavity:

$$\epsilon(a-0) \left(\frac{\partial\psi}{\partial r} \right)_{r=a-0} = \epsilon(a+0) \left(\frac{\partial\psi}{\partial r} \right)_{r=a+0} \quad (8b)$$

* The molecules of solvent are under the influence of both the S-A and S-S interactions together with the thermal agitation.

** The energy of interaction, U , between the dipole μ_A and the R.F. is given by:

$$U = -\mu_A \cdot E_R \quad (7)$$

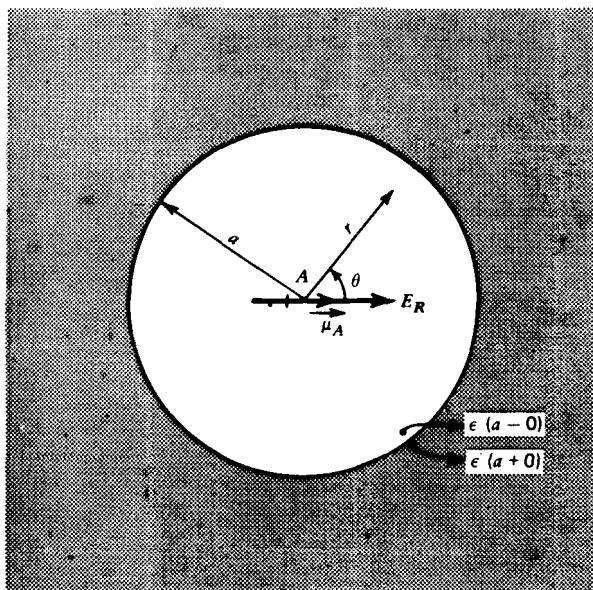


Figure 2 Solute cavity model used by Kirkwood, Block, Walker, and Onsager.

where $E(a - 0)$ and $E(a + 0)$ stand for the values of the dielectric constant at the inner and outer edges of the cavity, respectively. In the original treatment it is assumed that the perturbation induced by the solute is weak (compared to the thermal agitation). The function $\epsilon(r)$ is then a step function that changes abruptly from a constant value of one within the cavity to the macroscopic value of the bulk dielectric constant, ϵ_B , when the boundary is crossed (Fig. 2).

The solution of Equation 8a within the cavity is:

$$\psi = \frac{\mu_A \cdot \mathbf{r}}{r^3} - \mathbf{E}_R \cdot \mathbf{r} \quad (9a)$$

or:

$$\psi = \frac{\mu_A \cos\theta}{r^2} - E_r r \cos\theta \quad (9b)$$

where

$$\mathbf{E}_R = \frac{2(\epsilon_B - 1) \mu_A}{2\epsilon_B + 1} \frac{1}{a^3} \quad (10)$$

The first term in Equations 9a and 9b is the potential produced by the dipole, a constant quantity independent of the environment, \mathbf{E}_R is the reaction field.

The Block-Walker (6) Model: Although the isotropic approximation

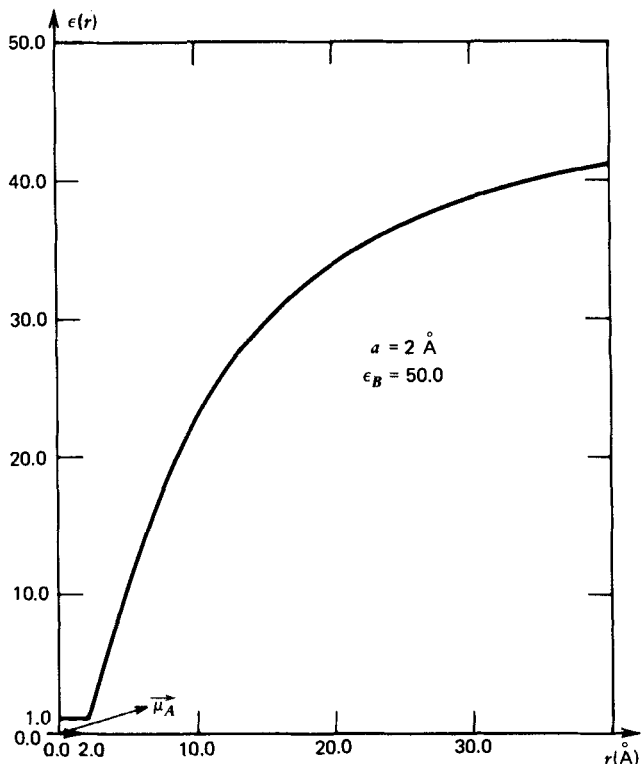


Figure 3 The shape of $\epsilon(r)$ for a solute cavity of radius 2 Å in a solvent of bulk dielectric constant 50. $\epsilon(r)$ vs. $r(\text{\AA})$.

probably holds for very low polarity systems, it likely breaks down when solvents and/or solutes are appreciably polar. A considerable degree of "solvent freezing" around the solute can take place when the dipolar solvent-solute interaction becomes significant compared to RT . In fact, as we shall see, there is a growing body of evidence indicating that the effects of polar media on polar solutes are determined to a large extent by multipolar complexation. Block and Walker suggested in 1973 that the form of the function $\epsilon(r)$ could be modified to account for the dielectric saturation likely to be brought about by the "solvent freezing." These authors suggest that $\epsilon(r)$ be taken as:

$$\epsilon(r) = \epsilon_B e^{-K/r} \quad (11)$$

for $r > a$ and $\epsilon(r) = 1$ for $0 \leq r \leq a$. K is determined as $K = a \ln \epsilon_B$ by the requirement that $\epsilon(a - 0) = \epsilon(a + 0) = 1$. In Fig. 3 we have represented the shape of $\epsilon(r)$ for a solute cavity of radius 2 Å in a solvent of bulk dielectric constant 50.

The integration of the Laplace equation with the expression of $\epsilon(r)$ given by Equation 11 yields the following expression for the potential within the cavity:

$$\psi = \frac{\boldsymbol{\mu}_A \cdot \mathbf{r}}{r^3} - \mathbf{E}_R \cdot \mathbf{r} \quad (12a)$$

or

$$\psi = \frac{\mu_A \cos\theta}{r^2} - \mathbf{E}_R \mathbf{r} \cos\theta \quad (12b)$$

where \mathbf{E}_R , the reaction field, is now given by

$$\mathbf{E}_R = \left[\frac{3\epsilon_B \ln\epsilon_B}{\epsilon_B \ln\epsilon_B - \epsilon_B + 1} - \frac{6}{\ln\epsilon_B} - 2 \right] \frac{\boldsymbol{\mu}_A}{a^3} \quad (13)$$

(It is assumed, once again, that A is a nonpolarizable dipole.) It can be noticed that the limiting expressions of E_R for $\epsilon_B \rightarrow \infty$ are the same for both models: μ_A/a^3 .

Recent calculations by Miles and Watts (7) on aqueous solutions of a variety of metal ions seem to indicate that Equation 11 likely overestimates the spatial range of the saturation effect; that is, the bulk value ϵ_B would be approached faster than predicted by that equation. In fact, as pointed out by Block and Walker, their expression of $\epsilon(r)$ is as approximate and arbitrary as Onsager's step function but has the advantage of reflecting the experimental fact of dielectric saturation and leads to mathematically tractable equations.

The Kirkwood-Eyring-Laidler Theory.

Simplified Form. Consider first a nonpolarizable point dipole $\boldsymbol{\mu}_A$ (solute molecule) located at the center of a sphere of radius a and dielectric constant one which is immersed in a medium of bulk dielectric constant ϵ_B . The electrostatic contribution to the chemical potential μ_{chem} of the dipole is given by Kirkwood's (8) Equation 14.

$$\mu_{chem} = -\frac{\mu_A^2}{a^3} \frac{\epsilon_B - 1}{2\epsilon_B + 1} = -\frac{\mu_A^2}{a^3} \varphi(\epsilon_B) \quad (14)$$

This expression was derived in a much more general form without reference to the R. F. formalism. It is clear, however, that this chemical potential is equal to the electrical work of charging the dipole $\boldsymbol{\mu}_A$ (9) in the presence of the electrostatic potential V ,

$$V = -\frac{2(\epsilon_B - 1)}{2\epsilon_B + 1} \frac{\boldsymbol{\mu}_A \cdot \mathbf{r}}{a^3} \quad (15)$$

from which Onsager's reaction field \mathbf{E}_R derives according to ($\mathbf{E}_R = -\text{grad } V$)

$$E_R = \frac{2(\epsilon_B - 1) \mu_A}{2\epsilon_B + 1} \frac{\mu_A}{a^3} \quad (16)$$

in the absence of dielectric saturation.

Insertion of the expression of the chemical potential given by Equation 14 into Equation 5 yields, in principle, the value of the electrostatic contribution to the solvent effect on equilibria.

For the equilibrium 2:



$$\begin{aligned} \Delta G^\circ(S,T) - \Delta G^\circ(\text{gas},T) &= -RT \ln \frac{(k_X)_S}{(k_X)_{\text{gas}}} \\ &= \left[\frac{\mu_C^2}{a_C^3} - \frac{\mu_A^2}{a_A^3} - \frac{\mu_B^2}{a_B^3} \right] \varphi(\epsilon_B) \end{aligned} \quad (17)$$

The extension to reaction rates in solution, via the activated complex theory has been carried out by Laidler and Eyring (10). For process 2,



$$\begin{aligned} \Delta G^{\circ\dagger}(S,T) - \Delta G^{\circ\dagger}(\text{gas},T) &= -RT \ln \frac{(k_1)_S}{(k_1)_{\text{gas}}} \\ &= \left[\frac{\mu_{C^\ddagger}^2}{a_{C^\ddagger}^3} - \frac{\mu_A^2}{a_A^3} - \frac{\mu_B^2}{a_B^3} \right] \varphi(\epsilon_B) \end{aligned} \quad (18)$$

Extensions and Modifications. Within the isotropic approximation, Equations 17 and 18 can be modified in different ways.

a. By taking the dielectric constant of the solute cavity as equal to 2.0 (a value close to that of ϵ_B for aliphatic hydrocarbons (11)). This is an indirect way of allowing for some solute polarization and is, for instance, the procedure followed by Laidler and Landskroenner (12). The consequence is that $\varphi(\epsilon_B)$ in Equations 17 and 18 is now replaced by $\varphi'(\epsilon_B)$:

$$\varphi'(\epsilon_B) = \frac{3 \epsilon_B - 1}{8 \epsilon_B + 1}$$

As pointed out by Koppel and Palm (13), this choice has little importance for semiquantitative purposes since $\varphi(\epsilon_B)$ and $\varphi'(\epsilon_B)$ are very nearly proportional except for the low values of ϵ_B .

This is a consequence of the crudeness of the models and the lack of independent methods for the evaluation of the dipole moments of transition states. These quantities are obtained from the slopes of the approximately linear plots of ΔG^\ddagger vs. $\varphi(\epsilon_B)$ or $\varphi'(\epsilon_B)$ (see, e.g., Ref. 14). As pointed out by

Abraham (14), there is not even a reliable method to determine the cavity radius a . Equation 17 opens an interesting possibility since, in principle, all the quantities involved are experimentally available (a is not, but the geometry of the molecule is). It is therefore somewhat surprising that so little attention has been paid so far to the experimental determination of the free energies of transfer of highly polar species of *known* dipole moments and geometries.

b. By removing the point-dipole assumption and considering higher multipoles. Although the functional dependence on the dielectric constant is still the same as in Equations 17 and 18, the dipole moments are now replaced by the more complex "charge configuration functions" (15). This treatment obviously needs a rather detailed model of the charge distribution.

c. Recently, Abraham (16) has included both the dipole and quadrupole moments of the solute and its polarization under the influence of the reaction field. The expression of the change in free energy of a polarizable dipole-quadrupole transferred from the gas phase into a solvent of dielectric constant ϵ_B becomes:

$$\Delta G^\circ(\text{S,T}) - \Delta G^\circ(\text{gas, T}) = -\frac{\mu_A^2}{a^3} \frac{x}{1-lx} - \frac{3q^2x}{5-x}$$

where

$$x = \frac{\epsilon_B - 1}{2\epsilon_B + 1}, \quad l = 2 \frac{n^2 - 1}{n^2 + 1}$$

and n and q , respectively, stand for the refractive index and quadrupole moment of the solute. It is instructive to examine the "solvent effect" on an "average solute" of refractive index $2^{1/2}$: 1 becomes $1/2$ and the quadrupole term simplifies considering that $x \ll 5$ (since $0 \leq x < 0.5$) and $(\epsilon_B - 1)/(2\epsilon_B + 1) \approx 1/2 (\epsilon_B - 1)/(\epsilon_B + 1)$

$$\Delta G^\circ(\text{S,T}) - \Delta G^\circ(\text{gas, T}) \approx - \left[\frac{2\mu_A^2}{3a^3} + \frac{3}{10}q^2 \right] \frac{\epsilon_B - 1}{\epsilon_B + 1} \quad (19)$$

The dependence on the dielectric constant still is essentially that of Laidler's theory.

Mathematically, $\varphi(\epsilon_B)$ and the cognate functions $\varphi'(\epsilon_B)$ and $(1 - 1/\epsilon_B)$ converge towards a limiting value when $\epsilon_B \rightarrow \infty$, for example, $\lim \varphi(\epsilon_B) = 1/2$. In Fig. 4 we have plotted $\varphi(\epsilon_B)$ versus ϵ_B and indicated the position of several common solvents. It appears that for $\epsilon_B > 10$, $\varphi(\epsilon_B)$ changes very slowly and predicts small differences in solvent effects between materials like EtBr ($\epsilon_B = 9.50$) and DMSO ($\epsilon_B = 48.9$). This is contrary to practically any experimental evidence, which indicates, for instance, a sizable difference in solvent efficiency even between DMF ($\epsilon_B = 36.7$) and DMSO. This important shortcoming is shared by all the preceding theories and the inclusion of the solute polarizability and multipoles does not improve the picture. This fact has been recognized by

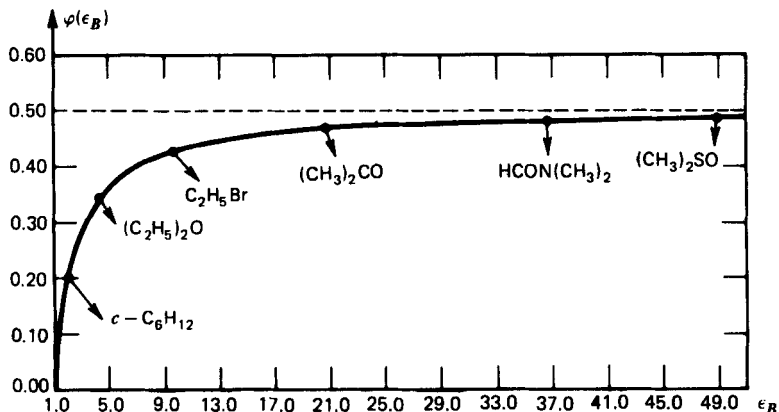


Figure 4 The function $\varphi(\epsilon_B)$ plotted vs. ϵ_B . The position of several common solvent is shown.

Abraham et al., who add an extra term to Equation 19 to allow for direct dipolar interactions between solvent and solute (17). This term is small for solvents of low dielectric constant but becomes significant for those having $\epsilon_B > 10$. The theory, thus modified, seems to give fairly satisfactory descriptions of polar effects on conformational equilibria (18), free energies of transfer of ion-pairs (19), and activation free energies of reactions²⁰.

The Inclusion of Dielectric Saturation. The phenomenon of dipolar association in solution has attracted attention since 1928 (21). A substantial body of experimental evidence has since been accumulated. Both the self-association of polar molecules and solvent-solute multipolar complexation (including that of transition states) have been detected and studied:

1. The self-association of highly polar liquids has been detected by a number of methods including ir spectroscopy (22), Brillouin scattering (23), dielectric polarization (24), H nmr (25), ¹³C nmr (26), ¹⁹F nmr (27), and cryoscopy (28). Quite recently, X-ray diffraction studies have conclusively shown that acetonitrile (29) and higher nitriles form clusters in the liquid state (30).

Some representative values for the dimerization constants of polar aprotic species in solution at 25°C are given in Table 1.

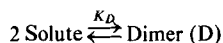
2. In studies published between 1962 and 1964 Ritchie and co-workers (31) used the study of infrared band intensities to detect complexes between dimethyl sulfoxide (DMSO) and acetone (Me₂CO), DMSO and substituted benzonitriles, benzonitrile and pyridine (Py), and acetonitrile and DMSO. In several cases the formation constants were measured.

3. Taft, Klingersmith, Price and Fox (27) and Uschold and Taft (32) used ¹⁹F nmr spectroscopy to measure the formation constants of dipolar complexes between *p*-fluoronitrosobenzene and thirteen different compounds [with

TABLE 1
Dimerization of Polar Aprotic Species in Solution

Solute	Solvent	K_D^a (1 mole ⁻¹)	Technique	Ref.
<i>c</i> -C ₄ H ₈ CO	<i>c</i> -C ₆ H ₁₂	0.13	D.P. ^b	24b
<i>c</i> -C ₅ H ₁₀ CO	<i>c</i> -C ₆ H ₁₂	0.11	D.P.	24b
C ₂ H ₅ CN	<i>c</i> -C ₆ H ₁₂	0.23	D.P.	24b
<i>t</i> -C ₄ H ₉ CN	<i>c</i> -C ₆ H ₁₂	0.04	D.P.	24b
<i>n</i> -C ₃ H ₇ CN	<i>c</i> -C ₆ H ₁₂	0.26	D.P.	24b
C ₆ H ₅ CN	<i>c</i> -C ₆ H ₁₂	0.18	D.P.	24b
<i>p</i> -F-C ₆ H ₄ NO ₂	CCl ₄	0.25	¹⁹ F nmr	27
3,4 DiF-C ₆ H ₃ NO ₂	CCl ₄	0.22	¹⁹ F nmr	27
<i>p</i> -F-C ₆ H ₄ NO	CCl ₄	0.08	¹⁹ F nmr	27

^a Equilibrium constants K_D at 25°C for the dimerization of dipolar aprotic compounds in solution.



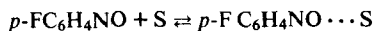
^b Dielectric polarization.

polarities between those of ethyl acetate (EtOAc) and DMSO], as well as a number of self-association formation constants. Both series of studies were consistent in showing that multipolar complexation essentially involves localized groups. It was also concluded that "complexing agents with one predominant polar center tend to form increasingly stable complexes with a given solute the larger the group dipole moment." The influence of the polarity on the stability of the multipolar complexes is illustrated by the results given in Table 2, extracted from Ref. 27.

4. We have recently developed (33) a "generalized solvent polarity scale" π which for aliphatic, aprotic, monofunctional solvents (henceforth called "select solvents") correlates quite well with all the other most widely used "empirical polarity scales" based on a variety of chemical and physical properties (34). It is significant that both the π scale and the other solvent polarity scales show excellent correlations with the molecular dipole moments of the select solvents.

5. As pointed out by Taft and co-workers (27) on the basis of linear free energy relationships, highly polar transition states are prime candidates to undergo specific solvation by polar or polarizable species. This concept was already set forth in 1935 by Wynne-Jones and Eyring (35) on an entirely different basis, namely, the interpretation of kinetic results in mixed solvents (36). The study of reaction rates in mixed solvents is an almost untapped source of information on the solvation of transition states. Recently, Drougard and Decroocq (37) have studied the kinetics of the Menshutkin reaction between Et₃N and MeI in binary and ternary solvent systems. From their experimental data it appears that

TABLE 2
Formation Constants, K , Corresponding to the Equilibria



in Carbon Tetrachloride Solution at 25°C as Determined
by Means of ^{19}F NMR Spectroscopy (27)

Polar component S	K (1 mole $^{-1}$)
(CH ₃) ₂ SO	0.6
CH ₃ CN	0.5
C ₆ H ₅ NO ₂	0.5
<i>m</i> -CF ₃ C ₆ H ₄ NO ₂	0.5
<i>m</i> -F C ₆ H ₄ NO ₂	0.5
<i>p</i> -F C ₆ H ₄ NO ₂	0.5
HCON (CH ₃) ₂	0.5
(CH ₃ CO) ₂ O	0.4
C ₆ H ₅ NO	0.4
C ₅ H ₅ N	0.2
CH ₃ COC ₂ H ₅	0.3
CH ₃ COOC ₂ H ₅	0.1

the transition state in carbon tetrachloride and cyclohexane solutions is relatively tightly bound to a small number (one to three) of the adduct molecules (benzene (38) or propionitrile). This is just but one example in which the well-known catalytic role of polar solvents has been examined quantitatively. Some representative results are given in Table 3. Experience has shown that theories aiming at the description of solvent effects on infrared frequencies (39) or nmr shifts (40) of polar solutes in polar solvents often perform poorly as long as they ignore direct dipole interactions. This has prompted several authors to develop theories in which only pairwise interactions are considered (41).

In view of these facts, it can be reasonably inferred that some degree of

TABLE 3
Rate Constant k for the Quaternarization of Triethylamine by
Ethyl Iodide in Cyclohexane-Propionitrile Solutions (37)

Volume fraction of propionitrile	$10^2 k$ (mole $^{-1}$ l min $^{-1}$) at 20°C
0.00	≈0.000
0.05	0.86
0.10	2.02
0.20	5.18
0.40	15.4
0.60	33.0
0.80	62.7
1.00	112.5

dielectric saturation takes place around a polar species in a polar solvent. On the other hand, the R.F. formalism is an extremely attractive way of treating solvent effects, especially considering that:

a. Little is known regarding the structure of the cybotactic environment of a polar solute.

b. The R.F. is determined under equilibrium conditions. If ψ is the potential acting on the solute dipole, the work of charging the dipole under ψ measures the electrostatic contribution to the chemical potential of the solute.

c. Polar effects on several physical properties can be (at least formally) related to the R.F.

It has recently been proposed (42) that the Block and Walker modification of the Onsager theory be used to treat solvent effects. The fact that this model leads to values of dipole moments that agree quite well with those measured in the gas phase is indeed encouraging. The expression of the R.F. given by Equation 13 can be used to determine the work of charging the unpolarizable solute dipole along the lines of Kirkwood's original treatment. The expression of the electrostatic contribution to the chemical potential μ_{chem} of the solute dipole is:

$$\mu_{chem}^0 = -\frac{1}{2} \frac{\mu_A^2}{a^3} \left[\frac{3\epsilon_B \ln \epsilon_B}{\epsilon_B \ln \epsilon_B - \epsilon_B + 1} - \frac{6}{\ln \epsilon_B} - 2 \right] \quad (20)$$

or

$$\mu_{chem} = -\frac{1}{2} \frac{\mu_A^2}{a^3} \Theta(\epsilon_B) \quad (21)$$

where

$$\Theta(\epsilon_B) = \left[\frac{3\epsilon_B \ln \epsilon_B}{\epsilon_B \ln \epsilon_B - \epsilon_B + 1} - \frac{6}{\ln \epsilon_B} - 2 \right] \quad (22)$$

Equations formally identical to Equations 17 and 18 wherein the function $\varphi(\epsilon_B)$ is replaced by $\Theta(\epsilon_B)$ can be derived. In Fig. 5 we have plotted $\frac{1}{2} \Theta(\epsilon_B)$ versus $\varphi(\epsilon_B)$. Clearly, for $\epsilon_B > 5$, $\Theta(\epsilon_B)$ changes more than $\varphi(\epsilon_B)$, the slope actually increasing with ϵ_B . This result agrees at least qualitatively with most of the experimental data available. It is also apparent that over the range $2 < \epsilon_B < 50$, which covers most of the solvents commonly used, $\varphi(\epsilon_B)$ varies by about 0.29 whereas $\Theta(\epsilon_B)/2$ varies by about 0.18. The immediate implication is that the dipole moments calculated by means of Equation 21 will be larger than those obtained on the basis of Equation 14 by at least a factor of $\sqrt{0.29/0.18}$, that is, 1.27. Although a 27% difference is by no means negligible, we feel that further elaboration would be untimely since the assumptions made in establishing

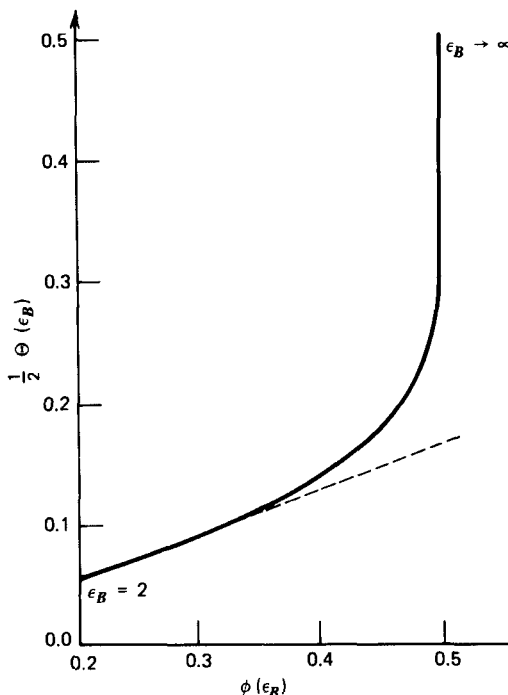


Figure 5 $1/2 \Theta(\epsilon_B)$ vs. $\phi(\epsilon_B)$.

Equations 14 and 20, are such that even larger departures can be expected (43).

The insertion of Equation 21 into Equations 5 and 5' leads to linear correlations between the free energies of transfer of polar species and the function $\Theta(\epsilon_B)$. As examples we consider here:

a. The free energy of transfer of the $\text{Me}_4\text{N}^+\text{Cl}^-$ ion pair (44), ΔG_{tr}° . The correlation is quite satisfactory (Fig. 6), $n = 9$, $\sigma = 0.35 \text{ kcal mole}^{-1}$, and $r = 0.999$.

b. The free energy of activation for the Menshutkin reaction between $n\text{-Pr}_3\text{N}$ and MeI (45), $\delta\Delta G^\ddagger$, relative to DMF. Here $n = 21$, $\sigma = 0.30 \text{ kcal mole}^{-1}$, and $r = 0.984$ (Fig. 7).

These kinds of correlations can only be expected to apply when other intermolecular forces are either excluded or kept reasonably constant. This requirement thus excludes hydroxylic and other hydrogen-bonding solvents together with aromatic and polyhalogenated compounds. Unfortunately, most experimental studies either include too few of these "select solvents" (33*a*) or those examined span a range of polarities which is too narrow. A typical example is provided by

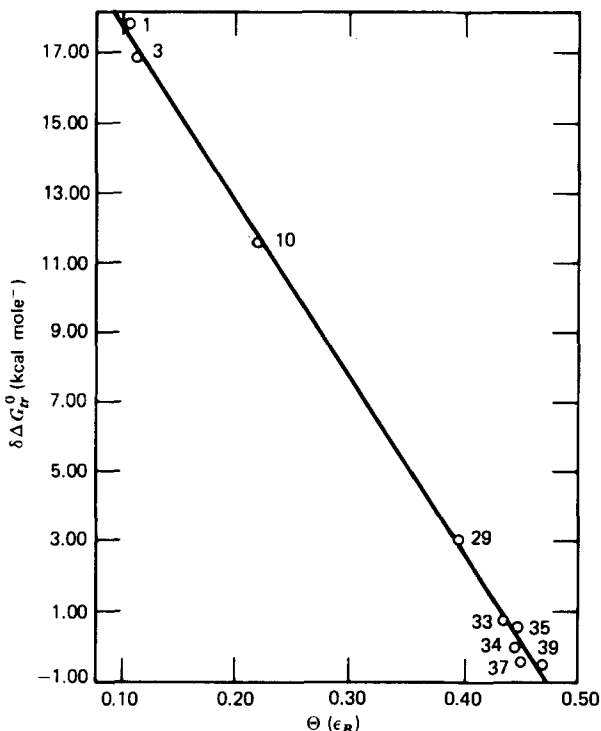


Figure 6 Free energies of transfer of the $\text{MeN}_4^+\text{Cl}^-$ ion pair from DMF to various solvents, $\delta\Delta G_{tr}^0$ vs. $\Theta(\epsilon_B)$.

Smith, Fainberg, and Winstein's (46) classical study of solvent effects on the solvolysis of *p*-methoxyneophyl tosylate at 75°C. It provides data for nine "select solvents" ranging from Et_2O to DMSO. The free energy of activation (in kcal mole $^{-1}$ in the mole l^{-1} scale) is related to $\Theta(\epsilon_B)$ by Equation 23:

$$\Delta G^\ddagger = 8.110 - 21.43 \Theta(\epsilon_B) \quad (23)$$

with $n = 8$,* $\sigma = 0.34$ kcal mole $^{-1}$, and $r = 0.984$ (Fig. 8), whereas the correlation with $\varphi(\epsilon_B)$ is of nearly the same quality (Fig. 8):

$$\Delta G^\ddagger = 17.01 - 38.15 \varphi(\epsilon_B) \quad (24)$$

with $n = 8$, $\sigma = 0.36$ kcal mole $^{-1}$, and $r = 0.978$. Figure 8 shows that studies in solvents of dielectric constants between those of THF and Me_2CO or below that of Et_2O (which were not possible in this instance) would have been valuable;

* The value in EtOAc has not been included in the correlations.

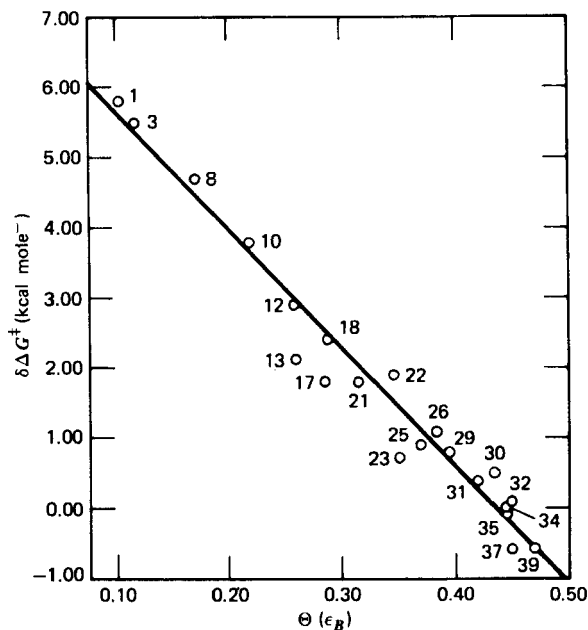


Figure 7 Relative free energies of activation (in the mole fraction scale) for the Menshutkin reaction between $n\text{-Pr}_3\text{N}$ and MeI at 20°C (relative to DMF).

for example, Equations 23 and 24 predict for the ΔG^\ddagger in $c\text{-C}_6\text{H}_{12}$, the values 5.72 and 9.28 kcal mole⁻¹, respectively.

2. Empirical Approach

A different approach consists in the application of the principles of linear free energy relationships to medium effects. In general, some property XYZ , susceptible of taking the values $XYZ_0, XYZ_1, \dots, XYZ_n$ in the solvents S_0, S_1, \dots, S_n , is expressed as a linear function of a standard property Σ in the same solvents:

$$XYZ_i = XYZ_0 + s(\Sigma_i - \Sigma_0) \quad (25)$$

where XYZ_0 and Σ_0 are the respective values of XYZ and Σ in the solvent S_0 taken as reference. The slope s of the linear relationship 25 is a measure of the relative sensitivities of XYZ and the standard property to medium effects. This formalism has been thoroughly discussed by Leffler and Grunwald (47) and Koppel and Palm (48). The merit of expressions such as Equation 25 in terms of understanding the mechanism of the solvent effects on XYZ is obviously limited by the amount of information available on the reference property Σ .

The development of "empirical solvent scales" was originally prompted

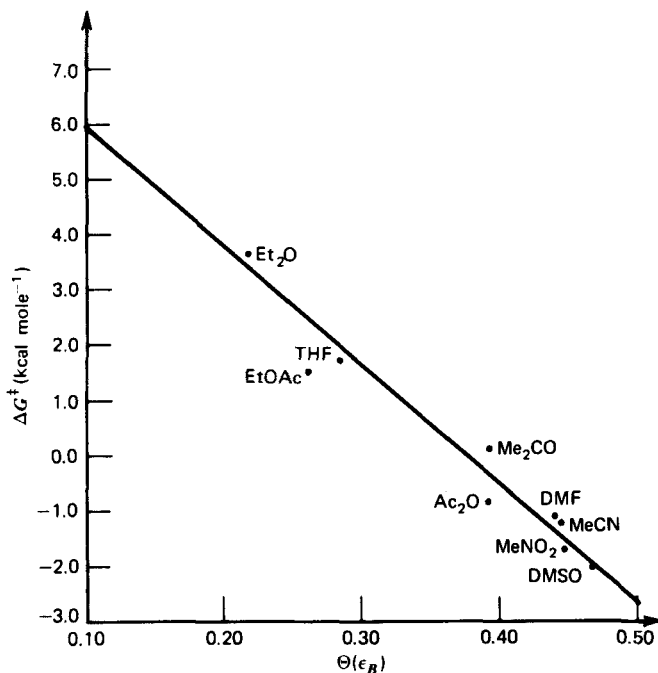


Figure 8 The free energy of activation for the solvolysis of para-methoxy neophyl tosylate at 75°C plotted vs. the $\Theta(\epsilon_B)$ solvent function.

by the need of quantifying solvent effects in systems which were (and mostly still are) beyond the reach of theoretical tools. The leading concept was that a dissolved species would be a “molecular probe” able to reflect the different interactions playing at the microscopic level. As is shown in a forthcoming section, the very concept of “molecular probe” has lately become the object of close scrutiny (34e).

Here, we briefly summarize some of the most important solvent scales based on reactivity. Recent reviews on the subject have been given by Reichardt (50) and Schwetlik (51).

Solvolytic Scales.

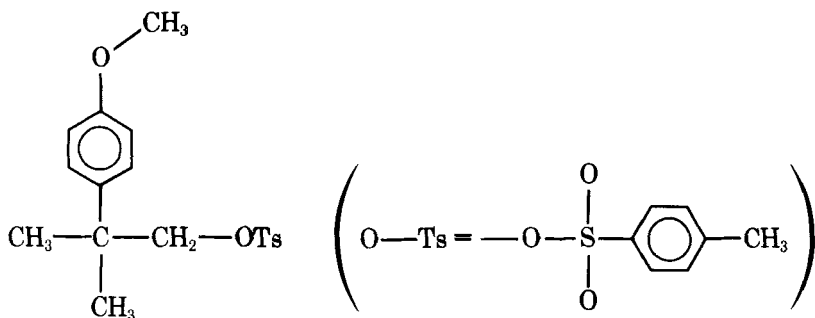
The Y Scale. It was first defined by Winstein and Grunwald in 1948 (52) and extensively used during the following decade (53). The standard property and medium chosen are the rate of solvolyses of *t*-butyl chloride in 80% aqueous ethanol at 25°C, the value of *Y* for a solvent *S* is given by:

$$Y = \log \frac{k_s}{k_0}$$

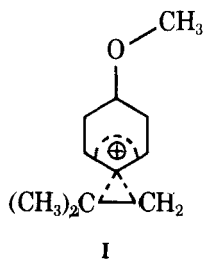
In accordance with the Hughes–Ingold model, it was assumed that the solvolysis

proceeds through a polar transition state and the activation barrier is influenced by the ability of the solvent to stabilize the intermediate $(\text{CH}_3)_3\text{C}^+ \rightarrow \text{Cl}^-$ by effects others than nucleophilic assistance. Y was thus considered a measure of the "ionizing power" of the solvent. Y values have been determined for several pure hydroxylic solvents and hydroorganic mixtures. Table 4 contains a collection of values of Y taken from Ref. 53b.

The Solvolysis of p-Methoxyneophyl Tosylate (46). The rate of solvolysis of



at 75°C was chosen as a process suitable to extend the measurement of "ionizing powers" to nonhydroxylic solvents. It was further established that the rate-determining process of the reaction is the formation of the anchimerically stabilized ion (I) which was shown to be practically free from such problems as



ion-pair return and solvent nucleophilicity participation. The rates of solvolysis, k , were measured in several protic and aprotic solvents and in various hydroorganic mixtures. When compared to Y for mixed hydroxylic solvents, good correlations of the form

$$\log k = \log k_0 + mY$$

were found but they generated separate lines for different binary mixtures. The values of $\log k$ at 75°C are given in Table 5.

The Diels-Alder Reaction. In a study published in 1962, Berson, Hamlet

TABLE 4
Y Values for Hydroxylic Solvents

Solvent ^a (vol. %)	Y	Solvent ^a (vol. %)	Y
EtOH-H₂O		MeOH-H₂O	
100	-2.033	100	-1.090
98	-1.681	90	-0.301
95	-1.287	80	0.381
90	-0.747	70	0.961
80	0.000	60	1.492
70	0.595	50	1.972
60	1.124	40	2.391
50	1.655	30	2.753
45	1.924	20	3.025
40	2.196	10	3.279
37.5	2.338	AcOH-HCOOH^b	
35	2.473	100	-1.639
30	2.721	90 ^c	-0.929
25	2.908	75	-0.175
20	3.051	50	0.757
15	3.189	25	1.466
10	3.312	10	1.862
5	3.397		
0(H ₂ O)	3.493		
HCOOH-H₂O		Dioxane-H₂O	
100	2.054	90 ^d	-2.030
95	2.163	80 ^d	-0.833
90	2.222	70	0.013
80	2.318	60	0.715
66.67	2.456	50	1.361
50	2.644	40	1.945
33.33	2.951	30	2.455
25	3.100	20	2.877
14.29	3.244	10	3.217
CH₃-COOH-H₂O^b		Me₂CO-H₂O^c	
0.50 M H ₂ O	-1.400	95.2 ^e	-2.76 ^e
2.00 M H ₂ O	-0.863	90	-1.856
4.00 M H ₂ O	-0.404	80	-0.673
8.00 M H ₂ O	0.193	70	0.130
16.0 M H ₂ O	0.984	60	0.796
60	1.519	50	1.398
50	1.938	40	1.981
40	2.312	30	2.482
25	2.843	25	2.689
		20	2.913
		10	3.230

TABLE 4
Y Values for Hydroxylic Solvents

Solvent ^a (vol. %)	Y	Solvent ^a (vol. %)	Y
Dioxane-HCOOH ^b		HCONH ₂ -H ₂ O	
80	-2.96 ^c	100	0.604
60	-0.677	80	1.383
40	0.402	97.5 Ac ₂ O-AcOH	-3.29
20	1.291	<i>n</i> -C ₃ H ₇ COOH	+1.7 ^f
		<i>i</i> -C ₃ H ₇ OH	-2.73 ^g
		<i>t</i> -C ₄ H ₉ OH	-3.26 ^g

^a For all the mixtures, X volume of A-B means X volumes of A plus 100-X volumes of B, each at 25°C, before mixing.

^b These solutions contained 0.065-0.068 M lithium salts (acetate and/or formate).

^c Calculated from data at 50 and 75°C.

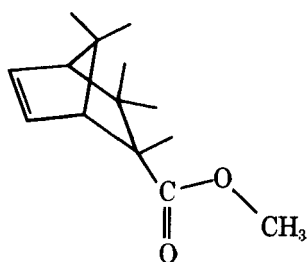
^d Initial rate constant.

^e Estimated from data on *t*-BuBr in acetone containing 0.170 mole fraction of water.

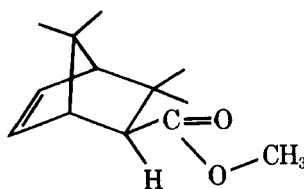
^f Estimated from data on α -phenylethyl chloride in this solvent.

^g Estimated from data on *t*-BuBr in these solvents.

and Mueller (54) examined the influence of solvents on the stereo-selectivity of the kinetically controlled reactions between cyclopentadiene and the dienophiles methyl acrylate, methyl metacrylate, and methyl-transcrotonate. The products depending on whether the *endo*(N) or *exo*(X) adduct is formed are:



(N)



(X)

The authors showed that the ratio of the isomers, [N]/[X] is solvent dependent and proposed the use of the quantities $\Omega = \log [N]/[X]$ as a measure of solvent polarity. Although Ω increases with the polarity of the solvent (as measured for example by the $\varphi(\epsilon_B)$ function), a result which seems to confirm their contention that the transition state corresponding to N is slightly more polar than that corresponding to X, the use of the *endo/exo* ratio for these reactions as a general measure of polarity is questionable. Besides experimental difficulties appearing in highly polar solvents, the effects that can be ascribed to polarity

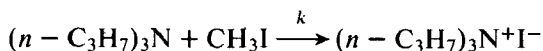
TABLE 5
Rate Constant k for the Solvolysis at 75°C of *p*-Methoxyneophyl
Tosylate in Different Solvents (46)

Solvent	$10^5 k(\text{sec}^{-1})$
(C ₂ H ₅) ₂ O	0.005
(CH ₂) ₄ O	0.0847
CH ₃ CO ₂ C ₂ H ₅	0.113
(CH ₃) ₂ CO	0.857
C ₅ H ₅ N	2.14
(CH ₃ CO) ₂ O	3.41
HCON(CH ₃) ₂	4.96
CH ₃ CN	6.01
CH ₃ NO ₂	12.3
(CH ₃) ₂ SO	18.2
C ₇ H ₁₅ COOH	7.26

are very small and can be easily blurred by even a slight imperfection in the cancellation of the contribution from nondipolar contributions. The Ω values are given in Table 6.

The Quaternarization of Tertiary Amines. This is a most suitable reaction since (a) it is very sensitive to medium effects, (b) it is easy to monitor, and (c) the mechanism is fairly well understood.

In 1968, Lassau and Jungers (34c) published a study of the reaction



in which the second order rate constant k was determined in 78 solvents (55).

TABLE 6
Solvent Polarity Parameter, Ω , for Various Solvents (54)

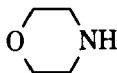
Solvent	Ω (at 30°C)
CH ₃ OH	0.845
C ₂ H ₅ OH	0.718
CH ₃ CO ₂ H	0.823
CH ₃ NO ₂	0.680
CH ₃ CN	0.692
HCONH ₂	0.620
(CH ₃) ₂ CO	0.619 (at 20°C)
ClCH ₂ CH ₂ Cl	0.600
C ₅ H ₅ N	0.595
(CH ₃ OCH ₂) ₂	0.543
(C ₂ H ₅) ₃ N	0.445
C ₁₀ H ₁₈ (decalin)	0.54 (interpolated)

TABLE 7
Second-Order Rate Constant k for the Reaction between
 n -Pr₃N and MeI at 20°C in Different Solvents (34c)

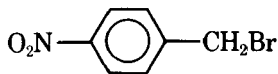
Solvent	k (1 mole ⁻¹ min ⁻¹) at 20°C
C ₆ H ₁₄	≈0.00001
<i>c</i> -C ₆ H ₁₂	0.0002
(<i>n</i> -C ₄ H ₉) ₂ O	0.0004
(C ₂ H ₅) ₂ O	0.0012
CS ₂	0.0025
<i>n</i> -C ₄ H ₉ OH	0.0046
<i>n</i> -C ₃ H ₇ OH	0.0074
<i>n</i> -C ₆ H ₁₃ Cl	0.0078
C ₂ H ₅ OH	0.0095
C ₆ H ₅ CH ₃	0.0095
<i>n</i> -C ₄ H ₉ Cl	0.013
<i>n</i> -C ₄ H ₉ Br	0.013
CH ₃ OH	0.013
C ₆ H ₆	0.018
CH ₃ CO ₂ C ₂ H ₅	0.022
C ₂ H ₅ Br	0.024
(CH ₂) ₄ O	0.029
Cl ₃ C-CO ₂ Et	0.040
C ₂ H ₅ COC ₄ H ₉	0.042
C ₆ H ₅ CH ₂ OH	0.058
C ₆ H ₅ Cl	0.070
CH ₂ Cl-CH ₂ Cl	0.075
C ₆ H ₅ Br	0.089
C ₆ H ₅ OCH ₃	0.089
CH ₃ COC ₂ H ₅	0.098
<i>o</i> -C ₆ H ₄ Cl ₂	0.100
CH ₂ Br-CH ₂ Br	0.130
Cl ₃ CH	0.130
<i>cis</i> Cl ₂ C=CH ₂	0.140
(CH ₃) ₂ CO	0.150
<i>c</i> -C ₅ H ₁₀ CO	0.160
<i>n</i> -PrCN	0.21
<i>c</i> -C ₄ H ₈ CO	0.22
C ₂ H ₅ CN	0.28
CH ₂ Cl ₂	0.28
<i>n</i> -C ₃ H ₇ NO ₂	0.29
Cl ₂ CH-CH ₂ Cl	0.33
CH ₂ Cl-CH ₂ Cl	0.38
C ₆ H ₅ CN	0.39
C ₂ H ₅ NO ₂	0.46
CH ₃ CN	0.47
C ₆ H ₅ NO ₂	0.48
HCON(CH ₃) ₂	0.60
CHCl ₂ -CHCl ₂	0.87
CH ₃ NO ₂	1.10
C ₆ H ₅ CH ₂ CN	1.10

Representative values are shown in Table 7. By examining the influence of the dielectric constant of the medium on $\log k$, they were able to classify the solvents into three groups: (a) hydroxylic, (b) aromatic and polyfunctional (mainly polyhalogenated), and (c) polar, monofunctional aliphatic solvents. It was further noticed that, for this last group, the plot $\log k$ versus ϵ_B is a smooth curve. They also examined the catalytic effect of some of these solvents on the rate of reaction in carbon tetrachloride and showed that the effect is proportional to the dipole moment of the "catalyst." More generally, they concluded that "... the kinetic efficiency [of group (c) solvents] ... originates to a large extent in their functional dipoles."

It is a fact that at least for these "select solvents," other Menshutkin reactions show excellent correlations (20b). An interesting exception is the reaction between morpholine,



and *p*-nitrobenzyl bromide (56),



The possibility of contributions from hydrogen bonding by the amino hydrogen is obvious and, it can be shown that the inclusion of this effect, together with the polarity, allows an excellent quantitative description of the results (57).

B. Physical Properties

1. Theoretical Approach

Electronic Absorption Spectra (58, 59). As seen earlier, solvent effects on reactivity and electronic absorption have the same origin.* Historically, however, the former were studied in terms of classical electrostatics, whereas the latter generally underwent (at least, formally) a quantum-mechanical treatment. Liptay (58f) has shown that the results of both theories are the same (at the level of the second order perturbation theory) except for a term corresponding to dispersion interactions. Assuming that the polar, radiation-absorbing species is in a very dilute solution, the main contributors to the energy of the

* Some subtle differences exist: in dealing with "chemical" effects, the important quantity to evaluate is the change in free energy ΔG° at constant temperature and pressure. In spectral studies, the relevant quantity is the change in energy ΔU at constant temperature and pressure. Although closely related, both quantities are not strictly the same. Furthermore, the system [solvent + excited molecule (Franck-Condon)] is not in equilibrium.

ground state are: (a) the interaction between the dipole of the solute and the R.F. of the solvent and (b) the dispersion forces. In the excited state the energetic contributions have the same origin but (a) the polarizability and dipole moment of the excited state are generally different from that in the ground state and (b) the time scale of the transition is much shorter than that of nuclear and solvent relaxation so that the solvent permanent orientation in the excited state is the same as in the ground state. Only the electronic component can "follow" the transition.

Consider now an idealized solute molecule of permanent dipole μ_g in its ground state. Let E_{Rg} be the corresponding R.E.; Equation 6 still holds:

$$E_{Rg} = C_g \mu_g$$

The dipole moment of the solute in the excited state is μ_e and the corresponding R.F. is E_{Re} . E_{Re} can be considered as having two components: $(E_{Re})_{orient}$, corresponding to the orientation of the solvent dipoles, still "frozen" in their ground-state configuration, and $(E_{Re})_{inst}$ arising from the instantaneous polarization of the solvent:

$$E_{Re} = (E_{Re})_{orient} + (E_{Re})_{inst}$$

where, from Equation 6:

$$(E_{Re})_{orient} = (C_e)_{orient} \mu_g$$

and

$$(E_{Re})_{inst} = (C_e)_{inst} \mu_e$$

From Equation 7 we obtain Equations 26 and 27 that yield the contributions to the electrostatic energy both in the ground and excited states:

$$U_g = -\mu_g \cdot E_{Rg} \quad (26)$$

$$U_e = -\mu_e \cdot E_{Re} \quad (27)$$

The difference ΔU between the ground and excited states is:

$$\Delta U = U_g - U_e = C_g \mu_g^2 - (C_e)_{orient} \mu_g \cdot \mu_e - (C_e)_{inst} \mu_e^2 \quad (28)$$

On very general grounds, $(C_e)_{inst}$ is taken as a function of the refractive index n of the solvent, C_g as a function of the bulk dielectric constant ϵ and $(C_e)_{orient}$ as a function of ϵ_B and n . So far, the various theories use the expressions of E_R given by Onsager's theory. As a first approximation, the various coefficients are taken as:

$$C_g \propto \varphi(\epsilon_B)$$

$$(C_e)_{inst} \propto \varphi(n^2)$$

$$(C_e)_{orient} \propto [\varphi(\epsilon_B) - \varphi(n^2)]$$

On the other hand, for the majority of solvents, n and $\varphi(n^2)$ vary within rather narrow limits. In Fig. 9 is represented $\varphi(n^2)$ versus ϵ_B for a variety of common solvents (27 solvents). Excluding aromatic solvents, no trend appears, and the variations of $\varphi(n^2)$ are ± 0.025 around an average value of 0.200. (This result should dictate circumspection on the use of linear combinations of $\varphi(\epsilon_B)$ and $\varphi(n^2)$ to describe solvent effects (60).) The solvent-induced variations of C_g , $(C_e)_{orient}$, and $(C_e)_{inst}$

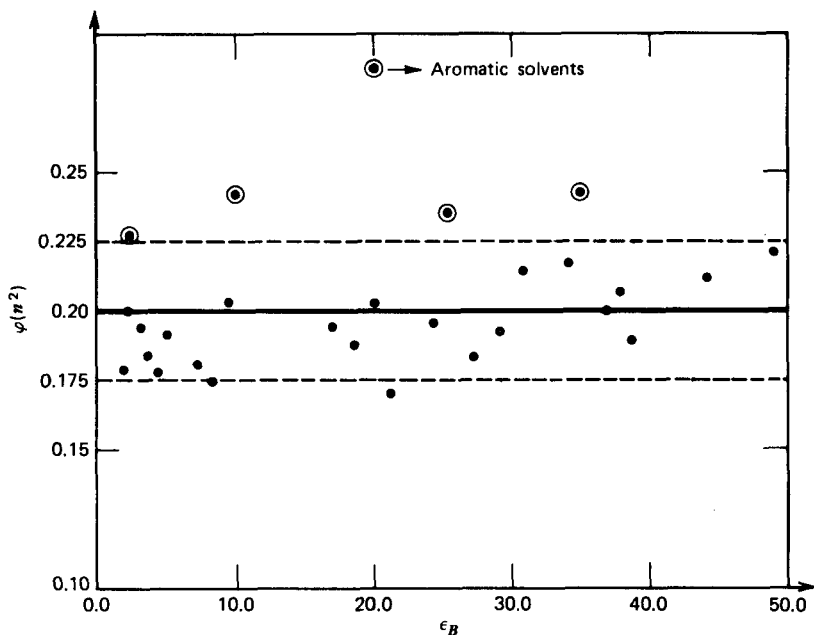


Figure 9 The refractive index function, $\varphi(n^2) = n^2 - 1/2n^2 + 1$, plotted vs. the bulk dielectric constant, ϵ_B , for twenty seven common solvents. Aromatic solvents are denoted separately.

can, therefore, undergo substantial simplifications:

$$\Delta_{S_1 \rightarrow S_2} C_g = k \Delta_{S_1 \rightarrow S_2} \varphi(\epsilon_B) = k[\varphi(\epsilon_B)_{S_2} - \varphi(\epsilon_B)_{S_1}]$$

$$\Delta_{S_1 \rightarrow S_2} (C_e)_{\text{inst}} \approx 0$$

$$\Delta_{S_1 \rightarrow S_2} (C_e)_{\text{orient}} \approx k \Delta_{S_1 \rightarrow S_2} \varphi(\epsilon_B)$$

and, consequently, the solvent effect on ΔU can, as a first approximation, be expressed as:

$$\Delta_{S_1 \rightarrow S_2} \Delta U \approx k \mu_g (\mu_g - \mu_e) \Delta_{S_1 \rightarrow S_2} \varphi(\epsilon_B) \quad (29)$$

A noticeable simplification takes place when μ_g and μ_e are orthogonal (since $\mu_g \cdot \mu_e = 0$):

$$\Delta_{S_1 \rightarrow S_2} \Delta U \approx k \mu_g^2 \Delta_{S_1 \rightarrow S_2} \varphi(\epsilon_B) \quad (30)$$

In both cases, the quantity $\Delta_{S_1 \rightarrow S_2} \Delta U$ can be identified to $\Delta_{S_1 \rightarrow S_2} h\nu$, where ν is the frequency of the transition under scrutiny. This approach therefore predicts a linear relationship between $\Delta\nu$ and $\varphi(\epsilon_B)$. Although it has become customary to plot $\Delta\nu$ versus $\varphi(\epsilon_B)$ or some cognate function (61), it is important to stress that this kind of relationship is only a consequence of adopting Onsager's model in its original form, since the coefficients C_g , $(C_e)_{\text{orient}}$ and $(C_e)_{\text{inst}}$ are not obtained from first principles. If, for instance, the Block-Walker model is used, an approximate linear relationship between $\Delta\nu$ and the function $\Theta(\epsilon_B)$ is predicted.

Nuclear Magnetic Resonance Spectra. The shielding constant σ for a given nucleus within a molecule in solution is generally expressed (62) as:

$$\sigma = \sigma_g + \sigma_b + \sigma_a + \sigma_L + \sigma_E \quad (31)$$

where σ_g is the chemical shift in the gas phase, σ_b and σ_a are the contributions from the bulk susceptibility of the solvent and its molecular anisotropy. The terms σ_L and σ_E , respectively, represent the effects of London forces and the electrostatic solvent-solute interactions.

In terms of differential solvent effects, Equation 31 yields:

$$\Delta_{S_1 \rightarrow S_2} \sigma = \Delta_{S_1 \rightarrow S_2} (\sigma_b + \sigma_a + \sigma_L) + \Delta_{S_1 \rightarrow S_2} \sigma_E \quad (32)$$

The first term on the right-hand side of Equation 32 can be either calculated (62) or, better yet, eliminated by a proper choice of the standard (27). The σ_E term is relevant for our present study. According to Buckingham's (62*b*) basic assumption, the screening constant* can be expressed as a power series of the electric field E acting on the nucleus. In the case of an X-H bond, it is shown that the shielding constant is of the form:

$$\sigma_E = \sigma_0 - AE_z - BE^2 \quad (33)$$

where E is the value of the field and E_z is the value of its component along the direction of the bond. In esu, A and B are estimated for the proton to be 2×10^{-12} and 10^{-18} . The differential solvent shift of a proton can then be expressed as:

$$\Delta_{S_1 \rightarrow S_2} \sigma_E \approx -2 \times 10^{-12} \Delta_{S_1 \rightarrow S_2} E_z - 10^{-18} \Delta_{S_1 \rightarrow S_2} E^2 \quad (34)$$

provided that the other contributions are eliminated.

This result is extremely important, in the sense that with a proper choice of the reference standard, the change in chemical shift is a measure of the variation of the electric field acting along the direction of the bond. When confronted with the actual problem of evaluating solvent effects, Buckingham used the expression of the field given by Onsager's model. All other factors being kept constant, Equations 33 and 34 should then establish as a first approximation a linear relationship between σ and $\varphi(\epsilon_B)$.** It is unfortunate that most of the experimental work directed to substantiate this kind of dependence has been carried out in mixed solvents (40). It is also a fact that these experimental results do not seem to support the theoretical expectations.

Infrared Absorption Spectra. Following West and Edwards (63), Bauer and Magat (64) examined the electrostatic effect of the solvent on the stretching frequency of a polar bond. Mathematically, their approach is simple: to the restoring force acting on the bond in the gas phase (Hooke law type) the treatment incorporates the perturbing force created by the R.F. on the polar bond. This contribution is proportional to the solvent R.F. Let ν_0 be the frequency of the vibrator in the gas phase, ν_2 , the frequency in the solvent S and $\Delta\nu$ the difference

* Actually, the components of the screening tensor.

** Or closely related functions.

$\nu_S - \nu_0$. The theory establishes that:

$$\frac{\Delta\nu_S}{\nu_0} = -k(A) C(S,A) \quad (35)$$

where $k(A)$ is a constant depending on the nature of the solute and $C(S,A)$ is the proportionality constant defined by Equation 6

$$E_R = C(S,A) \mu_A$$

If, according to the original work, $C(S,A)$ is taken from the Onsager-Kirkwood model, then:

$$\frac{\Delta\nu_S}{\nu_0} = -2k(A) \varphi(\epsilon_B)_S \quad (36)$$

Once again a solvent effect on a physical property is linked to the R.F. The presence of $\varphi(\epsilon_B)$ follows from the model used. Obviously, this is no longer the only possibility left: if the Block-Walker formalism is utilized then:

$$\frac{\Delta\nu_S}{\nu_0} = -k(A) \Theta(\epsilon_B)_S \quad (37)$$

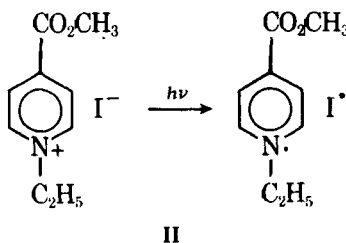
Fulton (65) has recently examined the problem by means of a discrete lattice model for the solvent. The form of his equation is the same as Equations 36 and 37 but the functional dependence on ϵ_B is indeed different.

2. Empirical Approach

The same criteria that lead to the development of polarity scales based on reactivity has stimulated the establishment of scales based upon physical properties. Spectral properties have become undisputed favorites since (a) the results are freer of mechanistic models* and (b) the experimental protocol is much simpler than in kinetic studies.

Polarity Scales Based on Electronic Absorption Spectra.

The Z Scale. It was developed by Kosower (34h) in 1958. The property chosen as a standard is the energy of the electronic transition



* See, however, Ref. 34e.

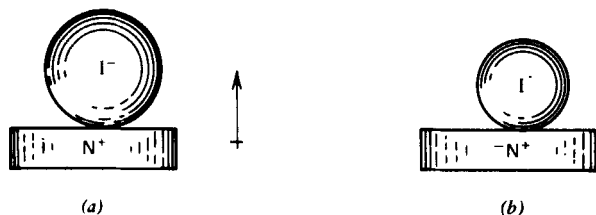


Figure 10 Models for electronic states of 1-alkylpyridinium diode complex: (a) ground state, (b) excited state. (Taken from *J.A.C.S.*, **80**, 3258 (1958).)

of 1-ethyl-4 carbomethoxypyridinium iodide (**II**) which is strongly solvent dependent. According to Kosower, this "internal charge transfer" process involves a drastic dipole reorientation (Cf. Fig. 10).

In this model, $|\mu_g| > |\mu_e|$ but, most important, μ_g and μ_e are orthogonal, so that $\mu_g \cdot \mu_e = 0$. This is the case described by equation 30'.

$$\Delta_{S_1 \rightarrow S_2} \Delta U \neq k \mu_g^2 \Delta_{S_1 \rightarrow S_2} \varphi(\epsilon_B) = -\frac{2 \mu_g^2}{\sigma^3} \Delta_{S_1 \rightarrow S_2} \varphi(\epsilon_B)$$

TABLE 8
Polarity Parameters Z from Ref. 49

Solvent	Z (kcal mole ⁻¹)
H ₂ O	94.6
CH ₃ OH	83.6
C ₂ H ₅ OH	79.6
<i>n</i> -C ₃ H ₇ OH	78.3
<i>n</i> -C ₄ H ₉ OH	77.7
<i>i</i> -C ₃ H ₇ OH	76.3
<i>t</i> -C ₄ H ₉ OH	71.3
(CH ₂ OH) ₂	85.1
CH ₂ Cl ₂	64.2
HCONH ₂	83.3
CH ₃ CO ₂ H	79.2
CH ₃ CN	71.3
(CH ₃) ₂ CO	65.7
(CH ₃) ₂ SO	71.1
OP [N(CH ₃) ₂] ₃	62.8
C ₅ H ₅ N	64.0
CH ₃ CON (CH ₃) ₂	66.9
(CH ₂) ₄ SO ₂	77.5
CH ₃ OCH ₂ CH ₂ OCH ₃	62.1
C ₆ H ₅ OC ₂ H ₅	58.9
C ₆ H ₆	54

or

$$\Delta_{S_1 \rightarrow S_2} \Delta U \approx -\frac{2\mu_g^2}{\sigma^3} \Delta_{S_1 \rightarrow S_2} \varphi(\epsilon_B) \quad (30')$$

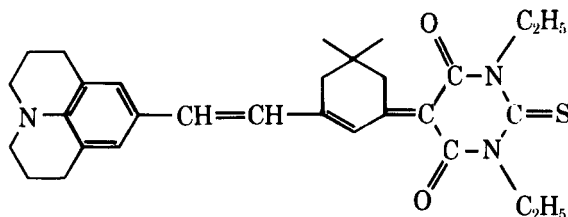
This expression of $\Delta_{S_1 \rightarrow S_2} \Delta U$ is exactly the same as $\Delta_{S \rightarrow S_2} \Delta U_g$ in the Onsager model and this result is still valid for the use of Block-Walker model.

This result lends support to Kosower's remarkable contention that the difference in the transition energies of the charge-transfer band of **II** in two solvents is a reasonable measure of the difference in energies of the ground-state solute in both media. It is unfortunate that this reasoning can not be extended to the gas phase.

Owing to the poor solubility of **II** in many organic solvents, directly measured values of Z are quite scarce. The original set of values was therefore extended by means of other indicators whose solvatochromic shifts yield good linear correlations with Z .

The Z values for a number of solvents are given in Table 8.

The χ_R Scale. In 1964, Brooker and co-workers (34b) suggested the use of the solvent induced bathochromic shifts of the 1,3 diethyl-5-[5-(2,3,6,7-tetrahydro-1H,5H-benzo-[ij]-quinolizin-9-yl)-1,3-neopentylene-2,4-pentadienylidene]-2-thiobarbituric acid (**III**) as measures of medium polarity.



III

This compound has the advantage of being soluble in most organic media and there is a reasonably large amount of available data (Table 9). Here, as in the following scales to be examined, μ_g and μ_e are not orthogonal and the simplification $\mu_g \cdot \mu_e = 0$ is no longer valid.

The E_T Scale. Dimroth, Reichardt, and co-workers (34a) suggested the use of the "solvatochromic band" shifts of 4-(2,4,6-triphenylpyridinium)-2,6-diphenylphenoxide (**IV**) and its trimethyl derivative (**V**) to probe solvent polarities (Table 10).

So far, the E_T scale is one of the most comprehensive in terms of number and variety of solvents and is widely used. For the betaines (**IV** and **V**), $|\mu_g| > |\mu_e|$ and an increase in polarity brings about a hypsochromic shift (i.e., the opposite

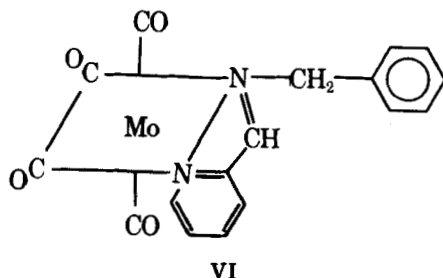
TABLE 9
Solvent Polarity Parameter χ_R^a

Solvent	χ_R (kcal mole ⁻¹)
iso-C ₈ H ₁₈	50.9
<i>n</i> -C ₆ H ₁₄ , <i>n</i> -C ₇ H ₁₆	50.9
<i>c</i> -C ₆ H ₁₁ -CH ₃	50.1
<i>c</i> -C ₆ H ₁₂	50.0
(C ₂ H ₅) ₃ N	49.3
CCl ₄	48.7
(<i>i</i> -C ₃ H ₇) ₂ O	48.6
(<i>n</i> -C ₄ H ₉) ₂ O	48.6
(CH ₂) ₄ O ₂	48.4
(C ₂ H ₅) ₂ O	48.3
<i>p</i> -(CH ₃) ₂ C ₆ H ₄	47.7
CH ₃ CO ₂ <i>n</i> C ₄ H ₉	47.5
<i>o</i> -(CH ₃) ₂ C ₆ H ₄	47.3
CH ₃ -C ₆ H ₅	47.2
CH ₃ CO ₂ C ₂ H ₅	47.2
C ₆ H ₆	46.9
(CH ₂) ₄ O	46.6
CH ₃ COC ₆ H ₁₃	45.8
<i>n</i> -C ₃ H ₇ CN	45.4
CH ₃ COC ₂ H ₅	45.4
C ₆ H ₅ Cl	45.2
C ₆ H ₅ Br	44.6
<i>c</i> -C ₅ H ₁₀ CO	44.3
C ₅ H ₅ N	43.9
HCON(CH ₃) ₂	43.7
C ₆ H ₅ CN	43.3
CH ₃ CON(CH ₃) ₂	43.0
C ₆ H ₅ NO ₂	42.6
CH ₂ -CH ₂ -CH ₂ CO-O	42.6
(CH ₃) ₂ SO	42.0
(CH ₃) ₂ CO	45.7
CH ₃ CN	45.7
<i>i</i> -C ₃ H ₇ OH	44.5
<i>n</i> -C ₄ H ₉ OH	44.5
CHCl ₃	44.2
<i>n</i> -C ₃ H ₇ OH	44.1
CH ₃ NO ₂	44.0
C ₂ H ₅ OH	43.9
CH ₃ OH	43.1
CH ₂ OH-CH ₂ OH	40.4

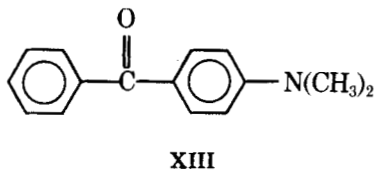
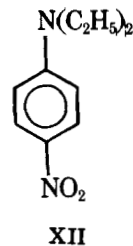
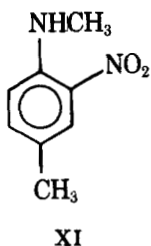
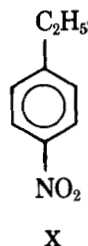
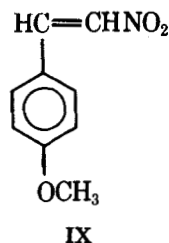
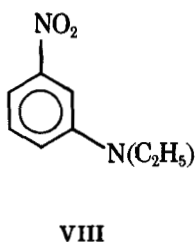
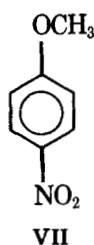
^a From Ref. 34b.

TABLE 10
Polarity Scale E_T (34a)

Solvent	E_T (kcal/mole ⁻¹)
C ₆ H ₁₄	30.9
<i>c</i> -C ₆ H ₁₂	31.2
CCl ₄	32.5
CS ₂	32.6
(<i>n</i> -C ₄ H ₉) ₂ O	33.4
C ₆ H ₅ -CH ₃	33.9
(<i>i</i> -C ₃ H ₇) ₂ O	34.0
C ₆ H ₆	34.5
(C ₂ H ₅) ₂ O	34.6
(CH ₂) ₄ O	36.0
C ₆ H ₅ OCH ₃	37.2
(CH ₂) ₄ O	37.4
(C ₂ H ₅ -OCH ₂) ₂	37.5
C ₆ H ₅ Cl	37.5
C ₆ H ₅ Br	37.5
CH ₃ CO ₂ C ₂ H ₅	38.1
(CH ₃ -OCH ₂) ₂	38.2
C ₅ H ₅ N	40.2
<i>c</i> -C ₅ H ₁₀ CO	40.8
OP[N(CH ₃) ₂] ₃	40.9
OC[N(CH ₃) ₂] ₂	41.0
CH ₃ COC ₂ H ₅	41.3
C ₆ H ₅ CN	42.0
C ₆ H ₅ NO ₂	42.0
Me ₂ CO	42.2
CH ₃ CON(CH ₃) ₂	43.7
HCON(CH ₃) ₂	43.8
(CH ₂) ₄ SO ₂	44.0
(CH ₃) ₂ SO	45.0
CH ₃ -CHCH ₂ OCOO	46.6
Cl ₃ CH	39.1
CH ₂ Cl ₂	41.1
<i>t</i> -C ₄ H ₉ OH	43.9
CH ₃ CN	46.0
CH ₃ NO ₂	46.3
<i>i</i> -C ₃ H ₇ OH	48.6
<i>n</i> -C ₄ H ₉ OH	50.2
<i>n</i> -C ₃ H ₇ OH	50.7
C ₆ H ₅ CH ₂ OH	50.8
CH ₃ CO ₂ H	51.1
C ₂ H ₅ OH	51.9
CH ₃ -CONHCH ₃	52.0
CH ₃ OCH ₂ CH ₂ OH	52.3
CH ₃ OH	55.5
(CH ₂ OH) ₂	56.3
HCONH ₂	56.6
H ₂ O	63.1



The π^ Scale.* Proposed in 1977 by the present authors (33b); this scale is based on the solvent-induced shifts of the frequency maxima of the $\pi \rightarrow \pi^*$ transitions of seven indicators: 4-nitroanisole (VII), N,N-diethyl-3-nitro-aniline (VIII), 4-methoxy- β -nitrostyrene (IX), 1-ethyl-4-nitrobenzene (X), N-methyl-2-nitro-*p*-toluidine (XI), N,N-diethyl-4-nitroaniline (XII) and 4-dimethylaminobenzophenone (XIII).



The choice of several indicators, whose solvatochromic shifts are averaged, is aimed at preventing the inclusion of specific effects or spectral anomalies. The optimized average values given in Table 12 are normalized so that $(\pi^*)_{C-C_6H_{12}}$

TABLE 12
 π^* Scale of Solvent Polarities

Solvent	N^0	π^*
<i>n</i> -C ₆ H ₁₄ , <i>n</i> -C ₇ H ₁₆	1	-0.081
<i>c</i> -C ₆ H ₁₂	2	0.000
(C ₂ H ₅) ₃ N	3	0.140
(<i>i</i> -C ₃ H ₇) ₂ O ^a	4	(0.271) ⁵
(<i>n</i> -C ₄ H ₉) ₂ O	5	0.239
CCl ₄	6	0.294
(C ₂ H ₅) ₂ O	7	0.273
C ₆ H ₅ CH ₃	8	0.535
(CH ₂) ₄ O ₂	9	0.553
Cl ₂ CCHCl	10	0.534
CH ₃ CO ₂ C ₂ H ₅	11	0.545
Cl ₃ CCH ₃	12	0.490
(CH ₂) ₄ O	13	0.576
C ₆ H ₆	14	0.588
C ₆ H ₅ Cl	15	0.709
CH ₃ COC ₂ H ₅	16	0.674
C ₆ H ₅ OCH ₃	17	0.734
(CH ₃) ₂ CO	18	0.683
OP(OC ₂ H ₅) ₃	19	0.715
CH ₂ Cl CH ₂ Cl	20	0.807
CH ₂ Cl ₂	21	0.802
CHCl ₂ CH ₂ Cl	22	0.829
CH ₃ CON(CH ₃) ₂	23	0.882
C ₅ H ₅ N	24	0.87
HCON(CH ₃) ₂	25	0.875
OPN(CH ₃) _{2,3}	26	0.871
$\overline{\text{CH}_2\text{CH}_2\text{CH}_2\text{COO}}$	27	0.873
$\overline{\text{CH}_2\text{CH}_2\text{CH}_2\text{CONCH}_3}$	28	0.921
(CH ₃) ₂ SO	29	1.000
HCCl ₃	30	0.760
C ₆ H ₅ NO ₂	31	1.006
CH ₃ NO ₂	32	0.85
$\overline{\text{C}_6\text{H}_5\text{Br}}$	33	0.794
(CH ₃ CO) ₂ O ^a	34	0.84
<i>p</i> -C ₆ H ₄ (CH ₃) ₂	35	0.426
CS ₂ ^d	36	[0.514] ²
C ₆ H ₅ CN	37	0.933
CH ₃ CO ₂ <i>n</i> -C ₄ H ₉	38	0.460
ClCH ₂ CO ₂ C ₂ H ₅	39	0.704
(CH ₂) ₅ O	40	0.513
<i>c</i> -C ₅ H ₁₀ CO	41	0.750
OP(OC ₄ H ₉) ₃	42	0.653
C ₂ Cl ₄	43	0.277
CHCl ₂ CHCl ₂	44	0.948
(C ₂ H ₅) ₂ SO ₄	45	(0.692) ³
(C ₆ H ₅ CH ₂) ₂ O ^a	46	(0.800) ⁵
C ₆ H ₅ CO ₂ C ₂ H ₅	47	0.739

TABLE 12
 π^* Scale of Solvent Polarities

Solvent	N^0	π^*
(<i>n</i> -C ₄ H ₉) ₃ N	48	0.162
C ₆ H ₅ CH ₂ N(CH ₃) ₂	49	0.494
CH ₃ CN	50	0.76
<i>c</i> -C ₄ H ₈ CO	51	0.756
CH ₃ CO ₂ CH ₃	52	0.556
(CH ₃) ₃ C ₆ H ₃	53	0.402
<i>n</i> -C ₄ H ₉ Cl	54	0.398
HCO ₂ CH ₃ ^a	55	0.605
(CH ₂) ₄ SO ₂ ^a	56	0.95
C ₆ H ₅ N(CH ₃) ₂	57	0.902
C ₆ H ₅ COCH ₃	58	0.901
(C ₆ H ₅) ₂ O ^a	59	(0.658) ³
<i>o</i> -C ₆ H ₄ Cl ₂ ^a	60	(0.796) ³
(CH ₃ OCH ₂) ₂ ^a	61	(0.526) ³
C ₆ H ₅ I ^a	62	(0.810) ³
C ₆ H ₅ CH ₂ CN ^a	63	(1.063) ³
C ₆ H ₅ -C ₂ H ₅ ^b	64	0.482
C ₆ H ₅ - <i>i</i> -C ₃ H ₇ ^b	65	0.458
α -C ₁₀ H ₇ CH ₃ ^b	66	[0.904] ²
<i>m</i> -C ₆ H ₄ Cl ₂	67	[0.690] ²
C ₆ H ₅ CHCH ₂	68	[0.682] ²
<i>t</i> -C ₄ H ₉ OH ^c	101	[0.43]
<i>i</i> -C ₃ H ₇ OH ^c	102	[0.46]
<i>n</i> -C ₄ H ₉ OH	103	0.46
C ₂ H ₅ OH	104	0.54
CH ₃ OH	105	0.60
(CH ₂ OH) ₂ ^c	107	[0.85] ²
H ₂ O	111	1.09
<i>n</i> -C ₃ H ₇ OH	112	0.51
CF ₃ CH ₂ OH ^c	113	[0.73] ²
HCONH ₂ ^c	204	[0.98] ²
(CF ₃) ₂ CHOH ^c	114	[0.65]
CF ₃ CO ₂ H ^c	203	[0.50] ²
CH ₃ CO ₂ H ^c	201	[0.62] ²
HCO ₂ H ^c		(0.96)

For select solvents, $\pi = \pi^*$ by definition.

^a Secondary values, still subject to revision. The superscript are numbers of π_i^* values averaged.

^b Tertiary values, to be used with caution.

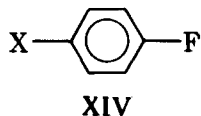
^c These values have been obtained by means of ¹³C nmr spectroscopy. A full discussion is given in Section II.

^d The experimental π^* values ranged from 0.233 to 0.547. The "temperamental" behavior of this solvent is discussed in Section II.

These improved and extended series of values supersede those given in Ref. 33b.

= 0.00 and $(\pi^*)_{DMSO} = 1.00$. The case of amphiprotic solvents is discussed in detail in Section II.

A Polarity Scale Based on NMR Spectroscopy. Taft and co-workers (27) showed that the ^{19}F chemical shifts in compounds of the type **XIV**



where X is an electron withdrawing group, were solvent sensitive; the sensitivity is actually much larger than that of the proton. To minimize the contributions from $(\sigma_a + \sigma_b + \sigma_L)$, the shifts were measured relative to that of fluoro-benzene in the same solution. The solvent P values were defined as

$$P = \left[\int_H^{NO} \right]_S - \left[\int_H^{NO} \right]_0$$

where $\left[\int_H^{NO} \right]_0$ is the corresponding value in the reference cyclohexane. It was shown that these P values gave excellent correlations with the ^{19}F shifts of eight other p -substituted fluorobenzenes with electron-withdrawing substituents and with reactivity and spectral data. Representative values of P for a variety of solvents are given in Table 13.

TABLE 13
Polarity Parameters P (from Ref. 27)

Solvent	P
$c\text{-C}_6\text{H}_{12}^a$	0.00
$\text{C}_{10}\text{H}_{18}$ (decalin) ^a	0.15
CCl_4^a	0.50
$(\text{C}_2\text{H}_5)_2\text{O}^a$	0.90
$n\text{-C}_6\text{H}_{13}\text{F}^a$	1.05
$\text{CH}_3\text{COOC}_2\text{H}_5^a$	1.45
$\text{C}_6\text{H}_5\text{Cl}^a$	1.50
$(\text{CH}_3)_2\text{CO}^a$	1.95
$cis\text{-(CH-CO}_2\text{C}_2\text{H}_5)_2^a$	2.00
$(\text{CH}_3\text{CO})_2\text{O}^a$	2.15
HCONHCH_3^a	2.15
$\text{HCON}(\text{CH}_3)_2^a$	2.25
$\text{C}_6\text{H}_5\text{NO}_2^a$	2.25
CH_3CN^a	2.30
$\overline{\text{CH}_2\text{CH}_2\text{CH}_2\text{COO}}^a$	2.35
CH_3NO_2^a	2.40
$(\text{CH}_3)_2\text{O}^b$	1.75
$o\text{-C}_6\text{H}_4\text{Cl}_2^b$	1.80
CH_3OH	1.85

TABLE 13
Polarity Parameters P (from Ref. 27)

Solvent	P
HCOOCH ₃ ^b	1.85
C ₆ H ₅ I ^c	1.90
C ₂ H ₅ NO ₃	1.90
C ₆ H ₅ COCH ₃ ^c	1.95
C ₅ H ₅ N	2.05
C ₆ H ₅ CN ^b	2.20
CH ₂ Cl CH ₂ Cl ^b	2.20
CH ₂ Cl ₂	2.30
HCCl ₃	2.30
CH ₂ I ₂	2.35
CH ₃ SCN ^c	2.35
CH ₃ SO ₂ F	2.50
(CH ₃) ₂ SO	2.60
(CH ₂) ₄ SO ₂	2.70
(C ₂ H ₅) ₂ CHCH ₃ ^b	-0.40
<i>n</i> -C ₇ H ₁₆ ^b	-0.10
(C ₂ H ₅) ₃ N ^c	0.20
C ₆ H ₅ CH ₃ ^c	0.55
C ₆ H ₆ ^b	0.80
(CH ₂) ₄ O ₂	1.25
(C ₆ H ₅) ₂ O	1.25
(CH ₂) ₄ S	1.30
(CH ₃) ₂ S ^b	1.30
<i>m</i> -C ₆ H ₄ Cl ₂ ^b	1.35
(CH ₂) ₄ O	1.45
C ₆ H ₅ OCH ₃ ^c	1.50
CCl ₃ CN	1.55
C ₆ H ₅ Br ^c	1.55
CH ₃ CO ₂ H	1.60
<i>t</i> -C ₄ H ₉ OH	1.60
C ₂ H ₅ OH	1.70

^a Primary values obtained from measurements with nine + *R* *p*-substituted fluorobenzenes.

^b Based upon $\int_{H}^{p,NO}$ and \int_{H}^{p,NO_2} .

^c Based on $\int_{H}^{p,NO}$ only.

A Polarity Scale Based on IR Spectroscopy. Allerhand and Schleyer (34*f*) observed a nice correlation between the stretching frequencies of various X = 0 vibrators and the ν_{X-H} stretching frequencies of X—H ... B hydrogen-bonded systems in a variety of solvents. This experimental result was taken as proof that "solvent interacts in a similar manner with the X = 0 and X—H ... B stretching frequencies." These effects were attributed to variations in polarity and used to construct a polarity scale, G , defined as:

TABLE 14
Polarity Scale G (34f)

Solvent	G
Vacuum	0
$n\text{-C}_8\text{F}_8$	36
$n\text{-C}_6\text{H}_{14}$	44
$c\text{-C}_6\text{H}_{12}$	49
$(\text{C}_2\text{H}_5)_3\text{N}$	62
$(\text{C}_2\text{H}_5)_2\text{O}$	64
C_2Cl_4	64
CCl_4	69
CS_2	74
$\text{C}_6\text{H}_5\text{CH}_3$	74
$(\text{CH}_2)_4\text{O}_2$	86
CH_3I	89
CH_3CN	93
$\text{C}_5\text{H}_5\text{N}$	94
$\text{CH}_2\text{ClCH}_2\text{Cl}$	95
CH_3NO_2	99
CH_2Cl_2	100
CHCl_3	106
CH_2Br_2	108
CBr_3H	118

$$\frac{\nu^0 - \nu^s}{\nu^s} = aG$$

In this expression, ν^0 and ν^s respectively stand for the stretching frequencies of the vibrators in the gas phase and in the solvent S.

As standard properties, the carbonyl bands of DMF and benzophenone and the sulfonyl band of DMSO were chosen. The origin of the scale was anchored by taking $G_{\text{CH}_2\text{Cl}_2} = 100$ by definition. Values of G are given in Table 14.

C. Toward a Generalized Scale of Solvent Polarities

The proliferation of polarity scales over the last two decades is alarming. The first question it raises is whether they really measure a single "property" of the solvent. The answer is generally negative.

Knauer and Napier (34e) have suggested a division of current polarity parameters into two classes: (1) those that involve no model reaction and which do not probe the solvent at the molecular level (in the cybotactic region) and (2) those that do involve a model and do probe the solvent at the molecular level. As examples of the former class they cite the dielectric constant ϵ_B , and dipole moment μ , and as examples of the latter class, $Y, Z, E_T(30)$ and Ω . Nitrogen hyperfine splitting

TABLE 15a
 Correlation of Various Solvent Scales for Select Solvents

Correlation ^a	<i>n</i>	<i>R</i>	Correlation	<i>n</i>	<i>R</i>	Correlation	<i>n</i>	<i>R</i>
μ vs. π^*	23	0.985 ^b	E_K vs. $\log k$	7	0.985	E_T vs. μ	12	0.979
E_T vs. π^*	12	0.987	A_N vs. $\log k$	6	0.970	χ_R vs. μ	16	0.987
χ_R vs. π^*	16	0.987	G vs. $\log k$	5	0.997	$\log k$ vs. μ	13	0.958
$\log k$ vs. π^*	13	0.985	P vs. $\log k$	8	0.985	$\log k$ vs. μ	12 ^c	0.981
E_K vs. π^*	9	0.977	S vs. $\log k$	7	0.998	E_K vs. μ	9	0.983
A_N vs. π^*	6	0.978	A_N vs. E_K	6	0.981	A_N vs. μ	6	0.997
G vs. π^*	8	0.993	G vs. E_K	^d	^d	G vs. μ	8	0.987
P vs. π^*	12	0.989	P vs. E_K	7	0.994	P vs. μ	12	0.957
S vs. π^*	10	0.981	S vs. E_K	5	0.969	P vs. μ	11 ^c	0.972
χ_R vs. E_T	10	0.987	G vs. A_N	^d	^d	S vs. μ	10	0.968
$\log k$ vs. E_T	9	0.988	P vs. A_N	6	0.986	$\log k$ vs. χ_R	11	0.966
E_K vs. E_T	7	0.982	S vs. A_N	^d	^d	E_K vs. χ_R	7	0.969
A_N vs. E_T	^d	^d	P vs. G	6	0.978	A_N vs. χ_R	6	0.985
G vs. E_T	5	0.996	S vs. G	6	0.996	G vs. χ_R	6	0.997
P vs. E_T	7	0.986	P vs. S	8	0.987	P vs. χ_R	9	0.966
S vs. E_T	7	0.950				S vs. χ_R	10	0.968

^a Values of E_T , χ_R , $\log k$, E_K , A_N , G and S are from reference 34. Values of P are from reference 27 and π^* from Reference 33b (solvent numbers are as given in Table 12). Dipole moments, μ , were taken from A. L. McClellan, *Tables of Experimental Dipole Moments*, W. H. Freeman, San Francisco, 1963. Wherever possible, the values are those measured in the gas phase otherwise values are those determined in saturated hydrocarbons.

^b The inclusion of solvents 13, 40, 52, and 55 (solvents of particularly small steric requirements) brings R down to 0.965 and raises σ to 0.079 (compared to 0.985 and 0.057).

^c Excluding solvent 56.

^d These correlations would involve less than five common solvents and were not considered.

^e Excluding solvent 55.

constants of nitroxides, A_N , they contend, fall into still a third category, since they involve no model reaction but are nevertheless cybotactic probes. Why Z and $E_T(30)$ should be regarded as involving a model reaction, whereas A_N for a specific indicator should not, is unclear to us. In fact, a spectral property can be considered as the difference between two "cybotactic non-model" reactions (corresponding to the ground and excited state).

The elimination of solvents that interact specifically (hydrogen-bond donors, polyhalogenated and aromatic materials) seems necessary. It then appears that for the group of "select solvents"* (i.e., polar, monofunctional aprotic, aliphatic compounds) left, all the scales correlate with each other to a good approximation (Table 15a). This has led present authors to define a scale of polarity π (32a) such that $\pi = (\pi^*)_c$, where $(\pi^*)_c$ is the value of π^* for a "select solvent."** (Cf. Table 15b).

Considering the wide variety of properties correlated, it seems safe to as-

* Practically those defined by Abraham (20a) as "normal solvents."

** This list can be considerably extended.

TABLE 15b
 π Values for Select Solvents

Solvent	π ($\equiv \pi^*$)
<i>n</i> -C ₆ H ₁₄ , <i>n</i> -C ₇ H ₁₈	-0.081
<i>c</i> -C ₆ H ₁₂	0.000
(C ₂ H ₅) ₃ N	0.140
(<i>n</i> -C ₄ H ₉) ₃ N	0.162
(<i>n</i> -C ₄ H ₉) ₂ O	0.239
(<i>i</i> -C ₃ H ₇) ₂ O	0.271
(C ₂ H ₅) ₂ O	0.273
CH ₃ CO ₂ C ₄ H ₉ - <i>n</i>	0.460
(CH ₂) ₅ O	0.513
CH ₃ CO ₂ C ₂ H ₅	0.545
CH ₃ CO ₂ CH ₃	0.61
(CH ₂) ₄ O	0.576
HCO ₂ CH ₃	0.605
HC(OCH ₃) ₃	0.63
OP(OC ₄ H ₉ - <i>n</i>) ₃	0.653
CH ₃ COC ₂ H ₅	0.674
(CH ₃) ₂ CO	0.72
ClCH ₂ CO ₂ C ₂ H ₅	0.704
OP(OC ₂ H ₅) ₃	0.715
(CH ₃ CO) ₂ O	0.76
<i>c</i> -C ₅ H ₁₀ CO	0.750
<i>c</i> -C ₄ H ₈ CO	0.756
<u>CH₂CH₂CH₂COO</u>	0.873
HCON(CH ₃) ₂	0.875
CH ₃ CON(CH ₃) ₃	0.882
(CH ₂) ₄ SO ₂	0.95
(CH ₃) ₂ SO	1.000

sume that π (and all other scales for that matter) is indeed probing an intrinsic property of the "select solvents." This is further supported by some new and still unpublished results.

The recent development of ¹³C ftmnr spectroscopy (67) has enabled the study of solvent effects on ¹³C spectra. Among others, these spectra have two distinct advantages: (a) great sensitivity, and (b) the possibility of probing different atoms within the same molecules, particularly the "inner" ones, which, according to Buckingham (62*b,c*) would better satisfy the requirements of the models used to define the R.F. and, at any rate, are less prone to undergo specific solvation.

Dr. B. Chawla (68*a*) in this laboratory has recently carried out a study of solvent effects on the ¹³C shifts of several aromatic compounds. A series of typical results is given in Table 16. It shows the influence of the environment on the chemical shifts of the para and meta carbon atoms of α,α,α -trifluoromethylbenzene relative to the signal of benzene.

TABLE 16
Solvent Effects on the ^{13}C NMR Shifts of α, α, α -Trifluoromethylbenzene Relative to Benzene

Solvent	$\int_H^{m-CF_3}$ (ppm)	$\int_H^{p-CF_3}$ (ppm)	$\int_{m-CF_3}^{p-CF_3}$ (ppm)
$n\text{-C}_6\text{H}_{14}^a$	0.28	3.06	2.78
$c\text{-C}_6\text{H}_{12}^a$	0.28	3.09	2.81
$\text{C}_{10}\text{H}_{18}$ (decalin)	0.32	3.10	2.78
$(\text{C}_2\text{H}_5)_3\text{N}^a$	0.46	3.34	2.88
CCl_4	0.32	3.21	2.89
$(\text{CH}_2)_4\text{O}_2$	0.57	3.63	3.06
HCCl_3	0.35	3.35	3.00
$\text{CF}_3\text{CO}_2\text{CH}_3$	0.57	3.61	3.04
$t\text{-C}_4\text{H}_9\text{OH}$	0.60	3.59	2.99
$\text{CF}_3\text{CO}_2\text{H}$	0.13	3.16	3.03
$\text{CH}_3\text{CO}_2\text{C}_2\text{H}_5^a$	0.75	3.80	3.05
$\text{C}_2\text{H}_5\text{OH}^a$	0.73	3.78	3.05
$\text{CH}_3\text{CO}_2\text{H}$	0.65	3.73	3.08
$(\text{CH}_2)_4\text{O}^a$	0.76	3.84	3.08
$\text{CH}_3\text{CO}_2\text{CH}_3^a$	0.76	3.86	3.10
CH_2Cl_2	0.49	3.59	3.10
CH_3OH^a	0.73	3.83	3.10
$\text{CH}_3\text{COC}_2\text{H}_5^a$	0.86	3.96	3.10
$\text{HC}(\text{OCH}_3)_3$	0.75	3.88	3.13
$\text{CH}_3\text{OCH}_2\text{CH}_2\text{OH}$	0.86	3.99	3.13
$\text{C}_5\text{H}_5\text{N}$	0.56	3.71	3.15
$(\text{C}_2\text{H}_5\text{O})_3\text{PO}$	1.05	4.18	3.13
$(\text{CH}_3)_2\text{CO}^a$	0.85	4.00	3.15
$(\text{CH}_3\text{CO})_2\text{O}^a$	0.78	3.96	3.18
$(\text{CH}_2\text{OH})_2$	0.82	4.03	3.21
$\text{CH}_3\text{CO N}(\text{CH}_3)_2^a$	1.04	4.23	3.19
$\text{FCH}_2\text{CH}_2\text{OH}$	0.67	3.86	3.19
CH_3NO_2	0.67	3.88	3.21
CH_3CN^a	0.73	3.94	3.21
$\text{HCON}(\text{CH}_3)_2^a$	0.97	4.21	3.24
60% aq. $\text{C}_2\text{H}_5\text{OH}$	0.70	3.94	3.24
HCONH_2	0.57	3.86	3.29
$\text{CH}_3\text{CH}(\text{CH}_2\text{COO})_2$	0.78	4.07	3.29
$(\text{CH}_3)_2\text{SO}^a$	0.94	4.24	3.30

^a Solvents used to establish Equation 37'.

The correlation of these shifts with the polarity parameters π , is, here again, quite satisfactory:

$$\int_H^{pCF_3} = 3.11 + 1.23 \pi; r = 0.997, n = 15$$

$$\int_H^{m-CF_3} = 0.34 + 0.68 \pi; r = 0.971, n = 15$$

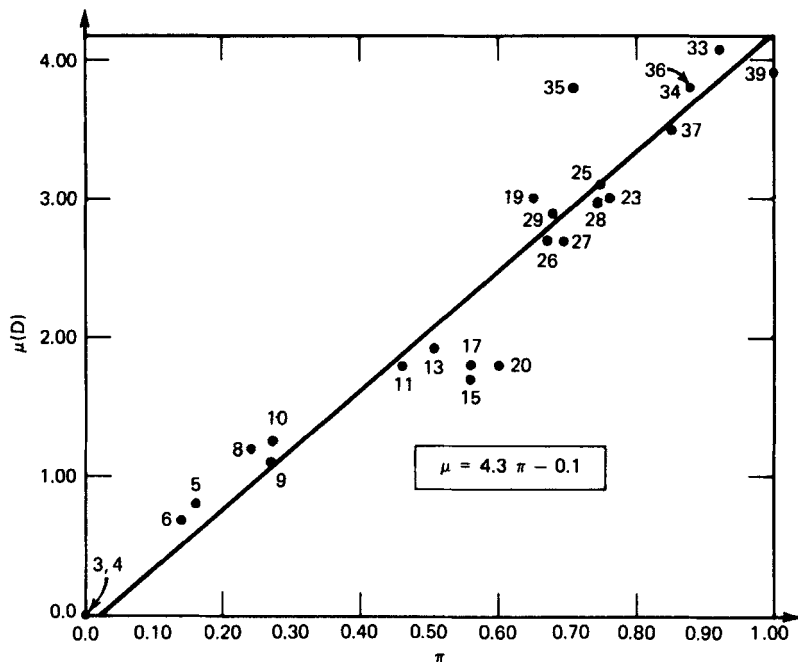


Figure 11 Correlation between the dipole moment and the polarity parameters π . Solvents numbered as in Table 17.

The quantity $\int_{m-CF_3}^{p-CF_3}$ is likely to be freer of specific solvation effects than the preceding shifts. The correlation equation is:

$$\int_{m-CF_3}^{p-CF_3} = 2.80 + 0.48 \pi \quad (37')$$

with $r = 0.988$, $\sigma = 0.03$, $n = 21$

It is of some interest that the ratio of the sensitivities of $\int_H^m-CF_3$ and $\int_H^p-CF_3$ to polar effects, $0.68/1.23 = 0.55$, is in good agreement with the ratio to be expected if these polar effects are proportional to the values of the reaction field acting on the meta and para carbons. If the R.F. acts along the dipole axis of the molecule (i.e., dipole moment axis), then (R.F.) *meta*/(R.F.) *para* $\approx \cos 60^\circ = 0.500$. (Cf., also, Ref. 68*b*).

At this stage, it is tempting to try to rationalize these results in terms of solvent properties.

At the microscopic level, the dipole moment of the isolated solvent molecule is a quantitative measure of polarity. Table 15*a* shows that there is a very good linear relationship between the different scales and the dipole moment of the "select solvents." (see also Fig. 11). The polarizability of the solvent, as measured for example by $\varphi(n^2)$ also plays a role (33*d*); the small but distinct difference

between the values of cyclohexane and *n*-hexane is likely a consequence thereof. However this contribution is nearly constant throughout the series considering the very narrow range of variation of $\varphi(n^2)$.

As a first approximation, therefore, "the elusive idealized solute-independent solvent polarity parameter is indicated to be the molecular dipole moment" (33a). For instance, the correlation equation between the π parameters and μ is:

$$\mu = -0.1 + 4.3 \pi; n_s = 28, r = 0.972, \text{av. dev.} = 0.3 \text{ D} \quad (38)$$

These results are strongly in favor of those theories of solvent effects on nmr and ir spectra in which only pairwise interactions are considered.

Indeed, it has recently been concluded (69) that "aprotic polar solvent effects are mostly determined by solvent-solute dipolar interactions rather than by a bulk effect of the solvent as a *continuous* dielectric."

These facts are deceitfully simple since a solute molecule actually interacts with a large number of solvent molecules. Looking back at Sections I.A and I.B it appears that *all the solvent effects considered are linear functions of the R.F. acting on the solute*. Now, the concept of R.F. does not need to be explicitly linked to any theory. The R.F. is the field generated by all the solvent molecules within the solute cavity and the actual calculation of the R.F., if at all possible, is an ancillary problem. *The linear dependence on the R.F. immediately rationalizes the linear relationships among scales*: For the "select solvents," they are probing the same property. The establishment of a functional dependence between the R.F. and experimentally accessible quantities is a strong challenge. We have already examined two alternative formalisms: the Kirkwood-Onsager's (isotropic solvent) and the Block-Walker's (dielectrically saturated solvent). For all the large simplifications involved, the latter seems to give a reasonable expression of the R.F. acting on a polar solute. Figure 12 shows a plot of the nmr parameters P versus $\Theta(\epsilon_B)$. The correlation is quite good: $n = 17$, $\sigma = 0.18$ and $r = 0.983$.

It is instructive to compare the polarity parameters π with both $\Theta(\epsilon_B)$ and $\varphi(\epsilon_B)$ (Figs. 13 and 14). $\Theta(\epsilon_B)$ gives a rather satisfactory linear correlation:

$$\pi = 2.52 \Theta(\epsilon_B) - 0.23; n = 28, \sigma = 0.10, r = 0.964$$

The linear relationship of π with the dipole moments and $\Theta(\epsilon_B)$ implies that these two quantities must be linearly related. Mathematically, however, *no such relationship can be proved*.

On an empirical basis, we have examined 39 widely used solvents that meet the definition of being a select solvent. There is indeed a good linear relationship between the dipole moment μ and $\Theta(\epsilon_B)$, as shown by the agreement between observed and calculated values given in Table 17. The correlation equation is:

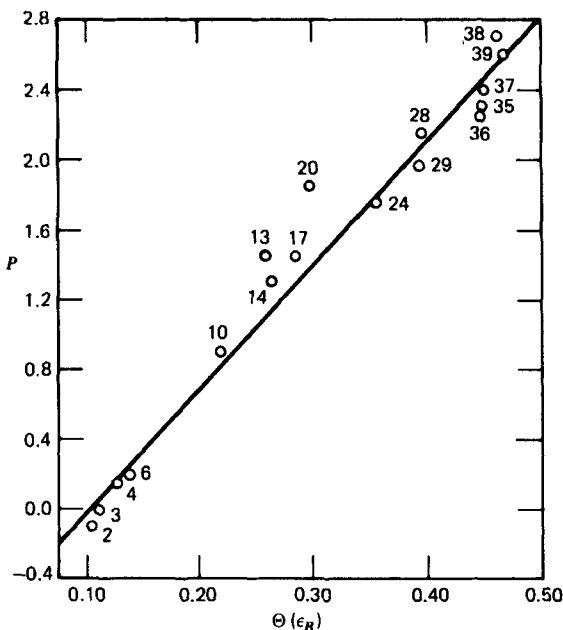


Figure 12 ^{19}F nmr solvent effects scale P vs. $\Theta(\epsilon_B)$.

$$\mu = 10.80 \Theta(\epsilon_B) - 1.03 \quad (39)$$

with $n = 39$, $r = 0.961$, and av. dev. = 0.3 D.

The quality of the correlation Equations 38 and 39 for select solvents is very similar, and, because the available data are relatively small in number, it is not possible to ascertain which property [$\Theta(\epsilon_B)$ or μ] is generally superior as an index of solvent polarity. It can be seen in Table 17 that for solvents with a given functionality, the calculated values are too large for solvents with small carbon content, whereas the calculated μ values are too small for solvents that carry large hydrocarbon residues. For example, there are 12 solvents in Table 17 that may be regarded as methyl derivatives [including $(\text{CH}_2)_2\text{O}$]. For these, deviations range from 0.0 to 1.0 D, the average deviation being +0.3 D. There are 8 solvents in Table 17 for which the functional groups are substituted with six or more carbon atoms. For these, deviations range from 0.1 to -0.9 D, the average deviation being -0.3 D. The behavior of some ethers and nitrocompounds further illustrates this behavior, as shown in Table 18. Although the dipole moment is fairly insensitive to an increase in the carbon content, the dielectric constant steadily falls off as the chain lengthens. Obviously, these results are not a consequence of the form of $\Theta(\epsilon_B)$. Any monotonical function of ϵ_B alone would display analogous behavior. The most common polar solvents are formed

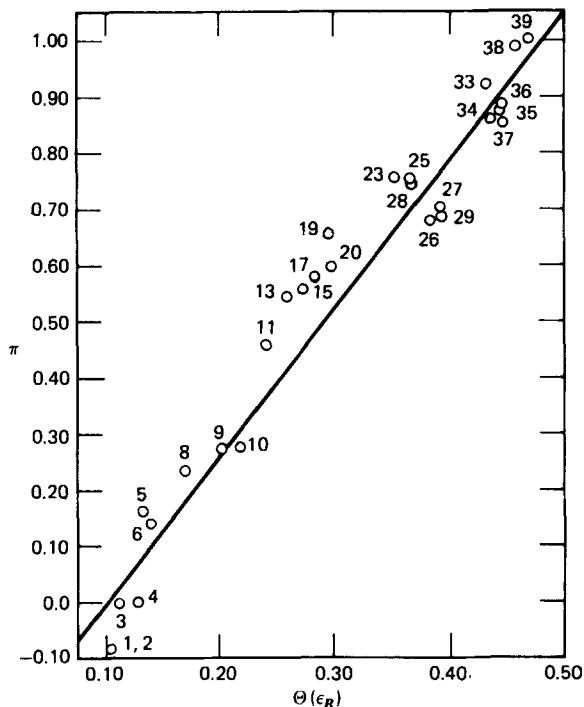


Figure 13 Generalized polarity parameter π vs. $\Theta(\epsilon_B)$.

by a small, polar functionality, generally containing heteroatoms, linked to one or more aliphatic or aromatic chains. The value of the dipole moment is essentially determined by the nature of the polar group and is nearly independent of the length of the chain beyond the second carbon atom. The dielectric constant ϵ_B , on the other hand, reflects the contribution of *all* the atoms in the molecule and decreases as the solvent becomes more hydrocarbon-like. A polar solute is likely to be able to "sort out" the polar terminus of the molecule, thus offsetting the decrease in ϵ_B . The solvents *n*-Bu₃N, *n*-Bu₂O, and (*n*-BuO)₃PO probably belong to this category, since their experimental μ values are substantially larger than the values predicted by Equation 39 whereas the π values for these solvents give better agreement with the calculated (Equation 38) and observed dipole moments. Thus Equation 39 seems to be more restrictive in that it is best represented by solvents having four to six carbon atoms. On the other hand, other structural features can be noted which favor Equation 39.

Cyclization of the hydrocarbon moiety frequently leads to pronounced increases in the *permanent* dipole moments of functional groups. Thus, N-methyl pyrrolidone has a moment 0.6 D greater than that of N,N-dimethylacetamide.

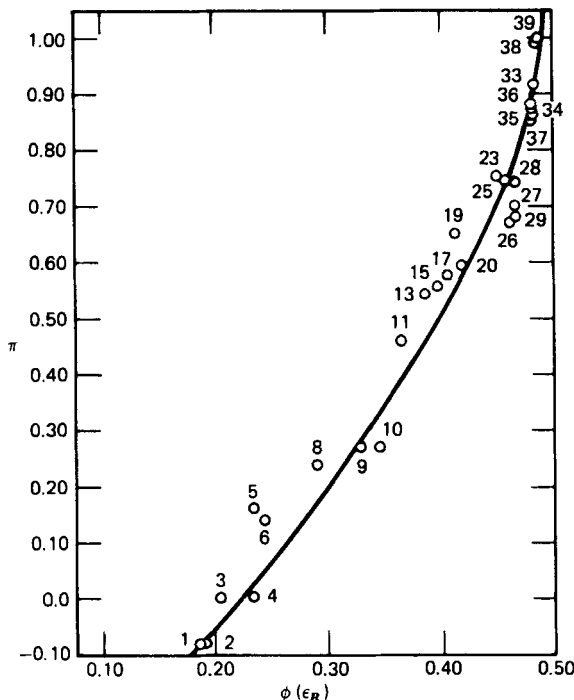


Figure 14 Generalized polarity parameter π vs. $\phi(\epsilon_B)$.

By the dipole moment criterion, the cyclic compounds would be expected to show appreciably greater polarities. They do not. For example, the π values (Table 17) are essentially the same for the open-chain and cyclic compounds. These results are in accord with the $\Theta(\epsilon_B)$ function, which has nearly the same values for the corresponding open-chain and cyclic compounds. Propylene carbonate (PC) provides a further case of interest. This solvent has a dipole moment and a dielectric constant (4.9 D and 65.1, respectively (70)) which are both substantially larger than those of DMSO (3.9 D and 48.9, respectively). According to the π - μ correlation (Equation 38) their π values would be $(\pi)_{DMSO} = 0.93$ and $(\pi)_{PC} = 1.16$, that is, PC would be 25% more polar than DMSO. The $\pi - \Theta(\epsilon_B)$ correlation, on the other hand, predicts $(\pi)_{DMSO} = 0.947$ and $(\pi)_{PC} = 1.000$, that is, the latter would be some 5% more polar than DMSO. Experimentally, DMSO and PC are extremely close, as shown in Table 19. These results seem indeed to favor the correlation with $\Theta(\epsilon_B)$.

It should be emphasized that the physical meaning of a correlation with the dipole moment is somewhat different from that of a correlation with the $\Theta(\epsilon_B)$ function. A strictly linear relationship with the dipole moment can only

TABLE 17
Dielectric Constants, Dielectric Functions, and Dipole Moments for Common
(Select) Aprotic Solvents

No.	Solvent	π^a	ϵ_B^b	$\Theta(\epsilon_B)^c$	$\varphi(\epsilon_B)^d$	$\mu_{(D)obs}^e$	$\mu_{(D)calc}^f$
1.	<i>n</i> -C ₆ H ₁₄	-.08	1.907	.103	.188	0.0	0.1
2.	<i>n</i> -C ₇ H ₁₆	-.08	1.924	.104	.191	0.0	0.1
3.	<i>c</i> -C ₆ H ₁₂	.00	2.023	.112	.203	0.0	0.2
4.	decalin	.00	2.26	.128	.232	0.0	0.3
5.	(<i>n</i> -C ₄ H ₉) ₃ N	.16	2.3	.131	.232	0.8	0.4
6.	(C ₂ H ₅) ₃ N	.14	2.42	.138	.243	0.7	0.5
7.	OC(OC ₂ H ₅) ₂	—	2.82	.160	.274	0.9	0.7
8.	(<i>n</i> -C ₄ H ₉) ₂ O	.24	3.06	.172	.289	1.2	0.8
9.	(<i>i</i> -C ₃ H ₇) ₂ O	.27	3.88	.204	.329	1.1	1.2
10.	(C ₂ H ₅) ₂ O	.27	4.34	.219	.345	1.2	1.3
11.	CH ₃ CO ₂ <i>n</i> -C ₄ H ₉	.46	5.01	.242	.364	1.8	1.6
12.	<i>n</i> -C ₆ H ₁₃ Cl	—	5.90	.258	.383	2.1	1.8
13.	CH ₃ CO ₂ C ₂ H ₅	.55	6.02	.260	.385	1.9	1.8
14.	(CH ₃) ₂ S	—	6.20	.264	.388	1.5	1.8
15.	CH ₃ CO ₂ CH ₃	.61	6.68	.273	.396	1.7	1.9
16.	HCO ₂ C ₂ H ₅	.61	7.16	.281	.402	1.9	2.0
17.	(CH ₂) ₄ O	.58	7.39	.285	.405	1.8	2.0
18.	C ₄ H ₉ Cl	—	7.39	.285	.405	2.1	2.0
19.	OP(O-C ₄ H ₉) ₃	.65	7.97	.294	.412	3.0	2.1
20.	HCO ₂ CH ₃	.61	8.37	.299	.415	1.8	2.2
21.	C ₂ H ₅ Br	—	9.50	.313	.425	2.0	2.3
22.	(<i>n</i> -C ₃ H ₇) ₂ CO	—	12.90	.347	.444	2.7	2.7
23.	<i>c</i> -C ₄ H ₈ CO	.76	13.50	.351	.446	3.0	2.8
24.	(CH ₂) ₂ O	—	13.90	.354	.448	1.8	2.8
25.	<i>c</i> -C ₅ H ₁₀ CO	.75	15.71	.367	.454	3.1	2.9
26.	CH ₃ COC ₂ H ₅	.67	18.51	.383	.461	2.7	3.1
27.	ClCH ₂ CO ₂ C ₂ H ₅	.70	20.0	.390	.463	2.7	3.2
28.	(CH ₃ CO) ₂ O	.76	20.5	.393	.464	3.0	3.2
29.	(CH ₃) ₂ CO	.72	20.74	.394	.465	2.9	3.2
30.	<i>n</i> -C ₃ H ₇ NO ₂	—	24.20	.408	.470	3.6	3.4
31.	C ₂ H ₅ CN	—	27.2	.419	.473	4.0	3.5
32.	C ₂ H ₅ NO ₂	—	29.11	.425	.475	3.7	3.6
33.	CH ₃ N(CH ₂) ₃ CO	.92	33.0	.433	.478	4.1	3.6
34.	HCON(CH ₃) ₂	.88	36.7	.444	.480	3.8	3.8
35.	CH ₃ CN	.85	37.5	.446	.480	3.7	3.8
36.	CH ₃ CON(CH ₃) ₂	.88	37.8	.447	.480	3.8	3.8
37.	CH ₃ NO ₂	.85	38.6	.448	.481	3.5	3.8
38.	(CH ₂) ₄ SO ₂	.95	44.0	.459	.483	4.7	3.9
39.	(CH ₃) ₂ SO	1.00	48.9	.467	.485	3.9	4.0

^a See Table 12 and Ref. 33*b*.

^b These values have generally been taken from Ref. 13.

^c See Equation 22.

^d $\varphi(\epsilon_B) = (\epsilon_B - 1)/(2\epsilon_B + 1)$

^e Most of the values are from A. L. McClellan's *Tables of Experimental Dipole Moments*, W. H. Freeman, San Francisco, 1963. Whenever possible, the values are those measured in the gas phase, otherwise, we use the values determined in saturated hydrocarbons.

^f Calculated from Equation 39.

TABLE 18
Effect of Carbon Content on the Dielectric Constants and Dipole Moments of Some Aliphatic Ethers and Nitro Compounds

Compound	ϵ_B	$\Theta(\epsilon_B)$	μ (experimental) ^a	μ (calculated) ^b	No. of carbon atoms
Et ₂ O	4.34	0.219	1.2	1.3	4
<i>i</i> -Pr ₂ O	3.88	0.204	1.1	1.2	6
<i>n</i> -Bu ₂ O	3.06	0.172	1.2	0.8	8
CH ₃ NO ₂	38.57	0.448	3.5	3.8	1
C ₂ H ₅ NO ₂	29.11	0.425	3.7	3.6	2
<i>n</i> -C ₃ H ₇ NO ₂	24.20	0.408	3.6	3.4	3

^a See Table 17.

^b Values calculated by means of Equation 39.

be expected in the cases of a 1:1 interaction between solvent and solute dipoles in the absence of contributions from the neighboring solvent molecules. This is the situation that might prevail in the gas phase under moderate pressures. In contradistinction, the function $\Theta(\epsilon_B)$ allows for strong solvent-solute and solvent-solvent dipolar interactions. On the other hand, it seems probable to us that the existence of Equation 39 depends upon the fact that there is short-lived clustering of a few polar solvent molecules around the dipolar solute.

Another test of Equation 39 is provided by its application to nonselect solvents, that is, polyhalogenated hydrocarbons, aromatic hydrocarbons, and protonic solvents. Such solvents generally involve specific interactions with polar solutes so that no general scale of polarity (alone) can be applied to correlate their observed solvent effect properties. These solvents generally give large deviations from Equation 39 (although C₆H₅CN and C₆H₅NO₂ were shown to satisfactorily follow this relationship). In Table 20, some typical nonselect solvents are given together with their observed dipole moments and those calculated using Equation 39.

TABLE 19
Comparative Polarity Effects of Dimethylsulfoxide (DMSO) and Propylene Carbonate (PC)

Property <i>p</i>	<i>c</i> -C ₆ H ₁₂	DMSO	PC	$(p)_{PC} - (p)_{C_6H_{12}}$
				$(p)_{DMSO} - (p)_{C_6H_{12}}$
E _T (30) Kcal	31.2	45.0	46.6	1.12
$\int_{m-CF_3}^{p-CF_3}$	2.81	3.30	3.29	0.98
$\delta\Delta G_{tr}^\ddagger$ Et ₄ N ⁺ I ⁻ (a) (Kcal/mol)	4.19	0.15	0.28	0.94

^a Free energy of transfer (relative to DMF) of the transition state of the quaternarization of Et₃N by EtI (20*b*).

TABLE 20
Observed and Calculated Dipole Moments for Some Typical Nonsolvent Solvents

Solvent	ϵ_B	$\Theta(\epsilon_B)$	μ (obs)	μ (calc Eq. 39)
CCl ₄	2.238	.127	0.0	0.3
HCCl ₃	4.806	.232	1.3	1.5
H ₂ CCl ₂	9.08	.308	1.6	2.3
C ₆ H ₆	2.284	.132	0.0	0.4
C ₆ H ₅ OCH ₃	4.33	.219	1.3	1.4
C ₆ H ₅ Cl	5.62	.252	1.6	1.7
<i>ortho</i> -C ₆ H ₄ Cl ₂	9.93	.319	2.3	2.4
C ₅ H ₅ N	12.3	.342	2.2	2.7
C ₆ H ₅ CN	25.20	.412	3.9	3.8
C ₆ H ₅ NO ₂	34.82	.440	3.9	3.8
HO ₂ CCH ₃	6.15	.263	1.7	1.8
EtOH	24.3	.408	1.7	3.4
MeOH	32.65	.434	1.7	3.7
H ₂ O	80.1	.504	1.7	4.4

The agreement between calculated and observed values of Table 20 is comparable to that obtained in Table 17 for the select solvents, except for water and alcohols. The latter solvents self-associate through H bonds to form very polar clusters giving rise to much larger ϵ_B values than might be anticipated from the permanent dipole moments of the monomers. Evidently, the formation of cyclic acetic acid dimer does not produce such an effect so that this hydroxylic solvent has "normal" values of both $\Theta(\epsilon_B)$ and μ —very similar to those for the aprotic derivatives methyl and ethyl acetates.

In conclusion, we note that the systems we have been dealing with are very polar. These systems necessarily display the largest effects and in practice have received considerable attention. It is a pity that relatively little effort has been directed so far to the study of low-polarity systems (probably because of the small magnitude of the effects). They are interesting, among other reasons because they present, at least in principle, the possibility of showing a different functional dependence with the dielectric constant of the solvent, perhaps along the lines predicted by Onsager's or Fulton's theories.

II. LINEAR SOLVATION ENERGY RELATIONSHIPS (LSER)

A. General Formalism

In general, a property XYZ of a species A in a solvent S can be expressed as,

$$(XYZ)_{A,S} = \sum_i \varphi_i (A,S) \quad (40)$$

and for a species B,

$$(XYZ)_{B,S} = \sum_i \varphi_i(B,S) \quad (41)$$

where the φ_i s are complex functions of both solvents and solutes. Since, in general, $\varphi_i(A,S) \neq \varphi_i(B,S)$, the possibility of a "universal scale" seems remote.

On the other hand, it is an experimental fact that for certain families of solvents a good correlation may exist between two different properties of two different solutes in a series of solvents (see Section I). The rationale is that in some cases, as a first approximation, the quantities $\varphi_i(A,S)$ and $\varphi_i(B,S)$ can be factorized as:

$$\varphi_i(A,S) = f_i(A) g_i(S)$$

and

$$\varphi_i(B,S) = f_i(B) g_i(S)$$

so that Equations 40 and 41 become:

$$(XYZ)_{A,S} = \sum_i f_i(A) g_i(S) = \sum_i \lambda_{A_i} g_i(S) \quad (40')$$

$$(XYZ)_{B,S} = \sum_i f_i(B) g_i(S) = \sum_i \lambda_{B_i} g_i(S) \quad (41')$$

If the g_i s are linearly independent, medium effects on $(XYZ)_A$ are not expected to correlate with $(XYZ)_B$ except if for all the λ s,

$$\lambda_{B_i} = k \lambda_{A_i}$$

The main physical implication of this condition is that good correlations involving "all solvents" will be limited to compounds and/or properties that are extremely closely related. This seems to be the main reason for the proliferation of solvent property scales.

Equations 40' and 41' can be written as:

$$(XYZ)_A = \lambda_{A_m} g_m(S) + \sum_{i \neq m} \lambda_{A_i} g_i(S) \quad (40'')$$

$$(XYZ)_B = \lambda_{B_m} g_m(S) + \sum_{i \neq m} \lambda_{B_i} g_i(S) \quad (41'')$$

If, for a given couple $(XYZ)_A$ and $(XYZ)_B$,

$$|\lambda_{A_m} g_m(S)| \gg \left| \sum_{i \neq m} \lambda_{A_i} g_i(S) \right|$$

and

$$|\lambda_{B_m}g_m(S)| \gg \left| \sum_{i \neq m} \lambda_{B_i}g_i(S) \right|$$

a linear medium effect relationship between $(XYZ)_{A,S}$ and $(XYZ)_{B,S}$ is to be expected. The same obviously holds in the cases, probably more frequent, where $\sum_{i \neq m} \lambda_{A_i}g_i(S)$ and $\sum_{i \neq m} \lambda_{B_i}g_i(S)$ are practically constant. It is then clear that by a proper choice of the reference systems and properties, the $g_i(S)$ s can be evaluated. This has been the underlying philosophy in the linear solvation energy relationships (LSER) concept.

We consider that, when using multiparameter expressions like Equations 40' and 41', the following requirements must be met: (a) The $g_i(S)$ s must be linearly independent; (b) the $g_i(S)$ s must represent physically meaningful properties which can be (at least approximately) explained and quantified in terms of current theories.

The following treatment is based on the use of three different scales [i.e., $g_1(S)$, $g_2(S)$, and $g_3(S)$] which have been determined empirically: the polarity scale π^* , the α scale of solvent hydrogen bond donor (HBD) acidities (71), and the β scale of solvent hydrogen bond acceptor (HBA) basicities (72). To avoid possible pitfalls resulting from experimental errors or from specific solvent effects, the solvatochromic parameters* have been arrived at by averaging multiple g_i s determined for each solvent with a variety of different indicators. Quite generally, the purpose of this study is the systematic correlation of solvent effects on diverse properties and reactivity parameters, XYZ , by means of expressions of the type,

$$XYZ = XYZ_0 + s\pi^* + a\alpha + b\beta \quad (42)$$

and the use of these equations to gain structural and mechanistic information.

B. Methodology

1. The β Scale of Solvent HBA Basicity

The initial construction of this scale involved the systematic application of the solvatochromic comparison method (72). Documentation of solvent-solute hydrogen bonding interactions by this method requires that three important

* Although the equations have been extended to cover many nonspectroscopic properties, we find it convenient to continue to refer to the method as the solvatochromic comparison method, the equations as the solvatochromic equations, the π^* , α , β , and δ terms as the solvatochromic parameters, and the s , a , b , and d terms as the solvatochromic coefficients (cf Eq. 96).

TABLE 21
Spectral Data (in kK) for 4-Nitroaniline (1), *N,N*-Diethyl-4-nitroaniline (2), 4-Nitrophenol (3), and 4-Nitroanisole (4)

Solvent	$\nu(1)_{\max}$		$\nu(2)_{\max}$		$\nu(1)_{\max}$		$\nu(2)_{\max}$		$\nu(3)_{\max}$		$-\Delta\Delta\nu-$ $(3-4)^B-HO$
	Obsd	Eq. 43	Obsd	Eq. 43	Obsd	Eq. 43	Obsd	Eq. 43	Obsd	Eq. 45	
1. Hexane, heptane	27.71		31.30						34.31		
2. Cyclohexane	27.40		31.01						34.13		
6. CCl_4	26.70		30.30						33.56		
8. Toluene	24.87		29.41								
10. $Cl_2C=CHCl$	25.76		29.63								
14. Benzene	25.60		29.07						32.84		
15. Chlorobenzene	25.38		28.82								
20. $ClCH_2CH_2Cl$	25.06		28.37						32.36		
21. CH_2Cl_2	24.96		28.65						32.25		
Non-Hydrogen Bonding or Weak Hydrogen Bonding											
Hydrogen-bond Acceptors											
17. Anisole	25.31		28.17		28.83		0.67		32.41		0.63
39. Ethyl chloroacetate	25.28		27.89		28.80		0.91		32.57		0.82
9. Dioxane	25.77		28.25		29.31		1.06		32.89		0.90
46. Dibenzyl ether	25.09		27.47		28.61		1.14				
47. Ethyl benzoate	25.31		27.66		28.84		1.22				
7. Ethyl ether	26.52		28.65		30.09		1.44		33.45		1.19
5. Butyl ether	26.85		29.03		30.43		1.40		33.56		1.23
11. Ethyl acetate	25.74		27.93		29.28		1.35		32.79		1.13
18. Acetone	25.22		27.32		28.74		1.42				

conditions be fulfilled: (a) a plot of corresponding ν_{\max} values (or other appropriate spectroscopic or thermodynamic properties), for two solutes of differing hydrogen bonding ability in a series of solvents of varying polarity but wherein hydrogen bonding is excluded, should show a linear relationship with a statistically acceptable correlation coefficient; (b) data points representing solvents in which hydrogen bonding occurs should be displaced from the regression line (all in the same direction) by statistically significant amounts; (c) the direction of the displacements should be consistent with the chemistry involved, and the relative magnitudes should reflect a reasonable order of solvent hydrogen bond donor strengths in the case of solvent to solute (type A) bonding, or solvent hydrogen bond acceptor strengths where the effects derive from solute to solvent (type B) hydrogen bonds.

As an example, ν_{\max} values for the [$>\dot{N}^+=C(1) \rightarrow C(4)=NO_2^-$] electronic transition of 4-nitroaniline (**1**) are compared in Table 21 and Fig. 15 with results in corresponding solvents for *N,N*-diethyl-4-nitroaniline (**2**).



Figure 15 shows that the first requirement is satisfied; the correlation equation for the results in 9 non-hydrogen-bonding and very weak HBA solvents is

$$\nu(\mathbf{1})_{\max} = 1.035 \nu(\mathbf{2})_{\max} + 2.64 \text{ kK} \quad (43)$$

$$r = 0.989, \sigma = 0.16 \text{ kK}.$$

It is also seen in Figure 15 that the second requirement is satisfied; displacements of the data points for HBA solvents from the regression line all reflect lower transition energies for the HBD solute **1**, and range from 2.4 standard deviations of Equation 43 for the very weak HBA solvent trichloroacetone to 17.5 σ for the very strong HBA solvent, hexamethylphosphoramide. Values of the enhanced solvatochromic displacements, $-\Delta\Delta\nu(\mathbf{1}-\mathbf{2})_{-H_2N}^B$, calculated from,

$$-\Delta\Delta\nu(\mathbf{1}-\mathbf{2})_{-H_2N}^B = \nu(\mathbf{1})_{\text{Eq. 43}}^{\text{calcd}} - \nu(\mathbf{1})_{\max}^{\text{obs}} \quad (44)$$

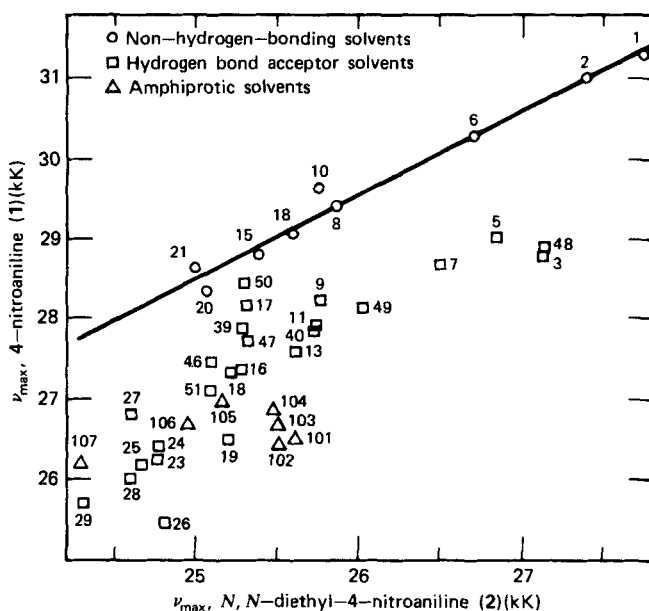


Figure 15 Solvatochromic comparison of 4-nitroaniline (1) and *N,N*-diethyl-4-nitroaniline (2) uv spectral data.

are included in Table 21.*

When the same type of analysis is carried out on the couple 4-nitrophenol (3) and 4-nitroanisole (4), exactly parallel effects are found. For nonhydrogen bonding solvents the regression equation is

$$\nu(3)_{\max} = 0.901 \nu(4)_{\max} + 4.16 \text{ kK} \quad (45)$$

$$n = 6, r = 0.997, \sigma = 0.06 \text{ kK}$$

As before, displacements of the points representing the HBA and amphiprotic solvents are in the direction that indicates that hydrogen bonding produces an enhanced bathochromic effect for the HBD relative to the nonprotic solute. Also as before, magnitudes of the vertical displacements from the re-

* In this system of nomenclature, which makes descriptions of the phenomenology much less confusing and cumbersome when several types of hydrogen bonding with concomitant spectral effects occur simultaneously, the $\Delta\Delta$ term denotes an enhanced or reduced effect due to hydrogen bonding; the negative sign indicates a bathochromic shift; the (1-2) term indicates that the effect is for indicator 1 relative to indicator 2; the superscript *B* indicates that the effect is due to type B hydrogen bonding; and the subscript $\leftarrow H_2N$ indicates that the bonding is by the amine protons of the indicator.

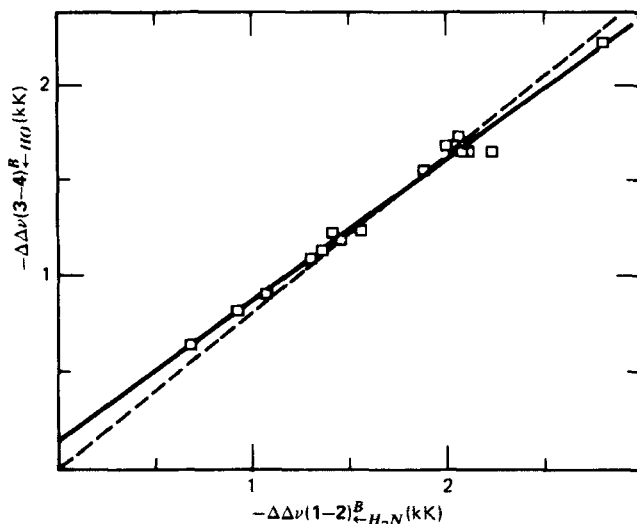


Figure 16 Enhanced bathochromic shifts for 4-nitroaniline (1) in HBA solvents plotted against enhanced bathochromic shifts for 4-nitrophenol (3).

gression line, represented by the $-\Delta\Delta\nu(3-4)_{\leftarrow HO}^B$ values in Table 21 increase with increasing HBA ability of the solvents.

That both sets of results are highly self-consistent is shown by their excellent correlation (Fig. 16):

$$-\Delta\Delta\nu(3-4)_{\leftarrow HO}^B = 0.740[-\Delta\Delta\nu(1-2)_{\leftarrow H_2N}^B] + 0.14 \text{ kK} \quad (46)$$

$$n = 15, f = 0.993, \sigma = 0.14 \text{ kK}$$

The relatively small intercept in Equation 46 (0.14 kK compared with $\sigma = 0.16$ for antecedent Equation 43) supports the concept that the quantities being compared are directly proportional to one another. *This behavior is required if both sets of $-\Delta\Delta\nu$ values are to be considered as proportional to the same intrinsic properties of the solvents.* Imposing direct proportionality in a regression line force fitted through the origin (the dashed line in Fig. 16) gives

$$-\Delta\Delta\nu(3-4)_{\leftarrow HO}^B = 0.825[-\Delta\Delta\nu(1-2)_{\leftarrow H_2N}^B] \pm 0.05 \text{ kK} \quad (47)$$

At the time of the development of the β scale (1974–1975), it was important to secure *independent evidence* showing that the magnitudes of the enhanced bathochromic shifts resulting from hydrogen bonding by HBD indicators to HBA solvents depend on some intrinsic measure of the ability of these solvents to act as hydrogen bond bases. Such evidence was available in some earlier findings by Gurka and Taft (73).

Using 0.01 *M* *p*-fluoroanisole as an internal reference standard in CCl₄, these workers had quantitatively evaluated the shielding effects of hydrogen bonded complex formation by 0.01 *M* *p*-fluorophenol (**5**). They determined formation constants K_f , and limiting ¹⁹F nmr shifts Δ , for the 1:1 hydrogen bonded complexes of **5** with a large number of bases of widely differing structures in CCl₄ at 25°C. Logarithms of the formation constants served as the basis for a pK_{HB} scale of HBA (hydrogen bond acceptor) basicity (74).

Both $-\Delta\Delta\nu(1-2)$ and $-\Delta\Delta\nu(3-4)$ were shown to be linearly related to pK_{HB} , the corresponding equations being,

$$pK_{HB} = 1.591[-\Delta\Delta\nu(1-2)_{-H_2N}^B] - 1.00 \quad (48)$$

$$n = 24, r = 0.979, \sigma = 0.18$$

and

$$pK_{HB} = 2.179[-\Delta\Delta\nu(3-4)_{-HO}^B] - 1.32 \quad (49)$$

$$n = 15, r = 0.972, \sigma = 0.23$$

The quality of the linear relationships between the enhanced solvatochromic shifts and the limiting ¹⁹F nmr shifts is even better:

$$\Delta(\mathbf{5}) = 1.307[-\Delta\Delta\nu(1-2)_{-H_2N}^B] + 0.09 \text{ ppm} \quad (50)$$

$$n = 15, r = 0.989, \sigma = 0.09 \text{ ppm}$$

$$\Delta(\mathbf{5}) = 1.737[-\Delta\Delta\nu(3-4)_{-HO}^B] - 0.13 \text{ ppm} \quad (51)$$

$$n = 10, r = 0.989, \sigma = 0.11 \text{ ppm}$$

Considering the low values of the intercepts relative to the standard deviations of Equations 50 and 51, it again seemed legitimate to force fit the correlations through the origins. Hence, to reflect direct proportionality, the correlation equations become:

$$\Delta(\mathbf{5}) = 1.365[-\Delta\Delta\nu(1-2)_{-H_2N}^B] \pm 0.07 \text{ ppm} \quad (50')$$

and

$$\Delta(\mathbf{5}) = 1.642[-\Delta\Delta\nu(3-4)_{-HO}^B] \pm 0.06 \text{ ppm} \quad (51')$$

The precision of the solvatochromic method was further tested against the association constants K_f , between phenol (**5a**) and a variety of HBA bases in CCl₄ as determined by Gramstad and co-workers (75). As in the case of *p*-fluorophenol, a good linear relationship was found to exist between $\log K_f$ and the enhanced solvatochromic shifts:

$$\log K_f(\mathbf{5a}) = 1.54[-\Delta\Delta\nu(1-2)_{-H_2N}^B] - 1.05 \quad (52)$$

$$n = 18, r = 0.982, \sigma = 0.16.$$

These five sets of properties were then used for the determination of the initial set of β values, labeled β_{1-5} to denote that they derived from five averaged β_i values. The value of 2.80 kK for $-\Delta\Delta\nu(1-2)$ of hexamethylphosphoramide (solvent **26**) was taken as the single fixed reference point and the β_i value corresponding to this datum was set equal to unit by definition, i.e., $\beta_1(\mathbf{26}) = 1.00$. (In this term, the subscript indicates that the value of β_i is obtained from property 1 and **26** stands for the solvent number). Other $\beta_1(i)$ values were then calculated from the expression,

$$\beta_1(i) = \frac{-\Delta\Delta\nu(1-2)}{2.80} \quad (53)$$

Equation 53 was then combined with Equations 47, 48, 50', and 52 to obtain the equations for the other β_i s:

$$\beta_2(i) = \frac{-\Delta\Delta\nu(3-4)}{(2.80)(0.825)} \quad (54)$$

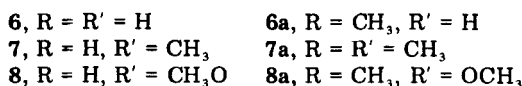
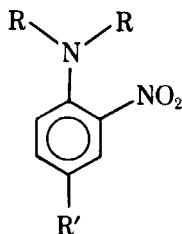
$$\beta_3(i) = \frac{(\text{p}K_{HB} + 1.00)}{(2.80)(1.571)} \quad (55)$$

$$\beta_4(i) = \frac{\Delta(\mathbf{5})}{(2.80)(1.365)} \quad (56)$$

$$\beta_5(i) = \frac{[\log K_f(\mathbf{5a}) + 1.05]}{(2.80)(1.54)} \quad (57)$$

Values of β_1 to β_5 calculated from the above equations are assembled in Table 22.

The β scale has been amended and expanded through three subsequent studies. In the first of these (76), the solvatochromic comparison method was applied to three HBD indicators, 2-nitroaniline (**6**), 2-nitro-*p*-toluidine (**7**), and 2-nitro-*p*-anisidine (**8**), and their corresponding N,N-dimethyl derivatives (**6a**, **7a**, **8a**).



It was shown that ν_{\max} values for these three systems satisfy the standard re-

quirements of the solvatochromic comparison method, and most particularly that the correlations between the $\Delta\Delta\nu$ terms and the β_{1-5} values are highly satisfactory:

$$-\Delta\Delta\nu(\mathbf{6-6a})_{\leftarrow H_2N}^B = 1.107 \beta_{1-5} - 0.025 \text{ kK} \quad (58)$$

$$n = 16, r = 0.959, \sigma = 0.065 \text{ kK}$$

$$-\Delta\Delta\nu(\mathbf{7-7a})_{\leftarrow H_2N}^B = 1.025 \beta_{1-5} - 0.06 \text{ kK} \quad (59)$$

$$n = 16, r = 0.963, \sigma = 0.063 \text{ kK}$$

$$-\Delta\Delta\nu(\mathbf{8-8a})_{\leftarrow H_2N}^B = 0.812 \beta_{1-5} + 0.11 \text{ kK} \quad (60)$$

$$n = 16, r = 0.959, \sigma = 0.05 \text{ kK}$$

It is seen that in these three cases also, the regression lines are sufficiently close to the origin to lend confidence that the experimental results reflect direct proportionality. β_6 to β_8 values were obtained by inverting Equations 58–60, and are included in Table 22.

$$\beta_6(\mathbf{i}) = \frac{[-\Delta\Delta\nu(\mathbf{6-6a}) + 0.025]}{1.107} \quad (58')$$

$$\beta_7(\mathbf{i}) = \frac{[-\Delta\Delta\nu(\mathbf{7-7a}) + 0.06]}{1.025} \quad (59')$$

$$\beta_8(\mathbf{i}) = \frac{[-\Delta\Delta\nu(\mathbf{8-8a}) - 0.11]}{0.812} \quad (60')$$

Although the basic principles remained the same, the next study (133) used a somewhat modified version of the solvatochromic comparison method. This was because the development of the polarity scale allowed the use of π^* values as reference measures of solvent polarity, rather than ν_{\max} for a related non-hydrogen-bonding indicator as in the previous examples. Thus, since where HBD solvents are excluded, total solvatochromic equations for $p \rightarrow \pi^*$ and $\pi \rightarrow \pi^*$ electronic spectral transitions take the form,

$$\nu(\mathbf{i})_{\max} = \nu(\mathbf{i})_0 + s\pi^* + b\beta \quad (42')$$

regression equations between $\nu(\mathbf{i})_{\max}$ and π^* of non-hydrogen-bonding solvents were determined in the first step, after which $-\Delta\Delta\nu(\mathbf{i-\pi^*})_{\leftarrow H_2N}^B$ results for HBA solvents were correlated with corresponding values of β_{1-8} .

The indicators whose solvatochromic behavior was analyzed in terms of Equation 42' were ethyl 4-aminobenzoate (**9**), 4-aminobenzophenone (**10**), 3,5-dinitroaniline (**11**), 3-nitroaniline (**12**), and N-ethyl-3-nitroaniline (**13**). Because, with amphiprotic HBA–HBD solvents, these indicators form type-AB

TABLE 22
 β_i Values Determined by the Solvatochromic Comparison Method

Solvent	β_1	β_2	β_3	β_4	β_5	β_6	β_7	β_8	β_9	β_{10}	β_{11}	β_{12}	β_{13}
3. Et ₃ N	.70	—	.66	.70	—	—	—	—	—	—	—	.72	.75
5. <i>n</i> -Bu ₂ O	.50	.53	.46	—	.47	—	—	—	—	.38	.53	.42	.33
7. Et ₂ O	.51	.52	.46	.48	.47	—	—	—	.44	.48	.49	.48	.41
8. Toluene	—	—	—	—	—	—	—	—	—	.08	.16	.14	.07
9. Dioxane	.38	.39	.39	.38	—	.41	.36	.34	.36	.40	.41	.36	.34
11. CH ₃ COOEt	.48	.49	.48	.48	.47	.46	.49	.44	.40	.43	.42	.44	.39
13. (CH ₂) ₄ O	.55	.52	.51	.52	.50	.62	.63	.59	.56	.54	.55	.55	.53
14. Benzene	—	—	—	—	—	—	—	—	—	.09	.13	.09	.10
15. C ₆ H ₅ Cl	—	—	—	—	—	—	—	—	—	.02	.10	.04	.11
16. CH ₃ COC ₂ H ₅	.51	—	.50	.53	.48	—	—	—	—	—	.50	.41	.48
17. C ₆ H ₅ OCH ₃	.24	.27	.23	—	.24	—	—	—	—	.19	.23	.21	.20
18. CH ₃ COCH ₃	.51	—	.50	—	.50	—	—	—	—	—	.48	.47	.47
19. (EtO) ₃ PO	.79	.72	.84	—	.83	.70	.71	.80	.75	.74	.75	.81	.84
23. CH ₃ CON(CH ₃) ₂	.73	.75	.77	.75	.75	—	—	—	.72	.77	.74	.79	.77
24. Pyridine	.67	.67	.66	.65	—	—	—	—	—	.66	.60	.61	.69
25. DMF	.71	.73	.70	.71	—	.63	.66	—	.69	.69	.65	.71	.72
26. [(CH ₃) ₂ N] ₃ PO	1.00	.97	1.04	.97	.98	—	—	—	1.06	1.13	1.04	1.19	1.14
27. Butyrolactone	.46	.47	.53	—	.53	—	—	—	.47	.46	.52	.47	.50
28. N-MePyrrolidone	.75	.71	.77	.79	.76	.73	.72	.70	.82	.81	.76	.85	.87
29. DMSO	.74	.72	.80	.79	.79	.74	.77	.71	.77	.79	.71	.81	.79

TABLE 23
Total Solvatochromic Equations in Non-HBD Solvents. Spectral Data in kK

$$\nu(i)_{\max} = \nu_0 + s\pi^* + b\beta$$

A: Stepwise, by successive single parameter correlations.

B: By multiple linear regression analysis.

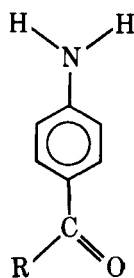
Equation	i	s	b	ν_0	r^a	SD ^a	n
A-1	9	-1.258	-2.951	36.86	0.996 ^b	0.11	21
B-1		-1.297	-3.005	36.89	0.996	0.12	
A-2	10	-1.664	-2.139	33.07	0.995 ^b	0.10	28
B-2		-1.738	-2.207	33.14	0.995	0.11	
A-3	11	-1.420	-2.800	27.60	0.995 ^b	0.10	32
B-3		-1.357	-2.815	27.57	0.996	0.10	
A-4	12	-1.652	-2.642	28.86	0.991 ^b	0.14	33
B-4		-1.741	-2.700	28.96	0.991	0.15	
A-5	13	-1.986	-1.408	27.08	0.995 ^b	0.08	32
B-5		-2.031	-1.494	27.14	0.995	0.09	

^a Values of r and SD determined by least-squares correlation of $\nu(i)_{\text{calc}}$ with $\nu(i)_{\text{obs}}$.

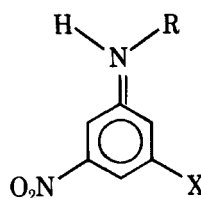
^b Correlation coefficients in the single parameter least squares fits were: A-1, 0.989, 0.986; A-2, 0.983, 0.983; A-3, 0.985, 0.985; A-4, 0.990, 0.974; A-5, 0.993, 0.978.

hydrogen bonds rather than pure type-B hydrogen bonds at the amine sites,* these correlations were limited to non-HBD solvents, including, however, CHCl_3 (solvent **30**) and CH_3CN (**50**), weak HBD solvents that seem to behave as non-HBD solvents to these weak HBA indicators.

Similar sequential operations are involved for indicators **9–13**. The pro-



9, R = $\text{C}_2\text{H}_5\text{O}$
10, R = C_6H_5



11, X = NO_2 , R = H
12, X = R = H
13, X = H, R = C_2H_5

* In type-A hydrogen bonding the solute acts as HBA base and the solvent as HBD acid. The converse applies in type-B bonding. In type-AB hydrogen bonding, the solute acts simultaneously as HBD acid and HBA base *at the same site*, associating with at least two molecules of amphiprotic HBA-HBD solvent in a probably cyclic complex. We have thus far observed type-AB bonding only with sp^3 -hybridized aromatic amine indicators.

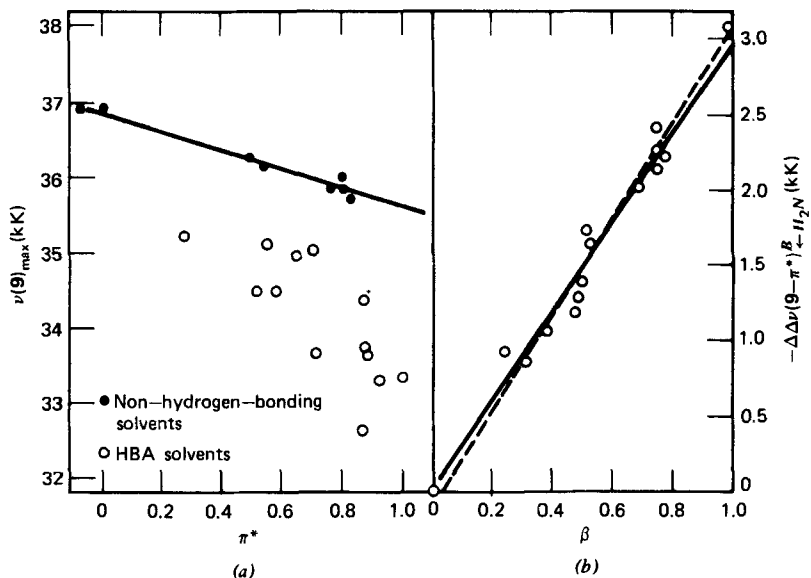


Figure 17 Solvatochromic comparison plots for ethyl 4-aminobenzoate. Sequential method. (a) $\nu(9)_{\max}$ vs. π^* . (b) $-\Delta\Delta\nu(9-\pi^*)_{\leftarrow H_2N}$ vs. β .

cedure is therefore illustrated in detail for **9** and summarized for **10–13** in the form of total solvatochromic equations in Table 23. As the first step, the correlation equation in nonhydrogen bonding solvents represented by the regression line in Fig. 17a is determined to be

$$\nu(9)_{\max} = -1.252 \pi^* + 36.86 \text{ kK} \quad (61)$$

$$n = 8, r = 0.989, \sigma = 0.075 \text{ kK}$$

Next, the enhanced bathochromic shifts attributable to type-B hydrogen bonding by **9** to HBA solvents (and corresponding to vertical displacements of the HBA solvent data points from the regression line in Fig. 17a) are calculated from

$$-\Delta\Delta\nu(9-\pi^*) = \nu(9)_{\text{Eq. 61}}^{\text{calcd}} - \nu(9)_{\max}^{\text{obs}} \quad (62)$$

When the enhanced solvatochromic shifts are next compared with solvent β_{1-8} values, it is seen that the relationship is linear and very nearly directly proportional (the broken line in Fig. 17b). The least squares regression equation for 14 data points (13 HBA solvents and one zero/zero point representing all non-HBA solvents) is

$$-\Delta\Delta\nu(9-\pi^*)_{\leftarrow H_2N}^B = 3.167 \beta_{1-8} - 0.12 \text{ kK} \quad (63)$$

$$r = 0.986, \sigma = 0.10 \text{ kK}$$

Force fitted through the origin to reflect the necessary direct proportionality (the solid line in Fig. 17*b*), this becomes

$$-\Delta\Delta\nu(\mathbf{9}-\pi^*)_{-H_2N}^B = 2.951 \beta_{1-8} \pm 0.13 \text{ kK} \quad (64)$$

$\beta_9(\mathbf{i})$ values, calculated by inverting Equation 64 that is,

$$\beta_9(\mathbf{i}) = \frac{-\Delta\Delta\nu(\mathbf{9}-\pi^*)}{2.951} \quad (65)$$

are included in Table 22, as are $\beta_{10}(\mathbf{i})$ to $\beta_{13}(\mathbf{i})$ values arrived at by carrying out the same sequence of steps with indicators **10–13**.

These results have been averaged with the β_1 to β_8 values determined earlier to arrive at a set of β_{1-13} parameters which we now consider satisfactory and do not propose to revise further unless warranted by the weight of further evidence. These are included in the comprehensive table of solvatochromic parameters (Table 35) at the end of this chapter.

Total Solvatochromic Equations. The slope and intercept in Equation 61 correspond to the *s* and ν_0 terms in Equation 42' and the proportionality constant in Equation 64 corresponds to the *b* coefficient. Combining the appropriate terms from Equations 61 and 64, we therefore obtain the stepwise total solvatochromic equation for indicator **9**,

$$\nu(\mathbf{9})_{\max} = 36.86 - 1.252 \pi^* - 2.951 \beta \text{ kK} \quad (66)$$

$$n = 21, r = 0.996, \sigma = 0.11 \text{ kK}$$

An alternative route to the total solvatochromic equation is by the method of multiple linear regression analysis (multiple parameter least squares correlation), which has become quite convenient with the recent availability of inexpensive programmable computers. In this one-step procedure, correlation of $\nu(\mathbf{9})_{\max}$ results with solvent π^* and β values leads directly to the equation,

$$\nu(\mathbf{9})_{\max} = 36.89 - 1.297 \pi^* - 3.005 \beta \text{ kK} \quad (66')$$

$$n = 21, r = 0.995, \sigma = 0.12 \text{ kK}$$

Observed values of $\nu(\mathbf{9})_{\max}$ are compared with values calculated through Equation 66' in Fig. 18. Considering that thirteen solvent π^* values which served as input to Equation 66' did not contribute to the determination of *s* in Equation 66, the fact that the agreement between the two equations is well within the precision of the individual spectral determinations must be regarded as highly satisfactory.

Agreement between the two methods is equally good for the other four indicators. Values of ν_0 , *s*, and *b* determined by the two versions of the solvatochromic comparison method are compared for **10–13** in Table 23.

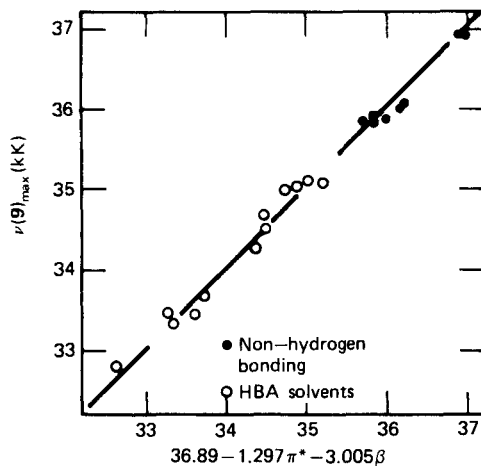


Figure 18 Solvatochromic comparison plot for ethyl-4-aminobenzoate. Multiple linear regression method.

The close correspondance between the two methods is quite important to us because in other studies we have sometimes had insufficient data in non-hydrogen-bonding solvents to determine solvatochromic equations by the stepwise method, so that it was necessary to use the method of multiple linear regression analysis. Since Equation 42' involves three adjustable parameters, the latter correlations were statistically less rigorous. We therefore emphasize the excellent agreement between the two methods (Table 23), since we believe that it is difficult to find statistical fault with the stepwise method, which involves successive single-parameter correlations and wherein the goodness of the fit is confirmed at every stage.

Structure-Property Relationships. The studies aimed at construction of the β scale and related investigations have uncovered some interesting relationships between indicator structures and solvatochromic effects. It was found (78c, 134) for example, that 4-nitroaniline (**1**) forms two hydrogen bonds to HBA solvents, that the ratio of the hydrogen bond strengths is about 1.5/1, and that the ratio of the bathochromic spectral effects is $1/(0.93 \pm 0.13)$. Comparable effects have also been observed with 3-nitroaniline (**12**).

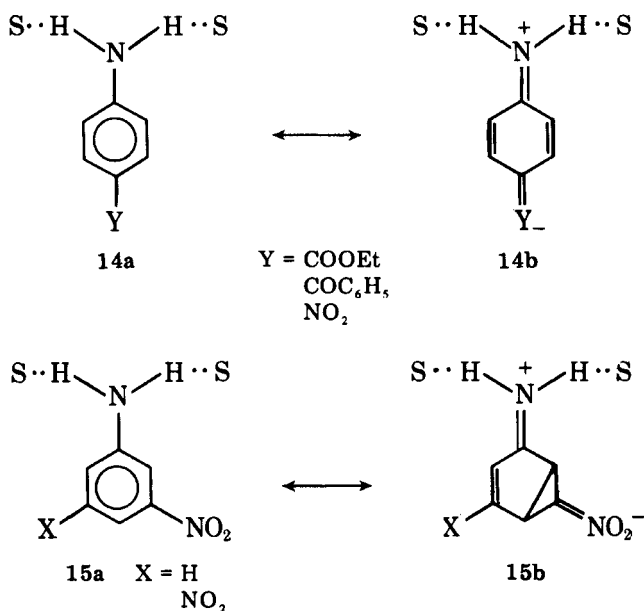
In a related unpublished study it was found that HBD acid strengths of the aromatic amine indicators are in the order: 3,5-dinitroaniline (**11**) > 4-nitroaniline (**1**) \sim N-ethyl-4-nitroaniline (**1a**) > 3-nitroaniline (**12**) \sim N-ethyl-3-nitroaniline (**13**) > 4-aminobenzophenone (**10**). This ordering reflects the $\Sigma\sigma_s$ of the aniline substituents.

It was of particular interest that the ordering of the $-b$ values in the solvatochromic equations (i.e., the spectral sensitivities to solvent HBA basicities)

did not follow the above progression of indicator HBD acidities, but rather followed the order: ethyl 4-aminobenzoate (**9**), $\mathbf{b} = -3.01 >$ 3,5-dinitroaniline (**11**), $\mathbf{b} = -2.80 >$ 4-nitroaniline (**1**), $\mathbf{b} = -2.79 >$ 3-nitroaniline (**12**), $\mathbf{b} = -2.64 >$ 4-aminobenzophenone (**10**), $\mathbf{b} = -2.14 >$ N-ethyl-3-nitroaniline (**13**), $\mathbf{b} = -1.41 >$ N-ethyl-4-nitroaniline, $\mathbf{b} = -1.14$.

By comparing the solvatochromic shifts attributable to hydrogen bonding with spectral displacements caused by N-alkylation and N,N-dialkylation, it was concluded (133) that six interacting effects contribute to the solvatochromic coefficient \mathbf{b} for an aromatic amine indicator: (a) the number of type-B hydrogen bonds formed by the indicator to HBA solvents; (b) the strengths of these bonds as influenced by indicator HBD acidity; (c) the increase in ground-state electron density on amine nitrogen caused by the type-B hydrogen bonding; (d) the effect of this increased ground state electron density on the electronic transition energy; (e) the amount of rehybridization on amine nitrogen (from nearer sp^3 to nearer sp^2) caused by type-B hydrogen bonding; and (f) the effect of rehybridization on transition energy. That the spectrum of the weakest HBD acid, **9**, showed the greatest susceptibility to solvent HBA basicity was attributed to the fact that significant rehybridization effects contribute to the bathochromic shifts, whereas with **1** and **11** rehybridization effects are negligible.

As concerns the *signs* of the \mathbf{s} and \mathbf{b} terms in the solvatochromic equations for the aromatic amine indicators, these are readily rationalized in terms of canonical structures **14** and **15** and electronic transitions from ground states



more closely resembling **14a** and **15a** to excited states more closely resembling **14b** and **15b**.*

Charge generation in the electronic excitation leads to lowered transition energies in more polar solvents (minus *s*); hydrogen bond strengthening leads to lower transition energies in stronger HBA solvents (minus *b*).

Correlations with Infrared $\Delta\nu$ Results. A number of workers have suggested that infrared $\Delta\nu$ values (free minus hydrogen bonded) of X-H stretching vibrations of protic indicators complexed with hydrogen bond acceptors might serve as reasonably sensitive measures of HBA basicity. Most recently, Koppel and Paju (131*b*) have proposed a general nucleophilicity (hydrogen bond basicity) scale, labeled *B*, based on solvent shifts of the ir stretching frequencies of the free and hydrogen bonded OH group of phenol in CCl₄ media,

$$B = \Delta\nu_{PhOH}^{CCl_4} = \nu_{PhOH}^{CCl_4} - \nu_{PhOH \cdots B}^{CCl_4} \text{ (cm}^{-1}\text{)} \quad (67)$$

Excellent linear correlations were reported between *B* and fourteen other sets of $\Delta\nu_{HX}$ (HX = *t*-BuOH, MeOH, 4-fluorophenol, pyrrole, HCl, PhC≡CH, HNCO, etc.).

If relative HBA basicities of electron donor solvents were correctly represented by the Koppel-Paju *B* scale on the one hand, and the present β scale on the other, it would logically follow that solvent *B* and β values must be proportional to one another. Unfortunately, however, no such direct correlation is observed. Indeed, the nonproportionality between the *B* and β indexes is so marked and so readily evident as to indicate that one or the other of these measures of hydrogen bond basicity must be incorrect in concept, as must be, to a greater or lesser extent, the many linear free energy relationships based thereon in the recent chemical literature.

Thus, following Gramstad and co-workers (136-138) whose cogent observations in this regard have been largely ignored by later workers, we have found the relationship between *B* and β to be as shown in Fig. 19 (139). It is seen that *B* values exhibit good linear regression with corresponding β values (but not passing through the origin) if the comparisons are restricted to families of solvents with similar hydrogen bond acceptor sites, that is, single-bonded oxygen bases, double-bonded oxygen bases, pyridine bases, and single-bonded nitrogen bases. It is also seen, however, that the correlation would be significantly poorer, indeed virtually a scatter plot, if HBA bases from the different families should be considered together. Correlation equations for the separate families are as follows:

Double-bonded oxygen bases:

* Structure **15b** is a "bond pusher's" way of accommodating to Murrell's suggestion that absorption bands near 400 nm for *o*-, *m*-, and *p*-nitroaniline derive from similarly founded electronic transitions (135).

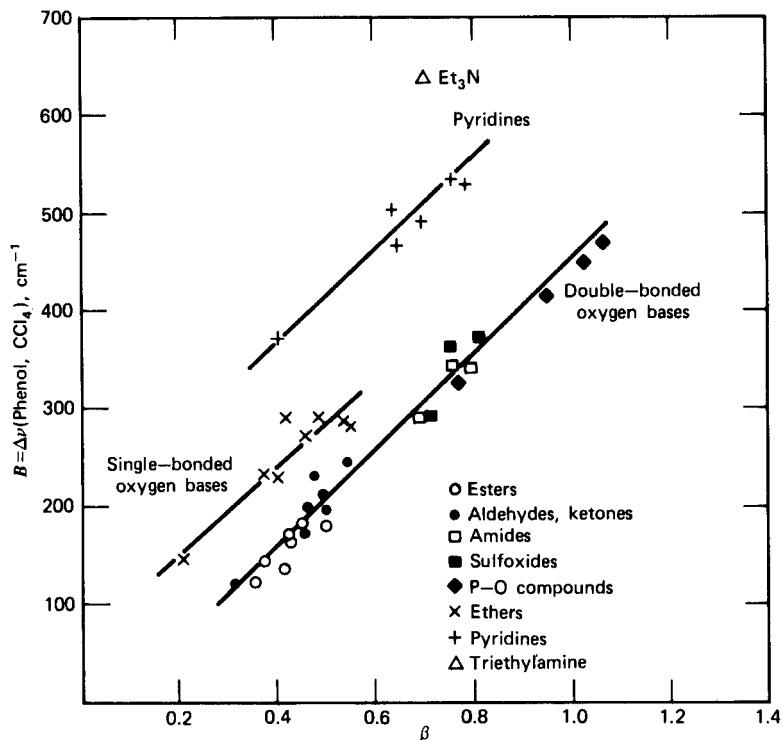


Figure 19 The relationship between B (Eq. 67) and β .

$$\Delta\nu = -37.1 + 487 \beta \text{ cm}^{-1} \quad (68a)$$

$$n = 23, r = 0.991, \sigma = 13.8 \text{ cm}^{-1}$$

Single-bonded oxygen bases:

$$\Delta\nu = 67.1 + 436 \beta \text{ cm}^{-1} \quad (68b)$$

$$n = 8, r = 0.991, \sigma = 18.5 \text{ cm}^{-1}$$

Pyridine bases:

$$\Delta\nu = 180.2 + 473 \beta \text{ cm}^{-1} \quad (68c)$$

$$n = 6, r = 0.974, \sigma = 14.8 \text{ cm}^{-1}$$

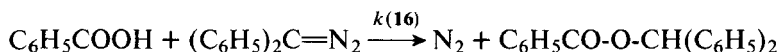
We have found similar separations into families and similarly good correlations within families in comparisons of β with other $\Delta\nu_{HX}$ stretching frequencies, including 4-fluorophenol in CCl_4 , methanol in CCl_4 , and methan[^2H]ol in the pure base media. These relationships *within families* appeared to us to be sufficiently precise to warrant using the wealth of available experi-

mental information to back-calculate otherwise not readily accessible β_i values. The comprehensive table of solvatochromic parameter (Table 35) therefore contains about thirty β values (mainly for solutes), arrived at by averaging β_i s from Equations 55 and 56 with values back-calculated from Equations 68a-c and corresponding equations for 4-fluorophenol, methanol, and methan[²H]ol.

As concerns the separation into families illustrated by Fig. 20, we consider that it derives from two effects: (a) differing geometrical relationships between the axis of vibration of the X—H bond of the HBA acid and the direction of the dominant dipole of the HBA base, (e.g., 60° for dialkyl ketones, 0° for pyridines and tertiary amines) affecting the energetics of the vibrations, and (b) differing hybridization on the acceptor atoms affecting the mobility of the hydrogen bonding electron pair. Taking these effects into account, we have suggested that it is reasonable that $\Delta\nu$ should be linear with HBA strength where the geometries of the hydrogen bonds and hybridization on the acceptor atoms are similar. We see no reason, however, to expect that such relationships should apply with differing geometries or hybridizations (139).

Correlations with Reactivity Results. In addition to the correlations described previously, we have used the β scale, alone or in combination with the π^* scale (in which case all correlations have been by the method of multiple linear regression analysis) to rationalize solvent effects on many additional types of properties and reactivity parameters. Representative examples are as follows.

Chapman and co-workers (140) have studied the kinetics of the reaction of benzoic acid with diphenyldiazomethane (**16**) at 37°C in a large number of solvents, and have reported that the reaction rate is influenced by both HBA and HBD properties of the solvents.



In HBD solvents the multiple hydrogen bonding effects and competing solvent self association effects (*vide infra*) are too complex to unravel but, if consideration is limited to aliphatic nonprotic solvents of the "select solvent set" discussed earlier (**4,5,11,16,18,23,25,29,41,50,51,52**) (see Section I), the logarithm of the rate constant is well correlated by a linear combination of π^* and β ,

$$\log k(16) = 0.130 + 3.06 \pi^* - 5.63 \beta \quad (68d)$$

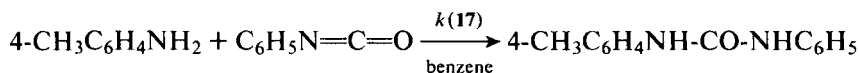
$$r = 0.989$$

If the result in dioxane (specifically excluded previously since it is not a select solvent) is included, the correlation breaks down completely, $r = 0.864$.

This reaction is one of relatively few that we have encountered in which **s** and **b** in Equation 42 are of comparable magnitudes and opposite signs. The

effect of increasing solvent polarity appears here to be rate accelerating (as is the case with most reactions which we have examined), whereas type-B hydrogen bonding by benzoic acid to HBA solvents tends to retard the rate.

Grekov and Otroshko (141) have reported that the reaction rate of *p*-toluidine with phenyl isocyanate (17) in benzene at 25°C is strongly accelerated by HBA catalysts.



We have found that these workers' "catalytic second order rate constants" correlate well with β values of the catalysts (solvents 7,11,14,23,25,26,29,31 in catalytic amounts in benzene).

$$\log k(17) = -3.61 + 3.64 \beta \quad (69)$$

$$r = 0.990, \sigma = 0.13$$

If the preceding HBA bases are used as solvents for the reaction rather than as catalysts in benzene solvent, the rate shows also a relatively small negative dependence on solvent polarity,

$$\log k(17) = -2.38 - 0.52 \pi^* + 2.43 \beta \quad (70)$$

$$r = 0.977, \sigma = 0.15$$

Evidently type-B hydrogen bonding by the amine protons to HBA bases increases the nucleophilicity of the *p*-toluidine, and hence the reactivity with the phenyl isocyanate.

Correlations with NMR Spectral Data. Together with the limiting ^{19}F nmr shifts of 4-fluorophenol with HBA bases in CCl_4 , used in the initial construction of the β scale, solvent effects on many other types of nmr spectral properties are well correlated by β . As an example, pmr shifts of fluorodinitromethane (18) at 18°C, as reported by Okhlobystina and co-workers (142) in 12 solvents for which β values are known (2,6,7,13,18,25,26,28,50,61,75) follow the relationship,

$$\Delta\delta_\infty(18) = 0.14 + 2.32 \beta \text{ ppm} \quad (71)$$

$$r = 0.968, \sigma = 0.18 \text{ ppm}$$

the $\Delta\delta$ value being relative to the result in cyclohexane. Correlation is improved slightly when a dependence on π^* is also allowed in a multiple parameter least squares correlation,

$$\Delta\delta_\infty(18) = 0.13 + 0.20 \pi^* + 2.15 \beta \text{ ppm} \quad (72)$$

$$r = 0.979$$

but the low s/b ratio indicates that the hydrogen bonding effect is by far the dominant (if not the only) influence.

A similar pattern is seen in solvent effects on pmr shifts of chloroform (**19a**) as reported by Lichter and Roberts (143). The shifts in nine solvents for which β values are known (2,3,6,7,18,24,25,26,50) follow the regression equation,

$$\Delta\delta(\mathbf{19a}) = -0.04 + 1.76 \beta \text{ ppm} \quad (73)$$

$$r = 0.971, \sigma = 0.16 \text{ ppm}$$

As before, allowing a partial dependence on π^* in a multiple linear regression analysis improves the correlation only slightly,

$$\Delta\delta(\mathbf{19a}) = -0.10 + 0.28 \pi^* + 1.59 \beta \text{ ppm} \quad (74)$$

$$r = 0.979$$

The situation is somewhat different with the ^{13}C nmr spectrum of chloroform (**19b**) as also reported by Lichter and Roberts (143). Here the correlation (in the same solvents as above +14) is improved significantly in the multiple parameter least squares treatment, i.e., single parameter,

$$\Delta\delta(\mathbf{19b}) = 0.06 + 3.56 \beta \text{ ppm} \quad (75)$$

$$r = 0.960, \sigma = 0.39 \text{ ppm}$$

compared with multiple parameter,

$$\Delta\delta(\mathbf{19b}) = -0.26 + 1.05 \pi^* + 3.02 \beta \text{ ppm} \quad (76)$$

$$r = 0.984$$

It seems quite reasonable that the ratio of the hydrogen bonding to the polarity coefficients (b/s) in the solvatochromic equations should be higher for the pmr shift of the hydrogen bonded proton than for the ^{13}C nmr shift, involving an atom once removed from the hydrogen bonding site.

Another carbon acid for which solvent effects on the pmr spectrum are well correlated by β , is 2-methylbut-1-en-3-yne (**20**), $\text{CH}_2=\text{C}(\text{CH}_3)-\text{C}\equiv\text{CH}$. The correlation equation for results reported by Lapuka and co-workers (144) in 9 solvents (6,16,23,24,25,26,28,29,50) is

$$\delta_c(\mathbf{20}) = 2.635 + 1.972 \beta \text{ ppm} \quad (77)$$

$$r = 0.993, \sigma = 0.08 \text{ ppm}$$

In this case, multiple parameter least squares correlation with β and π^* gives no improvement in the goodness of the fit ($r = 0.993$).

In a similar vein, the correlation of Vasyanina and co-workers' results (145) on pmr spectra of *t*-butanol (**21**) (relative to internal TMS) in eight solvents

(18,23,25,26,28,29,61,75) with solvent β values leads to

$$\delta_{\infty}(21) = 1.534 + 3.47 \beta \text{ ppm} \quad (78a)$$

$$r = 0.987, \sigma = 0.12 \text{ ppm}$$

Here, however, there is significant improvement in the goodness of the fit when we also allow a partial dependence on π^* (same solvents, except 75, for which π^* is not known),

$$\delta_{\infty}(21) = 1.173 + 0.74 \pi^* + 3.14 \beta \text{ ppm} \quad (78b)$$

$$r = 0.996$$

Finally, as an example involving an N-H acid, limiting ^{19}F nmr shifts, Δ , of 5-fluoroindole (22) with HBA bases in CCl_4 (relative to N-methyl-5-fluoroindole internal standard), as reported by Mitsky, Joris, and Taft (146), are also nicely linear with β . The regression equation for 14 bases (3,13,23,24,25,26,29,41,48,70,72,75,83,84, plus one zero-zero point for neat CCl_4) is

$$\Delta(22) = 0.07 + 2.06 \beta \text{ ppm} \quad (79)$$

$$r = 0.992, \sigma = 0.06 \text{ ppm}$$

It is of interest to compare the **b** value for $\Delta(22)$ with the **b** value of 3.8 for limiting ^{19}F nmr shifts of 4-fluorophenol (Equation 56). The difference must be due, at least in part, to the differing HBD strengths of the indicators.

Heats of Transfer between Solvents. Kurkchi and Iogan (147) have used gas-liquid chromatography to determine specific retention volumes of acetylene (23), propyne (24), and 1-butyne (25) in eight solvents (isooctane, 9,18,25,26,28,41,52) at a number of temperatures, and thence have derived heats of solution, ΔH_V , and of transfer between solvents, ΔH_{ij} . The later quantities (transfer from isooctane to HBA solvents) are well correlated by β and π^* :

$$\Delta H_{ij}(23) = 0.04 + 0.82 \pi^* + 1.76 \beta \text{ kcal mole}^{-1} \quad (80)$$

$$r = 0.996, (\mathbf{b}/\mathbf{s} = 2.14)$$

$$\Delta H_{ij}(24) = 0.06 + 1.30 \pi^* + 1.11 \beta \text{ kcal mole}^{-1} \quad (81)$$

$$r = 0.979, (\mathbf{b}/\mathbf{s} = 0.85)$$

$$\Delta H_{ij}(25) = 0.04 + 1.17 \pi^* + 0.83 \beta \text{ kcal mole}^{-1} \quad (82)$$

$$r = 0.974, (\mathbf{b}/\mathbf{s} = 0.70)$$

It is of interest that, as might be expected, the **b/s** ratios in the solvatochromic equations reflect smaller relative effects of solvent HBA basicity as the hydrocarbon moiety R in $\text{R}-\text{C}\equiv\text{CH}$ grows larger.

Gas-liquid partition coefficients, K , reported for acetylene in five solvents (9,18,25,26,28) by the same workers also show excellent correlation with β , with a minor (if any) dependence on π^* .

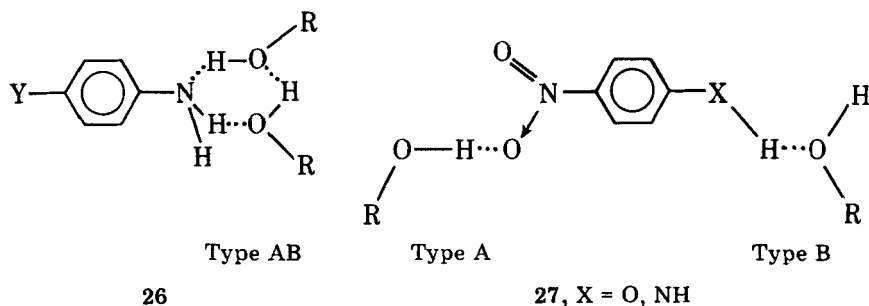
$$\log K = 0.85 + 0.088 \pi^* + 0.91 \beta \quad (83)$$

$$r = 1.000, \sigma = 0.004$$

β Values of Amphiprotic Solvents. Three important complications prevented us from using certain of the indicators discussed earlier to determine β_i values of the amphiprotic HBA-HBD solvents, and led to uncertainties in the β_i values determined with the other indicators.

(a) The HBA basicity of an amphiprotic solvent depends on the extent of its self-association, which is quite different in dilute solution in CCl_4 than in the bulk solvent. Since the β_3 - β_5 values for the HBA bases were based on ^{19}F nmr shifts and formation constants which were determined in dilute solutions in CCl_4 , Equations 55-57 were not appropriate for amphiprotic solvents.

(b) Indicators 9-13 form type-AB rather than type-B hydrogen bonds at the amine sites (26), so that, depending on the acidity and basicity of the amphiprotic solvent, the solvatochromic effect of the hydrogen bonding may be bathochromic or hypsochromic, that is, $\pm \Delta\Delta\nu(i-\pi^*)_{\rightleftharpoons \text{H}_2\text{N}}$.



(c) 4-Nitroaniline (1) and 4-nitrophenol (3) associate with amphiprotic solvents at multiple sites, the indicator protons forming type-B hydrogen bonds to the solvent and the solvent protons forming type-A hydrogen bonds to the nitro groups of the indicators (27). Effects of both type hydrogen bonds are to stabilize $[^+\text{Y}=\text{C}(1) \rightarrow \text{C}(4)=\text{NO}_2^-]$ electronic excited states, and are hence bathochromic.

In the determination of the initial β_1 and β_2 values, where ν_{max} of N,N-diethyl-4-nitroaniline (2) and 4-nitroanisole (4) were taken as reference measures of solvent polarity for 1 and 3, it was assumed that effects of hydrogen bonding to the nitro groups were similar for 1 and 2 and for 3 and 4; that is,

$$-\Delta\Delta\nu(\mathbf{1-2})_{\rightarrow O_2N}^A = 0 \quad (84)$$

$$-\Delta\Delta\nu(\mathbf{3-4})_{\rightarrow O_2N}^A = 0 \quad (85)$$

It can be seen in Table 22, however, that for weak HBA base-strong HBD acid solvents (**107,110,111**), the β_1 values determined from the **1-2** indicator pair differ significantly from the β_2 values determined from the **3-4** indicator pair. This could arise if the assumptions leading to Equations 84 or 85 or both were incorrect. Either or both of two possibilities might apply: The β_2 values may be too high because HBA-HBD solvents form a stronger hydrogen bond to the nitro of **3** than of **4**. Alternatively, the β_1 values may be too low because the type-A hydrogen bond to **2** is stronger than to **1**. Using our new notational system, these possibilities can be represented by,

$$-\Delta\Delta\nu(\mathbf{1-2})_{\text{total}} = [-\Delta\Delta\nu(\mathbf{1-2})_{\leftarrow H_2N}^B] - [-\Delta\Delta\nu(\mathbf{2-1})_{\rightarrow O_2N}^A] \quad (86)$$

and

$$-\Delta\Delta\nu(\mathbf{3-4})_{\text{total}} = [-\Delta\Delta\nu(\mathbf{3-4})_{\leftarrow HO}^B] + [-\Delta\Delta\nu(\mathbf{3-4})_{\rightarrow O_2N}^A] \quad (87)$$

We prefer the possibility wherein Equations 84 and 87 and the β_1 values are more nearly correct than Equations 85 and 86 and the β_2 results. Our reasoning is that a through-conjugated molecule like **1** or **3**, acting at one resonance terminus as an HBD acid, should be a stronger, not weaker, HBA base at its other resonance terminus than its O-alkyl or N,N-dialkyl derivative. Further, the β_6 - β_8 results determined by the solvatochromic comparisons of the *ortho*-nitroanilines, **6-8**, with their N,N-dialkyl derivatives, **6a-8a**, agree best with the β_1 results, and arguments have been presented that type-A hydrogen bonding effects to nitro are similar for the *o*-nitroanilines and their N-alkyl and N,N-dialkyl derivatives (76).

The question is far from closed, however, and we are particularly uncertain about the β values for the stronger HBD acid-weaker HBA base R-OH compounds (particularly water) in the comprehensive table of solvatochromic parameters. As concerns the stronger HBA base-weaker HBD acid alcohols, **101-105**, the differences between the β_1 and β_2 values in Table 22 are not so great, and we are reasonably comfortable with the average β values for these solvents.

2. The π^* Scale of Solvent Polarity

The *raison d'être* of a solvent polarity scale is the systematic correlation and analysis of chemical and physicochemical properties in solution. The standards and procedures used to establish the π^* scale (Table 35) have been dealt with in Section I, and more detailed considerations are to be found in the original papers (33*b*, 148).

A systematic scanning of experimental results from our own laboratories and a comprehensive search of the literature led the present authors to divide solvent polarity effects into three main groups: (a) “ π^* -type properties” for which correlations are good when all solvents are considered together, (b) the more general case of properties for which correlations with solvent π^* values are improved significantly when aliphatic, polychlorinated aliphatic, and aromatic solvents are treated separately, and (c) the special case of protic solvents.

Solvent Effects on “ π^* -Type Properties”. Where hydrogen bonding effects are excluded, solvent effects on “ π^* -type properties” are simply related to the π^* scale by equations of the form,

$$XYZ = XYZ_0 + s\pi^* \quad (88)$$

that is, Equation 42 with $a = b = 0$. Good examples (33b) are provided by the correlations of solvatochromic shifts of $p \rightarrow \pi^*$ and $\pi \rightarrow \pi^*$ electronic spectral transitions of 47 indicators in up to 60 solvents with the π^* parameters (Table 24).

The statistics of these correlations are informative. For example, of a total of 839 spectra, including 288 from the literature, only two literature results needed to be excluded as probably being too strongly influenced by impurities or spectral anomalies (See footnotes of Table 24). Of the 47 correlation coefficients, 19 were above 0.99; 21 between 0.98 and 0.99; 5 between 0.97 and 0.98; and 2 between 0.95 and 0.97. The correlation coefficients seemed to be more strongly influenced by variations in the s terms than by the standard deviations. The average standard deviation was 0.11 kK, which compares well with the 0.10 kK precision limit of the solvatochromic comparison method.

Structure-Property Relationships. In addition to the excellent statistics of the correlations in Table 24, the s and ν_0 terms in the solvatochromic equations reflect structure-property relationships that are consistent with both theory and experimental experience. Thus, the s terms show reasonable trends with systematic variations in indicator structure that lend confidence that this new parameter may serve as a convenient and meaningful indicator of the interaction of a chromophore with its cybotactic environment.*

Nature of Auxichrome. For example, it has long been known that spectral maxima for [$^+X=C(1) \rightarrow C(4)=Y^-$] electronic transitions are displaced to lower energies with increasing electron-donor ability of X and electron-acceptor ability of Y. As is shown in Table 25a for *para*-donor substituted nitrobenzene derivatives, such a progressive red shift in the ν_0 terms with increasing elec-

* The cybotactic region is the volume around a solute molecule in which the ordering of the solvent molecules has been influenced by the solute.

TABLE 24
Correlations of Electronic Spectral Data with the π^* Scale of Solvent Polarities: $\nu_{\max} = \nu_0 + \delta\pi^*$

No.	Spectrum	ν_0 , kK	$-\delta$	r	SD	n	Solvent types	Data ref.
1	4-Nitroanisole	34.17	2.410	0.994	0.079	27 ^a	NHB, HBA	b
1a.		34.12	2.343	0.994	0.071	51	NHB, HBA, HBA-D	b
2.	<i>N,N</i> -Diethyl-3-nitroaniline	25.52	2.212	0.991	0.088	28 ^a	NHB, HBA	c
2a.		25.52	2.214	0.992	0.076	60	NHB, HBA, HBA-D	c
3.	4-Methoxy- β -nitrostyrene	30.00	2.329	0.992	0.084	28 ^a	NHB, HBA	c
3a.		29.96	2.250	0.986	0.101	56	NHB, HBA, HBA-D	c
4.	1-Ethyl-4-nitrobenzene	37.60	2.133	0.994	0.066	18 ^a	NHB, HBA	c
4a.		37.67	2.259	0.990	0.090	32	NHB, HBA, HBA-D	c
5.	<i>N</i> -Methyl-2-nitro- <i>p</i> -toluidine	23.83	1.632	0.999	0.026	14 ^a	NHB, HBA	d
6.	<i>N,N</i> -Diethyl-4-nitroaniline	27.52	3.182	0.994	0.099	28 ^a	NHB, HBA	b
7.	<i>N,N</i> -Dimethyl-4-aminobenzophenone	30.41	2.013	0.986	0.101	27	NHB, HBA	c
8.	4,4'-Bis(dimethylamino)benzophenone	29.96	2.094	0.984	0.113	14	NHB, HBA	c
9.	Ethyl 4-dimethylaminobenzoate	33.31	1.407	0.979	0.082	30	NHB, HBA	c
10.	<i>N,N</i> ,3,5-Tetramethyl-4-nitroaniline	27.36	2.747	0.991	0.099	42	NHB, HBA	c
11.	<i>N,N</i> -Diethyl-3-methyl-4-nitroaniline	27.69	3.073	0.988	0.125	37	NHB, HBA	h
12.	4-Dimethylamino- β -nitrostyrene	25.25	3.354	0.990	0.131	16'	NHB, HBA	e
13.	<i>N,N</i> -Dimethyl-4-nitroaniline	28.10	3.436	0.988	0.150	33	NHB, HBA	g
14.	4-Nitroaniline	31.10	3.138	0.988	0.207	6	NHB	b
15.	3,5-Dimethyl-4-nitroaniline	28.68	1.813	0.988	0.104	11	NHB	c
16.	3-Methyl-4-nitroaniline	31.40	3.377	0.994	0.143	9	NHB	h
17a.	<i>N</i> -Methyl-4-nitroaniline	29.37	3.364	0.994	0.166	6	NHB	h
17b.	<i>N</i> -Ethyl-4-nitroaniline	29.17	3.327	0.995	0.148	6	NHB	h
17c.	<i>N</i> -Isopropyl-4-nitroaniline	28.96	3.237	0.995	0.138	6	NHB	h
18.	<i>N</i> -Ethyl-3-methyl-4-nitroaniline	29.35	3.341	0.994	0.131	10	NHB	h
19.	4-Dimethylaminobenzaldehyde	30.98	1.682	0.987	0.097	12	NHB, HBA	i
20.	Ethyl 4-aminobenzoate	36.85	1.261	0.989	0.074	8	NHB	c
21.	4-Aminobenzophenone	33.09	1.682	0.983	0.111	10	NHB	c
22.	<i>N,N</i> -Dimethyl-2-nitro- <i>p</i> -toluidine	24.81	2.070	0.993	0.081	15	NHB, HBA	d
23.	2-Nitro- <i>p</i> -toluidine	25.72	1.621	0.997	0.052	6	NHB	d
24.	Nile blue A oxazone	20.07	1.784	0.982	0.113	17	NHB, HBA	j

25.	Tolyldipropyl Nile blue base	20.19	1.508	0.992	0.072	11	NHB, HBA	<i>j</i>
26.	4-Nitro-4'-dimethylaminobiphenyl	26.63	2.860	0.987	0.166	10	NHB, HBA	<i>k</i>
27.	4-Nitro-4'-dimethylaminostilbene	24.31	2.131	0.988	0.121	10	NHB, HBA	<i>k</i>
28.	3-Nitroaniline	28.87	1.664	0.986	0.100	10	NHB	<i>c</i>
29.	<i>N</i> -Ethyl-3-nitroaniline	27.10	2.030	0.992	0.093	10	NHB	<i>c</i>
30.	3,5-Dinitroaniline	27.61	1.436	0.980	0.112	9	NHB	<i>c</i>
31.	<i>N,N</i> -Dimethyl-2-nitroaniline	25.30	2.023	0.988	0.097	16	NHB, HBA	<i>d</i>
32.	<i>N</i> -Methyl-2-nitroaniline	24.59	1.593	0.993	0.055	25	NHB, HBA, HBA-D	<i>n</i>
33.	2-Nitroaniline	26.55	1.536	0.992	0.079	6	NHB	<i>d</i>
34.	<i>N,N</i> -Dimethyl-2-nitro- <i>p</i> -anisidine	23.72	2.142	0.994	0.071	15	NHB, HBA	<i>d</i>
35.	2-Nitro- <i>p</i> -anisidine	24.33	1.596	0.988	0.094	6	NHB	<i>d</i>
36.	Brooker's mercocyanine	17.74	2.780	0.978	0.180	30 ^m	NHB, HBA	<i>l</i>
37.	Phenol blue	18.12	1.445	0.988	0.073	21	NHB, HBA	<i>o</i>
38.	Di(<i>tert</i> -butyl) phenol blue	18.54	1.281	0.954	0.126	11	NHB, HBA	<i>o</i>
39.	<i>p</i> -Nitrosodimethylaniline	25.39	1.852	0.976	0.120	13	NHB, HBA	<i>c</i>
40.	<i>N</i> -(4-Nitrophenyl)aziridine	32.11	2.510	0.980	0.124	15	NHB, HBA	<i>g</i>
41.	<i>N</i> -(4-Nitrophenyl)pyrrolidine	27.56	3.274	0.986	0.131	16	NHB, HBA	<i>g</i>
42.	<i>N</i> -(4-Nitrophenyl)piperidine	27.93	3.405	0.988	0.126	16	NHB, HBA	<i>g</i>
43.	2-(<i>p</i> -Dimethylaminophenylimino)-3-keto-2,3-dihydrothionaphthene	20.94	1.577	0.979	0.110	14	NHB, HBA	<i>p</i>
44.	2-(<i>p</i> -Dimethylaminobenzylidene)-3-keto-2,3-dihydrothionaphthene	21.59	1.198	0.964	0.116	14	NHB, HBA	<i>p</i>
45.	2-Nitroanisole	32.56	2.428	0.977	0.195	13	NHB, HBA, HBA-D	<i>i</i>

^a Initial round-robin least-squares correlation.

^b Ref. 72.

^c Ref. 33b.

^d Ref. 76.

^e Ref. 78a.

^f Exclude diethyl ether.

^g Ref. 78b.

^h Ref. 78c.

ⁱ Ref. 78d.

^j Ref. 78e.

^k Ref. 78f.

^l Ref. 34b.

^m Exclude dioxane.

ⁿ Ref. 78g.

^o Ref. 78h.

^p Ref. 78i.

TABLE 25
Structural Effects on Solvatochromic Parameters

A. Electron Donor Ability of Auxichrome				
No. (from Table 24)	$p\text{-XC}_6\text{H}_4\text{NO}_2$, X =		$\nu_0(\text{kK})^g$	$-s$
		σ^{+a}		
13.	(CH ₃) ₂ N-	-1.67	28.10	3.44
14.	H ₂ N-	-1.47	31.10	3.14
1.	CH ₃ O-	-0.79	34.17	2.41
4.	CH ₃ CH ₂ -	-0.31	37.60	2.13
<i>b</i>	F-	-0.08	38.89	1.70
<i>c</i>	H-	0.00	39.58	1.69

B. Electron Acceptor Terminus of Chromophore				
No.	$p\text{-YC}_6\text{H}_4\text{N}(\text{CH}_3)_2$, Y =		$\nu_0(\text{kK})$	$-s$
11.	COOC ₂ H ₅		33.31	1.41
19.	CH=O		30.97	1.68
7.	COC ₆ H ₅		30.41	2.01
13.	NO ₂		28.10	3.44
39.	N=O		25.39	1.85

C. Chromophore Length				
No.	$p\text{-RC}_6\text{H}_4\text{XNO}_2$, R = X =		$\nu_0(\text{kK})$	$-s$
13.	(CH ₃) ₂ N-	Direct bond	28.10	3.44
12.		-CH=CH-	25.25	3.35
26.		-C ₆ H ₄ -	26.63	2.86
27.		-CH=CHC ₆ H ₄ -	24.31	2.15
1.	CH ₃ O-	Direct bond	34.17	2.41
3.		-CH=CH-	30.00	2.33

D. Insulation of Chromophore by N-Alkylation				
No.	$p\text{-RR}'\text{NC}_6\text{H}_4\text{NO}_2$, R = R' =		$\nu_0(\text{kK})$	$-s$
14.	H-	H-	31.10	3.14
17a.	H-	CH ₃ -	29.37	3.36
17b.	H-	CH ₃ CH ₂ -	29.17	3.33
17c.	H-	(CH ₃) ₂ CH-	28.96	3.24
13.	CH ₃ -	CH ₃ -	28.10	3.44
6.	CH ₃ CH ₂ -	CH ₃ CH ₂ -	27.52	3.18

^a J. Hine, *Structural Effects on Equilibria in Organic Chemistry*, Wiley, New York, 1975, p. 72.

^b By correlation of results of W. M. Schubert, J. Robins, and J. L. Haun [*J. Am. Chem. Soc.*, 79, 910 (1957)] for nitrobenzene (NB) with our results in corresponding solvents (including HBA-D solvents) for **4**. The correlation equation was $\nu(\text{NB}) = 0.811 \nu(\mathbf{4}) + 9.09 \text{ kK}$, $n = 8$, $r = 0.991$, $\text{SD} = 0.10 \text{ kK}$.

^c By correlation of results of W. M. Schubert, H. Steady, and J. M. Craven [*J. Am. Chem. Soc.*, 82, 1353 (1960)] for *p*-fluoronitrobenzene (FNB) with earlier results for nitrobenzene. The correlation equation was $\nu(\text{FNB}) = 1.005 \nu(\text{NB}) - 0.89 \text{ kK}$, $n = 6$, $r = 0.995$, $\text{SD} = 0.09 \text{ kK}$.

tron-donor ability of the auxichrome is accompanied by a progressive increase in the magnitudes of the s terms. Indeed, there appear to be reasonably good linear correlations of both ν_0 and s for p -X-C₆H₄-NO₂ with σ^+ of X. The correlation equations are:

$$\nu_0 = 6.390 \sigma^+ + 39.50 \text{ kK} \quad (89)$$

$$n = 8, r = 0.992, \sigma = 0.65 \text{ kK}$$

and

$$s = 1.021 \sigma^+ - 1.685 \quad (90)$$

$$n = 8, r = 0.994, \sigma = 0.09$$

Other workers, including Bagal (149) and Rao (150) have reported correlations between ν_{\max} values of *para*-complementary substituted nitrobenzene derivatives and various of the σ substituent constants. However, Brownlee and Topsom (151) have pointed out that these correlations have limited scope and significance, and break down when electron-withdrawing *para* substituents are included. Similar limitations are probably applicable to the correlation of s with σ^+ (Equation 90).

Electron-Acceptor Terminus of Chromophore. The limited scope of ρ - σ relationships involving electronic spectral data is also evident from the results in Table 25*b* for chromophores containing the (CH₃)₂N-auxichrome at one terminus, and various electron-acceptor substituents, Y, at the other. Although the general trends of decreasing transition energy and increasing sensitivity to solvent polarity with increasing electron withdrawing ability of Y are readily seen (except for the —N=O substituent), we were unable to discern any satisfactory correlations of either s or ν_0 with any of the various σ sets.

In both the X-C₆H₄-NO₂ and Y-C₆H₄-N(CH₃)₂ series, the trends are toward increasing s values with increasing quinoidal character of the electronic excited states. These trends therefore reflect greater stabilization by more polar solvents of charge-concentrated electronic excited states relative to charge-diffuse ground states.

Chromophore Length. The effects of increasing the lengths of chromophores on sensitivities of transition energies to solvent polarity are shown in Table 25*c*. Incorporation of a —CH=CH— or —C₆H₄— moiety into a chromophore leads to more charge separation in the electronic excitation, a result being to shift transition maxima to lower energies. However, in contradistinction to the trends of increasing $-s$ with decreasing ν_0 in the earlier examples, the red shifts are here accompanied by *lowered* $-s$ values. The increased distances between centers of maximum and minimum electron density in the excited state molecules are evidently accompanied by charge delocalization from (or less charge con-

centration at) these centers in the electronic excitations. The net effects are to lessen both the energy of the transition and the dependence of that energy on solvent polarity.

Insulation of Chromophore from Solvent. The effects of N-alkylation and N,N-dialkylation of 4-nitroaniline (**1**) on ν_0 and s are relatively easily unraveled (Table 25*d*). On going from **1** to its N-methyl derivative, and thence to the N,N-dimethyl derivative, we see progressive decreases in ν_0 and increases in $-s$; these trends reflect the $(\text{CH}_3)_2\text{N} > \text{CH}_3\text{NH} > \text{H}_2\text{N}$ order of electron donor ability of these auxichromes. On going from the N-methyl to the N-ethyl and N-isopropyl derivatives, and from N,N-dimethyl to N,N-diethyl-4-nitroaniline, we see further bathochromic displacements of ν_0 , again reflecting the electron donor orders: $(\text{CH}_3)_2\text{CHNH} > \text{CH}_3\text{CH}_2\text{NH} > \text{CH}_3\text{NH}$ and $(\text{CH}_3\text{CH}_2)_2\text{NH} > (\text{CH}_3)_2\text{NH}$. Here, however, the effects of the ethyl and isopropyl groups relative to the methyl are to *decrease* the $-s$ values. The rationale obviously involves a steric effect. By virtue of their greater steric requirements, these substituents serve both to increase the size of the solvent cavity and to interpose themselves between the chromophore and the solvent molecules; both effects should reduce the interactions of the chromophore with its cybotactic environment. In comparing N-methyl or N,N-dimethyl-4-nitroaniline with **1**, the greater electron donor ability overcomes the steric effect, and the net result is to increase the $-s$ term in accordance with Equation 90; in going from methyl to higher alkyl, however, the increase in *para* donor ability is smaller and the steric effect dominates.

Infrared Spectral Correlations with π^ .* Certain infrared spectral vibration frequencies and parameters derived therefrom show good linearity with the π^* scale and may also qualify as " π^* -type properties." That linear solvation energy relationships (LSERs) apply to ir spectra was first pointed out by Allerhand and Schleyer (34*f*), who reported that solvent shifts of various types of ir stretching frequencies are proportional to one another. Based on this proportionality, they proposed an empirical LSER for the correlation of solvent sensitive ir vibration frequencies,

$$\frac{(\nu^o - \nu^s)}{\nu^o} = aG \quad (91)$$

where ν^o is the vibration frequency in the vapor phase, ν^s the observed frequency in a solvent, a a function of the particular ir vibration of a given molecule, and G a function of the solvent only. An arbitrary G value of 100 was assigned to methylene chloride to fix the scale, and values of G for 20 additional solvents were determined from the best fit of solvent shifts for a number of $\text{X}=\text{O}$ and $\text{X}-\text{H}\cdots\text{B}$ stretching vibrations. In effect, although not used to correlate other types of XYZs, Allerhand and Schleyer's set of G values comprised an ir-based

TABLE 26
 Solvent π^* and G Values

No.	Solvent ^a	π^*	G
1.	<i>n</i> -Hexane (SSS)	-0.081	44
2.	Cyclohexane (SSS)	0.000	49
3.	Triethylamine (SSS)	0.140	62
5.	Di- <i>n</i> -butyl ether (SSS)	0.239	61
6.	Carbon tetrachloride	0.294	69
7.	Diethyl ether (SSS)	0.273	64
8.	Toluene	0.535	74
9.	1,4-Dioxane	0.553	86
14.	Benzene	0.588	80
20.	1,2-Dichloroethane	0.807	95
21.	Dichloromethane	0.802	100
24.	Pyridine	0.867	94
29.	Dimethyl sulfoxide (SSS)	1.000	108 ^b
30.	Chloroform	0.760	106
32.	Nitromethane (SSS)	0.848	99
43.	Tetrachloroethylene	0.277	64
50.	Acetonitrile (SSS)	0.85	93

^a SSS = select solvent set; see text.

^b Not included in table of G values in Ref. 34f, but discussed in text.

solvent polarity scale, similar in concept to the present uv-based π^* scale. Values of G and π^* are compared in Table 26 and Fig. 20.

As follows from the LSER concept, when hydrogen bonding effects are eliminated by excluding the HBD solvents CH_2Cl_2 and CHCl_3 , the solvent G values are nicely linear with corresponding π^* values (154). For the 15 non-HBD solvents for which G and π^* values have been reported, the regression equation is,

$$G = 56.2 \pi^* + 49.8 \quad (92)$$

$$r = 0.986, \sigma = 3.4$$

If the correlation is limited to the eight solvents of the *select solvent set* (for which π^* is proportional to μ (33a); see Section I), the goodness of the statistical fit improves significantly,* the regression equation becoming

$$G = 59.0 \pi^* + 49.4 \quad (93)$$

$$r = 0.996, \sigma = 0.23$$

* Despite the improvement in correlation when only the select solvents are considered, we believe G to be a " π^* -type property" because, as is readily seen in Fig. 20, there is no *systematic* displacement of the data points for the aromatic or polychloroaliphatic solvents relative to the select solvents, the higher r value being due to the somewhat lesser scatter of the SSS results.

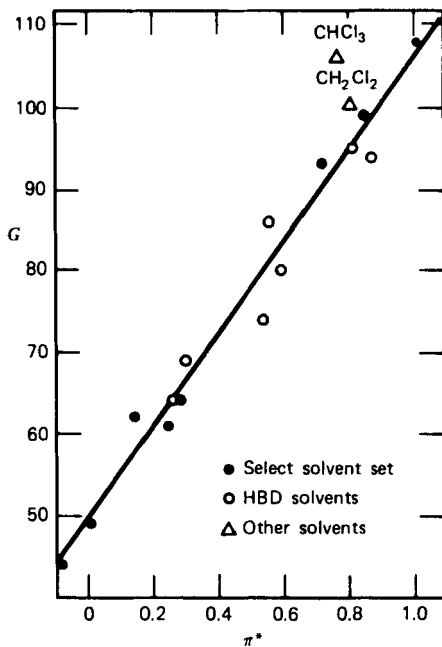


Figure 20 Allerhand and Schleyer's G values plotted against solvent π^* values.

Individual Correlations. Solvatochromic displacements of 25 single- and double-bond ir stretching frequencies of various types are correlated with solvent π^* values in Table 27. Correlations are given for (a) all non-HBD solvents for which $\bar{\nu}$ values have been reported in the cited references and π^* values are known, and (b) members of the *select solvent set*.

It is seen that the statistical fits of the "all data" correlations in Table 27 are quite respectable. All r values are >0.90 , 23 of the 25 are >0.97 . Also, the two r values that are <0.95 do not reflect lower σ_s , but result instead from lower s values (slopes) in the regression equations. The goodness of the fits improves significantly for the *select solvent set*, all r values being >0.96 , and 7 of 13 being >0.99 . In a number of instances, as before, the lower r s for the "all data" correlations result from a greater scatter of the non-SSS data points, but in other instances there are systematic separations into families of solvents, as discussed next for the more general case of solvent effects. For a more detailed discussion of structure-property relationships involving the data in Table 27, see the original paper (154).

Solvent Effects on Other Properties. The More General Case. It was shown in Section I that the gross features of solvent effects induced by the *select solvents* could be rationalized in terms of classical electrostatics. There is evidence,

however, that in the case of aromatic and polyhalogenated aliphatic solvents other factors are relevant. In the case of aromatic solvents, these factors include: (a) the strong anisotropy of the aromatic rings (79), (b) the possibility of donor-acceptor complexes with molecules having low-lying LUMOs, and (c) the often large and still incompletely understood effects of aromatic solvents on nmr spectra.

Factor (b) is a well-known phenomenon (80). Recently Skulski and Kanabus (81) presented experimental results hinting at the formation of such complexes between benzene and *p*-nitroanisole, one of the indicators used to establish the π^* scale. Since the work of Winstein and Feldman (82) has established the existence of C.T. complexes between aromatic hydrocarbons and tropylium cation, the possibility of weak nucleophilic attack by aromatics on incipient carbonium ions seems reasonable.

Factor (c) appears to depend on complex interacting effects and deserves detailed discussion. When the proton nmr spectrum of a polar substance, typically but not always a ketone (83), dissolved in an aromatic hydrocarbon is compared with that obtained in a saturated hydrocarbon, large shifts of up to 1.5 ppm are frequently observed. These shifts are either upfield or downfield, depending on the stereochemistry of each proton-bearing group (84). This general behavior, known as ASIS (aromatic solvent-induced shifts), has been reviewed by Foster and Lazlo (85).

It is likely that the ASIS effect originates in the short-lived clustering of aromatic molecules around the terminus of the solute through dipole-induced dipole (or eventually C.T.) interactions (86). These effects would be superimposed onto any "normal" R. F. effects. Abraham (157) has determined the chemical shifts of the proton signal of methyl iodide in a number of solvents (Table 28), and introduced the concept of "excess high field shift" (EHS). The EHS is defined as the difference between the chemical shifts in aromatic and aliphatic solvents of similar structure.

It is noteworthy that solvents such as nitrobenzene and benzonitrile, for which the EHS is practically nil, behave almost as "select solvents" (87). Inspection of the tables in Section I shows that very often benzene and toluene and, to a lesser extent, other more polar aromatic solvents display a solvation efficiency comparable to that of "select solvents" of much larger dipole moment. Benzene, for instance, has a π^* value comparable to that of THF. The rationale is that some of the factors that favor the EHS may also contribute to the solvent efficiency in chemical reactivity and spectral shifts.

The adverse effect of polar substituents on the enhanced reactivity of aromatics can be tentatively rationalized in several ways. (a) The orientation of solvent molecules relative to the solute dipole could be determined by the condition of optimal dipole-dipole interaction, rather than by the condition of maximum overlap (88) or larger dipole-induced dipole interactions. (b) The

TABLE 27
Correlations of Infrared Spectral Data with the π^* -Scale of Solvent Polarity-Polarizabilities

Stretch band	Solvent ^a	$\bar{\nu}$ $\bar{\nu}_0$	$\bar{\nu} = \bar{\nu}_0 + s\pi^*$, All data in cm^{-1}	r	SD	n	Ref.
1. <i>n</i> -Propyl chloride, <i>trans</i> C-Cl	All	734.2	-18.70	0.981	1.2	10	152
	SSS	733.8	-18.47	0.997	0.6	7	
	All	655.3	-14.19	0.972	1.0	10	
	SSS	654.7	-13.81	0.998	0.3	7	
2. Isobutyl chloride, <i>trans</i> C-Cl	All	734.6	-14.91	0.982	0.9	10	152
	SSS	734.1	-14.54	0.997	0.5	7	
	All	691.5	-13.91	0.978	0.9	10	
	SSS	691.1	-13.62	0.997	0.4	7	
3. $\text{CH}_3\text{OCH}(\text{CH}_3)\text{CH}_2\text{CH}_2\text{OH}$ bonded O-H	All	3552.0	-50.46	0.989	2.7	7 ^b	34 ^f
	All	3553.4	-54.90	0.992	2.6	7 ^c	34 ^f
4. $\text{CH}_3\text{CHOH-CH}_2\text{CHOH-CH}_3$ bonded O-H	All	3517.2	-49.81	0.994	1.9	7 ^b	34 ^f
	All	3359.2	-75.86	0.993	3.0	7 ^b	34 ^f
5. Methanol-ether, bonded O-H	All	3545.8	-70.49	0.995	2.2	5 ^b	34 ^f
	All	1083.0	-29.59	0.983	2.0	11 ^c	153
6. Phenol-ether, bonded O-H	All	1056.4	-13.00	0.938	1.7	12 ^c	153
	SSS	1055.6	-11.16	0.981	1.1	5	
7. Methanol dimer, bonded O-H	All	1041.2	-9.40	0.974	0.7	11 ^d	153
	All	1310.4	-16.89	0.981	1.2	8 ^d	153
8. Dimethyl sulfoxide, S=O	All						
	All						
9. Diphenyl sulfoxide, S=O	All						
	All						
10. Thionyl chloride, S=O	All						
	All						
11. Phosphorus Oxychloride, P=O	All						
	All						

12. (CH ₃) ₂ HPO, P=O, band I	All	1291.2	-26.09	0.957	2.7	10 ^c	153
band 2	SSS	1291.3	-30.48	0.992	1.6	6	
	All	1271.8	-16.97	0.928	2.3	10 ^c	
	SSS	1272.8	-20.89	0.991	1.1	6	
13. Methyl nitrite, <i>trans</i> N=O	All	1665.5	-22.48	0.961	2.6	6 ^{b,e}	153
<i>cis</i> N=O	All	1614.4	-10.12	0.962	1.1	6 ^{b,e}	
14. Isopropyl nitrite, <i>trans</i> N=O,	All	1650.0	-21.42	0.957	2.6	7 ^{c,e}	153
15. (CH ₃) ₂ N=N=O, >N-N	All	1024.0	+31.72	0.961	2.9	9 ^d	153
16. Acetophenone, C=O	All	1696.4	-13.23	0.960	1.3	16 ^c	155
	SSS	1696.2	-12.71	0.981	1.0	7	
17. Benzophenone, C=O	All	1670.2	-12.20	0.982	0.8	16 ^c	155
	SSS	1670.3	-11.64	0.991	0.6	7	
18. Cyclohexanone, C=O	All	1723.4	-18.68	0.973	1.4	17 ^{c,f}	156
	All	1725.2	-18.90	0.955	2.0	16 ^c	155
	SSS	1724.9	-19.40	0.960	2.1	7	
19. Acetone, C=O	All	1723.3	-12.63	0.961	1.2	16 ^c	155
	SSS	1723.2	-12.15	0.978	1.2	7	
20. Dimethylformamide, C=O	All	1694.5	-22.80	0.972	1.9	16 ^c	155
	SSS	1694.2	-23.55	0.993	1.1	7	
21. Methyl acetate, C=O	All	1753.9	-16.63	0.957	1.7	16 ^c	155
	SSS	1754.2	-15.36	0.967	1.6	7	

^a All includes nonchlorinated aliphatics, polychlorinated aliphatics, and aromatic solvents. SSS = selected solvent set; see text and Ref. 33a.

^b CH₂Cl₂ and CHCl₃ excluded from correlations; behave as HBD solvents.

^c CHCl₃ excluded from correlations and/or CH₂Cl₂ included.

^d CHCl₃ and CHCl₃ included in correlations. Do not behave as HBD acid solvents as indicator is evidently an insufficiently strong HBD base.

^e Ether excluded; spectrum obviously influenced by an impurity.

^f Tetrahydrofuran result obviously in error and excluded from correlation. Also, it is assumed that the ether and dioxan data are inverted due to a misprint.

TABLE 28
Excess High Field Shifts for the Proton Signal of Methyl Iodide

Solvent	Observed shift	EHS ^a
C ₆ H ₆	88.0	32.0
C ₆ H ₅ CH ₃	90.7	29.3
<i>m</i> -C ₆ H ₄ (CH ₃)	92.2	27.8
<i>p</i> -C ₆ H ₄ (CH ₃) ₂	92.3	27.7
<i>i</i> -C ₃ H ₇ C ₆ H ₅	93.0	27.0
<i>n</i> -C ₃ H ₇ C ₆ H ₅	95.0	25.0
C ₆ H ₃ (CH ₃) ₃	94.1	25.9
C ₆ H ₅ Cl	105.6	23.6
<i>o</i> -C ₆ H ₄ Cl ₂	116.9	12.2
C ₆ H ₅ CHO	121.5	8.5
C ₆ H ₅ CN	125.7	3.0
C ₆ H ₅ NO ₂	127.7	1.0
<i>c</i> -C ₆ H ₁₂	120.0	0.0

^a In H₂ at 60 Mc from (CH₃)₄Si at 35°C

grafting of strong electron-withdrawing groups (+*R* effect) on the aromatic ring greatly reduces the ability of the ring to act as an electron donor. (*c*) It has been shown (89) that the polarizability of conjugated and aromatic systems (i.e., highly anisotropic molecules) undergoes a large increase under the influence of high electric field strengths. Highly polar species in solution can indeed generate fields of the proper order of magnitude. In this context, Coulson and Davies (90) have reexamined the problem of the dispersion forces acting between polyenes or aromatic molecules and have shown them to be *significant* (compared to dipolar forces) and *highly directional*.

Incompletely understood interaction effects have also been observed with polyhalogenated aliphatic solvents. Thus, the existence of solid complexes between CCl₄ and electron donors has been reported (91), and Prausnitz (92) has offered evidence that CCl₄ and aromatic hydrocarbons form weak complexes in *n*-hexane solution. Also, over the last decade, a great deal of attention has been

TABLE 29
Formation Constants for Complexes of CCl₄ with Bases
in Cyclohexane at 20°C.

Base	K(1 mole ⁻¹) ^a
Pyridine	0.14 ± 0.04
4-Methylpyridine	0.32 ± 0.07
2,6-Dimethylpyridine	0.10 ± 0.02
2,4,6-Trimethylpyridine	0.09 ± 0.02
Tetrahydrofuran	0.08 ± 0.05

^a Ref. 93b.

TABLE 30
Formation Constants of Weak Complexes between Polyhalogenated
Compounds and Bases

Halogenated compound	K (1 mole ⁻¹) ^{a,b}	
	Pyridine	Tetrahydrofuran
Cl ₂ C=CCl ₂	0.13 ± 0.04	0.15 ± 0.04
<i>trans</i> -ClCH=CHCl	0.25 ± 0.08	0.40 ± 0.10
ClCH ₂ CH ₂ Cl	0.60 ± 0.15	0.60 ± 0.20

^a Cyclohexane solvent, 25°C.

^b Ref. 93c.

devoted to the interactions between different n or π bases and compounds of the type EX₄ (E = C, Si; X = Cl, Br), notably by Gomel and co-workers (158). A number of techniques, including dielectric polarization (93) ir spectroscopy (94), and calorimetry (95) are coincident in showing that CCl₄ and both n and π bases are able to form complexes in solution. Typical values of the formation constants of such complexes are given in Table 29. Considering the difficulties inherent in the measurement of such small constants, the uncertainties are probably large.

Carbon tetrachloride is by no means the only halocarbon solvent which associates by mechanism(s) other than hydrogen bonding. Tetrachloroethylene, *trans*-dichloroethylene, and 1,2-dichloroethane form somewhat stabler complexes as shown in Table 30.

Sandorfy and co-workers (96) have shown by means of ir spectroscopy that fluorocarbons containing heavier halogens can act as hydrogen bond breakers in moderately self-associating systems such as hindered alcohols and phenols, secondary amines, thiols, and amides. Typical solvents are CF₃Cl, C₂F₅Cl, CF₃Br, C₂F₅Br, *n*-C₃F₇Br, CF₃I, C₂F₅I, *n*-C₃F₇I, and BrCF₂CF₂Br. Some general trends appear: (a) Perfluorinated molecules have no hydrogen bond breaking potency.* (b) Fluorocarbons containing only chlorine in addition to carbon and fluorine have only a weak effect. (c) Fluorocarbons containing Br and I are strong hydrogen bond breakers and the order of potency is I > Br > Cl. It has been suggested that these solvents act as electron acceptors, and thus compete with the self-association through hydrogen bonding.** Interestingly, the hydrogen bond breaking ability of these solvents closely parallels their effectiveness as inhalation anesthetics.

Henceforth we use the term "polarizability" (with the quotation marks)

* It is interesting that *n*-C₈F₁₈ has a G value that is even smaller than that of straight chain saturated hydrocarbons.

** It has recently been suggested (97) that solvents such as methylene chloride and chloroform, well known as HBD solvents, also act as electron acceptors by a "pure" charge-transfer mechanism.

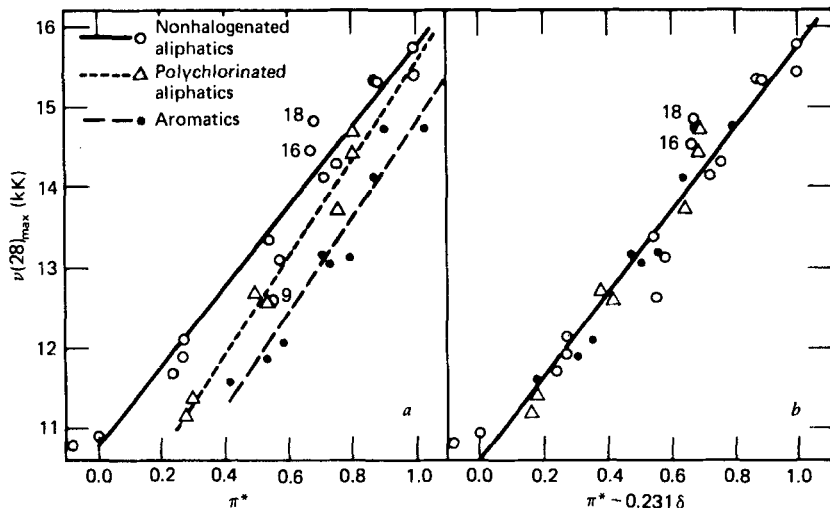
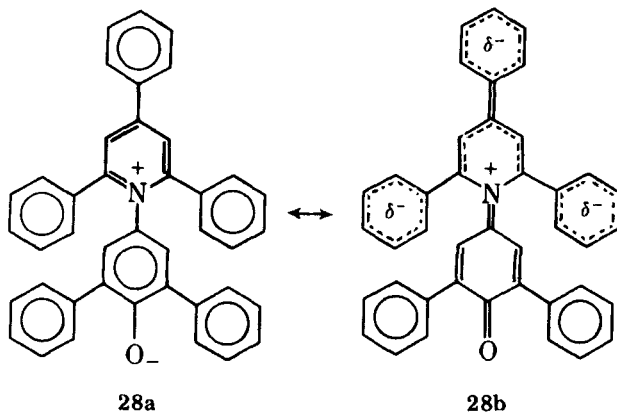


Figure 21 Solvatochromic comparison plots of ν_{\max} for Dimroth's betaine against solvent π^* values and against $\pi^* + d\delta$ of non-HBD solvents.

to characterize these still incompletely understood contributions to solvatochromic effects. It should be understood that this terminology is only loosely related to the classical concept of polarizability.

Solvatochromic Behavior of Dimroth's Betaine. In contrast with the highly satisfactory correlations between π^* and the " π^* -type properties" in Tables 24 and 26, the linear regression was significantly poorer when ν_{\max} values for Dimroth's betaine (34a), 4-(2,4,6-triphenylpyridinium)-2,6-diphenylphenoxide (28) in 32 non-hydrogen-bond donor solvents (Table 10) were plotted against the solvent π^* values (Fig. 21a).



The correlation coefficient was very much lower than had been observed for any of the 47 spectra of Table 24, and the standard deviation was well beyond the experimental precision of usual spectral determinations,

$$\begin{aligned}\nu(\mathbf{28})_{\max} &= 10.42 + 4.65 \pi^* \text{ kK} & (94a) \\ r &= 0.905, \sigma = 0.63 \text{ kK}\end{aligned}$$

This result could not be dismissed lightly, since the solvatochromic behavior of $\nu(\mathbf{28})_{\max}$ was the basis of the “ $E_T(30)$ ” scale, the most widely used and frequently cited measure of the polarity of pure solvents. For this reason, the correlation between $\nu(\mathbf{28})_{\max}$ and π^* for non-HBD solvents was subjected to more detailed analysis, whereupon it was found that the goodness of the fits was improved very much when consideration was limited to families of structurally similar solvents. Thus, for 16 nonchlorinated aliphatic solvents,

$$\begin{aligned}\nu(\mathbf{28})_{\max} &= 10.80 + 4.84 \pi^* \text{ kK} & (94b) \\ r &= 0.974, \sigma = 0.39 \text{ kK}\end{aligned}$$

Similarly, for seven polychlorinated aliphatic solvents,

$$\begin{aligned}\nu(\mathbf{28})_{\max} &= 9.56 + 5.93 \pi^* \text{ kK} & (94c) \\ r &= 0.985, \sigma = 0.26 \text{ kK}\end{aligned}$$

and for nine aromatic solvents,

$$\begin{aligned}\nu(\mathbf{28})_{\max} &= 8.88 + 5.82 \pi^* \text{ kK} & (94d) \\ r &= 0.967, \sigma = 0.32 \text{ kK}\end{aligned}$$

In light of the previous discussion, it seems reasonable that these results originate in the different “blend” of solvent polarity and “polarizability” in the case of **28** compared with the indicators of Table 24. This may derive from the fact that the directions of electron migration in the electronic transitions for the indicators in Table 24 were coincident with the directions of their ground state dipoles, whereas in the transition **28a** ($h\nu$) \rightarrow **28b** the direction of electron migration is converse to the direction of the ground state dipole. Also, there is charge concentration in the electronic transitions for the indicators of Table 24 as compared with charge delocalization for **28** (Liptay and co-workers (182) have reported decreases in dipole moments from near 15 D in the ground states to near 6 D in the electronic excited states for betaines like **28**). This accounts for the bathochromic shifts with increasing solvent polarity for the former compounds compared with a hypsochromic shift for **28** (for a more detailed discussion of these effects, see the original paper) (33b). Thus, the three regression lines in Fig. 22a characterize the solvatochromic behavior in three families of solvents with common “polarizability characteristics.”

To adapt the solvatochromic equations and the π^* scale to properties and phenomena involving different relative contributions of polarity and "polarizability," we have modified Equations 42, 42' and 89 by the addition of a $d\delta$ term. The d coefficient is intended to serve as a measure of the difference between the polarity-"polarizability" blend for XYZ and the " π^* blend." The δ parameter is taken to be 0.00 for all "select solvents," 0.50 for polychlorinated aliphatics, and 1.00 for all aromatic solvents.

Thus, where solvent HBD or HBA effects are excluded, the general solvent effects equation takes the form,

$$XYZ = XYZ_0 + s(\pi^* + d\delta) \quad (95)$$

We calculate the d term by dividing the difference in XYZ at $\pi^* = 0.7$ (which is near the average π^* value for aromatic solvents), as obtained separately through Equation 88 for "select solvents" and for aromatic solvents, by the average of the slopes, that is,

$$d = \frac{[XYZ_{\text{aliphatics}}^{\text{Eq. 88}} - XYZ_{\text{aromatics}}^{\text{Eq. 88}}] \text{ at } \pi^* = .7}{1/2 [s_{\text{aliphatics}}^{\text{Eq. 88}} + s_{\text{aromatics}}^{\text{Eq. 88}}]} \quad (96)$$

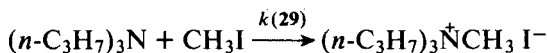
It is evident that correlations could have been improved even further if we had carried out least squares fits to obtain optimal d values for each case rather than calculating them by Equation 96. We felt, however, that the introduction of the additional parameter into the solvatochromic equations would be statistically more sound if the parameter were fixed by the calculational method rather than adjusted to optimize the correlation.

In the case of **28**, Fig. 21*b* shows how the data points for the three families of solvents are combined around a single regression line when $\nu(\mathbf{28})_{\text{max}}$ is plotted against $(\pi^* + d\delta)$, $d = -0.231$. The correlation equation becomes

$$\nu(\mathbf{28})_{\text{max}} = 10.60 + 5.12(\pi^* - 0.231 \delta) \text{ kK} \quad (94e)$$

the "all data" correlation coefficient becoming 0.971 (versus 0.905 for the original correlation by Equation 94*a*) and σ becoming 0.35 kK (versus 0.65 kK).

Additional Correlations with $(\pi^ + d\delta)$. Menshutkin Reaction Rates.* The most extensive single source set of accurate reactivity data in pure solvents in the chemical literature is for the Menshutkin reaction of tri-*n*-propylamine with methyl iodide at 20°C.



Lassau and Jungers (34*c*) have reported rate constants for this reaction in 78 solvents, of which 70 are non-hydrogen-bond donors (or have α values below

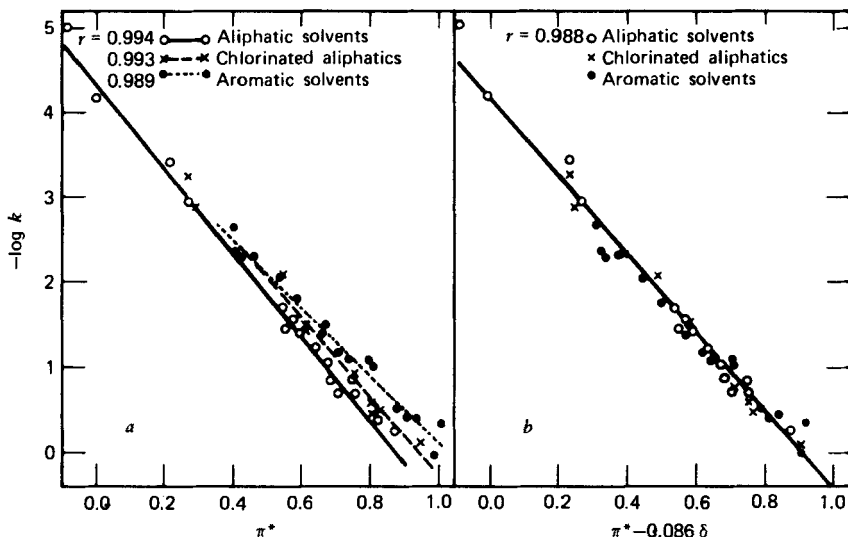


Figure 22 Log k (29) for the Menschutkin reaction of tri- n -propylamine with methyl iodide plotted against π^* and $(\pi^* + d\delta)$ of non-HBD solvents.

0.2) so that hydrogen bonding effects were essentially eliminated (Table 7). Values of π^* are known for 44 of these solvents.

An "all data" least squares correlation of the log k (29) results with solvent π^* values leads to the regression equation,

$$\log k(29) = -4.24 + 4.43 \pi^* \quad (97a)$$

$$r = 0.981, \sigma = 0.21 \text{ log unit}$$

Although the preceding measures of the goodness of the linear fit are highly satisfactory by the standards usually applied to linear free energy relationships, inspection of a plot of the results (Fig. 22a) shows systematic displacements of the data points for polychloroaliphatic and aromatic solvents relative to those for nonchlorinated aliphatic solvents. Correspondingly, significant improvements in r and σ are observed when the correlations are limited to families of solvents with similar "polarizability" characteristics, that is, for 15 nonchlorinated aliphatic solvents, $r = 0.994$, $\sigma = 0.16$; for 11 polychlorinated aliphatics, $r = 0.993$, $\sigma = 0.13$; for 18 aromatic solvents, $r = 0.989$, $\sigma = 0.12$.

Alternatively, if the results are fitted to Equation 95, the d term is calculated (from Equation 96) to be -0.086 , and the preferred all data correlation equation becomes

$$\log k(29) = -4.18 + 4.66 (\pi^* - 0.086 \delta) \quad (97b)$$

$$r = 0.988, \sigma = 0.17 \text{ log unit}$$

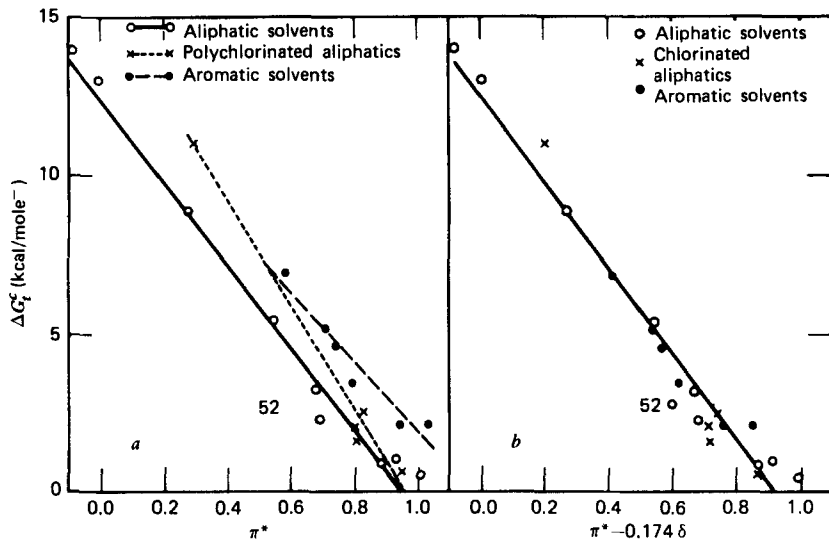


Figure 23 $\Delta G_i^c(30)$ from methanol to a variety of other solvents for the $\text{Et}_4\text{N}^+\text{I}^-$ ion pair plotted against π^* and $(\pi^* + d\delta)$.

A plot of $\log k(29)$ against $(\pi^* - 0.086 \delta)$ is shown in Fig. 22b.

Free Energies of Transfer of $\text{Et}_4\text{N}^+\text{I}^-$. Another somewhat different set of properties which is well correlated by the π^* and δ parameters involves the free energies of transfer of the tetraethylammonium iodide ion pair (30) from methanol to various other solvents. Abraham (44b) has reported 34 ΔG_i^c values, of which 21 are for non-HBD solvents whose π^* values are known.

The "all data" least-squares correlation of Abraham's results with π^* (Fig. 23a) gives the regression equation,

$$\Delta G_i^c(30) = 12.79 - 12.51 \pi^* \text{ kcal mole}^{-1} \quad (98a)$$

$$r = 0.954, \sigma = 0.92 \text{ kcal mole}^{-1}$$

As before, the correlations are improved significantly when the families of solvents with similar "polarizability" characteristics are considered separately. For the results in 10 nonchlorinated aliphatic solvents, $r = 0.985$, $\sigma = 0.72$; for the 5 polychlorinated aliphatic solvents, $r = 0.990$, $\sigma = 0.68$; and for the 6 aromatic solvents, $r = 0.961$, $\sigma = 0.58$. The three separate regression lines are shown in Fig. 23a.

Again the data points coalesce to cluster around a single regression line when plotted against $(\pi^* + d\delta)$, $d = -0.174$ (Fig. 23b). The "all data" least-squares regression equation becomes

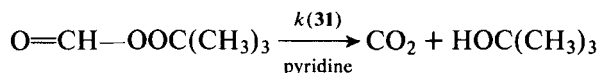
$$\Delta G_f^c(30) = 12.67 - 13.67 (\pi^* - 0.174 \delta) \text{ kcal mole}^{-1} \quad (98b)$$

$$r = 0.984, \sigma = 0.76 \text{ kcal mole}^{-1*}$$

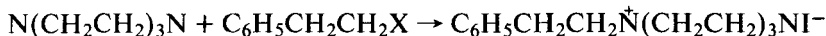
We will have occasion to refer to this property again in the discussion of the α scale.

Miscellaneous Correlations. To demonstrate the versatility and widespread applicability of the π^* scale, we have carried out least squares correlations through Equations 88 and 95 of non-HBD (or weak-HBD) solvent effects on many diverse types of properties. The results are summarized in Table 31. The properties correlated are:

(31) the second order rate constant for the pyridine-catalyzed ionic decomposition of *tert*-butyl peroxyformate at 90°C, as reported by Pincock (106):

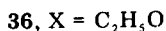
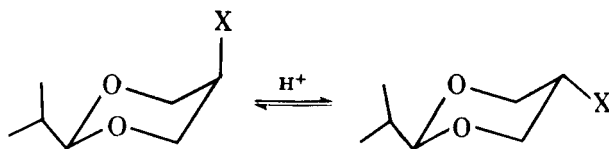


(32-34) second-order rate constants for the Menschutkin reactions of 1,4-diazabicyclo[2.2.2]octane (DABCO) with 2-chloroethylbenzene (32), 2-bromoethylbenzene (33), and 2-iodoethylbenzene (34) at 54.5°C, as reported by Auriel and de Hoffman (104):



(35) Y' values for solvolyses of *tert*-butyl chloride, as reported by Koppel and Pal'm (105), where $Y' = 1.800 [\log k_{\text{solvent}}^{120^\circ\text{C}} - \log k_{\text{gas phase}}^{120^\circ\text{C}}] \text{ kcal mole}^{-1}$;

(36) free energy changes, ΔG° in kcal mole^{-1} in the *cis-trans* conformational equilibrium of 2-isopropyl-5-ethoxy-1,3-dioxane (36), as reported by Eliel and Hofer (107):



(37,38) nitrogen hyperfine splitting constants of di-*tert*-butyl nitroxide

* Methyl formate (solvent 52) has been excluded from the correlation. It is noteworthy that 52 also fell somewhat out of line in the π^* vs. dipole moment correlation (33a). It was suggested that this was because 52 is a solvent of particularly small steric requirements.

TABLE 31
Correlations with π^* and $(\pi^* + \delta b)$. Non-HBD Solvents

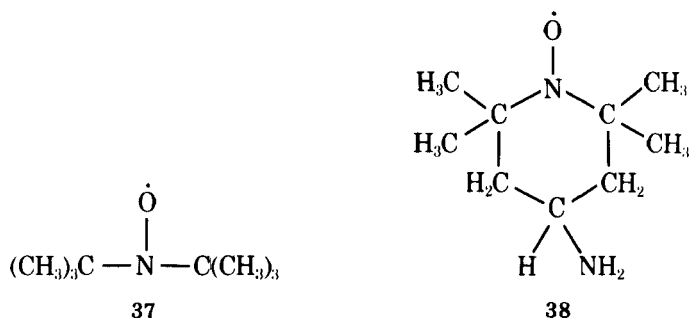
Property (see text)	XYZ =	Eq.	Solvents ^a	XYZ ₀	s	d	r	σ	n	Ref.
31	log k	88	All	0.30	1.96		0.986	0.11	15	106
		88	NCA	0.32	2.12		0.994	0.09	6	
		88	ARO	0.25	2.00		0.983	0.09	6	
32	log k	95	All	0.32	2.05	-0.074	0.989	0.09	15	104
		88	All	-6.16	3.84		0.886	0.35	14	
		88	NCA	-6.40	4.58		0.991	0.12	7	
		88	ARO	-6.26	3.59		0.958	0.20	7	
33	log k	95	All	-6.06	4.08	-0.133	0.974	0.17	14	104
		88	All	-3.94	3.71		0.923	0.35	16	
		88	NCA	-4.07	4.33		0.994	0.11	8	
		88	ARO	-3.87	3.24		0.952	0.19	7	
		95	All	-3.79	3.95	-0.153	0.979	0.19	16	
34	log k	88	All	-3.17	3.56		0.910	0.37	16	104
		88	NCA	-3.31	4.21		0.991	0.14	8	
		88	ARO	-3.15	3.11		0.957	0.18	7	
		95	All	-3.07	3.86	-0.169	0.981	0.17	16	
		88	All	5.89	7.33		0.928	2.17	13	
35	Y'	88	NCA	5.93	8.91		0.991	0.51	9	105
		88	ARO	4.95	6.82		0.948	0.54	4	
		95	All	5.97	8.75	-0.279	0.987	0.52	13	
		88	All	1.29	-0.93		0.930	0.11	13	
36	ΔG ⁰	88	NCA	1.22	-0.81		0.956	0.10	5	107
		88	ARO	1.56	-1.16		0.992	0.05	4	
		88	PCA	1.50	-1.38		0.990	0.06	4	
		95	All	1.28	-1.01	-0.089	0.956	0.09	13	

37	A_N	88	All	15.154	0.505		0.943	0.054	14	34c
		88	NCA	15.167	0.510		0.978	0.043	7	
38	A_N	88	ARO	14.992	0.673		0.952	0.035	5	34c
		95	All	15.164	0.528	-0.103	0.956	0.048	14	
		88	All	15.254	0.479		0.960	0.042	14	
		88	NCA	15.260	0.489		0.983	0.037	7	
		88	ARO	15.221	0.479		0.912	0.034	5	
		95	All	15.263	0.496	-0.092	0.969	0.036	14	
39	P	88	All	-0.10	2.60		0.934	0.31	25	159
		88	NCA	0.01	2.67		0.991	0.13	13	
40	δ	88	ARO	-1.28	3.68		0.967	0.17	8	b
		95	All	-0.04	2.81	-0.185	0.971	0.20	25	
		88	All	10.48	2.47		0.952	0.25	22	
		88	NCA	10.51	2.67		0.987	0.16	13	
		88	ARO	9.49	3.33		0.956	0.18	7	
		95	All	10.52	2.72	-0.197	0.981	0.16	22	
41	ν_{\max}	88	All	17.34	3.00		0.852	0.58	19	34d
		88	NCA	17.45	3.57		0.976	0.29	11	
		88	ARO	16.83	3.00		0.885	0.32	6	
		95	All	17.44	3.54	-0.314	0.957	0.32	19	
		88	All	2.56	0.519		0.955	0.058	11	
		88	NCA	2.58	0.556		0.997	0.021	5	
42	AI	88	ARO	2.51	0.462		0.992	0.008	3	101
		95	All	2.58	0.589	-0.257	0.991	0.026	11	

^a NCA = nonchlorinated aliphatics; PCA = polychlorinated aliphatics; ARO = aromatics.

^b Data (solvent no., δ value) are: **1**, 10.46; **2**, 10.50; **3**, 10.70; **6**, 11.10; **7**, 11.35; **9**, 11.60; **11**, 12.00; **13**, 11.98; **14**, 11.50; **15**, 11.95; **17**, 12.00; **18**, 12.45; **20**, 12.75; **24**, 12.55; **25**, 12.85; **27**, 13.00; **28**, 12.85; **29**, 13.20; **31**, 12.65; **33**, 12.05; **34**, 12.65; **37**, 12.65.

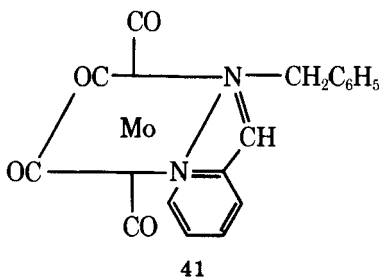
(37) and 4-amino-2,2,6,6-tetramethylpiperid-1-yloxy (38), A_N in G , as reported by Knauer and Napier (34e):



(39) Taft and co-workers' solvent polarity parameter P , based on solvent effects on F-nmr shielding in fluorobenzene derivatives (159);

(40) F-nmr shifts of *p*-fluoronitrobenzene relative to fluorobenzene internal standard, δ in ppm (values determined in these laboratories are given in footnote *b* of Table 31);

(41) absorption maxima, ν_{\max} , in the metal to ligand charge transfer band of the molybdenum complex, N-(2-pyridinecarboxylidene)benzylamine-molybdenum(0)tetracarbonyl (41), as reported by Walther, (34d)*:



(42) the absorption intensity, AI (in $1 \text{ mole}^{-1} \text{ cm}^{-2}$), of the $\text{C}\equiv\text{N}$ stretching band in the ir spectrum of propionitrile, as reported by Tanaka and co-workers (101).

* The solvatochromic behavior of 41 was proposed by Walther as the basis for still another solvent polarity scale, labeled E_K . This E_K index is of particular historical interest to us in that, in plotting E_K against corresponding E_T (30) values, Walther evidently noted poor correlation when all the data were considered together, but better correlation when families of data were considered separately. Walther's families comprised: (1) protic solvents, (2) alkyl halides, (3) substituted benzenes, and (4) nonprotic oxygen and nitrogen containing aliphatics. It is likely that Walther's considerations in the layout of his plot were similar to those which prompted us to the formulation of separate π^* and α scales, and to the inclusion of the $d\delta$ term in the solvatochromic equations.

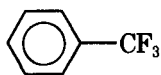
It is seen in Table 31 that the correlations of XYZs 31–42 with π^* follow the same now familiar pattern. “All data” correlations by Equation 89, which range from very poor to fairly good, are improved significantly when results in NCA and ARO solvents are treated separately. With the addition of the $d\delta$ term, “all data” correlations by Equation 95, although not quite as good as the individual family correlations by Equation 88, are usually much better than the earlier “all data” correlations. It is also to be noted that with these, as with most correlations through Equation 95 that we have carried out, the d coefficient has a negative sign.

π^* Values of Protic Solvents. For reasons that are too involved and incorrect (and which it serves no purpose) to repeat here, but which were discussed at great length in the original paper on the π^* scale (33*b*), our initial estimates of the π^* values of protic solvents were based on faulty assumptions. We assumed, incorrectly, that uv-visible spectra of 4-nitroanisole, N,N-diethyl-3-nitroaniline, 4-methoxy- β -nitrostyrene, and 1-ethyl-4-nitrobenzene (indicators 1–4 of Table 24) were only very slightly, if at all, influenced by type-A hydrogen bonding effects of HBD solvents, that is, $a \approx 0$ in Equation 42. Since the indicators are nonprotic (b also = 0), it therefore appeared to us that π^* values of protic solvents should be directly calculable from solvatochromic Equations 1–4 of Table 24, and the original π^* values for the HBD solvents were determined in this manner (33*b*).

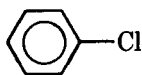
We have since come to the conclusion that solvatochromic effects of the stronger HBD solvents on indicators 1–4 of Table 24 include important contributions from type-A hydrogen bonding to the nitro groups, that is, $-\Delta\Delta\nu(\mathbf{i}-\pi^*)_{O_2N}^A$. From this it followed that some of our original estimates of HBD solvent π^* values were incorrect and required revision.

Further, as we compared magnitudes of a coefficients in solvatochromic equations for many additional types of $n \rightarrow \pi^*$, $p \rightarrow \pi^*$, $\pi \rightarrow \pi^*$, and intra- and intermolecular charge transfer bands, and as we encountered measurable HBA properties in such weak π -bases as benzene, chlorobenzene, and bromobenzene ($\beta = 0.10, 0.07,$ and 0.06), it became increasingly obvious to us that we were unlikely to find a satisfactory uv-visible spectral indicator for π^* of protic solvents, that is, an indicator whose spectrum was sufficiently sensitive to solvent polarity, yet was relatively little influenced by type-A hydrogen bonding by HBD solvents. This is because type-A hydrogen bonding is so pervasive that any chromophore or auxochrome that could lead to absorption of light in an experimentally accessible region of the electronic spectrum (i.e., beyond the cutoff point of most solvents) would almost necessarily contain a site of ground state electron density sufficiently high to induce hydrogen bonding by at least some HBD solvents (*vide infra* for discussion of competition between self-association of amphiprotic HBA–HBD solvents and bonding to other HBA bases).

No such restrictions exist as concerns nmr spectra, however, and it was in this direction we turned to find an indicator for π^* of protic solvents. Earlier studies had indicated that the ^{13}C chemical shift of the *para* carbon of mono-substituted benzenes relative to internal benzene was suitably sensitive to solvent polarity (160,161), and the problem became one of finding a substituent which was "chemically inert"* so that the solvent effect involved only the mutual dipolar interactions of the solvent and the substituent leading to modification of the substituent-induced polarization of the benzene ring (162). Based on analogous behavior of the ^{19}F chemical shifts of *m*- and *p*-substituted fluorobenzenes (163), benzotrifluoride (**43**) and chlorobenzene (**44**) were chosen for study.



43



44

Table 32 reports the ^{13}C chemical shifts of compounds **43** and **44**, referenced to the benzene carbon atom, in 43 pure solvents of interest. The solute concentration was 0.1–0.2 *M* and the benzene standard was present in each solution at approximately .05 *M* concentration. The chemical shifts were found to be reproducible (different samples and spectra) to ± 0.03 ppm.

Solvents are listed in Table 32 according to increasing value of the shift for the *para* carbon atom of **43** (i.e., increasing shift to lower magnetic field strength). The *ortho* and *meta* carbon shifts for **43** and the *para* carbon shifts for **44** tend to follow the same order, although some exceptions will be noted. Generally, for non-HBD solvents, the observed solvent orders for the shifts of **43** and **44** follow π^* values (the correlation is especially good for "select" solvents). However, our initial reaction to the solvent shifts tended to be somewhat reserved due to the unusual position of a number of the HBD solvents, for example, $\text{CF}_3\text{CO}_2\text{H}$, $(\text{CF}_3)_2\text{CHOH}$, and CH_3NO_2 .

The recognition that the benzene ring can act as a hydrogen bond acceptor (164) affords an immediate rationale for the anomalous solvent shifts of Table 32. Since benzene is a weak HBA base, it does not compete well with strong self-association of HBD–HBA solvents. However, for weakly associated HBD solvents, the shifts are strongly complicated by type-A hydrogen bonding to benzene. Since the substituents of **43** and **44** are strongly electron-attracting, less hydrogen bonding should occur to their ring positions. That is, the shifts of Table 32 involve internal benzene which has been downfield shifted compared to the carbons of **43** and **44** in the weakly self-associated HBD solvents.

If we use an intramolecular carbon atom standard rather than the benzene standard (as was done in earlier ^{19}F -nmr studies (165)), the results of Table 32

* A "chemically inert" substituent is one that is not itself an HBA site and which reduces the weak HBA tendency of the benzene ring.

indicate that none of the weaker strongly self-associated HBD solvents detectably affect the ring positions of **43**. This is shown by the following analysis of results. The *para* carbon shifts relative to the *ortho* or *meta* carbon of **43**, designated as $\int_{o-CF_3}^{p-CF_3} = \int_H^{p-CF_3} - \int_H^{o-CF_3}$ and $\int_{m-CF_3}^{p-CF_3} = \int_H^{p-CF_3} - \int_H^{m-CF_3}$, respectively, give excellent correlations with previously established π^* values for "select" solvents and strongly self associated HBD solvents (aliphatic alcohols), with s values that are of sufficient magnitudes to be useful. Furthermore, it will be noted that, in contrast to the shifts referenced to benzene, $\int_{m-CF_3}^{p-CF_3}$ shifts in acetic acid, formic acid, and trifluoroacetic acid are *strikingly* similar to those for their corresponding methyl esters. Likewise, these shifts can be seen to be very similar to trifluoroethanol, hexafluoroisopropanol and ethanol, and for formamide and dimethylformamide, a rational result only if variations in $\int_{m-CF_3}^{p-CF_3}$ shift values are determined by solvent polarities only (no type-A hydrogen bonding contributions).

The correlations of the $\int_{o-CF_3}^{p-CF_3}$ and $\int_{m-CF_3}^{p-CF_3}$ shifts with solvent π values are

$$\int_{o-CF_3}^{p-CF_3} (\mathbf{43}) = 6.09 + 1.51 \pi \text{ ppm} \quad (99)$$

$n = 18$ (except solvents **21, 30, 32, 50, 56, 113, 114, 201, 203**), $r = 0.996$,
and $\sigma = 0.02$ ppm

$$\int_{m-CF_3}^{p-CF_3} (\mathbf{43}) = 2.80 + 0.48 \pi \text{ ppm} \quad (100)$$

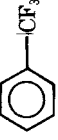
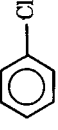
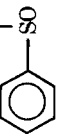
$n = 21$, $r = 0.988$, $\sigma = 0.03$ ppm

We have used Equations 99 and 100 to back-calculate π^*_i (π^*_1 and π^*_2) values which are assembled in Table 33.

It is to be noted that excellent agreement is found between π^*_1 and π^*_2 results and the earlier π^* values for the following 21 solvents: *n*-hexane, cyclohexane, triethylamine, isopropanol, dioxane, *n*-propanol, ethanol, tetrahydrofuran, ethyl acetate, methyl acetate, ethyl formate, ethanol, methyl orthoformate, 2-butanone, acetone, acetic anhydride, nitromethane, dimethylacetamide, dimethylformamide, sulfolane, and dimethyl sulfoxide. The aromatic and polychlorinated aliphatic solvents give lower π^*_1 and π^*_2 results than the uv-based π^* values (as expected in the light of the fact that these are really ($\pi^* + d\delta$) terms; all nmr shifts so far studied have involved negative d values in Equation 95).

However, it is of particular importance that the π^*_1 and π^*_2 results are also smaller than the earlier π^* values for the following solvents: *tert*-butanol, acetic acid, trifluoroethanol, ethylene glycol, and formamide, all relatively strong HBD solvents. These results strongly suggest that the initially obtained π^* values

TABLE 32
 C^{13} -NMR Shifts for Substituted Benzenes Relative to Internal Benzene (ppm)

Solvent						
	<i>p</i> -	<i>o</i> -	<i>p</i> -	<i>o</i> -	<i>p</i> -	<i>o</i> -
<i>n</i> -hexane	3.06	-2.92	-2.18	-2.92	1.70	-4.77
<i>c</i> -hexane	3.09	-2.94	-2.19	-2.94	1.78	-4.75
decalin	3.10	—	-2.13	—	—	—
(CF ₃) ₂ CHOH	3.12	-3.64	-1.97	-3.64	4.67	-4.22
CF ₃ CO ₂ H	3.16	-3.40	-2.02	-3.40	3.48	—
CCl ₄	3.21	-2.97	-2.08	-2.97	2.07	—
Et ₃ N	3.34	-2.94	-2.02	-2.94	1.86	—
CHCl ₃	3.35	-3.12	-1.91	-3.12	2.67	-4.77
CF ₃ CH ₂ OH	3.43	-3.37	-1.83	-3.37	4.06	-4.80
CF ₃ CO ₂ Me	3.61	-3.18	-1.78 (?) ^a	-3.18	2.35 (?) ^a	-4.41
CH ₂ Cl ₂	3.59	-3.05	-1.83	-3.05	2.52	-4.87 (?)
<i>i</i> -BuOH	3.59	-3.18	-1.83	-3.18	2.80	-4.85
dioxane	3.64	-3.04	-1.75	-3.04	1.13	-4.43
<i>n</i> -BuOH	3.64	-3.14	—	-3.14	1.94	-4.93
HOAc	3.73	-3.17	-1.73	-3.17	2.99	-4.47
<i>i</i> -PrOH	3.69	-3.18	—	-3.18	3.40	-4.02
C ₅ H ₅ N	3.71	-3.29	1.73	-3.29	3.04	-4.45
<i>n</i> -PrOH	3.71	-3.17	—	-3.17	2.18	—
HC(OEt) ₃	3.75	-3.18	-1.70	-3.18	3.10	-4.48
HCO ₂ H	3.78	-3.19	—	-3.19	—	—

THF	3.84	0.76	-3.09	-1.67	2.10	0.76	-4.85
C ₂ H ₅ OH	3.78	0.73	-3.12	-1.67	3.13	1.23	-4.48
EtOAc	3.80	0.75	-3.18	-1.62	2.13	0.86	-4.80
CH ₃ OH	3.83	0.73	-3.13	-1.62	3.26	1.34	-4.45
HCO ₂ Et	3.84	0.73	-3.13	—	—	—	—
MeOAc	3.86	0.76	-3.10	-1.62	2.13	0.86	-4.80
HCONH ₂	3.86	0.57	-3.45	-1.59	3.08	1.15	-4.53
FCH ₂ CH ₂ OH	3.86	0.67	-3.24	-1.53	3.26	1.24	-4.48
HC(OMe) ₃	3.88	0.75	-3.13	-1.59	—	—	—
CH ₃ NO ₂	3.88	0.67	-3.37	-1.57	2.51	0.94	-4.91
CF ₃ COCH ₂ COCH ₃	—	—	—	—	2.91	1.32	-4.56
CH ₃ CN	3.94	0.73	-3.29	-1.54	2.43	0.97	-4.88
2-butanone	3.96	0.86	-3.18	-1.51	2.27	0.92	-4.85
F ₂ CHCH ₂ OH	—	—	—	—	3.45	1.35	-4.37
acetone	4.00	0.85	-3.24	-1.55	2.29	0.91	-4.88
CH ₃ COCH ₂ COCH ₃	—	—	—	—	2.40	0.94	-4.85
Ac ₂ O	3.96	0.78	-3.25	-1.54	2.89 (?) ^a	1.14 (?) ^a	-4.47 (?)
CH ₃ O(CH ₂) ₂ OH	3.99	0.86	-3.24	-1.48	2.83	1.13	-4.53
(CH ₂ OH) ₂	4.03	0.82	-3.26	-1.51	3.37	1.35	-4.40
propylene carbonate	4.07	0.78	-3.21	-1.43	2.43	0.95	-4.90
sulfolane	4.16	0.86	-3.27	-1.37	2.43	1.03	-4.82
(EtO) ₃ PO	4.18	1.05	-3.20	—	—	—	—
DMF	4.21	0.97	-3.21	-1.38	2.32	0.94	-4.80
DMA	4.23	1.04	-3.19	-1.35	2.26	0.94	-4.83
DMSO	4.24	0.94	-3.29	-1.35	2.35	0.92	-4.77
HMPA	4.40	1.34	-3.25	-1.24	2.10	0.84	-4.78
86% (vol)H ₂ O-14% EtOH	—	—	—	—	3.75	1.38	-4.23

^a We question whether there may have been partial hydrolysis in these solvents.

for these solvents (33*b*) are not correct polarity measures but include some (α type) contributions from their hydrogen bond donor effects.

We have also carried out correlations of the $\int_H^{p-CF_3}$ (43) and \int_H^{p-Cl} (44) results with solvent π^* values, excluding only the data for the weakly self-associated HBD solvents:

$$\int_H^{p-CF_3} (43) = 3.11 + 1.22 \pi^* \text{ ppm} \quad (101)$$

$$n = 21, r = 0.993$$

and

$$\int_H^{p-Cl} (44) = -2.16 + 0.88 \pi^* \text{ ppm} \quad (102)$$

$$n = 20, r = 0.990^*$$

Values of π_3^* and π_4^* , back calculated by means of Equations 101 and 102 are included in Table 33.

The π_1^* to π_4^* results in Table 33 have been averaged to give a set of ^{13}C -nmr-based π^* values. We have compared these with the earlier set of π^* s, and for each solvent we have chosen a value (third data column of the table) which in our judgment best accomodates the total body of available experimental information. These are the results included in the comprehensive table of solvatochromic parameters at the end of the chapter (Table 35).

It is particularly to be noted that the recommended π^* values for many of the HBD solvents in Tables 33 and 35 are given in parentheses, indicating that we are still not completely comfortable with these results and consider them still subject to revision as additional information comes in. We are also particularly uncomfortable with the π^* value of 1.09 for water. This is because indicators 43 and 44 are insufficiently soluble in water to determine ^{13}C nmr spectra, so that the uv-based result has not at present been confirmed by other measurements.

It is also to be noted that the nmr-based π^*_i values for hexamethylphosphoramide (solvent 26, specifically excluded from the *select solvent set*) differ appreciably from the uv-based π^* . This solvent has been particularly troublesome. We have seen π^*_i values ranging from 0.5 to 1.2,** and when we have fixed on a π^* value of 0.87 in multiple-parameter least-squares correlations, we have seen β_i values ranging from 0.8 to 1.2.

* If we redo the correlations using the final recommended π^* values (third data column of Table 33) rather than the preliminary π^* s (second data column), the r values are only slightly improved.

** For example, Eq. 94*b*, which describes the solvatochromic behavior of Dimroth's betaine (28) in the *select solvent set*, gives $\pi^*_i = 0.723$ for hexamethylphosphoramide.

3. *The α Scale of Solvent HBD Acidity*

The purpose of the α scale is to provide a quantitative measure of the ability of a bulk solvent to act as a hydrogen bond donor toward a solute (71,166,167). Where type-B hydrogen bonding effects are excluded, as when solutes, reactants, or indicators are nonprotic, total solvatochromic equations for HBD solvents can take either of two forms: when all solvents are considered together,

$$XYZ = XYZ^0 + s(\pi^* + d\delta) + a\alpha \quad (103)$$

or when the families of solvents with similar polarizability characteristics are considered separately,

$$XYZ = XYZ_0 + s\pi^* + a\alpha \quad (104)$$

that is, Equation 42, $b = 0$. We have used equations in the form of Equation 104 with the method of multiple linear regression analysis in the construction of the revised α scale.

Problems Encountered in Determining α Values. Considerably greater difficulties were encountered in the formulation of the α scale than with the other solvatochromic parameter indexes. Complications were of three main types:

(a) The importance of the polarizability term, $d\delta$, was not known at the time of our initial efforts to evaluate HBD acidities. This caused us to consider the various classes of solvents together, when they might better have been treated separately.

(b) The incorrect assumptions (discussed previously) that type-A hydrogen bonding did not influence the solvatochromism of indicators 1–4 of Table 24, which led us to assign too-high π^* values to certain of the weakly self-associating HBD solvents, also led us to assign correspondingly too-low α values to those same solvents.

(c) Complications caused by the competition between self-association of amphiprotic HBA–HBD solvents and type-A bonding to HBA solutes, which have been alluded to in our earlier discussions, have frequently led to incorrect rankings of apparent HBD strengths.

In extreme examples of the latter effect, stronger HBD acids that can self-associate cause only minor solvatochromic effects, whereas larger effects are observed with weaker non-self-associating HBD solvents. Such a condition occurs when an indicator, which is a weak HBA base, has a property which is particularly sensitive to type-A hydrogen bonding interactions. The stronger HBD solvents achieve greater stability by remaining tied up with themselves, rather than by disrupting their self-association patterns to form hydrogen bonds to the solute. Thus, the aliphatic alcohols may remain as cyclic trimers or tetramers (114); benzyl alcohol and phenylethanol (which behave particularly

TABLE 33
Solvent Polarity Parameters from ^{13}C Shifts

Solvent	Earlier $\pi^{*a,b}$	Preliminary π^{*c}	Recommended π^{*d}	Eq. 99 π_1^*	Eq. 100 π_2^*	Eq. 101 π_3^*	Eq. 102 π_4^*	π_{ave}^*
<i>n</i> -hexane	-.08	-.08	-.08	-.07	-.01	-.04	-.02	-.04
cyclohexane	.00	.00	.00	-.04	-.05	-.02	-.03	-.01
decalin	—	—	—	—	.00	-.01	.03	.01
CCl ₄	.29	—	—	.05 ^e	.15 ^e	.06 ^e	.09 ^e	.08 ^e
Et ₃ N	.14	.14	.14	.13	.17	.16	.16	.14
CHCl ₃	.76	(.24 ^e)	—	—	.42 ^e	—	—	—
CH ₂ Cl ₂	.80	(.35 ^e)	—	—	.63 ^a	—	—	—
CF ₃ CO ₂ H	—	(.48)	—	—	.48	—	—	—
CF ₃ CO ₂ Me	—	(.44)	—	—	—	—	—	—
<i>t</i> -BuOH	[.53]	(.40)	(.41)	.45	.40	.38	—	.41
<i>i</i> -PrOH	[.51]	(.47)	.46	.52	.40	.46	—	.46
<i>n</i> -BuOH	[.50]	(.50)	.46	.45	.42	.43	—	.43
CH ₃ CO ₂ H	[.66]	(.62)	—	—	.58	—	—	—
dioxane	.55	—	—	.38	.54	.41	.47	—
pyridine	.87	—	—	—	(.73) ^e	—	—	—
<i>n</i> -PrOH	(.53)	(.50)	.51	.52	.48	.48	—	.50
HC(OEt) ₃	—	—	(.53)	.55	(.37) ^f	.52	.52	.53
(CF ₃) ₂ CHOH	—	(.65)	—	—	.65	—	—	—
C ₂ H ₅ OH	(.54)	(.54)	.54	.54	.52	.54	—	.54
CF ₃ CH ₂ OH	[1.02]	(.73)	—	—	.67	—	—	—
THF	.58	.58	.58	.56	.58	.59	.56	.56
EtOAc	.55	.55	.55	.59	.52	.56	.61	.57
MeOAc	.53	.56	.60	.58	.63	.61	.61	.60

HCO ₂ H	—	(.96)	—	(.96)	—	—	—
CH ₃ OH	(.59)	(.60)	.60	.59	.58	.61	.60
HCO ₂ Et	(~.60)	—	(.60)	.58	.60	—	.60
HC(OMe) ₃	.58	(.63)	.61	.63	.63	.65	.63
2-butanone	.67	(.67)	.67	.70	.69	.74	.69
acetone	.68	.68	.72	.72	.73	.69	.72
CH ₃ O(CH ₂) ₂ OH	—	—	(.71)	.66	.72	.77	.71
FCH ₂ CH ₂ OH	—	—	(.72)	.66	—	.72	.72
HOCH ₂ CH ₂ OH	[.93]	(.72)	(.73)	—	.72	.74	.73
Ac ₂ O	.76	(.74)	.76	.74	—	—	.76
CH ₃ CN	[.71]	(.76)	(.85)	—	—	—	.85
propylene carbonate	—	—	(.81)	.79	.79	.83	—
CH ₃ NO ₂	[.85]	(.80)	(.85)	—	—	—	.85
(EtO) ₃ PO	.72	—	—	.86	(.65) ^f	—	—
HCONH ₂	[1.12]	—	(.98)	—	1.02	—	—
CH ₃ CONMe ₂	.88	.88	.88	.88	.92	.92	.88
HCONMe ₂	.88	.88	.88	.88	.91	.93	.91
sulfolane	.98	—	.95	.89	.86	.90	.92
DMSO	1.00	1.00	1.00	.95	.93	.92	.97
HMPA	.87	—	—	1.04	1.07	1.05	1.05

^a From Refs. 33b and 148.

^b Square brackets, [], designate π^* value to be abandoned on the basis of the present results.

^c Preliminary π^* value used in the correlations leading to Eqs. 99–102.

^d Recommended π^* value based upon this and all previous work. A value given in parentheses, (), needs further confirmation before it is accepted as a primary value.

^e For polyhalogenated and aromatic solvents, these are probably ($\pi^* + \delta\delta$) terms.

^f Out-of-line values not included in averages.

erratically, sometimes acting in effect as non-hydrogen-bond donors) (115) may hydrogen bond to their own π systems (116); and formamide and acetic acid may remain as cyclic dimers. The weaker HBD solvents, CHCl_3 and CH_2Cl_2 (117,154), do not have this self-association option, and self-association complexes of CH_3CN (if any) are probably not cyclic. The latter solvents may therefore associate weakly with the solute and induce noticeable solvatochromic effects.

In more usual examples, often encountered where the solute undergoes type-A hydrogen bonding at multiple sites, the reversals of apparent solvent HBD strengths are not so dramatic. Moderately strong solvent-to-solute hydrogen bonds are sufficient to partially disrupt the solvent self-association patterns, but differing self-association equilibrium constants (114) lead to certain of the amphiprotic solvents seemingly exhibiting proper relative HBD strengths, while others fall out of line in their solvatochromic effects. In such instances, the aliphatic alcohols are usually well behaved,* with benzyl alcohol, ethylene glycol, acetic acid, and water most likely to fall out of line.

The least frequent instances of type-A solvation, but those which are best suited for the determination of the α_i values which are used in the formulation of the α scale, are those in which the indicator or reactant is such a strong HBA base that competitive self-association has only a minor influence on the $\Delta\Delta$ terms attributable to hydrogen bonding.

The complication caused by competitive self-association has introduced serious uncertainties in the determination and use of the solvent α values, and is probably a main reason why LSER's involving type-A hydrogen bonding and the α scale have usually been less precise than those involving type-B bonding and the β scale. We have seen many examples of breakdowns in correlation due to this effect which, while a complication, can be quite a revealing phenomenon if properly recognized.** In such instances, limited solvent effect relationships, involving only the monofunctional alkanols, have sometimes given satisfactory statistical correlations.

Requirements for Indicators. For the reasons cited previously, we felt that relatively stringent requirements should be fulfilled by the properties and reactivity parameters used in formulating the current version of the α scale (which

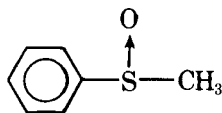
* A contributing factor here may be that the self-association equilibrium constants may also be very nearly linear with solvent α values for the aliphatic alcohols.

** For example, in a plot of ν_{max} values for N,N-diethyl-4-nitroaniline against results in corresponding solvents for 4-nitroanisole, the data points for benzyl alcohol and 2-phenylethanol fall directly on the regression line for non-HBD solvents (behaving, in effect as nonhydrogen-bond donors), while the data points for other alcohols are displaced from that line due to a $-\Delta\Delta\nu(2-4)_{O_2N}$ effect. This seems to us to be strong evidence that inter- or intramolecular hydrogen bonding by benzyl alcohol and 2-phenylethanol to their own π systems is stronger than intermolecular hydrogen bonding to oxygen in a self-association complex (115).

supersedes the version in Refs. 166 and 167) and we have established the following criteria of suitability: (a) The properties should involve sufficiently strong HBA reactants or indicators that competitive solvent self-association should not materially influence the $\Delta\Delta$ terms (the enhanced solvatochromic effects due to hydrogen bonding). (b) Ratios of the \mathbf{a}/\mathbf{s} terms in Equation 104 should not be too low (i.e., \mathbf{a}/\mathbf{s} necessarily >0.6 and preferably >1.0) so that uncertainties in the π^* values, which (as has been abundantly demonstrated) are necessarily less reliable for the HBD than for the non-HBD solvents, should not introduce unacceptable uncertainties in the α values.

We have chosen 16 diverse properties involving 13 indicators which meet these criteria for the construction of the α scale. As before, α values were arrived at by a process of successive approximations. Preliminary correlation equations for a few XYZs involving only unquestioned π^* and α values in Equation 104 were used to back-calculate a larger preliminary set of α values. These were then used in a further set of multiple-parameter least-squares fits to arrive at the regression equations that are described below. These regression equations were then used to back-calculate the 16 sets of α_i values that are assembled in Table 34, the latter, in turn, being averaged to arrive at the α_{1-16} values in Table 34 and the comprehensive table of solvatochromic parameters (Table 35). We next describe the 16 properties and correlation equations *seriatim*, pausing along the way to discuss any features of the solvatochromic equations that may illuminate aspects of the chemistry involved.

(45a-d) $^{13}\text{C-NMR}$ Shifts of Phenyl Methyl Sulfoxide. Phenyl methyl sulfoxide (**45**) is a strong hydrogen bond acceptor indicator, for which $^{13}\text{C-nmr}$ shifts (Table 32) arise predominantly from charge transferred by HBD solvents via type-A hydrogen bonding.



45

The data of Table 32 have been used to arrive at four distinct sets of shifts for **45**: **(45a)** the *para*-carbon shift of **45** referenced to the *meta*-carbon of benzo-trifluoride (**43**), that is, $\int_{m-CF_3}^{p-SOCH_3}(\mathbf{45a}) = \int_H^{p-SOCH_3}(\mathbf{45}) - \int_H^{m-CF_3}(\mathbf{43})$; **(45b)** the *para*-carbon shift of **45** referenced to the *para*-carbon of **43**, that is, $\int_{p-CF_3}^{p-SOCH_3}(\mathbf{45b}) = \int_H^{p-SOCH_3}(\mathbf{45}) - \int_H^{p-CF_3}(\mathbf{43})$; **(45c)** the *para*-carbon shift of **45** referenced to its own *ortho*-carbon shift, that is, $\int_{o-SOCH_3}^{p-SOCH_3}(\mathbf{45c}) = \int_H^{p-SOCH_3}(\mathbf{45}) - \int_H^{o-SOCH_3}(\mathbf{45})$; and **(45d)** the *para*-carbon shift of **45** referenced to its own *meta*-carbon shift, that is, $\int_{m-SOCH_3}^{p-SOCH_3}(\mathbf{45d}) = \int_H^{p-SOCH_3}(\mathbf{45}) - \int_H^{m-SOCH_3}(\mathbf{45})$. The individual correlation equations with π^* and α , determined by the method

TABLE 34
Construction of the α Scale of Solvent HBD Acidities

Solvent	α_1	Eq.	α_2	Eq.	α_3	Eq.	α_4	Eq.	α_5	Eq.	α_6	Eq.	α_7	Eq.	α_8	Eq.	α_9	Eq.	α_{10}	Eq.	α_{11}	Eq.	α_{12}	Eq.	α_{13}	Eq.	α_{14}	Eq.	α_{15}	Eq.	α_{16}	π		
16. 2-butanone	.03	.04	[.16]	.07	—	—	—	—	—	—	—	—	—	—	—	—	—	—	—	—	—	—	—	—	—	—	—	—	—	—	—	.05 \pm .02	5	
18. acetone	.08	.06	[.22]	.11	[-.02]	.11	.09	.08	[-.01]	.05	.03	.05	.05	.06	.12	—	—	—	—	—	—	—	—	—	—	—	—	—	—	—	—	—	.07 \pm .02	13
50. MeCN	.27	.23	.24	.19	—	.27	.27	.22	.28	—	.20	.25	.23	—	.20	.22	—	—	—	—	.20	.22	—	—	—	—	—	—	—	—	—	—	.24 \pm .03	13
32. MeNO ₂	.38	.37	.45	.33	.25	—	—	.36	[.10]	[.05]	.21	—	.28	—	.19	.30	.07	9	—	—	—	—	—	—	—	—	—	—	—	—	—	.30 \pm .07	9	
101. <i>t</i> -BuOH	.66	.66	.53	.67	—	.51	[.30]	—	[.44]	[.41]	—	.59	.57	—	.71	.67	—	—	—	—	—	—	—	—	—	—	—	—	—	—	—	.63 \pm .06	9	
102. <i>i</i> -PrOH	.77	.81	.81	.75	—	.73	[.44]	.75	.66	.76	.77	.77	.75	.75	.71	.71	—	—	—	—	—	—	—	—	—	—	—	—	—	—	—	.73 \pm .05	14	
103. <i>n</i> -BuOH	.79	.83	.77	.72	—	.80	.74	.75	.80	.80	—	.81	.74	.81	.89	—	—	—	—	—	—	—	—	—	—	—	—	—	—	—	—	.75 \pm .06	13	
112. <i>n</i> -PrOH	.84	.76	.92	.81	—	.80	.75	.79	.84	.82	—	.81	.80	.82	—	—	—	—	—	—	—	—	—	—	—	—	—	—	—	—	—	.81 \pm .03	12	
104. EtOH	.83	.84	.91	.80	—	.87	.84	.88	.92	.85	.85	.86	.89	.82	.84	.80	—	—	—	—	—	—	—	—	—	—	—	—	—	—	—	.85 \pm .03	15	
105. MeOH	.94	.94	1.00	.93	.97	1.04	1.06	1.00	.92	.97	.95	1.00	1.03	1.00	.98	.99	.99	—	—	—	—	—	—	—	—	—	—	—	—	—	—	.98 \pm .04	16	
107. HOCH ₂ CH ₂ OH	.97	.96	.98	1.02	—	.96	.97	.95	.99	.95	—	.96	—	.97	.96	1.04	—	—	—	—	—	—	—	—	—	—	—	—	—	—	—	.97 \pm .03	13	
111. H ₂ O	—	—	.96	1.35	—	1.01	—	1.07	—	—	—	1.11	1.07	1.10	—	1.12	1.21	(1.12 \pm .10)	9	—	—	—	—	—	—	—	—	—	—	—	—	—	—	—
113. CF ₃ CH ₂ OH	1.92	1.92	2.02	1.88	—	—	—	—	—	—	—	—	—	—	—	—	—	—	—	—	—	—	—	—	—	—	—	—	—	—	—	—	1.55 (1.86 \pm .12)	5
114. (CF ₃) ₂ CHOH	2.66	2.68	2.60	2.73	—	—	—	—	—	—	—	—	—	—	—	—	—	—	—	—	—	—	—	—	—	—	—	—	—	—	—	—	2.19 (2.57 \pm .15)	5
204. HCONH ₂	.93	.87	.69	.84	.84	.88	—	—	—	—	—	—	—	—	—	—	—	—	—	—	—	—	—	—	—	—	—	—	—	—	—	—	.73	
201. CH ₃ CO ₂ H	1.13	1.14	.70	1.21	—	—	—	—	—	—	—	—	—	—	—	—	—	—	—	—	—	—	—	—	—	—	—	—	—	—	—	—	.80 \pm .06	12
115. FCH ₂ CH ₂ OH	—	—	—	.99	1.00	—	—	—	—	—	—	—	—	—	—	—	—	—	—	—	—	—	—	—	—	—	—	—	—	—	—	—	(1.01 \pm .18)	5
203. CF ₃ CO ₂ H	—	—	—	—	—	—	—	—	—	—	—	—	—	—	—	—	—	—	—	—	—	—	—	—	—	—	—	—	—	—	—	—	(1.00 \pm .01)	2

^a Square brackets, [], denote results excluded in taking average α .

^b Parentheses, (), denote α_{1-16} values which are particularly uncertain.

Note: This Table has been out-dated by additional results, cf reference 108. Revised π^* and α values are listed in Table 35.

of multiple linear regression analysis are as follows:

$$^{13}\text{C}-\int_{m\text{-CF}_3}^{p\text{-SOCH}_3} \text{ (45a) } = 1.44 - 0.00 \pi^* + 1.15 \alpha \text{ ppm} \quad (105)$$

$$n = 11, r = 0.994, \sigma = 0.07 \text{ ppm, (a/s} = \infty)$$

$$^{13}\text{C}-\int_{p\text{-CF}_3}^{p\text{-SOCH}_3} \text{ (45b) } = -1.38 - 0.50 \pi^* + 1.18 \alpha \text{ ppm} \quad (106)$$

$$n = 11, r = 0.996, \sigma = 0.05 \text{ ppm, (a/s} = -2.36)$$

$$^{13}\text{C}-\int_{o\text{-SOCH}_3}^{p\text{-SOCH}_3} \text{ (45c) } = 6.56 + 0.62 \pi^* + 0.78 \alpha \text{ ppm} \quad (107)$$

$$n = 22, r = 0.990, \sigma = 0.09 \text{ ppm, (a/s} = 1.26)$$

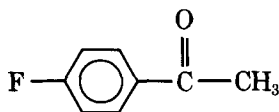
and

$$^{13}\text{C}-\int_{m\text{-SOCH}_3}^{p\text{-SOCH}_3} \text{ (45d) } = 1.05 + 0.38 \pi^* + 0.72 \alpha \text{ ppm} \quad (108)$$

$$n = 12, r = 0.990, \sigma = 0.05 \text{ ppm, (a/s} = 1.89)$$

Solvatochromic Equations 105 and 106 are particularly noteworthy, the former because it indicates that property **45a** shows almost no dependence on solvent polarity (which, in the light of our earlier experience, makes it a particularly attractive and unambiguous indicator for α), and the latter because it is one of relatively few properties for which **a** and **s** in Equation 104 are of opposite signs. It is also quite significant that the r values for these correlations are among the highest that we have encountered. Values of α_1 to α_4 for the HBD solvents, back-calculated from Equations 105–106, are included in Table 34.

(46) ^{19}F -NMR Shift of 4-Fluoroacetophenone. 4-Fluoroacetophenone (**46**) is also a reasonably strong HBA base indicator, for which ^{19}F -nmr



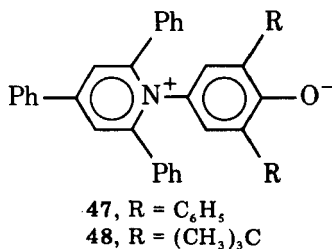
46

shifts, referenced to internal fluorobenzene, were determined in an earlier study (163). This property is also nicely correlated by a linear combination of π^* and α ,

$$^{19}\text{F}-\int_H^{p\text{-COCH}_3} \text{ (46) } = 6.09 + 0.70 \pi^* + 1.17 \alpha \text{ ppm} \quad (109)$$

$$n = 11, r = 0.982, \sigma = 0.11 \text{ ppm, (a/s} = 1.67)$$

(47,48) *Electronic Spectra of Dimroth's Betaines.* We have mentioned earlier that Dimroth and co-workers " $E_T(30)$ " scale, (34a), based on solvent effects on the lowest energy band of 4-(2,4,6-triphenylpyridinium)-2,6-diphenylphenoxide (47), is the most frequently cited measure of the polarity of pure bulk solvents, and we have already pointed out that " $E_T(30)$ " values correlate better with π^* values of nonprotic solvents when families of solvents with similar polarizability characteristics are treated separately.



In the present correlations with π^* and α (as in all 16 correlations leading to the α scale) only aliphatic solvents are considered, so that fits to Equation 105 can be carried out directly by the method of multiple linear regression analysis.

Based on results in 19 solvents (11,13,18,19,23,25,29,50,52,61,101,-102,103,104,105,107,111,112,204, except 9,34; Table 10),* the multiple linear regression equation for the "solvatochromiebande" of 47 is

$$\begin{aligned}
 "E_T(30)" = E_T(47) &= 29.35 + 16.3 \pi^* + 15.8 \alpha \text{ kcal mole}^{-1} \quad (110) \\
 r &= 0.993, \sigma = 0.89 \text{ kcal mole}^{-1} (\text{a/s} = 0.97)
 \end{aligned}$$

The signs of the solvatochromic coefficients in Equation 110 are consistent with an electronic transition from a ground state resembling 28a to an electronic excited state more closely resembling 28b. Charge delocalization in the electronic excitation leads to the +s terms; weakening of the hydrogen bond to phenoxide oxygen in the excitation leads to the +a term, that is, a + $\Delta\Delta\nu(47-\pi^*)^A_{\leftarrow-O-A}$ solvatochromic effect.

The appreciable a/s ratio in Equation 110 indicates that the " $E_T(30)$ " scale, usually considered to be a generalized measure of solvent polarity, is for protic solvents at least as much a measure of solvent hydrogen bond donor ability. On reviewing the literature on correlations with the " $E_T(30)$ " solvent polarity scale in light of Equation 110, it becomes evident that the best linear fits have been with properties that coincidentally have had a/s ratios near that for 47. Thus, the widespread acceptance of the " $E_T(30)$ " scale has resulted in part from

* A number of the E_T values for the less polar solvents in Table 10 were not determined from the spectrum of 47, but were based on secondary correlations with " $E_T(30)$." These are not included in the correlation.

its excellent linearity with Kosower's Z values for corresponding solvents (discussed subsequently). The relatively similar a/s ratios of 0.97 for " $E_T(30)$ " and 1.06 for Z account for the fact that, even though both scales incorporate strong effects of type-A hydrogen bonding by HBD solvents, Dimroth and Reichardt observed excellent, though purely fortuitous, correlations between the two "polarity" measures.

The same workers (34a) have also described solvent effects on the spectra of 4-(2,4,6-triphenylpyridinium)-2,6-di-*tert*-butylphenoxide (**48**). The total solvatochromic equation for this betaine in 13 solvents (**9,11,13,18,25,29,50,61,103,104,105,107,112**; except **101,102**, see below) is

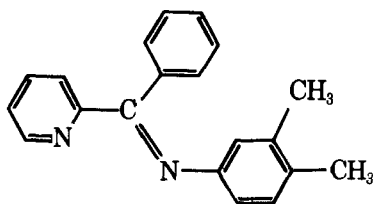
$$E_T(\mathbf{48}) = 28.21 + 12.4 \pi^* + 14.4 \alpha \text{ kcal mole}^{-1} \quad (111)$$

$$r = 0.993, \sigma = 0.75 \text{ kcal mole}^{-1}, (a/s = 1.16)$$

The somewhat different a/s ratios for **47** and **48** account for the curvature noted by Dimroth and co-workers when they plotted $E_T(\mathbf{47})$ against $E_T(\mathbf{48})$. Also, the relative a and s values in Equations 110 and 111 appear to conform with an observation we have made in other correlations, that is that sterically insulating a chromophore from its cybotactic environment seems to lessen nonspecific polarity effects to a greater extent than specific hydrogen-bonding effects.

Equations 110 and 111 have been used to back-calculate α_6 and α_7 values in Table 34. Following Dimroth's suggestion that hydrogen bonding by *t*-butanol (**101**) and isopropanol (**102**) to the phenoxide oxygen is particularly sterically hindered by the *ortho t*-butyl groups, we have excluded the α_7 s for these solvents from the α_{1-16} averages.

(49) **Electronic Spectra of $[\text{Fe}(\text{LL})_2(\text{CN})_2]^0$** . Burgess (109) has described solvent effects on the metal to ligand C.T. band in the spectrum of bis[α -(2-pyridyl)benzylidene-3,4-dimethylaniline]bis(cyano)iron(II) (**49**), which can be represented by $[\text{Fe}(\text{LL})_2(\text{CN})_2]^0$, where LL is **49a**.



49a

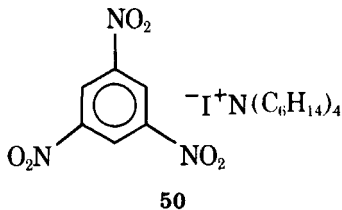
Results in 13 aliphatic solvents (**7,18,25,29,32,50,102,103,104,105,109,111,112**) correlate well with π^* and α ,

$$\nu(\mathbf{49})_{\max} = 14.02 + 0.98 \pi^* + 1.56 \alpha \text{ kK} \quad (112)$$

$$r = 0.999, \sigma = 0.04 \text{ kK}, (a/s = 1.59)$$

The differing a/s ratios in Equations 110 and 112 account for Burgess' observation that the data points formed two separate regression lines for protic and nonprotic solvents when $\nu(49)_{\max}$ was plotted against " $E_T(30)$." We have used Equation 112 with Burgess' data to generate the α_8 values in Table 34.

(50) **1,3,5- $C_6H_3(NO_2)_3 \cdot (C_6H_{14})_4N^+I^-$ Charge Transfer Band.** Davis (110) has reported solvent effects on the I^- to TNB charge transfer band of the 1,3,5-trinitrobenzene-tetra-*n*-hexylammonium iodide complex (50).



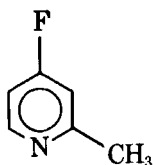
The total solvatochromic equation for 11 aliphatic solvents (7,11,13,18,29,50,102,103,104,105,107,112; except 32,101) is,

$$\begin{aligned} \nu(50)_{\max} &= 20.03 + 1.79 \pi^* + 6.22 \alpha \text{ kK} & (113) \\ r &= 0.993, \sigma = 0.37 \text{ kK}, (a/s = 3.47) \end{aligned}$$

The very much larger a/s ratio for $\nu(50)_{\max}$ than for either " $E_T(30)$ " or Z explains why Davis observed poor correlation when he plotted his results against these latter parameters.

The signs and magnitudes of the a and s terms of Equation 113 are consonant with an iodide to trinitrobenzene electron transfer in the electronic excitation, the positive s term being due to charge delocalization in the excited state, and the positive a term resulting from a $+\Delta\Delta\nu(50-\pi^*)^{\downarrow}_{-I}$ effect; that is, a weakening of the hydrogen bond to iodide as charge is delocalized into the TNB ring. We have occasion later to compare the magnitude of the s term for this ($I^- \rightarrow$ neutral molecule) charge transfer band with that for an ($I^- \rightarrow$ positive ion) C.T. band. The α_9 values in Table 34 were back-calculated through Equation 114.

(51) **^{19}F -NMR Shifts of 4-Fluoro-2-picoline.** ^{19}F -nmr shifts of 4-fluoro-2-picoline relative to internal fluorobenzene have been reported by Giam and Lyle (111) in a number of HBD and non-HBD aliphatic solvents.



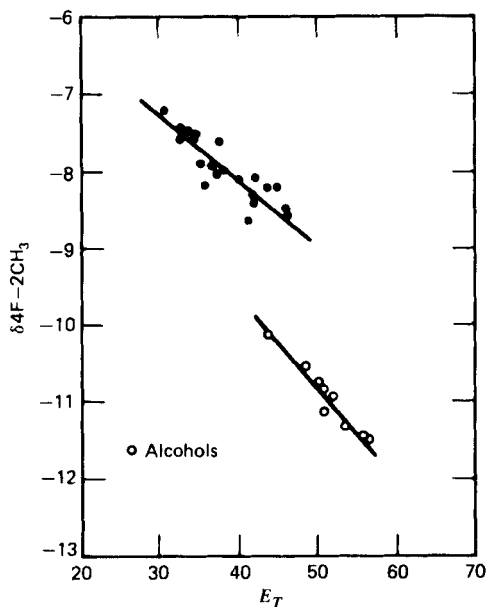


Figure 24 Plot of the solvent induced ^{19}F shifts of 4-fluoro-2-picoline (**51**) (relative to internal fluorobenzene) vs. " $E_T(30)$."

The correlation equation with π^* and α of their results in 13 of these solvents (**1,2,7,11,13,18,29,102,103,104,105,107,112**; except **25,32,101**) is

$$\delta(\mathbf{51}) = -7.25 - 0.95 \pi^* - 3.76 \alpha \text{ ppm} \quad (114)$$

$$r = 0.998, \sigma = 0.11 \text{ ppm, (a/s} = 3.96)$$

As with a number of the other properties discussed here, Giam and Lyle found their data points separating into two families of solvents, protic and nonprotic, when they plotted $\delta(\mathbf{51})$ against " $E_T(30)$." Because their results are quite typical of the correlational situation encountered by many workers when they compared two properties having different $\mathbf{a/s}$ ratios in Equation 104, their plot is shown here as Fig. 24.

(**52**) *Gutmann's Acceptor Number (AN)*. Mayer, Gutmann, and Gerger (112) have used infinite dilution ^{31}P -nmr shifts of triethylphosphine oxide (**52**) as the basis for what they describe as "Acceptor Number (AN), a quantitative empirical parameter for the electrophilic properties of solvents" (the conversion factor is $-\delta_{\infty}^{\text{corr}} = \text{AN}/2.349$). For protic solvents AN is intended to serve as a measure of HBD acidity; for nonprotic solvents it is seemingly intended as a measure of Lewis-type acidity. Compared with α values which range from 33.5 to 41.3 for the aliphatic alcohols, AN values of representative non-HBD solvents are: THF, 8.0; ethyl acetate, 10.8; DMSO, 19.3. Thus, the latter solvents are

considered to have reasonably strong Lewis acid-type electron acceptor properties. Together with a scale of "Donor Numbers (DN)," measures of solvent nucleophilicity which, for most solvents, correlate reasonably well with our β scale, the AN scale was intended to correlate solution properties through a generalized two-parameter equation.

This AN solvent parameter scale is of interest to us in that, whereas in many other instances we have found that solvent property scales intended to serve as measures of solvent polarity, that is, π^* -equivalent, were in fact measures of combined polarity and HBD acidity properties, that is, equivalent to a linear combination of π^* and α (as has been shown for " $E_T(30)$ " and will be shown for Z , χ_R , and A_N), here we have a property intended as an electrophilicity measure, that is, α -equivalent, which is also, in fact, a combined function of π^* and α .

Thus, when only data for aliphatic *non-HBD* solvents are considered, the AN results show statistically respectable linear regression with solvent π^* values:

$$\text{AN} = 15.15 \pi^* + 0.64, r = 0.933, \sigma = 2.1 \quad (115a)$$

If the datum for hexamethylphosphoramide (solvent **26** which, as has been mentioned, frequently misbehaves) is excluded, the r value goes up to 0.960.

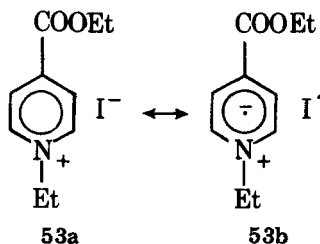
Combining the results in 16 HBD and non-HBD solvents (**1,7,9,11,13,18,23,25,29,28,50,102,104,105,111,204**; except **26,32,201**), the correlation equation with π^* and α is

$$\text{AN} = 0.16 + 16.7 \pi^* + 32.9 \alpha \quad (115b)$$

$$r = 0.996, \sigma = 1.54, (\text{a/s} = 1.97).$$

The α_{11} values in Table XXXIV were back-calculated through Eq. 115b.

(53) **Kosower's Z Scale.** Another widely used dye indicator polarity scale is Kosower's Z index (168), based on energies (in kilocalories per mole) for the charge transfer band of N-ethyl-4-carbethoxypyridinium iodide (**53**), an electronic transition from a ground state like **53a** to an excited state more closely resembling **53b**.



Z values in 14 solvents (18,25,29,50,101,102,103,104,105,107,111,112,201,204; Table 8), when correlated with π^* and α , lead to the multiple linear regression equation,

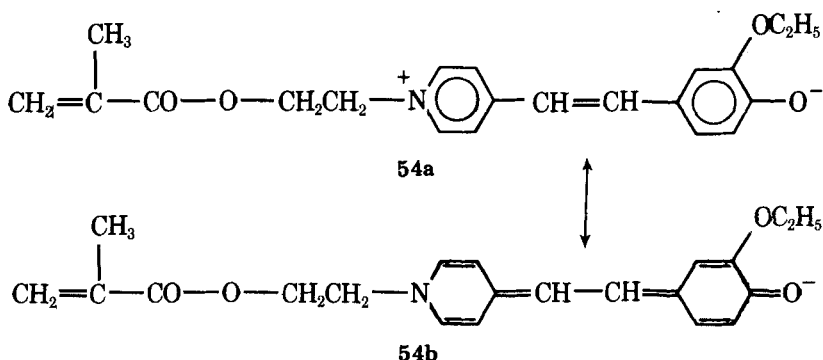
$$Z = E_T(\mathbf{53}) = 51.46 + 19.4 \pi^* + 20.5 \alpha \text{ kcal mole}^{-1} \quad (116)$$

$$r = 0.998, \sigma = 0.52 \text{ kcal mole}^{-1}, (\mathbf{a/s} = 1.06)$$

The α_{12} values in Table 34 were back-calculated from the Z values through Equation 116.

It is of interest to compare the solvatochromic parameters for $\nu(\mathbf{53})_{\max}$ with those for $\nu(\mathbf{50})_{\max}$ discussed earlier. Expressed in kK (1 kcal mole⁻¹ = 2.86 kK), the s and a values for **53** are 6.68 and 7.16, compared with $s = 1.79$ and $a = 6.22$ for **50**. Thus, whereas the a values are about the same for the two C.T. transitions, the s value is about four times as high for **53** as for **50**. This is consistent with spectral absorption where for **50** the transition (in its extreme termini) is from a charge-concentrated I⁻ and a charge-neutral TNB to a charge-neutral I and a charge-diffuse TNB⁻, whereas the transition for **53** is from a charge-concentrated I⁻ and a charge-diffuse 4-EtOOC-C₅H₄N⁺-Et to two charge-neutral moieties (**53b**). Hence, there is much more dissipation of charge in the **53a**($h\nu$)→**53b** electronic transition, with the correspondingly greater dependence on solvent polarity.

(**54**) E_T for Another Betaine. The next property correlated, leading to the α_{13} values in Table 34, is the transition energy for the intramolecular C.T. band of 1-(2-methacryloyloxyethyl)-4-(3-ethoxy-4-oxystyryl)-pyridinium betaine (**54**), as reported by Strop, Mikes, and Kalal (113).



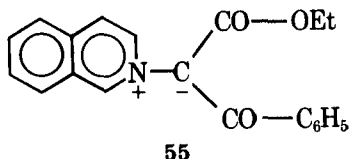
Based on results in 14 solvents (11,16,18,25,29,50,101,102,103,104,-105,111,112,205; except 9,32), the total solvatochromic equation for this betaine is

$$E_T(\mathbf{54}) = 39.86 + 9.14 \pi^* + 8.52 \alpha \text{ kcal mole}^{-1} \quad (117)$$

$$r = 0.995, \sigma = 0.39 \text{ kcal mole}^{-1} (\mathbf{a/s} = 0.93)$$

The positive signs of **a** and **s** suggest a more delocalized charge and a weaker hydrogen bond in the excited state, and are thus consistent with a **54a**($h\nu$) \rightarrow **54b** electronic transition, rather than vice versa. Also, Strop and co-workers found that their E_T (**54**) results were nicely linear with Dimroth's " $E_T(30)$," as is quite reasonable on the basis of the similar **a/s** ratios for the two electronic transitions.

(55) **Intramolecular C.T. Transition in an Isoquinolinium Ylide.** Dorohoi and his co-workers (119) have described solvent effects on the transition energies of a series of isoquinolinium ylides, including **55**.



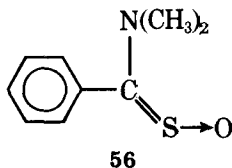
Solvent effects on this property are exceedingly well correlated by π^* and α , the total solvatochromic equation based on results in 11 solvents (**11,18,29,101,102,103,104,105,107,112,201**) being

$$E_T(\mathbf{55}) = 61.07 + 4.47 \pi^* + 8.64 \alpha \text{ kcal mole}^{-1} \quad (118)$$

$$r = 0.999, \sigma = 0.18 \text{ kcal mole}^{-1} (\mathbf{a/s} = 1.93)$$

Poor correlation of E_T (**55**) with Kosower's Z was observed by these workers, as is consistent with the almost doubled **a/s** ratio for **55** compared with **53**. We have used Equation 118 with the E_T (**55**) values to back-calculate the α_{14} values in Table 34.

(56) **The "S-Oxide" Band of *N,N*-Dimethylthiobenzamide-S-oxide.** Solvent effects on an electronic transition which they characterize as an "S-oxide band" of **56** have been reported by Walter and Bauer (120) and are the basis for the α_{15} results in Table 34.



The total solvatochromic equation for this band in 15 aliphatic solvents (**2,3,9,18,25,26,29,101,102,103,104,105,107,111,201**; except **204**) is

$$E_T(\mathbf{56}) = 80.1 + 1.65 \pi^* + 4.90 \alpha \text{ kcal mole}^{-1} \quad (119)$$

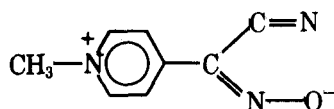
$$r = 0.990, \sigma = 0.10 \text{ kcal mole}^{-1} (\mathbf{a/s} = 2.97)$$

The large **a/s** ratio for **56** suggests that hydrogen bonding is to the oxygen

rather than to the amide nitrogen, and the positive sign of \mathbf{a} suggests hydrogen bond weakening in the excited state. Hence, electron migration in the electronic excitation must be away from oxygen.

In company with many already discussed, these workers found acceptable correlations with " $E_T(30)$ " only when the solvents were divided into families of hydrogen bond donors and non-hydrogen-bond donors, $r = 0.978$ in both instances. Again, this is consonant with the differing $\mathbf{a/s}$ ratios in Equations 110 and 119.

(57) *4-Cyanoformyl-1-methylpyridinium Oximate C.T. Band.* The final property employed in the construction of the α scale is the more intense of two *C.T.* bands in the spectrum of 57, reported by Mackay and Poziomek (121).



57

The total solvatochromic equation for 57 in 15 solvents (11,18,-29,50,102,104,105,111 (121); 3,7,25,32,101,107,201 (169)) is

$$E_T(57) = 67.8 + 7.51 \pi^* + 6.45 \alpha \text{ kcal mole}^{-1} \quad (120)$$

$$r = 0.992, \sigma = 0.70 (\mathbf{a/s} = 0.86)$$

Although the $\mathbf{a/s}$ ratio in Equation 120 is smaller than desired for a property used in constructing the α scale, it was included because it allowed independent confirmation of α for trifluoroethanol (solvent 113) and hexafluoroisopropanol (114), whose other α_i s were all based on the ^{13}C -nmr spectrum of phenyl methyl sulfoxide.

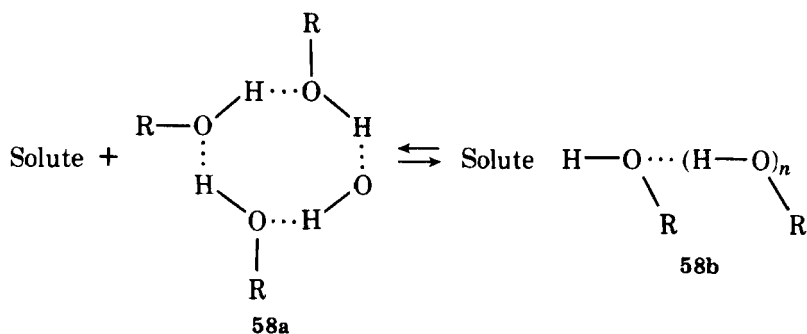
General Comments Regarding the α Scale. In constructing the α scale we were more concerned with arriving at equations that would yield accurate values of the α_i s than with demonstrating the statistical precision of the solvatochromic comparison method, so that we were more free in excluding individual results than had earlier been the case. If these results had been included, most r values would not have been as high as shown for Equations 109–120, but would still be quite respectable. The solvents most frequently excluded have been: *tert*-butanol (101), which is particularly susceptible to steric complications; nitromethane (32), whose effects may be strongly influenced by small amounts of the very acidic *aci*-nitromethane; acetic acid (204), which is very strongly self-associated (*vide infra*), and which also may act in specific situations as a proton transfer acid rather than as a hydrogen-bond donor acid; and hexamethylphosphoramide (26) whose troublesome behavior has already been mentioned. Further, when $\mathbf{a/s}$ ratios in the solvatochromic equations are high, solvent effects are strongly influenced by small amounts of hydroxylic impurities. In

the further correlations with π^* and α discussed subsequently, we exclude no results unless for specific reasons cited.

The 16 sets of α_i 's, determined as discussed previously have been averaged to obtain the α_{1-16} values which are included in Table 34 and in the comprehensive table of solvatochromic parameters (Table 35). We wish again to emphasize that we are not as comfortable with many of these as with the π^* and β values, and that they remain subject to further revision as additional results come in.

Some points of interest regarding ordering of the HBD acidities are as follows: (a) α_{1-16} values of monofunctional alcohols, R-OH, including trifluoroethanol and (probably) hexafluoroisopropanol, but not including water, correlate well with σ_I values for the substituents, R. It is particularly significant that the α value for water is lower than called for by the inductive order. (b) The HBD carbon acids, CH_3R (2-butanone, acetone, acetonitrile, nitromethane) also have α values that correlate well with σ_I of R. (c) The α values of $\text{CH}_3\text{CO}_2\text{H}$ and $\text{CF}_3\text{CO}_2\text{H}$ increase with increasing acidity, but are both less than the α values for trifluoroethanol and (especially) hexafluoroisopropanol. (d) Hydrogen bond acidities are quite similar for methanol, water, and acetic acid, so that most of the differences in effects of these three solvents derive from their differing polarities and HBA basicities.

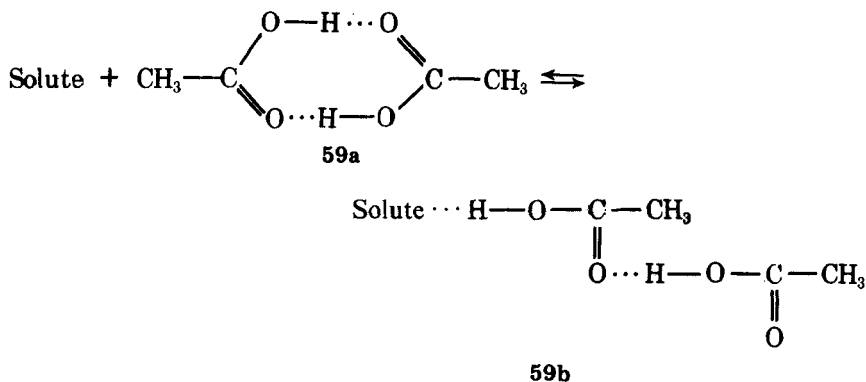
A Rationale for the Ranking of the α Values. We rationalize the ranking of the HBD acidities in terms of the differing structures of the self-associating solvent clusters. We have shown by solvatochromic dilution studies (134) that, in neat R-OH solvents, $(\text{R-OH})_n$ dimers or polymers are the type-B solvating species, and it is likely that similar considerations apply with type-A hydrogen bonding. For example, for hydrogen bonding by monofunctional alkanols, the dominant equilibrium probably takes the form,



The important aspect of structure **58b** is that the solvent hydroxyl group, whose proton serves as donor to the solute, acts on its oxygen as acceptor in a hydrogen bond with another R-OH molecule. Huyskens (170) has recently pointed out that, when an amphiprotic molecule acts simultaneously as hydrogen

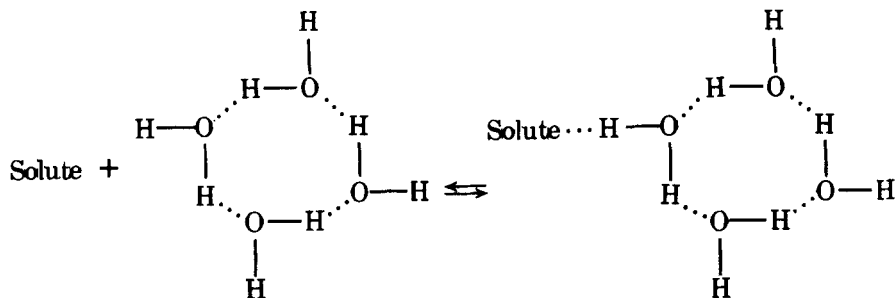
bond acceptor and donor at the same site, both the donor and acceptor strengths *are enhanced substantially* relative to the same species when acting only as acceptor or only as donor.

In the case of acetic acid solvent, the equilibrium can probably be represented by

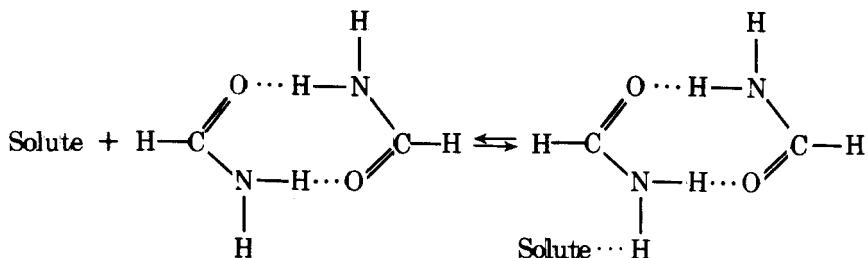


with the self-association complex of acetic acid (**59a**) substantially stronger than the alkanol self-association complex (**58a**). Again the acetic acid molecule acting as a hydrogen bond donor to the solute in **59b** is also acting simultaneously as an acceptor. Here, however, the acceptor site is two additional atoms removed from the donor site, with a consequently lessened HBD strengthening effect than in **58b**. We attribute the greater proclivity of acetic acid to fall out of line in solvatochromic comparisons to the stronger self-association in **59a** relative to **58a** and the lower than might be expected α (on the basis of relative proton transfer acidities) to the lesser HBD acid strengthening by the neighboring hydrogen bond in **59b** relative to **58b**.

With water and formamide, considerations of solvent structure suggest an entirely different rationale for the lower than expected α values. Here, minimization of free energy *in the total system* may be achieved by *retaining the primary solvent structure*, and having the solvent molecule form a *second* hydrogen bond to the solute, for example,



and



Huyskens has also shown that when a molecule forms two donor or acceptor hydrogen bonds at the same site, the second hydrogen bond is weaker than it would have been in the absence of the first such bond (170). Such a situation would very neatly explain the relative hydrogen bond strengths of **111**, **204**, and the monofunctional alkanols to HBA solutes.

4. Additional Correlations with π^* , α , and β

***t*-Butyl Chloride Solvolysis.** Solvent effects on the S_N1 solvolysis of *t*-butyl chloride (**60**) have been the subject of two important studies. Koppel and Pal'm (105) have extrapolated kinetics by various workers to 120°C and have reported rates in terms of a Y' factor, where $Y' = 1.800 [\log k_{\text{solvent}}^{120^\circ\text{C}} - \log k_{\text{gas phase}}^{120^\circ\text{C}}]$ kcal mole⁻¹. Data have been recorded in 11 aliphatic HBD and 6 non-HBD solvents for which π^* and α are known (**1,2,3,7,18,50,25,29,32,101,102,103,104,105,111,112,201**). Multiple-parameter least-squares correlation leads to the total solvatochromic equation,

$$Y' = 5.6 + 8.54 \pi^* + 7.06 \alpha \text{ kcal mole}^{-1} \quad (121)$$

$$r = 0.992, \sigma = 0.65 \text{ kcal mole}^{-1} (\mathbf{a/s} = 0.83)^*$$

Because Equation 121 is typical of many of the better correlations with π^* and α , a plot of Y' (observed) versus Y' (calculated) is shown in Fig. 25.

Abraham (44b) has assembled 25°C first-order rate constants for the same reaction in a number of solvents, of which 13 are aliphatic and of known π^* and α (**1,7,9,18,25,28,32,50,103,104,105,111,201**). The total solvatochromic equation for Abraham's data set is

$$\log k(\mathbf{60}) = -15.0 + 7.05 \pi^* + 5.01 \alpha \quad (122)$$

$$r = 0.995, \sigma = 0.36 (\mathbf{a/s} = 0.71)$$

* A Y' value of 24.1 was used for water. Arguments have been offered (71) that an alternative extrapolation of near-room-temperature results, leading to $Y' = 22.2$, might be equally appropriate. If the latter value is used, the r term becomes 0.994.

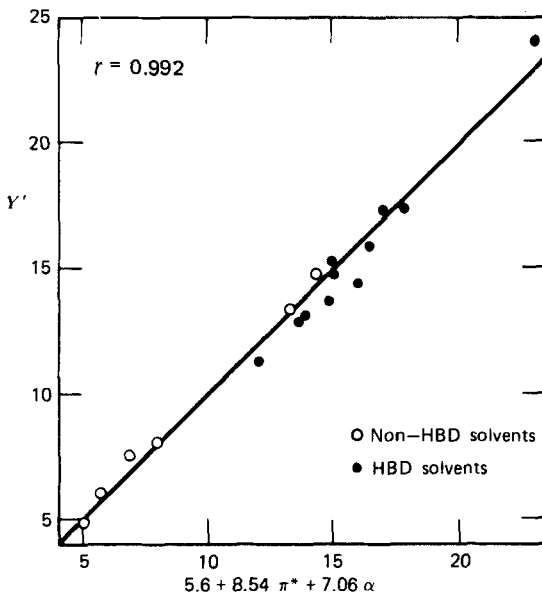


Figure 25 Observed vs. calculated Y' for *tert*-butyl chloride solvents.

The lower a and s values in Equation 121 compared with Equation 122 (a and s in Equation 121 must be divided by 1.8 for this comparison) undoubtedly reflect a temperature effect; the higher a/s ratio in Equation 121 appears to indicate that the temperature effect on the solvent polarity term is greater than that on the hydrogen bonding term.*

The correlations leading to Equations 121 and 122 are of considerable interest to us in the light of the large amount of attention devoted to *tert*-butyl chloride solvolysis in the 1950s (171), as well as the fact that Winstein and Grunwald, in their pioneering LSER studies (52,53) had based their Y scale of "solvent ionizing power" on solvent effects on the rate of this reaction. The solvatochromic coefficients in Equations 121 and 122 leave little doubt that there is significant rate acceleration in HBD solvents due to type-A hydrogen bonding to the leaving chlorine atom (in the terminology used by workers in this field (171), this corresponds to *electrophilic assistance* of S_N1 solvolysis). The a/s ratios of 0.83 for Y' and 0.71 for $\log k(60)$ provide measures of the relative sensitivities of this reaction to solvent polarity and solvent HBD acidity. They show, for example, that on going from acetone solvent to methanol, the $\Delta \log k(60)$ of 3.8 is due totally to the *electrophilic assistance* effect, whereas on going from methanol to water, the $\Delta \log k(60)$ of 4.6 is 83% due to solvent polarity and 17% due to *electrophilic assistance*.

* However, this comparison may involve placing more reliance than warranted on Koppel and Pal'm's extrapolations to 120°C.

Although the participation of electrophilic assistance in S_N1 and S_N2 solvolyses has long been suspected (51,52) most treatments of solvent effects on solvolytic reactions, including that of Schleyer and co-workers as recently as 1976 (171), have been on the implicit assumption that a single mY term accounts adequately for each reactant's sensitivity to both general solvent power and specific electrophilic solvation of the leaving group. Schleyer et al. have expressed concern that this assumption might not be justified, and our findings offer abundant reason for such concern.

Further, we have found that for *tert*-butyl bromide solvolysis (61), based on Abraham's collection of rate data (44b) (solvents 18,25,28,32,104,105,111,201) at 25°C, the total solvatochromic equation for aliphatic solvents is

$$\log k(61) = -12.72 + 7.81 \pi^* + 3.57 \alpha \quad (123)$$

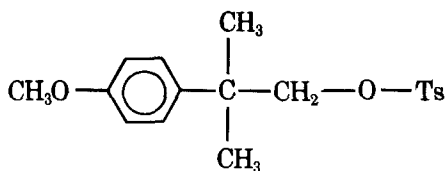
$$r = 0.992, \sigma = 0.27 (a/s = 0.46)$$

The a/s value of 0.46 in Equation 123, compared with 0.71 for *tert*-butyl chloride is consonant with the leaving bromide ion being a weaker HBA base than chloride.

For *p*-methoxyneophyl tosylate (62) solvolysis at 75°C (46), based on Smith, Fainberg, and Winstein's data for 6 HBD and 6 non-HBD aliphatic solvents (7,11,13,18,25,29,32,34,50,104,105,201), the total solvatochromic equation is

$$\log k(62) = -8.61 + 4.86 \pi^* + 3.12 \alpha \quad (124)$$

$$r = 0.987, \sigma = 0.23 (a/s = 0.64)^*$$



62

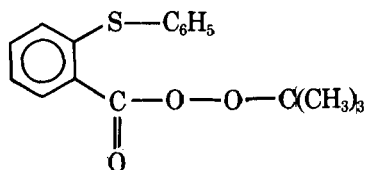
It is noteworthy that these correlations are also quite acceptable without the inclusion of any nucleophilic participation terms. The lower a value than for the *tert*-butyl halides is partially a temperature effect, but probably also reflects charge delocalization in the leaving tosylate group as well as in the forming carbonium ion (through anchimeric assistance by the *p*-methoxyphenyl group).

The varying a/s ratios for these three reactions suggest strongly that solvent effects on S_N1 and S_N2 solvolyses need to be reconsidered with greater attention

* The datum for water, which the original authors had considered suspect, is excluded from the correlation. If this datum were included, the r value would be 0.977.

paid to the variable role of electrophilic assistance. The existence of the three solvent parameter scales now makes such a study in pure solvents feasible.

Radical Decomposition of *t*-Butyl *o*-Phenylthioperbenzoate. Martin and co-workers (172) have reported solvent effects on first-order rate constants for the radical decomposition of **63** at 40°C.

**63**

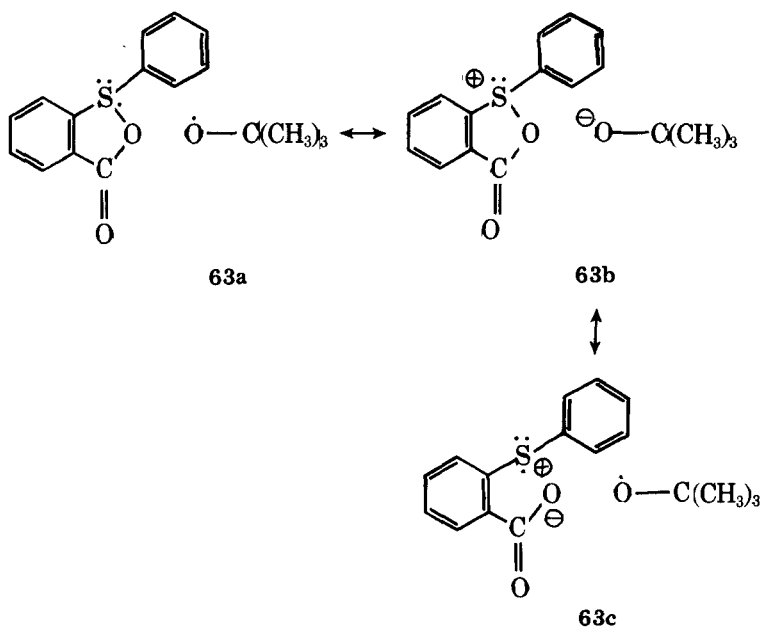
The total solvatochromic equation for this reaction in nine aliphatic solvents (**2,13,18,29,32,101,102,104,105**) is

$$\log k(63) = -5.32 + 1.91 \pi^* + 1.77 \alpha \quad (125)$$

$$r = 0.986, \sigma = 0.16 (a/s = 0.93)$$

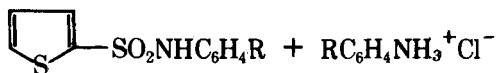
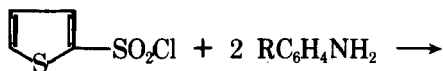
Good correlation was observed between $\log k(63)$ and Z , as is consistent with the not too dissimilar a/s ratios in Equations 116 and 125.

The authors suggested structure **63a-c** for the transition state, and the solvatochromic equation is consistent with such a mechanism.



The appreciable contribution of the α term to the total solvatochromic equation is probably due to type-A hydrogen bonding by the protic solvents to a carboxyl oxygen of **63**, that is, $\Delta\Delta\log k(63-\pi^*)^A_{O=C}$.

Reactions of 2-Thiophenesulfonyl Chloride with Anilines. Arcoria and co-workers (126) have studied solvent effects on the kinetics of the reactions of 2-thiophenesulfonyl chloride with a series of ring-substituted aniline derivatives. Using the data in the eight of their solvents which are aliphatic and whose solvatochromic parameters are known (18,50,102,103,104,105,111,112), we have found correlations with π^* and α to be excellent.



64a, R = *p*-CH₃

b, R = H

c, R = *p*-Cl

For the reaction in which R = *p*-CH₃, the total solvatochromic equation is,

$$\log k(\mathbf{64a}) = -5.29 + 3.05 \pi^* + 1.66 \alpha \quad (126a)$$

$$r = 0.988, \sigma = 0.20$$

for R = H,

$$\log k(\mathbf{64b}) = -5.83 + 3.11 \pi^* + 1.94 \alpha \quad (126b)$$

$$r = 0.991, \sigma = 0.18$$

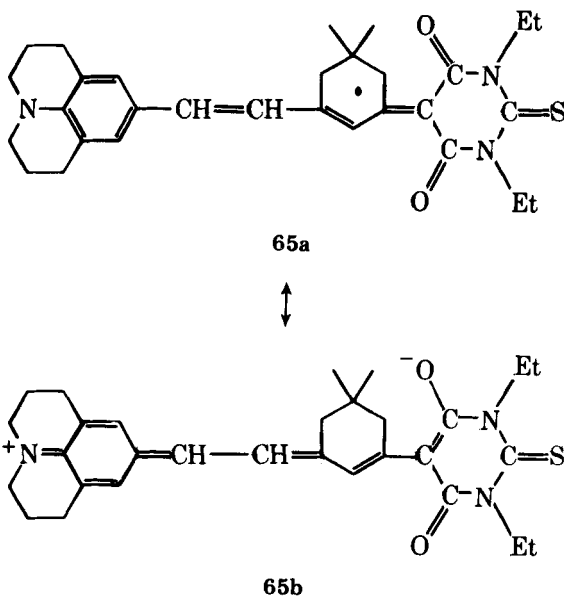
and for R = *p*-Cl,

$$\log k(\mathbf{64c}) = -6.85 + 2.83 \pi^* + 2.45 \alpha \quad (126c)$$

$$r = 0.989, \sigma = 0.17$$

There appears to be an unmistakable trend toward increasing α values with decreasing basicity of the aniline derivative. This can be rationalized in terms of a "push-pull" mechanism where the lower the nucleophilicity of the attacking group, the greater is the importance of type-A hydrogen bonding (electrophilic assistance) to the leaving group. Equations 126a—c may also include minor rate-decelerating effects of type-A hydrogen bonding to the anilines, which should lessen their nucleophilicity, with the effect being greater the more basic the amine.

The χ_R "Solvent Polarity" Scale. A solvent polarity scale proposed by Brooker and co-workers and labeled χ_R represents a ranking based on transition energies for the longest wavelength band in the uv-visible spectrum of the merocyanine, **65** (*34b*).



The electronic transition **65** involves an increase in charge in an electronic excited state that is more like **65b** relative to a ground state that is more like **65a**, so that, unlike " $E_T(30)$ " or Z , increased solvent polarity leads to lower transition energy. Also, this is a $p \rightarrow \pi^*$ transition ($d = 0$ in Equation 103), so that aliphatic and aromatic solvents can be considered together in the solvatochromic comparison.

Based on results in 32 solvents (ex **9**; Table 9),* the total solvatochromic equation for χ_R is,

$$\chi_R = E_T(\mathbf{65}) = 50.8 - 7.91 \pi^* - 3.48 \alpha \text{ kcal mole}^{-1} \quad (127)$$

$$r = 0.967, \sigma = 0.60 \text{ kcal mole}^{-1} (\mathbf{a/s} = 0.44)$$

A plot of Brooker's χ_R values against values calculated through Eq. 127 is shown in Fig. 26.

The negative sign of \mathbf{a} (bathochromic effect) indicates that there is hydrogen-bond strengthening in the electronic excitation, which is consistent with

* If dioxan (**9**) is included, the r value becomes 0.958. If CH_3CN were also excluded, the r value would be 0.978.

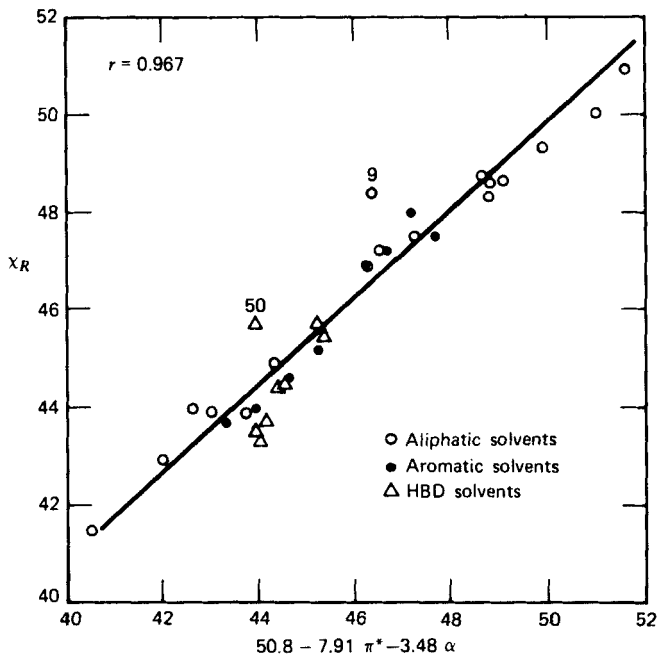


Figure 26 Plot of χ_R values reported by Brooker against values calculated through Eq. 126.

type-A hydrogen bonding by protic solvents to the carboxamide oxygens, that is, $-\Delta\Delta E_T(65 - \pi^*) \xrightarrow{O=C}$. Again, like Z and " $E_T(30)$," χ_R is an index, based on the solvatochromic behavior of an indicator dye, which was represented as a solvent polarity scale, but which is in fact a combined measure of solvent polarity and hydrogen bonding effects.

Nitrogen Hyperfine Splitting Constants of Nitroxides. We have already mentioned (in Section I) Napier and Knauer's suggestion (34e) that solvent polarity scales fall into two classes; (a) those that involve no model reaction and that do not probe the solvent at the molecular level (dielectric constant ϵ , and dipole moment, μ), and (b) those that do involve a model reaction and do probe the solvent at the molecular level (Y, Z , " $E_T(30)$," etc.). Nitrogen hyperfine splitting constants, A_N , they contended, fall into still a third category, since they involve no model reaction, but are, nevertheless, cybotactic probes (although it is not clear to us why Z and " $E_T(30)$ " should be regarded as involving a model reaction, whereas A_N for a specific indicator should not, we suppose that the π^* , α , and β scales also fall into the third class).

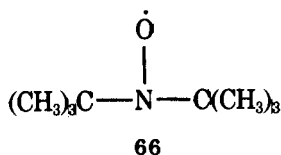
Since A_N values for specific indicators correlated poorly with ϵ and μ , but fairly well with " $E_T(30)$ " and Z , Knauer and Napier suggested that it is more

important that a solvent polarity scale should be a cybotactic probe than that it should involve a model reaction. They suggested also that A_N might serve as a useful solvent polarity parameter, especially in cases where values for the other parameters cannot be obtained because of solubility limitations, spectral interference, and so on.

Again we have found, however, that like the earlier examples cited, A_N values of nitroxides in protic solvents reflect combined effects of solvent polarity and solvent HBD acidity. Thus, the total solvatochromic equation for the nitrogen hyperfine splitting constant of di-*tert*-butyl nitroxide (66) in 17 aliphatic solvents (1,7,9,13,18,25,29,32,50,61,101,102,103,104,105,107,111) is

$$A_N(66) = 15.009 + 0.709 \pi^* + 0.888 \alpha \text{ G} \quad (128)$$

$$r = 0.958, \sigma = 0.12 \text{ G}$$



For reasons that we cannot now explain, but which probably relate to a specific solvent effect, the data points for water fall out of line on the high side in a consistent manner for all the nitroxides studied by Napier and Knauer. If this datum is excluded, the r value becomes 0.981, and the σ value becomes 0.07 G.

Heats of Transfer of the $\text{Et}_4\text{N}^+\text{I}^-$ Ion Pair. The $\Delta G'_c$ terms from methanol into nonprotic solvents for the tetraethylammonium iodide ion pair (30), reported by Abraham (44*b*), were discussed earlier in connection with the π^* and δ parameters. When results in the 18 protic and nonprotic aliphatic solvents (1,2,7,11,16,18,25,28,29,32,50,101,102,103,104,105,111,112)* are considered together, the effects of type-A hydrogen bonding by HBD solvents to iodide become evident. The multiple linear regression equation becomes,

$$\Delta G'_c(30) = 12.62 - 13.0 \pi^* - 5.3 \alpha \text{ kcal mole}^{-1} \quad (129)$$

$$r = 0.995, \sigma = 0.5 \text{ kcal mole}^{-1}$$

Pyridine ^{15}N -NMR Shifts. A property that is highly sensitive to solvent HBD acidity, and which might in the future prove to be quite useful for the determination of new α values is the ^{15}N -nmr spectrum of pyridine (67). Shifts (relative to external 1.0 M H^{15}NO_3) in five aliphatic solvents (2,29,105,111,113), as reported by Duthaler and Roberts (173) show excellent correlation with π^*

* A heat of transfer of -7.5 was used for water for reasons cited in ref. 166.

and α and a high $\mathbf{a/s}$ ratio:

$$\begin{aligned}\delta(\mathbf{67}) &= 53.9 + 4.55 \pi^* + 18.4 \alpha \text{ ppm} & (130a) \\ r &= 0.999 (\mathbf{a/s} = 4.0)\end{aligned}$$

The $\mathbf{d\delta}$ term for this property is probably not very high, because when results in four aromatic and polychloroaliphatic solvents (**6,14,24,43**) are included in the multiple-parameter least-squares correlation, there is no decrease in the goodness of the fit,

$$\begin{aligned}\delta(\mathbf{67}) &= 53.8 + 4.59 \pi^* + 18.6 \alpha \text{ ppm} & (130b) \\ r &= 0.999\end{aligned}$$

The combination of the high $\mathbf{a/s}$ ratio and the probably low $\mathbf{d\delta}$ term for this property allow an estimate of the α values of CH_2Cl_2 and CHCl_3 . If we assume that $(\pi^* + \mathbf{d\delta})$ for each of these HBD solvents equals 0.6 ± 0.2 , the $\delta(\mathbf{67})$ values of 60.5 and 63.9 in Equation 130b lead to $\alpha = 0.21 \pm 0.05$ for CH_2Cl_2 and 0.40 ± 0.05 for CHCl_3 . These values are consistent with the $\Delta\Delta G$ displacements for these solvents in Fig. 20.

Additional Correlations with β . Formation Constants of Bu_3NH^+ Complexes. All the indicators used for the correlations with solvent β values in Equations 53–83 and Table 22 were neutral molecules. To explore the scope and versatility of the β scale, we have also carried out correlations involving formation constants of hydrogen-bonded complexes of HBA bases (**7,13,18,23,24,26,29,37,48**) with tri-*n*-butylammonium ion (**68**) in *o*-dichlorobenzene, as reported by Gilkerson and co-workers (174). The regression equation with β is

$$\begin{aligned}\log K_f(\mathbf{68}) &= -1.83 + 7.90 \beta & (131a) \\ r &= 0.952, \sigma = 0.53\end{aligned}$$

Correlation is improved significantly in a multiple-parameter least-squares fit with β and π^* :

$$\begin{aligned}\log K_f(\mathbf{68}) &= -2.30 + 1.40 \pi^* + 7.10 \beta & (131b) \\ r &= 0.982, \sigma = 0.33\end{aligned}$$

The latter correlation raises the question of why formation constants with HBA bases, acting as solutes in *o*-dichlorobenzene, should show a dependence on π^* , which is a bulk solvent property. The rationale lies in the proportionality between solvent π^* values and molecular dipole moments discussed in Section I. The partial dependence on π^* in Equation 131b evidently reflects the complex-stabilizing effect of the interaction between the tributylammonium ion charge and the HBA base dipole. In future papers we shall show even more ex-

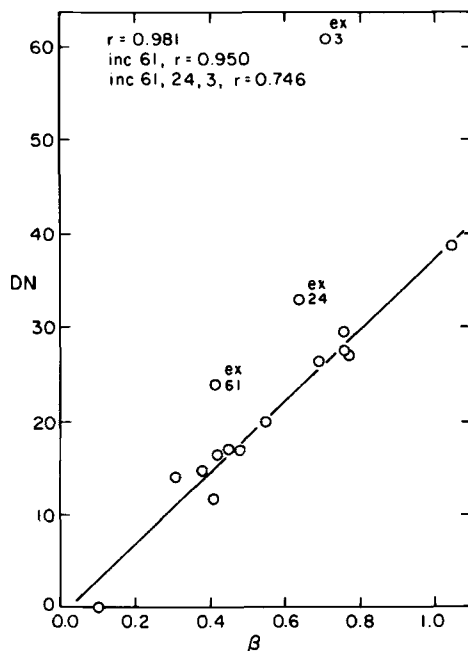


Figure 27 Gutmann's solvent donicity number, DN, plotted against β for corresponding solvents.

treme examples where dipole-dipole interactions between weak HBD acids and HBA bases provide major proportions of the free energies of formation of their hydrogen-bonded complexes.

Correlation of β with Gutmann's DN. The relationship between the β scale and Gutmann's "Solvent Donicity (DN)" numbers provides a context for several additional interesting correlations. Gutmann has defined donicity as "the negative ΔH -value in kcal mole⁻¹ for the interaction of the nucleophilic solvent (Lewis base) with SbCl₅ in a highly diluted solution in dichloroethane." DN values have been reported for 17 HBA solvents whose β values are known (3,7,9,11,13,14,18,23,24,25,26,28,29,37,50,52,61) (175).

A plot of DN versus β is shown in Fig. 27, where it is seen that if the results for 1,2-dimethoxyethane (61), pyridine (24); and triethylamine (3) are excluded, linear correlation is quite good. The correlation equation (ex 3,24,61) is,

$$\begin{aligned} \text{DN} &= -0.78 + 38.4 \beta \\ r &= 0.982, \sigma = 1.86 \end{aligned} \quad (132)$$

If 61 is included, the correlation coefficient is 0.950; if 3 and 24 are also included, $r = 0.746$.

The behavior of pyridine and triethylamine in Fig. 28 is reminiscent of the separations into families of HBA bases in an aqueous pK_a versus pK_{HB} plot reported earlier (74), and in the $\Delta\nu$ versus β plot in Fig. 19. It seems likely that, as with pK_a and with $\Delta\nu$, $\Delta H_f(\text{SbCl}_5)$ and β show differing responses to hybridization, electron mobility, and/or electronegativity of the HBA atom.

The behavior in Fig. 27 is also reminiscent of a plot by Arnett and co-workers (176), wherein they show very poor correlation (indeed almost a scatter diagram) when all solvents were considered together in a plot of ΔH_f^0 for 4-fluorophenol with various bases against ΔG_f^0 for the same HBD acid with the same HBA bases. When families of HBA bases were considered separately, however, a series of crudely parallel lines was observed.

This raises a very fundamental question regarding the scope and applicability of the DN scale. If ΔG_f s of 4-fluorophenol complexes with a series of HBA bases are not linear with ΔH_f s of the self-same complexes when bases with different type HBA sites are considered together, why should they, or any free energy-proportional, solvent-dependent properties be linear with ΔH_f s of complexes of the solvents with the particular electrophile chosen by Gutmann? It is of particular interest in this regard to compare correlations between β and properties which, like DN, depend upon interactions between nonprotonic Lewis acid indicators and bases. Preferably the comparisons should involve sets that include triethylamine (3) and/or pyridine (24), the out-of-line solvents in Fig. 28.

NMR Coupling Constant of Me_3SnCl . The $J(^{119}\text{Sn}-\text{CH}_3)$ coupling constant of $(\text{CH}_3)_3\text{SnCl}$, reported by Bolles and Drago (177), represents such a property. Coupling constants in 10 solvents including pyridine (6,7,8,13,18,23,24,26,29,50) show a fair correlation with β :

$$J(^{119}\text{Sn}-\text{CH}_3) = 57.1 + 14.6 \beta \text{ cps} \quad (133a)$$

$$r = 0.938, \sigma = 1.79 \text{ cps}$$

If we also allow a partial dependence on π^* , the goodness of the fit is improved significantly:

$$J(^{119}\text{Sn}-\text{CH}_3) = 54.2 + 7.8 \pi^* + 10.2 \beta \text{ cps} \quad (133b)$$

$$r = 0.980$$

and the correlation is improved even more if we include a $d\delta$ term with a d value of about -0.20 in the total solvatochromic equation:

$$J(^{119}\text{Sn}-\text{CH}_3) = 54.8 + 8.8(\pi^* - 0.20 \delta) + 8.5 \beta \text{ cps} \quad (133c)$$

$$r = 0.988$$

DN numbers have been reported for eight of Bolles and Drago's solvents

(7,13,18,23,24,26,29,50) and we have assigned DN = 0 (like ClCH₂CH₂Cl) to CCl₄ and DN = 0.1 (like benzene) to toluene in order that the comparison with Equation 133a be more fair. The correlation equation for the coupling constants in these 10 solvents is

$$J(^{119}\text{Sn}-\text{CH}_3) = 57.9 + 0.342 \text{ DN cps} \quad (134a)$$

$$r = 0.922, \sigma = 1.98 \text{ cps}$$

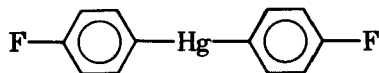
Acceptor numbers (AN) have also been reported (175) for the solvents treated previously (again using the benzene AN number for toluene), which allows a multiparameter treatment according to Gutmann's donor-acceptor approach to solvent effects. In light of the near proportionality between AN and π^* for non-HBD solvents shown in Equation 115a, this is roughly equivalent to a multiple-parameter correlation with DN and π^* . The correlation equation with DN and AN is

$$J(^{119}\text{Sn}-\text{CH}_3) = 55.5 + 0.309 \text{ DN} + 0.257 \text{ AN cps} \quad (134b)$$

$$r = 0.956$$

Comparing Equations 133a,b with Equations 134a,b, it is seen that the correlations with the solvatochromic parameters are somewhat better (but not convincingly so) than with Gutmann's parameters. It is therefore also useful to compare the J values calculated by the two multiparameter equations with the observed J value for pyridine (24), one of the out-of-line data points in Fig. 28. The results are J (Equation 133b) = 67.5 cps, J (Equation 134b) = 69.4 cps, $J(\text{obs}) = 67.0$ cps, which seems to indicate that although the indicator is a nonprotonic Lewis acid, this property shows β -type rather than DN-type behavior.

¹⁹F-NMR Spectrum of Bis(4-fluorophenyl)mercury. Another comparison of the two sets of solvent parameter scales involves ¹⁹F-nmr solvent shifts of 69 (relative to internal fluorobenzene) as reported by Kravtsov and co-workers (178). Results were given in 12 solvents for which both β and DN are known (2,6,9,11,13,14,18,24,26,29,50,61; we assume DN = 0 for C₆H₁₂).



69

The correlation equation of $\delta(69)$ with β is

$$\delta(69) = -0.96 + 2.85 \beta \text{ cps} \quad (135a)$$

$$r = 0.974, \sigma = 0.22 \text{ cps}$$

Allowing also a partial dependence on π^* , the multiple linear regression equation becomes,

$$\delta(\mathbf{69}) = -1.22 + 0.83 \pi^* + 2.27 \beta \text{ cps} \quad (135b)$$

$$r = 0.985$$

For comparison, the correlation equation of $\delta(\mathbf{69})$ with DN is

$$\delta(\mathbf{69}) = -0.90 + 0.067 \text{ DN cps} \quad (136a)$$

$$r = 0.953, \sigma = 0.28 \text{ cps}$$

and the multiple parameter correlation with DN and AN (preceding solvents ex **11** and **61**; DN not known) is

$$\delta(\mathbf{69}) = -1.06 + 0.063 \text{ DN} + 0.022 \text{ AN cps} \quad (136b)$$

$$r = 0.965$$

As before, the solvatochromic parameters give somewhat better correlations (but not convincingly so) than Gutmann's parameters, so that a comparison of the results for pyridine is again appropriate. The results are: δ (Equation 135b) = 0.96 cps, δ (Equation 136b) = 1.34 cps, δ (obs) = 0.94 cps.* Again, although the indicator is a nonprotonic Lewis acid, the property shows β -type behavior.

The Solvent-Cation Complexation Parameter, L_s . Also of interest are effects of pure solvents on the ^{19}F -nmr spectra of a series of *m*- and *p*-fluorophenyl alkyl- and aryl-substituted "onium" ions (ammonium, carbonium, phosphonium, and sulfonium) as reported by Rakshys and Taft (74,179). The solvent effects were found to be well correlated by the product of a solvent-cation complexation parameter, L_s , and a cation sensitivity parameter, M_{R^+} . L_s was considered to be an approximate measure of the stability of a generalized class of weak organic cation-molecule complexes which appeared specifically not to involve hydrogen bonding interactions (although for certain of the *p*-fluorophenyl onium ions, such as $\text{F-C}_6\text{H}_4\text{-}\overset{\oplus}{\text{S}}\text{-Me}_2$, the possibility of HBD acidity of a proton on the alkyl group cannot be excluded).

Correlation is quite good between the L_s values for nine solvents (**23,24,25,26,28,29,50,70,75**) and corresponding β values:

$$L_s = 1.85 + 3.30 \beta \quad (137a)$$

$$r = 0.984, \sigma = 0.12$$

* Since the data point for hexamethylphosphoramide (**26**) was out of line in the correlations of π^* and α with AN (Eqs. 116a,b) it is also of interest to compare the observed and calculated $J(^{119}\text{Sn}-\text{CH}_3)$ and $\delta(\mathbf{69})$ values in this solvent. The results are: $J(\pi^*,\beta) = 71.6$, $J(\text{AN},\text{DN}) = 70.2$; $J(\text{obs}) = 71.6$; $\delta(\pi^*,\beta) = 1.89$, $\delta(\text{AN},\text{DN}) = 1.62$, $\delta(\text{obs}) = 1.93$.

Here, however, the high r value for Equation 137a masks an important contribution of solvent polarity to medium effects on L_s . Multiple linear regression analysis (ex solvents 70,75 for which π^* values are not yet known) leads to

$$L_s = 0.79 + 1.41 \pi^* + 3.05 \beta \quad (137b)$$

$$r = 0.990$$

For comparison, the correlation equation between L_s and DN (preceding solvents, ex 75) is

$$L_s = 2.13 + 0.075 \text{ DN} \quad (138a)$$

$$r = 0.795, \sigma = .45$$

and the correlation with DN and AN is

$$L_s = 2.32 - 0.018 \text{ AN} + 0.076 \text{ DN} \quad (138b)$$

$$r = 0.836$$

From the above (admittedly limited) comparisons, it does appear that certain types of nonprotonic Lewis acid-base type solvent effects parallel type-B hydrogen bonding (proton sharing) effects in their dependences on β . It also goes without saying that, for the thirty-odd sets of hydrogen bonding effects discussed in connection with the solvent HBA basicity scale, the demonstrated correlations with β are significantly better than corresponding correlations with DN. Indeed, from our evaluation of the latter parameter, we conclude that DN is a reasonably good measure of solvent nucleophilicity when only oxygen bases (and a few R—CN nitrogen bases) are considered, but that correlations of solvent effects on free energy-proportional properties are likely to break down if the solvent set includes other type bases.

5. Concluding Remarks

The Comprehensive Table of Solvatochromic Parameters. The β , π^* , and α parameters, determined as described previously for 124 solvents, are assembled in Table 35. Where conflicting values have been published, the results listed here supersede those that have appeared in Parts 1–8 of our Solvatochromic Comparison Method series and Parts 1–6 of the Linear Solvation Energy Relationships (LSER) series. Findings published in Part 7 and later papers of the LSER series will take precedence over present results.

The assembled parameters have been assigned five levels of reliability. Results not in brackets or parentheses are *primary* values. These are based on averages of $(\pi^*, \beta, \alpha)_i$ s back-calculated from correlation equations for at least six properties. Average deviations of these results have usually been <0.05 .

TABLE 35
Comprehensive Table of Solvatochromic Parameters^a

Solvent	π^*	β	α	(SSS?) ^b
Aliphatic Hydrocarbons				
1. <i>n</i> -Hexane, <i>n</i> -Heptane	-.08	nil	nil	SSS
2. Cyclohexane	nil	nil	nil	SSS
Ethers and Orthoesters				
4. Diisopropyl ether	(.27)	(.49)	nil	SSS
5. Di- <i>n</i> -butyl ether	.24	.46	nil	SSS
7. Diethyl ether	.27	.47	nil	SSS
9. Dioxan	(.55)	.37	nil	EXCL
13. Tetrahydrofuran	.58	.55	nil	SSS
17. Anisole	.73	.22	nil	AROM
40. Tetrahydropyran	.51	.54	nil	SSS
46. Dibenzyl ether	(.80)	.41	nil	AROM
59. Diphenyl ether	(.66)	(.13)	nil	AROM
61. Dimethoxyethane	(.53)	(.41)	nil	—
86. Di- <i>n</i> -propyl ether	—	[.46]	nil	—
87. Phenetole	—	[.20]	nil	AROM
88. Bis(2-methoxyethyl) ether	.64	—	nil	—
133. Trimethyl orthoacetate	.35	—	nil	—
134. Trimethyl orthoformate	.58	—	nil	—
Aldehydes and Ketones				
16. 2-Butanone	.67	(.48)	(.05)	SSS
18. Acetone	.72	.48	(.07)	SSS
36. Trichloroacetone	—	[.14]	—	—
41. Cyclohexanone	(.76)	.53	—	SSS
51. Cyclopentanone	.76	.52	—	SSS
58. Acetophenone	.90	(.49)	—	AROM
65. Methyl <i>t</i> -butyl ketone	—	[.45]	—	—
66. Benzaldehyde	—	(.44)	nil	AROM
71. Dimethyl- γ -pyrone	—	[.82]	—	—
76. Benzophenone	—	[.46]	nil	AROM
77. Biacetyl	—	[.31]	—	—
98. 3-Heptanone	.59	—	—	—
131. Phenylacetone	.88	—	—	AROM
Esters				
11. Ethyl acetate	.55	.45	nil	SSS
27. Butyrolactone	.87	.49	nil	SSS
38. Butyl acetate	.46	—	nil	SSS
39. Ethyl chloroacetate	.70	.35	nil	SSS
47. Ethyl benzoate	.74	.41	nil	AROM
52. Methyl acetate	.60	(.42)	nil	SSS
55. Methyl formate	.61	—	nil	SSS
85. Diethyl carbonate	—	[.38]	nil	—

TABLE 35
Comprehensive Table of Solvatochromic Parameters^a

Solvent	π^*	β	α	(SSS?) ^b
94. Diethyl malonate	.64	—	—	—
95. Ethyl acetoacetate	.61	—	—	—
64. Ethyl propionate	—	(.42)	nil	—
96. Ethyl trichloroacetate	.61	—	nil	—
136. Methyl trifluoroacetate	(.39)	—	nil	—
137. Propylene carbonate	(.81)	—	nil	—
138. Ethyl formate	(.61)	—	nil	—
Amides and Ureas				
23. Dimethylacetamide	.88	.76	nil	SSS
25. Dimethylformamide	.88	.69	nil	SSS
28. <i>N</i> -Methylpyrrolidone	.92	.77	nil	—
69. Dimethyltrifluoroacetamide	—	[.46]	nil	—
72. Dimethyl chloroacetamide	—	(.62)	nil	—
75. Tetramethylurea	—	(.78)	nil	—
204. Formamide	(.98)	—	(.66)	—
Amines				
3. Triethylamine	.14	.71	nil	SSS
48. Tri- <i>n</i> -butylamine	.16	.62	nil	SSS
49. <i>N,N</i> -Dimethylbenzylamine	.49	.57	nil	AROM
57. Dimethylaniline	[.90]	—	nil	AROM
Sulfur Compounds				
29. Dimethyl sulfoxide	1.00	.76	nil	SSS
45. Ethyl sulfate	(.69)	—	nil	—
56. Sulfolane	.98	—	nil	SSS
67. Diphenyl sulfoxide	—	(.70)	nil	AROM
74. Di- <i>n</i> -butyl sulfoxide	—	(.83)	nil	—
Phosphorus Compounds				
19. Triethyl phosphate	(.72)	.77	nil	SSS
26. Hexamethylphosphoramide	((.87))	((1.05))	nil	EXCL
42. Tri- <i>n</i> -butyl phosphate	.65	—	nil	SSS
68. Triphenylphosphine oxide	—	(.94)	nil	—
70. Trimethyl phosphate	—	[.73]	nil	—
73. Trimethylphosphine oxide	—	(1.02)	nil	—
Nitro Compounds and Nitriles				
31. Nitrobenzene	1.01	[.39]	nil	AROM
32. Nitromethane	(.85)	—	(.23)	EXCL ^c
37. Benzotrile	.90	(.41)	nil	AROM
50. Acetonitrile	(.85)	(.31)	(.15)	EXCL ^c
63. Phenylacetoneitrile	(.99)	—	—	AROM
89. Butyronitrile	.71	—	—	—

TABLE 35
Comprehensive Table of Solvatochromic Parameters^a

Solvent	π^*	β	α	(SSS?) ^b
Pyridines				
24. Pyridine	.87	.64	nil	AROM
78. 4-Methylpyridine	—	(.67)	nil	AROM
79. 2,6-Dimethylpyridine	—	(.76)	nil	AROM
80. 2,4,6-Trimethylpyridine	—	(.78)	nil	AROM
81. Quinoline	—	(.64)	nil	AROM
82. 3,5-Dichloropyridine	—	(.42)	nil	AROM
83. 3-Bromopyridine	—	(.51)	nil	AROM
84. 4-Dimethylaminopyridine	—	(.87)	nil	AROM
Aromatics and Haloaromatics				
8. Toluene	.54	(.11)	nil	AROM
14. Benzene	.59	(.10)	nil	AROM
15. Chlorobenzene	.71	(.07)	nil	AROM
33. Bromobenzene	.79	(.06)	nil	AROM
35. <i>p</i> -Xylene	.43	—	nil	AROM
53. Mesitylene	.41	—	nil	AROM
60. <i>o</i> -Dichlorobenzene	(.80)	—	nil	AROM
62. Iodobenzene	(.81)	—	nil	AROM
90. Cumene	.41	—	nil	AROM
92. <i>m</i> -Dichlorobenzene	.67	—	nil	AROM
97. Fluorobenzene	.62	—	nil	AROM
135. <i>m</i> -Xylene	.47	—	nil	AROM
Haloaliphatics				
6. Carbon tetrachloride	.29	nil	nil	HA
10. Trichloroethylene	.53	nil	nil	HA
12. 1,1,1-Trichloroethane	.49	nil	nil	HA
20. 1,2-Dichloroethane	.81	nil	nil	HA
21. Methylene chloride	[(.80)]	nil	[.22]	HA
22. 1,1,2-Trichloroethane	[(.83)]	nil	—	HA
30. Chloroform	[(.76)]	nil	[.34]	HA
43. Tetrachloroethylene	.28	nil	nil	HA
44. 1,1,2,2-Tetrachloroethane	[(.95)]	nil	—	HA
54. <i>n</i> -Butyl chloride	[.39]	nil	nil	HA
91. 1,2-Dibromoethane	.75	nil	nil	HA
93. <i>trans</i> -1,2-dichloroethylene	.44	nil	nil	HA
132. Pentachloroethane	[(.62)]	nil	—	HA
Alcohols and Water				
101. <i>tert</i> -Butanol	(.41)	(1.01)	(.62)	EXCL
102. 2-Propanol	(.46)	(.95)	(.78)	EXCL
103. 1-Butanol	(.46)	(.88)	(.79)	EXCL
104. Ethanol	.54	(.77)	.86	EXCL
105. Methanol	.60	(.62)	.98	EXCL

TABLE 35
Comprehensive Table of Solvatochromic Parameters^a

Solvent	π^*	β	α	(SSS?) ^b
106. 2-Phenylethanol	[(.88)]	((.61))	—	EXCL
107. Ethylene glycol	(.85)	((.52))	(.92)	EXCL
109. Benzyl alcohol	[(.98)]	((.50))	[(.43)]	EXCL
110. 2-Chloroethanol	—	((.31))	—	EXCL
111. Water	((1.09))	((.18))	((1.13))	EXCL
112. 1-Propanol	(.51)	—	(.80)	EXCL
113. Trifluoroethanol	(.73)	—	(1.35)	EXCL
114. Hexafluoroisopropanol	(.65)	—	—	EXCL
115. 2-Fluoroethanol	(.72)	—	—	EXCL
116. 2-Methoxyethanol	(.71)	—	—	EXCL
Carboxylic Acids and Anhydrides				
34. Acetic anhydride	.76	—	nil	SSS
201. Acetic acid	((.62))	—	((1.09))	EXCL
203. Trifluoroacetic acid	(.50)	—	—	EXCL

^a Square brackets, [] denote tertiary value; based on less than three properties. Parentheses, (), denote secondary value; either based on less than six properties or there is more than usual scatter. Double parentheses, (()), uncertain; either a generally bad acting solvent, or insufficient information of the right type, or conflicting measurements. Bracketed parentheses, [()], denote a published value that is based on an incorrect mixture of π^* and α properties, and is almost certain to be changed.

^b SSS = Member of select solvent set for which $\pi^* \sim K\mu$; EXCL = solvent specifically excluded from select solvent set; AROM = aromatic solvent; HA = haloaliphatic solvent.

^c EXL = Initially considered as SSS, but now excluded on the basis of its HBD acidity.

Secondary values are in parenthesis (). These are either based on three to five individual correlations, or there is more than usual scatter (>0.05) in the $(\pi^*, \beta, \alpha)_i$. π^* Values for dioxan and triethyl phosphate fall into the latter category. Despite the poorer than usual precision (which may be due to hygroscopicity or a proclivity of the solvent to contain protic impurities), however, we are satisfied that the listed values are probably nearly correct. Secondary values are to be promoted to primary when additional results become available and/or when the averages “settle down” to an average deviation of <0.05 .

Tertiary values are in square brackets []. These are based on less than three correlations, and are to be promoted to secondary when additional information becomes available. We have not used tertiary values in the correlations in the present report.

We are particularly uncertain about the results in double parentheses (()) for one or several of a number of reasons. The solvent may be a generally “bad actor” like hexamethylphosphoramide (**26**), which usually behaves as if its π^* value were about 0.9, but in a number of occasions (like the correlation of AN

with π^*) produced effects consonant with a π^*_i like 0.4–0.5. This may be because of a greater than usual proclivity toward specific solvent association effects (it will be recalled that **26** was specifically found not to be a member of the *select solvent set*). The uncertainty in π^* for **26** has led to a corresponding uncertainty in β .

Another reason for the double parentheses is that, as a consequence of uncertainties in unraveling multiple hydrogen-bonding effects, different sets of solvatochromic equations have given internally consistent but conflicting sets of results. As discussed earlier, this was the case with the β values for the more acidic alcohols and water.

A third reason for the double parentheses is that the result, although more likely than not to be nearly correct, is based on properties that were later found to be inappropriate for the measurement, and have not yet been confirmed by more appropriate measurements. The π^* value (and hence the α value) for water falls into this class.

Finally, values in bracketed parentheses [()] are published results that we believe to be wrong by more than 0.1 unit, and are very likely eventually to be changed. These were usually based on inappropriate measurements (e.g., assuming HBD effects were nil when basing π^* values of CHCl_3 and CH_2Cl_2 on spectra of indicators 1–7 of Table 24). Most of these parameters will be difficult to determine accurately, because their solvatochromic equations usually involve $\delta\delta$ terms which are not easily assessed.

The Current Status of the Solvatochromic Parameters. The parameters for the protic solvents in Table 35 represent a second set of published π^* s and a third set of published α s, and we are not yet satisfied that these results are final. We are aware that the differing values in the literature have the potential of confusing the user and hindering development in the field. However, our shortcomings in this regard should be viewed in light of the fact that *all earlier workers on solvent effects* (and if we include mixed solvent effects, they number in the dozens) have, to a greater or lesser extent, *demonstrably failed to unravel solvent polarity and multiple hydrogen bonding effects*. Further, many years after serious shortcomings or inconsistencies have been pointed out (e.g., by Koppel and Pal'm (13), Figueras (180), Fowler, Katritzky and Rutherford (181), and Gramstad and co-workers (136–138), misleading solvent property scales like “ $E_T(30)$,” Z , DN , AN , and B continue to be widely and incorrectly used.

That the π^* and β values of nonprotic solvents are now fairly well defined is a result of the fact that determining these parameters involved unraveling only two types of effects, solvent polarity and type-B hydrogen bonding at a single site. With the π^* , β , and α values of protic solvents, however, the interacting effects are usually far more complex and more difficult to unravel. Solvent self-association effects compete with type-B and type-A hydrogen bonding ef-

fects, and the latter (which are pervasive) usually occur at multiple sites. Type-AB hydrogen bonding phenomenology, which we have touched on briefly in the present report (and which will be quite difficult to quantify and incorporate in the solvatochromic equations) represents still another source of uncertainty that is unlikely to be resolved in the near future.

In retrospect, we can recognize the naivité in some of the assumptions which contributed to our earlier false starts. We hope that when in the future we look back to the present report, we will not expect that it is correct in all regards, but rather that we will see it as having resolved some, and significantly narrowed others, of the areas of uncertainty in the field of linear solvation energy relationships.

ACKNOWLEDGMENT

The work by MJK was done under Naval Surface Weapons Center Independent Research Task IR-201. The work by J.L.A. and R.W.T. was supported in part by a grant from the Public Health Service.

References

1. The reaction studied was the quaternarization of triethylamine by ethyl iodide at 100 °C [N. Menshutkin, *Z. Physik. Chem.*, **6**, 41 (1890)]. Menshutkin's first discussion on solvent effects dealt with the reactions between acetic anhydride and alcohols [*Z. Physik. Chem.*, **1**, 611 (1887)]. The catalytic role of solvents was already recognized in 1862 by Berthelot and Péan de Saint Gilles in their *Recherches sur les Affinités* [see, e.g., H. G. Grimm, H. Ruf, and H. Wolff, *Z. Physik. Chem.*, **B13**, 301 (1931)].
2. (a) J. G. Kirkwood and I. Oppenheim, *Chemical Thermodynamics*, McGraw-Hill, New York, 1961, Chapter 11.; (b) G. N. Lewis and M. Randall, *Thermodynamics* (revised by K. S. Pitzer and L. Brewer), McGraw-Hill, New York, 1961, Chapter 20.; (c) E. Fermi, *Termodinamica*, Boringhieri, Ed., Torino, 1977, Chapter 5.; (d) M. Diaz Pěna and A. Roig Muntaner, *Quimica Fisica*, Alhambra, Ed., Madrid 1978, Chapters 10 and 22.
3. See, e.g., Ref 2b, pp. 239–240.
4. (a) H. Eyring, *J. Chem. Phys.*, **3**, 107 (1934).; (b) E. A. Molwyn-Hughes, *The Kinetics of Reactions in Solution*, Clarendon, Oxford, 1947.; (c) S. Glasstone, K. J. Laidler, and H. Eyring, *The theory of Rate Processes*, McGraw-Hill, New York 1941, p. 400.
5. L. Onsager, *J. Am. Chem. Soc.*, **58**, 1486 (1936).
6. M. Block and S. M. Walker, *Chem. Phys. Lett.*, **19**, 363 (1973).
7. W. A. Millen and D. W. Watts, *J. Am. Chem. Soc.*, **89**, 6051 (1967). Laidler, using a different treatment, also calculates a somewhat faster increase of $\epsilon(r)$, K. J. Laidler, *Can. J. Chem.*, **37**, 138 (1959).
8. J. G. Kirkwood, *J. Chem-Phys.*, **2**, 351 (1934).
9. This is the original procedure used by Kirkwood to develop Equation 14. See also, e.g., (a) M. Jauquet and P. Laszlo, in *Solutions and Solubilities*, Part I, Chapter IV, Wiley, New York, 1974.; (b) Ref. 2b, Chapter 23.
10. (a) K. J. Laidler and H. Eyring, *Ann. N.Y. Acad. Sci.*, **39**, 303 (1940); (b) K. J. Laidler, *Chemical Kinetics*, Chapter 5, McGraw-Hill, New York, 1950.

11. J. G. Kirkwood and F. H. Westheimer, *J. Chem. Phys.*, **6**, 506 (1936).
12. K. J. Laidler and P. A. Landskroener, *Trans. Faraday Soc.*, **52**, 200 (1956).
13. I. A. Koppel and V. A. Palm, in *Advances in Linear Free Energy Relationships*, Chapter 5, N. B. Chapman and J. Shorter, Eds., Plenum, London, 1972.
14. M. H. Abraham, in *Progress in Physical Organic Chemistry*, Chapter 1, Vol. 12, R. W. Taft, Ed., Wiley, 1974.
15. K. Hiromi, *Bull. Chem. Soc. Japan*, **33**, 1521 (1960); see also Ref. 12.
16. R. J. Abraham and M. A. Cooper, *J. Chem. Soc.*, (B), 202 (1967).
17. (a) R. J. Abraham, *J. Phys. Chem.*, **73**, 1192 (1968); (b) R. J. Abraham and R. Bretschneider, in *Internal Rotation in Molecules*, W. J. Orville-Thomas, Ed., Academic, London, 1974, Chapter 13 and references therein.
18. R. J. Abraham and Z. L. Rossetti, *J. Chem. Soc., Perkin II*, 582 (1973), and previous papers in that series.
19. M. H. Abraham and R. J. Abraham, *J. Chem. Soc., Perkin II*, 47 (1974).
20. (a) M. H. Abraham and R. J. Abraham, *J. Chem. Soc., Perkin II*, 1677 (1975); (b) M. H. Abraham and P. L. Grellier, *J. Chem. Soc., Perkin II*, 1735 (1976).
21. K. Højendahl, Ph.D. Thesis, Copenhagen, 1928, quoted by J. R. Partington in *An Advanced Treatise in Physical Chemistry*, Longman, Green, and Co., London, 1966, Vol. V, p. 384.
22. Self-association of DMSO pure and in CCl₄, e.g., R. H. Figueroa, E. Roig, and H. H. Szmant, *Spectrochim. Acta*, **22**, 587 (1966); self-association of substituted benzonitriles, e.g., L. Deady, A. R. Katritzky, R. A. Shanks, and R. D. Topsom, *Spectrochim. Acta*, **29A**, 115 (1973).
23. Self-association of DMSO, J. B. Kisinger, M. M. Tannahill, M. S. Greenberg, and A. I. Popov, *J. Phys. Chem.*, **77**, 2444 (1973).
24. This technique has been used to determine the dimerization constants of ketones and nitriles in cyclohexane and carbon tetrachloride solutions: (a) M. Guérin, Ph.D. Thesis, University of Poitiers (France), 1975.; (b) J. Monteau, H. Huser, M. Guérin, and M. Gomel, *J. Chem. Research (S)*, 256 (1978).
25. Self-association of N-N, dimethylformamide, N,N-dimethylacetamide, and N-methylpyrrolidone, T. Yonezawa and I. Morishima, *Bull. Chem. Soc. Japan*, **39**, 2346 (1966).
26. Self-association of ketones, esters, amides, nitriles, and nitrocompounds, H. Saito, Y. Tanaka, S. Nagata, K. Nukada, *Can. J. Chem.*, **51**, 2118 (1973).
27. Self-association of *p*-fluoronitrobenzene in carbon tetrachloride, R. W. Taft, G. B. Klingsmith, E. Price, and I. R. Fox, Symposium on Linear Free Energy Correlations, Reprints of Papers, Durham, 1964, pp. 275-278; also, cf. Ref. 32.
28. Self-association of aromatic nitrocompounds, A. A. Leichenko, Y. Y. Maksimov, *Zh. Fiz. Khim.*, **47**, 1265 (1973) [*C.A.*, **79**, 5767a (1973)].
29. A. Kratchowill, J. V. Zeidner, V. Joerg, and H. Zimmerman, *Ber. Bunsenges. Phys. Chem.*, **77**, 408 (1973).
30. T. B. Borgunova, V. V. Shilov, and G. I. Batalin, *Zh. Fiz. Khim.*, **48**, 2571 (1974) [*C.A.*, **82**, 57331f (1975)].
31. (a) C. D. Ritchie, B. A. Bierl, and R. J. Honour, *J. Am. Chem. Soc.*, **84**, 4687 (1962); (b) C. D. Ritchie and A. L. Pratt, *ibid.*, **86**, 1571 (1964).
32. R. E. Uschold and R. W. Taft, *Org. Mag. Resonance*, **1**, 375 (1969).
33. (a) J. L. M. Abboud, M. J. Kamlet, and R. W. Taft, *J. Am. Chem. Soc.*, **99**, 8325 (1977); (b) M. J. Kamlet, J. L. M. Abboud, and R. W. Taft, *ibid.*, **99**, 6027 (1977).
34. The Scales correlated are (a) $E_T(30)$, K. Dimroth, C. Reichardt, T. Seipman, and F. Bohlman; *Justus Liebig Ann. Chem.*, **661** 1(1963); C. Reichardt, *ibid.*, **752**, 64 (1971), C. Reichardt, *Angew. Chem., Int. Ed. Engl.*, **4**, 29 (1965); (b) χ_R , L. G. S. Brooker, A. C. Craig, D. W. Heseltine, P. W. Jenkins, and L. L. Lincoln, *J. Am. Chem. Soc.*, **87**, 2433 (1965); (c) the logarithm of the rate constant of the Menschutkin reaction between Pr₃N and MeI at 20°C.,

- C. Lussan and J. C. Jungers, *Bull. Soc. Chim. (France)*, 2678 (1968); (d) E_K . D. Walther, *J. Prakt. Chem.*, 316, 604 (1974); (e) A_N : B. R. Knauer and J. J. Napier, *J. Am. Chem. Soc.*, 98, 4395 (1976); (f) G. A. Allerhand and P. V. Schleyer, *J. Am. Chem. Soc.*, 85, 374 (1963); (g) P. Ref. 27; (h) S. S. Brownstein, *Can. J. Chem.*, 38, 1590 (1960). This scale has been included as an extension of Kosower's Z parameters [E. M. Kosower, *J. Am. Chem. Soc.*, 80, 3253 (1958)].
35. W. F. K. Wynne-Jones and H. Eyring, *J. Chem. Phys.*, 3, 493 (1935).
 36. The reaction examined was that between Et_3N and EtBr in benzene-acetone solutions [data from A. von Hempfing and A. Bekaert, *Z. Physik. Chem.*, 28, 255 (1895)].
 37. Y. Drougard and D. Decroocq, *Bull. Soc. Chim. (France)*, 2972 (1969).
 38. The short-lived clustering of benzene and other highly polarizable molecules around polar solutes, likely through a dipole-induced dipole mechanism is also known: (a) R. D. Bertrand, R. D. Compton, and J. G. Verkade, *J. Am. Chem. Soc.*, 92, 2702 (1970); (b) R. S. Armstrong, M. J. Aroney, R. K. Duffin, H. J. Stootman, and R. J. W. Le Fevre, *J. Chem. Soc., Perkin 2*, 1272 (1973).
 39. (a) For a recent survey of solvent effects on spectroscopic properties, see, e.g., Ref. 9a; (b) concerning the use and limitations of the dielectric functions to correlate infrared shifts, see, e.g., W. D. Horrocks, Jr., and R. M. Mann, *Spectrochim. Acta*, 19, 1375 (1963); S. Tanaka, K. Tanabe, and H. Kamada, *Spectrochim. Acta*, 23A, 209, 1967, A. D. Buckingham, *Proc. Roy. Soc. (London)*, A248, 169 (1958); *ibid.*, A255, 32 (1960); M. L. Josien and N. Fuson, *J. Chem. Phys.*, 22, 1169, 1264 (1954); *J. Chim. Phys.*, 52, 162 (1955).
 40. (a) B. Fontaine, M. T. Chenon, and N. Lumbroso-Bader, *J. Chim. Phys.*, 62, 1075 (1965); (b) P. Laszlo and J. I. Musher, *J. Chem. Phys.*, 41, 3906 (1964) and references cited therein.
 41. See, e.g., (a) A. M. Benson, Jr. and H. C. Drickamer, *J. Chem. Phys.*, 27, 1164 (1957); R. R. Wiederkehr and M. G. Drickamer, *J. Chem. Phys.*, 27, 1164 (1957); R. R. Wiederkehr and M. G. Drickamer, *ibid.*, 28, 311 (1958); and (b) R. L. Schmidt, R. S. Butler, and J. H. Goldstein, *J. Phys. Chem.*, 73, 1117 (1969) and references cited therein.
 42. J. L. M. Abboud and R. W. Taft, *J. Phys. Chem.*, 83, 412 (1979).
 43. (a) E. Lippert, *Z. Elektrochem.*, 61, 967 (1957); (b) C. J. F. Böttcher, *Theory of Dielectric Polarization*, Elsevier, Amsterdam, 1952, pp. 135-138.
 44. (a) Ref. 14; (b) M. H. Abraham, *J. Chem. Soc., Perkin II*, 1343 (1972).
 45. Although most of the information available on this system comes from Ref. 34c we have used the values given by Abraham and Abraham (19)
 46. S. G. Smith, A. H. Fainberg, and S. Winstein, *J. Am. Chem. Soc.*, 83, 618 (1961).
 47. J. E. Leffler and E. Grunwald, *Rates and Equilibria of Organic Reactions*, Wiley, 1963, Chapter 8.
 48. I. A. Koppel and V. A. Palm, *Advances in Linear Free Energy Relationships*, 1972, Chapter 5. Cf. reference 13.
 49. E.g., E. M. Kosower, *An Introduction to Physical Organic Chemistry*, Wiley, New York, 1968.
 50. C. Reichardt, *Angew. Chem. Int. Ed. Engl.*, 4, 29 (1965).
 51. K. Schwetlick, *Kinetische Methoden Zur Untersuchung von Reaktions-mechanismen*, VEB Deutscher Verlag der Wissenschaften, Berlin, 1971, Chapter 4.
 52. E. Grunwald and S. Winstein, *J. Am. Chem. Soc.*, 70, 846 (1948).
 53. (a) S. Winstein, E. Grunwald, and W. H. Jones, *J. Am. Chem. Soc.*, 73, 2700 (1951); (b) A. H. Fainberg and S. Winstein, *J. Am. Chem. Soc.*, 78, 2770 (1956); (c) A. H. Fainberg and S. Winstein, *ibid.*, 79, 1597 (1957); (d) A. H. Fainberg and S. Winstein, *ibid.*, 79, 1602 (1957); (e) A. H. Fainberg and S. Winstein, *ibid.*, 79, 1608 (1957).
 54. A. Berson, E. Hamlet, and W. A. Mueller, *J. Am. Chem. Soc.*, 84, 297 (1962).

55. In this connection, see Ref. 20a.
56. M. Kerfanto and G. Barion, *C. R. Acad. Sci.*, 948 (1966).
57. J. L. M. Abboud and M. J. Kamlet, unpublished results.
58. (a) Y. Ooshika, *J. Phys. Soc., Japan*, 9, 594 (1954); (b) N. S. Bayliss and E. G. MacRae, *J. Phys. Chem.*, 58, 1002 (1954); (c) E. G. MacRae, *ibid.*, 61, 562 (1957); (d) Ref. 43a; [(e) N. G. Bakshiev, *Opt. Spektrosk.*, 10, 717 (1961); *ibid.*, 16, 821 (1964); N. G. Bakshiev, O. P. Girin, and I. V. Pitserskaya, *ibid.*, 24, 901 (1968), all through Ref. 48 (f) W. Liptay, in *Modern Quantum Chemistry*, Part II, O. Sinanoglu, Ed. Academic, New York, 1965, Chapter 5, and references herein; (g) M. B. Ledger and P. Suppan, *Spectrochim. Acta*, 23A, 641 (1967).
59. (a) The formal extension to fluorescence spectra has been carried out by Mataga, Kaifu, and Koizumi [N. Mataga, Y. Kaifu, and M. Koizumi, *Bull. Chem. Soc. Japan*, 29, 465 (1956)]; (b) See also Ref. 43a.
60. For an exhaustive study on the use of dielectric and refractive index functions to correlate solvent effects, see, e.g., F. W. Fowler, A. R. Katritzky, and R. J. D. Rutherford, *J. Chem. Soc. (B)*, 460 (1971). We are not considering here the contribution from dispersion forces as discussed in Refs. 58a and 58b and by Longuet-Higgins and Pople [H. C. Longuet-Higgins and J. A. Pople, *J. Chem. Phys.*, 27, 192 (1957)]. These forces will introduce a red shift (relative to the gas phase) even in the case of nonpolar solutes in nonpolar solvents.
61. For a recent application of this technique to the uv-visible and fluorescence spectra of azulene and cyclopenta [ef]heptalene, see H. Yamaguchi, T. Ikeda, and H. Mametsuka, *Bull. Chem. Soc. Japan*, 49, 1762 (1976).
62. (a) J. A. Pople, W. G. Schneider, and H. J. Bernstein, *High-Resolution Nuclear Magnetic Resonance*, McGraw-Hill, New York, 1959, Chapter 16; (b) A. D. Buckingham, *Can. J. Chem.*, 38, 300 (1960); (c) A. D. Buckingham, T. Schaefer, and W. G. Schneider, *J. Chem. Phys.*, 32, 1227 (1960).
63. W. West and R. T. Edwards, *J. Chem. Phys.*, 5, 14 (1937).
64. E. Bauer and M. Magat, *J. Phys. Radium*, 9, 319 (1938).
65. R. L. Fulton, *J. Chem. Phys.*, 61, 4141 (1974).
66. (a) Ref. 34h; (b) E. M. Kosower, *J. Am. Chem. Soc.*, 80, 3262 (1958); Ref. 49.
67. (a) G. C. Levy and G. L. Nelson, *C-13 NMR Spectroscopy for Organic Chemists*, Wiley, New York, 1972; (b) F. W. Wherli and T. Wirtmlin, *Interpretation of ¹³C NMR Spectra*, Heyden and Son, 1976.
68. (a) B. Chawla, M. Fujio, and R. W. Taft, unpublished results; (b) W. Adcock and T. C. Khor, *J. Am. Chem. Soc.*, 100, 7799 (1978).
69. K. Kalyanasundaram and J. K. Thomas, *J. Am. Chem. Soc.*, 99, 2039 (1977).
70. Taken from C. V. Krishnan and H. L. Friedman, *J. Phys. Chem.*, 73, 1572 (1969).
71. R. W. Taft and M. J. Kamlet, *J. Am. Chem. Soc.*, 98, 2886 (1976).
72. M. J. Kamlet and R. W. Taft, *J. Am. Chem. Soc.*, 98, 377 (1976).
73. D. Gurka and R. W. Taft, *J. Am. Chem. Soc.*, 91, 4797 (1969).
74. R. W. Taft, D. Gurka, L. Joris, P. V. R. Schleyer, and J. W. Rakshys, *J. Am. Chem. Soc.*, 91, 4801 (1969).
75. (a) T. Gramstad and J. Sandstrom, *Spectrochim. Acta*, 25A, 31 (1969); (b) T. Gramstad, *ibid.*, 19, 497, 829 (1963); T. Gramstad and W. J. Fuglevik, *ibid.*, 21, 343 (1965); (c) V. Bindheim and T. Gramstad, *ibid.*, 21, 1073 (1965).
76. T. Yokoyama, R. W. Taft, and M. J. Kamlet, *J. Am. Chem. Soc.*, 98, 3233 (1976).
77. (a) B. Gosh and S. Basu, *Trans. Faraday Soc.* 61, 2097 (1965); (b) C. M. Huggins and G. C. Pimentel, *J. Phys. Chem.*, 60, 1615 (1956); (c) P. J. Krenger and B. F. Hawkins, *Can. J. Chem.*, 51, 3250 (1973); (d) A. L. Smolyanskii, *Opt. Spektrosk.*, Suppl. 2, 254 (1963); *EE* 133 (1966); (e) B. B. Wayland and R. S. Drago, *J. Am. Chem. Soc.*, 86, 5240 (1964).

78. The effects of band overlap (usually with higher intensity, higher energy bands), of hidden underlying lower intensity bands, and of changing band shape with changing solvent, all of which we include in the term spectral anomalies, can cause shifts in ν_{\max} of as much as 0.4–0.5 kK. We have attempted to minimize such complications by taking ν_{\max} as the midpoint between the two positions on the spectral envelope where OD (optical density) = 0.90 OD_{max}. We consider that for “well-behaved” spectra, combined uncertainties in ν_{\max} due to usual spectral anomalies and experimental precision limits in measuring the spectra are about 0.10 kK. (a) D. J. Cowley, *J. Chem. Soc., Perkin Trans. II*, 287 (1975); (b) M. J. Kamlet, R. R. Minesinger, E. G. Kayser, M. M. Aldrige, and J. W. Eastes, *J. Org. Chem.*, 36, 3852 (1971); (c) R. R. Minesinger, M. E. Jones, R. W. Taft, and M. J. Kamlet; *J. Org. Chem.*, 42, 1929 (1977); (d) A. E. Lutskii, V. V. Bocharova, and M. R. Kreslavskaya, *Zh. Obshch. Khim.*, 45, 2276 (1975); (e) M. M. Davis and H. B. Hetzer, *Anal. Chem.*, 38, 451 (1966); (f) A. E. Lutskii, V. V. Vochareva, and Z. I. Kanevskaya, *Zh. Obshch. Khim.*, 45, 2731 (1975); (g) T. Yokoyama, *Aust. J. Chem.*, 29, 1469 (1976); (h) J. Figueras, *J. Am. Chem. Soc.*, 93, 3255 (1971); (i) M. A. Mostoslavskii and V. A. Ismailskii, *Dokl. Akad. Nauk SSSR*, 142, 600 (1962).
79. J. O. Hirschfelder, C. F. Curtiss, and R. B. Bird; *Molecular Theory of Gases and Liquids*, Wiley, New York, Chapters 12 and 13, particularly p. 947 and ff.
80. W. B. Person and R. B. Mulliken; *Molecular Complexes: A Lecture and Reprint Volume*, Wiley, New York 1969.
81. L. Skulski and J. M. Kanabus, *Bull. Acad. Pol. Sci., Ser. Sci. Chim.*, 17, 311 (1969).
82. M. Feldman and S. Winstein, *J. Am. Chem. Soc.*, 83, 3338 (1961).
83. Other polar materials have been studied: e.g., ethers, amines, lactones, acid anhydrides, coumarines and cyanine dyes. Detailed references are given by R. Foster, in *Organic Charge-Transfer Complexes*, Academic, London–New York, 1969, p. 108.
84. P. Laszlo and P. J. Stang, *Spectroscopie Organique*, Hermann, Paris, 1972, p. 284.
85. (a) R. Foster and C. A. Fyfe, in *Progress in Nuclear Magnetic Resonance Spectroscopy*, J. W. Emsley, J. Feeney, and L. H. Sutcliffe, Eds., Pergamon, Oxford–New York, 1969; Vol. 4; Chapter 1; (b) P. Laszlo, *ibid.*, Vol. 3, Chapter 6.
86. (a) Ref. 84; (b) Ref. 38.
87. As shown in Table 20, for example.
88. (a) R. S. Mulliken, *J. Am. Chem. Soc.*, 72, 600 (1950); (b) Ref. 83, p. 21; (c) R. S. Mulliken, 74, 811 (1952); (d) C. Reid and R. S. Mulliken, *J. Am. Chem. Soc.*, 76, 3869 (1954).
89. C. A. Coulson, A. Maccoll, and L. Sutton, *Trans. Faraday Soc.*, 48, 106 (1952).
90. (a) C. A. Coulson and P. L. Davis, *Trans. Faraday Soc.*, 48, 777 (1952); (b) Ref. 79, pp. 974–983.
91. H. O. Hooper, *J. Chem. Phys.*, 41, 599 (1964).
92. (a) R. Anderson and J. M. Pransnitz, *J. Chem. Phys.*, 39, 1225 (1963); (b) *ibid.*, 40, 3443 (1964); (c) R. F. Weimer and J. M. Pransnitz, *J. Chem. Phys.*, 42, 3643 (1965).
93. (a) J-M. Dumas, C. Geron, H. Peurichard, and M. Gomel, *Bull. Soc. Chim. (France)*, 720 (1976); (b) J-M. Dumas, H. Peurichard, and M. Gomel, *J. Chem. Res. (S)*, 54 (1978); (c) B. Castagna, J-M. Dumas, M. Guérin and M. Gomel, *J. Chim. Phys.*, 960 (1973).
94. J-M. Dumas, Ph.D. Thesis, University of Poitiers, 1975.
95. J-M. Dumas, M. Kern, and J-L. Hanier-Dubry, *Bull. Soc. Chim. (France)* (1976).
96. See, e.g., T. Di Paolo and C. Sandorfy, *Can. J. Chem.*, 52, 3612 (1974) and references therein.
97. (a) J. P. Sheridan, D. E. Martire, and Y. B. Tewari, *J. Am. Chem. Soc.*, 94, 3294 (1972); (b) D. E. Martire, J. P. Sheridan, J. W. King, and S. E. O'Donnell, *ibid.*, 98, 3101 (1976); (c) C. Geron and M. Gomel, *J. Chim. Phys.*, 75, 241 (1978).
98. W. P. Hayes and C. J. Timmons, *Spectrochim. Acta*, 21A, 529 (1965).
99. P. Jacques and J. Faure, *J. Chem. Phys.*, 70, 653 (1973).

100. L. J. Bellamy and R. L. Williams, *Trans. Faraday Soc.*, **55**, 14 (1959).
101. S. Tanaka, K. Tanabe, and H. Kamada, *Spectrochim. Acta*, **23A**, 300 (1967).
102. U. Hayer, V. Gutmann, and W. Geiger, *Monatsh. Chem.*, **106**, 1235 (1975).
103. C. J. MacDonald and T. Schaefer, *Can. J. Chem.*, **45**, 3157 (1967).
104. M. Auriel and E. de Hoffmann, *J. Am. Chem. Soc.*, **97**, 7433 (1975).
105. I. A. Koppel and V. A. Palm, *Reakts. Sposobn. Org. Soedin.*, **6**, 504 (1969).
106. R. E. Pincock, *J. Am. Chem. Soc.*, **86**, 1820 (1964).
107. E. L. Eliel and O. Hofer, *J. Am. Chem. Soc.*, **94**, 8041 (1972).
108. B. Chawla, M. Fujio, L. Symani, S. Pollack, C. Lebrilla, R. W. Taft, unpublished results.
109. J. Burgess, *Spectrochim. Acta*, **A**, **26**, 1957 (1970).
110. K. M. C. Davis, *J. Chem. Soc. (B)*, 1128 (1963).
111. C. S. Giam and J. L. Lyle, *J. Am. Chem. Soc.*, **95**, 3253 (1973).
112. (a) V. Mayer, V. Gutmann, and W. Gerger, *Monatsh. Chem.*, **106**, 1235 (1975); (b) V. Gutmann, *Electrochim. Acta*, **21**, 661 (1976).
113. P. Strop, F. Mikes, and J. Kalal, *J. Phys. Chem.*, **80**, 694 (1976).
114. C. Duboc, *Spectrochim. Acta*, **30A**, 431, 440 (1974).
115. See, e.g., M. J. Kamlet, E. G. Kayser, J. W. Eastes, and W. H. Gilligan, *J. Am. Chem. Soc.*, **95**, 5210 (1973).
116. For a discussion of HBA properties of the benzene π -system, see G. C. Pimentel and A. L. McClellan, *The Hydrogen Bond*, W. H. Freeman, San Francisco, 1960, pp. 22-24; also, B. B. Wayland and R. S. Drago, *J. Am. Chem. Soc.*, **86**, 5240 (1964).
117. For examples of hydrogen bonding by methylene chloride, see, e.g., E. F. Meyer and F. A. Baiocchi, *J. Am. Chem. Soc.*, **99**, 6206 (1977).
118. (a) R. W. Taft, E. Price, I. R. Fox, I. C. Lewis, K. K. Anderson, and G. T. Davis, *J. Am. Chem. Soc.*, **85**, 709 (1963); (b) *ibid.*, **85**, 3146 (1963).
119. D. Dorohoi, L. Sitaru, G. Surpatenan, and C. Mihul, *An. Stiint. Univ. "Al. I. Cuza," Sect. Ib*, **20**, 147 (1974).
120. W. Walter and O. H. Bauer, *Ann.* **421** (1977).
121. R. A. Mackay and E. Z. Poziomek, *J. Am. Chem. Soc.*, **97**, 6107 (1975).
122. J. Moskal, A. Moskal, and W. Pietrzycki, *J. Chem. Soc., Perkin II*, 1893 (1975).
123. T. M. Krygowski and W. R. Fawcett, *J. Am. Chem. Soc.*, **97**, 2143 (1975).
124. (a) M. J. Kamlet, E. G. Kayser, J. W. Eastes, and W. H. Gilligan, *J. Am. Chem. Soc.*, **95**, 5210 (1973).
125. L. S. Kaminsky and M. Lamchen, *J. Chem. Soc. (B)*, 1087 (1968).
126. A. Arcoria, V. Librando, E. Maccarone, G. Musumarra, and G. A. Tomaselli, *Tetrahedron*, **33**, 105 (1977).
127. F. P. Ballistrei, E. Maccarone, G. Musumarra, and G. A. Tomaselli, *J. Org. Chem.*, **42**, 1415 (1977).
128. L. E. Cramer and K. G. Spears, *J. Am. Chem. Soc.*, **100**, 221 (1978).
129. L. A. Kazitsyna and V. V. Mischenko, *Zhur. Org. Khim.*, **1**, 617 (1965).
130. (a) J. Hires, *Acta Univ. Szegediensis, Acta Phys. Chim.*, **4**, 120 (1958); (b) J. Hires and L. Hackel, *ibid.*, **5**, 19 (1959).
131. (a) I. A. Koppel and V. A. Palm, *Reakts. Sposobnost. Org. Soedin.*, **8**, (1971); (b) I. A. Koppel and A. I. Paju, *ibid.*, **11**, 137 (1974).
133. M. J. Kamlet, M. E. Jones, J. L. Abboud, and R. W. Taft, *J. Chem. Soc., Perkin Trans. II*, 342 (1979).
134. M. J. Kamlet, E. G. Kayser, M. E. Jones, J. L. Abboud, J. W. Eastes, and R. W. Taft, *J. Phys. Chem.*, **82**, 2477 (1978).
135. J. N. Murrell, *The Theory of Electronic Spectra of Organic Molecules*, Methuen, London, 1963, p. 244ff.

136. T. Gramstad, *Spectrochim Acta*, **19**, 497, 829, 1363 (1963).
137. T. Gramstad and O. Mundheim, *Spectrochim. Acta*, **28A**, 1405 (1972).
138. T. Gramstad and J. Sandstrom, *Spectrochim. Acta*, **25A**, 31 (1969).
139. M. J. Kamlet, A. Solomonvici, and R. W. Taft, *J. Am. Chem. Soc.*, **101**, 3734 (1979).
140. N. B. Chapman, M. R. J. Dack, D. J. Newman, J. Shorter, and R. Wilkinson, *J. Chem. Soc., Perkin Trans. II*, 962 (1974).
141. A. P. Grekov and G. V. Otroshko, *Zhur. Organ. Khim.*, **10**, 783 (1974).
142. L. V. Okhlobystina, V. M. Khutoretskii, A. D. Naumov, and A. V. Kessenikh, *Izv. Akad. Nauk SSSR, Ser. Khim.*, 545 (1971).
143. R. L. Lichten and J. D. Roberts, *J. Phys. Chem.*, **74**, 912 (1970).
144. L. E. Lapuka, O. P. Yablonskii, S. Tu. Pavlov, and B. A. Saraev, *Russ. J. Phys. Chem., Engl. Ed.*, **47**, 516 (1973).
145. L. K. Vosyanina, V. A. Marchenko, Yu. S. Bogachev, F. S. Yakushin, N. N. Shapet'ko, and A. I. Shatenshtein, *Zhur. Obshch. Khim.*, **42**, 447 (1972).
146. J. Mitsky, L. Joris, and R. W. Taft, *J. Am. Chem. Soc.*, **94**, 3442 (1972).
147. G. A. Kurkchoi and A. V. Iogansen, *Russ. J. Phys. Chem., Engl. Ed.*, **41**, 81, 283 (1967).
148. M. J. Kamlet, T. N. Hall, J. Boykin, and R. W. Taft, *J. Org. Chem.*, **44**, 2599 (1979).
149. I. L. Bagal, *Reakts. Sposobn. Organ. Soedin.*, **5**, 402 (1968); *Engl. ed.*, p. 166.
150. C. N. R. Rao, *Ultraviolet and Visible Spectroscopy*. Chemical Applications, 2nd ed., Butterworths, London, pp. 66ff.
151. R. T. C. Brownlee and R. D. Topsom, *Spectrochim. Acta*, **29A**, 385 (1973).
152. N. Oi and J. F. Coetzee, *J. Am. Chem. Soc.*, **91**, 2473 (1963).
153. L. J. Bellamy, C. P. Conduit, R. J. Pace, and R. L. Williams, *Trans. Faraday Soc.*, **55**, 1677 (1959).
154. M. J. Kamlet and R. W. Taft, *J. Chem. Soc., Perkin Trans. II*, 337 (1969).
155. L. J. Bellamy and R. L. Williams, *Trans. Faraday Soc.*, **55**, 14 (1959).
156. K. C. James and M. Ramgoolam, *Spectrochim. Acta*, **31A**, 599 (1975).
157. In ref. 20a, p. 1681
158. M. Guérin and M. Gomel, *J. Chim. Phys.*, **953** (1973).
159. Ref. 27, p. 265.
160. G. L. Nelson, G. C. Levy, and J. D. Cargioli, *J. Am. Chem. Soc.*, **94**, 3089 (1972).
161. J. Bromilow, R. T. C. Brownlee, R. D. Topsom, and R. W. Taft, *J. Am. Chem. Soc.*, **98**, 2020 (1976).
162. (a) W. F. Reynolds, I. R. Peat, M. H. Freedman, and J. R. Lyster, *Can. J. Chem.*, **51**, 1857 (1973); (b) W. Adcock and T. C. Khor, *J. Am. Chem. Soc.*, **100**, 7799 (1978) and references cited therein.
163. (a) R. W. Taft, E. Price, I. R. Fox, I. C. Lewis, K. K. Anderson, and G. T. Davis, *J. Am. Chem. Soc.*, **85**, 709, 3146 (1963); (b) Ref. 160.
164. (a) B. B. Wayland and R. S. Drago, *J. Am. Chem. Soc.*, **86**, 5240 (1964); (b) Ref. 133.
165. R. E. Uschold and R. W. Taft, *Organic Mag. Resonance*, **1**, 375 (1969).
166. R. W. Taft and M. J. Kamlet, *J. Chem. Soc., Perkin Trans. II*, 0000 (1979).
167. M. J. Kamlet and R. W. Taft, *J. Chem. Soc., Perkin Trans. II*, 349 (1979).
168. (a) Ref. 49, p. 301; (b) E. M. Kosower, *J. Am. Chem. Soc.*, **80**, 5253 (1958).
169. Unpublished results of T. N. Hall and M. J. Kamlet.
170. F. L. Huyskens, *J. Am. Chem. Soc.*, **99**, 2579 (1977).
171. For a recent discussion see T. W. Bentley and P. v. R. Schleyer, *J. Am. Chem. Soc.*, **98**, 7658 (1976); F. L. Schadt, T. W. Bentley, and P. v. R. Schleyer, *ibid.*, **98**, 7667 (1976).
172. D. L. Tuleen, W. G. Bentrude, and J. C. Martin, *J. Am. Chem. Soc.*, **85**, 1938 (1963).
173. R. O. Duthaler and J. D. Roberts, *J. Am. Chem. Soc.*, **100**, 4969 (1978).
174. H. W. Aitkin and W. R. Gilkerson, *J. Am. Chem. Soc.*, **95**, 8551 (1973); W. R. Gilkerson

- and J. B. Ezell, *ibid.*, 89, 809 (1967); H. B. Flora and W. R. Gilkerson, *ibid.*, 92, 3273 (1970); M. D. Jackson and W. R. Gilkerson, *ibid.*, 101, 328 (1979).
175. V. Gutmann, *Chemtech*, 255 (1977).
176. E. M. Arnett, E. J. Mitchell, and T. S. S. R. Murty, *J. Am. Chem. Soc.*, 96, 3875 (1974).
177. T. F. Bolles and R. S. Drago, *J. Am. Chem. Soc.*, 88, 5730 (1966).
178. D. N. Kravtsov, B. A. Kvasov, F. N. Fedin, B. A. Faingor, and L. S. Golovchenko, *Izv. Akad. Nauk SSSR, Ser. Khim.*, 536 (1969).
179. J. W. Raksy, Jr., PhD. Thesis, University of California, Irvine, 1967.
180. J. Figueras, *J. Am. Chem. Soc.*, 93, 3255 (1971).
181. F. W. Fowler, A. R. Katritzky, and R. J. D. Rutherford, *J. Chem. Soc. (B)*, 460 (1971).
182. W. Liptay, D. Dumbacher, and H. Weisenberger, *Z. Naturforsch.*, 23A 1601 (1968); C. Reichardt and R. Muller, *Ann. Chem. Liebigs*, 1937 (1976).

Index

- Alkenes, molecular properties of, cf compounds:
 chemical compound index, 454-484
- Anilide anions, 36
- Anilines, effect of π -acceptor, σ -acceptor substituents, 25
 acidity of, 46
 basicity of, 46
 effect of σ -donor, π -acceptor substituents, 27
 inversion barriers in, 31
- Anilinium cations, 43
- Basicity, of allenes, 344
- Benzonitriles, 32
- π -Bond order, cf compound index, 454-484
- ^{13}C chemical shifts:
 of allenes and cumulenes, cf compound index, 454-484
 compound index, 454-484
- Chemical potentials:
 electrostatic contributions to, 491
 and the role of solvents, 486
- CISGEN computer program, 70
- C_nH_{2n} and $\text{C}_n\text{H}_{2n-2}$ families, 75
- $\text{C}_n\text{H}_{2n-4}$ hydrocarbons, 79
 stabilomers of, 82
- $\text{C}_n\text{H}_{2n-6}$ hydrocarbons, 97
- $\text{C}_n\text{H}_{2n-8}$ hydrocarbons, 103
 saturated vs. aromatics, 108
- Cumulenes:
 chemical compound index, 454-484
 molecular properties of, cf compound index, 454-484
- Cyanobenzenes, 32
- Delocalized electrical effects, 120
 parameters for, 131, 177, 197
 separation of:
 by Exner method, 242
 percentage of total effect, 247
 by Swain-Lupton method, 238
- Dielectric constants, of bulk solvents, 531
- Dielectric saturation, 490
- Dipole moments:
 of allenes and cumulenes, 331
 also cf compound index, 454-484
- Disubstituted benzenes, 18
- Electron densities, in allenes and cumulenes, cf compound index, 454-484
- Electronic absorption spectra:
 of pyridino betaines, 572, 594
 solvent effects on, 507, 538, 549, 559, 580, 595, 596, 598, 599, 600, 601
- Electron paramagnetic resonance spectroscopy, 273, 282, 285
 hyperfine coupling constants from, 285
 influence of trifluoromethyl group on, 287
 for miscellaneous fluorinated radicals, 298
 of nitrobenzene anion radicals, 292
 of nitroxide radicals, 289
 for fluorinated semiquinones, 302
 theoretical interpretation of the fluorine hyperfine splittings, 304
- Enthalpy contributions to hydrocarbon standard, free energies of formation, 65, 67
- Entropy contributions to hydrocarbon standard, free energies of formation, 65, 66
- Field effect, 120, 255, 264
 parameters for, 127
- Fluorinated aliphatic free radicals, 279
- Fluorinated anilines, contact shifts for, 292
- Fluorinated nitrobenzene anion radicals, 292
- Fluorinated nitroxide radicals, 289
- Fluorinated semiquinones, 302
- Fluorine substituent chemical shifts, 269

- Fluorobenzenes:
 effect of π -acceptor, σ -acceptor substituents, 25
 effect of σ -donor, π -acceptor substituents, 27
- Four-electron interaction, 9
- ¹H chemical shifts of allenes and cumulenes, cf compound index, 454-484
- Heats of formation of polycyclic alkanes, 68
 calculation of, 73
 calculations for 1-alkyladamantanes, 94
 calculations for 2-alkyladamantanes, 94
- Heats of isomerization of adamantanes, 69
- Heats of transfer between solvents, 498, 556, 576, 611
- Hydrogen atom exchange reactions, of aliphatic fluorocarbons, 264
- Hydrogen-bonding types, AB, A, and B, 557
- Inductive effect, 120, 254
- π -effect, 10, 42, 254, 255
- Infrared absorption spectra:
 the B scale of solvent HBA basicity, 551
 solvent effects on, 510, 551, 564, 580
- Interaction saturation, 8
- Ionization energies of allenes and cumulenes, cf compound index, 454-484
- Isomerism, in cumulenes, 323
- Linear solvation energy relationships, 533, 548, 604
- Lithiobenzenes, 34
- Localized electrical effects, 120
 of alkyl groups, 161, 172
 comparison of substituent constants for, 169
 criteria for reference set parameters, 129
 parameters for, 121, 122, 125, 127
 separation of:
 by Ehrenson, Brownlee and Taft method, 238
 by Exner method, 242
 by modification of Hanch, 238
 by Swain-Lupton method, 238
 by Yukawa-Tsuno method, 126
- Molecular orbital theory:
Ab initio, 4
 perturbation, 5
- Monofluoroacetamide radical, 275
- Monosubstituted benzenes:
 conformations of, 9
 π -electron populations for, 10
 HOMO and LUMO coefficients, 12, 13, 14, 15
- Mulliken population analysis, 4, 8
- 2-nitro-4-trifluoromethylchlorobenzene, 262
- Nuclear magnetic resonance spectra:
 the AN solvent scale from, 597
 the P scale of solvent polarity from, 520
 solvent effects on, 509, 554, 580, 582, 591, 593, 596, 597, 614
- Nucleophilic aromatic substitution reactions, 262
- Perfluorosuccinate radical, 276
- Phenols:
 acidity of, 46
 effect of π -acceptor, σ -acceptor substituents, 25
 effect of σ -donor, π -acceptor substituents, 27
 rotational barriers in, 29
 trifluoromethyl substituted, 261
- Phenoxide anions, 36
- Photoelectron spectroscopy, 271
 of allenes and cumulenes, cf compound index, 454-484
 core-electron binding energy from, 272
 coupling constant tensors from, 275
- Polysubstituted benzenes, 51
 polycyanobenzenes, 52
 polyfluorobenzenes, 51
 polythiobenzenes, 52
- Pyridines, substituent effect on basicities of, 210
- Reaction field theory, 488
 Block-Walker modification, 489
 the $\psi(\epsilon_B)$ function, 491, 498
 the $\theta(\epsilon_B)$ function, 497, 499, 500
 influence of solute dipole, 493
 influence of solute polarizability, 494

- influence of solute quadripole, 493
 of Onsager, 488
 Reaction rates, solvent effects on, 501, 553,
 575, 577, 604, 607, 608
 Self-association of dipolar solute, 494
 SEMA algorithm, 70
 Shielding-desielding mechanism, 7
 Solvent effects, contributions of dipoles,
 488
 Solvent polarizability, 508, 571, 574
 Solvent polar scales:
 α scale of HBD acidity, 587, 592, 617
 AN scale, 597
 β scale of HBA basicity, 535, 544, 617
 $\chi(\epsilon_B)$ scale, 491, 530
 χ_R scale, 513, 609, 610
 dipole moment scale for select solvents,
 526
 DN scale, 613
 E_K scale, 516
 E_T scale, 513, 572, 594
 G scale, 521, 564
 L_s scale, 616
 π^* scale, 517, 558, 581, 588, 617
 the π scale, 523
 P scale, 520
 $\theta(\epsilon_B)$ scale, 497, 527, 529
 Y value, 501, 503
 Z scale, 511, 598
 Spin-spin coupling constants in allenes and
 cumulenes, cf compound index, 454-
 484
 Stabilities of hydrocarbons, 64, 114
 experimental methods for determination
 of, 64
 thermodynamic stability rules, 72
 Stabilization energy, 5
 Stabilomer:
 C_nH_{2n} stabilomers, 77
 C_nH_{2n-2} stabilomers, 78
 C_nH_{2n-4} stabilomers, 82
 C_nH_{2n-6} stabilomers, 82
 C_nH_{2n-8} stabilomers, 82
 definition of, 64
 Steric effects, 157, 163
 dependence on degree of branching, 163
 Substituent constants:
 F , 127
 σ^* , 121
 σ_D , 120, 131
 σ_i , 126
 σ_I , 125, 127, 136, 142
 σ_I^q , 129
 σ_L , 120, 131
 σ_m , 178, 180, 191, 196
 σ^+ , 122
 σ_p , 178, 181, 191, 196
 σ_R , 191, 197
 σ_R^q , 201, 269
 σ_R^- , 215
 σ_R^+ , 202
 errors in, 141
 estimation of, 225, 226, 232, 236
 for hydroxylic groups, 166, 246
 for ionic groups, 166, 245
 methods for evaluation of, 138
 validity in non-protonic media, 166, 190,
 196, 215, 220
 Substituent effects:
 on acidity and basicity, 46
 in allenes compared to benzenes and ethyl-
 enes, 412
 in amide anions, 36
 in anilines, 19
 in anilinium cations, 43
 composition of electrical effect of,
 120
 in cyanobenzenes, 32
 in fluorobenzenes, 19
 in lithiobenzenes, 34
 nature of, 9, 10
 in phenols, 19
 in phenoxide anions, 36
 Substituent interaction energies, 5
 Trifluoromethyl group:
 C-F hyperconjugation in, 254, 256
 dipole moment in compounds containing,
 267
 polar effect in, 262
 1,3 p p interactions in, 254, 274, 279
 σ_R^q value for, 269
 Tri- n -butylammonium ion, H-bonded com-
 plex formation constants for, 612
 UV spectra, of allenes and cumulenes, cf
 compound index, 454-484

Cumulative Index, Volumes 1-13

	VOL.	PAGE
<i>Acetals, Hydrolysis of, Mechanism and Catalysis for</i> (Cordes)	4	1
<i>Acetonitrile, Ionic Reactions in</i> (Coetzee)	4	45
<i>Active Sites of Enzymes, Probing with Conformationally Restricted Substrate Analogs</i> (Kenyon and Fee)	10	381
<i>Activity Coefficient Behavior of Organic Molecules and Ions in Aqueous Acid Solutions</i> (Yates and McClelland)	11	323
<i>Alkyl Inductive Effect, The, Calculation of Inductive Substituent Parameters</i> (Levitt and Widing)	12	119
<i>Allenes and Cumulenes, Substituent Effects in</i> (Runge)	13	315
<i>Amines, Thermodynamics of Ionization and Solution of Aliphatic, in Water</i> (Jones and Arnett)	11	263
<i>Aromatic Nitration, A Classic Mechanism for</i> (Stock)	12	21
<i>Barriers, to Internal Rotation about Single Bonds</i> (Lowe)	6	1
<i>Benzenes, A Theoretical Approach to Substituent Interactions in Substituted</i> (Pross and Radom)	13	1
<i>Benzene Series, Generalized Treatment of Substituent Effects in the A Statistical Analysis by the Dual Substituent Parameter Equation</i> (Ehrenson, Brownlee, and Taft)	10	1
<i>¹³C Nmr, Electronic Structure and</i> (Nelson and Williams)	12	229
<i>Carbonium Ions</i> (Deno)	2	129
<i>Carbonyl Group Reactions, Simple, Mechanism and Catalysis of (Jencks)</i>	2	63
<i>Catalysis, for Hydrolysis of Acetals, Ketals, and Ortho Esters</i> (Cordes) ..	4	1
<i>Charge Distributions in Monosubstituted Benzenes and in Meta- and Para-Substituted Fluorobenzenes, 4b Initio Calculations of: Com- parison with ¹H, ¹³C, and ¹⁹F Nmr Substituent Shifts</i> (Hehre, Taft, and Topsom)	12	159
<i>Charge-Transfer Complexes, Reactions through</i> (Kosower)	3	81
<i>Conformation, as Studied by Electron Spin Resonance of Spectroscopy (Geske)</i>	4	125
<i>Delocalization Effects, Polar and Pi, an Analysis of</i> (Wells, Ehrenson, and Taft)	6	147
<i>Deuterium Compounds, Optically Active</i> (Verbic)	7	51
<i>Electrolytic Reductive Coupling: Synthetic and Mechanistic Aspects (Baizer and Petrovich)</i>	7	189

	VOL.	PAGE
<i>Electronic Structure and ¹³C Nmr</i> (Nelson and Williams)	12	229
<i>Electron Spin Resonance, of Nitrenes</i> (Wasserman)	8	319
<i>Electron Spin Spectroscopy, Study of Conformation and Structure by</i> (Geske)	4	125
<i>Electrophilic Substitutions at Alkanes and in Alkylcarbonium Ions</i> (Brouwer and Hogeveen)	9	179
<i>Enthalpy-Entropy Relationship</i> (Exner)	10	411
<i>Fluorine Hyperconjugation</i> (Holtz)	8	1
<i>Gas-Phase Reactions, Properties and Reactivity of Methylene from</i> (Bell)	2	1
<i>Group Electronegativities</i> (Wells)	6	111
<i>Hammett and Derivative Structure-Reactivity Relationships, Theoretical</i> <i>Interpretations of</i> (Ehrenson)	2	195
<i>Heats of Hydrogenation A Brief Summary</i> (Jenson)	12	189
<i>Hydrocarbons, Acidity of</i> (Streitwieser and Hammons)	3	41
<i>Hydrocarbons, Pyrolysis of</i> (Badger)	3	1
<i>Hydrolysis, of Acetals, Ketals, and Ortho Esters, Mechanism and</i> <i>Catalysis for</i> (Cordes)	4	1
<i>Internal Rotation, Barriers to, about Single Bonds</i> (Lowe)	6	1
<i>Ionic Reactions, in Acetonitrile</i> (Coetzee)	4	45
<i>Ionization and Dissociation Equilibria, in Solution, in Liquid Sulfur</i> <i>Dioxide</i> (Lichtin)	1	75
<i>Ionization Potentials, in Organic Chemistry</i> (Streitwieser)	1	1
<i>Isotope Effects, Secondary</i> (Halevi)	1	109
<i>Ketals, Hydrolysis of, Mechanism and Catalysis for</i> (Cordes)	4	1
<i>Kinetics of Reactions, in Solutions under Pressure</i> (le Noble)	5	207
<i>Linear Solvation Energy Relationships, An Examination of</i> (Abboud, Kamlet, and Taft)	13	485
<i>Methylene, Properties and Reactivity of, from Gas-Phase Reactions</i> (Bell)	2	1
<i>Molecular Orbital Structures for Small Organic Molecules and Cations</i> (Lathan, Curtiss, Hehre, Lisle, and Pople)	11	175
<i>Naphthalene Series, Substituent Effects in the</i> (Wells, Ehrenson, and Taft)	6	147
<i>Neutral Hydrocarbon Isomer, The Systematic Prediction of the Most</i> <i>Stable</i> (Godleski, Schleyer, Osawa and Wipke)	13	63
<i>Nitrenes, Electron Spin Resonance of</i> (Wasserman)	8	319
<i>Non-Aromatic Unsaturated Systems, Substituent Effects in</i> (Charton)	10	81

	VOL.	PAGE
<i>Nucleophilic Displacements, on Peroxide Oxygen</i> (Behrman and Edwards)	4	93
<i>Nucleophilic Substitution, at Sulfur</i> (Ciuffarin and Fava)	6	81
<i>Optically Active Deuterium Compounds</i> (Verbict)	7	51
<i>Organic Bases, Weak, Quantitative Comparisons of</i> (Arnett)	1	223
<i>Organic Polarography, Mechanisms of</i> (Perrin).....	3	165
<i>Ortho Effect, The Analysis of the</i> (Fujita and Nishioka)	12	49
<i>Ortho Effect, Quantitative Treatment of</i> (Charton)	8	235
<i>Ortho Esters, Hydrolysis of, Mechanism and Catalysis for</i> (Cordes)	4	1
<i>Ortho Substituent Effects</i> (Charton)	8	235
<i>Physical Properties and Reactivity of Radicals</i> (Zahradnik and Carsky) ..	10	327
<i>Pi Delocalization Effects, an Analysis of</i> (Wells, Ehrenson, and Taft)	6	147
<i>Planar Polymers, The Influence of Geometry on the Electronic Structure and Spectra of</i> (Simmons)	7	1
<i>Polar Delocalization Effects, an Analysis of</i> (Wells, Ehrenson, and Taft).	6	147
<i>Polarography, Physical Organic</i> (Zuman)	5	81
<i>Polyalkylbenzene Systems, Electrophilic Aromatic Substitution and Related Reactions in</i> (Baclocchi and Illuminati)	5	1
<i>Protonated Cyclopropanes</i> (Lee)	7	129
<i>Proton-Transfer Reactions in Highly Basic Media</i> (Jones)	9	241
<i>Radiation Chemistry to Mechanistic Studies in Organic Chemistry, The Application of</i> (Fendler and Fendler)	7	229
<i>Radical Ions, The Chemistry of</i> (Szwarc)	6	323
<i>Saul Winstein: Contributions to Physical Organic Chemistry and Bibliography</i>	9	1
<i>Semiempirical Molecular Orbital Calculations for Saturated Organic Compounds</i> (Herndon)	9	99
<i>Solutions under Pressure, Kinetics of Reactions in</i> (le Noble)	5	207
<i>Solvent Effects on Transition States and Reaction Rates</i> (Abraham)	11	1
<i>Solvent Isotope Effects, Mechanistic Deductions from</i> (Schowen)	9	275
<i>Solvolysis, in Water</i> (Robertson)	4	213
<i>Solvolytic Substitution in Simple Alkyl Systems</i> (Harris)	11	89
<i>Steric Effects, Quantitative Models of</i> (Unger and Hansch)	12	91
<i>Structure, as Studied by Electron Spin Resonance Spectroscopy</i> (Geske)	4	125
<i>Structure-Reactivity and Hammett Relationships, Theoretical Interpretations of</i> (Ehrenson)	2	195
<i>Structure-Reactivity Relationships, Examination of</i> (Ritchie and Sager).	2	323
<i>Structure-Reactivity Relationships, for Ortho Substituents</i> (Charton)	8	235
<i>Structure-Reactivity Relationships, in Homogeneous Gas-Phase Reactions</i> (Smith and Kelley)	8	75
<i>Substituent Constants for Correlation Analysis, Electrical Effect</i> (Charton)	13	119

	VOL.	PAGE
<i>Substituent Effects, in the Naphthalene Series</i> (Wells, Ehrenson and Taft)	6	147
<i>Substituent Electronic Effects, The Nature and Analysis of</i> (Topsom) ...	12	1
<i>Substitution Reactions, Electrophilic Aromatic</i> (Berliner)	2	253
<i>Substitution Reactions, Electrophilic Aromatic, in Polyalkylbenzene Systems</i> (Baclocchi and Illuminati)	5	1
<i>Substitution Reactions, Nucleophilic Aromatic</i> (Ross)	1	31
<i>Sulfur, Nucleophilic Substitution at</i> (Ciuffarin and Fava)	6	81
<i>Thermal Rearrangements, Mechanisms of</i> (Smith and Kelley)	8	75
<i>Thermal Unimolecular Reactions</i> (Wilcott, Cargill and Sears)	9	25
<i>Thermolysis in Gas-Phase, Mechanisms of</i> (Smith and Kelley)	8	75
<i>Trifluoromethyl Group in Chemistry and Spectroscopy Carbon-Fluorine Hyperconjugation, The</i> (Stock and Wasielewski).....	13	253
<i>Ultra-Fast Proton-Transfer Reactions</i> (Grunwald)	3	317
<i>Vinyl and Allenyl Cations</i> (Stang)	10	205
<i>Water, Solvolysis in</i> (Robertson)	4	213